Tyrosinase-induced cross-linking of collagen

Master's thesis

prepared by

Matthias Pretzler

at the

Institute for Environmental Biotechnology
Graz University of Technology

under the supervision of

Ao.Univ.-Prof. Dipl.-Ing. Dr.techn. Georg M. Gübitz

Graz, March 2012

This page was intentionally left blank.

Abstract

The aim of the present work was the investigation of the cross-linking of collagen evoked by the action of tyrosinase on said substrate with particular emphasis on the amino acids involved in the covalent bonds formed therein.
Experiments were carried out with bovine acid soluble collagen as the principle substrate, the oxidised β-chain of bovine insulin which functioned as a substitute easier to analyse and also with free amino acids in combination with derivatised tyrosine. Free, underivatised tyrosine treated with tyrosinase under aerobic conditions also results in the formation of an *o*-quinone which is not stable and undergoes intramolecular cyclisation and subsequent formation of a black precipitate – melanin. As a result of the formation of melanin any other reaction involving the reactive quinone has to compete for it against this (intramolecular) reaction and is therefore suppressed by lack of educts. Therefore, an N-protected tyrosine derivative was used from which a stable *o*-quinone was formed by tyrosinase in the presence of atmospheric oxygen.
Fungal tyrosinases from *Botryosphaeria obtusa* (an ascomycete causing frogeye leaf spot, black rot and canker in many trees and shrubs) and *Agaricus bisporus* (the common mushroom, a basidiomycete which is best known for its culinary use) were added to aqueous solutions of the respective substrates. This treatment caused an increase in molecular weight for the proteinaceous substrates accompanied by a slightly yellow shade of colour and resulted in strong colours for the individual free amino acids treated in presence of the N-protected tyrosine derivative.
Molecular size was determined with gel electrophoresis under denaturing conditions for all proteins and by gel permeation chromatography for untreated collagen as well as for samples with the oxidised β-chain of insulin. For the free amino acids treated with tyrosinase as well as for hydrolysed protein samples mass spectrometry was employed. The progress of the enzymatic reactions was monitored by UV-Vis spectroscopy and fluorometry as well as by visual sampling. As the proteinaceous samples were too big to be directly analysed by multistage mass spectrometry, a hydrolysis step (4 h at 145 °C in 4 M hydrochloric acid) was interposed yielding free amino acids. These amino acids were quantified by reversed-phase high performance liquid chromatography after pre-column derivatisation with *o*-phthaldialdehyde employing an UV-detector.
Gel electrophoresis and gel permeation chromatography showed a clear increase of apparent molecular weight in collagen and the oxidised β-chain of insulin treated with tyrosinase as compared to the respective untreated substrate which was markedly more pronounced in proteins treated with tyrosinase from *B. obtusa* as compared to the effect of treatment with tyrosinase from *A. bisporus*. For collagen as the tyrosinase´s substrate a gel-formation could also be observed. Amino acid analysis of hydrolysed samples indicated the impact of the incubation of collagen with tyrosinase on the levels of Ala, Arg, Gly, His, Ile, Leu and Val while liquid chromatography with subsequent multistage mass spectrometry showed the presence of amino acid derived, covalently bound units heavier than a single amino acid in the tyrosinase treated samples.

Zusammenfassung

Die Zielstellung der vorliegenden Arbeit lag in der Untersuchung der Quervernetzung von Kollagen hervorgerufen durch Einwirkung von Tyrosinase auf ebendieses Substrat mit besonderem Augenmerk auf die an im Zuge dieses Prozesses gebildeten kovalenten Bindungen beteiligten Aminosäuren.
Säurelösliches Rinderkollagen kam in den Experimenten als Zielsubstrat zum Einsatz, als einfacher analysierbares Substitut war die oxidierte Form der β-Kette von Rinderinsulin in Verwendung und außerdem wurden freie Aminosäuren in Kombination mit einem derivatisiertem Tyrosin eingesetzt. Freies, underivatisiertes Tyrosin das mit Tyrosinase unter aeroben Bedingungen behandelt wird führt ebenfalls zur Bildung eines *o*-Chinons welches allerdings nicht stabil ist und beginnend mit einem intramolekularen Ringschluss einen schwarzen Niederschlag bildet – Melanin. Diese Bildung von Melanin stellt eine Konkurrenzreaktion gegenüber allen anderen Reaktionen mit demselben reaktiven *o*-Chinon dar welche infolgedessen durch Eduktmangel unterdrückt werden. Daher wurde ein N-geschützten Tyrosinderivat eingesetzt, welches durch enzymatische Umsetzung mit Tyrosinase in Anwesenheit von atmosphärischem Sauerstoff in ein stabiles *o*-Chinon umgesetzt werden kann.
Pilzliche Tyrosinasen von *Botryosphaeria obtusa* (ein Ascomycet der Blattflecken-Nekrose, Fruchtfäule und Rindenbrand in vielen Bäumen und Sträuchern verursacht) und *Agaricus bisporus* (Zuchtchampignon, ein Basidiomycet der zu den beliebtesten Speisepilzen zählt) wurden wässrigen Lösungen der jeweiligen Substrate zugesetzt. Diese Behandlung bewirkte für die proteinösen Substrate eine Zunahme der molekularen Masse während gleichzeitig ein blass gelblicher Farbton ausgebildet wurde und kräftige Farben im Falle der freien Aminosäuren die in Anwesenheit des N-geschützten Tyrosinderivats behandelt wurden.
Zur Bestimmung der Molekülgröße kam für alle Proteine Gelelektrophorese unter denaturierenden Bedingungen sowie Gelpermeationschromatographie für sowohl unbehandeltes Kollagen als auch Proben mit oxidierter β-Kette von Insulin zum Einsatz. Freie Aminosäuren behandelt mit Tyrosinase und hydrolysierte Proteinproben wurden per Massenspektrometrie vermessen. Der Fortschritt der enzymatischen Reaktionen wurde per UV-Vis Spektroskopie, Fluorometrie und auch mittels visueller Bemusterung verfolgt. Da die Proteinproben zu groß waren um direkt per mehrstufiger Massenspektrometrie analysiert zu werden wurde ein Hydrolyseschritt (4 h bei 145 °C in 4 M Salzsäure) zwischengeschalten, der freie Aminosäuren lieferte. Diese Aminosäuren wurden per Umkehrphasenhochleistungsflüssigkeitschromatographie nach Vorsäulenderivatisierung mit o-Phthaldialdehyd unter Verwendung eines UV-Detektors quantifiziert.
Gelelektrophorese und Gelpermeationschromatographie zeigten einen klaren Anstieg der scheinbaren molekularen Masse von tyrosinasebehandeltem Kolllagen bzw. der oxidierten β-Kette von Insulin im Vergleich zu dem jeweiligen unbehandeltem Substrat. Diese Zunahme der Molekülgröße war deutlich stärker in Proben die mit Tryosinase von *B. obtusa* behandelt worden waren ausgeprägt als es für die mit Tyrosinase von *A. bisporus* behandelten Proteine der Fall war. Im Falle von Kollagen als Substrat für die Tyrosinase konnte zusätzlich die Bildung eines Gels beobachtet werden. Die Aminosäurenanalyse von hydrolysierten Proben wies auf die Auswirkung der Inkubation von Kollagen mit Tyrosinase auf die Menge an Ala, Arg, Gly, His, Ile, Leu und Val hin während mittels Flüssigchromatographie mit anschließender mehrstufiger Massenspektrometrie die Anwesenheit von kovalent verknüpften, von Aminosäuren abgeleiteten Einheiten mit Massen größer einer einzelnen Aminosäure in den mit Tyrosinase behandelten Proben gezeigt werden konnte.

1. Introduction

The present work aimed at the investigation of the cross-linking of collagen by the enzymatic action of tyrosine. This introduction will consequently provide a short review of the substrate and enzyme involved in the aforementioned reaction.

1.1. Collagen

The word collagen stems from the greek κόλλα /kólːa/ ("glue") and γένος /génos/ ("origin", "kind") and is used for "that constituent of connective tissue which yields gelatin on boiling" (*A New English Dictionary on Historical Principles*[1], Vol. II, 1893).
Collagen is a key element in the solution to a problem that arised when multicellular organisms evolved: the formation of functionally diverse tissues. The need to provide the tissue with a defined shape and mechanical properties fitting its function was met not just by changes inside the involved cells but also by the implementation of a specialised filling material between the cells: the extracellular matrix. The main components of this extracellular material are proteoglycans, adhesive glycoproteins and collagens [1]. Owing to the critical function for the evolution of metazoa, the main collagens evolved circa 800 – 900 million years ago [2] in accordance with the fossil record of primitive metazoa dating approximately one billion years back [3, 4].
Collagens (and the less abundant elastin) are among the most important insoluble proteins in connective tissue and responsible for its considerable tensile strength. The structure, post-translational modifications and the degree of intermolecular crosslinking of the collagen molecules significantly influence the physiological and biochemical properties of the connective tissue [5].

1.1.1. Structure of collagens

27 types of collagen are known in vertebrates, each consisting of 3 out of 42 distinct polypeptide chains [6]. The three polypeptide chains, called α-chains, each contain at least one repeating Gly-X-Y sequence where X and Y can be any amino acid but at the X position Pro can often be found while at the Y position the probability of encountering 4-hydroxyproline is greatly enhanced. Some collagens are composed of three identical α-chains whereas others contain two or even three different types of α-chains. Each of these α-chains coils into a left-handed helix with approximately 18 amino acids per turn which are in turn wound around a common axis to form a triple helix with a right-handed superhelical pitch. The presence of one glycine per 3 amino acid residues is necessary to allow the packing of this coiled-coil structure as only Gly is small enough to fit in the restricted place in the center of the triple-helix where the three α-chains come together [7].
Hydroxyproline is especially important for the stability of the final triple helix as it forms hydrogen bonds between its hydroxyl group and coordinated water. Collagen consisting of α-chains lacking Hyp can form a triple helix at low temperature which is however not stable at mammalian body temperature [7].
At the N- and C-terminus of the protein no Gly-X-Y triplets are found so that the helical domain doesn't extend into the terminal regions where unordered telopeptides are found. These terminal telopeptides are crucial to the assembly of the diverse supramolecular structures formed by collagens.

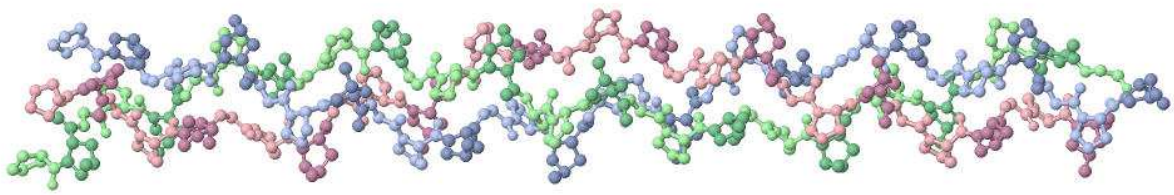

Figure 1-1 triple helical structure of collagen (PDB entry 1CAG, [8])

[1] Later editions published as "Oxford English Dictionary"

1.1.2. Classification of collagens

Collagens are distinguished with roman numerals which denote the order of their discovery. The polypeptide chains making up the collagen (α-chains) are specified using arabic numerals and the collagen type in round parentheses (e.g. α1(I) and α2(I) are the α1 and α2 chains of collagen I respectively). The α-chains of procollagen molecules (unprocessed fibrillar collagens, *vide infra*) are labelled by prefixing the name of the corresponding α-chain with "pro".
The name for the genes encoding the α-chains is formed by "COL" for collagen, an arabic number for the type of the collagen, the letter 'A' for α-chain and another arabic number for the chain in question (e.g. the aforementioned α-chains α1(I) and α2(I) are encoded by COL1A1 and COL1A2).

The collagen superfamily of proteins can be divided into eight subgroups (and one associated family of noncollagenous proteins) on the basis of the differences in the formed supramolecular assemblies and other properties like location and biological function [6]:

- **Fibril-forming** collagens: I, II, III, V, XI, XXIV and XXVII
  - COL1A1, COL1A2, COL2A1, COL3A1, COL5A1, COL5A2, COL5A3, COL5A4, COL11A1, COL11A2, COL24A1 and COL27A1
- **FACIT** (fibril-associated collagens with interrupted triple helices) located on the surface of fibrils and related collagens: IX, XII, XIV, XVI, XIX, XX, XXI, XXII and XXVI
  - COL9A1, COL9A2, COL9A3, COL12A1, COL14A1, COL16A1, COL19A1, COL20A1, COL21A1, COL22A1 and COL26A1
- Collagens forming **hexagonal networks**: VIII and X
  - COL8A1, COL8A2 and COL10A1
- Family of **type IV** collagens located in basement membranes: IV
  - COL4A1, COL4A2, COL4A3, COL4A4, COL4A5 and COL4A6
- **Type VI** collagen forming beaded filaments: VI
  - COL6A1, COL6A2 and COL6A3
- **Type VII** collagen forming anchoring fibrils for basement membranes: VII
  - COL7A1
- Collagens with **transmembrane domains**: XIII, XVII, XXIII and XXV
  - COL13A1, COL17A1, COL23A1 and COL25A1
- Family of **type XV and XVIII** collagens: XV and XVIII
  - COL15A1 and COL18A1
- Proteins containing triple-helical **collagenous domains**:
  e.g. Acetyl-cholinesterase, C1q complex, macrophage receptors …

Collagen type I is the most common of all collagens in vertebrates and is responsible for much of the mechanical resistance of skin, arteries, tendons, ligaments, intervertebral disks, bones, dentins etc. [5, 9]. It accounts for more than 90 % of the extracellular matrix of bone tissue [10] and is also the most abundant structural protein in tendons and skin [11]. Even in cartilage, which was believed to contain exclusively type II collagen traces of type I collagen have been found [9].
The fibril forming collagen I is a heterotrimer consisting of 2 α1(I) and one α2(I) chains [12].
Due to its widespread nature, collagen type I is often what is implied if the term "collagen" is used colloquially. It is used in the gelatine industry, in many biomaterials and is also the main component of leather [9].

1.1.3. Biosynthesis of fibrillar collagens

Collagen biosynthesis is a multistep process that can be roughly separated into two distinct phases: intracellular peptide synthesis with the subsequent assembly to triple helices and extracellular modification leading to the formation of the respective supramolecular assembly.

The synthesis of fibrillar collagens is one of the essential features of stromal cells [5]. Fibroblasts and osteoblasts account for the main part of the collagen synthesis capacity though many other cells are able to synthesise collagens as well.

Translation:

The spliced mRNAs encoding the (for fibrillar collagens: pre-pro) α-chains are translated on membrane-bound ribosomes of the rough endoplasmic reticulum. The translation product, the pre-pro α-chain, protrudes into the lumen of the rough endoplasmic reticulum as it has a signal recognition domain which is recognized by the corresponding receptors [13]. A signal peptidase then cleaves off a short N-terminal rest (the signal sequence) [14] yielding the pro α-chain. The pro α-chain features two non-helical sequences at its N- and C-terminus: the pN and the pC propeptide. The pC propeptide is important for the water solubility of the pro α-chain under physiological conditions, while the pN propeptide has a regulatory effect on the mRNA translation [5].

Intracellular posttranslational modifications:

The nascent pro α-chain is enzymatically hydroxylated on certain prolyl and lysyl residues [5]. The enzymes responsible for this modification crucial to the stability of the triple helix to be formed later on are prolyl-4-hydroxylase (EC 1.14.11.2), prolyl-3-hydroxylase (EC 1.14.11.7) and lysyl hydroxylase (EC 1.14.11.4). These enzymes catalyse the hydroxylation of proline to 4-hdroxyproline (Hyp) or 3-hydroxyproline (only prolines in X position [9]) and lysine to 5-hydroxylysine (Hyl) (see **Scheme 13-1**) and need therefore 2-oxoglutarate, molecular oxygen, Fe^{2+} and ascorbate as cofactors [13]. Hyl is involved in the subsequent glycosylation and is also the initial amino acid for the cross-linking of collagen triple helices (*vide infra*). The increased polarity of the chain is also important for the formation of hydrophilic domains which play a crucial role in the formation of fibrils in the extracellular matrix [15].
While the level of hydroxylysine varies, Hyp is specific for collagen as a posttranslational modification and relatively constant as the proportion of Hyp is critical for the stability of the collagen triple helix [16-18]. Due to these constraints, a measurement of Hyp can be used to determine the levels of collagen present in a given sample. This approach found its way into legal regulations for example in Austria where the allowed level of connective tissues in marketable meat products is monitored via a determination of the hydroxyproline content[2].

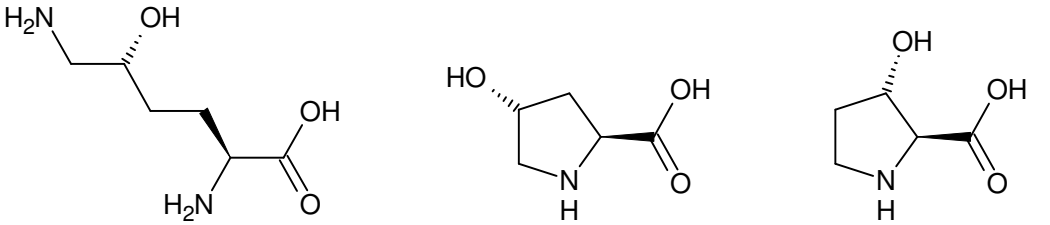

5-Hydroxy-L-lysine **(Hyl**) 4-Hydroxy-L-proline (**Hyp**) 3-Hydroxy-L-proline

Scheme 1-1 posttranslationally modified amino acids in procollagen

Glycosylation of the procollagen also takes place in the lumen of the endoplasmic reticulum [5, 6]. Hyl residues are O-glycosidically linked to galactose and glucosygalactose by the action of

[2] **Codex Alimentarius Austriacus, chapter B 14:**

$$Kollagenwert = \frac{Hydroxyprolin\ x\ 100\ x\ 8}{N\ x\ 6{,}25}$$

Kollagenwert .....value used in the legal regulations (proportion of protein from connective tissue on total protein content, in %)
Hydroxyprolin.....hydroxyproline content (in the unmodified food product), in mg g^{-1}
N.....total nitrogen content as determined by the Kjeldahl method, in mg g^{-1}

hydroxylysine galactosyltransferase (EC 2.4.1.50) and galactosylhydroxylysine glucosyltransferase (EC 2.4.1.66) [19].
These O-glycosidic bonds are stable under alkaline conditions and the degree of glycosylation influences the properties of the final collagen molecules like the diameter of the formed microfibrils. More extensive glycosylation is believed to promote interaction with other molecules of the extracellular matrix and to hinder close staggering of the collagen molecules. Overglycosylation results in copolymerisation with other molecules which is quite detrimental to the organisation of the collagen fibrils.
In addition to the glycosylation on the Hyl residues by collagen specific enzymes, the telopeptide regions are also glycosylated at certain asparagine residues [6].

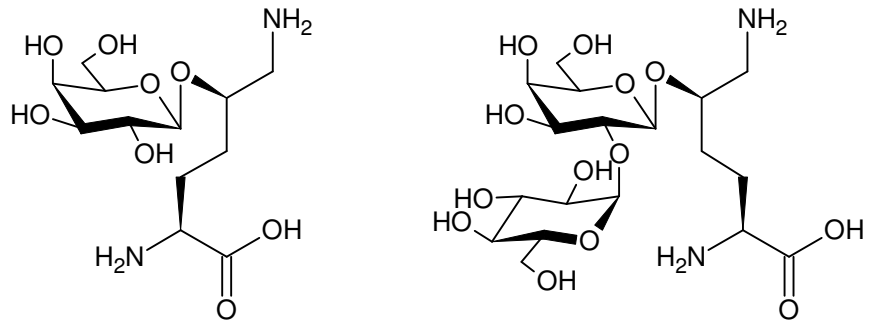

Scheme 1-2 glycosylated hydroxylysines in procollagen

Formation of the triple helix:

The globular C-terminal propeptides (pC) play an important role in the assembly of three collagen α-chains to one triple helical collagen monomer. The specific recognition sequences of the pC direct the association of three compatible α-chains. This so-called nucleation process is stabilised by the formation of intra- and intermolecular disulphide bonds in the region of the pC [5, 6, 13] and the addition of a N-linked carbohydrate by the oligosaccharyl transferase complex (OST, EC 2.4.1.119) [13]. When the three C-terminal propeptides are associated and approximately 100 proline residues have been hydroxylated to Hyp in all of the three α-chains [6] the formation of the triple helix is initiated at the C-terminus and proceeds then towards the N-terminus in a zipper-like fashion. For this process to be initiated and also to proceed efficiently, the presence of other enzymes in the lumen of the endoplasmic reticulum is necessary:
The rearrangement of -S-S- bonds in proteins is catalysed by the enzyme protein disulphide isomerase (PDI, EC 5.3.4.1) which is identical to the β-subunit of collagen prolyl-4-hydroxylase and also acts as a chaperon binding nascent collagen pro α-chains and thereby preventing their agglomeration.
The rate limiting step in the propagation of the newly forming triple helix is the cis-trans-isomerization of prolyl peptide bonds in the α-chains. Catalysis by peptidyl-prolyl cis-trans-isomerase (PPI, EC 5.2.1.8) accelerates the process to a physiologically reasonable level [9].
Another important ingredient for the biosynthesis of collagens is a specific chaperone, Hsp47 (heat shock protein 47) which seems to be indispensable, as knockout of its gene is lethal in mice at the embryonic stage [20].

Secretion of collagen monomers:

After formation of the triple helical collagen monomer, the enzymes responsible for posttranslational modification of amino acids can no longer access the pro α-chains and the collagen molecule is transported to the Golgi apparatus from where secretion of the pro collagen monomers by exocytosis ensues [5].

Extracellular modifications:

After secretion and also in late secretory vesicles the N- and C-propeptides of the procollagen α-chains are cleaved off by the specific Zn^{2+} dependent metalloproteinases procollagen N-proteinase (EC 3.4.24.14) and procollagen C-proteinases (EC 3.4.24.19) [13]. The group of enzymes exhibiting procollagen C-endopeptidase activity (EC 3.4.24.19, cleavage of the C-terminal propeptide at Ala-/-Asp in type I and II procollagens and at Arg-/-Asp in type III procollagens) includes bone morphogenic protein-1 (BMP-1), mammalian tolloid (mTLD) and mammalian tolloid-like protein (mTLL) [10]. Besides cleaving off pC, the procollagen C-proteinases also cleave the pro-lysyloxidase (Pro-LOX), yielding the active lysyl oxidase (LOX, EC 1.4.3.13) [21] which is the key enzyme for collagen crosslinking.
The cleavage of pC reduces the solubility of the collagen triple helical monomer approximately 10000-fold [22] which initiates in concert with the cleavage of pN the self-assembly of the resulting collagen monomers (also known as tropocollagen) into ordered, fibrillar structures.
This process is driven mainly by hydrophobic and electrostatic of the involved collagen monomers [13] and is therefore significantly influenced by the nature of the amino acids at X and Y position of the Gly-X-Y triplet in the helical domain of the collagen α-chains. These amino acids are located at the surface of the triple helix and are thus one of the key factors of fibril formation [5] which adds another condition to be met in terms of hydroxyproline content.

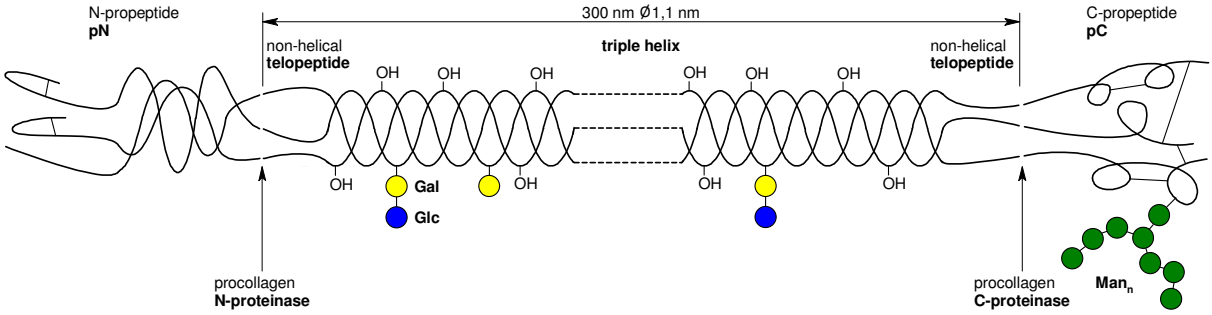

Figure 1-2 Structure of (pro)collagen I [13, 23]

The monomers of fibrillar collagen self-assemble into periodic cross-striated fibrils with a characteristic axial periodicity D of 67 nm [24]. The tropocollagens are thereby parallel to each other with a staggering and a gap between consecutive triple helices. The microfibrils of type I collagen are formed with an overlap (staggering) between parallel tropocollagens of approximately 10 % of the length of one tropocollagen molecule and a gap between two tropocollagens sharing the same axis of approximately 12 % of one molecule's length [23].
In tendons the type I collagen microfibrils align parallel to each other forming bundles of fibers whereas in skin a complex network of interlaced fibers is formed [13]. The diameter of a collagen fibril in a tendon can reach values of 50 – 500 µm whereby a greater mechanical strain results in thicker fibrils [5].

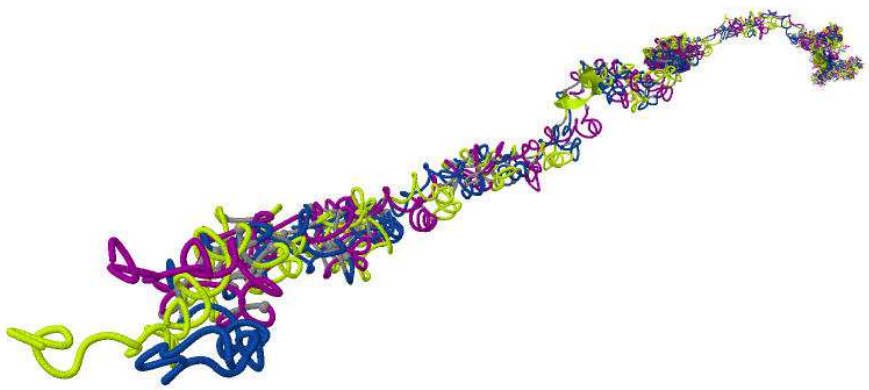

Figure 1-3 Structure of a single collagen I triple helix in a microfibril (PDB entry 3HQV, [23])

Cross-linking of collagen fibers:

The arrangement into fibrils initiates the formation of covalent cross-links between the collagen monomers which further stabilise the fibril and are a key factor for the mechanical properties of the tissue in question. Number, type and the proportion of the different cross-links varies for a given type of collagen and is closely entangled with the physiological function of the connective tissue or pathological derivations thereof.

The study of collagen cross-links came into the focus of research when in 1956 the experimental gerontologist Verzár postulated the existence of covalent linkages between collagens which he used as model molecules for his general model of cell aging that introduced the idea of an age-dependent cross-linking of protein molecules as the mayor biological determinant for the alterations brought forward as cells age [25, 26]. This model predicted two general types of cross-linking: enzymatically formed and unspecifically, indirectly formed cross-links.
The first experimental proof, i.e. evidence for covalent linkages between collagen molecules were attained 12 years later using [^{3}H]$NaBH_4$ which reduced the labile cross-links and preserved them that way during the acid-hydrolysis which was employed to obtain fragments of analysable size while at the same time providing a specific signal allowing the radiometric detection[3] of the reduced compounds [27]. The cross-links discovered using tritiated sodium borohydride were termed reducable cross-links and are presently also termed “inmature” or divalent cross-links. This type of cross-link disappears over the life time of the sample donor [28, 29] which couldn’t be explained satisfyingly until the trivalent, “mature” cross-links were detected.
With the detection of histidine in cross-linked structures from bovine skin collagen that were not reducible by $NaBH_4$ [30] in 1975 one maturation mechanism of the reducable collagen cross-links had been elucidated but the majority of the missing divalent cross-links still awaited explanation.
The one enzyme known to be indispensable for the formation of cross-links in collagen [5, 31], lysyl oxidase (EC 1.4.3.13) which catalyses the oxidative deamination of lysyl and hydroxylysyl residues was identified one year later by Sigel et al. [32, 33], eight years after the identification of the enzymatic activity in crude bone extract [34].
One year later an explanation for the phenomenon of the age-correlated decline of the reducible cross-links of collagen presented itself as a fluorescent amino-acid with three amino acid side chains was isolated from ox tendon and bone collagen [35] which was shown to be a 3-hydroxypyridinium derivative [36].
Proteinase digests of collagenous tissue were also found to give a pink colour with *para*-Dimethylaminobenzaldehyde in hydrochloric acid (Ehrlich’s reagent) which provoked the postulation of a pyrrole-type cross-link [37, 38].

[3] Tritium transmutes into ^{3}He (β-decay).: ${}^3_1T \rightarrow {}^3_2He^+ + e^- + \bar{\nu}_e + 18{,}5912\ keV$; $t_{½}$ = 4500 ± 8 days [207]
The average kinetic energy of the emitted electron is 5,69 keV (soft β-radiation, average track length in water: 0,56 µm, max. track length in water: 6 µm [208]).

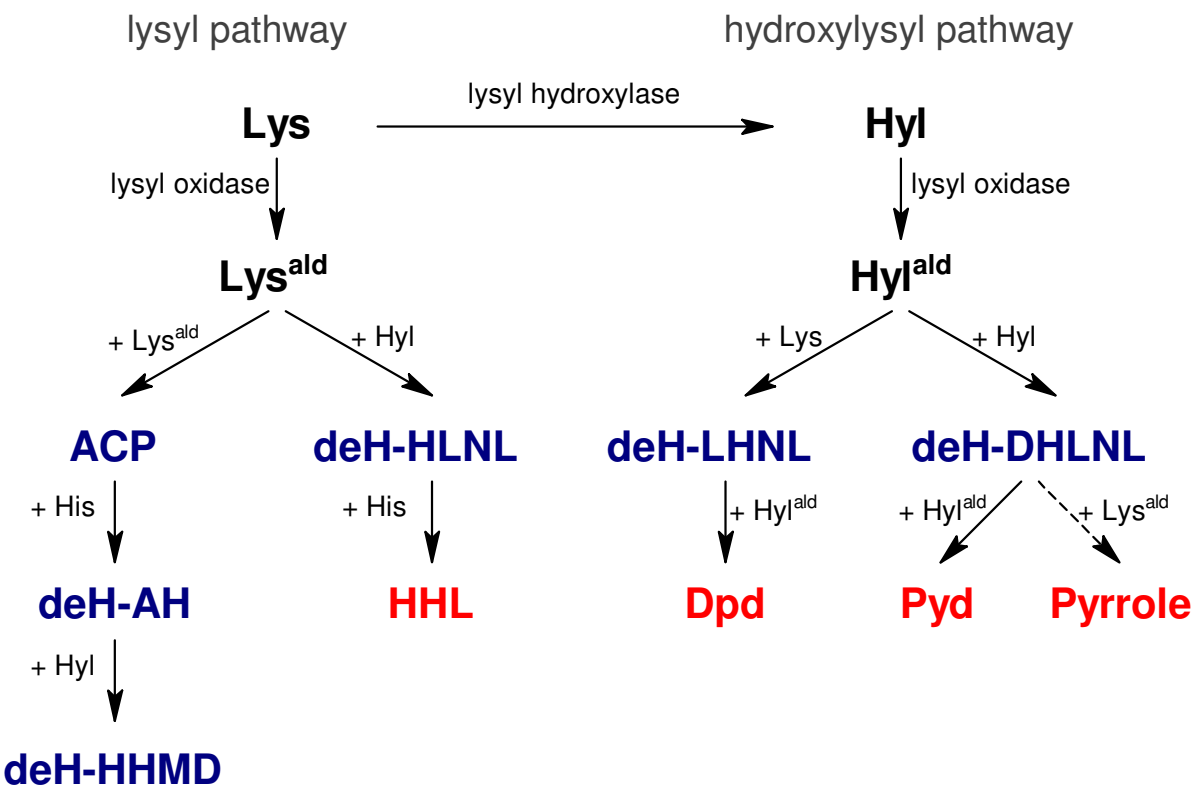

Scheme 1-3 formation of the naturally occurring reducible and mature cross-links in fibrillar collagen

Lys .....*L*-Lysine
Hyl .....*L*-Hydroxylysine
Lys^{ald} .....*L*-Allysine
Hyl^{ald} .....*L*-Hydroxylysinealdehyde
His .....*L*-Histidine

HHL.....Histidinohydroxylysinonorleucine
Dpd.....Deoxypyridinoline
Pyd .....Pyridinoline
Pyrrole.....putative pyrrole-containing cross-link

ACP ..... Aldol condensation product
deH- ..... dehydro
AH ..... Aldolhistidine
HHMD ..... Histidinohydroxymerodesmosine
HLNL ..... Hydroxylysinonorleucine
LHNL ..... Lysinohydroxynorleucine
DHLNL ..... Dihydroxylysinonorleucine

Cross-linking is initiated by the oxidative deamination of a lysino ε-amino group by the action of the lysyl oxidase (EC 1.4.3.13) yielding reactive aldehydes which condense with other lysyl, hydroxylysyl or histidino sidechains in reach forming covalent intermolecular cross-links (see Scheme 1-3). Knockout of lysyl oxidase is incompatible with life in the mouse model where the few homozygous $LOX^{-/-}$ mice that were still alive after parturition died soon afterwards from ruptured arterial aneurysms and diaphragmatic ruptures [39].
The cross-linking of fibrillar collagens can be divided into two classes: the lysyl pathway (proceeding from allysine, the aldehyde derivative of lysine) which predominates for example in skin (soft-tissue) and the hydroxylysyl pathway (starting from 5-hydroxy allysine) which is the principal route in cartilage and bone (hard-tissue) [5].
Intermolecular cross-linking starts with the coupling of an allysine or an 5-hydroxyallysine to a helical lysyl- or hydroxylysyl residue or another aldehyde located on a neighbouring tropocollagen molecule within the same microfibril yielding difunctional and reducible cross-links [5]. Among the divalent cross-links of the lysyl pathway are the aldol condensation product (ACP), formed from two condensed allysine residues [40] and the imine (Schiff base) dehydro-hydroxylysinonorleucine (deH-HLNL) generated by the condensation of an allysine residue with a helical hydroxylysine of a neighbouring tropocollagen molecule [41]. Within the hydroxylysyl pathway emerge on the one hand the imine dehydro-lysinohydroxynorleucine (deH-LHNL) which is the product of the reaction between hydroxyallysine and lysine [5] and on the other hand dehydro-dihydroxylysinonorleucine (deH-

DHLNL), an imine resulting from the condensation of hydroxyallysine and hydroxylysine [41]. These two divalent, “inmature” cross-links are found predominately in bone and dentin [5].

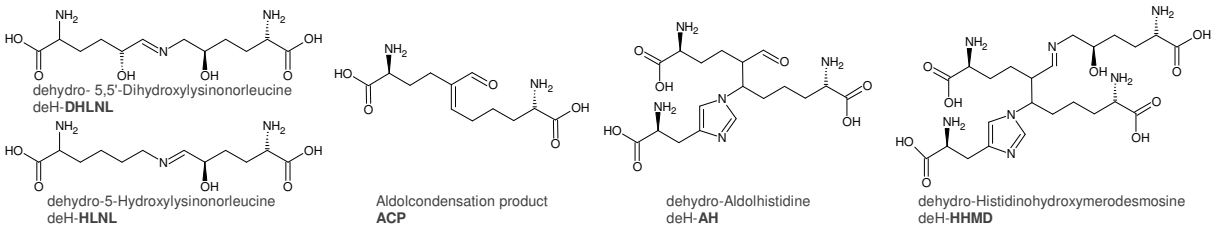

Scheme 1-4 Reducible natural cross-links of collagen: DHLN, HLNL [41], ACP [40], AH, HHMD [42]

In the process of tissue maturation the reducible, divalent cross-links are replaced by multivalent, “mature” cross-links. A determining factor for the control of this process is the degree of hydroxylation of the lysyl residues during the intracellular posttranslational modification [5]. The multivalent cross-links play an important role for the physiological properties of a given tissue, especially its mechanical properties and increase with the age of the tissue in question [43]. Within the lysyl pathway the tetravalent imine with an N-linked histidino residue at the β-carbon dehydro-histidinohydroxymerodesmosine (deH-HHMD) is formed by addition of one histidyl to the divalent ACP and subsequent condensation of a hydroxylysine residue [42]. DeH-HHMD occurs primarily in soft tissue like ligaments or skin. It is found in concentrations initially increasing with age until the concentrations start to decrease again which is attributed to the formation of cross-links more stable than the (still reducable) imine deH-HHMD [5]. The other important “mature” cross-link in the lysyl pathway is the trivalent histidinohydroxylysinonorleucine (HHL) which is formed by coupling of a helical hystidino residue to the divalent deH-HLNL [44, 45]. HHL is the main cross-link found in soft tissue like skin and its concentration does increase with age [5, 45]. The quantitatively most prominent products of the hydroxylysyl pathway are pyridinoline (Pyd) and deoxypyridinoline (Dpd) which are the predominate cross-links in hard tissue like bone or dentin [46] but have also been found in skin [47]. Pyd is the “maturation product” of deH-DHLNL which is formed upon condensation of a hydroxyallysine residue [41] while the structurally similar Dpd is the product of a condensation of deH-LHNL and a hydroxyallysine residue [48] and has consequently one hydroxyl group less. The pyridinolines Pyd and Dpd are non-reducible by $NaBH_4$, stable under acidic conditions and fluorescent (at neutral pH: $\lambda_{ex,max}$ = 325 nm, $\lambda_{em,max}$ = 410 nm) [35]. In bone, the ratio of Pyd to Dpd is fairly constant over the whole adult life span and amounts to approximately 3,5 : 1 [49]. A high proportion of Dpd correlates with the mineralisation of the extracellular matrix in bone tissue whereupon the distribution of collagen cross-links is believed to support the spatial organisation of mineralisation crystals in bone tissue [10]. With increasing age the reducible cross-links (deH-DHLNL, deH-LHNL) are converted to non-reducible, “mature” cross-links (Pyd, Dpd), i.e. the proportion of pyridinolins increases [49]. The formation of these “mature” crosslinks provides the bone with the biomechanical properties like rigidity, tenacity and viscoelasticity that are crucial to its physiological function [11].

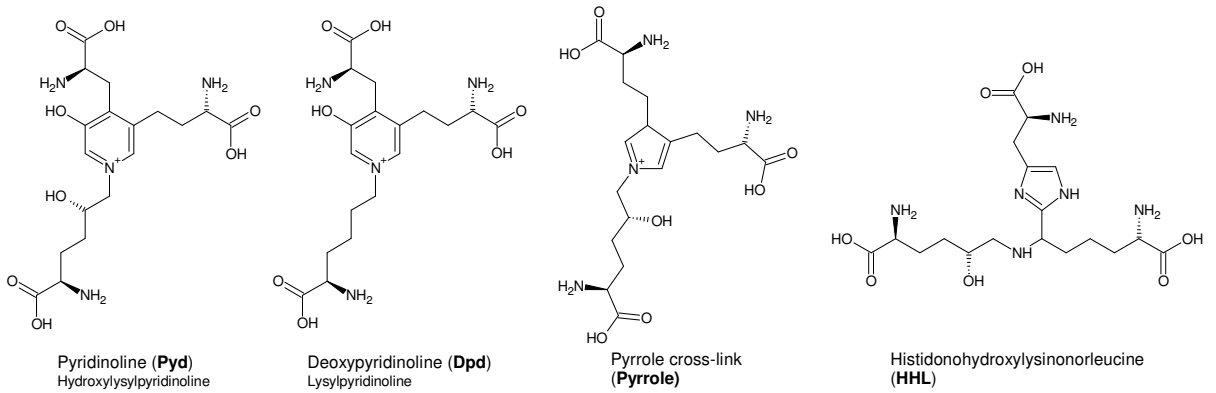

Scheme 1-5 Mature natural cross-links of collagen: Pyd [41], Dpd [48], HHL [44, 45], Pyrrole [41]

Besides the cross-linking initiated by the action of the lysyl oxidase an adventituos non-enzymatic glycation ensues as tissue ages. Reducing sugars or metabolic intermediates like glyoxal or Glyceraldehyde 3-phosphate react with the free ε-amino group of lysyl, hydroxylysl or arginine residues forming imines (Maillard reaction) which can in turn react with other free amino groups or undergo a variety of rearrangements, oxidations and/or dehydrations. The stable protein adducts formed this way are known as advanced glycation end products (AGEs) and can be both protein adducts and cross-links between proteins. AGEs increase with exposition time, i.e. the biological age of the protein, and are believed to contribute significantly to the various dysfunctions of collagenous tissues in old age [50-52].

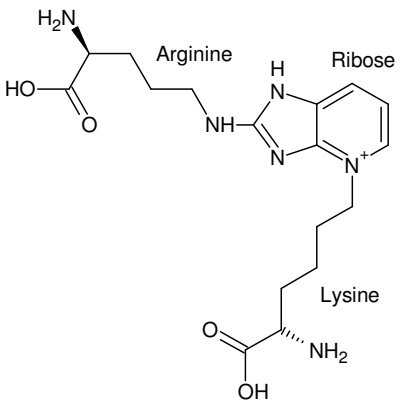

Scheme 1-6 Pentosidine, an AGE [51]

1.1.4. *In vitro* cross-linking of collagen

Its excellent biocompatibility, low antigenic potential and toxicity, its controllable resorbability (primarily by the degree of crosslinking) and its well-established safety profile emphasizes the eligibility of collagen for use as a biomaterial applied *in vivo* [53-56]. Unmodified collagenous materials are however not suitable for most applications owing to their sensitivity towards humidity, elevated temperatures and enzymatic degradation.

The most important application area for modified collagen as a biomaterial is medicine where uses include artificial tissue, carrier systems for targeted drug delivery, prostheses and matrices to assist wound healing [53-58]. The physiological properties of collagen-based biomaterials are also exploited in fermentation technology where beads made from or covered with collagen are used in the culture of anchorage-dependent cells [59, 60] or collagen is used to immobilize cells in high density cultures in order to increase the productivity [61].

In most *in vivo* applications of collagenous biomaterials the degradation and resorption of the introduced collagen is controlled by cross-linking of the used collagen material, usually reconstituted acid soluble collagen I. The cross-linking is usually done chemically, applying acyl azide [62], carbodiimides [63, 64], chromium tanning [65], formaldehyde [65, 66], glutardialdehyde [67], hexamethylene diisocyanate [68] or polyepoxy compounds [69]. The toxicity and especially the uncontrolled release of these species is a severe disadvantage of the chemical cross-linking which would disappear if enzymes were used instead.

1.2. Tyrosinase

Tyrosinases catalyse the *ortho*-hydroxylation of monophenols to o-diphenols (monophenol monooxygenase, EC 1.14.18.1) and the two-electron oxidation of o-diphenols to the corresponding o-quinones (catechol oxidase, EC 1.10.3.1), each coupled with the reduction of molecular oxygen to water [70]. The formed o-quinones are usually unstable in aqueous environments and undergo spontaneous, non-enzymatic reactions including the formation of high molecular weight compounds like melanin [71-74], intermolecular nucleophilic 1,4-Michael additions [75-77] or direct coupling of two quinones [75, 78, 79].

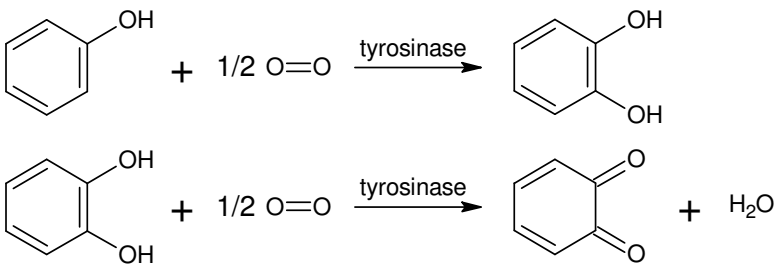

Scheme 1-7 hydroxylation of monophenols and oxidation of *o*-diphenols catalysed by tyrosinase

Tyrosinases are widely distributed in animals, higher plants and microorganism and are of central importance for the melanin pigmentation in vertebrates as the reactions catalysed by tyrosinase start the melanin biosynthesis pathway [80]. Mutations of the gene encoding the human tyrosinase (TYR) resulting in impaired tyrosinase production or function cause the hereditary disease oculocutaneous albinism type 1 which has a prevalence of circa 1 per 40000 and is characterised by the absence (type 1a) or the markedly reduced and slow production (type 1b) of pigments [81, 82]. The activity of tyrosinase in plant tissue (commonly referred to as polyphenol oxydase, PPO) is responsible for enzymatic browning in vegetables and fruits [83] and also contributes to the defence against herbivores by reducing the nutritive quality of the ingested plant material [84, 85].
Tyrosinases belong to the group of metalloproteins containing a type III copper centre at the active site. The division of copper binding proteins is historically done according to their spectroscopic properties whereat type I centers are found in the so-called “blue copper proteins” and are mostly connected with electron transfer, type II centers are the “non-blue copper centers” and type III centers contain two copper atoms [86]. These type III copper centers bind dioxygen in a characteristic, “side-on” bridging mode which results in the activation of O_2 and the characteristic spectral features of the oxy form of proteins like tyrosinase containing such a copper center; A strong antiferromagnetic coupling between the electrons on the two copper centres, a raman-active O-O stretching vibration at 750 cm^{-1} and an adsorption spectrum with two typical charge-transfer bands at ca. 600 nm ($\varepsilon \approx 1\ mM^{-1}\ cm^{-1}$) and ca. 350 nm ($\varepsilon \approx 20\ mM^{-1}\ cm^{-1}$) [87].

1.2.1. Structure and mechanism

The active site of tyrosinase is made up by a dinuclear (type III) copper centre whose copper atoms are coordinated by three histidyl residues each [88, 89].

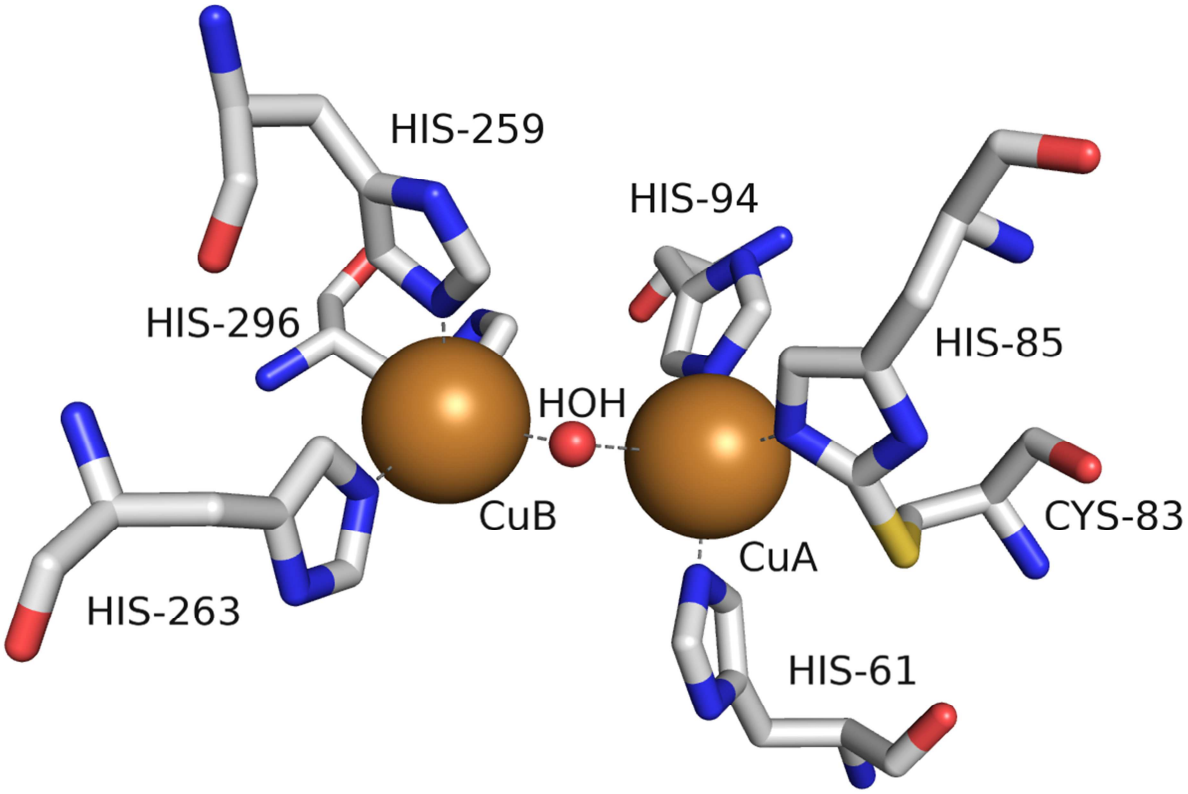

Figure 1-4 active site of desoxy-AbT
showing the two copper ions (brown spheres), a coordinated μ-H_2O (red sphere) and the six histidines coordinating the copper ions whereby His85 is covalently linked to Cys83 via a thioether bond between the γ-S of Cys83 and the ε-C of His85 that is not conserved within tyrosinases (PDB entry 2Y9W, [88])

A similar active site is found in the related metalloproteins hemocyanin, the oxygen transport protein of molluscs and arthropods and in catechol oxidase, an ubiquitous plant enzyme which catalyses the oxidation of *o*-diphenoles to *o*-quinones but cannot hydroxylate monophenols as tyrosinases do [87, 90, 91]. These dinuclear copper centres bind molecular oxygen in a (μ-η^2:η^2-peroxo)dicopper(II) complex yielding the oxy-form of the different proteins. Despite the chemically identic active oxygen species present in the active sites the reactivities towards external substrates differ quite a bit. The inability of catechol oxidase to hydroxylate monophenoles and the absence of redox activity towards external substrates in native hemocyanin are commonly attributed to sterical hindrances originating in the protein structure [90] as the enzymatic activities can be induced by denaturing conditions [92] or partial proteolysis [93].
The molecular details of the reaction mechanism of tyrosinase have not yet been definitively clarified but kinetic studies [70, 80, 83, 94-104], structural data from diverse techniques including x-ray scattering [87-89, 105-108] and a wide variety of tested model substrates and inhibitors [102, 109-122] allow the formulation of a model for the action of tyrosinase on mono- and diphenolic substrates (Scheme 1-8, for a proposed structural mechanism see Scheme 13-11).

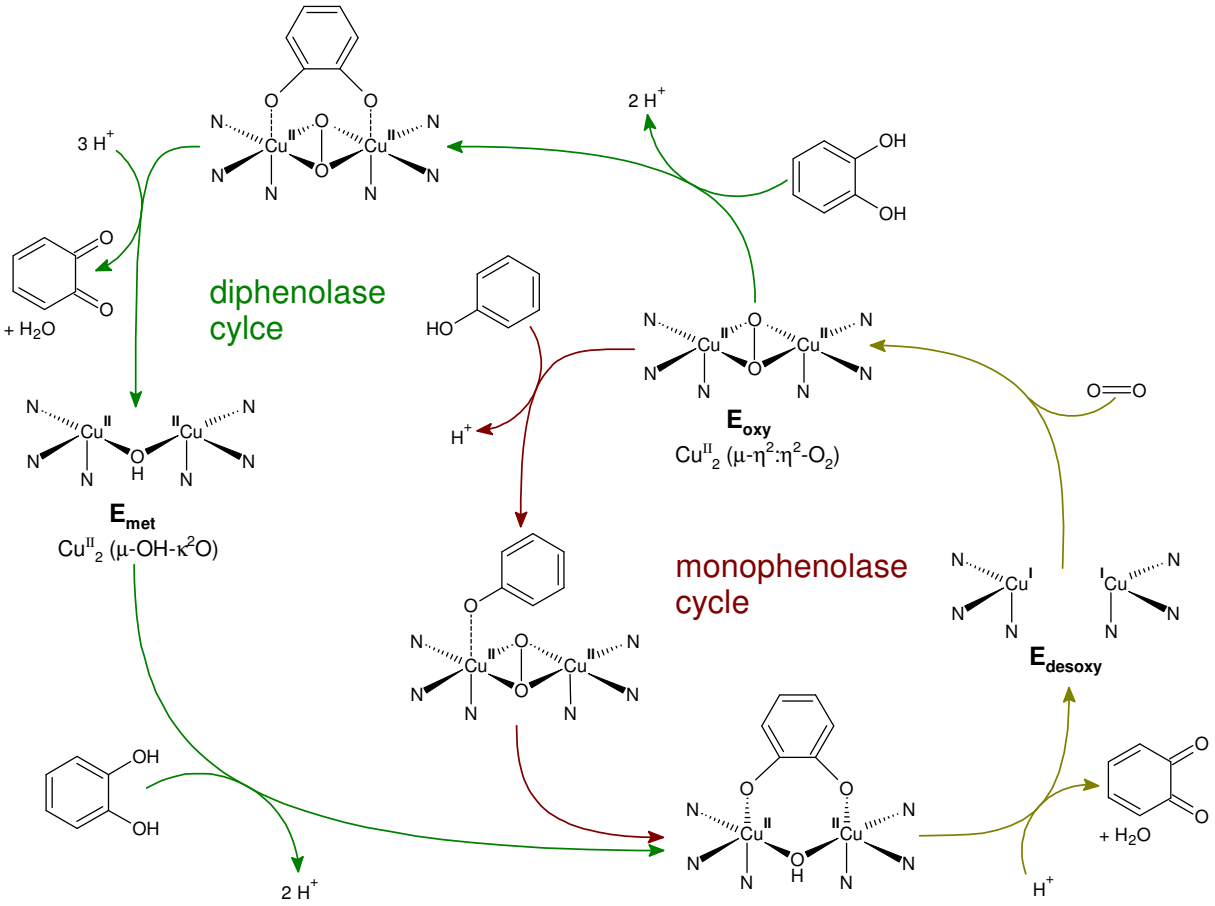

Scheme 1-8 tyrosinase acting on mono- and diphenols [91]

The desoxy form of tyrosinase (E_{desoxy}) with the oxidation state of Cu(I)-Cu(I) binds molecular oxygen in in the characteristic side-on bridging (μ-η^2:η^2) geometry as peroxide forming the oxy form of the enzyme. The oxidation state is thereby converted to a Cu(II)-Cu(II) configuration and the resulting state of the enzyme (E_{oxy}) can bind mono- as well as diphenols [123]. E_{oxy} can *ortho*-hydroxylate monophenols forming *o*-diphenols (monophenolase activity) that are released [121] or subsequently oxidised to *o*-quinones whereupon the desoxy form of tyrosinase is reformed which can again bind molecular oxygen. Besides the hydroxylation of monophenols E_{oxy} can also bind external *o*-diphenols which are in turn oxidised to *o*-quinones (diphenolase activity) by what the met form of tyrosinase is generated that is able to bind diphenols and carry out the two-electron oxidation which results in the release of another *o*-quinone. One passage through the diphenolase cycle, for which one molecule O_2

is required, oxidises therefore two *o*-diphenols to *o*-quinones while within the monophenolase cycle only one monophenol is converted to one *o*-quinone per molecule of O_2 consumed.
Tyrosinase as obtained after protein purification, referred to as "resting tyrosinase", was found to be a mixture of ≤ 15 % oxy-tyrosinase and ≥ 85 % met-tyrosinase [124]. The slow step in the enzymatic cycle is the hydroxylation of the monophenol [102] which is consistent with the observation of a lag-period when tyrosinase acts on monophenols until the steady-state concentration of the corresponding diphenol has been reached [70, 102].
While the molecular details of this step, which is the mechanistically most demanding in the tyrosinase-catalysed formation of *o*-quinones out of monophenols, are not yet clarified completely Hammett-analysis[4] [125] of the oxygenation of differently substituted monophenols hints towards an electrophilic aromatic substitution mechanism (ρ = -2,4 [126]) [90, 127].

1.3. Objective of the present work

The aim of this work was to investigate the enzymatic action of tyrosinase on collagen in presence of oxygen with emphasis on the amino acids involved in the cross-linking of said substrate. The systems used to investigate the cross-linking reactions initiated by tyrosinase-effected generation of reactive *o*-quinons from tyrosyl residues were acid soluble collagen as the substrate of interest, the oxidised β-chain of insulin as well as the free amino acids Arg, His, Ile, Leu, Lys, Ser and Val.
While in collagen type I (a heterotrimer of two α1(I) and one α2(I) chains) only approximately 3,5 ‰ of all amino acids are tyrosine residues the β-chain of insulin contains 6,6̇ % tyrosine (2 tyrosines out of a total of 30 amino acids making up the β-chain) resulting in an approximately 19-fold increase of convertible amino acid side chains for the same mass of collagen I and the β-chain of insulin respectively. In addition to the higher tyrosine content the relatively small molecular mass of the insulin β-chain (The α-chain of insulin is even lighter with only 21 amino acids.) makes it easier to handle analytically as for example the cross-linked peptides are still water soluble for degrees of cross-linking that do result in gel formation for collagen which creates a heterogeneous system.
Amino acids which's concentrations were influenced by the enzymatic treatment of collagen (see 12.1.2) as well as Lys, the amino acid crucial for the natural cross-linking of fibrillar collagen (see 1.1.3), were tested in incubations with tyrosinase both individually and in combination with an *o*-quinone-forming substrate in an effort to differentiate between direct action of tyrosinase and transfer of redox equivalents from reactive *o*-quinons.

[4]The Hammett-equation is an empirical linear free energy relationship: $\log(k) = \log(k_0) + \rho \cdot \sigma$
k..... reaction rate with *m*- or *p*-substituted benzene derivative
k_0 ..... rate of the reference reaction with the unsubstituted (= H as substituent) benzene derivative
σ ..... Hammett substituent constant, tabulated
ρ ..... reaction constant, depends on the type of reaction: accessible via a plot of log(k) versus σ for different substituents (same reaction, unchanged conditions)

2. Materials and devices

The used chemicals and analytical devices are given in the annex (II).

2.1. Tyrosinases and substrates

- **BoT1**: native tyrosinase from *Botryosphaeria obtusa*, kindly provided by Novozymes, Denmark (luna 2007-46082)
- **BoT2**: C-terminally processed tyrosinase from *Botryosphaeria obtusa*, kindly provided by Novozymes, Denmark (luna 2006-50861-01)
- **AbT**: tyrosinase from *Agaricus bisporus*, Fluka 93898, Lot# 1331446
- **K**: acid soluble collagen type I, extracted with 0,1 M acetic acid from bovine split; kindly provided by the Forschungsinstitut für Leder und Kunstoffbahnen (FILK) Freiberg, Germany (A001398)
- **I-b new**: insulin chain B oxidised, from bovine pancreas; Sigma I6383, Lot# 020M5056
- **N-Boc-*L*-Tyr**: N-[(1,1-dimethylethoxy)carbonyl]-L-tyrosine, see 10.1

2.2. Used abbreviations

%A..... volume ratio of the aqueous component in liquid chromatography
%B..... volume ratio of the organic modifier in liquid chromatography
ATR ..... attenuated total reflectance
bis-Tris ..... 2,2'-bis(hydroxymethyl)-2, 2', 2''-nitrilo-triethanol
Boc..... 1,1-dimethylethoxy)carbonyl (amino protection group)
CBB ..... coomassie brilliant blue
CID ..... collision-induced dissociation
DBE ..... double bond equivalent
ddH_2O ..... deionized water, ρ > 12 MΩ cm
dH_2O ..... demineralised water
DOPA ..... (S)-2-amino-3-(3,4-dihydroxyphenyl) propanoic acid (L-3,4-dihydroxyphenylalanine)
EC..... Enzyme Commission (providing a numerical identification system for enzymes)
EDTA ..... ethylenediamine-tetraacetic acid = 2,2',2'',2'''-(ethane-1,2-diyldinitrilo)tetraacetic acid
ESI ..... electro spray ionisation
FTIR..... Fourier transform infrared (spectroscopy)
HCl ..... hydrochloric acid
HPLC..... high-performance liquid chromatography
Hyl..... L-hydroxylysine
I-b..... β-chain of insulin
IT..... ion trap
K..... acid soluble collagen
LCAO-MO..... linear combination of atomic orbitals - molecular orbital theory
\d M..... \d mol · l^{-1}
$[M+H]^+$ ..... protonated pseudomolecular ion (M: molecule, H: proton)
$[M-H]^-$..... deprotonated pseudomolecular ion
MALDI-MS..... matrix-assisted laser desorption/ionisation mass spectroscopy
MeOH ..... methanol
MES..... 2-(N-morpholino)ethanesulfonic acid
MS^n ..... multistage mass spectrometry
$NaBH_4$ ..... sodium borohydride
N-Boc-*L*-Tyr... (2*S*)-2-[(*tert*-butoxycarbonyl)amino]-3-(4-hydroxyphenyl)propanoic acid
NH_4Ac..... ammonium acetate

o..... *ortho*, descriptor for the relative position of two substituents on an aromatic ring:
o: *ortho*: vicinal substituents (bond to two adjacent C-atoms: 1,2 isomer)
m: *meta*: 1,3 isomer
p: *para*: 1,4 isomer
OPA..... o-pthalaldehyde (benzene-1,2-dicarboxaldehyde)
pC..... C-terminal propeptide of procollagen
pN ..... N-terminal propetide of procollagen
PP..... Polypropene
PS..... Polystyrene
QTOF..... quadrupole time-of-flight
RI..... refractive index
RID ..... refractive index detector
RP-HPLC..... reversed-phase HPLC
SDD-AGE ..... semi-denaturing detergent agarose gel electrophoresis
SDS..... Sodium lauryl sulphate (sodium dodecyl sulphate)
SDS-PAGE..... sodium dodecyl sulphate polyacrylamide gel electrophoresis
TEMED ..... N, N, N', N'-tetramethylethylenediamine
TFA..... 2,2,2-trifluoroacetic acid
Tris ..... tris-(hydroxymethyl)-aminomethane
U ..... unit (of enzymatic activity, 1 U := 1 µmol of processed substrate per min)
UV ..... ultraviolet
UVD..... ultraviolet detector / detection
Vis ..... visible

3. Protein hydrolysis with HCl

3.1. Choice of method

The conventional hydrolysis method uses 6M HCl at 110 °C for 20 – 24 h in vacuo with 2‰ phenol as stabilizing agent [128]. Under these conditions, tryptophan is destroyed completely, the conservation of cysteine residues is unsure and the amide moieties of asparagine and glutamine are both converted to carboxylic acids.
The key benefit of using hydrochloric acid as the hydrolysing agent is constituted by its volatility, a property which is rather unique among the substances routinely used for protein hydrolysis.
Since the present study focused on phenolic moieties, it was refrained from adding phenol to the hydrolysis mixture. As a result of this limitation, the problem of loss of analyte during the hydrolysis became somewhat more pronounced.
Pursuant to the idea that in order for protein hydrolysis to yield meaningful fragments at all the activation energy of the processes leading to loss of amino acids should be considerably higher than that of the one leading to hydrolysis of the amide bonds an increase of the process temperature accompanied by shorter residence time should result in slightly increased losses for a given degree of depolymerisation. As ultrasound devices capable of that task were not available, a higher hydrolysis temperature was chosen (145 °C) and the concentration of acid was reduced to 4M.

3.2. Procedure

3.2.1. Pre-tests of hydrolysis vessels

The tested vessels were filled with 6M hydrochloric acid, closed by applying the respective cap and subjected to elevated temperature for a prolonged period of time using a drying cabinet.

1,5 ml glass vials with crimp caps

The aluminium crimp caps with rubber septa exhibited insufficient mechanical strength under the corrosive conditions of steam of hydrochloric acid to withstand the internal pressure which results from the generation of the steam in a closed vessel.

Table 3-1 HPLC-vials with 6M hydrochloric acid at 170 °C for 20h

#	Tare / g	+ 1 ml HCl 6N / g	m_{20h} / g	Δm / %
1	2,88946	3,99948	3,84494	13,92
2	2,87023	3,96503	3,10889	78,20
3	2,86009	3,95482	2,86006	100,0

The rubber seal in the caps of the vials 1 & 2 was black and visibly porous while the one of vial three was lacerated centrally.

4 ml glass vials with screw caps

The liner of the 10 mm screw cap (butyl rubber with PTFE-coating) showed no visible signs of deterioration but after only two hours all the liquid was gone.

Table 3-2 Screw cap vials with 6M hydrochloric acid at 170 °C for 2h

#	Tare / g	+ 1 ml HCl 6N / g	m_{2h} / g	Δm / %
1	4,66481	5,77817	4,66729	99,78
2	4,65390	5,76838	4,65631	99,78
3	4,65906	5,77303	4,65973	99,94

The experiment was stopped after 2h because the vials did contain a few solid residues but no longer any liquid at that time.

Pyrex®-tubes

Glass tubes (Pyrex®) with 13 mm screw caps and PTFE-liner exhibited reasonable losses (around 1%) and no visible deterioration neither of the liner material nor the glass itself even after repeated use.
One tube (15,82266 g) was filled with 1 ml of 6M HCl (16,94832 g) and heated to 145 °C for 4 h in an oil bath (wrapped in aluminium foil, immersion depth approximately 2,5 cm with the liquid surface at about 1 cm). After 4 h 1,16 % of mass was lost from this tube (m_{4h} = 16,93529 g).

3.2.2. Method

For each preparation 150 µl of sample (possibly with dispersed solids) and 300 µl of 6M HCl (concentration determined by titration with sodium hydroxide of known titer) were pipetted into a glass (Pyrex®) tube with screw cap equipped with a PTFE-liner. After complete dissolution of possibly present solids (or immediately after mixing of the two constituents, given both were homogenous solutions) the solution was stirred with a jet of pure N_2 (N 5.0) in order to reduce the residual concentration of dissolved oxygen in the liquid as well as in the headspace of the glass tube. The tube was the closed firmly while the nitrogen jet was still maintained and the hydrolysis was started by placing the tube in a preheated (145 °C) metal cylinder with 21 drill holes. The tubes remained in this apparatus for 4 hours and were removed from the heating block after this time had elapsed and allowed to cool to approximately 50 °C before further processing.
20 of the 21 cavities were used to keep the glass tubes at 145 °C while the 21th was filled with heat transfer oil which was used to establish thermal contact to the resistance thermometer (Pt 1000) of the thermo shaker which used the thermometer as actual value transducer for the control loop of its thermostat.
Once sufficiently cooled down the hydrolysis solution was transferred to labelled 1,5 ml HPLC glass vials which were in turn placed in a 48-well plate (for increased tilting stability) and dried in an exsiccator over blue gel (silica gel impregnated with $CoCl_2$ – blue: dry, rose: humid) at approximately 40 mbar. During the drying process (60 h) the silica gel was replaced twice, the used silica gel was regenerated in the drying cabinet at 170 °C and used again.
Once all the liquid was evaporated, the solid residues were reconstituted in 80 µl ddH_2O (from a Barnstead NANOpure Analytical Deionization System, ρ > 12 MΩ cm), vortexed and after 2 min at room temperature transferred to 100 µl glass inserts which were placed inside the same vial used for the preceding drying process. Those were then sealed and the aqueous solution was measured by RP-HPLC-UVD after derivatisation with *o*-phthalaldehyde.

In the beginning a wire cage immersed in an oil bath was used for the heating of the glass tubes but this approach was discontinued because of the unproportional time and effort required to clean the tubes after each round of hydrolysis.

3.3. Mathematical modelling

The principal assumption of this model is that the release of all the amino acid residues anywhere in the protein chain can be described by the same rate constant, thus all residues are treated as equal without regard for their specific position in the polypeptide chain or the influence of neighbouring residues (e.g. steric hindrance of the hydrolytic attack).
All reactions are assumed as irreversible or – which is equivalent – are net reaction rates.
In addition to this first assumption the influence of already released free amino acids and the decrease in the concentration of water as the hydrolysis proceeds on the rate of release of so far bonded amino acids is neglected. This seems to be reasonable given the much higher concentration of species promoting hydrolysis compared to the released amino acids:
Amino acids in the hydrolysis solution: circa 19 mM (for 5 g/l collagen in the sample solution)

$$\frac{HCl}{\sum amino\ acids} \approx 200 \qquad \frac{water}{\sum amino\ acids} \approx 2800$$

3.3.1. Model 1-1

This model assumes first-order kinetics for both release and degradation of amino acids during the period of hydrolysis [129].

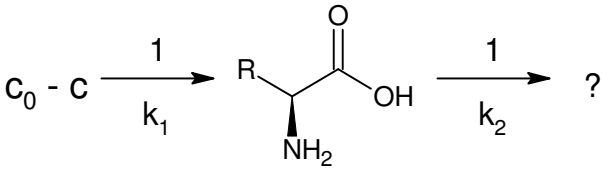

$$c(t)\frac{k_1 \cdot c_0}{k_1 - k_2} \cdot e^{-k_2 \cdot t} \cdot \left(1 - e^{(k_2 - k_1) \cdot t}\right)$$

Scheme 3-1 Model 1-1

The mathematical derivation of the three kinetic models is given in the annex (III.I).

3.3.2. Model 1-0

Contrary to model 1-1 this model assumes zero order kinetics for the degradation of amino acids. As this imposes a constant rate for the degradation of the amino acids discounting their available concentration at any given time this models presents an unsound approximation of reality.

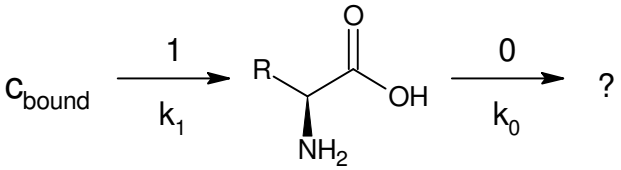

$$c(t) = c_0 \cdot \left(1 - e^{-k_1 \cdot t}\right) - k_0 \cdot t$$

Scheme 3-2 Model 1-0

3.3.3. Model 1-1 2x

As the nonlinear regression for the amino acids aspartic acid and glutamic acid resulted in initial concentrations below the level of the highest measured amino acid concentrations in solution the model had to be adapted. This adaptation consists in adding a second bound species which is converted instantaneously to the respective free amino acid. The rationale for the introduction of another independently released species is constituted by the observation that Asn and Gln are converted to Asp and Glu respectively during the acidic hydrolysis. As neither asparagine nor glutamine were detected in hydrolysed samples, no information concerning the rate of conversion

from amide to carboxylic acid could be determined beside the general conclusion that the rate of conversion surpasses the rate of release significantly. Within this model the rate of conversion is set to infinity, which is mathematically equivalent to the identification of the two released species (Asn ≡ Asp, Gln ≡ Glu).

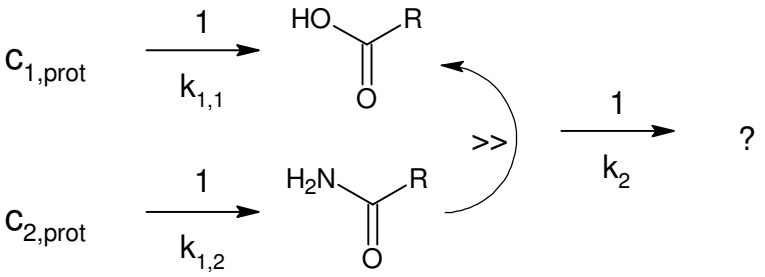

$$[c_1] + [c_2] = [c]$$

$$c(t) = \frac{k_{1,1} \cdot c_{1,0}}{k_{1,1} - k_2} \cdot \left(e^{-k_2 \cdot t} - e^{-k_{1,1} \cdot t}\right) + \frac{k_{1,2} \cdot c_{2,0}}{k_{1,2} - k_2} \cdot \left(e^{-k_2 \cdot t} - e^{-k_{1,2} \cdot t}\right))$$

Scheme 3-3 Model 1-1 2x

A series of identical samples containing 150 µl of 5 g l^{-1} acid soluble collagen dissolved in 1 % (v/v) acetic acid was prepared in triplicates and hydrolysed after addition of 300 µl of 6 M HCl as described in 3.2.2.

The measured amino acid concentrations (cp. Table III-III) were utilised to fit the parameters of the kinetic models applying the gaussian principle of least squares. The non-linear regression was carried out using the program Dataplot™ in the version 2/2005 with the maximal measured concentration or signal area as initial guess for the free parameter c_0. To avoid bias arising from the uneven spacing of the measuring points data from each point (representing a triplicate measurement for a given hydrolysis time) was used multiple times in order to simulate a spacing of 15 min. As such an artificial inflation of data would abate the variance of the calculated parameters, the standard deviation of the regression parameters was calculated from the data set with one entry for each measured value (see III.III).

4. Amino acid analysis after pre-column derivatisation with OPA

The reaction of amino acids with o-phthaldialdehyde yields an isoindole derivate that can be detected fluorometrically [130] or – featuring a somewhat reduced sensitivity – by absorption photometry.

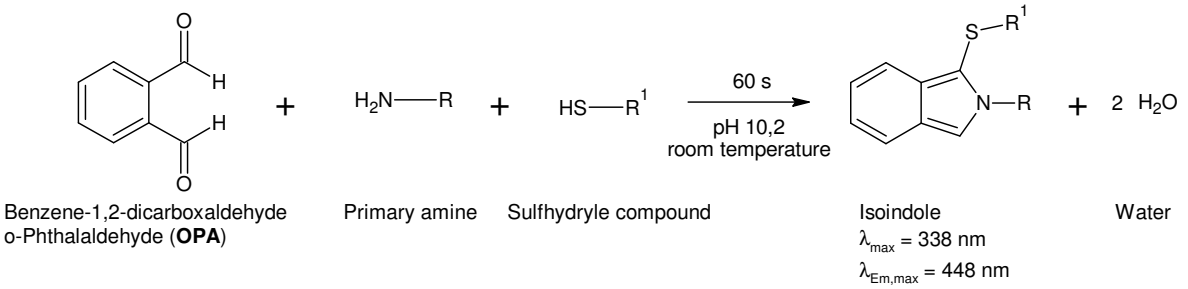

Scheme 4-1 Derivatisation of amino acids with OPA

4.1. Detectability of free amino acids

The amino acids were to be sampled using a HPLC system, for which either UV- or RI-detection was available. For specific questions, a mass spectrometer interface able with an LC-system was available but due to limitations concerning the workload of this machine and even more the general use of buffer salts for the resolution of amino acids the principal mode of detection had to be spectroscopic.

In order to check the detectability of free amino acids, seven amino acids representing the range of spectroscopically active functional groups were chosen, dissolved in water at a concentration of 10 mM (dissolved in 1% formic acid) and injected into the HPLC system which was operated with a zero void union in place of a chromatographic column.

Table 4-1 spectroscopic detectability of underivatised amino acids

Substance	g mol^{-1}	signal area per µmol of substance[a]			
		RI	205 nm	228 nm	280 nm
Proline	115,13	23,0	81,9	3,20	-
Tyrosine[b]	181,19	104	2100*	1980*	628
Tryptophan	204,23	44,8	2850*	2730*	2050
Histidine	155,16	27,6	2090*	645	0,820
Phenylalanine	165,19	34,1	2100*	35,6	1,06
Isoleucine	131,18	21,6	91,6	3,67	-
Alanine	89,09	13,9	71,7	3,14	-

a… in mAU min µmol^{-1} for the UVD, in µRIU min µmol^{-1} for the RID
b… dissolved in 1% formic acid
*… detector saturation

The refractive index detection exhibited insufficient sensitivity; the aromatic amino acids can be detected by ultra violet absorption while for the nonaromatic amino acids a derivatisation step is necessary before an UVD can be applied successfully.

4.2. Method

4.2.1. Original method

The method presented in [131] was adjusted to the available instrumentation while omitting the use of preformulated reagents.

The initial method development was carried out with bovine casamino acids, 1 g/l in ddH_2O as a test sample of comparable complexity and similar production route (hydrolysis with hydrochloric acid) to the hydrolysates of collagen. The samples were derivatised without any further processing using 2-mercaptoethanol as the sulfhydryl component.
The initially used mobile phase (10 mM NaH_2PO_4, 10 mM $Na_2B_4O_7$ to pH 8,2 with HCl) was changed when the pump started to leak and white crusts emerged close to almost every valve of the pump (a model of the exact manufacturer who published the method used) – see II.V.

Mobile Phase:

A: 10 mM NaH_2PO_4, 10 mM $Na_2B_4O_7$ in ddH_2O; pH 8,2 with HCl
B: ACN : MeOH : ddH_2O 45:45:10 (v + v + v)

Reaction buffer:

$Na_2B_4O_7$, saturated in ddH_2O; to pH 10,2 with NaOH

OPA-reagent:

o-Phthalaldehyde (OPA) 10 g l^{-1} dissolved in 10 % of the final volume MeOH, after complete solvation (10 – 20 s when shaken by hand) reaction buffer was added to the final volume
2-Mercaptoethanol 6 ‰ (v + v) (115 % based on OPA content)

Derivatisation in the autosampler:

- wash needle (100 µl ddH_2O)
- draw 50 µl reaction buffer
- draw 20 µl sample
- eject 70 µl to reaction vial (equipped with a 100 µl glass insert)
- mix 2 times (40 µl)
- draw 10 µl OPA-reagent
- eject 10 µl to reaction vial
- mix 2 times (50 µl)
- wait: 30 s
- inject 20 µl to column

RP-HPLC:

column: Eurospher 100-5 C18 4,6x250 mm
column oven temperature: 40 °C
detection: UVD 170U @ 338 nm (bandwidth 10 nm), reference wavelength 390 nm (b.w. 20 nm)
flow: 1,5 ml min^{-1}
gradient: (%A = 100 - %B)

time after injection /min	%B
0	2
0,84	2
33,4	57
33,5	100
39,3	100
39,4	2
40,0	2 (end)

4.2.2. Revised method

Sodium borate and sodium dihydrogen phosphate were replaced according to [132] by sodium acetate at pH 5 (adjusted with glacial acetic acid) which affected the resolution a bit but ameliorated the problems with the leaking pump.

Mobile Phase:

A: ddH_2O : MeOH : THF : NaOAc 1M pH 5,0
72,5 20 2,5 5,0 (v + v + v + v)

B: ddH_2O : MeOH : THF : NaOAc 1M pH 5,0
12,5 80 2,5 5,0 (v + v + v + v)

When preparing the mobile phase constituents using graduated cylinders shifts in the retention times of up to 50 s were observed from different preparations of mobile phase constituents. A change to volumetric pipettes for the measurement of the required volumes mitigated the problem.

Reaction buffer:

$Na_2B_4O_7$, saturated in ddH_2O; to pH 10,2 with NaOH

OPA-reagent:

o-Phthalaldehyde (OPA) 10 g l^{-1} dissolved in 10 % of the final volume MeOH, after complete solvation (10 – 20 s when shaken by hand) reaction buffer was added to the final volume
3-Mercaptopropionic acid 8,25 ‰ (v + v) (155 % based on OPA content)

Derivatisation in the autosampler:

- draw 10 µl internal standard (*L*-Norvalin 1 mM in ddH_2O)
- draw 10 µl sample
- eject 20 µl to reaction vial (equipped with a 100 µl glass insert)
- wash needle (100 µl ddH_2O)
- draw 40 µl OPA-reagent
- eject 40 µl to reaction vial
- mix (3 x 40 µl)
- wait: 28 s
- inject 20 µl to column
- wash needle (100 µl ddH_2O)

In addition to this standard derivatisation program a second program with lower derivatisation capacity but higher sensitivity (due to less dilution) was also used:

- draw 5 µl internal standard
- draw 20 µl sample
- eject 25 µl to reaction vial (equipped with a 100 µl glass insert)
- wash needle (100 µl ddH_2O)
- draw 20 µl OPA-reagent
- eject 20 µl to reaction vial
- mix (3 x 30 µl)
- wait: 30 s
- inject 20 µl to the column
- wash needle (80 µl ddH_2O)

Under perfect analytical conditions the calibration functions derived from this two derivatisation protocols will differ by a constant factor of 0,25 (for normalised signals; 0,375 for unreferenced signals), derived from the different dilution of sample and internal standard only as the regression function (signal = k · concentration + d) is linear.

$$sample\text{: } \frac{\frac{10}{60}}{\frac{20}{45}} = 0{,}375;\ IS\text{: } \frac{\frac{10}{60}}{\frac{5}{45}} = 1{,}5;\ \frac{0{,}375}{1{,}5} = 0{,}25;$$

upper numerator..... volume of sample/internal standard used in protocol 1
upper denominator ..... total derivatisation volume of protocol 1
lower numerator ..... volume of sample/internal standard used in protocol 2
lower denominator..... total derivatisation volume of protocol 2

RP-HPLC:

column: Eurospher 100-5 C18 4,6x250 mm
column oven temperature: 40 °C
detection: UVD 170U @ 338 nm (bandwidth 10 nm), reference wavelength 390 nm (b.w. 20 nm)
flow: 1,0 ml min^{-1}
gradient: (%A = 100 - %B)

time after injection /min	%B
0	5
7	5
17	25
27	50
35	50
35	100
40	100
40	5
45	5 (end)

Alternatively to the binary gradient presented above, a ternary approach was also used resulting in the same concentration profile as the binary gradient:

A: ddH_2O
B: NaOAc 250 mM pH 5,0 & THF 12,5 % (v + v) in ddH_2O
C: MeOH
gradient: %B = 20; %A = 80 - %C

time after injection /min	%C
0	23
7	23
17	35
27	50
35	50
35	80
40	80
40	23
45	23 (end)

To correct for potentially different derivatisation efficiencies (e.g. due to deterioration of the OPA reagent with time), the measured signal areas were normalised to the respective signal area of the internal standard (*L*-Norvalin).

4.2.3. Shortened method without buffer salts for 7 AS

As the model system comprising seven amino acids didn't place the same demands on resolution as did the hydrolysed proteins, a method generating fractions eligible for direct infusion into an ESI source while at the same time saving one third of solvent volume and occupation time was applied.

Mobile Phase:

A: ddH2O

B: ACN : MeOH : ddH2O
45 45 10 (v + v + v)

C: 1 % (v + v) formic acid in ddH_2O

The reaction buffer, the OPA reagent and the derivatisation protocol were identical to those used in the revised method (4.2.2).

RP-HPLC:

column: Eurospher 100-5 C18 4,6x250 mm
column oven temperature: 20 °C
detection: UVD 170U @ 338 nm (bandwidth 10 nm), reference wavelength 390 nm (b.w. 20 nm)
flow: 1,0 ml min^{-1}
gradient: %C = 10; %A = 90 - %B

time after injection /min	%B
0	40
5	45
7	68
15	68
18	80
20	80
22	90
26	90
26	40
29	40 (end)

4.3. Previous approaches

4.3.1. Variation of the reaction buffer

The medium for the derivatisation of free amino acids with OPA was also varied in an attempt to completely exclude borate from the method.
A first test with OPA dissolved in MeOH and water instead of reaction buffer clearly indicated the lability of the reagent used under non-basic conditions: a white precipitate was formed which could be redissolved using an ultrasonic bath but all the peaks in the resulting chromatogram were extremely small and generally shifted in an erratic manner.
When ammonium hydrogen carbonate (at pH 10,2 with NH_3) was used as reaction buffer, a yellow precipitate was immediately formed and no signals could be detected. Unsurprisingly the reaction for the detection of primary amines (see Scheme 4-1) also works with ammonia.
With a tertiary amine (triethylamine, to pH 10,2 with glacial acetic acid) the reaction works in principle but the amount of fluorophor derivate formed is greatly reduced, on average 2 % of the signal area observed using borate buffer were detected.

Finally, given its far superior performance in derivatisation of free amino acids and reasonably low amounts brought into the HPLC system by the protocol used, borax buffer was used as described above (4.2.2).

4.3.2. Neutralisation of hydrochloric acid in the autosampler

As the drying of the hydrolysed samples constitutes the most time-consuming step in the preparation of protein hydrolyzates for subsequent amino acid determination, it was tried to avoid it by directly neutralizing the acid in the hydrolysis solution. As no buffer of sufficient capacity at pH 10,2 which also mustn't affect the derivatisation reaction could not be procured, the acid was to be neutralized by addition of the appropriate amount of base. This base was chosen to be sodium hydroxide for its unproblematic reaction products with hydrochloric acid and its high solubility in water.
At first, an aqueous solution of lye was made and titrated with a volumetric solution of hydrochloric acid to determine its exact concentration. In turn, this solution was then used to determine the concentration of the hydrochloric acid used for the preparation of the 6 M HCl for the protein hydrolysis and the formulation of the relationship between measured pH and concentration of hydrochloric acid.

Titration

Piston Burette Schott Titronic® 97/20; beaker with magnetic stir bar on a magnetic stirrer
Titrant solution: NaOH, 50 % (19 M) 1:50 in ddH_2O: 20 ml (volumetric pipette) in 1 l (volumetric flask)

Table 4-2 Titration of hdrochloric acid with sodium hydroxide

analyte	endpoint	consumption of titrant / ml			c / M
titrant (with 25 ml 0,1009 N HCl)	pH 7	6,92	6,92	6,92	**0,365**
200 µl "37 %" HCl	pH 7	5,81	5,80	5,80	**10,58**
titrant (with 25 ml 0,1009 N HCl)	pH 7	6,92	6,92	-	**0,365**
500 µl NaOH in borax buffer pH	pH 10,25	1,56	1,52	1,53	**3,93**
10,25 + 25 ml 0,1009 N HCl	pH 7,0	1,04	1,00	1,00	4,32
400 µl NaOH circa 5M + 25 ml 0,1009 N HCl	pH 7	1,47	1,48	1,49	**4,958**

$$N(HCl) = \frac{N(NaOH) \cdot V(NaOH)}{V(HCl)}$$

With the concentration of the NaOH used for neutralisation known, the required volume of NaOH for the neutralisation of 20 µl (using the original method, cp. 4.2.1) of acidic sample in the autosampler can be determined using the titration of 200 µl of hydrolysis solution as base.

$$V(5M\ NaOH) = 7{,}35\ \mu l \cdot \frac{V(NaOH)}{ml}$$

The pH-values were measured after 100-fold dilution of the hydrochloric acid with ddH_2O to better match the conditions of samples after acid hydrolysis where only a small volume could be used for the determination on the pH. All pH-values were measured using the Mettler Toledo InlabExpert Pt 1000 pH electrode.
Hydrochloric acid being a strong acid the relation between pH and acid concentration is pretty straightforward.

Table 4-3 pH – hydrochloric acid concentration

c(HCl) / M	pH (1:100 with ddH_2O)		
10,6	1,35	1,35	1,34
8,82	1,49	1,48	1,48
7,05	1,52	1,53	1,52
5,29	1,61	1,61	1,62
3,53	1,76	1,75	1,75
1,76	2,01	2,00	2,00
0,882	2,27	2,28	2,27
0,0882	3,19	3,20	3,20

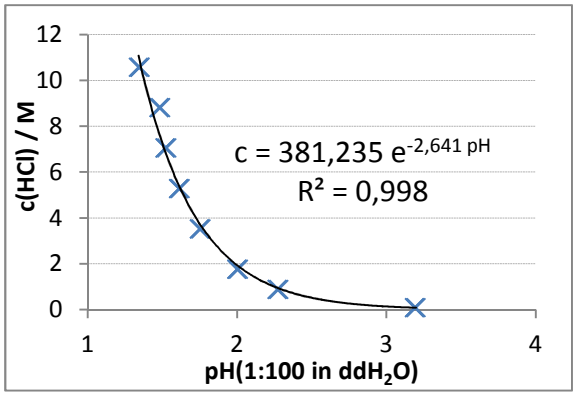

Figure 4-1 pH – hydrochloric acid concentration

In combination with the concentration of the used sodium hydroxide as determined by titration (Table 4-2), the amount of NaOH needed to neutralize the acid in the sample can be estimated as follows (for the original method, cp. 4.2.1; for the revised method, cp. 0, simply divide by 2):

$$V(5M\ NaOH) = 1538\ \mu l \cdot e^{-2{,}641 \cdot pH(sample\ 1{:}100\ in\ ddH_2O)}$$

As the drying and reconstitution of the hydrolysis solution has as a side effect a considerable concentration (circa 5,5 for 150 µl of sample, cp. 3.2.2) while the addition of an extra volume adds extra variance being an additive step to carry out as well as increasing the effort of data interpretation, the samples were dried and reconstituted in ddH_2O, as described in 3.2.2.

4.3.3. Masking of ammonia as urotropine

Ammonia being a volatile compound, the ammonia content of the samples should drop to almost zero during the drying process of the hydrolysed samples. As it turned out, the removal is not really quantitative and some ammonia is still present when the sample is brought into contact with the derivatising reagent OPA. As a result, some of the OPA reacts with the ammonia giving a product which manifests itself as a few negative peaks eluting after all the isoindoles formed with primary amino acids.
To avoid this side reaction, ammonium can be masked using formaldehyde [133].

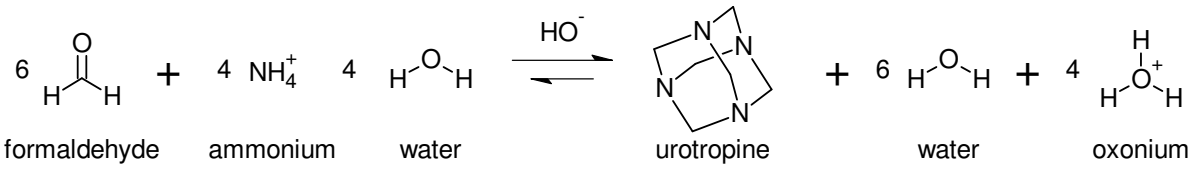

Scheme 4-2 reaction of ammonium with formaldehyde yielding urotropine

This reaction was done in the autosampler using an additional vial containing 1 % formaldehyde in water and a reaction time before the addition of OPA reagent of 20 min at room temperature. Using this additional step, it was possible to get rid of the negative peaks but as with the neutralisation of hydrochloric acid (4.3.2) the additional step is detrimental to the repeatability of the protocol. Instead of masking the residual ammonium the negative peaks were either ignored or the buffer used in the sample preparations was changed in order to not contain ammonium.

5. Gel electrophoresis

Denaturating gel electrophoresis was used to check for changes in molecular weight and size which are inevitable side effects of cross linking.
The competing technology of gel permeation chromatography was not applicable for a considerable part of the samples because of the size of the gels resulting from cross linking which slightly exceeds the selective permeative region of the columns available – blatantly speaking: It's difficult to separate a gel in another gel.
Another possibly applicable technology, MALDI-MS, requires the cocrystallisation of the analyte with the MALDI matrix compound. These compounds generally feature at least one phenolic moiety, which is a potential point of attack for the enzymes used in this study. A pre-test with the standard matrix for larger proteins, sinapic acid, showed indeed the formation of a yellow colour immediately after the dissolved matrix was brought into contact with the solutions containing the individual enzymes (tyrosinases as well as laccases).

5.1. SDS-PAGE

The gels were polymerised radically with ammonium persulfate and TEMED, the anode- and cathode puffer contained Tris, glycine and SDS [134].
The gel electrophoresis system used was the BioRad Mini Protean® 3 (vertical gels).

5.1.1. Gel casting

2 gels of 1 mm thickness each were produced in compliance to the following protocol:

- assemble the gel cassette sandwich
- prepare the monomer solution for the polymerisation of the resolving gel (10 ml)
  - (% of acrylamide in the gel) / 4 ml 40 % acrylamide : bis-acrylamide 37,5 : 1
  - 2,5 ml 1,5 M Tris-HCl buffer pH 8,8
  - {10 – 2,657 – ml(40 % acrylamide)} ml dH_2O
  - 100 µl SDS 100 g/l in dH_2O
  - 50 µl ammonium persulphate 100 g/l in dH_2O
  - 7 µl TEMED, mix well and pour into the gel cassette (using a 1000 µl piston pipette)
- overlay the resolving gel with approximately 1 cm of isopropanol
- allow to polymerize for 1 h
- decant the alcohol and rinse the gel surface with dH_2O
- prepare the monomer solution for the polymerisation of the stacking gel (4 ml)
  - (% of acrylamide in the gel) / 4 ml 40 % acrylamide : bis-acrylamide 37,5 : 1
  - 1,0 ml 0,5 M Tris-HCl buffer pH 6,8
  - {4 – 1,063 – ml(40 % acrylamide)} ml dH_2O
  - 40 µl SDS 100 g/l in dH_2O
  - 20 µl ammonium persulphate 100 g/l in dH_2O
  - 3 µl TEMED, mix well
- dry the surface between the glass plates above the resolving gel using a piece of filter paper
- pour the solution for the stacking gel into the gel cassette (using a 1000 µl piston pipette)
- insert the comb (make sure there are no trapped air bubbles) and allow to polymerize for approximately 1 h

5.1.2. Running buffer

For 1 l of 5x buffer (dilute 1 + 4 with dH_2O prior to use):

- 15 g Tris
- 72 g glycine
- 5 g SDS

dissolved in 1 l dH_2O (SDS foams up strongly)

5.1.3. Loading buffer

2x loading buffer (standard):

- 250 mM Tris-HCl buffer pH 6,8
- 46 g l^{-1} SDS
- 20 % glycerine (v/v)
- 100 mg l^{-1} bromophenol blue

For 2 ml of reductive 10x buffer:

- 800 µl SDS 100 g l^{-1} in ddH2O
- 200 µl 2-mercaptoethanol
- 500 µl 0,5 M Tris-HCl buffer pH 6,8
- 500 µl glycerine
- 1 mg bromophenol blue

5.1.4. Mass standard

Table 5-1 Mass standards for gel electrophoresis

MW / kDa	Protein
29	carbonic anhydrase (from bovine erythrocytes)
66	albumin (bovine)
150	alcohol dehydrogenase (yeast)
200	β-amylase (sweet potato)
443	apoferritin (horse spleen)
669	thyroglobulin (bovine)

Each protein was prepared at 125 mg l^{-1} in ddH_2O.

5.1.5. Sample preparation

An aliquot of the sample (12 µl) was mixed with the 2x loading puffer and put for 10 min on an Eppendorf thermomixer which was set and preheated to 95 °C (unless specifically noted otherwise).

5.1.6. Electrophoresis

The polymerized gel was removed from the casting stand, the comb was removed and the gel was installed into the electrophoresis chamber.
The chamber was then filled with running buffer (approximately 950 ml) and the whole assembly was placed in a box made of expanded polystyrene filled with ice.
20 µl of the sample solution with loading buffer was then pipetted into the wells of the gel, the power supply was connected and the gel was run at 100 V till the band of bromophenol blue had almost reached the bottom of the resolving gel.
After electrophoresis the gel was dismounted from the gel cassette, rinsed with dH_2O and stained.

5.1.7. Composite gels

As the mechanical stability of polyacrylamide gels with an acrylamide content of less than 2 % is insufficient for gel electrophoresis, much less for the handling afterwards, while the samples to be separated called for a degree of cross-linking equivalent to a content well below that agarose was added to the monomer solution to provide mechanical stabilisation.
Agarose contents below 0,5 % resulted in brittle gels which couldn't even stand the strain of assembling the gel chamber but for agarose contents of 1 % and higher a sufficient mechanical stabilisation was achieved.
An additional problem arised when using agarose within the used electrophoretic system (BioRad Protean® 3): the gel combs made from PC exhibited strong adhesion to the gels containing agarose. So when the idea was to remove the comb from the gel what was achieved was the removal of the gel, still attached to the comb, from the gel cassette resulting in the loss of the newly polymerised gel. This problem could be overcome by applying a releasing agent to the surface of the combs before inserting those into the prospective gel (amresco E319 Acryl-Glide™: siloxanes and ethyl sulphate in ethanol and isopropanol).
Agarose was added to the monomer solution is solid form just prior to the addition of the radical starters ammonium persulphate and TEMED. The monomer solution was then heated up using a microwave oven at 800 W under constant supervision to avoid bumping and boiling over of the cancerogenic mixture until the agarose was completely dissolved. The gel casting cassette was preheated with boiling water to avoid local cooling of the agarose containing solution which would result in the formation of inhomogeneities in the gel as the polymerisation reaction couldn't reach the already solid spots or even in the generation of cavities in the gel due to a viscosity too high to fill the mould completely. To the hot solution the radical starters were added and the mixture was poured quickly into the gel casting cassette. Due to the higher temperature the radical polymerisation was speeded up considerably which seriously reduced the pot life but also allowed for the polymerisation to form a cross-linked polymer before the diffusion was hindered by the solidifying agarose.

5.2. SDD-AGE

As SDS-PAGE was unable to separate the products of the crosslinking experiments with collagen, a method reportedly suitable for separation of proteins in the MDa range [135] was applied (SDD-AGE: semi-denaturating detergent agarose gel electrophoresis).
The main difference to the SDS-PAGE (5.1) was the use of agarose instead of polyacrylamide and a different composition of the running buffer.
For the gels of 10 mm thickness used with this protocol, the Savant H6370 Electrophoretic Gel System was used (horizontal gel).

5.2.1. Running buffer

TAE-buffer (Tris-Acetate-EDTA):

For 250 ml of 20 x TAE buffer:

- 24,2 g Tris
- 1,86 g Na-EDTA
  - Dissolved in 225 ml dH_2O
  - pH adjusted with glacial acetic acid to pH 8,0 (approximately 5,6 ml)
  - with dH_2O filled up to 250 ml

The running buffer used was 0,5 x TAE-buffer with 1 ‰ (1 g l^{-1}) SDS for both anode and cathode.

5.2.2. Gel casting

The appropriate mass of agarose was placed in an Erlenmeyer flask, 20x TAE buffer was added to a final concentration of 0,5x (1,25 ml for a 10 mm gel with a volume of 50 ml) and dH_2O was added to make up the rest of the volume. The flask was then put into a microwave oven and heated at 800 W till the agarose was completely dissolved. To this hot solution 1 ‰ SDS was added using a solution of 10 % SDS in water (e.g. 0,5 ml to what is left of the 50 ml applied originally; Adding the SDS before the heating step results in generation of huge amounts of foam as the flask needs to be agitated in order to prevent bumping and boiling over of the prospective solution.).
This solution was then poured into the gel mould, the comb was put in place and the agarose solution was allowed to cool down and solidify.

5.2.3. Loading buffer

2x loading buffer:

- 1x TAE buffer
- 40 g l^{-1} SDS
- 50 % glycerine (w/v)
- 0,5 g l^{-1} bromophenol blue

5.2.4. Sample preparation

Aliquots of the samples were mixed with the loading puffer and put for 10 min on an Eppendorf thermomixer which was set and preheated to 50 °C and 500 min^{-1}. As an alternative solid urea was added to the mixture of sample and loading buffer to a final concentration of 8 M and no treatment at higher temperature was applied [136].

5.2.5. Electrophoresis

The comb was removed from the agarose gel and the gel chamber was filled with running buffer. 30 µl of the samples mixed with loading buffer were then pipetted into the wells of the gel, the power supply was connected and the gel was run at 30 V for 15 min and then at 90 V till the band of bromophenol blue had almost reached the bottom of the resolving gel.
After electrophoresis the gel was dismounted from the gel cassette, rinsed with dH_2O and stained.
The 10 mm gels could be stained quicker and more sensitively if the gel was reduced in thickness prior to staining. This was done by squeezing the gel between two paper filters assembled in a sandwich of paper towels and weighted with 3,8 kg (an exsiccator) for 24 h. This reduced the thickness to about 1 mm and speeded up the staining quite a bit (hours instead of days).

5.3. bis-Tris SDS-PAGE

This protocol used exclusively for samples containing insulin is based on [137] and was applied using the modifications released online (http://openwetware.org/wiki/Sauer:bis-Tris_SDS-PAGE,_the_very_best, retrieved 2011-04-04).
As for the SDS-PAGE using the Laemmli buffer system (5.1) the gel electrophoresis system used was the BioRad Mini Protean® 3.

5.3.1. Acryl amide

The acrylamide mixture used contains 30 % (w/v) Acrylamide and 2 % (w/v) bis-acrylamide.
The acrylamide in stock was a 40 % mixture of 37,5 : 1 acrylamide : bis-acrylamide which adds up to 38,96 % acrylamide and 1,04 % bis-acrylamide (w/v) assuming that "%" denotes weight by unmodified volume at a density of 1 g cm^{-3} (thus 1 % ≡ 10 g l^{-1}).

$$a + b = 40 \wedge 37{,}5 \cdot b = a \Longrightarrow b = \frac{40}{38{,}5} \approx 1{,}04$$

To arrive at the ratio of the above mixture (15 : 1), the mixture in stock was spiked with bis-acrylamide to obtain the 2,5 fold concentration (37,5/15 = 2,5) of said compound. 15,58 g l^{-1} of bis-acrylamide (2,5 · 1,04 - 1,04 = 1,56) were dissolved in the acrylamide mixture in stock yielding a 41,6 % acrylamide solution.
For the specification of the separating gels used, the acrylamide content indicated refers to the content of acrylamide only (the fifteenth part of that number being the additional bis-acrylamide content).

5.3.2. Gel buffer

The gel is polymerised in bis-Tris buffer pH 6,8.
For 3,5x buffer 1,25 M bis-Tris in dH_2O,brought to pH 6,5 – 6,8 with hydrochloric acid is used.

5.3.3. Running buffer

For 5x buffer (dilute 1 + 4 with dH_2O prior to use):

- 250 mM MES
- 250 mM Tris
- 5 mM EDTA
- 5 g l^{-1} SDS

The reducing agent sodium bisulfite is added from a concentrated solution to a final concenctration of 5 mM.

5.3.4. Reducing agent

To maintain a reducing environment sodium bisulfite is included in the running buffer.
Sodium disulfite is prepared at 500 mM in dH_2O constituting a 200x concentrate which is added to the running buffer immediately before use.
Sodium disulfite hydrolyses to two molecules of sodium bisulfite if it is brought in contact with water.
$Na_2S_2O_5 + H_2O \rightleftharpoons 2\ NaHSO_3$

5.3.5. Gel casting

The resolving gel of 1 mm thickness was cast in accordance with the following recipe.

- $3{,}5^{-1}$ of the final volume of 3,5x gel buffer
- acrylamide to the preferred final concentration
- dH_2O for the rest up to the final volume
- 5 µl ammonium persulphate 100 g l^{-1} in dH_2O per ml of final volume
- 1,5 µl TEMED per ml of final volume, mix well
- cast gel (fast, pot life approximately 90 s)
- overlay the gel with *tert*-butanol saturated with gel buffer
- allow to polymerise (approximately 20 min for 10 % acrylamide)

On the resolving gel, a stacking gel containing about 4 % acrylamide was cast.

- decant the butanol, rinse with dH_2O and remove the residual water with a piece of filter paper
- prepare and cast the stacking gel analogous to the resolving gel
- insert comb
- allow to polymerise (approximately 60 min for 4 % acrylamide)

5.3.6. Loading buffer

As loading buffer the same formulation as used for SDD-AGE was used (see 5.2.3).

5.3.7. Sample preparation

Aliquots of the samples to be run were mixed with loading buffer (1v + 1v) and subjected to 85 °C for 10 min on a preheated thermomixer.

5.3.8. Electrophoresis

After removal of the comb from the polyacrylamide gel the gel chamber was filled with running buffer (to which the reducing agent was now added). Per well of the 1 mm gel 20 µl of pretreated sample were transferred, the connection to the power supply was established and the gel was run at 150 V while providing external cooling in the form of box filled with crashed ice. As the bromophenol blue travels with the proteins weighting 3 – 5 kDa the electrophoresis was stopped when the band of the bromophenol blue reached the lower third of the gel (The used substrate, chain B of insulin can only boast 3,5 kDa). The gel chamber was the disassembled, the gel rinsed with dH_2O and stained.

5.4. Staining

5.4.1. Coomassie blue staining

Staining solution:

- 0,25 % (2,5 g l^{-1}) coomassie brilliant blue R-250
- 5,5 % (v/v) acetic acid
- 50 % (v/v) methanol
- dH_2O up to the final volume

Staining:

The gel is immersed into the staining solution and rests there for 20 min during which the vessel with the staining solution is shaken at approx. 150 min^{-1}.

Destaining solution:

- 10 % (v/v) acetic acid
- 40 % (v/v) methanol
- 50 % (v/v) dH_2O

Destaining:

The staining solution is decanted (and can be reused), the gel rinsed with water.
For the destaining the gel is shaken in destaining solution until the desired degree of destaining is reached. To speed up the process, the destaining solution should be changed 1 or 2 times, given this is done the destaining is usually adequate after 1 – 2 h.
The destained gel is then rinsed with dH_2O, placed between two transparent foils and documented using a scanner.

5.4.2. Staining with Biebrich scarlet

Using Ponceau S, proteins in agarose gels can be reversibly stained (destaining with water) [135]. Since this dye was not in stock but the structurally similar Biebrich scarlet (two sulfonic acid groups on the naphtalene system less) was available that was used instead.

Staining solution:

1 g l^{-1} Biebrich scarlet in 5 % (v/v) acetic acid (aqueous)

Staining:

The agarose gel is immersed into the staining solution and rests there for 2 days during which the vessel containing the staining solution is shaken at approx. 150 min^{-1}.

Destaining:

The destaining with water did not, well work – propably due to the structural differences to the original molecule Ponceau S (two sulfonic acid groups) which are sure to negatively inflict the solubility of the dye in water.
Using the destaining solution for the coomassie blue staining (5.4.1) a destaining was possible although it was kind of slow (4 days for a 10 mm agarose gel).

5.4.3. Coomassie blue staining with Al^{3+}

The addition of Al^{3+} increases the sensitivity of the stain as well as the rapidity of the staining process [138]. Another advantage of this modified protocol is that for many applications a destaining is not necessary because the polyacrylamide itself is stained quite slowly.

Staining solution:

- 200 mg l^{-1} coomassie brilliant blue G-250
- 50 g l^{-1} aluminium sulphate $Al_2(SO_4)_3 \cdot (H_2O)_x$, x = 14 - 18
- 10 % (v/v) ethanol 96 %
- 20 g l^{-1} orthophosphoric acid

First, the aluminium sulphate is dissolved in 50 % of the final volume dH_2O, the ethanol is added and the solution is homogenised. The Coomassie brilliant blue G-250 and phosphoric acid is added and water is added to the final volume. The resulting, dark-green to bluish dispersion contains colloidal coomassie blue which is crucial to the staining process.

Staining:

Since SDS hinders the binding of the colloidal coomassie blue to the proteins and in addition accounts for a strong background the gel should be washed at least 2 times for 10 min each in dH_2O if the running buffer contained SDS.
The staining solution is shaken immediately before use; the gels to be stained are covered with staining solution and are shaken at approx. 150 min^{-1} during the staining process which takes usually 20 min – 3 h.

Destaining solution:

- 10 % (v/v) ethanol 96 %
- 20 g l^{-1} orthophosphoric acid
- dH_2O up to the final volume

Destaining:

The gels are rinsed with dH_2O and are then either documented directly or, if further destaining is in order, are washed 2 x for 20 min each in dH_2O and then 10 – 60 min in destaining solution and again 2 x 20 min in water.

5.4.4. Silver staining

If the sensitivity of the other staining methods is unsatisfactory [139] or the gel dimensions or pore sizes impose diffusion limitations on the relatively big commassie blue molecules, silver staining can still be applied successfully.

Required solutions:

- A: fixing solution
  - 120 ml glacial acetic acid (12 %)
  - 500 ml ethanol (50 %)
  - 500 µl formaldehyde 37 % (w/v, formalin, 0,5 ‰)
  - fill to 1 l with dH_2O
- B: washing solution
  - 200 ml ethanol (20 %)
  - 800 ml dH_2O (80 %)
- C: sensibilising solution
  - sodium thiosulphate 200 mg l^{-1} in dH_2O (0,2 ‰)
- D: staining
  - silver nitrate 2 g l^{-1} (2 ‰)
  - 760 µl formaldehyde 37 %
  - fill to 1 l with dH_2O
  - cool to 4 °C prior to use
- E: developing
  - sodium carbonate (soda) 60 g l^{-1} (6 %)
  - sodium thiosulphate 4 mg l^{-1} (4 ppm)
  - 500 µl formaldehyde 37 %
  - fill to 1 l with dH_2O
- F: stopping solution
  - 120 ml glacial acetic acid (12 %)
  - fill to 1 l with dH_2O

The solutions A, B and F are stable for several months if stored at room temperature.

Staining:

- gel pivoted for 2 h or overnight in the fixing solution (A)
- 20 min washing (B) – changing the solution at least 3 times
- 2 min in the sensibilising solution (C)
- 2 x washing with dH_2O for 1 min each
- 20 min in (cold!) staining solution (D)
- gel shortly rinsed with a large volume of dH_2O for 20 – 40 s
- 2 – 5 min in the developing solution (E): constant supervision, stopping as soon as the desired degree of staining is almost reached
- washing with stopping solution (F) until no more bubbles are released: usually no more than 10 min; A slight darkening is observed.

For documentation the gel is rinsed with dH_2O, brought between two transparent foils and scanned.

6. MS^n analysis

The analysis of fragmentation trees was carried out using an Agilent 1100 Series LC/MSD Trap SL mass spectrometer which features a scannable mass range of ± 25 Th – ± 2200 Th at a mass accuracy of ±0,25 Th within the calibrated mass range in standard scan mode (±0,5 Th for fragmentation experiments).
The analytes were taken from fractions collected from a RP-HPLC run which was done immediately before the MS^n analysis. As most of the analytes were OPA-modified amino acids (see 4) and as such didn't exactly exhibit exceptional stability the collected fractions were stored at -18 °C until the analysis (for 2 min – 6 h).
The ions for mass spectrometry were generated using an ESI source with nitrogen (purity: N 5.0) as both nebulizer and drying gas which was charged using a syringe pump operated at 5 µl min^{-1}. The collision gas used for CID (and passive cooling) of the ions entrapped in the mass analyser was He (He 6.0) at a partial pressure of approximately 0,6 mPa.
The mass spectrometer was calibrated using a manufacturer supplied calibration mix (Agilent ESI Tuning Mix (for Ion Trap), part number G2431A) and was operated in standard mode (scan speed 2500 Th s^{-1}) using the settings given in 6.2.

6.1. Fraction collection

Since direct coupling of the LC system to the MS was not possible due to the salts used in the mobile phase. Even more restrictive (as it could not be overcome by changing the separation conditions) was the fact that such a direct attachment would have limited the time available for MS^n analysis to the peak width (approximately 0,2 – 0,5 min) which was distinctly too short a time for the analysis in question (A typical MS^n analysis was finished in 80 min.).
The fraction collector used was a Teledyne Isco Foxy® R1 controlled via integration into the Chromeleon® operated HPLC system.

6.1.1. Determination of the delay volume

The delay volume is the volume between the device generating the primary trigger signal (the UVD of the HPLC system in the setup used) and the next (following the flow of the mobile phase) device to be controlled.
In order to determine the actual delay volume, 6 M HCl was injected into the HPLC system whose column had been replaced by a zero void volume union. As mobile phase ddH_2O was used and the detection of the injected acid was done using the UVD @ 220 nm. For the detection of the acid in the collected fraction, one drop of a solution of phenolphthalein in ethanol (2 % w/v) with 10 mM NaOH was placed in the tube of the fraction collector which was then swirled while the mobile phase was collected dropwise. The time between injection and the colour change from pink to colourless was measured using an electronic time clock and from the difference to the time of the UVD signal the volume between the two optically detected events was calculated to 218 µl (cp. VI.I).

6.1.2. Desalting of collected fractions

As the mobile phase used by default contains 50 mM sodium acetate (cp. 4.2.2) the fractions collected from such a separation needed to be desalted before it was reasonable to conduct an analysis by ESI-MS.

Sodium acetate clusters:

When the desalting step was omitted and the collected fractions were injected without further purification into the ESI interface, no specific signals were generated. All that could be detected were clusters of sodium acetate.

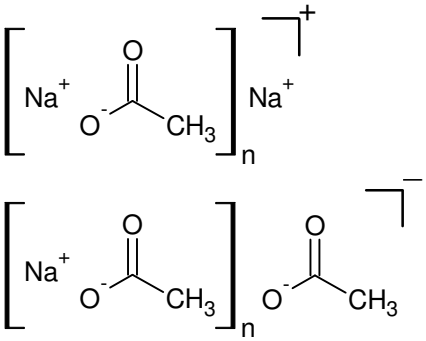

formula weight /Th: 82,00 ·n + 22,99 $n \in \mathbb{N}\backslash\{0\}$

measured /Th: 105; 187; 269; 351; 433; 515; 597; 679; 761; 843; (925); (1007)

formula weight /-Th: 82,00 ·n + 59,01 $n \in \mathbb{N}\backslash\{0\}$

measured /-Th: 141; 223; 305; 387; 469; 551; 633; 715; 797; 879; 961; 1043; 1125; 1207; 1289; (1371); (1453); (1535)

Figure 6-1 clusters of sodium acetate

Desalting via RP-HPLC:

Desalting was done using the same column as for the first round of chromatographic separation which had been flushed with 4 column volumes of 1 ‰ formic acid in ddH_2O with 50 % (v + v) ACN. The collected fraction from the primary run was reinjected and the analyte was recollected from this isocratic run. The content of organic modifier was adjusted to give a retention factor of approximately 1 for the analyte in question.
As this procedure brought forth a certain dilution in combination with a limited recovery (an effect that became more pronounced as the amount of the analyte decreased), derivatised amino acids which were only present in minute amount could not be analysed using this approach. A further limitation which also excludes this method from application with most of the scarcely produced derivatised amino acids is the time needed to finish the desalting, a period of time which was too long for some of the substances analysed – those decomposed before they could be brought into the mass analyser.

6.1.3. RP-HPLC without the addition of a buffer salt

For increased recovery and generally milder conditions during the preparation of the samples for MS^n analysis the chromatographic step was modified in order to exclude especially all addition of non-volatile salts. While this compromised the chromatographic resolution it allowed the analysis of scarcely present compounds as well as the capture of labile ones. To compensate for the buffer capacity lost with the exclusion of salts from the mobile phase, 1 ‰ (v/v) formic acid was added to the mobile phase to provide a sufficiently acidic environment to allow for the protonation of all basic side chains whose presence in a charged state would seriously compromise the retention under reversed phase conditions. In order to further decrease the exposure for labile compounds the temperature of the analytic column was lowered from 40 °C (cp. 4.2.2) to 20 °C.

RP-HPLC:

column: Eurospher 100-5 C18 4,6x250 mm
column oven temperature: 20 °C
detection: UVD 170U @ 338 nm (bandwidth 10 nm), reference wavelength 390 nm (b.w. 20 nm)
flow: 1,0 ml min^{-1}

mobile phase
A: ddH_2O
B: ACN
C: formic acid 1 % (v/v) in ddH_2O

gradient: %C = 10%; %A = 90 - %B

time after injection /min	%B
0	25
64	60
64	90
68	90
68	25
70	25 (end)

6.2. Mass spectrometer settings

The spray capillary, arranged orthogonally to the ion transfer capillary and made of stainless steel, was at ground potential and placed approximately 2 mm above the entrance of the ion transfer capillary equipped with a round spray shield.

Data acquisition was done using the MSD Trap Control software in the version 12.86, which notation is used here to term the adjustable parts of the MS.

Table 6-1 MS^n analysis settings for the Agilent 1100 Series LC/MSD Trap SL

Component	Parameter	Positive mode	Negative mode
Ion source	Dry gas temperature	325 °C	
	Dry gas flow rate	5 l/min	
	Nebulizer pressure	15 psi	
	HV Capillary	-3,5 kV	3,5 kV
	HV End Plate	-3 kV	3 kV
	Skimmer	40 V	-40 V
	Lens 1	-5 V	5 V
	Lens 2	-60 V	60 V
	Octopole 1 DC	12 V	-12 V
	Octopole 2 DC	1,7 V	-1,7 V
	Octopole RF amplitude	(100 – 220) V_{pp}*,sps	
	Capillary exit	(90 – 160) V^{sps}	(-160 – -90) V^{sps}
Ion trap	Ion charge control target	30000 ions	
	Max. accumulation time	300 ms	
	Averages	5 spectra	
	Isolation width	4 Th	
	Fragmentation delay	0 µs	
	Fragmentation time	40 ms	
	Fragmentation width	10 Th	
	Fragmentation amplitude	(0,1 – 2,6) V^{ma}	
	Normalize to accu. time	On	
Detector	Electron multiplier voltage	2137 V**	
	Dynode voltage	10 kV	-10 kV
	Scan delay	0 µs	
	Skimmer block	0 V	-0 V
	Lens 1 block	-200 V	200 V
	Octopole RF amplitude block	0 V_{pp}*	
	Lens 2 block	0 V	-0 V
	Capillary exit block	-200 V	200 V

*.....Volts, AC peak-to-peak

sps.....adjusted for optimal transmission of ions with selected m/z using the "smart parameter settings" option of the control software

ma.....manually adjusted for maximal abundance of the daughter ion to be fragmented in the next step of isolation and fragmentation

**.....set using the "calibrate detector gain" functionality of the control software

6.3. Selection of signals of interest

Signals to be investigated more closely were chosen based on two scans of the full accessible mass range (± 25 Th – ± 2200 Th) for which the ion lens parameters were optimised for maximal transmission in intervals of 200 Th (using the "smart parameter settings" option of the control software). From the resulting 2 spectra those signals appearing in positive as well as in negative mode and with absolute values of the two corresponding signal differing by exactly 2 Th were selected for fragmentation tree analysis using CID-MS^n. A further check was done for the charge state of each signal which was carried out by measuring the distance between the monoisotopic signal (corresponding to a molecule made up entirely of the most abundant isotopes) and the isotopic +1 peak (mainly due to the contribution of molecules with one ^{13}C instead of the "standard" ^{12}C in organic molecules without isotopic labelling; a result of the natural isotopic composition of carbon: 1,07 % ^{13}C [140]). The deplacement of these two signals on the mass over charge axis reveals the charge state n of the detected molecule, which is related to the deplacement Δx by the simple formula $n = \frac{1\,Th}{\Delta x}$.
The signals with an assigned charge state of one and a difference of the absolute values between the corresponding signals in positive and negative ionisation mode of 2 Th should correspond to the quasi-molecular ions $[M+H]^+$ and $[M-H]^-$ respectively, thus an ion formed by either protonation or deprotonation of the analyte molecule (or clusters thereof).

6.4. Interpretation of fragmentation trees

The measured fragments and especially the neutral losses (having lower molecular masses and therefore exhibiting a significantly lower number of possibly matching molecular formulas for a given precision) were analysed and molecular formulas and structures were assigned to the neutral losses [141-144] and finally also to the pseudo-molecular ions themselves. In doing so, available additional information derived from other measurements (mostly photospectroscopic data) or the experimental conditions (especially the educts provided and the general mode of the reaction used) was taken into consideration to somewhat limit the number of candidate structures.
Photoabsorption occurring above approximately 350 nm couldn't be fully exploited because no suitable matching between the position of the absorption band and the molecular structure could be established for structures containing longwave chromophores, especially such derived from quinone structures. While for conjugated olefins and related structures the rules derived by Woodward and Fieser allow an estimation of the position of the energetically lowest absorption band with adequate precision, the rules fail for chromophores based even partially on different principles.
While semi-empirical methods of quantum chemistry can be applied to systems containing such chromophores, the precision attainable without the introduction of experimental values renders them useless for the task described above.
LCAO-MO in the Hückel approximation can be used to establish an order of frontier orbital energy gaps [145], adjusting the central parameters of a ("the" semi-empirical) method for the calculation of electronic absorption spectra (ZINDO/S [146]) to match experimental data can be successful [147, 148] but working with the structure only the results are generally unsatisfactory [149].
Ab-initio calculation on the other hand are able to yield the desired information [149-153] but neither the time and computational power required nor the expertise necessary to carry out one of these calculations, let alone dozens of them, were at hand.

Possibly matching molecular formulas were calculated using the software Molecular Weight Calculator in the version 6.46. By default, the elements C, H, N, O, S and, if in order, Na were included in the search with an accepted mass window of 0,5 Da. Changing this mass window to 0,2 or 0,8 Da usually didn't change the number or identity of the formulas found; the discriminatory capacity of the mass spectrometer used was thus at unit resolution.
The list of results was then, if applicable and of a length justifying the additional mouse clicks, filtered for Double Bond Equivalents (DBEs) using a Microsoft batch file (given in the Annex, see VI.II).

The precision of the measured isotopic distributions of a single signal was generally useful to distinguish between the possible general types of the compound in question (at the level of: organic compound, halogenated organic compound or inorganic compound) but for the extraction of more detailed information like the number of carbon atoms in the pseudo-molecular ion (Which is accessible from the relative abundance of the +1 isotopic peak because the natural abundance of heavy isotopes for the most abundant elements in organic compounds (^{2}H: 0,115 ‰; ^{13}C: 10,7 ‰; ^{15}N: 3,68 ‰; ^{17}O: 0,38 ‰; ^{33}S: 7,6 ‰; all values taken from [140]) in combination with the general abundance of these elements in organic molecules allows for the simplification of considering only ^{13}C as the sole isotope accountable for the isotopic +1 peak.) the quality of the data did not suffice.

6.5. MS^n analysis of known OPA-derivatised amino acids

6.6. Known OPA-derivatised amino acids

To get an idea of the fragmentations to be expected, four amino acids were derivatised under conditions identical to those used for the unknown samples (chromatogram: see VI.III).
In the fragmentation trees the precursor and fragment ions are given in Th (Thomson [154], 1 Th ≡ 1 $u \cdot e^{-1} \approx 1{,}036427 \cdot 10^{-8}$ kg C^{-1}) connected by an arrow with labels indicating the mass of the neutral loss in u (= Da) above the arrow and the molecular formula(s) of the lost neutral(s) beneath it. For this label, the two appreviations **ACA**: acrylic acid ($C_3H_4O_2$) and **AA**: acetic acid ($C_2H_4O_2$) are used to indicate the two corresponding species. The most abundant ion in the MS^1 scan and within any particular order of daughter ions is underlined to allow the quick identification of the main fragmentation route. *Italic, grey fragments* indicate ions that could not be isolated in the subsequent step (or only in a single scan therein) and were only detectable in the fragment spectrum of their precursor ion.
The fractions given for the isotopic fingerprint are relative abundances based on the monoisotopic pseudo-molecular ion. For the measured values this is given by the peak area normalised to the mono-isotopic peak's area.

Table 6-2 monoisotopic masses of pseudo-molecular ions of amino acids derivatised with OPA and 3-mercaptopropionic acid

Amino acid	abbreviation		(COOH)H_2NCH-R	FW(R) / (g mol^{-1})	OPA-amino acid / ±Th	
					$[M - p]^-$	$[M + p]^+$
Glycine	**Gly**	G	–H	1,01	**278,05**	**280,06**
Alanine	**Ala**	A	$–CH_3$	15,02	**292,06**	**294,08**
Serine	**Ser**	S	$–CH_2OH$	31,02	**308,06**	**310,07**
Proline	**Pro**	P	$–CH_2CH_2CH_2–$	42,05	-	-
Valine	**Val**	V	$–CH(CH_3)_2$	43,05	**320,09**	**322,11**
Threonine	**Thr**	T	$–CH(OH)CH_3$	45,03	**322,07**	**324,09**
Cysteine	**Cys**	C	$–CH_2SH$	47,00	**324,04**	**326,05**
Isoleucine	**Ile**	I	$–CH(CH_3)CH_2CH_3$	57,07	**334,11**	**336,13**
Leucine	**Leu**	L	$–CH_2CH(CH_3)_2$	57,07	**334,11**	**336,13**
Asparagine	**Asn**	N	$–CH_2CONH_2$	58,03	**335,07**	**337,08**
Aspartic acid	**Asp**	D	$–CH_2COOH$	59,01	**336,05**	**338,07**
Glutamine	**Gln**	Q	$–CH_2CH_2CONH_2$	72,04	**349,08**	**351,10**
Lysine	**Lys**	K	$–CH_2CH_2CH_2CH_2NH_2$	72,08	**349,12**	**351,14**
Glutamic acid	**Glu**	E	$–CH_2CH_2COOH$	73,03	**350,07**	**352,08**
Methionine	**Met**	M	$–CH_2CH_2SCH_3$	75,03	**352,07**	**354,08**
Histidine	**His**	H	$–CH_2(C_3H_3N_2)$	81,05	**358,08**	**360,10**
Phenylalanine	**Phe**	F	$–CH_2(C_6H_5)$	91,05	**368,09**	**370,11**
Arginine	**Arg**	R	$–CH_2CH_2CH_2NH$-C(NH)NH_2	100,09	**377,13**	**379,14**
Tyrosine	**Tyr**	Y	$–CH_2(C_6H_4)OH$	107,05	**384,09**	**386,10**
Tryptophan	**Trp**	W	$–CH_2(C_8H_6N)$	130,07	**407,11**	**409,12**
Dityrosine	-	-	$–CH_2(C_6H_3)OH–(C_6H_3)OHCH_2–$	212,08	**739,18**	**741,19**

6.6.1. Arg

The fragmentation of electrospray ionised unmodified arginine (in positive mode) has been recorded by Rasche et al. on a QTOF instrument with a mass accuracy of 20 ppm [155]. While the fragments from the mercaptopropionic acid moiety are dominant in the fragmentation tree of the OPA-derivatised arginine, the neutral losses from arginine could not be replicated in full. The dominant neutral loss in the QTOF fragmentation tree – NH_3 – is blocked by incorporation in the isoindole moiety of the OPA-derivatised amino acid, thereby cutting the biggest branch right at the root of the tree. The remaining neutral losses, with the exception of guanidinium (60 Th), which's signal was below the scanned range (> 100 Th), could be found in the OPA-Arg fragmentation tree, although in different combinations.

+MS^n

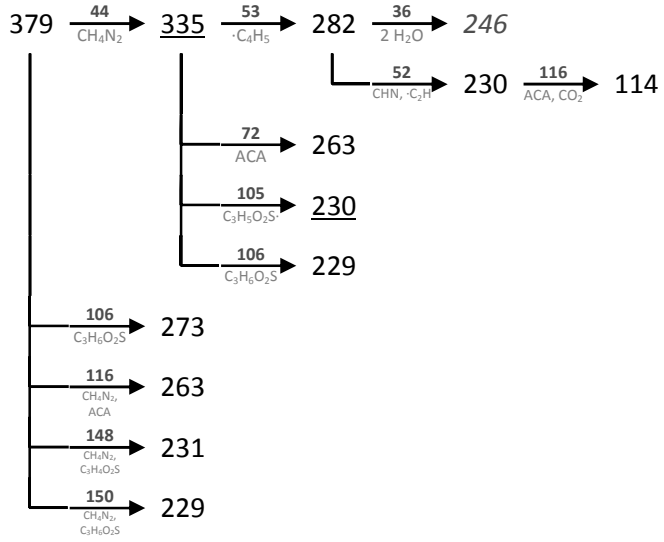

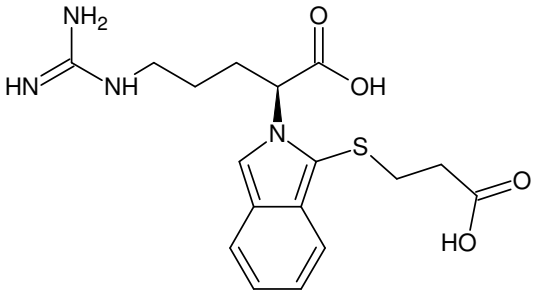

OPA-Arg
Molecular Formula = $C_{17}H_{22}N_4O_4S$
Monoisotopic Mass = 378.136175 Da

-MS^n

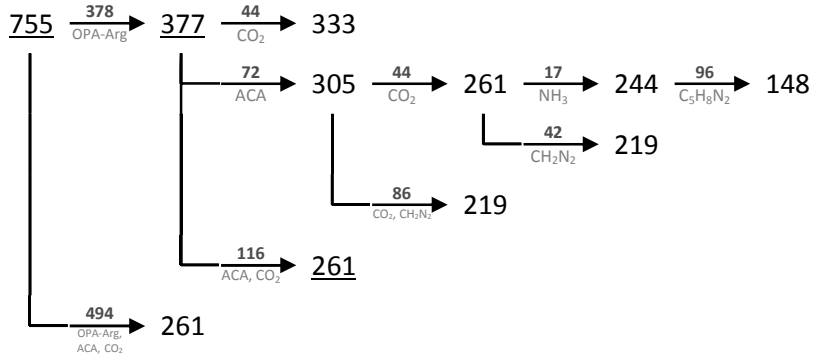

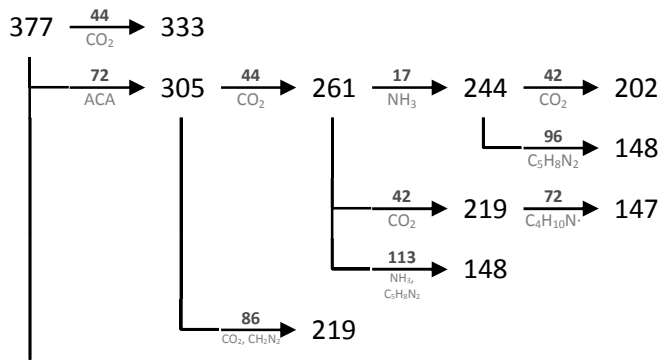

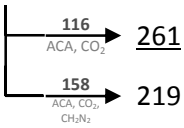

isotopic fingerprint:

peak area / % of monoisotopic	+1	+2	+3
theoretical ($C_{17}H_{13}N_4O_4S^+$):	21,2	7,5	1,2
measured (379,2 Th):	21,3	6,5	1,0
measured (-376,9 Th):	19,6	6,4	1,0

Figure 6-2 MS^n analysis of OPA-Arg

6.6.2. Glu

+MS^n

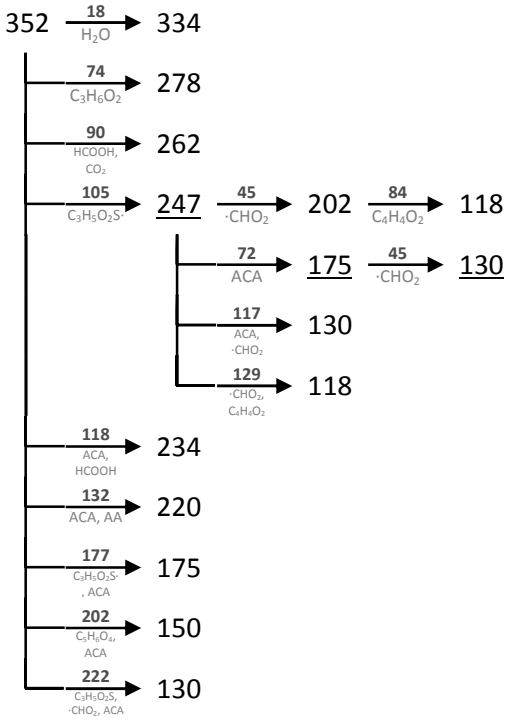

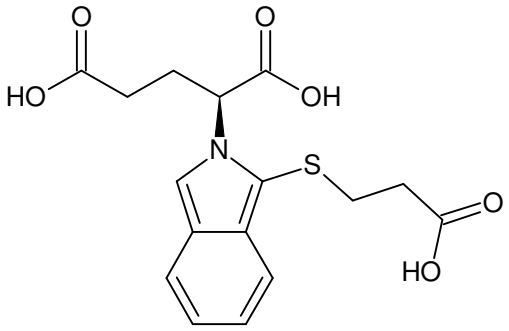

OPA-Glu

Molecular Formula = $C_{16}H_{17}NO_6S$

Monoisotopic Mass = 351.077657 Da

-MS^n

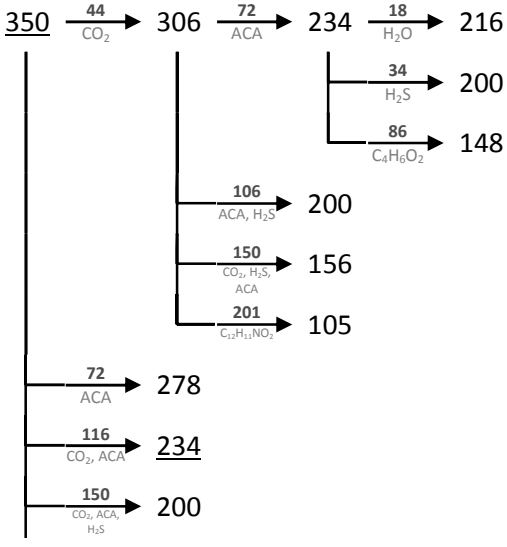

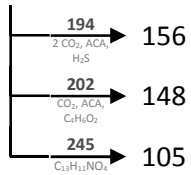

isotopic fingerprint:

peak area / % of monoisotopic	+1	+2	+3
theoretical ($C_{16}H_{16}NO_6S^-$):	18,9	7,5	1,2
measured (-349,8 Th):	17,8	6,3	1,4
measured (352,1 Th):	31,4	8,6	4,1

Figure 6-3 MS^n analysis of OPA-Glu

6.6.3. His

As for arginine (6.6.1), Rasche et al. presented a fragmentation tree for histidine [155]. As the derivatisation chemistry generating OPA-His was the same as for arginine, the primary amino moiety was blocked, what deprived the fragmentation tree of 9 from a total of 13 vertices. The remaining neutral losses could be reproduced from the fragmentation data derived from OPA-His.

+MS^n

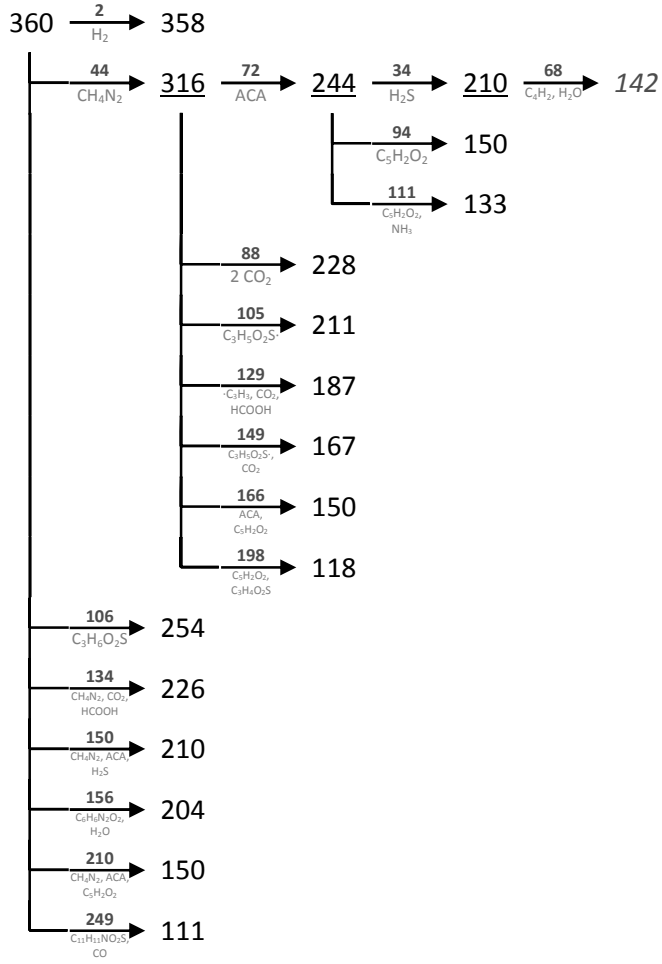

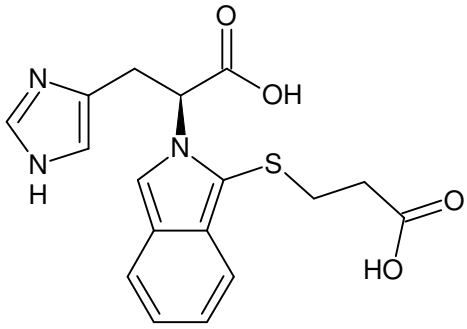

OPA-His

Molecular Formula = $C_{17}H_{17}N_3O_4S$

Monoisotopic Mass = 359.093976 Da

-MS^n

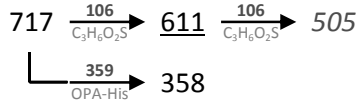

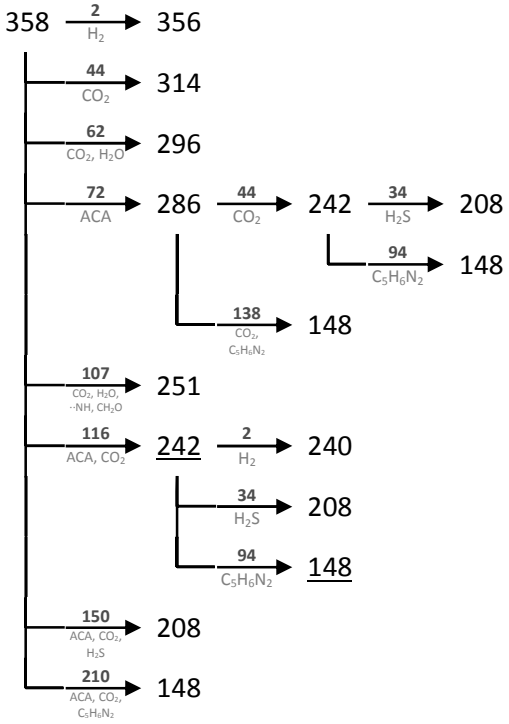

isotopic fingerprint:

peak area / % of monoisotopic	+1	+2	+3
theoretical ($C_{16}H_{16}NO_6S^-$):	20,7	7,4	1,2
measured (360,1 Th):	21,4	7,9	1,3
measured (-357,8 Th):	20,2	7,6	4,4

Figure 6-4 MS^n analysis of OPA-His

6.6.4. Met

+MS^n

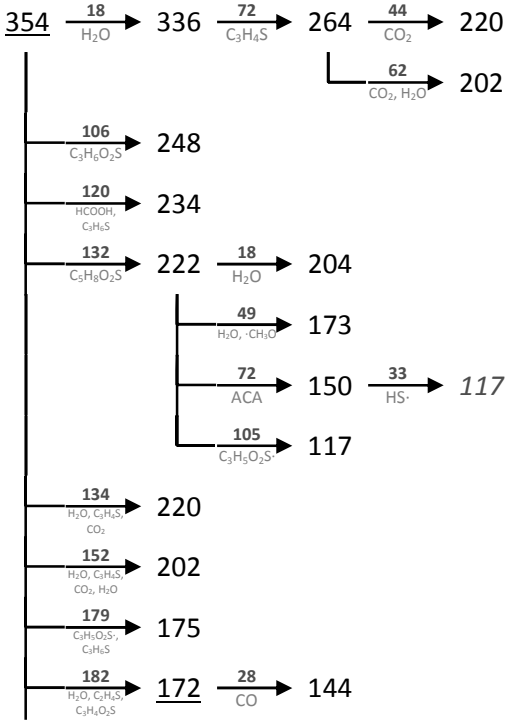

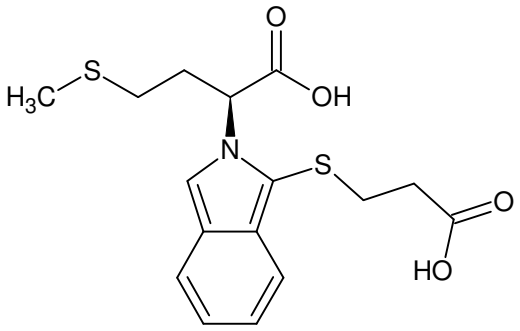

OPA-Met

Molecular Formula = $C_{16}H_{19}NO_4S_2$

Monoisotopic Mass = 353.075548 Da

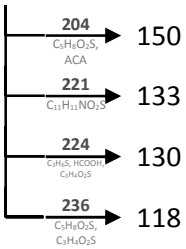

-MS^n

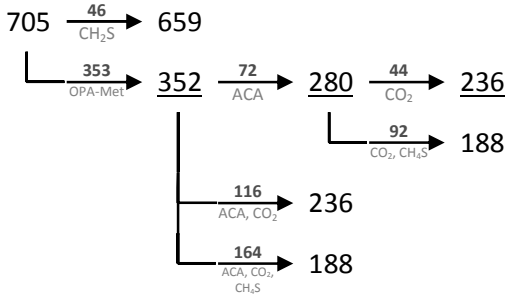

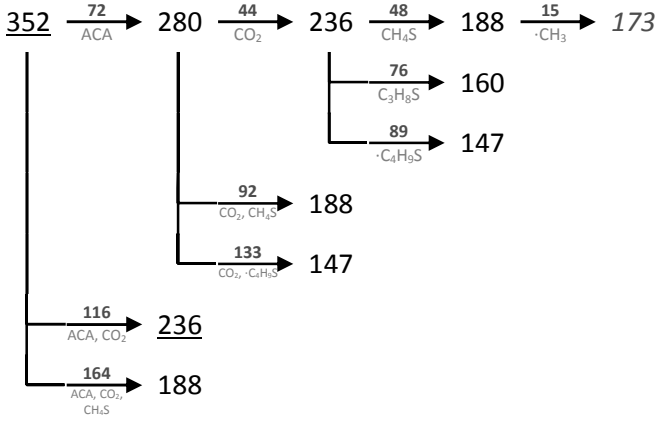

isotopic fingerprint:

peak area / % of monoisotopic	+1	+2	+3
theoretical ($C_{16}H_{20}NO_4S_2^+$):	19,7	11,7	2,0
measured (354,1 Th):	18,3	12,7	1,6
measured (-351,8 Th):	17,1	10,3	1,9

Figure 6-5 MS^n analysis of OPA-Met

7. Photo- and flourometry

The photospectroscopic properties of soluble compounds were measured with the Tecan Infinite® M200 plate reader with 200 µl of dissolved product in one well of a flat-bottom 96 well microtitre plate (transparent PS for absorbance measurements, black PS for fluorescence measurements) without any cover plate. The optical path length (in liquid) for this setup was 6,05 mm.
For fluorescence measurements the detector gain was set manually to 100 and the radiation incident on the detector was integrated for 20 µs starting from the pulse of the illumination light source (@ 20 Hz) with no interjacent lag time. Each data point captured was calculated from at least 4 individual measurements, the step size used for both the excitation and the emission wavelength as well as for the wavelength used in absorbance measurement was 1 nm.
Routinely, blanks (well filled with solvent only) were measured parallel to the samples but the signals generated from those generally were virtually non-existent or at least of a constant nature so that a correction of the sample's data was not necessary for the majority of the samples processed using the plate reader.

For solvents which would dissolve the well plates made from polystyrene, if the application called for enhanced sensitivity or if measurements in the UV range around 200 nm were necessary the absorbance was measured in cuvettes made from fused silica with an optical path length of 1 cm using a Hitachi U-2001 double beam spectrophotometer. Owing to the adjustment of the optical elements as well as to the lack of a second monochromator between sample and detector only absorption measurements are possible using this instrument. The instrument was calibrated using the pure solid as a base line and measuring against air (no cuvette) in the reference beam.
Blank correction was done by measuring separately the pure solvent in the same cuvette as was used for the sample and subtracting the absorbance for the system with pure solvent from that of the system with dissolved sample. In opposition to the situation with the samples measured on the plate reader (Which mostly consisted of aqueous solutions.) the measured signal was always corrected for the blank's contribution.

7.1. Enzymatic activity assays

The assays used for the determination of the volumetric activity of the used enzymes are based on the generation of a product with distinctive optical properties whose concentration can be determined using photometry. With the molar decadic absorption coefficient ε of the formed compound and the optical path length d of the used setup known the concentration of the compound in question can be calculated using the Lambert-Beer law.

$$lg\left(\frac{I_0}{I_T}\right) = E = \varepsilon \cdot c \cdot d$$

$$\dot{E} = \varepsilon \cdot \dot{c} \cdot d \implies \dot{c} = \frac{\dot{E}}{\varepsilon \cdot d}$$

I_0.....incident light intensity, $[I_0]$ = cd
I_T.....transmitted light intensity, $[I_T]$ = cd
E.....absorbance (extinction), [E] = 1
ε.....molar decadic absorption coefficient, $[\varepsilon] = 10^3$ cm^2 mol^{-1} = M^{-1} cm^{-1}
c.....molar concentration of the analyte, [c] = mol l^{-1} = M
d.....optical path length, [d] = cm
$\dot{}$.....first derivative with respect to time, $[\dot{}] = s^{-1} = 60$ min^{-1}
ċ.....gradient of the analyte concentration, $[\dot{c}] = $ mol l^{-1} s^{-1} = 60 · 10^3 U ml^{-1}
U := µmol min^{-1}

The actual measurement result was Ė, which was taken from the linear part of the graph depicting absorbance over time. For the laccase activity measurements this part started usually at the beginning of the measurement while the tyrosinases typically exhibited an initial lag period.

7.1.1. Laccase activity on ABTS

50 mM 2,2'-azino-bis(3-ethylbenzthiazoline-6-sulphonic acid) (ABTS; 13,72 mg for 500 µl) was prepared in NH_4Ac 50 mM pH 6,5 and pH 4,5 (adjusted with acetic acid) accordingly. Photometry was done in 96 well plates with 20 µl of 50 mM ABTS solution, 160 µl of NH_4Ac buffer and 20 µl of the enzyme solution to be tested. The sum of this volumes (ΣV = 200 µl) in combination with the geometry of the 96 well microtitre plate made from transparent PS with flat base results in an optical path length of 6,05 mm.

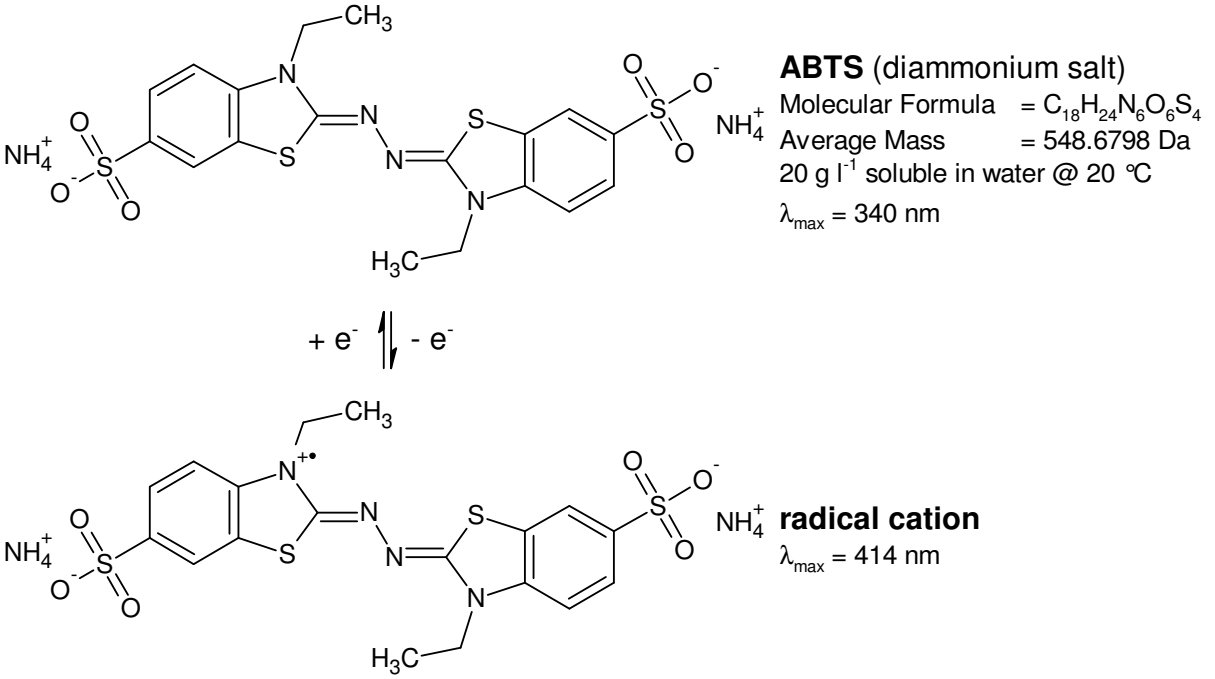

Figure 7-1 ABTS

Oxidised, ABTS forms a stable, green radical cation which is soluble in aqueous media and can be determined photometrically at 420 nm with an absorption coefficient of ε_{420} = 36000 M^{-1} cm^{-1} [156, 157].
Given this value and the experimental conditions stated above, the volumetric activity of a tested enzyme solution can be calculated from the experimental slope of the absorbance at 420 nm using the first derivative with respect to time of the Lambert-Beer law.

$$\dot{c} = \dot{E}_{420}[s^{-1}] \cdot 27{,}548 \, \frac{U \cdot s}{ml} \cdot f$$

Ė.....slope of the absorbance at 420 nm, [Ė] = s^{-1}
f.....dilution factor of the measured sample, [f] = 1

7.1.2. Tyrosinase activity on *L*-tyrosine

A solution of 2 mM *L*-tyrosine (362,38 mg l^{-1}) was prepared in the reaction buffer (NH_4Ac 50 mM pH 6,5 or sodium phosphate buffer 50 mM pH 6,8), heated to 25 °C and 180 µl each were mixed in one flat-bottomed well of a 96 well microtitre plate with 20 µ of the enzyme solution to be characterised. As was the case for the laccase activity assay (7.1.1) the optical path length filled with liquid was 6,05 mm.

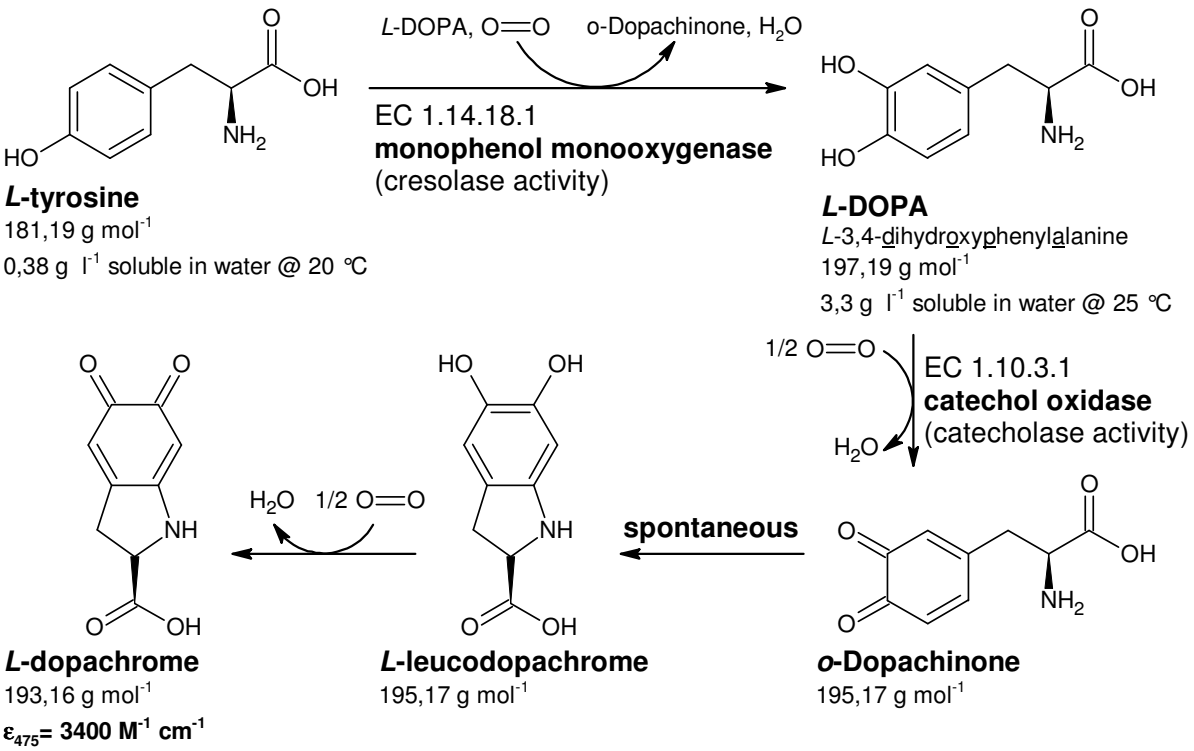

Scheme 7-1 Tyrosinase activity assay

Analogous to the laccase activity assay, the volumetric activity of the tested enzyme solutions was determined using the derivative with respect to time of the Lambert-Beer law and the absorption coefficient ε_{475} = 3400 M^{-1} cm^{-1} [158, 159] of the formed semistable dopachrome. As the oxidation of DOPA to its quinoid form occurs considerably faster than the initial hydroxylation of tyrosine [70], the measured turnover rate should resemble the rate of the monophenol monooxygenase reaction given the bottleneck approach holds.

$$\dot{c} = \dot{E}_{475}[s^{-1}] \cdot 291{,}69 \; \frac{U \cdot s}{ml} \cdot f$$

Ė.....slope of the absorbance at 475 nm, [Ė] = s^{-1}
f.....dilution factor of the measured solution, [f] = 1

Tyrosinase activity assay in 1 cm cuvettes:

The enzyme solution to be tested was diluted 10-fold with reaction buffer (NH_4Ac 50 mM pH 6,5 or sodium phosphate buffer 50 mM pH 6,8) (6,5 µl + 58,5 µl).
L-tyrosine was prepared at a concentration of 2 mM (362,38 mg l^{-1}) in the reaction buffer; the resulting solution was heated to 25 °C prior to use. 440 µl of Tyr 2 mM were pipetted into a PS cuvette with 10 mm optical path length, 60 µl of the diluted enzyme solution were added and the solutions were mixed by repeated drawing and dispensing using the pipette used to add the enzyme solution. The development of dopachrome was monitored at 475 nm against air (no cuvette in the reference beam).

$$\dot{c} = \dot{E}_{475}[min^{-1}] \cdot 24{,}510 \; \frac{U \cdot min}{ml} \cdot f$$

Ė.....slope of the absorbance at 475 nm, [Ė] = min^{-1}
f.....additional dilution factor of the measured solution, [f] = 1

8. Vibrational spectroscopy

Samples that were available as powder were measured directly in the form of a small pile on aluminium foil. Aqueous solutions were dispensed on aluminium foil in 2 or 3 steps of 25 µl each on the exact same spot marked with a circumferring (inner margin 2 mm) line drawn by a black permanent marker. Between each step the solutions were desiccated to dryness in an exsiccator over silica gel at approximately 40 mbar.
Blanks and references were treated in the exact same way as the samples using the same piece of aluminium foil for all the preparations that were to be analysed together.

8.1. Raman spectroscopy

Scattering experiments were performed on a PerkinElmer RamanStation 400 equipped with a red laser (λ = 785 nm).
The samples were measured on aluminium foil which was mounted on a microscope slide to plan its surface. If the sample present had the form of powder, pressing the pile with a second microscope slide gave it a defined form and, most importantly, a smooth surface which allowed all the parts of the sample in the focal area of the laser measuring approximately one millimetre in diameter to contribute to the final scattering signal.
All measurements were carried out after the laser source had been stabilised and the CCDs of the detector had been cooled down to -50 °C. The focal plane was set roughly using the build-in camera and was then varied for maximal scattering intensity. The scattered light was scavenged for 12 s each; each spectrum recorded was calculated from 16 individual scans preceded by 4 scans of identical duration without laser illumination to determine the dark current of the CCD array used.

8.2. FTIR-ATR spectroscopy

The infrared absorption of the samples was measured using a PerkinElmer Spectrum 100 equipped with an Universal ATR head.
Baseline correction was achieved by recording a blank spectrum without any sample on the ATR head (thus using the ambient atmosphere). All measurements including the background scan were done employing two mathematical corrections, namely for water vapour and carbon dioxide, provided by the control software of the device.
Powdered samples were measured by depositing a small amount directly on the diamond window of the ATR head and applying pressure with the attached screw-driven piston (140 N as measured by the strain gauge integrated in the arm linking the piston to the base of the ATR head). Samples dried on aluminium foil were measured likewise, with the side of the foil carrying the sample facing the window of the ATR head.
Aluminium foil without sample didn't exhibit any absorbance in the range probed (4000 cm^{-1} – 650 cm^{-1}).
All the samples were measured at a constant force pressing the specimen towards the crystal (diamond) of the ATR head (140 N ± 5 N); 16 individual scans were averaged to yield one recorded spectrum.

9. Synthesis of dityrosine

As among the candidate structures for the cross-links formed by the action of tyrosinase on tyrosyl-containing proteins dityrosine made the top of the list [160-165], it seemed important to have dityrosine available as a reference in substance.
The conventional production of dityrosine via enzymatic oxidation usually requires several purification steps using a variety of chemical purification methods [166]. As only a small quantity of dityrosine was needed, an easier alternative was sought and found; namely the Mn(III)-mediated oxidation of tyrosine [167].

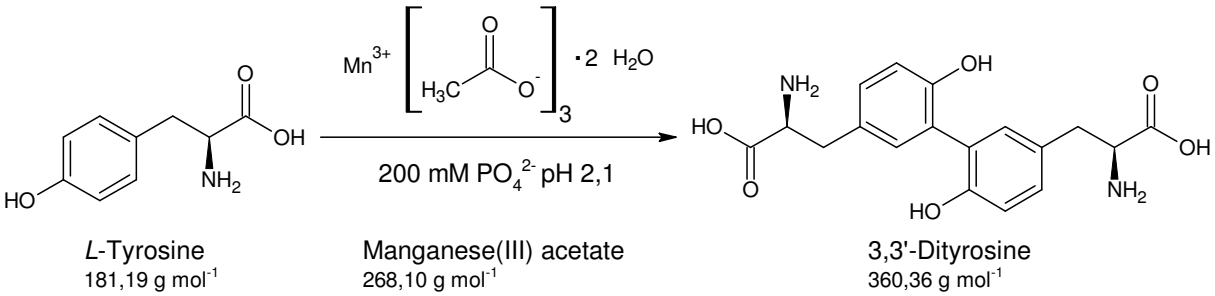

Scheme 9-1 preparation of dityrosine via Mn(III)-mediated oxidation of tyrosine

9.1. Dityrosine preparation

The reaction medium used was a 200 mM sodium phosphate buffer in ddH_2O at pH 2,1:

- 96,8 mM NaH_2PO_4; 156,01 g mol^{-1} (dihydrate) => 15,102 g l^{-1}
- 103,2 mM H_3PO_4; 98,00 g mol^{-1} => 10,114 g l^{-1}
  - concentrations calculated for pH 2,1 with CurTiPot v. 3.5.4; measured (Mettler Toledo InlabExpert Pt 1000 pH): pH 2,10

- 50 ml of both tyrosine and Mn(III) acetate were prepared in reaction medium at 5 mM.
  - tyrosine; 181,19 g mol^{-1} => 45,30 mg (actual: 53,60 mg)
  - manganese triacetate; 268,10 g mol^{-1} => 37,03 mg (actual: 69,94 mg)
- The solutions were mixed in a 250 ml beaker and were reacted for 60 s at room temperature (25 °C), of which the beaker was immersed in an ultrasonic bath for 10 s.
- 100 ml of aqueous ammonia (30 – 33 % w/v) were added to precipitate the phosphate present in the reaction medium. ⇒ The solution became turbid.
  - filtrated (glass frit Schott Duran®, porosity 4: 10 – 16 µm pore size) => yellow solution
  - filtrate evaporated (in a 500 ml single-neck round-bottom flask using a Heidolph VV 2000 rotary evaporator): 75 °C water bath temperature, 120 mbar system pressure
    ⇒ yellow (ochre) oil; solid, hard lump after solidification
    > crushed using a mortar and pestle made of porcelain: pale yellow powder
- To remove most of the unreacted tyrosine still present in the preparation, the powder was washed with cold acidified water (pH 2,0 with hydrochloric acid, prechilled to 4 °C) which should dissolve preferentially the monomeric tyrosine and filtrated (glass frit; Schott Duran®, porosity 4).
  - In the filtrate, a lot of fluorescence specific to dityrosine was found (λ_{ex} = 230 nm, λ_{em}= 400 nm; device: Tecan Infinte® 200 plate reader). Therefore the filtrate was reevaporated and the resulting yellow solid was grinded again (pale yellow powder).
    ⇒ The method used by [167] was therefore modified and the removal of the unreacted reactant was replaced by an extraction of the product.
    > The washing step was omitted and the powder was desiccated at 75 °C for 100 min in a drying cabinet. ⇒ melted material

> After cooling to room temperature, which was accompanied by solidification of the material, the resulting lump was grinded using mortar and pestle and weighted in a 2 ml PP vial: 1015,15 mg ⇒ mainly phosphate (dityrosine at a yield of 1: 53,3 mg).

- The raw dityrosine ($(NH_4)_3PO_4$ with a little tyrosine and dityrosine) was extracted using different solvents which were chosen in order to minimise the cosolvation of ammonium phosphate.
  - A small amount (covering the tip of a spatula) of raw dityrosine was suspended in 400 µl of the respective solvent to be tested. After 20 s in an ultrasonic bath the dispersion was filtrated (glass frit, porosity 4) and the supernatant was checked for fluorescence on the plate reader.
    - ⇒ n-heptane, diethyl ether, acetone, cyclohexane, toluene, chloroform, dichloromethane, n-butanol, isopropanol and ethanol: No fluorescence was found.
    - ⇒ methanol: Fluorescence at 400 nm was found (λ_{ex}= 230 nm).
- Raw dityrosine was washed with methanol: 80 ml MeOH, 1015 mg raw dityrosine
  - The filtrate (4- frit) was evaporated (60 °C, 350 mbar) and desiccated on the rotary evaporator (60 °C, 100 mbar). ⇒ 57,26 mg of an ochre substance

9.1.1. RP-HPLC

Polishing of the crude dityrosine (and removal of unreacted tyrosine) was effected using RP-HPLC with an analytical column (dictated by the high resolution needed to resolve tyrosine and dityrosine).

column: Eurospher 100-5 C18 4,6x250 mm
column oven temperature: 25 °C
detection: UVD 170U @ 210 nm (bandwidth 10 nm), reference wavelength 600 nm (b.w. 10 nm)
flow: 1,0 ml min^{-1}

mobile phase
A: ddH_2O + 1 ‰ (v + v) TFA (trifluoroacetic acid)
B: ACN + 1 ‰ (v + v) TFA

gradient: %A = 100 - %B

time after injection /min	%B
0	5
5	11
8,8	12,5
11,0	15,5
11,0	60
16,0	60
16,0	5
20,0	5 (end)

purging of the fraction collector: 0 – 2 min
collected fraction: 8,8 – 9,3 min (dityrosine, identified by fluorescence: λ_{ex}= 230 nm, λ_{em}= 400nm)

The crude dityrosine was not soluble in the mobile phase A at neither 40 g l^{-1} nor 20 g l^{-1} but at 10 g l^{-1} a homogenous solution could be achieved.
In 32 runs of 60 µl each (max. injection volume of 10 gl^{-1} solution for sufficient resolving power; At larger injected volumes the overloading of the column became insupportably detrimental to the

retention characteristics of tyrosine end dityrosine.) the dityrosine contained in 19,2 mg of crude dityrosine was collected in 16 ml of mobile phase.

Preliminary MS^n analysis:

400 µl of the purified fractions containing dityrosine were subjected to MS^n analysis as described in 66.3.
In positive mode, a signal at 361,1 Th was found which was attributed to 3,3'-dityrosine (monoisotopic mass 360,132 Da; $[DiTyr + H]^+$):

+MS^n

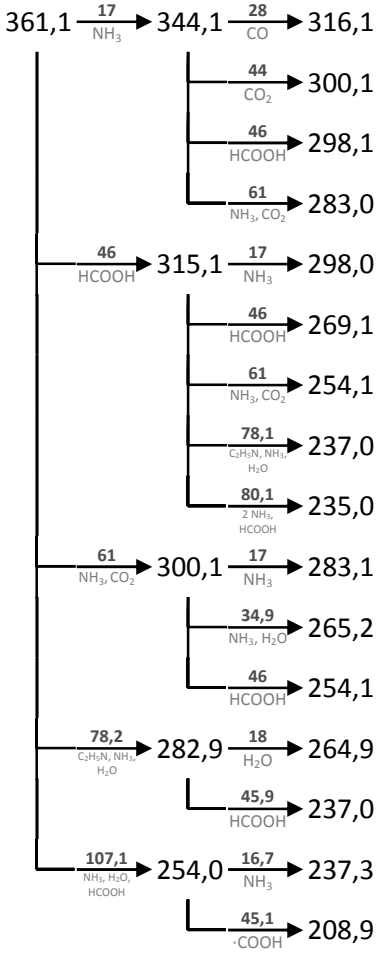

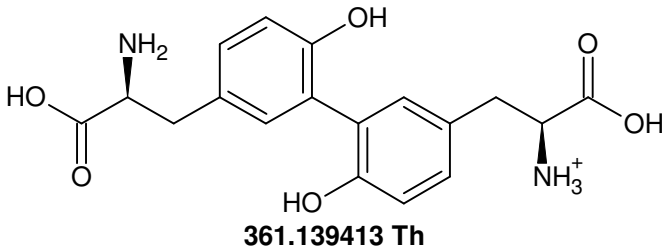

361.139413 Th

Scheme 9-2 preliminary MS^n analysis of dityrosine after purification by RP-HPLC

In negative mode no signal corresponding to dityrosine could be detected, presumably due to the suppressing effect of trifluoroacetic acid on the generation of negative ions [168, 169].

Yield after purification by RP-HPLC:

The combined purified fractions were placed in a 50 ml round-bottom flask, evaporated (75°C, 120 mar) and scraped off the inner surface of the glass flask using a spatula made from stainless steel. The resulting solids were dried in an exsiccator over silica gel at 38 mbar and room temperature for 24 h.
The resulting ochre powder's mass was determined to add up to 8,27 mg, which equals to an yield of **47,5 %** based on stoichiometric conversion of tyrosine to dityrosine (cp. Scheme 9-1).

- 53,60 mg of tyrosine were employed for the reaction.
  - Total conversion of this amount of tyrosine would result in 53,30 mg dityrosine.
- 1920 µl of 5726 µl total (raw dityrosine 10 g l^{-1} in mobile phase A) were processed. (0,3353)

- 16 ml of purified dityrosine solution were collected. Of these, 400 µl were used for the preliminary MS^n analysis. (0,975)
  - ⇒ A fraction of 0,3269 of the set up was processed; 53,60 mg · 0,3269 = 17,43 mg eq. 100 %
    - > 8,27 mg of substance ⇒ 8,27 · $17,43^{-1}$ = 0,475

9.2. MS^n analysis of dityrosine

1 mM dityrosine was prepared in MeOH and injected into the ESI interface. Other than the solution containing 1 ‰ TFA the methanolic solution of dityrosine prepared from the purified and dried material – a procedure which removed most of the TFA [170] – yielded positive as well as negative ions.
The strongest fragment peak encountered in positive mode (262,8 Th) didn't show an isotopic +1 peak (as did all the other peaks in spectra containing 262,8 Th) and was therefore excluded from the fragmentation tree as a probable artefact.
In positive mode, a contaminant was encountered which sodium adduct interfered with the pseudo-molecular ion of dityrosine due to its isobaricity. Consulting a list of common contaminants in mass spectroscopy [171] and the fragmentation spectra of the ionised contaminant the two signals at 338,3 Th and 360,3 Th were assigned to the pseudo-molecular ion and the sodium adduct respectively of erucamide, a slip additive used in the manufacture of polyolefin films which is suitable for food packing materials. As this isobaric contamination rendered the determination of the pseudo-molecular ion of dityrosine unreliable (with the isotopic +1 peak of the contaminant's sodium adduct at 363,3 Th and $[M+H]^+$ at 361,1 Th), the isotopic fingerprint of dityrosine was taken from the negative pseudo-molecular ion only which didn't suffer from isobaric contamination.

+MS^n

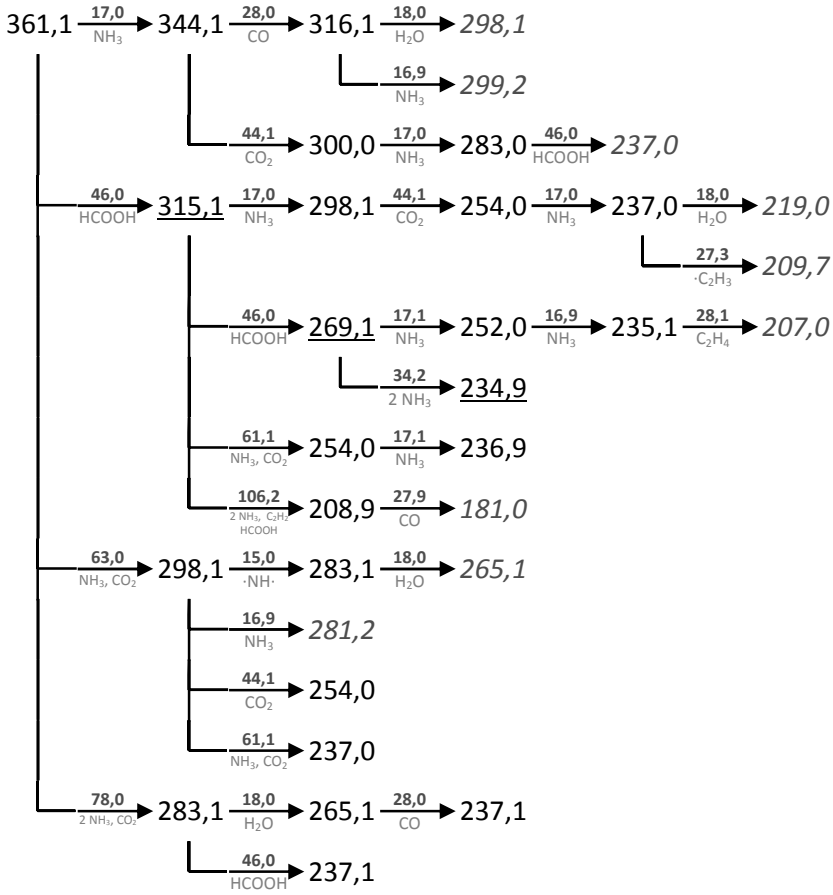

-MS^n

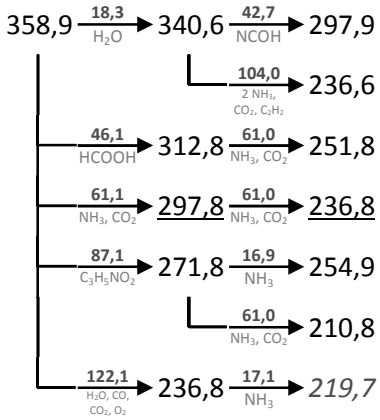

Italic ..... signal which could not be confirmed in the subsequent isolation step (no signal at all) or signal derived from one single scan (here: 207,0 Th and 236,9 Th)

underlined ..... most abundant fragment

isotopic fingerprint of $[M-H]^-$

theoretical ($C_{18}H_{20}N_2O_6^-$):	20,7 %	3,28 %
	+1	+2
measured (-359,2 Th):	18,2 %	3,59 %

Scheme 9-3 MS^n analysis of purified dityrosine

9.3. Fluorometry

Dityrosine can be characterised by its fluorescence in the range of 400 nm which can be measured after excitation within the absorption bands at 284 nm (in acidic solution) or 315 nm (in alkaline solutions) [160, 166, 172, 173]. Differentiation from tyrosine, which shares the absorbance maximum at 278 nm with dityrosine, is possible using fluorometry as the fluorescence of tyrosine at 300 – 305 nm [166] doesn't contribute to the emission peak of dityrosine at 400 nm.

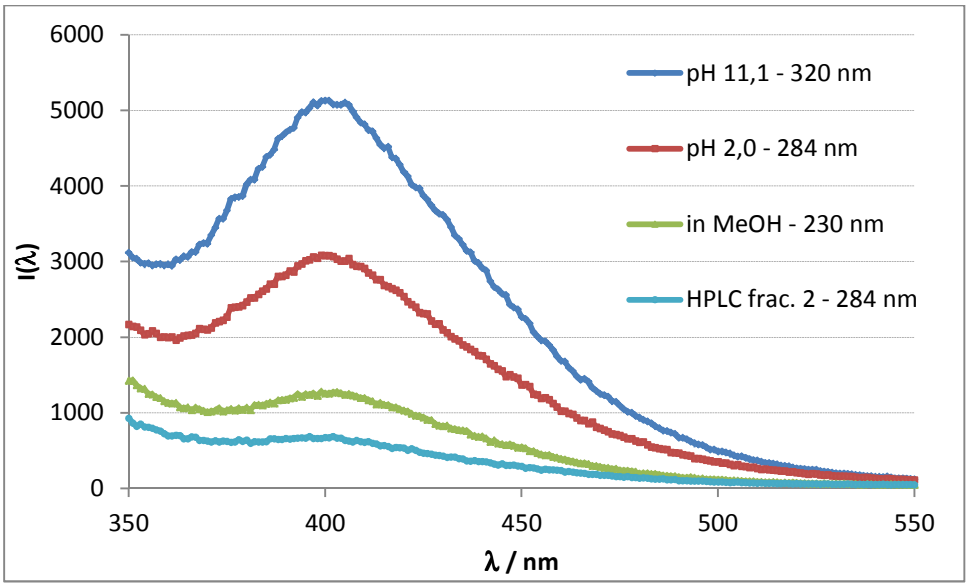

Figure 9-1 Fluorescence spectra of dityrosine

The wavelength indicated in the legend of the diagram gives the excitation wavelength used for the measurement of the respective emission spectrum.

in MeOH: see 9.1, HPLC frac. 2: see 9.1.1 (fraction 1 = Tyr)

Solvents: 10 mM sodium carbonate for pH 11,1; 10 mM hydrochloric acid for pH 2,0

10. Protection of the tyrosine amino group

Free tyrosine in solution confronted with tyrosinase activity has a strong tendency to form a black precipitate, melanin [71, 174, 175]. As this precipitate is analytically challenging and the oxidised tyrosine expended in its formation is lost for any other reactions including those at the centre of the present study a way had to be found to prevent the formation of this precipitate while conserving at the same time the affinity of the used oxidoreductase towards its substrate.

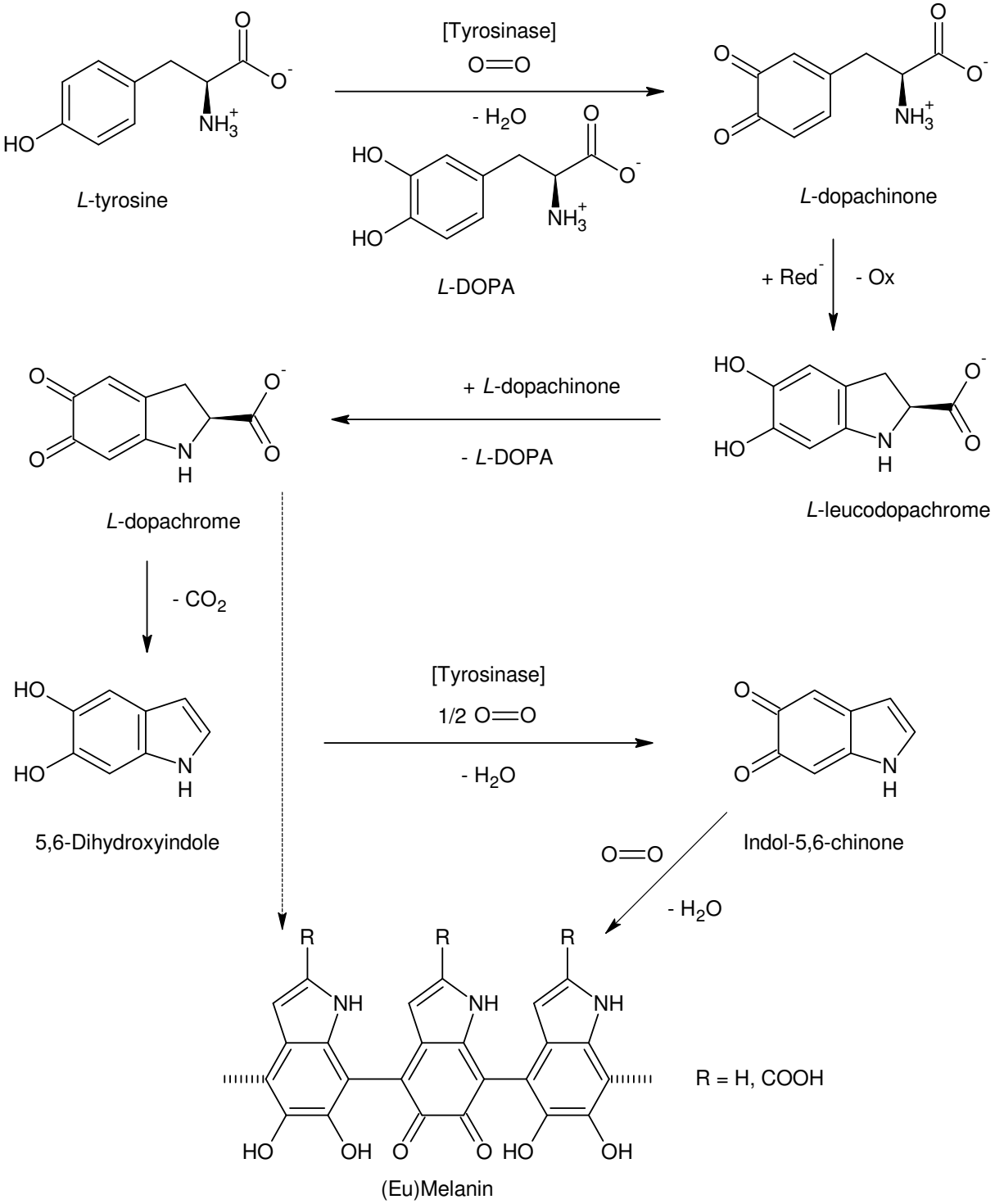

Scheme 10-1 Formation of melanin by the action of tyrosinase on tyrosine

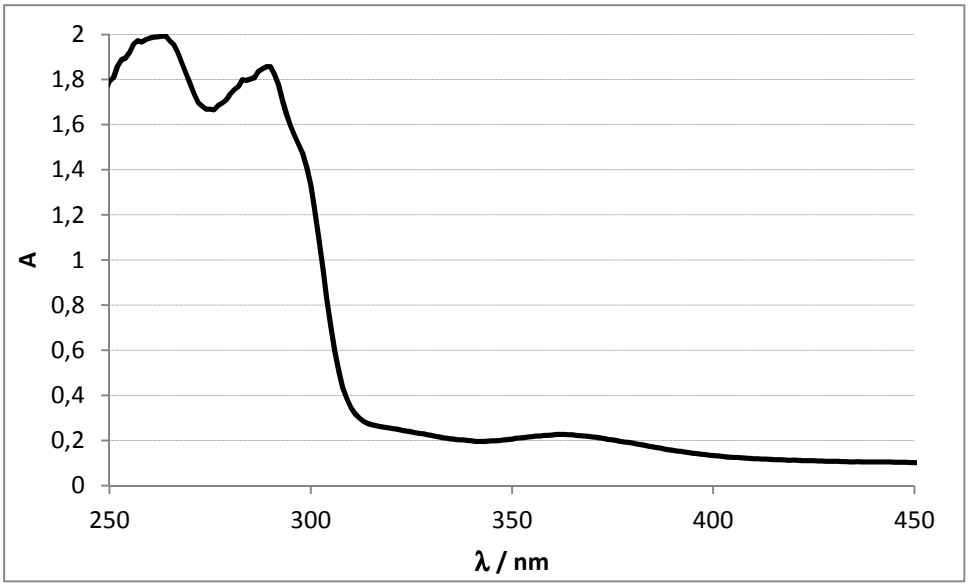

Figure 10-1 UV-Vis spectrum of the black precipitate formed from tyrosine upon oxidation with tyrosinase, dissolved in 2-Chloroethanol [174]

The key step in the formation of melanin presents itself as the cyclisation of *L*-dopachinone to *L*-leucodopachrome. Crucial to this step is the availability of the primary amino group if *L*-dopachinone which should be less important to the enzymatic oxidation of *L*-tyrosine given the activity of all (to my knowledge) tested tyrosinases on catechol (1,2-benzenediol) which lacks the additional nitrogen.
Based on this assumption the amino group of *L*-tyrosine was blocked in order to keep the formed chinone in solution and in doing so clearing the path for other reactions involving the very same chinone. These reactions could be mimetic to the cross-linking reactions in proteins where tyrosyl residues are also incorporated in a way that prevents the cyclisation, namely in an amide bond.

While the reaction with OPA (cp. Scheme 4-1) indeed yields a product with a blocked amino function the resulting isoindole is however only stable under reducing conditions what is not exactly the best choice for an enzymatic reaction employing an oxidoreductase with a somewhat elevated redox potential like tyrosinase (e.g. 0,36 V for the enzyme from *Agaricus bisporus* [106]).
To resemble the conditions in a peptide chain more closely, the protective group was decided to be an amide and a standard reagent to achieve the protection of the amino group in such a way was chosen: Boc_2O, which forms an urethane with the primary amino group.

10.1. Synthesis and purification of N-Boc-*L*-Tyr

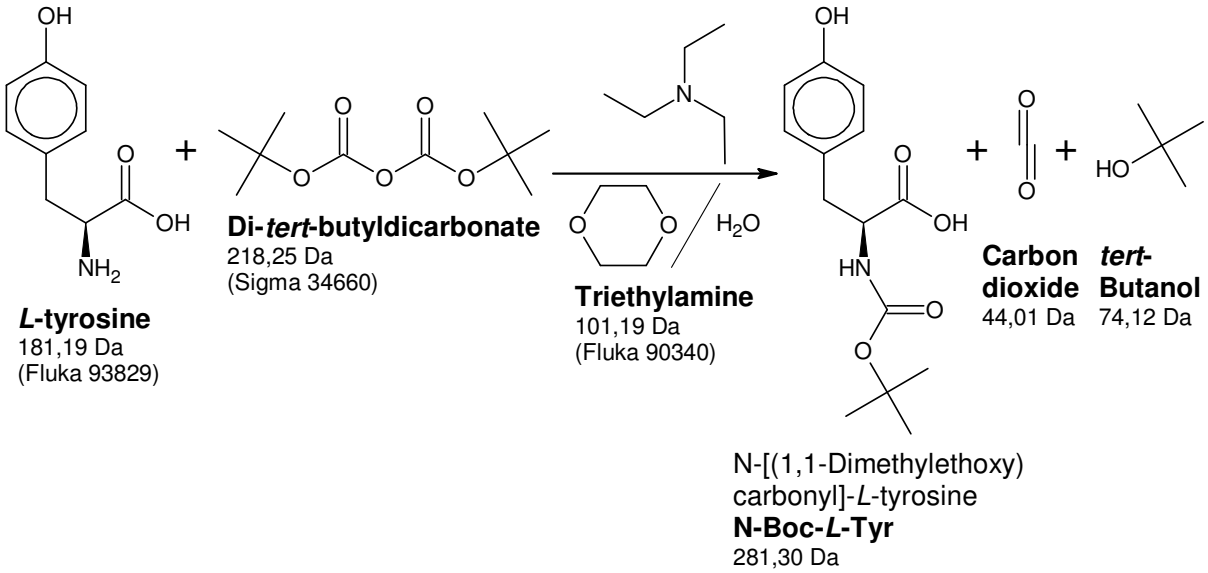

Scheme 10-2 Protection of the amino group of tyrosine with (tBuO$_2$C)$_2$O [176]

- The synthesis was carried out in a 250 ml round bottom flask equipped with a stirring bar and cooled externally by immersion in a bath of water and crushed ice. In this flask, all the constituents of the reaction laid out in Scheme 10-2 were put.
  - Tyr: 4,37 g (24,1 mmol) in 50 ml 1-4 dioxane and 50 ml dH$_2$O
    - ⇒ Tyrosine was not dissolved; instead a turbid suspension was formed.
  - Triethylamine: 1,5 equivalents => 36,2 mmol ≙ 5,08 ml
    - ⇒ 101,19 g mol^{-1}, ρ = 0,72 g cm^{-3}
  - Di-*tert*-butyldicarbonate: 1,2 equivalents => 28,9 mmol ≙ 6,31 g (actual: 6,45 g)
    - ⇒ 218,25 g mol^{-1}, fp 21 – 22 °C, ρ = 0,94 g cm^{-3}
- The suspension was stirred at 300 min^{-1}, the first 20 min of the reaction were carried out in the ice bath. After that time had elapsed the ice bath was removed and the suspension was stirred at room temperature (23 – 25 °C) for a total reaction time of 18 h.
  - After 18 h the suspension had become a grey to white solution with a few white flakes.
    - ⇒ The solution was concentrated to approximately 20 ml using a rotary evaporator (50 °C bath temperature, 150 mbar pressure). => no precipitate
      - > vapour pressure of 1-4 dioxane: 159 mbar @ 50 °C
- For purification the concentrated solution was diluted with 50 ml each of dH$_2$O and ethyl acetate and extracted using a separatory funnel made of glass. The phase separation was complete after 2 min of resting in earth's gravitational field.
  - The aqueous phase (lower layer, ρ(ethyl acetate) = 0,90 g cm^{-3}) was washed with 25 ml of ethyl acetate.
    - ⇒ After shaking and phase separation the aqueous phase was adjusted to pH 1,5 with 6 M HCl and backextracted 3 times with 25 ml of ethyl acetate each.
  - The combined organic phases (including the first ethyl acetate fraction) were cleaned by extraction with 150 g l^{-1} sodium chloride in dH$_2$O.
    - ⇒ 1 x 50 ml, 2 x 25 ml, separatory funnel rinsed with dH$_2$O, 2 x 25ml
      - > clear, colourless solution
- The purified solution was desiccated over CaCl$_2$, filtrated (glass fritt, porosity 5: pore size 1,0 - 1,6 µm) and transferred to a 500 ml round bottom flask in which the solvent was evaporated on a rotary evaporator (50 °C, 90 mbar; vapour pressure of ethyl acetate: 380 mbar @ 50 °C).

- After 2 h of drying on the rotary evaporator, the product presented itself as white foam occupying the complete inner volume of the round bottom flask.

10.1.1. Yield

foam and flask:	178,67 g
tare flask:	172,40 g
product:	**6,27 g** ≙ 22,3 mmol ≙ **92,4 %**

Further drying in an exsiccator over NaOH at 40 mbar didn't give any mass change over 24 h. The foam was then scraped off the inner surface of the round bottom flask using a stainless steel spatula and the resulting white powder was stored in a tinted glass vessel at room temperature.

10.2. Vibronic analysis of N-Boc-*L*-Tyr

The white powder yielded from the synthesis and purification procedure was measured without any further modifications.
The FTIR-ATR spectrum of the purified products shows five strong absorption peaks in the region above 1500 cm^{-1}: 3329, 2980, 1682, 1615 and 1515 cm^{-1}.
In [176] the four ν_{max} bands are given at 3445, 2962, 1690 and 1518 cm^{-1} as measured in transmission mode (neat).
The seven strongest scattering peaks in the product's raman spectrum exhibit a raman shift of 3064, 2982, 2933, 1615, 1450, 1207 and 850 cm^{-1}, which is in good agreement with the reference spectrum of the commercially available N-Boc-*L*-Tyr (from Sigma).
All the mentioned spectra are given in the annex (see X.I, Figure X-I and Figure X-II).

10.3. Test for acceptance by tyrosinase

As the reason for the synthesis of N-Boc-*L*-Tyr was the idea to use it as a non-melanogenic substitute for tyrosine in the oxidation catalysed by tyrosinase, the acceptance of the latter for the first as a substrate was crucial. The test was carried out by simply incubating a solution of 1 mM N-Boc-*L*-Tyr in 100 mM sodium phosphate puffer pH 6,8 with 2 mU of the tyrosinase from *Agaricus bisporus* in 1,5 ml glass vials at room temperature. In parallel, the same reaction was carried out with unprotected *L*-tyrosine to act as a reference.
Both solutions turned pink after 1 min of reaction; After 18 h the reaction with N-Boc-*L*-Tyr had developed a nut brown colour and was still clear while the reaction containing unprotected tyrosine had turned grey and a lot of black precipitate had been formed.

10.3.1. Photo- and fluorometry

As new functional groups adsorbing in the VIS or the near UV range are neither introduced nor removed from tyrosine in the protection process, the photospectroscopic properties of reactant and product should be qualitatively the same in the specified energy range.

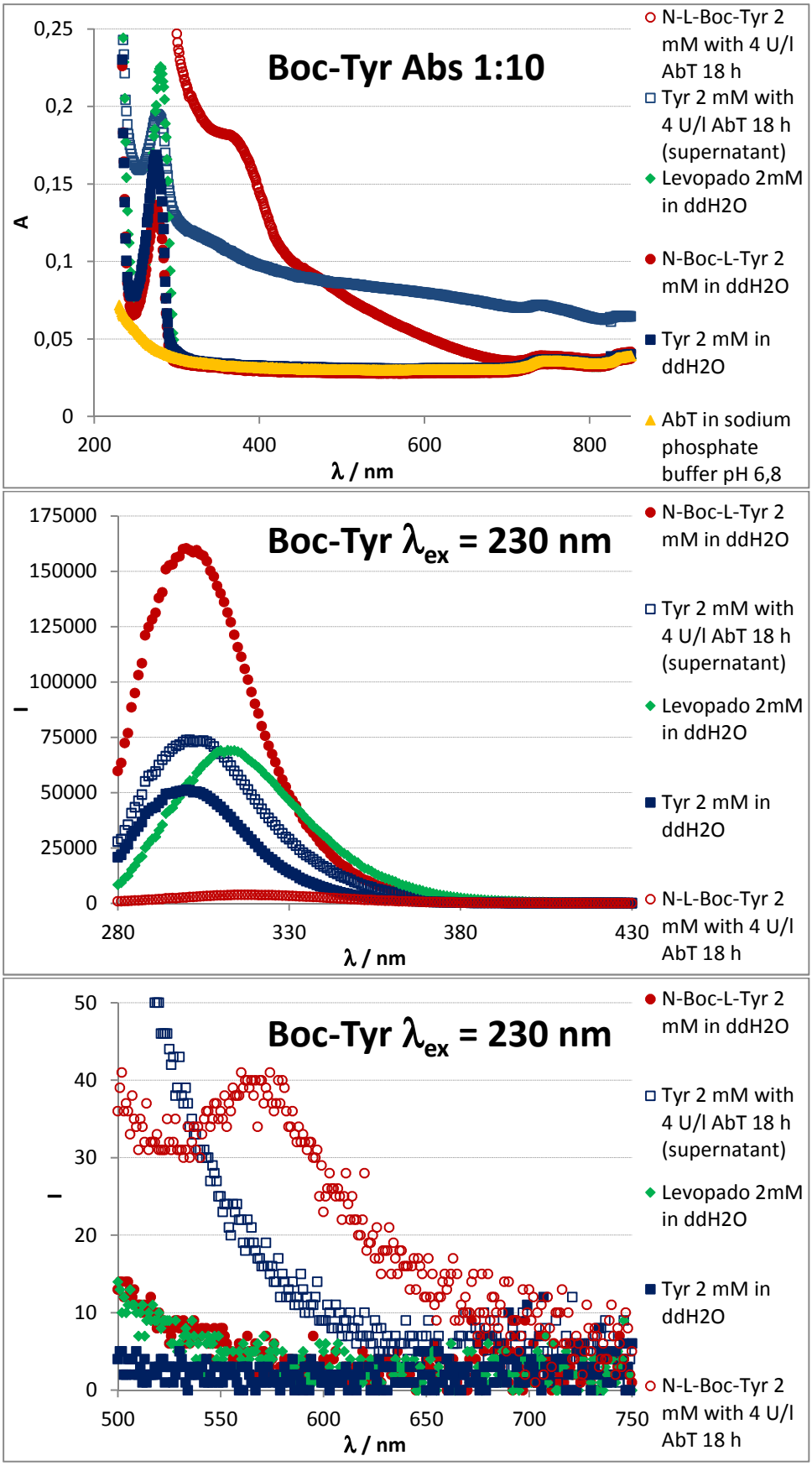

Figure 10-2 Photo- and fluorometry of N-Boc-*L*-Tyr

Tyrosin 2 mM was measured with a gain setting of 80 while N-Boc-L-Tyr was measured with the standard setting (as defined in 7) of 100. The reason for this different setting was that tyrosine was measured parallelly to its OPA-derivatised counterpart which (being an isoindole, cp. Scheme 4-1) exhibits strong fluorescence that would saturate the detector at a gain setting of 100.

The oxidised N-Boc-*L*-Tyr exhibits strong absorbance around 390 nm, which indicates the formation of N-Boc-*o*-dopachinone [113], and also fluorescence at 570 nm which can be measured after excitation within the adsorption band at 454 nm (for the spectra see X.III, Figure X-VI).

10.4. MS^n analysis of N-Boc-*L*-Tyr

A solution of 2 mM N-Boc-*L*-Tyr in methanol was prepared and infused into the ESI source.

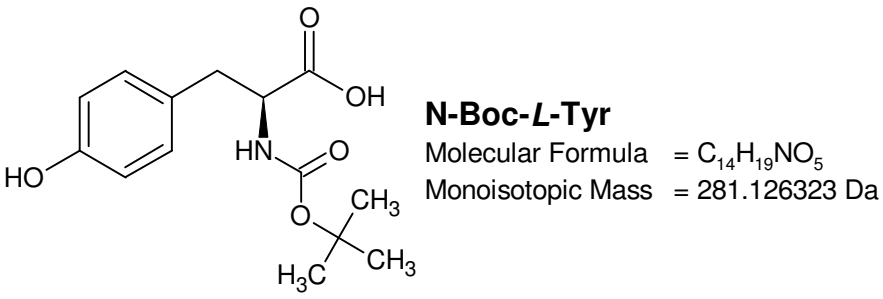

Figure 10-3 N-[(1,1-Dimethylethoxy)carbonyl]-*L*-tyrosine

In the full scan, the dominating signals are 585,1 Th and -560,9 Th in positive and negative mode respectively (cp. the mass spectra given in the annex, X.II). These signals were assigned to the dimer sodium adduct and the negatively charged dimer respectively.
The addition of NH_3 and formic acid respectively to the methanolic solution increased the intensity of the measured signals, an effect that was particularly pronounced for the generation of negative ions from a basic solution.

+MS^n

882,1 $\xrightarrow{280,9\ \text{Boc-Tyr}}$ 601,2 $\xrightarrow{100,0\ C_4H_8,\ CO_2}$ 501,2 $\xrightarrow{100,1\ C_4H_8,\ CO_2}$ 401,1

585,1 $\xrightarrow{281,0\ \text{Boc-Tyr}}$ 304,1 $\xrightarrow{56,1\ C_4H_8}$ 248,0 $\xrightarrow{44,0\ CO_2}$ 204,0 $\xrightarrow{17,1\ NH_3}$ *186,9*
585,1 $\xrightarrow{381,1\ \text{Boc-Tyr},\ C_4H_8,\ CO_2}$ 204,0

304,1 $\xrightarrow{56,1\ C_4H_8}$ 248,0 $\xrightarrow{44,0\ CO_2}$ 204,0 $\xrightarrow{17,2\ NH_3}$ 186,8

282,1 $\xrightarrow{56,1\ C_4H_8}$ 226,0 $\xrightarrow{46,2\ HCOOH}$ 179,8 $\xrightarrow{43,8\ CO_2}$ 136,0
226,0 $\xrightarrow{17,0\ NH_3}$ *209,0*

-MS^n

660,8 $\xrightarrow{280,9\ \text{Boc-Tyr}}$ 379,9 $\xrightarrow{74,1\ C_4H_8,\ H_2O}$ 305,8 $\xrightarrow{43,1\ \text{HNCO}}$ 262,7 $\xrightarrow{56,1\ C_4H_8}$ 206,6 $\xrightarrow{43,8\ CO_2}$ 162,8 $\xrightarrow{44,0\ CO_2}$ 118,8
660,8 $\xrightarrow{381,1\ \text{Boc-Tyr},\ C_4H_8,\ CO_2}$ 279,7 $\xrightarrow{74,1\ t\text{-ButOH}}$ 205,6 $\xrightarrow{42,9\ \text{HNCO}}$ 162,7 $\xrightarrow{43,9\ CO_2}$ 118,8

561,0 $\xrightarrow{281,2\ \text{Boc-Tyr}}$ 279,8 $\xrightarrow{74,1\ t\text{-ButOH}}$ 205,7 $\xrightarrow{43,0\ \text{HNCO}}$ 162,7 $\xrightarrow{43,9\ CO_2}$ 118,8
561,0 $\xrightarrow{355,3\ \text{Boc-Tyr},\ t\text{-ButOH}}$ 205,7 $\xrightarrow{43,0\ \text{HNCO}}$ 162,7 $\xrightarrow{44,0\ CO_2}$ 118,7

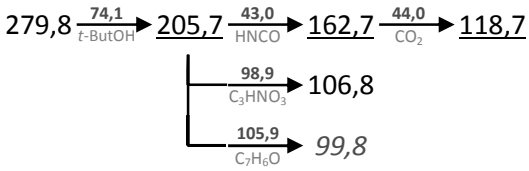

isotopic fingerprint:

peak area / % of monoisotopic	+1	+2	+3
theoretical ($C_{14}H_{19}NO_5Na^+$):	16,0	2,2	0,2
measured (304,1 Th):	14,1	2,4	0,4
measured (-279,8 Th):	17,0	0,7	0,6
theoretical ($C_{28}H_{38}N_2O_{10}Na^+$):	32,0	7,0	1,2
measured (585,1 Th):	27,8	4,8	0,9
measured (-560,9 Th):	22,0	5,5	1,0

Scheme 10-3 MS^n analysis of N-Boc-*L*-Tyr

10.5. MS^n analysis of oxidised N-Boc-*L*-Tyr

As already deduced from the reaction with oxygen in the presence of tyrosinase (10.3), N-Boc-*L*-Tyr is oxidised to a chinon (absorption around 390 nm [113], see Figure 10-2).

Solutions of 2 mM N-Boc-*L*-Tyr were prepared in ddH_2O and sodium phosphate buffer 100 mM pH 6,8 respectively and incubated with 4 U l^{-1} of tyrosinase from *Agaricus bisporus* (5 d @ 25 °C and 145 min^{-1}). The final pH of the (virtually unbuffered) reaction batch in water was determined to be around 4 while the pH of the buffered batch didn't differ significantly from 6,8. The batch in buffer exhibited a dark brown colour while the batch in water had formed a little brown precipitate and was also brown in colour but quite pale in comparison to the batch in buffer.

The enzyme was removed by filtration (Vivaspin® 2, 3 kDa molecular weight cut-off) and the filtrate of the batch prepared in water was introduced into the electrospray ion source.

+MS^n

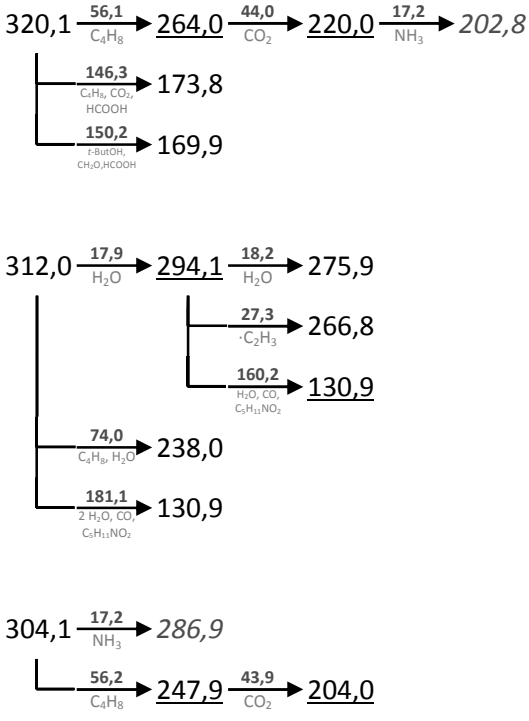

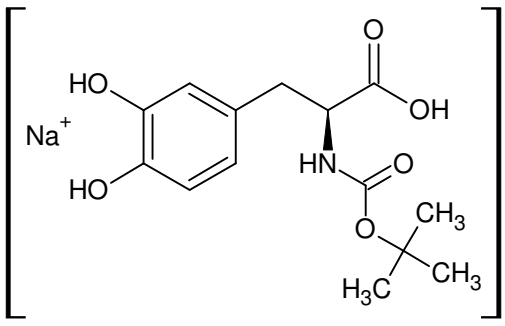

320.110459 Th

-MS^n

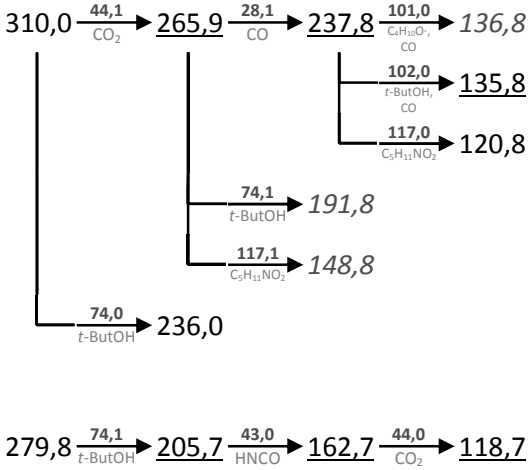

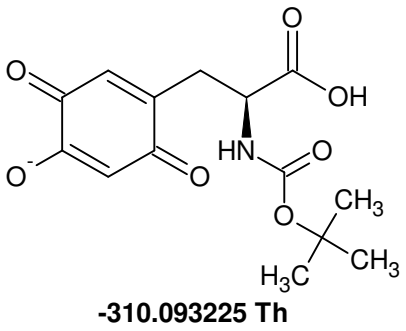

-310.093225 Th

isotopic fingerprint:

peak area / % of monoisotopic	+1	+2	+3
theoretical ($C_{14}H_{18}NO_7^+$):	16,0	2,6	0,3
measured (312,1 Th):	30,6	3,7	3,0
measured (-309,9 Th):	15,1	-	-

Figure 10-4 MS^n analysis of oxidised N-Boc-*L*-Tyr

In the full scan signals with a spacing of 16 Th each (assigned to ^{16}O) were found for the monomeric signals as well as (and in much higher abundances) for the dimeric signals (mass spectra given in the annex, see X.IV). The maximal number of 16 Th steps observed was 4 for the dimeric signals in negative ionisation mode. In addition to the expected formation of the hydroxylation product N-Boc-*L*-DOPA, which explains the additional signals up to the second step, this indicates a second hydroxylation and a twofold oxidation of the monophenolic substrate. Taking into account the fragments generated from the corresponding signals in the MS^n analysis (and assuming the correctness of the respective interpretations), this additional oxygen can neither be located on the protecting group nor on the carboxyl group or the short aliphatic chain of the compound what leaves only the aromatic ring as the sole point of modification possible. The pH of the tested solution was acidid (pH 4) which was found to promote the formation of the dihydroxylated tyrosine derivative trihydroxyphenylalanine (TOPA) [109, 115].

11. Reduction with $NaBH_4$

Reduction of collagen with tritiated sodium borohydride has been used to isolate and identify reducible crosslinks [5, 9, 40, 41, 177-182] and modified amino acids [183] in the peptide chain.
These reducible crosslinks are generally not stable under acidic conditions and would therefore be destroyed if subjected to an acidic hydrolysis like the one used in this study (see 3.2.2). While the naturally occurring crosslinks in collagen were not within the scope of this study, any new crosslinks of a similar chemical nature formed over the course of the oxidoreductase treatment would also be destroyed in any subsequent sample pre-treatment step involving acidic conditions and therefore had to be protected prior to acidic hydrolysis.

Sodium borohydride was dissolved in aqueous ammonium carbonate buffer 600 mM pH 9:

- 340 mM $(NH_4)_2CO_3$ 69,09 Da ⇒326,71 mg per 10 ml
- 260 mM NH_4HCO_3 79,06 Da ⇒205,56 mg per 10 ml

The amount of reducing agent used was calculated to be 4 moles of sodium borohydride per mole of lysyl residues in the collagen to be reduced (300% excess if no $NaBH_4$ was destroyed before reacting with the collagen). For 100 µl of a 3,75 g l^{-1} collagen solution (as used for the enzymatic reactions), the molecular weight of a type 1 collagen triple helix (2 α-1(I) + α-2(I), *Bos Taurus*) of 280447 Da and 107 lysine residues in the trimer this resulted in 143 nmol Lys ≙ 4 · 143 = 572 nmol $NaBH_4$ which were added as 25 µl of a 22,88 nmol $µl^{-1}$ ≙ 0,866 g l^{-1} (M($NaBH_4$) = 37,83 g mol^{-1}) solution.
Before the sodium borohydride solution was added to the sample solution, the latter was adjusted to pH 9 with aqueous NH_3. This step was necessary because sodium borohydride exhibits insufficient stability in aqueous solutions below pH 9 where the hydrolysis reaction is quite fast.

$$NaBH_4 + 4\ H_2O \rightarrow NaB(OH)_4 + 4\ H_2\uparrow$$

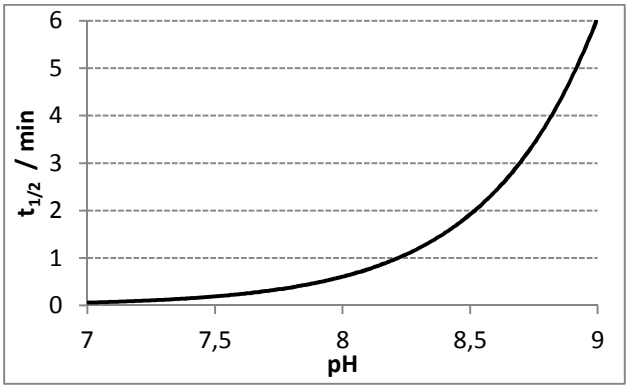

Figure 11-1 Half-life of sodium borohydride in aqueous solution at 25 °C
calculated using $log_{10}\left(\frac{t_{1/2}}{min}\right) = pH - 0{,}034 \cdot \frac{T}{K} + 1{,}92$ [184]

The necessary amount of ammonia needed to achieve that adjustment was determined by titration of a test sample containing the same constituents as the sample to be reduced with 5 % (w/v) NH_3 (aq.). For the routinely used ammonium acetate buffer 50 mM pH 6,5 at a fraction of one third (v+v) the pH adjustment was facilitated by adding 25 µl of a 0,6 ‰ (w/v) NH_3 (aq.) solution per 100 µl of sample solution.
The reduction was carried out in 1,5 ml PP reaction vials at 25 °C and 400 min^{-1} on a thermal shaker for 10 min. After the reaction time had elapsed, the excess $NaBH_4$ was destroyed by adding an thousandfold excess of acetone – 21 µl for the aforementioned 100 µl of sample solution (acetone: 58,079 g mol^{-1}, 0,79 g cm^{-3} @ 25 °C ⇒ pure ≙ 13,6 M) – and the reaction was allowed to continue overnight.
$NaBH_4$ could have been destroyed much quicker by adding a strong acid but such a procedure would have compromised the specificity of the reduction by greatly enhancing the reducing power of the sodium borohydride [185].
Samples that were reduced with $NaBH_4$ are marked with a minuscule “r” after the sample name.

12. Preparations

All enzymatic reactions were carried out in 1,5 ml or 2 ml PP micro tubes at a fixed temperature and with constant agitation – both provided by one (or multiple instances of) thermomixer.
To avoid constraining the enzymatic reactions by insufficient concentrations of the oxidant used, each tube was opened two times a day, the head space was filled with air of tested oxygen content (namely by breathing it) and the content of the tube was brought in direct contact with the renewed gas volume by reversing the tube four times after the cap had been closed again. The "refilling" routine was concluded by exchanging the gas in the head space one more time, closing the micro tube and putting it back on the thermomixer.

Sample naming convention:

(K|I-b|Boc-Tyr)? ?(BoT1|BoT2|AbT|T4|TvL|ThL|Null|6,5|4,5){1} ?\+?\|{0,2} ?\d*(h|d|min)?\b

K..... substrate: acid soluble collagen
I-b..... substrate: insulin β-chain oxidised (Cys(SO_3H))
Boc-Tyr..... substrate: N-[(1,1-Dimethylethoxy)carbonyl]-*L*-tyrosine
no indicated substrate: blank with buffer instead of substrate solution
BoT1 - ThL..... used enzyme
Null ..... reference without enzyme solution (volume substituted with buffer)
6,5..... reference without enzyme, buffered at pH 6,5
4,5..... reference without enzyme, buffered at pH 4,5
+..... preparation contains 20 µM $CuCl_2$
|, || ..... replicates 1 and 2 respectively
\d ..... incubation time (in multiples of the following unit)
h, d, min..... incubation time given in hours, days or minutes accordingly

12.1. Acid soluble collagen with tyrosinases and laccases in NH_4Ac

Ammonium acetate buffer was prepared at a concentration of 50 mM in ddH_2O.

- NH_4Ac 77,08 g mol^{-1} 50 mM ⟹ 770,8 mg for 200 ml (pH ≈ 7,0)
  - pH 6,5 with 10 % acetic acid (buffer capacity 1,8 mM pH^{-1})
  - pH 4,5 with glacial acetic acid (buffer capacity 69,0 mM pH^{-1})

Table 12-1 Volumetric activities of the used enzyme solutions in NH_4Ac 50 mM

Enzyme	laccase activity / (U ml^{-1})		tyrosinase activity (U ml^{-1})	
	pH 4,5	pH 6,5	pH 4,5	pH 6,5
BoT1	-	-	0,0266	0,389
BoT2	-	-	0,204	1,39
AbT	-	-	n.a.	0,264
T4 10 g l^{-1}	0,232	0,0234	-	-
TvL 2 g l^{-1}	29,9	3,14	-	-
ThL	298	41,8	-	-

n.a. ..... not analysed

12.1.1. K with BoT1, BoT2, AbT, T4, TvL and ThL

Preparation:

- 1000 µl substrate: acid soluble collagen, 4 g l^{-1} in 1 % (v/v, 175 mM) acetic acid
- Enzyme solution: volume containing 1 dU
- NH_4Ac buffer pH 4,5 (laccases) and pH 6,5 (tyrosinases) respectively to a final volume of 1500 µl

- Incubation on the thermomixer: 25 °C, 400 min^{-1} for 16 h (stored in the deep freezer until the acid hydrolysis)

K BoT2 16h exhibited increased viscosity and a slight yellow colour as compared to the reference treated alike but with buffer instead of the enzyme solution.

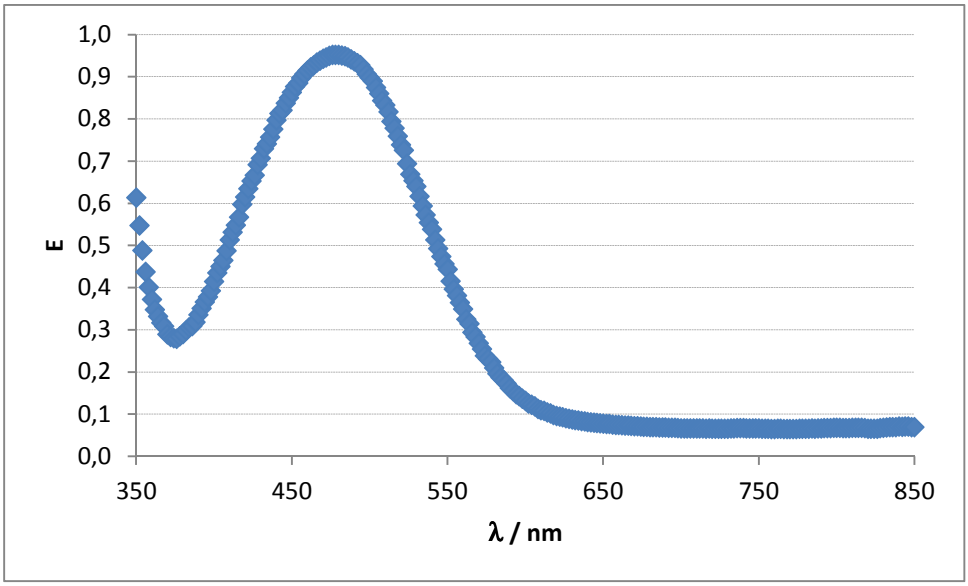

Figure 12-1 Vis spectra of Dopachrome in NH_4Ac 50 mM pH 6,5 (Tyr with AbT after 30 min)

Amino acid analysis:

The analysis of amino acid content was done using the method of neutralising the hydrochloric acid with sodium hydrochloride instead of evaporating it (cp. 4.3.2). The residual concentration of hydrochloric acid varied from 4,2 – 5,9 M. Additionally, the resulting solution was quite diluted what also didn't exactly enhance the accuracy of the measured concentrations.

12.1.2. K with BoT1, BoT2, AbT, T4, TvL and ThL

In addition to the cross-linking, this preparation was designed to test for an influence of copper-ions in the reaction medium [94]. In the study presented in [94], the generated signal from a biosensor (Clark electrode coated with immobilised AbT and gelatine crosslinked with glutaraldehyde) exhibited saturation starting at 20 µM Cu^{2+}; this concentration was therefore chosen for the test with acid soluble collagen.

Preparation:

- 1000 µl substrate: acid soluble collagen, 5 g l^{-1} in 1 % (v/v, 175 mM) acetic acid
- Enzyme solution: volume containing 1 dU (BoT1, BoT2, AbT), 1 U (TvL, ThL) and 1,7 dU (T4, due to the limited solubility of the brown powder)
- 30 µl of a 1 mM $CuCl_2$ solution (in NH_4Ac buffer 50 mM pH 6,5): samples labelled "**+**"
- NH_4Ac buffer pH 4,5 (laccases) and pH 6,5 (tyrosinases) respectively to a final volume of 1500 µl
    - Incubation on the thermomixer in **open** micro tubes: 25 - 30 °C, 400 min^{-1} for 24 h; then with closed lid, without agitation and further aeration at 25 - 30 °C for 3 additional days (stored at 4 °C)

Sampling:

Aliquots of the preparations were taken immediately after mixing the constituents (0 h) and after 1 h, 6 h, 12 h, 18 h and 24 h of reaction.

- 200 µl of the respective sample were mixed with 200 µl ice-cooled MeOH (on ice, to precipitate the enzymes and thereby stopping the reaction [186-188]) in 1,5 ml micro tubes, vortexed and kept on ice for 10 minutes.
  - With two samples a precipitate was formed immediately: BoT1 (white), T4 (brown).
- The stopped samples were stored at 4 °C in the refrigerator until acid hydrolysis.

Observations 5 min – 60 min:

BoT1: higher viscosity, a lot of small bubbles entrapped in the collagen
BoT2: higher viscosity, a few big bubbles entrapped in the collagen
AbT, TvL, ThL, References: clear and colourless
T4: a few small bubbles entrapped in the collagen (disappeared after 12 h), formation of yellow colour; immediately after the combination of the preparation's constituents insoluble clots were formed.

Correction for evaporation losses:

As the incubation in open vessels is bound to introduce volume losses due to evaporation, the concentration of the dissolved solids will increase with time without the need for any chemical reaction. To correct the measured concentrations for this purely physical contribution, a quadratic model of the evaporation has been set up; the model parameters have been fit to weight data obtained from model samples made up of the solvents used for the preparations with collagen:

- 1000 µl 1 % (v/v) acetic acid
- 500 µl NH_4Ac buffer pH 6,5 or 4,5: indicated in the name of the respective tube
  - Incubation in open 2 ml micro tubes at 27,2 °C (average temperature during the 24 h of the test with collagen and oxidoreductases) and 400 min^{-1}

The model assumes that the rate of evaporation depends on ambient temperature and exposed surface of the liquid only. Both parameters were kept constant during the trial with the model samples: the temperature by means of the employed thermomixer's thermostat and the liquid surface doesn't change with volume as the used vessel has cylindrical geometry (until the last 100 µl with the micro tubes used).
The data for fitting the model parameters to has been taken from the tubes 6,5 III; 6,5 IV; 4,5 II; 4,5 III and 4,5 IV (cp. Figure XII-II).

$\Delta m / mg = 9{,}66549 \cdot t / h - 0{,}0624672 \cdot t^2 / h^2$
$R^2 = 0{,}999511$ (coefficient of determination)

The initially chosen linear model was rejected due to systematic deviations of the calculated residues from normal distribution (cp. Figure XII-III) indicating improper modelling.

Table 12-2 correction factors for evaporation losses in open tubes

Sample	V_{ev} / µl	V_{rest} / µl	c / %	f_{corr}
0 h	0,00	1500	100	**1,000**
1 h	9,60	1290	101	**0,9926**
6 h	46,8	1044	105	**0,9500**
12 h	55,7	788	113	**0,8873**
18 h	55,7	532	125	**0,8031**
24 h	55,7	276	150	**0,6683**

V_{ev}: evaporated volume, V_{rest}: volume at the time of sampling; c: actual relative concentration in the taken sample; f_{corr}: correction factor, normalising concentrations to the 0 h level

Amino acid determination:

Table 12-3 changes in amino acid composition after enzymatic treatment (cp. Table XII-IV)

Amino acid	effect of the enzymatic treatment (l = lower, h = higher content)							
	K BoT1	K BoT2	K AbT	K 6,5	K T4	K TvL	K ThL	K 4,5
Ala	(l)	l	l		l	l	(l)	(l)
Arg	l	l			h			
Asp		h^{Cu}	(h)					(l)
Cys	h	h^{Cu}	(l)				(h)	
Glu								
Gly	l	l	(l)			l		
His		l					(l)	
Ile	l	l	l	(l)	(l)	(l)	l	(l)
Leu	l	l	l					
Lys		l						
Met								
Phe		l	l					
Ser		h						
Thr						l	l	(l)
Tyr		h			(l)	(l)	l	
Val	l	l	l				(l)	(l)

Cu .....only in preparations with 20 µM $CuCl_2$

Parantheses mark observations that could only be reproduced in 3 out of 4 replicates.

The addition of 20 µM Cu^{2+} seems to be of no pronounced effect for the changes in the amino acid composition due to enzymatic treatment. Solely the levels of Arg seem to increase for BoT2 with added copper and to increase steeper with Cu^{2+} added to preparations with AbT. For the rest of the amino acids, the values measured in preparations with and without copper resembled simple replicates.

Test for microbial contamination:

To make sure that any observed change in amino acid composition is due to enzymatic activity of the deliberately added enzymes only, the preparations were checked for microorganisms which could potentially use the collagen in the preparations as nutrients. As such microbial growth would undoubtedly be adequate for altering the amino acid pattern, the presence of such had to be confirmed or ruled out.

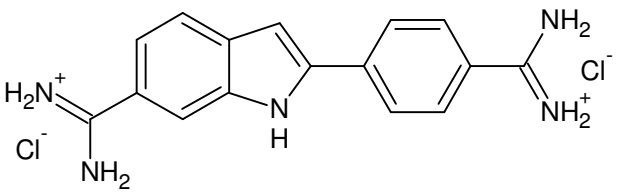

DAPI . 2 HCl
4',6-Diamidino-2-phenylindole dihydrochloride
with dsDNA: $\lambda_{ex,max}$ = 358 nm
$\lambda_{em,max}$ = 461 nm

Figure 12-2 DAPI

The samples K BoT2 | 24h (aliquot with 50 % MeOH) and K AbT +|| 4d were checked for microbial growth using the fluorescence microscope in transmissive mode. No microorganisms were discernible using this approach.
Additionally the sample K AbT +|| 4d was stained with DAPI (+ SlowFade®) and analysed in fluorescent mode. Only particles without defined form and in particular not a single colony were visible; the test was therefore interpreted as negative, thus no microbial contamination was detected.
The tests on the fluorescence microscope were carried out by Dr. Massimiliano Cardinale.

Four additional samples were plated on LB agar plates to check not only for viable microorganism but also for bacterial or fungal spores.

- 15 g l^{-1} agar-agar Kobe I and 25 g l^{-1} LB-media in ddH_2O
  - autoclaved for 20 min @ 121 °C
    - ⇒ Plates were poured at 20 ml each and allowed to solidify and cool down
- 100 µl of each sample were plated on one agar plate.
  - 24 h @ 37 °C (petri dish upside down)

Table 12-4 colonies on LB plates grown at 37 °C

Sample	Colonies	CFU per ml	Notes
+	18	-	Surface sample of the laboratory door handle; small, round colonies
K BoT2 || 24h	127	1270	Big, irregularly limited colonies with white texture
K BoT2 | 4d	(651)	(6500)	Big, irregularly limited colonies with white texture
K AbT +|| 24h	(1)	(10)	Yellow, round colony
K AbT +|| 4d	0	0	
Ø |	0	-	Blank: only opened, nothing plated
Ø ||	0	-	Blank: only opened, nothing plated
Ø |||#	1	-	Blank: autoclaved LB medium only
K BoT2 +| 4d#	4	400	"Colonies" yellowish and quite big (diameter up to 8 mm after 20 h), margin irregular, white texture
BoT1#	91	9100	
BoT2#	124	12400	

#..... 10 µl sample and 90 µl autoclaved LB medium, 20 h @ 37 °C
Samples 24h were aliquots with 50 % (v/v) methanol.

10 µl of K BoT2 || 4d were used to inoculate approximately 9,7 ml of LB medium which was then incubated at 37 °C for 7 d. After one day white filaments were visible in the liquid medium which was covered by a thin white layer starting from that day.
Microscopic analysis of this liquid sample and BoT2 plated on solid agar (cp. Table 12-4) suggests that the contaminating microorganism is fungal in nature as structures attributed to hyphae, chlamydospores and sclerotia were found.

The solutions of BoT1 and BoT2 were sterile-filtered using a 0,5 ml centrifuge vessel equipped with a PET-membrane of 0,20 µm pore size before any further use in cross-linking assays.

12.1.3. K with BoT1 and BoT2

For these preparations the volumetric activities of the used tyrosinase solutions were reassessed using the Hitachi U-2001 spectrophotometer and NH_4Ac 50 mM pH 6,5 exclusively.

Table 12-5 activity of BoT1 and BoT2 in NH_4Ac

Enzyme	tyrosinase activity (U ml^{-1})
BoT1	0,489
BoT2	1,33
BoT2 0,2 µm#	0,631

..... sterile-filtrated

Preparation:

- 1500 µl acid soluble collagen, 5 g l^{-1} in 1 % (v/v, 175 mM) acetic acid
- Enzyme solution: volume containing 100 mU for BoT1 and 15 mU for BoT2
- NH_4Ac buffer pH 6,5 to the final volume of 2000 µl
    - Incubation on the thermomixer in closed 2 ml micro tubes: 25 °C, 400 min^{-1} for 5 d (stored at 4 °C pending further analyses)

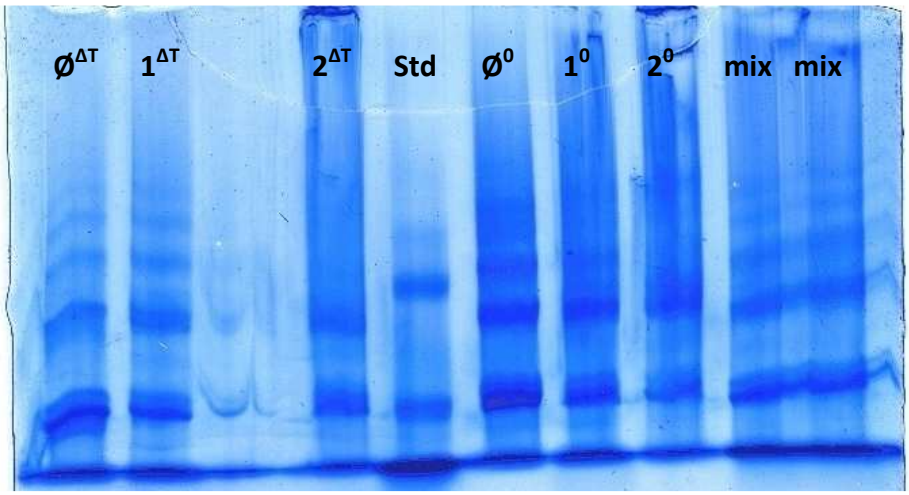

Figure 12-3 SDS-PAGE: composite gel 2 % acryl amide & 1 % agarose, stained with CBB-G250,no destaining
The 1 mm vertical gel was run for 18 min @ 50 V followed by 90 min @ 10 V and 45 min @ 50 V.
Std .....Standard (globular proteins, see 5.1.4)
Ø.....K Null 5d
1 .....K BoT1 5d
2 .....K BoT2 5d
Sample preparation after mixing with 2x loading buffer (see 5.1.3):
ΔT .....15 min @ 50 °C, 400 min^{-1}
0 .....15 min at room temperature

As illustrated inFigure 12-3 the treatment with tyrosinases from *B. obtuse* (especially BoT2) does increase the apparent molecular weight of the acid soluble collagen (cp. also further gels presented in the annex, XII.I.III).

12.1.4. K with BoT1, BoT2 and AbT

The volumetric activities of the used tyrosinase solutions were redetermined in NH_4Ac 50 mM pH 6,5 (see Figure XII-XIV and Figure XII-XVI).

Table 12-6 activity of sterile-filtered BoT1, BoT2 and AbT in NH_4Ac

Enzyme	tyrosinase activity (U ml^{-1})
BoT1[#]	0,0405
BoT2	1,70
AbT[15]	0,513

.....5-fold diluted (to squeeze out the last drops), 7 min lag time
15 .....15 min lag time

Preparation:

- 1500 µl acid soluble collagen, 5 g l^{-1} i**n ddH_2O**
- Enzyme solution: volume containing 15 mU (BoT2, AbT) and 3,2 mU (BoT1, rest of the enzyme solution) respectively
- 20 µl of a 20 mM $CuCl_2$ solution (in NH_4Ac buffer 50 mM pH 6,5): samples labelled "**+**"
- NH_4Ac buffer 50 mM pH 6,5 up to the final volume of 2 ml
    - Incubation on the thermomixer in 2 ml micro tubes: 25 °C, 550 min^{-1} for 7 d; (stored at 4 °C pending further analyses)

Sampling:

One aliquot was taken after **18 h** of reaction (300 µl) and stopped by the addition of one volume of cold MeOH (analogous to the procedure used in 12.1.2).

As formed gels and smaller fluffs made a representative sampling impossible, the aggregates were reduced in size by the action of an injection cannula with sharp tip directly inside the reaction tubes. The resistance the formed aggregates put up against this breakup varied greatly between treated and untreated collagen as did the colour of the preparations after the initial hour of reaction.

Table 12-7 visual and mechanical properties of samples K 18 h

Sample	Yellow-brownish colour	Resistance[#]	appearance after stirring
K Null	- (white)	-	small white flakes
K BoT1	+++	++	small white-brownish flakes
K BoT2	+	+	small flakes and bigger lumps
K BoT2 +	++	++	small flakes and bigger lumps
K AbT and **K AbT +**	+	+	gel pieces and a few bigger flakes; The gel adheres strongly to stainless steel.

.....Resistance against separation into smaller units using an injection cannula

Reduction with $NaBH_4$:

100 µl of undiluted sample or 200 µl of the aliquots with MeOH respectively were subjected to reduction with $NaBH_4$ as described in 11.

Amino acid analysis:

The levels of His are generally lower after the enzymatic treatment, the treatment with BoT1 also diminished the Asp content (cp. Table XII-V).

MS^n analysis:

The sample with the most intense signals (in amino acid analysis after OPA-derivatisation) appearing in enzymatically treated but not in untreated collagen, K BoT1 r 18h, was chosen for MS^n analysis after chromatography without salts in the mobile phase (see 6.1.3 for the chromatographic conditions and XIII.I.I for the fragmentation trees).
Fractions containing the two most abundant signals ("BoT#4", "BoT#8") were also taken from K BoT2 + | 4d, desalted chromatographically (see 6.1.2) and subjected to MS^n analysis (XIII.I.II).

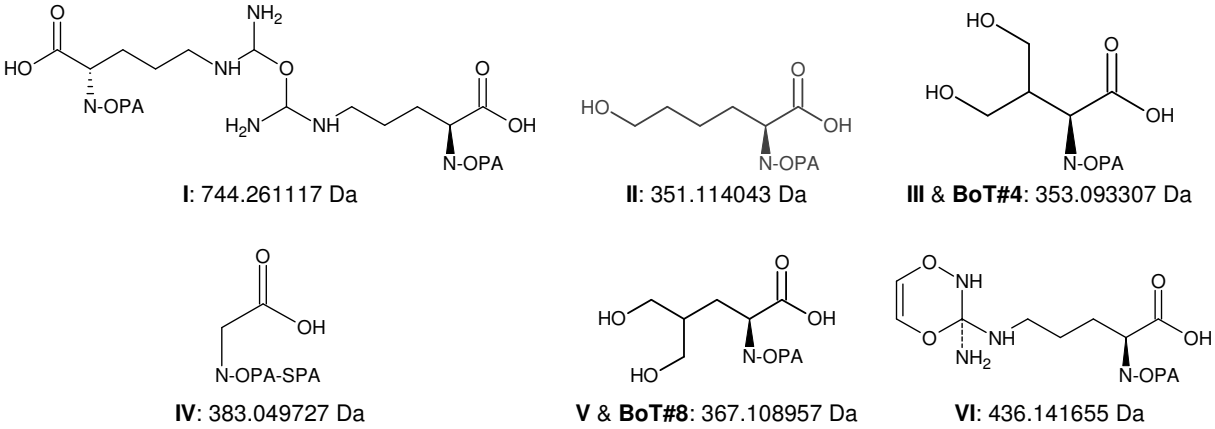

Figure 12-4 structures from the MS^n analysis of acid soluble collagen incubated with BoT1 / BoT2
For the abbreveations used for groups introduced by chemical derivatisation see Figure XII-XLI.

12.2. Insulin β-chain with BoT2 and AbT

The β-chain of insulin was used as a model substrate for the action of tyrosinase on proteins in lieu of acid soluble collagen. While the primary sequence of the collagen (extracted from bovine split) is not known precisely due to the blended character of the former, the β-chain of insulin is a defined substrate.

Phe–Val–Asn–Gln–His–Leu–Cys(SO_3H)–Gly–Ser–His–Leu–Val–Glu–Ala–Leu–
Tyr–Leu–Val–Cys(SO_3H)–Gly–Glu–Arg–Gly–Phe–Phe–**Tyr**–Thr–Pro–Lys–Ala
Figure 12-5 peptide sequence of the used oxidised β-chain of insulin

I-b old was dissolved in sodium phosphate buffer 100 mM pH 6,8 which was also used as reaction buffer instead of the volatile NH_4Ac to avoid some interference in the OPA-derivatisation caused by incomplete removal of ammonium (cp. 4.3.3).

- Sodium phosphate buffer 100 mM pH 6,8 in ddH_2O (buffer capacity 58 mM pH^{-1})
  - 50 mM NaH_2PO_4 . 2 H_2O 156,01 g mol^{-1} 7,801 g l^{-1}
  - 50 mM Na_2HPO_4 . 2 H_2O 177,99 g mol^{-1} 8,900 g l^{-1}

12.2.1. I-b old with BoT2 and AbT in NH_4Ac

Table 12-8 activity of sterile-filtered BoT2 and AbT in NH_4Ac

Enzyme	tyrosinase activity (U ml^{-1})
BoT2	0,0692
AbT	0,369

Preparation:

- 100 µl I-b 5 g l^{-1} in sodium phosphate buffer 100 mM pH 6,8
- Enzyme solution: volume containing 5 mU
- NH_4Ac buffer 50 mM pH 6,5 up to the final volume of 500 µl
    - Incubation on the thermomixer in 1,5 ml micro tubes: 25 °C, 300 min^{-1} for 24 h; (stored at 4 °C pending further analyses)

After 15 min of reaction, the preparations containing tyrosinase started to turn pink, after 5 h a black precipitate had been formed (UV-VIS spectra in 2-chloroethanol: see Figure 10-1) in the otherwise clear solutions.
After acidic hydrolysis, yellow needles were found in the desiccated samples (white needles for I-b without tyrosinase) which were soluble in ddH_2O. The derivatisation of the reconstituted samples with OPA didn't produce much of the fluorogenic isoindole but a lot of red precipitate which was formed immediately after adding the OPA reagent. The resulting chromatograms contained very little signal while for the standard solutions of dissolved amino acids no deviation from the routinely reached signal levels was observed.
Gel permeation chromatography revealed the inhomogeneous nature of the allegedly pure protein (see Figure XII-XXI and Figure XII-XXVI).

12.2.2. I-b old with BoT2 and AbT in sodium phosphate buffer

For the determination of the enzyme doses the activities in NH_4Ac were used (see Table 12-8).

Preparation:

- 100 µl I-b 5 g l^{-1} in sodium phosphate buffer 100 mM pH 6,8
- Enzyme solution: volume containing 5 mU
- up to the final volume of 500 µl with sodium phosphate buffer 100 mM pH 6,8
    - Incubation on the thermomixer in 1,5 ml micro tubes: 25 °C, 300 min^{-1} for 24 h; (stored at 4 °C pending further analyses)

After 10 min of reaction the preparations containing tyrosinase had turned red, after 6 h black precipitate was present in large amounts. For the UV-Vis and fluorescence monitoring, the signal measured stemmed primarily from the supernatant (cp. Figure XII-XXIII).

12.2.3. I-b new with BoT2 and AbT in NH_4Ac

Preparation:

- 100 µl I-b 5 g l^{-1} in ddH_2O
- Enzyme solution: volume containing 5 mU AbT or 1 mU BoT2 respectively
- up to the final volume of 500 µl with NH4Ac 50 mM pH 6,5
    - Incubation on the thermomixer in 1,5 ml micro tubes: 25 °C, 300 min^{-1} for 24 h; (stored at 4°C pending further analyses)

After 3 h of reaction, I-b BoT2 had developed a pale reddish colour, after 6 h I-b BoT2 and the reference I-b were turbid and contained white flakes (I-b AbT was clear and colourless.).
At the end of the incubation (24 h) all the preparations were clear (again), preparations containing tyrosinase and insulin had developed a pale yellow colour while the references and blanks were colourless (cp. UV-Vis and fluorescence monitoring: Figure XII-XXVII).

12.2.4. I-b new with BoT2 and AbT in sodium phosphate buffer

The activities in NH_4Ac were used (see Table 12-8) as estimates for the enzyme activities.

Preparation:

- 120 µl I-b 5 g l^{-1} in ddH_2O
- Enzyme solution: volume containing 5 mU AbT or 1 mU BoT2 respectively
- up to the final volume of 600 µl with sodium phosphate buffer 100 mM pH 6,8
    - Incubation on the thermomixer in 1,5 ml micro tubes: 25 °C, 350 min^{-1} for 27 h; (stored at -18 °C pending further analyses)

At the beginning of the incubation, all preparations were clear and colourless. After 4 hours all preparations were still homogenous (and stayed that way for the complete incubation), I-b BoT2 had developed a pink colour; the other preparations were still colourless (cp. UV-Vis and fluorescence monitoring: Figure XII-XXX).

Protein hydrolysis:

All samples (including references and blanks) exhibited water soluble white fringes, attributed to sodium phosphates (which are contrary to the volatile salt ammonium acetate non-volatile; theoretical concentration for 100 % recovery: 145 mM phosphates => soluble, cp. Table XII-VI). For the samples 24 h with tyrosinases yellow crystals were encountered additional to the white ones present in every sample. After reconstitution with ddH_2O I-b BoT2 6h showed a feeble yellowness, the samples with BoT2 or AbT after 24 h of incubation were yellow solutions.

Amino acid analysis:

For all enzymatically treated samples a consumption of tyrosine is observable; for I-b treated with BoT2 a decrease in the levels of Glu and an increase in the levels of Gly can also be stated (see Table XII-VIII).

MS^n analysis:

The elution volumes corresponding to differences in the UVD-signal at 338 nm for the OPA-derivatised acid hydrolysates of I-b BoT2 24h and I-b 24h as reference were collected and subjected to MS^n analysis (see XIII.II).

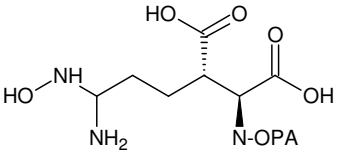

F3: 425.12567 Da

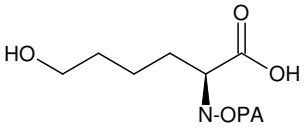

F5: 351.114043 Da

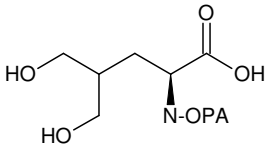

F6, **F7**: 367.108957 Da

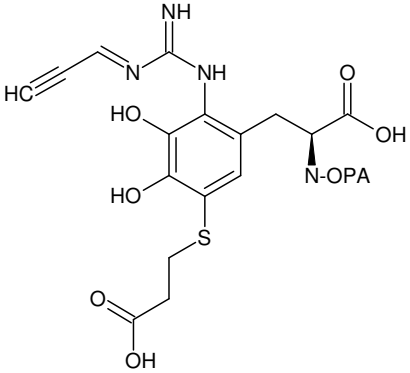

F6: 598.119204 Da

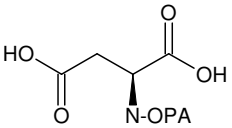

F9: 337.062007 Da

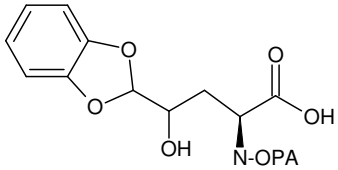

F9: 443.103872 Da

Figure 12-6 structures from the MS^n analysis of insulin β-chain treated with BoT2

12.3. 7 AS with BoT2 and AbT

To support the interpretation of the data from MS^n analysis, preparations with individual amino acids were tested for changes in the amino acid content as a result of enzymatic treatment.
The tested amino acids were Arg, Ile, Leu, Lys, Ser and Val in preparations containing only one specific amino acid and the six amino acids listed above and His in a composite sample termed 7 AS.

12.3.1. 7 AS with BoT2 and AbT in NH_4Ac

For the activities of the used enzyme solutions see Table 12-8.

Preparation:

- 400 µl amino acid solution 100 mM in ddH_2O
- Enzyme solution: volume containing 2 mU
- NH_4Ac buffer 50 mM pH 6,5 up to the final volume of 800 µl
    - Incubation on the thermomixer in 2 ml micro tubes: 25 °C, 250 min^{-1} for 5 d; (stored at 4 °C pending further analyses)

Amino acid analysis:

The enzymatic treatment didn't result in any modification of the levels of the amino acids originally provided (cp. Figure XII-XXXIV), the samples with and without added enzyme resembled replicates.

12.3.2. 7 AS with AbT in sodium phosphate buffer with 1,77 mM Tyr

The enzyme was metered according to the activities in NH_4Ac (see Table 12-8).

Preparation:

- 40 µl amino acid solution 100 mM in ddH_2O
- 5,4 µl AbT 1 g l^{-1} (2 mU)
- *L*-Tyr 2 mM in sodium phosphate buffer 100 mM pH 6,8 to 400 µl final volume
    - Incubation on the thermomixer in 1,5 ml micro tubes: 25 °C, 300 min^{-1} for 5 d; (stored at 4 °C pending further analyses)

All preparations with AbT exhibited a formation of a black precipitate which was removed by centrifugation (15 min @ 18620 g, 0 °C). The supernatant was used directly for amino acid analysis after OPA-derivatisation. Contrary to I-b old with AbT (cp. 12.2.1) the derivatisation worked well although monomeric Tyr was present and presumably oxidised by AbT in the preparations.

The amino acid analysis after 24 h of reaction did show a distinctly lower level of tyrosine in all preparations but the levels of the other amino acids didn't change at all (cp. Figure XII-XXXV).

12.3.3. 7 AS with N-Boc-*L*-Tyr and AbT in sodium phosphate buffer

The volumetric activity of the used AbT 1 g l^{-1} solution in sodium phosphate buffer 100 mM pH 6,8 was determined to amount to 2,38 U ml^{-1} (cp. Figure XII-XXXIX)

Preparation:

- 500 µl amino acid solution 20 mM in ddH_2O
- 500 µl N-Boc-*L*-Tyr 2 mM in sodium phosphate buffer 100 mM pH 6,8
- 5,4 µl AbT 1 g l^{-1} (12 mU), mixing
    - Incubation on the thermomixer in 2 ml micro tubes: 25 °C, 300 min^{-1} for 48 h; (stored at 4 °C pending further analyses)

After 10 min the preparations containing AbT and any of seven amino acids had turned pink while all blanks (without AbT or AbT with water only) were colourless.

Table 12-9 7 AS with N-Boc-*L*-Tyr and AbT: pink colour after 15 min of reaction

Amino acid	Arg	Ile	Leu	Lys	Ser	Val	7AS	Blanks
Colour intensity#	++	+	+/-	++	+	+	+	-

..... determined by visual sampling

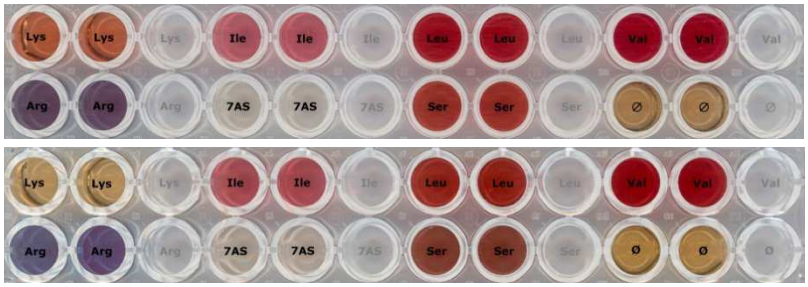

Figure 12-7 7 AS with N-Boc-*L*-Tyr after 16,5 h (above) and 48 h (below)
Ø.....N-Boc-*L*-Tyr and AbT without additional amino acids
grey .....blanks (no AbT)

The maxima of the absorption bands (as measured after 19 h, cp. UV-Vis and fluorescence monitoring, Figure XII-XXXVI) were at 625 nm (Arg), 502 nm (Val, Leu, Ser, Ile), 304 nm (Val, Ile) and 274 nm (all amino acids).

Amino acid analysis:

The reaction was stopped by precipitation with methanol (analogous to 12.1.2); the preparations were centrifuged (18600 g for 18 min at 0 °C) and the supernatant (no precipitate was visible) was used for the analysis of amino acids.
As the method used (see 4.2.3) differed from the chromatographic conditions used to establish the calibration (4.2.1) and especially the resolution of the internal standard norvaline (shoulder on the peak of valine) was quite unsatisfactory as basis of all calculations. To attenuate that problem, the concentrations were calculated applying the unreferenced calibration (see Table IV-VI) and measuring a solution on known concentration (10 mM) to act as a basis for correction of the measured concentrations (see Table XII-IX and Table XII-X).

Table 12-10 7 AS & Boc-Tyr: changes in amino acid levels after 24 h and 48 h

Amino	24h		48h	
acid	Δ / %	R_{rep} / %	Δ / %	R_{rep} / %
Arg	**31,3**	2,00	**32,1**	2,82
Ile	**11,7**	6,50	**14,6**	2,43
Leu	**18,5**	8,24	**25,1**	3,90
Lys	**12,7**	0,942	**20,1**	2,40
Ser	**26,2**	1,63	**37,7**	3,23
Val	**19,1**	1,60	**18,8**	1,88

Δ .....difference AbT – reference: $\Delta = \frac{c(Null) - \frac{1}{2} \cdot [c(AbT\ |) + c(AbT\ ||)]}{c(Null)}$

R_{rep}.....Range of the two replicates: $R_{rep} = \frac{2 \cdot |c(AbT\ |) - c(AbT\ ||)\ |}{c(AbT\ |) + c(AbT\ ||)}$

MS^n analysis:

Signals from the OPA-derivatised amino acid derivatives (from the amino acid analysis) present in the preparations with AbT but not in the respective references without tyrosinase were selected, collected as a single fraction per injection and injected into the ESI-interface of the MS. The signals at 2,9 and 13,3 min were seen in all the tested preparations containing AbT and N-Boc-*L*-Tyr.
Fractions from the samples Arg AbT | 24h, Ser AbT || 24h, Val AbT | 24h and Ile AbT | 48h were subjected to MS^n analysis (see XIII.III).

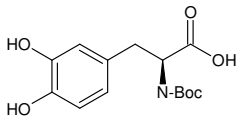

Arg 274nm 8min: 297.121237 Da

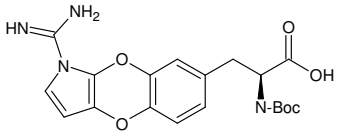

Arg 595nm 6,8min: 402.153934 Da

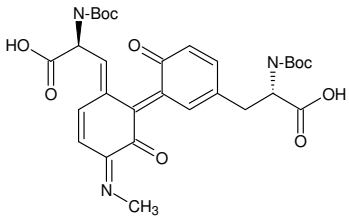

Arg 595nm 8,6min: 585.232244 Da

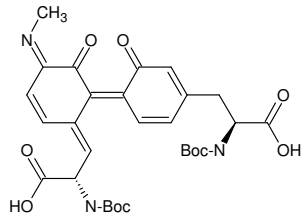

Arg 595nm 12,3min: 585.232244 Da
Isomer of Arg 595nm 8,6min 585Da

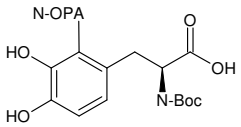

OPA-Ser 13,3min: 516.156636 Da
The corresponding UVD-signal is found in all the analysed samples (Lys, Ile, Leu, Val, Arg, Ser).

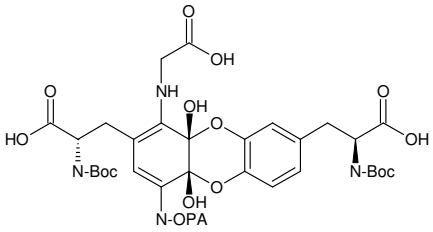

OPA-Ser 13,3min: 884.278601 Da

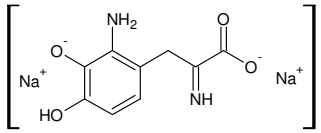

OPA-Val 2,9 min: 254.027947 Da
clusters with sodium
The corresponding UVD-signal is found in all the analysed samples (Lys, Ile, Leu, Val, Arg, Ser) and in the references with AbT and N-Boc-L-Tyr but not in the blanks (without AbT).

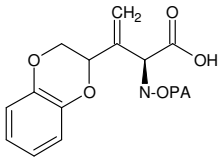

OPA-Ile 10,4min: 439.108957 Da
The corresponding UVD-signal appears only in preparations containing (**iso**)**leucine** treated with **AbT**.

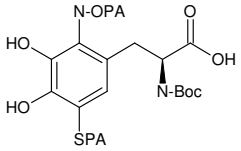

OPA-Ile 12,9min: 620.149835 Da
The corresponding UVD-signal can be found in preparations containing **Ile**, **Leu**, **Val**, **Arg** or **Ser** and **AbT**.

Figure 12-8 structures derived from the MS^n analysis of preparations with one amino acid, N-Boc-*L*-Tyr and AbT

Stability test with MeOH:

As a signal sensitive to methanol was encountered in the OPA-derivatised sample Ile AbT | 48h, 100 µl each of the preparations 48h were mixed with 100 µl MeOH and incubated in closed 1,5 ml micro tubes at 25 °C and 150 min^{-1} for 5 days.
The absorption band around 502 nm of the samples containing AbT and Val (E_{502} = 0,143), Leu (E_{502} = 0,128) or Ile (E_{502} = 0,090) disappeared almost completely in the course of 5 days (cp. UV-Vis monitoring and fluorescence, Figure XII-XXXVII).

Oxidised substrate without enzyme:

- 50 µl oxidised N-Boc-*L*-Tyr: samples AbT | 48h and AbT || 48h filtrated (Vivaspin 2, 3 kDa MWCO) => max. 0,5 mM oxidised N-Boc-*L*-Tyr for 5 mM amino acids (1:10, the fraction used also for the original preparations)
- 25 µl sodium phosphate buffer 100 mM pH 6,8
- 25 µ amino acid solution 20 mM in ddH_2O
    - Incubated in closed 1,5 ml micro tubes @ 25 °C, 150 min^{-1} for 5 d

Just two weak signals could be identified in the fluorescence spectra after 120 h: Ile @ 560 nm (λ_{ex} = 230 nm) and Arg @ 444 nm (λ_{ex} = 274 nm) (cp. Figure XII-XXXVIII).

pH-dependence of the spectroscopic properties of oxidised N-Boc-*L*-Tyr:

- N-Boc-*L*-Tyr 2 mM in sodium phosphate buffer 100 mM pH 6,8 or ddH_2O (for MS^n analysis cp 10.5) with 4 U l^{-1} AbT
  - In 2 ml micro tubes with perforated lid: 5d @ 24°C, 150 min^{-1}
- Sodium phosphate buffer 400 mM pH 2,5 in ddH_2O (buffer capacity 181 mM pH^{-1})
  - 297 mM Na_2HPO_4 . 2 H_2O 156,01 g mol^{-1} 46,335 g l^{-1}
  - 103 mM H_3PO_4 98,00 g mol^{-1} 10,094 g l^{-1}
    - $\Rightarrow$ measured pH: 2,50
- 100 µl N-Boc-*L*-Tyr oxidised with AbT 5d
- 100 µl sodium phosphate buffer pH 2,5 or pH 6,8
  - Incubation in closed 1,5 ml micro tubes: 20 min @ 500 min^{-1}; 18,6̇ h @ 0 min^{-1}, 25°C

The adsorption spectra didn't show any direct influence of pH, intensity of the fluorescence band at 570 nm was higher at pH 6,8 where it was excitable primarily from the absorption band around 454 nm than at pH 4,0 where excitation stemed primarily from the absorption band around 388 nm (cp. Figure XII-XL).

13. Discussion

The present work aimed at the mechanistical investigation of the enzymatic cross-linking of collagen. While tyrosinase has already been shown to possess the principal aptidude to induce cross-linking in collagen [189], the molecular details of the cross-linking and especially the formed cross-linking units do still await elucidation. In order to add another piece to this puzzle, this work focused on the identification of amino acids involved in cross-linking reactions apart from or occurring in succession to the oxidation of tyrosine forming an *o*-quinone.
New amino acid species brought about by incubation with tyrosinase were pinpointed by RP-HPLC amino acid analysis (4), isolated from the eluat stream and analysed by ESI-MS^n (6).

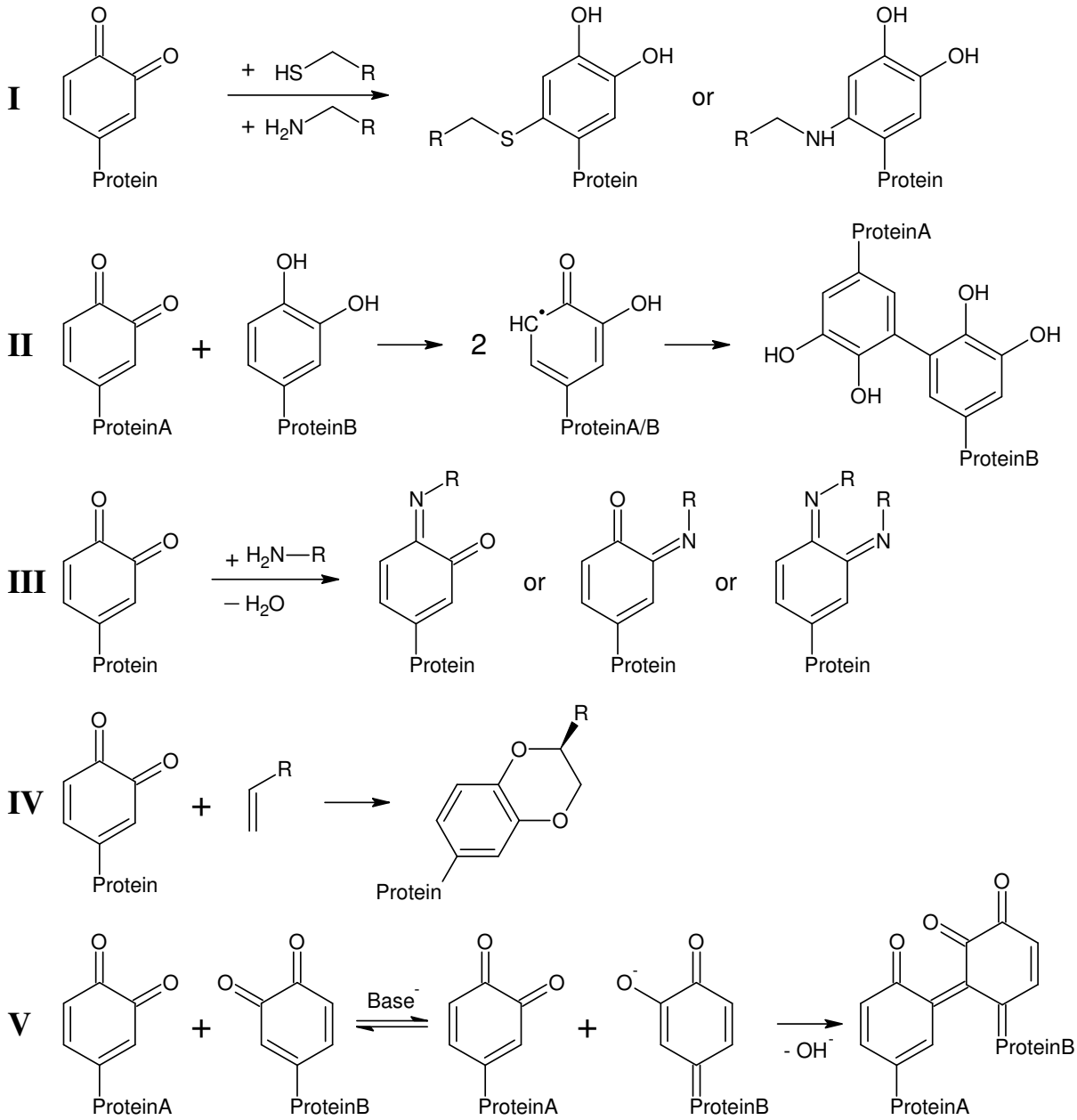

Figure 13-1 cross-linking reactions of *o*-dopaquinones
I: Michael-type 1,4-addition (nucleophilic addition) [77], II: radical-mediated, comproportional coupling of diphenol and *o*-quinone ("phenol coupling") [79], III: imine formation under condensation of water (Schiff base formation) [200], IV: [4+2] cycloadditon (hetero Diels-Alder reaction) [203], V: enolisation and subsequent aldol condensation

13.1. Cross-linking of Acid soluble collagen with tyrosinases and laccases in NH_4Ac

Due to the insufficient buffer capacity of the 50 mM ammonium acetate buffer used (1,8 mM pH^{-1} @ pH 6,5) the addition of the substrate dissolved in acetic acid (cp. 12.1.1, 12.1.2 and 12.1.3) lowered the pH of the reaction mixture by approximately 2,5 pH units so that the reactions took place at a pH of approximately 4. This pH-shift has an effect on the apparent activity of the used enzymes, the most severe being a reduction of 75 % in the diphenolase acitivity of AbT [189, unpublished data]. For the buffer at pH 4,5 (69 mM pH^{-1}) the same amount of acid resulted in a pH-shift of 0,7 units so that the reactions intended to run at two different pH-values were in fact separated by only 0,1 pH. As an enzyme load reduced by a factor of 30 (from 100 mU BoT1 in 12.2.3 to 3,2 mU in 12.1.4) did still yield cross-linked products, the aforementioned reduction was assumed non-critical. Even so, for the preparation determined to be subjected to MS^n-analysis acid soluble collagen dissolved in water instead of acetic acid was used (12.1.4).

Assuming validity of the applied amino acid measurements, RP-HPLC analysis of hydrolysed collagen treated with tyrosinases revealed that the amino acids affected by incubation with tyrosinases are Ala, Arg, Gly, His, Ile, Leu and Val (cp. Table 12-3, Table XII-IV and Table XII-V) which are all found in somewhat reduced levels after the enzymatic treatment. The conclusiveness of the determined amino acid concentrations and the respective fractions calculated thereof suffers from the different orders of magnitude of the amino acid concentrations and the respective changes thereof which are commonly in the range of the used analytical method's margin of deviation. A more severe problem for the conclusiveness of the determined values is the representativity of the taken samples, i.e the lack thereof. The preparations containing cross-linked material (i.e. comprising a heterogenous system with liquid buffer depleted of and some volumes containing more than their volume-average share of substrate), which were of special interest, were to be sampled in a way allowing comparability with the (homogenous and liquid) references and blanks. This problem was tackled by using the fractions of the individual amino acids calculated from the concentrations obtained from the application of the calibration (Table IV-VII) to the values of the numerical integrals over the corresponding peaks (signal areas). By using this approach the actual amount of sample used for the analysis no longer matters (which also makes an correction for the losses by evaporation, cp. Table 12-2, unnecessary) as long as the inhomogeneity of the current sample is significantly smaller than the method's margin of deviation and enough sample is brought into the analytical process to exceed the quantification limit for all the components of interest. For collagen treated with BoT1 and BoT2 this normalisation of data encountered the complication that the sum of all unmodified amino acids, which was used as the denominator for the calculation of the individual amino acids' fractions, didn't contain the most prominent peak(s) in the chromatogram (BoT#4 and the smaller BoT#8, cp. Figure XIII-XVI for a typical chromatogram) as no calibration was available for those unknown substances. The comparison of the figures calculated from the concentration of the known amino acids (applying the calibration) and those based on the measured signal areas and the integral over all the signals at the acquisition wavelength (total signal area) shows however no difference in the deductions derived thereof: the data looks qualitatively the same (cp. traces "c" and "A" in Figure XII-IV).

As perceptible from gel electrophoresis the incubation with tyrosinases did increase the molecular weight of acid soluble collagen (cp. Figure 12-3, Figure XII-VI for BoT1 and BoT2, Figure XII-VIII for AbT). Additional measurements employing size exclusion chromatography did only yield the qualitative information "bigger in size" as the separating matrix of the column used to separate untreated acid soluble collagen (Superdex 200 10/300 GL) wasn't permeable for the products of the enzymatic treatment.

The UV-Vis spectra of collagen didn't experience much change in the course of the enzymatic treatment (see Figure XII-XI for the absorption and Figure XII-XVII for the fluorescence spectra). This may be attributed to the small ratio of tyrosine in the substrate (3,5 ‰ of all amino acids in collagen I) and especially to the formation of functional units similar or identical to the ones already present in the protein.

FTIR analysis of dried collagen solutions (see 8) displays the amide I, II and III bands of collagen around 1630, 1525 and 1230 cm^{-1} respectively (Figure XII-XIII). Amide I, which is usually the most prominent peak in the IR spectrum of a protein, arises primarily from the stretching vibrations of C=O (70 – 85 %) and C-N (10 – 20 %) groups in the peptide linkages and is located between 1600 cm^{-1} and 1700 cm^{-1}. The amide II band (1510 – 1580 cm^{-1}) is derived mainly from in-plane N-H bending (40 – 60 %) with contributions from C-C (18 – 40 %) and C-N (≈ 10%) stretching vibrations while the amide III band (1200 – 1350 cm^{-1}) has a more complicated structure with components originating from the peptide linkages (C-N stretching and in-plane bending of N-H groups) as well as additional absorptions due to wagging vibrations of $–CH_2–$ groups of the glycine backbone and proline side-chains [190]. The absorption of the amide III band can be used to estimate the degree of denaturation as it is sensitive to the presence of the native tertiary structure of collagen [191]. The band at approximately 1450 cm^{-1}, which is due to vibrations of the pyrrolidine ring of proline and hydroxyproline side-chains [192], is insensitive to the tertiary structure of the collagen and can therefore be used as an internal standard to normalize the pathlength of the light within the specimen [191].

Table 13-1 ATR-FTIR of K 160h

sample	amide I			amide II			≈1450 cm^{-1}		amide III		
	cm^{-1}	A_I	A_I/A_r	cm^{-1}	A_{II}	A_{II}/A_r	cm^{-1}	A_r	cm^{-1}	A_{III}	A_{III}/A_r
K BoT1	1632	0,411	**1,74**	1551	0,340	**1,44**	1451	0,236	1237	0,253	**1,07**
BoT2	-	-	**-**	1547	0,016	**0,903**	1443	0,018	1243	0,020	**1,12**
K BoT2 |	1630	0,047	**1,40**	1542	0,045	**1,35**	1448	0,033	1233	0,037	**1,11**
K BoT2 ||	1630	0,077	**1,44**	1544	0,068	**1,28**	1448	0,053	1234	0,059	**1,11**
K BoT2 +	1630	0,104	**1,47**	1544	0,095	**1,34**	1449	0,071	1234	0,076	**1,07**
K AbT	1632	0,063	**1,32**	1521	0,056	**1,17**	1443	0,048	1229	0,048	**0,992**
K AbT +	1632	0,147	**1,37**	1521	0,129	**1,21**	1443	0,107	1231	0,102	**0,953**
K Null |	1630	0,131	**1,44**	1526	0,114	**1,26**	1444	0,091	1229	0,092	**1,01**
K Null ||	1632	0,244	**1,50**	1525	0,206	**1,26**	1444	0,163	1231	0,162	**0,994**

The position of the amide I band is not altered by the enzymatic treatment with tyrosinases while the amide II band is shifted by +25 cm^{-1} (BoT1) and +16 cm^{-1} (BoT2) in collagen treated with tyrosinases from *Botryosphaeria obtusa*. A slight shift is also noticed for the amide III band (+3 cm^{-1} with BoT2 and +7 cm^{-1} with BoT1) while treatment with AbT yields only marginal changes in the infrared spectrum of reconstituted acid soluble collagen. The ratio of the absorption at the peak of the amide III band and the peak around 1450 cm^{-1} is considered to be indicative for the structural integrity of the collagen triple helix with a value of 0,59 for gelatine cast at 60 °C [191]. Collagen treated with AbT, BoT1 or BoT2 has values for this ratio similar to untreated collagen of around 1 indicating an 50 % intact triple helix. The slight increase in preparations with BoT1 or BoT2 is probably due to the enzyme itself rather than its action on the collagenous substrate (cp. Table 13-1, BoT2).

Interpretation of the data from the MS^n analysis of acid soluble collagen treated with BoT1 (XIII.I.I) is summarised in Figure 12-4. While results from the incubation of free amino acids with AbT and BoT2 (see 12.3.1 and Figure XII-XXXIV) show no direct action of the tested tyrosinases with the free amino acids, the amount of modified amino acids formed from collagen treated with tyrosinases from *B. obtuse* (see Figure XIII-XVI for a typical chromatogram) either requires direct enzymatic attack on peptide-bound non-tyrosyl sidechains (which are especially electrostatically quite different to the usually zwitterionic free amino acids) or a tyrosine derived intermediate which can function as a mediator shuttling redox equivalents between the tyrosinase and other amino acids in the peptide chain. Since also the presence of free tyrosine does not produce any alterations in the levels of free amino acids beside the formation of melanin from the added tyrosine (see 12.3.2 and Figure

XII-XXXV), the free *o*-dopaquinone formed from the tyrosine upon hydroxylation and oxidation employing molecular oxygen doesn't convert a significant fraction of the other amino acids present before it undergoes cyclisation and subsequent melanin formation. While *o*-dopaquinone is not stable enough to function as said mediator, the quinone of a tyrosyl residue with a blocked amino function (as, for example, in a peptide bond) cannot cyclisize and experiences a greatly enhanced half-life in solution (cp. 10.5 and 12.3.3). Monooxygenation of exogenous aliphatic substrates mediated by dicopper peroxo complexes is common in monooxygenases which have two type II copper centres [193] but has also been reported for dicopper(II)-μ-1,2-peroxo (*end-on*) [194, 195] and dicopper(II)-μ-η^2:η^2-peroxo (*side-on*, active site of tyrosinase) [194] model complexes.

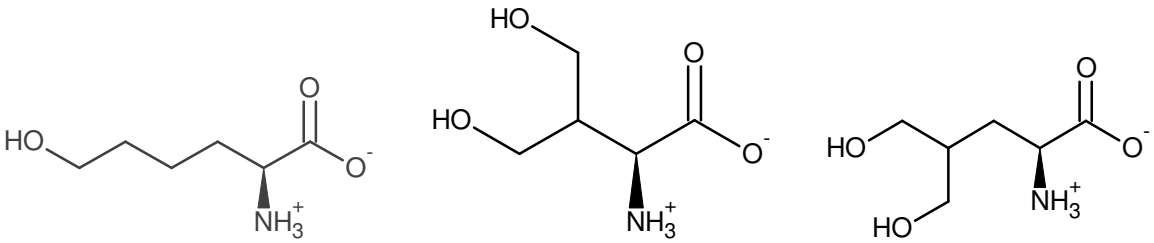

II, F5 **III, BoT#4, (F9)** **V, BoT#8, F6, F7**

Figure 13-2 MS^n analysis-derived structures common to collagen and insulin β-chain treated with BoT1/BoT2

13.2. Cross-linking of the Insulin β-chain with BoT2 and AbT

The oxidised β-chain of insulin which was used as an easier to analyse model substrate for collagen has a much higher content of tyrosine (6,6̇ %, see Figure 12-5) and should therefore be more susceptible to modification by tyrosinase. While the first batch of protein used ("I-b old") had become decomposed (cp. Figure XII-XXI and Figure XII-XXVI) and did practically just illustrate the formation of dopachrome out of tyrosine with the subsequent formation of melaninous polymers (cp. Figure XII-XX, Figure XII-XXIII and Figure 12-1 for the Vis-absorption of dopachrome), some cross-linking could be achieved by incubation with BoT2 (Figure XII-XXI).

A new batch of substrate ("I-b new"), which showed only one peak in size exclusion chromatography (Figure XII-XXVI), could be cross-linked successfully. In SEC analysis (Figure XII-XXXI) a big increase in hydrodynamic volume is monitored for I-b treated with BoT2 (base peak at 14,6 ml, new peak at 7,2 ml) while I-b incubated with AbT shows only a small shift towards higher apparent molecular weight (14,3 ml -> 13,2 ml).

The strongest UV-Vis absorption peak (for the spectra see Figure XII-XXVII and Figure XII-XXX) in all preparations containing the oxidised β-chain of insulin is centered at 276 nm and can be attributed to the π-π* transition of Tyr (cp. Figure 10-2, [196], no Trp present in the molecule). In preparations with AbT and substrate a peak at 469 nm (in NH_4Ac, 456 nm in sodium phosphate) develops in the course of the incubation. The same peak can be seen as a shoulder in preparations with BoT2 and I-b (where the absorption in this spectral range is generally higher). In all preparations with I-b and tyrosinase a shoulder around 330 nm arises as the incubation continues.

Upon excitation at λ_{ex} = 230 nm (the minimal possible excitation wavelength of the used fluorometer) the insulin β-chain fluoresces around 300 nm (tyrosine [166]) while the two tyrosinases emit fluorescence light with a wavelength around 323 nm (tryptophan [197]). The fluorescence intensity at 300 nm declines as the incubation continues indicating less unmodified tyrosine in the substrate. I-b treated with tyrosinases also shows a fluorescence signal around 500 nm (in NH_4Ac, 530 nm in sodium phosphate) that can be excited from absorption within the 276 nm absorption band (stronger for I-b treated with AbT) or, with higher quantum yield, within the 469 / 456 nm absorption band (similar intensities for I-b treated with either AbT or BoT2).

The amino acid analysis (Table XII-VIII) shows consumption of tyrosine for all samples containing I-b and tyrosinase; for BoT2-treated I-b a lower content of Glu and an increase in the Gly content is indicated while the changes for I-b incubated with AbT are generally less pronounced.

13.3. Treatment of 7 AS with BoT2 and AbT

The treatment of free amino acids with tyrosinases didn't yield any changes in the concentrations of the non-tyrosine amino acids (cp. Figure XII-XXXIV). The addition of free Tyr resulted in the formation of a red substance (dopachrome) which formed subsequently a black precipitate (melanin) but although the species involved in this reaction sequence (Scheme 10-1) include quite reactive *o*-quinons the other amino acids remained unperturbed (cp. Figure XII-XXXV).
After substitution of the free *L*-tyrosine with its N-protected analogon, N-Boc-*L*-Tyr (see 10), the preparations developed individual colours (see Figure 12-7) and consumption of 15 % - 38 % of the individual amino acids over the course of 48 h ensued (cp. Table 12-10). UV-Vis photometry showed absorption band maxima at 274 nm (for all the tested amino acids – arising primarily from the tyrosine analogon N-Boc-*L*-Tyr, cp. Figure 10-2), 304 nm (Val, Ile; shoulder for Leu, Ser, Arg), 502 nm (Val, Leu, Ser, Ile) and 625 nm (Arg, see Figure XII-XXXVI). The shoulder around 360 nm (from oxidised N-Boc-*L*-Tyr, cp. Figure X-VI) was at the beginning of the incubation present only in the reference without additional amino acids (N-Boc-*L*-Tyr and AbT only) and to a smaller extent also in the preparations containing all seven tested amino acids and arginine (even less intense) but appeared as a discernible shoulder in preparations with lysine or arginine after two days of incubation (The reference and 7AS preparations remained virtually unchanged. see Figure XII-XXXVI). Absorption around 502 nm remained virtually unchanged between one and two days of incubation for preparations with the single amino acids Val, Leu or Ile but appeared leved out for preparations with Ser as the only free amino acid which showed a shoulder at 625 nm instead.
In the fluorescence spectra (Figure XII-XXXVI), an emission band centered on 649 nm ($\lambda_{ex,max1}$ = 257 nm, $\lambda_{ex,max2}$ = 300 nm) was visible for preparations containing arginine (see Figure XII-XXXVI), 7AS (≈ 4 % of the intensity in preparations containing only Arg) and Ser (≈ 1 % signal intensity).
The species responsible for the absorption band around 502 nm seems to be unstable in the presence of methanol (cp. 12.3.3, Stability test with MeOH:) as the band in the spectra of the samples containing AbT and Val ($E_{502,\,0}$ = 0,143), Leu ($E_{502,\,0}$ = 0,128) or Ile ($E_{502,\,0}$ = 0,090) disappeared almost completely in the course of 5 days at 50 % (v+v) MeOH which had also seen the concomitant formation of a new peak at 600 nm (equivalent to the peak at 625 nm in sodium phosphate buffer without methanol, *vide supra*) for single amino acid preparations with Arg (which displayed that peak from the beginning of the stability test with methanol), Leu, Val, Ser and Ile (cp. Figure XII-XXXVII). The formation of the absorption band around 600 nm / 625 nm for all the tested amino acids except lysine indicates a chromophore that does not contain any specific amino acid sidechains but is rather formed from the functional units common to the individual preparations. The biggest common substructure of the tested free amino acids is (3-dehydro-) alanine and in all the preparations oxidised N-Boc-*L*-Tyr (N-Boc-*o*-dopaquinone) was present. The observation that the presence of arginine, the most basic of the proteinogenic amino acids with a pI of 11,76 [198], promoted the formation of the species responsible for the absorption at 625 nm was interpreted as indication for the contribution of base catalysis in its formation. As summarised in Figure 12-8, this assumption and the observation of an absorption peak at 625 nm in the Vis spectrum tilted the interpretation of the MS^n data in favour of an aldol condensation between two N-Boc-*o*-dopaquinons for the fractions absorbing at 595 nm (the maximally quantifiable wavelength of the used UVD) rather than a radical-mediated, comproportional coupling of a *o*-diphenolic moieties with its respective *o*-diquinone [75, 78, 79] that may also explain the observed absorption with λ_{max} > 500 nm.
The second proposed reaction type beyond Michael-type 1-4 additions between tyrosine-derived quinones and free amino groups (e.g. in Lys side chains) [199-201] is the hetero Diels-Alder reaction ([4 + 2] cycloaddition) with *o*-quinons in the role of the diene [202, 203]. This type of reaction is assumed for the interpretation of MS^n data for fractions taken from OPA-derivatised amino acids at an retention time of 13,3 min (Ser, the same signal was seen in all preparations containing AbT) and 10,4 min (Ile, the corresponding UVD-signal was seen in preparations containg Ile and Leu, see Figure 12-8 and XIII.III).

In conclusion, within the present work the participations of non-tyrosine amino acids (namely Ala, Arg, Gly, His, Ile, Leu and Val) in the cross-linking of collagen brought about by the enzymatic action of tyrosinase in presence of atmospheric oxygen was demonstrated. MS^n-experiments carried out with amino acids modified during the cross-linking also revealed the presence of covalently linked, amino acid derived units larger than the original amino acid for which structures were proposed based on their fragmentation trees.

I. Introduction

I.I. Biosynthesis of fibrillar collagens

Reaction catalysed by procollagen-proline dioxygenase (**1.14.11.2**):

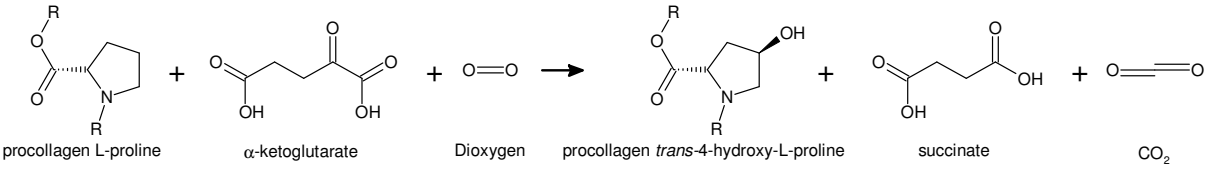

Reaction catalysed by procollagen-proline 3-dioxygenase (**1.14.11.7**):

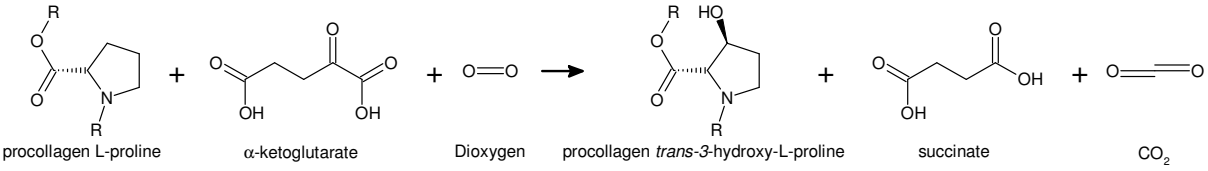

Reaction catalysed by procollagen-lysine 5-dioxygenase (**1.14.11.4**):

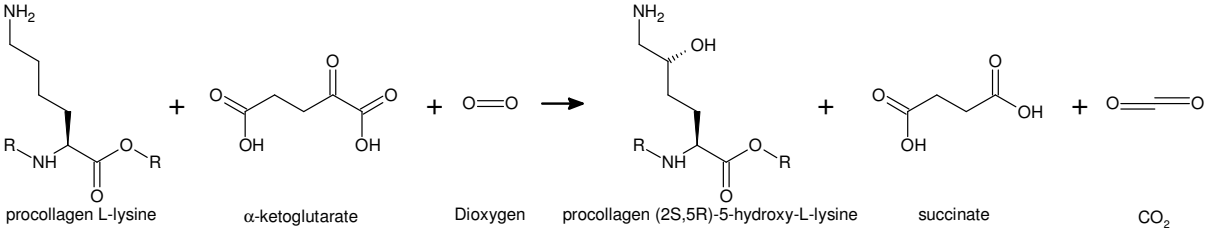

Scheme 13-1 hydroxylation of nascent collagen pro α-chains in the endoplasmic reticulum

Reaction catalysed by procollagen galactosyltransferase (**2.4.1.50**):

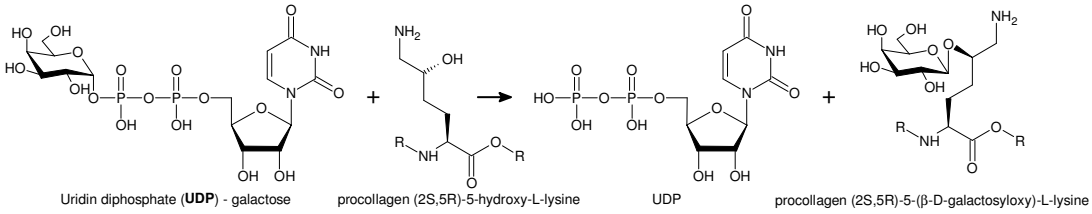

Reaction catalysed by procollagen glucosyltransferase (**2.4.1.66**):

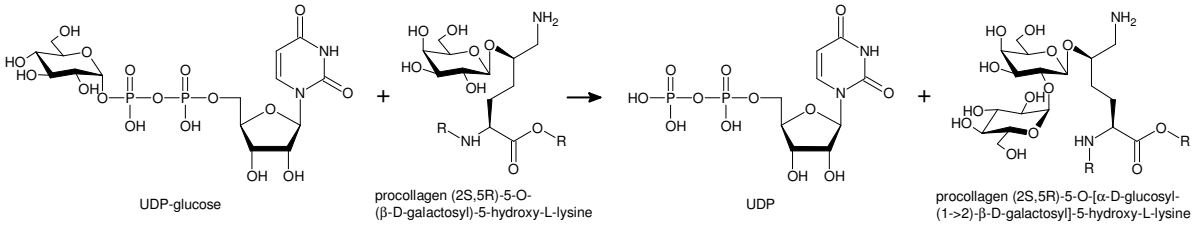

Scheme 13-2 glycosylation of Hyl in nascent collagen pro α-chains in the endoplasmic reticulum

Reaction catalysed by Peptidylprolyl isomerase (**5.2.1.8**):

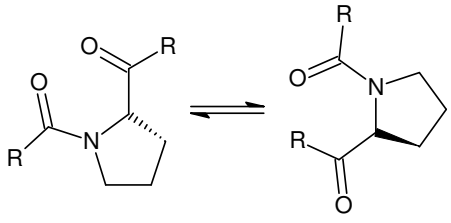

Scheme 13-3 *cis-trans* isomerisation of peptide bound proline catalysed by PPI

Reaction catalysed by protein-lysine 6-oxidase (**1.4.3.13**):

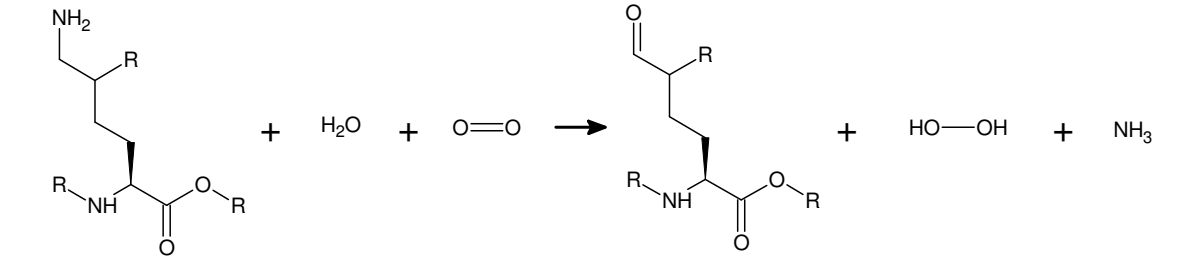

peptidyl-L-lysine (R = H) or L-5-hydroxy-lysine (R = OH) | water | dioxygen | peptidyl-L-lysine aldehyde (R = H, **allysine**) or L-5-hydroxy-lysine aldehyde (R = OH) | hydrogenperoxide | ammonia

Scheme 13-4 formation of allysine catalysed by lysyl oxidase

I.I.I. Formation of the natural cross-links of collagen

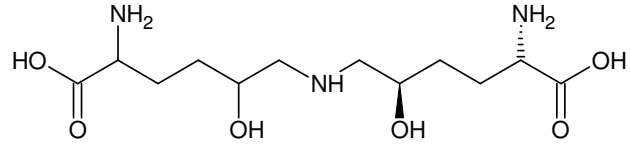

5,5'-Dihydroxylysinonorleucin (**DHLNL**)
Molecular Formula = $C_{12}H_{25}N_3O_6$
Monoisotopic Mass = 307.174336 Da

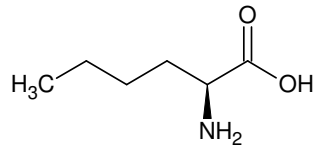

L-Norleucin

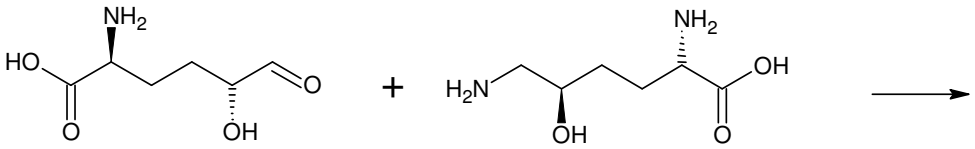

Hydroxylysinaldehyd + Hydroxylysin

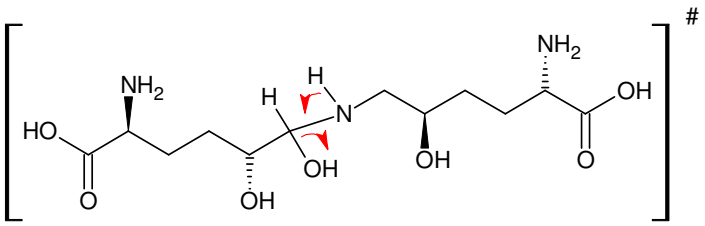

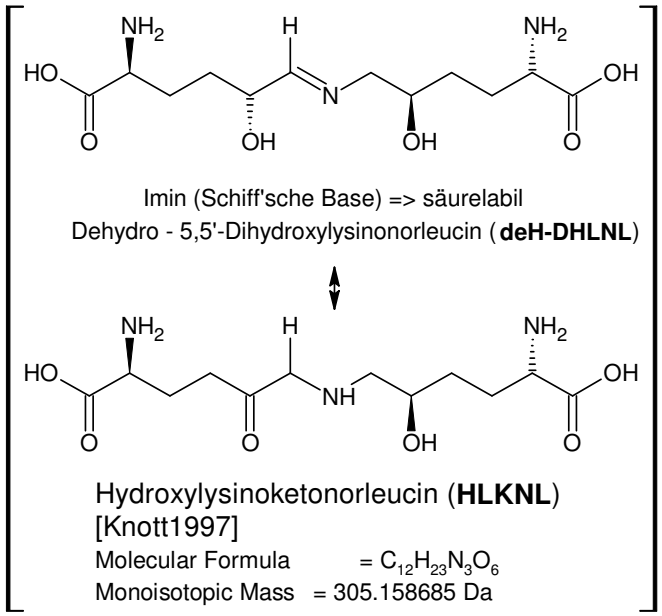

Imin (Schiff'sche Base) => säurelabil
Dehydro - 5,5'-Dihydroxylysinonorleucin (**deH-DHLNL**)

Hydroxylysinoketonorleucin (**HLKNL**)
[Knott1997]
Molecular Formula = $C_{12}H_{23}N_3O_6$
Monoisotopic Mass = 305.158685 Da

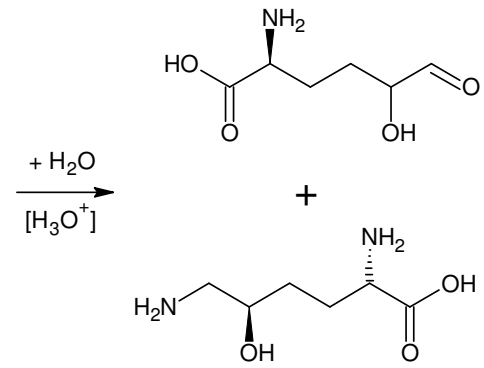

Die kürzere Abkürzung bezeichnet die **reduzierte Form** (historisch bedingt: Nachweis über **$NaBT_3$**), mit der Vorsilbe **deH-** ist die native Form (**Schiff'sche Base**) gemeint.

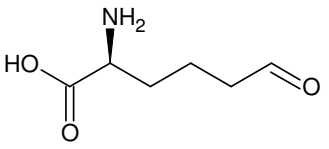

Lysinaldehyd

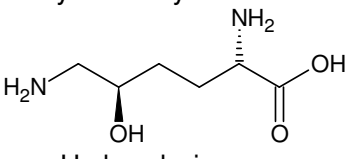

Hydroxylysin

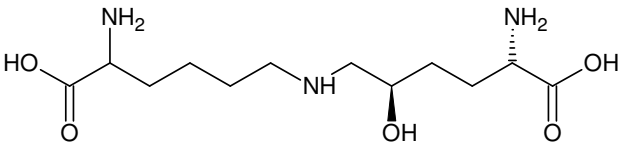

5-Hydroxylysinonorleucin (**HLNL**)
vor Reduktion: 5-Lysinoketonorleucin (**LKNL**)
[Knott1997]
Molecular Formula = $C_{12}H_{25}N_3O_5$
Monoisotopic Mass = 291.179421 Da

Scheme 13-5 formation of the reducible cross-links DHLNL and HLNL [41]

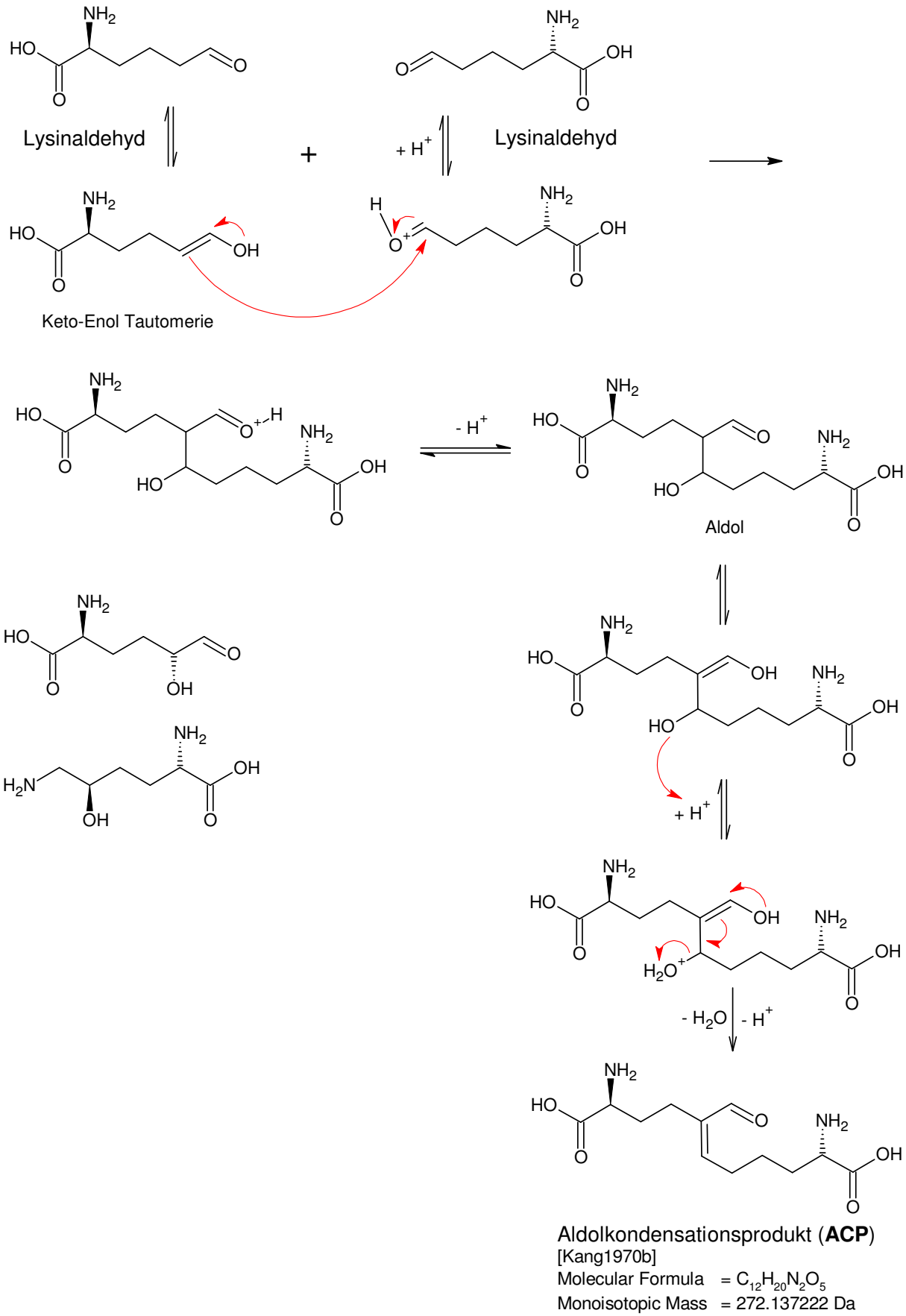

Aldolkondensationsprodukt (**ACP**)
[Kang1970b]
Molecular Formula = $C_{12}H_{20}N_2O_5$
Monoisotopic Mass = 272.137222 Da

Scheme 13-6 formation of the reducible aldol condensation product (ACP) [40]

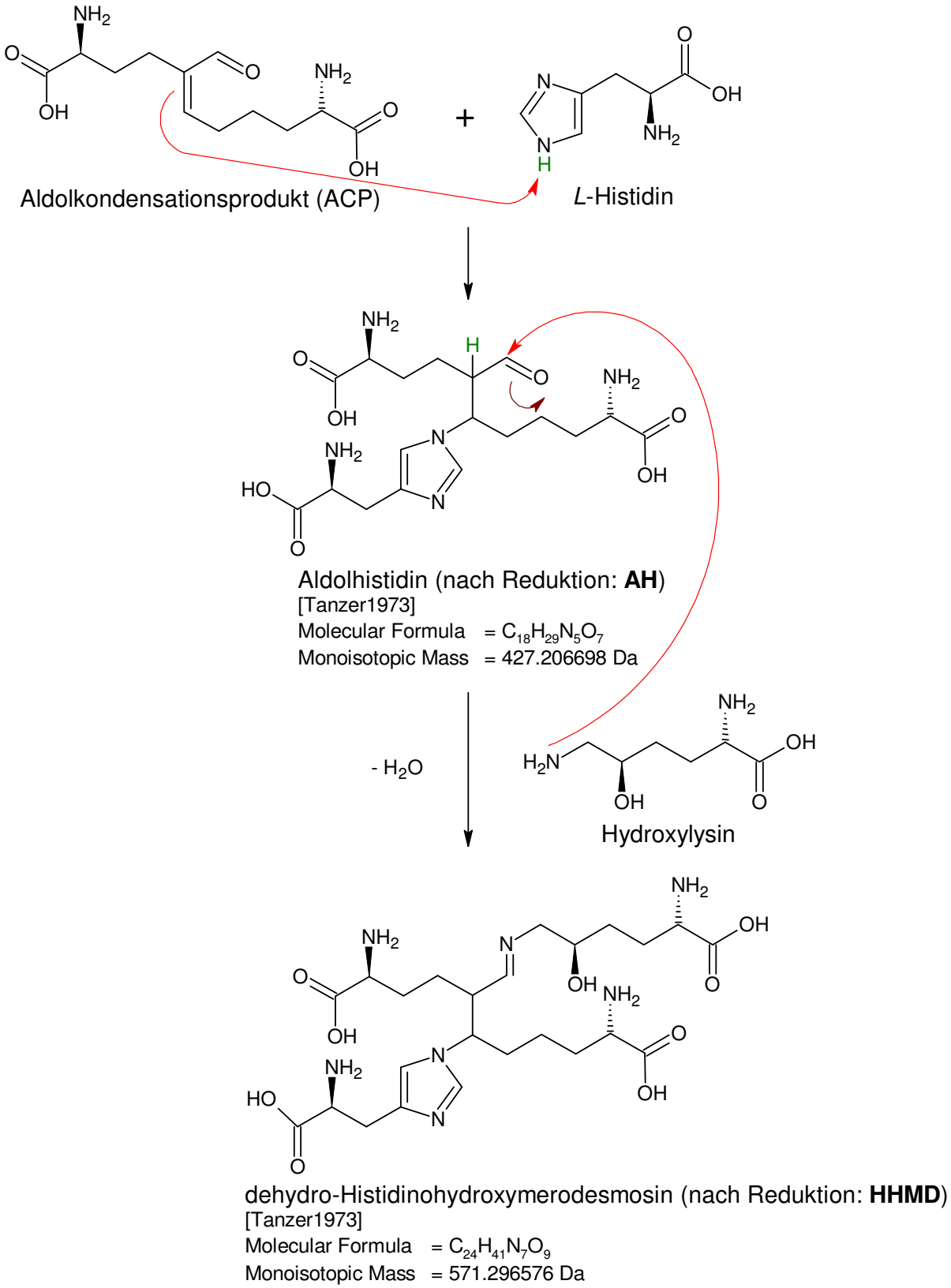

Scheme 13-7 formation of the reducible cross-links AH and HHMD [42]

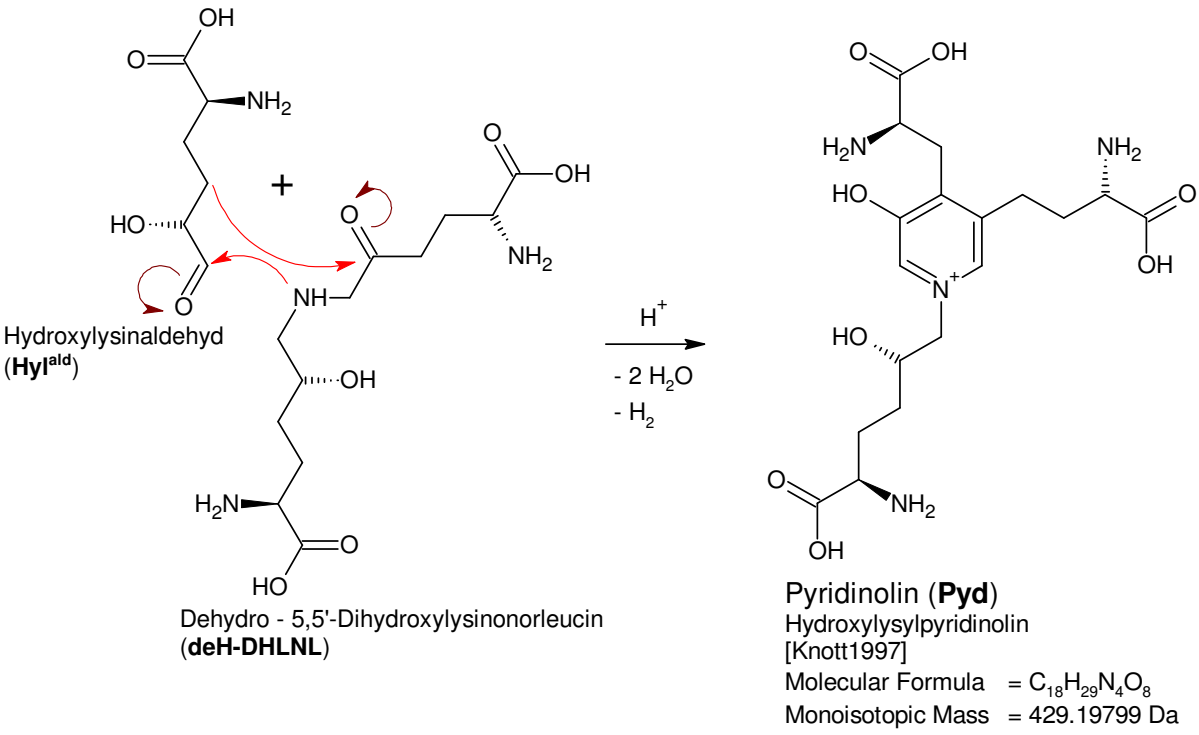

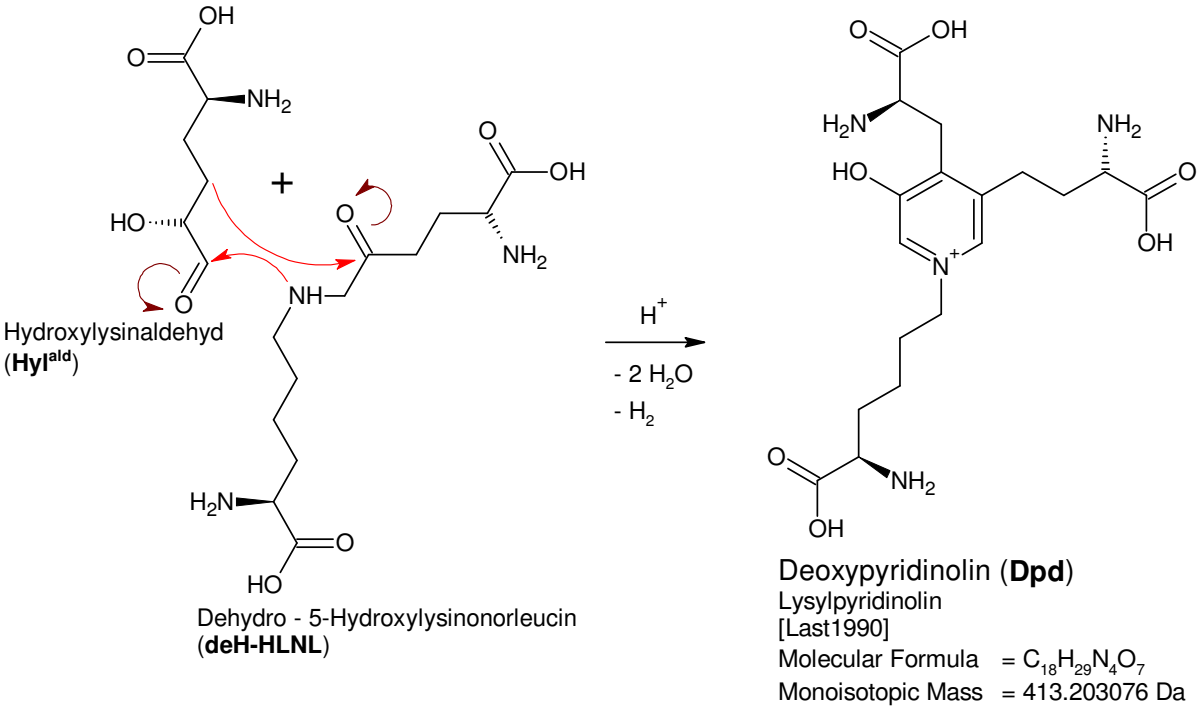

Scheme 13-8 formation of the mature pyridinium cross-links Pyd [41] and Dpd [48]

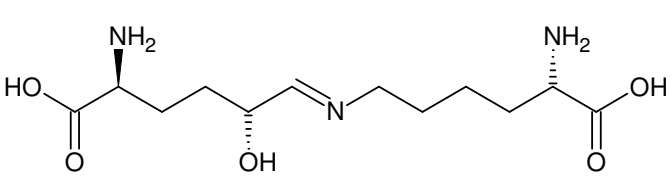

Dehydro - 5-Hydroxylysinonorleucin (**deH-HLNL**)

+

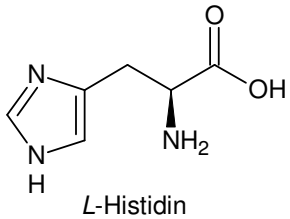

L-Histidin

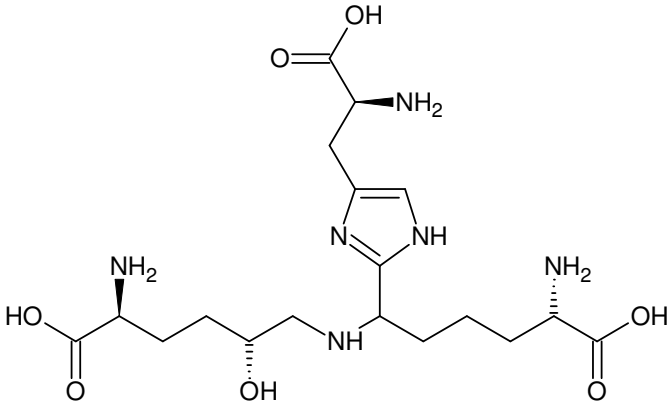

Histidonohydroxylysinonorleucin (**HHL**)
[Mechanic1987, Yamauchi1991]
Molecular Formula = $C_{18}H_{32}N_6O_7$
Monoisotopic Mass = 444.233247 Da

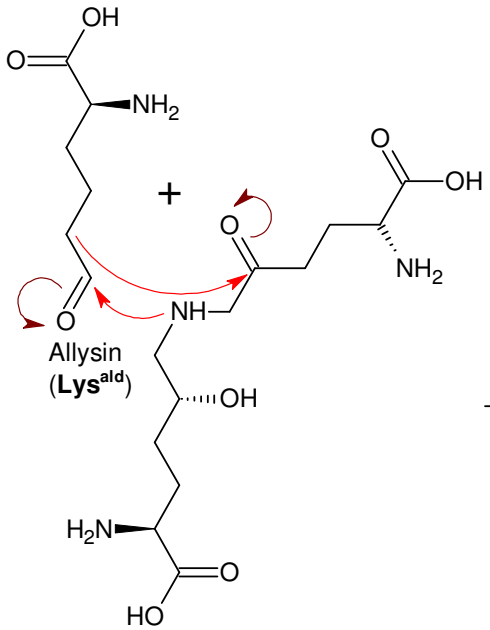

Allysin
(**Lys^{ald}**)

+

Dehydro - 5,5'-Dihydroxylysinonorleucin
(**deH-DHLNL**)

H^+
- 2 H_2O

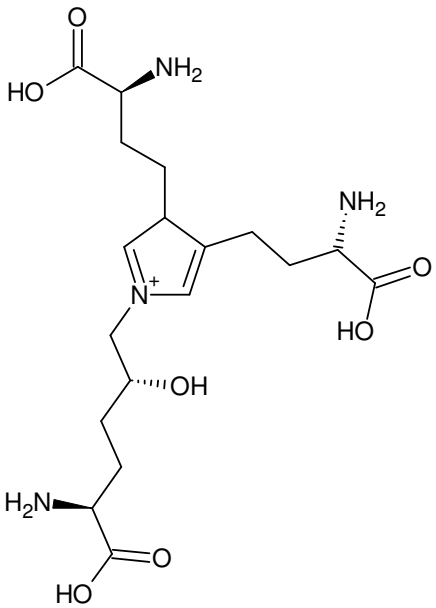

Pyrrolquervernetzung (**Pyrrol**)
[Knott1997]
Molecular Formula = $C_{18}H_{31}N_4O_7$
Monoisotopic Mass = 415.218726 Da

Scheme 13-9 formation of the mature cross-links HHL [44, 45] and the putative pyrrole [41]

I.II. Tyrosinase

Reaction catalysed by monophenol monooxygenase (**1.14.18.1**):

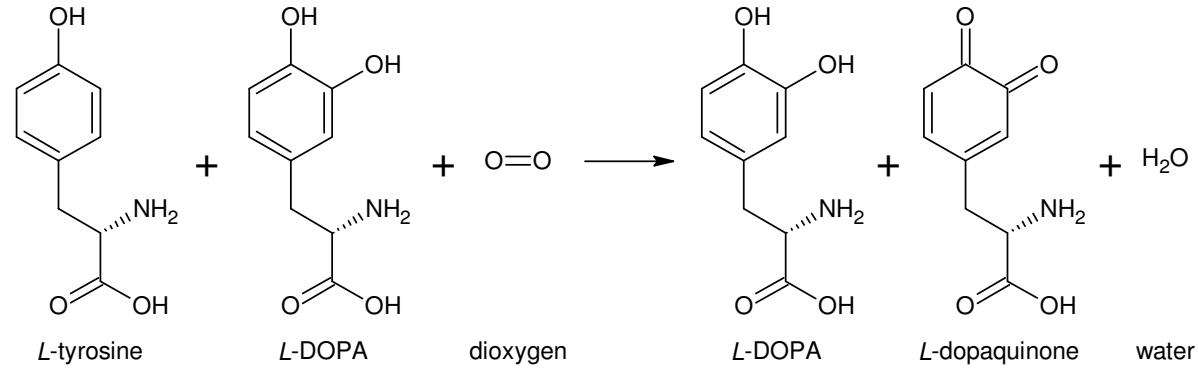

L-tyrosine *L*-DOPA dioxygen *L*-DOPA *L*-dopaquinone water

Reaction catalysed by catechol oxidase (**1.10.3.1**):

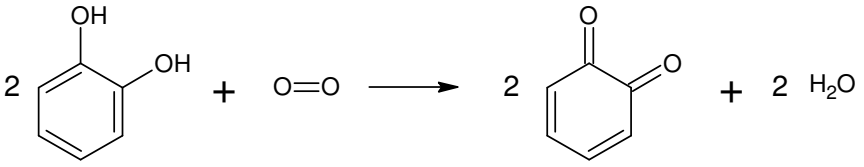

catechol dioxygen *o*-benzoquinone water

Scheme 13-10 catalytic activities of tyrosinase

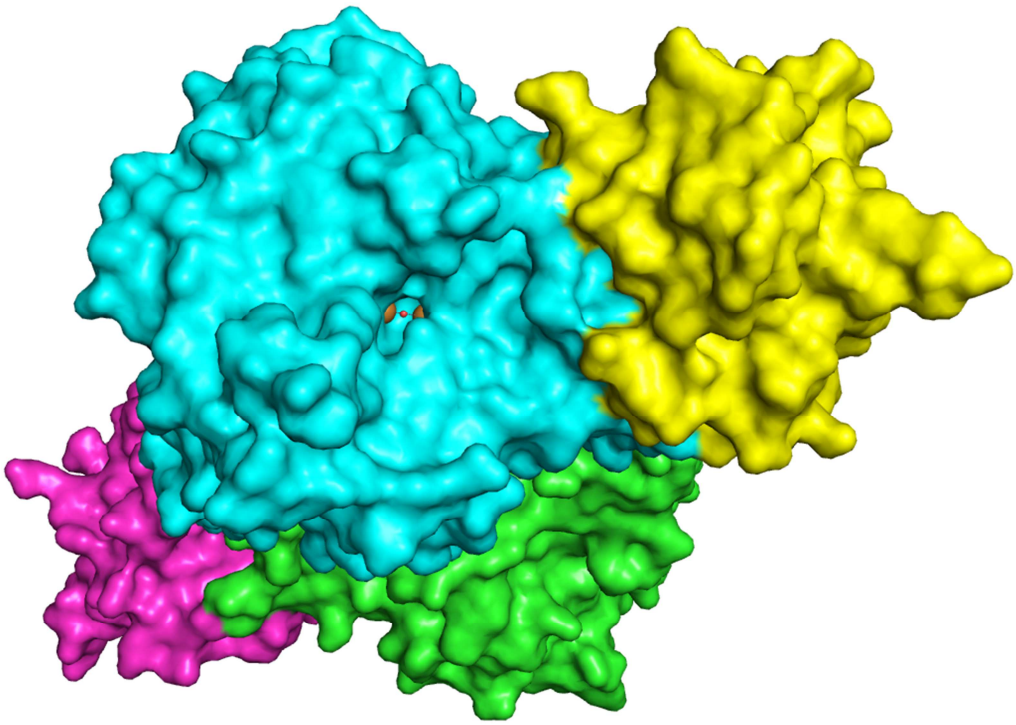

Figure I-I tetrameric H_2L_2 structure of *Agaricus bisporus* tyrosinase (PDB entry 2Y9W, [88], visual axis identical to Figure 1-4)

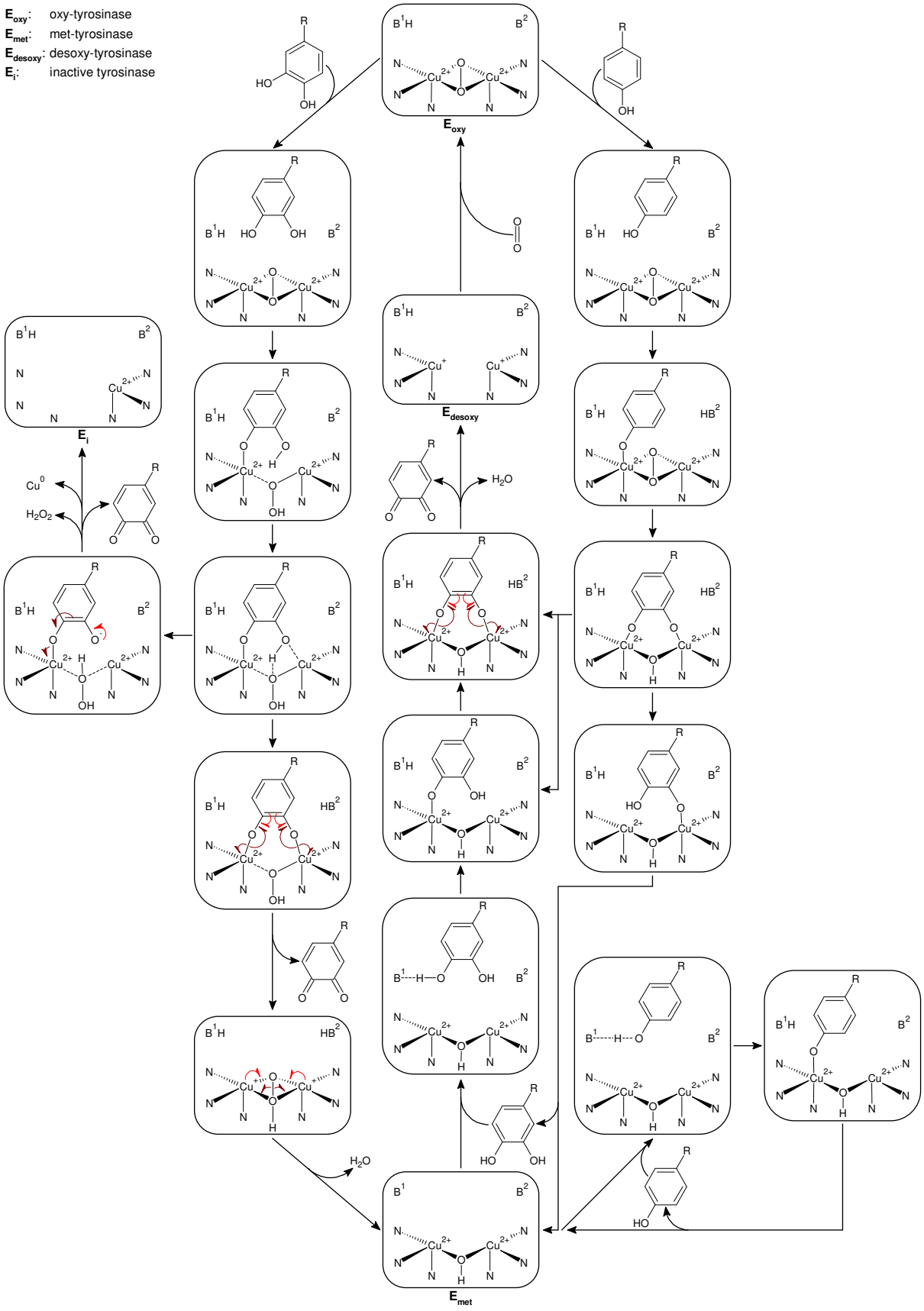

Scheme 13-11 proposed structural mechanism for the action of tyrosinase on mono- and diphenols [102, 103, 105, 106, 116, 118, 121, 124, 204]

II. Materials and devices

Character strings given in bold at the beginning of the line denote abbreviations used for the respective compound.

II.I. Enzymes

- **BoT1**: native tyrosinase from *Botryosphaeria obtusa*, kindly provided by Novozymes, Denmark (luna 2007-46082)
- **BoT2**: C-terminally processed tyrosinase from *Botryosphaeria obtusa*, kindly provided by Novozymes, Denmark (luna 2006-50861-01)
- **AbT**: tyrosinase from *Agaricus bisporus*, Fluka 93898, Lot# 1331446
- **T4**: peroxidase from *Bjerkandera adusta*, JenaBios EN-203 Lot# S-1-10-JB-06
- **TvL**: laccase from *Trametes versicolor*, Fluka 53739, Lot# 1350185
- **ThL**: laccase from *Trametes hirsuta*, isolated and purified as described in [205]

II.II. Substrates

- **K**: acid soluble collagen type I, extracted with 0,1 M acetic acid from bovine split; kindly provided by the Forschungsinstitut für Leder und Kunstoffbahnen (FILK) Freiberg, Germany (A001398)
- **I-b**: insulin chain B oxidised, from bovine pancreas; Sigma I6383, Lot# 078k5062 and 020M5056 (“new”)

II.III. General: solvents, pipettes, glassware and consumables

- **ddH_2O**: deionized water from a Barnstead NANOpure D4700 Analytical Deionization System, ρ > 12 MΩ cm
- **dH_2O**: demineralised water
- **ACN**: acetonitrile, Roth AE 70.2
- **MeOH**: methano,l Roth AE 71.2
- **THF**: tetrahydrofuran, Sigma 186562
- Glacial acetic acid, Roth 3738.5

Micro tube 2 ml PP, Sarstedt 72.695.500
Micro tube 1,5 ml PP, Sarstedt 72.690.001
Micropipettes 0,5 – 10; 5 – 50; 10 – 100; 20 – 200; 100 – 1000 µl, Socorex Acura® manual 825
Pipette tip 10 µl neutral, Sarstedt 70.1130
Pipette tip 200 µl yellow, Sarstedt 70.760.002
Pipette tip 1000 µl blue, Sarstedt 70.762
2004 MP6E analytical balance, Sartorius
S-4002 laboratory scales, Denver Instrument
Volumetric pipettes 25; 50; 100 ml, Hecht Assistent®
Volumetric pipettes 10; 15 ml, Brand Blaubrand®
Volumetric flasks 2; 5; 100; 250; 1000 ml, Brand Blaubrand®
Beakers 10; 25; 50; 100; 250; 500; 5000 ml, Schott Duran®

II.IV. Protein hydrolysis with HCl

- **HCl**: hydrochloric acid 37 % (w/v), Roth X942.2
- **Blue gel**: silica gel pellets with $CoCl_2$ as moisture indicator, Roth 9351.1
- Oil bath filling (lab) for oil baths up to approx. 250 °C, Merck 1.06900.5000

Culture tubes (Pyrex®) with 13 mm screw caps equipped with PTFE liners, SciLabware 1636/24MP
RCT basic magnetic stirrer/heater with PT1000.60 temperature sensor, IKA®-Werke
48-well microtitre plate, flat bottom, Greiner Bio-One
Vacuum exsiccator (flange i.d. 170 mm) filled with blue gel, Schott Duran®
UM 500 laboratory type drying cabinet, Memmert
Membrane pump, Ilmvac 113024

II.V. Amino acid analysis after pre-column derivatisation with OPA

- Casamino acids, BD Biosciences 223050, Bacto™
- Borax (disodium tetraborate, $Na_2B_4O_7$), Riedel-de Haën 11648
- **OPA**: Phthaldialdehyde, Fluka 79760
- β-Mercaptoethanol, Sigma M-3148
- 3-Mercaptopropionic acid, Aldrich M580-1
- Sodium dihydrogen phosphate dihydrate (NaH_2PO_4 . 2 H_2O), Roth T879.2
- **NaOAc**: Sodium acetate trihydrate, Roth 6779.2
- **Nor**: *L*-Norvaline, Sigma N7627
- **Ala**: *L*-Alanine, Merck 1007
- **Arg,** *L*-Arginine, Sigma A-5006
- **Asn**: *L*-Asparagine monohydrate, Merck 12117
- **Asp**: *L*-Aspartic acid, Fluka 11189
- **Cys**: *L*-Cysteine hydrochloride monohydrate, Sigma C6852
- **Gln**: *L*-Glutamine, Fluka 49419
- **Glu**: *L*-Glutamic acid, Fluka 49449
- **Gly**: Glycine, Roth 3908.3
- **His**: *L*-Histidine, Roth 3852.3
- **Ile**: *L*-Isoleucine, Merck 5362
- **Leu**: *L*-Leucine, Merck 5360
- **Lys**: *L*-Lysine hydrochloride, Sigma 8662
- **Met**: *L*-Methionine, Merck 5707
- **Phe**: *L*-Phenylalanine, Merck 7256
- **Pro**: *L*-Proline, Merck 7434
- **Ser**: *L*-Serine, Merck 7769
- **Thr**: *L*-Threonine, Merck 8411
- **Trp**: *L*-Tryptophan, Roth 4858.1
- **Tyr**: *L*-Tyrosine, Fluka 93829
- **Val**: *L*-Valine, Merck 8495.0100
- **Orn**: *L*-Ornithine hydrochloride, Merck 6906
- Ammonium hydrogen carbonate, Aldrich 28,509-9
- Ammonia 25 % (w/v) in water, Merck 5432
- Triethylamine, Sigma T0886
- HCl standard solution 0,1 M, Aldrich 318965
- Sodium hydroxide 50 % (w/v), Roth 8655.2

HPLC system:

Chromeleon® Version 6.80 SR7 Build 2528 controlling software, Dionex
SOR-100 solvent rack, Dionex
P680 HPLC pump, Dionex
UltiMate 3000 autosampler, Dionex
TCC-100 thermostatted colum compartement, Dionex
UVD 170U diode array detector, Dionex
Foxy® R1 fraction collector, Teledyne Isco

Eurospher 100-5 C18 250 x 4,6 mm analytical column with precolumn, Knauer 25VE181ESJ
1,5 ml glass vials, Markus Bruckner Analysentechnik 610 002
Crimp caps 11 mm NR/TEF red-orange, Markus Bruckner Analysentechnik 611 003
0,1 ml micro-insert 31 x 6 mm, Markus Bruckner Analysentechnik 06 09 0357
Vortex-Genie 2 mixer, Scientific Industries
Mikro 200R type 2405 benchtop centrifuge, Hettich
Sonorex Super RK 102 H ultrasonic cleaning unit, Bandelin electronic
InlabExpert Pt 1000 pH electrode, Mettler Toledo
Piston Burette Titronic® 97/20, Schott

II.VI. Gel electrophoresis

- Sinapic acid, Fluka 85429
- Acrylamide 40 % (acrylamide:bi-sacrylamide 37,5:1), Roth T802.1
- **Tris**: Tris-(hydroxymethyl)-aminomethane, Roth 4855.2
- **SDS**: Sodium lauryl sulphate (sodium dodecyl sulphate) pellets, Roth CN30.3
- Ammonium peroxodisulphate (ammonium persulphate), Merck K19701601, Roth 9529.3
- **TEMED**: N, N, N', N'-Tetramethylethylenediamine, Acros Organics 138450500
- Isopropanol, Roth 7343.1
- **Gly**: Glycine, Roth 3908.3
- β-Mercaptoethanol, Sigma M-3148
- Glycerin (glycerol), Roth 3783.2
- Bromophenol blue, Merck 8122
- Urea, Roth 2317.1
- Carbonic anhydrase from bovine erythrocytes, Sigma C7025
- Bovine albumin, Sigma A-8531
- Alcohol dehydrogenase from yeast, Sigma A-8656
- β-amylase from sweet potato, Sigma A-8781
- Apoferritin from equine spleen, Sigma A-3660
- Bovine thyroglobulin, Sigma T9145
- Agarose, Peqlab 35-1020
- Acryl-Glide™ (siloxanes and ethyl sulphate in ethanol and isopropanol), amresco E319
- N,N'-Methylenebis(acrylamide) (bis-acrylamide), Sigma 146072
- **bis-Tris**: 2,2'-Bis(hydroxymethyl)-2, 2', 2''-nitrilo-triethanol, Aldrich 15,666-3
- **EDTA**: Ethylenediamine-tetraacetic acid 2 Na . 2 H_2O, Roth 8043.2
- **MES**: 2-(N-morpholino)ethanesulfonic acid, Sigma M8250
- Sodium disulfite ($Na_2S_2O_5$), Merck 1.06528.0500
- *tert*-Butanol, Roth 4323.1
- **CBB R-250**: Coomassie brilliant blue R-250 (C.I. 42660), BioRad 161-0400
- Biebrich scarlet (C.I. 26905), Sigma B-6008
- **CBB G-250**: Coomassie brilliant blue G-250 (C.I. 42655), BioRad 161-0406
- Aluminium sulphate ($Al_2(SO_4)_3 \cdot (H_2O)_x$, x = 14 - 18), Merck 1102.1000
- Ethanol 96 % with 1 % MEK (methyl ethyl ketone, butanone), Roth T171.1
- Phosphoric acid (orthophosphoric acid, H_3PO_4), Sigma 79622

- Formaldehyde 37 % (w/v, formalin), Roth 4979.1
- Sodium thiosulphate, Merck 6516
- Silver nitrate, Merck 1512.0250
- Sodium carbonate (washing soda, Na_2CO_3) anhydrous, Riedel-de Haën 13419

Mini Protean® 3 gel electrophoresis system, BioRad
H6370 Electrophoretic Gel System, Savant
Thermomixer comfort with thermoblocks for 24 x 1,5 or 2 ml micro tubes, Eppendorf 5355
ZBE 30-10 ice machine, Ziegra
Promax 2020 reziprocating platform shaker, Heidolph
HP Scanjet 4890 photo scanner, Hewlett-Packard
CorelDraw X3 v. 13.0.0.667, Corel

II.VII. MS^n analysis

- ESI-T Tuning Mix, Agilent G2431A
- Phenolphthalein, Sigma P9750

1100 Series LC/MSD Trap SL mass spectrometer with ESI interface (Agilent G1948A), Agilent
E1M18 rotary vane dual stage mechanical vacuum pump, Edwards A34317984
1750 RN 500 µl glass syringe, Hamilton 81230/01
KDS100 syringe pump, KD Scientific

II.VIII. Photo- and flourometry

- **ABTS**: 2,2´-azinobis(3-ethylbenzthiazoline-6-sulfonic acid), Fluka 11557
- **Tyr**: *L*-Tyrosine, Fluka 93829
- **NH_4Ac**: Ammonium acetate, Merck 2376679
- Sodium dihydrogen phosphate dihydrate (NaH_2PO_4 . 2 H_2O), Roth T879.2
- Disodium hydrogen phosphate dihydrate (Na_2HPO_4 . 2 H_2O), Roth 4984.1

Infinite® M200 plate reader, Tecan
U-2001 double beam spectrophotometer, Hitachi
PS cuvettes with 10 mm optical path length and 750 µl max. volume, Sarstedt 67.742
Rotilabo®-precision glass cuvette with 10 mm optical path length and 700 µl volume, Roth X856.1
BD Falcon® microtiter plates, 96 wells, PS UV-transparent, flat bottom, BD Biosciences 353261
Microtiter plates, 96 wells, PS black, flat bottom, Greiner Bio-One 655079

II.IX. Vibrational spectroscopy

RamanStation 400 equipped with a red laser (λ = 785 nm), PerkinElmer
Spectrum 100 equipped with the matched Universal ATR head, PerkinElmer
Vacuum exsiccator (flange i.d. 170 mm) filled with blue gel, Schott Duran®
Aluminium foil, household quality
Microscope slides with cut edges 76 x 26 mm, Roth 0656.1

II.X. Synthesis of dityrosine

- **Tyr**: *L*-Tyrosine, Fluka 93829
- Manganese(III) acetate dihydrate, Aldrich 215880
- Ammonia solution 30 – 33 % (w/v) in water, Roth P093.1
- n-Heptane, Merck 1.04379.1000
- Diethyl ether, Roth 3942.2

- Acetone, Roth KK40.1
- Cyclohexane, Roth 6570.3
- Toluene, Roth 7346.1
- Chloroform, Roth Y015.2
- Dichloromethane, Roth KK47.1
- n-Butanol, Merck 1.01988.1000
- Isopropanol, Roth 7343.1
- Ethanol 100 %, AustrAlco Österr. Alkoholhandels GmbH
- **TFA**: Trifluoroacetic acid, Sigma T6508

Sonorex Super RK 102 H ultrasonic bath, Bandelin electronic
Glass frit porosity 4 (pore size 10 - 16 µm), Schott Duran®
VV 2000 rotary evaporator, Heidolph
Ceramic mortar (70 ml) and pestle, Haldenwanger

II.XI. Synthesis and purification of N-Boc-*L*-Tyr

- 2-Chloroethanol, Aldrich 18,574-4
- Ethyl acetate (acetic ester), Roth 7338.3
- 1-4 Dioxane, Sigma D-9553
- **Tyr**: *L*-Tyrosine, Fluka 93829
- Triethylamine, Fluka 90340
- Di-*tert*-butyldicarbonate, Sigma 34660
- Ethyl acetate (acetic ester), Roth 6784.2
- Sodium chloride (NaCl), Roth 3957.2
- Calcium chloride ($CaCl_2$) anhydrous, Acros Organics 300380010
- Sodium hydroxide pellets, Roth 6771.2
- *L*-DOPA (3,4-Dihydroxy-*L*-phenylalanine), Sigma D9628

Glass frit porosity 5 (pore size 1,0 - 1,6 µm), Schott Duran®
Separatory funnel 250 ml with stopcock and taper joint stopper, Schott Duran®
VV 2000 rotary evaporator, Heidolph
Vivaspin® 2 3000 MWCO PES centrifugal concentrator tubes, Vivaproducts VS0291

II.XII. Reduction with $NaBH_4$

- Sodium borohydride, Aldrich 71320
- Acetone, Roth KK40.1
- Ammonium carbonate ($(NH_4)_2CO_3$), Merck 938
- Ammonium hydrogen carbonate (ammonium bicarbonate, NH_4HCO_3), Aldrich 28,509-9

II.XIII. Preparations

- Copper(II) chloride dihydrate, Merck 1.02733.0250
- **DAPI**: 4',6-diamidino-2-phenylindole dihydrochloride, Invitrogen D1306
- SlowFade® Gold Antifade Reagent, Invitrogen S36936
- Agar-Agar, Kobe 1, Roth 5210.2
- LB-Broth, Roth X968.2
- Polypeptide SDS-PAGE standard, BioRad 161-0326
- PageRuler™ prestained protein ladder, Fermentas SM0671
- Silver stain SDS-PAGE standards, low Range, BioRad 161-0314

DM 5500 Q fluorescence microscope, Leica
N-400M optical microscope, Optika Microscopes
CV-EL 18 L GS autoclave, CertoClav
Petri dishes PS sterile, Roth TA19.1
Drigalski spatula, stainless steel, Roth K732.1
Teclu burner, Lactan 320507400
Centrifuge filter system Mini, for max. 500 µl, 0,2 µm pore size PET- membrane, Roth EL89.1
Dual Digital Model 20 oxygen measurement controller with 2 Clark-electrodes, Rank Brothers
Zorbax GF-250 4 µm 9,4 x 250 mm analytical GPC column, Agilent
Superdex 200 10/300 GL preparative GPC column, GE Healthcare

III. Protein hydrolysis with HCl

III.I. Mathematical modelling

III.I.I. Model 1-1

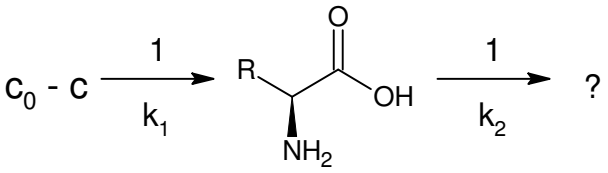

Release without degradation:

$\dot{c} = k_1 \cdot (c_0 - c) = k_1 \cdot c_0 - k_1 \cdot c$
$\frac{dc}{dt} + k_1 \cdot c = k_1 \cdot c_0$ lin. ODE of 1. order (1)

homogeneous first-order linear ordinary differential equation: $\frac{dc}{dt} + k_1 \cdot c = 0$
$\frac{dc}{dt} = -k_1 \cdot c \quad \frac{dc}{c} = -k_1 \cdot dt \quad \int \frac{1}{c} dc = -k_1 \int dt \qquad ln|c| = -k_1 \cdot t + ln(C)$
$c_h = C \cdot e^{-k_1 t}$

particular solution of the inhomogenous ODE: $c_p = C(t) \cdot e^{-k_1 t}$ (variation of constants)
$\dot{c_p} = \dot{C}(t) \cdot e^{-k_1 t} + C(t) \cdot e^{-k_1 t} \cdot (-k_1)$
in (1): $\dot{C}(t) \cdot e^{-k_1 t} + C(t) \cdot e^{-k_1 t} \cdot (-k_1) + k_1 \cdot C(t) \cdot e^{-k_1 t} = k_1 \cdot c_0$
$\dot{C}(t) = \frac{k_1 \cdot c_0}{e^{-k_1 t}} = k_1 \cdot c_0 \cdot e^{k_1 t}$
$C(t) = \int \dot{C}(t) dt = k_1 \cdot c_0 \cdot \int e^{k_1 t} dt = c_0 \cdot e^{k_1 t} + const$
$m = k_1 \cdot t \qquad \frac{dm}{dt} = k_1 \qquad dt = \frac{dm}{k_1} \qquad \int e^m dt = \int e^m \cdot \frac{1}{k_1} \cdot dt = k_1^{-1} \cdot e^m = k_1^{-1} \cdot e^{k_1 t}$
$C(t) = c_0 \cdot e^{k_1 t}$

$c_p = c_0 \cdot e^{k_1 t} \cdot e^{-k_1 t} = c_0$
$c = c_h + c_p = C \cdot e^{-k_1 t} + c_0$ (2)

initial value problem: $c(0) = 0 \implies 0 = C \cdot e^0 + c_0 \Longrightarrow C = -c_0$
$c(t) = c_0 \cdot \left(1 - e^{-k_1 t}\right)$

Release and degradation:

$\dot{c} = k_1 \cdot \left(c_0 - c_0 \cdot \left(1 - e^{-k_1 t}\right)\right) - k_2 \cdot c = k_1 \cdot c_0 \cdot e^{-k_1 t} - k_2 \cdot c$
$\frac{dc}{dt} + k_2 \cdot c = k_1 \cdot c_0 \cdot e^{-k_1 t}$ lin. ODE of 1. order (3)

General formula for first-order linear ordinary differential equations:
$y' + f(x) \cdot y = g(x) \implies y(x) = e^{-\int f(x) dx} \cdot \left(\int g(x) \cdot e^{\int f(x) dx} dx + const\right)$ (4)

$c(t) = e^{-\int k_2 dx} \cdot \left(\int k_1 \cdot c_0 \cdot e^{-k_1 t} \cdot e^{\int k_2 dx} dx + C\right)$
$= e^{-k_2 \cdot t} \cdot \left(k_1 \cdot c_0 \cdot \int e^{(-k_1 + k_2) \cdot t} dx + C\right)$
$m = (k_2 - k_1) \cdot t \qquad \frac{dm}{dt} = k_2 - k_1 \quad dt = \frac{dm}{k_2 - k_1} \qquad \int e^m dt = (k_2 - k_1)^{-1} \cdot e^{(k_2 - k_1) \cdot t}$

$$c(t) = e^{-k_2 \cdot t} \cdot \left(k_1 \cdot c_0 \cdot e^{(-k_1+k_2)\cdot t} \cdot \frac{1}{k_2-k_1} + C\right) \tag{5}$$

initial value problem: $c(0) = 0 \implies 0 = 1 \cdot \left(k_1 \cdot c_0 \cdot 1 \cdot \frac{1}{k_2-k_1} + C\right) \implies C = \frac{k_1 \cdot c_0}{k_1-k_2}$

$$c(t) = e^{-k_2 \cdot t} \cdot \left(k_1 \cdot c_0 \cdot e^{(-k_1+k_2)\cdot t} \cdot \frac{1}{k_2-k_1} + \frac{k_1 \cdot c_0}{k_1-k_2}\right) = \frac{k_1 \cdot c_0}{k_1-k_2} \cdot e^{-k_2 \cdot t} \cdot \left(1 - e^{(k_2-k_1)\cdot t}\right) \tag{6}$$

III.I.II. Model 1-0

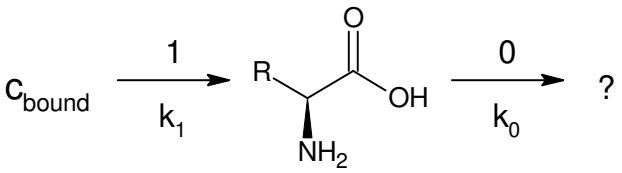

Release and degradation

$\dot{c} = k_1 \cdot c_{bound} - k_0$
$c_{bound} = c_0 - c - k_0 \cdot t$
$\dot{c} = k_1 \cdot (c_0 - c - k_0 \cdot t) - k_0$
$\dot{c} + k_1 \cdot c = k_1 \cdot c_0 - k_1 \cdot k_0 \cdot t - k_0$ lin. ODE of 1. order (7)

$$c(t) = e^{-\int k_1 dt} \cdot \left(\int (k_1 \cdot c_0 - k_1 \cdot k_0 \cdot t - k_0) \cdot e^{\int k_1 dt} dt + C\right)$$

$\int e^{k_1 \cdot t} \cdot (k_1 \cdot c_0 - k_1 \cdot k_0 \cdot t - k_0)\, dt =$ $\quad m = k_1 \cdot t \quad dt = \frac{dm}{k_1} \quad \int e^m dt = k_1^{-1} \cdot e^{k_1 t}$

$= \frac{1}{k_1} \cdot e^{k_1 \cdot t} \cdot (k_1 \cdot c_0 - k_0) + \int -e^{-k_1 \cdot t} \cdot k_1 \cdot k_0 \cdot t\, dt$

$\int -e^{-k_1 \cdot t} \cdot k_1 \cdot k_0 \cdot t\, dt =$

Integration by parts: $\int f' \cdot g\, dx = f \cdot g - \int f \cdot g'\, dx$

$$= \frac{1}{k_1} \cdot e^{k_1 \cdot t} \cdot (-k_1 \cdot k_0 \cdot t) - \int \frac{1}{k_1} \cdot e^{k_1 \cdot t} \cdot (-k_1 \cdot k_0)\, dt = e^{k_1 \cdot t} \cdot (-k_0 \cdot t) + e^{k_1 \cdot t} \cdot \frac{k_0}{k_1} + const$$

$$= \frac{k_0}{k_1} \cdot e^{k_1 \cdot t} \cdot (1 - k_1 \cdot t) + const$$

$$c(t) = e^{-k_1 \cdot t} \cdot \left(\frac{1}{k_1} \cdot e^{k_1 \cdot t} \cdot (k_1 \cdot c_0 - k_0) + \frac{k_0}{k_1} \cdot e^{k_1 \cdot t} \cdot (1 - k_1 \cdot t) + C\right)$$

$$= e^{-k_1 \cdot t} \cdot \left(e^{k_1 \cdot t} \cdot \left(c_0 - \frac{k_0}{k_1} + \frac{k_0}{k_1} - k_0 \cdot t\right) + C\right) = c_0 - k_0 \cdot t + e^{-k_1 \cdot t} \cdot C$$

initial value problem: $c(0) = 0 \implies 0 = c_0 - k_0 \cdot 0 + 1 \cdot C \implies C = -c_0$

$$c(t) = c_0 \cdot \left(1 - e^{-k_1 \cdot t}\right) - k_0 \cdot t \tag{8}$$

III.I.III. Model 1-1 2x

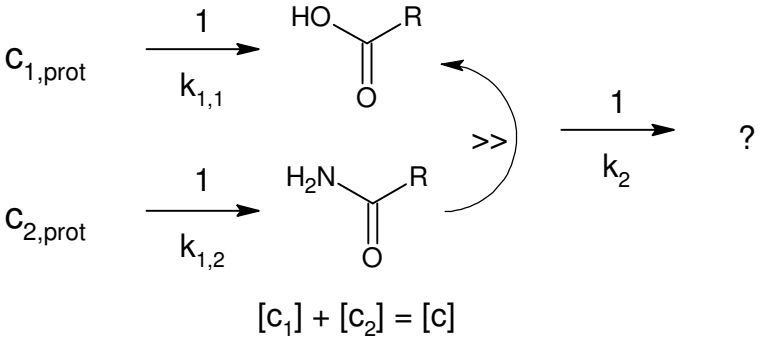

$[c_1] + [c_2] = [c]$

$$\dot{c} = k_{1,1} \cdot c_{1,prot} - k_2 \cdot c + k_{1,2} \cdot c_{2,prot} \quad (9)$$

Release independent of the concentration in the liquid phase:

$\dot{c}_{1,prot} = -k_{1,1} \cdot c_{1,prot}$ $\quad \dot{c}_{2,prot} = -k_{1,2} \cdot c_{2,prot}$

$\frac{dc}{dt} = -k \cdot c \quad \int \frac{dc}{c} = \int -k dt \quad ln|c| = -k \cdot t + ln(C)$

$c = e^{-k \cdot t + ln(C)} = C \cdot e^{-k \cdot t}$

Initial value problem: $c(0) = c_0 \implies M = c_0$

$$c_{prot}(t) = c_{prot,0} \cdot e^{-k_1 \cdot t} \quad (10)$$

Release and degradation:

(10) in (9): $\dot{c} = k_{1,1} \cdot c_{1,0} \cdot e^{-k_{1,1} \cdot t} - k_2 \cdot c + k_{1,2} \cdot c_{2,0} \cdot e^{-k_{1,2} \cdot t}$

$$\dot{c} + k_2 \cdot c = k_{1,1} \cdot c_{1,0} \cdot e^{-k_{1,1} \cdot t} + k_{1,2} \cdot c_{2,0} \cdot e^{-k_{1,2} \cdot t} \quad \text{1. order lin. ODE (11)}$$

$$c(t) = e^{-\int k_2 dt} \cdot \left(\int \left(k_{1,1} \cdot c_{1,0} \cdot e^{-k_{1,1} \cdot t} + k_{1,2} \cdot c_{2,0} \cdot e^{-k_{1,2} \cdot t} \right) \cdot e^{\int k_2 dt} dt + C \right)$$

$$\int k_2 dt = k_2 \cdot t + const$$

$$\int e^{k_2 \cdot t} \cdot \left(k_{1,1} \cdot c_{1,0} \cdot e^{-k_{1,1} \cdot t} + k_{1,2} \cdot c_{2,0} \cdot e^{-k_{1,2} \cdot t} \right) dt$$

$$= \int k_{1,1} \cdot c_{1,0} \cdot e^{(k_2 - k_{1,1}) \cdot t} \, dt + \int k_{1,2} \cdot c_{2,0} \cdot e^{(k_2 - k_{1,2}) \cdot t} \, dt$$

$$\int \mathrm{k} \cdot \mathrm{c}_0 \cdot e^{\mathrm{m} \cdot t} \, dt = \mathrm{k} \cdot \mathrm{c}_0 \cdot \frac{1}{m} \cdot e^{\mathrm{m} \cdot t}$$

$$c(t) = e^{-k_2 \cdot t} \cdot \left\{ \frac{k_{1,1} \cdot c_{1,0}}{k_2 - k_{1,1}} \cdot e^{(k_2 - k_{1,1}) \cdot t} + \frac{k_{1,2} \cdot c_{2,0}}{k_2 - k_{1,2}} \cdot e^{(k_2 - k_{1,2}) \cdot t} + C \right\}$$

Initial value problem: $c(0) = 0 \implies 0 = 1 \cdot \left\{ \frac{k_{1,1} \cdot c_{1,0}}{k_2 - k_{1,1}} \cdot 1 + \frac{k_{1,2} \cdot c_{2,0}}{k_2 - k_{1,2}} \cdot 1 + C \right\} \implies C = \frac{k_{1,1} \cdot c_{1,0}}{k_{1,1} - k_2} + \frac{k_{1,2} \cdot c_{2,0}}{k_{1,2} - k_2}$

$$c(t) = e^{-k_2 \cdot t} \cdot \left\{ \frac{k_{1,1} \cdot c_{1,0}}{k_2 - k_{1,1}} \cdot e^{(k_2 - k_{1,1}) \cdot t} + \frac{k_{1,2} \cdot c_{2,0}}{k_2 - k_{1,2}} \cdot e^{(k_2 - k_{1,2}) \cdot t} + \frac{k_{1,1} \cdot c_{1,0}}{k_{1,1} - k_2} + \frac{k_{1,2} \cdot c_{2,0}}{k_{1,2} - k_2} \right\}$$

$$c(t) = \frac{k_{1,1} \cdot c_{1,0}}{k_{1,1} - k_2} \cdot \left(e^{-k_2 \cdot t} - e^{-k_{1,1} \cdot t} \right) + \frac{k_{1,2} \cdot c_{2,0}}{k_{1,2} - k_2} \cdot \left(e^{-k_2 \cdot t} - e^{-k_{1,2} \cdot t} \right) \quad (12)$$

Comparison to model 1-1 (3.3.1):

$k_{1,2} = 0, c_{2,0} = 0; \; k_{1,1} \mapsto \mathrm{k}_1, c_{1,0} \mapsto c_0 \qquad \text{model } 1-1 \text{ 2x} \mapsto \text{model } 1-1$

$$c(t) = \frac{k_1 \cdot c_0}{k_1 - k_2} \cdot \left(e^{-k_2 \cdot t} - e^{-k_1 \cdot t} \right) = \frac{k_1 \cdot c_0}{k_1 - k_2} \cdot e^{-k_2 \cdot t} - \frac{k_1 \cdot c_0}{k_1 - k_2} \cdot e^{-k_1 \cdot t} = \frac{k_1 \cdot c_0}{k_1 - k_2} \cdot e^{-k_2 \cdot t} \cdot \left(1 - e^{(k_2 - k_1) \cdot t} \right) \text{cp. (6)}$$

III.II. Data evaluation scripts for Dataplot™

Model 1-1:

```
. kh.dpp
. Auswertungsschema für Dataplot Version 2/2005

ECHO OFF
SKIP 13
READ KH.txt t c
. unterschiedliche Startwerte für k1 und k2 nötig: gleiche Werte für k1 und k2 => Division
durch Null => Abbruch
PRE-FIT c = k1*c0/(k1-k2)*exp(-k2*t)*(1-exp((k2-k1)*t)) FOR c0=0.1 .18 1 FOR k1=0.01 0.099 1
FOR k2=0.0001 0.00999 0.1
. Schätzwerte für die freien Parameter als Ausgangspunkt für die nichtlineare Regression (mit
dem Levenberg-Marquardt Algorithmus)
. LET c0 = 1
. LET k1 = 0.2
. LET k2 = 0.1E-2
FIT ITERATIONS 500
FIT STANDARD DEVIATION 0.1E-12
FIT c = k1*c0/(k1-k2)*exp(-k2*t)*(1-exp((k2-k1)*t))
.
.  MULTIPLOT Zeilen Spalten ; .  MULTIPLOT CORNER COORDINATES (linke Ecke) rechts unten
(rechte Ecke) rechts unten (in % der Fensterausdehunung)
MULTIPLOT 2 2 ; MULTIPLOT CORNER COORDINATES 0 0 100 100
TITLE Messdaten
Y1LABEL c
XLABEL t
CHARACTERS + BLANK
LINES BLANK
PLOT c t
LINES BLANK SOLID
TITLE Hydrolyse: Kinetik 1. Ordnung
PLOT c PRED VS t
TITLE Residuen
Y1LABEL c(real) - c(Modell)
PLOT RES VS t
.
.   Probability Plot: The normal probability plot is formed by:
.     * Vertical axis: Ordered response values
.     * Horizontal axis: Normal order statistic medians
.
.  The observations are plotted as a function of the corresponding normal order statistic
medians which are defined as:
.
.      N(i) = G(U(i))
.
.  where U(i) are the uniform order statistic medians (defined below) and G is the percent
point function of the normal distribution. The percent point function is the inverse of the
cumulative distribution function (probability that x is less than or equal to some value).
That is, given a probability, we want the corresponding x of the cumulative distribution
function.
.
.  The uniform order statistic medians are defined as:
.       m(i) = 1 - m(n) for i = 1
.       m(i) = (i - 0.3175)/(n + 0.365) for i = 2, 3, ..., n-1
.       m(i) = 0.5(1/n) for i = n
.
TITLE Normalwahrscheinlichkeitsauftragung der Residuen
X1LABEL Normal N(0,1) Order Statistic Medians
NORMAL PROBABILITY PLOT RES
END MULTIPLOT
.
. Whenever a FIT command is executed, the coefficients and their standard deviations are
copied out to file dpst1f.dat in your current directory.
. since dpst1f.dat has no header lines
SKIP 0
. read in coefficients & standard deviations(coefficients) into vectors COEF and SDCOEF
READ DPST1F.DAT COEF SDCOEF
. copy the first element of SDCOEF into the parameter SDK1, …
LET SDK1 = SDCOEF(1)
LET SDC0 = SDCOEF(2)
LET SDK2 = SDCOEF(3)
.
WRITE "c0 = ^c0 (+/- ^SDC0)"
WRITE "k1 = ^k1 (+/- ^SDK1)"
WRITE "k2 = ^k2 (+/- ^SDK2)"
```

Model 1-1 2x:

```
. kh_2x.dpp
. Auswertungsschema für Dataplot Version 2/2005

ECHO OFF
SKIP 15
READ KH_2x.txt t c
.
LET FUNCTION cm = k11*c01/(k11-k2)*(exp(-k2*t)-exp(-k11*t)) + k12*c02/(k12-k2)*(exp(-k2*t)-
exp(-k12*t))
.
. HEAVE(X,C)   heavside function (==1 if X >= C, 0 otherwise)
.
. 20: 1,5 x cmax
LET FUNCTION cmod = cm + 100*HEAVE(k11+k12,2) + 100*HEAVE(c01+c02,20)
. LET k11 = 0.4
. LET k2 = 0.001
. LET k12 = 0.4
. LET c01 = 4
. LET c02 = 6
PRE-FIT c = cmod FOR c01=0.1 1.8 10 FOR k11=0.01 0.099 1 FOR k2=0.0001 0.00999 0.1
PRE-FIT c = cmod FOR c02=0.1 1.8 10 FOR k12=0.01 0.099 1 FOR k2=0.0001 0.00999 0.1
PRE-FIT c = cmod FOR c01=0.1 1.8 10 FOR c02=0.1 1.8 10
PRE-FIT c = cmod FOR c02=0.1 1.8 10 FOR k12=0.01 0.099 1 FOR k2=0.0001 0.00999 0.1
PRE-FIT c = cmod FOR c01=0.1 1.8 10 FOR k11=0.01 0.099 1 FOR k2=0.0001 0.00999 0.1
.
FIT ITERATIONS 500
FIT STANDARD DEVIATION 0.1E-12
FIT c = cmod
.
MULTIPLOT 2 2 ; MULTIPLOT CORNER COORDINATES 0 0 100 100
TITLE Messdaten
Y1LABEL c
XLABEL t
CHARACTERS + BLANK
LINES BLANK
PLOT c t
LINES BLANK SOLID
TITLE Hydrolyse: Kinetik 1. Ordnung
PLOT c PRED VS t
TITLE Residuen
Y1LABEL c(real) - c(Modell)
PLOT RES VS t
.
TITLE Normalwahrscheinlichkeitsauftragung der Residuen
X1LABEL Normal N(0,1) Order Statistic Medians
NORMAL PROBABILITY PLOT RES
END MULTIPLOT
.
SKIP 0
READ DPST1F.DAT COEF SDCOEF
LET SDK11 = SDCOEF(1)
LET SDC01 = SDCOEF(2)
LET SDK2 = SDCOEF(3)
LET SDK12 = SDCOEF(4)
LET SDC02 = SDCOEF(5)
.
WRITE "c01 = ^c01 (+/- ^SDC01)"
WRITE "k11 = ^k11 (+/- ^SDK11)"
WRITE "c02 = ^c02 (+/- ^SDC02)"
WRITE "k12 = ^k12 (+/- ^SDK12)"
WRITE "k2 = ^k2 (+/- ^SDK2)"
```

III.III. Data for the hydrolysis time series

Table III-I signal areas from RP-HPLC-UVD

Sample	Signal area / (mAU · min)																			
	Ala	Arg	Asn	Asp	Cys	Gln	Glu	Gly	His	Ile	Leu	Lys	Met	Phe	Ser	Thr	Trp	Tyr	Val	Nor
K Null 45min 1	55,77	14,63	-	57,96	-	-	39,28	189,34	0,91	2,36	11,94	11,83	4,78	6,57	17,39	11,86	1,12	1,49	9,06	28,29
K Null 45min 2	57,67	14,52	-	61,70	-	-	39,41	189,80	0,84	2,29	12,12	13,72	4,83	6,60	17,04	11,03	1,30	1,29	9,46	29,08
K Null 45min 3	56,28	14,51	-	59,87	-	-	41,10	195,54	0,97	2,53	12,66	14,72	5,09	6,96	18,09	12,07	1,22	1,65	9,20	28,52
K Null 1h 1	70,39	19,93	-	69,72	-	-	47,92	261,33	1,63	3,91	17,51	18,51	6,45	8,97	27,94	19,79	0,91	2,40	10,68	29,01
K Null 1h 2	62,65	17,20	-	62,37	-	-	40,53	219,51	1,22	2,94	14,44	16,94	5,34	7,42	22,09	14,21	1,03	1,95	9,29	28,39
K Null 1h 3	68,43	19,67	-	64,83	-	-	41,57	241,38	1,42	3,51	16,08	18,26	5,96	8,21	25,65	16,14	0,91	2,30	9,70	28,21
K Null 1,5h 1	86,55	29,91	-	77,29	-	-	53,10	334,62	2,58	6,69	23,88	22,41	8,14	12,34	40,56	31,13	0,61	3,25	14,14	27,84
K Null 1,5h 2	80,06	27,76	-	76,37	-	-	53,46	327,10	2,38	6,89	23,71	22,52	7,29	12,10	39,21	30,61	0,67	3,03	13,81	28,20
K Null 1,5h 3	84,12	30,88	-	74,66	-	-	54,21	338,04	2,67	7,75	26,06	24,44	7,72	13,39	42,91	35,07	0,50	3,36	15,62	27,95
K Null 2h 1	79,86	29,45	-	77,86	-	-	57,96	347,04	3,09	8,21	26,80	24,23	7,23	13,56	43,35	36,97	0,48	3,49	15,43	27,27
K Null 2h 2	87,90	33,81	-	76,14	-	-	56,55	351,92	3,03	9,28	28,96	25,79	7,27	14,11	44,69	39,09	0,47	3,65	16,50	27,25
K Null 2h 3	72,05	29,46	-	72,41	-	-	52,26	322,13	2,72	8,12	25,00	22,94	6,34	12,76	41,07	32,09	0,40	3,65	14,85	27,74
K Null 3h 1	101,57	43,93	-	86,33	-	-	71,55	420,32	4,28	16,18	39,80	33,08	8,42	20,55	55,92	51,51	-	5,78	28,05	25,89
K Null 3h 2	94,66	40,78	-	80,20	-	-	65,33	387,94	4,09	13,69	35,32	29,89	8,99	18,44	52,31	46,48	-	4,97	24,78	26,31
K Null 3h 3	115,25	51,72	-	94,49	-	-	65,02	452,28	4,60	17,67	43,14	36,16	9,60	20,97	62,98	57,57	-	5,80	29,65	29,27
K Null 4h 1	89,07	40,39	-	73,46	-	-	61,68	354,00	3,91	15,37	35,76	28,31	5,61	18,42	47,50	44,42	-	4,95	26,10	25,58
K Null 4h 2	90,55	42,12	-	75,72	-	-	62,61	365,94	4,23	16,68	37,95	28,48	6,78	19,32	49,12	48,98	-	5,20	28,09	24,91
K Null 4h 3	93,26	43,25	-	78,39	-	-	66,79	380,02	4,52	17,29	39,36	29,76	8,51	20,08	51,22	52,90	-	5,38	29,18	25,15
K Null 8h 1	95,63	47,10	-	79,28	-	-	68,52	385,68	5,06	22,09	42,97	31,33	6,51	21,65	49,42	50,44	-	6,12	35,00	24,48
K Null 8h 2	93,54	46,79	-	79,43	-	-	70,83	383,88	5,35	23,25	44,41	31,53	6,75	22,35	47,91	53,55	-	6,02	37,02	24,56
K Null 8h 3	90,28	44,37	-	77,53	-	-	64,52	362,97	4,39	22,47	43,23	30,68	6,79	21,79	44,07	53,32	-	6,40	35,67	24,82
K Null 24h 1	91,35	46,89	-	82,12	-	-	80,32	391,58	6,07	24,79	45,98	32,98	4,41	23,24	44,76	58,13	-	6,65	40,61	23,69
K Null 24h 2	89,09	48,07	-	87,45	-	-	83,93	411,69	6,44	25,70	46,91	37,53	3,71	24,06	46,20	60,63	-	5,76	43,30	24,61
K Null 24h 3	104,86	49,42	-	81,51	-	-	76,02	406,00	5,21	23,06	43,90	32,56	4,27	21,93	52,47	52,58	-	5,68	37,41	24,42
K Null 48h 1	81,97	41,99	-	73,68	-	-	70,40	342,99	5,35	22,79	41,93	29,96	5,47	21,32	31,86	50,81	-	6,30	38,41	24,24
K Null 48h 2	77,76	40,29	-	71,35	-	-	69,92	337,92	5,31	20,98	37,84	28,97	3,51	19,76	27,32	40,30	-	5,23	37,37	25,38
K Null 48h 3	79,62	40,94	-	68,90	-	-	68,28	326,30	5,04	21,39	39,24	27,98	4,60	19,79	29,51	43,03	-	5,95	36,00	24,43

Table III-II relative signal areas from RP-HPLC-UVD

Sample	Relative signal area / (mAU · min)																		
	Ala	Arg	Asn	Asp	Cys	Gln	Glu	Gly	His	Ile	Leu	Lys	Met	Phe	Ser	Thr	Trp	Tyr	Val
K Null 45min 1	1,972	0,517	-	2,049	-	-	1,388	6,694	0,032	0,083	0,422	0,418	0,169	0,232	0,615	0,419	0,040	0,053	0,320
K Null 45min 2	1,983	0,499	-	2,122	-	-	1,355	6,528	0,029	0,079	0,417	0,472	0,166	0,227	0,586	0,379	0,045	0,044	0,325
K Null 45min 3	1,973	0,509	-	2,099	-	-	1,441	6,855	0,034	0,089	0,444	0,516	0,178	0,244	0,634	0,423	0,043	0,058	0,323
K Null 1h 1	2,426	0,687	-	2,403	-	-	1,652	9,008	0,056	0,135	0,603	0,638	0,222	0,309	0,963	0,682	0,031	0,083	0,368
K Null 1h 2	2,207	0,606	-	2,197	-	-	1,428	7,733	0,043	0,104	0,509	0,597	0,188	0,261	0,778	0,500	0,036	0,069	0,327
K Null 1h 3	2,426	0,697	-	2,298	-	-	1,474	8,557	0,050	0,124	0,570	0,647	0,211	0,291	0,909	0,572	0,032	0,081	0,344
K Null 1,5h 1	3,109	1,074	-	2,776	-	-	1,907	12,019	0,093	0,240	0,858	0,805	0,292	0,443	1,457	1,118	0,022	0,117	0,508
K Null 1,5h 2	2,839	0,985	-	2,709	-	-	1,896	11,601	0,084	0,244	0,841	0,799	0,259	0,429	1,391	1,086	0,024	0,107	0,490
K Null 1,5h 3	3,010	1,105	-	2,671	-	-	1,940	12,095	0,096	0,277	0,933	0,874	0,276	0,479	1,535	1,255	0,018	0,120	0,559
K Null 2h 1	2,928	1,080	-	2,855	-	-	2,125	12,724	0,113	0,301	0,983	0,888	0,265	0,497	1,589	1,355	0,018	0,128	0,566
K Null 2h 2	3,226	1,241	-	2,795	-	-	2,076	12,917	0,111	0,341	1,063	0,947	0,267	0,518	1,640	1,435	0,017	0,134	0,606
K Null 2h 3	2,597	1,062	-	2,610	-	-	1,884	11,612	0,098	0,293	0,901	0,827	0,228	0,460	1,480	1,157	0,014	0,132	0,535
K Null 3h 1	3,923	1,697	-	3,334	-	-	2,764	16,235	0,165	0,625	1,537	1,278	0,325	0,794	2,160	1,990	-	0,223	1,083
K Null 3h 2	3,597	1,550	-	3,048	-	-	2,483	14,744	0,156	0,520	1,343	1,136	0,342	0,701	1,988	1,767	-	0,189	0,942
K Null 3h 3	3,938	1,767	-	3,228	-	-	2,222	15,453	0,157	0,604	1,474	1,235	0,328	0,716	2,152	1,967	-	0,198	1,013
K Null 4h 1	3,482	1,579	-	2,872	-	-	2,411	13,839	0,153	0,601	1,398	1,107	0,219	0,720	1,857	1,736	-	0,194	1,020
K Null 4h 2	3,635	1,691	-	3,040	-	-	2,513	14,689	0,170	0,670	1,523	1,143	0,272	0,776	1,972	1,966	-	0,209	1,127
K Null 4h 3	3,708	1,720	-	3,117	-	-	2,656	15,110	0,180	0,687	1,565	1,183	0,338	0,798	2,036	2,103	-	0,214	1,160
K Null 8h 1	3,906	1,923	-	3,238	-	-	2,799	15,752	0,206	0,902	1,755	1,280	0,266	0,884	2,018	2,060	-	0,250	1,429
K Null 8h 2	3,809	1,905	-	3,234	-	-	2,884	15,631	0,218	0,947	1,808	1,284	0,275	0,910	1,951	2,180	-	0,245	1,507
K Null 8h 3	3,637	1,787	-	3,123	-	-	2,599	14,621	0,177	0,905	1,741	1,236	0,274	0,878	1,775	2,148	-	0,258	1,437
K Null 24h 1	3,855	1,979	-	3,466	-	-	3,390	16,526	0,256	1,046	1,941	1,392	0,186	0,981	1,889	2,453	-	0,281	1,714
K Null 24h 2	3,621	1,954	-	3,554	-	-	3,411	16,732	0,262	1,044	1,906	1,525	0,151	0,978	1,878	2,464	-	0,234	1,760
K Null 24h 3	4,295	2,024	-	3,338	-	-	3,113	16,628	0,213	0,944	1,798	1,334	0,175	0,898	2,149	2,153	-	0,233	1,532
K Null 48h 1	3,382	1,732	-	3,039	-	-	2,904	14,150	0,221	0,940	1,730	1,236	0,226	0,880	1,315	2,096	-	0,260	1,584
K Null 48h 2	3,064	1,588	-	2,812	-	-	2,755	13,316	0,209	0,827	1,491	1,142	0,138	0,779	1,077	1,588	-	0,206	1,473
K Null 48h 3	3,259	1,676	-	2,820	-	-	2,795	13,355	0,206	0,875	1,606	1,145	0,188	0,810	1,208	1,761	-	0,244	1,473

Table III-III concentrations calculated from the relative signal areas

Sample	Concentration / mM																		
	Ala	Arg	Asn	Asp	Cys	Gln	Glu	Gly	His	Ile	Leu	Lys	Met	Phe	Ser	Thr	Trp	Tyr	Val
K Null 45min 1	2,540	0,620	-	8,754	-	-	1,958	13,444	0,058	0,100	0,454	0,321	0,203	0,269	0,716	0,612	0,066	0,064	0,274
K Null 45min 2	2,555	0,598	-	9,067	-	-	1,913	13,112	0,053	0,095	0,449	0,360	0,199	0,263	0,684	0,555	0,073	0,054	0,278
K Null 45min 3	2,542	0,609	-	8,968	-	-	2,030	13,768	0,061	0,105	0,477	0,392	0,213	0,282	0,739	0,617	0,070	0,070	0,276
K Null 1h 1	3,122	0,825	-	10,273	-	-	2,318	18,085	0,096	0,153	0,644	0,479	0,263	0,353	1,114	0,984	0,055	0,099	0,315
K Null 1h 2	2,841	0,727	-	9,389	-	-	2,012	15,528	0,075	0,120	0,545	0,449	0,224	0,301	0,903	0,727	0,062	0,083	0,280
K Null 1h 3	3,121	0,837	-	9,823	-	-	2,075	17,181	0,087	0,142	0,609	0,486	0,250	0,333	1,053	0,829	0,056	0,098	0,294
K Null 1,5h 1	3,996	1,293	-	11,873	-	-	2,668	24,123	0,154	0,262	0,910	0,599	0,341	0,501	1,678	1,602	0,042	0,140	0,434
K Null 1,5h 2	3,651	1,185	-	11,585	-	-	2,653	23,286	0,141	0,266	0,892	0,594	0,303	0,485	1,603	1,556	0,045	0,129	0,419
K Null 1,5h 3	3,869	1,330	-	11,424	-	-	2,713	24,276	0,158	0,300	0,988	0,648	0,323	0,540	1,768	1,795	0,037	0,144	0,478
K Null 2h 1	3,764	1,299	-	12,211	-	-	2,966	25,536	0,186	0,324	1,040	0,658	0,311	0,560	1,830	1,938	0,037	0,153	0,484
K Null 2h 2	4,146	1,494	-	11,953	-	-	2,899	25,924	0,183	0,365	1,124	0,700	0,313	0,583	1,888	2,050	0,036	0,160	0,518
K Null 2h 3	3,341	1,278	-	11,162	-	-	2,636	23,307	0,163	0,316	0,955	0,614	0,269	0,519	1,705	1,657	0,032	0,157	0,458
K Null 3h 1	5,039	2,045	-	14,269	-	-	3,840	32,576	0,269	0,659	1,620	0,938	0,378	0,886	2,481	2,836	-	0,266	0,927
K Null 3h 2	4,622	1,868	-	13,040	-	-	3,456	29,587	0,253	0,551	1,416	0,836	0,397	0,784	2,285	2,520	-	0,225	0,806
K Null 3h 3	5,058	2,130	-	13,815	-	-	3,098	31,010	0,256	0,637	1,554	0,907	0,382	0,801	2,472	2,804	-	0,236	0,866
K Null 4h 1	4,474	1,903	-	12,285	-	-	3,358	27,773	0,249	0,634	1,474	0,815	0,259	0,805	2,135	2,477	-	0,231	0,873
K Null 4h 2	4,670	2,038	-	13,004	-	-	3,497	29,478	0,276	0,705	1,605	0,841	0,319	0,866	2,266	2,803	-	0,249	0,964
K Null 4h 3	4,764	2,073	-	13,335	-	-	3,692	30,321	0,291	0,723	1,649	0,870	0,393	0,891	2,340	2,997	-	0,255	0,993
K Null 8h 1	5,017	2,319	-	13,856	-	-	3,888	31,609	0,334	0,945	1,847	0,939	0,311	0,985	2,320	2,936	-	0,298	1,223
K Null 8h 2	4,892	2,297	-	13,839	-	-	4,004	31,365	0,352	0,991	1,903	0,942	0,322	1,014	2,242	3,106	-	0,292	1,289
K Null 8h 3	4,672	2,155	-	13,363	-	-	3,615	29,341	0,287	0,948	1,833	0,907	0,320	0,978	2,042	3,060	-	0,307	1,229
K Null 24h 1	4,952	2,386	-	14,834	-	-	4,697	33,161	0,413	1,094	2,041	1,019	0,222	1,091	2,172	3,492	-	0,334	1,466
K Null 24h 2	4,652	2,356	-	15,212	-	-	4,726	33,573	0,421	1,092	2,006	1,115	0,182	1,088	2,159	3,508	-	0,279	1,505
K Null 24h 3	5,515	2,441	-	14,287	-	-	4,319	33,366	0,345	0,989	1,892	0,978	0,209	1,000	2,469	3,068	-	0,277	1,311
K Null 48h 1	4,345	2,088	-	13,004	-	-	4,033	28,396	0,356	0,984	1,821	0,908	0,266	0,980	1,516	2,987	-	0,309	1,355
K Null 48h 2	3,939	1,913	-	12,026	-	-	3,829	26,724	0,338	0,867	1,571	0,840	0,168	0,869	1,244	2,267	-	0,246	1,260
K Null 48h 3	4,188	2,020	-	12,063	-	-	3,883	26,803	0,334	0,917	1,692	0,843	0,224	0,904	1,394	2,512	-	0,290	1,260

Calibration functions: see Table IV-V, The regression parameters have been corrected for the different derivatisation protocol used (namely the standard revised method, see 4.2.2): $\boldsymbol{k' = 0,25 \cdot k}$; $\boldsymbol{d' = 0,25 \cdot d}$

Table III-IV fitted parameters for the models 1-1 (3.3.1) and 1-1 2x (3.3.3): based on measured relative signal area

Amino acid	A_0			k_1 / h^{-1}			k_2 / h^{-1}			A_0/A_{4h}
	value	std. dev.	RSD	value	std. dev.	RSD	value	std. dev.	RSD	
Ala	**4,104**	0,1162	2,83%	0,7043	0,07529	10,7%	0,004193	0,001213	28,9%	**1,137**
Arg	**2,152**	0,07798	3,62%	0,3618	0,03294	9,10%	0,005152	0,001325	25,7%	**1,294**
Asn*	**2,811**	0,9645	34,3%	1,609	0,4666	29,0%	0,02026	0,01109	54,7%	**2,319***
Asp*	**4,167**	1,430	34,3%	0,03065	0,009754	31,8%				
Cys	**-**	-	-	-	-	-	-	-	-	**-**
Gln*	**2,705**	0,5870	21,7%	1,805	0,2926	16,2%	0,02085	0,002153	10,3%	**2,766***
Glu*	**4,285**	0,4020	9,38%	0,0330	0,04035	122%				
Gly	**16,96**	0,4590	2,71%	0,6246	0,05657	9,06%	0,003644	0,001100	30,2%	**1,166**
His	**0,2672**	0,01543	5,78%	0,2097	0,03202	15,3%	0,005140	0,002023	39,4%	**1,597**
Ile	**1,151**	0,08754	7,60%	0,2131	0,02002	9,40%	0,006233	0,002422	38,9%	**1,764**
Leu	**2,061**	0,07380	3,58%	0,3122	0,02620	8,39%	0,005227	0,001271	24,3%	**1,378**
Lys	**1,484**	0,04894	3,30%	0,3749	0,05055	13,5%	0,004342	0,001307	30,1%	**1,296**
Met^{4h}	**0,8241**	2,378	289%	0,3571	1,516	424%	0,3575	1,225	343%	**2,979**
Phe	**1,031**	0,03546	3,44%	0,3226	0,02631	8,16%	0,004693	0,001216	25,9%	**1,348**
Ser	**2,330**	0,1201	5,15%	0,5146	0,06701	13,0%	0,01184	0,002360	19,9%	**1,192**
Thr	**2,733**	0,1652	6,04%	0,2643	0,04446	16,8%	0,008693	0,002321	26,7%	**1,412**
Trp	**-**	-	-	-	-	-	-	-	-	**-**
Tyr	**0,2638**	0,01318	5,00%	0,4005	0,03465	8,65%	0,002457	0,001632	66,4%	**1,284**
Val	**1,809**	0,08226	4,55%	0,2254	0,01834	8,13%	0,004094	0,001478	36,1%	**1,641**
Sum of all AA	42,91	1,178	2,75%	0,4725	0,04689	9,92%	0,004224	0,001098	26,0%	1,224

* ..... model 1-1 2x (3.3.3)

4h ..... data up to 4 h used

The parameters were fitted to the measured data applying the gaussian principle of the least sum of squared errors using the program Dataplot v. 2/2005.

Table III-V fitted parameters for the models 1-1 (3.3.1) and 1-1 2x (3.3.3): based on calculated concentration

Amino acid	c_0 / mM			k_1 / h^{-1}			k_2 / h^{-1}			c_0/c_{4h}
	value	std. dev.	RSD	value	std. dev.	RSD	value	std. dev.	RSD	
Ala	**5,270**	0,14857	2,82%	0,7066	0,07543	10,7%	0,004176	0,001209	29,0%	**1,137**
Arg	**2,596**	0,09473	3,65%	0,3606	0,03298	9,15%	0,005178	0,001334	25,8%	**1,295**
Asn*	**5,989**	2,294	38,3%	0,0812	0,06653	82,0%	0,008010	0,007176	89,6%	**1,396***
Asp*	**11,99**	4,614	38,5%	1,601	0,6975	43,6%				
Cys	-	-	-	-	-	-	-	-	-	-
Gln*	**2,720**	0,7062	26,0%	1,379	0,3079	22,3%	0,01392	0,001798	12,9%	**1,987***
Glu*	**4,265**	0,864	20,2%	0,05610	0,21291	380%				
Gly	**34,03**	0,9195	2,70%	0,6268	0,05658	9,03%	0,003632	0,001098	30,2%	**1,166**
His	**0,4283**	0,02304	5,38%	0,2152	0,03216	14,9%	0,004921	0,001896	38,5%	**1,575**
Ile	**1,2006**	0,08360	6,96%	0,2160	0,01923	8,90%	0,006105	0,002226	36,5%	**1,747**
Leu	**2,165**	0,07574	3,50%	0,3151	0,02616	8,30%	0,005154	0,001245	24,2%	**1,374**
Lys	**1,0757**	0,03443	3,20%	0,3986	0,05134	12,9%	0,003981	0,001264	31,8%	**1,278**
Met^{4h}	**0,9740**	0,6548	67,2%	0,356	0,6714	189%	0,3630	0,3734	103%	**3,009**
Phe	**1,1438**	0,03738	3,27%	0,3282	0,02632	8,02%	0,004566	0,001173	25,7%	**1,339**
Ser	**2,672**	0,1357	5,08%	0,5211	0,06674	12,8%	0,011714	0,002325	19,8%	**1,189**
Thr	**3,885**	0,2303	5,93%	0,2661	0,04434	16,7%	0,008612	0,002280	26,5%	**1,408**
Trp	-	-	-	-	-	-	-	-	-	-
Tyr	**0,3138**	0,0155	4,93%	0,4021	0,03450	8,58%	0,002438	0,001612	66,1%	**1,283**
Val	**1,548**	0,070	4,55%	0,2254	0,01833	8,13%	0,004095	0,001479	36,1%	**1,641**
Sum of all AA	75,12	1,925	2,56%	0,5520	0,05328	9,65%	0,003743	0,001046	27,9%	1,193

* ..... model 1-1 2x (3.3.3)

4h ..... data up to 4 h used

The parameters were fitted to the measured data applying the gaussian principle of the least sum of squared errors using the program Dataplot v. 2/2005.

Table III-VI percentages of the amino acids as measured by RP-HPLC UVD (excluding Pro)

Sample	Proportion of the amino acid on all unmodified primary amino acids / %																		
	Ala	Arg	Asn	Asp	Cys	Gln	Glu	Gly	His	Ile	Leu	Lys	Met	Phe	Ser	Thr	Trp	Tyr	Val
K Null 45min 1	8,34	2,03	-	28,75	-	-	6,43	44,15	0,19	0,33	1,49	1,06	0,67	0,88	2,35	2,01	0,22	0,21	0,90
K Null 45min 2	8,43	1,97	-	29,92	-	-	6,31	43,26	0,17	0,31	1,48	1,19	0,66	0,87	2,26	1,83	0,24	0,18	0,92
K Null 45min 3	8,14	1,95	-	28,73	-	-	6,50	44,10	0,20	0,34	1,53	1,25	0,68	0,90	2,37	1,98	0,22	0,22	0,88
K Null 1h 1	7,97	2,11	-	26,22	-	-	5,92	46,16	0,25	0,39	1,64	1,22	0,67	0,90	2,84	2,51	0,14	0,25	0,80
K Null 1h 2	8,29	2,12	-	27,40	-	-	5,87	45,31	0,22	0,35	1,59	1,31	0,65	0,88	2,64	2,12	0,18	0,24	0,82
K Null 1h 3	8,37	2,25	-	26,35	-	-	5,57	46,09	0,23	0,38	1,63	1,30	0,67	0,89	2,82	2,22	0,15	0,26	0,79
K Null 1,5h 1	7,90	2,55	-	23,46	-	-	5,27	47,66	0,30	0,52	1,80	1,18	0,67	0,99	3,32	3,16	0,08	0,28	0,86
K Null 1,5h 2	7,48	2,43	-	23,74	-	-	5,44	47,73	0,29	0,54	1,83	1,22	0,62	0,99	3,28	3,19	0,09	0,26	0,86
K Null 1,5h 3	7,62	2,62	-	22,49	-	-	5,34	47,79	0,31	0,59	1,94	1,28	0,64	1,06	3,48	3,53	0,07	0,28	0,94
K Null 2h 1	7,06	2,44	-	22,91	-	-	5,56	47,91	0,35	0,61	1,95	1,24	0,58	1,05	3,43	3,64	0,07	0,29	0,91
K Null 2h 2	7,63	2,75	-	22,00	-	-	5,33	47,71	0,34	0,67	2,07	1,29	0,58	1,07	3,47	3,77	0,07	0,29	0,95
K Null 2h 3	6,88	2,63	-	22,98	-	-	5,43	47,99	0,33	0,65	1,97	1,27	0,55	1,07	3,51	3,41	0,07	0,32	0,94
K Null 3h 1	7,30	2,96	-	20,67	-	-	5,56	47,19	0,39	0,95	2,35	1,36	0,55	1,28	3,59	4,11	-	0,39	1,34
K Null 3h 2	7,38	2,98	-	20,82	-	-	5,52	47,23	0,40	0,88	2,26	1,33	0,63	1,25	3,65	4,02	-	0,36	1,29
K Null 3h 3	7,66	3,23	-	20,92	-	-	4,69	46,97	0,39	0,96	2,35	1,37	0,58	1,21	3,74	4,25	-	0,36	1,31
K Null 4h 1	7,49	3,18	-	20,56	-	-	5,62	46,49	0,42	1,06	2,47	1,36	0,43	1,35	3,57	4,15	-	0,39	1,46
K Null 4h 2	7,34	3,21	-	20,45	-	-	5,50	46,36	0,43	1,11	2,52	1,32	0,50	1,36	3,56	4,41	-	0,39	1,52
K Null 4h 3	7,26	3,16	-	20,33	-	-	5,63	46,23	0,44	1,10	2,51	1,33	0,60	1,36	3,57	4,57	-	0,39	1,51
K Null 8h 1	7,29	3,37	-	20,13	-	-	5,65	45,93	0,49	1,37	2,68	1,36	0,45	1,43	3,37	4,27	-	0,43	1,78
K Null 8h 2	7,11	3,34	-	20,10	-	-	5,82	45,56	0,51	1,44	2,76	1,37	0,47	1,47	3,26	4,51	-	0,42	1,87
K Null 8h 3	7,18	3,31	-	20,54	-	-	5,56	45,10	0,44	1,46	2,82	1,39	0,49	1,50	3,14	4,70	-	0,47	1,89
K Null 24h 1	6,75	3,25	-	20,22	-	-	6,40	45,19	0,56	1,49	2,78	1,39	0,30	1,49	2,96	4,76	-	0,46	2,00
K Null 24h 2	6,30	3,19	-	20,59	-	-	6,40	45,45	0,57	1,48	2,72	1,51	0,25	1,47	2,92	4,75	-	0,38	2,04
K Null 24h 3	7,61	3,37	-	19,72	-	-	5,96	46,04	0,48	1,36	2,61	1,35	0,29	1,38	3,41	4,23	-	0,38	1,81
K Null 48h 1	6,86	3,30	-	20,53	-	-	6,37	44,83	0,56	1,55	2,87	1,43	0,42	1,55	2,39	4,71	-	0,49	2,14
K Null 48h 2	6,78	3,29	-	20,70	-	-	6,59	46,00	0,58	1,49	2,70	1,45	0,29	1,50	2,14	3,90	-	0,42	2,17
K Null 48h 3	7,06	3,40	-	20,33	-	-	6,54	45,18	0,56	1,55	2,85	1,42	0,38	1,52	2,35	4,23	-	0,49	2,12
Model 1-1 (2x)[#]	**6,41**	**3,16**	**7,28**	**14,57**	**-**	**3,31**	**5,18**	**41,37**	**0,52**	**1,46**	**2,63**	**1,31**	**1,18**	**1,39**	**3,25**	**4,72**	**-**	**0,38**	**1,88**

..... calculated from the fitted parameters c_0 (see Table III-V)

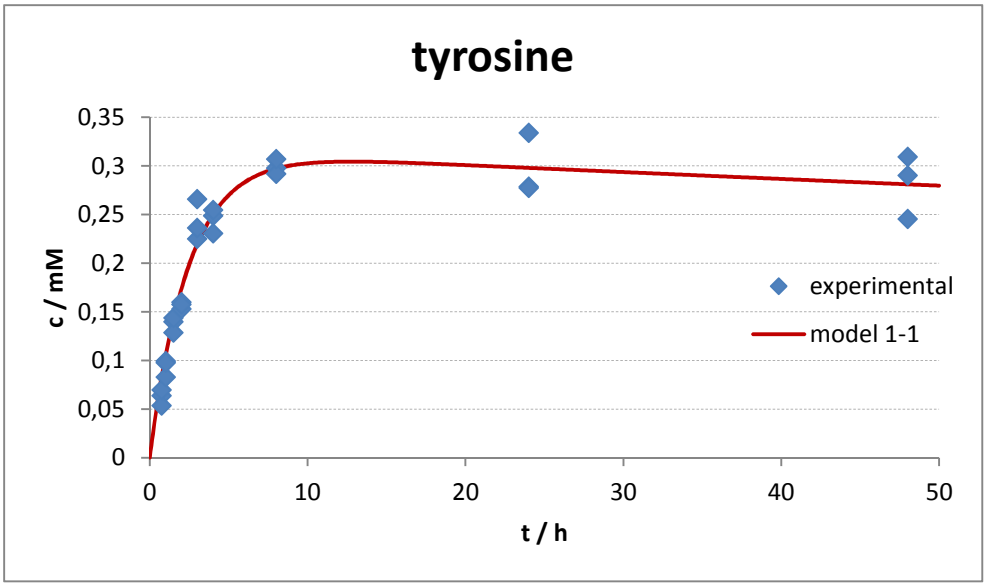
tyrosine
0,35
0,3
0,25
0,2
0,15
0,1
0,05
0
c / mM
0
10
20
30
40
50
t / h
experimental
model 1-1

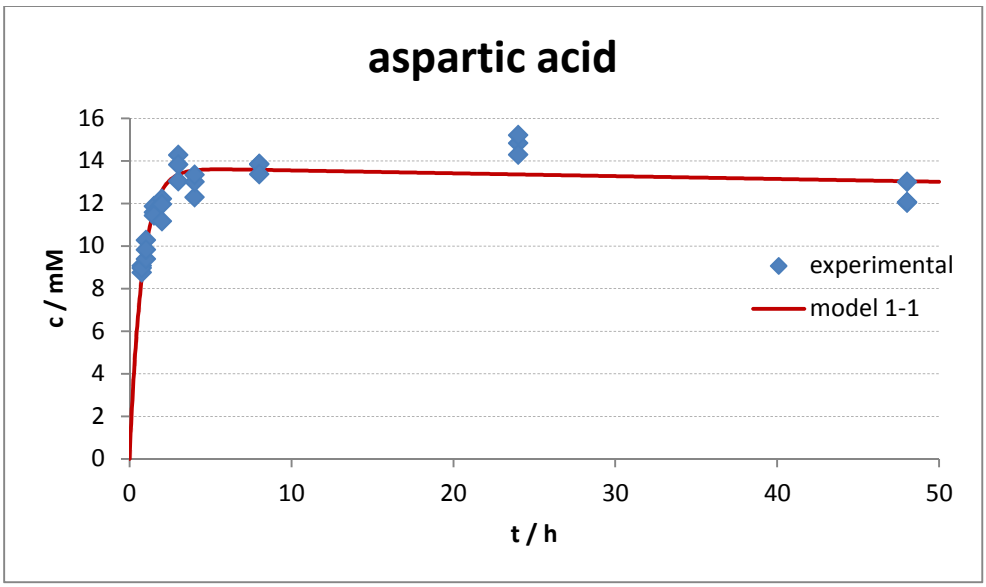
aspartic acid
16
14
12
10
8
6
4
2
0
c / mM
0
10
20
30
40
50
t / h
experimental
model 1-1

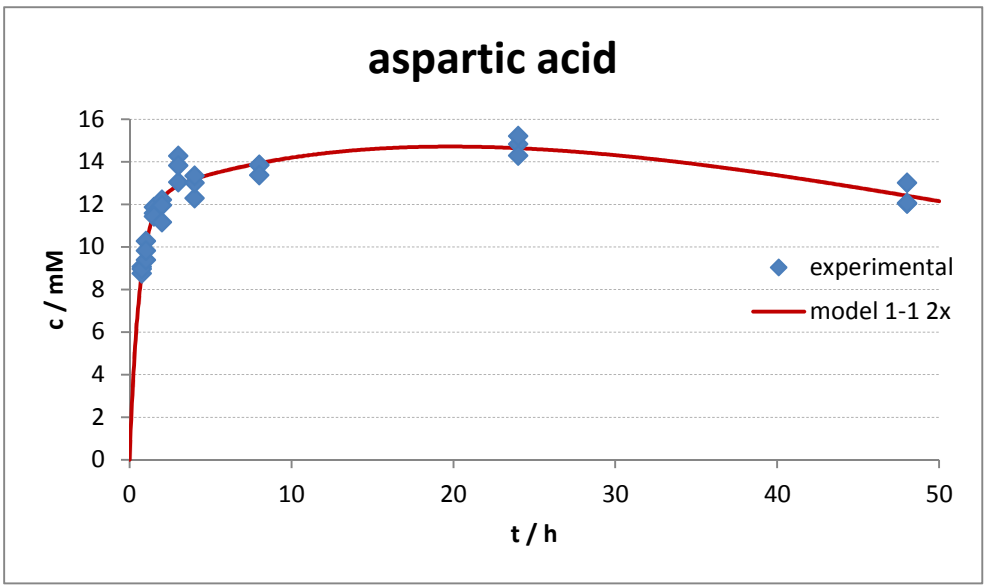
aspartic acid
16
14
12
10
8
6
4
2
0
c / mM
0
10
20
30
40
50
t / h
experimental
model 1-1 2x

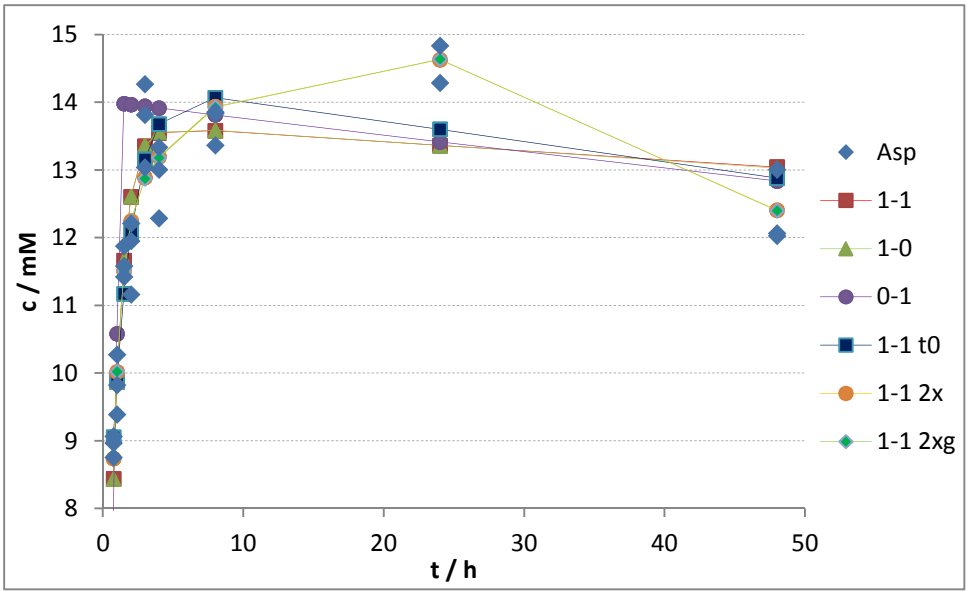

Figure III-I Comparison of the different models for the measured concentrations of aspartic acid
t_0.....start time of the hydrolysis as an additional free parameter

IV. Amino acid analysis after OPA-derivatisation

IV.I. Chromeleon® program for the revised method (4.2.2)

C18 4,6 x 250 mm: Aminosäuren mit OPA; 40 °C; A == ddH2O, B == MeOH+ddH2O+THF+50mM NaOAc, C = ddH2O+MeOH+THF+50mM NaOAc; B3 == 5 M NaOH; BE1 == OPA-Reagenz; BE2 == IS; BE8 == ddH2O; Pos+8 == leeres Vial

```
AcquireExclusiveAccess
;column oven
               TempCtrl =                                On
               ColumnOven.Temperature.Nominal =          40.0 [°C]
               ColumnOven.Temperature.LowerLimit =       5.0 [°C]
               ColumnOven.Temperature.UpperLimit =       50.0 [°C]
               EquilibrationTime =                       0.5 [min]
               ReadyTempDelta =                          1.0 [°C]
               HumidityLeakSensor =                      Low
               GasLeakSensor =                           Low
               MsvPosition =                             B
;Autosampler
               DrawSpeed =                               10.000 [µl/s]
               DrawDelay =                               3000 [ms]
               DispSpeed =                               20.000 [µl/s]
               DispenseDelay =                           0 [ms]
               WasteSpeed =                              32.000 [µl/s]
               SampleHeight =                            2.000 [mm]
               InjectWash =                              Both
               WashVolume =                              100.000 [µl]
               WashSpeed =                               20.000 [µl/s]
               Sampler.PumpDevice =                      "PumpLeft"
               InjectMode =                              Normal
               SyncWithPump =                            On
;UVD
               UV_VIS_1.Wavelength =                     210 [nm]
               UV_VIS_1.Bandwidth =                      10 [nm]
               UV_VIS_1.RefWavelength =                  600 [nm]
               UV_VIS_1.RefBandwidth =                   10 [nm]
               UV_VIS_1.Step =                           Auto
               UV_VIS_1.Average =                        On
               UV_VIS_2.Wavelength =                     338 [nm]
               UV_VIS_2.Bandwidth =                      10 [nm]
               UV_VIS_2.RefWavelength =                  600 [nm]
               UV_VIS_2.RefBandwidth =                   20 [nm]
               UV_VIS_2.Step =                           Auto
               UV_VIS_2.Average =                        On
               UV_VIS_3.Wavelength =                     338 [nm]
               UV_VIS_3.Bandwidth =                      10 [nm]
               UV_VIS_3.RefWavelength =                  390 [nm]
               UV_VIS_3.RefBandwidth =                   20 [nm]
               UV_VIS_3.Step =                           Auto
               UV_VIS_3.Average =                        On
               UV_VIS_4.Wavelength =                     280 [nm]
               UV_VIS_4.Bandwidth =                      10 [nm]
               UV_VIS_4.RefWavelength =                  600 [nm]
               UV_VIS_4.RefBandwidth =                   10 [nm]
               UV_VIS_4.Step =                           Auto
               UV_VIS_4.Average =                        On
;Pumps
               PumpLeft.Pressure.LowerLimit =            2 [bar]
               PumpLeft.Pressure.UpperLimit =            350 [bar]          ; Säule
Eurospher 100-5 C18: bis 400 bar
               PumpLeft.MaximumFlowRamp =                6.00 [ml/min²]
               PumpLeft.%A.Equate =                      "%A"
               PumpLeft.%B.Equate =                      "%B"
               PumpLeft.%C.Equate =                      "%C"
               PumpRight.Pressure.LowerLimit =           0 [bar]
               PumpRight.Pressure.UpperLimit =           400 [bar]
               PumpRight.MaximumFlowRamp =               6.00 [ml/min²]
               PumpRight.%A.Equate =                     "%A"
               PumpRight.%B.Equate =                     "%B"
               PumpRight.%C.Equate =                     "%C"
               PumpRight.Flow =                          0.000 [ml/min]
               PumpRight.%B =                            0.0 [%]
               PumpRight.%C =                            0.0 [%]
               PumpRight.Curve =                         5
;RI-Detector
               ;RI.Temperature.Nominal =                 45 [°C]
               ;Recorder_Range =                         512.00 [µRIU]
```

```
                ;Integrator_Range =                                  500 [µRIU/V]
                ;Rise_Time =                                         0.50 [s]
                ;Polarity =                                          Plus
                ;Baseline_Shift =                                    0 [mV]
                ;RI_1.Step =                                         Auto
                ;RI_1.Average =                                      On

;Fraction collector
                ;*********************************************************************
                ;* Definition of triggers for fraction collection starts here.
                ;*********************************************************************
                ;Trigger                                             FracStart
                FracStartDetected
                ;Valve =                                             On
                ;EndTrigger

                ;Trigger                                             TubeChange
                FracTubeChange
                ;Valve =                                             Off
                ;Tube =                                              tube+1
                ;Valve =                                             On
                ;EndTrigger

                ;Trigger                                             FracEnd
                FracEndDetected
                ;Valve =                                             Off
                ;Tube =                                              Tube+1
                ;EndTrigger

                ;*********************************************************************
                ;* Definition of triggers for fraction collection ends here.
                ;*********************************************************************

                ;Valve =                                             Off
                ;Tube =                                              sample.Foxy_tube
                ;FractionCollection.PumpDevice =                     "PumpLeft"
                ;TubeMaxVolume =                                     10.00 [ml]
                ;TotalNumberInstalled =                              144
                ;MaxTubesPerFraction =                               Unlimited
                ;TubeWrapping =                                      No
                ;TubeChangeDuration =                                2.0 [s]
                ;DetectionChannel1.Name =                            "UV_VIS_3"
                ;Detektorkanal zur Peakerkennung
                ;PeakStartThreshold =                                2.00 [signal]
                ;PeakStartSlope =                                    0.500 [signal/s]
                ;PeakStartTrueTime =                                 1.00 [s]
                ;PeakEndThreshold =                                  10.00 [signal]
                ;PeakEndSlope =                                      -1.000 [signal/s]
                ;PeakEndTrueTime =                                   1.00 [s]
                ;DerivStep =                                         1.00 [s]
                ;ThresholdNoPeakEnd =                                2000.00 [signal]
                ;ThresholdDoNotResolve =                             Off
                ;PeakMaxSlope =                                      Off
                ;PeakMaxTrueTime =                                   1.00 [s]
                ;BaselineDrift =                                     0.000 [signal/s]
                ;BaselineOffset =                                    0.000 [signal]
                ;DelayVolume =                                       219 [µl]            ;Volumen
zwischen UVD und Fraktionensammler
                ;OffsetVolume =                                      0 [µl]

;run-specific commands
                ;die Probenvorbereitung dauert insgesamt etwa 185 s bis zur Injektion
(Autosampler UltiMate 3000)
                InjectMode =                                         UserProg

                ReagentAVial =                                       BE2                 ; Norvalin
1 mM in ddH2O
                ;ReagentBVial =                                      BE8                 ; ddH2O
                ;ReagentBVial =                                      B3                  ; NaOH 5 M
                ReagentCVial =                                       BE1                 ; OPA-
Reagenz
                ;PrepVial =                                          Position+8          ; leeres,
offenes Glasvial mit 100 µl-Einsatz
                PositionCalculator =                                 Sampler.Position
                IncrementPositionCalculator                          By=8
                PrepVial =                                           PositionCalculator
```

```
                WashVolume =                                         100.000 [µl]
                WashSpeed =                                          20.000 [µl/s]


                ;internen Standard zusetzen (Nadel wurde gerade gewaschen <= InjectWash=Both)
                UdpDraw                                              From=ReagentAVial,
Volume=10.000, SyringeSpeed=GlobalSpeed, SampleHeight=GlobalHeight

                ;Probe aufziehen
                UdpDraw                                              From=SampleVial, Volume=10.00,
SyringeSpeed=GlobalSpeed, SampleHeight=GlobalHeight
                UdpDispense                                          To=PrepVial, Volume=20.00,
SyringeSpeed=GlobalSpeed, SampleHeight=GlobalHeight
                UdpMixWait                                           Duration=2

                ;Derivatisieren
                UdpDispense                                          To=Wash, Volume=0.000,
SyringeSpeed=GlobalSpeed, SampleHeight=GlobalHeight
                UdpMixNeedleWash                                     Volume=100
                ;Verunreinigung des OPA-Reagenz vermeiden
                UdpDraw                                              From=ReagentCVial,
Volume=40.000, SyringeSpeed=GlobalSpeed, SampleHeight=GlobalHeight
                UdpDispense                                          To=PrepVial, Volume=40.000,
SyringeSpeed=GlobalSpeed, SampleHeight=GlobalHeight
                UdpMixWait                                           Duration=2

                ;mischen
                DrawSpeed =                                          20.000 [µl/s]
                DispSpeed =                                          30.000 [µl/s]
                DrawDelay =                                          1000 [ms]
                UdpDraw                                              From=PrepVial, Volume=40.00,
SyringeSpeed=GlobalSpeed, SampleHeight=GlobalHeight
                UdpDispense                                          To=PrepVial, Volume=40.000,
SyringeSpeed=GlobalSpeed, SampleHeight=GlobalHeight
                UdpMixWait                                           Duration=2
                UdpDraw                                              From=PrepVial, Volume=40.00,
SyringeSpeed=GlobalSpeed, SampleHeight=GlobalHeight
                UdpDispense                                          To=PrepVial, Volume=40.000,
SyringeSpeed=GlobalSpeed, SampleHeight=GlobalHeight
                UdpMixWait                                           Duration=2
                UdpDraw                                              From=PrepVial, Volume=40.00,
SyringeSpeed=GlobalSpeed, SampleHeight=GlobalHeight
                UdpDispense                                          To=PrepVial, Volume=40.000,
SyringeSpeed=GlobalSpeed, SampleHeight=GlobalHeight
                UdpMixWait                                           Duration=2

                UdpMixWait                                           Duration=27 ;gesamte
Derivatisierungszeit 80 s, 3 s Wartezeit nach jedem Aufsaugen (beim Mischen: 1s)

                ;Spritzengeschwindigkeiten zurücksetzen
                DrawSpeed =                                          10.000 [µl/s]
                DrawDelay =                                          3000 [ms]
                DispSpeed =                                          20.000 [µl/s]

                ;Injektion: Verdünnung der Probe: 6-fach, 10 µl Probe pro Messung
                UdpSyringeValve Position =                           Needle
                UdpInjectValve                                       Position=Load
                UdpDraw                                              From=PrepVial, Volume=20.000,
SyringeSpeed=GlobalSpeed, SampleHeight=GlobalHeight
                UdpMixWait                                           Duration=5

                UdpInjectValve                                       Position=Inject
                UdpInjectMarker                                      ;erzeugt "Inject Response",
wenn Programm läuft
                UdpMixWait                                           Duration=40

                ;UdpDraw                                             From=SampleVial, Volume=0.000,
SyringeSpeed=GlobalSpeed, SampleHeight=GlobalHeight
                UdpSyringeValve                                      Position=Waste
                UdpMoveSyringeHome                                   SyringeSpeed=GlobalSpeed
                UdpSyringeValve                                      Position=Needle
                UdpMixNeedleWash                                     Volume=100



 0.000          PumpLeft.Flow =                                      1.000 [ml/min]
                PumpLeft.%B =                                        5.0 [%]
                PumpLeft.%C =                                        95.0 [%]
```

```
                ;CollectFractions =                         No
                UV.Autozero
                ;RI.Purge =                                 Off
                ;RI.Autozero
                Wait                                        ColumnOven.Ready and
Sampler.Ready

                Inject

                UV_VIS_1.AcqOn
                ;UV_VIS_2.AcqOn
                UV_VIS_3.AcqOn
                ;UV_VIS_4.AcqOn
                ;RI_1.AcqOn

                PumpLeft.Flow =                             1.000 [ml/min]
                PumpLeft.%B =                               5.0 [%]
                PumpLeft.%C =                               95.0 [%]

7.000           PumpLeft.%B =                               5.0 [%]
                PumpLeft.%C =                               95.0 [%]

17.000          PumpLeft.%B =                               25.0 [%]
                PumpLeft.%C =                               75.0 [%]

27.000          PumpLeft.%B =                               50.0 [%]
                PumpLeft.%C =                               50.0 [%]

35.000          PumpLeft.%B =                               50.0 [%]
                PumpLeft.%C =                               50.0 [%]

                PumpLeft.%B =                               100.0 [%]
                PumpLeft.%C =                               0.0 [%]

40.000          PumpLeft.%B =                               100.0 [%]
                PumpLeft.%C =                               0.0 [%]

                PumpLeft.%B =                               5.0 [%]
                PumpLeft.%C =                               95.0 [%]


45.000          PumpLeft.Flow =                             1.000 [ml/min]
                PumpLeft.%B =                               5.0 [%]
                PumpLeft.%C =                               95.0 [%]


                Sampler.WashBufferLoop                      Volume=300.000
                Wait                                        Sampler.Ready, Continue

                UV_VIS_1.AcqOff
                ;UV_VIS_2.AcqOff
                UV_VIS_3.AcqOff
                ;UV_VIS_4.AcqOff
                ;RI_1.AcqOff

                ;RI.Purge =                                 On                  ;während
der Vorbereitung der nächsten Probe spülen
                ReleaseExclusiveAccess
                End
;EOF
```

IV.II. Calibration

Table IV-I amino acid stock solution

Amino acid	Molecular weight / Da	Solubility in water @ 20 °C	200 µmol / mg	
			theoretical	actual
Ala	89,09	1,86 M*	17,82	17,84
Arg	174,20	853 mM	34,84	34,89
Asn . H_2O	150,14	151 mM	30,02	30,27
Asp	133,10	30 mM	26,62	26,75
Cys	121,16	2,31 M	24,23	24,22
Gln	146,15	178 mM**	29,23	29,42
Glu	147,13	75 mM*	29,43	29,50
Gly	75,07	3,0 M	15,01	15,12
His	155,16	246 mM	31,03	31,16
Ile	131,18	300 mM	26,24	26,38
Leu	131,18	180 mM	26,24	26,25
Lys . HCl	182,60	1,83 M	36,52	36,63
Met	149,21	320 mM	29,84	29,74
Phe	165,19	163 mM	33,04	33,25
Pro	115,13	13,0 M	23,03	23,16
Ser	105,09	3,42 M	21,02	21,02
Thr	119,12	671 mM	23,83	24,07
Trp	204,23	49 mM	40,84	40,76
Tyr	181,19	2,1 mM	36,24	36,42
Val	117,15	725 mM	23,43	23,57

Solubility data taken from the DGUV-IFA GESTIS Stoffdatenbank, accessed 2010-06-09

* .....@ 25 °C

** .....@ 18 °C

Table IV-II calibration solutions

#	c / µM	Pipetting scheme
①	2000	stock solution (S)
②	1500	750 µl S + 250 µl ddH_20
③	1000	500 µl S + 500 µl ddH_20
④	750	375 µl S + 625 µl ddH_20
⑤	500	250 µl S + 750 µl ddH_20
⑥	100	100 µl ③ + 900 µl ddH_20
⑦	50	100 µl ⑤ + 900 µl ddH_20
⑧	10	100 µl ⑥ + 900 µl ddH_20

Table IV-III Retention times of the individual amino acids

Amino acid	Retention	
	t_R / min	Δt_R / s
Ala	16,9	20
Arg	9,9	19
Asn	5,6	6
Asp	5,4	6
Cys	19,6	6
DiTyr	27,1	10
Gln	7,5	14
Glu	8,6	20
Gly	11,0	18
His	6,4	13
Ile	32,5	17
Leu	33,2	17
Lys	38,7	6
Met	26,4	15
Nor	28,8	10
Orn	34,6	22
Phe	29,2	13
Ser	6,9	15
Thr	12,0	15
Trp	27,8	12
Tyr	19,9	14
Val	28,3	14

Table IV-IV calibration functions and method parameters for the low capacity method (4.2.2): based on measured signal area

direct	20 µM – 1000 µM						20 µM – 2000 µM					
	k / μM^{-1} · mAU·min	d / mAU·min	r^2	σ_{rest} / mAU·min	σ_{method} / µM	LOD / µM	k / μM^{-1} · mAU·min	d / mAU·min	r^2	σ_{rest} / mAU·min	σ_{method} / µM	LOD / µM
Ala	0,05644	-0,2916	0,9979	1,11	19,7	50	0,05177	1,379	0,9965	2,32	44,7	100
Arg	0,05974	1,012	0,9984	1,03	17,2	44	0,05820	1,564	0,9993	1,15	19,7	45
Asn	0,06293	-0,4678	0,9992	0,767	12,2	31	0,06261	-0,3551	0,9998	0,700	11,2	26
Asp$^{!100}$	0,01679	0,9037	0,9945	0,560	33,4	100	0,02968	-4,549	0,9419	5,79	195	492
Cys	0,001557	0,1845	0,9745	0,109	69,7	180	0,001654	0,1497	0,9928	0,106	64,3	148
Gln	0,07533	1,622	0,9975	1,61	21,4	54	0,08466	-1,715	0,9952	4,42	52,2	120
Glu	0,05298	-2,716	0,9927	1,96	36,9	94	0,02897	5,873	0,8003	10,90	376	860
Gly	0,03607	-0,4452	0,9966	0,914	25,3	64	0,03567	-0,3030	0,9990	0,836	23,4	54
His	0,04569	0,1501	0,9973	1,02	22,4	57	0,04793	-0,6506	0,9986	1,36	28,3	65
Ile	0,06998	-0,2186	0,9994	0,729	10,4	27	0,06809	0,4566	0,9996	1,07	15,7	36
Leu	0,06915	-0,2040	0,9993	0,760	11,0	28	0,06774	0,3011	0,9997	0,929	13,7	31
Lys	0,1009	-1,231	0,9984	1,74	17,2	44	0,08913	2,991	0,9933	5,51	61,9	140
Met	0,06419	-0,1229	0,9990	0,888	13,8	35	0,06283	0,3649	0,9996	1,00	16,0	37
Phe	0,06576	-0,2159	0,9992	0,801	12,2	31	0,06310	0,7337	0,9991	1,39	22,0	50
Ser	0,06329	-0,2538	0,9979	1,24	19,5	50	0,07427	-4,180	0,9919	5,04	67,9	160
Thr	0,05106	-0,4384	0,9979	1,02	19,9	51	0,04928	0,1974	0,9989	1,21	24,5	56
Trp	0,05435	-0,1683	0,9991	0,715	13,1	33	0,05194	0,6955	0,9990	1,26	24,2	56
Tyr^{⅕}	0,06093	0,05622	0,9974	0,269	4,41	11	0,05997	0,1243	0,9992	0,255	4,25	10
Val	0,08437	0,9840	0,9969	2,02	24,0	61	0,07973	2,644	0,9979	2,76	34,6	79

!100.....without 100 µM

⅕ .....one-fifth of the concentration used: 4 µM – 400 µM

The limit of detection (LOD) has been calculated from the linear calibration curve with the 95 % confidence interval.

Table IV-V calibration functions and method parameters for the low capacity method (4.2.2): based on normalised signal area

norm.	20 µM – 1000 µM						20 µM – 2000 µM					
	k / µM^{-1}	d	r^2	σ_{rest}	σ_{method} / µM	LOD / µM	k / µM^{-1}	d	r^2	σ_{rest}	σ_{method} / µM	LOD / µM
Ala	0,003124	-0,04793	0,9981	0,0584	18,7	48	0,002795	0,06979	0,9945	0,156	56,0	130
Arg	0,003310	0,01768	0,9987	0,0505	15,3	39	0,003141	0,07808	0,9986	0,0881	28,1	64
Asn	0,003482	-0,06038	0,9988	0,0511	14,7	37	0,003377	-0,02299	0,9993	0,0655	19,4	44
Asp$^{!100}$	0,000932	0,03721	0,9949	0,0300	32,2	96	0,001595	-0,2435	0,9465	0,298	187	470
Cys	0,00008681	0,008555	0,9836	0,00483	55,6	140	0,00008944	0,007614	0,9956	0,00448	50,1	120
Gln	0,004177	0,03885	0,9983	0,0749	17,9	46	0,004566	-0,1004	0,9971	0,187	40,9	94
Glu	0,002923	-0,1696	0,9916	0,116	39,6	100	0,001568	0,3151	0,7863	0,616	393	900
Gly	0,001995	-0,04381	0,9975	0,0429	21,5	55	0,001924	-0,01850	0,9988	0,0498	25,9	59
His	0,002528	-0,01814	0,9993	0,0288	11,4	29	0,002585	-0,03839	0,9997	0,0361	14,0	32
Ile	0,003873	-0,05178	0,9993	0,0456	11,8	30	0,003674	0,01950	0,9987	0,0982	26,7	61
Leu	0,003827	-0,05051	0,9994	0,0413	10,8	27	0,003655	0,01120	0,9990	0,0857	23,4	54
Lys	0,005581	-0,1210	0,9997	0,0445	7,98	20	0,004811	0,1544	0,9909	0,347	72,2	170
Met	0,003553	-0,04355	0,9991	0,0456	12,8	33	0,003390	0,01480	0,9989	0,0837	24,7	57
Phe	0,003640	-0,04924	0,9990	0,0492	13,5	34	0,003405	0,03463	0,9980	0,114	33,5	77
Ser	0,003502	-0,04955	0,9987	0,0534	15,3	39	0,004002	-0,2285	0,9943	0,229	57,3	130
Thr	0,002825	-0,05207	0,9985	0,0472	16,7	43	0,002659	0,007224	0,9982	0,0854	32,1	74
Trp	0,003008	-0,04024	0,9991	0,0398	13,2	34	0,002803	0,03330	0,9978	0,0988	35,2	81
Tyr^{⅕}	0,003374	-0,004188	0,9978	0,0135	4,00	13	0,003236	0,005619	0,9987	0,0172	5,32	12
Val	0,004675	0,0008349	0,9970	0,110	23,5	60	0,004305	0,1334	0,9965	0,193	44,8	100

!100.....without 100 µM

⅕ .....one-fifth of the concentration used: 4 µM – 400 µM

The limit of detection (LOD) has been calculated from the linear calibration curve with the 95 % confidence interval.

Table IV-VI calibration functions for the standard method (4.2.2): based on measured signal area

direct	(10 - 2000) µM					
	k / μM^{-1} · mAU · min	d / mAU · min	r^2	σ_{rest} / mAU · min	σ_{method} / µM	LOD / µM
Ala	0,02194	0,02037	0,9996	0,313	14,2	22
Arg	0,02439	-0,1875	0,9988	0,599	24,6	38
Asn	0,02200	0,5196	0,9977	0,748	34,0	52
Asp	0,01363	0,8132	0,9949	0,685	50,2	77
Gln	0,02913	-0,6131	0,9984	0,832	28,5	44
Glu$^{<=100}$	0,06203	-1,374	0,8707	1,07	17,3	120
Gly	0,01463	-0,2620	0,9990	0,325	22,2	34
His	0,02504	-0,9820	0,9947	1,28	51,1	79
Ile	0,02814	-0,1907	0,9994	0,486	17,3	27
Leu	0,02777	-0,1944	0,9994	0,469	16,9	26
Lys	0,04263	-0,9110	0,9993	0,788	18,5	29
Met	0,02597	-0,1876	0,9994	0,457	17,6	27
Phe	0,02940	-0,7275	0,9979	0,957	32,6	50
Ser	0,03201	-0,9166	0,9988	0,773	24,1	37
Thr	0,02396	-0,1776	0,9995	0,370	15,4	24
Trp	0,02245	-0,07589	0,9993	0,412	18,3	28
Tyr	0,02566	0,008982	0,9996	0,340	13,3	20
Val	0,02782	-0,1294	0,9992	0,553	19,9	31

<=100 .....10 µM – 100 µM

Cysteine couldn't be resolved due to the deteriorating condition of the used analytical column.

Table IV-VII calibration functions for the standard method (4.2.2): based on normalised signal area

norm.	(10 - 2000) µM					
	k / μM^{-1}	d	r^2	σ_{rest}	σ_{method} / µM	LOD / µM
Ala	0,0007112	-0,01536	0,9986	0,0183	25,8	40
Arg	0,0007911	-0,02358	0,9959	0,0354	44,7	69
Asn	0,0007134	-0,0004349	0,9996	0,00981	13,7	21
Asp	0,0004426	0,01416	0,9987	0,0112	25,4	39
Gln	0,0009447	-0,03978	0,9949	0,0476	50,4	78
Glu$^{<=100}$	0,001824	-0,04041	0,8695	0,0317	17,4	120
Gly	0,0004742	-0,01852	0,9967	0,0193	40,7	63
His	0,0008117	-0,04774	0,9906	0,0555	68,4	110
Ile	0,0009124	-0,02633	0,9975	0,0323	35,3	55
Leu	0,0009003	-0,02607	0,9975	0,0318	35,3	54
Lys	0,001381	-0,05804	0,9971	0,0519	37,5	58
Met	0,0008419	-0,02445	0,9977	0,0285	33,8	52
Phe	0,0009529	-0,04318	0,9953	0,0462	48,4	75
Ser	0,001037	-0,05048	0,9958	0,0469	45,2	70
Thr	0,0007767	-0,02284	0,9981	0,0238	30,6	47
Trp	0,0007280	-0,01859	0,9979	0,0231	31,8	49
Tyr	0,0008322	-0,01855	0,9982	0,0247	29,7	46
Val	0,0009020	-0,02430	0,9975	0,0316	35,0	54

<=100 .....10 µM – 100 µM

Cysteine couldn't be resolved due to the deteriorating condition of the used analytical column.

VI. MS^n analysis

VI.I. Determination of the delay volume

Table VI-I delay volume UVD 170U – Foxy R1

Colour change /s	Peak @ 5% /min	Flow rate /(ml min^{-1})	Volume /µl
93	0,395	0,2	231
90	0,389	0,2	222
88	0,386	0,2	216
44	0,187	0,4	**218**
45	0,205	0,4	**218**
44	0,1833	0,4	220
17	0,0741	1,0	209
17	0,0740	1,0	209
18	0,0738	1,0	226
29	0,124	0,6	215
30	0,125	0,6	225
29	0,125	0,6	215
22	0,0945	0,8	**218**
22	0,0938	0,8	**218**
22	0,0939	0,8	**218**

Median(volume) = **218 µl**, average(volume) = 219 µl

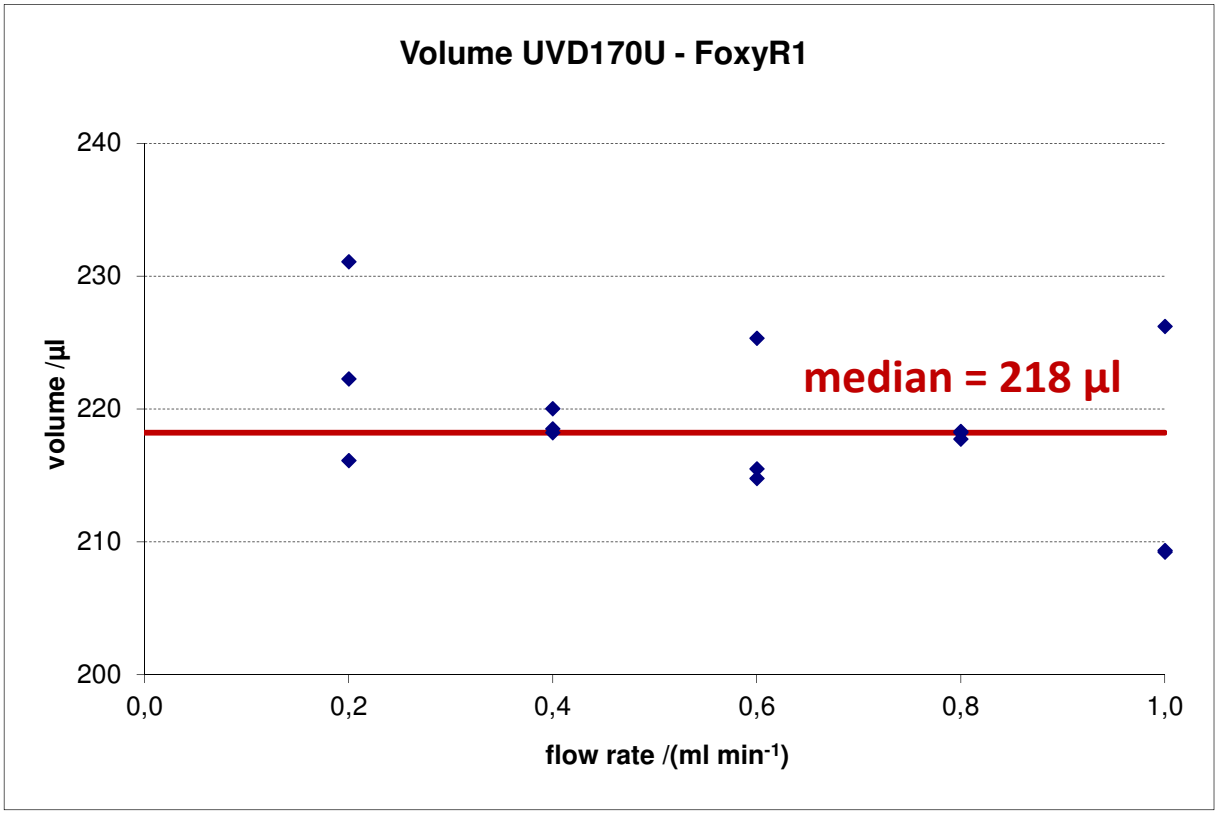

Figure VI-I delay volume UVD 170U – Foxy R1

VI.II. Windows batch file filtering the possible molecular formulas for DBEs

```
:: Liste von Summenformeln nach Doppelbindungsäquivalenten filtern
:: Listenformat: Molecular Weight Calculator 6.x, Formel-Finder
:: für organische Moleküle: CHNO mit S (2-wertig) und Halogenen: F, Cl, Br, I
:: DBE = 1/2 * (2 * 4-wertige Atome + 3-wertige Atome - 1-wertige Atome + 2)

@echo off
title DBEfilter
:: ------------------------------------------------------------------------------
:: Pfade mit Leerzeichen müssen in Hochkommata eingeschlossen werden,
:: ansonsten beginnt beim ersten Leerzeichen bereits %2 bzw. argv[2]
:: ohne Leerzeichen werden die einzelnen Worte als separate Argumente übergeben
:: Leerzeichen in den Befehlen der Batchdatei sind ebenfalls problematisch
:: ------------------------------------------------------------------------------

setlocal enableextensions enabledelayedexpansion
:: verzögerte Erweiterung von Umgebungsvariablen:
:: Inhalt der Variablen wird bei Verwendung von "!" anstatt "%" zur Laufzeit erweitert
("gefüllt")
:: anstatt zur Zeit des Einlesens in die logische Verarbeitungsstruktur des Interpreters
:: (Problem: Zusammenfassung logisch zusammengehörender Blöcke wie etwa ein If-Block, ...
:: und dementsprechend auch nur einmaliges Erweitern der Variablen)
:: - nur wenn Feature aktiviert (cmd /v oder setlocal enabledelayedexpansion in Batch-Dateien)

:: Anzahl der übergebenen Parameter überprüfen
if "%1"=="" goto para0
if "%2"=="" goto para1
goto paraN

:: Belegen mit den voreingestellten Standarwerten
:: keine Parameter => Standarddatei und Standardfilter
:para0
set szDatei=DBE.txt
goto para00
:: nur Datei angegeben, Standardfilter gültig
:: %~nxI erstellt den Dateinamen und die Dateierweiterung von %I.
:para1
set szDatei=%~nx1
:para00
:: Standardfilter: DBE -2 -> 8
:: iN ... Anzahl der akzeptierten DBEs (gespeichert in iFn)
set /a iN=11
set /a ii=0
for /L %%i in (-2,1,8) do (
    set /a iF!ii!=%%i
    ::echo [%%i - iF!ii!]
    set /a ii+=1
)
goto checkfile


:: übergebene Parameter auf ihren Typ überprüfen
:: ------------------------------------------------------------------------------
:: set /a liefert 0 bei Konvertierung eines Strings mit Elementen aus [^0-9]
:: beginnt der String mit (einer) Ziffer(n) und setzt mit Nichtziffern ([^0-9]) fort,
:: so führt dies zu einem schweren Fehler beim Interpretieren (errorlevel: 9167)
:: Besteht die "Zahl" nur aus " führt dies ebenfalls zu einem Interpreterfehler
:: (errorlevel 1073750990).

:: Else muss bei If-Else Konstrukten in derselben Zeile wie der Befehl nach If stehen
:: ohne die Klammern bei IF ... (goto ...) ELSE muss (!) der Befehl nach ELSE in der
:: nächsten Zeile stehen; ansonsten wird er ignoriert!
:: ------------------------------------------------------------------------------
:: 2> ... Umleitung der Ausgabe an stderr
:: Parameter einlesen: Datei (%1) und Filter (ab %2)
:: while-Schleife nicht verfügbar => if & goto
:paraN
set szDatei=%~nx1
set /a iN=0

:Schleife
:: alle Parameter eingelesen und geprüft
if "%2"=="" goto checkfile
set /a iF%iN%=%2 2>NUL
:: Zeichenketten, die nicht mit einer Ziffern beginnen, werden als 0 interpretiert.
if not errorlevel 0 goto numerror
::echo !iDBE%iN%!
```

```
set /a iN+=1
:: verschiebt alle Kommandozeilenparameter ab Nr. 2 eine Position nach unten (z.B. %5 -> %4)
shift /2
goto Schleife

:: übergebene "Textdatei" auf Existenz prüfen
:: iFilter ... Anzahl der gefundenen Summenformeln mit den spezifizierten DBEs
:: iZeile ... momentan bearbeitete Zeile in der Textdatei
:checkfile
set /a iFilter=0
set /a iZeile=0
if not exist "%szDatei%" goto EndeDatei
for /f "tokens=1 delims=    " %%i in (%szDatei%) do (
    :: Ende der Summenformeln, Einträge früherer Durchläufe folgen
    if %%i==-----D--B--E--f-i-l-t-e-r----- goto EndeSF
    set /a iZeile+=1
    if !iZeile!==1 (
        set szAnzahl=%%i
        :: in die Datei den verwendeten Filter eintragen
        echo.>> %szDatei%
        echo.>> %szDatei%
        echo.-----D--B--E--f-i-l-t-e-r----->> %szDatei%
        echo %date% - %time%>> %szDatei%
        echo akzeptierte DBE:>> %szDatei%
        set /a iN-=1
        for /l %%j in (0,1,%iN%) do (
            set szDBE=!szDBE! !iF%%j!
        )
        rem Im ersten Durchlauf der Schleife ist szDBE (der Rechtswert in der Zuweisung)
        rem undefiniert. => standardmäßig NULL (nicht druckbares Zeichen)
        rem => 1. Zeichen (NULL) und letztes Zeichen (Leerzeichen) entfernen
        rem Direkt beim Schreiben in die Datei funktioniert dies aber nicht, Ausgabe:
[szDBE:~1,-1].
        ::echo.[!szDBE:~1,-1!] >> %szDatei%
        set szDBE2=!szDBE:~1,-1!
        echo.!szDBE2!>>%szDatei%
        echo.>> %szDatei%
    ) else (
        for /f "tokens=1-9 delims=0123456789" %%j in ("%%i") do (
            ::echo %%j %%k %%l %%m %%n %%o %%p %%q %%r
            call :DBE %%i %%j %%k %%l %%m %%n %%o %%p %%q %%r
        )
    )
)
:EndeSF

:: Eintrag in der ersten Zeile: "Compounds found:  526"
:: tokens=3 wählt das 3. erkannte Element (abgetrennt durch das nach delims= angeführte
:: Zeichen), erstellt eine Variable dafür und führt die Befehle nach do dafür aus.
:: mehrere Einträge pro Zeile: tokens=x,y,m-n,* bedeutet eine Variable (die, die vor der
:: Schleife angeführt ist, 1 Buchstabe) für das x. Element, der nächste Buchstabe im Alphabet
:: als Variable für y und dasselbe für die Elemente m bis n. Der Stern erzeugt eine weitere
:: Variable (nach demselben Benennungsschema) für den Rest der Zeile - egal wie viel
:: dies noch ist und wie viele Begrenzungszeichen (delims) dort noch vorkommen.
for /f "tokens=3 delims= " %%i in ("%szAnzahl%") do set /a iAnzahl=%%i
set /a iZeile-=1

echo.>> %szDatei%
echo.%iFilter% von %iZeile% Summenformeln>> %szDatei%
echo.
echo.bearbeitete Datei: %szDatei%
echo Es wurden %iZeile% von %iAnzahl% Summenformeln eingelesen,
echo davon wiesen %iFilter% die spezifizierten DBE auf.

endlocal
pause > NUL
goto:EOF


:: Aufbereitung der Summenformel (übergeben in %1)
:: für organische Moleküle: CHNO mit S(2-wertig) und Halogenen: F, Cl, Br, I
:: iE ... Anzahl der beteiligten Elemente in der Summenformel
:: iDBE ... 2-mal die Doppelbindungsequivalente (initialisiert mit 2 da +2 in der Formel für
DBE)
:: iIndex ... Läuferposition im Summenformelstring (hier als %1 verfügbar)
:: iInk ... Inkrement auf iIndex für das jeweilige Elementsymbol
:: iZ ... Anzahl der Stellen des Index des jeweiligen Elements
:: iI ... Multiplikator des jeweiligen Elementes
```

```
:: iZahl ... Index des jeweiligen Elementes
:: iStart ... Beginn des Index
:: szSF ... String mit der Summenformel
:: szE ... String mit dem aktuellen Elementsymbol

:DBE
set szSF=%1
set sZE=%2
set /a iE=0
set /a iDBE=2
set /a iIndex=0
set /a iInk=0
set /a iZ=0
::echo szSF = %szSF%

:lesen
::echo [%szE%]
if "%szE%"=="" goto schreiben
if %szE%==C (
    set /a iI=2
    goto l
)
if %szE%==H (
    set /a iI=-1
    goto l
)
if %szE%==N (
    set /a iI=1
    goto l
)
if %szE%==O (
    set /a iI=0
    goto l
)
if %szE%==S (
    set /a iI=0
    goto l
)
if %szE%==F (
    set /a iI=-1
    goto l
)
if %szE%==Cl (
    set /a iI=-1
    set /a iInk=1
    goto l
)
if %szE%==Br (
    set /a iI=-1
    set /a iInk=1
    goto l
)
if %szE%==I (
    set /a iI=-1
    goto l
)
:: hier angekommen: 1-fach vorkommendes Element => trennen
:: für organische Moleküle: CHNO mit S(2-wertig) und Halogenen: F, Cl, Br, I
:: => an zweiter Stelle steht ein l bei Chlor und ein r bei Brom, ansonsten ist
:: das erste Zeichen ein eigenes Element
:ll
::echo [[%szE:~1,1%]]
if %szE:~0,2%==Cl (
    ::echo.[Cl]
    set /a iInk=2
    set /a iI=-1
    goto lll
)
if %szE:~0,2%==Br (
    ::echo.[Br]
    set /a iInk=2
    set /a iI=-1
    goto lll
)
if %szE:~0,1%==C (
    ::echo.[C]
    set /a iInk=1
    set /a iI=2
```

```
    goto lll
)
if %szE:~0,1%==H (
    ::echo.[H]
    set /a iInk=1
    set /a iI=-1
    goto lll
)
if %szE:~0,1%==O (
    ::echo.[O]
    set /a iInk=1
    set /a iI=0
    goto lll
)
if %szE:~0,1%==N (
    ::echo.[N]
    set /a iInk=1
    set /a iI=1
    goto lll
)
if %szE:~0,1%==S (
    ::echo.[S]
    set /a iInk=1
    set /a iI=0
    goto lll
)
if %szE:~0,1%==F (
    ::echo.[F]
    set /a iInk=1
    set /a iI=-1
    goto lll
)
if %szE:~0,1%==I (
    ::echo.[I]
    set /a iInk=1
    set /a iI=-1
    goto lll
)

:lll
set /a iZahl=1
::echo #_ iIndex = %iIndex% _#
::echo #_ iInk = %iInk% _#
set /a iIndex+=iInk


::letztes Element des Mehrfachelementes wurde bearbeitet
::echo szE:iInk=##!szE:~%iInk%!##
::echo szSF:iIndex=##!szSF:~%iIndex%!##
:: "!szSF:~%iIndex%,!"=="" - und zwar immer <= %Test:~3,% ist äquivalent zu %Test:~3,0%

if "!szE:~%iInk%!"=="" (
    :: Ende der gesamten Summenformel
    if "!szSF:~%iIndex%!"=="" (
        set /a iDBE+=iZahl*iI
        set /a iE+=1
        ::echo #_ iZahl = %iZahl% _#
        goto schreiben
    )
    :: Summenformel geht noch weiter => Index anpassen (+1 im Standardweg)
    set /a iIndex-=iInk
    set /a iInk=0
    ::echo #_[%szE%]_#
    goto lesen
)

::echo ##!szE:~%iInk%!##
::echo #_ iZahl = %iZahl% _#
:: Beitrag zu den DBEs berechnen
set /a iDBE+=iZahl*iI
::nächste Runde in der verkürzten Schleife (nur das Mehrfachelement)
set /a iE+=1
set szE=!szE:~%iInk%!
set /a iInk=0
goto ll

:l
:: 1 Stelle für alle Elemente, die zweistelligen Elementsymbole haben iInk bereits auf 1
```

```
set /a iInk+=1
:: Anzahl der Atome des jeweiligen Elements einlesen: aus der Summenformel
:: cSF ... aktuell bearbeitetes Zeichen
:: C3H37S
:: iIndex == 1
set /a iIndex+=iInk
set /a iStart=%iIndex%
::echo szSF = %szSF%

::echo _ iIndex = %iIndex% _

set /a iZ=0
:StartIndex
set cSF=!szSF:~%iIndex%,1!
::echo _ cSF = !szSF:~%iIndex%,1! _
:: ist cSF eine Ziffer? - Typüberprüfung gibt's nicht
if "%cSF%"=="0" goto Ziffer
if "%cSF%"=="1" goto Ziffer
if "%cSF%"=="2" goto Ziffer
if "%cSF%"=="3" goto Ziffer
if "%cSF%"=="4" goto Ziffer
if "%cSF%"=="5" goto Ziffer
if "%cSF%"=="6" goto Ziffer
if "%cSF%"=="7" goto Ziffer
if "%cSF%"=="8" goto Ziffer
if "%cSF%"=="9" goto Ziffer
:: Ende der gesamten Summenformel (analoges Kriterium im :lll-Zweig)
if "%cSF%"=="" (
    :: wenn letztes Zeichen der Summenformel Elementsymbol: iZahl == 1
    if %iZ%==0 (
        set /a iDBE+=iI
        set /a iE+=1
        ::echo [_ iZahl = 1 _]
        goto schreiben
    )

)
goto keineZiffer

:Ziffer
    set /a iZ+=1
    set /a iIndex+=1
    goto StartIndex
::echo _ iZ = %iZ% _

:keineZiffer
:: iIndex steht bereits auf dem nächsten Elementsymbol
:: Index auswerten
set /a iZahl=!szSF:~%iStart%,%iZ%!
::echo _ iZahl = %iZahl% _

:: Beitrag zu den DBEs berechnen
set /a iDBE+=iZahl*iI
::echo ## iDBE = %iDBE% ##

:: Anzahl der Elementsymbole aktualisieren und nächste Runde vorbereiten
set /a iE+=1
set /a iInk=0
shift /2
set szE=%2
goto lesen

:schreiben
::echo.Summenformel: %szSF%
::echo.Elemente: %iE%
:: set /a beherrscht nur Ganzzahldivision => mit 2x DBE rechnen
::set /a iDBE/=2
::echo.2x DBE: %iDBE%
::echo.-----------------------
:: Auf die Standardausgabe funktioniert echo.%szSF% DBE=%iDBE% tadellos,
:: mit Pipe nicht mehr.?
:: echo.%szSF%  DBE=!iDBE!>> %szDatei%
for /l %%j in (0,1,%iN%) do (
    set /a iTemp=2*!iF%%j!
    if !iDBE!==!iTemp! (
        echo.%szSF% DBE: !iF%%j!>> %szDatei%
        set /a iFilter+=1
    )
```

```
)

goto:EOF

:numerror
echo.
echo Ung ltige Zahl; Numerische Konstanten sind entweder dezimale (85),
echo hexadezimale (0x55), oder oktale (0125) Zahlen.
echo Buchstaben werden als Null interpretiert.
goto Ende

:EndeDatei
echo.
echo.Die Datei %szDatei% konnte nicht gefunden werden.
goto Ende

:Ende
echo.
echo.Verwendung: %~n0 [Pfad\zu\Textdatei = ".\DBE.txt"] [[akzeptierte DBE = -2 -1 0 1 2 3 4 5
6 7 8]]
endlocal
pause > NUL
goto:EOF

:EOF
```

VI.III. Known OPA-derivatised amino acids

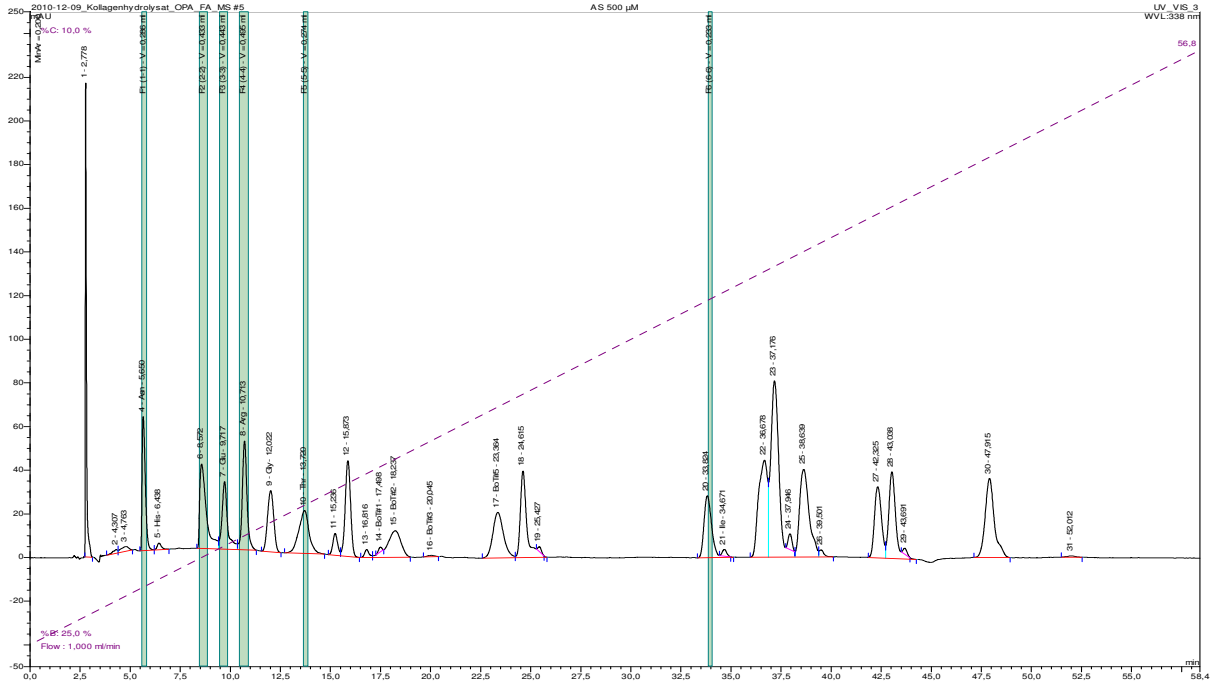

Figure VI-II AS 500 µM – RP-HPLC fractions for ESI-MS, collected: #1 (His), #2 (Arg), #5 (Glu), #6 (Met)

VI.III.I. Arg

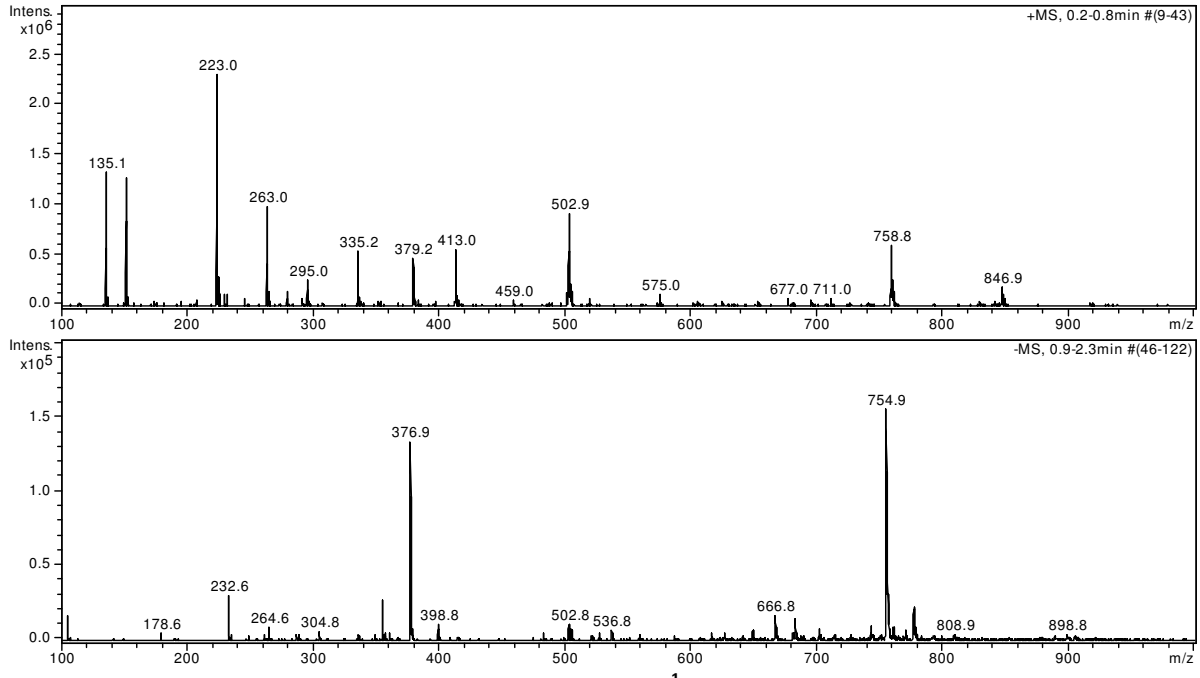

Figure VI-III HPLC fraction #2: 8,4 – 8,85 min, Arg; full scan MS[1]

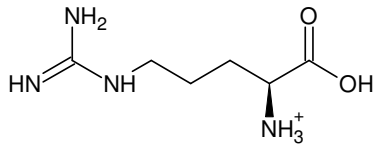

Monoisotopic Mass = 175.118952 Da

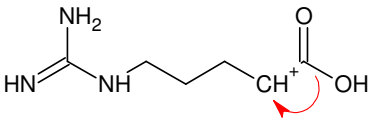

NH3
17.026549 Da

Monoisotopic Mass = 158.092403 Da

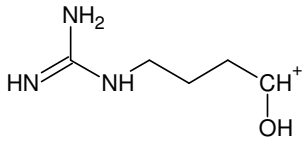

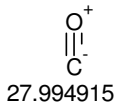

27.994915 Da

Monoisotopic Mass = 130.097488 Da

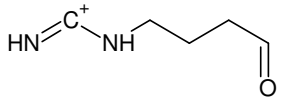

NH3
17.026549 Da

Monoisotopic Mass = 113.070939 Da

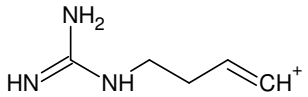

H2O
18.010565 Da

Monoisotopic Mass = 112.086924 Da

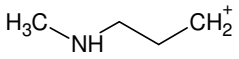

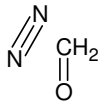

58.016713 Da

Monoisotopic Mass = 72.080776 Da

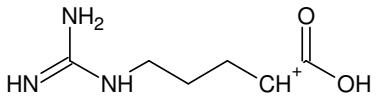

Monoisotopic Mass = 158.092403 Da

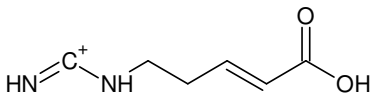

NH3
17.026549 Da

Monoisotopic Mass = 141.065854 Da

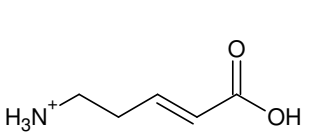

42.021798 Da

Monoisotopic Mass = 116.070605 Da

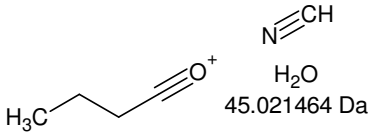

H2O
45.021464 Da

Monoisotopic Mass = 71.049141 Da

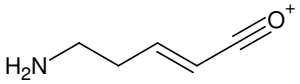

H2O
18.010565 Da

Monoisotopic Mass = 98.06004 Da

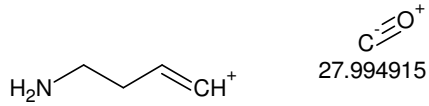

27.994915 Da

Monoisotopic Mass = 70.065126 Da

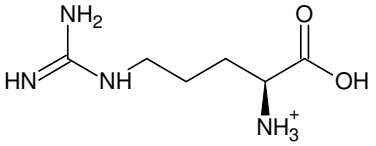

Monoisotopic Mass = 175.118952 Da

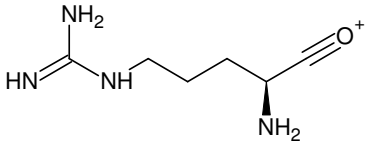

H2O
18.010565 Da

Monoisotopic Mass = 157.108387 Da

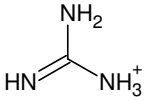

Monoisotopic Mass = 60.055624 Da

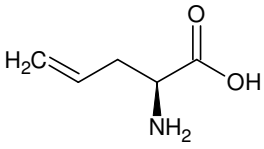

115.063329 Da

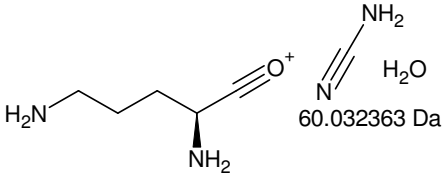

H2O
60.032363 Da

Monoisotopic Mass = 115.086589 Da

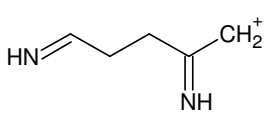

H2O
18.010565 Da

Monoisotopic Mass = 97.076025 Da

+MSn, reproduced from [155], Figure 4: fragmentation tree of Arg; 175 -> 158 -> 130 -> 113, 112, 72 and [175 -> 158) -> 141, 116 -> 71, 98 -> 70 as well as 175 -> 157, 60, 115 -> 122

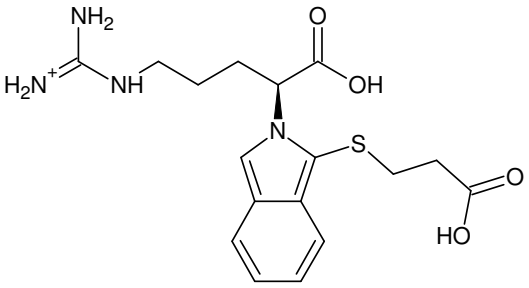

Monoisotopic Mass = 379.143452 Da

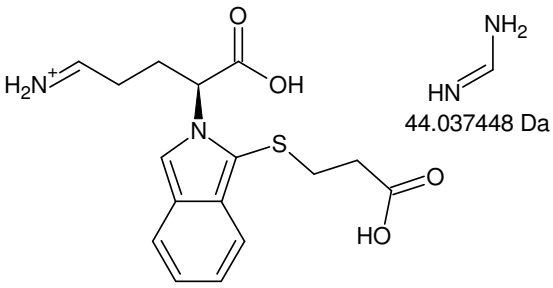

Monoisotopic Mass = 335.106003 Da

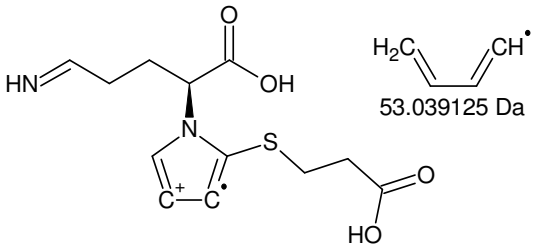

Monoisotopic Mass = 282.066878 Da

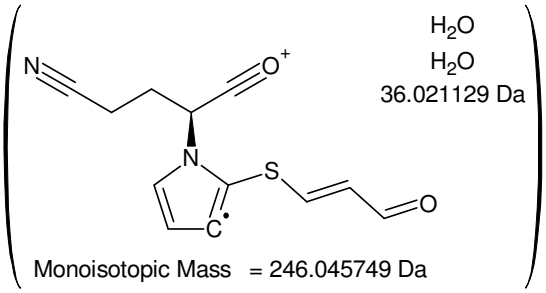

Monoisotopic Mass = 246.045749 Da

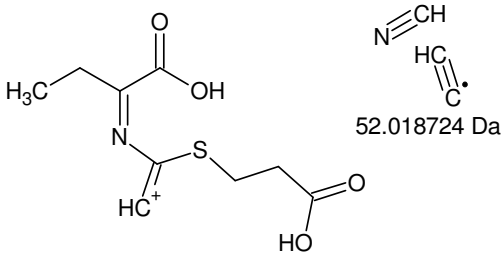

Monoisotopic Mass = 230.048154 Da

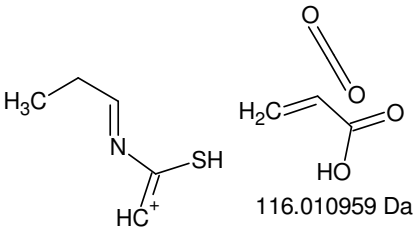

Monoisotopic Mass = 114.037196 Da

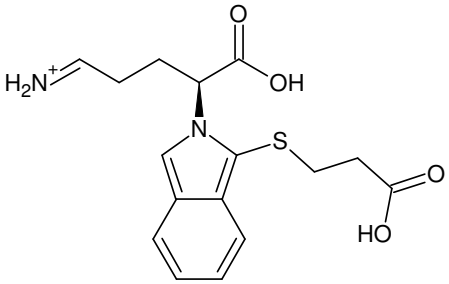

Monoisotopic Mass = 335.106003 Da

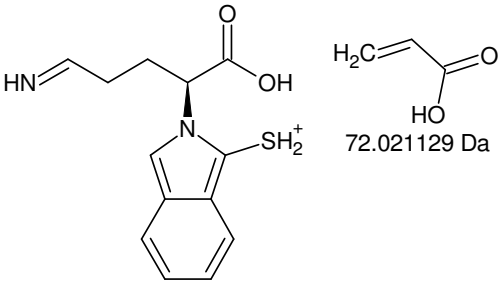

Monoisotopic Mass = 263.084874 Da

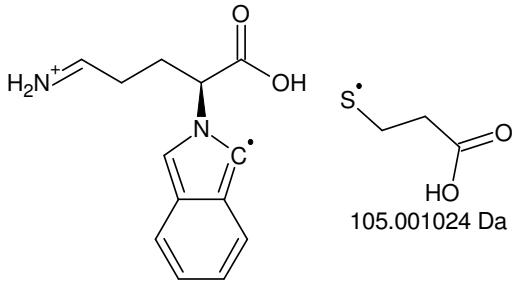

Monoisotopic Mass = 230.104979 Da

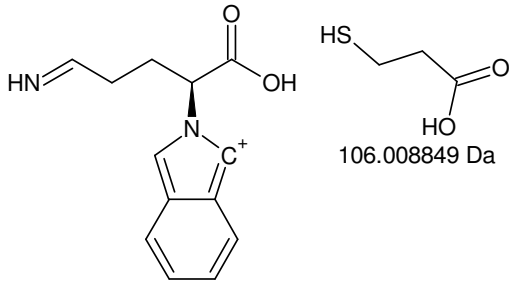

Monoisotopic Mass = 229.097154 Da

+MSn [OPA-Arg]: 379 -> 335 -> 282 -> (246), 230 -> 114 and [379 -> 335] -> 263, 205, 229

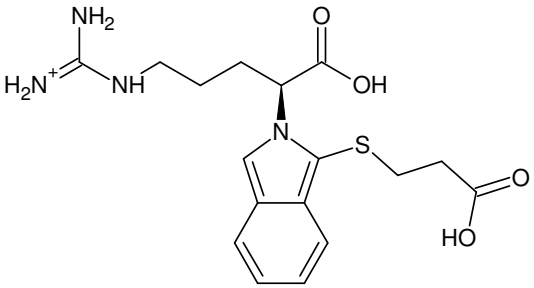

Monoisotopic Mass = 379.143452 Da

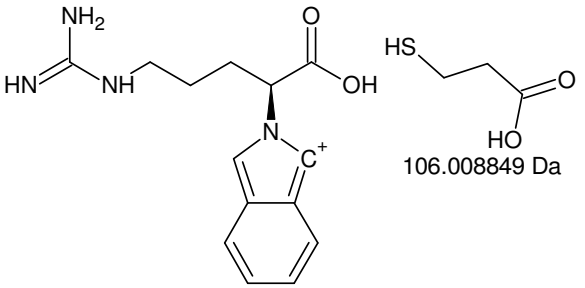

Monoisotopic Mass = 273.134602 Da

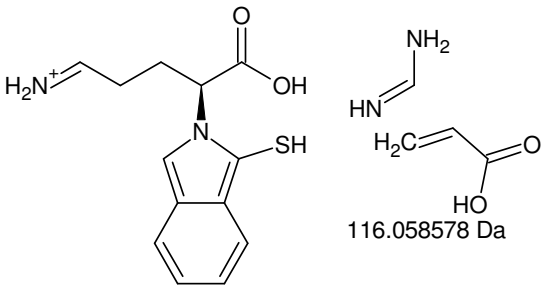

Monoisotopic Mass = 263.084874 Da

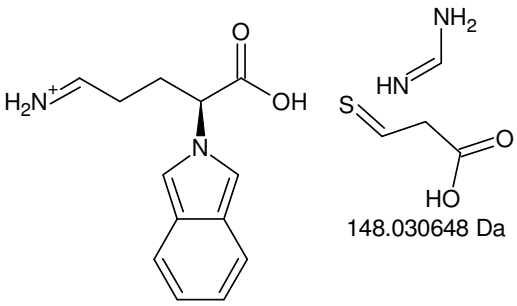

Monoisotopic Mass = 231.112804 Da

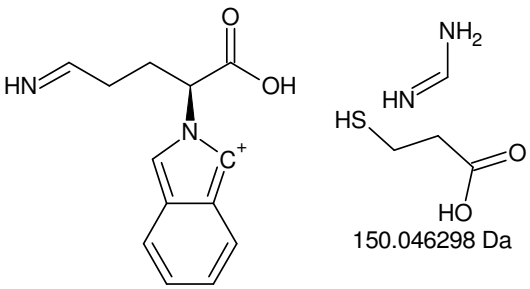

Monoisotopic Mass = 229.097154 Da

+MSn [OPA-Arg]: 379 -> 273, 263, 231, 229

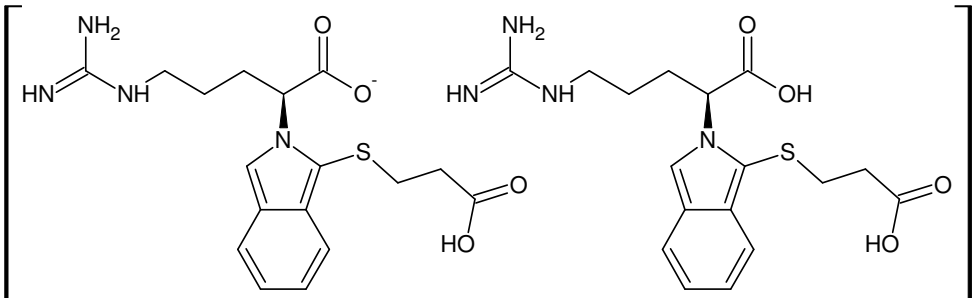

Monoisotopic Mass = 755.265074 Da

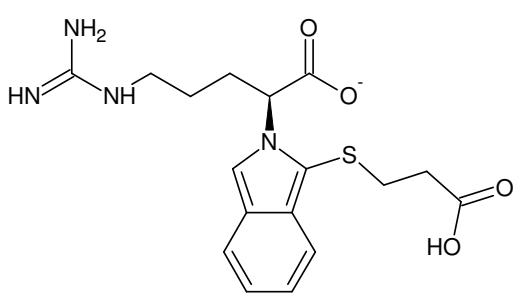

Monoisotopic Mass = 377.128899 Da

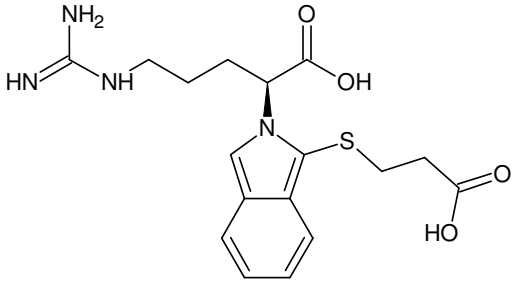

378.136175 Da

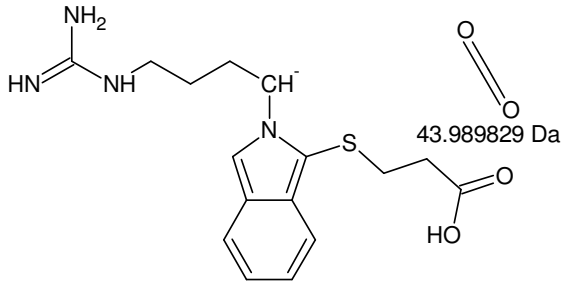

Monoisotopic Mass = 333.13907 Da

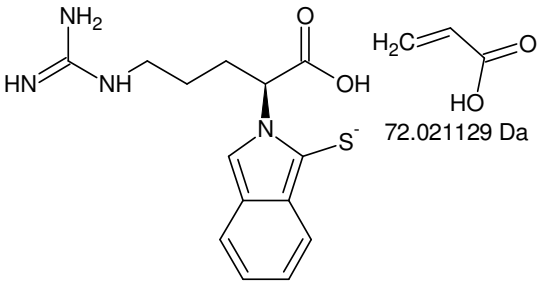

Monoisotopic Mass = 305.107769 Da

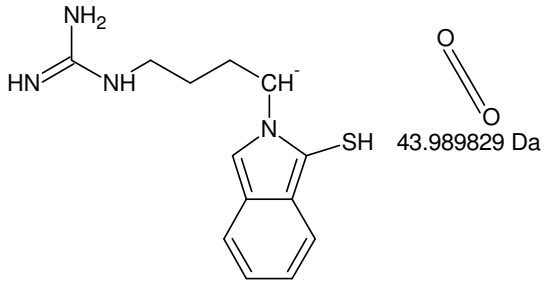

Monoisotopic Mass = 261.11794 Da

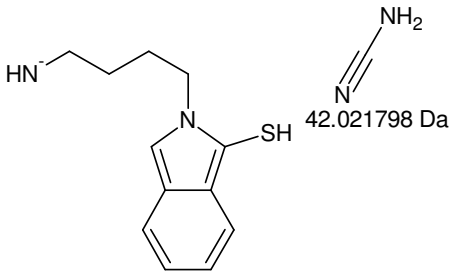

Monoisotopic Mass = 219.096142 Da

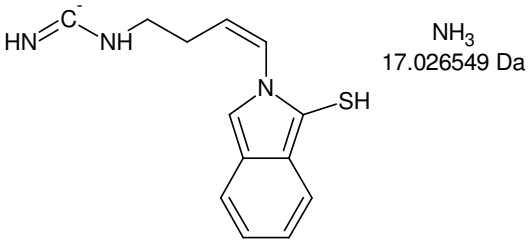

Monoisotopic Mass = 244.091391 Da

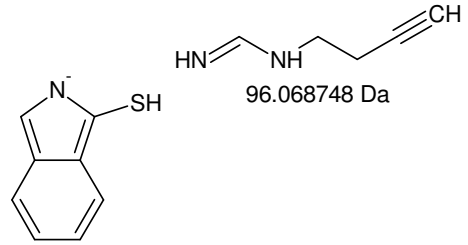

Monoisotopic Mass = 148.022643 Da

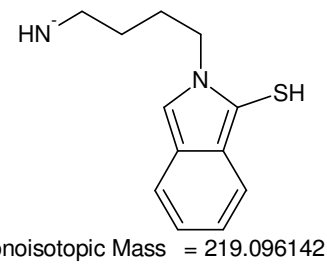

Monoisotopic Mass = 219.096142 Da

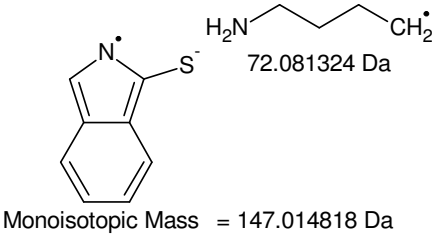

Monoisotopic Mass = 147.014818 Da

-MSn [OPA-Arg]: 755 -> 377 -> 333, 305 -> 261 -> 219, 244 -> 148 and [377 -> 305 -> 261 -> 219] -> 147

VI.III.II. Glu

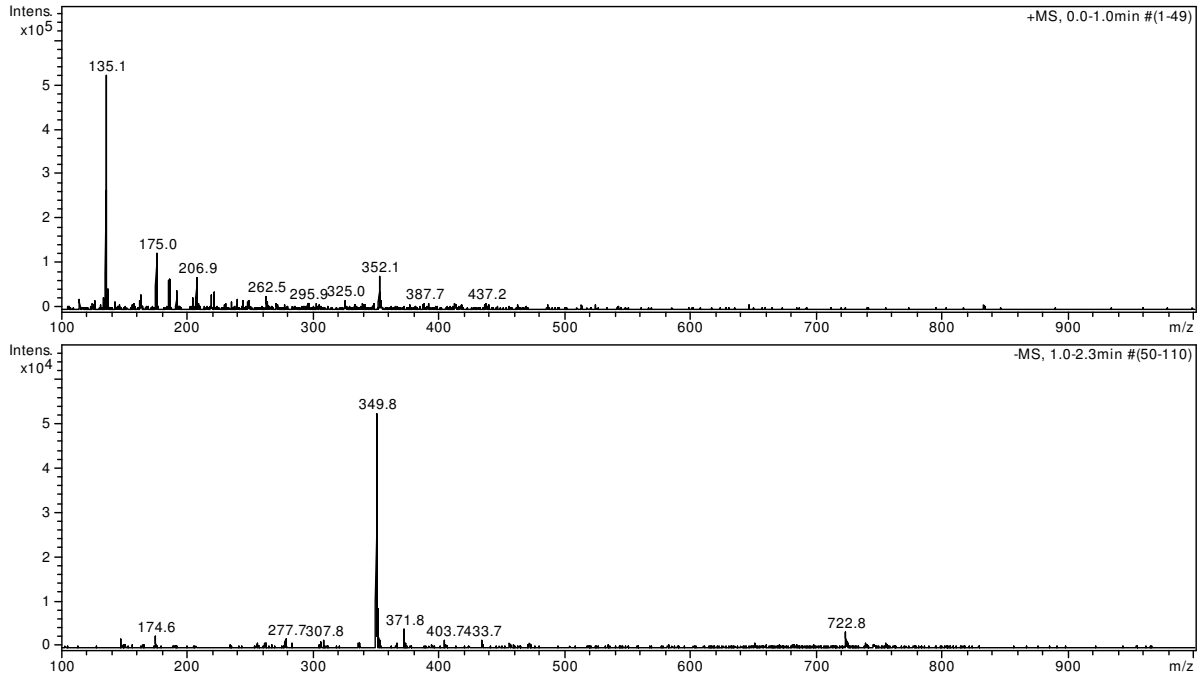

Figure VI-IV HPLC fraction #5: 13,6 – 13,9 min, Glu; full scan MS[1]

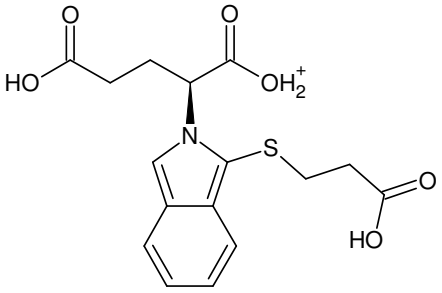

Monoisotopic Mass = 352.084934 Da

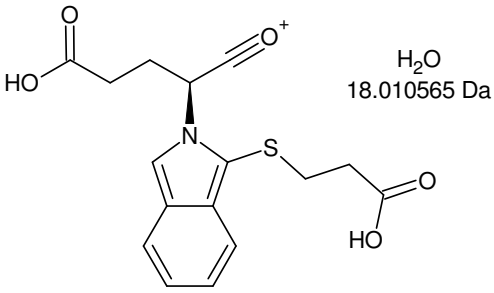

H_2O
18.010565 Da

Monoisotopic Mass = 334.074369 Da

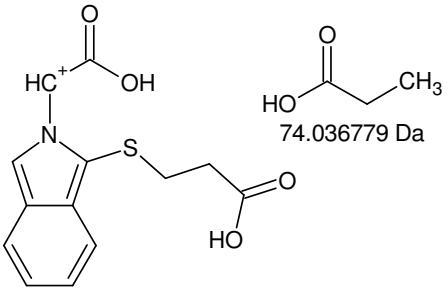

74.036779 Da

Monoisotopic Mass = 278.048154 Da

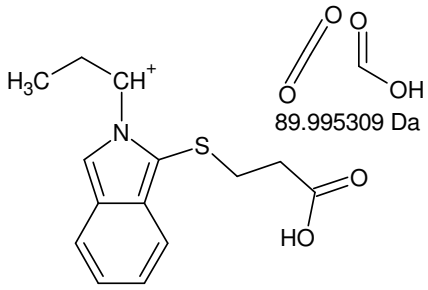

89.995309 Da

Monoisotopic Mass = 262.089625 Da

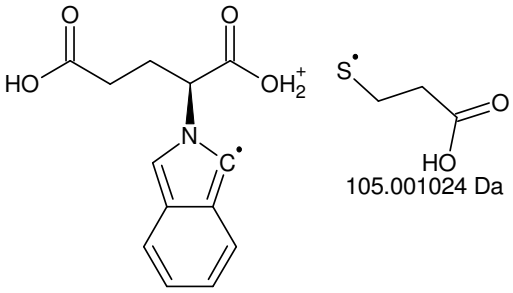

105.001024 Da

Monoisotopic Mass = 247.083909 Da

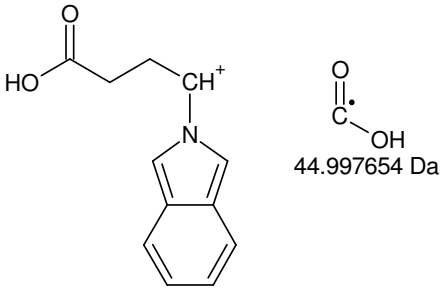

44.997654 Da

Monoisotopic Mass = 202.086255 Da

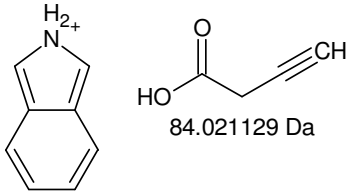

84.021129 Da

Monoisotopic Mass = 118.065126 Da

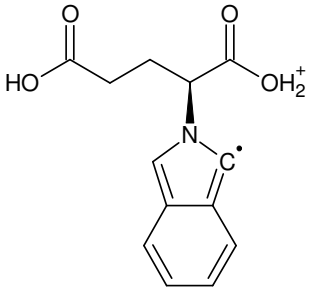

Monoisotopic Mass = 247.083909 Da

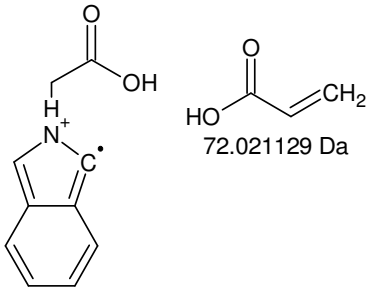

72.021129 Da

Monoisotopic Mass = 175.06278 Da

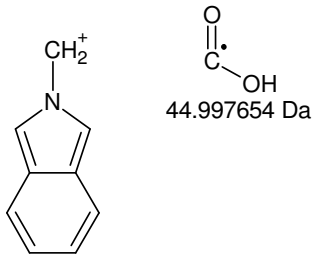

44.997654 Da

Monoisotopic Mass = 130.065126 Da

+MSn [OPA-Glu]: 352 -> 334, 278, 262, 247 -> 202 -> 118 and [352 -> 247] -> 175 -> 130

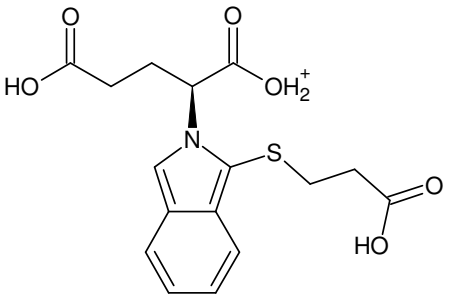

Monoisotopic Mass = 352.084934 Da

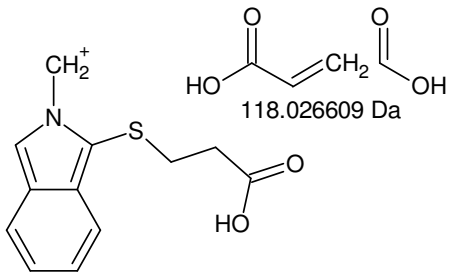

118.026609 Da

Monoisotopic Mass = 234.058325 Da

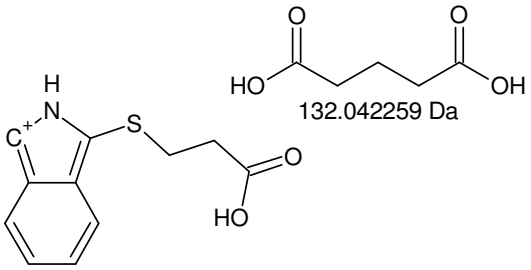

132.042259 Da

Monoisotopic Mass = 220.042675 Da

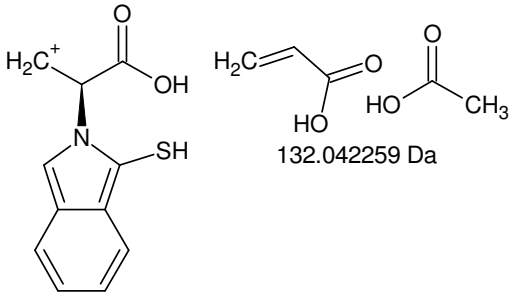

132.042259 Da

Monoisotopic Mass = 220.042675 Da

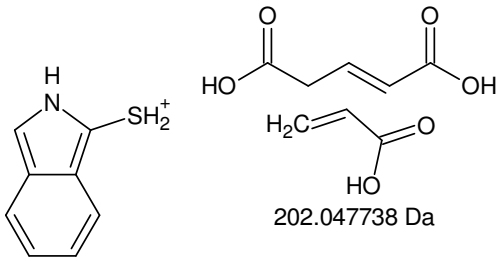

202.047738 Da

Monoisotopic Mass = 150.037196 Da

+MSn [OPA-Glu]: 352 -> 234, 220, 150

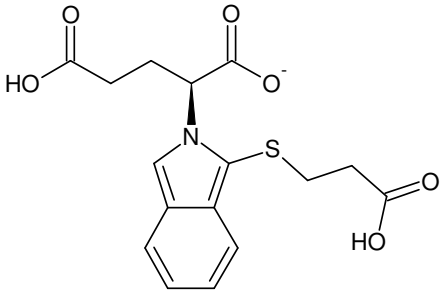

Monoisotopic Mass = 350.070381 Da

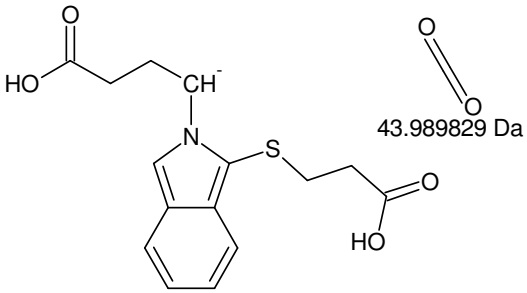

Monoisotopic Mass = 306.080552 Da

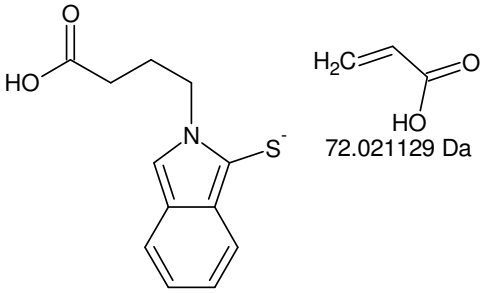

Monoisotopic Mass = 234.059422 Da

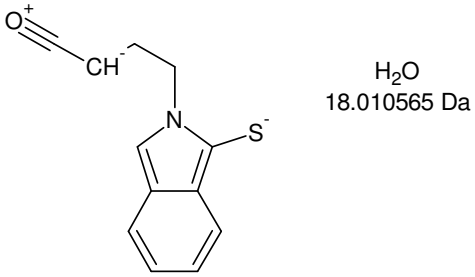

Monoisotopic Mass = 216.048858 Da

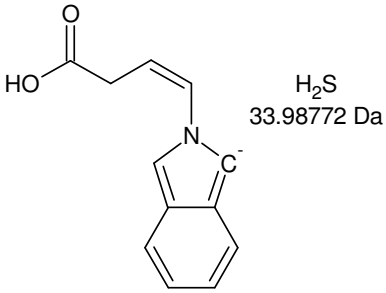

Monoisotopic Mass = 200.071702 Da

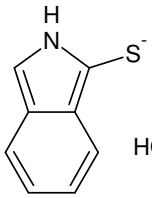

Monoisotopic Mass = 148.022643 Da

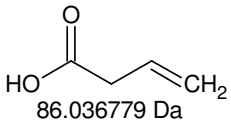

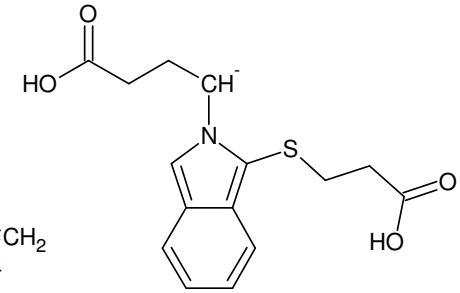

Monoisotopic Mass = 306.080552 Da

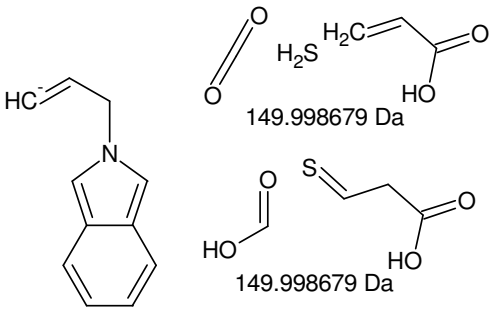

Monoisotopic Mass = 156.081873 Da

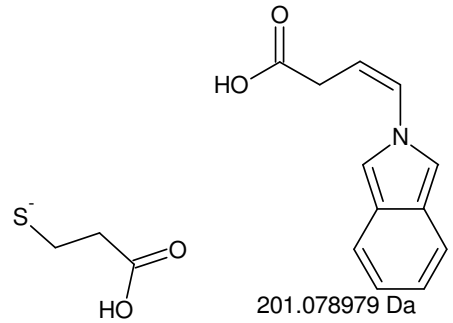

Monoisotopic Mass = 105.001573 Da

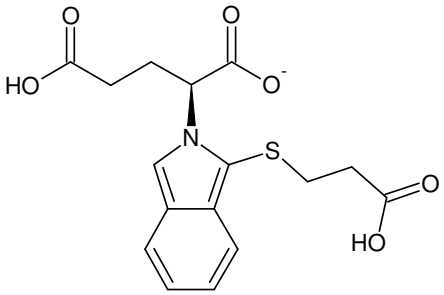

Monoisotopic Mass = 350.070381 Da

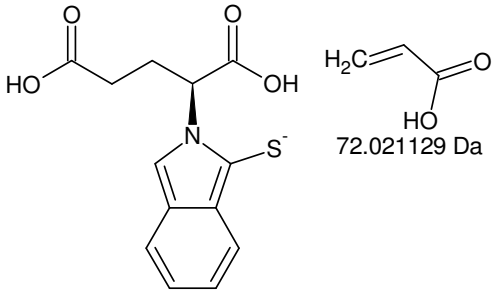

Monoisotopic Mass = 278.049251 Da

-MSn [OPA-Glu]: 350 -> 306 -> 234 -> 216, (200), 148 and [350 -> 306] -> 156, 105 as well as 350 -> 278

VI.III.III. His

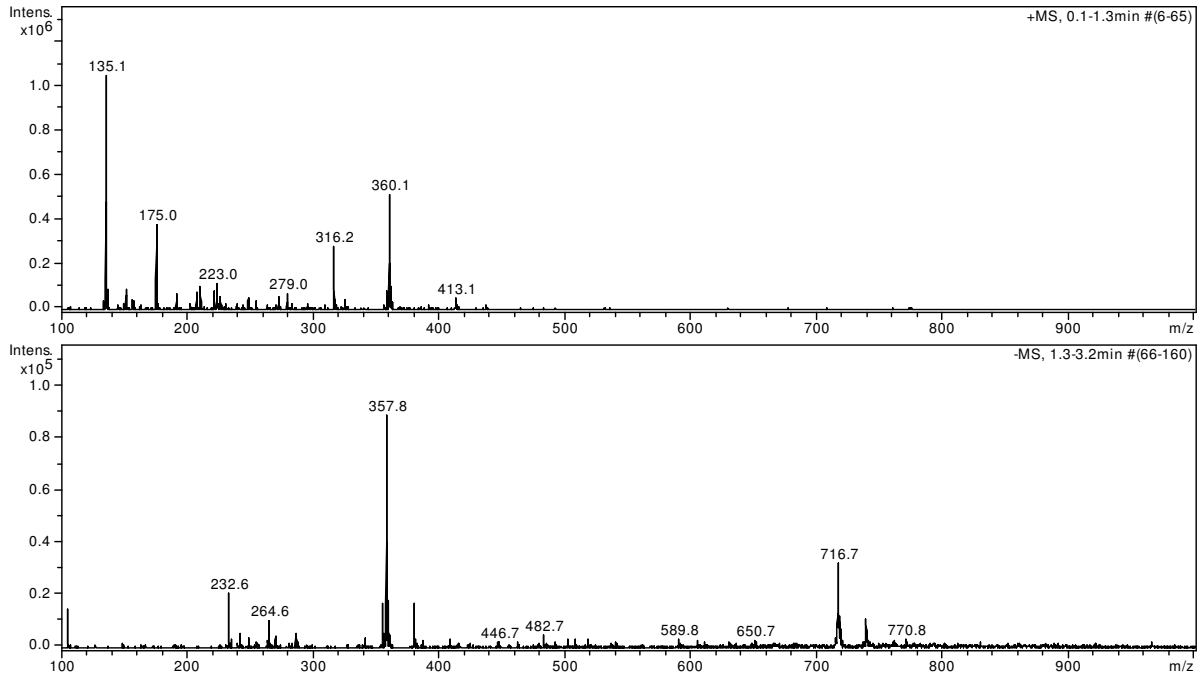

Figure VI-V HPLC fraction #1: 5,55 – 5,85 min min, His; full scan MS[1]

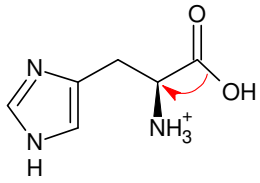

Monoisotopic Mass = 156.076753 Da

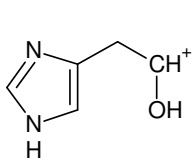

45.021464 Da

Monoisotopic Mass = 111.055289 Da

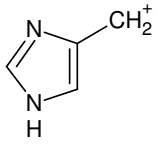

30.010565 Da

Monoisotopic Mass = 81.044725 Da

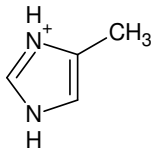

27.994915 Da

Monoisotopic Mass = 83.060375 Da

17.026549 Da

Monoisotopic Mass = 66.033826 Da

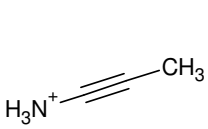

27.010899 Da

Monoisotopic Mass = 56.049476 Da

17.026549 Da

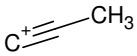

Monoisotopic Mass = 39.022926 Da

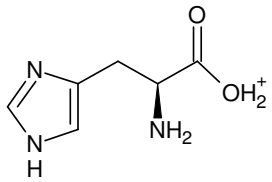

Monoisotopic Mass = 156.076753 Da

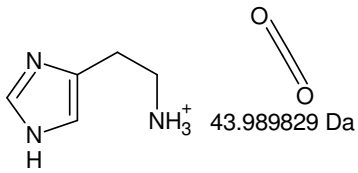

43.989829 Da

Monoisotopic Mass = 112.086924 Da

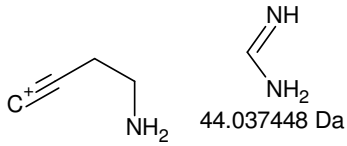

44.037448 Da

Monoisotopic Mass = 68.049476 Da

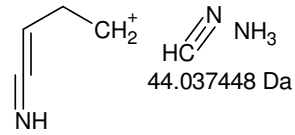

44.037448 Da

Monoisotopic Mass = 68.049476 Da

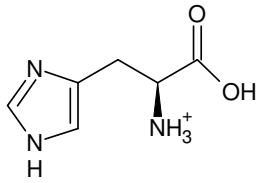

Monoisotopic Mass = 156.076753 Da

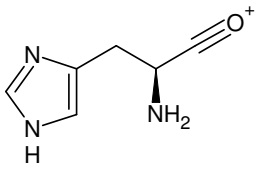

18.010565 Da

Monoisotopic Mass = 138.066188 Da

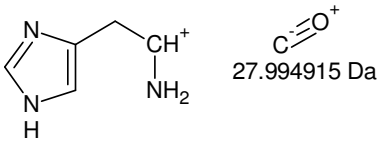

27.994915 Da

Monoisotopic Mass = 110.071274 Da

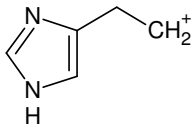

15.010899 Da

Monoisotopic Mass = 95.060375 Da

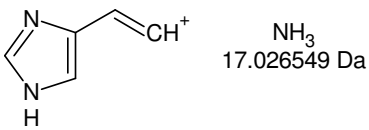

17.026549 Da

Monoisotopic Mass = 93.044725 Da

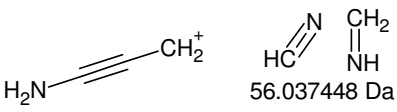

56.037448 Da

Monoisotopic Mass = 54.033826 Da

+MSn, reproduced from [155], Figure S-7: calculated fragmentation tree of His; 156 -> 111 -> 81, 83 -> 66, 56 -> 39 and 156 -> 112 -> 68 as well as 156 -> 138 -> 110 -> 95, 93, 54

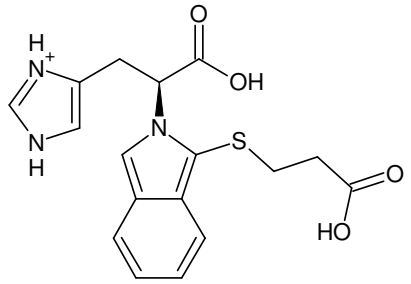

Monoisotopic Mass = 360.101252 Da

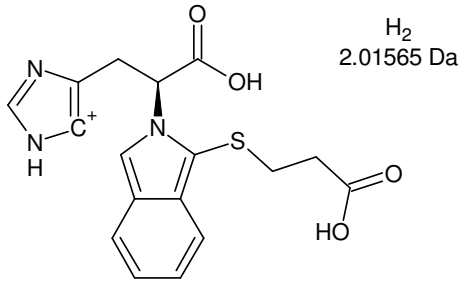

Monoisotopic Mass = 358.085602 Da

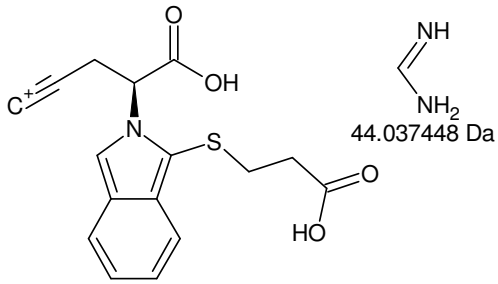

Monoisotopic Mass = 316.063804 Da

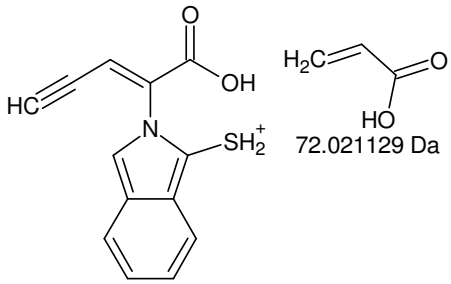

Monoisotopic Mass = 244.042675 Da

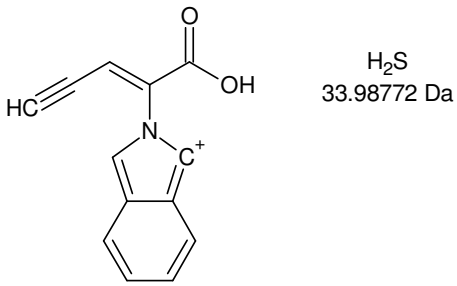

Monoisotopic Mass = 210.054955 Da

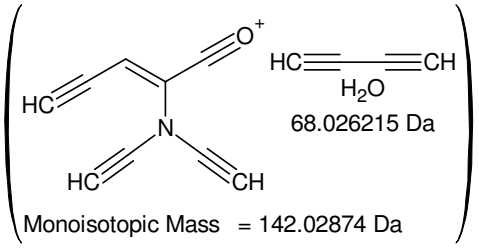

Monoisotopic Mass = 142.02874 Da

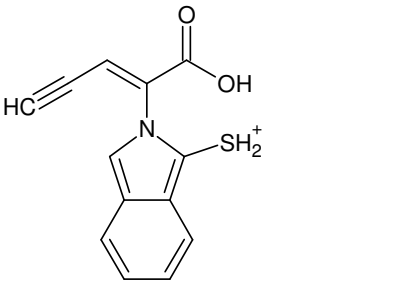

Monoisotopic Mass = 244.042675 Da

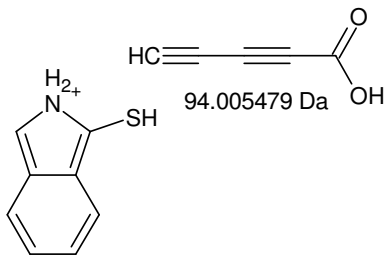

Monoisotopic Mass = 150.037196 Da

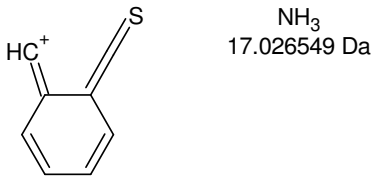

Monoisotopic Mass = 133.010647 Da

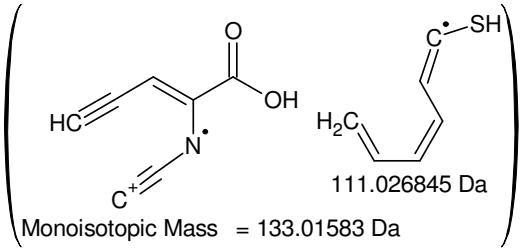

Monoisotopic Mass = 133.01583 Da

+MSn [OPA-His]: 360 -> 358, 316 -> 244 -> 210 -> (142) and [360 -> 316 -> 244] -> 150 -> 133

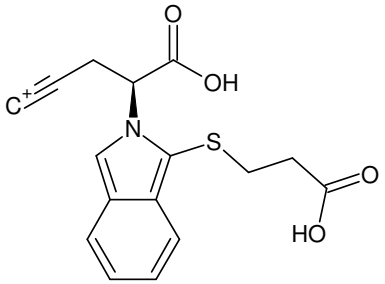

Monoisotopic Mass = 316.063804 Da

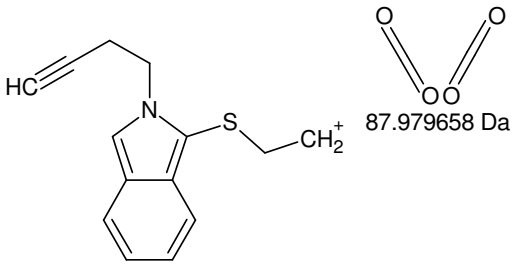

Monoisotopic Mass = 228.084146 Da

87.979658 Da

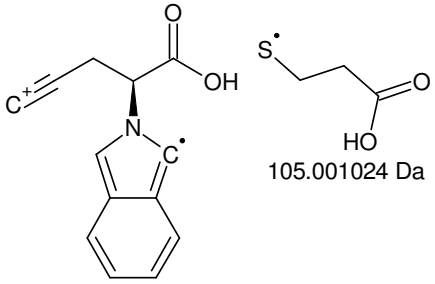

105.001024 Da

Monoisotopic Mass = 211.06278 Da

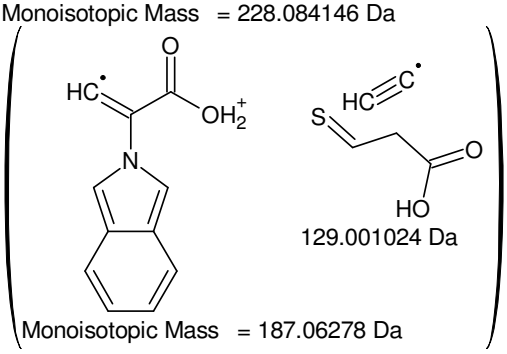

129.001024 Da

Monoisotopic Mass = 187.06278 Da

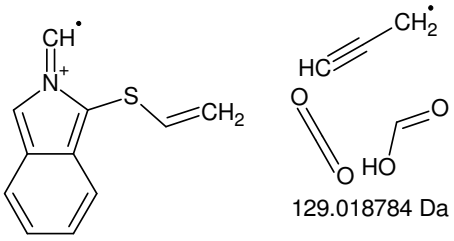

129.018784 Da

Monoisotopic Mass = 187.045021 Da

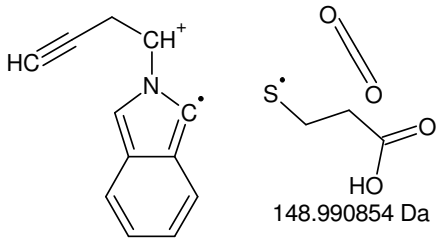

148.990854 Da

Monoisotopic Mass = 167.072951 Da

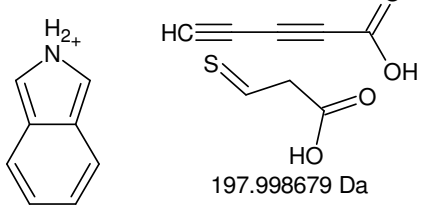

197.998679 Da

Monoisotopic Mass = 118.065126 Da

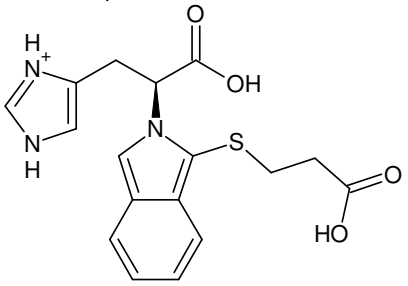

Monoisotopic Mass = 360.101252 Da

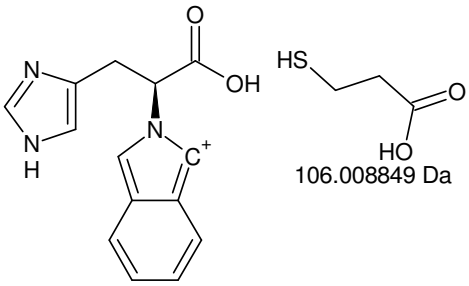

106.008849 Da

Monoisotopic Mass = 254.092403 Da

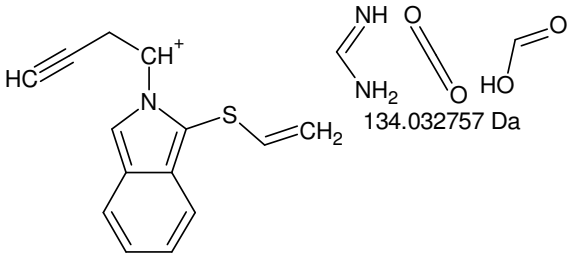

134.032757 Da

Monoisotopic Mass = 226.068496 Da

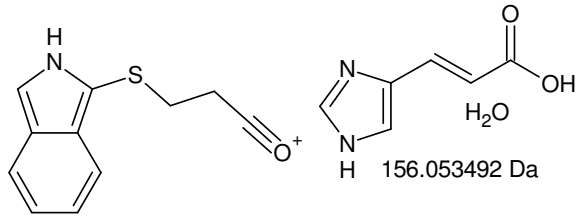

156.053492 Da

Monoisotopic Mass = 204.04776 Da

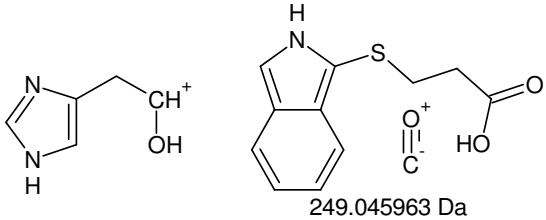

249.045963 Da

Monoisotopic Mass = 111.055289 Da

+MSn [OPA-His]: [360 -> 316] -> 228, 211, 187, 167, 118 and 360 -> 254, 226, 204, 111

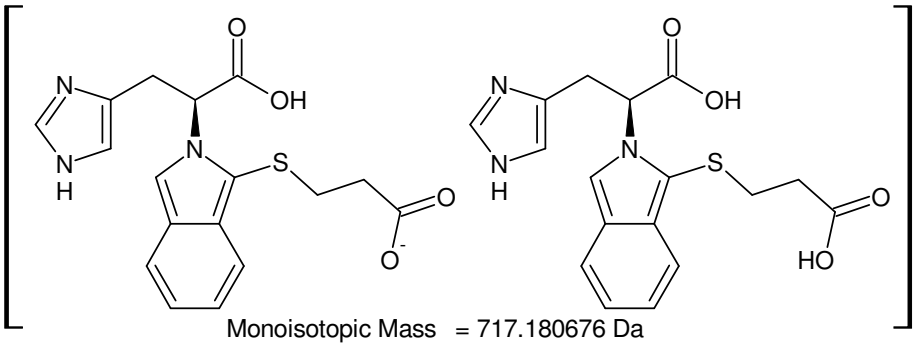

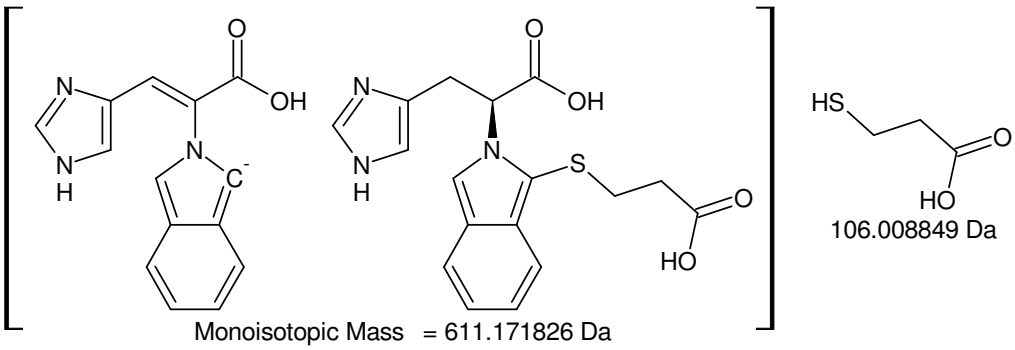

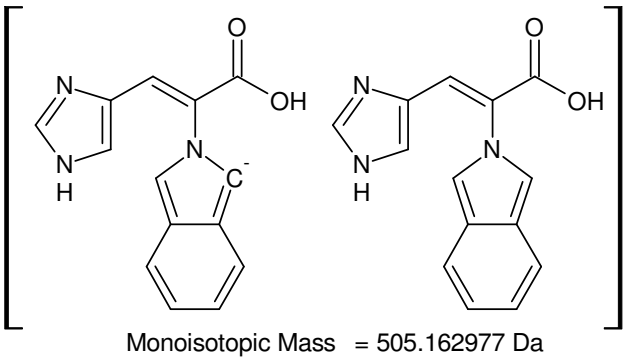

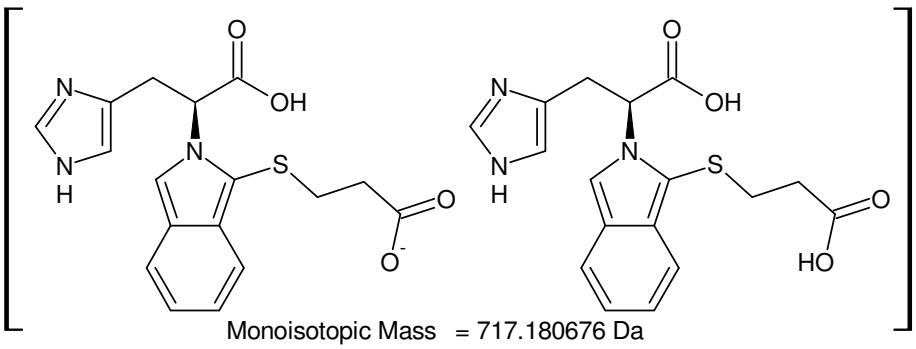

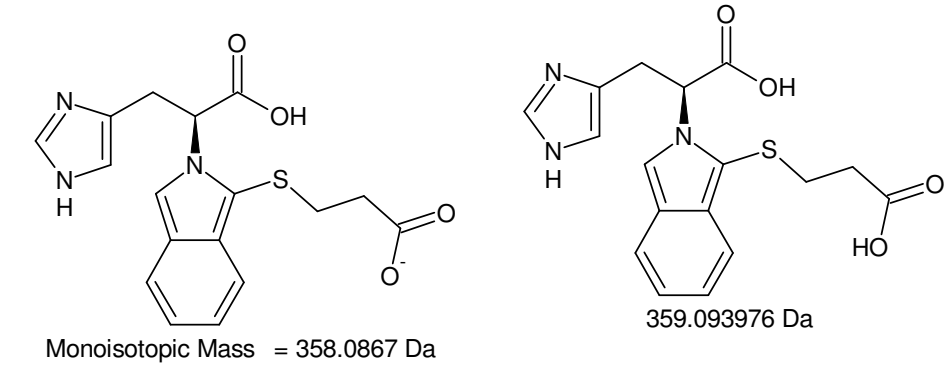

-MSn [OPA-His]: 717 -> 611 -> (505) and 717 -> 358

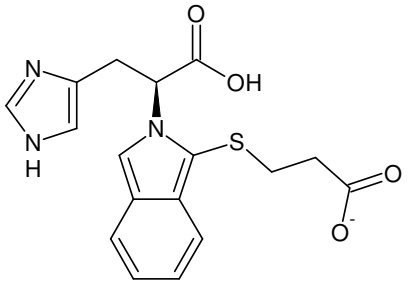

Monoisotopic Mass = 358.0867 Da

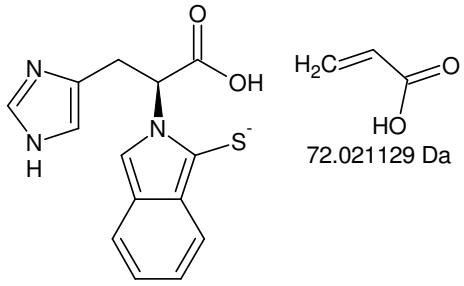

Monoisotopic Mass = 286.06557 Da

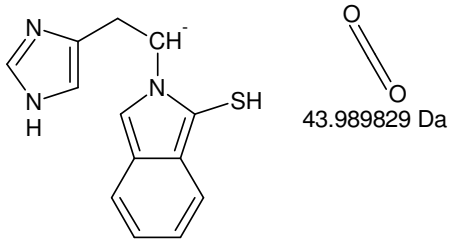

Monoisotopic Mass = 242.075741 Da

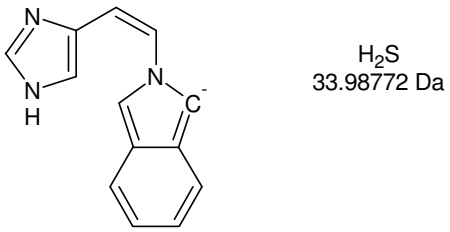

Monoisotopic Mass = 208.088021 Da

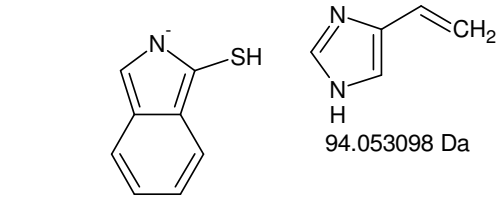

Monoisotopic Mass = 148.022643 Da

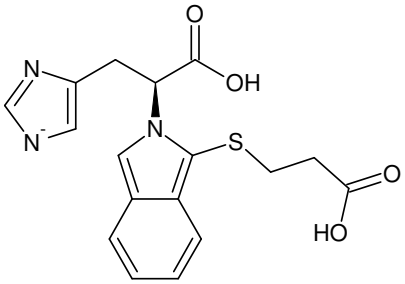

Monoisotopic Mass = 358.0867 Da

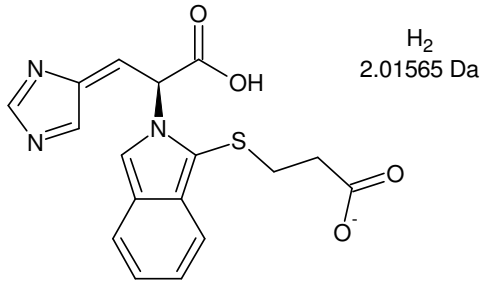

Monoisotopic Mass = 356.07105 Da

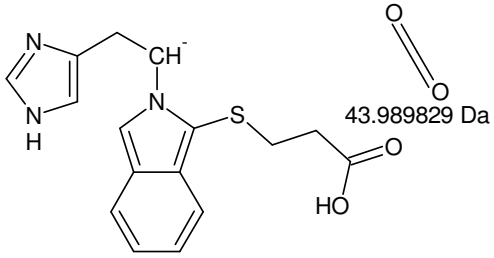

Monoisotopic Mass = 314.09687 Da

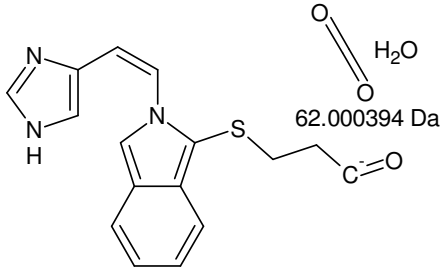

Monoisotopic Mass = 296.086306 Da

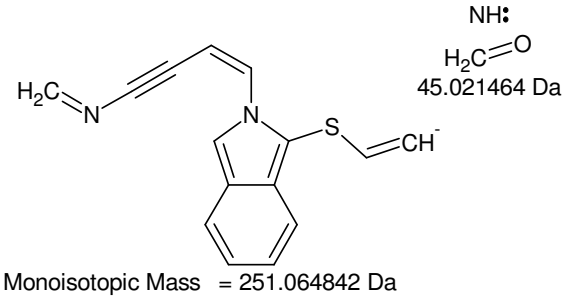

Monoisotopic Mass = 251.064842 Da

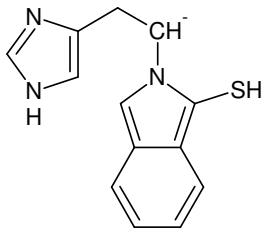

Monoisotopic Mass = 242.075741 Da

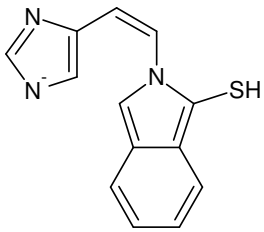

Monoisotopic Mass = 240.060091 Da

-MSn [OPA-His]: 358 -> 286 -> 242 -> 208, 148 and 358 -> 356, 314, 296 -> 251 as well as [358 -> 242] -> 240

VI.III.IV. Met

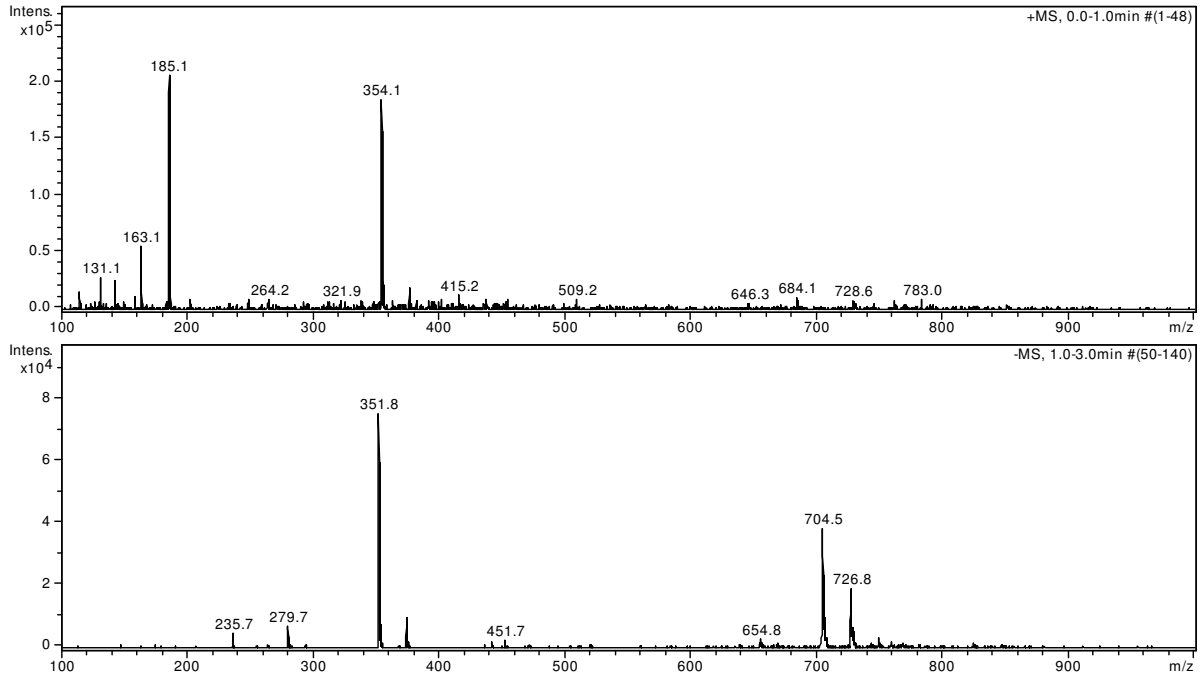

Figure VI-VI HPLC fraction #6: 33,85 – 34,1 min, Met; full scan MS[1]

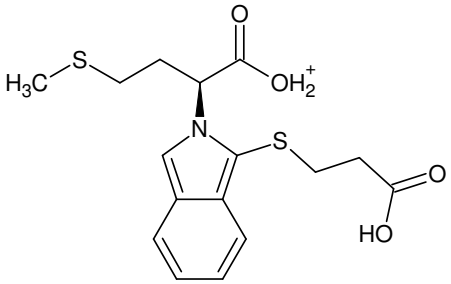

Monoisotopic Mass = 354.082825 Da

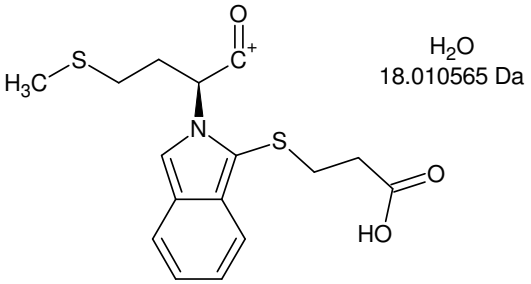

H_2O
18.010565 Da

Monoisotopic Mass = 336.07226 Da

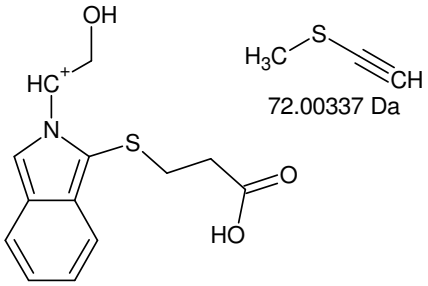

72.00337 Da

Monoisotopic Mass = 264.06889 Da

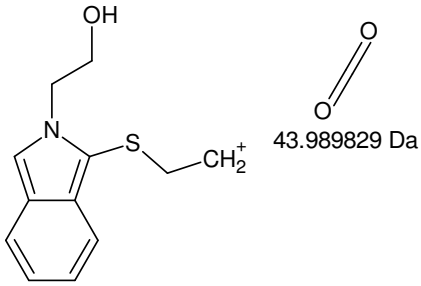

43.989829 Da

Monoisotopic Mass = 220.07906 Da

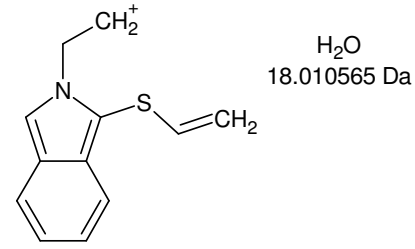

H_2O
18.010565 Da

Monoisotopic Mass = 202.068496 Da

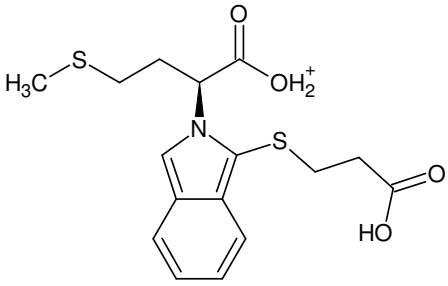

Monoisotopic Mass = 354.082825 Da

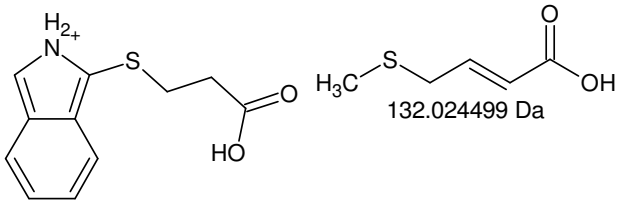

Monoisotopic Mass = 222.058325 Da

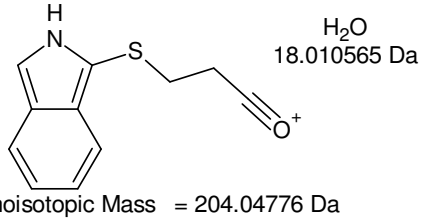

H_2O
18.010565 Da

Monoisotopic Mass = 204.04776 Da

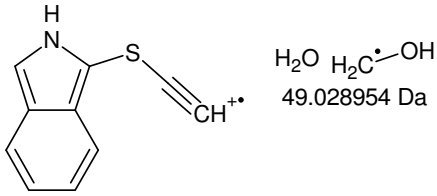

H_2O $H_2C^{\bullet}-OH$
49.028954 Da

Monoisotopic Mass = 173.029371 Da

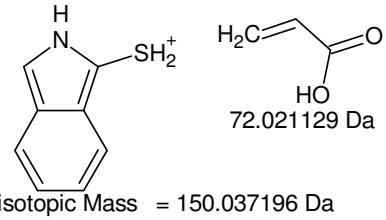

72.021129 Da

Monoisotopic Mass = 150.037196 Da

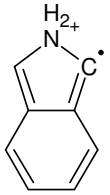

$HS^{\bullet}$
32.979895 Da

Monoisotopic Mass = 117.057301 Da

+MSn [OPA-Met]: 354 -> 336 -> 264 -> 220 -> 202 and 354 -> 222 -> 204, 173, 150 -> 117

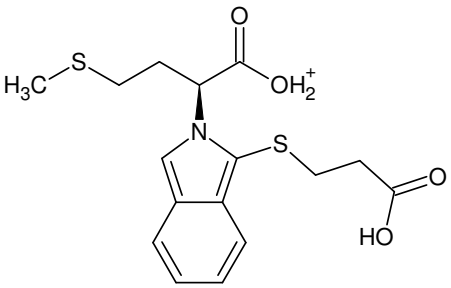

Monoisotopic Mass = 354.082825 Da

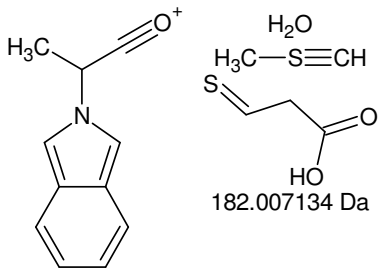

Monoisotopic Mass = 172.07569 Da

182.007134 Da

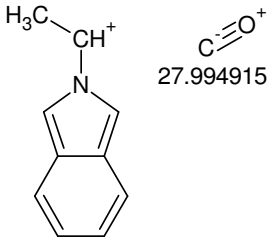

27.994915 Da

Monoisotopic Mass = 144.080776 Da

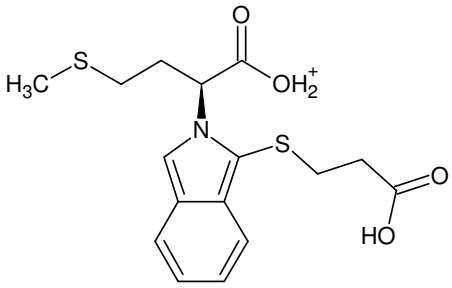

Monoisotopic Mass = 354.082825 Da

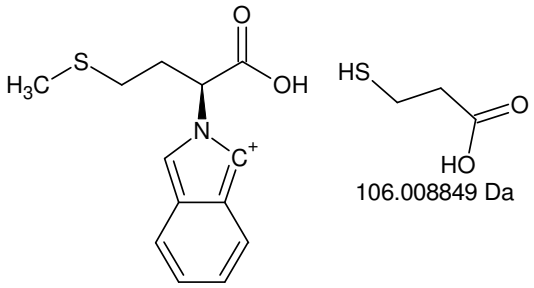

106.008849 Da

Monoisotopic Mass = 248.073975 Da

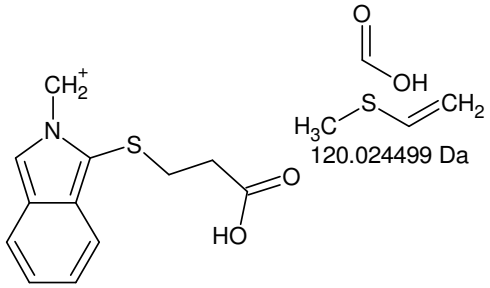

120.024499 Da

Monoisotopic Mass = 234.058325 Da

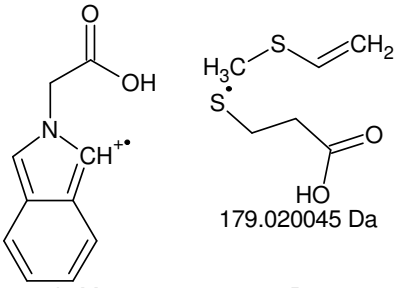

179.020045 Da

Monoisotopic Mass = 175.06278 Da

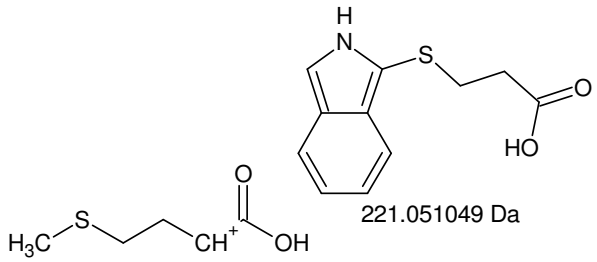

221.051049 Da

Monoisotopic Mass = 133.031776 Da

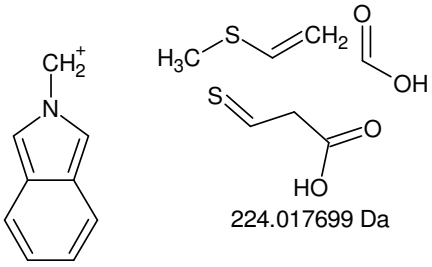

224.017699 Da

Monoisotopic Mass = 130.065126 Da

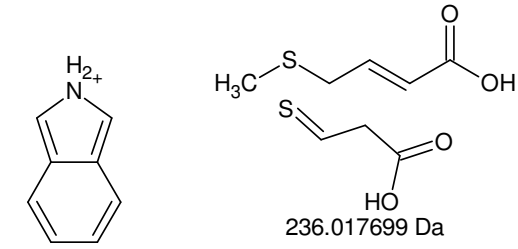

236.017699 Da

Monoisotopic Mass = 118.065126 Da

+MSn [OPA-Met]: 354 -> 172 -> 144 and 354 -> 248, 234, 175, 133, 130, 118

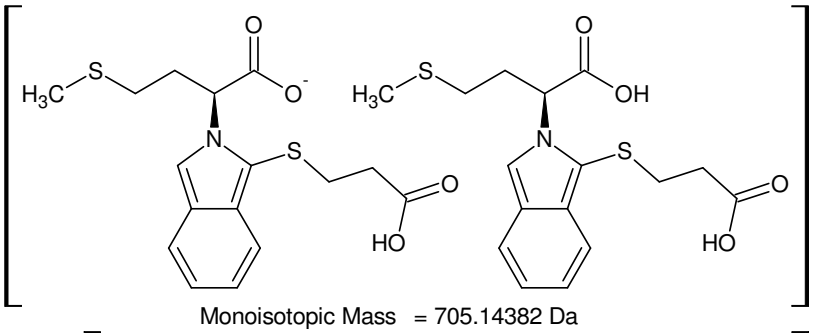

Monoisotopic Mass = 705.14382 Da

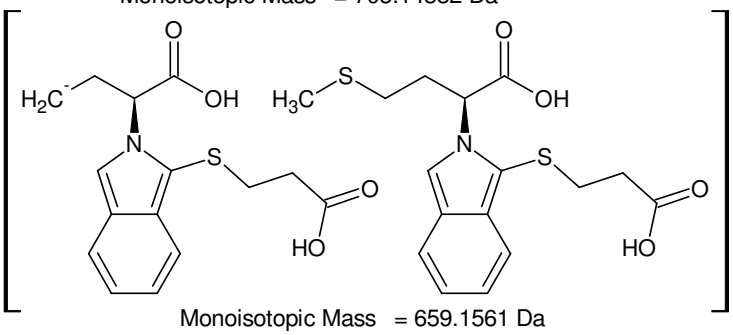

Monoisotopic Mass = 659.1561 Da

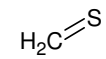

45.98772 Da

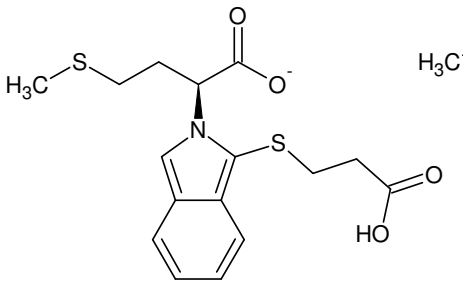

Monoisotopic Mass = 352.068272 Da

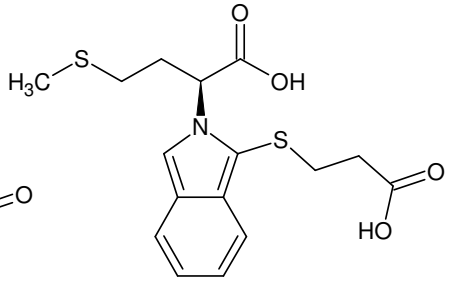

353.075548 Da

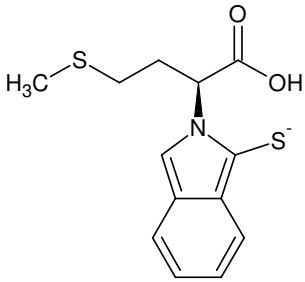

Monoisotopic Mass = 280.047142 Da

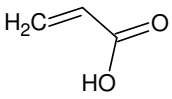

72.021129 Da

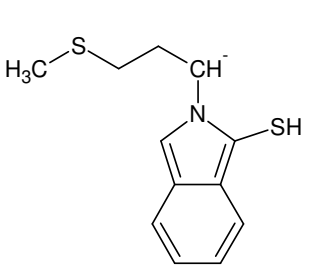

Monoisotopic Mass = 236.057313 Da

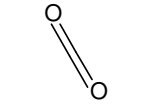

43.989829 Da

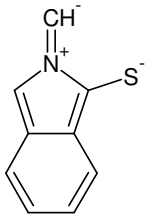

Monoisotopic Mass = 160.022643 Da

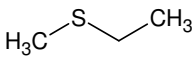

76.03467 Da

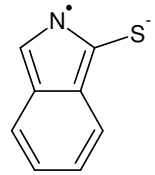

Monoisotopic Mass = 147.014818 Da

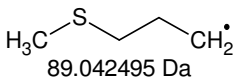

89.042495 Da

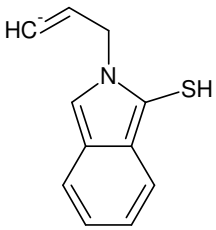

Monoisotopic Mass = 188.053943 Da

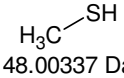

48.00337 Da

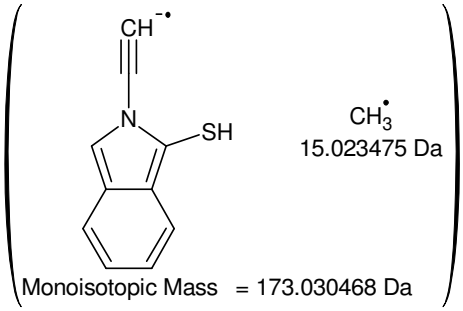

Monoisotopic Mass = 173.030468 Da

15.023475 Da

-MSn [OPA-Met]: 705 -> 659, 352 -> 280 -> 236 -> 160, 147, 188 -> (173)

IX. MS^n analysis of dityrosine

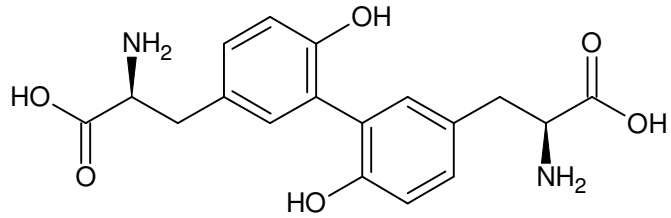

dityrosine
3,3'-dityrosine or 3,3'-bityrosine or o,o'-dityrosine or
(2*S*,2'*S*)-2-amino-3-[5'-(2-amino-2-carboxyethyl)-6,2'-dihydroxybiphenyl-propionic acid] or
(2*S*,2'*S*)-3,3'-(6,6'-dihydroxybiphenyl-3,3'-diyl)bis(2-aminopropanoic acid)
Molecular Formula = $C_{18}H_{20}N_2O_6$
Monoisotopic Mass = 360.132136 Da

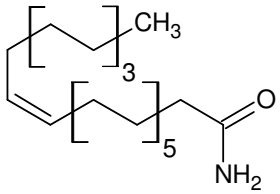

cis-13-docosenamide or **erucamide** or fatty acid amide ($C_{22}H_{43}NO$) or Kemamide-E
Molecular Formula = $C_{22}H_{43}NO$
Monoisotopic Mass = 337.334465 Da
Erucylamide; 13-Docosenamide; 13-Docosenoic acid amide; Erucic acid amide; (Z)-Docos-13-enamide; (Z)-13-Docosenamide; (13Z)-13-Docosenamide; (Z)-Docos-13-enamide

Scheme 13-12 Structures and names of dityrosine and the assumed contaminant (see 9.2)

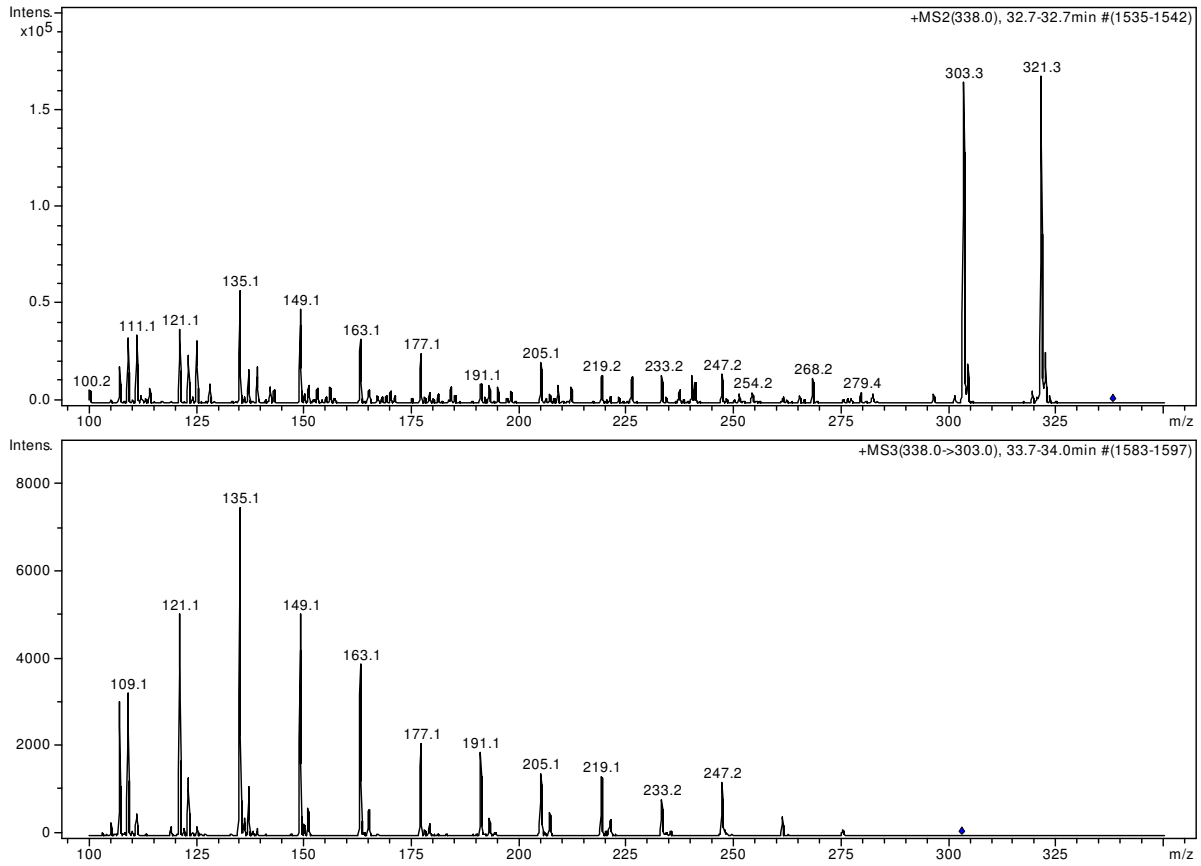

Figure IX-I Fragment spectra of the contaminant in the methanolic solution of dityrosine (cp. 9.2)

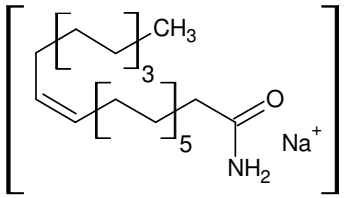

Monoisotopic Mass = 360.323686 Da

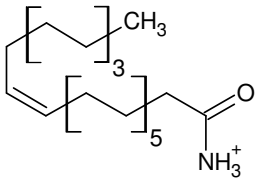

Monoisotopic Mass = 338.341741 Da

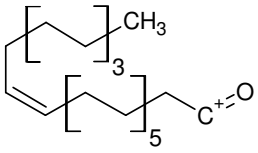

NH_3
17.026549 Da

Monoisotopic Mass = 321.315192 Da

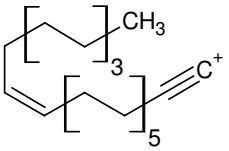

H_2O
18.010565 Da

Monoisotopic Mass = 303.304628 Da

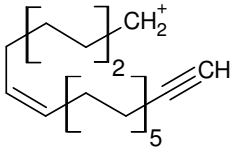

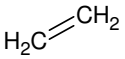

28.0313 Da

Monoisotopic Mass = 275.273328 Da

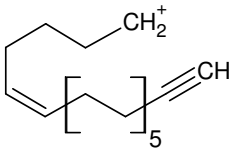

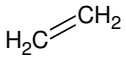

28.0313 Da

Monoisotopic Mass = 247.242027 Da

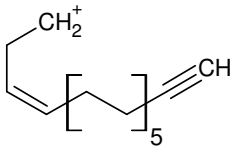

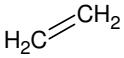

28.0313 Da

Monoisotopic Mass = 219.210727 Da

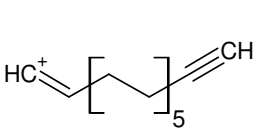

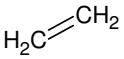

28.0313 Da

Monoisotopic Mass = 191.179427 Da

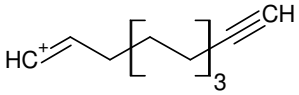

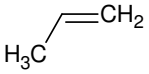

42.04695 Da

Monoisotopic Mass = 149.132477 Da

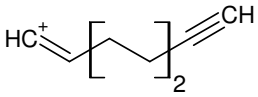

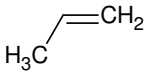

42.04695 Da

Monoisotopic Mass = 107.085527 Da

+MSn: 360 Th; 338 -> 321 -> 303 -> 275 -> 247 -> 219 -> 191 -> 149 -> 107

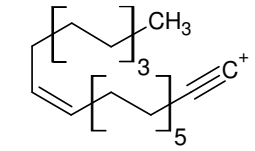

Monoisotopic Mass = 303.304628 Da

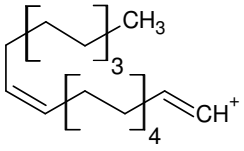
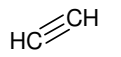

26.01565 Da

Monoisotopic Mass = 277.288978 Da

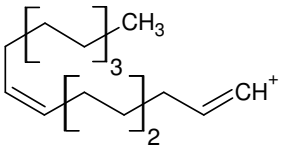
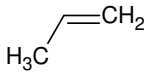

42.04695 Da

Monoisotopic Mass = 235.242027 Da

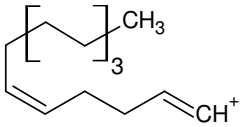
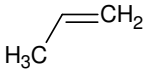

42.04695 Da

Monoisotopic Mass = 193.195077 Da

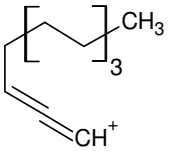
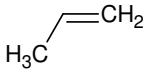

42.04695 Da

Monoisotopic Mass = 151.148127 Da

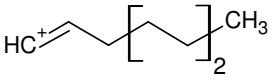
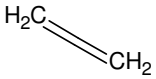

40.0313 Da

Monoisotopic Mass = 111.116827 Da

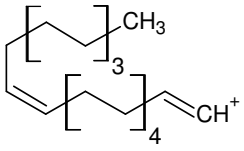

Monoisotopic Mass = 277.288978 Da

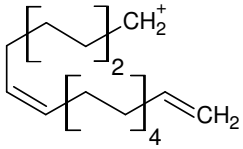
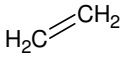

28.0313 Da

Monoisotopic Mass = 249.257677 Da

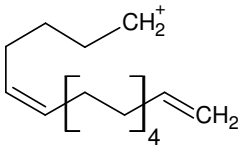
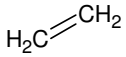

28.0313 Da

Monoisotopic Mass = 221.226377 Da

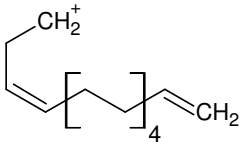
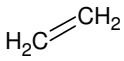

28.0313 Da

Monoisotopic Mass = 193.195077 Da

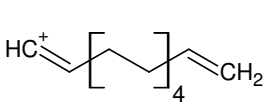
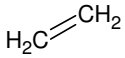

28.0313 Da

Monoisotopic Mass = 165.163777 Da

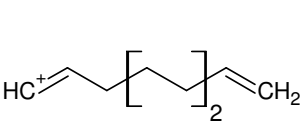
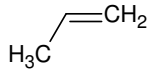

42.04695 Da

Monoisotopic Mass = 123.116827 Da

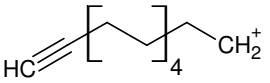

Monoisotopic Mass = 165.163777 Da

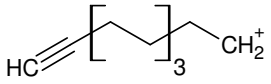
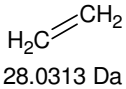

28.0313 Da

Monoisotopic Mass = 137.132477 Da

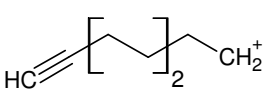
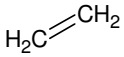

28.0313 Da

Monoisotopic Mass = 109.101177 Da

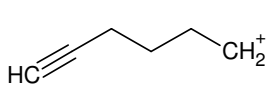
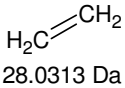

28.0313 Da

Monoisotopic Mass = 81.069877 Da

+MSn: [338 -> 321 -> 303] -> 277 -> 235 -> 193 -> 151 -> 111 and [338 -> 321 -> 303 -> 277] -> 249 -> 221 -> 193 -> 165 -> 123 as well as 165 -> 137 -> 109 (-> 81)

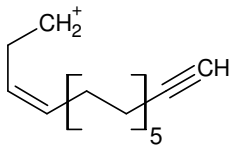

Monoisotopic Mass = 219.210727 Da

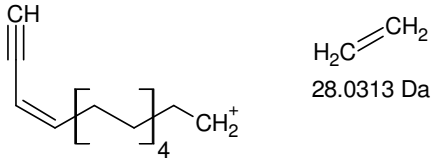

Monoisotopic Mass = 191.179427 Da

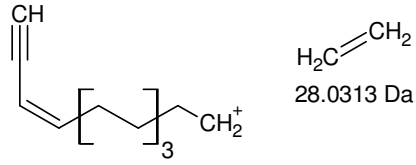

Monoisotopic Mass = 163.148127 Da

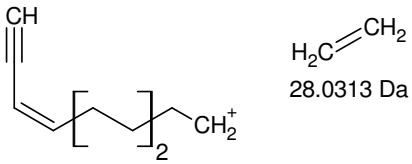

Monoisotopic Mass = 135.116827 Da

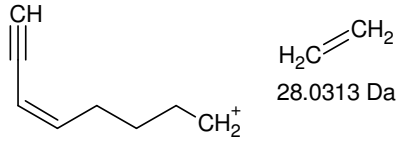

Monoisotopic Mass = 107.085527 Da

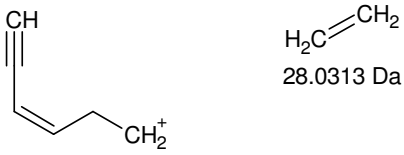

Monoisotopic Mass = 79.054227 Da

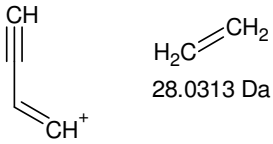

Monoisotopic Mass = 51.022926 Da

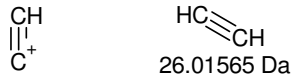

Monoisotopic Mass = 25.007276 Da

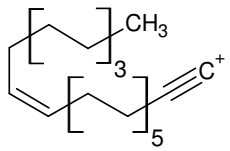

Monoisotopic Mass = 303.304628 Da

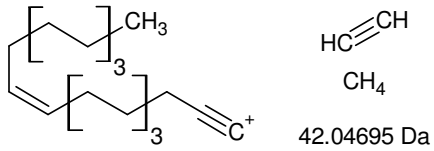

Monoisotopic Mass = 261.257677 Da

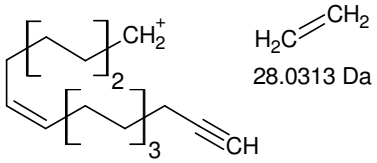

Monoisotopic Mass = 233.226377 Da

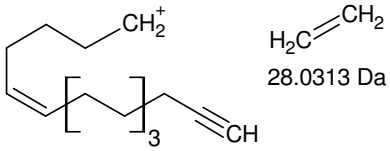

Monoisotopic Mass = 205.195077 Da

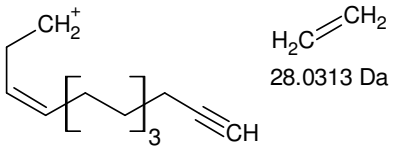

Monoisotopic Mass = 177.163777 Da

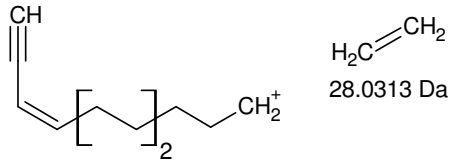

Monoisotopic Mass = 149.132477 Da

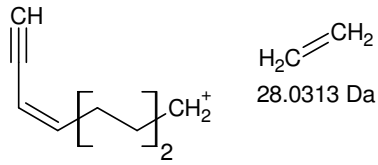

Monoisotopic Mass = 121.101177 Da

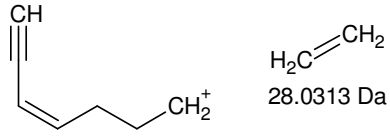

Monoisotopic Mass = 93.069877 Da

+MSn: [338 -> 321 -> 303 -> 275 -> 247 -> 219] -> 191 -> 163 -> 135 -> 107 (-> 79 -> 51 -> 25) and [338 -> 321 -> 303] -> 261 -> 233 -> 205 -> 177 -> 149 -> 121 (-> 93)

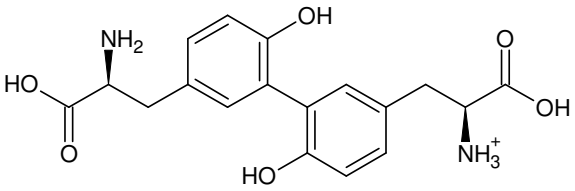

Monoisotopic Mass = 361.139413 Da

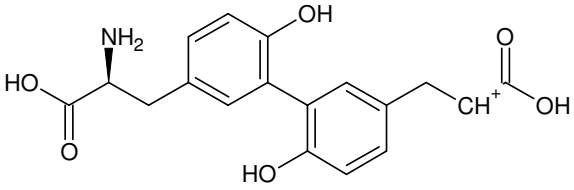

NH_3
17.026549 Da

Monoisotopic Mass = 344.112864 Da

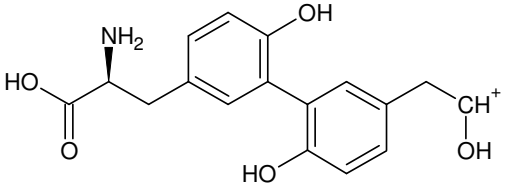

27.994915 Da

Monoisotopic Mass = 316.117949 Da

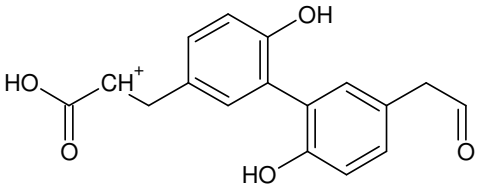

NH_3
17.026549 Da

Monoisotopic Mass = 299.0914 Da

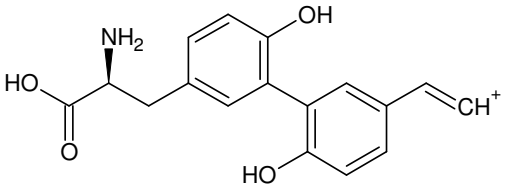

H_2O
18.010565 Da

Monoisotopic Mass = 298.107384 Da

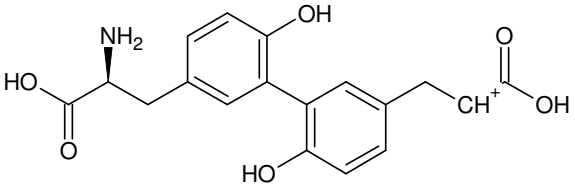

Monoisotopic Mass = 344.112864 Da

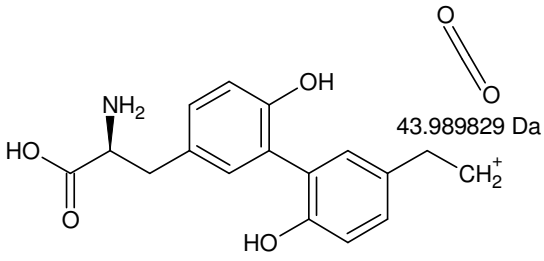

43.989829 Da

Monoisotopic Mass = 300.123034 Da

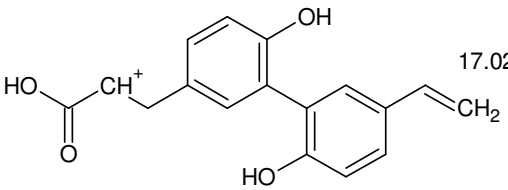

NH_3
17.026549 Da

Monoisotopic Mass = 283.096485 Da

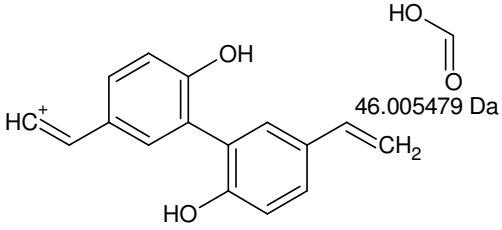

46.005479 Da

Monoisotopic Mass = 237.091006 Da

+MSn [DiTyr]: 361 -> 344 -> 316 -> 299, 298 and [361 -> 344) -> 300 -> 283 -> 237

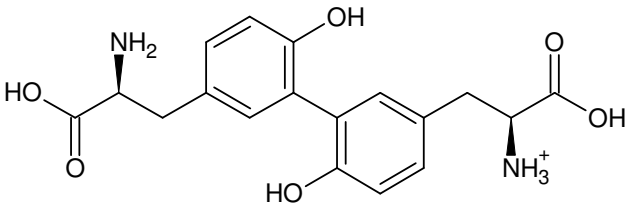

Monoisotopic Mass = 361.139413 Da

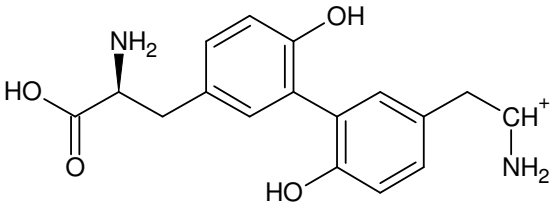

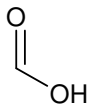

46.005479 Da

Monoisotopic Mass = 315.133933 Da

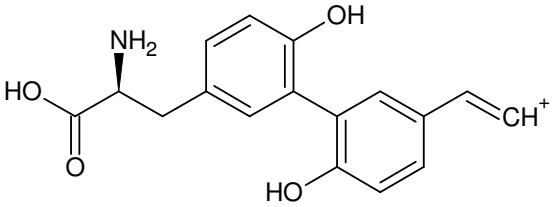

NH_3
17.026549 Da

Monoisotopic Mass = 298.107384 Da

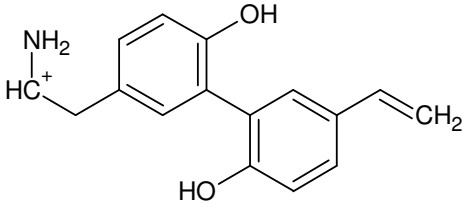

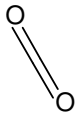

43.989829 Da

Monoisotopic Mass = 254.117555 Da

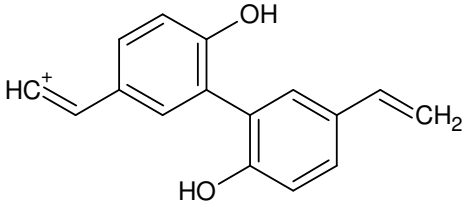

NH_3
17.026549 Da

Monoisotopic Mass = 237.091006 Da

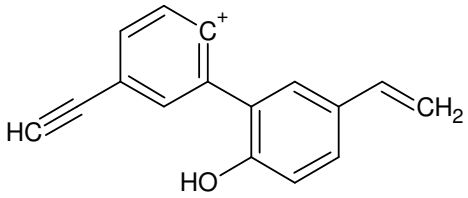

H_2O
18.010565 Da

Monoisotopic Mass = 219.080441 Da

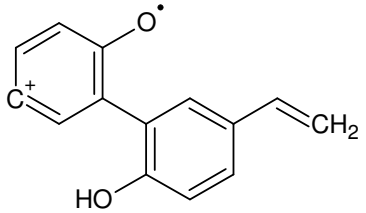

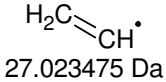

27.023475 Da

Monoisotopic Mass = 210.067531 Da

+MSn [DiTyr]: 361 -> 315 -> 298 -> 254 -> 237 -> 219, 210

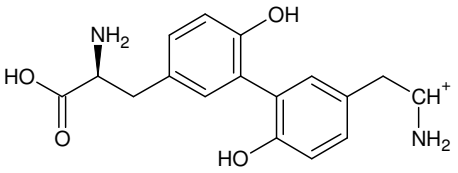

Monoisotopic Mass = 315.133933 Da

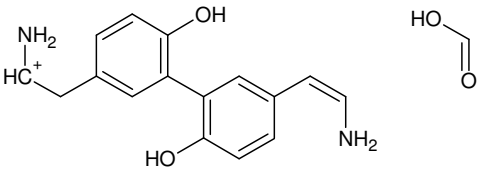

Monoisotopic Mass = 269.128454 Da

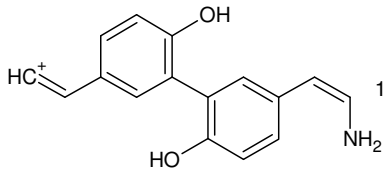

NH_3
17.026549 Da

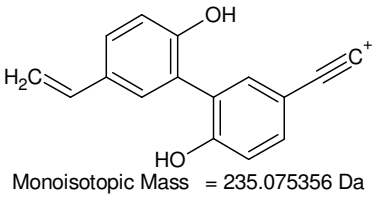

NH_3

Monoisotopic Mass = 235.075356 Da

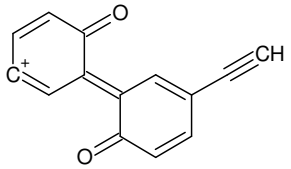

$H_2C{=}CH_2$
28.0313 Da

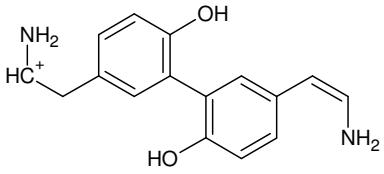

Monoisotopic Mass = 269.128454 Da

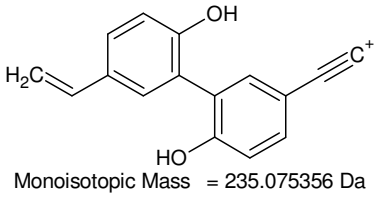

NH_3
NH_3

Monoisotopic Mass = 235.075356 Da

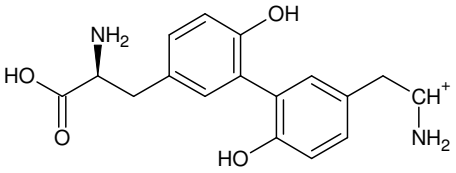

Monoisotopic Mass = 315.133933 Da

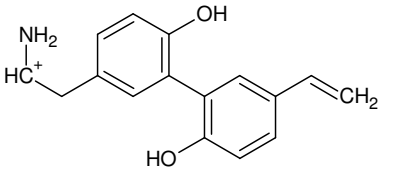

NH_3
O
O

Monoisotopic Mass = 254.117555 Da

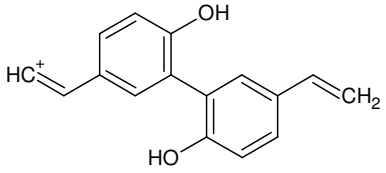

NH_3
17.026549 Da

Monoisotopic Mass = 237.091006 Da

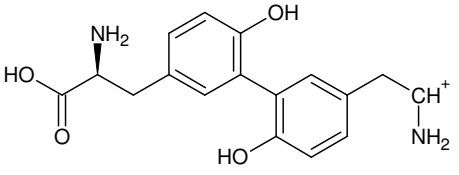

NH_3

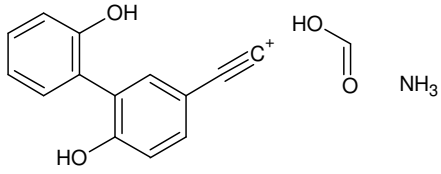

Monoisotopic Mass = 315.133933 Da

Monoisotopic Mass = 209.059706 Da

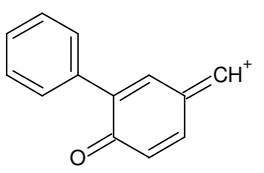

$C{\equiv}O^+$
27.994915 Da

Monoisotopic Mass = 181.064791 Da

+MSn [DiTyr]: [361 -> 315] -> 269 -> 252 -> 235 -> 207 and [361 -> 315 -> 269] -> 235 plus [361 -> 315] -> 254 -> 237 as well as [361 -> 315] -> 209 -> 181

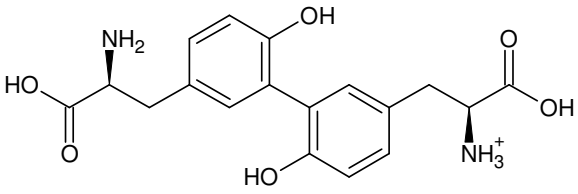

Monoisotopic Mass = 361.139413 Da

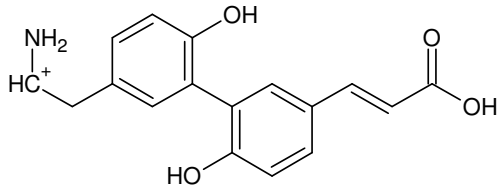

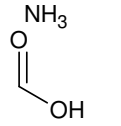

63.032028 Da

Monoisotopic Mass = 298.107384 Da

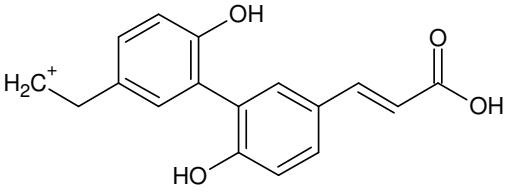

NH: 15.010899 Da

Monoisotopic Mass = 283.096485 Da

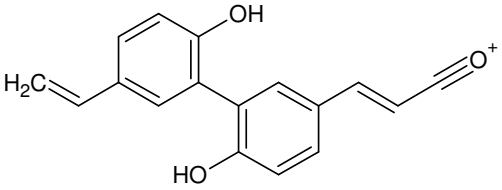

H_2O 18.010565 Da

Monoisotopic Mass = 265.085921 Da

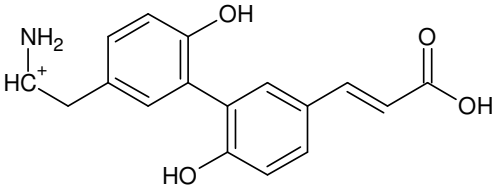

Monoisotopic Mass = 298.107384 Da

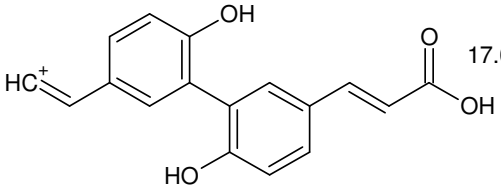

NH_3 17.026549 Da

Monoisotopic Mass = 281.080835 Da

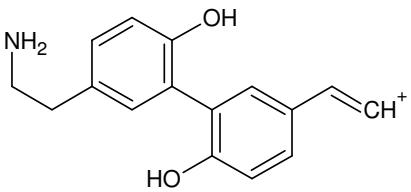

43.989829 Da

Monoisotopic Mass = 254.117555 Da

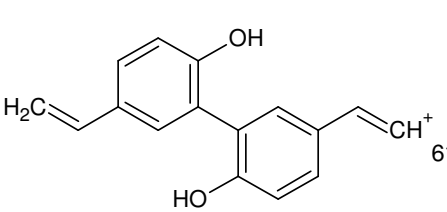

NH_3 61.016378 Da

Monoisotopic Mass = 237.091006 Da

+MSn [DiTyr]: 361 -> 298 -> 283 -> 265 and [361 -> 298] -> 281, 254, 237

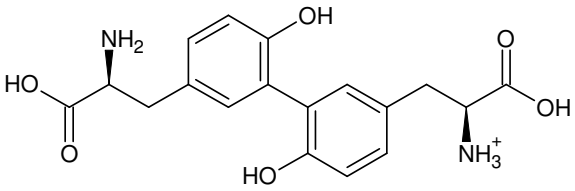

Monoisotopic Mass = 361.139413 Da

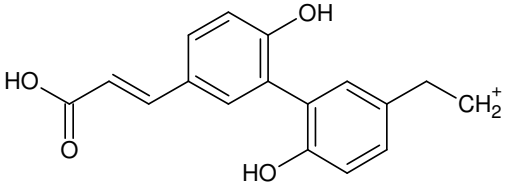

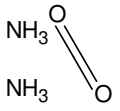

78.042927 Da

Monoisotopic Mass = 283.096485 Da

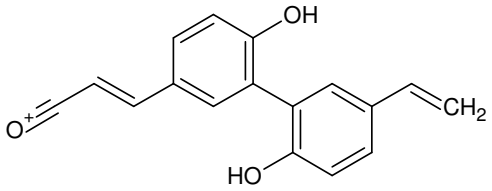

H_2O
18.010565 Da

Monoisotopic Mass = 265.085921 Da

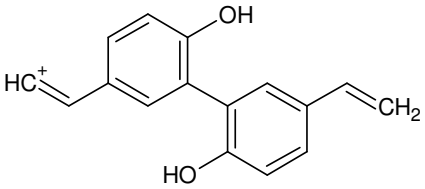

27.994915 Da

Monoisotopic Mass = 237.091006 Da

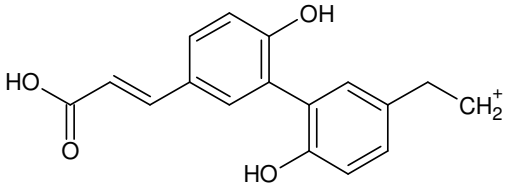

Monoisotopic Mass = 283.096485 Da

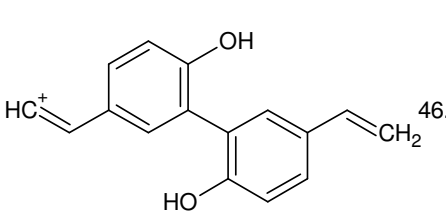

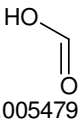

46.005479 Da

Monoisotopic Mass = 237.091006 Da

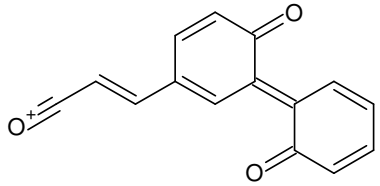

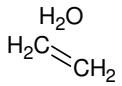

46.041865 Da

Monoisotopic Mass = 237.054621 Da

+MSn [DiTyr]: 361 -> 283 -> 265 -> 237 and [361 -> 283] -> 237

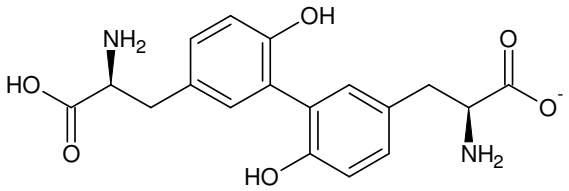

Monoisotopic Mass = 359.12486 Da

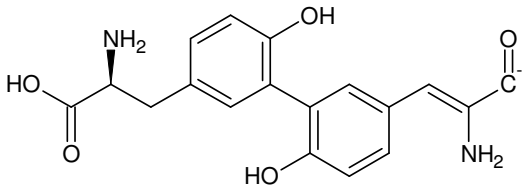

Monoisotopic Mass = 341.114295 Da

H_2O
18.010565 Da

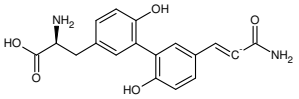

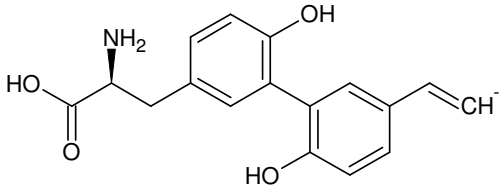

Monoisotopic Mass = 298.108482 Da

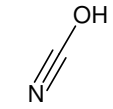

43.005814 Da

340,6 - 297,9 = **42,7**
Gefundene Verbindungen: 12
CHNO MG=43,0058136
CH3N2 MG=43,0296218
CH15O MG=43,112284
CH17N MG=43,1360922
C2H3O MG=43,0183888
C2H5N MG=43,042197
C2H19 MG=43,1486674
C3H7 MG=43,0547722
HN3 MG=43,0170466
H11O2 MG=43,0759006
H13NO MG=43,0997088
H15N2 MG=43,123517

-----D--B--E--f-i-l-t-e-r-----
07.10.2011 - 12:06:13,42
akzeptierte DBE:
-2 -1 0 1 2 3 4 5 6 7 8

CHNO DBE: 2
C_2H_5N DBE: 1
HN_3 DBE: 2

3 von 12 Summenformeln

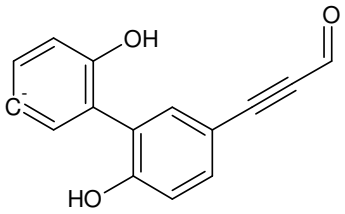

Monoisotopic Mass = 237.055718 Da

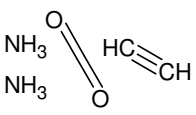

104.058578 Da

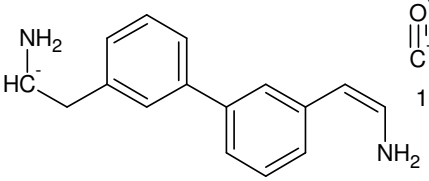

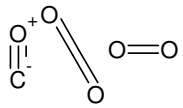

103.974573 Da

Monoisotopic Mass = 237.139722 Da

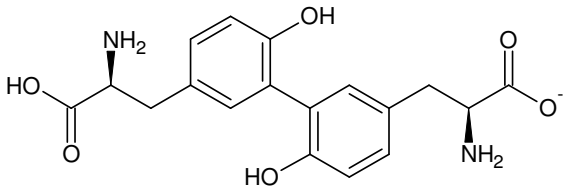

Monoisotopic Mass = 359.12486 Da

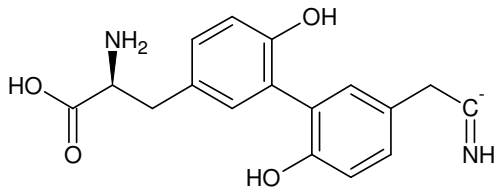

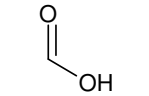

46.005479 Da

Monoisotopic Mass = 313.119381 Da

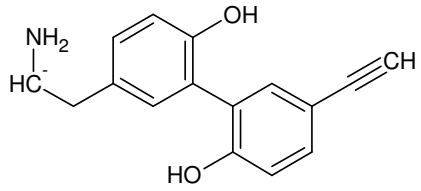

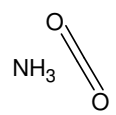

61.016378 Da

Monoisotopic Mass = 252.103002 Da

-MSn [DiTyr]: 359 -> 341 -> 280, 237 and 359 -> 313 -> 252

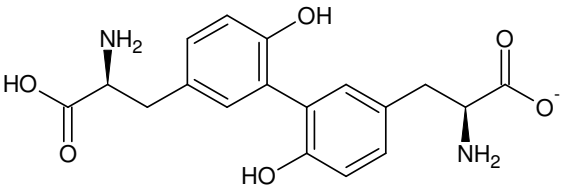

Monoisotopic Mass = 359.12486 Da

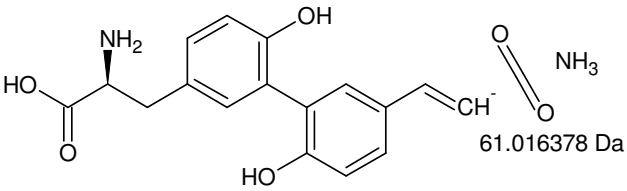

61.016378 Da

Monoisotopic Mass = 298.108482 Da

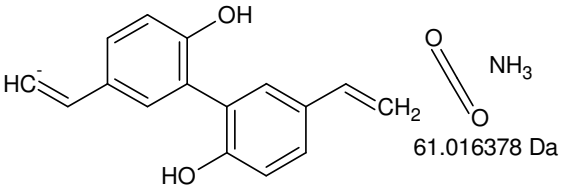

61.016378 Da

Monoisotopic Mass = 237.092103 Da

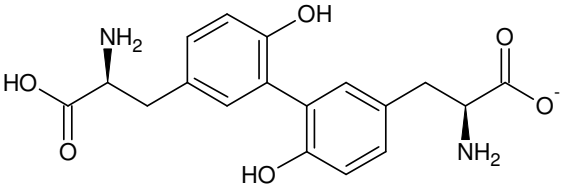

Monoisotopic Mass = 359.12486 Da

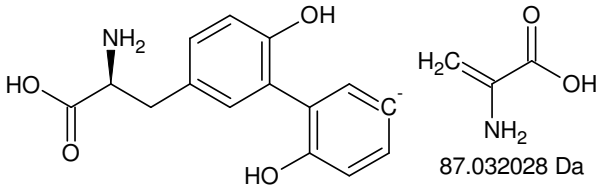

87.032028 Da

Monoisotopic Mass = 272.092832 Da

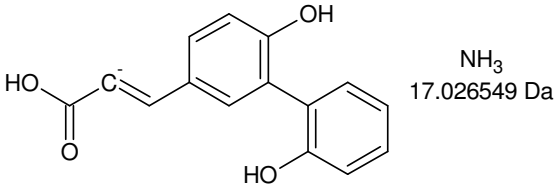

NH3
17.026549 Da

Monoisotopic Mass = 255.066282 Da

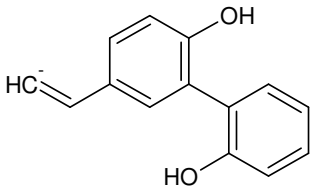

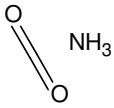

61.016378 Da

Monoisotopic Mass = 211.076453 Da

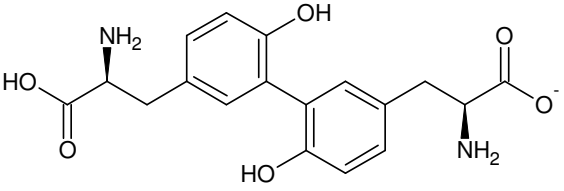

Monoisotopic Mass = 359.12486 Da

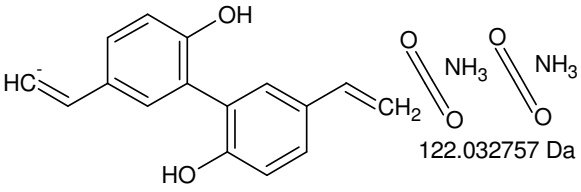

122.032757 Da

Monoisotopic Mass = 237.092103 Da

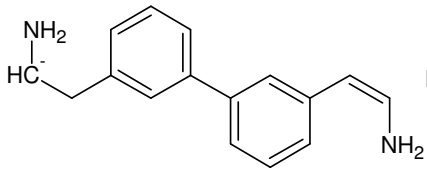

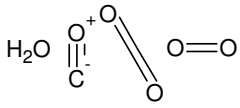

121.985138 Da

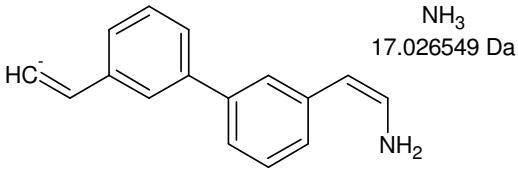

Monoisotopic Mass = 237.139722 Da

Monoisotopic Mass = 220.113173 Da

-MSn [DiTyr]: 359 -> 298 -> 237 and 359 -> 272 -> 255, 211 plus 359 -> 237 -> 220

X. Synthesis and purification of N-Boc-*L*-Tyr

X.I. Vibronic analysis of N-Boc-*L*-Tyr

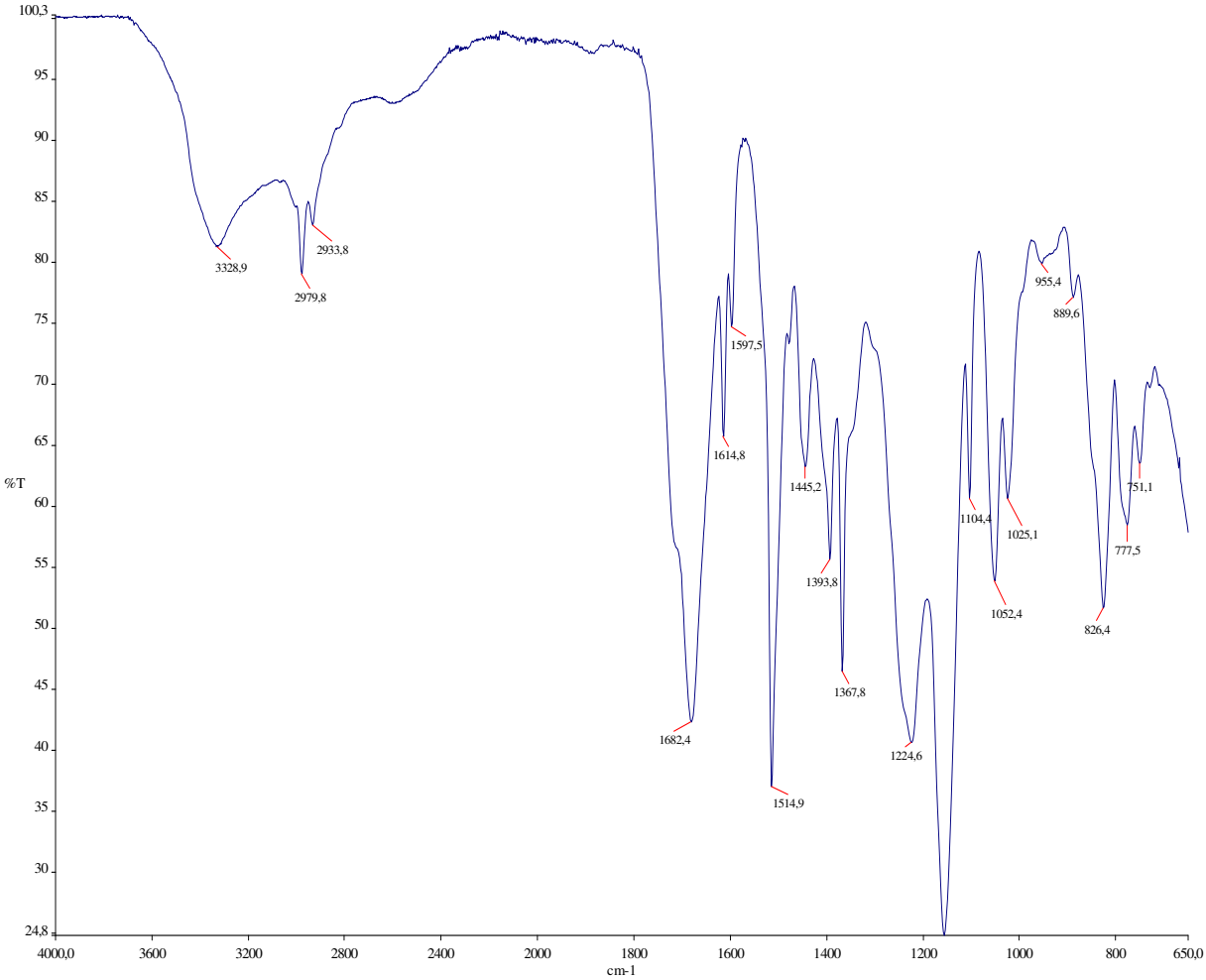

Figure X-I FTIR-ATR spectrum of N-Boc-*L*-Tyr

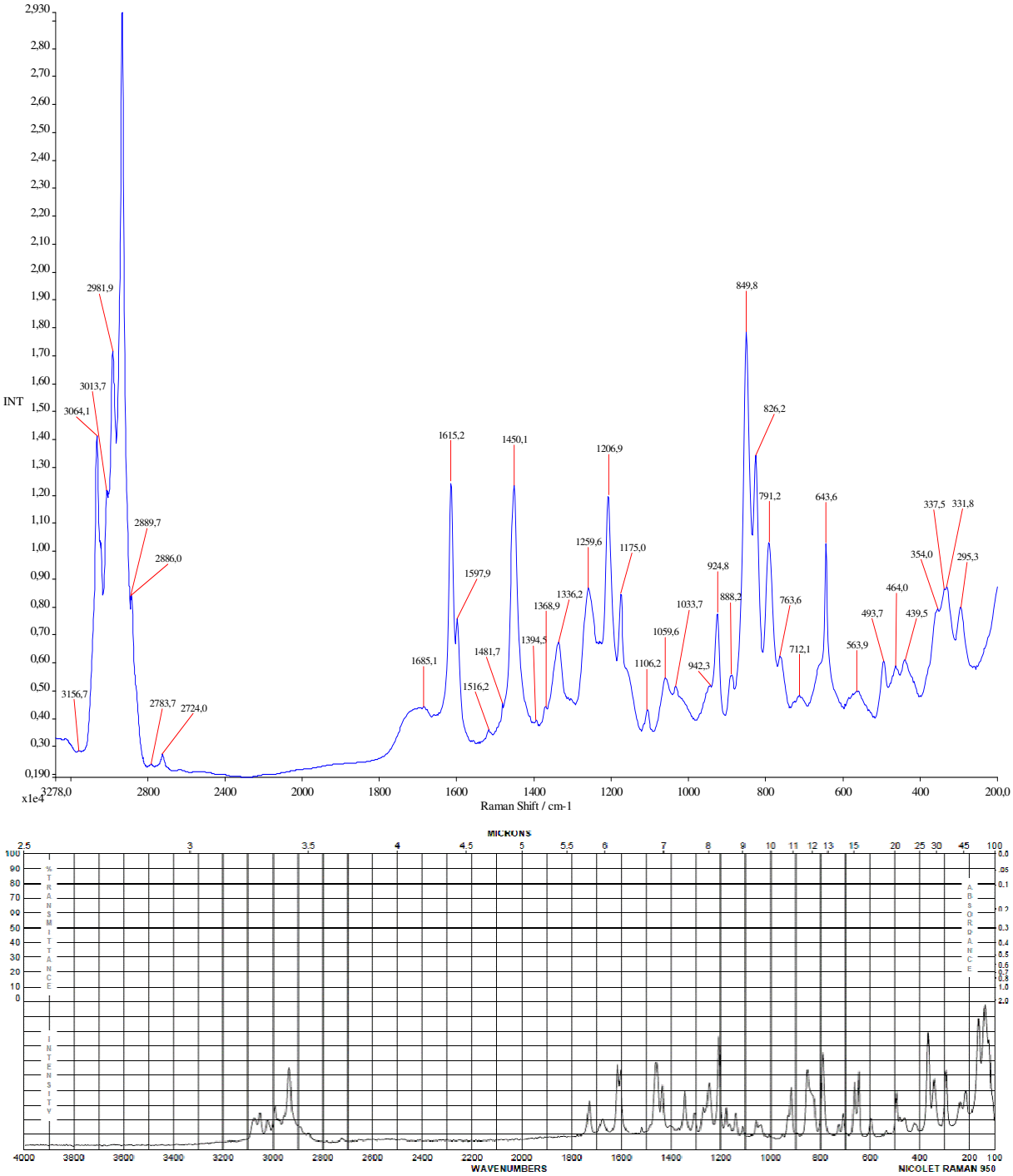

Figure X-IIRaman spectrum of N-Boc-*L*-Tyr (above) and a reference raman spectrum of N-Boc-*L*-Tyr (Sigma 374229, below)

X.II. MS^n analysis of N-Boc-*L*-Tyr

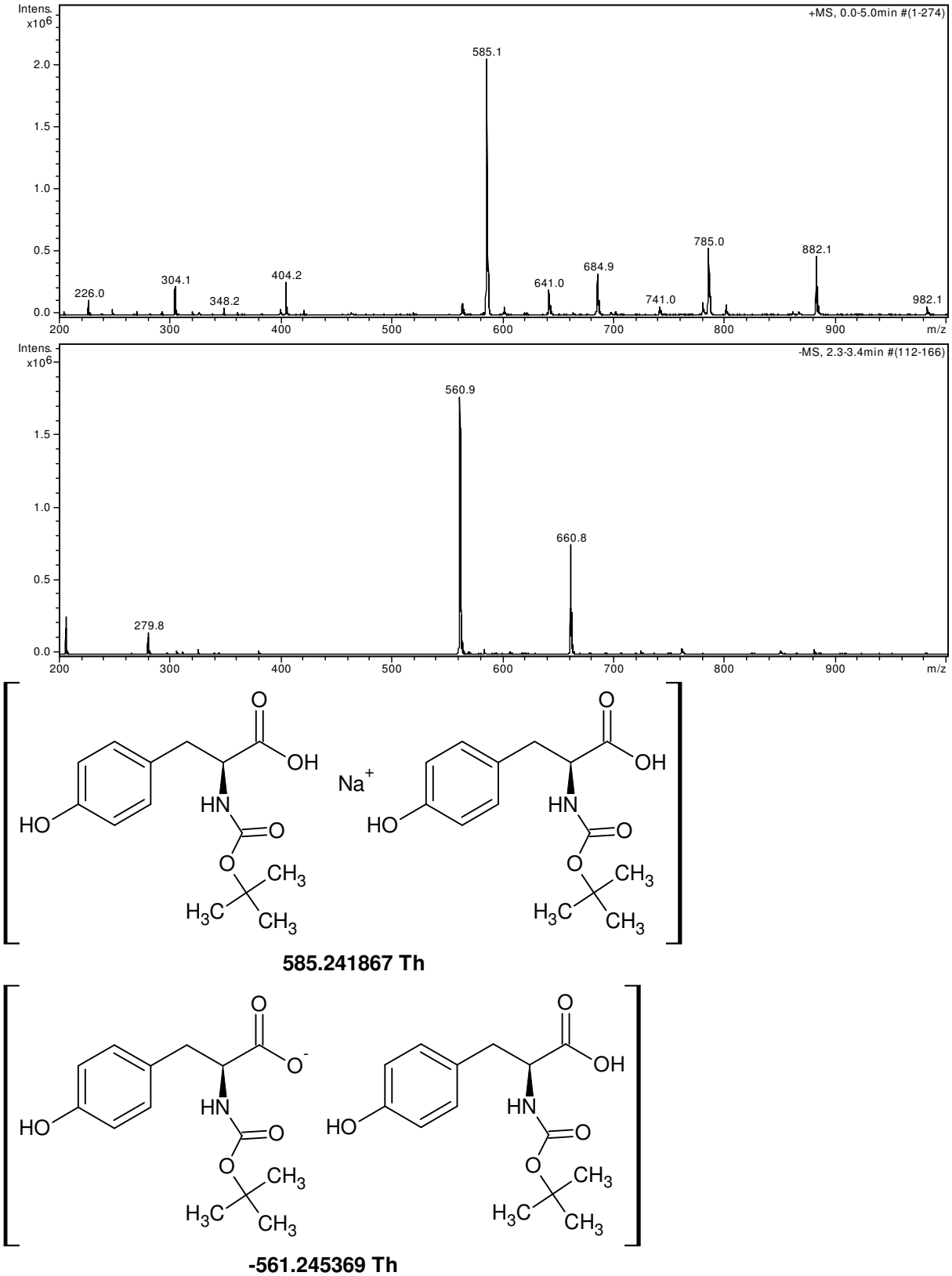

Figure X-III N-Boc-*L*-Tyr 2 mM in MeOH, full scan MS^1

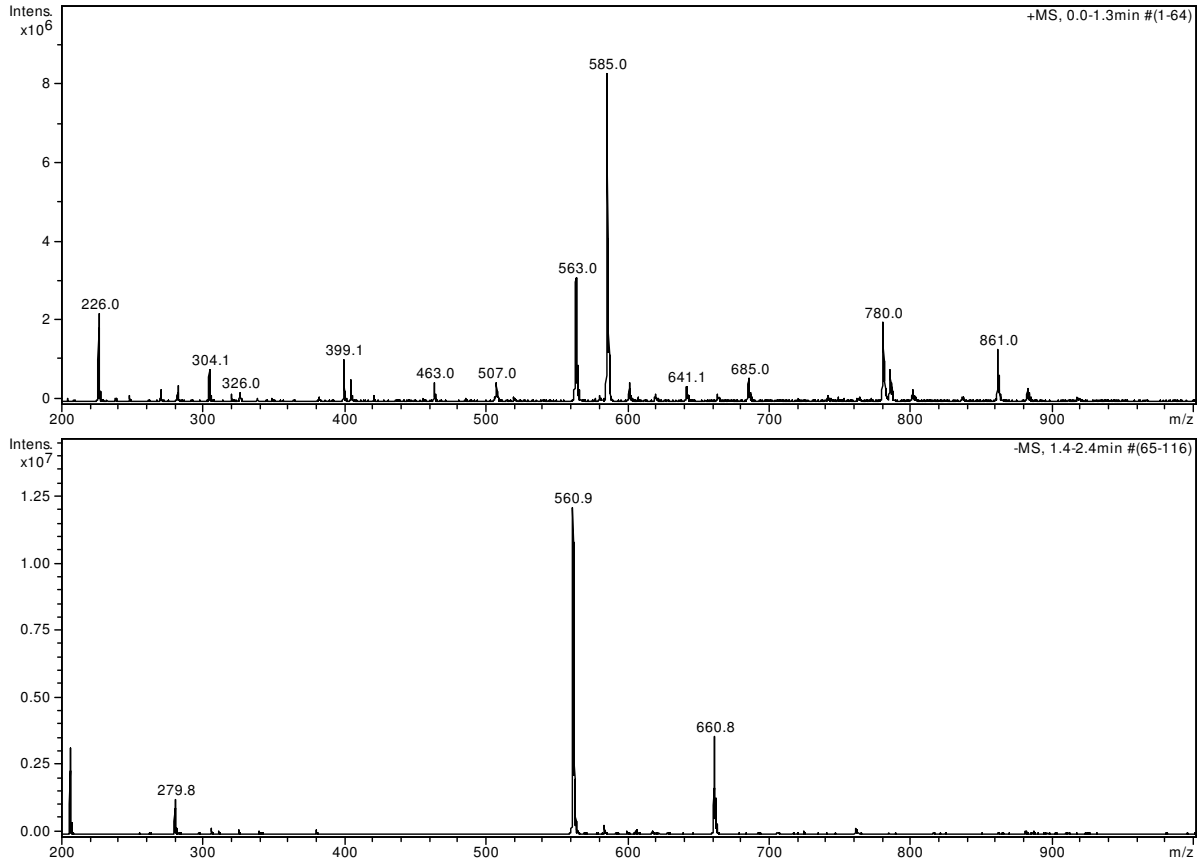

Figure X-IV N-*L*-Boc-Tyr 2 mM in MeOH with 1 % (v+v) 30 % aqueous NH_3 (pH 9); full scan MS^1

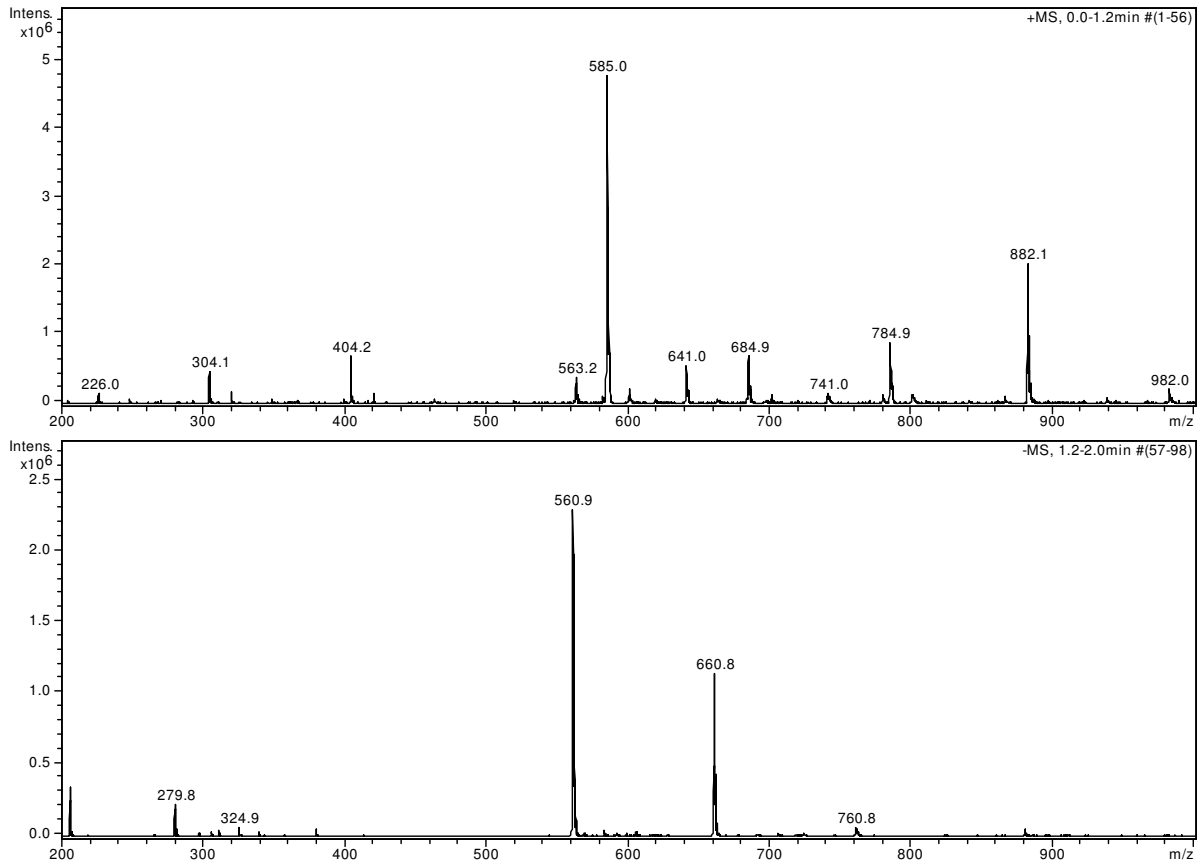

Figure X-V N-*L*-Boc-Tyr 2 mM in MeOH with 1 ‰ formic acid; full scan MS^1

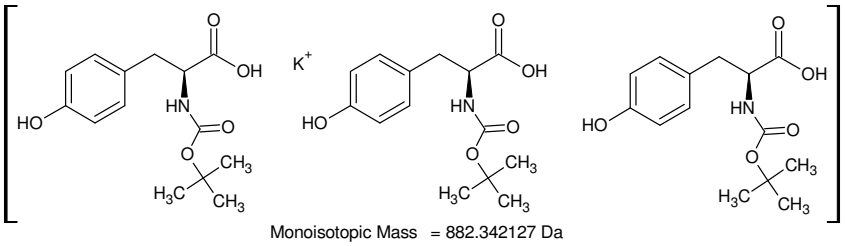

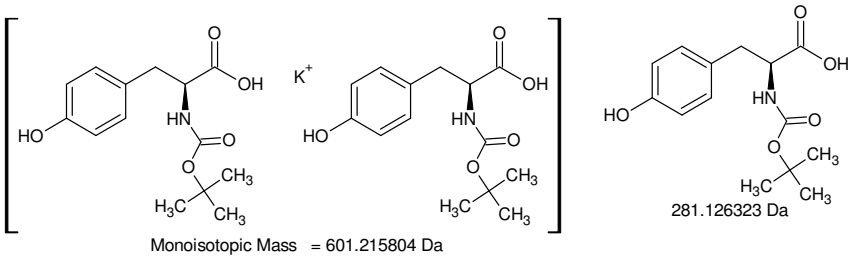

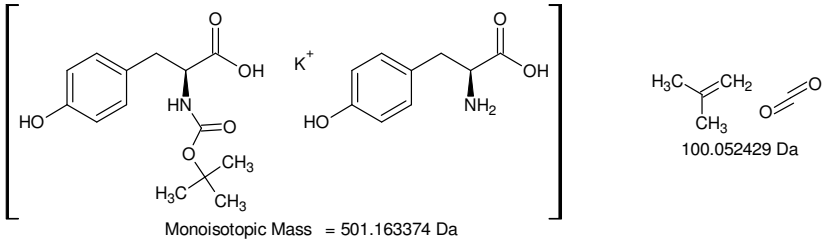

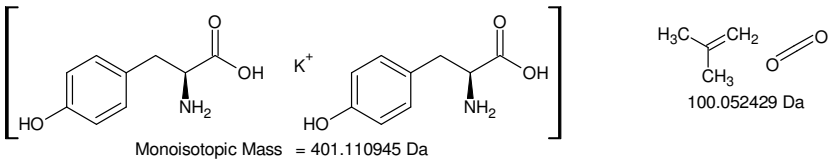

Gefundene Verbindungen: 91
CH2N5O MG=100,0259342
CH4N6 MG=100,0497424
(...)
H44N4 MG=100,3565784
N6O MG=100,013359

-----D--B--E--f-i-l-t-e-r-----
23.05.2011 - 15:38:02,40
akzeptierte DBEs:
0
1
2
3
4
5
6

CH_4N_6	DBE: 3
CN_4O_2	DBE: 4
$C_2H_4N_4O$	DBE: 3
$C_2N_2O_3$	DBE: 4
$C_3H_4N_2O_2$	DBE: 3
$C_3H_8N_4$	DBE: 2
C_3O_4	DBE: 4
$C_4H_4O_3$	DBE: 3
$C_4H_8N_2O$	DBE: 2
$C_5H_8O_2$	DBE: 2
$C_5H_{12}N_2$	DBE: 1
$C_6H_{12}O$	DBE: 1
C_7H_{16}	DBE: 0
N_6O	DBE: 4

14 von 91 Summenformeln

+MSn: 882 -> 601 -> 501 -> 401

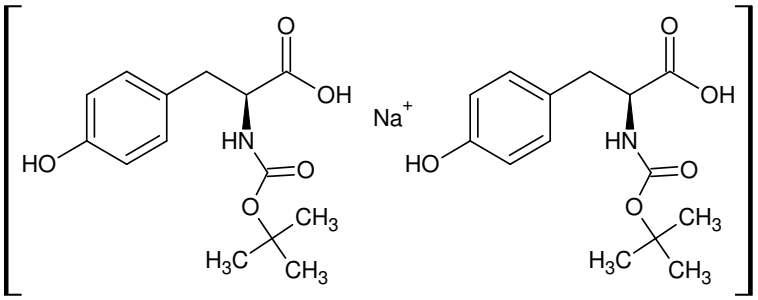

Monoisotopic Mass = 585.241867 Da

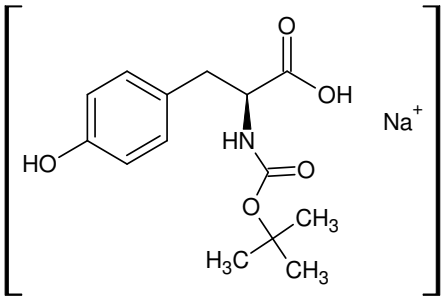

Monoisotopic Mass = 304.115544 Da

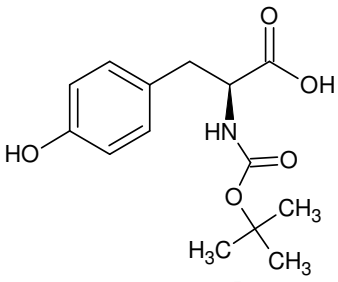

281.126323 Da

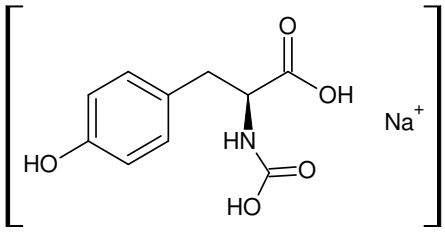

Monoisotopic Mass = 248.052944 Da

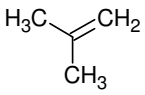

56.0626 Da

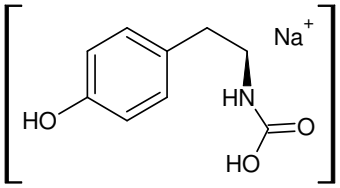

Monoisotopic Mass = 204.063115 Da

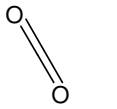

43.989829 Da

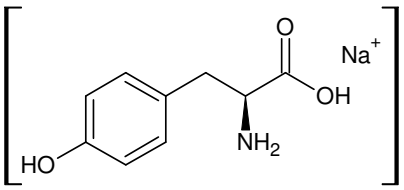

Monoisotopic Mass = 204.063115 Da

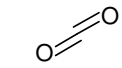

43.989829 Da

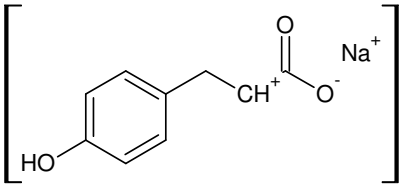

Monoisotopic Mass = 187.036566 Da

NH3
17.026549 Da

+MSn: 585 -> 304 -> 248 -> 2x 204 -> 187

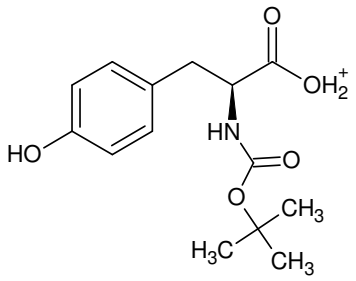

Monoisotopic Mass = 282.133599 Da

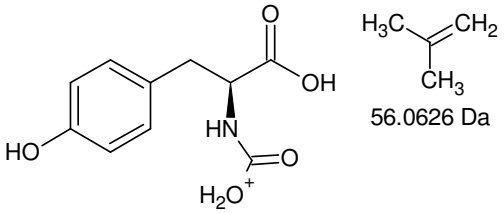

Monoisotopic Mass = 226.070999 Da

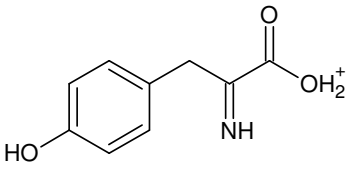

Monoisotopic Mass = 180.06552 Da

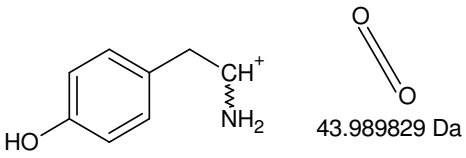

Monoisotopic Mass = 136.07569 Da

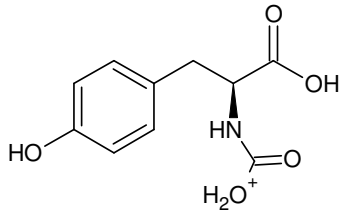

Monoisotopic Mass = 226.070999 Da

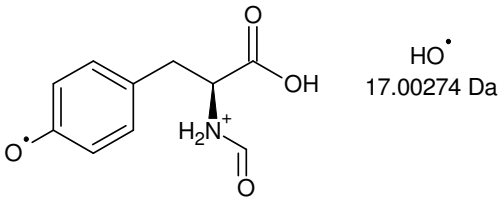

Monoisotopic Mass = 209.068259 Da

+MSn: 282 -> 226 -> 180 -> 136 and [282 -> 226] -> 209

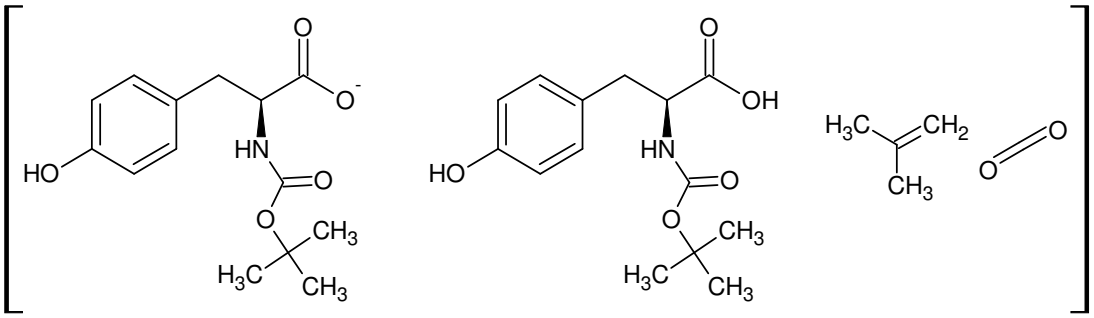

Monoisotopic Mass = 661.297798 Da

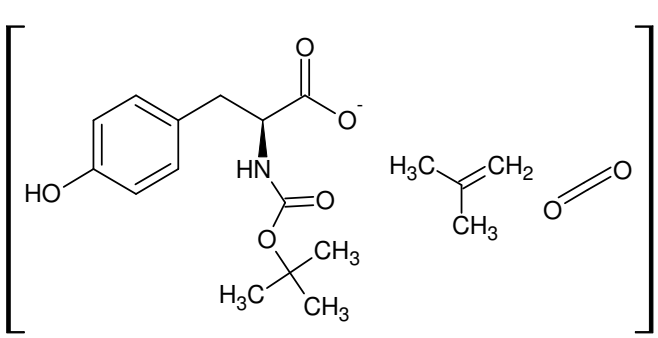

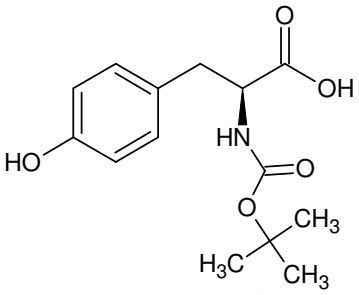

281.126323 Da

Monoisotopic Mass = 380.171476 Da

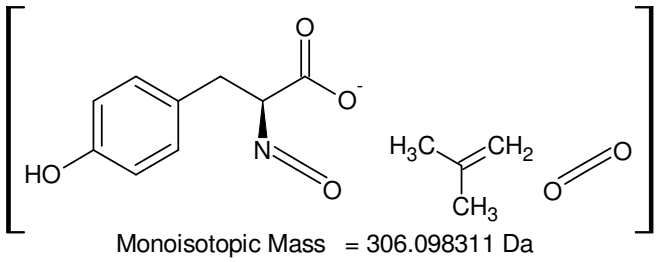

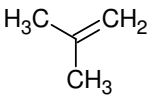

H_2O

74.073165 Da

Monoisotopic Mass = 306.098311 Da

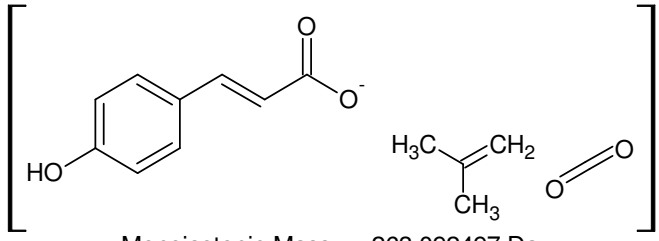

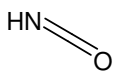

43.005814 Da

Monoisotopic Mass = 263.092497 Da

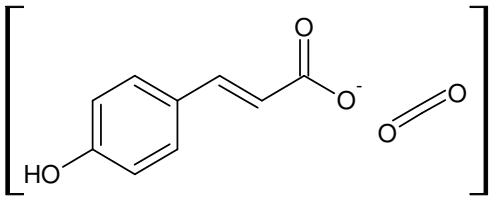

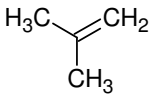

56.0626 Da

Monoisotopic Mass = 207.029897 Da

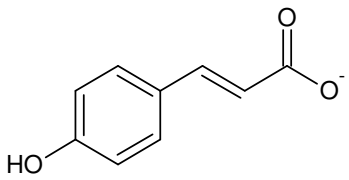

43.989829 Da

Monoisotopic Mass = 163.040068 Da

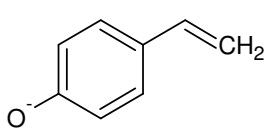

43.989829 Da

Monoisotopic Mass = 119.050238 Da

-MSn: 661 -> 380 -> 306 -> 263 -> 207 -> 163 -> 119

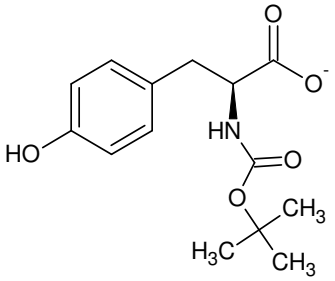

Monoisotopic Mass = 280.119046 Da

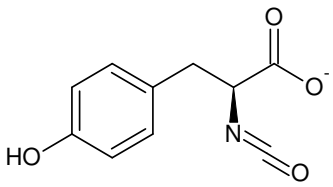

74.073165 Da

Monoisotopic Mass = 206.045881 Da

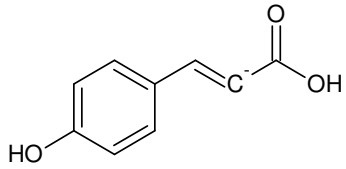

43.005814 Da

Monoisotopic Mass = 163.040068 Da

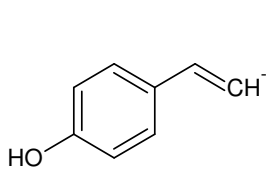

43.989829 Da

Monoisotopic Mass = 119.050238 Da

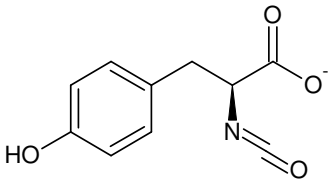

Monoisotopic Mass = 206.045881 Da

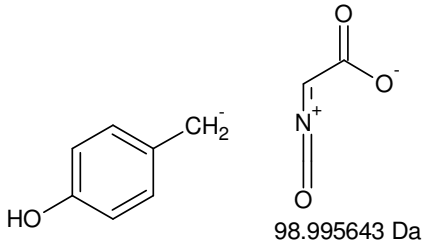

98.995643 Da

Monoisotopic Mass = 107.050238 Da

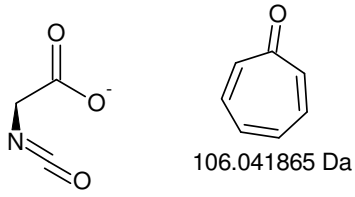

106.041865 Da

Monoisotopic Mass = 100.004017 Da

Gefundene Verbindungen: 44
CH2N2O2 MG=74,0116272
CH4N3O MG=74,0354354
(...)
H32N3 MG=74,2596092
N3O2 MG=73,999052

-----D--B--E--f-i-l-t-e-r-----
23.05.2011 - 14:26:09,56
akzeptierte DBEs:
0 1 2 3 4 5 6

$CH_2N_2O_2$	DBE: 2
CH_6N_4	DBE: 1
$C_2H_2O_3$	DBE: 2
$C_2H_6N_2O$	DBE: 1
$C_3H_6O_2$	DBE: 1
$C_3H_{10}N_2$	DBE: 0
$C_4H_{10}O$	**DBE: 0**
C_6H_2	DBE: 6
H_2N_4O	DBE: 2

9 von 44 Summenformeln

-MSn: 280 -> 206 -> 163 -> 119 and [280 -> 206] -> 107, 100

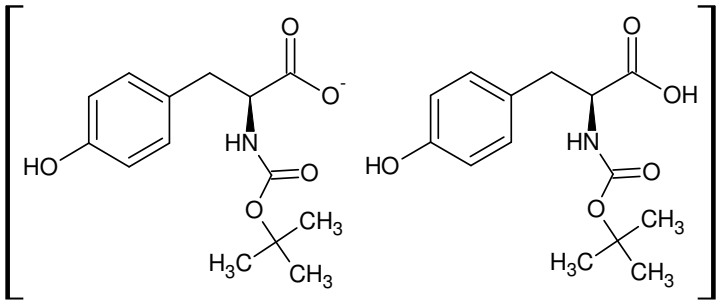

Monoisotopic Mass = 561.245369 Da

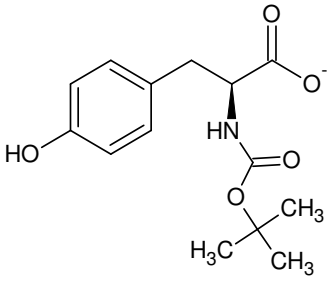

Monoisotopic Mass = 280.119046 Da

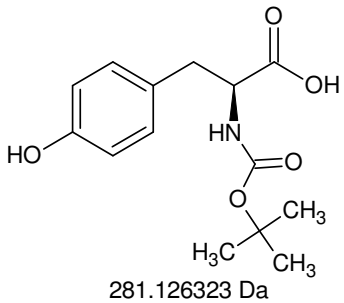

281.126323 Da

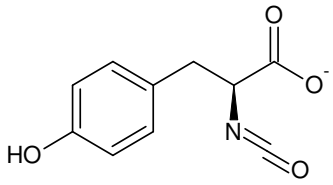

Monoisotopic Mass = 206.045881 Da

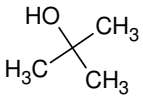

74.073165 Da

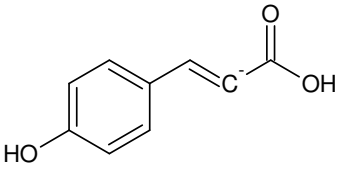

Monoisotopic Mass = 163.040068 Da

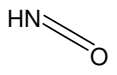

43.005814 Da

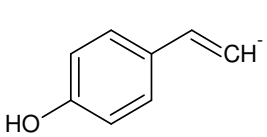

Monoisotopic Mass = 119.050238 Da

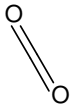

43.989829 Da

-MSn: 561 -> 280 -> 206 -> 163 -> 119

Gefundene Verbindungen: 14
CH2NO MG=44,0136382
CH4N2 MG=44,0374464
CH16O MG=44,1201086
CH18N MG=44,1439168
CO2 MG=43,98983
C2H4O MG=44,0262134
C2H6N MG=44,0500216
C2H20 MG=44,156492
C3H8 MG=44,0625968
H2N3 MG=44,0248712
H14NO MG=44,1075334
H12O2 MG=44,0837252
H16N2 MG=44,1313416
N2O MG=44,001063

-----D--B--E--f-i-l-t-e-r-----
23.05.2011 - 15:14:42,67
akzeptierte DBEs:
0 1 2 3 4 5 6

CH_4N_2 DBE: 1
CO_2 DBE: 2
C_2H_4O DBE: 1
C_3H_8 DBE: 0
N_2O DBE: 2

5 von 14 Summenformeln

X.III. Photo- and fluorometry of N-Boc-*L*-Tyr oxidised by AbT

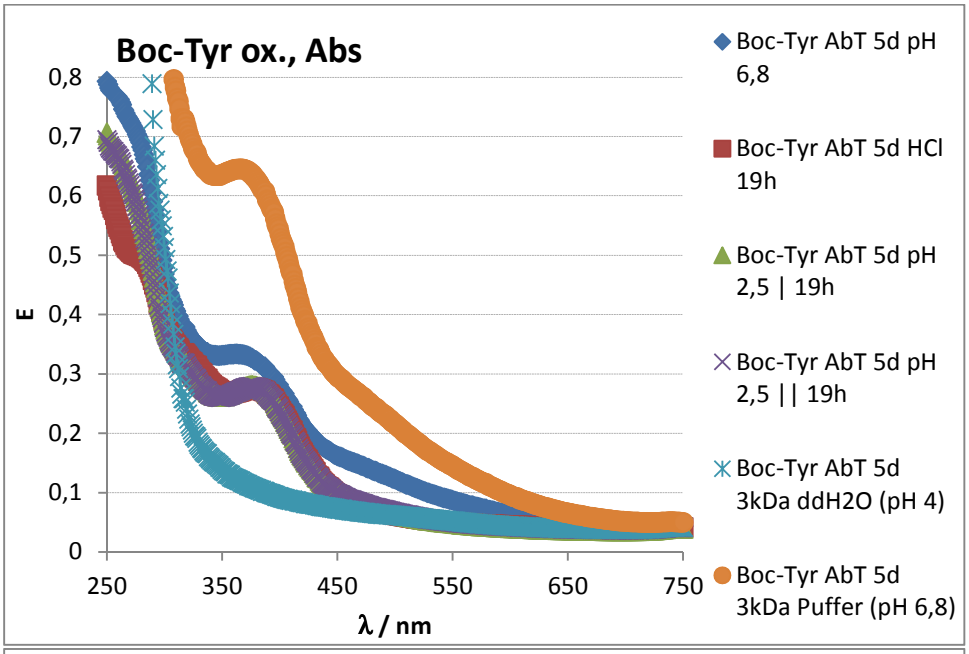

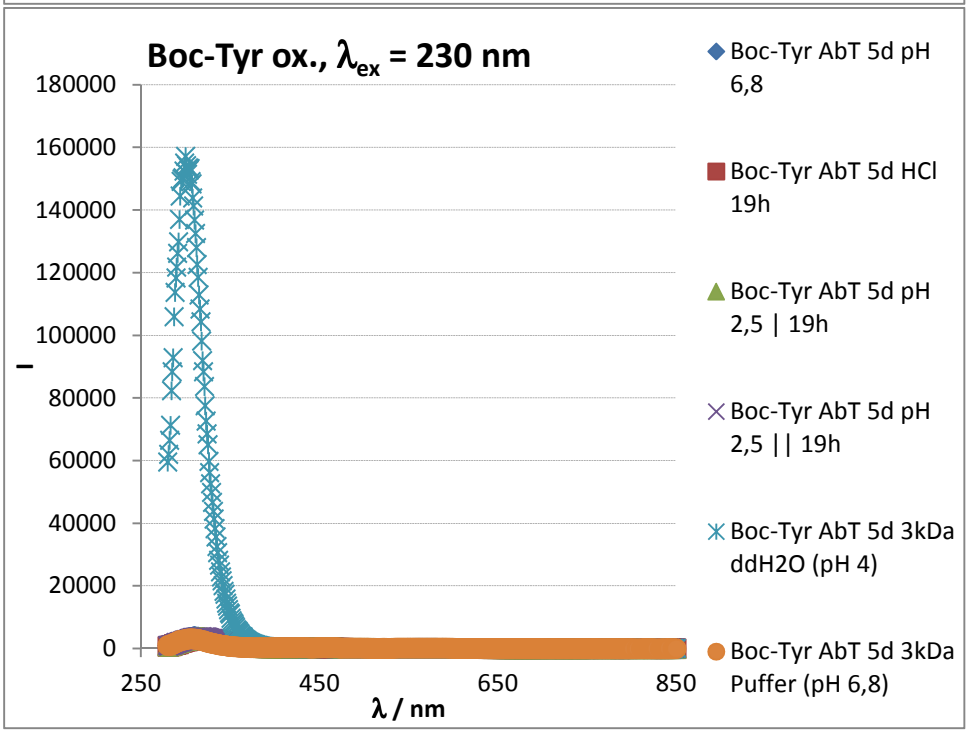

230 · 2 = 460

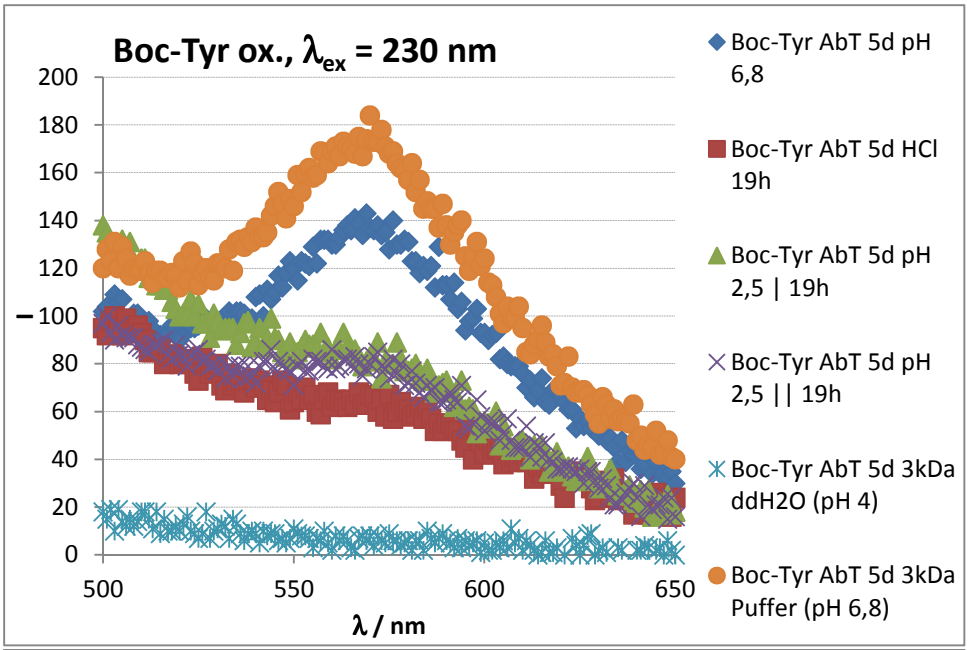
Boc-Tyr ox., λex = 230 nm
200
180
160
140
120
100
80
60
40
20
0
500
550
600
650
λ / nm
Boc-Tyr AbT 5d pH 6,8
Boc-Tyr AbT 5d HCl 19h
Boc-Tyr AbT 5d pH 2,5 | 19h
Boc-Tyr AbT 5d pH 2,5 || 19h
Boc-Tyr AbT 5d 3kDa ddH2O (pH 4)
Boc-Tyr AbT 5d 3kDa Puffer (pH 6,8)

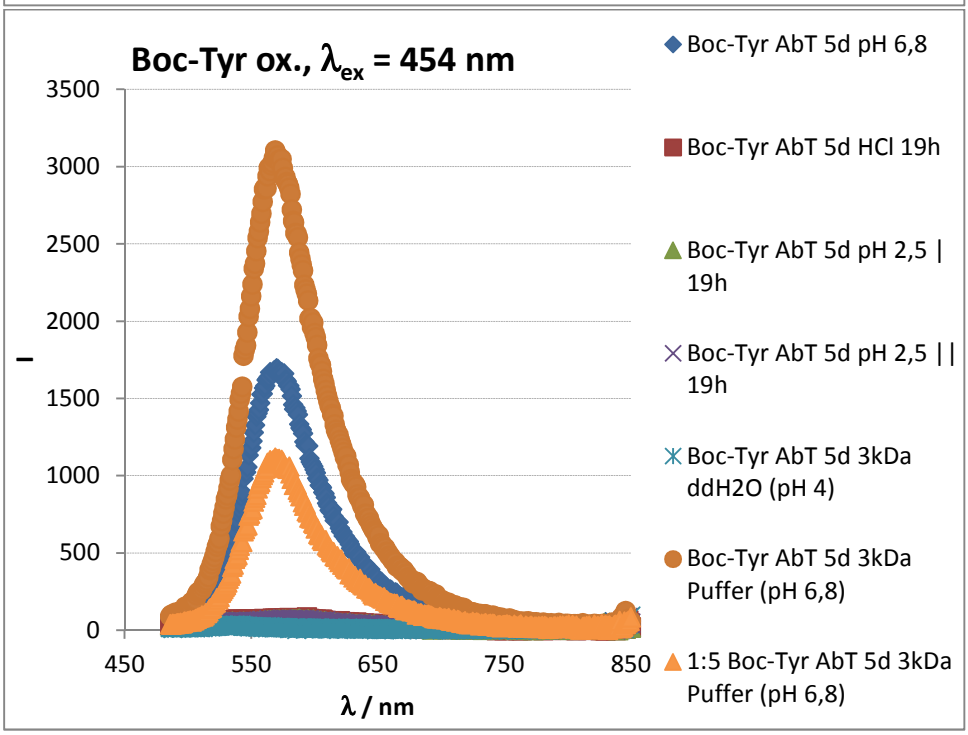
Boc-Tyr ox., λex = 454 nm
3500
3000
2500
2000
1500
1000
500
0
450
550
650
750
850
λ / nm
Boc-Tyr AbT 5d pH 6,8
Boc-Tyr AbT 5d HCl 19h
Boc-Tyr AbT 5d pH 2,5 | 19h
Boc-Tyr AbT 5d pH 2,5 || 19h
Boc-Tyr AbT 5d 3kDa ddH2O (pH 4)
Boc-Tyr AbT 5d 3kDa Puffer (pH 6,8)
1:5 Boc-Tyr AbT 5d 3kDa Puffer (pH 6,8)

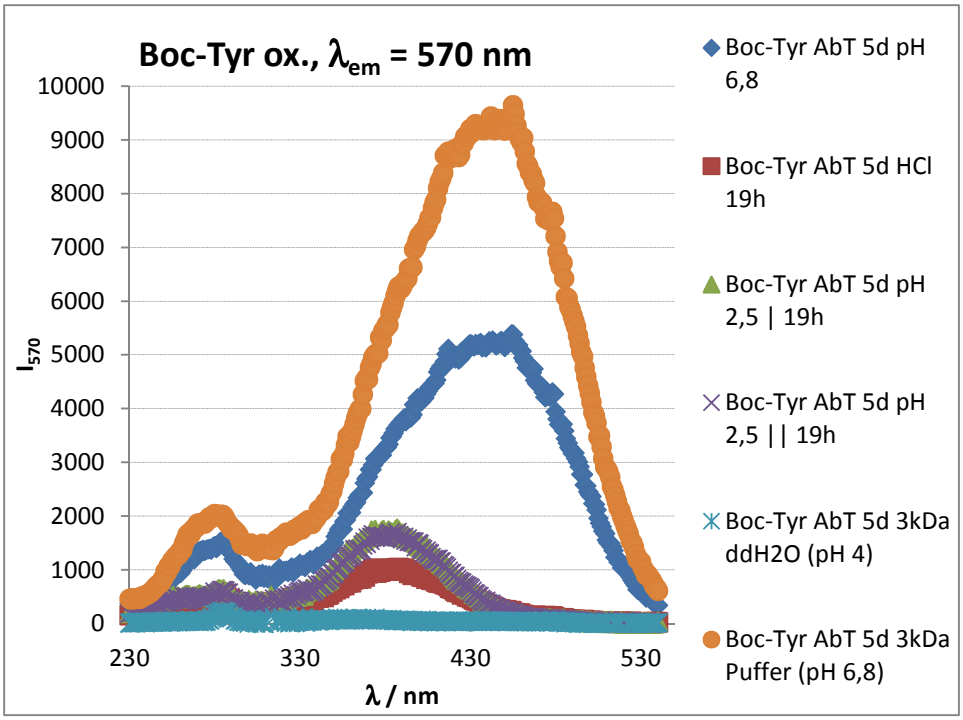

570 / 2 = 285: Artefact generated due to imperfect monochromatisation

(The measurement device uses grating monochromators for both emission and excitation light. For those devices the **grating equation** holds which states that the light diffracted by the grating exhibits maxima of intensity at angles α as a function of the grating constant g, the wavelength of the incident light λ and the order of the intensity maxima m: $\mathbf{g \cdot \sin(\alpha) = m \cdot \lambda}$, where m is an integer).

Figure X-VI Oxidised Boc-Tyr (5d @ 25 °C in 2 ml PP vials with perforated caps, 150 min^{-1} with 4 U l^{-1} AbT) after 20 h at the indicated pH (figure continued from the 2 previous pages)

3 kDa .....filtrated through a Vivaspin® 2 membrane with 3000 Da molecular weight cut-off

X.IV. MS^n analysis of oxidised N-Boc-*L*-Tyr

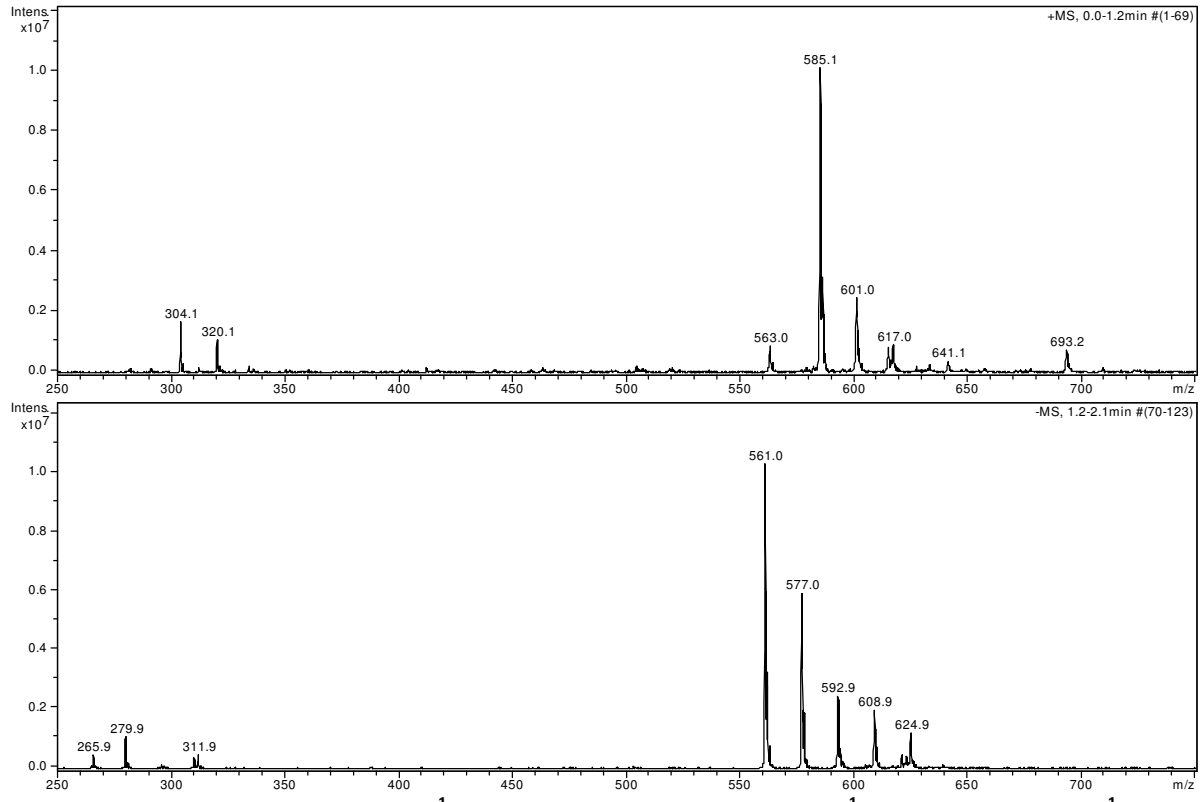

Figure X-VII 2mM N-Boc-*L*-Tyr with 1 U l^{-1} AbT in ddH_2O; 5 d @ 25 °C, 145 min^{-1}; filtrated: full scan MS^1

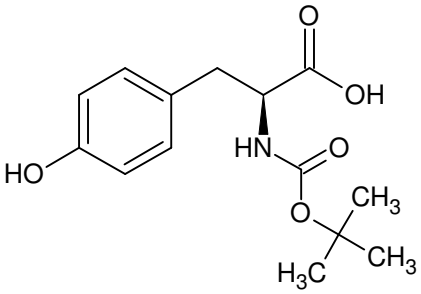

Boc-Tyr-OH
281.126323 Da

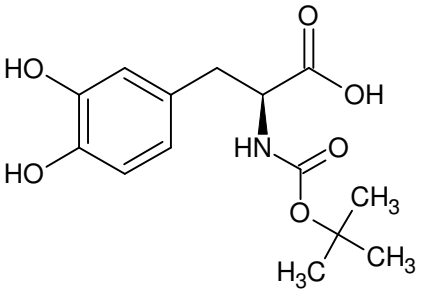

Boc-Tyr-$(OH)_2$
(DOPA)
297.121237 Da

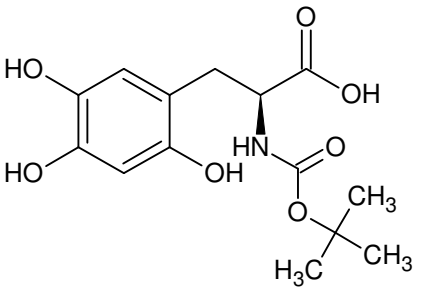

Boc-Tyr-$(OH)_3$
(TOPA)
313.116152 Da

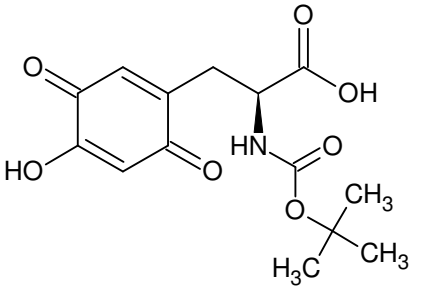

Boc-Tyr-$(OH)_3$ ox.
311.100502 Da

Scheme 13-13 Structure and oxidation products of N-Boc-*L*-Tyr

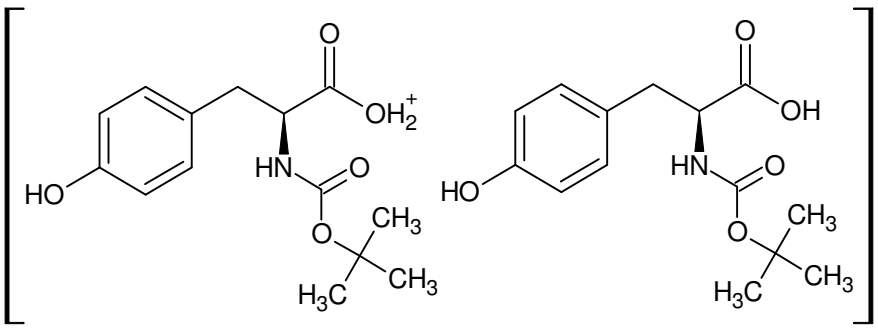

563.259922 Th

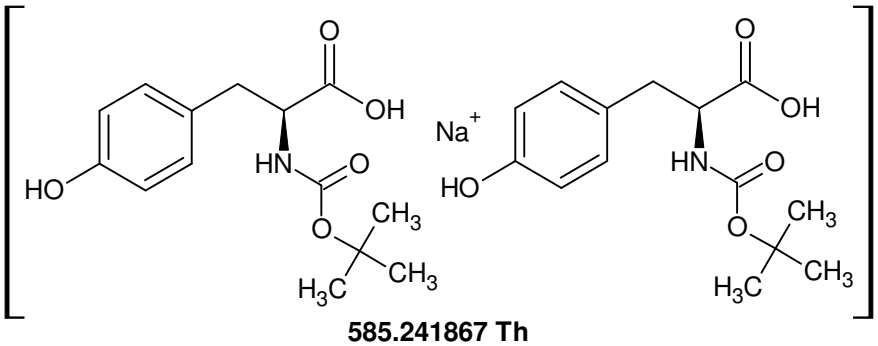

585.241867 Th

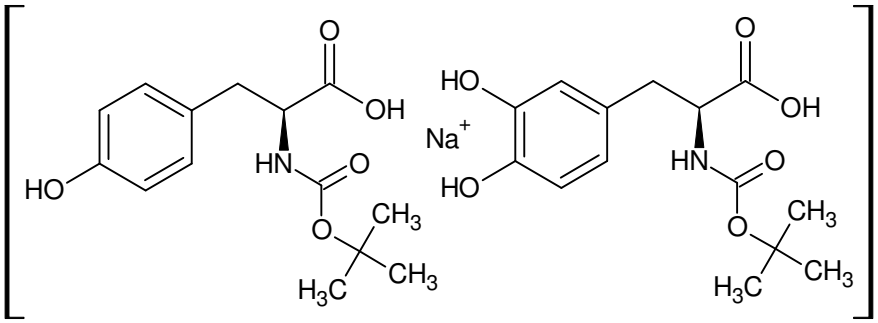

601.236781 Th

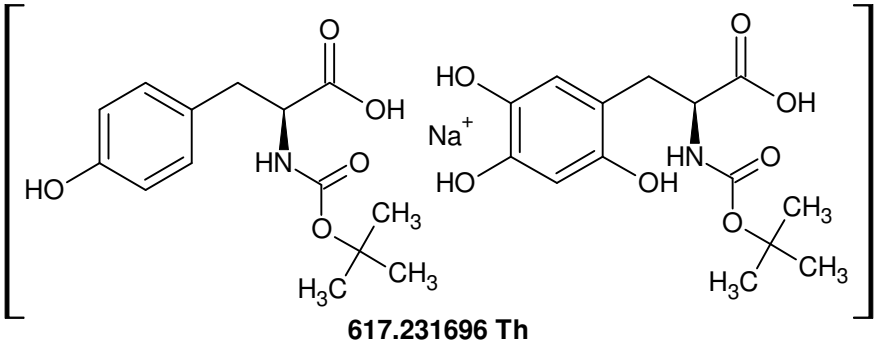

617.231696 Th

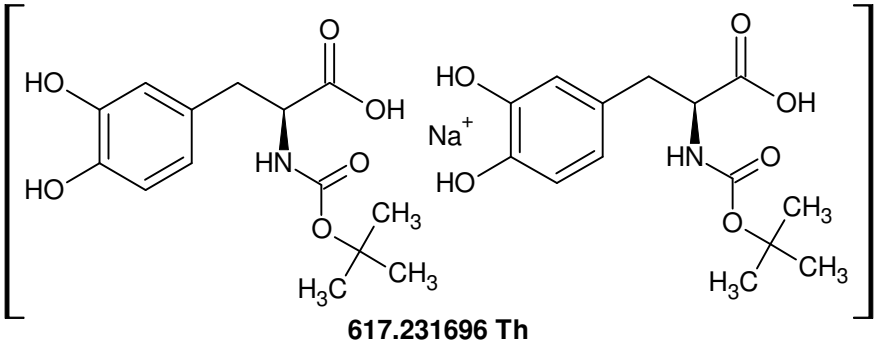

617.231696 Th

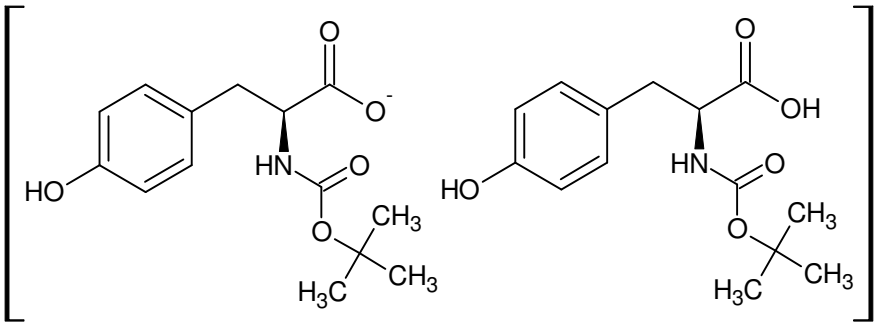

-561.245369 Th

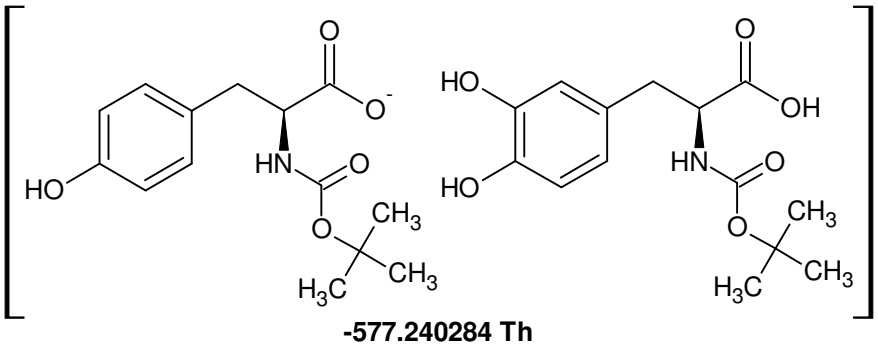

-577.240284 Th

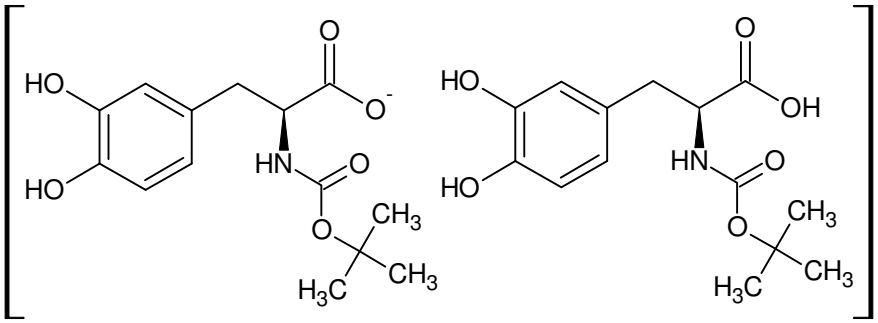

-593.235198 Th

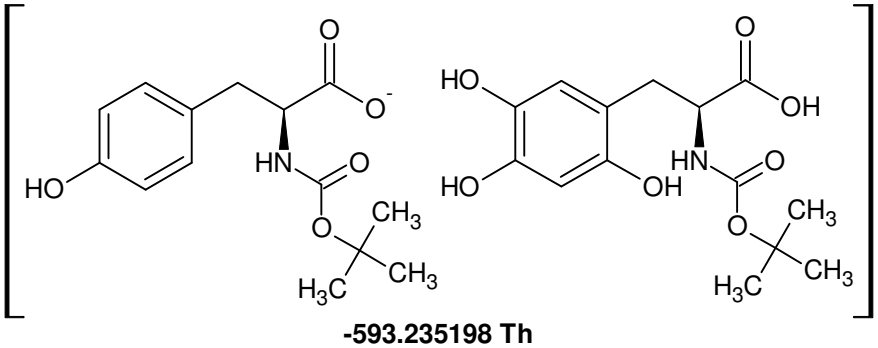

-593.235198 Th

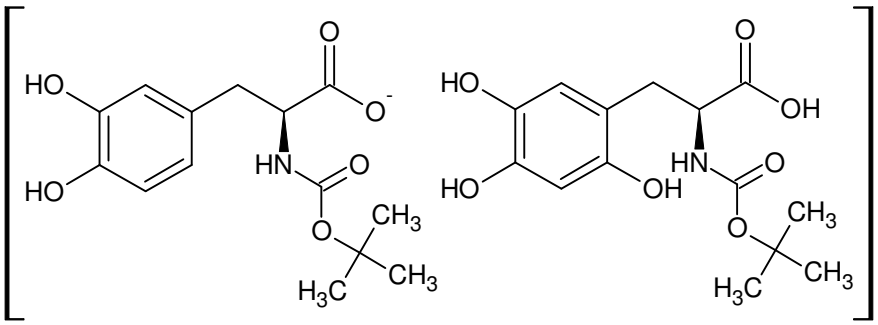

-609.230113 Th

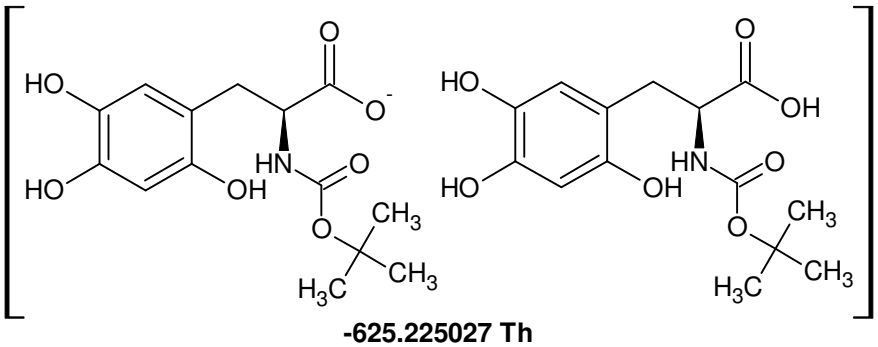

-625.225027 Th

Interpretation of the signals spaced 16 Th each

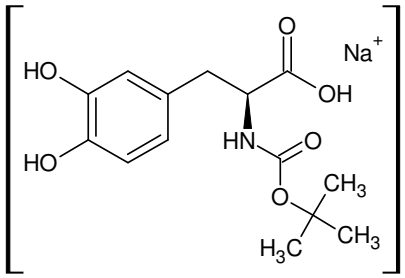

Monoisotopic Mass = 320.110459 Da

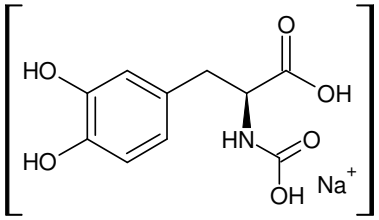

Monoisotopic Mass = 264.047858 Da

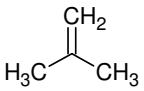

56.0626 Da

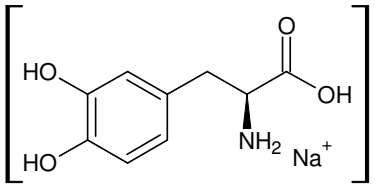

Monoisotopic Mass = 220.058029 Da

43.989829 Da

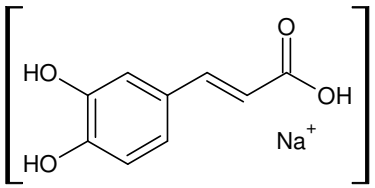

Monoisotopic Mass = 203.03148 Da

NH_3
17.026549 Da

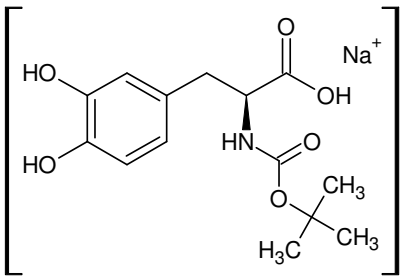

Monoisotopic Mass = 320.110459 Da

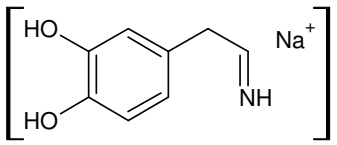

Monoisotopic Mass = 174.05255 Da

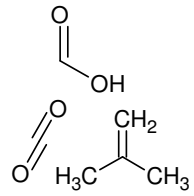

146.057909 Da

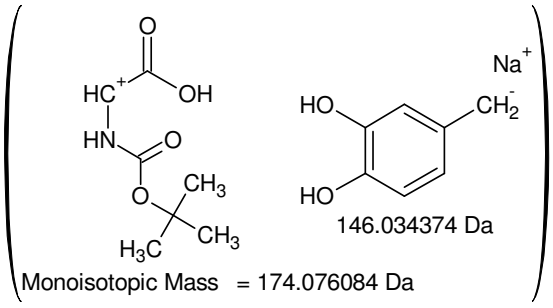

146.034374 Da

Monoisotopic Mass = 174.076084 Da

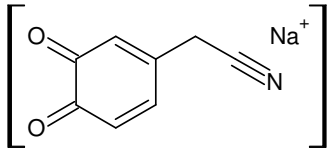

Monoisotopic Mass = 170.02125 Da

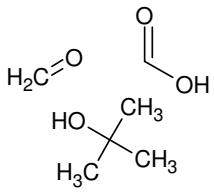

150.089209 Da

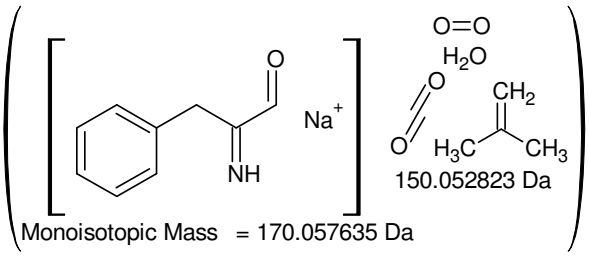

150.052823 Da

Monoisotopic Mass = 170.057635 Da

+MSn: 320 -> 264 -> 220 -> 203 and 320 -> 174, 170

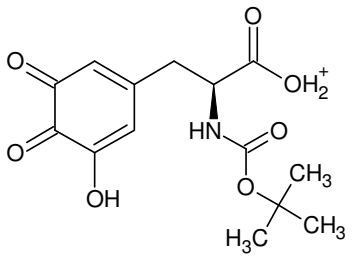

Monoisotopic Mass = 312.107778 Da

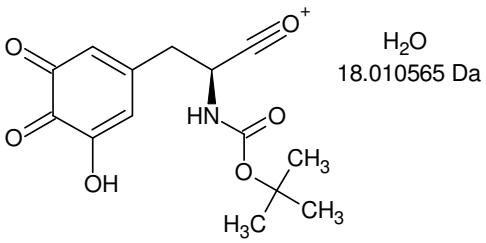

Monoisotopic Mass = 294.097214 Da

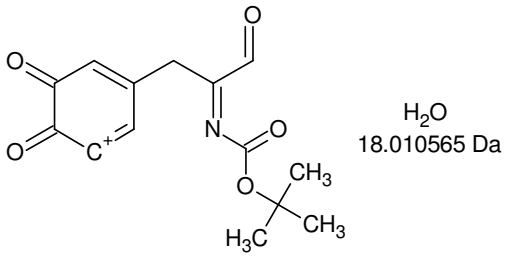

Monoisotopic Mass = 276.086649 Da

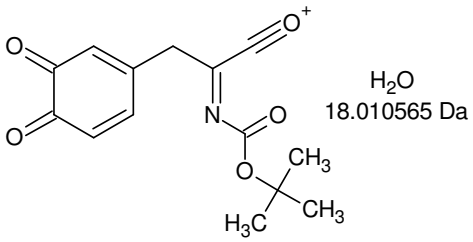

Monoisotopic Mass = 276.086649 Da

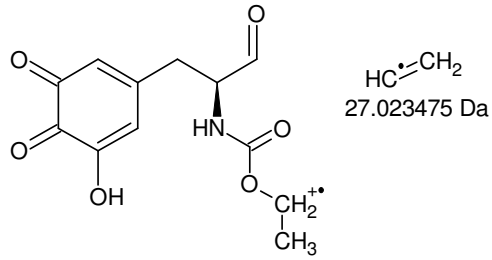

Monoisotopic Mass = 267.073739 Da

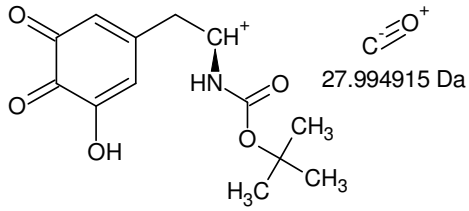

Monoisotopic Mass = 266.102299 Da

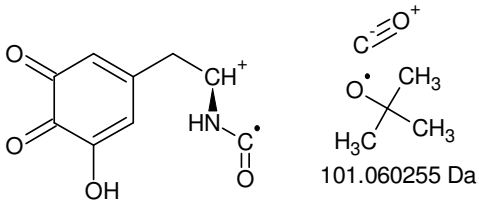

Monoisotopic Mass = 193.036959 Da

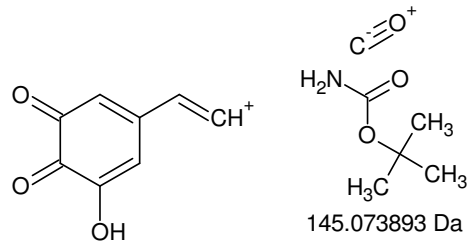

Monoisotopic Mass = 149.02332 Da

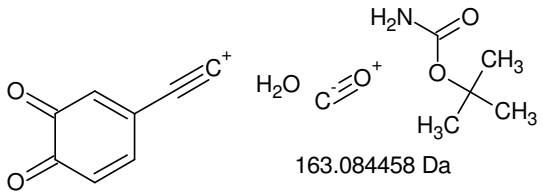

Monoisotopic Mass = 131.012756 Da

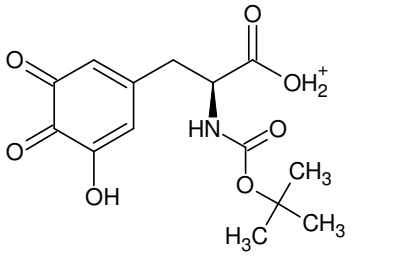

Monoisotopic Mass = 312.107778 Da

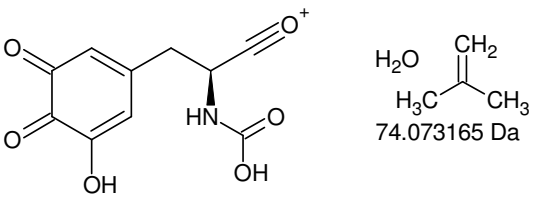

Monoisotopic Mass = 238.034613 Da

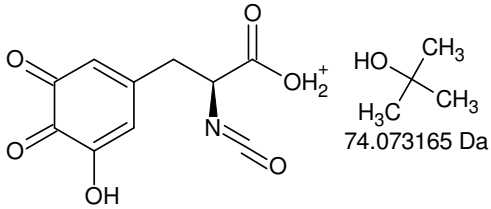

Monoisotopic Mass = 238.034613 Da

+MSn: 312 -> 294 -> 276, (267,) 266, 193, 149, 131 and 312 -> 238

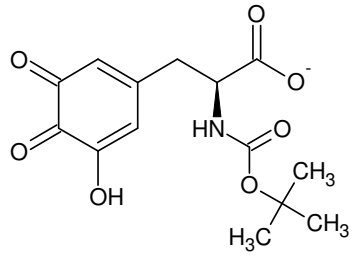

Monoisotopic Mass = 310.093225 Da

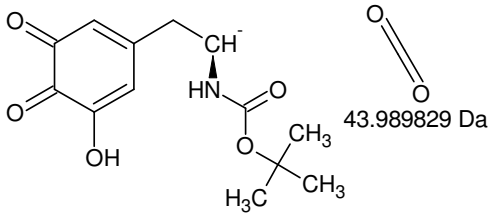

Monoisotopic Mass = 266.103396 Da

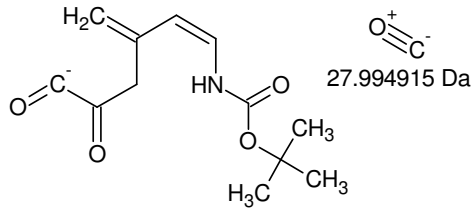

Monoisotopic Mass = 238.108482 Da

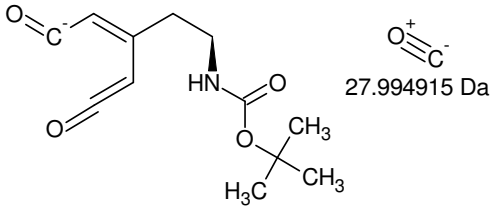

Monoisotopic Mass = 238.108482 Da

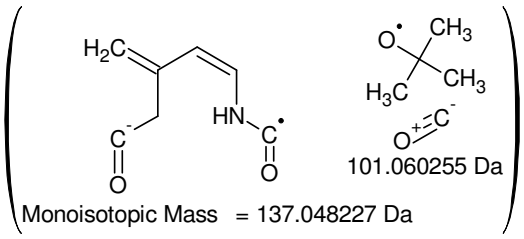

Monoisotopic Mass = 137.048227 Da

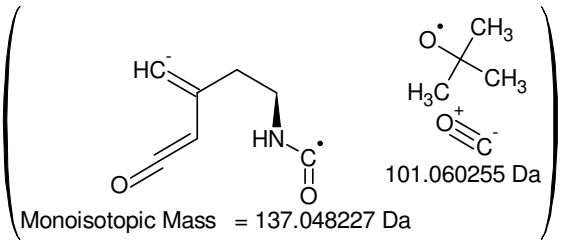

Monoisotopic Mass = 137.048227 Da

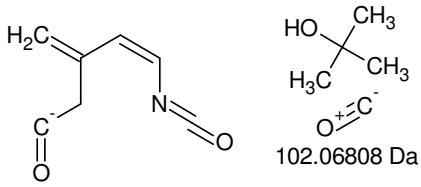

Monoisotopic Mass = 136.040402 Da

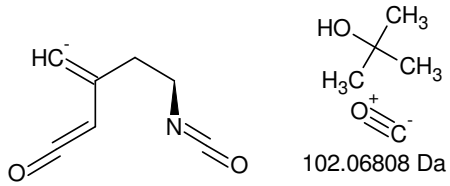

Monoisotopic Mass = 136.040402 Da

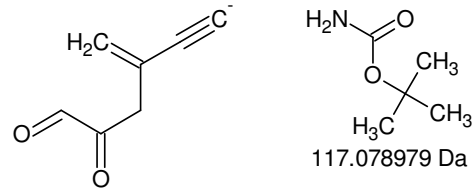

Monoisotopic Mass = 121.029503 Da

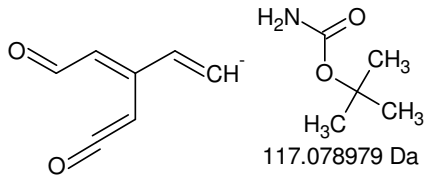

Monoisotopic Mass = 121.029503 Da

-MSn: 310 -> 266 -> 2x 238 -> (2x 137,) 2x 136, 2x 121

XI. Reduction with $NaBH_4$

P02453[162-1215], Collagen alpha-1(I) chain, Bos taurus

>sp|P02453|162-1215

QLSYGYDEKSTGISVPGPMGPSGPRGLPGPPGAPGPQGFQGPPGEPGEPGASGPMGPRGPPGPPGKNGDDGEA
GKPGRPGERGPPGPQGARGLPGTAGLPGMKGHRGFSGLDGAKGDAGPAGPKGEPGSPGENGAPGQMGPRGLP
GERGRPGAPGPAGARGNDGATGAAGPPGPTGPAGPPGFPGAVGAKGEGGPQGPRGSEGPQGVRGEPGPPGPA
GAAGPAGNPGADGQPGAKGANGAPGIAGAPGFPGARGPSGPQGPSGPPGPKGNSGEPGAPGSKGDTGAKGEP
GPTGIQGPPGPAGEEGKRGARGEPGPAGLPGPPGERGGPGSRGFPGADGVAGPKGPAGERGAPGPAGPKGSPG
EAGRPGEAGLPGAKGLTGSPGSPGPDGKTGPPGPAGQDGRPGPPGPPGARGQAGVMGFPGPKGAAGEPGKAG
ERGVPGPPGAVGPAGKDGEAGAQGPPGPAGPAGERGEQGPAGSPGFQGLPGPAGPPGEAGKPGEQGVPGDLG
APGPSGARGERGFPGERGVQGPPGPAGPRGANGAPGNDGAKGDAGAPGAPGSQGAPGLQGMPGERGAAGLP
GPKGDRGDAGPKGADGAPGKDGVRGLTGPIGPPGPAGAPGDKGEAGPSGPAGPTGARGAPGDRGEPGPPGPA
GFAGPPGADGQPGAKGEPGDAGAKGDAGPPGPAGPAGPPGPIGNVGAPGPKGARGSAGPPGATGFPGAAGRV
GPPGPSGNAGPPGPPGPAGKEGSKGPRGETGPAGRPGEVGPPGPPGPAGEKGAPGADGPAGAPGTPGPQGIAG
QRGVVGLPGQRGERGFPGLPGPSGEPGKQGPSGASGERGPPGPMGPPGLAGPPGESGREGAPGAEGSPGRDGS
PGAKGDRGETGPAGPPGAPGAPGAPGPVGPAGKSGDRGETGPAGPAGPIGPVGARGPAGPQGPRGDKGETGE
QGDRGIKGHRGFSGLQGPPGPPGSPGEQGPSGASGPAGPRGPPGSAGSPGKDGLNGLPGPIGPPGPRGRTGDAG
PAGPPGPPGPPGPPGPPSGGYDLSFLPQPPQEKAHDGGRYY

P02465[80-1100], Collagen alpha-2(I) chain, Bos taurus

>sp|P02465|80-1100

QFDAKGGGPGPMGLMGPRGPPGASGAPGPQGFQGPPGEPGEPGQTGPAGARGPPGPPGKAGEDGHPGKPGR
PGERGVVGPQGARGFPGTPGLPGFKGIRGHNGLDGLKGQPGAPGVKGEPGAPGENGTPGQTGARGLPGERGRV
GAPGPAGARGSDGSVGPVGPAGPIGSAGPPGFPGAPGPKGELGPVGNPGPAGPAGPRGEVGLPGLSGPVGPPG
NPGANGLPGAKGAAGLPGVAGAPGLPGPRGIPGPVGAAGATGARGLVGEPGPAGSKGESGNKGEPGAVGQPGP
PGPSGEEGKRGSTGEIGPAGPPGPPGLRGNPGSRGLPGADGRAGVMGPAGSRGATGPAGVRGPNGDSGRPGEP
GLMGPRGFPGSPGNIGPAGKEGPVGLPGIDGRPGPIGPAGARGEPGNIGFPGPKGPSGDPGKAGEKGHAGLAGA
RGAPGPDGNNGAQGPPGLQGVQGGKGEQGPAGPPGFQGLPGPAGTAGEAGKPGERGIPGEFGLPGPAGARGE
RGPPGESGAAGPTGPIGSRGPSGPPGPDGNKGEPGVVGAPGTAGPSGPSGLPGERGAAGIPGGKGEKGETGLRG
DIGSPGRDGARGAPGAIGAPGPAGANGDRGEAGPAGPAGPAGPRGSPGERGEVGPAGPNGFAGPAGAAGQPG
AKGERGTKGPKGENGPVGPTGPVGAAGPSGPNGPPGPAGSRGDGGPPGATGFPGAAGRTGPPGPSGISGPPGP
PGPAGKEGLRGPRGDQGPVGRSGETGASGPPGFVGEKGPSGEPGTAGPPGTPGPQGLLGAPGFLGLPGSRGERG
LPGVAGSVGEPGPLGIAGPPGARGPPGNVGNPGVNGAPGEAGRDGNPGNDGPPGRDGQPGHKGERGYPGNA
GPVGAAGAPGPQGPVGPVGKHGNRGEPGPAGAVGPAGAVGPRGPSGPQGIRGDKGEPGDKGPRGLPGLKGHN
GLQGLPGLAGHHGDQGAPGAVGPAGPRGPAGPSGPAGKDGRIGQPGAVGPAGIRGSQGSQGPAGPPGPPGPP
GPPG

Figure XI-I Primary sequence of the proteins making up type I collagen: one α-2(I) and two α-1(I) chains

XII. Preparations

XII.I. Acid soluble collagen with tyrosinases and laccases in NH4Ac

XII.I.I. K with BoT1, BoT2, AbT, T4, TvL and ThL

Table XII-I Amino acid analysis of hydrolysed K after 16 h @ 25 °C - mM

Amino acid	Change after enzymatic treatment / mM (K treated - K untreated - enzyme only)									
	BoT1	BoT1 |	BoT2	AbT	T4	T4 |	TvL	TvL |	ThL	ThL |
Asp	0,15	-0,19	0,19	0,037	-0,27	0,77	-0,11	0,10	-0,14	0,068
Glu	0,22	-0,12	0,65	0,12	0,060	1,59	0,031	0,15	-0,004	0,045
Asn	-0,12	-0,25	-0,033	0,13	-0,060	-0,16	**0,22**	**0,18**	0,10	0,065
Ser	0,029	-0,13	0,54	0,064	-0,077	0,53	**-0,23**	**-0,13**	**-0,32**	**-0,33**
Gln	-0,017	-0,057	-0,0054	-0,021	-0,071	-0,0055	-0,021	-0,009	-0,072	-0,056
Gly&Thr	**0,95**	**0,71**	5,75	0,32	2,84	8,23	**-1,87**	**-2,15**	-0,99	-2,17
Arg	**-0,42**	**-0,25**	0,79	0,08	0,39	1,25	0,021	0,051	0,066	0,015
Ala	0,46	0,27	2,75	0,13	0,94	3,34	**-0,82**	**-0,91**	-0,35	-0,95
Tyr	-0,52	-0,17	0,49	-0,227	-0,059	0,57	**0,14**	**0,15**	0,053	-0,092
Val	0,024	-0,13	0,028	0,035	-0,091	0,29	-0,017	0,055	-0,039	0,033
Met	0,000	0,000	0,23	0,000	-0,0044	0,040	-0,0066	-0,110	0,042	-0,110
Trp	**-0,093**	**-0,091**	-0,24	-0,053	0,010	0,17	-0,068	-0,20	-0,059	-0,017
Phe	0,036	-0,067	0,12	-0,0036	0,035	0,27	**0,064**	**0,076**	-0,038	0,043
Ile	-0,0044	-0,042	0,26	-0,012	-0,20	0,034	**-0,058**	**-0,078**	**-0,054**	**-0,066**
Leu	**0,056**	**0,054**	0,68	0,010	0,22	0,80	**-0,11**	**-0,15**	-0,048	-0,18
Lys	-0,0053	-0,20	0,056	0,030	0,033	0,64	**0,11**	**0,088**	0,0049	0,047

Table XII-II Amino acid analysis of hydrolysed K after 16 h @ 25 °C - %

Amino acid	Change after enzymatic treatment / % (relative to K untreated)									
	BoT1	BoT1 |	BoT2	AbT	T4	T4 |	TvL	TvL |	ThL	ThL |
Asp	12	-16	16	3	-24	67	-10	9	-12	6
Glu	11	-6	34	6	3	86	2	8	0	2
Asn	-25	-52	-7	28	-24	-66	**87**	**70**	42	26
Ser	3	-13	54	6	-7	45	**-20**	**-11**	**-27**	**-28**
Gln	-15	-50	-5	-19	-57	-4	-17	-7	**-58**	**-45**
Gly&Thr	**17**	**13**	102	6	36	105	**-24**	**-28**	-13	-28
Arg	-31	-18	58	6	30	96	2	4	5	1
Ala	13	8	78	4	21	76	**-18**	**-21**	-8	-22
Tyr	-100	-34	96	-44	-25	240	**57**	**65**	22	-38
Val	4	-21	5	6	-17	53	-3	10	-7	6
Met	-	-	-	-	-4	36	-6	-100	38	-100
Trp	-36	-35	-91	-21	8	133	-53	-152	-45	-13
Phe	10	-18	33	-1	12	89	**21**	**25**	-13	14
Ile	-1	-11	68	-3	-41	7	**-12**	**-16**	**-11**	**-14**
Leu	6	6	70	1	19	69	**-9**	**-13**	-4	-16
Lys	-1	-34	10	5	7	134	**23**	**18**	1	10

XII.I.II. K with BoT1, BoT2, AbT, T4, TvL and ThL

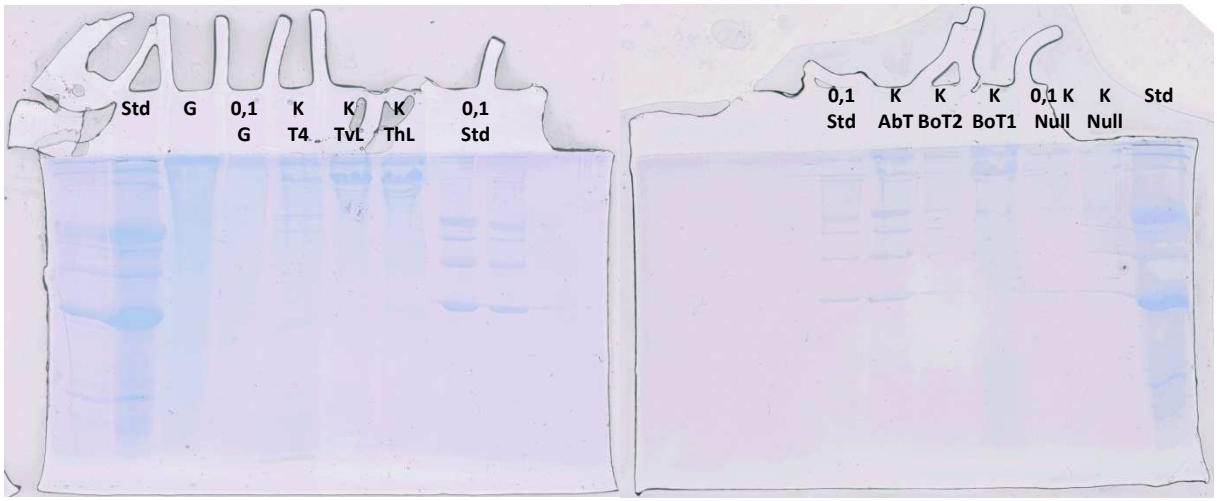

Figure XII-I 2x SDS-PAGE: 13,4 % acryl amide, stained with CBB R-250; samples 4d (K precipitated)
The 1 mm vertical gel was run for 90 min @ 150 V.
Std .....standard (globular proteins, see 5.1.4)
G.....gelatine
0,1 .....10-fold diluted with ddH_2O
Samples were mixed 1+9 with 10x reductive loading buffer (see 5.1.3) and loaded after 10 min at room temperature.

Table XII-III Evaporation losses from 2 ml micro tubes @ 27,2 °C & 400 min^{-1}

tube	tube / g	+1,5 ml /g	1,0 h /g	16,5 h /g	18,0 h /g	21,5 h /g	24,0 h /g
6,5 I	1,03004	2,52834	2,50562	2,30747	2,29076	2,25735	2,23494
6,5 II	1,02648	2,52378	2,51425	2,36047	2,34601	2,31756	2,28601
6,5 III	1,02614	2,52475	2,51593	2,38601	2,37377	2,35023	2,33182
6,5 IV	1,03476	2,53280	2,52279	2,38792	2,37595	2,35074	2,33395
6,5 V	1,02644	2,52345	2,52345	2,52342	2,52353	2,52356	2,52344
6,5 VI	1,02580	2,52522	2,52521	2,52523	2,52520	2,52520	2,52521
6,5 VII	1,02774	2,52702	2,52704	2,52707	2,52704	2,52704	2,52703
4,5 I	1,02947	2,52852	2,51862	2,36162	2,34723	2,31876	2,30142
4,5 II	1,02797	2,52529	2,51649	2,38340	2,37066	2,34545	2,32922
4,5 III	1,02604	2,52347	2,51479	2,38176	2,36943	2,34408	2,32821
4,5 IV	1,02650	2,52264	2,51286	2,37969	2,36793	2,34295	2,32684
4,5 V	1,03530	2,53327	2,53340	2,53331	2,53329	2,53330	2,53330
4,5 VI	1,02805	2,52523	2,52535	2,52534	2,52530	2,52529	2,52527
4,5 VII	1,02800	2,53776	2,53782	2,53780	2,53777	2,53778	2,53775

I – IV..... open tube
V – VII..... lid closed

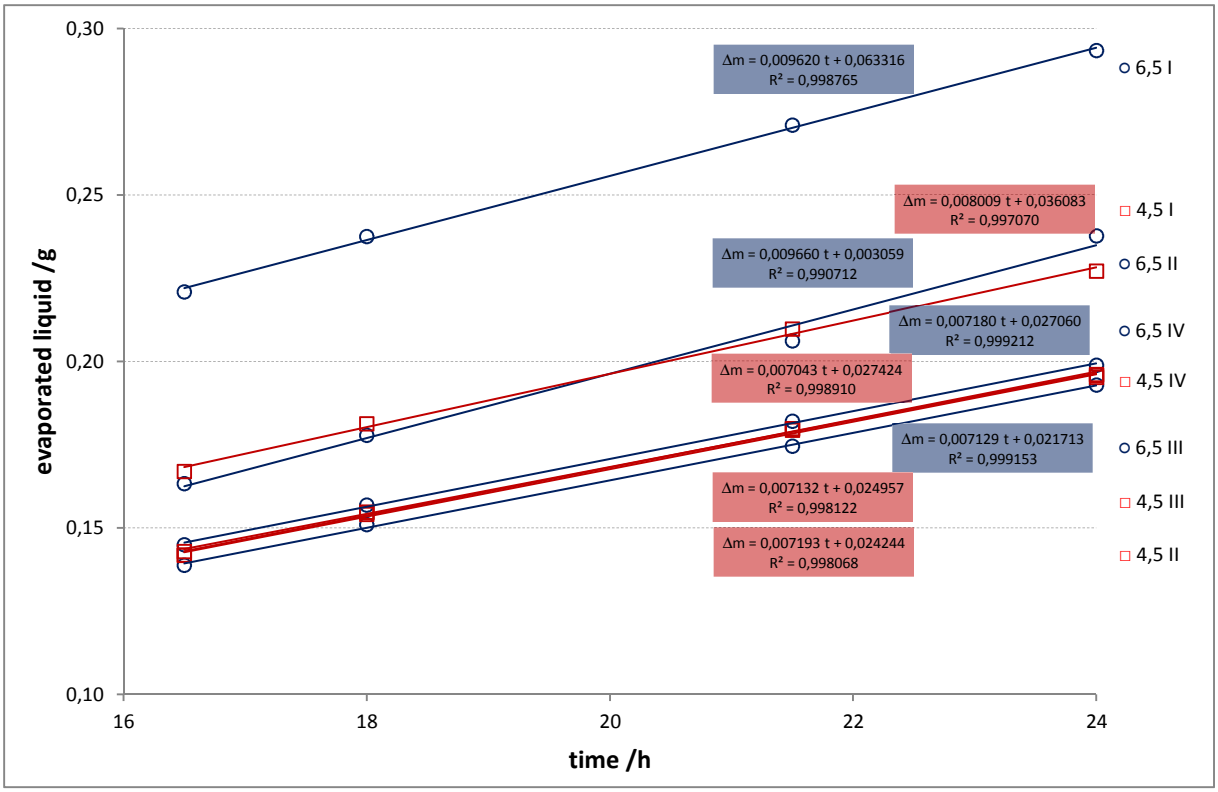

Figure XII-II evaporated liquid from open 2 ml micro tubes: 16,5 – 24 h
No significant amount of liquid evaporated from the closed tubes (V – VII).

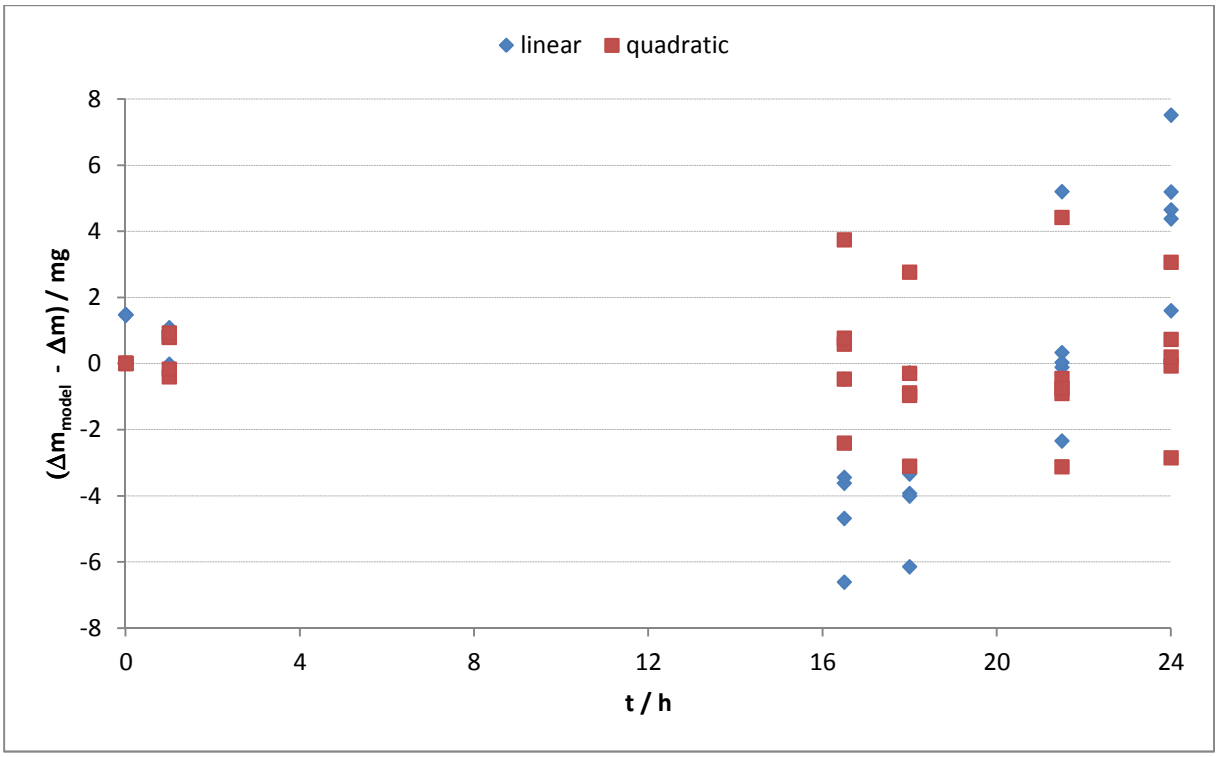

Figure XII-III residues for the linear and quadratic model of evaporation
linear: $\Delta m / mg = 8{,}36353 \cdot t / h$; $R^2 = 0{,}998037$; Note the curvature in the distribution of the residuals plotted vs. the independent variable (time).
quadratic: $\Delta m / mg = 9{,}66549 \cdot t / h - 0{,}0624672 \cdot t^2 / h^2$; $R^2 = 0{,}999511$

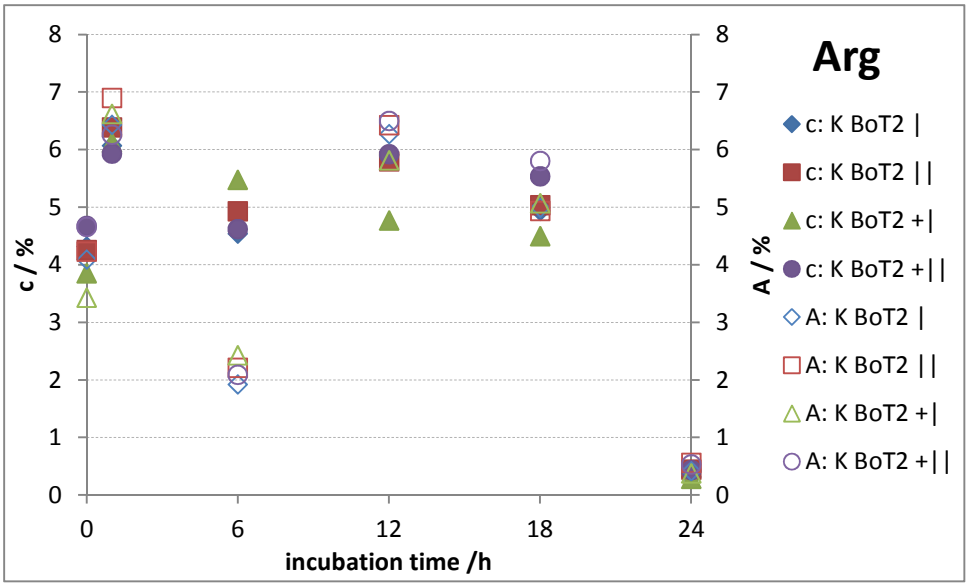
Arg
c / %
A / %
incubation time /h
0
6
12
18
24
c: K BoT2 |
c: K BoT2 ||
c: K BoT2 +|
c: K BoT2 +||
A: K BoT2 |
A: K BoT2 ||
A: K BoT2 +|
A: K BoT2 +||

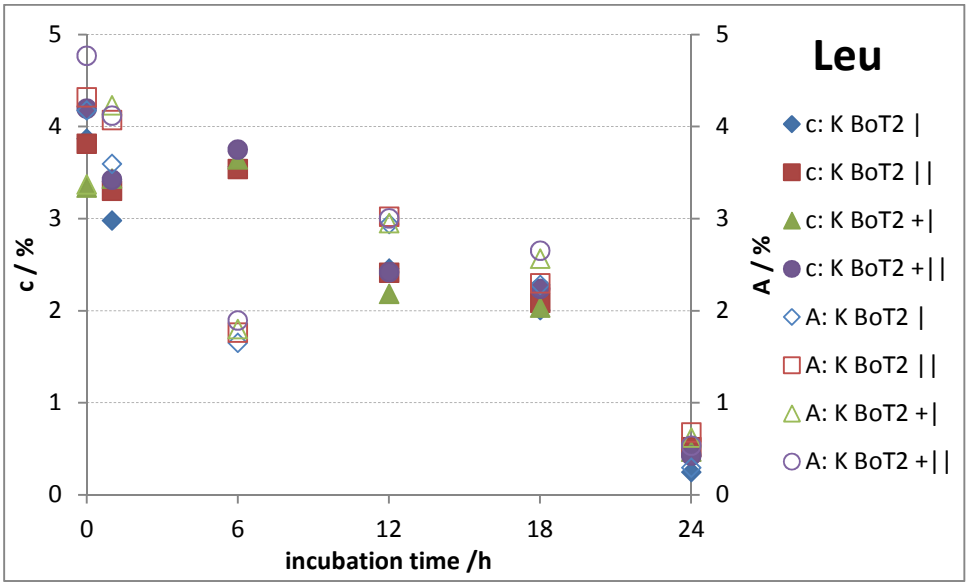
Leu
c / %
A / %
incubation time /h
0
6
12
18
24
c: K BoT2 |
c: K BoT2 ||
c: K BoT2 +|
c: K BoT2 +||
A: K BoT2 |
A: K BoT2 ||
A: K BoT2 +|
A: K BoT2 +||

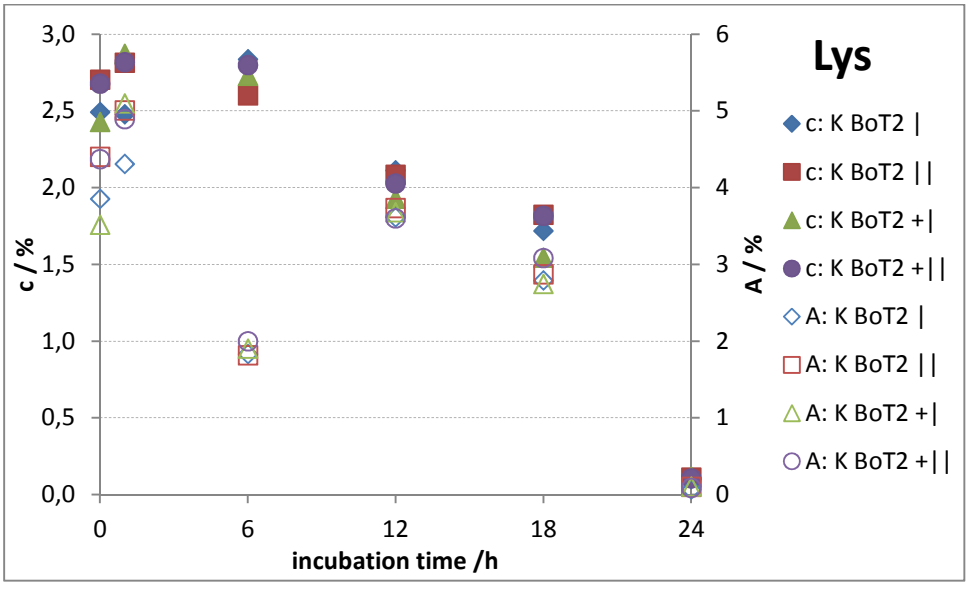
Lys
c / %
A / %
incubation time /h
0
6
12
18
24
c: K BoT2 |
c: K BoT2 ||
c: K BoT2 +|
c: K BoT2 +||
A: K BoT2 |
A: K BoT2 ||
A: K BoT2 +|
A: K BoT2 +||

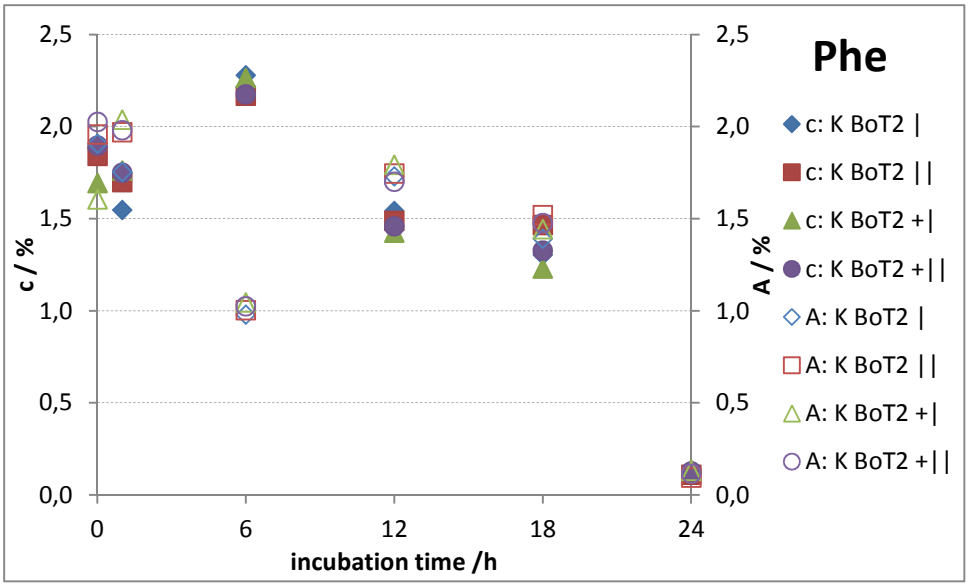
Phe
c / %
A / %
incubation time /h
0
6
12
18
24
0,0
0,5
1,0
1,5
2,0
2,5
c: K BoT2 |
c: K BoT2 ||
c: K BoT2 +|
c: K BoT2 +||
A: K BoT2 |
A: K BoT2 ||
A: K BoT2 +|
A: K BoT2 +||

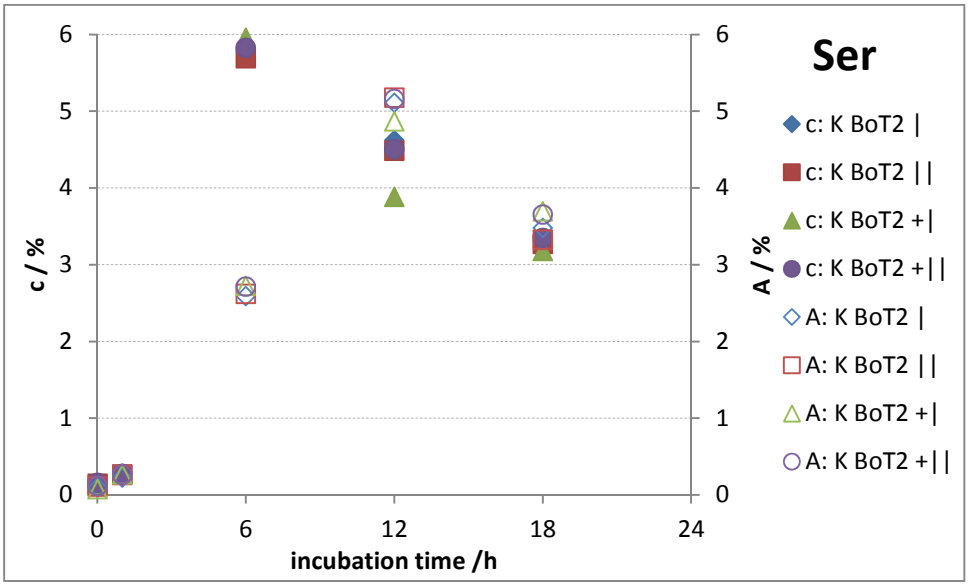
Ser
c / %
A / %
incubation time /h
0
1
2
3
4
5
6
c: K BoT2 |
c: K BoT2 ||
c: K BoT2 +|
c: K BoT2 +||
A: K BoT2 |
A: K BoT2 ||
A: K BoT2 +|
A: K BoT2 +||

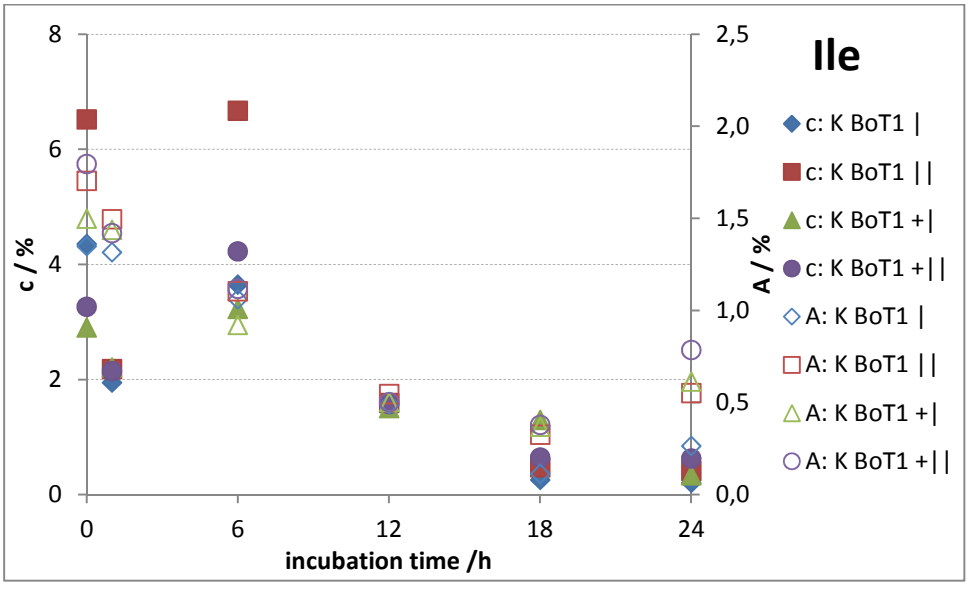
Ile
c / %
A / %
incubation time /h
0
2
4
6
8
0,0
0,5
1,0
1,5
2,0
2,5
c: K BoT1 |
c: K BoT1 ||
c: K BoT1 +|
c: K BoT1 +||
A: K BoT1 |
A: K BoT1 ||
A: K BoT1 +|
A: K BoT1 +||

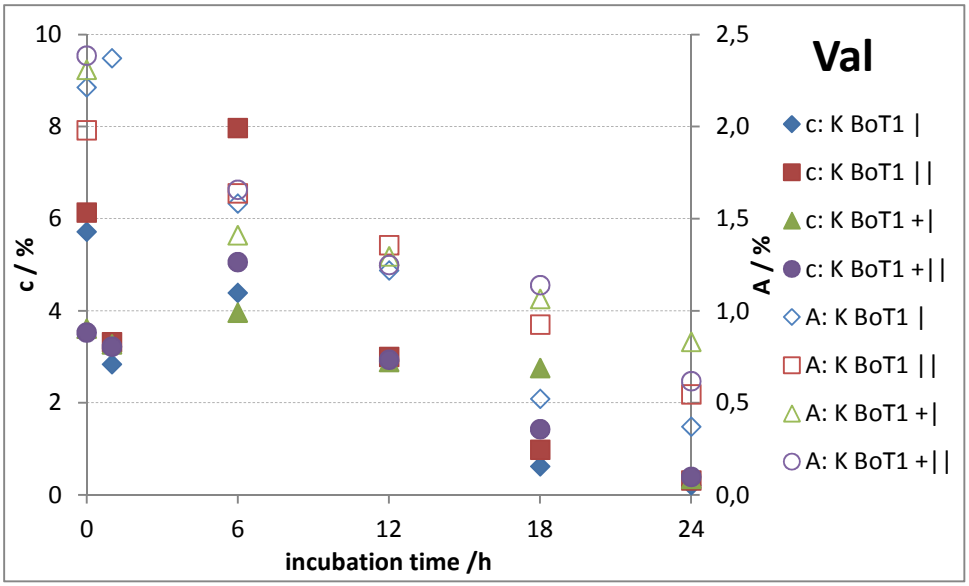

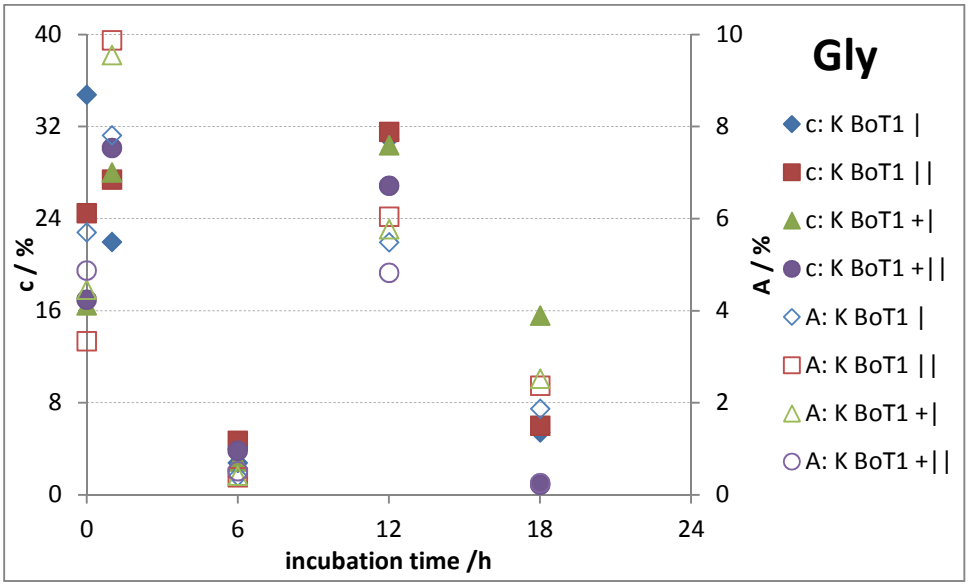

Figure XII-IV effect of enzymatic treatment with tyrosinases from *Botryosphaeria obtuse*
c:.....fraction of the concentration on the sum of all unmodified amino acids
A: .....fraction of the signal area on the integral over the complete retention range

Table XII-IV effect of enzymatic treatment on the levels of amino acids as determined by RP-HPLC-UVD after acid hydrolysis and OPA-derivatisation

Sample	Coefficients of determination (R^2) and orientation of trend (+: upwards, -: downwards) for a linear fit with data from the samples 0 h – 24 h[#]															
	Ala	Arg	Asp	Cys	Glu	Gly	His	Ile	Leu	Lys	Met	Phe	Ser	Thr	Tyr	Val
K BoT1 |		**0,19-**		**0,84+**		**0,21-**		**0,71-**	**0,55-**	0,20-					0,14-	**0,77-**
		0,21-		**0,67+**		**0,27-**		**0,90-**	**0,40-**	0,09+					0,18+	**0,96-**
K BoT1 ||	0,34-	**0,25-**		**0,70+**		**0,16-**		**0,54-**	**0,70-**	0,59-					0,09-	**0,59-**
	0,15-	**0,15-**		**0,73+**		**0,10-**		**0,81-**	**0,30-**	0,11-					0,30+	**0,85-**
K BoT1 +|		**0,01-**		**0,93+**		**0,00-**	0,71+	**0,76-**	**0,12-**	0,13-					0,00-	**0,70-**
		0,11-		**0,92+**		**0,16-**	0,63+	**0,74-**	**0,30-**	0,13-		0,31-			0,23+	**0,83-**
K BoT1 +||	0,14-	**0,16-**		**0,86+**		**0,23-**		**0,60-**	**0,37-**	0,05-					0,03-	**0,67-**
	0,25-	**0,22-**		**0,70+**		**0,39-**		**0,65-**	**0,33-**	0,01+					0,19+	**0,91-**
BoT1 6,5		0,33+				0,13-		|	0,51+					0,88+	
		0,23+				0,10-		0,62-				0,08+			0,16+	0,41-
K BoT2 |	**0,47-**	**0,41-**				**0,56-**	**0,74-**	**0,27-**	**0,85-**	**0,76-**		**0,28-**	**0,32+**		**0,01+**	**0,33-**
	0,29-	**0,20-**				**0,34-**	**0,68-**	**0,66-**	**0,67-**	**0,57-**		**0,13-**	**0,70+**		**0,45+**	**0,86-**
K BoT2 ||	**0,54-**	**0,42-**				**0,54-**	**0,85-**	**0,28-**	**0,91-**	**0,84-**		**0,65-**	**0,34+**		**0,01+**	**0,34-**
	0,37-	**0,24-**				**0,37-**	**0,61-**	**0,53-**	**0,69-**	**0,60-**		**0,55-**	**0,66+**		**0,37+**	**0,79-**
K BoT2 +|	**0,59-**	**0,50-**	**0,20+**	**0,70+**	0,59-	**0,67-**	**0,84-**	**0,27-**	**0,87-**	**0,85-**		**0,70-**	**0,29+**		**0,00+**	**0,34-**
	0,23-	**0,20-**	**0,20+**	**0,70+**	0,49-	**0,31-**	**0,77-**	**0,54-**	**0,59-**	**0,55-**		**0,49-**	**0,75+**		**0,26+**	**0,84-**
K BoT2 +||	**0,51-**	**0,37-**	**0,28+**	**0,58+**	0,16-	**0,56-**	**0,80-**	**0,31-**	**0,87-**	**0,83-**		**0,74-**	**0,34+**		**0,02+**	**0,33-**
	0,35-	**0,17-**	**0,27+**	**0,60+**	0,14-	**0,33-**	**0,49-**	**0,60-**	**0,68-**	**0,61-**		**0,59-**	**0,71+**		**0,38+**	**0,82-**
BoT2 6,5		0,77+	0,16+				0,42-		0,17+	0,60-	0,24+	0,37-			0,34+	
		0,61+	0,11+			0,05+	0,70-		0,13-	0,05-		0,05+			0,00+	0,69-
K AbT |	**0,11-**					**0,20-**	0,67-	**0,42-**	**0,16-**			**0,18-**			0,02-	**0,29-**
	0,08-					**0,05-**	0,74-	**0,45-**	**0,21-**			**0,24-**			0,01-	**0,35-**
K AbT ||	**0,12-**		**0,27+**	0,11-		**0,03-**	0,07+	**0,30-**	**0,11-**			**0,14-**			0,11-	**0,20-**
	0,13-		**0,26+**	0,08-			0,06+	**0,33-**	**0,15-**			**0,21-**			0,15-	**0,24-**
K AbT +|	**0,32-**		**0,41+**	0,29-		**0,11-**	0,03+	**0,13-**	**0,15-**			**0,11-**			0,18+	**0,17-**
	0,21-		**0,41+**	0,25-		**0,02-**	0,20+	**0,09-**	**0,09-**			**0,30-**			0,43+	**0,25-**
K AbT +||	**0,15-**		**0,58+**	0,05-			0,07+	**0,22-**	**0,07-**			**0,11-**			0,18+	**0,17-**
	0,21-		**0,57+**	0,07-			0,17+	**0,27-**	**0,13-**			**0,27-**			0,23+	**0,23-**
AbT 6,5			0,25+			0,27-		0,42-	0,05-	0,67-		0,46-				0,32-
	058+		0,35+			0,53+		0,06+	0,34+	0,15+		0,41+				0,20+
K 6,5 |	0,57-	0,50-				0,69-		**0,47-**	0,34-	0,30-		0,48-			0,26-	0,45-
	0,08-		0,23+					**0,34-**	0,11-	0,06-		|			0,02+	0,31-
K 6,5 ||	0,22-		0,16+			0,07-	0,10-	**0,38-**	0,11-						0,27-	0,29-
			0,16+					**0,38-**	0,08-			0,12-				0,30-
K 6,5 +|	0,66-	0,32-	0,49+			0,59-	0,73-	**0,48-**	0,34-			0,43-		0,28-	0,13+	0,43-
	0,12-		0,56+	0,45+				**0,32-**	0,10-			0,13-		0,04-	0,37+	0,27-
K 6,5 +||	0,19+	0,13+	0,18-											0,07+	0,56-	0,00+
	0,29+	0,25+													0,42-	0,03+
K Null	0,30-	0,04+						0,33-	0,35-	0,25-	0,97+	0,33-	0,26-		0,72+	0,32-
	0,27-	0,45+						0,29	0,22-		0,93+	0,19-	0,11-		0,59+	0,31-

Table XII-IV effect of enzymatic treatment on the levels of amino acids as determined by RP-HPLC-UVD after acid hydrolysis and OPA-derivatisation (continued)

Sample	Coefficients of determination (R^2) and orientation of trend (+: upwards, -: downwards) for a linear fit with data from the samples 0 h – 24 h[#]															
	Ala	Arg	Asp	Cys	Glu	Gly	His	Ile	Leu	Lys	Met	Phe	Ser	Thr	Tyr	Val
K T4 |	**0,23-**	**0,07+**		0,16+				**0,24-**	0,12-						**0,32-**	
	0,18-	**0,40+**		0,16+										0,18-		
K T4 ||	**0,12-**	**0,31+**														
	0,39-	**0,15+**													**0,36-**	
K T4 +|	**0,30-**	**0,52+**						**0,26-**	0,25-						**0,21-**	0,23-
	0,27-	**0,45+**						**0,18-**		0,16+					**0,15-**	0,14-
K T4 +||	**0,66-**	**0,04+**						**0,24-**	0,15-			0,17-			**0,18-**	0,19-
	0,72-	**0,15+**				0,34+		**0,21-**						0,57-	**0,12-**	
T4 4,5	0,13+		0,12-			0,27+	0,07+									
	0,17+	0,48+				0,89+	0,04+							0,03+		
K TvL |	**0,34-**					**0,47-**	0,67-	**0,40-**						**0,32-**	**0,52-**	
	0,04-		0,08-				0,20-	**0,25-**						**0,20-**	**0,52-**	
K TvL ||	**0,04-**		0,09-			**0,15-**		**0,16-**						**0,17-**	**0,65-**	
	0,06-		0,07-			**0,03-**		**0,20-**						**0,28-**	**0,62-**	
K TvL +|	**0,01-**		0,02-			**0,27-**										
	0,06-		0,01-			**0,04-**		**0,17-**						**0,19-**		
K TvL +||	**0,43-**					**0,50-**	0,43-	0,42-				0,36-			**0,60-**	
	0,04-		0,22-			**0,00-**	0,00-	0,22-						**0,20-**	**0,61-**	
TvL 4,5						0,03-										0,52-
														0,82-		|
K ThL |	**0,37-**					0,14-	**0,35-**	**0,38-**				0,20-		**0,85-**	**0,63-**	**0,23-**
	0,06-					0,36+	**0,24-**	**0,25-**						**0,81-**	**0,52-**	**|**
K ThL ||	**0,39-**			0,41+		0,11-	**0,69-**	**0,40-**	0,24-			0,29-		**0,66-**	**0,26-**	**0,32-**
	0,13-			0,46+			**0,56-**	**0,32-**	|			|		**0,55-**	**0,15-**	**0,25-**
K ThL +|	**0,38-**			0,45+		0,00-		**0,36-**	0,18-					**0,78-**	**0,10-**	**0,21-**
	0,16-			0,46+		0,42+		**0,23-**						**0,36-**	**0,10-**	
K ThL +||	**0,12-**	0,09-				0,01+	**0,21-**	**0,15-**	0,13-	0,19-		0,14-		**0,80-**	**0,03-**	**0,14-**
						0,70+	**0,18-**								**0,00-**	
ThL 4,5							0,74-	0,19-		0,06-		0,41-	0,71+			0,27-
						0,32+	0,56-		0,30+	0,03+		0,06+	0,58+			
K 4,5 |	0,22-	0,17-		0,22+		0,09-	0,14-	**0,27-**	0,21-	0,26-		0,35-		**0,65-**	0,34-	**0,30-**
				0,18+		0,20+		**0,21-**	0,13-	0,15-		0,25-		**0,32-**		**0,24-**
K 4,5 ||	0,44-	0,40-	**0,66-**	0,31-			0,17-	**0,50-**	0,49-			0,31-		**0,48-**	0,35-	**0,51-**
	0,44-		**0,76-**	0,09-			0,07-			0,07+		0,03+		**0,14-**	0,03-	
K 4,5 +|	0,55-		**0,45-**	0,06-		0,48+				0,01+					0,12+	
	0,49-	0,00+	**0,40-**	0,06-		0,51+				0,05+					0,13+	**0,24-**

..... upper line: R^2 for % of total concentration of all unmodified amino acids versus time, lower line: R^2 for % of total signal area (of all signals including modified amino acids) vs. time

Time series were filtered prior to the determination of the fit parameters to have at least four (of six) measurements points and the sign of the difference of the proportions at 24 and 0 h to be in accordance with the direction of the trend in the respective data.

XII.I.III. K with BoT1 and BoT2

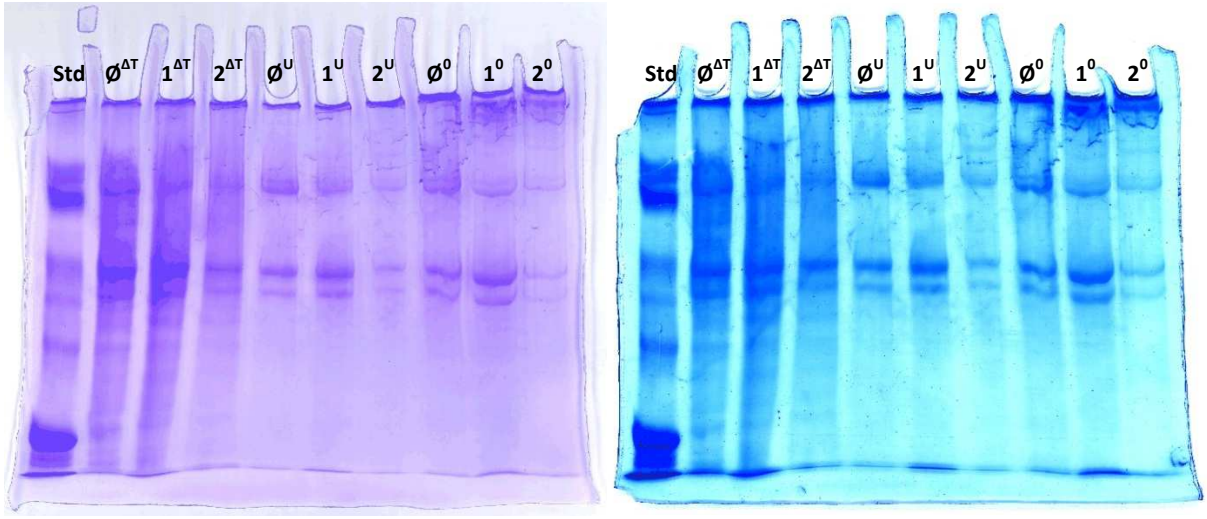

Figure XII-V SDS-PAGE, 6% acryl amide, stained with CBB R-250, 2 h destaining (left); restained with CBB G-250, no destaining (right)

The 1 mm vertical gel was run for 80 min @ 120 V whilst being constantly cooled with ice.
Std .....Standard (globular proteins, see 5.1.4)
Ø.....K Null 5d
1 .....K BoT1 5d
2 .....K BoT2 5d
Sample preparation after mixing with 2x loading buffer (see 5.1.3):
ΔT .....5 min @ 95 °C, 400 min^{-1}
U.....containing 4 M urea
0 .....5 min at room temperature

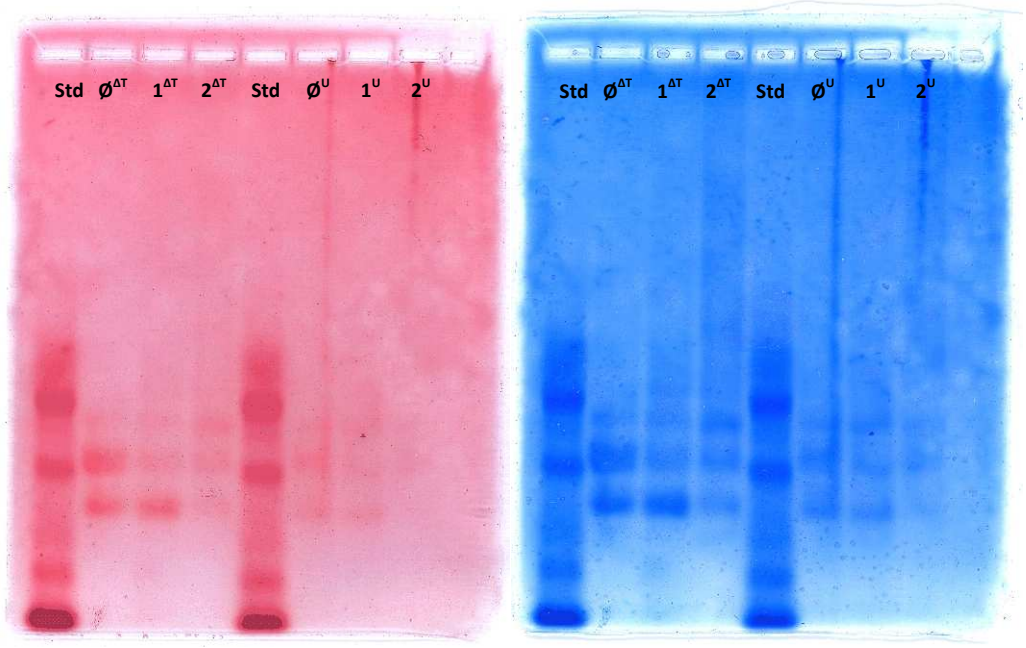

Figure XII-VI SDD-AGE: 1,8 % agarose, stained with Biebrich-Scarlet, no destaining (left); restained with CBB-G250, 2 d destaining (right)

The 10 mm horizontal gel was run for 15 min @ 30 V followed by 90 min @ 100V on the Savant H6370 system.
Lane assignments: see Figure XII-V
Sample preparation after mixing with loading buffer (see 5.2.3):
ΔT .....10 min @ 50 °C, 500 min^{-1}
U.....containing 4 M urea

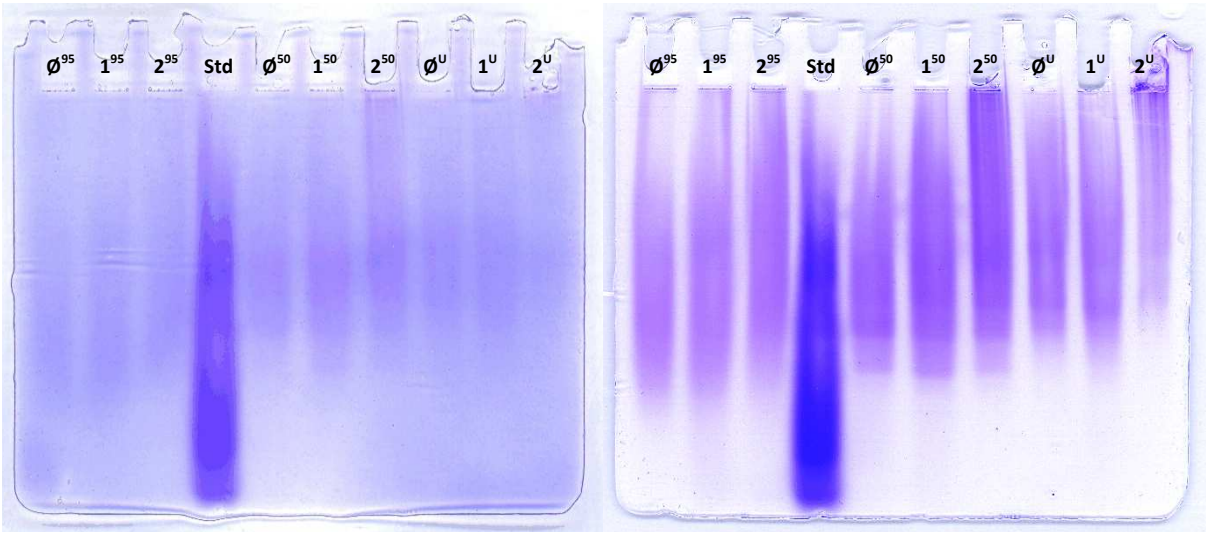

Figure XII-VII SDD-AGE: 2 % agarose, stained with CBB R-250, 1,5 h destaining (left); restaining with CBB-G250, 16 h destaining (right)

The 1 mm vertical gel was run for 18 min @ 50 V followed by 90 min @ 10 V and 45 min @ 50 V.
Lane assignments: see Figure XII-V
Sample preparation after mixing with loading buffer (see 5.2.3):
95 .....15 min @ 95 °C, 400 min^{-1}
50 .....15 min @ 50 °C, 400 min^{-1}
U.....containing 2 M urea

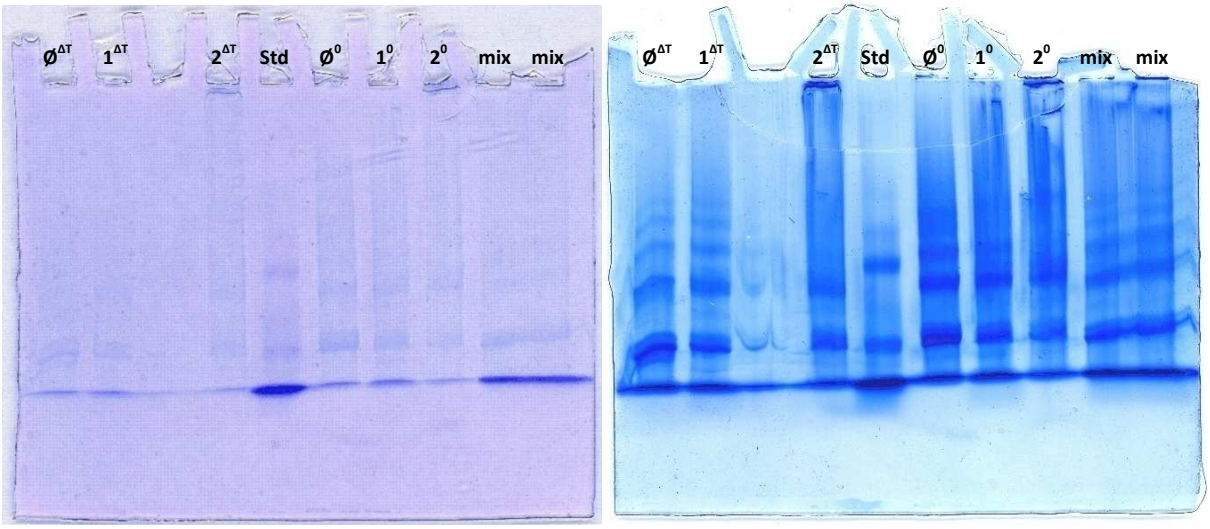

Figure XII-VIII SDS-PAGE: composite gel 2 % acryl amide & 1 % agarose, stained with CBB R-250, 16 h destaining (left); restaining with CBB-G250,no destaining (right)

The 1 mm vertical gel was run for 18 min @ 50 V followed by 90 min @ 10 V and 45 min @ 50 V.
Lane assignments: see Figure XII-V
Sample preparation after mixing with 2x loading buffer (see 5.2.3):
ΔT .....15 min @ 50 °C, 400 min^{-1}
0 .....15 min @ room temperature

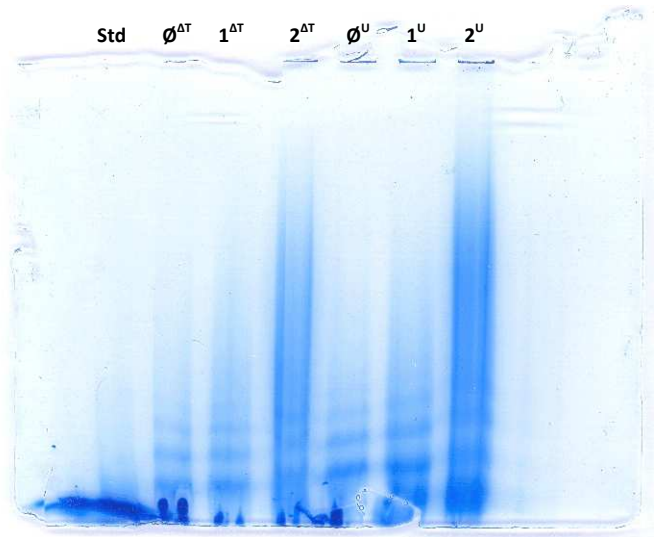

Figure XII-IX SDS-PAGE: composite gel 1 % acryl amide & 2 % agarose, stained with CBB G-250, 40 min destaining

The 1 mm vertical gel was run for 105 min @ 120 V.
Lane assignments: see Figure XII-V
Sample preparation after mixing with 2x loading buffer (see 5.2.3):
ΔT .....15 min @ 50 °C, 400 min^{-1}
U .....containing 8 M urea

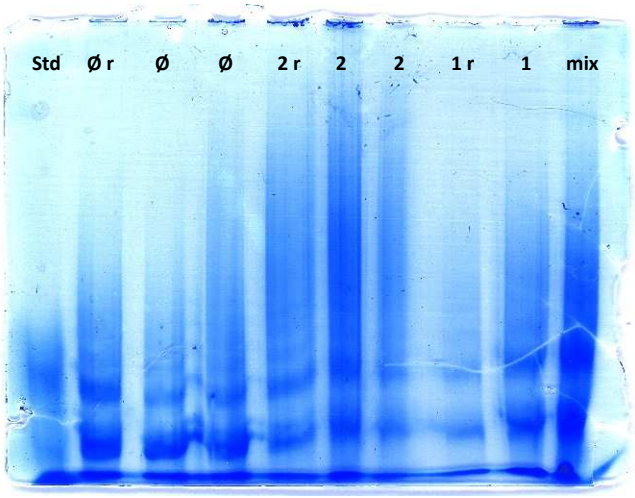

Figure XII-X SDS-PAGE: composite gel 1,5 % acryl amide & 1,5 % agarose, stained with CBB G-250, no destaining

The 1 mm vertical gel was run for 90 min @ 120 V.
Lane assignments: see Figure XII-V
r .....reduced with $NaBH_4$ (see 11)
All sample were pretreated for 15 min @ 50 °C, 400 min^{-1} after mixing with 2x loading buffer (see 5.2.3).

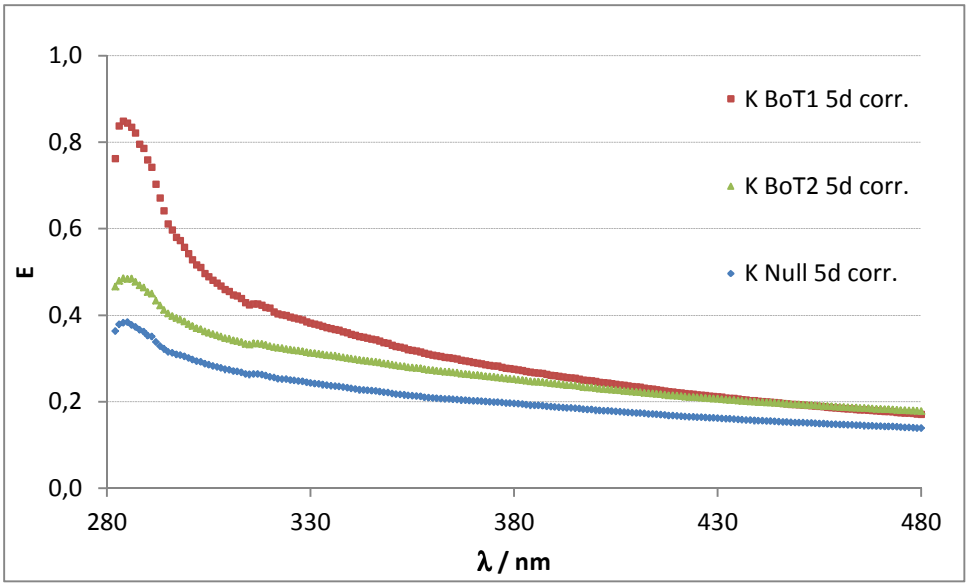

Figure XII-XI UV-VIS spectra of samples K 5d corrected for the absorbance of the microtitre plate

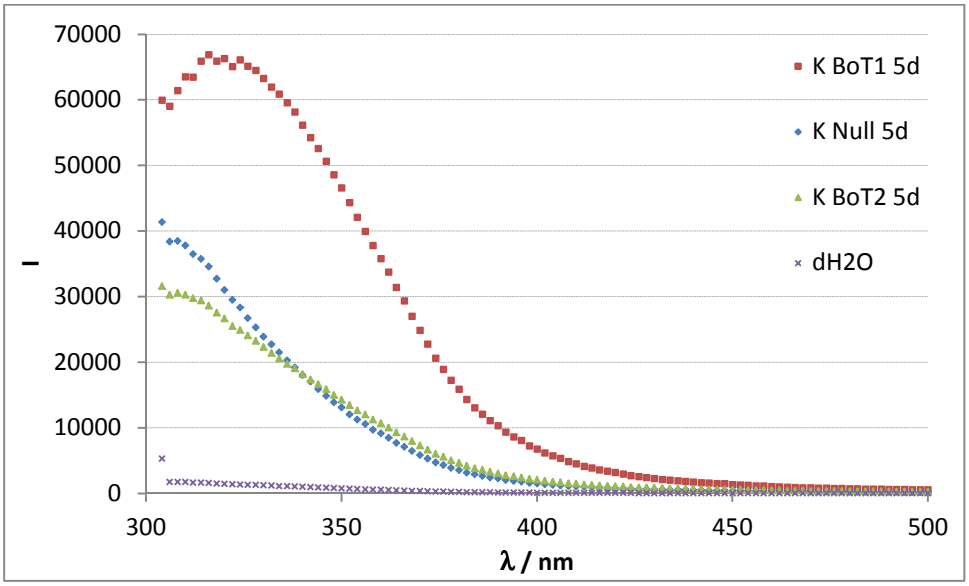

Figure XII-XII emission spectra of samples K 5d, λ_{ex} = 280 nm

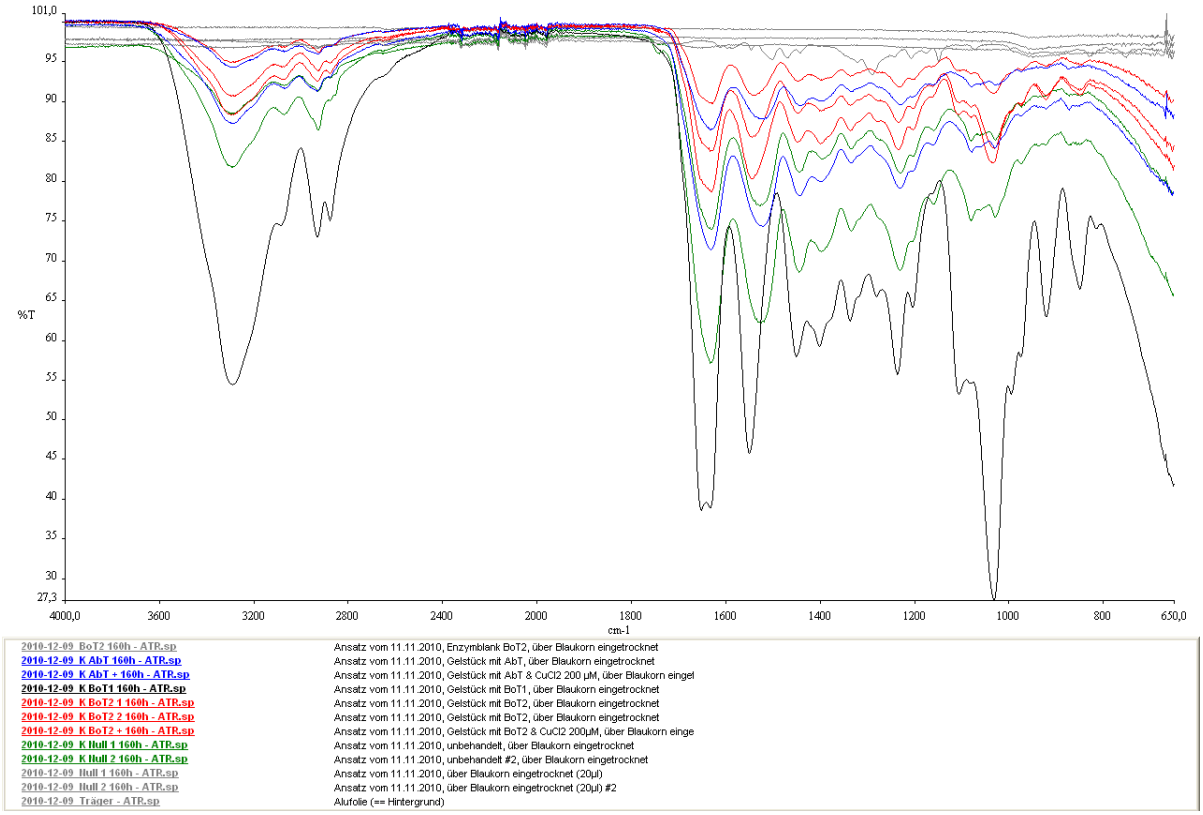

Figure XII-XIII FTIR-ATR spectra of samples K 160h

New signals at 815 cm^{-1} wsh (K BoT1), 995 cm^{-1} wsh (K BoT1, K BoT2, **BoT2**), 1105 cm^{-1} wsh (K BoT1, K BoT2), shift from 1525 cm^{-1} m (K Null, K AbT) to 1550 cm^{-1} m (K BoT1) and 1545 cm^{-1} m (K BoT2, **BoT2**) respectively, 1650 cm^{-1} wsh (K BoT1, K BoT2); K AbT and K Null resembles replicates.

w.....weak absorption
m .....medium absorption
s.....strong absorption
sh.....shoulder (after intensity indicator)
br.....broad (after intensity indicator)

XII.I.IV. K with BoT1, BoT2 and AbT

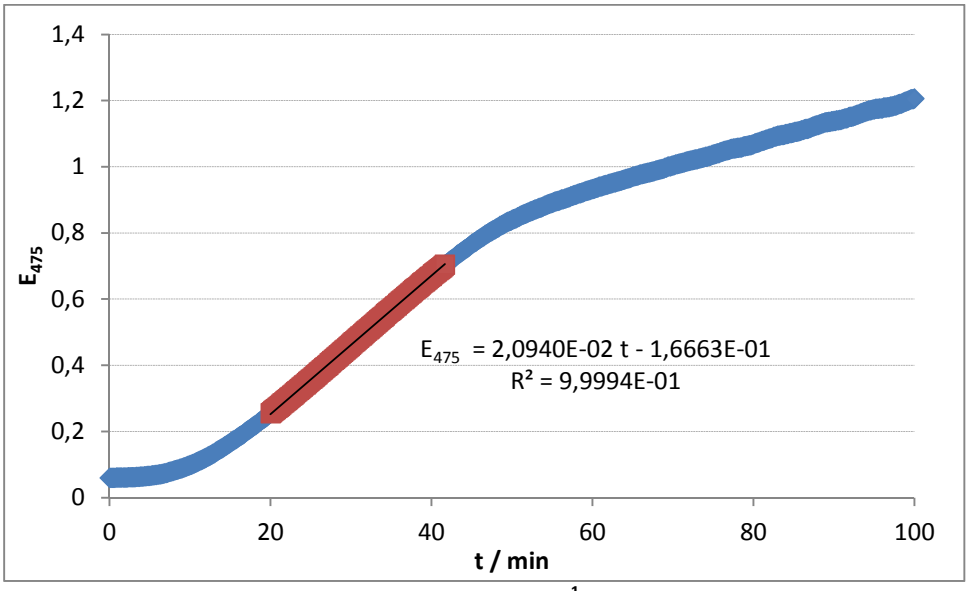

Figure XII-XIV tyrosinase activity assay for AbT 1 g l^{-1} in NH_4Ac pH 6,5: significant lag time

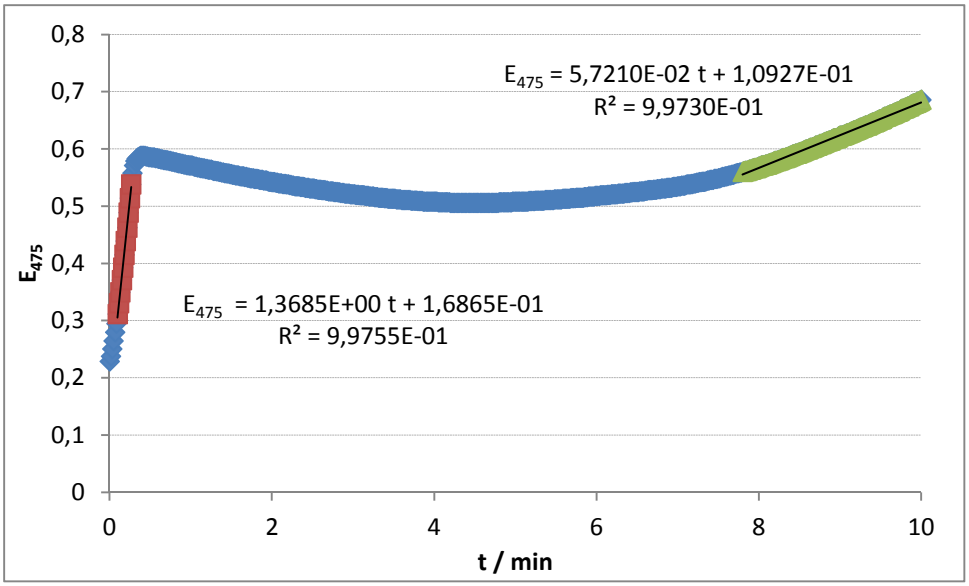

Figure XII-XV tyrosinase activity assay for BoT2 with 260 µm $CuCl_2$ added to the enzyme solution prior to mixing with the substrate solution

Without $CuCl_2$, it takes 400 s to reach the same level of absorption as this solution does after 10 s.

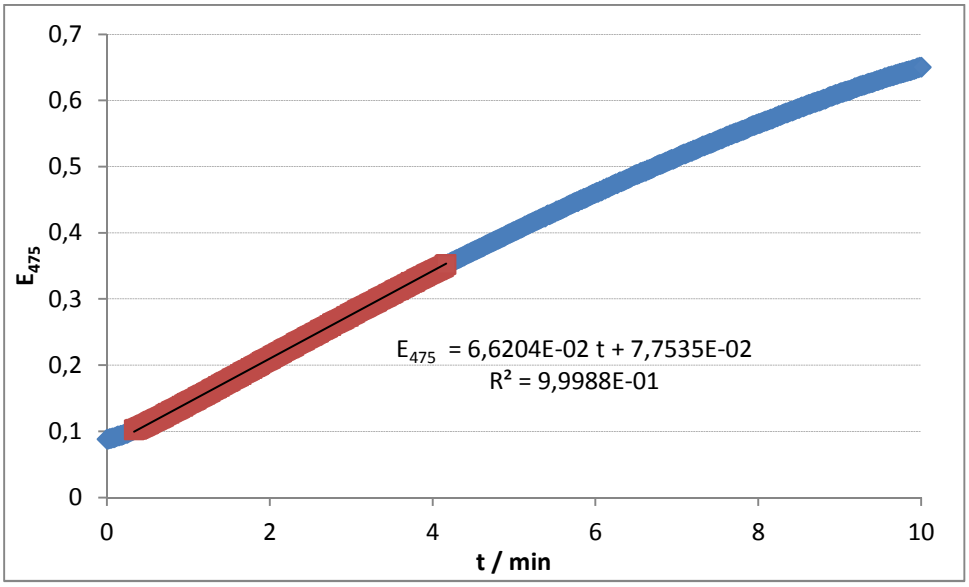

Figure XII-XVI tyrosinase activity assay for BoT2 in NH_4AH pH 6,5 without addition of $CuCl_2$

Table XII-V samples K 18h: percentages of the amino acids as measured by RP-HPLC UVD (excluding Pro)

Sample	Proportion of the amino acid on all unmodified primary amino acids / %																		
	Ala	Arg	Asn	Asp	Cys	Gln	Glu	Gly	His	Ile	Leu	Lys	Met	Phe	Ser	Thr	Trp	Tyr	Val
K Null | 18h	13,23	5,10		9,42			3,14	46,36	1,32	2,64	3,67	3,12	1,61	2,24	3,34	2,39		0,42	2,00
K Null | r 18h	12,66	3,02		9,91			4,55	50,36	1,91	2,19	4,28	1,13	0,16	1,72	3,16	1,96		0,55	2,45
K Null || 18h	13,27	5,60		9,56			2,67	47,06	1,53	2,20	3,38	3,24	1,62	1,76	3,22	2,23		0,43	2,21
K Null || r 18h	12,44	3,72		9,61			3,78	50,92	2,34	2,00	3,75	1,37	0,38	1,75	3,22	2,00		0,49	2,23
K BoT1 18h	12,84	5,03		**4,61**			**0,88**	**55,72**	**0,72**	2,21	3,43	2,69	1,61	1,68	**3,40**	1,98		**0,81**	2,40
K BoT1 r 18h	12,44	5,42		**4,07**			**1,35**	**57,36**	**0,66**	1,95	3,39	2,43	0,69	1,66	**3,35**	1,94		**0,79**	2,49
K BoT2 | 18h	12,68	5,24		9,11			0,55	49,27	**0,90**	2,32	3,70	3,24	1,37	2,81	3,22	2,26		0,84	2,50
K BoT2 | r 18h	12,31	2,97		9,44			4,95	51,33	**1,53**	1,82	3,69	1,38	0,25	2,39	3,07	2,29		0,35	2,20
K BoT2 || 18h	12,91	5,11		9,14			2,39	47,40	**0,79**	2,22	3,54	3,63	1,63	2,83	3,32	2,39		0,53	2,18
K BoT2 || r 18h	12,76	4,33		7,70			3,28	52,78	**1,41**	2,36	3,63	1,73	0,41	1,65	3,19	2,18		0,31	2,27
K BoT2 + 18h	12,53	4,65		9,16			3,51	47,46	**0,87**	2,49	3,93	3,67	0,87	2,73	3,42	2,28		0,22	2,22
K BoT2 + r 18h	12,99	5,31		5,90			0,69	56,05	**0,89**	1,84	3,53	2,13	0,56	1,64	3,32	2,25		0,45	2,45
BoT2 18h	2,28			13,55			38,13	18,53							11,48	8,96		1,75	5,34
BoT2 r 18h				8,49			22,11	45,77							11,20	7,09			5,33
K AbT 18h	**14,20**	6,02		4,54			**0,33**	54,02	**0,65**	2,31	3,31	3,54	1,35	1,59	3,44	1,90		**0,39**	**2,42**
K AbT r 18h	**14,24**	5,98		3,50			**0,60**	59,29	**0,32**	2,41	3,64	2,45	0,55	1,52	0,11	2,47		**0,34**	**2,58**
K AbT + 18h	**13,46**	5,28		9,74			**2,98**	45,42	**0,78**	3,33	3,66	3,75	1,08	2,46	3,13	2,33		**0,17**	**2,42**
K AbT + r 18h	**12,92**	4,47		9,85			**1,39**	53,57	**1,02**	2,15	3,65	1,49	0,25	1,63	2,89	1,98		**0,30**	**2,44**
Replicates	**Relative standard deviation of replicates / %**																		
K Null	**3,2**	**27**		**2,2**			**23**	**4,7**	**25**	**12**	**9,9**	**51**	**83**	**13**	**2,4**	**9,5**		**12**	**8,3**
K Null |&||	0,23	6,6		1,1			11	1,1	11	13	5,7	2,7	0,64	17	2,6	4,8		1,8	7,0
K Null |&|| r	1,3	15		2,2			13	0,79	14	6,2	9,2	14	58	1,2	1,3	1,6		8,8	6,8
K BoT1	2,2	5,3		8,8			30	2,1	6,1	9,0	0,85	7,1	56	0,67	1,0	1,2		1,8	2,5
K BoT2	**2,0**	**19**		**16**			**67**	**6,6**	**30**	**13**	**4,0**	**38**	**65**	**24**	**3,8**	**2,9**		**49**	**6,0**
K BoT2 |&||&+	1,5	6,2		0,31			70	2,2	6,4	5,8	5,3	6,8	30	2,0	3,1	3,0		59	7,5
K BoT2 |&||&+ r	2,7	28		23			72	4,5	27	15	2,3	21	38	23	3,9	2,3		19	5,7
K AbT	**4,6**	**13**		**49**			**90**	**11**	**42**	**21**	**4,8**	**37**	**62**	**25**	**64**	**13**		**32**	**3,1**
K AbT |&+	3,8	9,2		52			110	12	13	25	7,2	4,1	15	30	6,8	14		56	0,12
K AbT |&+ r	6,9	20		67			56	7,2	73	7,8	0,044	34	52	4,7	130	15		9,3	4,0

Bold proportions mark **significantly different averages** of the respective preparations with the same enzyme compared to K Null (F- and T-tests, **α = 0,05**).

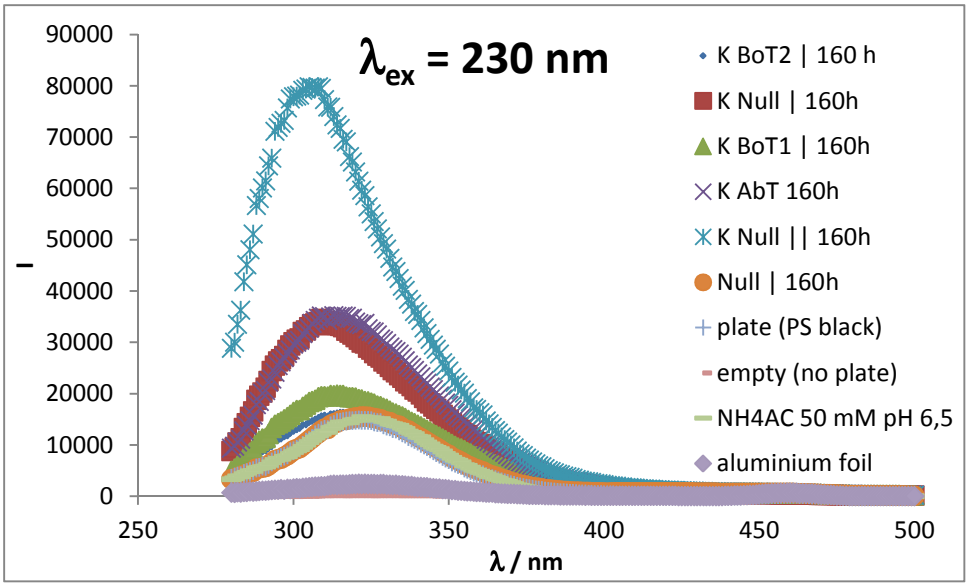

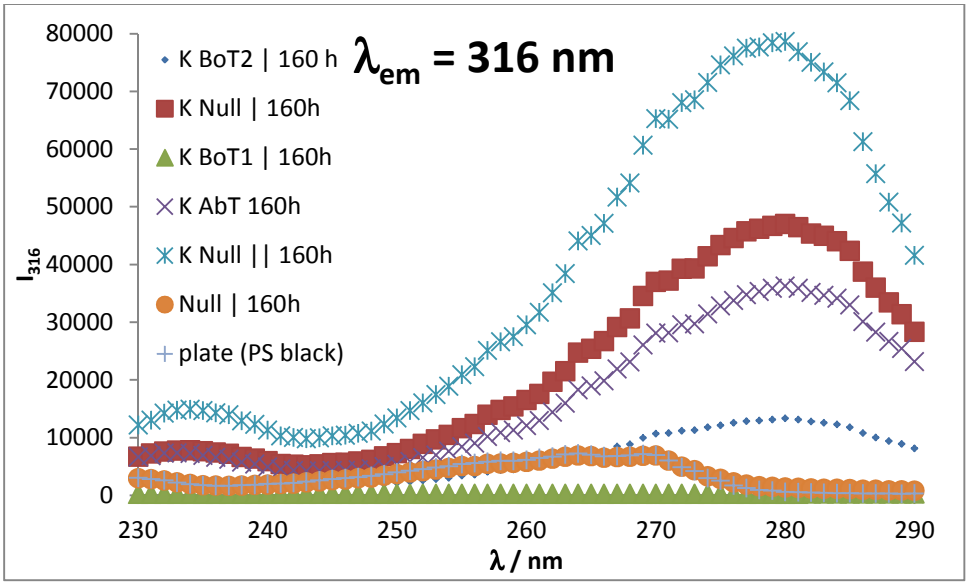

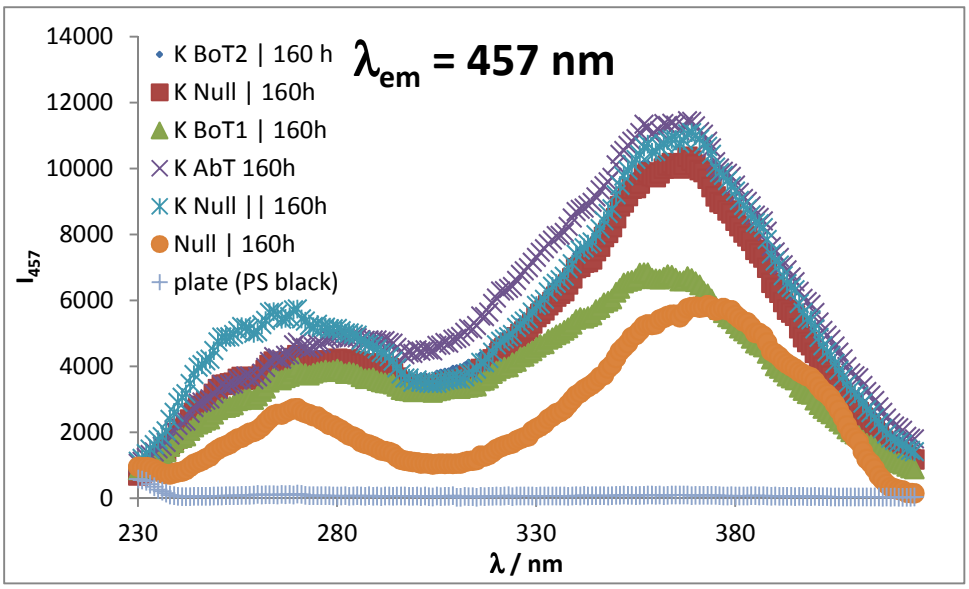

Figure XII-XVII Fluorescence spectra of samples K 160h: no specific changes recognizable

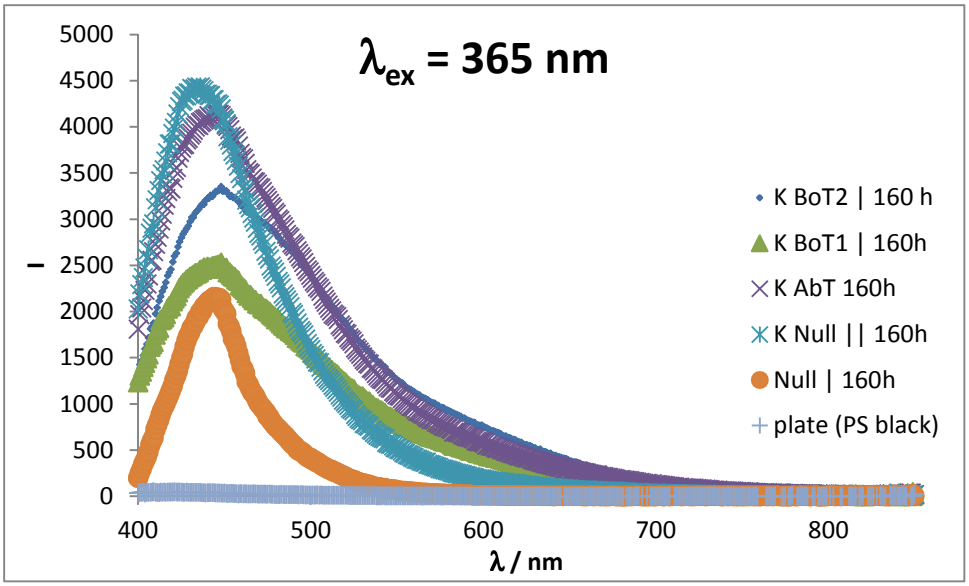

Figure XII-XVII Fluorescence spectra of samples K 160h: no specific changes recognizable (continued)

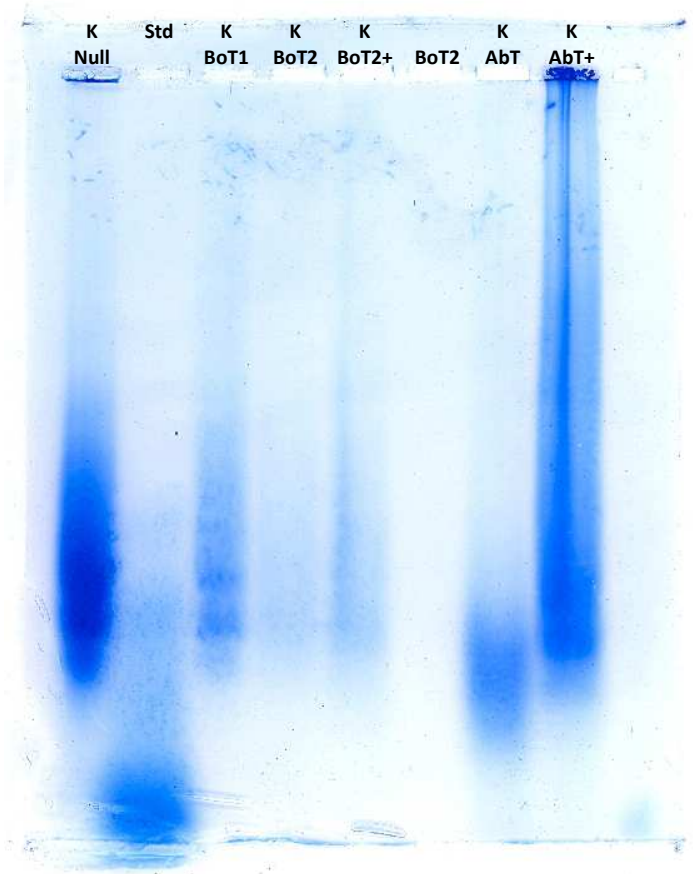

Figure XII-XVIII SDD-AGE, 1,6% agarose, compressed to 10 % thickness, stained with CBB G-250, no destaining
The 10 mm horizontal gel was run for 15 min @ 30 V followed by 90 min @ 90 V on the Savant H6370 system.
Std .....Standard (globular proteins, see 5.1.4)
Samples 7d were prepared in 2x loading buffer (see 5.2.3) with 10 % (v/v) acetic acid and 10 % SDS (which was intended to dissolve the collagen – what it did not do for the samples with K and BoT1 or BoT2) and conditioned at 50 °C for 15 min followed by 15 min in the ultrasonic bath.

XII.II. Insulin β-chain with BoT2 and AbT

XII.II.I. I-b old with BoT2 and AbT in NH4Ac

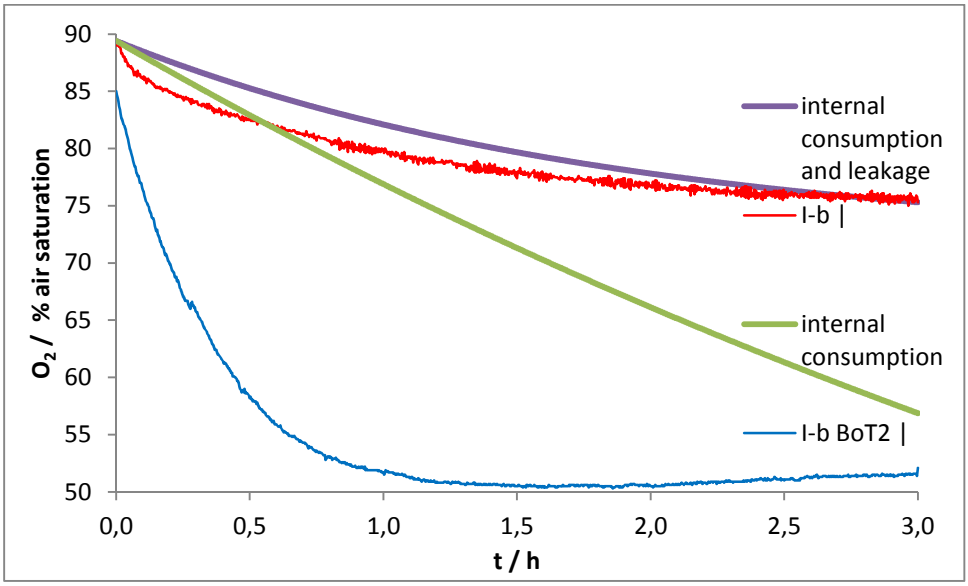

Figure XII-XIX Insulin β-chain old with 5 mU BoT2 and reference in 500 ml, measured with Clark-electrodes

Internal consumption of the oxygen electrode (according to manufacturer specifications):

Cathode (Pt): $O_2 + 2\ H_2O + 4\ e^-$ → $4\ OH^-$
Anode (Ag): $4\ Ag + 4\ Cl^-$ → $4\ AgCl \downarrow + 4\ e^-$

Sum: $4\ Ag + O_2 + 2\ H_2O + 4\ Cl^-$ → $4\ AgCl \downarrow + 4\ OH^-$

Current for polarising voltages at the platinum electrode < -0,6 V:

$$i_d = 4 \cdot F \cdot \frac{P_m}{d} \cdot A \cdot p_{O_2}$$

F ..... Faraday constant (electric charge of 1 mol e^-); F = 96 485,34 C mol^{-1}
P_m ..... permeability (Henry's law constant^{-1} · diffusion coefficient) of the used Teflon membrane for O_2; typically 1,05 · 10^{-13} mol atm^{-1} s^{-1} mm^{-1}
d ..... thickness of the Teflon membrane; typically 12,5 µm
A ..... surface of the platinum working electrode in contact with electrolyte; typically 3,1 mm^2

$$\%D = 12{,}5 \cdot \frac{i_d}{p_{O_2} \cdot V_{Test}}$$

%D ..... percentage of the total amount of oxygen lost per minute, in % min^{-1}
12,5 ..... construction specific proportionality constant, in % min^{-1} A^{-1} atm dm^3
i_d ..... current at the working electrode, in A
pO_2 ..... partial pressure of O_2, in atm = 1013,25 mbar = 101325 Pa
V_{Test} ..... volume of the tested solution, in dm^3 = l

$$\%D = 12{,}5 \cdot \frac{4 \cdot F \cdot \frac{P_m}{d} \cdot A \cdot p_{O_2}}{p_{O_2} \cdot V_{Test}} = 50 \cdot \frac{F \cdot P_m \cdot A}{d \cdot V_{Test}} = \frac{1{,}26 \cdot 10^{-4}\ \frac{\% \cdot dm^3}{min}}{V_{Test}}$$

gastight: $c(t) = c_0 \cdot e^{-\%D \cdot t}$

leakage: $c(t) = e^{-(\%D + f_{leak}) \cdot t} \cdot \left[\frac{\%D \cdot pO_{2,external}}{\%D + f_{leak}} \cdot e^{(\%D + f_{leak}) \cdot t} + c_0 - \frac{f_{leak} \cdot pO_{2,external}}{\%D + f_{leak}}\right]$

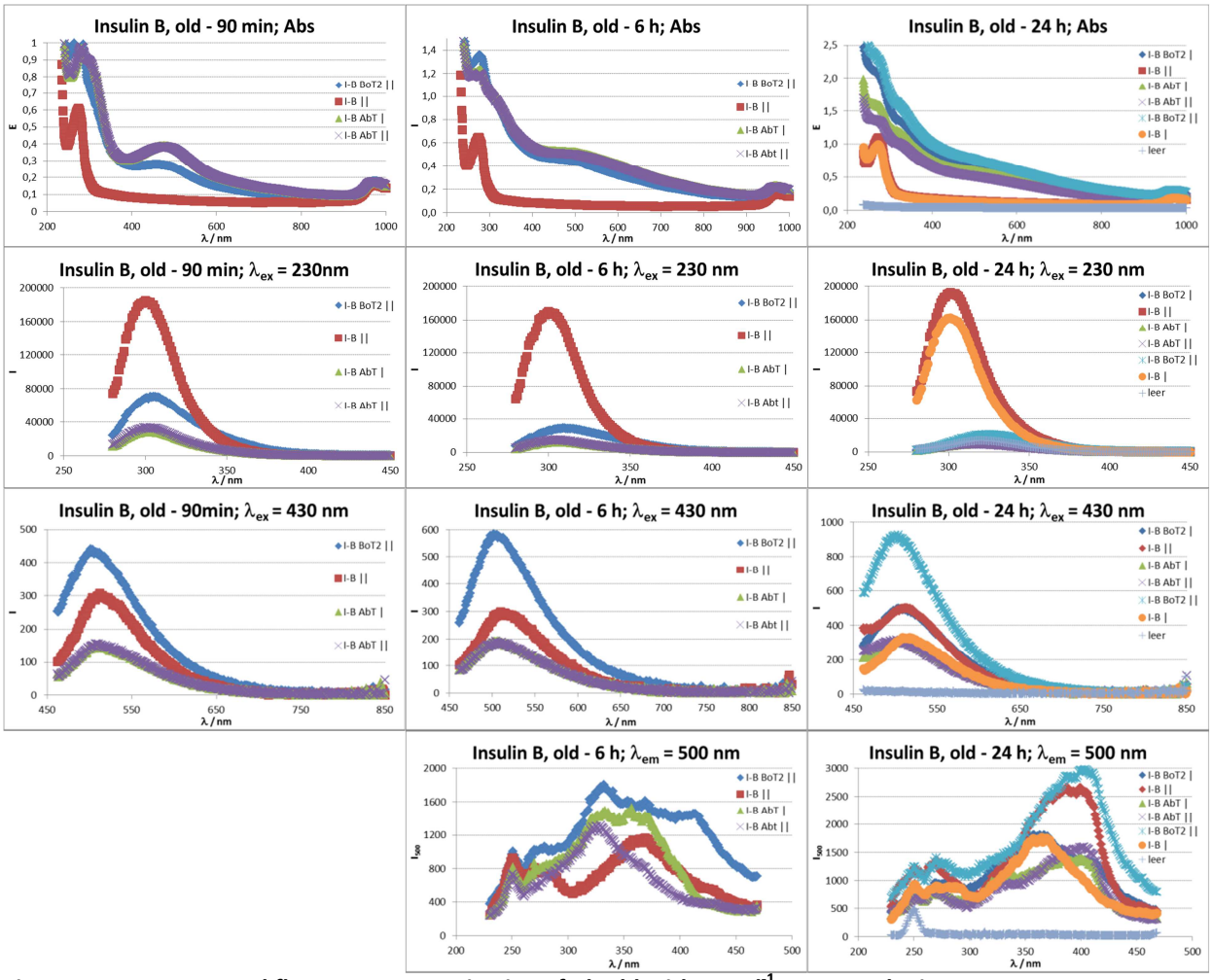

Figure XII-XX UV-VIS and fluorescence monitoring of I-b old with 10 U l^{-1} BoT2 or AbT in NH_4Ac

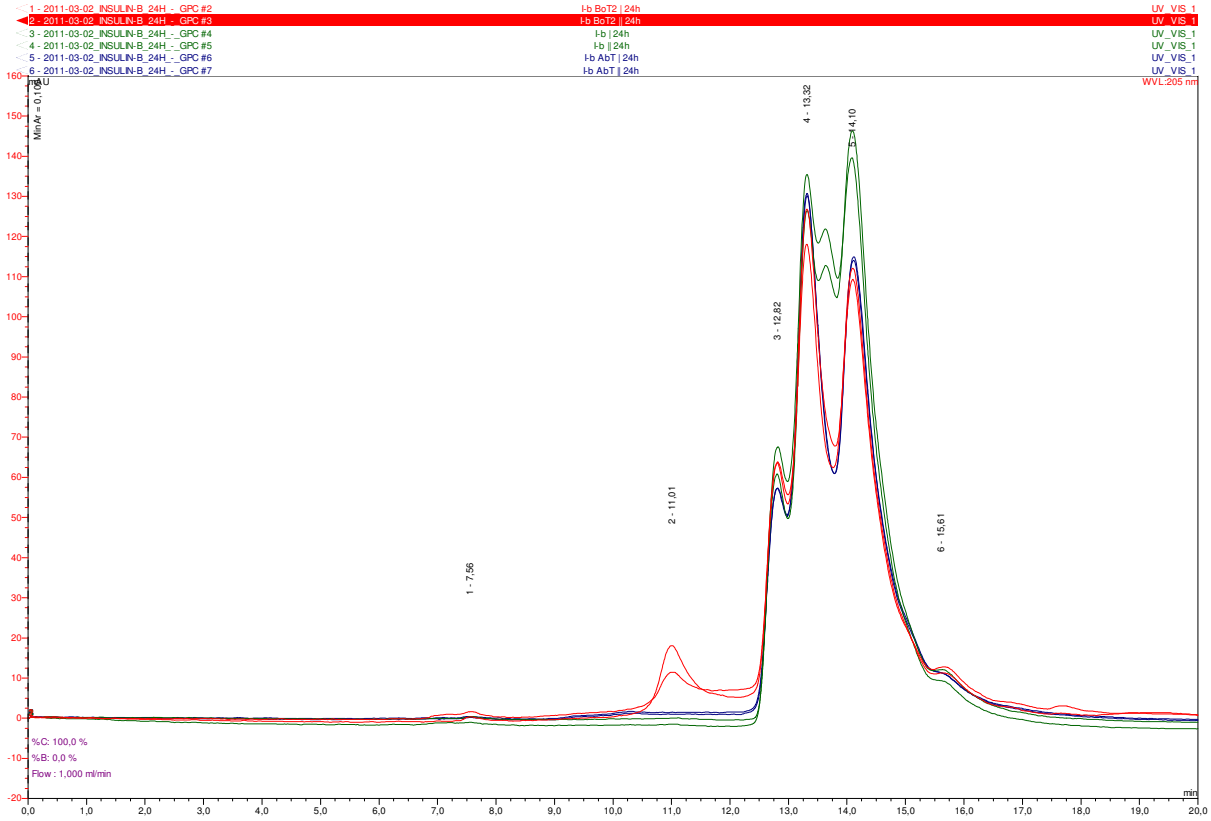

Figure XII-XXI GPC of samples I-b old 24h: increased apparent molecular weight with BoT2, UVD @ 205 nm
Column: Zorbax GF-250 4 µm 9,4 x 250 mm, Agilent
Mobile phase: sodium phosphate buffer 200 mM pH 6,8 (100 mM Na_2HPO_4, 100 mM NaH_2PO_4)

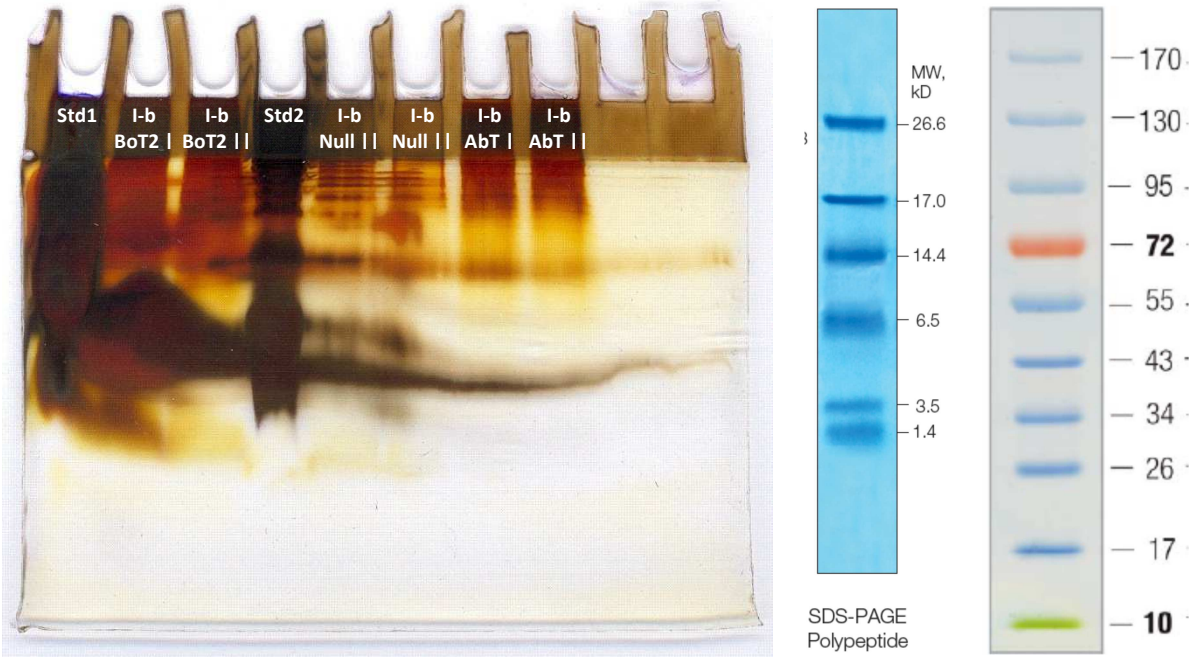

Figure XII-XXII SDS-PAGE, 18 % acryl amide, silver staining (overstained)
The 1 mm vertical gel was run for 150 min @ 100 V whilst being cooled with crushed ice.
Std1 .....BioRad Polypeptide SDS-PAGE Standard (middle)
Std2 .....Fermentas PageRuler™ (right)
Staining with CBB G-250 wasn't successful, supposedly because of diffusion limitations of the CBB pigments into the small pores of the 18 % acryl amide gel.

XII.II.II. I-b old with BoT2 and AbT in sodium phosphate buffer

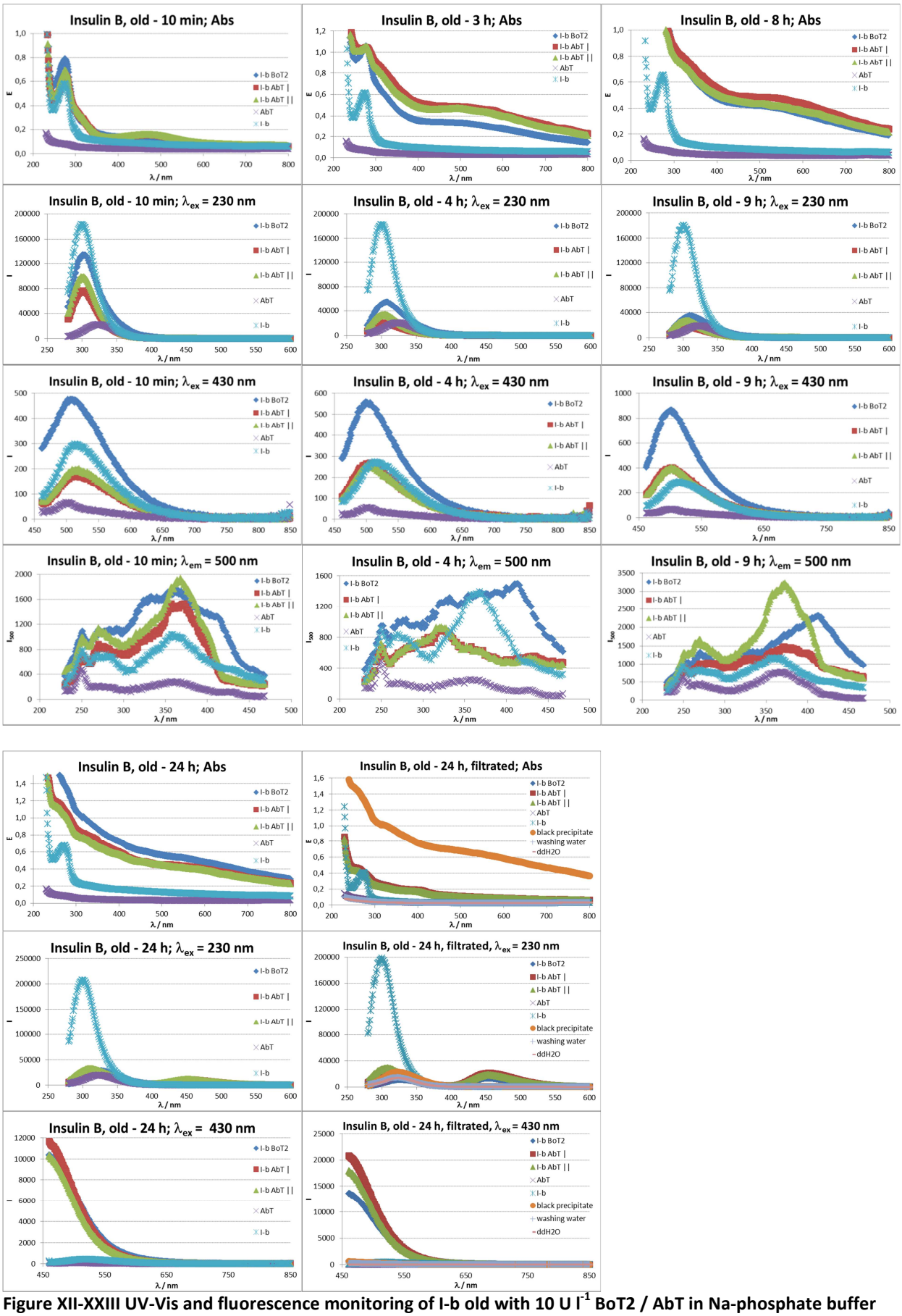

Figure XII-XXIII UV-Vis and fluorescence monitoring of I-b old with 10 U l^{-1} BoT2 / AbT in Na-phosphate buffer

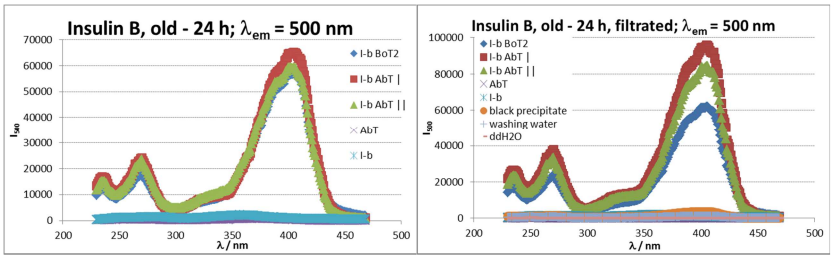

Figure XII-XXIII UV-Vis and fluorescence monitoring of I-b old with 10 U I-1 BoT2 / AbT in Na-phosphate buffer (continued)

The samples "filtrated" are the filtrate of the respective sample filtered through a 0,2 µm PET membrane. The black precipitate that had been separated that way was washed with 4 x 400 µl ddH_2O (=> washing water) and suspended in 200 µl ddH_2O (=> black precipitate, see also the black curve "SNS_gewaschen" in Figure XII-XXIV) for the UV-Vis and fluorescence measurements.

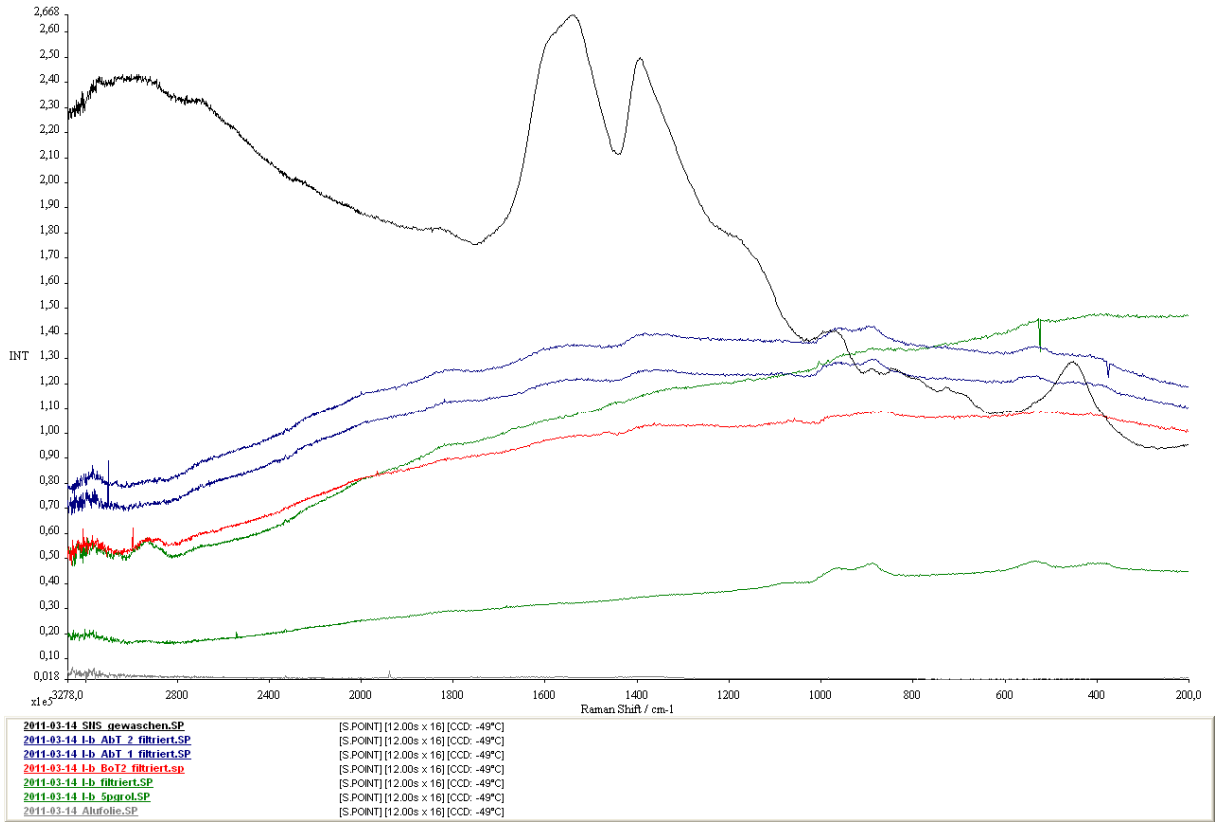

Figure XII-XXIV Raman spectra of samples I-b old 24h filtrated (25 µl dried on aluminium foil)

No specific signals were found in the spectra of insuline which might be attributed to the detrimental effect of the fluorescence exhibited by these substrates on the detection of scattered light.

According to [206] the Raman spectrum of melanin is marked by two intense and broad peaks at about 1580 and 1380 cm^{-1}, which may be attributed to the in-plane stretching of the aromatic rings and the linear stretching of the C-C bonds within the rings, along with some contributions from the C-H vibrations in the methyl and methylene groups.

This supports the assumption of the melaninous nature of the black precipate generated from melanin ("SNS_gewaschen", black curve, cp. also the UV-Vis spectrum given in Figure 10-1) which's Raman spectrum has peaks at 455 cm^{-1} m, 970 cm^{-1} w, 1390 cm^{-1} s and 1540 cm^{-1} sbr.

For peak annotations see Figure XII-XIII.

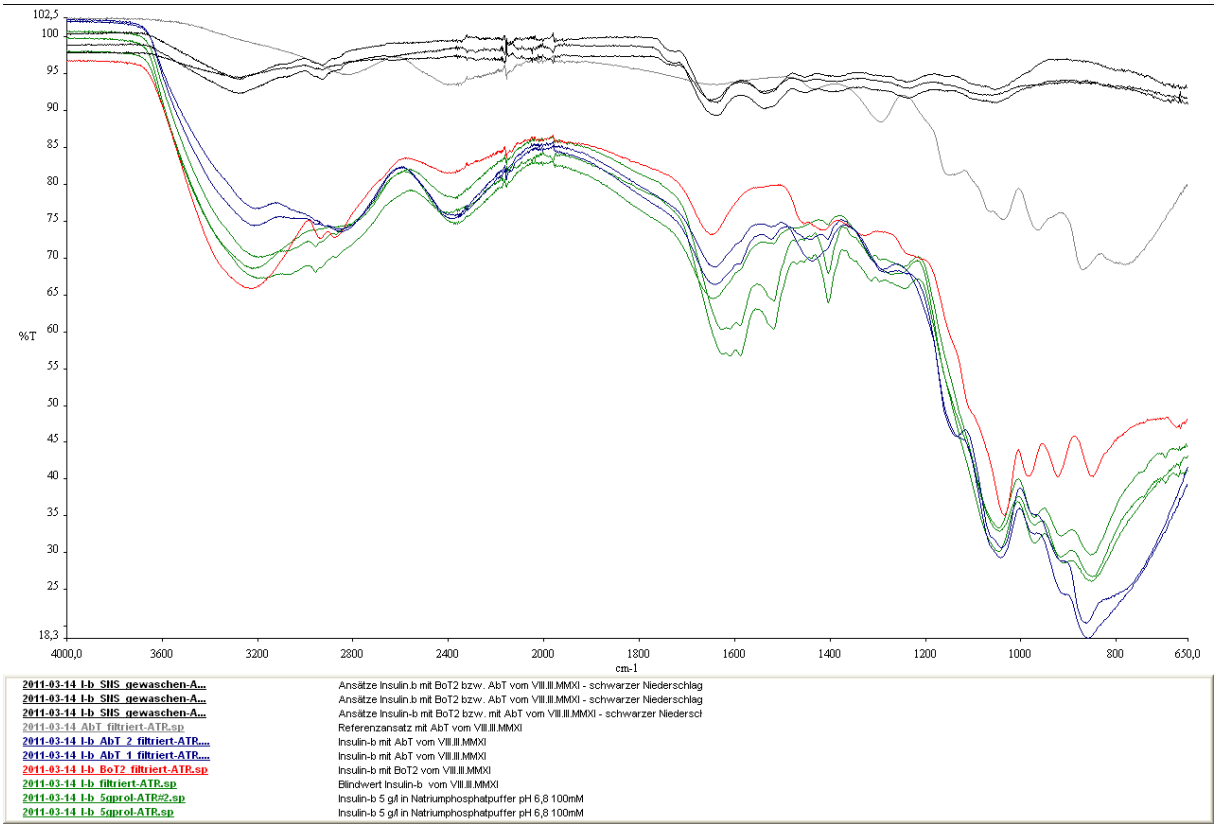

Figure XII-XXV FTIR-ATR spectra of samples I-b old 24h filtrated (25 µl dried on aluminium foil)

No specific new signals are found in the spectra of enzyme treated insuline. A lesser absorbance at 1530 cm^{-1} m and 1410 cm^{-1} m due to incubation alone (no need for enzymes) is recognized.

XII.II.III. I-b new with BoT2 and AbT in NH4Ac

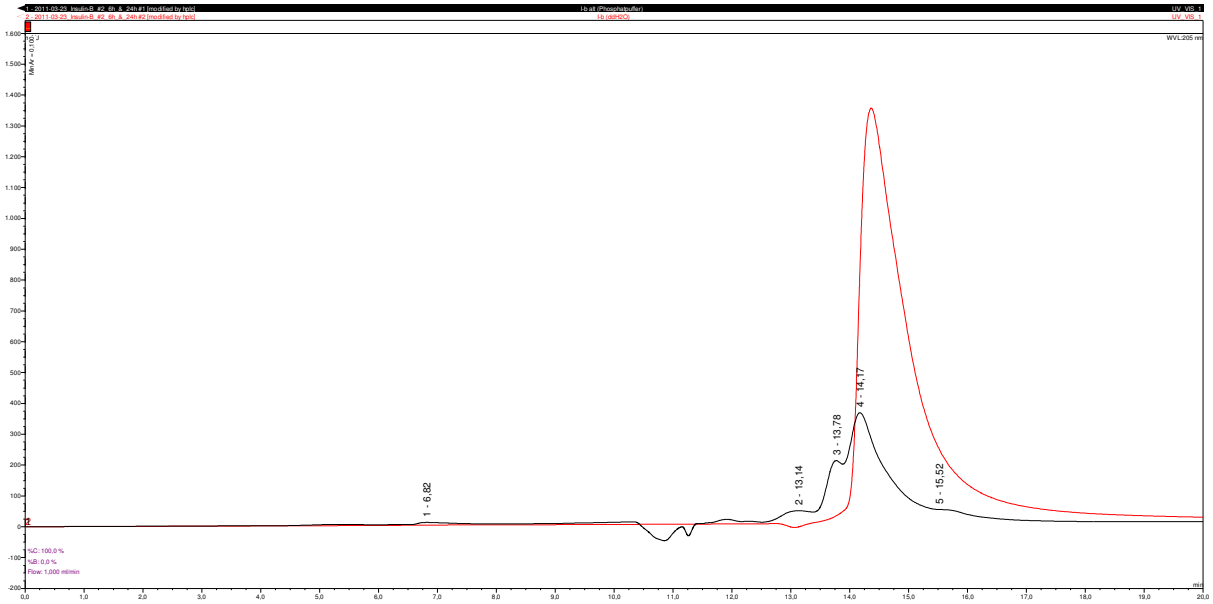

Figure XII-XXVI GPC of I-b old and I-b new 5 g l^{-1} each, UVD @ 205 nm

Column: Zorbax GF-250 4 µm 9,4 x 250 mm, Agilent

Mobile phase: sodium phosphate buffer 200 mM pH 6,8 (100 mM Na_2HPO_4, 100 mM NaH_2PO_4)

I-b old is not a pure protein as at least five fractions of different hydrodynamical volume are visible in the UVD at 205 nm. The fraction responsible for the pink colour and the formation of black precipitate upon treatment with tyrosinase (cp. 12.2.1) is #3 at approximately 13,8 min.

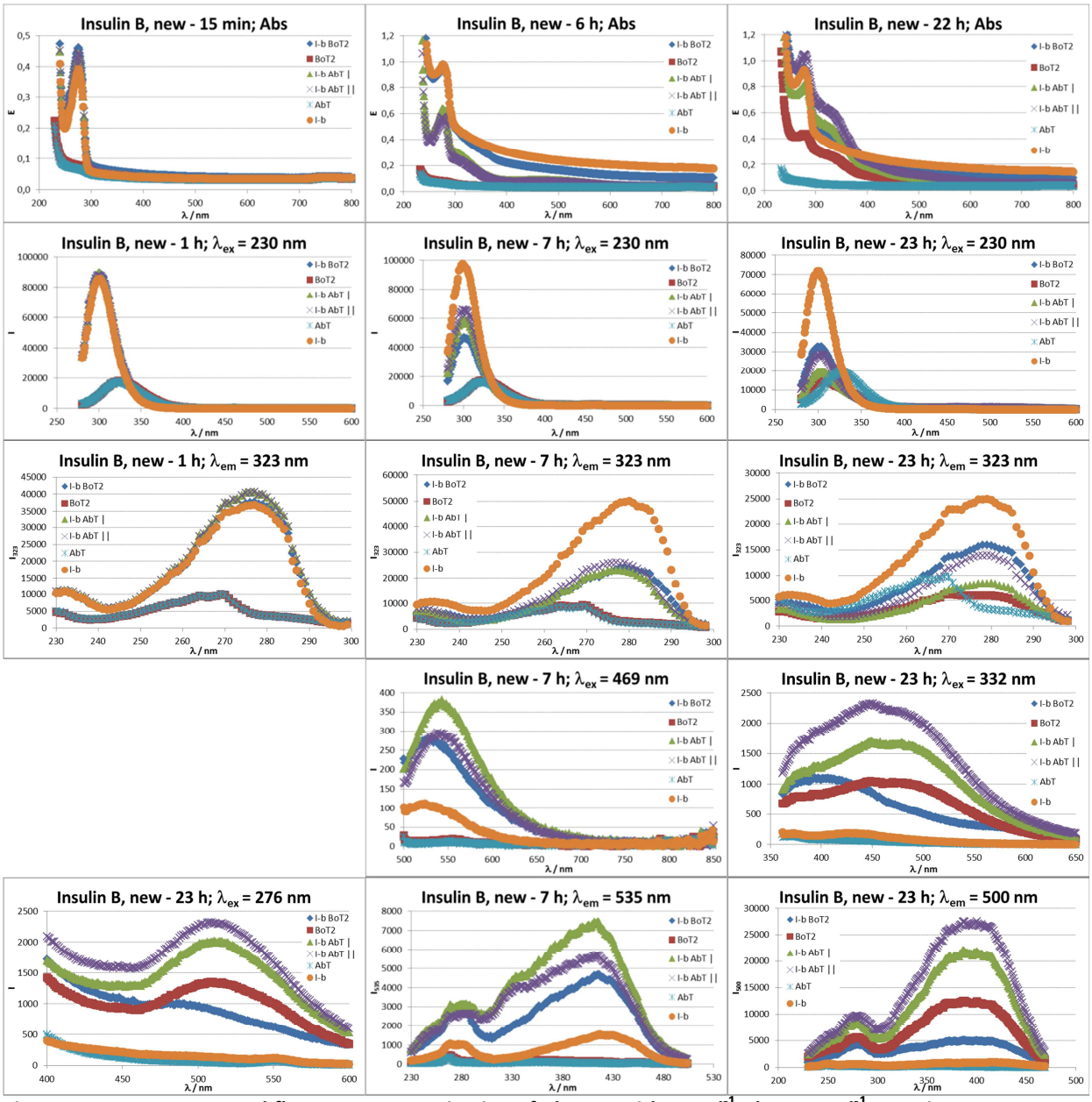

Figure XII-XXVII UV-VIS and fluorescence monitoring of I-b new with 10 U l^{-1} AbT or 2 U l^{-1} BoT2 in NH_4Ac
Starting from 22 h the preparation BoT2 contains I-b AbT | (pipetting error).

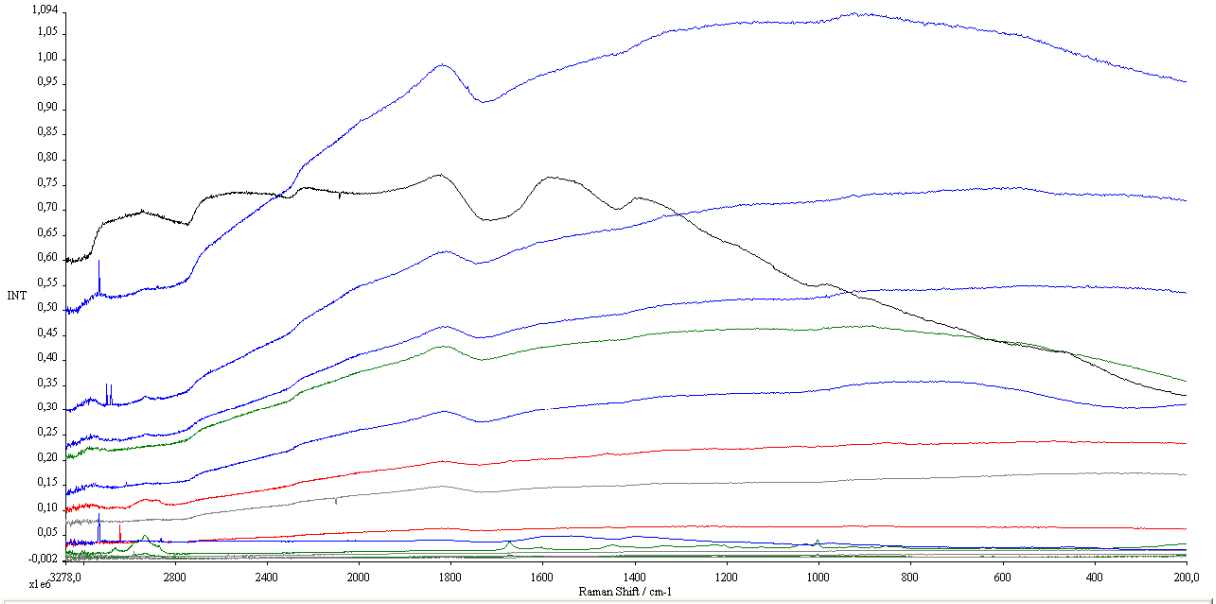

Figure XII-XXVIII Raman spectra of samples I-b new 6h & 24h in NH_4Ac (2 x 25 µl dried on aluminium foil)
no specific signals (substrates are fluorescent)

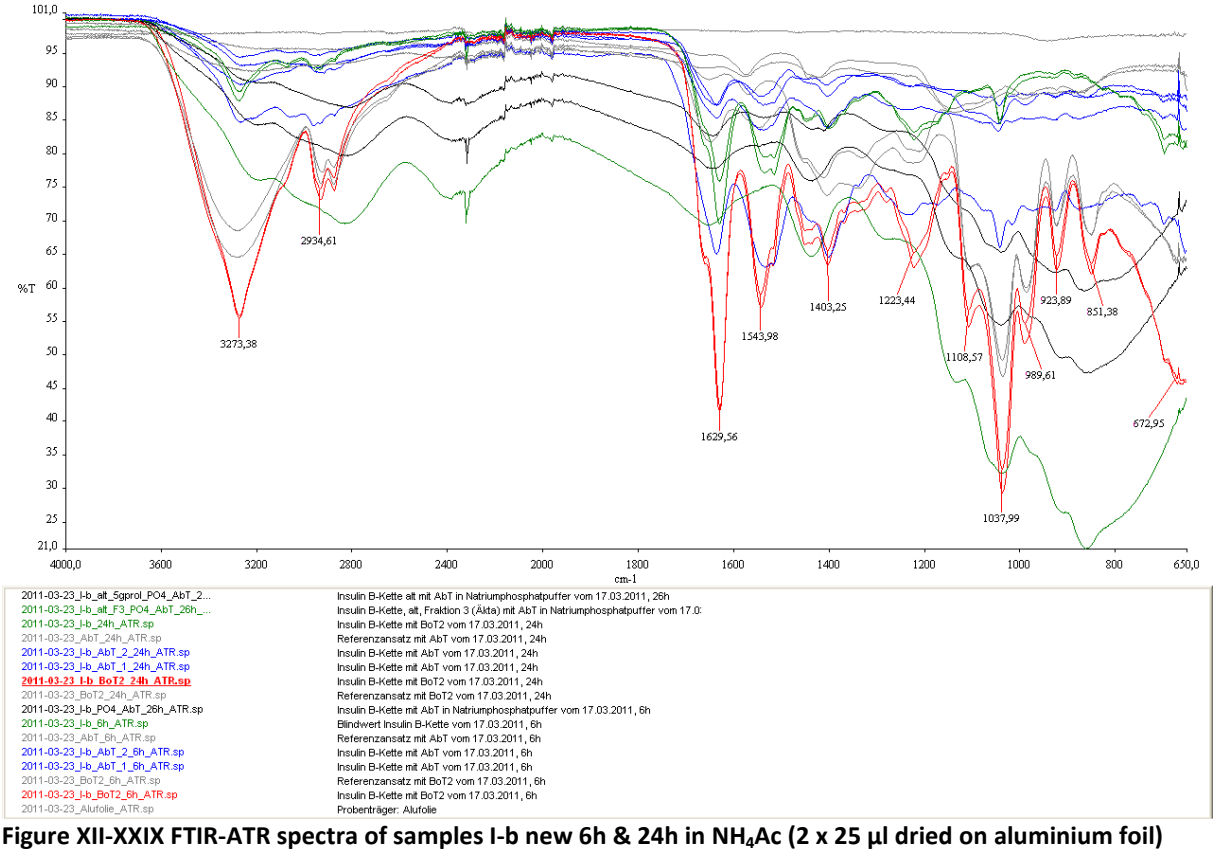

Figure XII-XXIX FTIR-ATR spectra of samples I-b new 6h & 24h in NH_4Ac (2 x 25 µl dried on aluminium foil)
No signals specific for enzymatically treated insulin β-chain were detected (all frequencies are also present in I-b Null or AbT or BoT2 in comparable intensities).

XII.II.IV. I-b new with BoT2 and AbT in sodium phosphate buffer

Table XII-VI solubility of sodium phosphates

Species	Molecular weight / Da	Solubility in water @ 20 °C	
		g l^{-1}	M
NaH_2PO_4	119,98	850	7,08
Na_2HPO_4	141,96	77	0,542
Na_3PO_4	163,49	121	0,740

Data taken from the IFA GESTIS-Stoffdatenbank

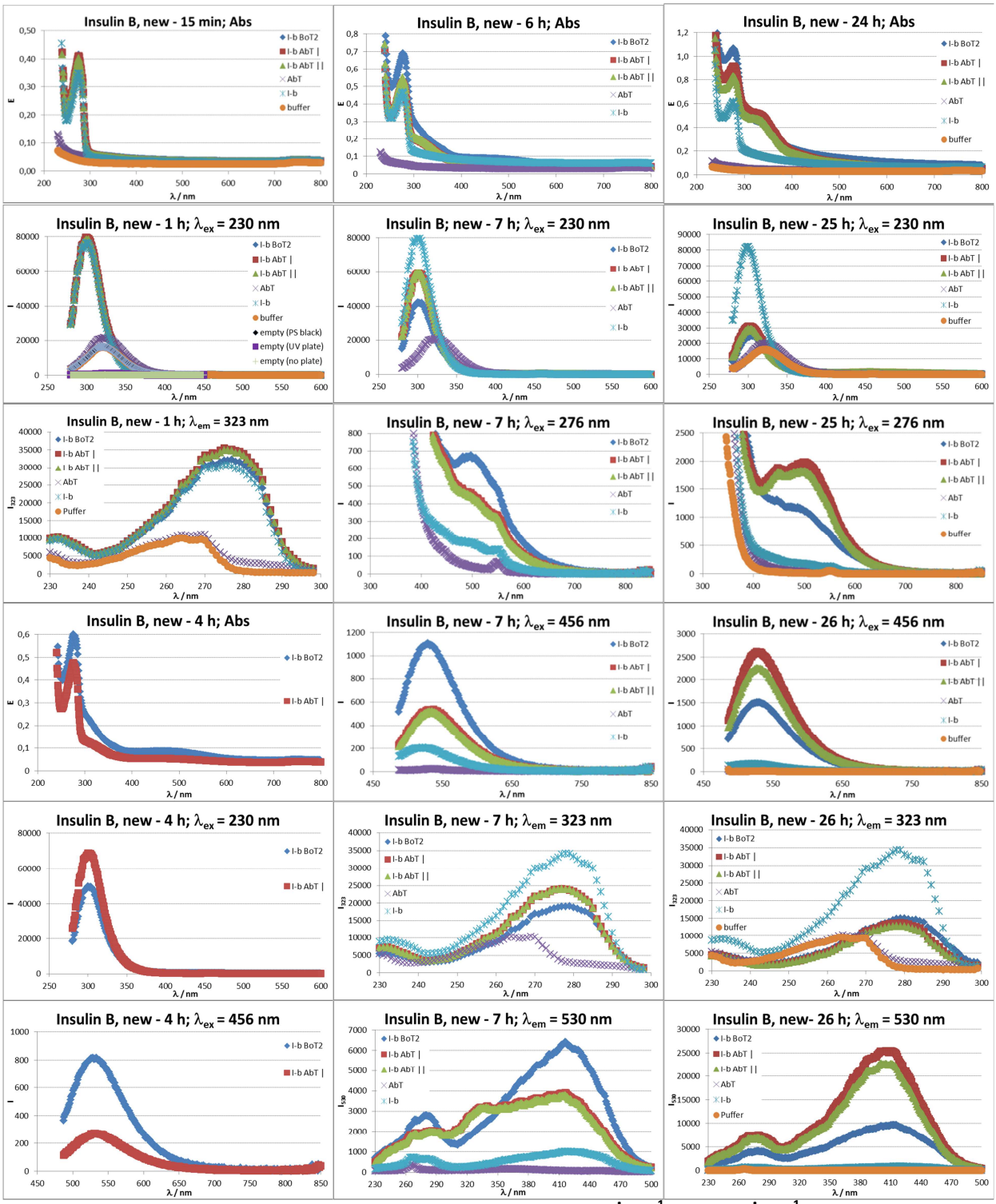

Figure XII-XXX UV-VIS and fluorescence monitoring of I-b new with 8,3̇ U l^{-1} AbT or 1,6̇ U l^{-1} BoT2 in sodium phosphate buffer

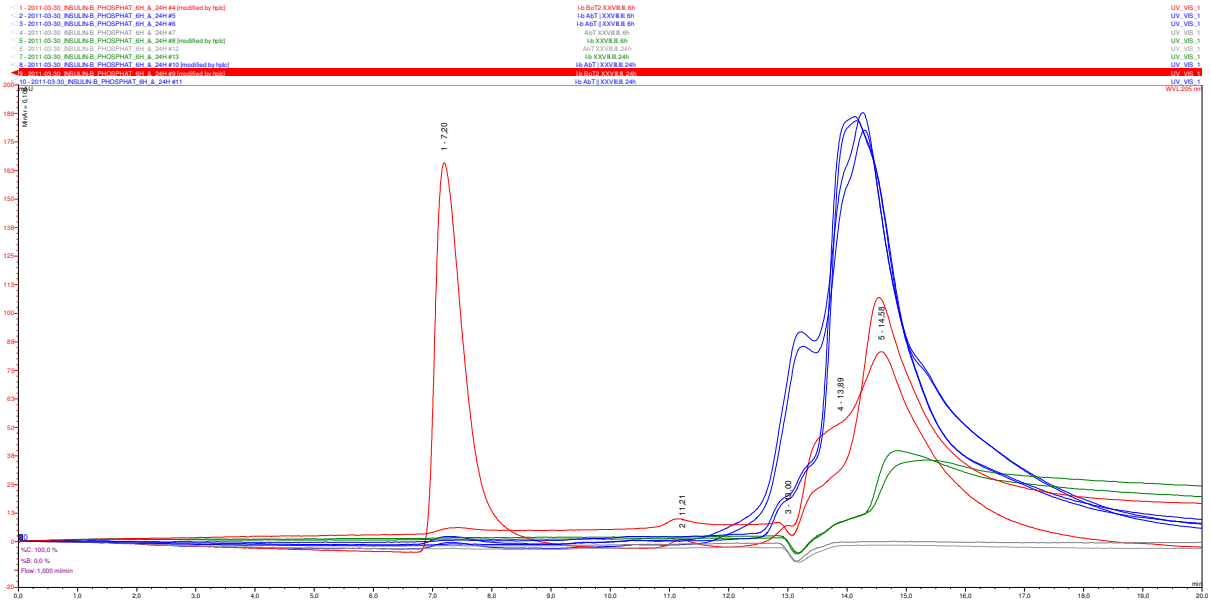

Figure XII-XXXI GPC of samples I-b new 6h & I-b new 24h: increased apparent molecular weight with BoT2, UVD @ 205 nm

Chromatographic conditions: identical to Figure XII-XXI

Table XII-VII samples I-b 6h & I-b 24h: concentrations of the amino acids as measured by RP-HPLC UVD

Sample	Concentration / mM																		
	Ala	Arg	Asn	Asp	Cys	Gln	Glu	Gly	His	Ile	Leu	Lys	Met	Phe	Ser	Thr	Trp	Tyr	Val
7 AS 10mM		9,12		0,0585			0,0792		6,29	9,20	8,26	5,52			6,65			0,0911	8,94
AS 750 µM	0,613	0,648	0,639	1,19		0,613	0,495	0,604	0,539	0,763	0,735	0,601	0,567	0,719	0,464	0,681	0,755	0,726	1,04
I-b BoT2 6h	0,530	0,359		0,678			0,592	1,61	0,585	0,0386	1,83	0,415		1,34	0,278	0,428		0,648	1,32
I-b AbT | 6h	0,644	0,411		0,810			0,814	1,23	0,650	0,0432	1,95	0,450		1,51	0,311	0,461		0,676	1,42
I-b AbT || 6h	0,667	0,432		0,865			0,849	1,36	0,717	0,0441	1,99	0,463		1,56	0,349	0,510		0,797	1,45
AbT 6h	0,0253			0,0142			0,160	0,0464		0,0350	0,0374	0,0483			0,0486	0,033			0,0354
I-b 6h	0,466	0,333		0,636			0,678	1,05	0,573	0,0320	1,58	0,36		1,20	0,270	0,380		0,76	1,16
I-b BoT2 24h	0,694	0,466		1,03			0,753	2,35	0,840	0,0695	2,35	0,543		1,75	0,433	0,563		0,57	1,82
I-b AbT | 24h	0,487	0,424		1,03			0,980	1,58	0,811	0,0587	2,30	0,504		1,79	0,442	0,546		0,678	1,72
I-b AbT || 24h	0,532	0,454		1,03			0,975	1,60	0,819	0,0551	2,32	0,481		1,79	0,427	0,532		0,64	1,78
AbT 24h	0,0246			0,00788			0,158	0,0437		0,0343	0,0383	0,0484			0,0494	0,0337			0,0367
I-b 24h	0,514	0,350		0,718			0,719	1,07	0,605	0,0424	1,68	0,372		1,30	0,283	0,374		0,761	1,29

Table XII-VIII samples I-b 6h & I-b 24h: percentages of the amino acids as measured by RP-HPLC UVD

Sample	Proportion of the amino acid on all unmodified primary amino acids / %																		
	Ala	Arg	Asn	Asp	Cys	Gln	Glu	Gly	His	Ile	Leu	Lys	Met	Phe	Ser	Thr	Trp	Tyr	Val
7 AS 10mM		17		0,11			0,15		12	17	15	10			12			0,17	16
AS 750 µM	4,9	5,2	5,2	9,6		4,9	4,0	4,9	4,3	6,2	5,9	4,9	4,6	5,8	3,7	5,5	6,1	5,9	8,4
I-b BoT2 6h	**5,0**	**3,4**		**6,4**			**5,6**	**15**	**5,5**	**0,36**	**17**	**3,9**		**13**	**2,6**	**4,0**		**6,1**	**12**
I-b AbT | 6h	**5,7**	**3,6**		**7,1**			**7,1**	**11**	**5,7**	**0,38**	**17**	**4,0**		**13**	**2,7**	**4,0**		**5,9**	**12**
I-b AbT || 6h	**5,5**	**3,6**		**7,2**			**7,0**	**11**	**5,9**	**0,37**	**16**	**3,8**		**13**	**2,9**	**4,2**		**6,6**	**12**
AbT 6h	5,2			2,9			33	9,6		7,2	7,7	10			10	6,8			7,3
I-b 6h	**4,9**	**3,5**		**6,7**			**7,2**	**11**	**6,0**	**0,34**	**17**	**3,8**		**13**	**2,8**	**4,0**		**8,0**	**12**
I-b BoT2 24h	**4,9**	**3,3**		**7,3**			**5,3**	**17**	**5,9**	**0,49**	**17**	**3,8**		**12**	**3,0**	**4,0**		**4,0**	**13**
I-b AbT | 24h	**3,6**	**3,2**		**7,7**			**7,3**	**12**	**6,1**	**0,44**	**17**	**3,8**		**13**	**3,3**	**4,1**		**5,1**	**13**
I-b AbT || 24h	**4,0**	**3,4**		**7,7**			**7,3**	**12**	**6,1**	**0,41**	**17**	**3,6**		**13**	**3,2**	**4,0**		**4,8**	**13**
AbT 24h	5,2			1,7			33	9,2		7,2	8,1	10			10	7,1			7,7
I-b 24h	**5,1**	**3,5**		**7,1**			**7,1**	**11**	**6,0**	**0,42**	**17**	**3,7**		**13**	**2,8**	**3,7**		**7,5**	**13**
Theoretical#	**7,4**	**3,7**	**3,7**			**3,7**	**7,4**	**11**	**7,4**		**15**	**3,7**		**11**	**3,7**	**3,7**		**7,4**	**11**

..... Calculated from the peptide sequence of I-b (see Figure 12-5) excluding Cys(SO_3H) (2x) and Pro (1x)

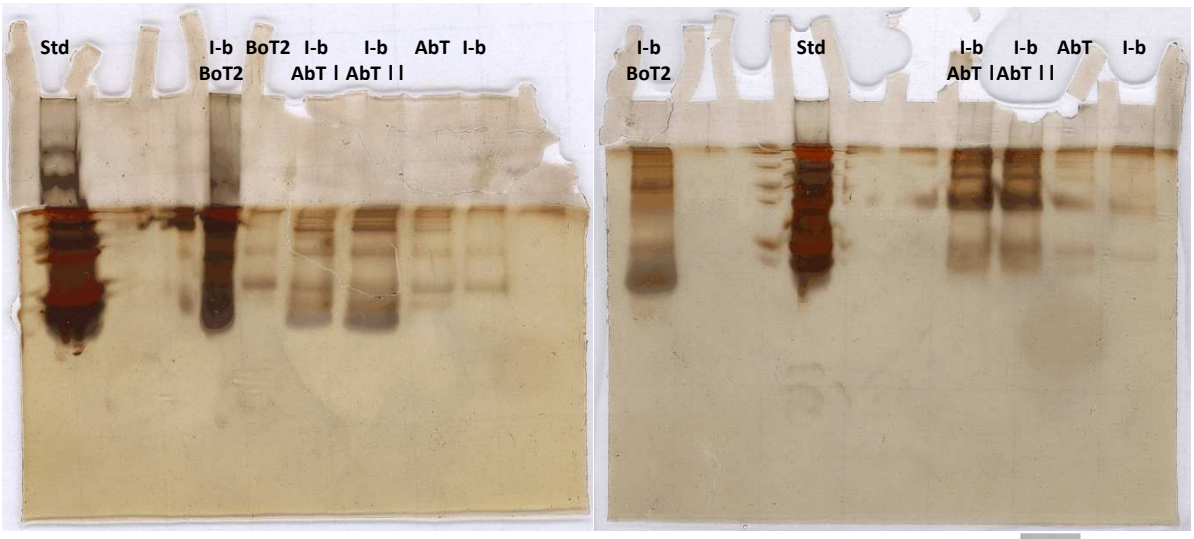

Figure XII-XXXII 2x bis-Tris SDS-PAGE, 10 % acryl amide, silver staining: samples I-b 24h in NH_4Ac (left) or sodium phosphate buffer (right)

The 0,75 mm vertical gels were run for 90 min @ 100 V whilst being constantly cooled with ice.

Std .....BioRad silver stain SDS-PAGE standards, low range (see right)

The samples were kept for 10 min @ 80 °C after mixing with 2x loading buffer (see 5.2.3) prior to loading.

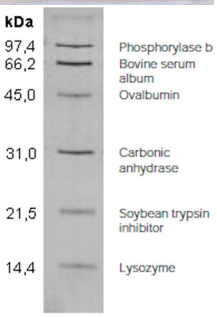

XII.III. 7 AS with BoT2 and AbT

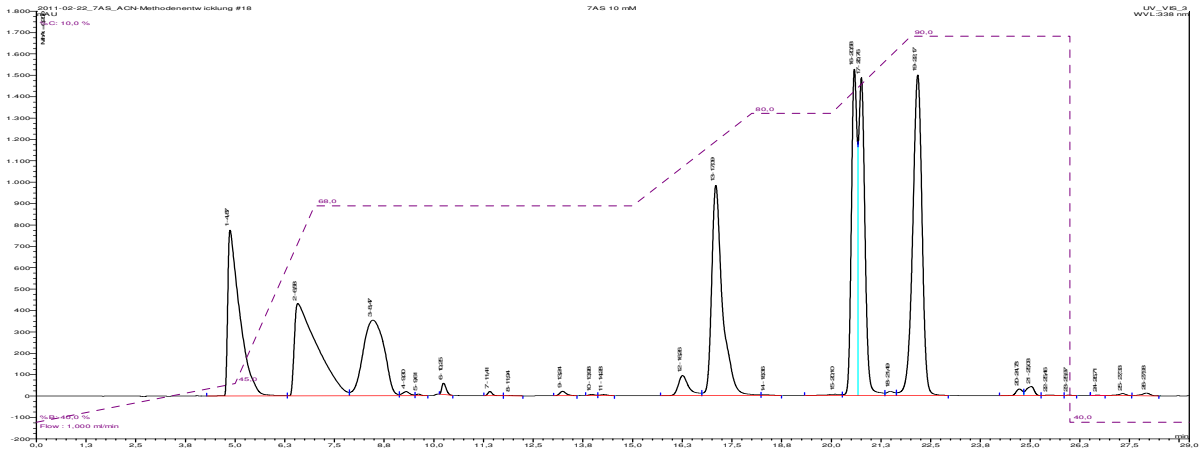

Figure XII-XXXIII RP-HPLC-UVD of 7AS 10mM after OPA-derivatisation

mobile phase: A == 1 ‰ formic acid (v/v) in ddH_2O; B == ACN:MeOH:ddH2O 45:45:10 (v+v+v)

column: Eurospher 100-5 C18 4,6x250mm

XII.III.I. 7 AS with BoT2 and AbT in NH_4Ac

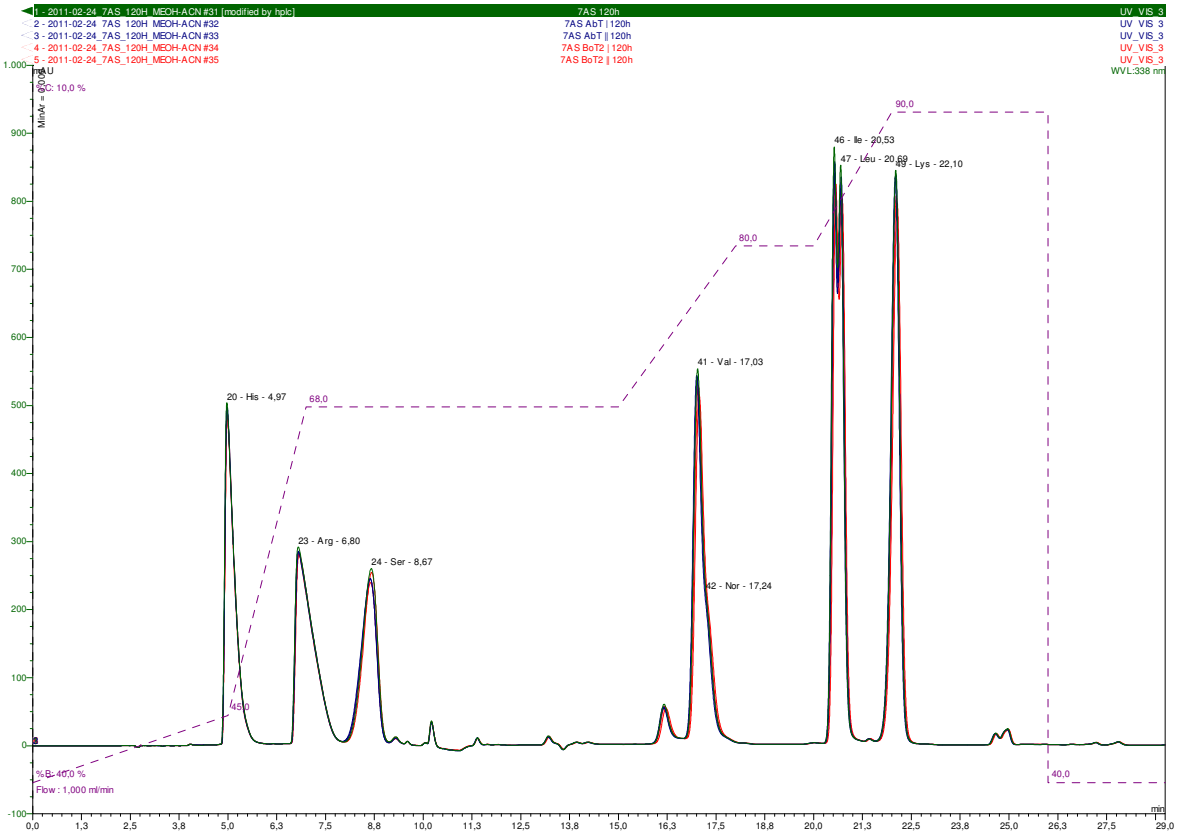

Figure XII-XXXIV 7 AS with 25 U l-1 BoT2 and AbT in NH_4Ac pH 6,8: no changes after 5 days @ 25 °C

XII.III.II. 7 AS with AbT in sodium phosphate buffer with 1,77 mM Tyr

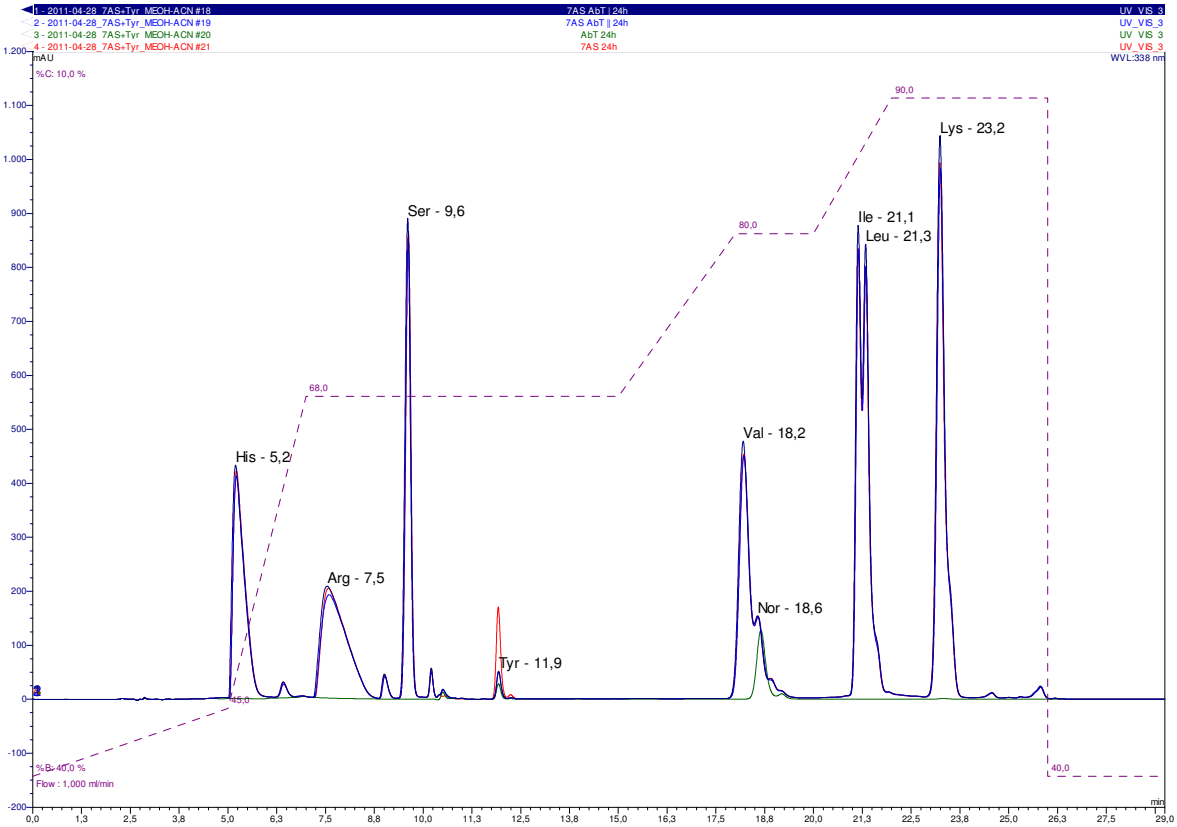

Figure XII-XXXV 7 AS with Tyr and 5 U l^{-1} AbT in sodium phosphate buffer pH 6,8: no changes after 24 h @ 25 °C apart from the consumption of tyrosine

XII.III.III. 7 AS with N-Boc-L-Tyr and AbT in sodium phosphate buffer

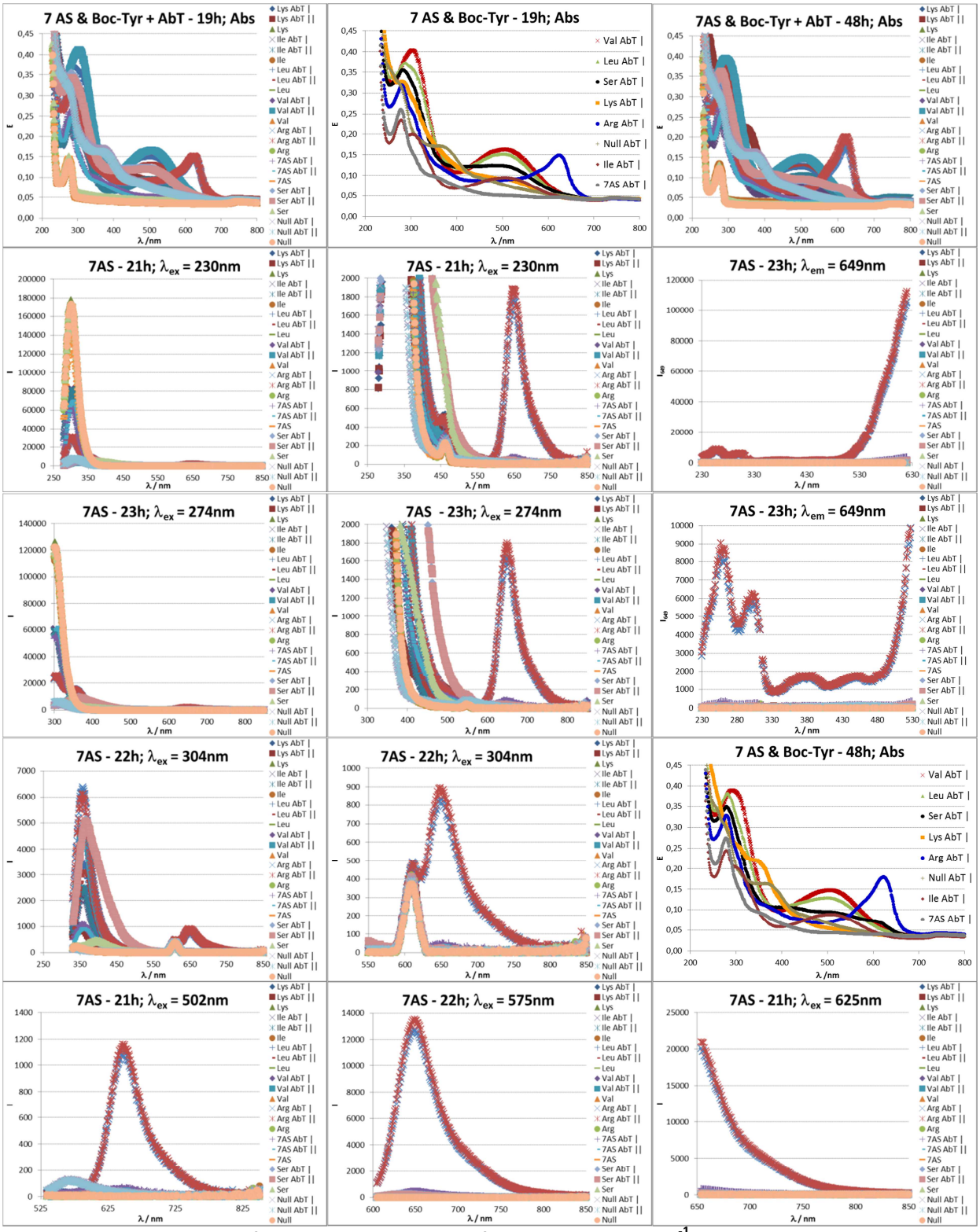

Figure XII-XXXVI UV-VIS and fluorescence monitoring of 7 AS & Boc-Tyr + 2 U l^{-1} AbT in sodium phosphate buffer

Table XII-IX samples 7 AS & Boc-Tyr 24 h: amino acid concentrations as measured by RP-HPLC-UVD

Sample	Concentration / mM								Sum /mM
	Arg	His	Ile	Leu	Lys	Ser	Tyr	Val	
7AS 10 mM	9,97	9,90	10,1	9,98	9,72	9,98	0,00821	9,47	**69,1**
Lys AbT | 24h					**4,75**		0,00541		**4,76**
Lys AbT || 24h					**4,80**		0,00559		**4,80**
Lys 24h					**5,47**		0,00440		**5,47**
Ile AbT | 24h			**5,18**	0,288	0,0327	0,0384	0,0116		**5,55**
Ile AbT || 24h			**4,85**	0,217	0,0196	0,0376	0,00771		**5,13**
Ile 24h			**5,68**	0,279	0,0203		0,00985		**5,99**
Leu AbT | 24h				**3,09**	0,0204	0,0381	0,00549		**3,15**
Leu AbT || 24h				**3,36**	0,0206	0,0381	0,00569		**3,42**
Leu 24h				**3,96**	0,0219		0,00926		**3,99**
Val AbT | 24h				0,00802	0,0208		0,00577	**4,30**	**4,34**
Val AbT || 24h				0,00855	0,0213		0,00537	**4,37**	**4,41**
Val 24h				0,00852	0,0215		0,00556	**5,36**	**5,40**
Arg AbT | 24h	**3,41**	0,0355			0,0197	0,0364	0,00290		**3,50**
Arg AbT || 24h	**3,34**				0,0195	0,0365	0,00309		**3,40**
Arg 24h	**4,91**	0,0359			0,0201	0,0386	0,00489		**5,01**
7AS AbT | 24h	5,28	5,35	4,02	5,69	5,45	5,05	0,00637	3,25	**34,1**
7AS AbT || 24h	7,91	7,60	5,55	7,79	8,51	7,42	0,00636	4,58	**49,4**
7AS 24h	5,34	5,56	4,03	5,62	5,49	5,04	0,00908	3,21	**34,3**
Ser AbT | 24h		0,0362			0,0306	**3,58**	0,00457		**3,65**
Ser AbT || 24h						**3,52**	0,00476		**3,53**
Ser 24h		0,0361				**4,81**	0,00613		**4,85**
Null AbT | 24h		0,0366					0,00680		**0,0434**
Null AbT || 24h		0,0360					0,00721		**0,0432**
Null 24h		0,0368					0,00862		**0,0454**
7AS 10 mM	10,0	10,1	9,93	10,0	10,3	10,0	0,00280	10,5	**70,9**

Table XII-X samples 7 AS & Boc-Tyr 48 h: amino acid concentrations as measured by RP-HPLC-UVD

Sample	Concentration / mM								Sum /mM
	Arg	His	Ile	Leu	Lys	Ser	Tyr	Val	
7AS 10 mM	9,85	9,71	9,81	9,75	9,28	9,84	0,0131	10,4	**68,6**
Lys AbT | 48h					**4,39**		0,0137		**4,41**
Lys AbT || 48h					**4,50**		0,0137		**4,51**
Lys 48h					**5,57**		0,0058		**5,57**
Ile AbT | 48h		0,0356	**5,30**		0,0351	0,0383	0,00997		**5,42**
Ile AbT || 48h		0,0357	**5,18**		0,0234	0,0385	0,00915		**5,28**
Ile 48h		0,0359	**6,13**		0,0231		0,0127		**6,21**
Leu AbT | 48h		0,0362		**2,92**	0,0220	0,0367	0,00506		**3,02**
Leu AbT || 48h		0,0359		**3,04**	0,0220	0,0365	0,00553		**3,14**
Leu 48h		0,0357		**3,97**	0,0232		0,00545		**4,04**
Val AbT | 48h		0,0358		0,0117	0,0222		0,00579	**3,86**	**3,94**
Val AbT || 48h		0,0356		0,0101	0,0225		0,00815	**3,79**	**3,87**
Val 48h		0,0361		0,0115	0,0225		0,00626	**4,71**	**4,79**
Arg AbT | 48h	**2,83**	0,0365		0,00694	0,0203	0,0372	0,00302		**2,93**
Arg AbT || 48h	**2,75**	0,0361		0,00833	0,0204	0,0376	0,00338		**2,86**
Arg 48h	**4,11**	0,0358		0,00800	0,0203	0,0392	0,00361		**4,21**
7AS AbT | 48h	5,19	5,35	4,18	5,74	5,70	5,02	0,00936	3,27	**34,5**
7AS AbT || 48h	4,99	5,13	3,97	5,37	5,39	4,74	0,00867	3,13	**32,7**
7AS 48h	4,93	5,31	3,90	5,35	5,37	4,65	0,0104	3,07	**32,6**
Ser AbT | 48h		0,0361			0,0284	**2,68**	0,00524		**2,75**
Ser AbT || 48h		0,0368			0,0200	**2,77**	0,00393		**2,83**
Ser 48h		0,0360			0,0200	**4,38**	0,00755		**4,44**
Null AbT | 48h		0,0366	0,00912	0,00654	0,0209		0,00717		**0,0804**
Null AbT || 48h		0,0362	0,00940	0,00770			0,00895		**0,0622**
Null 48h		0,0362	0,00931	0,00769	0,0204		0,00759		**0,0812**
7AS 10 mM	10,1	10,3	10,2	10,3	10,7	10,2	0,00725	9,63	**71,4**

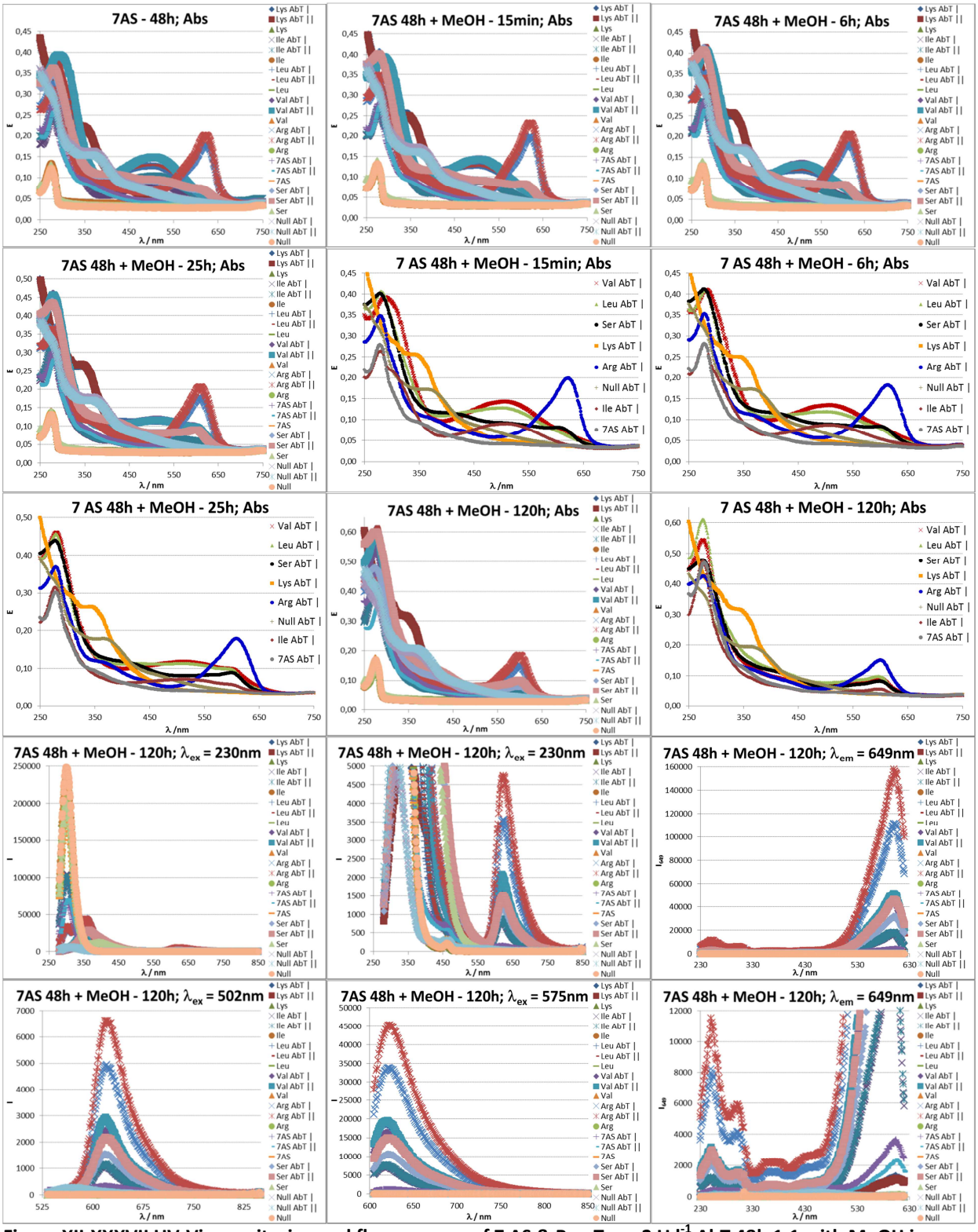

Figure XII-XXXVII UV-Vis monitoring and fluorescence of 7 AS & Boc-Tyr + 2 U l^{-1} AbT 48h 1:1 with MeOH in sodium phosphate buffer

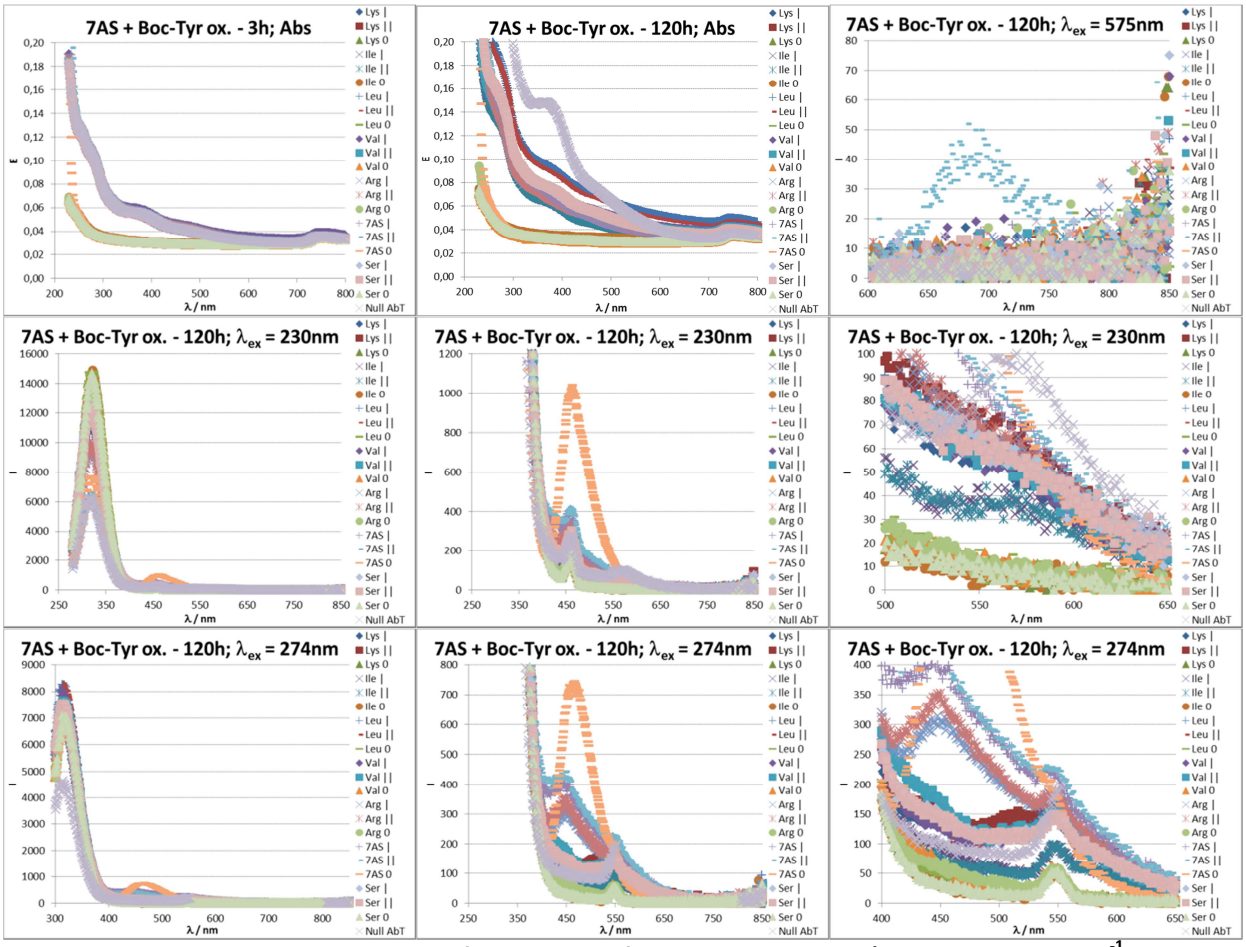

Figure XII-XXXVIII UV-Vis monitoring and fluorescence of oxidised N-Boc-*L*-Tyr (7AS & Boc-Tyr + 2 U l^{-1} AbT 48h, filtrated 3 kDa MWCO) with 7 AS in sodium phosphate buffer, diluted 1:5 with ddH_2O

Null AbT.....7AS & Boc-Tyr + 2 U l-1 AbT 48h, filtrated: 3 kDa MWCO

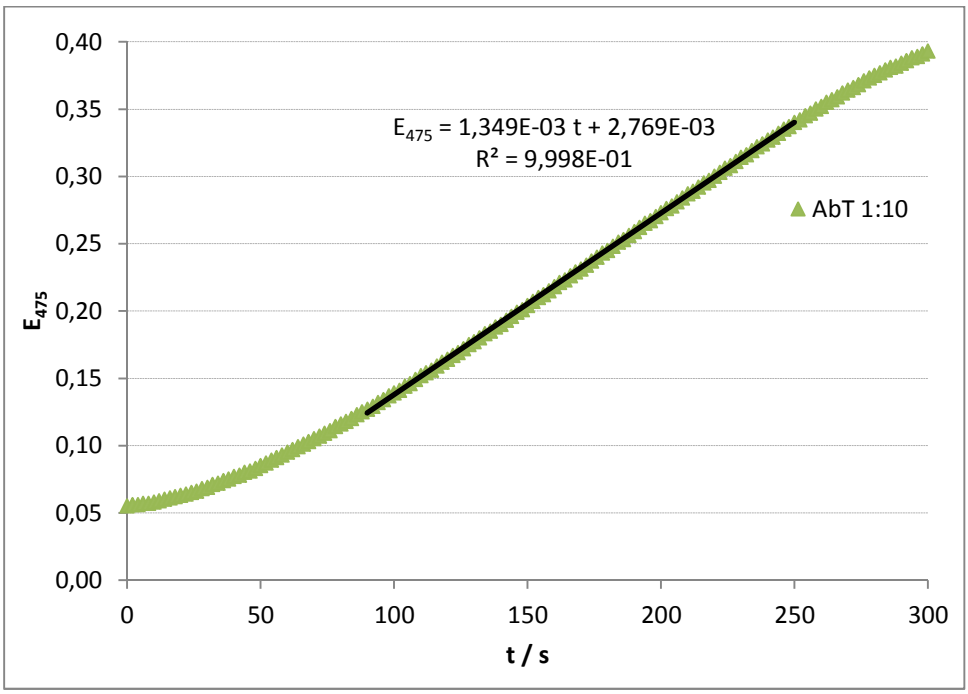

Figure XII-XXXIX Tyrosinase activity of AbT in sodium phosphate buffer pH 6,5

50 µl enzyme solution + 450 µl Tyr 2 mM in 1 cm cuvettes @ 25 °C

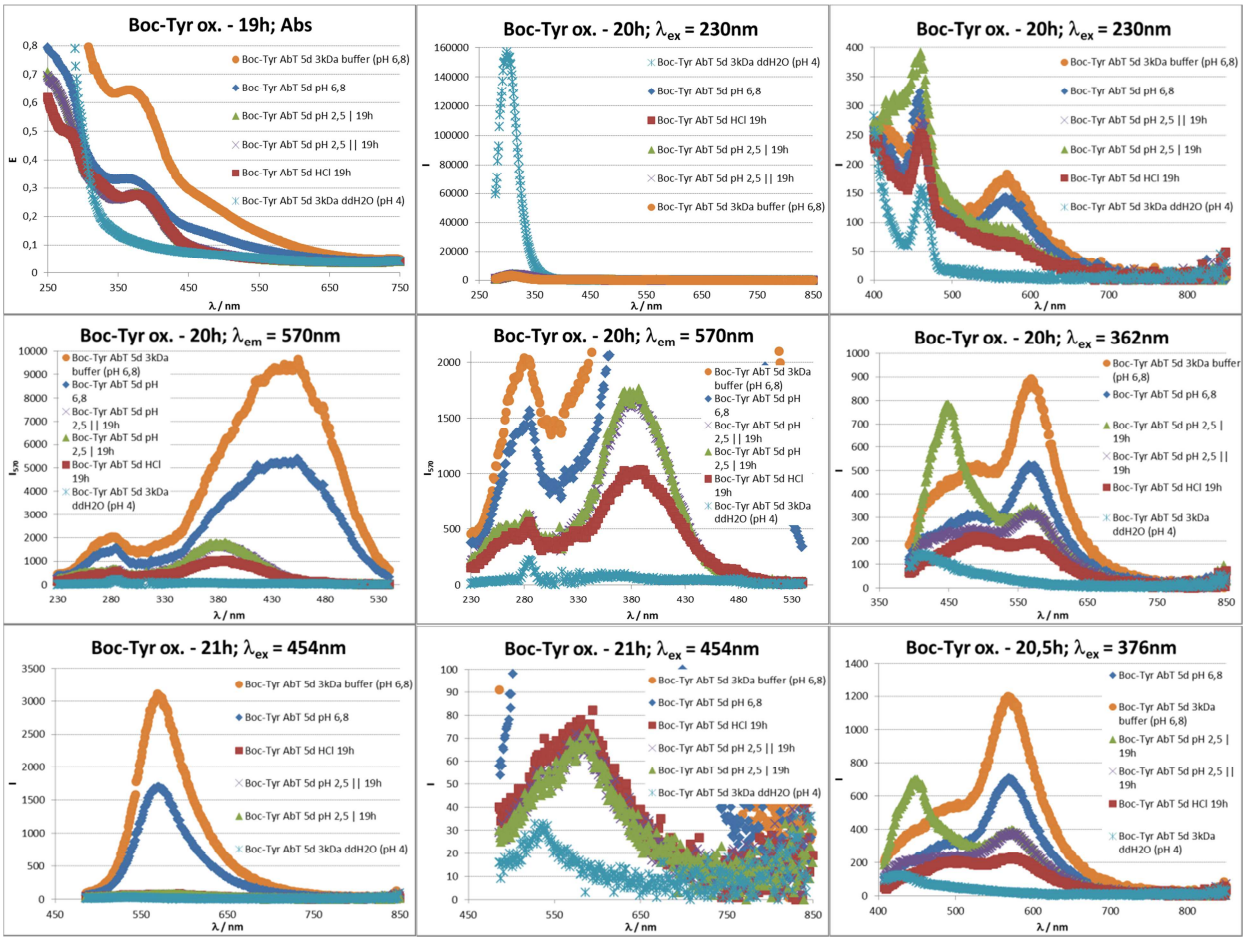

Figure XII-XL UV-Vis and fluorescence spectra of oxidised N-Boc-*L*-Tyr in sodium phosphate buffer of different pH

3kDa .....filtrated: Vivaspin 2, 3 kDa MWCO

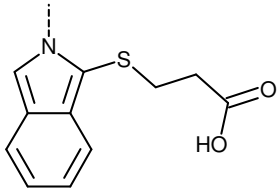

N-OPA
1-[(2-carboxyethyl)sulfanyl]-2*H*-isoindol-2-yl
Molecular Formula = $C_{11}H_{10}NO_2S$
Monoisotopic Mass = 220.043224 Da

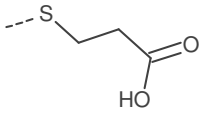

SPA
(2-carboxyethyl)sulfanyl
Molecular Formula = $C_3H_5O_2S$
Monoisotopic Mass = 105.001024 Da

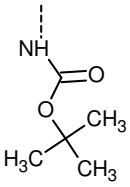

N-Boc
(*tert*-butoxycarbonyl)amino
Molecular Formula = $C_5H_{10}NO_2$
Monoisotopic Mass = 116.071154 Da

Figure XII-XLI structures and abbreviations for groups derived from pre-column derivatisation with OPA and N-protection with Boc_2O

XIII. Fragmentation trees

XIII.I. K with BoT1, BoT2 and AbT

XIII.I.I. K BoT1 r 18h: Fractions I - VII

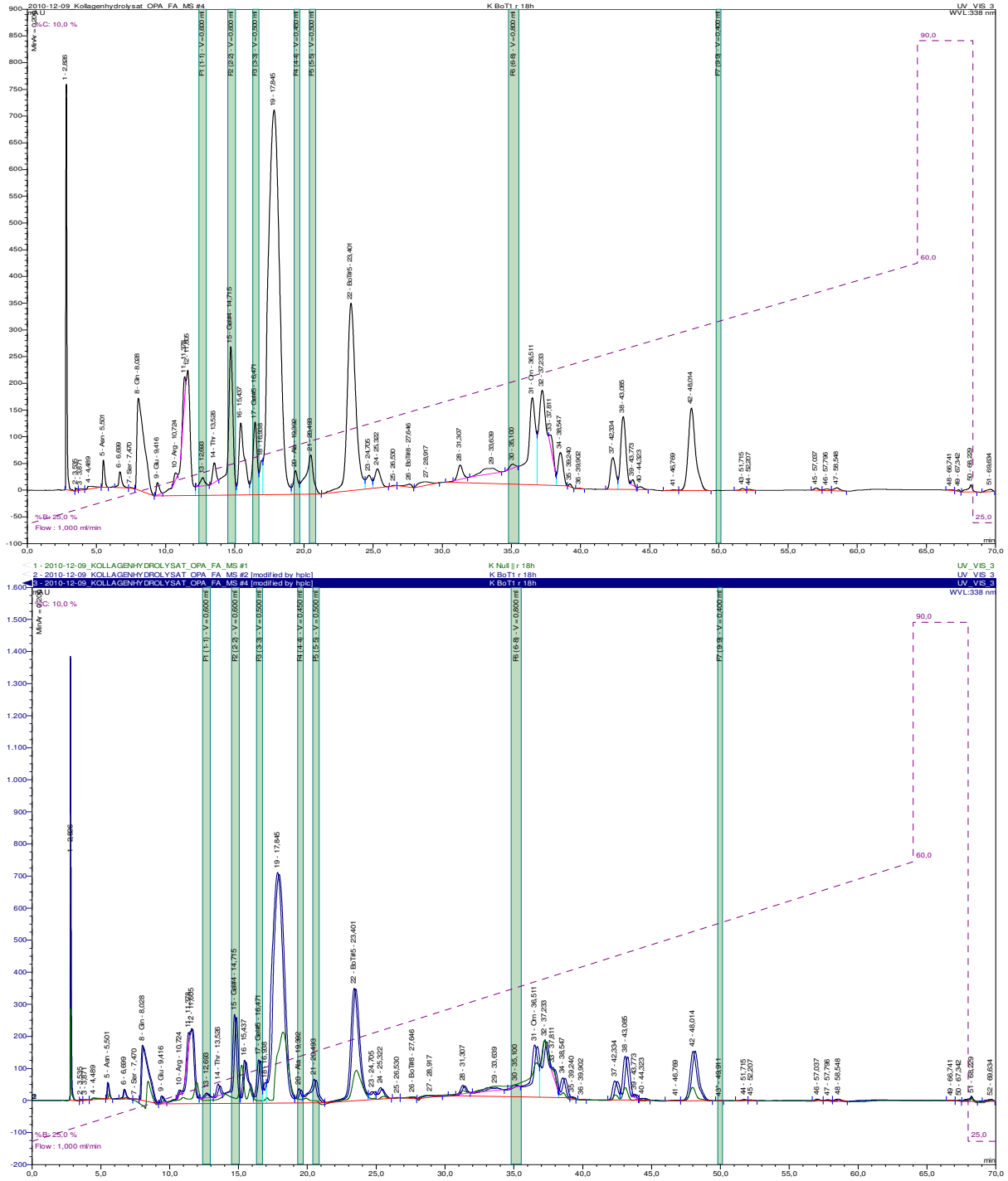

Figure XIII-I K BoT1 r 18h – RP-HPLC fractions I-VII for ESI-MS, UVD @ 338 nm

The chromatographic signals present in the enzymatically treated samples but neither in the blank (containing only enzyme and buffer but no substrate) nor the reference (acid soluble collagen without enzymes) were chosen for MS^n-analysis.

541 Th / **-539 Th** have been found in each and every one of the seven samples. **322 Th** can also be found in all of the seven fractions while -320 Th is only significant in I. As these signals appear in different samples at various abundances (An abundance decreasing over the length of the chromatogram may be attributed to cross-contamination brought forth by the fraction collector.) the corresponding substance cannot contain any moieties characteristic for neither of the seven samples. Due to this observation and the measured fragmentation trees (which are identic in all of the seven samples) these signals have been attributed to a decomposition product which could stem from every OPA-derivatised amino acid.

I

+MS^n

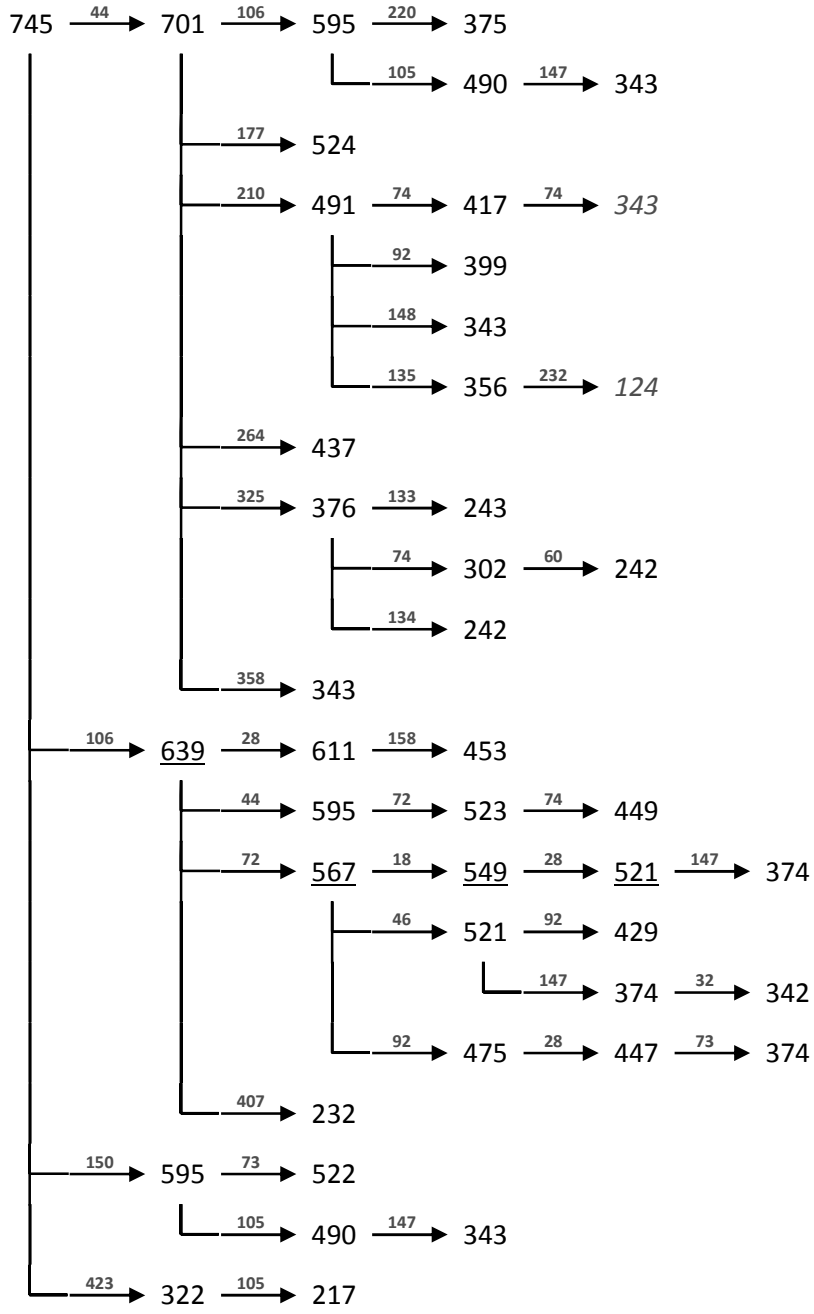

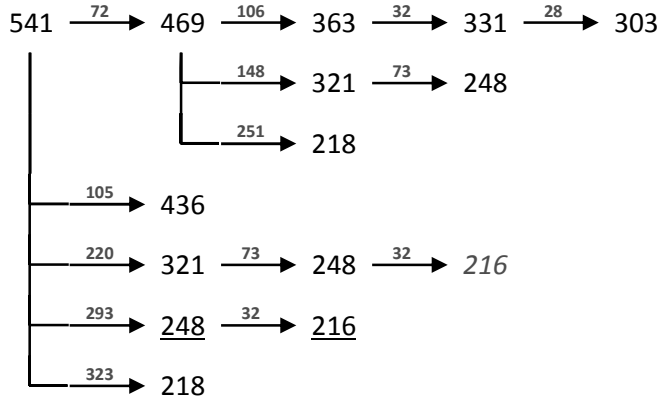

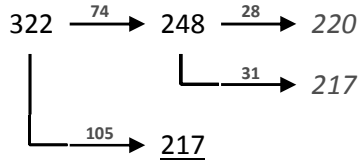

-MS^n

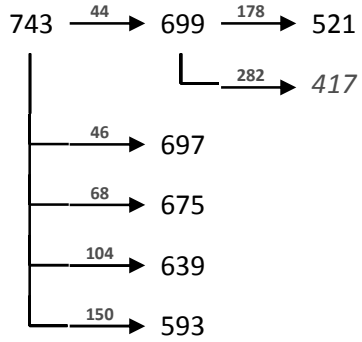

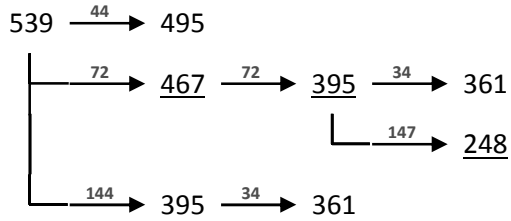

isotopic fingerprint:

peak area / % of monoisotopic	**+1**	**+2**	**+3**
theoretical ($C_{34}H_{45}N_6O_9S_2^+$):	41,6	19,3	5,6
measured (745,3 Th):	50,9	20,4	7,8
measured (-742,8 Th):		(S/N too low)	
theoretical ($C_{26}H_{25}N_2O_7S_2^+$):	31,1	15,2	3,6
measured (541,2 Th):	32,9	12,6	5,3
measured (-538,9 Th):		(S/N too low)	
theoretical ($C_{16}H_{20}NO_4S^+$):	18,9	7,0	1,1
measured (322,2 Th):	20,0	9,6	2,2
measured (-319,8 Th):	(27,6)	-	-

Figure XIII-II MS^n analysis of I

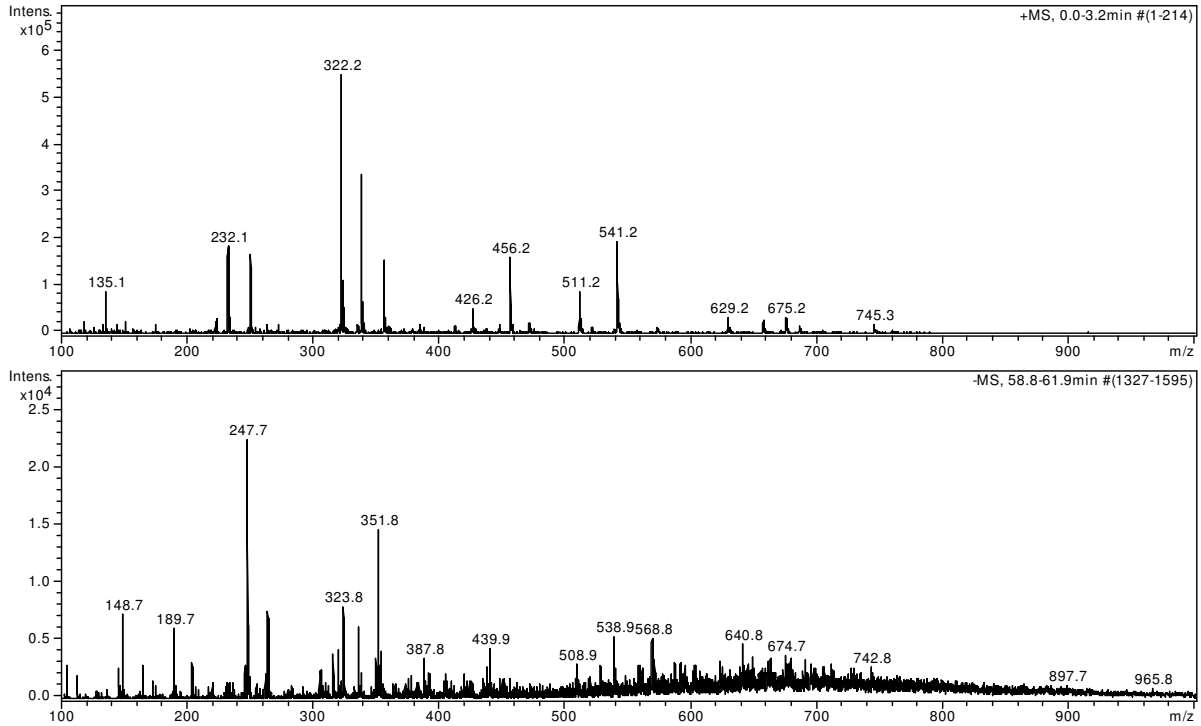

Figure XIII-III I: 12,4 – 13,0 min, 1 ‰ FA, 30 % ACN in ddH_2O; full scan MS^1

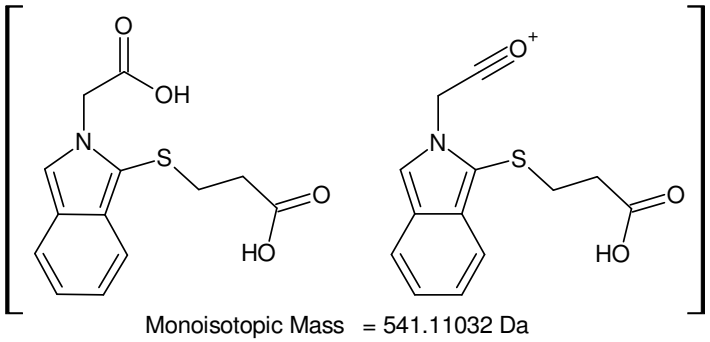

Monoisotopic Mass = 541.11032 Da

541 Th kommt in jeder der 7 Proben vor.

Dimer aus 2x OPA-Gly bzw.
nach Seitenkettenverlust?

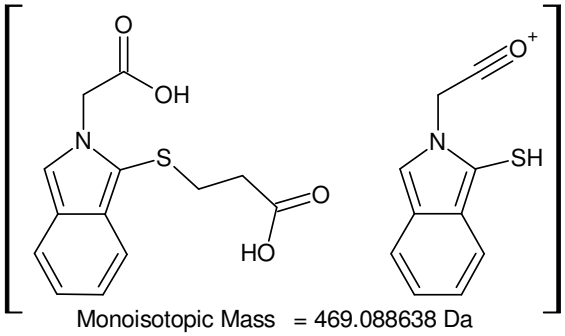

Monoisotopic Mass = 469.088638 Da

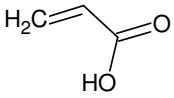

acrylic acid
72.021129 Da

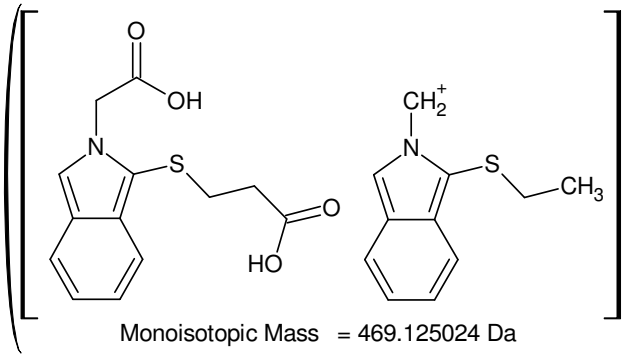

Monoisotopic Mass = 469.125024 Da

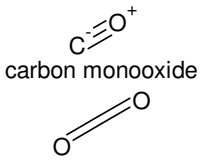

carbon monooxide

carbon dioxide
71.984744 Da

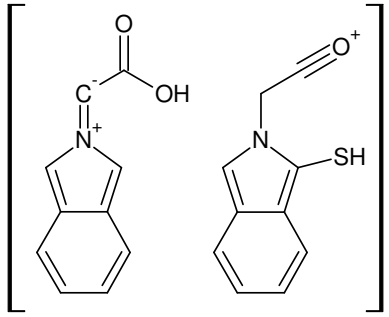

Monoisotopic Mass = 363.080339 Da

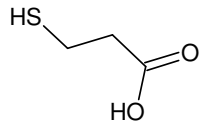

3-mercaptopropanoic acid
106.008849 Da

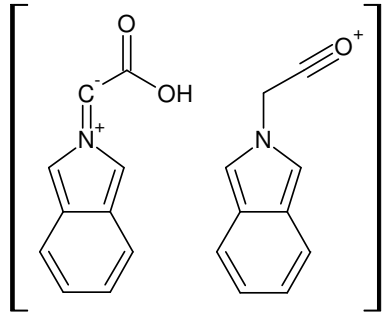

Monoisotopic Mass = 331.108268 Da

S:
sulfanylidene
31.97207 Da

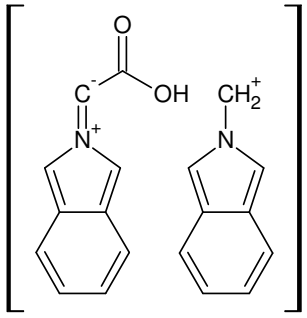

Monoisotopic Mass = 303.113353 Da

carbon monooxide
27.994915 Da

+MSn [I-VII]: 541 -> 2x 469 -> 363 -> 331 -> 303

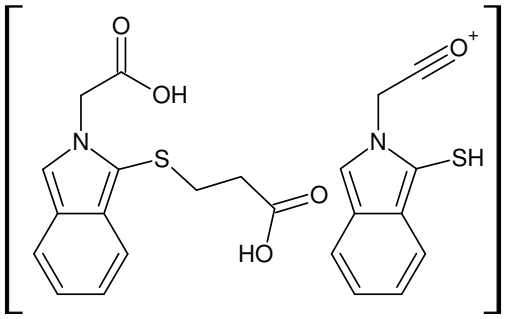

Monoisotopic Mass = 469.08919 Da

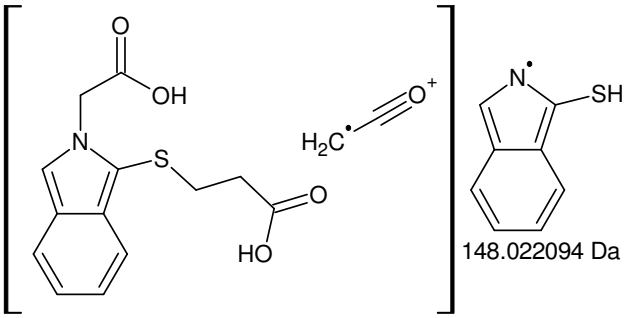

148.022094 Da

Monoisotopic Mass = 321.066544 Da

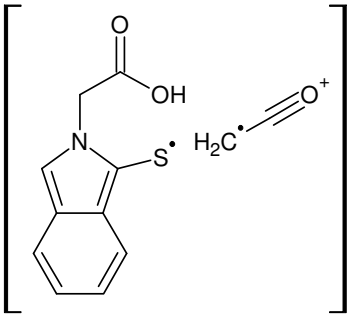

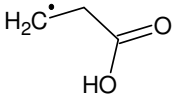

73.028954 Da

Monoisotopic Mass = 248.03759 Da

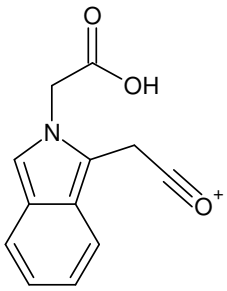

S:
31.97207 Da

Monoisotopic Mass = 216.06552 Da

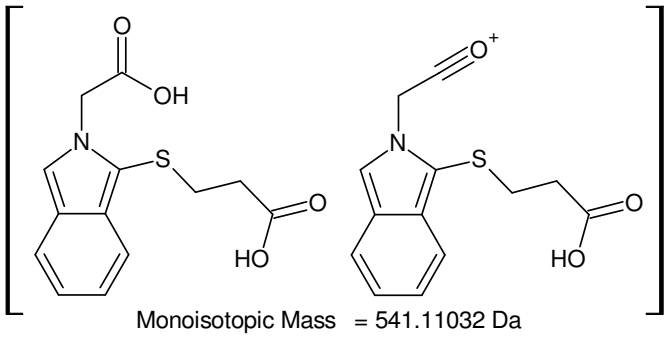

Monoisotopic Mass = 541.11032 Da

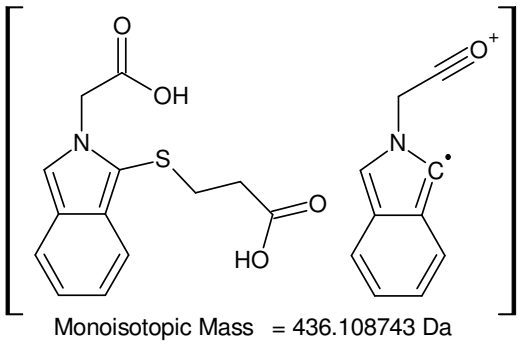

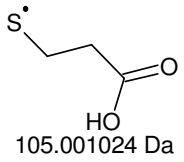

105.001024 Da

Monoisotopic Mass = 436.108743 Da

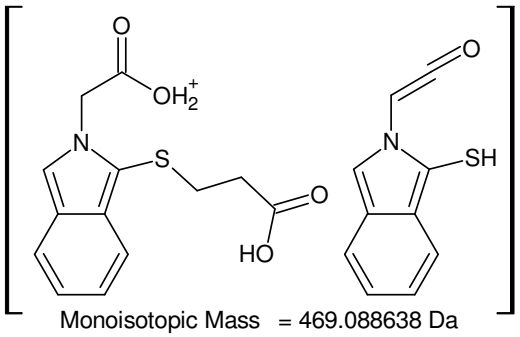

Monoisotopic Mass = 469.088638 Da

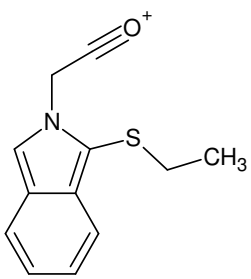

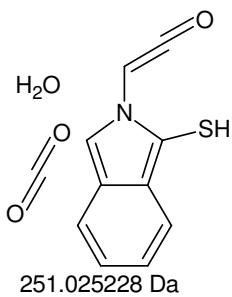

251.025228 Da

Monoisotopic Mass = 218.06341 Da

+MSn [I-VII]: [541 -> 469] -> 321 -> 248 -> 216 and 541 -> 436 as well as [541 -> 469] -> 218

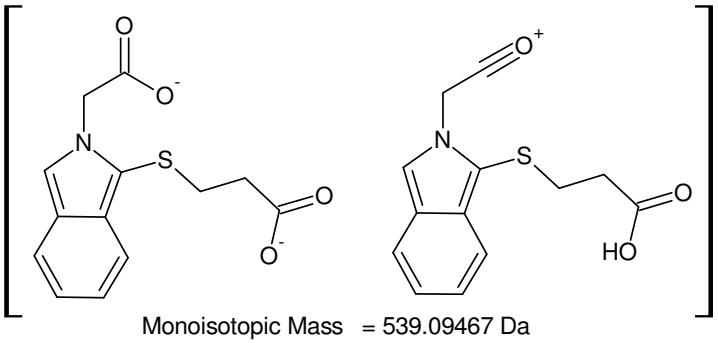

Monoisotopic Mass = 539.09467 Da

539 Th kommt in jeder der 7 Proben vor.

Die Intensität der Signale ist gegenüber +MS sehr gering.

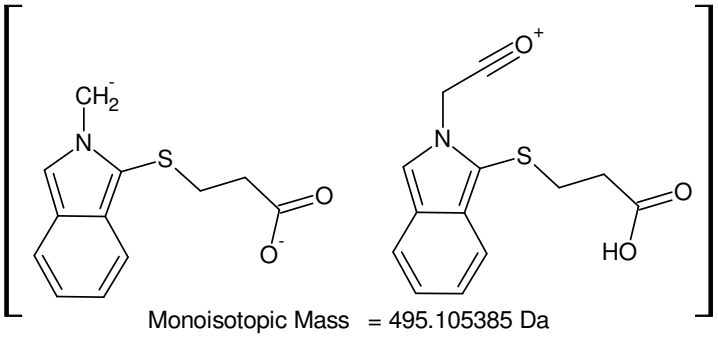

Monoisotopic Mass = 495.105385 Da

43.989829 Da

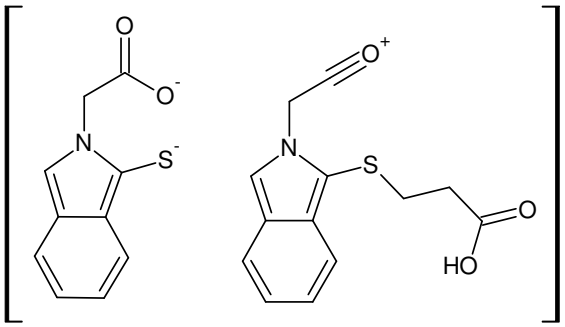

Monoisotopic Mass = 467.07354 Da

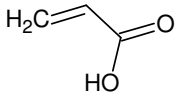

72.02113 Da

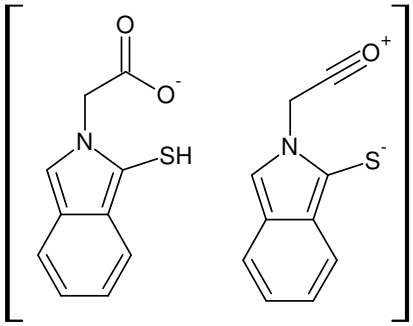

Monoisotopic Mass = 395.05241 Da

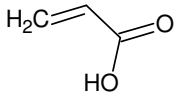

72.02113 Da

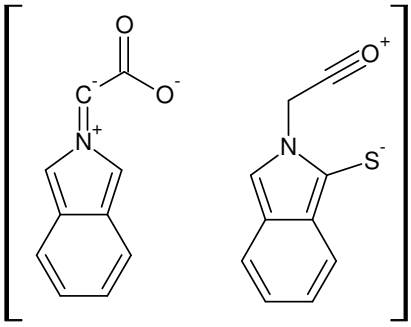

Monoisotopic Mass = 361.064689 Da

H_2S

33.987721 Da

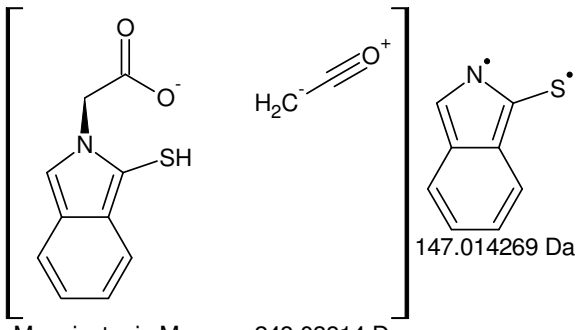

Monoisotopic Mass = 248.03814 Da

147.014269 Da

-MSn [I-VII]: 539 -> 495, 467 -> 395 -> 361, 248

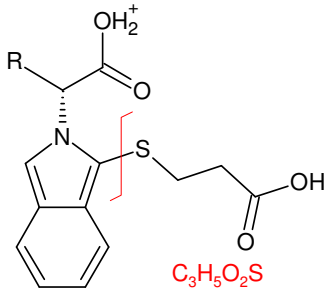

322 Th

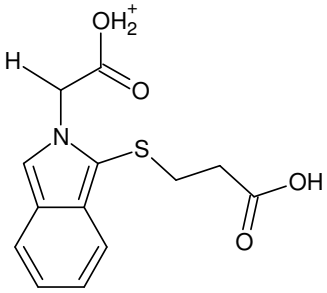

Monoisotopic Mass = 280.063804 Da

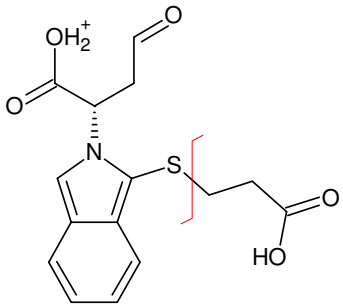

Monoisotopic Mass = 322.074369 Da

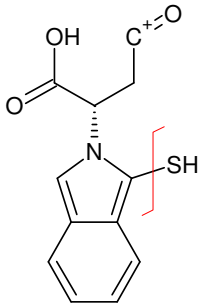

Monoisotopic Mass = 248.03759 Da

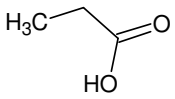

Monoisotopic Mass = 74.036779 Da

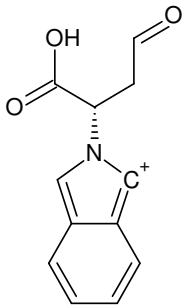

Monoisotopic Mass = 216.06552 Da

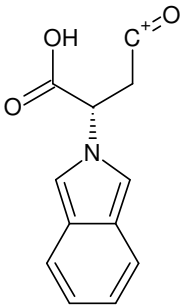

Monoisotopic Mass = 216.06552 Da

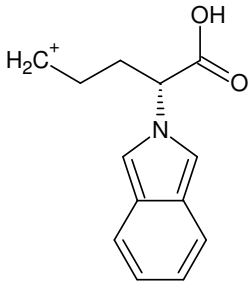

Monoisotopic Mass = 216.101905 Da

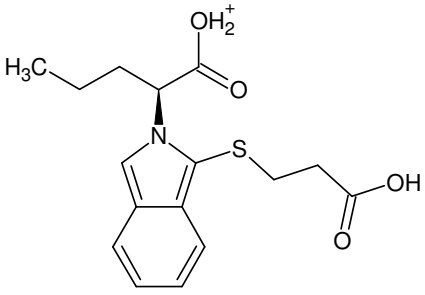

Monoisotopic Mass = 322.110755 Da

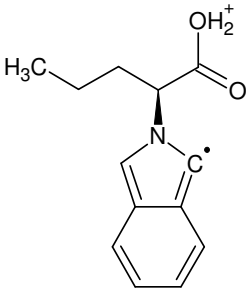

Monoisotopic Mass = 217.10973 Da

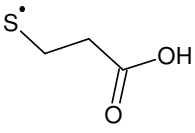

105.001024 Da

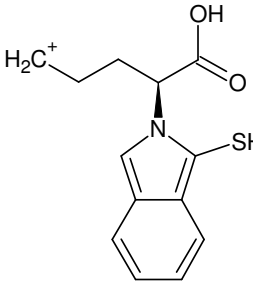

74.036779 Da

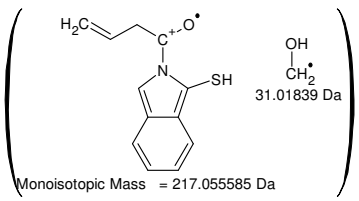

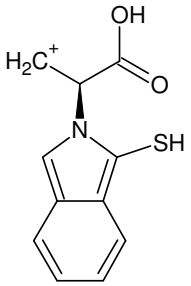

28.0313 Da

Monoisotopic Mass = 248.073975 Da

Monoisotopic Mass = 220.042675 Da

+MSn [I-VII]: 322 Th & 322 -> 217, 248 -> 220 {I/II}

322 - 280 = **42**
Compounds found: 13
CH2N2 MW=42,0217972
CH14O MW=42,1044594
CH16N MW=42,1282676
CNO MW=41,997989
C2H2O MW=42,0105642
C2H4N MW=42,0343724
C2H18 MW=42,1408428
C3H6 MW=42,0469476
H10S MW=42,050318
H12NO MW=42,0918842
H10O2 MW=42,068076
H14N2 MW=42,1156924
N3 MW=42,009222

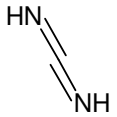

(keine AS)

Molecular Formula = C H_2 N_2

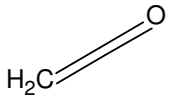

Thr

Molecular Formula = C_2 H_2 O

-----D--B--E--f-i-l-t-e-r-----
08.02.2011 - 13:24:30,10
akzeptierte DBEs:
0
1
2
3
4

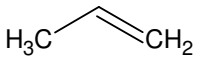

Arg oder Orn

Molecular Formula = C_3 H_6

CH2N2 DBE: 2
C2H2O DBE: 2
C3H6 DBE: 1

3 von 13 Summenformeln

248 - 217 = **31**
Gefundene Verbindungen: 6
CH3O MG=31,0183888
CH5N MG=31,042197
C2H7 MG=31,0547722
HNO MG=31,0058136
H3N2 MG=31,0296218
H15O MG=31,112284

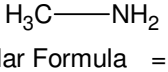

Molecular Formula = C H_5 N

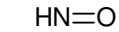

Molecular Formula = H N O

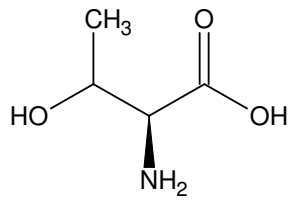

L-Threonin

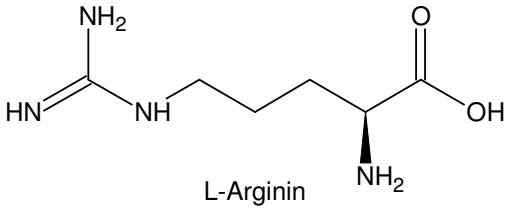

L-Arginin

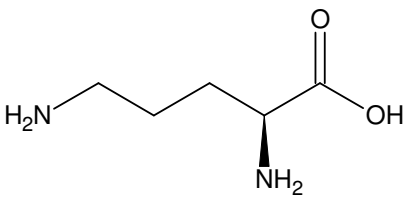

L-Ornithin

+MSn [I-VII]: 322 Th & 322 -> 217, 248 -> 220 {II/II}

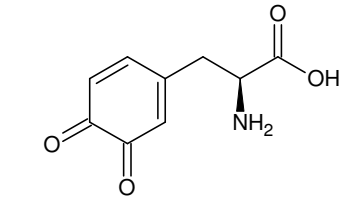

Monoisotopic Mass = 195.053158 Da

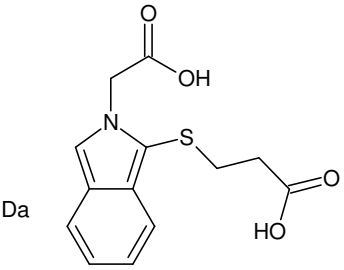

Monoisotopic Mass = 279.056528 Da

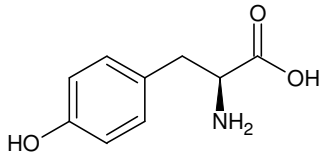

Monoisotopic Mass = 181.073893 Da

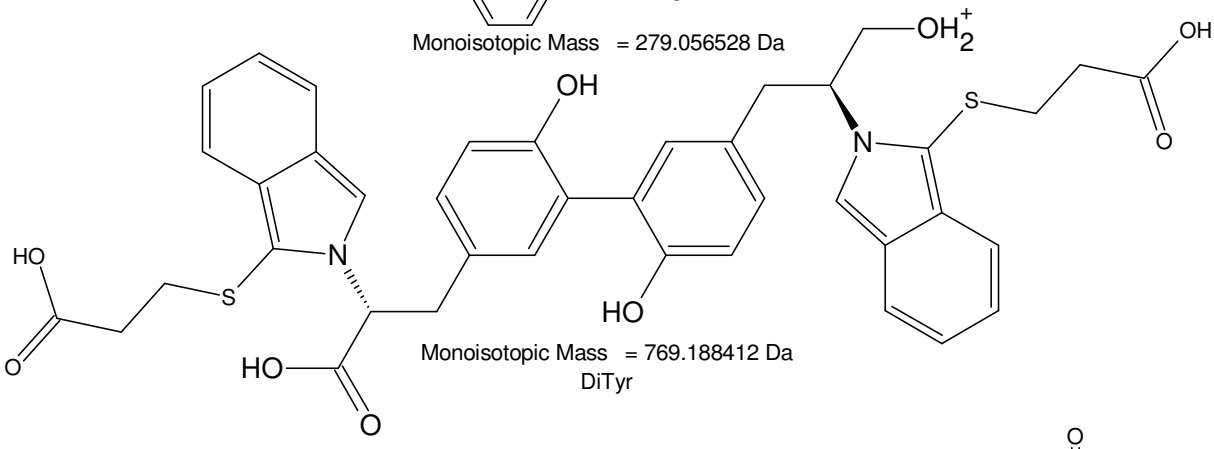

Monoisotopic Mass = 769.188412 Da
DiTyr

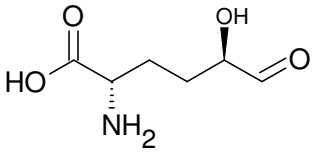

Hydroxylysinaldehyd

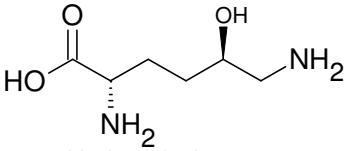

Hydroxylysin

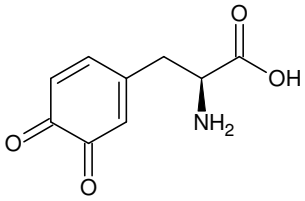

o-Dopachinon

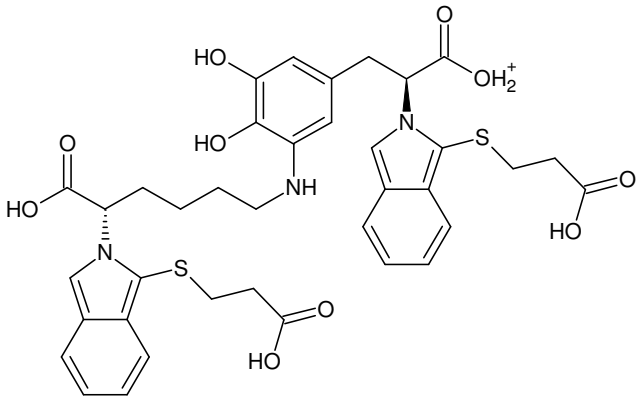

Monoisotopic Mass = 750.214961 Da

Lys-Tyr

<u>Kollagen alpha 1</u>: Trimer aus alpha-2 (I) + 2 alpha-1 (I) (Bos Taurus, UniProt)

Ala	**A**	**349**	**11,2%**
Arg	**R**	**158**	**5,0%**
Asn	N	47	1,5%
Asp	D	90	2,9%
Cys	C	0	0,0%
Gln	Q	84	2,7%
Glu	E	142	4,5%
Gly	**G**	**1036**	**33,1%**
His	H	14	0,4%
Ile	I	36	1,2%
Leu	L	78	2,5%
Lys	K	107	3,4%
Met	M	18	0,6%
Phe	F	39	1,2%
Pro	**P**	**689**	**22,0%**
Ser	S	110	3,5%
Thr	T	52	1,7%
Trp	W	0	0,0%
Tyr	Y	11	0,4%
Val	V	69	2,2%
Pyl	O	0	0,0%
Sec	U	0	0,0%
		3129	100,0%

+MSn [I]: 745 Th – structural elements

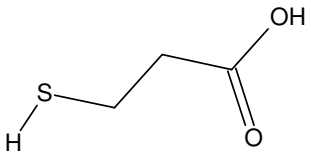

106

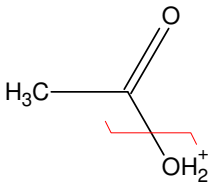

H_2O
18.0106 Da

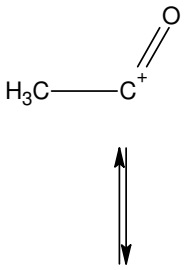

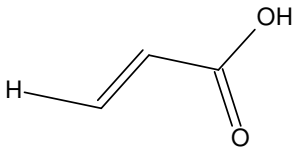

72

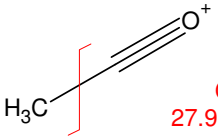

CO
27.9949 Da

H_2O 18

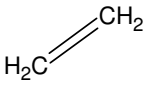

28

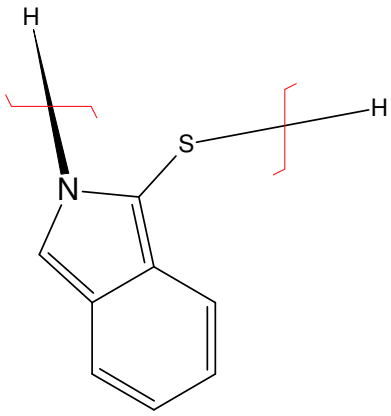

147

Nominal Mass = 147 Da

=> 374

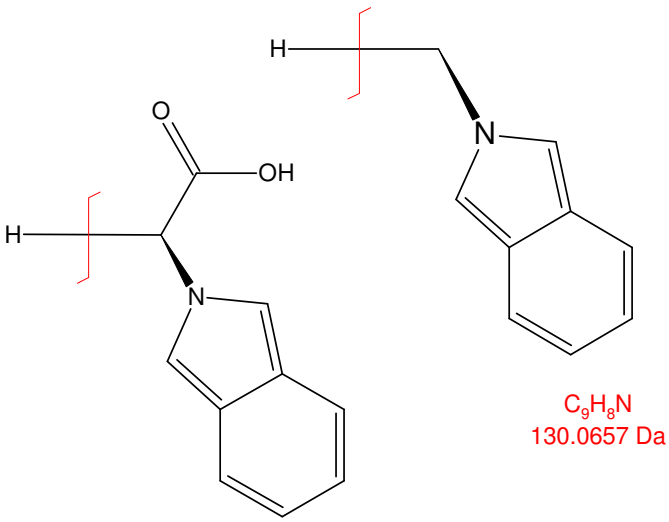

C_9H_8N
130.0657 Da

H_3C—OH 32

$C_{10}H_8NO_2$
174.0555 Da

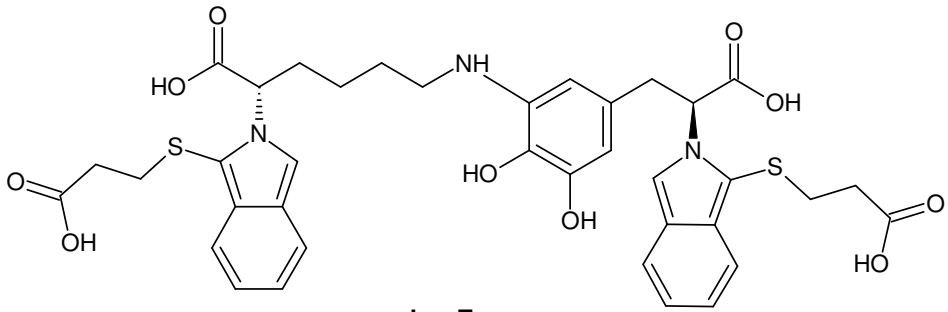

Lys-Tyr

Monoisotopic Mass = 749.207684 Da

+MSn [I]: 745 Th main fragmentation route {I/VIII}

745

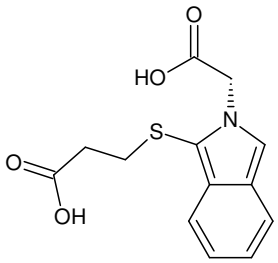

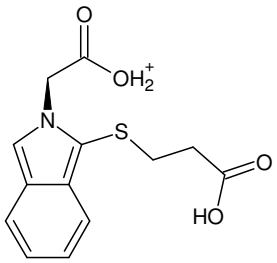

639

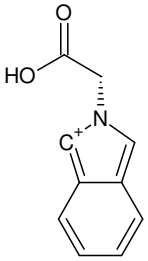

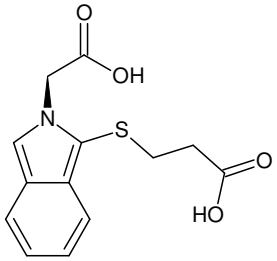

567

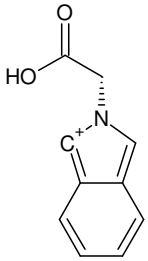

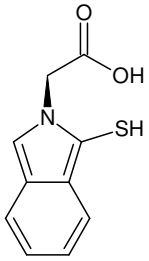

549

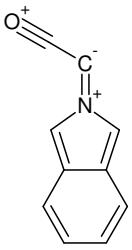

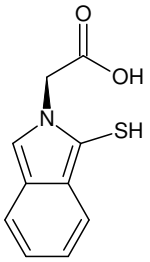

521

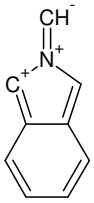

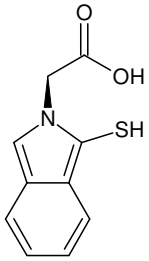

374

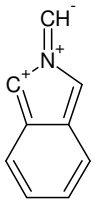

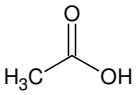

MS_6 und noch keine spezifischen Fragmente...

Monoisotopic Mass = 188.071154 Da

+MSn [I]: 745 Th main fragmentation route {II/VIII}

nächste Fragmentierung: 374 -> 342: -32 Th =>$H_3C—OH$

374-188 = 186

745 - 279 -280 = 186

Compounds found: 594
CH4N3O2S3 MW=185,9465664
CH4N3O4S2 MW=185,9643244
(...)
C12H26O MW=186,1983546
C13H14O MW=186,1044594

-----D--B--E--f-i-l-t-e-r-----
02.02.2011 - 16:48:28,47
akzeptierte DBEs:
2
3
4

C4H10N8O DBE: 4
C5H10N6O2 DBE: 4
C6H10N4OS DBE: 4
C6H10N4O3 DBE: 4
C6H14N6O DBE: 3
C7H10N2O2S DBE: 4
C7H10N2O4 DBE: 4
C7H14N4O2 DBE: 3
C8H10OS2 DBE: 4
C8H10O3S DBE: 4
C8H10O5 DBE: 4
C8H14N2OS DBE: 3
C8H14N2O3 DBE: 3
C8H18N4O DBE: 2
C9H14O2S DBE: 3
C9H14O4 DBE: 3
C9H18N2O2 DBE: 2
C10H18OS DBE: 2
C10H18O3 DBE: 2

19 von 594 Summenformeln

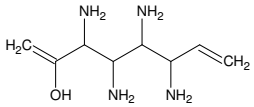

Molecular Formula = $C_8H_{18}N_4O$

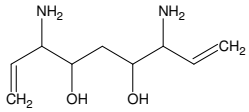

Molecular Formula = $C_9H_{18}N_2O_2$

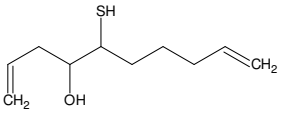

Molecular Formula = $C_{10}H_{18}OS$

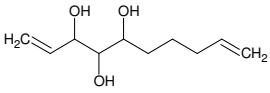

Molecular Formula = $C_{10}H_{18}O_3$

AKP aus zwei Diolen; 10 C sind zu viel für 2 aliphatische Aminosäureseitenketten (max. 8 C).

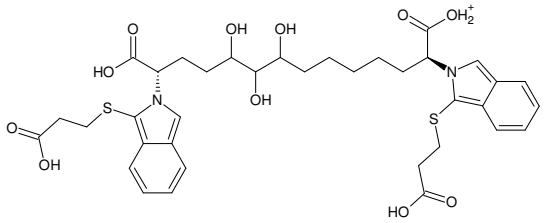

Monoisotopic Mass = 745.24648 Da

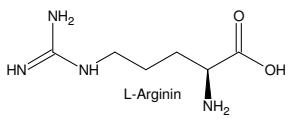

L-Arginin

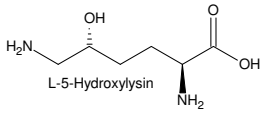

L-5-Hydroxylysin

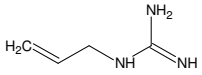

Arginin

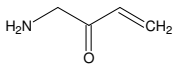

Hydroxylysin-O-aldehyd

1 O zu wenig bei Kondensation => Iminbildung ohne Wasserabspaltung? - eher weniger

S könnte nur aus Met stammen (Cys nicht in der Kollagen-alpha-1-Kette)

Compounds found: 594
CH4N3O2S3 MW=185,9465664
CH4N3O4S2 MW=185,9643244
(...)
C12H26O MW=186,1983546
C13H14O MW=186,1044594

-----D--B--E--f-i-l-t-e-r-----
02.02.2011 - 17:06:30,14
akzeptierte DBEs:
5
6
7
8

C2H6N10O DBE: 5
C3H6N8O2 DBE: 5
C4H6N6OS DBE: 5
C4H6N6O3 DBE: 5
C5H6N4O2S DBE: 5
C5H6N4O4 DBE: 5
C6H6N2OS2 DBE: 5
C6H6N2O3S DBE: 5
C6H6N2O5 DBE: 5
C7H6O2S2 DBE: 5
C7H6O4S DBE: 5
C7H6O6 DBE: 5
C11H10N2O DBE: 8
C12H10O2 DBE: 8
C13H14O DBE: 7

15 von 594 Summenformeln
keine SF mit 6 DBEs => nichts mit Tyr & Amin

+MSn [I]: 745 Th main fragmentation route {III/VIII}

Compounds found: 16
CH2NO MW=44,0136382
CH4N2 MW=44,0374464
CH16O MW=44,1201086
CH18N MW=44,1439168
CO2 MW=43,98983
CS MW=43,972072
C2H4O MW=44,0262134
C2H6N MW=44,0500216
C2H20 MW=44,156492
C3H8 MW=44,0625968
H2N3 MW=44,0248712
H12O2 MW=44,0837252
H12S MW=44,0659672
H14NO MW=44,1075334
H16N2 MW=44,1313416
N2O MW=44,001063

-----D--B--E--f-i-l-t-e-r-----
02.02.2011 - 15:37:16,67
akzeptierte DBEs:
0
1
2
3
4

CH4N2 DBE: 1
CO2 DBE: 2
CS DBE: 2
C2H4O DBE: 1
C3H8 DBE: 0
N2O DBE: 2

6 von 16 Summenformeln

C, H, N, O & S; 1/2 Da Toleranz

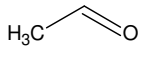
Molecular Formula = C_2H_4O

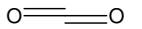
Molecular Formula = CO_2

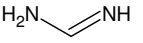
Molecular Formula = CH_4N_2

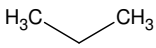
Molecular Formula = C_3H_8


oxadiazirene

Molecular Formula = N_2O

Compounds found: 55
CH2N3O MW=72,0197862
CH4N4 MW=72,0435944
(...)
H30N3 MW=72,24396
N4O MW=72,007211

-----D--B--E--f-i-l-t-e-r-----
02.02.2011 - 14:58:46,66
akzeptierte DBEs:
0
1
2
3
4

CH4N4 DBE: 2
CN2O2 DBE: 3
CN2S DBE: 3
C2H4N2O DBE: 2
C2OS DBE: 3
C2O3 DBE: 3
C3H4O2 DBE: 2
C3H4S DBE: 2
C3H8N2 DBE: 1
C4H8O DBE: 1
C5H12 DBE: 0
N4O DBE: 3

12 von 55 Summenformeln

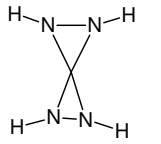
Molecular Formula = CH_4N_4

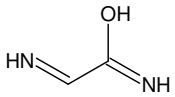
Molecular Formula = $C_2H_4N_2O$

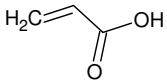
Molecular Formula = $C_3H_4O_2$

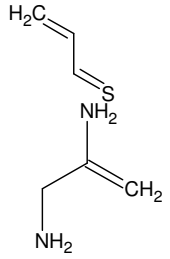
Molecular Formula = C_3H_4S

Molecular Formula = $C_3H_8N_2$

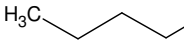
Molecular Formula = C_5H_{12}

Compounds found: 478
CHN5O2S MW=146,9850966
CHN5O4 MW=147,0028546
(...)
H72N3S MW=146,5446652
H74N4O MW=146,5862314

-----D--B--E--f-i-l-t-e-r-----
02.02.2011 - 15:46:14,87
akzeptierte DBEs:
0
1
2
3
4

CHN5O2S DBE: 4
CHN5O4 DBE: 4
CHN5S2 DBE: 4
CH5N7O2 DBE: 3
CH5N7S DBE: 3
CH9N9 DBE: 2
C2HN3OS2 DBE: 4
C2HN3O3S DBE: 4
C2HN3O5 DBE: 4
C2H5N5OS DBE: 3
C2H5N5O3 DBE: 3
C2H9N7O DBE: 2
C3HNO2S2 DBE: 4
C3HNO4S DBE: 4
C3HNO6 DBE: 4
C3HNS3 DBE: 4
C3H5N3O2S DBE: 3
C3H5N3O4 DBE: 3
C3H5N3S2 DBE: 3
C3H9N5O2 DBE: 2
C3H9N5S DBE: 2
C3H13N7 DBE: 1
C4H5NOS2 DBE: 3
C4H5NO3S DBE: 3
C4H5NO5 DBE: 3
C4H9N3OS DBE: 2
C4H9N3O3 DBE: 2
C4H13N5O DBE: 1
C5H9NO2S DBE: 2
C5H9NO4 DBE: 2
C5H9NS2 DBE: 2
C5H13N3O2 DBE: 1
C5H13N3S DBE: 1
C5H17N5 DBE: 0
C6H13NOS DBE: 1
C6H13NO3 DBE: 1
C6H17N3O DBE: 0
C7H17NO2 DBE: 0
C7H17NS DBE: 0
HN7OS DBE: 4
HN7O3 DBE: 4
H5N9O DBE: 3

42 von 478 Summenformeln

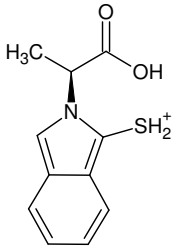
Monoisotopic Mass = 222.058875 Da

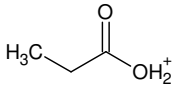
Monoisotopic Mass = 75.044605 Da

222 - 75 = 147


Molecular Formula = C_8H_5NS
C8H5NS DBE: 7

Monoisotopic Mass = 147.01427 Da

+MSn [I]: 745 Th main fragmentation route {IV/VIII}

745 - 279 - 280 = **186**

"mit H_4N_2"

Compounds found: 596
CH4N3O2S3 MW=185,9465664
CH4N3O4S2 MW=185,9643244
(...)
H93N2O4 MW=185,7134958
H93N2S2 MW=185,6779798

-----D--B--E--f-i-l-t-e-r-----
08.02.2011 - 12:42:42,97
akzeptierte DBEs:
2
3
4

C3H10N10 DBE: 4
C4H10N8O DBE: 4
C5H10N6O2 DBE: 4
C5H10N6S DBE: 4
C5H14N8 DBE: 3
C6H10N4OS DBE: 4
C6H10N4O3 DBE: 4
C6H14N6O DBE: 3
C7H10N2O2S DBE: 4
C7H10N2O4 DBE: 4
C7H10N2S2 DBE: 4
C7H14N4O2 DBE: 3
C7H14N4S DBE: 3
C7H18N6 DBE: 2
C8H14N2OS DBE: 3
C8H14N2O3 DBE: 3
C8H18N4O DBE: 2
C9H18N2O2 DBE: 2
C9H18N2S DBE: 2

19 von 596 Summenformeln

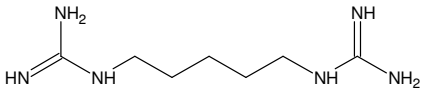

Molecular Formula = $C_7H_{18}N_6$

zu wenig C für 2 x Arg, zu viel N für andere Kombinationen

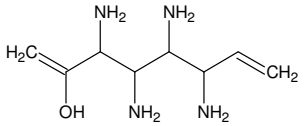

Molecular Formula = $C_8H_{18}N_4O$

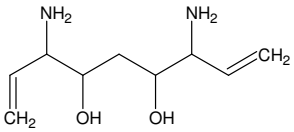

Molecular Formula = $C_9H_{18}N_2O_2$

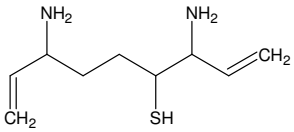

Molecular Formula = $C_9H_{18}N_2S$

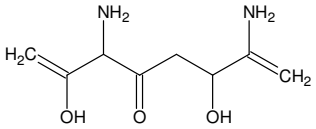

Molecular Formula = $C_8H_{14}N_2O_3$

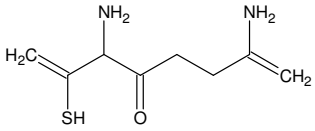

Molecular Formula = $C_8H_{14}N_2OS$

Compounds found: 596
CH4N3O2S3 MW=185,9465664
CH4N3O4S2 MW=185,9643244
(...)
H93N2O4 MW=185,7134958
H93N2S2 MW=185,6779798

-----D--B--E--f-i-l-t-e-r-----
08.02.2011 - 12:45:09,97
akzeptierte DBEs:
5
6
7
8

CH6N12 DBE: 5
C2H6N10O DBE: 5
C3H6N8O2 DBE: 5
C3H6N8S DBE: 5
C4H6N6OS DBE: 5
C4H6N6O3 DBE: 5
C5H6N4O2S DBE: 5
C5H6N4O4 DBE: 5
C5H6N4S2 DBE: 5
C6H6N2OS2 DBE: 5
C6H6N2O3S DBE: 5
C6H6N2O5 DBE: 5
C10H10N4 DBE: 8
C11H10N2O DBE: 8
C12H14N2 DBE: 7

15 von 596 Summenformeln

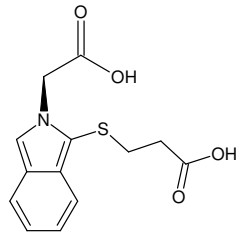

Monoisotopic Mass = 279.05653 Da

+MSn [I]: 745 Th main fragmentation route {V/VIII}

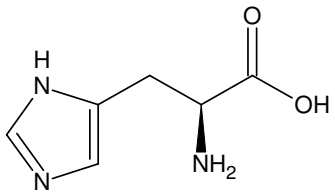

Compounds found: 138
C4H2N4O5 MW=186,0025202
C4H4N5O4 MW=186,0263284
(...)
C12N3 MW=186,009222
C13H2N2 MW=186,0217972

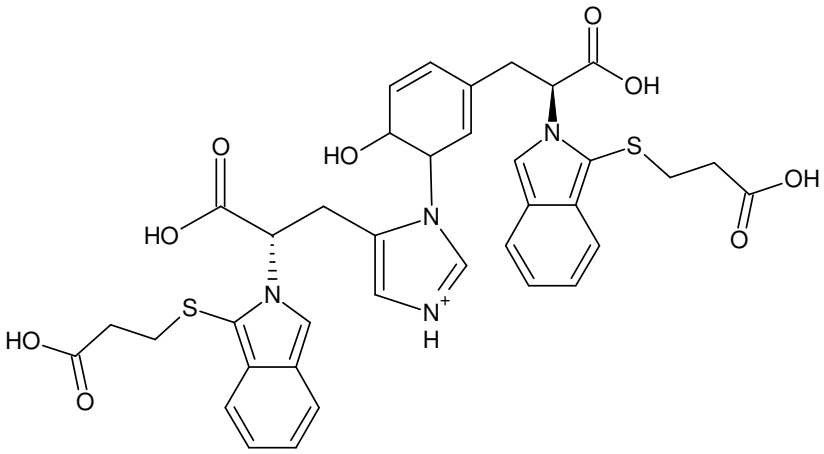

-----D--B--E--f-i-l-t-e-r-----
09.02.2011 - 23:11:58,65
akzeptierte DBEs:
5
6
7
8
9
10

Monoisotopic Mass = 745.200198 Da

C4H2N4O5 DBE: 6
C4H6N6O3 DBE: 5
C5H2N2O6 DBE: 6
C5H6N4O4 DBE: 5
C6H2N8 DBE: 10
C6H6N2O5 DBE: 5
C7H2N6O DBE: 10
C8H2N4O2 DBE: 10
C8H6N6 DBE: 9
C9H2N2O3 DBE: 10
C9H6N4O DBE: 9
C10H6N2O2 DBE: 9
C10H10N4 DBE: 8
C11H10N2O DBE: 8
C12H14N2 DBE: 7

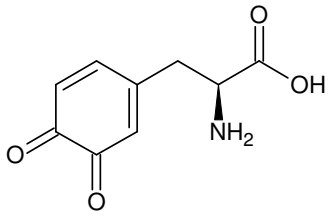

o-Dopachinon

15 von 138 Summenformeln

+MSn [I]: 745 Th main fragmentation route {VI/VIII}

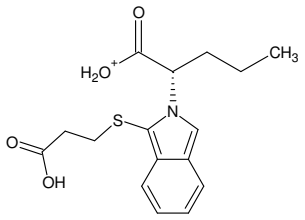

Monoisotopic Mass = 322.111305 Da

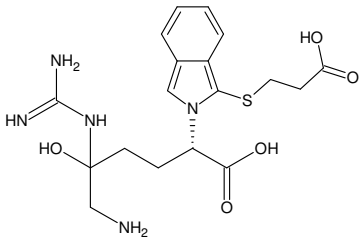

Monoisotopic Mass = 423.157641 Da

745 -> 322: Fragmentierung am zentralen N?

nächste Fragmentierung: 322 -> 217 (- 105 Da) => mod(nN, 2) == 1

322 - 280 = 42

Compounds found: 13
CH2N2 MW=42,0217972
CH14O MW=42,1044594
CH16N MW=42,1282676
CNO MW=41,997989
C2H2O MW=42,0105642
C2H4N MW=42,0343724
C2H18 MW=42,1408428
C3H6 MW=42,0469476
H10S MW=42,050318
H12NO MW=42,0918842
H10O2 MW=42,068076
H14N2 MW=42,1156924
N3 MW=42,009222

-----D--B--E--f-i-l-t-e-r-----
03.02.2011 - 20:18:36,53
akzeptierte DBEs:
0
1
2
3
4

CH2N2 DBE: 2
C2H2O DBE: 2
C3H6 DBE: 1

3 von 13 Summenformeln

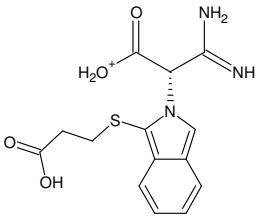

Monoisotopic Mass = 322.086153 Da

Molecular Formula = C H$_2$ N$_2$

Molecular Formula = C$_2$ H$_2$ O

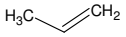

Molecular Formula = C$_3$ H$_6$

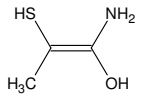

Molecular Formula = C$_3$ H$_7$ N O S
Monoisotopic Mass = 105.024835 Da

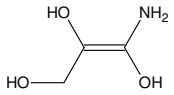

Molecular Formula = C$_3$ H$_7$ N O$_3$
Monoisotopic Mass = 105.042594 Da

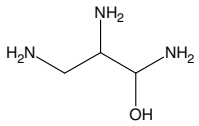

Molecular Formula = C$_3$ H$_{11}$ N$_3$ O
Monoisotopic Mass = 105.090212 Da

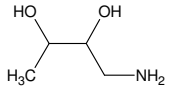

Molecular Formula = C$_4$ H$_{11}$ N O$_2$
Monoisotopic Mass = 105.078979 Da

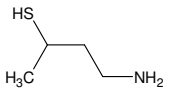

Molecular Formula = C$_4$ H$_{11}$ N S
Monoisotopic Mass = 105.06122 Da

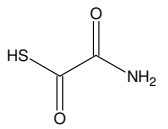

Molecular Formula = C$_2$ H$_3$ N O$_2$ S
Monoisotopic Mass = 104.98845 Da

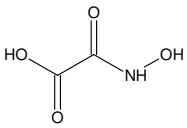

Molecular Formula = C$_2$ H$_3$ N O$_4$
Monoisotopic Mass = 105.006209 Da

+MSn [I]: 745 Th main fragmentation route {VII/VIII}

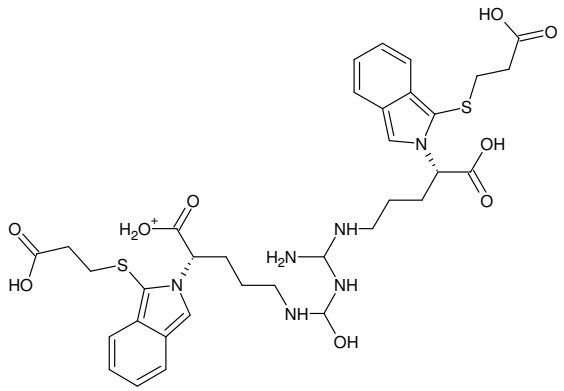

Monoisotopic Mass = 745.268946 Da
AKP aus 2x Citrullin

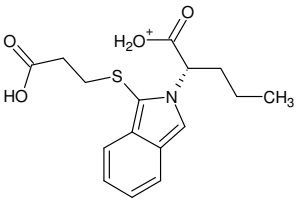

Monoisotopic Mass = 322.111305 Da

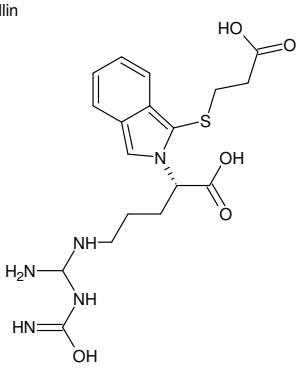

Monoisotopic Mass = 423.157641 Da

423 - 279 = 144
Compounds found: 459

CH2N7O2	MW=144,0269972
CH2N7S	MW=144,0092392
(...)	
O7S	MW=143,936477
O9	MW=143,954235

-----D--B--E--f-i-l-t-e-r-----
03.02.2011 - 20:42:04,96
akzeptierte DBEs:
1
2
3
4

CH4N8O	DBE: 4
C2H4N6O2	DBE: 4
C2H4N6S	DBE: 4
C2H8N8	DBE: 3
C3H4N4OS	DBE: 4
C3H4N4O3	DBE: 4
C3H8N6O	DBE: 3
C4H4N2O2S	DBE: 4
C4H4N2O4	DBE: 4
C4H4N2S2	DBE: 4
C4H8N4O2	DBE: 3
C4H8N4S	DBE: 3
C4H12N6	DBE: 2
C5H4OS2	DBE: 4
C5H4O3S	DBE: 4
C5H4O5	DBE: 4
C5H8N2OS	DBE: 3
C5H8N2O3	DBE: 3
C5H12N4O	DBE: 2
C6H8O2S	DBE: 3
C6H8O4	DBE: 3
C6H8S2	DBE: 3
C6H12N2O2	DBE: 2
C6H12N2S	DBE: 2
C6H16N4	DBE: 1
C7H12OS	DBE: 2
C7H12O3	DBE: 2
C7H16N2O	DBE: 1
C8H16O2	DBE: 1
C8H16S	DBE: 1
H4N10	DBE: 4
OS4	DBE: 1
O3S3	DBE: 1
O5S2	DBE: 1
O7S	DBE: 1
O9	DBE: 1

36 von 459 Summenformeln

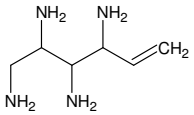

Molecular Formula = $C_6H_{16}N_4$

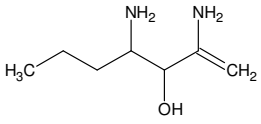

Molecular Formula = $C_7H_{16}N_2O$

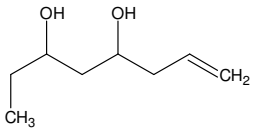

Molecular Formula = $C_8H_{16}O_2$

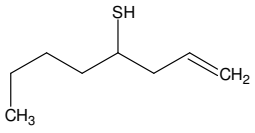

Molecular Formula = $C_8H_{16}S$

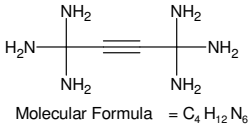

Molecular Formula = $C_4H_{12}N_6$

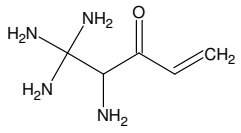

Molecular Formula = $C_5H_{12}N_4O$

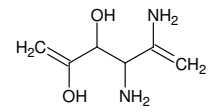

Molecular Formula = $C_6H_{12}N_2O_2$

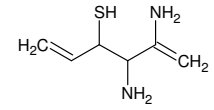

Molecular Formula = $C_6H_{12}N_2S$

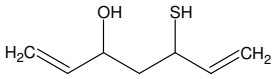

Molecular Formula = $C_7H_{12}OS$

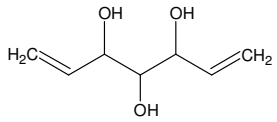

Molecular Formula = $C_7H_{12}O_3$

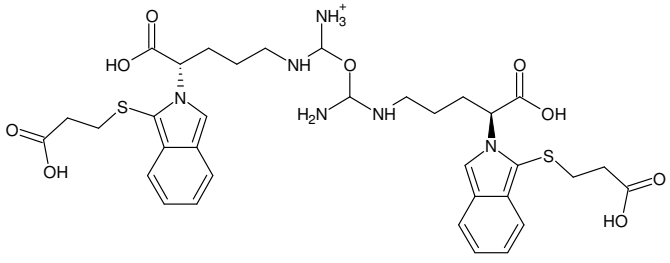

Monoisotopic Mass = 745.268946 Da

+MSn [I]: 745 Th main fragmentation route {VIII/VIII}

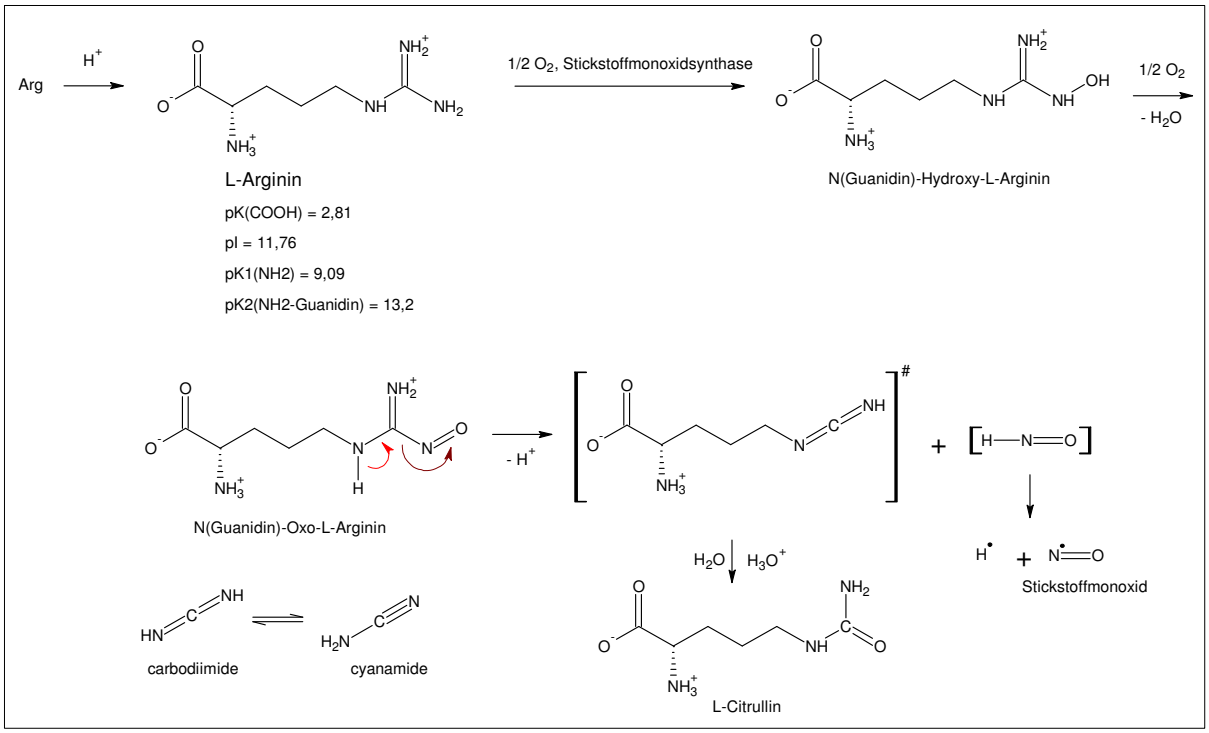

Arginin zu Citrullin: nitric-oxide synthase (**1.14.13.39**) oder protein-arginine deiminase (**3.5.3.15**) - Die Hydrolase funktioniert nachgewiesenermaßen mit proteingebundenem Arginin.

Tyrosinase: EC **1.14.18.1** - monophenol monooxygenase & EC **1.10.3.1** - catechol oxidase

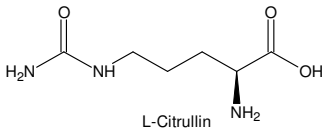

EC

1 Oxidoreductases

1.14 Acting on paired donors, with O2 as oxidant and incorporation or reduction of oxygen. The oxygen incorporated need not be derived from O2

1.14.18 With another compound (other than 2-oxoglutarate, NADH, NADPH, reduced flavin or flavoprotein, reduced iron-sulfur protein, reduced pteridin or reduced ascorbate) as one donor, and incorporation of one atom of oxygen into the other donor

1.14.18.1 **monophenol monooxygenase**

1.10 Acting on diphenols and related substances as donors

1.10.3 With oxygen as acceptor

1.10.3.1 **catechol oxidase**

1.14.13 With NADH or NADPH as one donor, and incorporation of one atom of oxygen into the other donor

1.14.13.39 **nitric-oxide synthase**

3 Hydrolases

3.5 Acting on carbon-nitrogen bonds, other than peptide bonds

3.5.3 In linear amidines

3.5.3.15 **protein-arginine deiminase**

+MSn [I]: 745 Th – reaction mechanism of nitric-oxide synthase

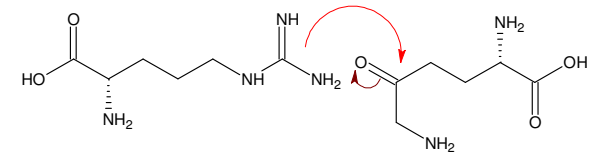

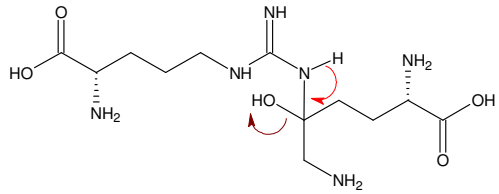

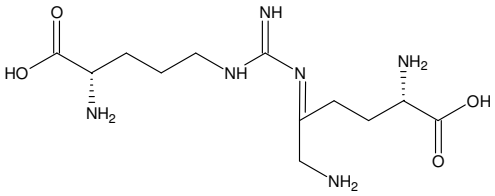

um 20 Da zu leicht (bzw. nach Reduktion 18 Da)

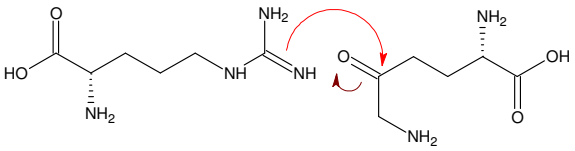

Würden Imine so reagieren, so wären sie nicht isolierbar.

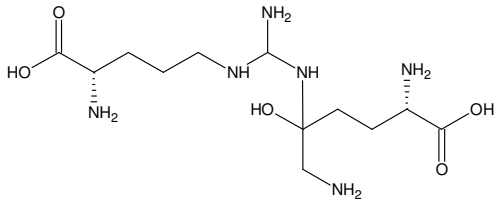

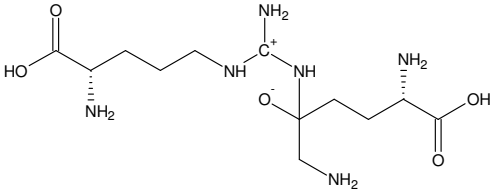

De- / Reprotonierung

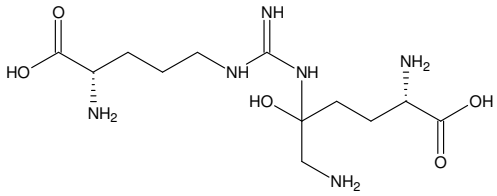

+MSn [I]: 745 Th – putative reactions at the guanidino-N

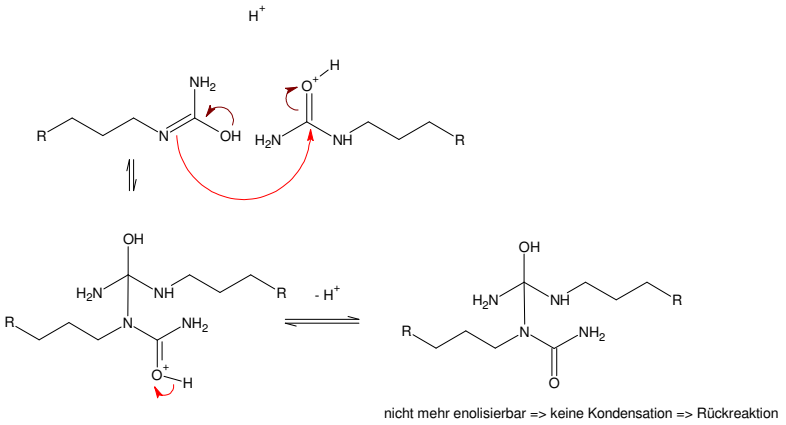

Citrullin ist aber in reiner Form und in wässriger Lösung stabil.

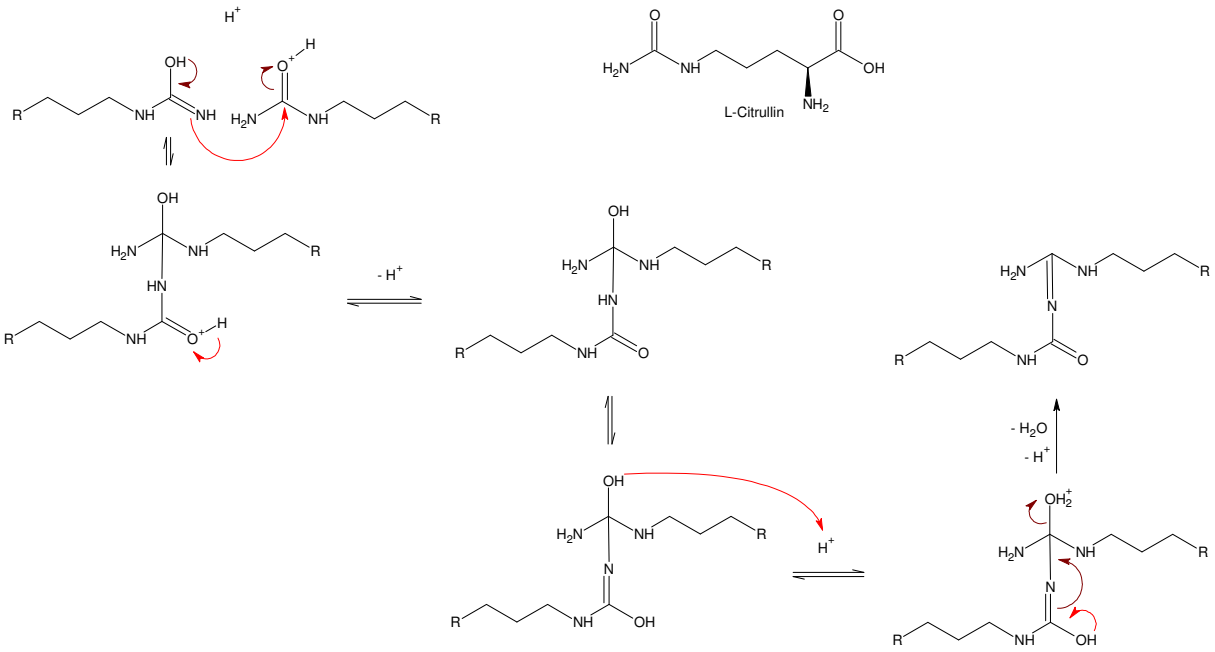

+MSn [I]: 745 Th – aldol condensation with citrulline

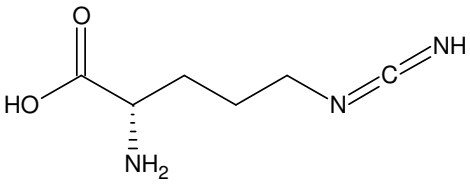

L-N-(Iminomethylen)ornithin

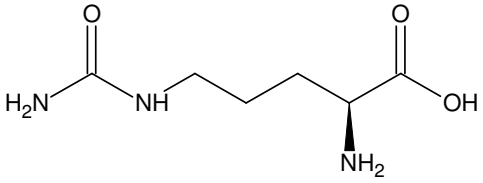

L-Citrullin

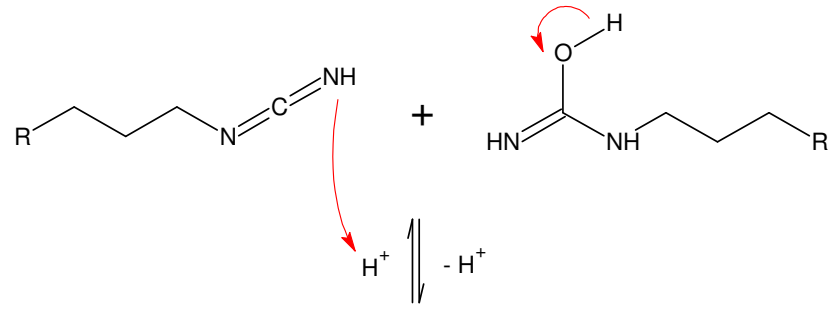

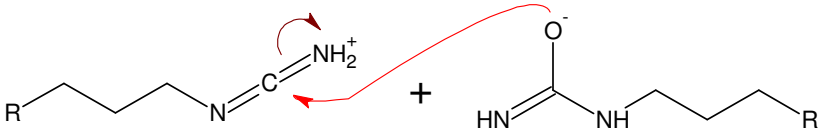

C im Carbodiimid aktiviert (Peptidknüpfungsmethode mit DCC)

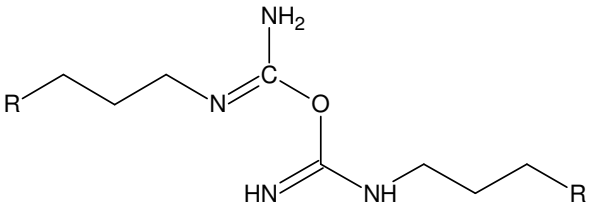

+MSn [I]: 745 Th – coupling between the intermediate and the hydrolysed product of nitric-oxide synthase

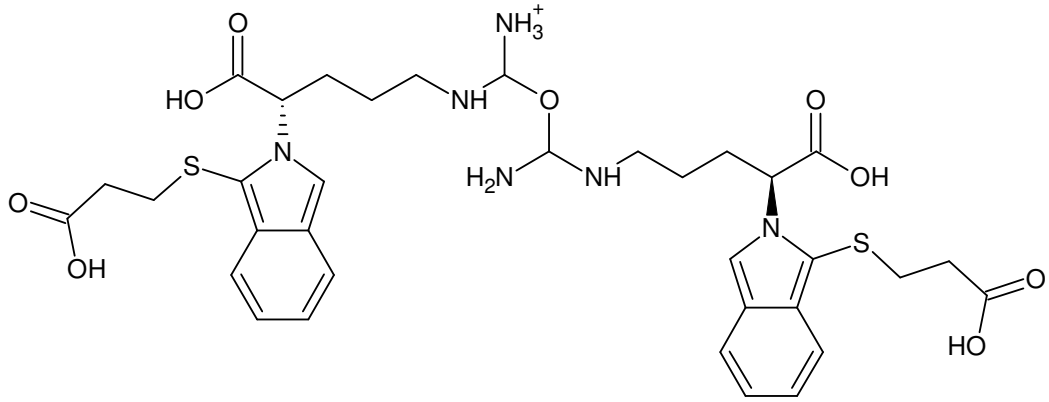

Monoisotopic Mass = 745.268946 Da

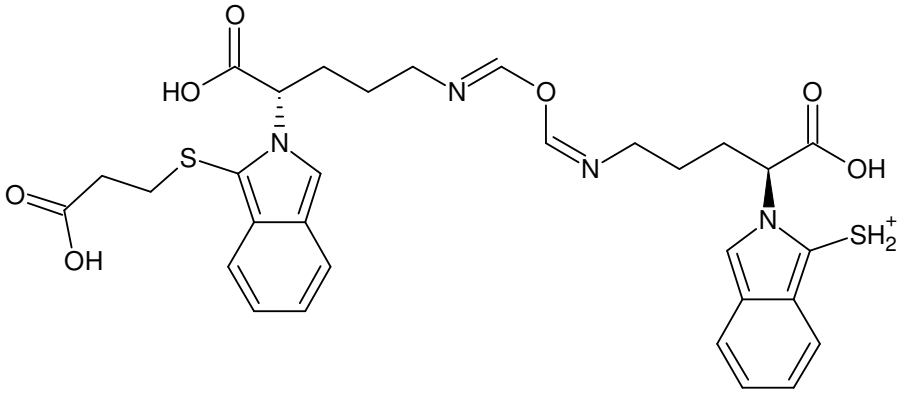

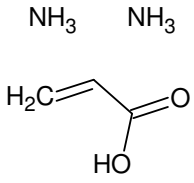

106.074228 Da

Monoisotopic Mass = 639.194718 Da

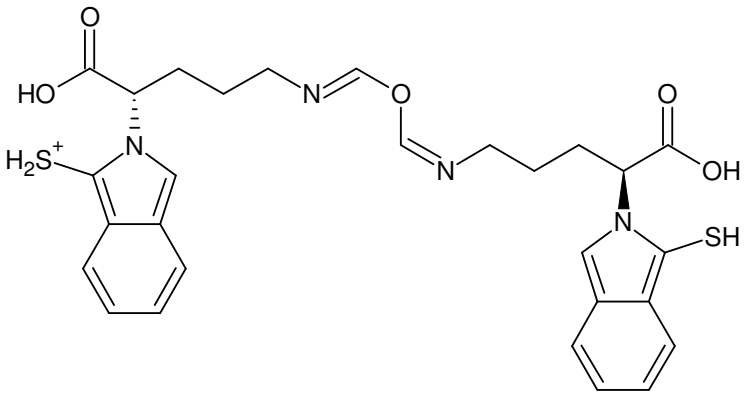

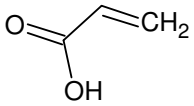

72.02113 Da

Monoisotopic Mass = 567.173588 Da

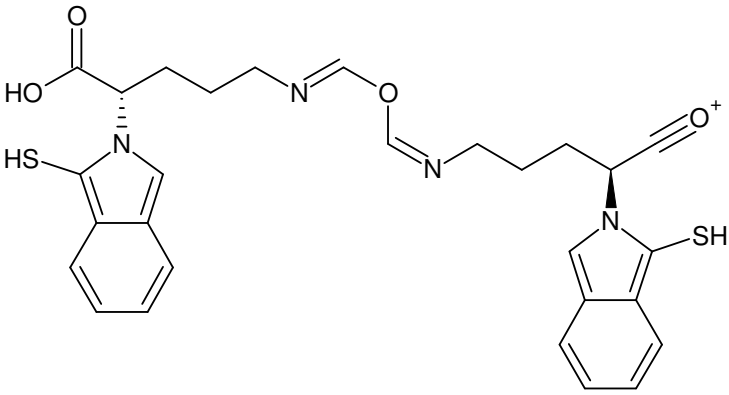

H_2O

18.010565 Da

Monoisotopic Mass = 549.163023 Da

+MSn [I]: 745 -> 639 -> 567 -> 549

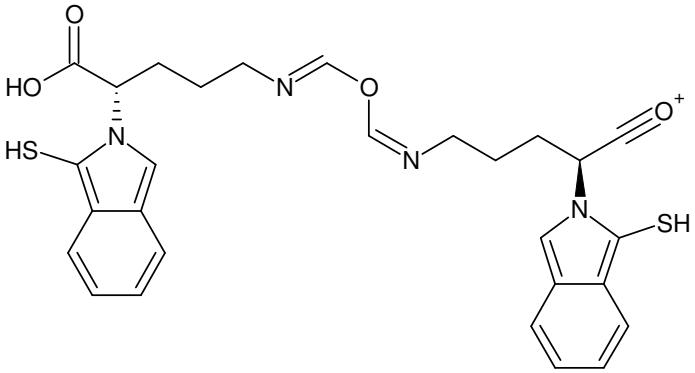

Monoisotopic Mass = 549.163023 Da

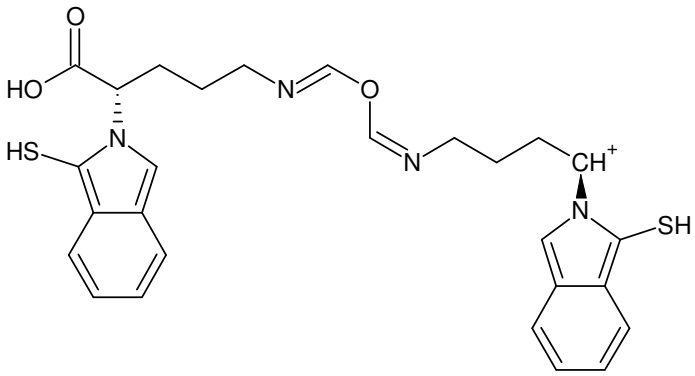

27.994915 Da

Monoisotopic Mass = 521.168108 Da

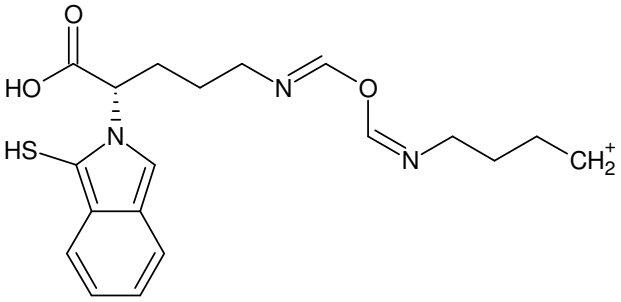

147.01427 Da

Monoisotopic Mass = 374.153838 Da

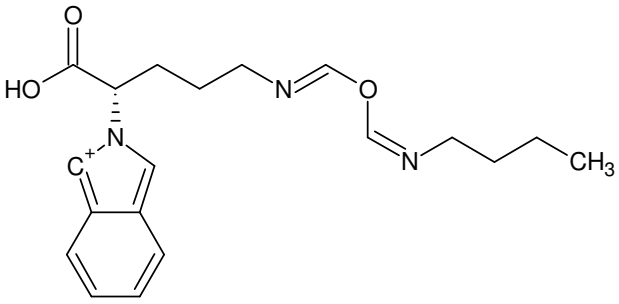

S:

31.972071 Da

Monoisotopic Mass = 342.181767 Da

+MSn [I]: [745 -> 639 -> 567 -> 549] -> 521 -> 374 -> 342

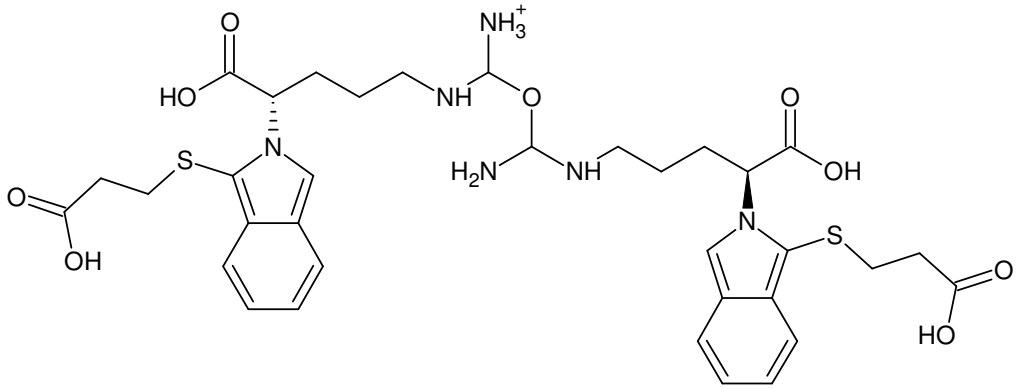

Monoisotopic Mass = 745.268946 Da

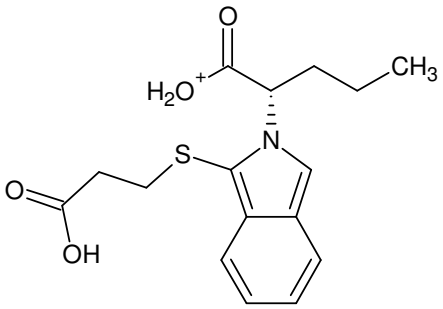

Monoisotopic Mass = 322.111305 Da

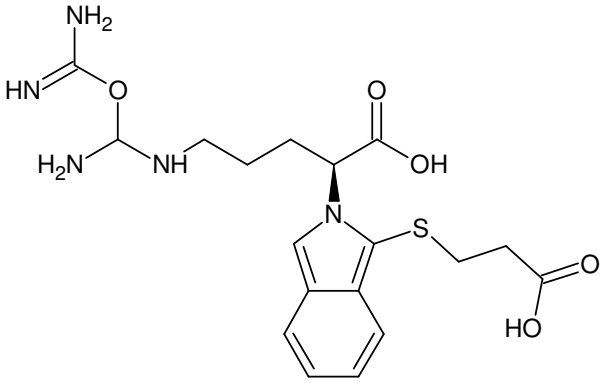

423.157641 Da

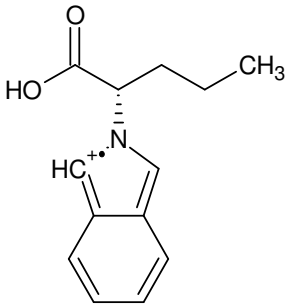

Monoisotopic Mass = 217.110279 Da

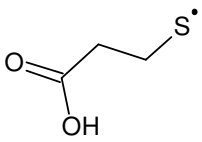

105.001026 Da

+MSn [I]: 745 -> 322 -> 217

II

+MS^n

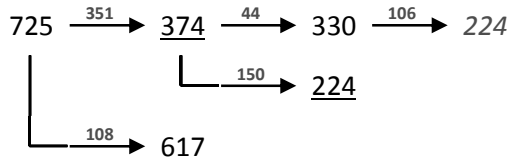

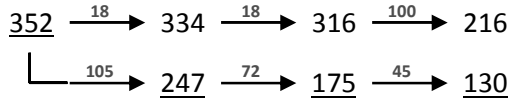

-MS^n

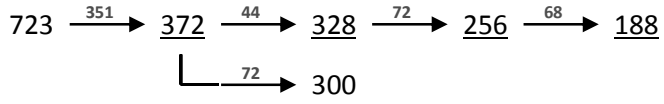

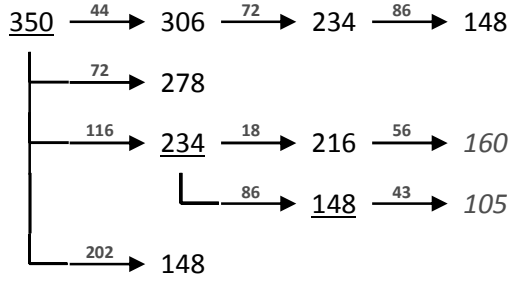

isotopic fingerprint:

peak area / % of monoisotopic	**+1**	**+2**	**+3**
theoretical ($C_{34}H_{40}N_2NaO_{10}S_2^-$):	40,1	18,9	5,4
measured (-722,8 Th):	30,3	17,4	4,5
measured (725,0 Th):	27,8	19,4	8,1
theoretical ($C_{17}H_{22}NO_5S^+$):	20,1	7,5	1,2
measured (352,2 Th):	15,5	8,2	0,9
measured (-349,8 Th):	18,4	6,8	0,9

Figure XIII-IV MS^n analysis of II

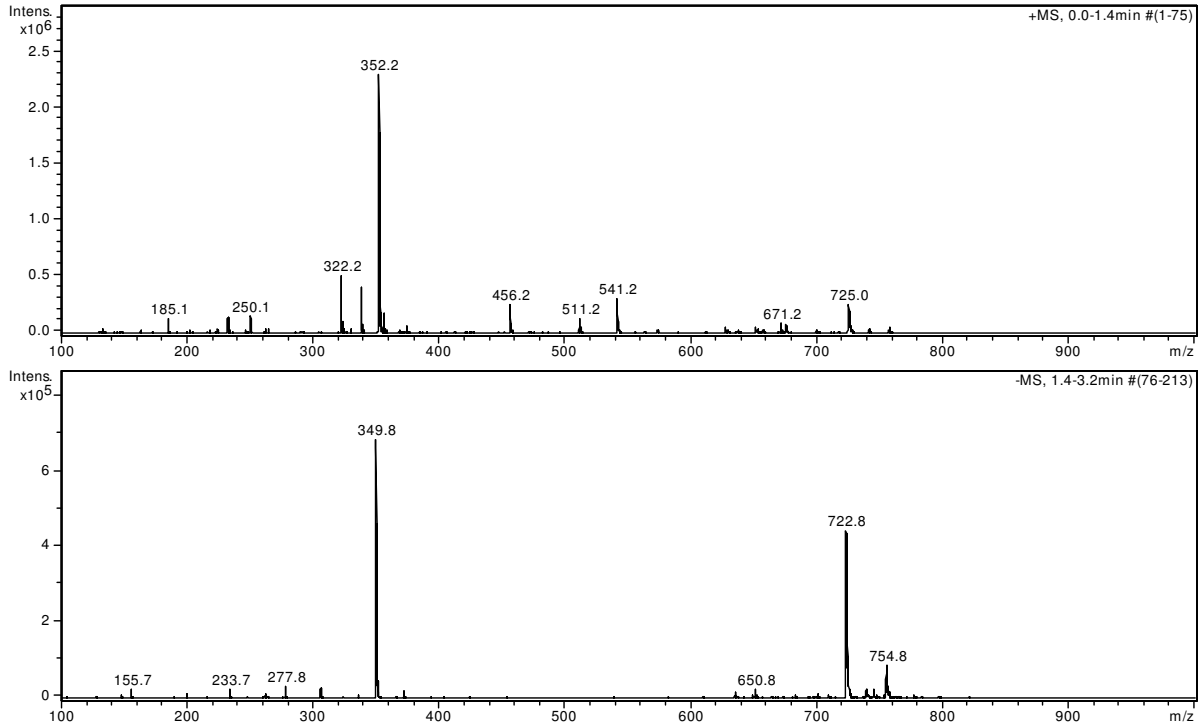

Figure XIII-V II: 14,5 – 15,1 min, 1 ‰ FA, 33 % ACN in ddH_2O; full scan MS^1

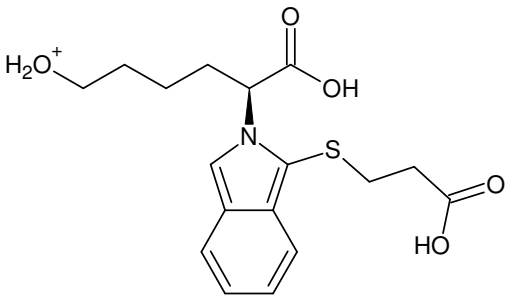

Monoisotopic Mass = 352.12187 Da

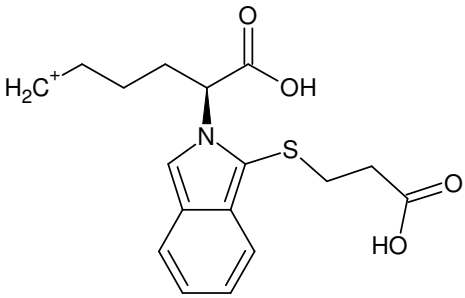

H_2O
water

Monoisotopic Mass = 334.111305 Da

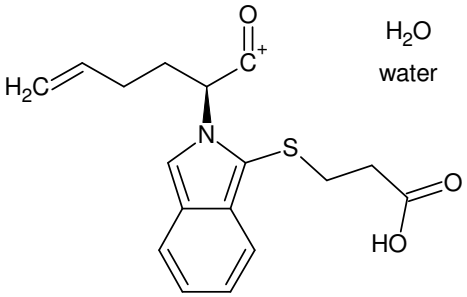

H_2O
water

Monoisotopic Mass = 316.10074 Da

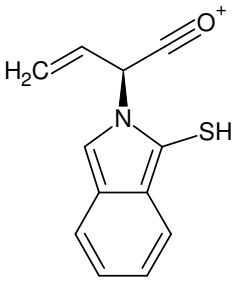

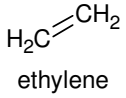

ethylene

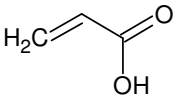

acrylic acid

Monoisotopic Mass = 216.04831 Da

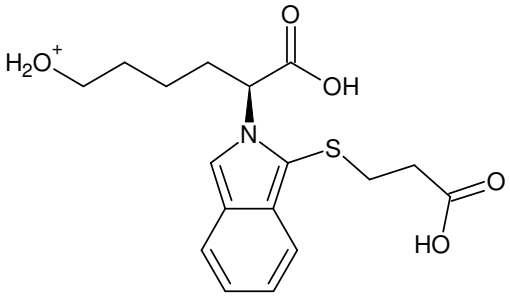

Monoisotopic Mass = 352.12187 Da

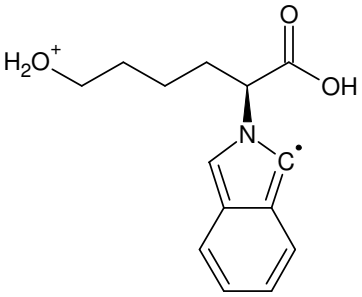

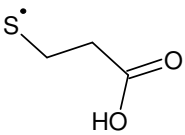

105.001024 Da

Monoisotopic Mass = 247.120295 Da

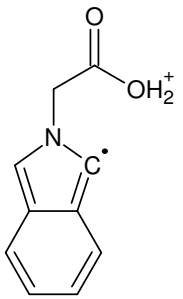

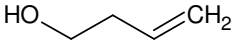

72.057515 Da

Monoisotopic Mass = 175.06278 Da

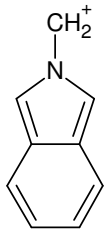

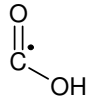

44.997654 Da

Monoisotopic Mass = 130.065126 Da

+MSn [II]: 352 -> 334 -> 316 -> 216 and 352 -> 247 -> 175 -> 130

352 - 247 = **105**
Compounds found: 163
CHN2O2S MW=104,9758746
CHN2O4 MW=104,9936326
(...)
H47N3O MW=105,3718932
H49N4 MW=105,3957014

-----D--B--E--f-i-l-t-e-r-----
10.02.2011 - 14:37:29,73
akzeptierte DBEs:
-1
0
1
2

CH3N3OS DBE: 2
CH3N3O3 DBE: 2
CH7N5O DBE: 1
C2H3NO2S DBE: 2
C2H3NO4 DBE: 2
C2H3NS2 DBE: 2
C2H7N3O2 DBE: 1
C2H7N3S DBE: 1
C2H11N5 DBE: 0
C3H7NOS DBE: 1
C3H7NO3 DBE: 1
C3H11N3O DBE: 0
C4H11NO2 DBE: 0
C4H11NS DBE: 0
C4H15N3 DBE: -1
C5H15NO DBE: -1
H3N5O2 DBE: 2
H3N5S DBE: 2
H7N7 DBE: 1

19 von 163 Summenformeln

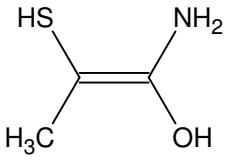

Molecular Formula = $C_3 H_7 N O S$

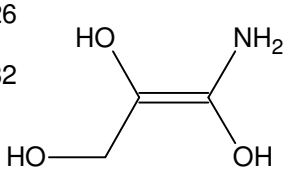

Molecular Formula = $C_3 H_7 N O_3$

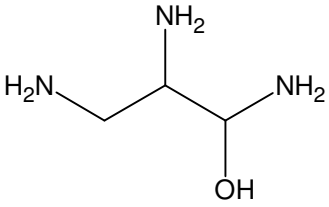

Molecular Formula = $C_3 H_{11} N_3 O$

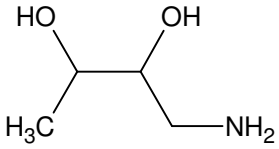

Molecular Formula = $C_4 H_{11} N O_2$

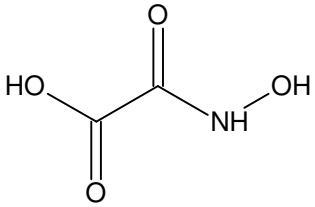

Molecular Formula = $C_2 H_3 N O_4$

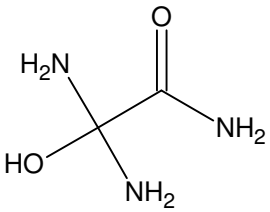

Molecular Formula = $C_2 H_7 N_3 O_2$

+MSn [II]: 352 -> 247; possible 105 Da even-electron losses

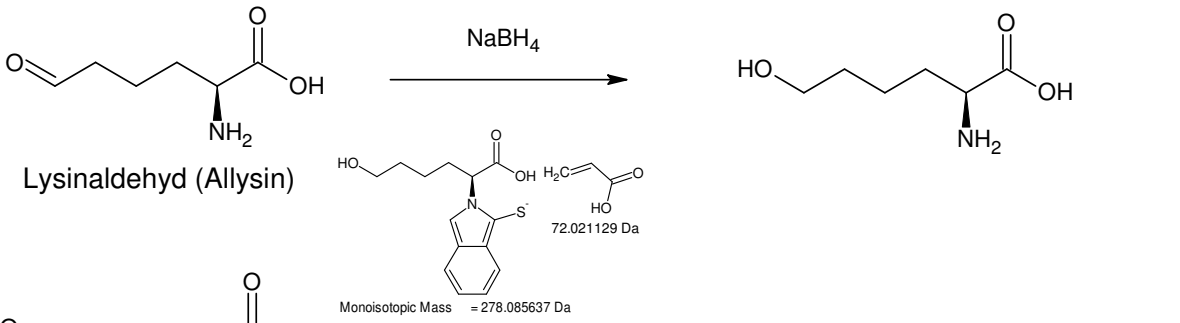

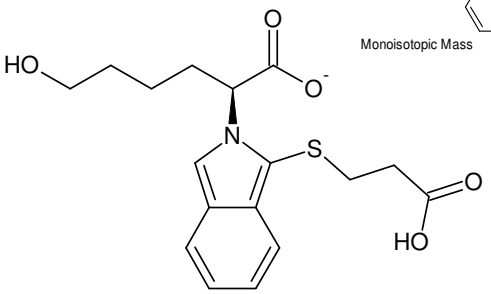

Monoisotopic Mass = 350.10622 Da

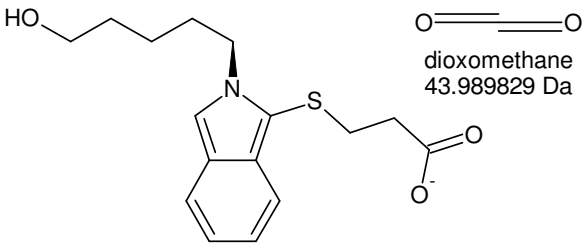

Monoisotopic Mass = 306.11639 Da

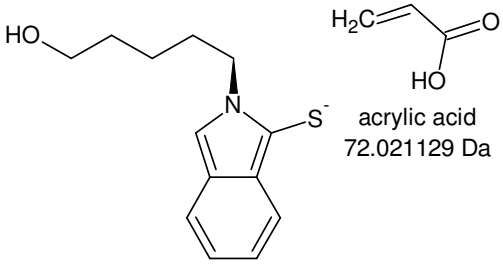

Monoisotopic Mass = 234.09526 Da

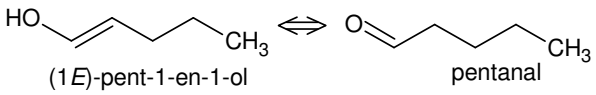

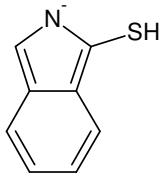

86.073165 Da

Monoisotopic Mass = 148.022095 Da

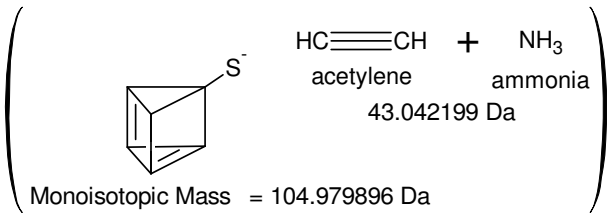

Monoisotopic Mass = 104.979896 Da

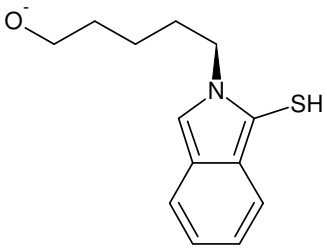

Monoisotopic Mass = 234.09526 Da

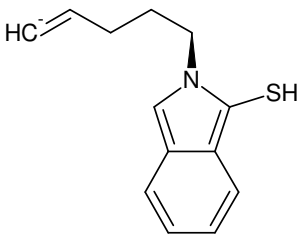

Monoisotopic Mass = 216.084695 Da

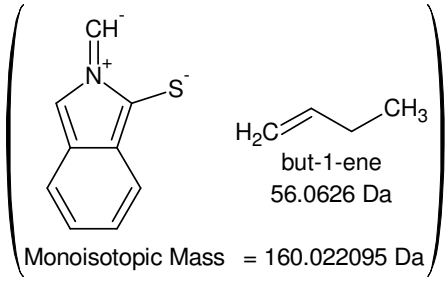

Monoisotopic Mass = 160.022095 Da

-MSn[II]: 350 -> 278, 306 -> 234 -> 148 -> (105) and [350 -> 306 -> 234] -> 216 -> (160)

-MSn: 350 - 278 = **72**
+MSn: 247 - 175 = **72**
Compounds found: 55
CH2N3O MW=72,0197862
CH4N4 MW=72,0435944
(...)
H30N3 MW=72,24396
N4O MW=72,007211

-----D--B--E--f-i-l-t-e-r-----
10.02.2011 - 13:09:16,27
akzeptierte DBEs:
1
2
3
4
5
6
7
8

CH4N4 DBE: 2
CN2O2 DBE: 3
CN2S DBE: 3
C2H4N2O DBE: 2
C2OS DBE: 3
C2O3 DBE: 3
C3H4O2 DBE: 2
C3H4S DBE: 2
C3H8N2 DBE: 1
C4H8O DBE: 1
C6 DBE: 7
N4O DBE: 3

12 von 55 Summenformeln

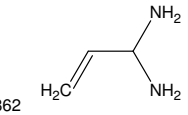

Molecular Formula = $C_3H_8N_2$

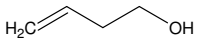

Molecular Formula = **C_4H_8O**

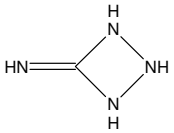

Molecular Formula = CH_4N_4

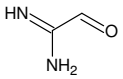

Molecular Formula = $C_2H_4N_2O$

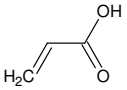

Molecular Formula = **$C_3H_4O_2$**

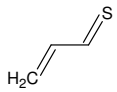

Molecular Formula = C_3H_4S

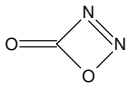

Molecular Formula = CN_2O_2

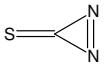

Molecular Formula = CN_2S

Molecular Formula = C_2OS

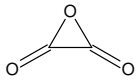

Molecular Formula = C_2O_3

Molecular Formula = N_4O

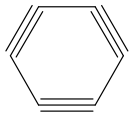
Molecular Formula = C_6

148 - 105 = **43**
Compounds found: 13
CHNO MW=43,0058136
CH3N2 MW=43,0296218
CH15O MW=43,112284
CH17N MW=43,1360922
C2H3O MW=43,0183888
C2H5N MW=43,042197
C2H19 MW=43,1486674
C3H7 MW=43,0547722
HN3 MW=43,0170466
H11O2 MW=43,0759006
H11S MW=43,0581426
H13NO MW=43,0997088
H15N2 MW=43,123517

-----D--B--E--f-i-l-t-e-r-----
10.02.2011 - 13:34:31,62
akzeptierte DBEs:
-1
0
1
2
3
4

CHNO DBE: 2
C2H5N DBE: 1
HN3 DBE: 2

3 von 13 Summenformeln

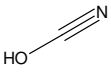

cyanic acid

Molecular Formula = C H N O

prussic acid + CH_4 methane

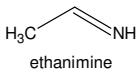

ethanimine

Molecular Formula = C_2H_5N

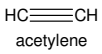

acetylene + NH_3 ammonia

1*H*-triazirene

Molecular Formula = HN_3

-MSn[II]: 350 -> 278 and [350 -> 306 -> 234 -> 148] -> (105); possible even-electron losses

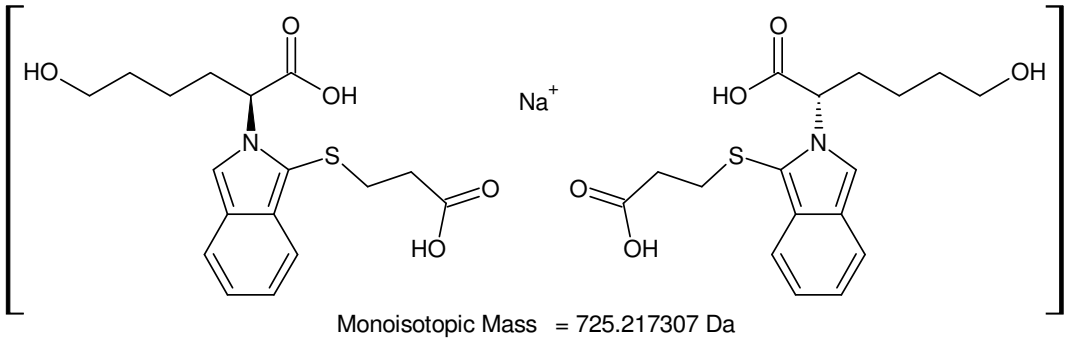

Monoisotopic Mass = 725.217307 Da

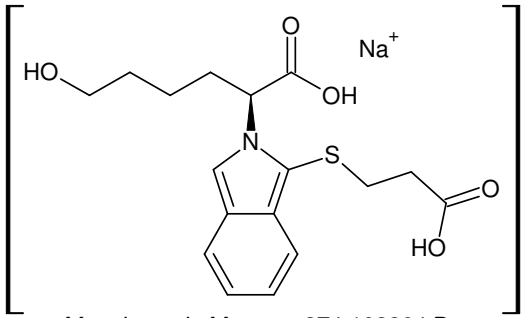

Monoisotopic Mass = 374.103264 Da

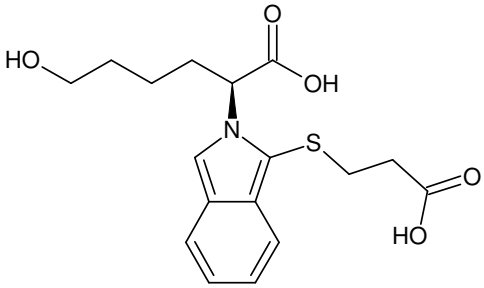

351.114043 Da

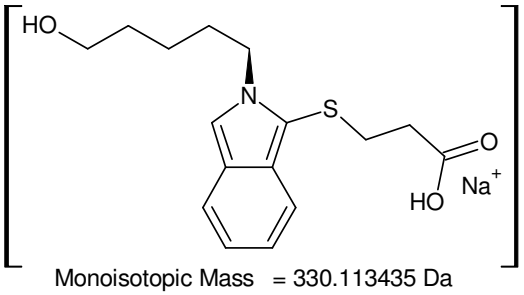

Monoisotopic Mass = 330.113435 Da

O=O
43.989829 Da

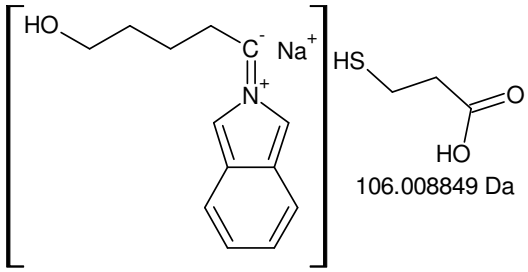

106.008849 Da

Monoisotopic Mass = 224.104586 Da

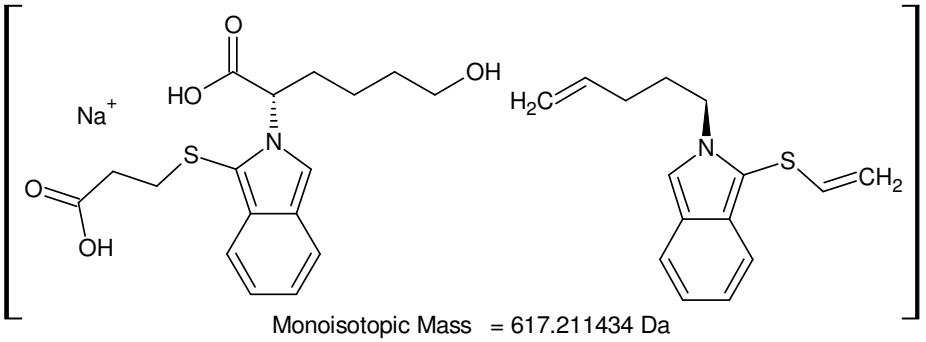

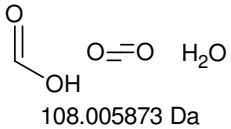

108.005873 Da

Monoisotopic Mass = 617.211434 Da

+MSn [II]: 725 -> 374 -> 330 -> 224 and [725] -> 617

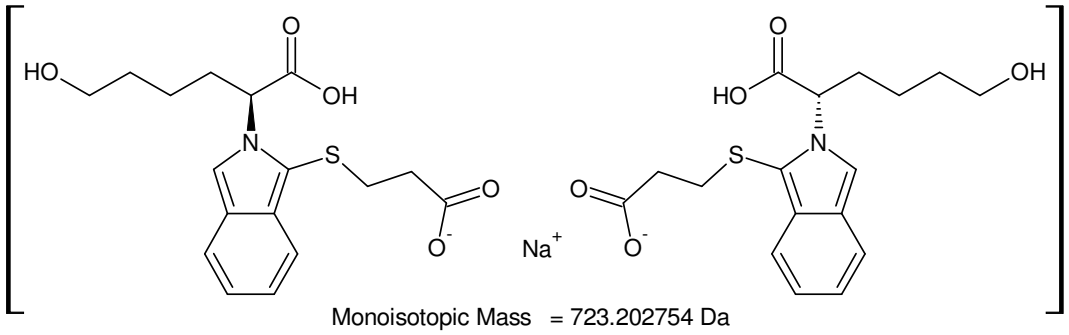

Monoisotopic Mass = 723.202754 Da

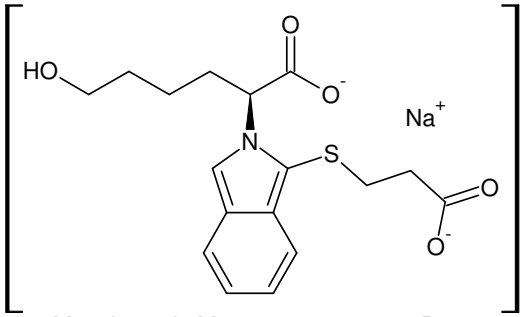

Monoisotopic Mass = 372.088711 Da

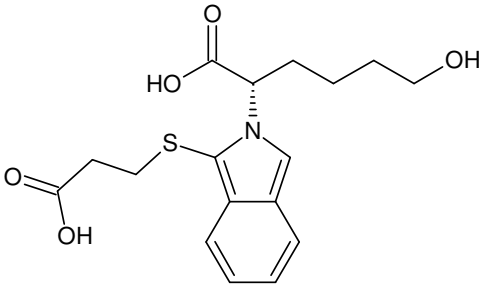

351.114043 Da

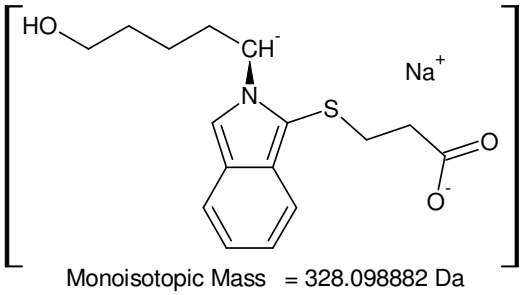

Monoisotopic Mass = 328.098882 Da

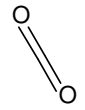

43.989829 Da

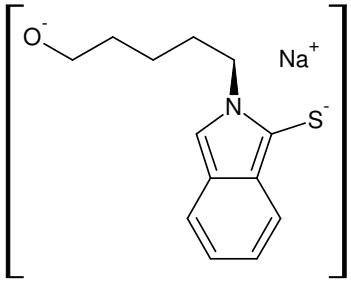

Monoisotopic Mass = 256.077753 Da

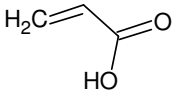

72.021129 Da

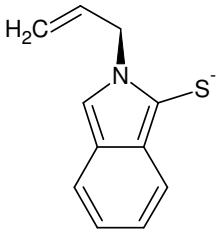

Monoisotopic Mass = 188.053943 Da

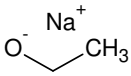

68.02381 Da
sodium ethanolate

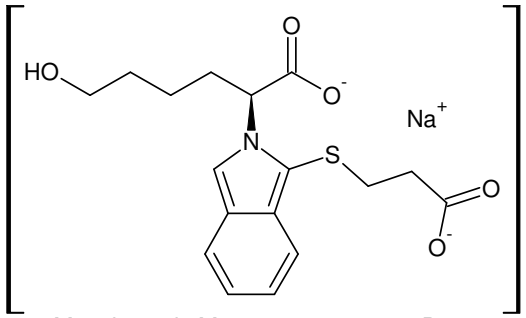

Monoisotopic Mass = 372.088711 Da

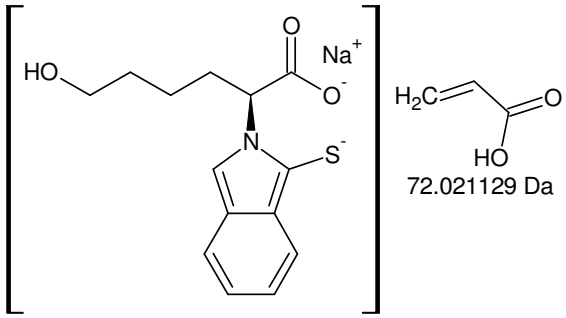

72.021129 Da

Monoisotopic Mass = 300.067582 Da

-MSn [II]: 723 -> 372 -> 328 -> 256 -> 188 and [723 -> 372] -> 300

III

The fragmentation pattern of 354 Th / -352Th of fraction III is identical to that of the (desalted) sample BoT#4 (cp. XIII.I.II, BoT#4).

+MS^n

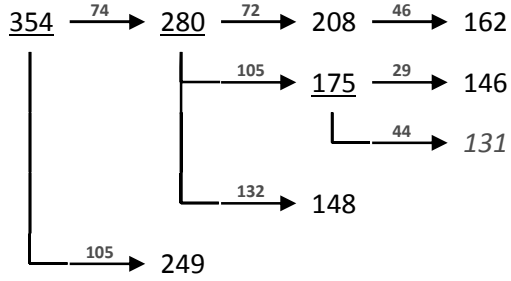

-MS^n

isotopic fingerprint:

peak area / % of monoisotopic	**+1**	**+2**	**+3**
theoretical ($C_{16}H_{18}NO_6S^-$):	19,0	7,5	1,2
measured (-351,8 Th):	18,9	7,3	1,5
measured (354,2 Th):	20,3	16,5	3,5

Figure XIII-VI MS^n analysis of III

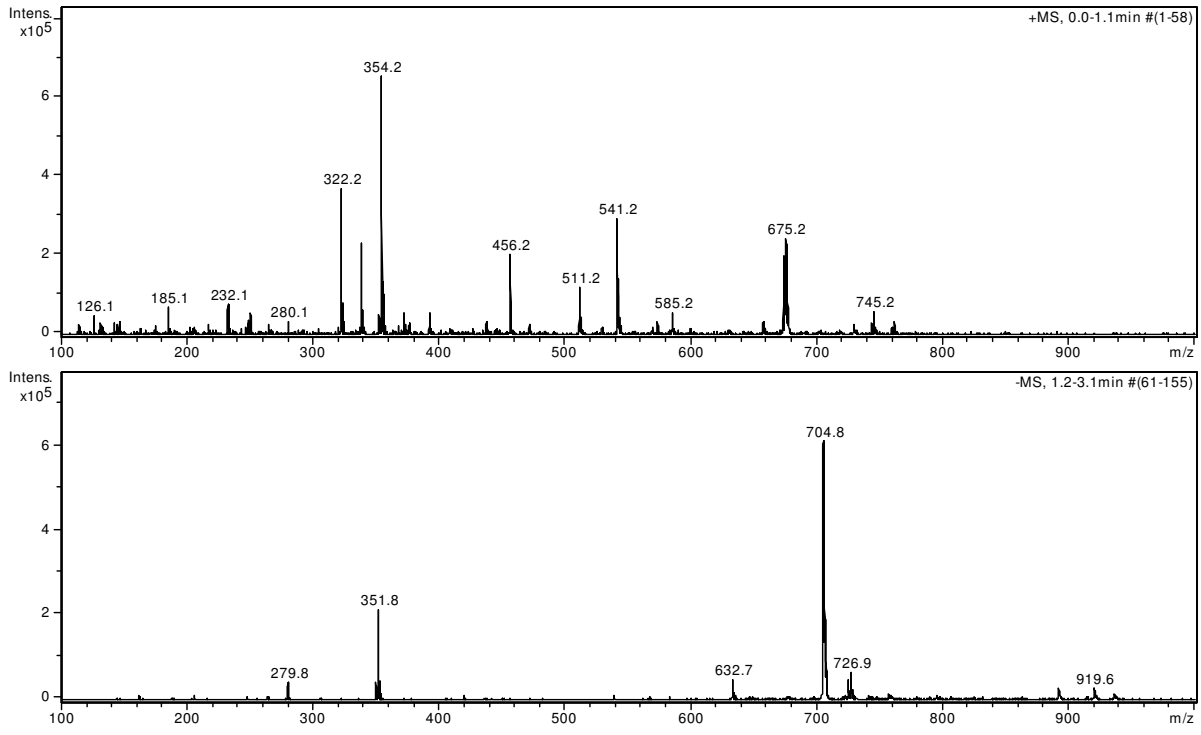

Figure XIII-VII III: 16,3 – 16,8 min, 1 ‰ FA, 34 % ACN in ddH_2O; full scan MS^1

Beobachtete Fragmente stimmen mit BoT#4 überein.

Fragmente von OPA-Met (+MSn: 236, 188; -MSn: 337, 264, 220, 150) wurden nicht beobachtet.

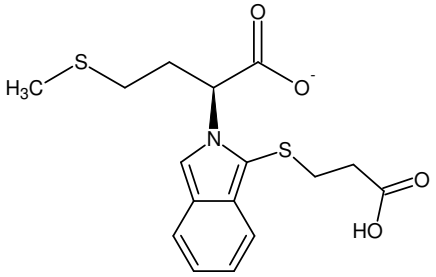

OPA-Met

Monoisotopic Mass = 352.067726 Da

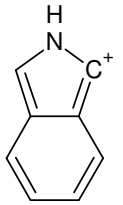

$H_2C{=}S$

thioxomethane

45.98772 Da

Monoisotopic Mass = 116.050024 Da

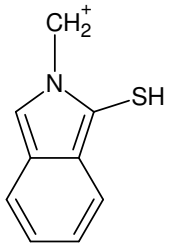

$C^-{\equiv}O^+$

carbon monoxide

27.994915 Da

Monoisotopic Mass = 162.037745 Da

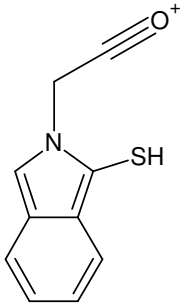

H_2O

water

18.010565 Da

Monoisotopic Mass = 190.03266 Da

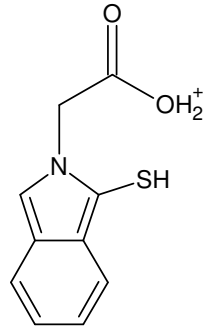

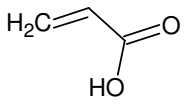

acrylic acid

72.021129 Da

Monoisotopic Mass = 208.043225 Da

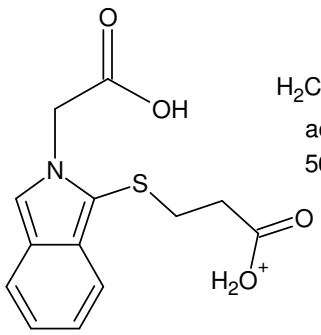

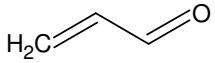

acrylaldehyde

56.026215 Da

Monoisotopic Mass = 280.064355 Da

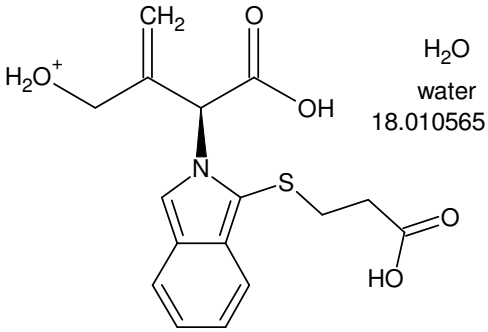

H_2O

water

18.010565 Da

Monoisotopic Mass = 336.09057 Da

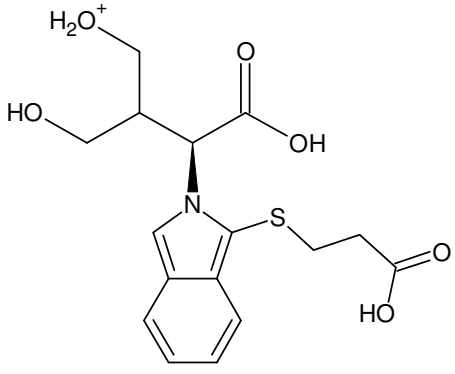

Monoisotopic Mass = 354.101135 Da

+MSn [III, BoT#4]: 116 <- 162 <- 190 <- 208 <- 280 <- 336 <- 354

354 - 280 = **74**
Compounds found: 60
CH2N2O2 MW=74,0116272
CH2N2S MW=73,9938692
(...)
N3O2 MW=73,999052
N3S MW=73,981294

-----D--B--E--f-i-l-t-e-r-----
10.02.2011 - 15:14:38,72
akzeptierte DBEs:
1
2
3
4

CH2N2O2 DBE: 2
CH2N2S DBE: 2
CH6N4 DBE: 1
C2H2OS DBE: 2
C2H2O3 DBE: 2
C2H6N2O DBE: 1
C3H6O2 DBE: 1
C3H6S DBE: 1
H2N4O DBE: 2

9 von 60 Summenformeln

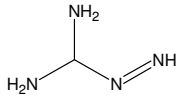

Molecular Formula = $C H_6 N_4$
zu viel N: keine AS-Seitenkette

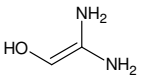

Molecular Formula = $C_2 H_6 N_2 O$
2 C & 2 N: Fragment in keiner AS zu finden

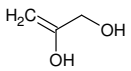

Molecular Formula = $C_3 H_6 O_2$
3 C: Orn, Gln, Glu, Nvl, Val
2 O: Ornithinaldehyd + 1 OH
Glu reduziert => geminales Diol...
Val 2-fach hydroxyliert

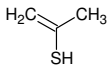

Molecular Formula = $C_3 H_6 S$
(Met)

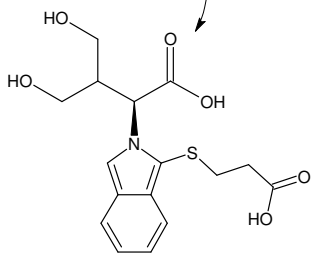

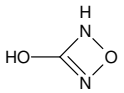

Molecular Formula = $C H_2 N_2 O_2$

Molecular Formula = $C H_2 N_2 S$

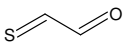

Molecular Formula = $C_2 H_2 O S$

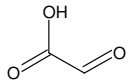

Molecular Formula = $C_2 H_2 O_3$
2C & 3 O: Asp oxidiert (Persäure => eher weniger) oder hydroxyliert

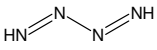

Molecular Formula = $H_2 N_4$

190 - 162 = **28**
Compounds found: 6
CH2N MW=28,0187232
CO MW=27,994915
C2H4 MW=28,0312984
H12O MW=28,0888102
H14N MW=28,1126184
N2 MW=28,006148

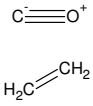

280 - 208 = **56**
Compounds found: 28
CH2N3 MW=56,0248712
CH12O2 MW=56,0837252
(...)
H28N2 MW=56,2252368
N4 MW=56,012296

-----D--B--E--f-i-l-t-e-r-----
10.02.2011 - 16:08:11,76
akzeptierte DBEs:
1
2
3
4

CN2O DBE: 3
C2H4N2 DBE: 2
C2O2 DBE: 3
C2S DBE: 3
C3H4O DBE: 2
C4H8 DBE: 1
N4 DBE: 3

7 von 28 Summenformeln

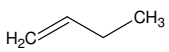

Molecular Formula = $C_4 H_8$

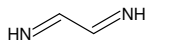

Molecular Formula = $C_2 H_4 N_2$

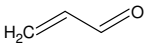

Molecular Formula = $C_3 H_4 O$

Molecular Formula = $C N_2 O$

Molecular Formula = $C_2 O_2$

Molecular Formula = $C_2 S$

Molecular Formula = N_4

+MSn [III, BoT#4]: 162 <- 190 <- 208 <- 280 <- 354: even-electron losses 74, 28 and 56 Da

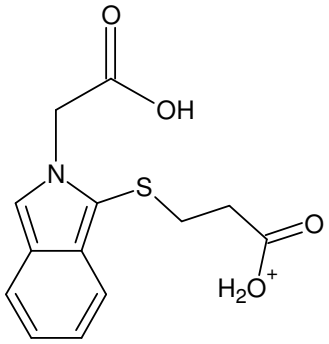

Monoisotopic Mass = 280.064355 Da

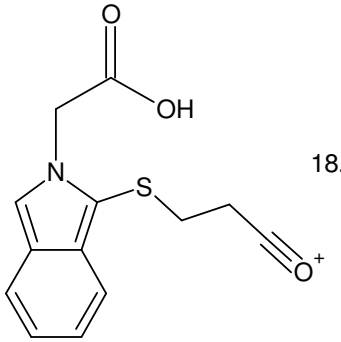

H_2O
water
18.010565 Da

Monoisotopic Mass = 262.05379 Da

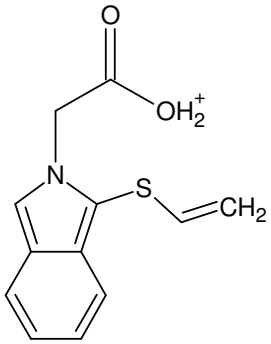

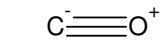

carbon monoxide
27.994915 Da

Monoisotopic Mass = 234.058875 Da

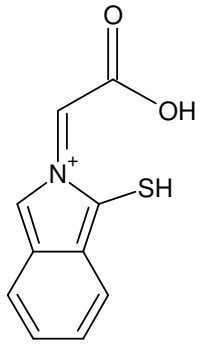

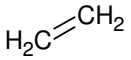

ethylene
28.0313 Da

Monoisotopic Mass = 206.027575 Da

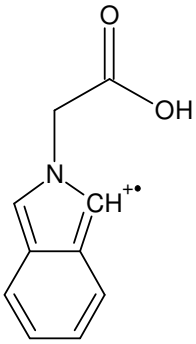

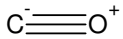

carbon monoxide

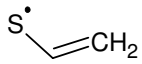

ethylenethiolyl
86.99046 Da

Monoisotopic Mass = 175.063329 Da

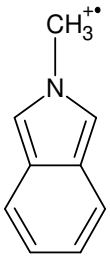

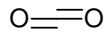

carbon dioxide
43.989829 Da

Monoisotopic Mass = 131.073499 Da

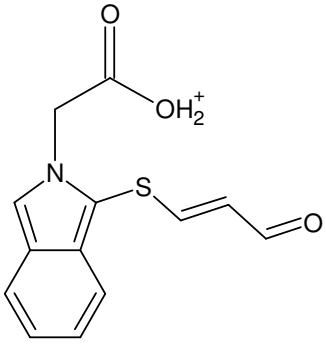

Monoisotopic Mass = 262.05379 Da

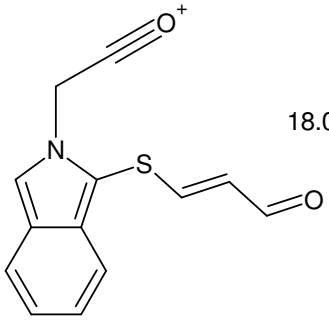

H_2O
water
18.010565 Da

Monoisotopic Mass = 244.043225 Da

+MSn [III, BoT#4]: [354 -> 336 -> 280] -> 262 -> 234 -> 206 -> 175 -> 131 and [354 -> 336 -> 280 -> 262] -> 244

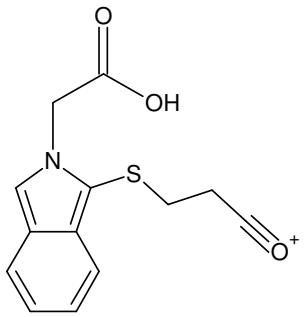

Monoisotopic Mass = 262.05379 Da

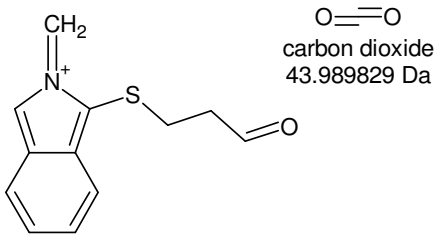

Monoisotopic Mass = 218.06396 Da

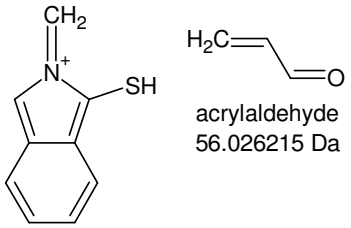

Monoisotopic Mass = 162.037745 Da

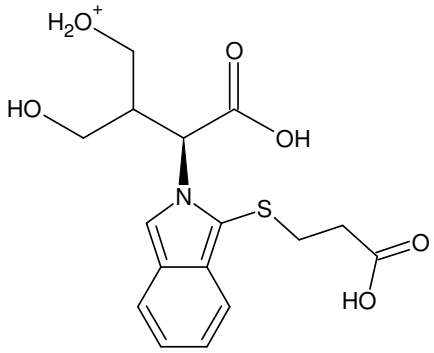

Monoisotopic Mass = 354.101135 Da

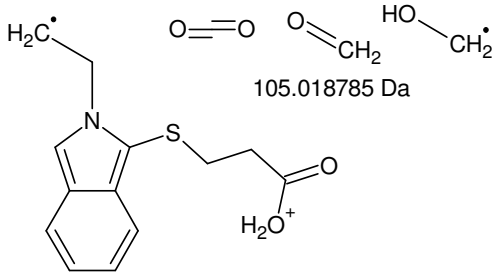

Monoisotopic Mass = 249.08235 Da

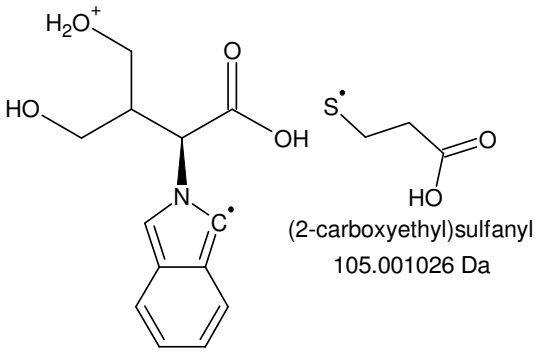

Monoisotopic Mass = 249.100109 Da

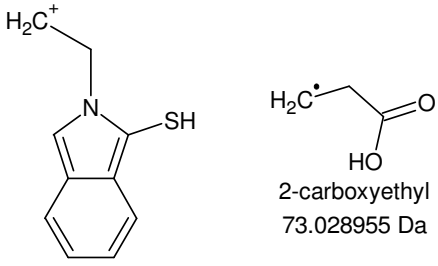

Monoisotopic Mass = 176.053395 Da

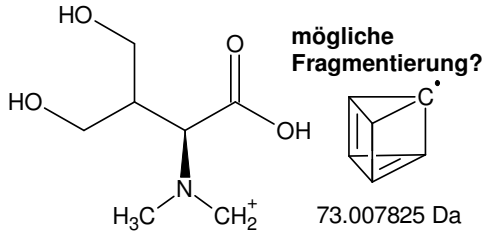

Monoisotopic Mass = 176.092284 Da

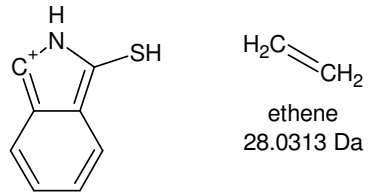

Monoisotopic Mass = 148.022095 Da

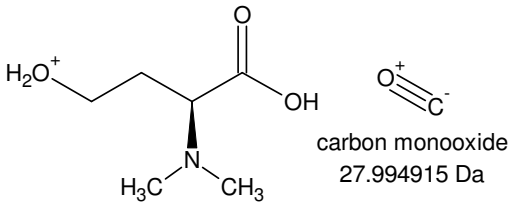

Monoisotopic Mass = 148.097369 Da

+MSn [III, BoT#4]: [354 -> 336 -> 280 -> 262] -> 218 -> 162 and 354 -> 249 -> 176 -> 148

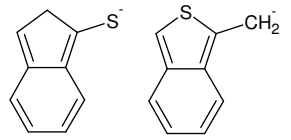

15 Da?

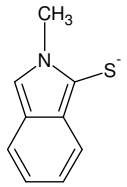

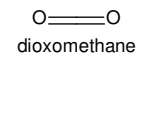

Monoisotopic Mass = 147.026846 Da

Monoisotopic Mass = 162.037745 Da

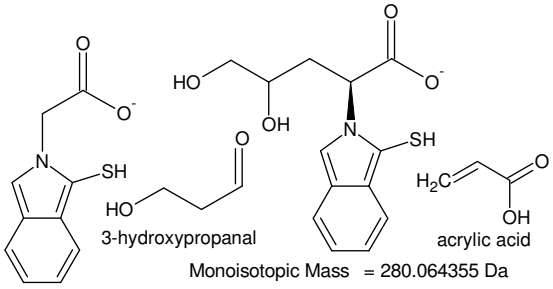

Monoisotopic Mass = 280.064355 Da

Monoisotopic Mass = 206.027575 Da

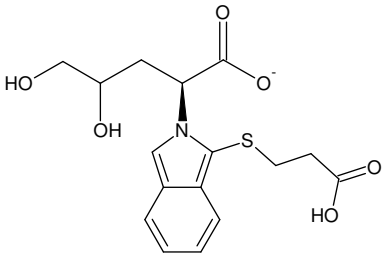

Monoisotopic Mass = 352.085485 Da

72 Da (Acrylsäure) stellt die erste Fragmentrierung dar. => Das Seitenkettenfragment hat 74 Da.

mögliche Fragmente (CHONS, mit 1/2 Da Massentoleranz, min. 2 C, chemisch sinvoll - Wertigkeitssummenregel)

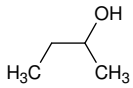

Molecular Formula = $C_4H_{10}O$
Monoisotopic Mass = 74.073165 Da

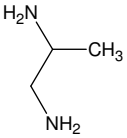

Molecular Formula = $C_3H_{10}N_2$
Monoisotopic Mass = 74.084398 Da

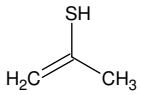

Molecular Formula = C_3H_6S
Monoisotopic Mass = 74.019021 Da

Methionin: 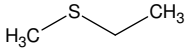

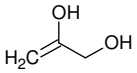

Molecular Formula = $C_3H_6O_2$
Monoisotopic Mass = 74.03678 Da

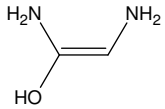

Molecular Formula = $C_2H_6N_2O$
Monoisotopic Mass = 74.048013 Da

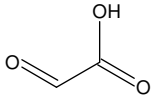

Molecular Formula = $C_2H_2O_3$
Monoisotopic Mass = 74.000395 Da

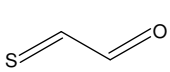

Molecular Formula = C_2H_2OS
Monoisotopic Mass = 73.982636 Da

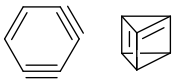

Molecular Formula = C_6H_2
Monoisotopic Mass = 74.01565 Da

Compounds found: 60
CH2N2O2 MW=74,0116272
CH2N2S MW=73,9938692
(...)
N3O2 MW=73,999052
N3S MW=73,981294

-----D--B--E--f-i-l-t-e-r-----
14.02.2011 - 16:14:35,40
akzeptierte DBEs:
0 1 2 3 4 5 6

CH2N2O2 DBE: 2
CH2N2S DBE: 2
CH6N4 DBE: 1
C2H2OS DBE: 2
C2H2O3 DBE: 2
C2H6N2O DBE: 1
C3H6O2 DBE: 1
C3H6S DBE: 1
C3H10N2 DBE: 0
C4H10O DBE: 0
C6H2 DBE: 6
H2N4O DBE: 2

12 von 60 Summenformeln

-MSn [BoT#4]: 147 <- 162 <- 206 <- 280 <- 352

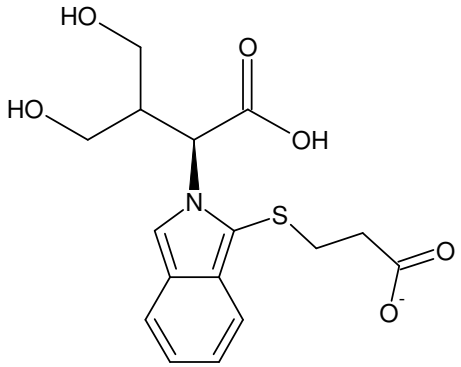

Monoisotopic Mass = 352.085485 Da

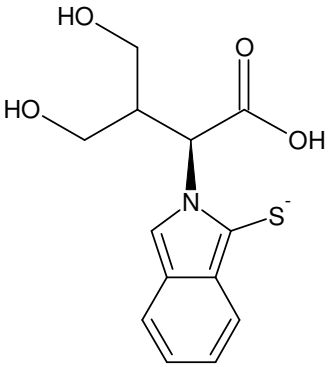

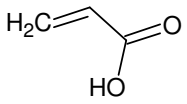

prop-2-enoic acid
72.02113 Da

Monoisotopic Mass = 280.064355 Da

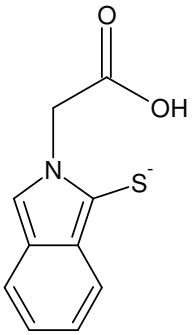

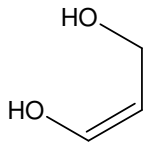

(1*Z*)-prop-1-ene-1,3-diol
74.03678 Da

Monoisotopic Mass = 206.027575 Da

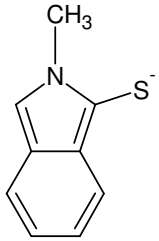

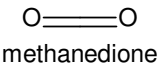

methanedione
43.98983 Da

Monoisotopic Mass = 162.037745 Da

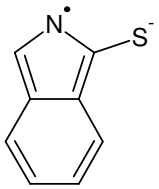

$CH_3^{\bullet}$
methyl
15.023475 Da

Monoisotopic Mass = 147.01427 Da

-MSn [III, BoT#4]: 352 -> 280 -> 206 -> 162 -> 147

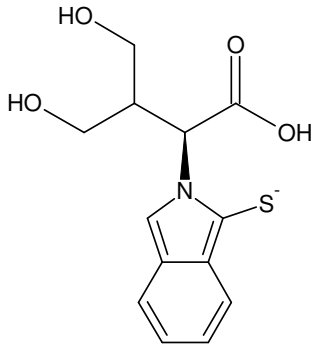

Monoisotopic Mass = 280.064355 Da

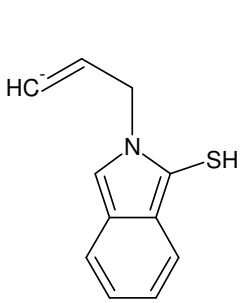

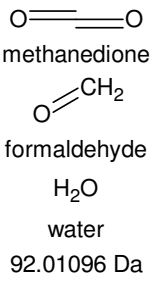

Monoisotopic Mass = 188.053395 Da

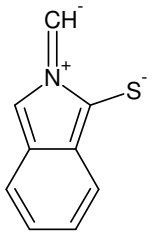

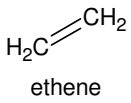

Monoisotopic Mass = 160.022095 Da

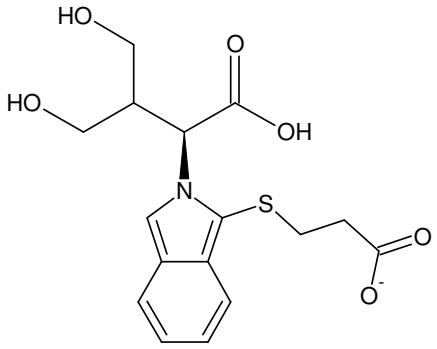

Monoisotopic Mass = 352.085485 Da

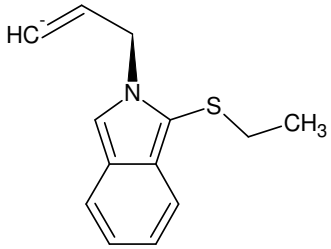

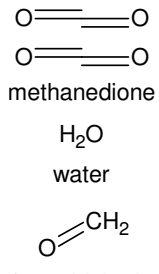

Monoisotopic Mass = 216.084695 Da

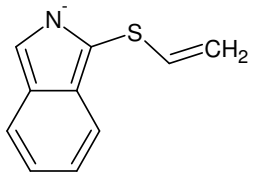

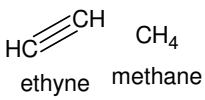

Monoisotopic Mass = 174.037745 Da

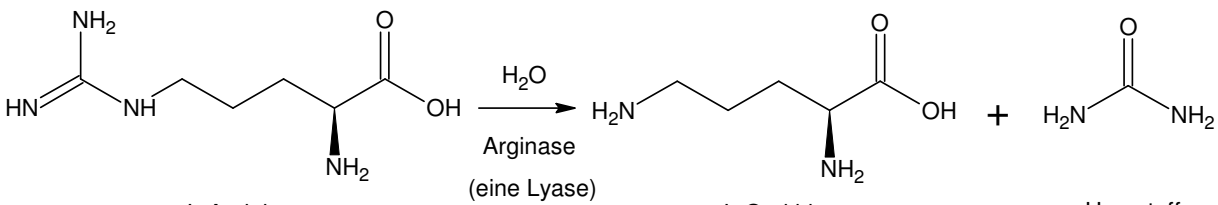

L-Arginin L-Ornithin Harnstoff

-MSn [III, BoT#4]: [352 -> 280] -> 188 -> 160 and 352 -> 216 -> 174

IV

+MS^n

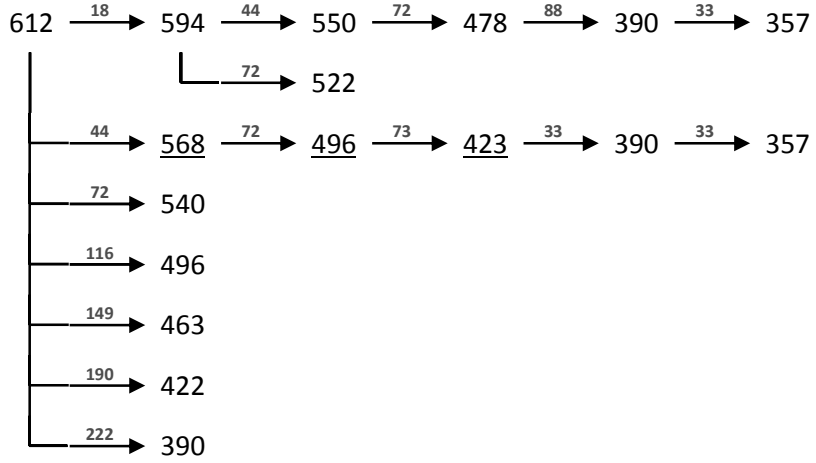
612 18 594 44 550 72 478 88 390 33 357
72 522
44 568 72 496 73 423 33 390 33 357
72 540
116 496
149 463
190 422
222 390

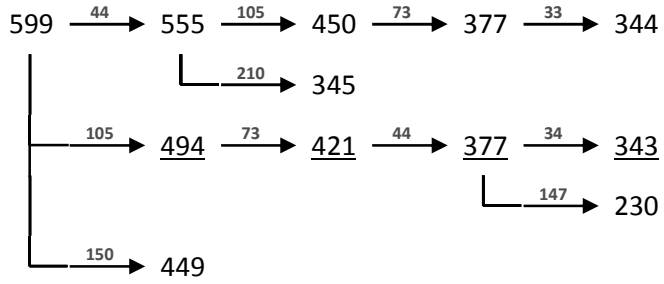
599 44 555 105 450 73 377 33 344
210 345
105 494 73 421 44 377 34 343
147 230
150 449

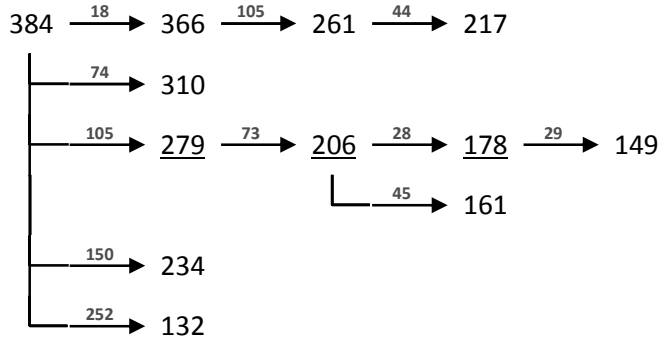
384 18 366 105 261 44 217
74 310
105 279 73 206 28 178 29 149
45 161
150 234
252 132

-MS^n

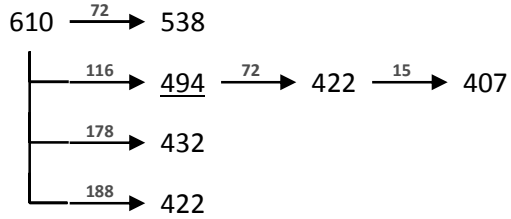
610 72 538
116 494 72 422 15 407
178 432
188 422

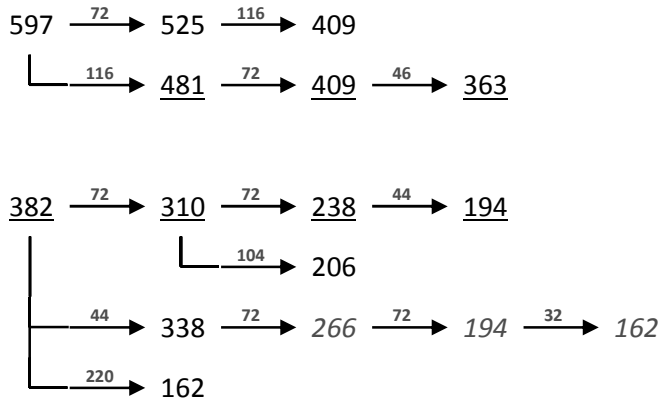

isotopic fingerprint:

peak area / % of monoisotopic	**+1**	**+2**	**+3**
measured (612,2 Th):	71,8	21,3	9,7
measured (-609,9 Th):	35,3	(38,2)	(16,1)
theoretical ($C_{28}H_{27}N_2O_9S_2^+$):	33,4	16,6	4,1
measured (599,2 Th):	36,6	17,4	5,8
measured (-596,9 Th):	41,4	14,0	5,2
theoretical ($C_{16}H_{18}NO_6S_2^+$):	19,8	12,1	2,1
measured (384,2 Th):	26,6	11,6	2,7
measured (-381,8 Th):	22,6	12,5	3,0

Figure XIII-VIII MS^n analysis of IV

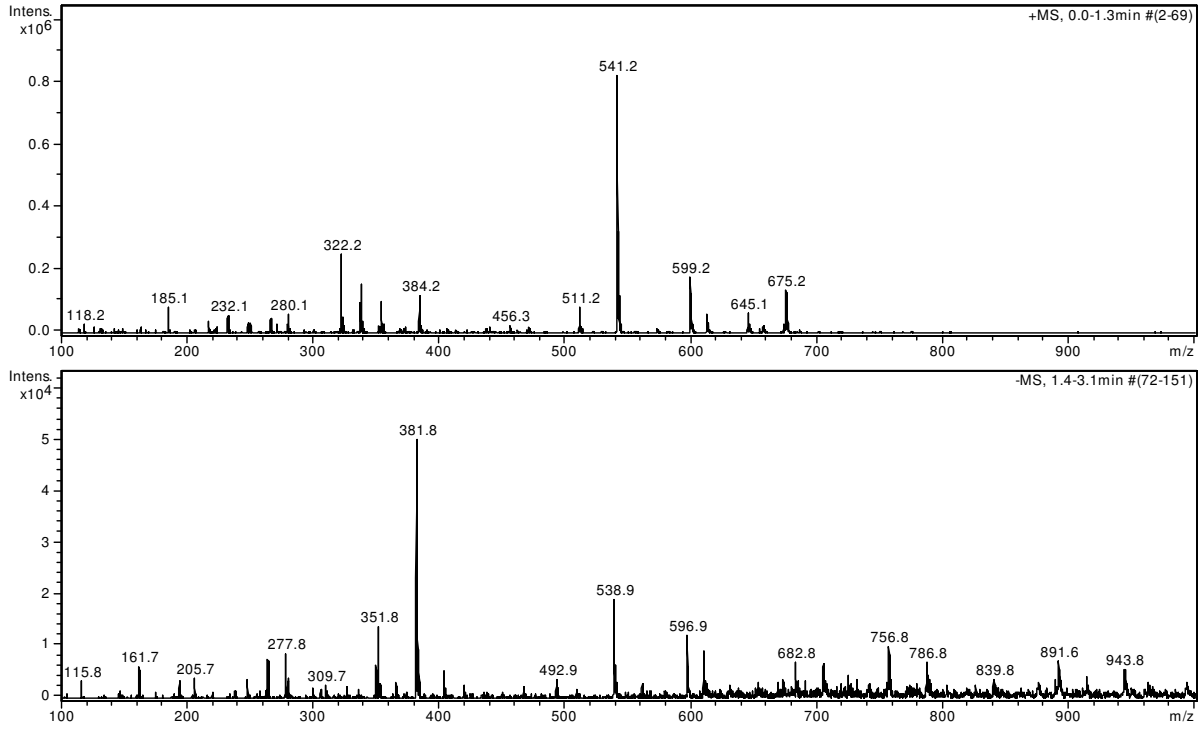

Figure XIII-IX IV: 19,3 – 19,75 min, 1 ‰ FA, 38 % ACN in ddH_2O; full scan MS^1

Compounds found: 53

$C_3H_5O_2S$	MW=105,001025
$C_3H_5O_4$	MW=105,018783
$C_3H_5S_2$	MW=104,983267
C_3H_7NOS	MW=105,0248332
$C_3H_7NO_3$	MW=105,0425912
$C_3H_9N_2O_2$	MW=105,0663994
$C_3H_9N_2S$	MW=105,0486414
$C_3H_{11}N_3O$	MW=105,0902076
$C_3H_{13}N_4$	MW=105,1140158
$C_3H_{21}OS$	MW=105,1313036
$C_3H_{21}O_3$	MW=105,1490616
$C_3H_{23}NO_2$	MW=105,1728698
$C_3H_{23}NS$	MW=105,1551118
$C_3H_{25}N_2O$	MW=105,196678
$C_3H_{27}N_3$	MW=105,2204862
$C_3H_{37}O_2$	MW=105,2793402
$C_3H_{37}S$	MW=105,2615822
$C_3H_{39}NO$	MW=105,3031484
$C_3H_{41}N_2$	MW=105,3269566
$C_3H_{53}O$	MW=105,4096188
C_4HN_4	MW=105,0201206
C_4H_9OS	MW=105,0374084
$C_4H_9O_3$	MW=105,0551664
$C_4H_{11}NO_2$	MW=105,0789746
$C_4H_{11}NS$	MW=105,0612166
$C_4H_{13}N_2O$	MW=105,1027828
$C_4H_{15}N_3$	MW=105,126591
$C_4H_{25}O_2$	MW=105,185445
$C_4H_{25}S$	MW=105,167687
$C_4H_{27}NO$	MW=105,2092532
$C_4H_{29}N_2$	MW=105,2330614
$C_4H_{41}O$	MW=105,3157236
$C_4H_{43}N$	MW=105,3395318
C_5HN_2O	MW=105,0088876
$C_5H_3N_3$	MW=105,0326958
$C_5H_{13}O_2$	MW=105,0915498
$C_5H_{13}S$	MW=105,0737918
$C_5H_{15}NO$	MW=105,115358
$C_5H_{17}N_2$	MW=105,1391662
$C_5H_{29}O$	MW=105,2218284
$C_5H_{31}N$	MW=105,2456366
C_5H_{45}	MW=105,352107
C_6HO_2	MW=104,9976546
C_6HS	MW=104,9798966
C_6H_3NO	MW=105,0214628
$C_6H_5N_2$	MW=105,045271
$C_6H_{17}O$	MW=105,1279332
$C_6H_{19}N$	MW=105,1517414
C_6H_{33}	MW=105,2582118
C_7H_5O	MW=105,034038
C_7H_7N	MW=105,0578462
C_7H_{21}	MW=105,1643166
C_8H_9	MW=105,0704214

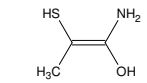

Molecular Formula = C_3H_7NOS

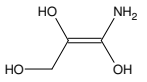

Molecular Formula = $C_3H_7NO_3$

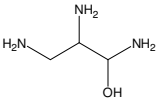

Molecular Formula = $C_3H_{11}N_3O$

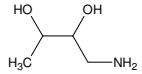

Molecular Formula = $C_4H_{11}NO_2$

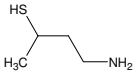

Molecular Formula = $C_4H_{11}NS$

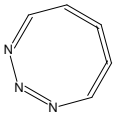

Molecular Formula = $C_5H_3N_3$

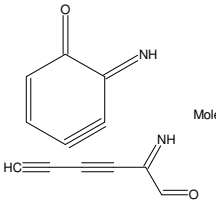

Molecular Formula = C_6H_3NO

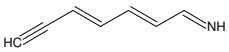

Molecular Formula = C_7H_7N

105 Da even-electron neutral loss {I/II}

CH_4 CH_4 CH_4 H_2
NH_3 H_2O H_2O H_2

Molecular Formula = $C_3H_{23}NO_2$

CH_4 CH_4 CH_4 H_2
NH_3 H_2S H_2 H_2

Molecular Formula = $C_3H_{23}NS$

CH_4 CH_4 CH_4 H_2 H_2
NH_3 NH_3 NH_3 H_2

Molecular Formula = $C_3H_{27}N_3$

CH_4 CH_4 CH_4 H_2 H_2 H_2
NH_3 H_2O H_2 H_2 H_2 H_2
H_2 H_2 H_2 H_2

Molecular Formula = $C_3H_{39}NO$

CH_4 CH_4 CH_4 CH_4
NH_3 H_2O H_2 H_2 H_2

Molecular Formula = $C_4H_{27}NO$

CH_4 CH_4 CH_4 CH_4 H_2
NH_3 H_2 H_2 H_2 H_2 H_2
H_2 H_2 H_2 H_2 H_2

Molecular Formula = $C_4H_{43}N$

CH_4 CH_4 CH_4 CH_4 CH_4
NH_3 H_2 H_2 H_2 H_2

Molecular Formula = $C_5H_{31}N$

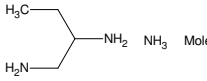

NH_3 Molecular Formula = $C_4H_{15}N_3$

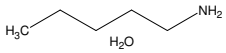

Molecular Formula = $C_5H_{15}NO$

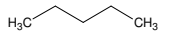

CH_4 NH_3 Molecular Formula = $C_6H_{19}N$

Compounds found: 163
CHN2O2S MW=104,9758746
CHN2O4 MW=104,9936326
(...)
H47N3O MW=105,3718932
H49N4 MW=105,3957014

-----D--B--E--f-i-l-t-e-r-----
02.02.2011 - 18:08:11,25
akzeptierte DBEs:
-1
0
1
2
3
4
5
6
7
8

CH3N3OS DBE: 2
CH3N3O3 DBE: 2
CH7N5O DBE: 1
C2H3NO2S DBE: 2
C2H3NO4 DBE: 2
C2H3NS2 DBE: 2
C2H7N3O2 DBE: 1
C2H7N3S DBE: 1
C2H11N5 DBE: 0
C3H7NOS DBE: 1
C3H7NO3 DBE: 1
C3H11N3O DBE: 0
C4H11NO2 DBE: 0
C4H11NS DBE: 0
C4H15N3 DBE: -1
C5H3N3 DBE: 6
C5H15NO DBE: -1
C6H3NO DBE: 6
C7H7N DBE: 5
H3N5O2 DBE: 2
H3N5S DBE: 2
H7N7 DBE: 1

22 von 163 Summenformeln

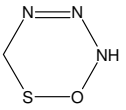

Molecular Formula = $C H_3 N_3 O S$

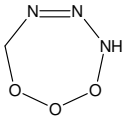

Molecular Formula = $C H_3 N_3 O_3$

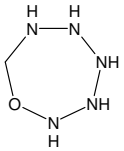

Molecular Formula = $C H_7 N_5 O$

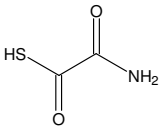

Molecular Formula = $C_2 H_3 N O_2 S$

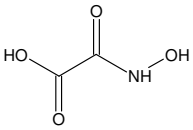

Molecular Formula = $C_2 H_3 N O_4$

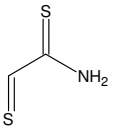

Molecular Formula = $C_2 H_3 N S_2$

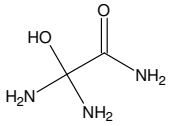

Molecular Formula = $C_2 H_7 N_3 O_2$

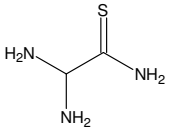

Molecular Formula = $C_2 H_7 N_3 S$

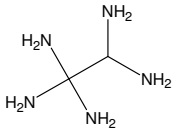

Molecular Formula = $C_2 H_{11} N_5$

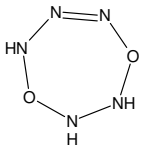

Molecular Formula = $H_3 N_5 O_2$

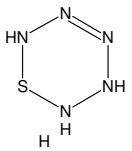

Molecular Formula = $H_3 N_5 S$

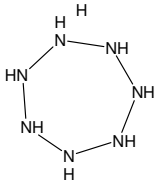

Molecular Formula = $H_7 N_7$

105 Da even-electron neutral loss {II/II}

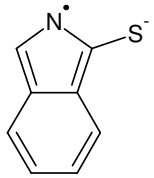

162 - 147 = **15**
Verbindungen: 2
CH3 MG=15,0234738
HN MG=15,0108986

Monoisotopic Mass = 147.014818 Da

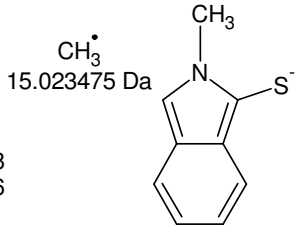

15.023475 Da

194 - 162 = **32**
Gefundene Verbindungen: 8
CH4O MG=32,0262134
CH6N MG=32,0500216
C2H8 MG=32,0625968
H2NO MG=32,0136382
H4N2 MG=32,0374464
H16O MG=32,1201086
O2 MG=31,98983
S MG=31,972072

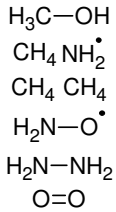

Monoisotopic Mass = 162.038293 Da

Die möglichen Summenformeln (außer O_2 und **S**) haben **weniger als 1 DBE**. => nicht zu montieren

=> kein Standard-OPA-Derivat

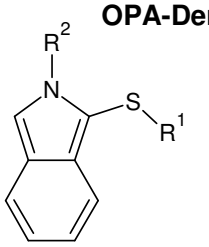

147.014269 Da
6 DBE

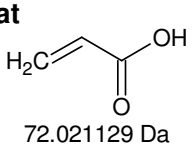

72.021129 Da

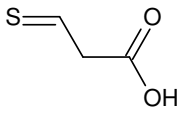

103.993199 Da

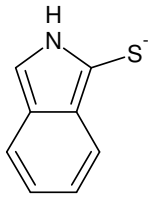

148.022643 Da

194 - 147 = **47**
Gefundene Verbindungen: 18
CH3O2 MG=47,0133038
CH3S MG=46,9955458
...
H17NO MG=47,1310072
H19N2 MG=47,1548154

-----D--B--E--f-i-l-t-e-r-----
14.11.2011 - 15:55:58,10
akzeptierte DBE:
-2 -1 0 1 2 3 4 5 6 7 8

CH5NO DBE: 0
C2H9N DBE: -1
HNO2 DBE: 1
HNS DBE: 1
H5N3 DBE: 0

5 von 18 Summenformeln

194 - C8H5NS
Gefundene Verbindungen: 22
C8H6N2O2S MG=194,0149976
C8H6N2S2 MG=193,9972396
...
C10H28NS MG=194,1942348
C11H16NS MG=194,1003396

-----D--B--E--f-i-l-t-e-r-----
14.11.2011 - 16:00:18,77
akzeptierte DBE:
-2 -1 0 1 2 3 4 5 6 7 8

C8H6N2O2S	DBE: 7	**HNO2**
C8H6N2S2	DBE: 7	**HNS**
C8H10N4S	DBE: 6	**H5N3**
C8H22N2OS	DBE: -1	H17NO
C9H10N2OS	DBE: 6	**CH5NO**
C9H26N2S	DBE: -2	CH21N
C10H14N2S	DBE: 5	**C2H9N**

7 von 22 Summenformeln

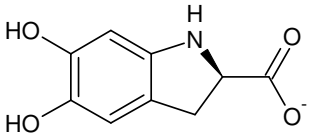

Monoisotopic Mass = 194.045881 Da
L-Leucodopachrom

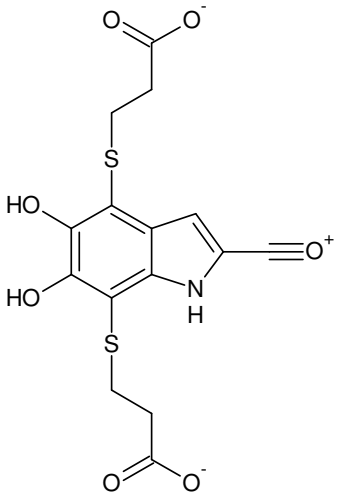

Monoisotopic Mass = 382.006065 Da

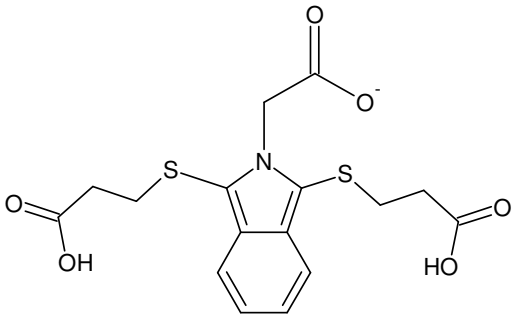

Monoisotopic Mass = 382.042451 Da

-MSn [IV]: 147 <- 162 <X 194 <- 266 <- 338 <- 382

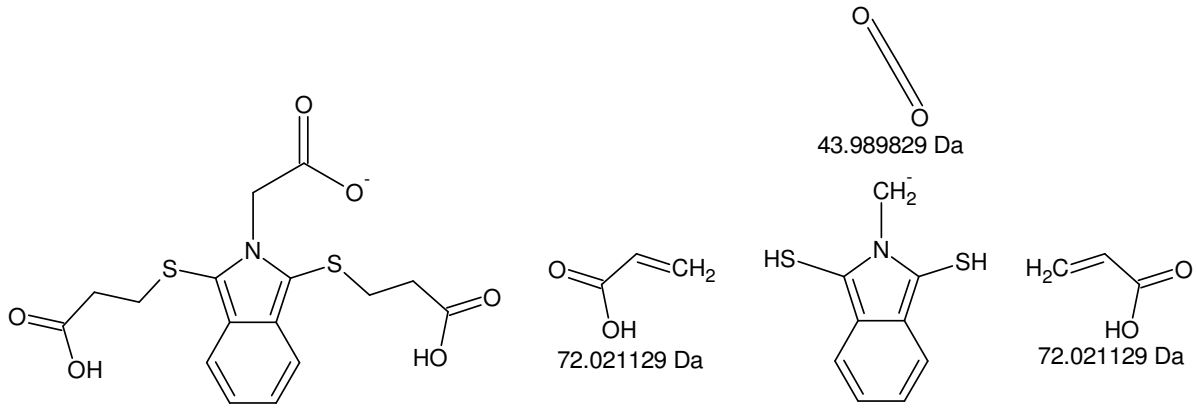

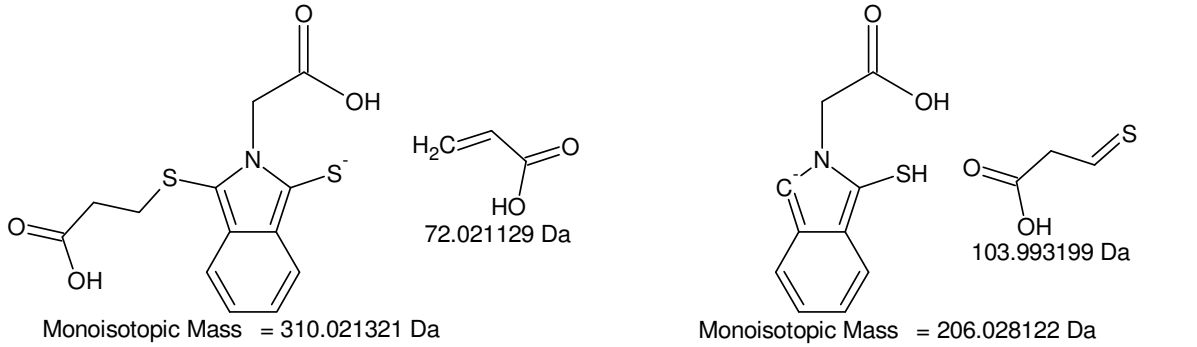

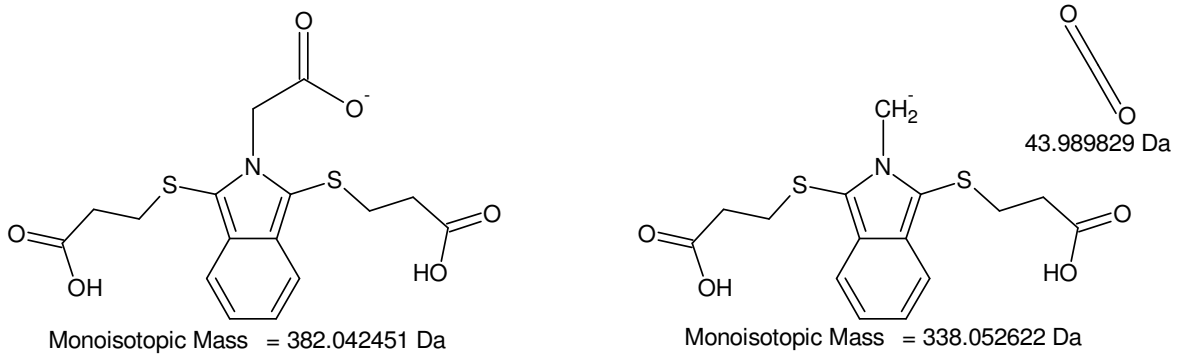

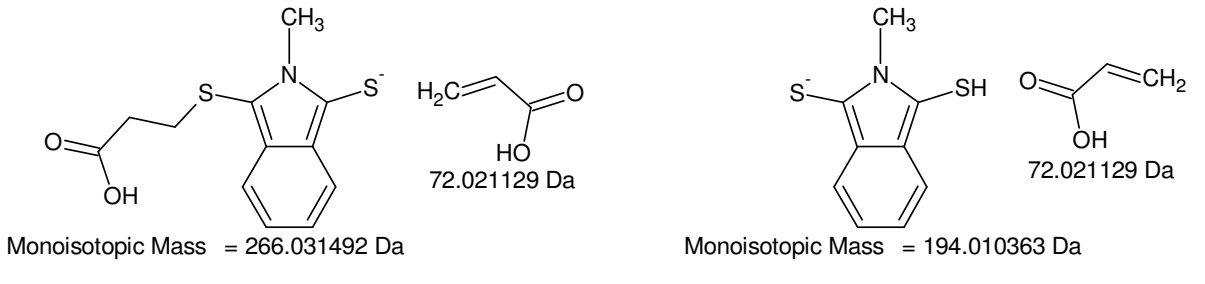

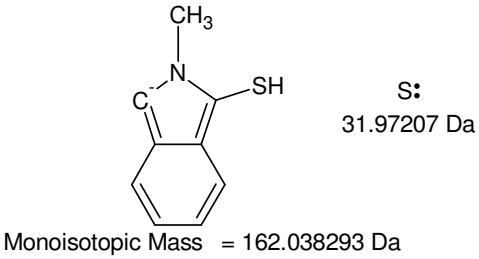

-MSn [IV]: 382 -> 310 -> 238 -> 194 and [382] -> 310 -> 206 as well as 382 -> 266 -> 194 -> 162

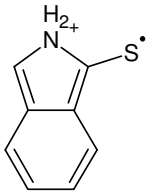

178 - 149 = **29**
Gefundene Verbindungen: 6

CHO	MG=29,0027396
CH3N	MG=29,0265478
C2H5	MG=29,039123
HN2	MG=29,0139726
H13O	MG=29,0966348
H15N	MG=29,120443

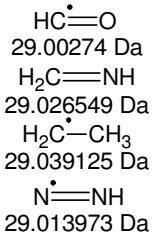

Monoisotopic Mass = 149.029371 Da

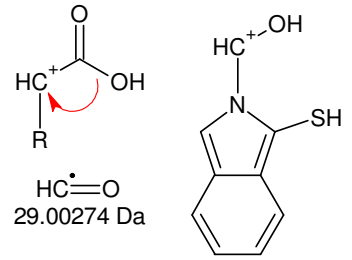

Monoisotopic Mass = **178.03211 Da**
[384 -> 279 -> 206] -> 161: ·**COOH**

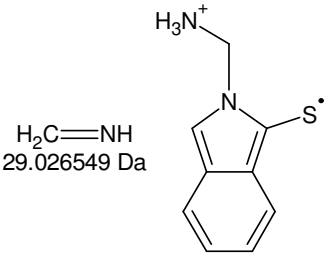

Monoisotopic Mass = 178.05592 Da

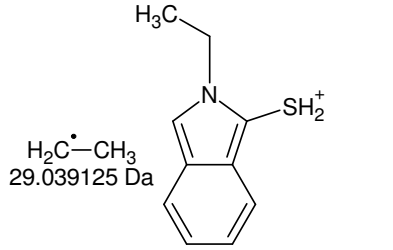

Monoisotopic Mass = 178.068496 Da

206 - 178 = **28**
Gefundene Verbindungen: 6

CH2N	MG=28,0187232
CO	MG=27,994915
C2H4	MG=28,0312984
H12O	MG=28,0888102
H14N	MG=28,1126184
N2	MG=28,006148

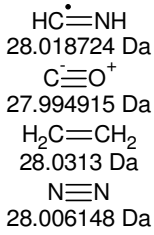

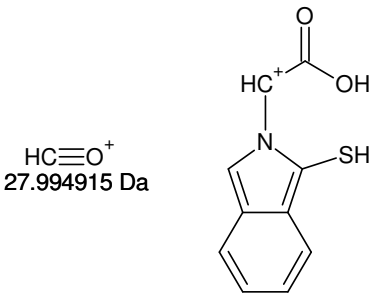

Monoisotopic Mass = **206.027025 Da**

+MSn: 279 - 206 = **73**
Gefundene Verbindungen: 60

CH2N2O2	MG=74,0116272
CH2N2S	MG=73,9938692
...	
N3O2	MG=73,999052
N3S	MG=73,981294

-----D--B--E--f-i-l-t-e-r-----
14.11.2011 - 12:09:18,87
akzeptierte DBE:
-2 -1 0 1 2 3 4 5 6 7 8

CH2N2O2	DBE: 2
CH2N2S	DBE: 2
CH6N4	DBE: 1
C2H2OS	DBE: 2
C2H2O3	DBE: 2
C2H6N2O	DBE: 1
C3H6O2	DBE: 1
C3H6S	DBE: 1
C3H10N2	DBE: 0
C4H10O	DBE: 0
C5H14	DBE: -1
C6H2	DBE: 6
H2N4O	DBE: 2

13 von 60 Summenformeln

-MSn: 310 - 238 = **72**
Gefundene Verbindungen: 55

CH2N3O	MG=72,0197862
CH4N4	MG=72,0435944
...	
H30N3	MG=72,24396
N4O	MG=72,007211

-----D--B--E--f-i-l-t-e-r-----
14.11.2011 - 12:14:06,27
akzeptierte DBE:
-2 -1 0 1 2 3 4 5 6 7 8

CH4N4	DBE: 2
CN2O2	DBE: 3
CN2S	DBE: 3
C2H4N2O	DBE: 2
C2OS	DBE: 3
C2O3	DBE: 3
C3H4O2	DBE: 2
C3H4S	DBE: 2
C3H8N2	DBE: 1
C4H8O	DBE: 1
C5H12	DBE: 0
C6	DBE: 7
N4O	DBE: 3

13 von 55 Summenformeln

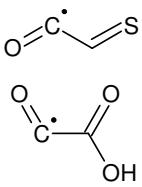

C_2HOS
72.97481 Da

C_2HO_3
72.992569 Da

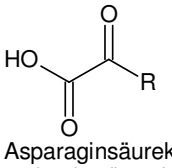

Asparaginsäureketon
=> decarboxyliert sehr leicht

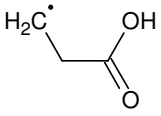

$C_3H_5O_2$
73.028954 Da

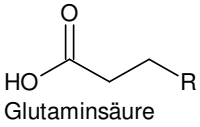

Glutaminsäure

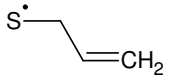

C_3H_5S
73.011195 Da

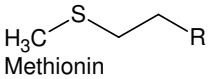

Methionin

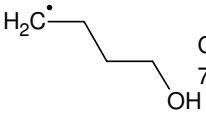

C_4H_9O
73.06534 Da

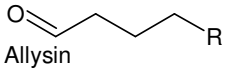

Allysin

C_6H
73.007825 Da

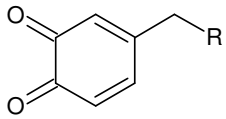

o-Dopachinon?

+MSn [IV]: 149 <- 178 <- 206 {<- 279 <- 384}

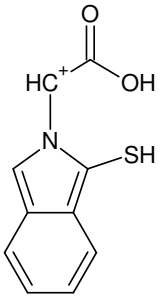

Monoisotopic Mass = 206.027025 Da

384 - 279 = **105**

[106 Da, min. 1 H]: -10 Treffer

Gefundene Verbindungen: 163

CH2N2O2S MG=105,9836992

CH2N2O4 MG=106,0014572

...

H48N3O MG=106,3797178

H50N4 MG=106,403526

-----D--B--E--f-i-l-t-e-r-----

14.11.2011 - 17:49:06,85

akzeptierte DBE:

-2 -1 0 1 2 3 4 5 6 7 8

CH2N2O2S	DBE: 2
CH2N2O4	DBE: 2
CH2N2S2	DBE: 2
CH6N4O2	DBE: 1
CH6N4S	DBE: 1
CH10N6	DBE: 0
C2H2OS2	DBE: 2
C2H2O3S	DBE: 2
C2H2O5	DBE: 2
C2H6N2OS	DBE: 1
C2H6N2O3	DBE: 1
C2H10N4O	DBE: 0
C3H6O2S	**DBE: 1**
C3H6O4	DBE: 1
C3H6S2	DBE: 1
C3H10N2O2	DBE: 0
C3H10N2S	DBE: 0
C3H14N4	DBE: -1
C4H2N4	DBE: 6
C4H10OS	DBE: 0
C4H10O3	DBE: 0
C4H14N2O	DBE: -1
C5H2N2O	DBE: 6
C5H14O2	DBE: -1
C5H14S	DBE: -1
C5H18N2	DBE: -2
C6H2O2	DBE: 6
C6H2S	DBE: 6
C6H6N2	DBE: 5
C6H18O	DBE: -2
C7H6O	DBE: 5
C8H10	DBE: 4
H2N4OS	DBE: 2
H2N4O3	DBE: 2
H6N6O	DBE: 1

35 von 163 Summenformeln

-MSn: C3H5O2S·

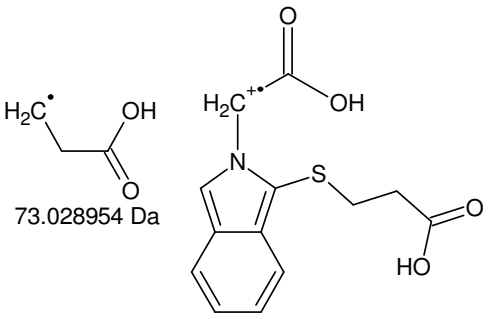

73.028954 Da

Monoisotopic Mass = 279.055979 Da

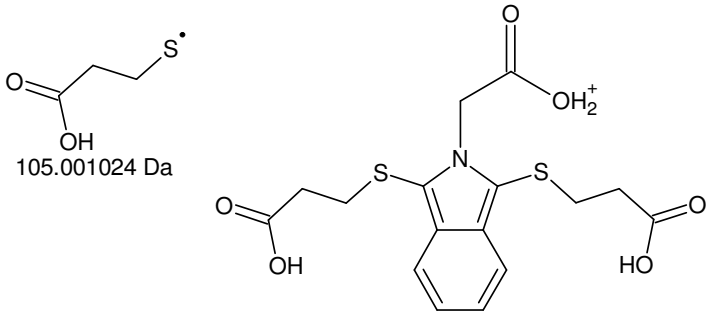

105.001024 Da

Monoisotopic Mass = 384.057004 Da

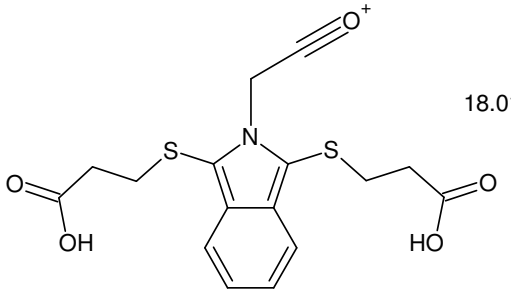

H_2O
18.010565 Da

Monoisotopic Mass = 366.046439 Da

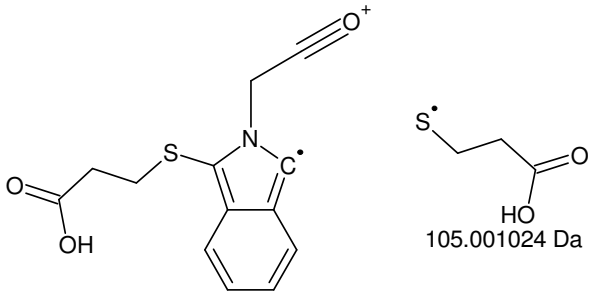

105.001024 Da

Monoisotopic Mass = 261.045415 Da

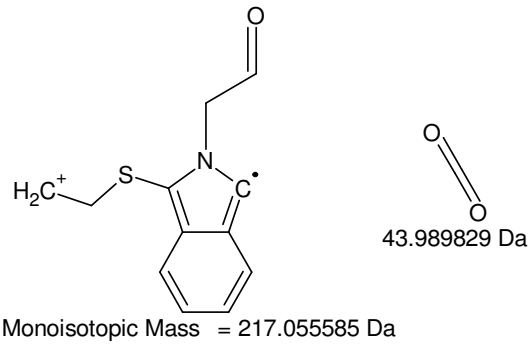

43.989829 Da

Monoisotopic Mass = 217.055585 Da

+MSn [IV]: [149 <- 178 <- 206] <- 279 <- 384 -> 366 -> 261 -> 217

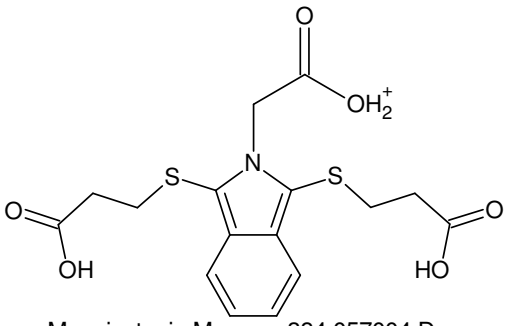

Monoisotopic Mass = 384.057004 Da

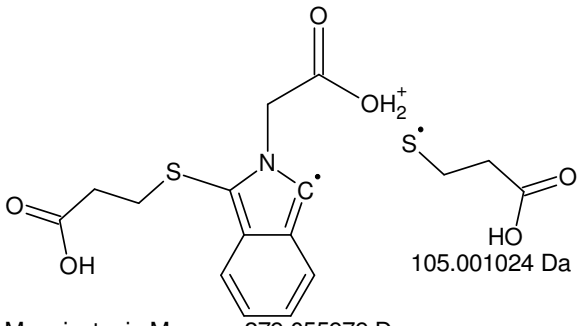

Monoisotopic Mass = 279.055979 Da

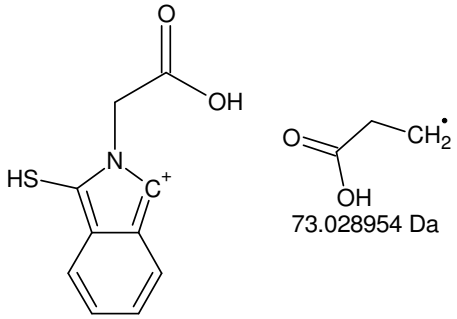

Monoisotopic Mass = 206.027025 Da

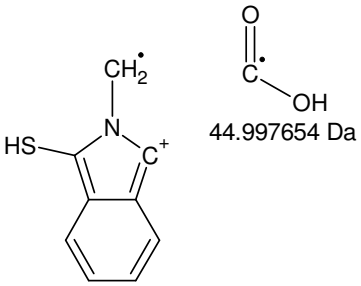

Monoisotopic Mass = 161.029371 Da

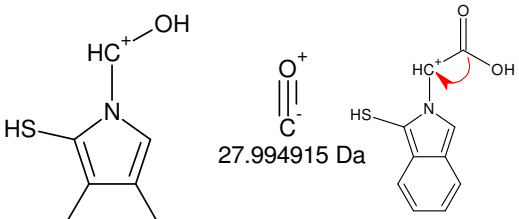

Monoisotopic Mass = 178.03211 Da

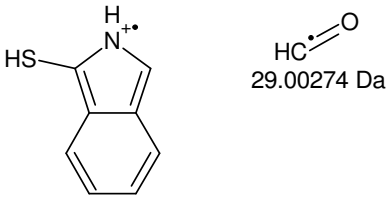

Monoisotopic Mass = 149.029371 Da

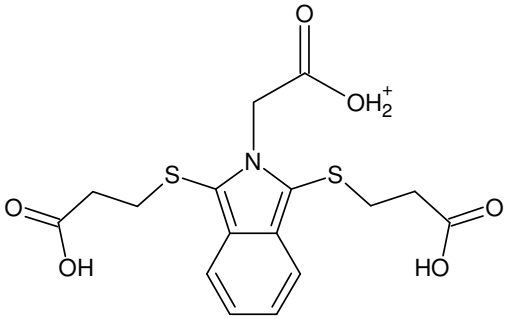

Monoisotopic Mass = 384.057004 Da

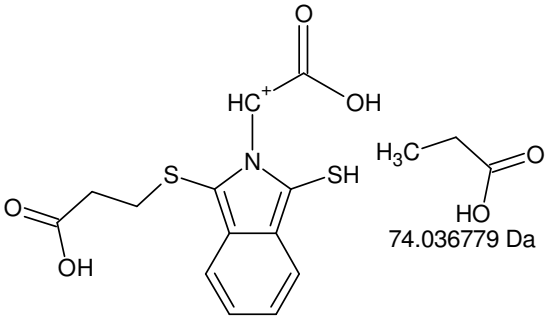

Monoisotopic Mass = 310.020224 Da

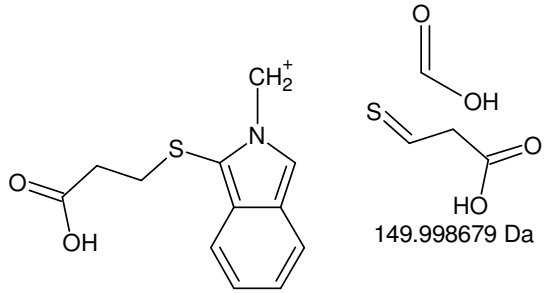

Monoisotopic Mass = 234.058325 Da

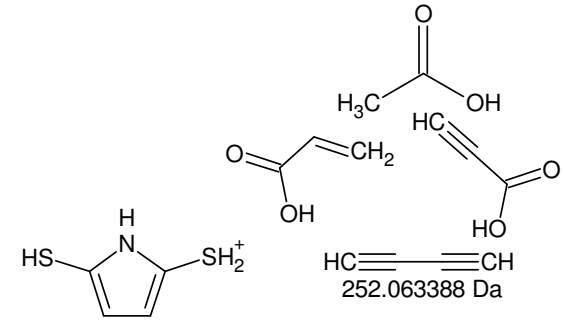

Monoisotopic Mass = 131.993616 Da

+MSn [IV]: 384 -> 279 -> 206 -> 161, 178 -> 149 und 384 -> 310, 234, 132

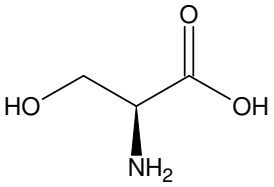

L-Serin

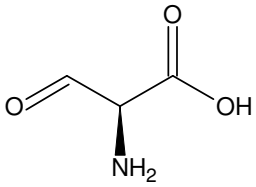

L-Serinaldehyd

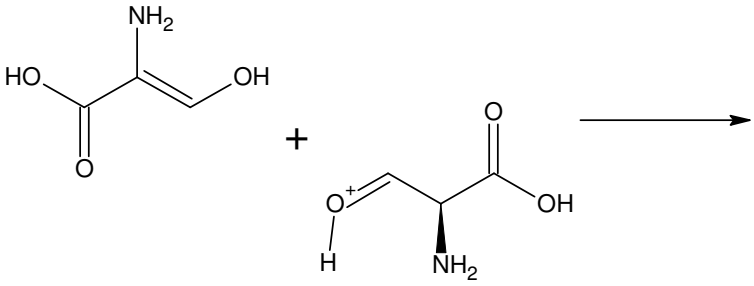

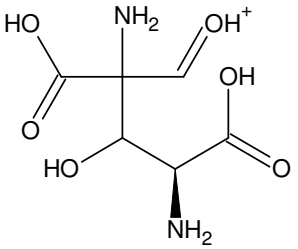

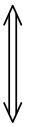

Tautomerie

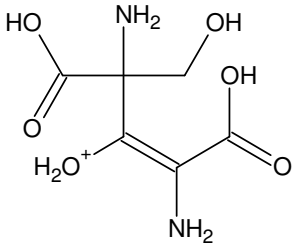

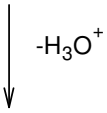

1.1. $NaBH_4$

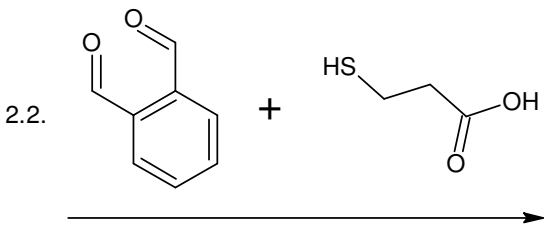

2.2.

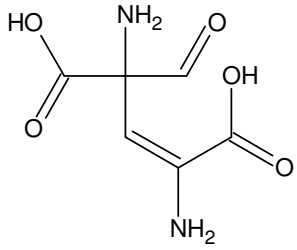

Monoisotopic Mass = 188.043323 Da

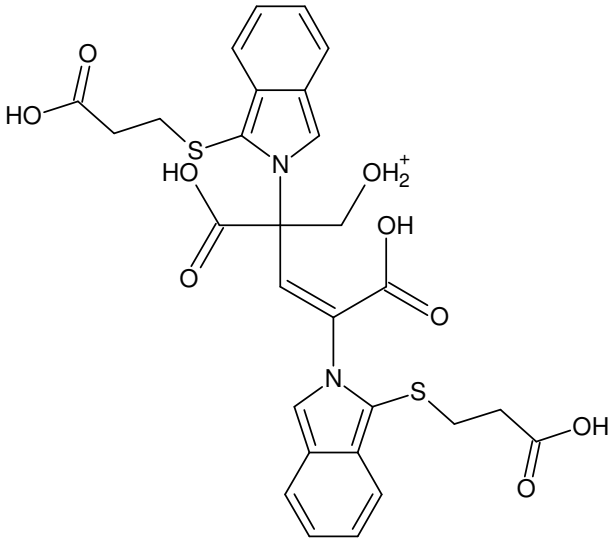

Monoisotopic Mass = 599.1158 Da

599 Th [IV]: ACP Ser-Ser

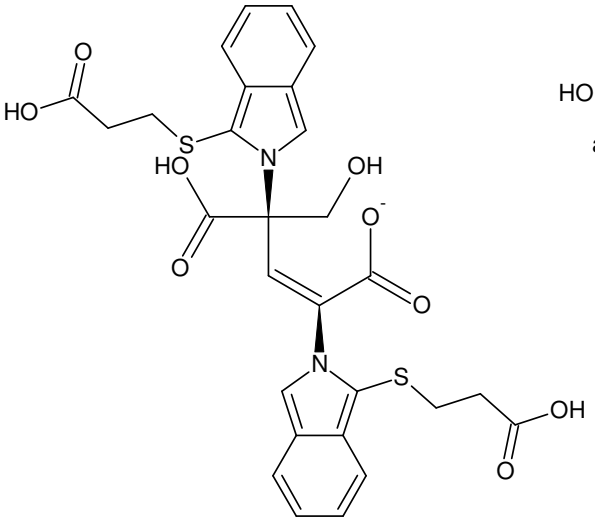

Monoisotopic Mass = 597.10015 Da

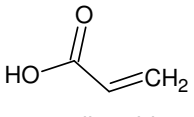

acrylic acid

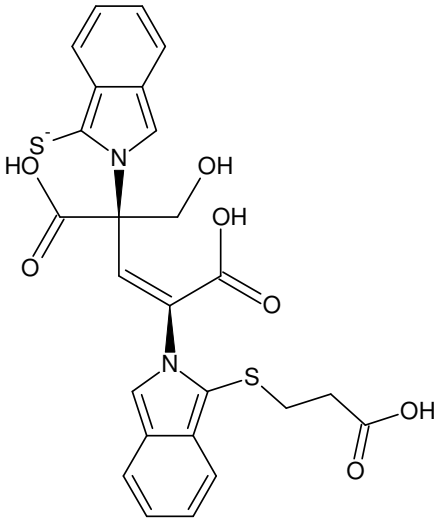

Monoisotopic Mass = 525.07902 Da

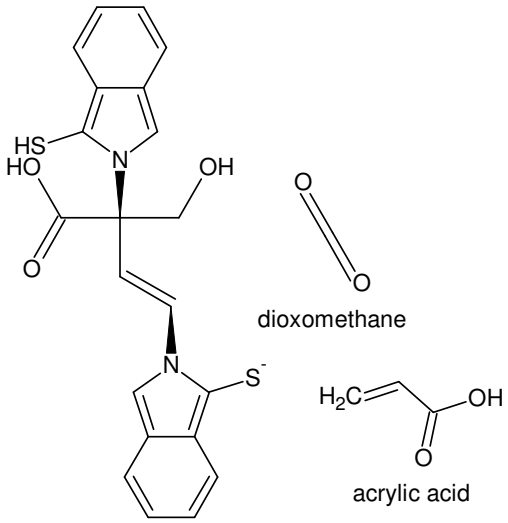

Monoisotopic Mass = 409.06806 Da

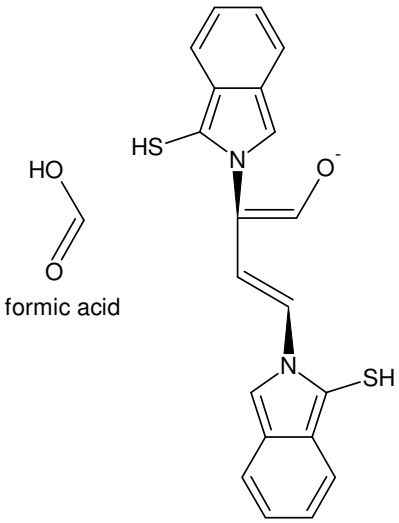

Monoisotopic Mass = 363.06258 Da

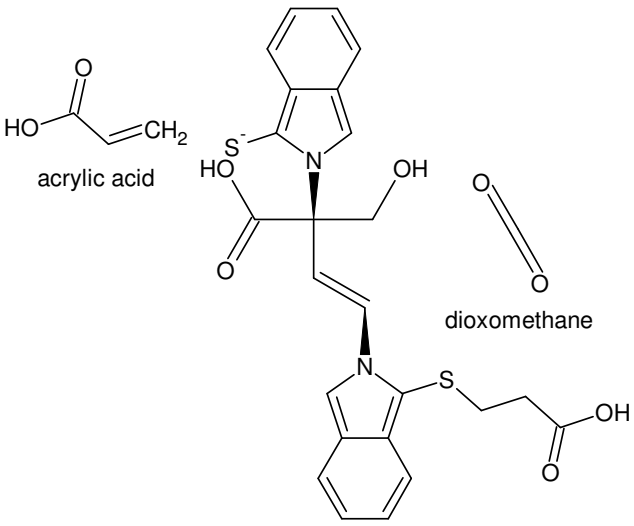

Monoisotopic Mass = 481.08919 Da

-MSn [IV]: 597 -> 525 -> 409 -> 363 and 597 -> 481

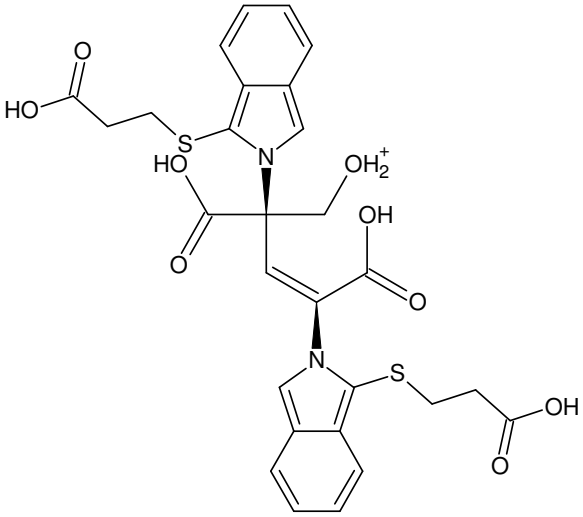

Monoisotopic Mass = 599.1158 Da

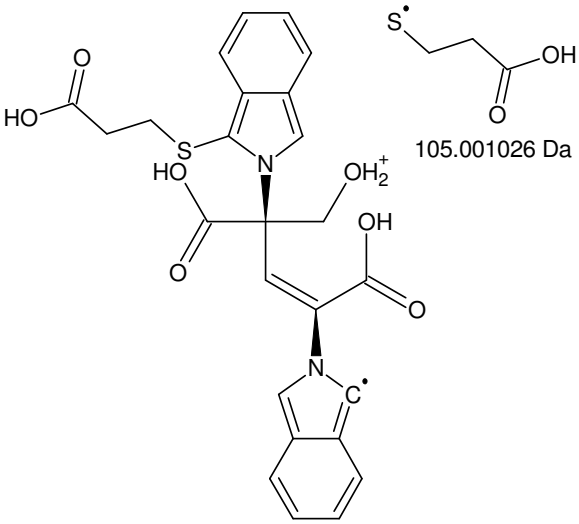

105.001026 Da

Monoisotopic Mass = 494.114774 Da

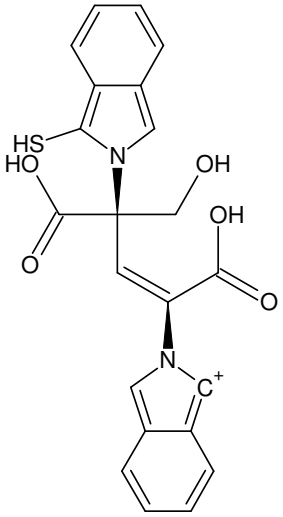

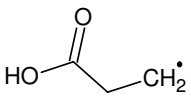

73.028955 Da

Monoisotopic Mass = 421.085819 Da

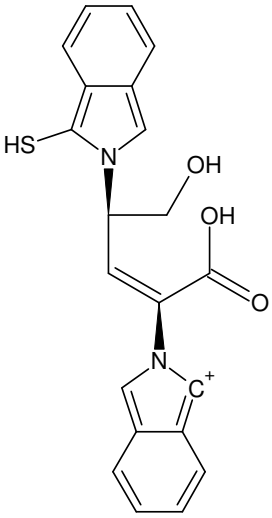

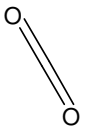

43.98983 Da

Monoisotopic Mass = 377.095989 Da

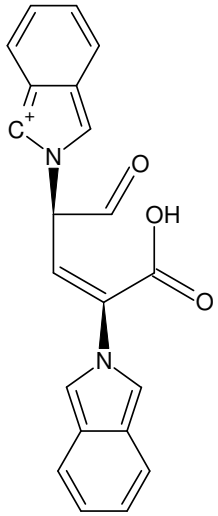

H_2S
33.987721 Da

Monoisotopic Mass = 343.108268 Da

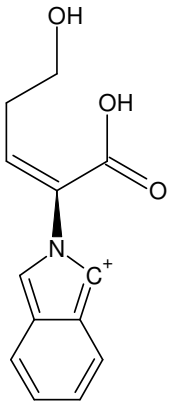

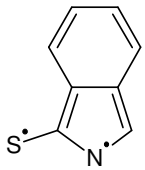

147.01427 Da

Monoisotopic Mass = 230.081719 Da

+MSn [IV]: 599 -> 494 -> 421 -> 377 -> 343, 230

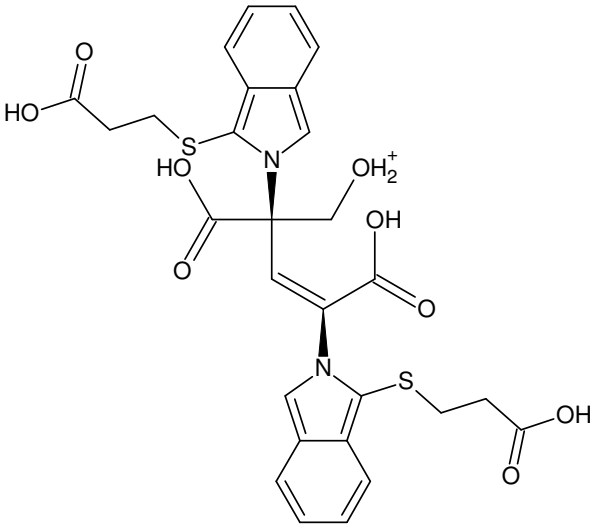

Monoisotopic Mass = 599.1158 Da

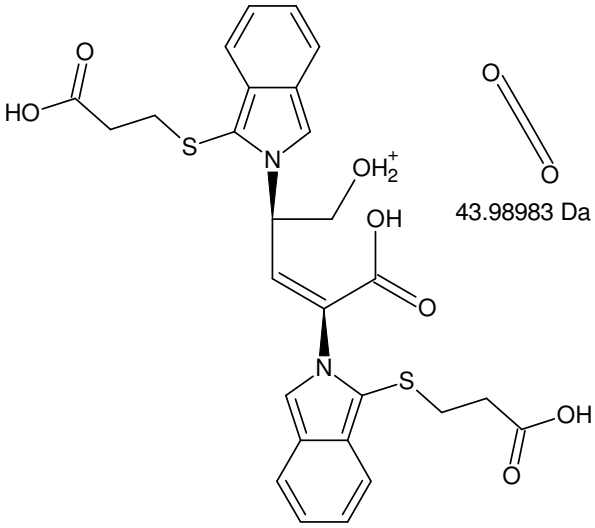

43.98983 Da

Monoisotopic Mass = 555.12597 Da

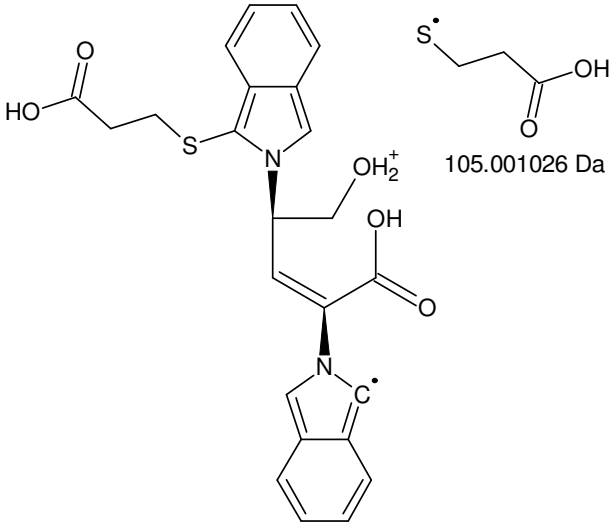

105.001026 Da

Monoisotopic Mass = 450.124944 Da

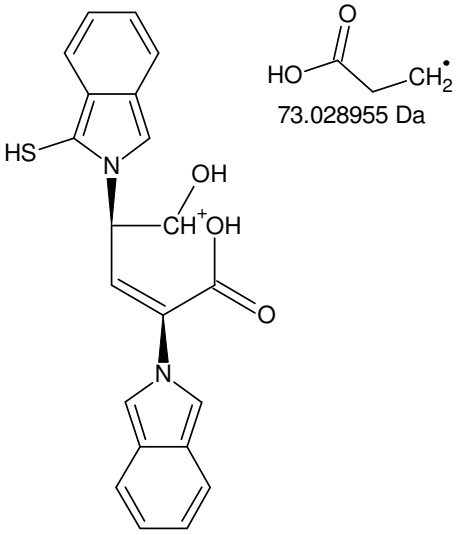

73.028955 Da

Monoisotopic Mass = 377.095989 Da

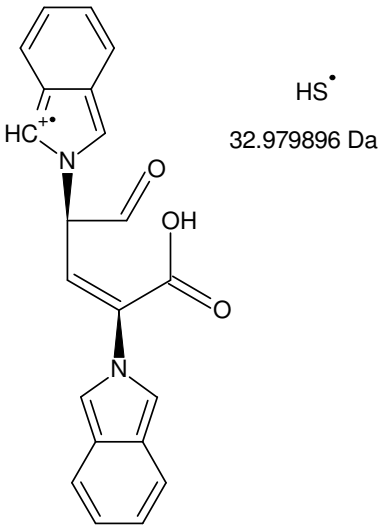

32.979896 Da

Monoisotopic Mass = 344.116093 Da

+MSn [IV]: 599 -> 555 -> 450 -> 377 -> 344

V

The fragmentation pattern of 368 Th / -366 Th of fraction V is identical to that of the (desalted) sample BoT#8 (cp. XIII.I.II, BoT#8).

+MS^n

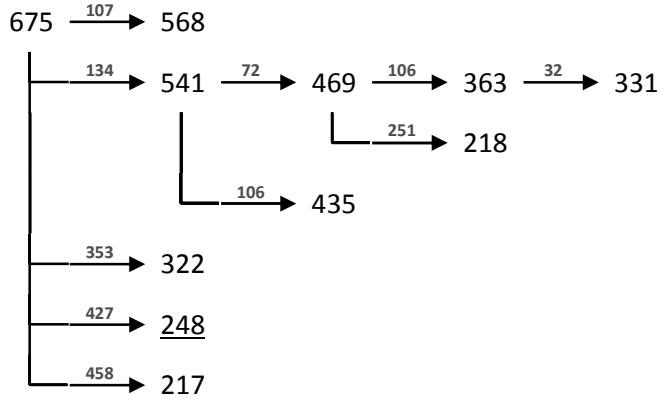

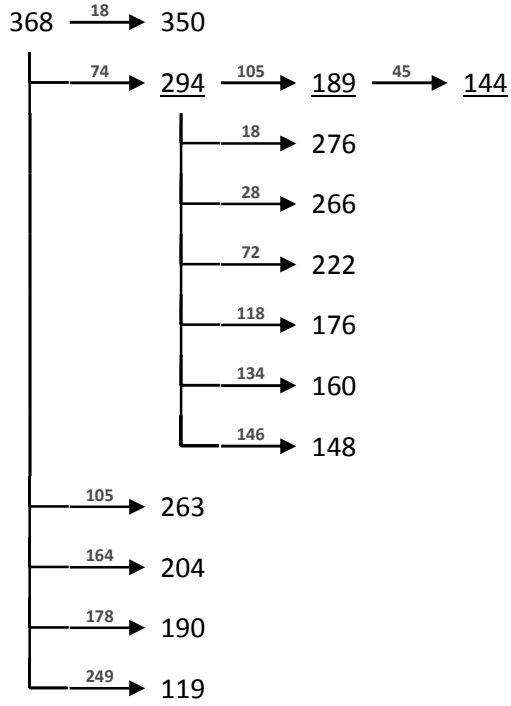

-MS^n

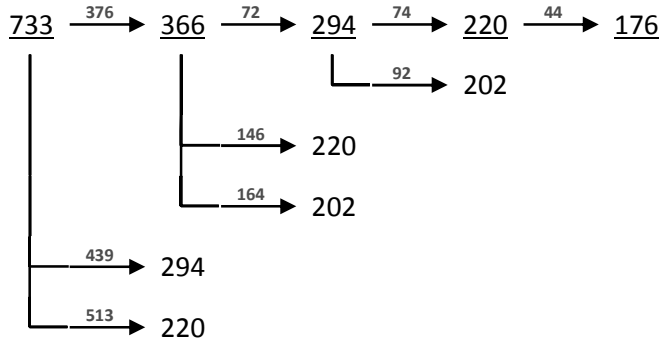

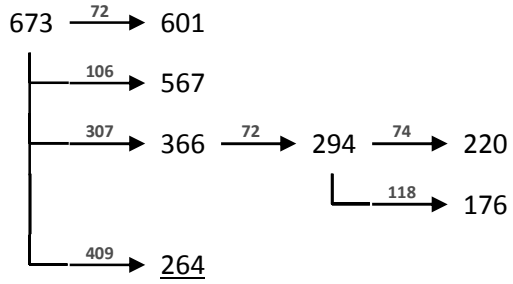

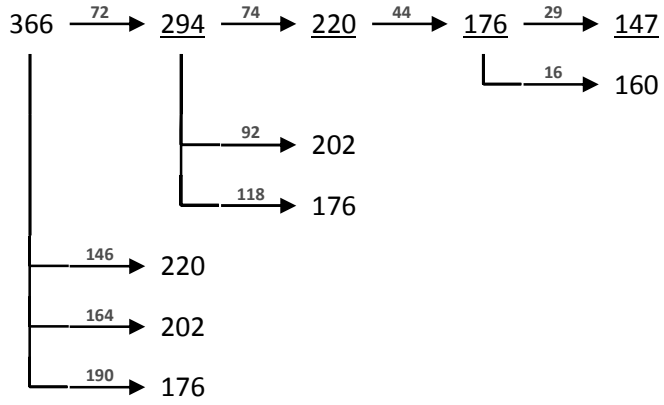

isotopic fingerprint:

peak area / % of monoisotopic	**+1**	**+2**	**+3**
theoretical ($C_{32}H_{39}N_2O_{10}S_2^+$):	37,9	18,1	5,0
measured (675,2 Th):	47,3	20,1	4,4
measured (-672,7 Th):	30,5	18,9	6,0
theoretical ($C_{17}H_{22}NO_6S^+$):	20,1	7,7	1,2
measured (368,2 Th):	22,6	9,2	2,7
measured (-365,9 Th):	20,5	5,7	1,3

Figure XIII-X MS^n analysis of V

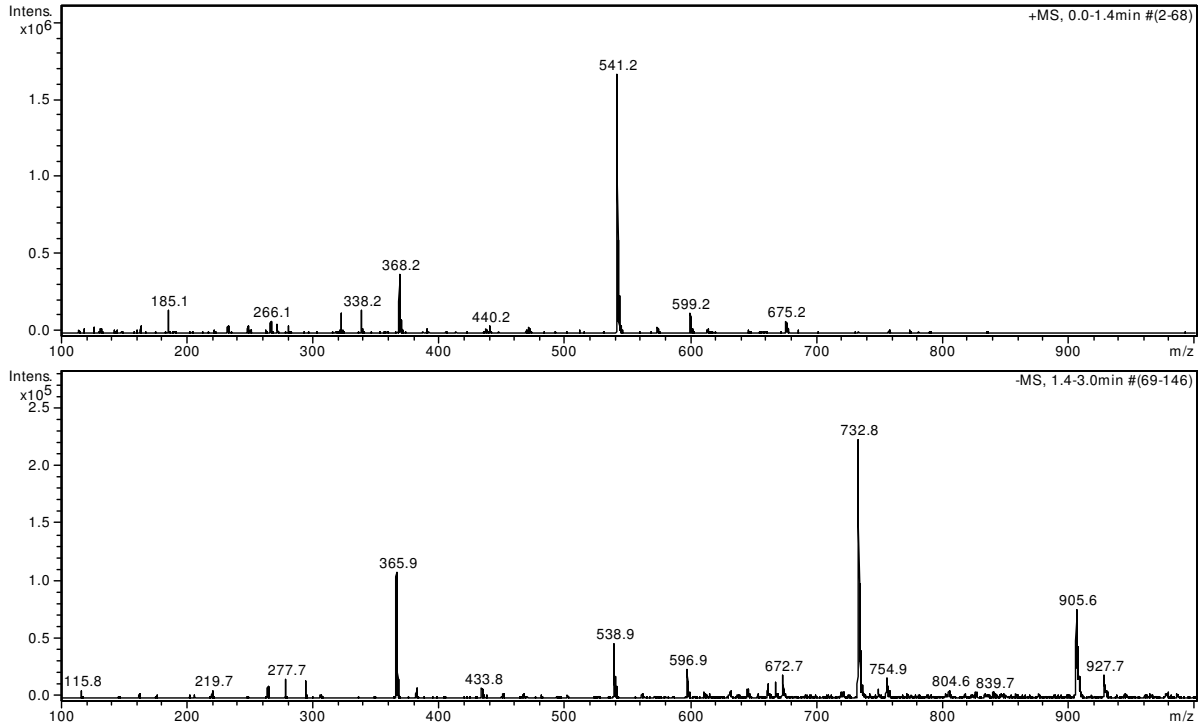

Figure XIII-XI V: 20,4 – 20,9 min, 1 ‰ FA, 39 % ACN in ddH_2O; full scan MS^1

Die beobachteten Fragmente stimmen mit BoT#8 überein.

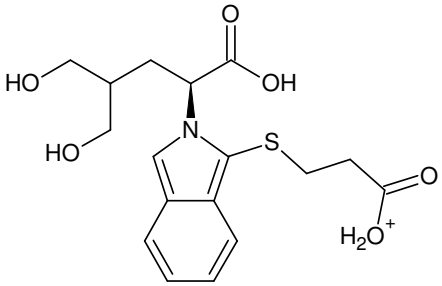

Monoisotopic Mass = 368.116234 Da

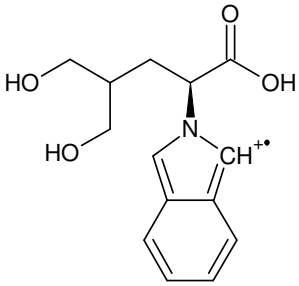

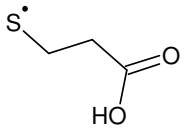

105.001024 Da

Monoisotopic Mass = 263.115209 Da

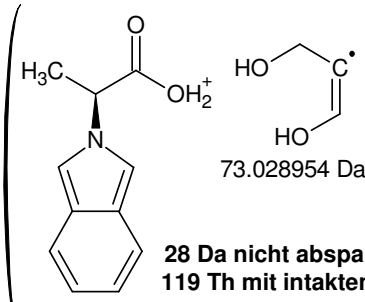

73.028954 Da

28 Da nicht abspaltbar.
119 Th mit intaktem Isoindol nicht realisierbar.

Monoisotopic Mass = 190.086255 Da

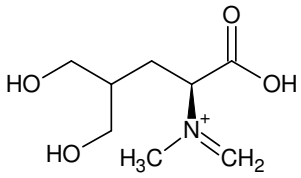

73.007825 Da

Monoisotopic Mass = 190.107384 Da

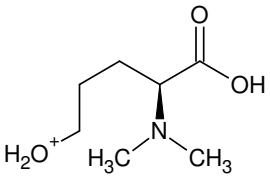

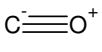

27.994915 Da

Monoisotopic Mass = 162.11247 Da

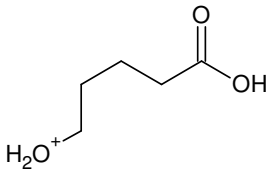

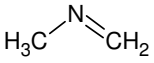

43.042199 Da

Monoisotopic Mass = 119.070271 Da

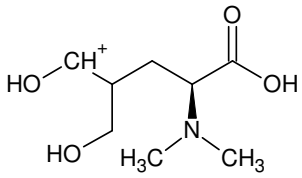

Monoisotopic Mass = 190.107384 Da

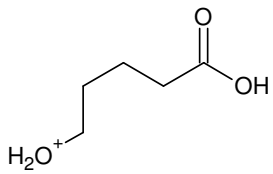

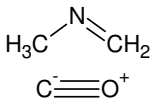

71.037114 Da

Monoisotopic Mass = 119.070271 Da

+MSn [V, BoT#8]: 368 -> 263 -> 190 -> 162 -> 119

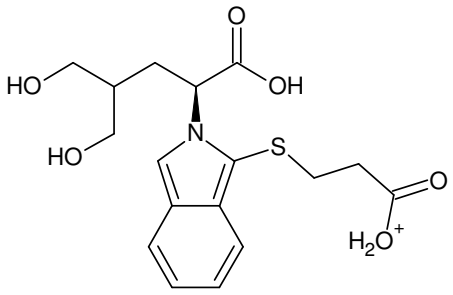

Monoisotopic Mass = 368.116234 Da

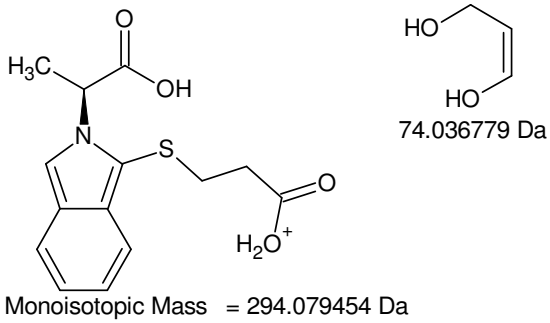

74.036779 Da

Monoisotopic Mass = 294.079454 Da

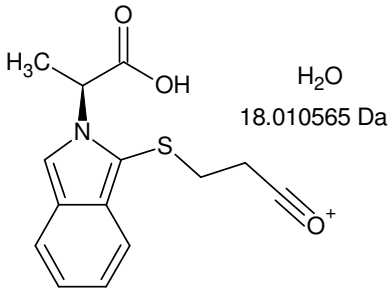

18.010565 Da

Monoisotopic Mass = 276.06889 Da

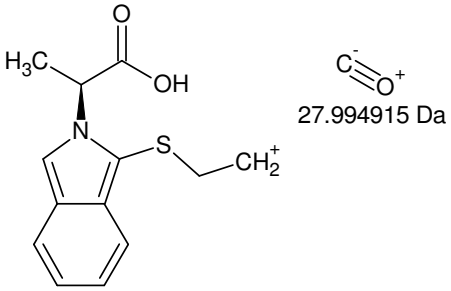

27.994915 Da

Monoisotopic Mass = 248.073975 Da

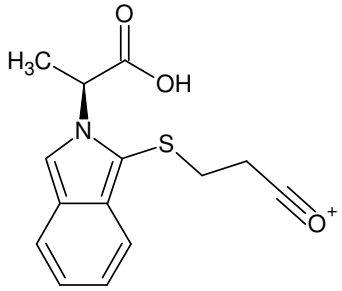

Monoisotopic Mass = 276.06889 Da

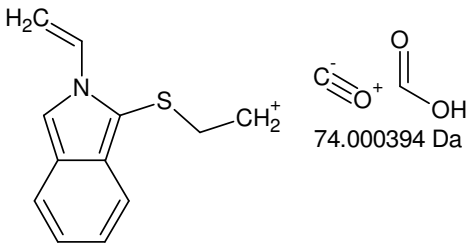

74.000394 Da

Monoisotopic Mass = 202.068496 Da

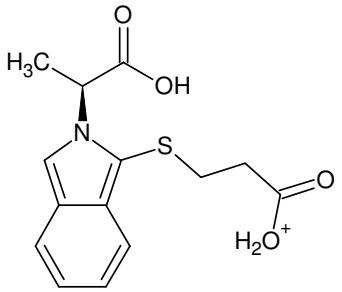

Monoisotopic Mass = 294.079454 Da

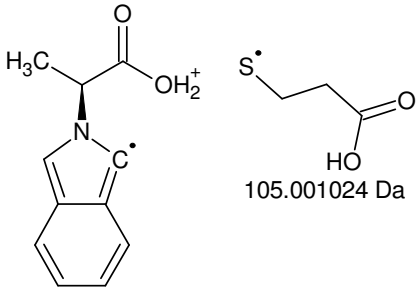

105.001024 Da

Monoisotopic Mass = 189.07843 Da

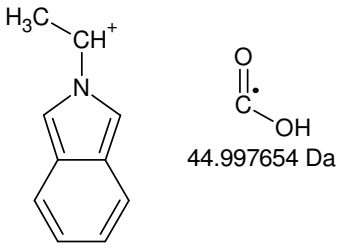

44.997654 Da

Monoisotopic Mass = 144.080776 Da

+MSn [V, BoT#8]: 368 -> 294 -> 276 -> 248 and [368 -> 294 -> 276] -> 202 as well as [368 -> 294] -> 189 -> 144

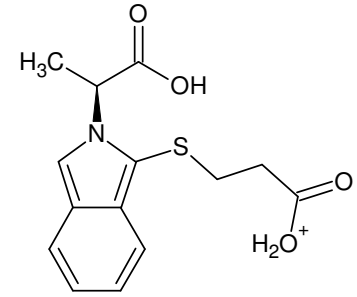

Monoisotopic Mass = 294.079454 Da

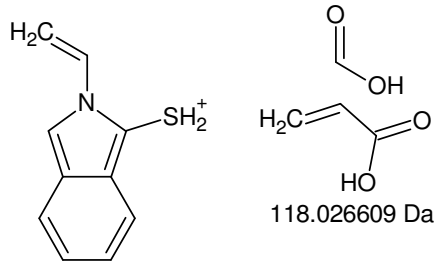

118.026609 Da

Monoisotopic Mass = 176.052846 Da

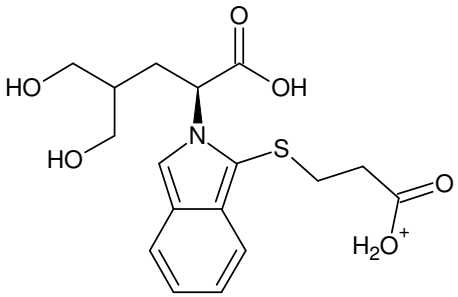

Monoisotopic Mass = 368.116234 Da

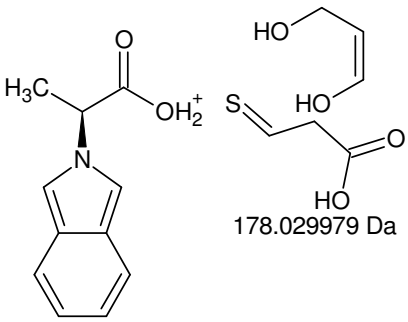

178.029979 Da

Monoisotopic Mass = 190.086255 Da

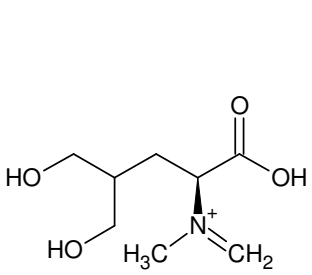

178.008849 Da

Monoisotopic Mass = 190.107384 Da

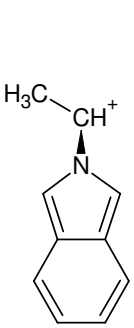

46.005479 Da

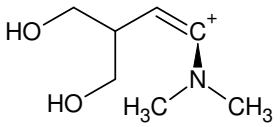

Monoisotopic Mass = 144.101905 Da

Monoisotopic Mass = 144.080776 Da

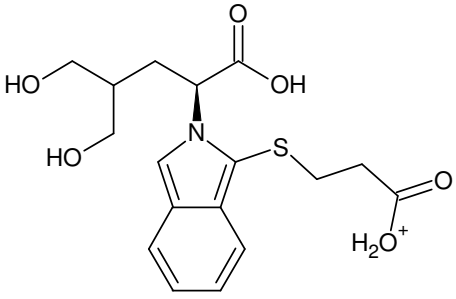

Monoisotopic Mass = 368.116234 Da

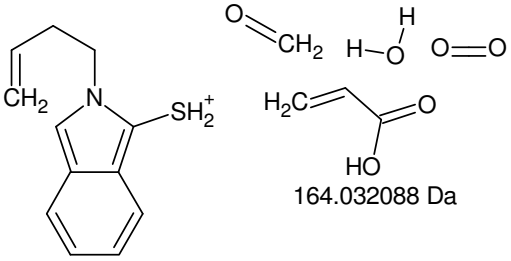

164.032088 Da

Monoisotopic Mass = 204.084146 Da

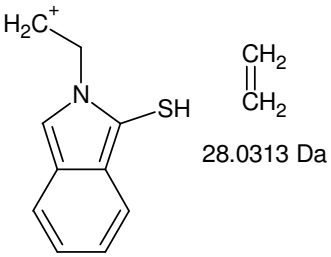

28.0313 Da

Monoisotopic Mass = 176.052846 Da

+MSn [V, BoT#8]: [368 -> 294] -> 176 sowie 368 -> 2x 190 -> 144 und 368 -> 204 -> 176

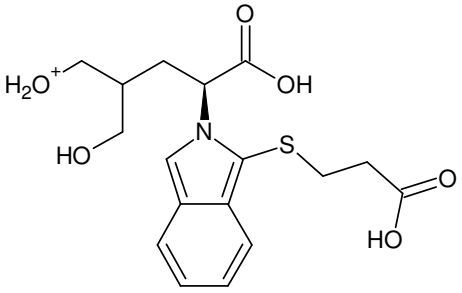

Monoisotopic Mass = 368.116234 Da

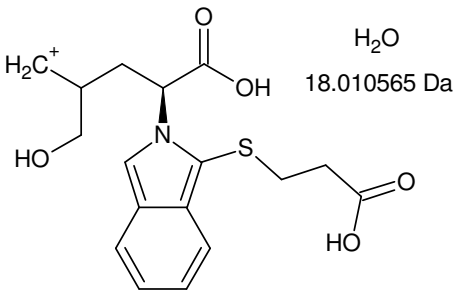

Monoisotopic Mass = 350.105669 Da

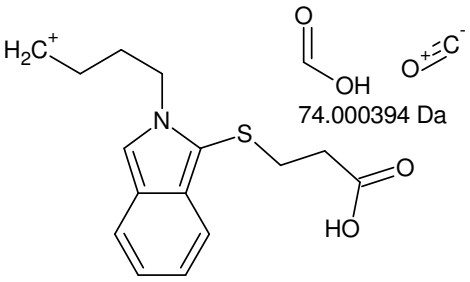

Monoisotopic Mass = 276.105275 Da

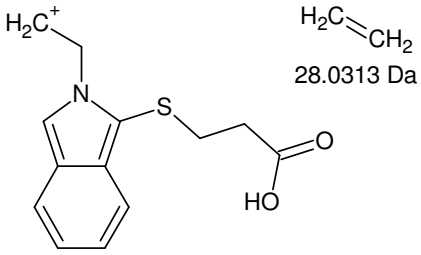

Monoisotopic Mass = 248.073975 Da

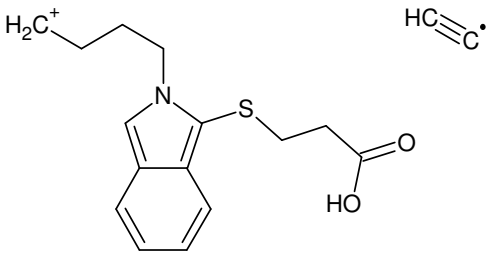

Monoisotopic Mass = 276.105275 Da

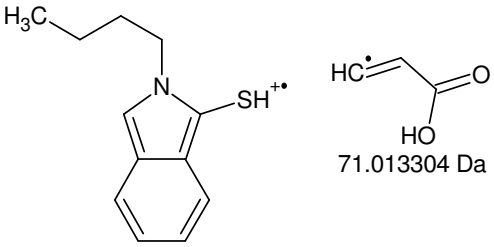

Monoisotopic Mass = 205.091971 Da

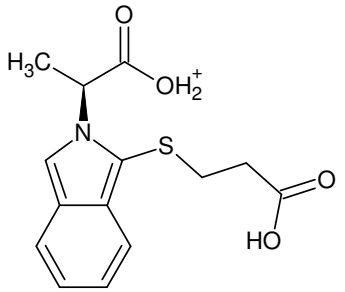

Monoisotopic Mass = 294.079454 Da

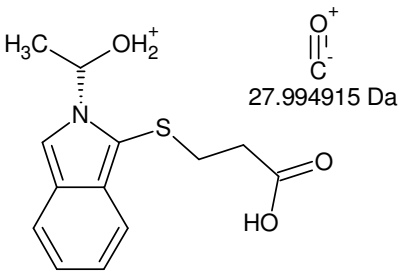

Monoisotopic Mass = 266.08454 Da

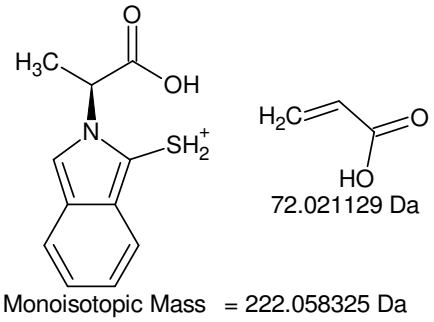

Monoisotopic Mass = 222.058325 Da

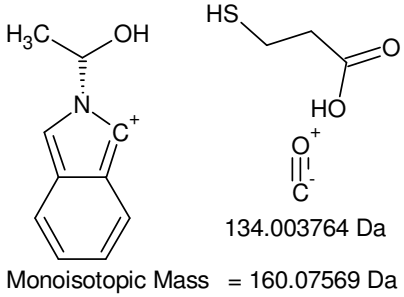

Monoisotopic Mass = 160.07569 Da

+MSn [V, BoT#8]: 368 -> 350 -> 276 -> 248, 205 and [368 -> 294] -> 266, 222, 160

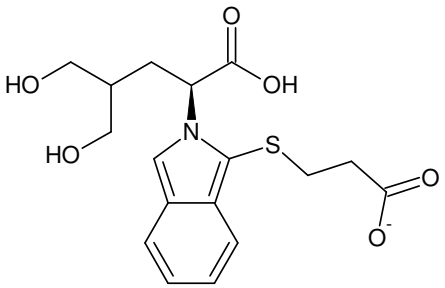

Monoisotopic Mass = 366.101681 Da

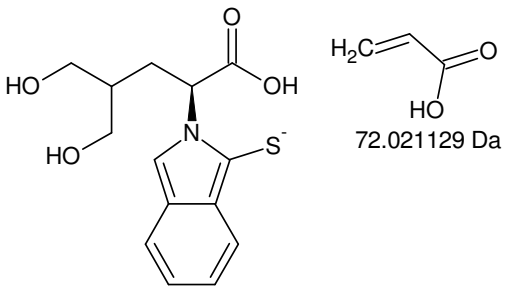

72.021129 Da

Monoisotopic Mass = 294.080552 Da

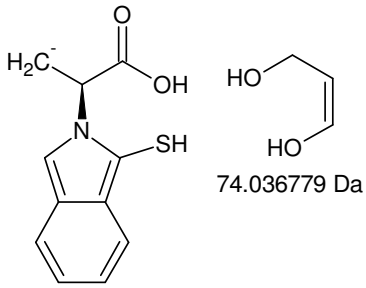

74.036779 Da

Monoisotopic Mass = 220.043772 Da

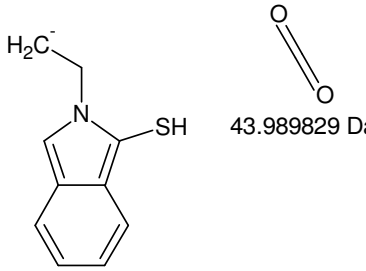

43.989829 Da

Monoisotopic Mass = 176.053943 Da

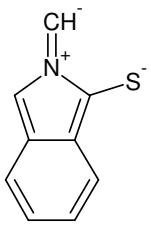

CH_4

16.0313 Da

Compounds found: 3

H2N	MW=16,0187232
CH4	MW=16,0312984
O	MW=15,994915

Monoisotopic Mass = 160.022643 Da

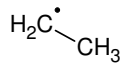

29.039125 Da

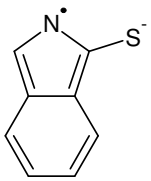

Compounds found: 6

CHO	MG=29,0027396
CH3N	MG=29,0265478
C2H5	MG=29,039123
HN2	MG=29,0139726
H13O	MG=29,0966348
H15N	MG=29,120443

Monoisotopic Mass = 147.014818 Da

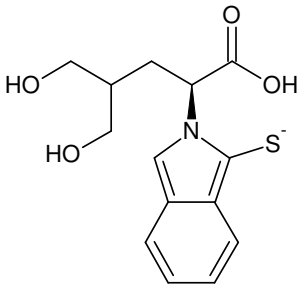

Monoisotopic Mass = 294.080552 Da

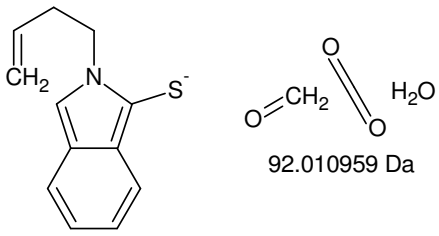

92.010959 Da

Monoisotopic Mass = 202.069593 Da

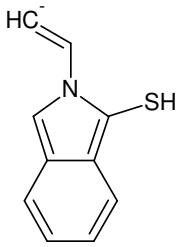

28.0313 Da

Monoisotopic Mass = 174.038293 Da

-MSn [V, BoT#8]: 366 -> 294 -> 220 -> 176 -> 160, 147 and [366 -> 294] -> 202 -> 174

675 = 368 + 307

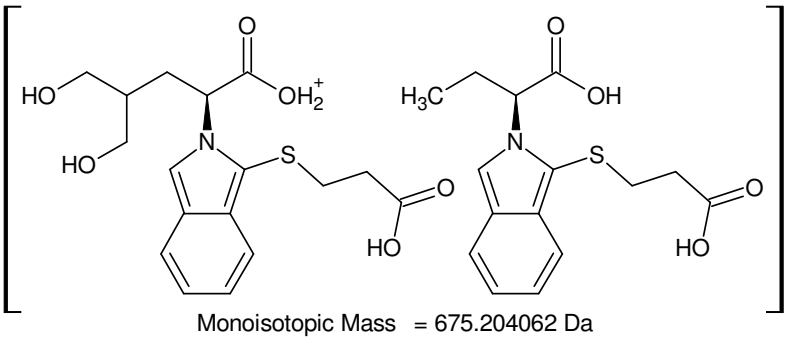

Monoisotopic Mass = 675.204062 Da

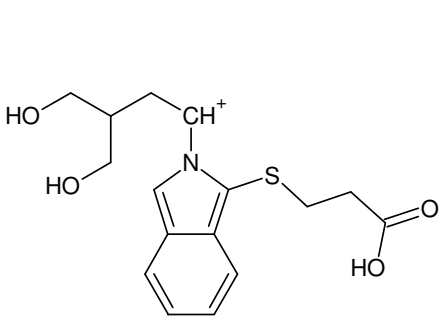

Monoisotopic Mass = 322.110755 Da

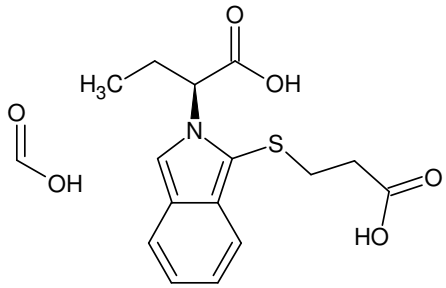

353.093307 Da

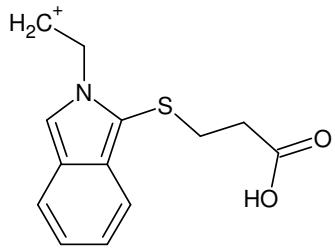

Monoisotopic Mass = 248.073975 Da

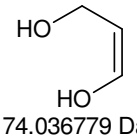

74.036779 Da

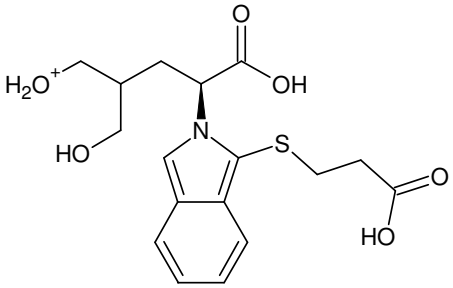

Monoisotopic Mass = 368.116234 Da

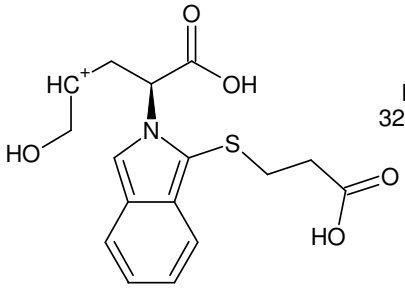

Monoisotopic Mass = 336.090019 Da

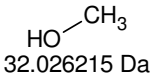

32.026215 Da

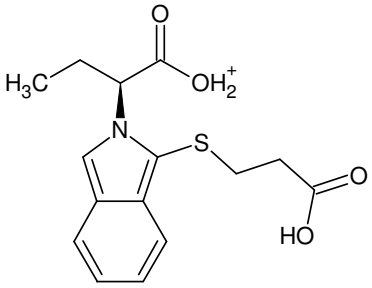

Monoisotopic Mass = 308.095104 Da

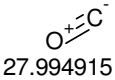

27.994915 Da

+MSn [V]: 675 -> 322 -> 248 and 368 -> 308

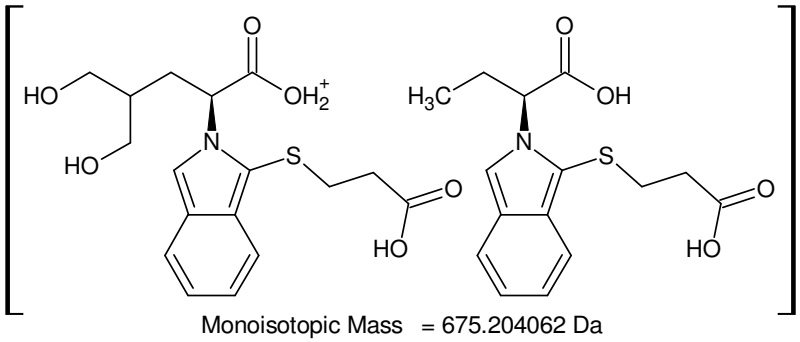

Monoisotopic Mass = 675.204062 Da

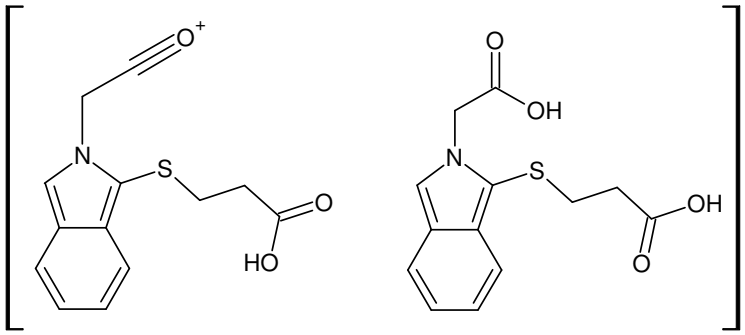

Monoisotopic Mass = 541.11032 Da

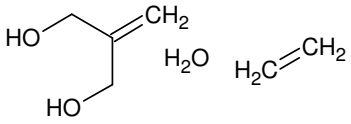

134.094294 Da

Fragmente von 541Th: siehe I

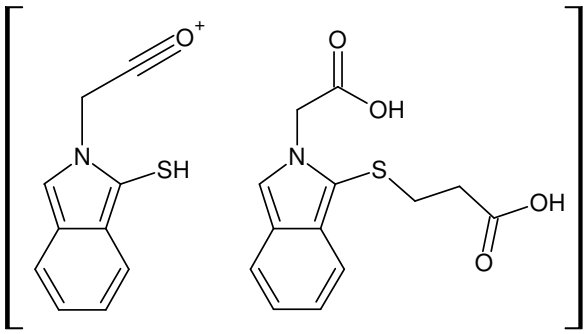

Monoisotopic Mass = 469.08919 Da

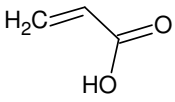

72.02113 Da

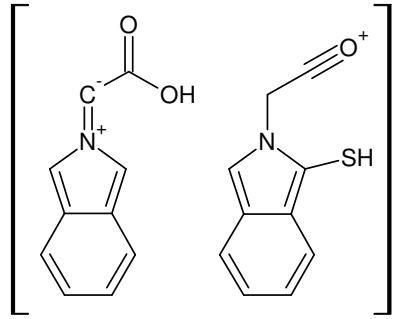

Monoisotopic Mass = 363.080339 Da

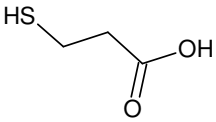

106.008851 Da

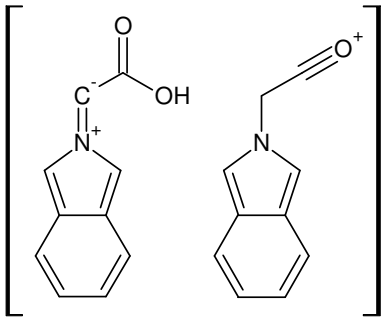

Monoisotopic Mass = 331.108268 Da

S**:**

31.972071 Da

+MSn [V]: 675 -> 541 -> 469 -> 363 -> 331

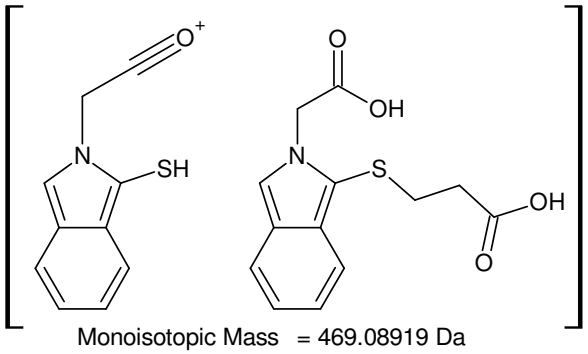

Monoisotopic Mass = 469.08919 Da

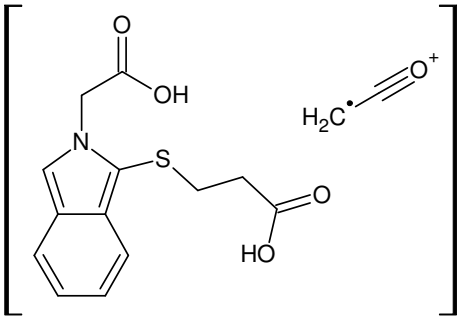

Monoisotopic Mass = 321.067095 Da

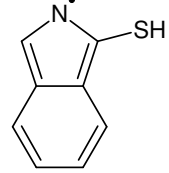

148.022095 Da

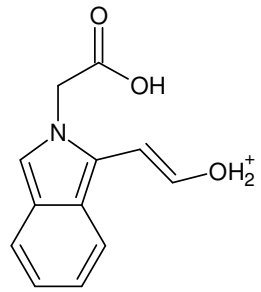

Monoisotopic Mass = 218.081719 Da

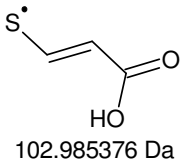

102.985376 Da

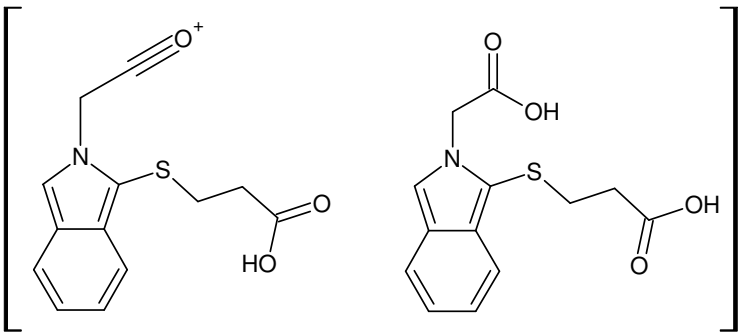

Monoisotopic Mass = 541.11032 Da

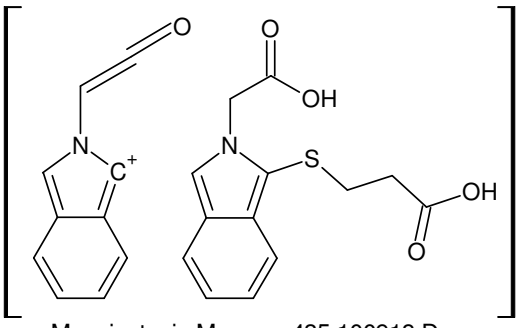

Monoisotopic Mass = 435.100918 Da

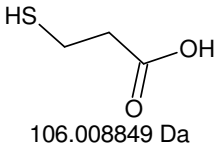

106.008849 Da

+MSn [V]: [675 -> 541 -> 469] -> 218 and [675 -> 541] -> 435

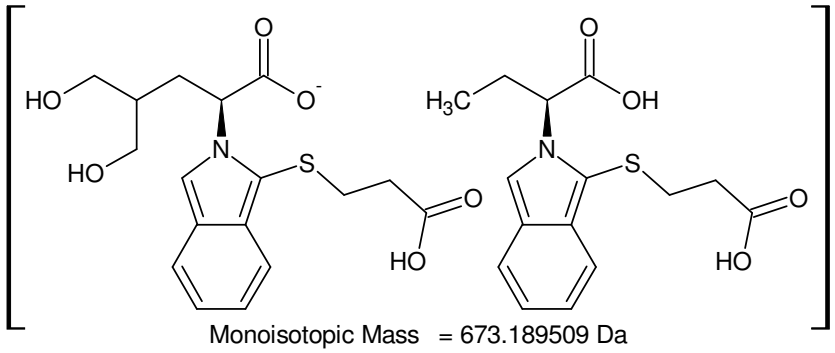

Monoisotopic Mass = 673.189509 Da

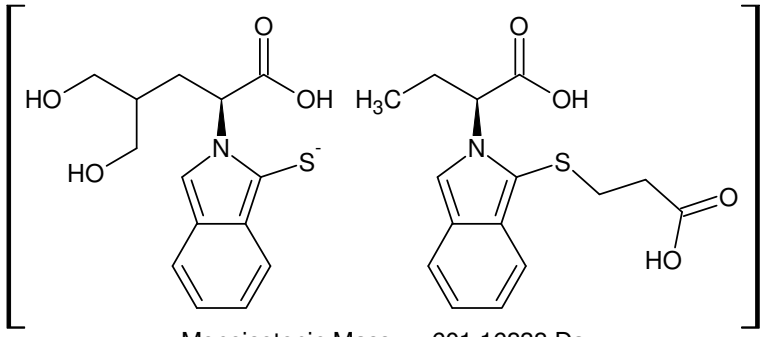

Monoisotopic Mass = 601.16838 Da

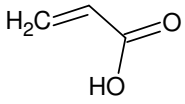

72.021129 Da

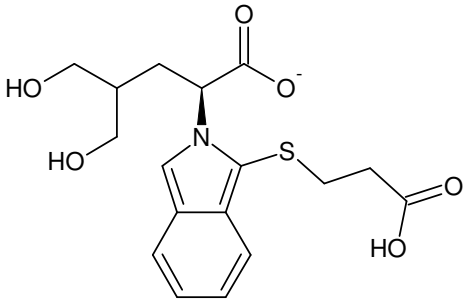

Monoisotopic Mass = 366.101681 Da

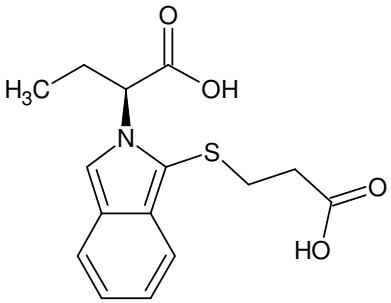

307.087828 Da

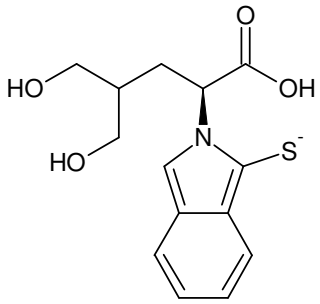

Monoisotopic Mass = 294.080552 Da

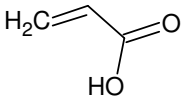

72.021129 Da

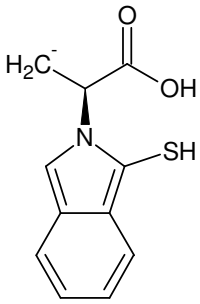

Monoisotopic Mass = 220.043772 Da

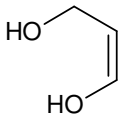

74.036779 Da

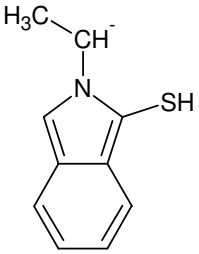

Monoisotopic Mass = 176.053943 Da

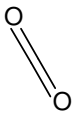

43.989829 Da

-MSn [V]: 673 -> 601, 366 -> 294 -> 220 -> 176

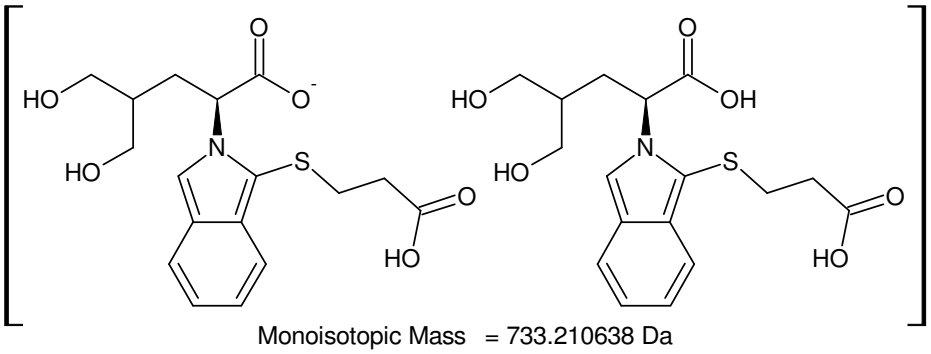

Monoisotopic Mass = 733.210638 Da

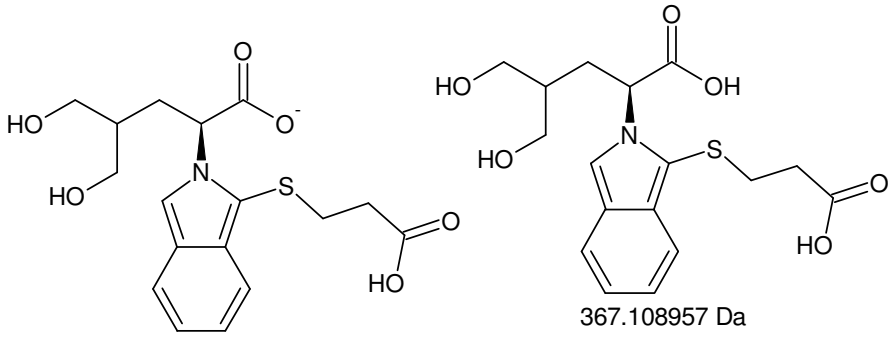

Monoisotopic Mass = 366.101681 Da

367.108957 Da

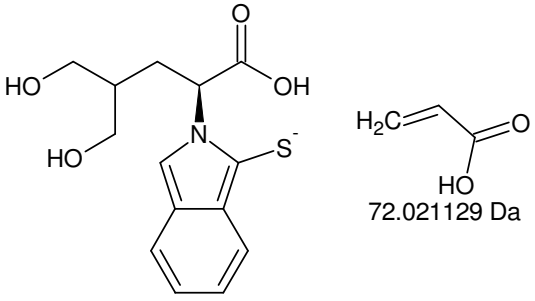

Monoisotopic Mass = 294.080552 Da

72.021129 Da

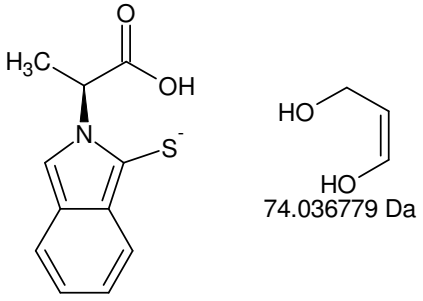

Monoisotopic Mass = 220.043772 Da

74.036779 Da

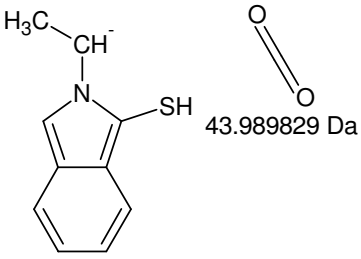

Monoisotopic Mass = 176.053943 Da

43.989829 Da

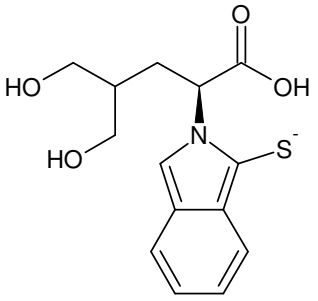

Monoisotopic Mass = 294.080552 Da

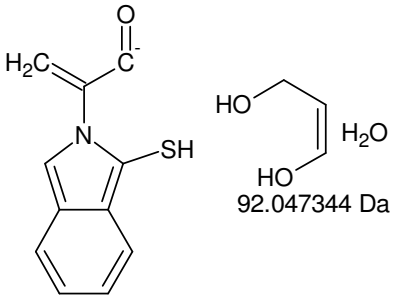

Monoisotopic Mass = 202.033207 Da

92.047344 Da

-MSn [V]: 733 -> 366 -> 294 -> 220 -> 176 and [733 -> 366 ->294] -> 202

VI

The target signal of fraction VI presented itself as a shoulder on the signal of an unmodified amino acid (Asp).

+MS^n

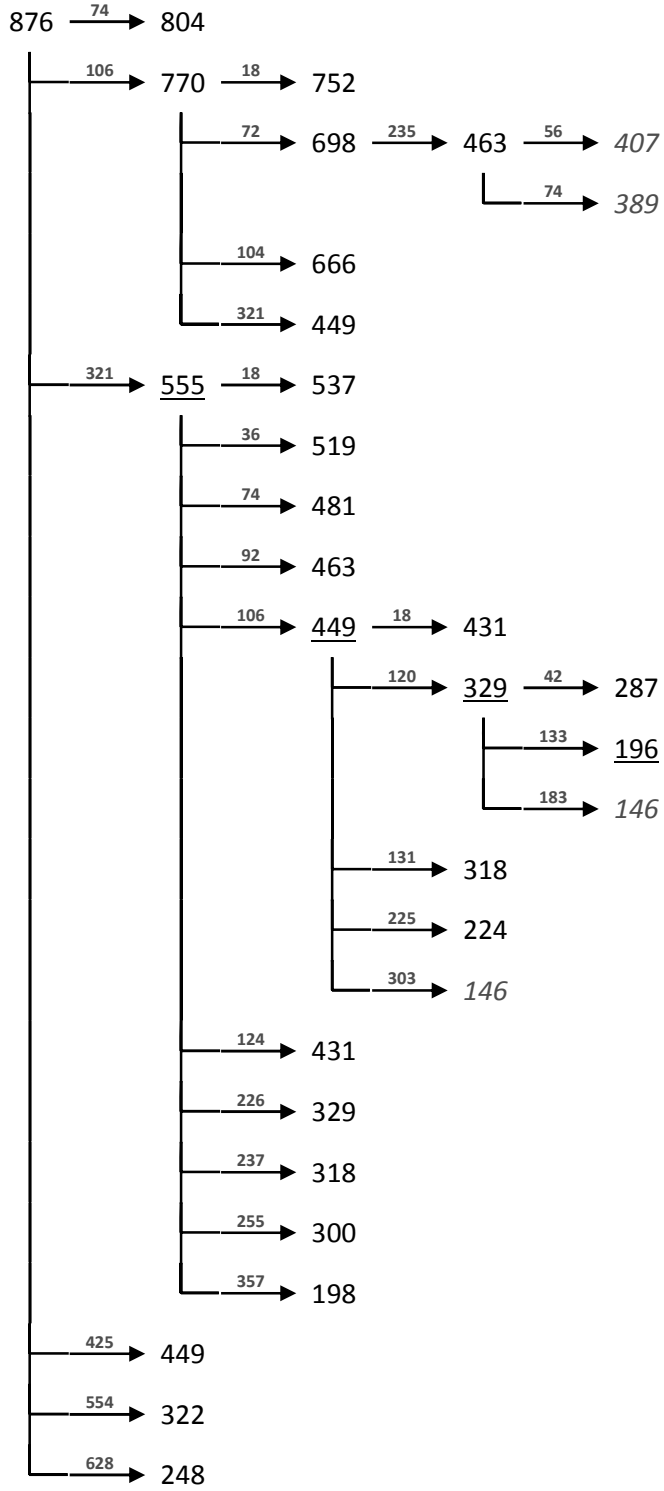

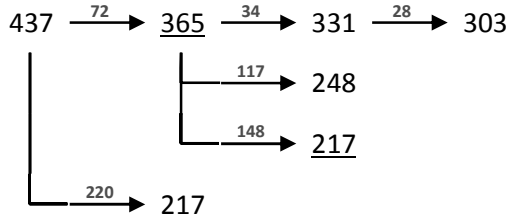
437
72
365
34
331
28
303
117
248
148
217
220
217

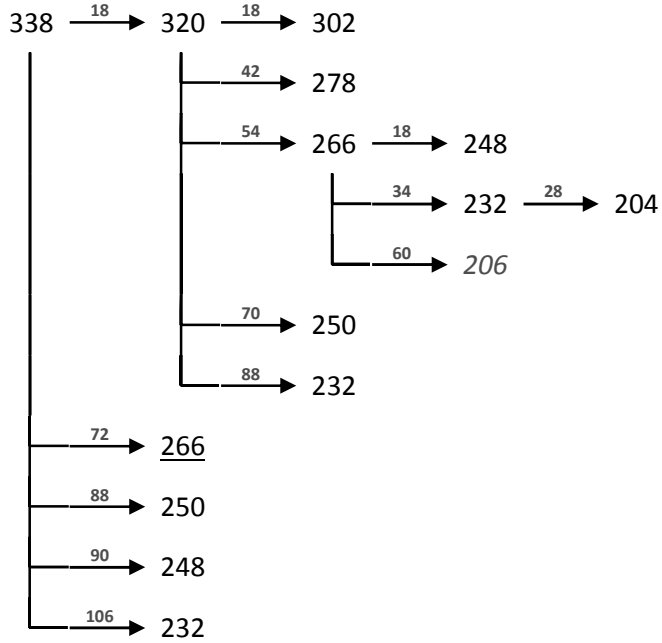
338
18
320
18
302
42
278
54
266
18
248
34
232
28
204
60
206
70
250
88
232
72
266
88
250
90
248
106
232

-MS^n

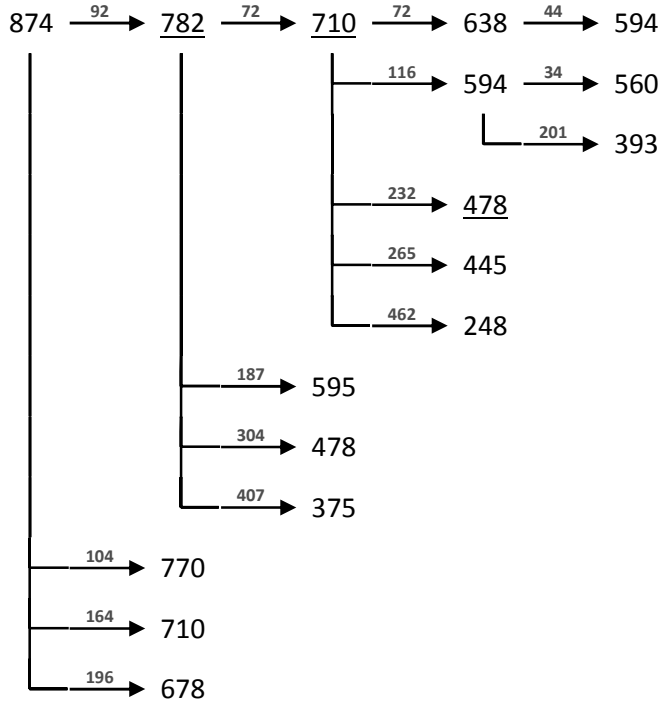
874
92
782
72
710
72
638
44
594
116
594
34
560
201
393
232
478
265
445
462
248
187
595
304
478
407
375
104
770
164
710
196
678

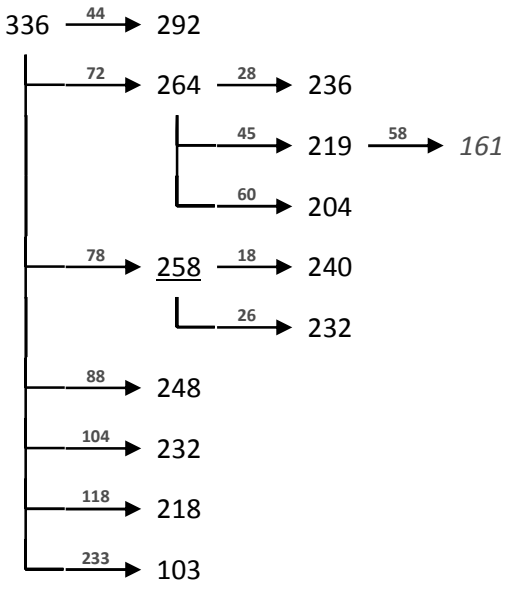

isotopic fingerprint:

peak area / % of monoisotopic	**+1**	**+2**	**+3**
measured (876,3 Th):	47,1	9,5	-
measured (-874,2 Th):	69,5	18,3	-
theoretical ($C_{19}H_{25}N_4O_6S^+$):	23,4	8,4	1,5
measured (437,2 Th):	46,4	12,7	9,0
measured (-434,9 Th):	47,6	17,3	-
theoretical ($C_{15}H_{16}NO_6S^+$):	17,9	7,1	1,1
measured (338,2 Th):	21,1	7,3	1,1
measured (-335,8 Th):	16,4	8,5	3,2

Figure XIII-XII MS^n analysis of VI

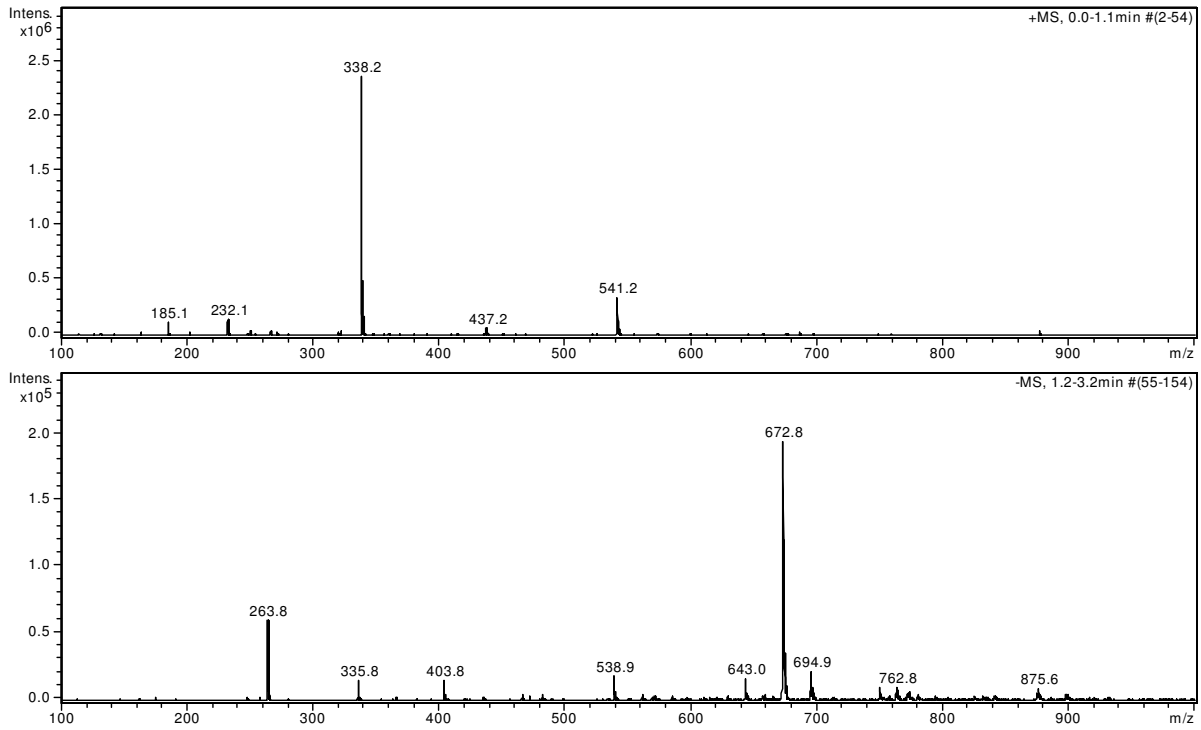

Figure XIII-XIII VI: 34,8 – 35,6 min, 1 ‰ FA, 45 % ACN in ddH_2O; full scan MS^1

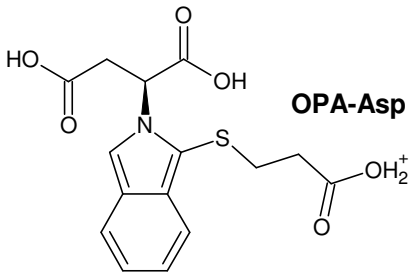

Monoisotopic Mass = 338.069284 Da

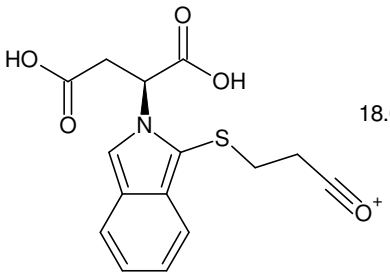

H_2O
water
18.010565 Da

Monoisotopic Mass = 320.058719 Da

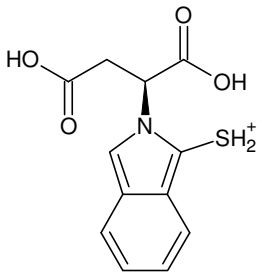

carbon monoxide

acetylene
54.010565 Da

Monoisotopic Mass = 266.048154 Da

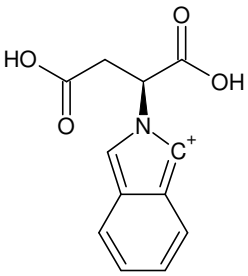

H_2S
hydrogen sulfide
33.98772 Da

Monoisotopic Mass = 232.060434 Da

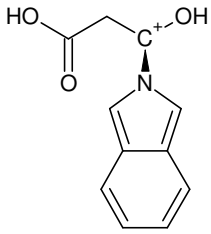

carbon monoxide
27.994915 Da

Monoisotopic Mass = 204.06552 Da

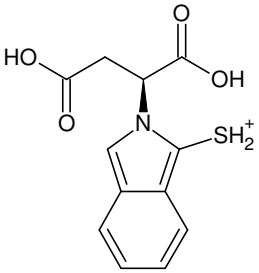

Monoisotopic Mass = 266.048154 Da

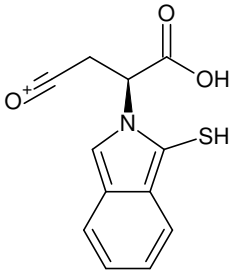

H_2O
water
18.010565 Da

Monoisotopic Mass = 248.03759 Da

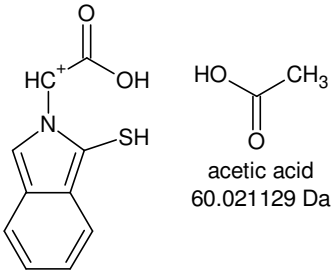

acetic acid
60.021129 Da

Monoisotopic Mass = 206.027025 Da

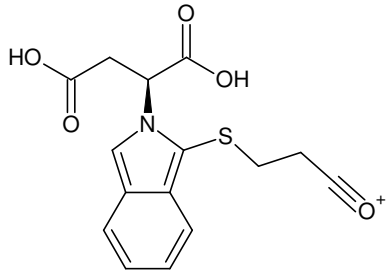

Monoisotopic Mass = 320.058719 Da

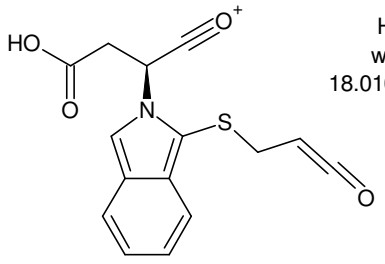

H_2O
water
18.010565 Da

Monoisotopic Mass = 302.048154 Da

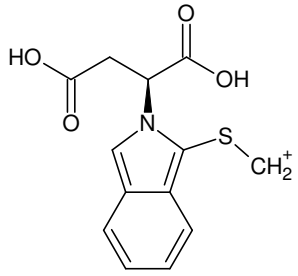

ethenone
42.010565 Da

Monoisotopic Mass = 278.048154 Da

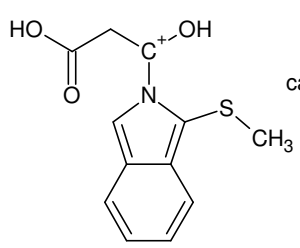

carbon monoxide
27.994915 Da

Monoisotopic Mass = 250.05324 Da

+MSn [VI]: 338 -> 320 -> 266 -> 232 -> 204 and [338 -> 320 -> 266] -> 248, 206 as well as [338 -> 320] -> 302, 278 -> 250

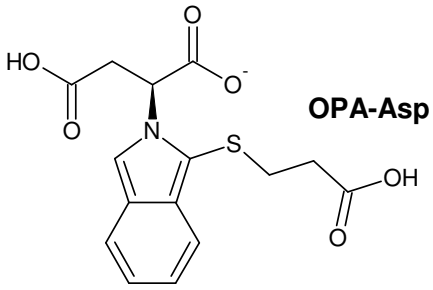

OPA-Asp

Monoisotopic Mass = 336.054731 Da

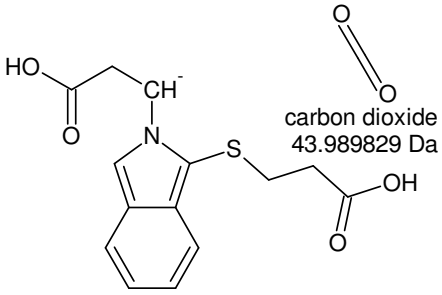

Monoisotopic Mass = 292.064902 Da

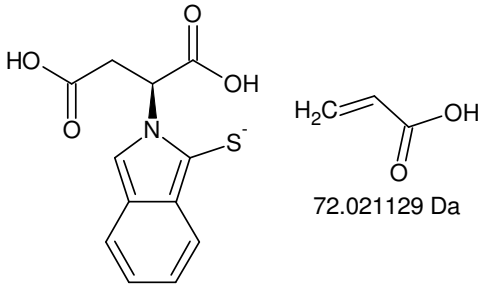

Monoisotopic Mass = 264.033601 Da

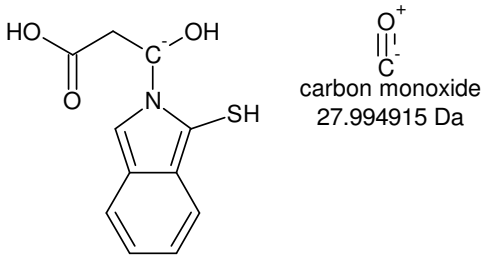

Monoisotopic Mass = 236.038687 Da

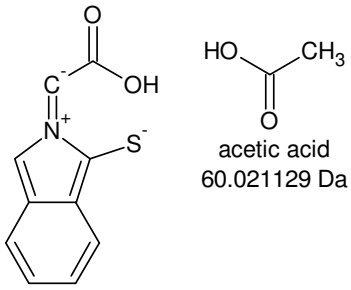

Monoisotopic Mass = 204.012472 Da

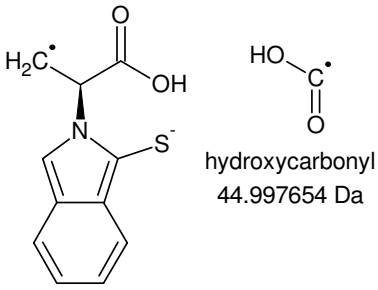

Monoisotopic Mass = 219.035947 Da

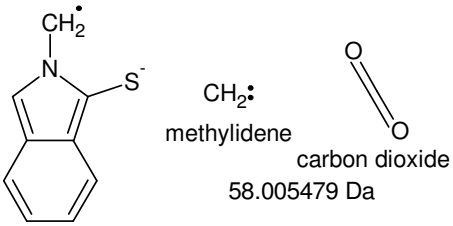

Monoisotopic Mass = 161.030468 Da

-MSn [VI]: 336 -> 292, 264 -> 236, 204, 219 -> (161)

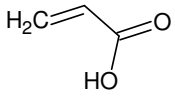

72.021129 Da

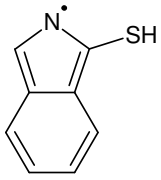

148.022094 Da

117.057849 Da

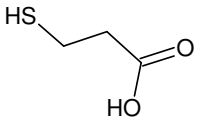

106.008849 Da

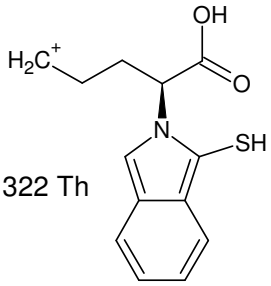

I: 322 Th

Monoisotopic Mass = 248.073975 Da

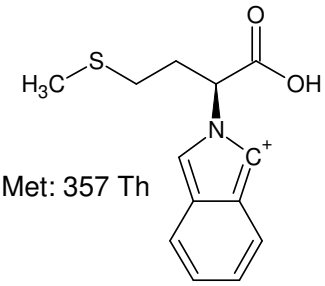

Met: 357 Th

Monoisotopic Mass = 248.073975 Da

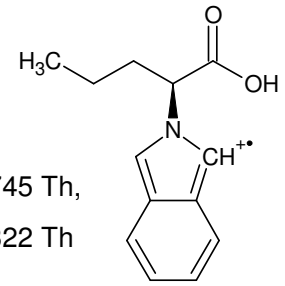

I: 745 Th,

I: 322 Th

Monoisotopic Mass = 217.10973 Da

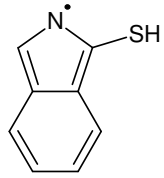

148.022094 Da

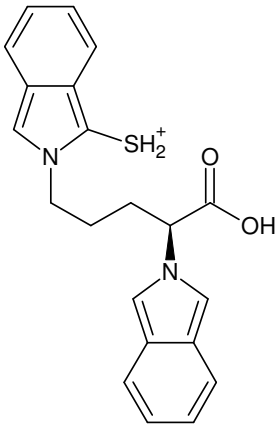

Monoisotopic Mass = 365.131824 Da

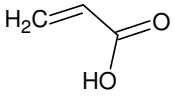

72.021129 Da

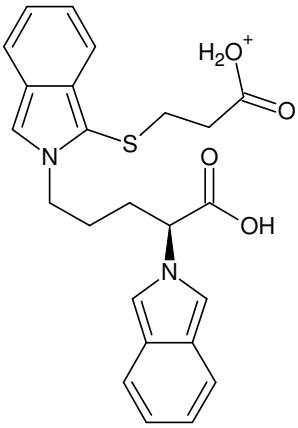

Monoisotopic Mass = 437.152954 Da

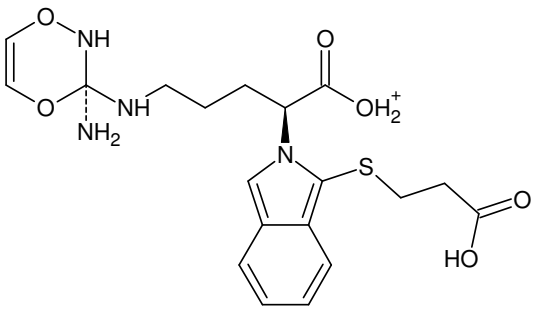

Monoisotopic Mass = 437.148931 Da

+MSn [VI]: 437 Th {I/III}

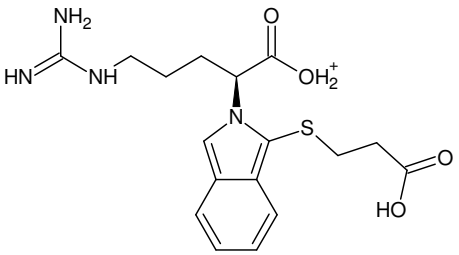

Monoisotopic Mass = 379.143452 Da

437 - 379 = **58**
Gefundene Verbindungen: 31
CH2N2O MG=58,0167122
CH4N3 MG=58,0405204
...
H30N2 MG=58,240886
N3O MG=58,004137

-----D--B--E--f-i-l-t-e-r-----
22.11.2011 - 13:42:29,51
akzeptierte DBE:
1 2 3 4 5 6 7 8

CH2N2O DBE: 2
C2H2O2 DBE: 2
C2H2S DBE: 2
C2H6N2 DBE: 1
C3H6O DBE: 1
H2N4 DBE: 2

6 von 31 Summenformeln

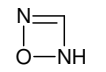

CH_2N_2O
58.016713 Da

$C_2H_2O_2$
58.005479 Da

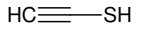

C_2H_2S
57.98772 Da

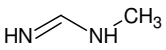

$C_2H_6N_2$
58.053098 Da

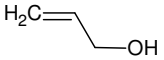

C_3H_6O
58.041865 Da

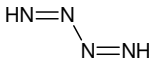

H_2N_4
58.027946 Da

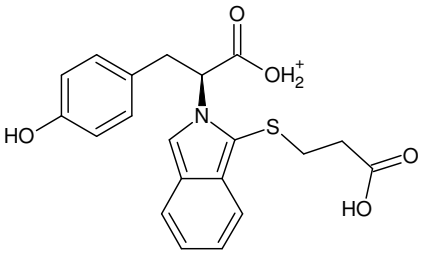

Monoisotopic Mass = 386.105669 Da

437 - 386 = **51**
Gefundene Verbindungen: 21
CH7O2 MG=51,0446022
CH7S MG=51,0268442
...
H21NO MG=51,1623056
H23N2 MG=51,1861138

-----D--B--E--f-i-l-t-e-r-----
22.11.2011 - 13:50:26,18
akzeptierte DBE:
1 2 3 4 5 6 7 8

C3HN DBE: 4

1 von 21 Summenformeln

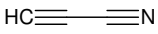

C_3HN
51.010899 Da

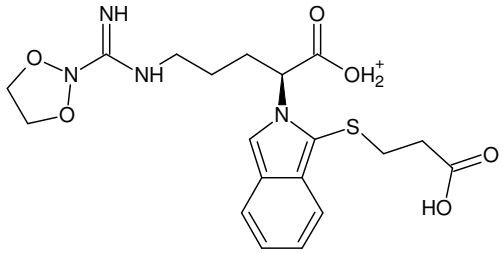

Monoisotopic Mass = 437.148931 Da

365 - 331 = **34**
Gefundene Verbindungen: 8
CH6O MG=34,0418626
CH8N MG=34,0656708
C2H10 MG=34,078246
H2O2 MG=34,0054792
H2S MG=33,9877212
H4NO MG=34,0292874
H6N2 MG=34,0530956
H18O MG=34,1357578

-----D--B--E--f-i-l-t-e-r-----
22.11.2011 - 14:01:00,37
akzeptierte DBE:
-2 -1 0 1 2 3 4 5 6 7 8

CH6O DBE: -1
C2H10 DBE: -2
H2O2 DBE: 0
H2S DBE: 0
H6N2 DBE: -1

5 von 8 Summenformeln

331 - 303 = **28**
Gefundene Verbindungen: 6
CH2N MG=28,0187232
CO MG=27,994915
C2H4 MG=28,0312984
H12O MG=28,0888102
H14N MG=28,1126184
N2 MG=28,006148

-----D--B--E--f-i-l-t-e-r-----
22.11.2011 - 14:07:04,51
akzeptierte DBE:
-2 -1 0 1 2 3 4 5 6 7 8

CO DBE: 2
C2H4 DBE: 1
N2 DBE: 2

3 von 6 Summenformeln

+MSn [VI]: 437 Th {II/III}

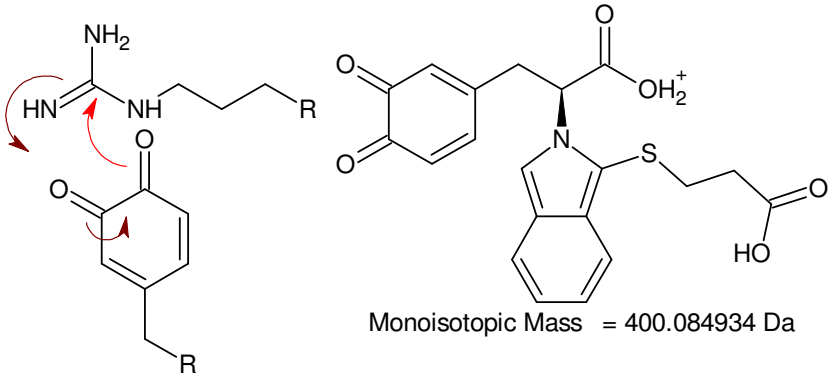

Monoisotopic Mass = 400.084934 Da

437 - 400 = 37
Gefundene Verbindungen: 8

CH9O	MG=37,0653364
CH11N	MG=37,0891446
C2H13	MG=37,1017198
C3H	MG=37,0078246
H5O2	MG=37,028953
H5S	MG=37,011195
H7NO	MG=37,0527612
H9N2	MG=37,0765694

-----D--B--E--f-i-l-t-e-r-----
22.11.2011 - 13:53:26,17
akzeptierte DBE:
1 2 3 4 5 6 7 8

0 von 8 Summenformeln

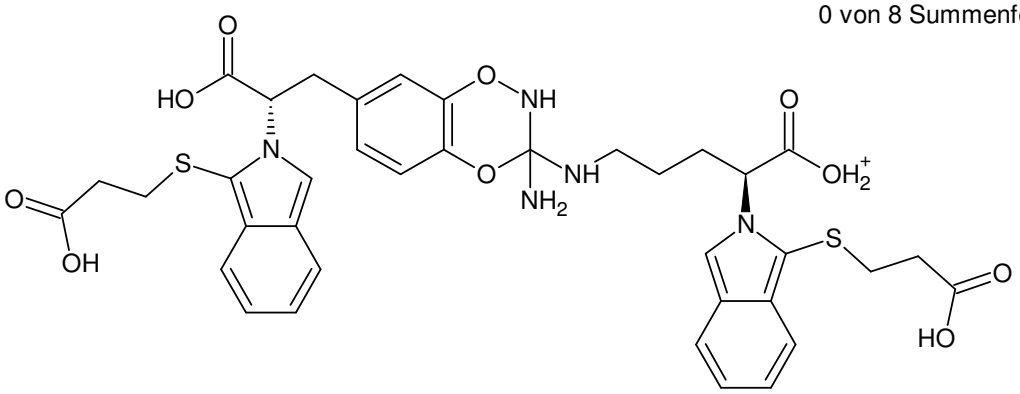

Monoisotopic Mass = 778.221109 Da

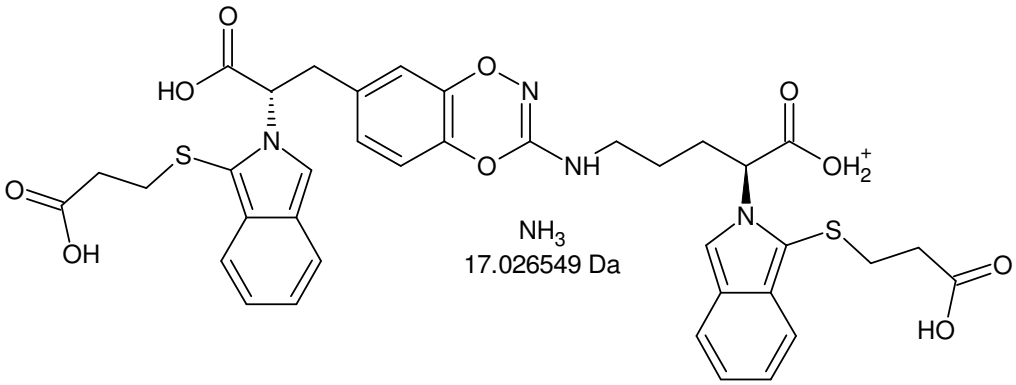

Monoisotopic Mass = 761.19456 Da

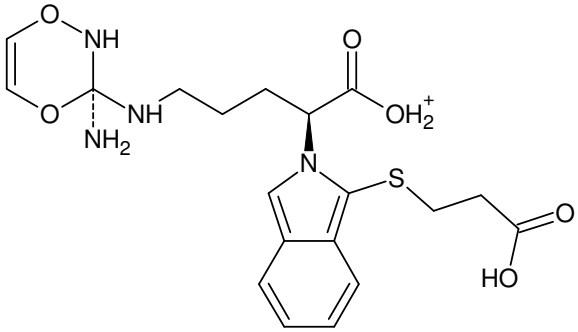

+MSn [VI]: 437 Th {III/III}

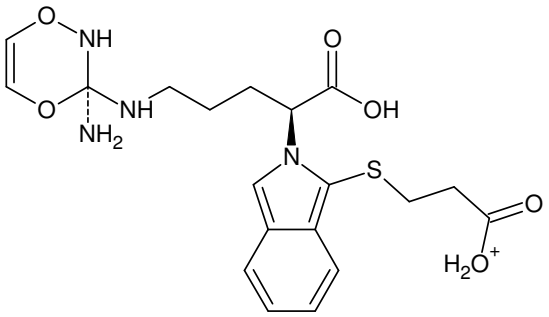

Monoisotopic Mass = 437.148931 Da

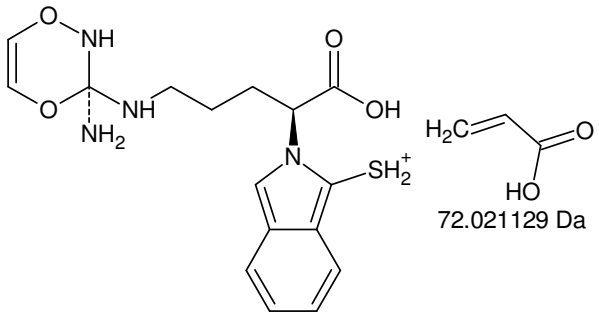

Monoisotopic Mass = 365.127802 Da

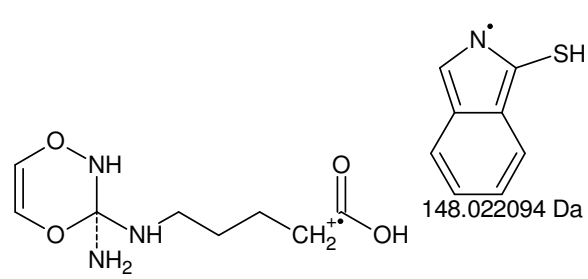

Monoisotopic Mass = 217.105707 Da

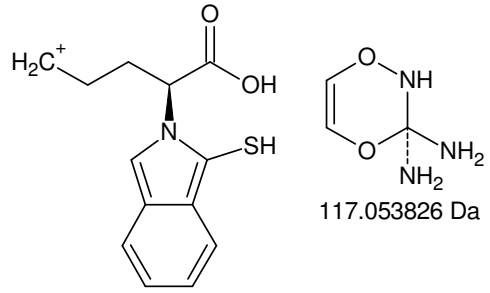

Monoisotopic Mass = 248.073975 Da

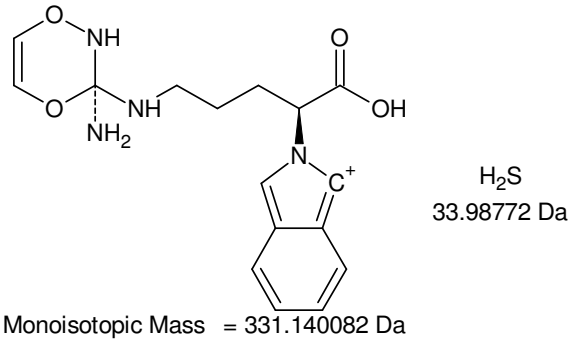

Monoisotopic Mass = 331.140082 Da

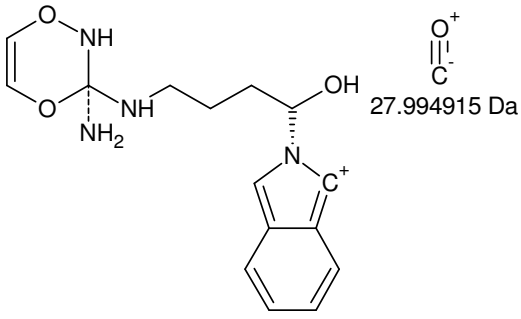

Monoisotopic Mass = 303.145167 Da

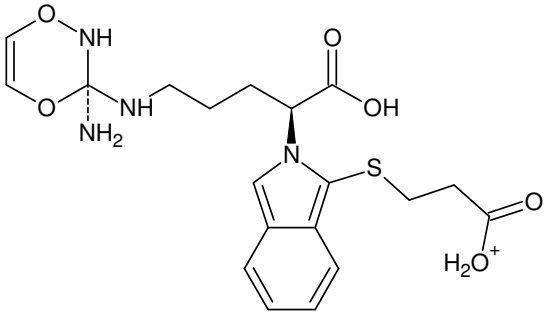

Monoisotopic Mass = 437.148931 Da

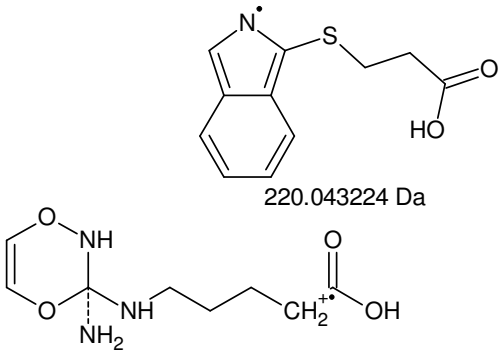

Monoisotopic Mass = 217.105707 Da

+MSn [VI]: 437 -> 365 -> 217, 248 , 331 -> 303

876 Th => 1, 3, 5, ... N

=> 1, 3, ... N in der verbindenden Seitenkette

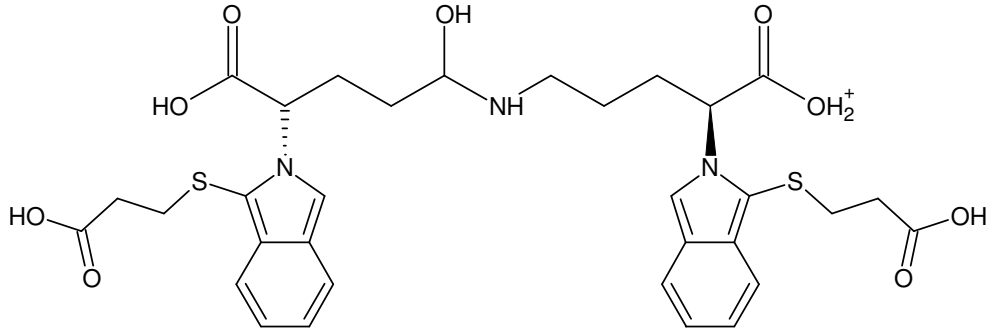

Monoisotopic Mass = 672.204949 Da

876 - 804 = **74**

Gefundene Verbindungen: 60

CH2N2O2 MG=74,0116272

CH2N2S MG=73,9938692

...

N3O2 MG=73,999052

N3S MG=73,981294

-----D--B--E--f-i-l-t-e-r-----

16.11.2011 - 14:40:35,18

akzeptierte DBE:

-2 -1 0 1 2 3 4 5 6 7 8

CH2N2O2 DBE: 2

CH2N2S DBE: 2

CH6N4 DBE: 1

C2H2OS DBE: 2

C2H2O3 DBE: 2

C2H6N2O DBE: 1

C3H6O2 DBE: 1

C3H6S DBE: 1

C3H10N2 DBE: 0

C4H10O DBE: 0

C5H14 DBE: -1

C6H2 DBE: 6

H2N4O DBE: 2

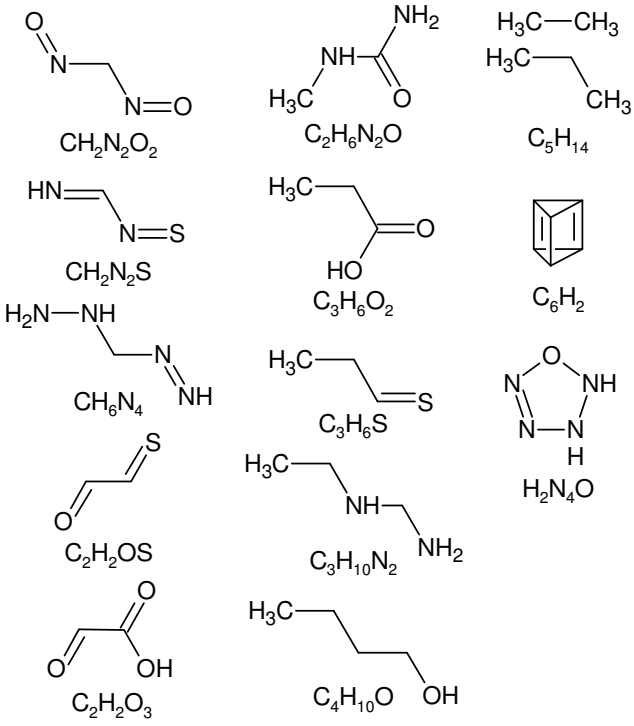

13 von 60 Summenformeln

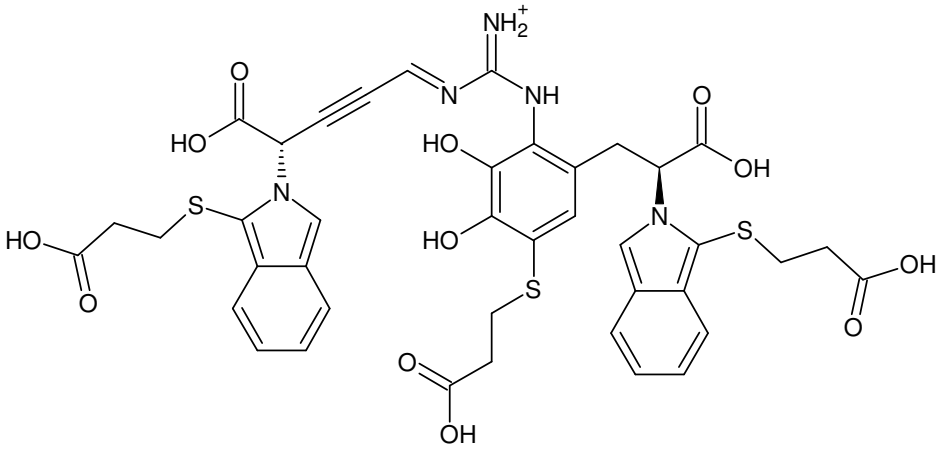

Monoisotopic Mass = 876.167358 Da

X +MSn [VI]: 876 Th

874 Th => 1, 3, 5, ... N

92 Da

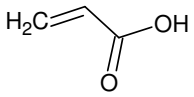

72.02113 Da

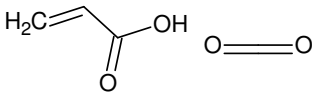

116.01096 Da

H_2S 33.987721 Da

874 - 782 = **92**
Gefundene Verbindungen: 113
CH2NO2S MG=91,9806252
CH2NO4 MG=91,9983832
...
N2O4 MG=91,985808
N2S2 MG=91,950292

-----D--B--E--f-i-l-t-e-r-----
16.11.2011 - 15:00:11,56
akzeptierte DBE:
-2 -1 0 1 2 3 4 5 6 7 8

CH4N2OS DBE: 1
CH4N2O3 DBE: 1
CH8N4O DBE: 0
COS2 DBE: 2
CO3S DBE: 2
CO5 DBE: 2
C2H4O2S DBE: 1
C2H4O4 DBE: 1
C2H4S2 DBE: 1
C2H8N2O2 DBE: 0
C2H8N2S DBE: 0
C2H12N4 DBE: -1
C3H8OS DBE: 0
C3H8O3 DBE: 0
C3H12N2O DBE: -1
C3N4 DBE: 6
C4H12O2 DBE: -1
C4H12S DBE: -1
C4H16N2 DBE: -2
C4N2O DBE: 6
C5H4N2 DBE: 5
C5H16O DBE: -2
C5O2 DBE: 6
C5S DBE: 6
C6H4O DBE: 5
C7H8 DBE: 4
H4N4O2 DBE: 1
H4N4S DBE: 1
H8N6 DBE: 0
N2O2S DBE: 2
N2O4 DBE: 2
N2S2 DBE: 2

32 von 113 Summenformeln
fett: 74 Da + H_2O

=> Fragment mit 594 Th sollte noch beinhalten:

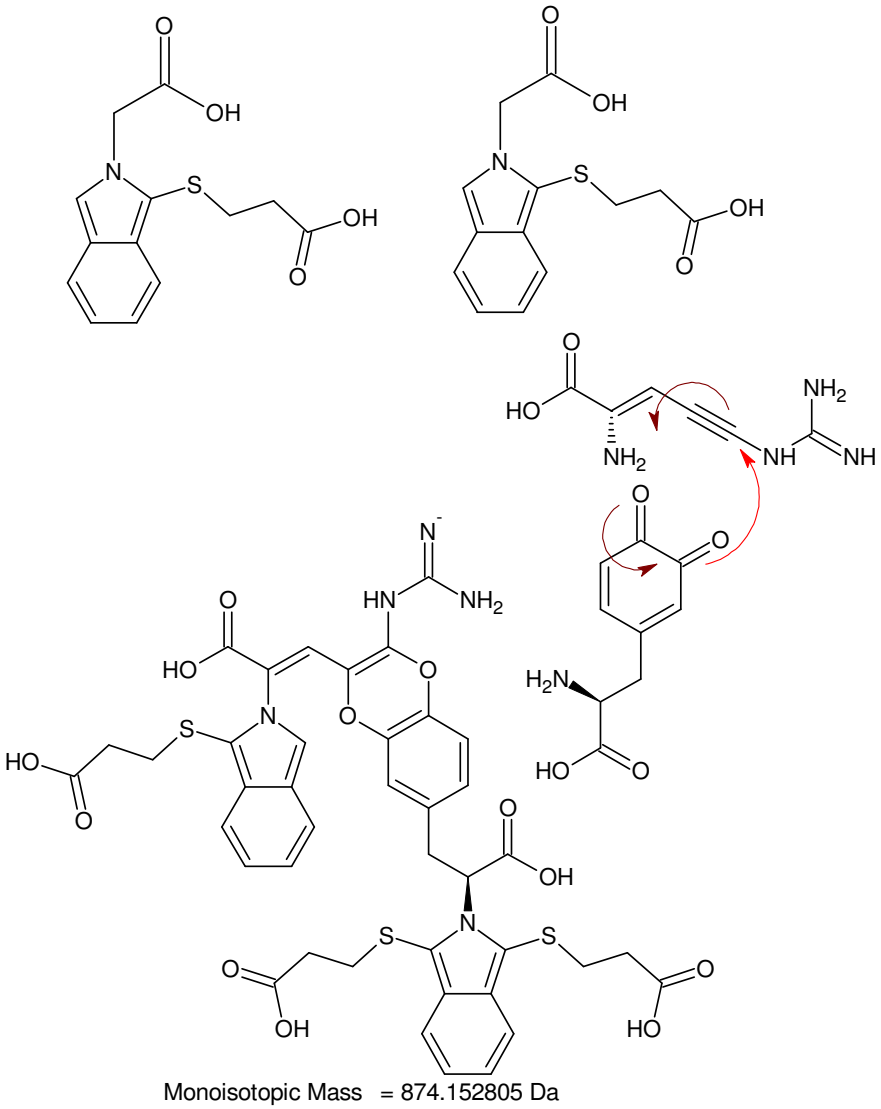

Monoisotopic Mass = 874.152805 Da

X -MSn [VI]: -874 Th

VII

+MS^n

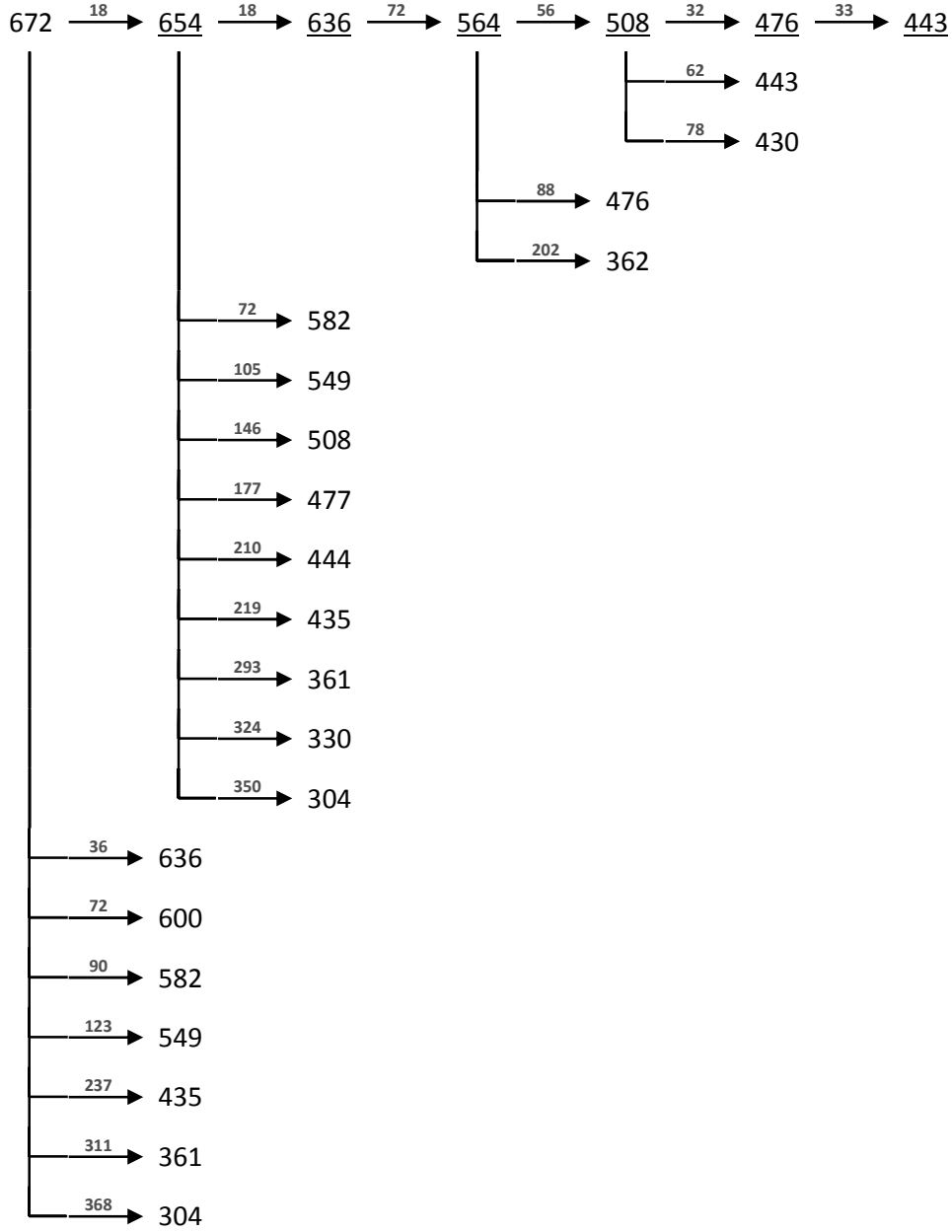
672
18
654
18
636
72
564
56
508
32
476
33
443
62
443
78
430
88
476
202
362
72
582
105
549
146
508
177
477
210
444
219
435
293
361
324
330
350
304
36
636
72
600
90
582
123
549
237
435
311
361
368
304

-MS^n

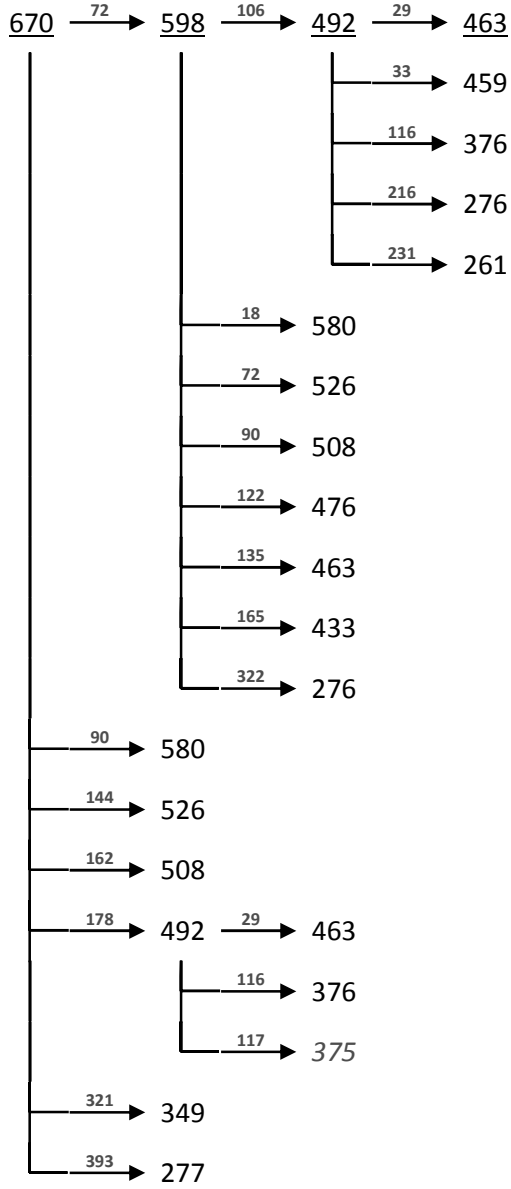

isotopic fingerprint:

peak area / % of monoisotopic	**+1**	**+2**	**+3**
measured (672,3 Th):	48,7	31,4	10,0
measured (-669,9 Th):	53,4	29,8	-

Figure XIII-XIV MS^n analysis of VII

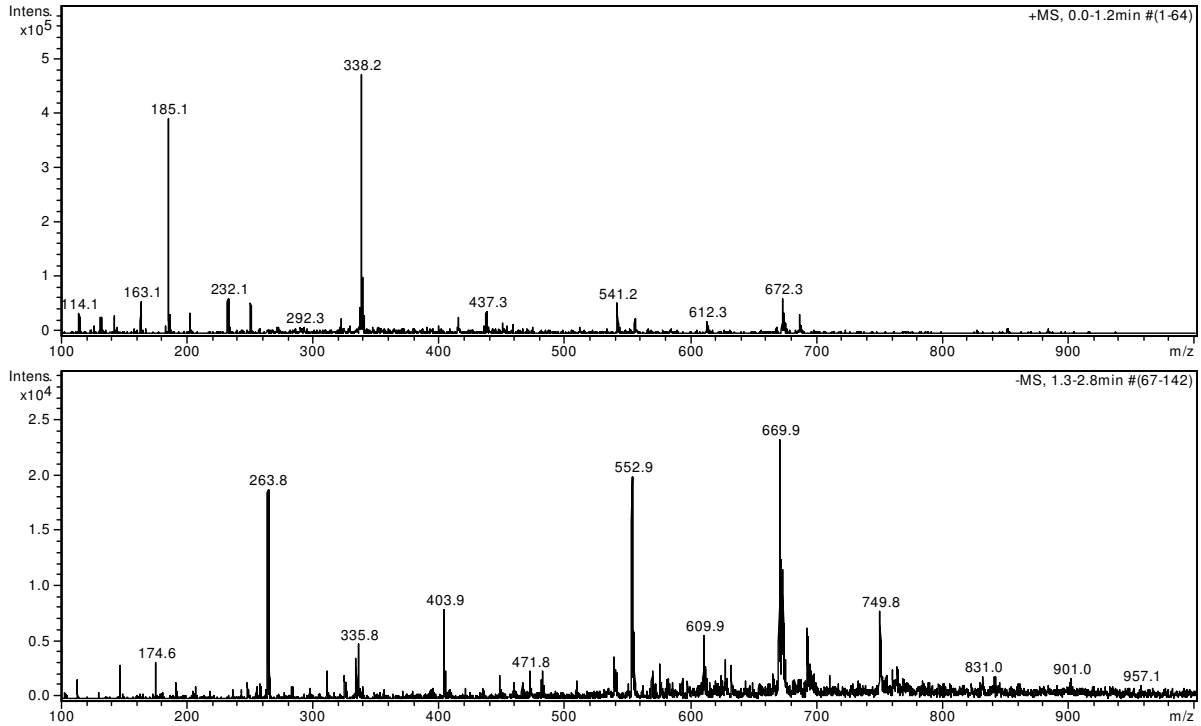

Figure XIII-XV VII: 49,8 – 50,2 min, 1 ‰ FA, 55 % ACN in ddH_2O; full scan MS^1

672 Th

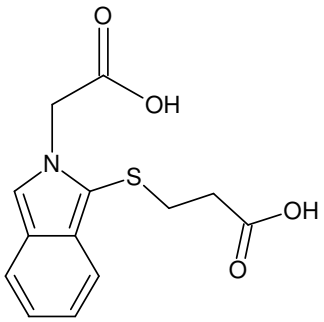

H_2O Monoisotopic Mass = 18.010565 Da

H_2O Monoisotopic Mass = 18.010565 Da

Compounds found: 3
H2O MW=18,0105642
CH6 MW=18,0469476
H4N MW=18,0343724

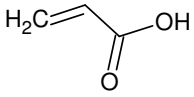

Monoisotopic Mass = 72.02113 Da

672 - 2 * 279 - 1 = 113

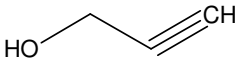

Monoisotopic Mass = 56.026215 Da

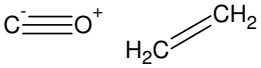

Monoisotopic Mass = 56.026215 Da

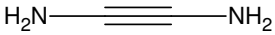

Monoisotopic Mass = 56.037448 Da

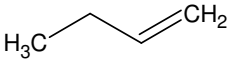

Monoisotopic Mass = 56.0626 Da

Compounds found: 209
CHN6O MW=113,0211836
CH3N7 MW=113,0449918
(...)
H55N3O MW=113,43449
H57N4 MW=113,4582982

-----D--B--E--f-i-l-t-e-r-----
31.01.2011 - 18:50:05,62
akzeptierte DBEs:
2
3
4
5
6

Monoisotopic Mass = 32.026215 Da

Monoisotopic Mass = 32.037448 Da

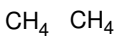

Monoisotopic Mass = 32.0626 Da

CH3N7 DBE: 4
C2H3N5O DBE: 4
C3H3N3O2 DBE: 4
C3H3N3S DBE: 4
C3H7N5 DBE: 3
C4H3NOS DBE: 4
C4H3NO3 DBE: 4
C4H7N3O DBE: 3
C5H7NO2 DBE: 3
C5H7NS DBE: 3
C5H11N3 DBE: 2
C6H11NO DBE: 2

12 von 209 Summenformeln

Monoisotopic Mass = 33.057849 Da

Monoisotopic Mass = 33.021464 Da

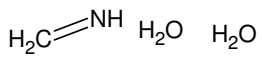

Monoisotopic Mass = 65.047679 Da

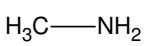

Monoisotopic Mass = 65.02992 Da

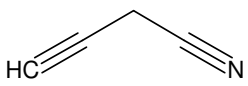

Monoisotopic Mass = 65.026549 Da

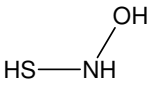

Monoisotopic Mass = 64.993535 Da

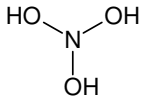

Monoisotopic Mass = 65.011294 Da

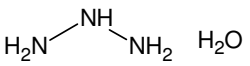

Monoisotopic Mass = 65.058912 Da

+MSn [VII]: main fragmentation route 672 Th

670 Th

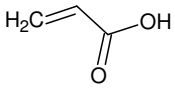

Monoisotopic Mass = 72.02113 Da

H_2O Monoisotopic Mass = 18.010565 Da

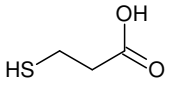

Monoisotopic Mass = 106.008851 Da

2 * 44 + 18 ?

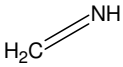

methanimine

Monoisotopic Mass = 29.026549 Da

aber: 3 x OPA wäre bereits zu schwer; Des weiteren ist die Abspaltung von S im negativen Modus nicht gerade typisch

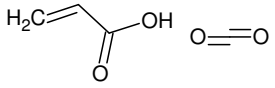

Monoisotopic Mass = 116.01096 Da

2 * 44 + 28 ?

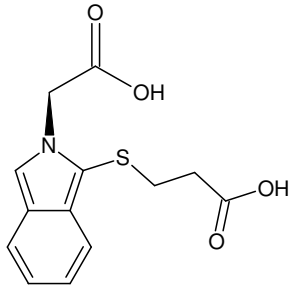

Monoisotopic Mass = 279.05653 Da

670 - 2 * 279 + 1 = 113

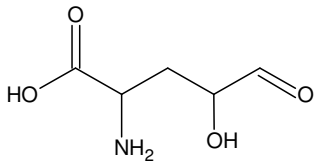

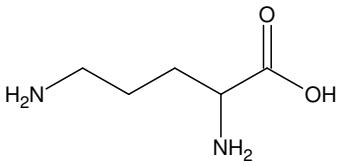

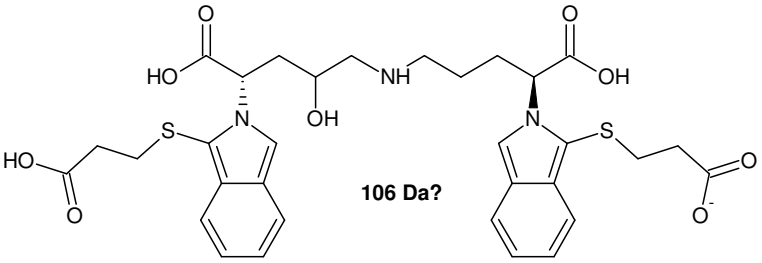

106 Da?

Monoisotopic Mass = 670.189299 Da

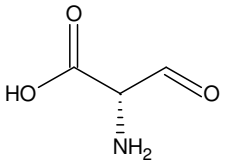

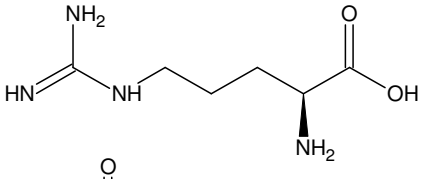

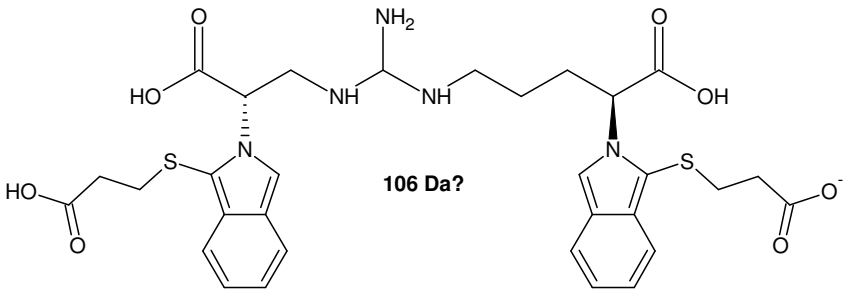

106 Da?

Monoisotopic Mass = 670.200532 Da

18 Da (598 -> 580) schwer hiervon abspaltbar; Dasselbe gilt für alle Isomere der Seitenketten.

-MSn [VII]: main fragmentation route -670 Th

XIII.I.II. K BoT2 +| 4d

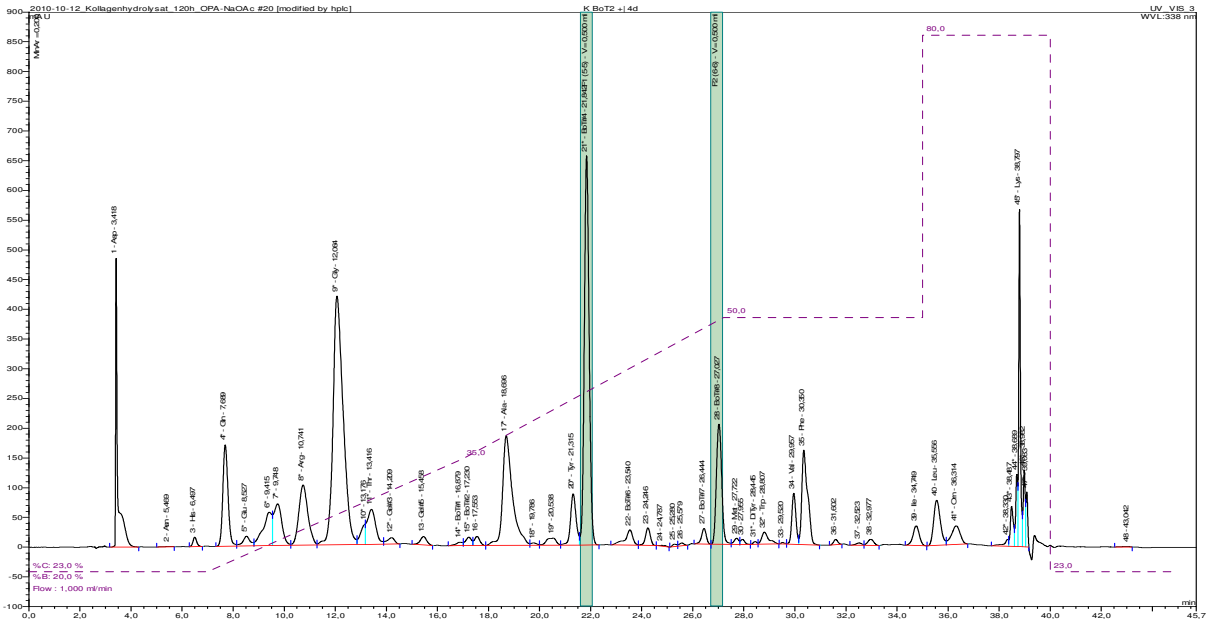

Figure XIII-XVI K BoT2 +| 4d – RP-HPLC fractions for desalting and subsequent MS^n-analysis

BoT#4

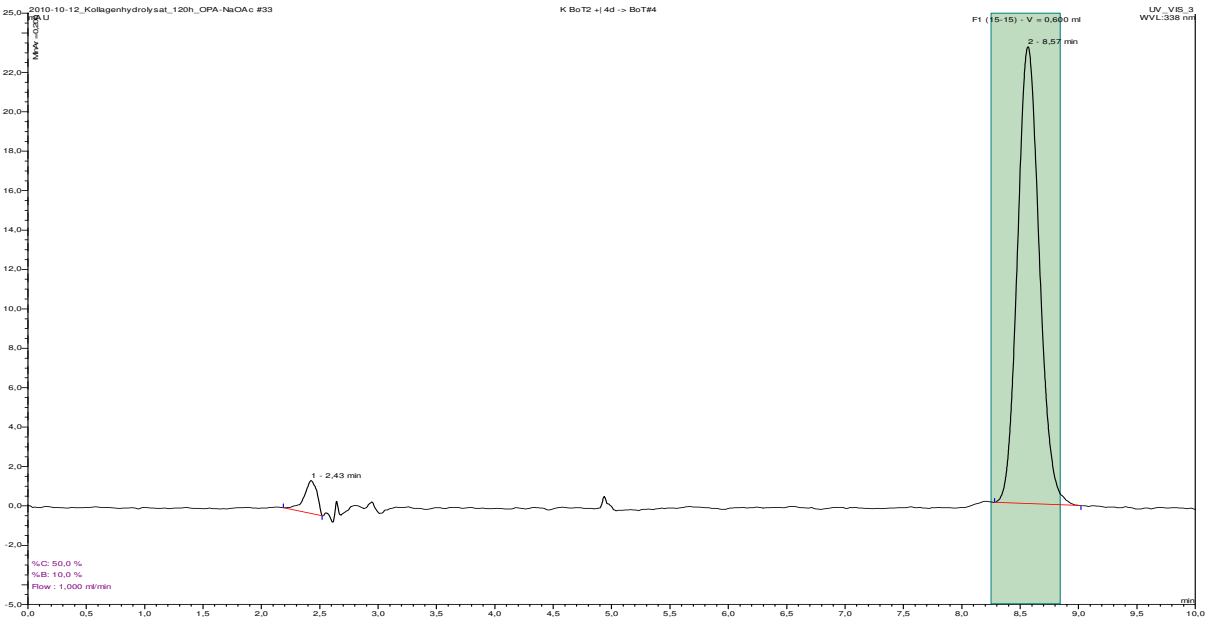

Figure XIII-XVII Desalting of fraction BoT#4: 50 % MeOH, 40 % ddH_2O, 10 % formic acid 265 mM (v+v+v)

+MS^n

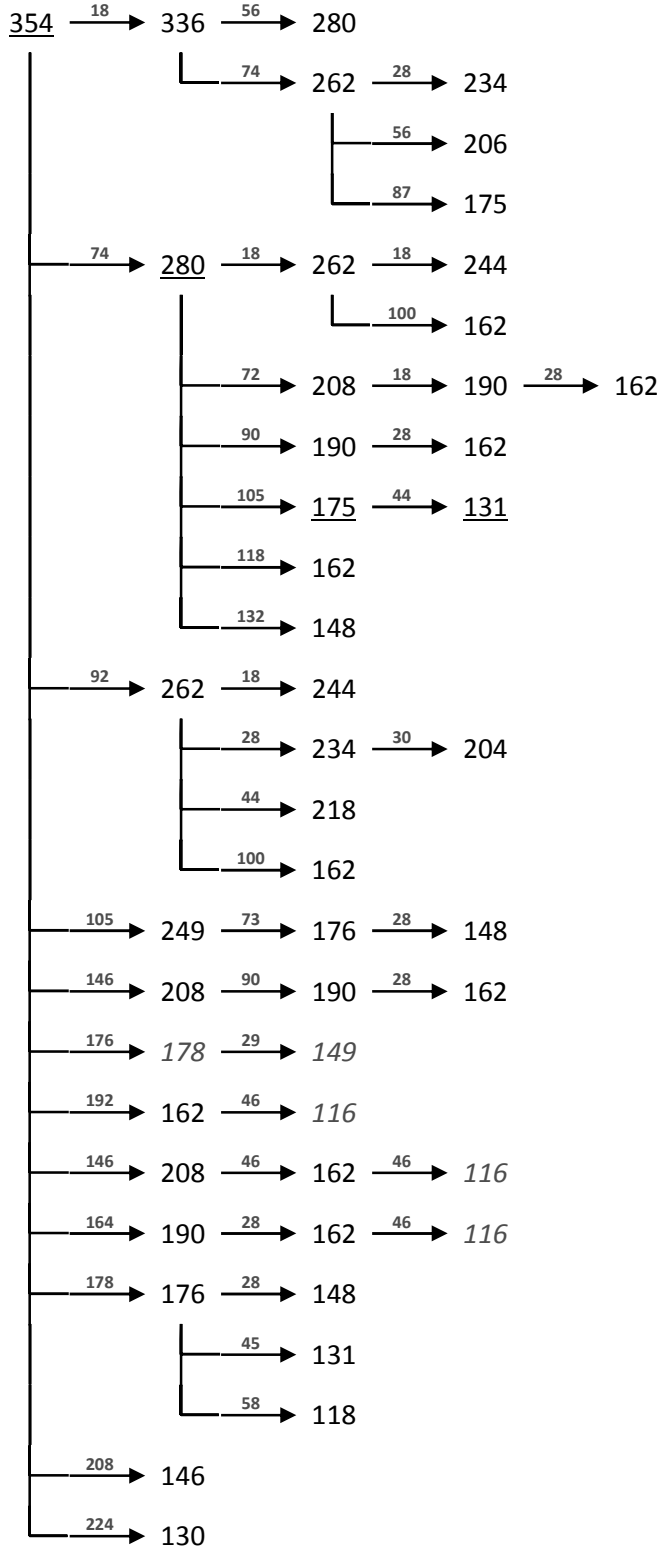
354
18
336
56
280
74
262
28
234
56
206
87
175
74
280
18
262
18
244
100
162
72
208
18
190
28
162
90
190
28
162
105
175
44
131
118
162
132
148
92
262
18
244
28
234
30
204
44
218
100
162
105
249
73
176
28
148
146
208
90
190
28
162
176
178
29
149
192
162
46
116
146
208
46
162
46
116
164
190
28
162
46
116
178
176
28
148
45
131
58
118
208
146
224
130

-MS^n

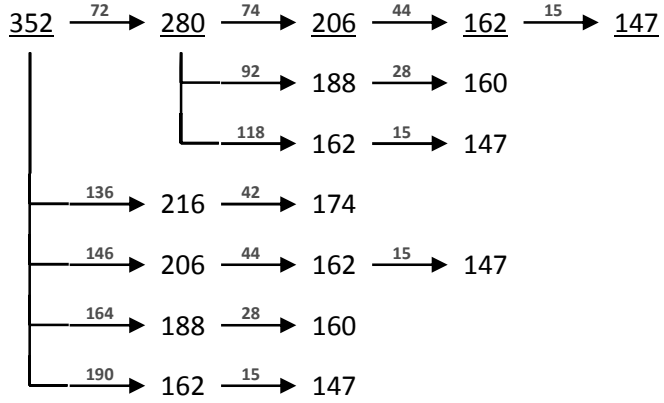

isotopic fingerprint:

peak area / % of monoisotopic	**+1**	**+2**	**+3**	**+4**
theoretical ($C_{16}H_{20}NO_6S^+$):	19,0	7,5	1,2	0,2
measured (354,1 Th):	20,8	10,5	4,4	1,4
measured (-351,8 Th):	20,2	6,8	2,1	0,7

Figure XIII-XVIII MS^n analysis of BoT#4

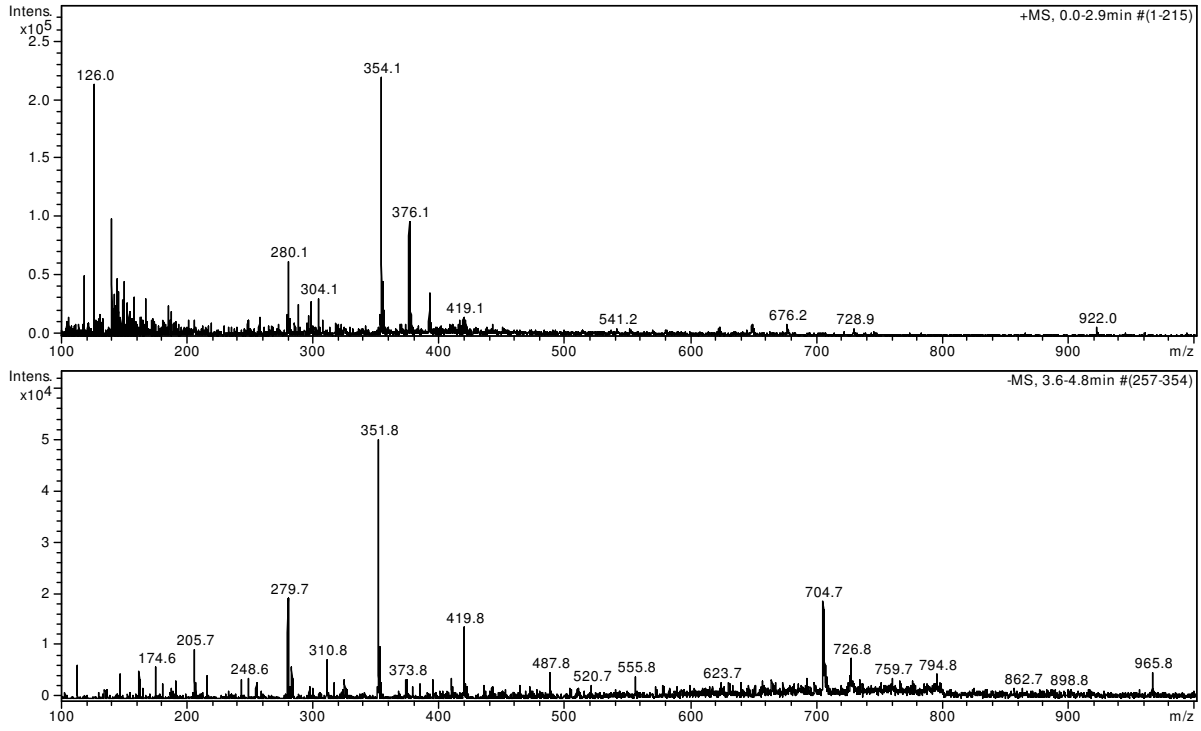

Figure XIII-XIX BoT#4: 1 ‰ FA, 50 % MeOH in ddH_2O; full scan MS^1

BoT#8

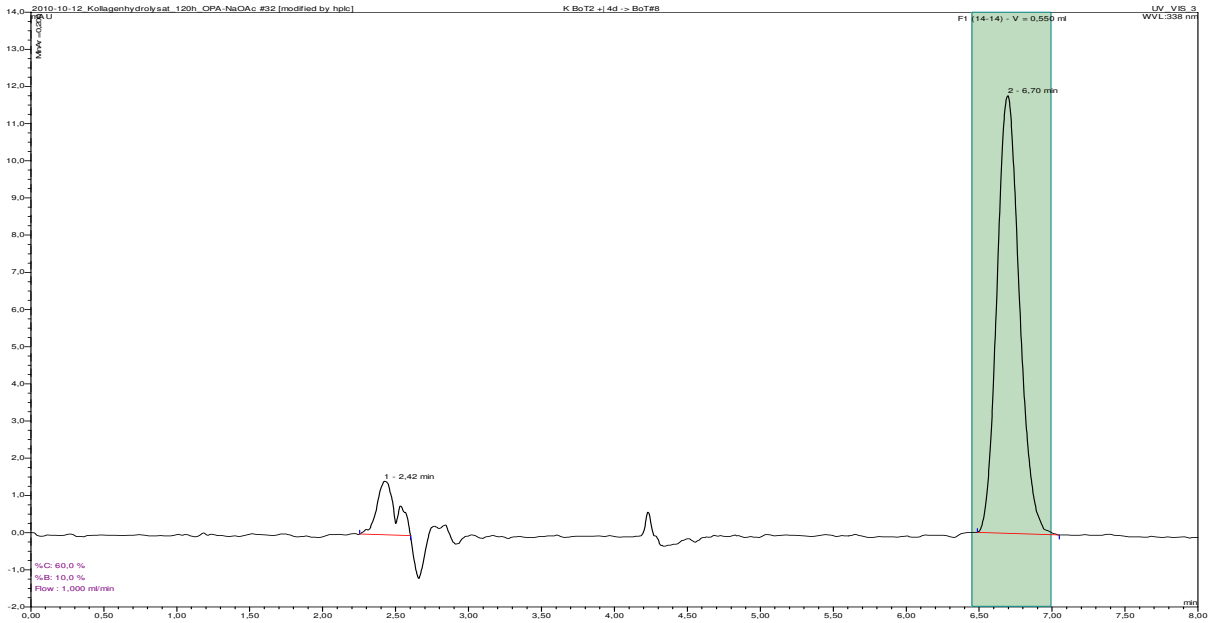

Figure XIII-XX Desalting of fraction BoT#8: 60 % MeOH, 30 % ddH_2O, 10 % formic acid 265 mM (v+v+v)

+MS^n

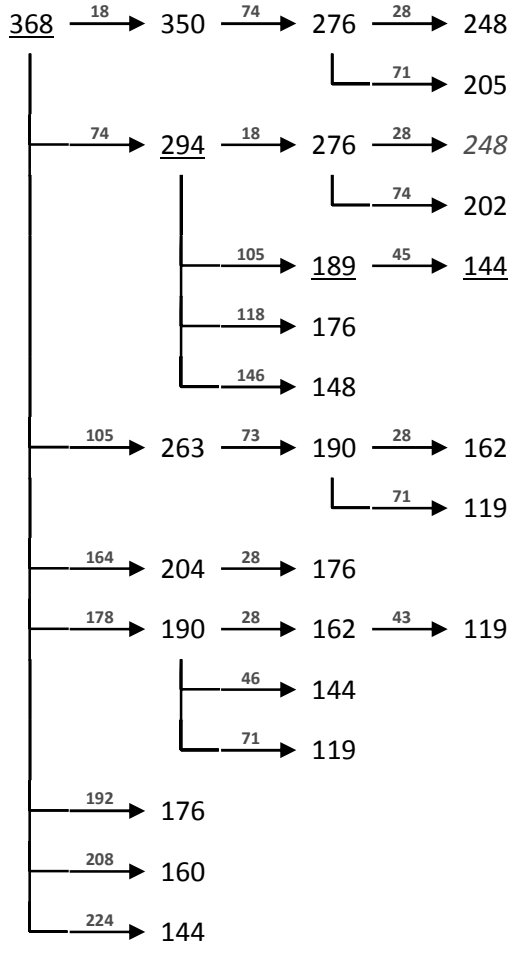

-MS^n

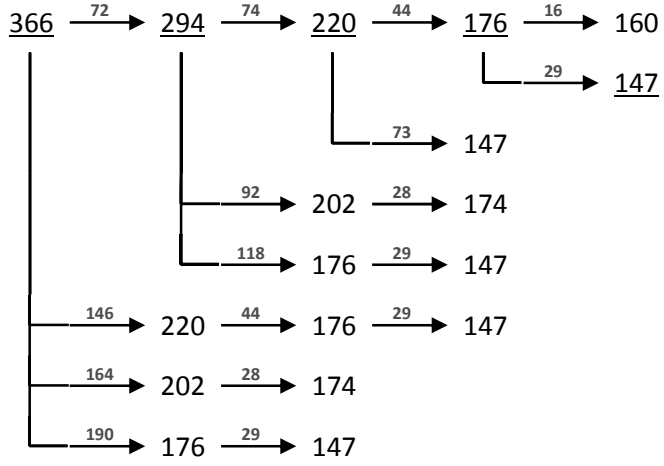

isotopic fingerprint:

peak area / % of monoisotopic	**+1**	**+2**	**+3**	**+4**
theoretical ($C_{17}H_{22}NO_6S^+$):	20,1	7,7	1,2	0,2
measured (368,1 Th):	20,7	8,5	3,5	0,7
measured (-365,8 Th):	21,5	7,0	6,1	1,2

Figure XIII-XXI MS^n analysis of BoT#8

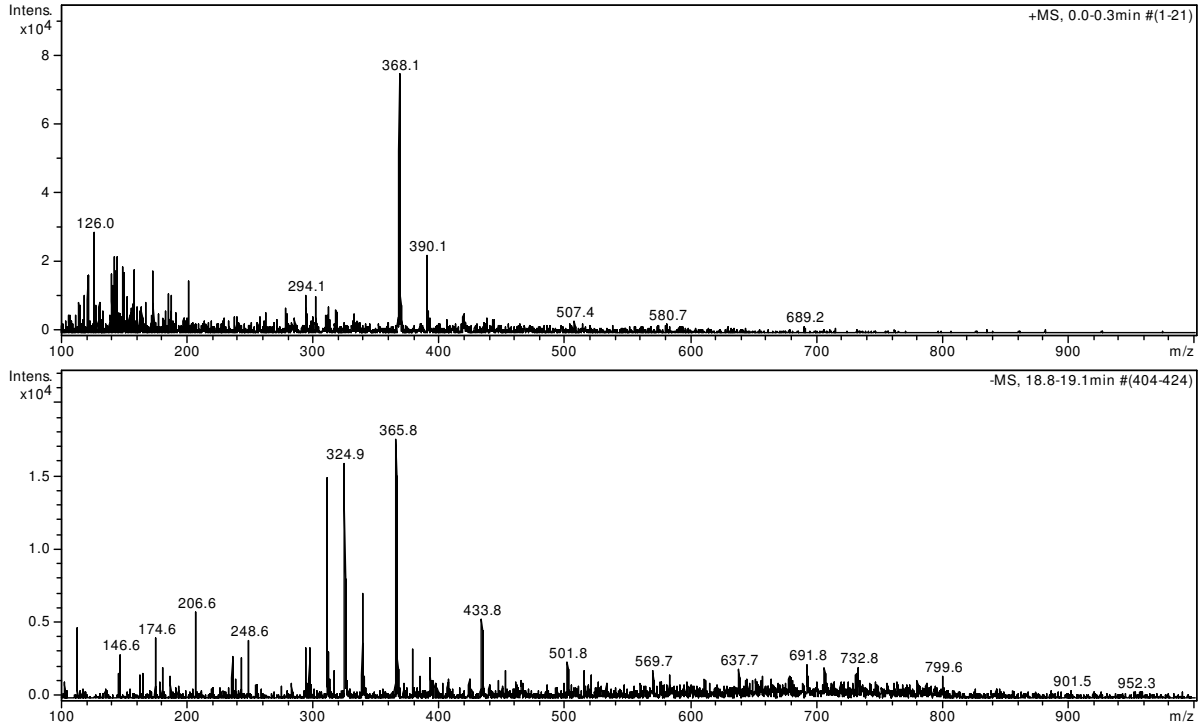

Figure XIII-XXII BoT#8: 1 ‰ FA, 60 % MeOH in ddH_2O; full scan MS^1

XIII.II. I-b new with BoT2 and AbT in sodium phosphate buffer

The signal at -966 Th which was encountered in all the measured fractions was found to stem from the Nanopure® water (see ddH_2O, Figure XIII-XXVI).

XIII.II.I. Chromeleon® program for the fractionation of I-b 24h

```
AS-OPA_20°C_C18-4,6x250mm_20µl_#3-1_Fraktionierung.pgm

C18 4,6 x 250 mm: Aminosäuren mit OPA; 20 °C; A == ddH2O, B == ACN, C == 1% FA; BE1 == OPA-
Reagenz; BE2 == IS; Pos+1 == leeres Vial

                AcquireExclusiveAccess
;column oven
                TempCtrl =                                  On
                ColumnOven.Temperature.Nominal =                                    20.0 [°C]
                ColumnOven.Temperature.LowerLimit =         15.0 [°C]
                ColumnOven.Temperature.UpperLimit =         45.0 [°C]
                EquilibrationTime =                         0.5 [min]
                ReadyTempDelta =                            1.0 [°C]
                HumidityLeakSensor =                        Low
                GasLeakSensor =                             Low
                MsvPosition =                               B
;Autosampler
                DrawSpeed =                                 10.000 [µl/s]
                DrawDelay =                                 3000 [ms]
                DispSpeed =                                 20.000 [µl/s]
                DispenseDelay =                             0 [ms]
                WasteSpeed =                                32.000 [µl/s]
                SampleHeight =                              2.000 [mm]
                InjectWash =                                Both
                WashVolume =                                100.000 [µl]
                WashSpeed =                                 20.000 [µl/s]
                Sampler.PumpDevice =                        "PumpLeft"
                InjectMode =                                Normal
                SyncWithPump =                              On
;UVD
                UV_VIS_1.Wavelength =                       228 [nm]
                UV_VIS_1.Bandwidth =                        10 [nm]
                UV_VIS_1.RefWavelength =                    600 [nm]
                UV_VIS_1.RefBandwidth =                     20 [nm]
                UV_VIS_1.Step =                             Auto
                UV_VIS_1.Average =                          On
                UV_VIS_2.Wavelength =                       338 [nm]
                UV_VIS_2.Bandwidth =                        10 [nm]
                UV_VIS_2.RefWavelength =                    600 [nm]
                UV_VIS_2.RefBandwidth =                     20 [nm]
                UV_VIS_2.Step =                             Auto
                UV_VIS_2.Average =                          On
                UV_VIS_3.Wavelength =                       338 [nm]
                UV_VIS_3.Bandwidth =                        10 [nm]
                UV_VIS_3.RefWavelength =                    390 [nm]
                UV_VIS_3.RefBandwidth =                     20 [nm]
                UV_VIS_3.Step =                             Auto
                UV_VIS_3.Average =                          On
                UV_VIS_4.Wavelength =                       280 [nm]
                UV_VIS_4.Bandwidth =                        10 [nm]
                UV_VIS_4.RefWavelength =                    600 [nm]
                UV_VIS_4.RefBandwidth =                     20 [nm]
                UV_VIS_4.Step =                             Auto
                UV_VIS_4.Average =                          On
;Pumps
                PumpLeft.Pressure.LowerLimit =              2 [bar]
                PumpLeft.Pressure.UpperLimit =              350 [bar]           ; Säule
Eurospher 100-5 C18: bis 400 bar
                PumpLeft.MaximumFlowRamp =                  6.00 [ml/min²]
                PumpLeft.%A.Equate =                        "%A"
                PumpLeft.%B.Equate =                        "%B"
                PumpLeft.%C.Equate =                        "%C"
                PumpRight.Pressure.LowerLimit =             0 [bar]
                PumpRight.Pressure.UpperLimit =             400 [bar]
                PumpRight.MaximumFlowRamp =                 6.00 [ml/min²]
                PumpRight.%A.Equate =                       "%A"
                PumpRight.%B.Equate =                       "%B"
                PumpRight.%C.Equate =                       "%C"
                PumpRight.Flow =                            0.000 [ml/min]
```

```
                PumpRight.%B =                                  0.0 [%]
                PumpRight.%C =                                  0.0 [%]
                PumpRight.Curve =                               5
;RI-Detector
                ;RI.Temperature.Nominal =                       45 [°C]
                ;Recorder_Range =                               512.00 [µRIU]
                ;Integrator_Range =                             500 [µRIU/V]
                ;Rise_Time =                                    0.50 [s]
                ;Polarity =                                     Plus
                ;Baseline_Shift =                               0 [mV]
                ;RI_1.Step =                                    Auto
                ;RI_1.Average =                                 On

;Fraction collector
                ;*********************************************************************
                ;* Definition of triggers for fraction collection starts here.
                ;*********************************************************************
                Trigger                                         FracStart
                FracStartDetected
                Valve =                                         On
                EndTrigger

                ;Trigger                                        TubeChange
                FracTubeChange
                ;Valve =                                        Off
                ;Tube =                                         tube+1
                ;Valve =                                        On
                ;EndTrigger

                Trigger                                         FracEnd
                FracEndDetected
                Valve =                                         Off
                Tube =                                          Tube+1
                EndTrigger

                ;*********************************************************************
                ;* Definition of triggers for fraction collection ends here.
                ;*********************************************************************

                Valve =                                         Off
                ;Tube =                                         sample.Foxy_tube
                FractionCollection.PumpDevice =                 "PumpLeft"
                TubeMaxVolume =                                 10.00 [ml]
                TotalNumberInstalled =                          144
                MaxTubesPerFraction =                           Unlimited
                TubeWrapping =                                  No
                TubeChangeDuration =                            2.0 [s]
                DetectionChannel1.Name =                        "UV_VIS_3"
                ;Detektorkanal zur Peakerkennung
                PeakStartThreshold =                            2.00 [signal]
                PeakStartSlope =                                0.500 [signal/s]
                PeakStartTrueTime =                             1.00 [s]
                PeakEndThreshold =                              10.00 [signal]
                PeakEndSlope =                                  -1.000 [signal/s]
                PeakEndTrueTime =                               1.00 [s]
                DerivStep =                                     1.00 [s]
                ThresholdNoPeakEnd =                            2000.00 [signal]
                ThresholdDoNotResolve =                         Off
                PeakMaxSlope =                                  Off
                PeakMaxTrueTime =                               1.00 [s]
                BaselineDrift =                                 0.000 [signal/s]
                BaselineOffset =                                0.000 [signal]
                DelayVolume =                                   219 [µl]            ;Volumen
zwischen UVD und Fraktionensammler
                OffsetVolume =                                  0 [µl]

;run-specific command
                ;die Probenvorbereitung dauert insgesamt etwa 185 s bis zur Injektion
(Autosampler UltiMate 3000)
                InjectMode =                                    UserProg

                ReagentAVial =                                  BE2                 ; Norvalin
1 mM in ddH2O
                ;ReagentBVial =                                 BE8                 ; ddH2O
                ;ReagentBVial =                                 B3                  ; NaOH 5 M
                ReagentCVial =                                  BE1                 ; OPA-
Reagenz
```

```
               ;PrepVial =                                   Position+1          ; leeres,
offenes Glasvial mit 100 µl-Einsatz
               PositionCalculator =                          Sampler.Position
               IncrementPositionCalculator                   By=1
               PrepVial =                                    PositionCalculator


               WashVolume =                                  100.000 [µl]
               WashSpeed =                                   20.000 [µl/s]

               ;internen Standard zusetzen (Nadel wurde gerade gewaschen <= InjectWash=Both)
               UdpDraw                                       From=ReagentAVial,
Volume=10.000, SyringeSpeed=GlobalSpeed, SampleHeight=GlobalHeight

               ;Probe aufziehen
               UdpDraw                                       From=SampleVial, Volume=10.00,
SyringeSpeed=GlobalSpeed, SampleHeight=GlobalHeight
               UdpDispense                                   To=PrepVial, Volume=20.00,
SyringeSpeed=GlobalSpeed, SampleHeight=GlobalHeight
               UdpMixWait                                    Duration=2

               ;Derivatisieren
               UdpDispense                                   To=Wash, Volume=0.000,
SyringeSpeed=GlobalSpeed, SampleHeight=GlobalHeight
               UdpMixNeedleWash                              Volume=100
               ;Verunreinigung des OPA-Reagenz vermeiden
               UdpDraw                                       From=ReagentCVial,
Volume=40.000, SyringeSpeed=GlobalSpeed, SampleHeight=GlobalHeight
               UdpDispense                                   To=PrepVial, Volume=40.000,
SyringeSpeed=GlobalSpeed, SampleHeight=GlobalHeight
               UdpMixWait                                    Duration=2

               ;mischen
               DrawSpeed =                                   20.000 [µl/s]
               DispSpeed =                                   30.000 [µl/s]
               DrawDelay =                                   1000 [ms]
               UdpDraw                                       From=PrepVial, Volume=45.00,
SyringeSpeed=GlobalSpeed, SampleHeight=GlobalHeight
               UdpDispense                                   To=PrepVial, Volume=45.000,
SyringeSpeed=GlobalSpeed, SampleHeight=GlobalHeight
               UdpMixWait                                    Duration=2
               UdpDraw                                       From=PrepVial, Volume=45.00,
SyringeSpeed=GlobalSpeed, SampleHeight=GlobalHeight
               UdpDispense                                   To=PrepVial, Volume=45.000,
SyringeSpeed=GlobalSpeed, SampleHeight=GlobalHeight
               UdpMixWait                                    Duration=2
               UdpDraw                                       From=PrepVial, Volume=45.00,
SyringeSpeed=GlobalSpeed, SampleHeight=GlobalHeight
               UdpDispense                                   To=PrepVial, Volume=45.000,
SyringeSpeed=GlobalSpeed, SampleHeight=GlobalHeight
               UdpMixWait                                    Duration=2

               UdpMixWait                                    Duration=27 ;gesamte
Derivatisierungszeit 80 s, 3 s Wartezeit nach jedem Aufsaugen (beim Mischen: 1s)

               ;Spritzengeschwindigkeiten zurücksetzen
               DrawSpeed =                                   10.000 [µl/s]
               DrawDelay =                                   3000 [ms]
               DispSpeed =                                   20.000 [µl/s]

               ;Injektion: Verdünnung der Probe: 6-fach, 10 µl Probe pro Messung
               UdpSyringeValve Position =                    Needle
               UdpInjectValve                                Position=Load
               UdpDraw                                       From=PrepVial, Volume=20.000,
SyringeSpeed=GlobalSpeed, SampleHeight=GlobalHeight
               UdpMixWait                                    Duration=5

               UdpInjectValve                                Position=Inject
               UdpInjectMarker                               ;erzeugt "Inject Response",
wenn Programm läuft
               UdpMixWait                                    Duration=40

               ;UdpDraw                                      From=SampleVial, Volume=0.000,
SyringeSpeed=GlobalSpeed, SampleHeight=GlobalHeight
               UdpSyringeValve                               Position=Waste
               UdpMoveSyringeHome                            SyringeSpeed=GlobalSpeed
               UdpSyringeValve                               Position=Needle
               UdpMixNeedleWash                              Volume=50
```

```
 0.000          PumpLeft.Flow =                          1.000 [ml/min]
                PumpLeft.%B =                            25.0 [%]
                PumpLeft.%C =                            10.0 [%]
                ;CollectFractions =                      No
                UV.Autozero
                ;RI.Purge =                              Off
                ;RI.Autozero

                Tube =                                   11                  ;
Initialspülung
                Valve =                                  On

                Wait                                     ColumnOven.Ready and
Sampler.Ready

                Inject

                UV_VIS_1.AcqOn
                UV_VIS_2.AcqOn
                UV_VIS_3.AcqOn
                UV_VIS_4.AcqOn
                ;RI_1.AcqOn


                PumpLeft.Flow =                          1.000 [ml/min]
                PumpLeft.%B =                            25.0 [%]
                PumpLeft.%C =                            10.0 [%]


1.750           Valve =                                  Off
                Tube =                                   sample.Foxy_tube

2.73            Tube =                                   sample.Foxy_tube
                CollectFractions =                       By_Time             ; größter
Peak
                CollectPeriod =                          6 [s]

2.83            CollectFractions =                       No

5.289           Tube =                                   11                  ; "Fenster"
von 5,07 - 5,48
                Valve =                                  On

5.699           Valve =                                  Off
                Tube =                                   sample.Foxy_tube+1


6.200           CollectFractions =                       By_Time             ; 6,2 - 6,4
                CollectPeriod =                          12 [s]

6.400           CollectFractions =                       No
                Tube =                                   11

10.919          Valve =                                  On                  ; "Fenster"
von 10,7 - 11,0

11.09           Valve =                                  Off
                Tube =                                   sample.Foxy_tube+2

11.100          CollectFractions =                       By_Time             ; 11,1 -
11,5
                CollectPeriod =                          24 [s]

11.500          CollectFractions =                       No
                Tube =                                   11

12.419          Valve =                                  On                  ; "Fenster"
von 12,2 - 12,45

12.499          Valve =                                  Off
                Tube =                                   sample.Foxy_tube+3

12.5            CollectFractions =                       By_Time             ; 12,5 -
12,9, Schulter
                CollectPeriod =                          24 [s]
```

```
12.9          CollectFractions =                    No
              Tube =                                11

14.719        Valve =                               On                  ; "Fenster"
von 14,5 - 14,71

14.929        Valve =                               Off
              Tube =                                sample.Foxy_tube+4

16.1          CollectFractions =                    By_Time             ; 16,1 -
16,6
              CollectPeriod =                       30 [s]

16.6          CollectFractions =                    No
              Tube =                                11

19.419        Valve =                               On                  ; "Fenster"
von 19,2 - 19,3

19.519        Valve =                               Off
              Tube =                                sample.Foxy_tube+5

20.1          CollectFractions =                    By_Time             ; 20,1 -
20,5
              CollectPeriod =                       18 [s]

20.4          CollectFractions =                    No

20.6          Tube =                                sample.Foxy_tube+6
              CollectFractions =                    By_Time             ; 20,5 -
20,9
              CollectPeriod =                       18 [s]

20.9          CollectFractions =                    No
              Tube =                                11

21.169        Valve =                               On                  ; Fenster
von 20,95 - 21,6

21.699        Valve =                               Off
              Tube =                                sample.Foxy_tube+7

21.7          CollectFractions =                    By_Time             ; 21,7 -
22,2
              CollectPeriod =                       30 [s]

22.2          CollectFractions =                    No
              Tube =                                11

26.119        Valve =                               On                  ; Fenster
von 25,9 - 27,9

28.119        Valve =                               Off
              Tube =                                sample.Foxy_tube+8

33.15         CollectFractions =                    By_Time             ; 33,15 -
33,85
              CollectPeriod =                       42 [s]

33.85         CollectFractions =                    No
              Tube =                                11

45.719        Valve =                               On                  ; Fenster
von 45,5 - 47,0

47.219        Valve = Off
              Tube =                                sample.Foxy_tube+9

56.75         CollectFractions =                    By_Time             ; 56,75 -
57,45
              CollectPeriod =                       42 [s]

57.45         CollectFractions =                    No
              Tube =                                36                  ; Entnahme
des Röhrchens ermöglichen


64.000        PumpLeft.%B =                         60.0 [%]
```

```
              PumpLeft.%B =                                 90.0 [%]

68.000        PumpLeft.%B =                                 90.0 [%]
              PumpLeft.%B =                                 25.0 [%]

70.000        PumpLeft.Flow =                               1.000 [ml/min]
              PumpLeft.%B =                                 25.0 [%]
              PumpLeft.%C =                                 10.0 [%]


              UV_VIS_1.AcqOff
              UV_VIS_2.AcqOff
              UV_VIS_3.AcqOff
              UV_VIS_4.AcqOff
              ;RI_1.AcqOff


              Sampler.WashBufferLoop                        Volume=300.000
              Wait                                          Sampler.Ready, Continue

              ;RI.Purge =                                   On                  ;während
der Vorbereitung der nächsten Probe spülen
              ReleaseExclusiveAccess
              End
;EOF
```

XIII.II.II. I-b BoT2 24h: F1 – F10

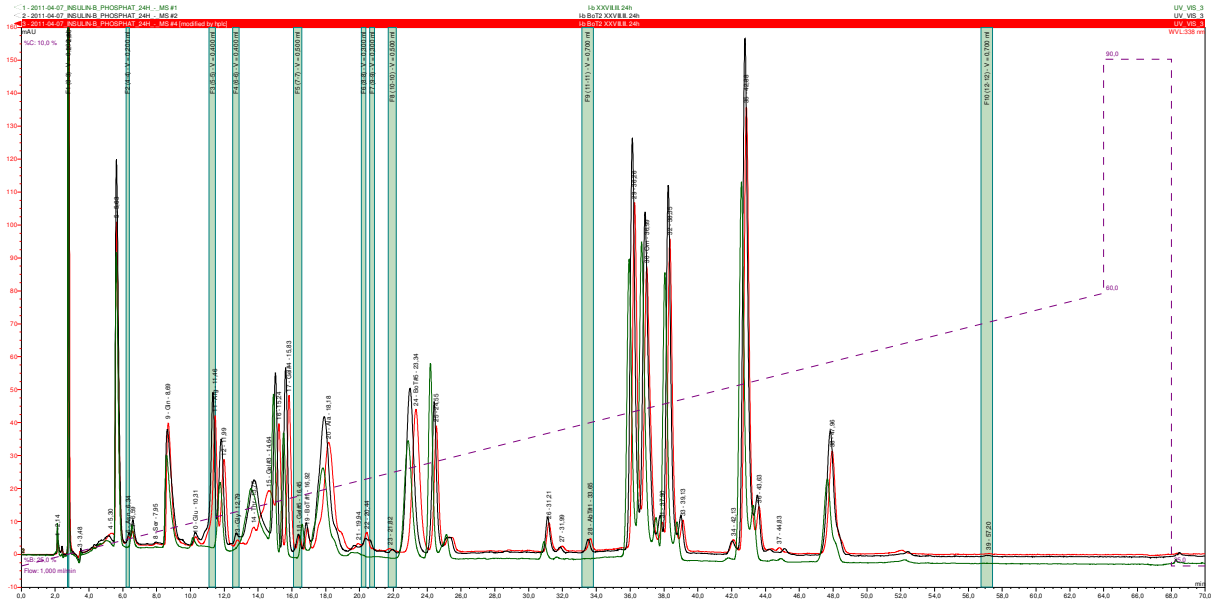

Figure XIII-XXIII RP-HPLC fractions of insulin β-chain after treatment with BoT2 for 24h and comparison to the reference (same treatment – without BoT2, green chromatogram) => ESI-IT MS^n F1 - F10 \{F2}

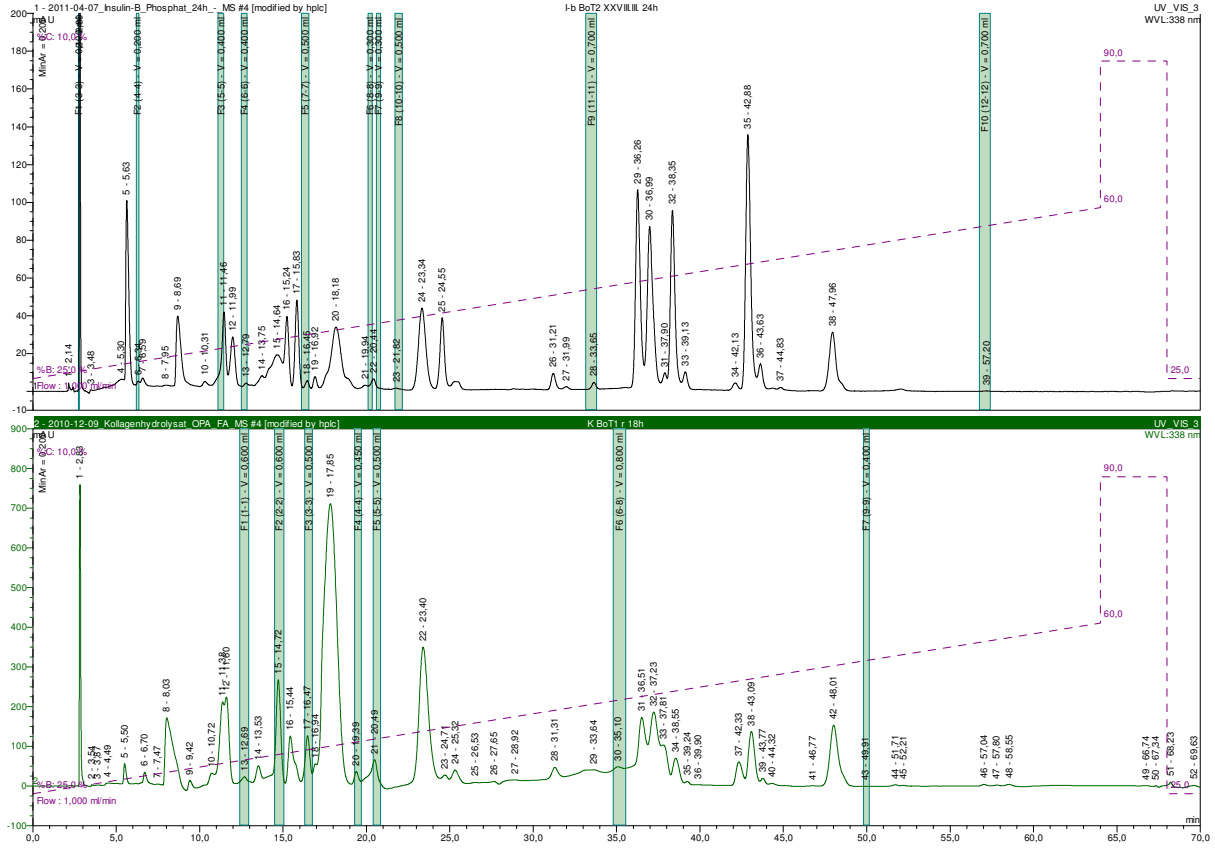

Figure XIII-XXIV comparison of the collected fractions F1 - F10 to I - VII (same chromatographic conditions)

ddH$_2$O

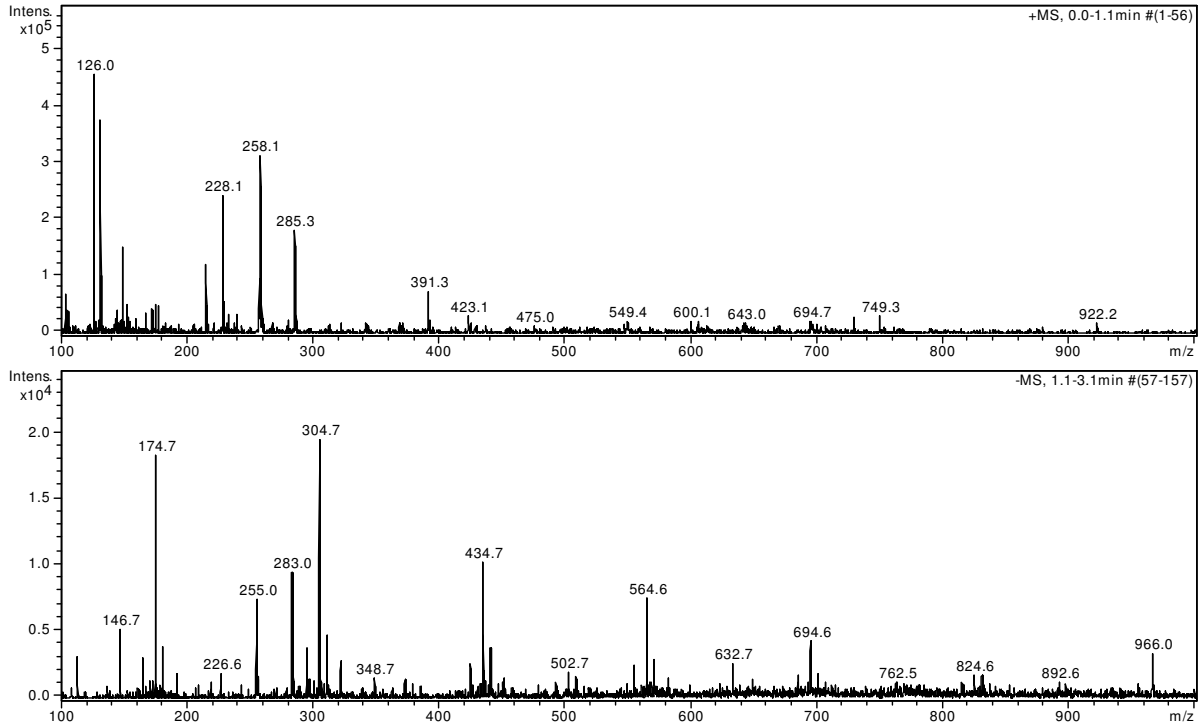

Figure XIII-XXV ddH$_2$O with 1 ‰ FA, full scan MS^1

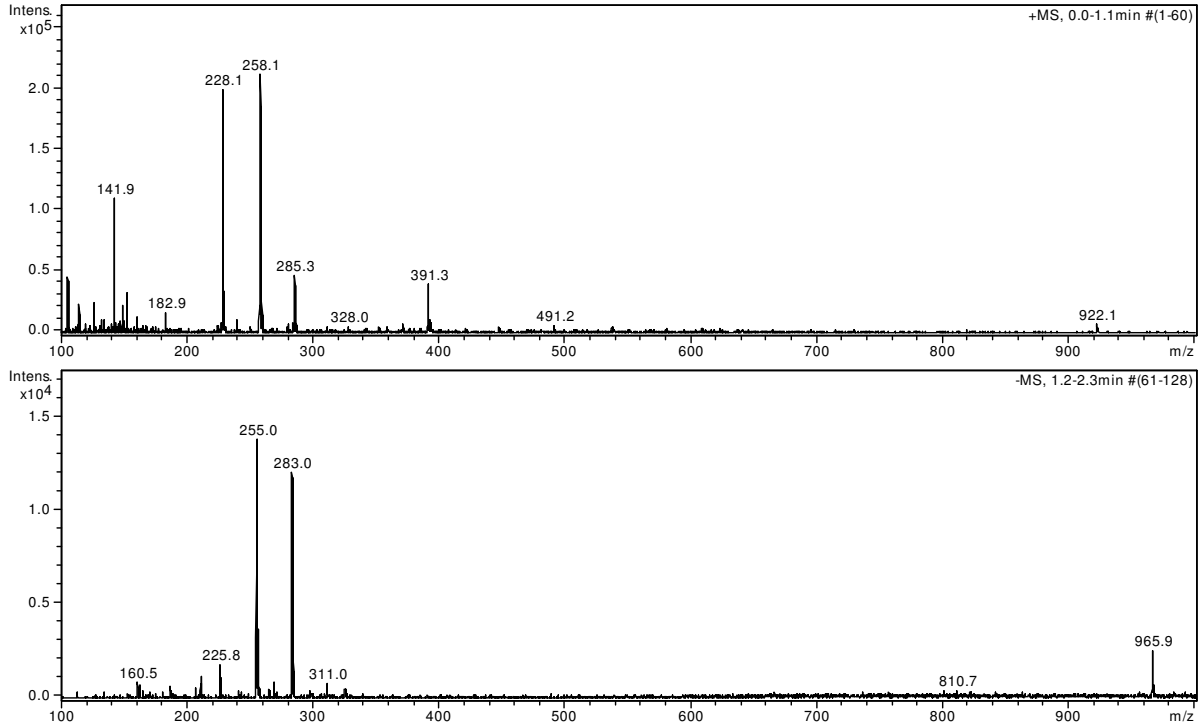

Figure XIII-XXVI ddH$_2$O, full scan MS^1

F1

No signals in compliance with the predefined selection rules ([M±p]$^{\pm}$, see 6.3) were encountered in the mass spectrum of fraction 1.

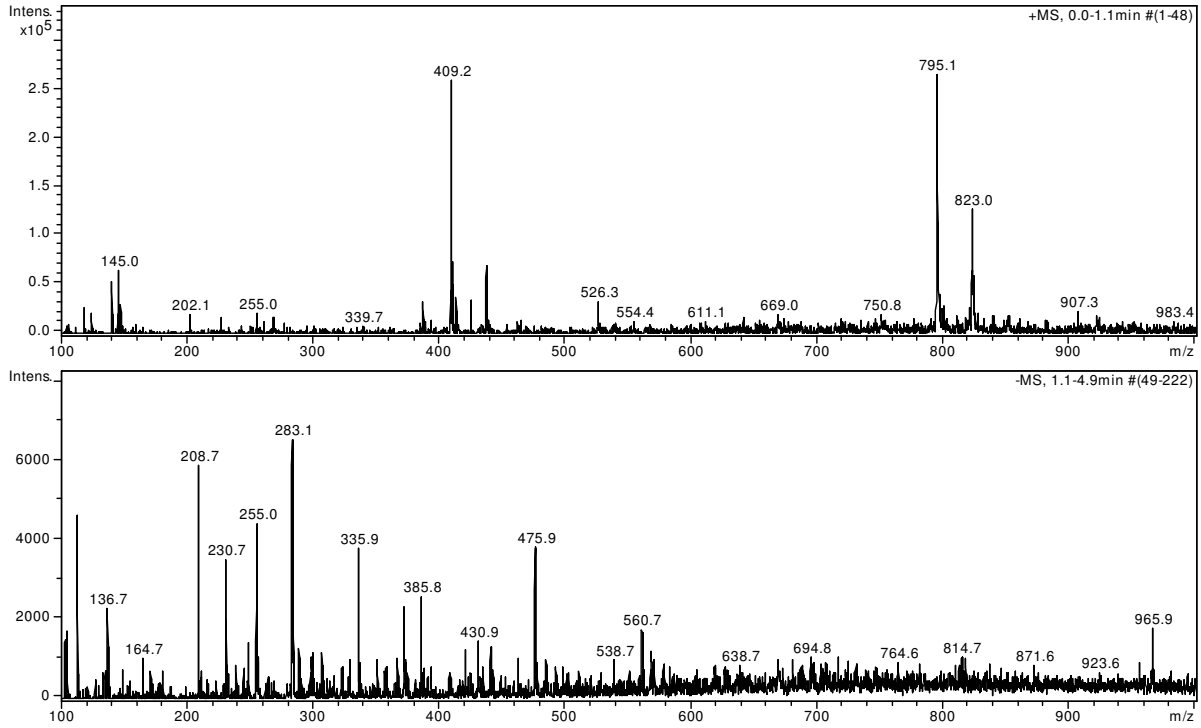

Figure XIII-XXVII F1: 2,73 – 2,85 min, 1 ‰ FA, 26 % ACN in ddH_2O; full scan MS^1

F2

Fraction 2 didn't make it to the collection tube.

F3

+MS^n

707,5 —258,4→ 449,1

426,1 —17,9→ 408,2
- 408,2 —84,9→ 341,2 —57,9→ 283,3
- 408,2 —106,0→ 320,1 —18,1→ 302,0 —28,0→ 274,0 —32,9→ 241,1
  - 274,0 —44,1→ 229,9
- 320,1 —46,1→ 274,0 —74,0→ 200,0
  - 200,0 —33,0→ 241,0
  - 200,0 —43,9→ 230,1
  - 200,0 —171,0→ 103,0
- 408,2 —142,0→ 284,1 —82,1→ 202,0 —56,7→ 145,3
  - 284,1 —100,1→ 184,0
- 408,2 —152,0→ 274,1 —56,0→ 218,1 —18,0→ 200,1
  - 218,1 —46,2→ 171,9

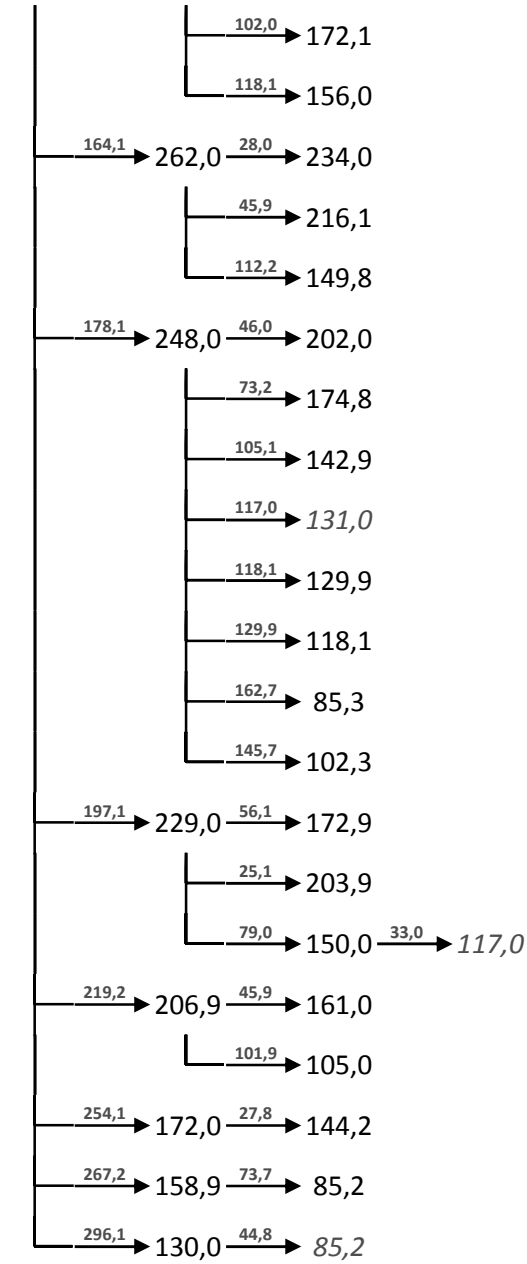
102,0 172,1
118,1 156,0
164,1 262,0 28,0 234,0
45,9 216,1
112,2 149,8
178,1 248,0 46,0 202,0
73,2 174,8
105,1 142,9
117,0 131,0
118,1 129,9
129,9 118,1
162,7 85,3
145,7 102,3
197,1 229,0 56,1 172,9
25,1 203,9
79,0 150,0 33,0 117,0
219,2 206,9 45,9 161,0
101,9 105,0
254,1 172,0 27,8 144,2
267,2 158,9 73,7 85,2
296,1 130,0 44,8 85,2

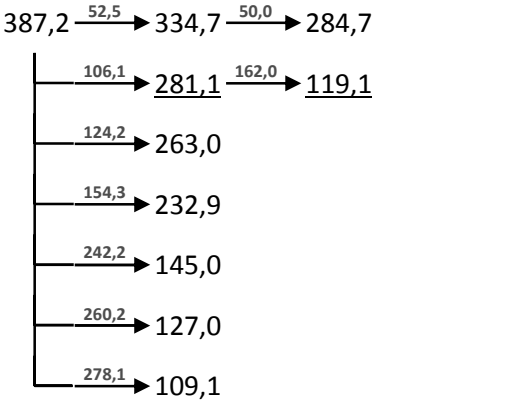
387,2 52,5 334,7 50,0 284,7
106,1 281,1 162,0 119,1
124,2 263,0
154,3 232,9
242,2 145,0
260,2 127,0
278,1 109,1

-MS^n

721,9 $\xrightarrow{46,8}$ 675,1

$\xrightarrow{386,1}$ 335,8

423,9 $\xrightarrow{44,0}$ 379,9

$\xrightarrow{72,1}$ 351,8 $\xrightarrow{92,1}$ 259,7 $\xrightarrow{44,0}$ 215,7

$\xrightarrow{136,1}$ 215,7

$\xrightarrow{92,1}$ 331,8 $\xrightarrow{72,0}$ 259,8

$\xrightarrow{164,2}$ 259,7 $\xrightarrow{44,0}$ 215,7

$\xrightarrow{208,2}$ 215,7 $\xrightarrow{33,9}$ 181,8

$\xrightarrow{56,0}$ 159,7

isotopic fingerprint:

peak area / % of monoisotopic	**+1**	**+2**	**+3**
theoretical ($C_{18}H_{24}N_3O_7S^+$):	22,0	8,3	1,4
measured (425,2 Th):	52,8	19,3	9,9
measured (-424,0 Th):	21,4	9,6	5,0

Figure XIII-XXVIII MS^n analysis of F3

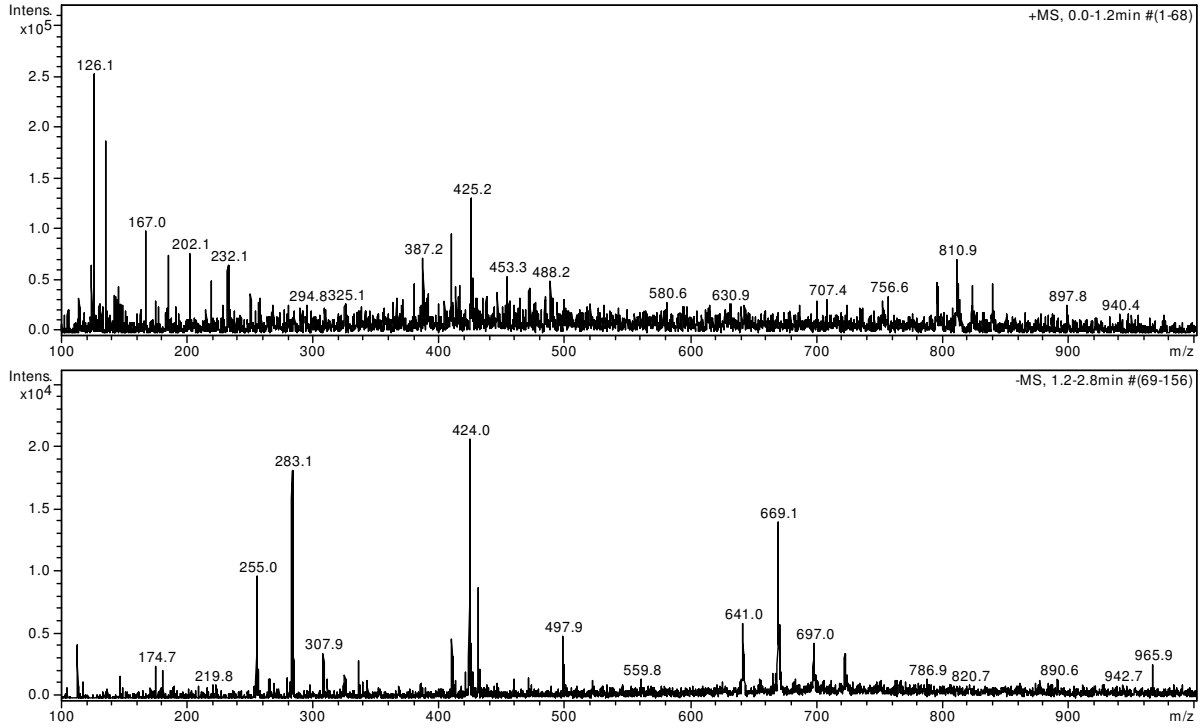

Figure XIII-XXIX F3: 11,1 – 11,5 min, 1 ‰ FA, 31 % ACN in ddH_2O; full scan MS^1

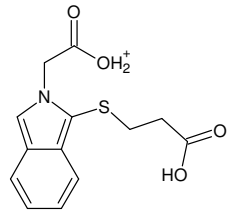

Monoisotopic Mass = 280.063804 Da

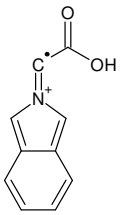

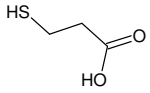

106.008849 Da

H_2O

18.010565 Da

$C\equiv O^+$

27.994915 Da

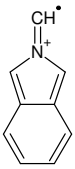

43.989829 Da

Fragment 85,2 Th
Gefundene Verbindungen: 27
CH8O2S MG=84,0244988
CH8O4 MG=84,0422568
CH10NO3 MG=84,066065
CH12N2O2 MG=84,0898732
CH24O3 MG=84,1725354
CH26NO2 MG=84,1963436
CH40O2 MG=84,302814
C2H12O3 MG=84,0786402
C2H14NO2 MG=84,1024484
C2H28O2 MG=84,2089188
C2N2O2 MG=83,995978
C3H2NO2 MG=84,0085532
C3H16O2 MG=84,1150236
C3O3 MG=83,984745
C4H4O2 MG=84,0211284
H4O3S MG=83,9881154
H4O5 MG=84,0058734
H6NO2S MG=84,0119236
H6NO4 MG=84,0296816
H8N2O3 MG=84,0534898
H10N3O2 MG=84,077298
H20O2S MG=84,118394
H20O4 MG=84,136152
H22NO3 MG=84,1599602
H24N2O2 MG=84,1837684
H36O3 MG=84,2664306
H38NO2 MG=84,2902388

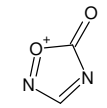

Monoisotopic Mass = 85.003254 Da

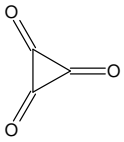

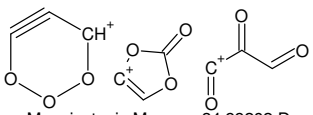

Monoisotopic Mass = 84.99202 Da

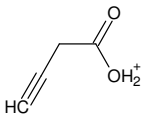

Monoisotopic Mass = 85.028406 Da

-----D--B--E--f-i-l-t-e-r-----
02.05.2011 - 14:25:04,48
akzeptierte DBEs:
0
1
2
3
4
5
6

C2N2O2 DBE: 4
C3O3 DBE: 4
C4H4O2 DBE: 3

3 von 27 Summenformeln

426,1 - 280,06 = **146,04**

Gefundene Verbindungen: 477
CH2N6OS MG=146,0010802
CH2N6O3 MG=146,0188382
...
N7OS MG=145,988505
N7O3 MG=146,006263

-----D--B--E--f-i-l-t-e-r-----
02.05.2011 - 12:06:14,89
akzeptierte DBEs:
1
2
3
4
5
6

CH2N6OS	DBE: 4
CH2N6O3	DBE: 4
CH6N8O	DBE: 3
C2H2N4O2S	DBE: 4
C2H2N4O4	DBE: 4
C2H2N4S2	DBE: 4
C2H6N6O2	DBE: 3
C2H6N6S	DBE: 3
C2H10N8	DBE: 2
C3H2N2OS2	DBE: 4
C3H2N2O3S	DBE: 4
C3H2N2O5	DBE: 4
C3H6N4OS	DBE: 3
C3H6N4O3	DBE: 3
C3H10N6O	DBE: 2
C4H2O2S2	DBE: 4
C4H2O4S	**DBE: 4**
C4H2O6	**DBE: 4**
C4H2S3	DBE: 4
C4H6N2O2S	DBE: 3
C4H6N2O4	DBE: 3
C4H6N2S2	DBE: 3
C4H10N4O2	DBE: 2
C4H10N4S	DBE: 2
C4H14N6	DBE: 1
C5H6OS2	DBE: 3
C5H6O3S	DBE: 3
C5H6O5	**DBE: 3**
C5H10N2OS	DBE: 2
C5H10N2O3	DBE: 2
C5H14N4O	DBE: 1
C6H10O2S	**DBE: 2**
C6H10O4	**DBE: 2**
C6H10S2	DBE: 2
C6H14N2O2	DBE: 1
C6H14N2S	DBE: 1
C7H14OS	**DBE: 1**
C7H14O3	**DBE: 1**
C9H10N2	DBE: 6
C10H10O	**DBE: 6**
C11H14	**DBE: 5**
H2N8O2	DBE: 4
H2N8S	DBE: 4
H6N10	DBE: 3

44 von 477 Summenformeln

+MSn [F3]: 85 Th

Gefundene Verbindungen: 86
CH2N5 MG=84,0310192
CH8O2S MG=84,0244988
(...)
H42N3 MG=84,3378552
N6 MG=84,018444

-----D--B--E--f-i-l-t-e-r-----
08.06.2011 - 12:11:33,68
akzeptierte DBEs:
0 1 2 3 4 5 6 7 8

CN4O DBE: 4
C2H4N4 DBE: 3
C2N2O2 DBE: 4
C2N2S DBE: 4
C3H4N2O DBE: 3
C3OS DBE: 4
C3O3 DBE: 4
C4H4O2 DBE: 3
C4H4S DBE: 3
C4H8N2 DBE: 2
C5H8O DBE: 2
C6H12 DBE: 1
C7 DBE: 8
N6 DBE: 4

14 von 86 Summenformeln

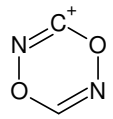

$C_2HN_2O_2$
85.003254 Da

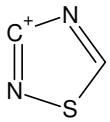

C_2HN_2S
84.985494 Da

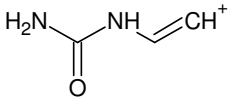

$C_3H_5N_2O$
85.039639 Da

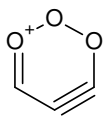

C_3HO_3
84.99202 Da

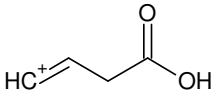

$C_4H_5O_2$
85.028406 Da

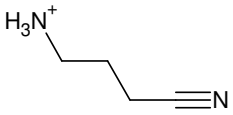

$C_4H_9N_2$
85.076025 Da

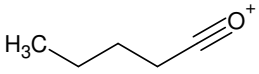

C_5H_9O
85.064791 Da

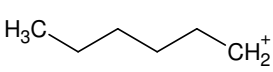

C_6H_{13}
85.101177 Da

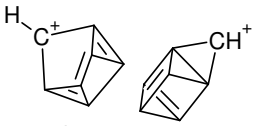

C_7H
85.007276 Da

Gefundene Verbindungen: 92
CH2N4O MG=86,0228602
CH4N5 MG=86,0466684
(...)
H44N3 MG=86,3535044
N5O MG=86,010285

-----D--B--E--f-i-l-t-e-r-----
08.06.2011 - 16:34:52,03
akzeptierte DBEs:
0 1 2 3 4 5 6 7 8

CH2N4O DBE: 3
C2H2N2O2 DBE: 3
C2H2N2S DBE: 3
C2H6N4 DBE: 2
C3H2OS DBE: 3
C3H2O3 DBE: 3
C3H6N2O DBE: 2
C4H6O2 DBE: 2
C4H6S DBE: 2
C4H10N2 DBE: 1
C5H10O DBE: 1
C6H14 DBE: 0
C7H2 DBE: 7
H2N6 DBE: 3

14 von 92 Summenformeln

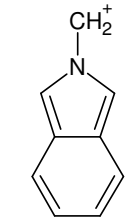

Monoisotopic Mass = 130.065126 Da

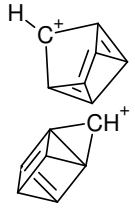

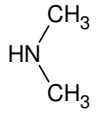

45.057849 Da

Monoisotopic Mass = 85.007276 Da

Gefundene Verbindungen: 16
CHO2 MG=44,9976546
CHS MG=44,9798966
CH3NO MG=45,0214628
CH5N2 MG=45,045271
CH17O MG=45,1279332
CH19N MG=45,1517414
C2H5O MG=45,034038
C2H7N MG=45,0578462
C2H21 MG=45,1643166
C3H9 MG=45,0704214
HN2O MG=45,0088876
H3N3 MG=45,0326958
H13O2 MG=45,0915498
H13S MG=45,0737918
H15NO MG=45,115358
H17N2 MG=45,1391662

-----D--B--E--f-i-l-t-e-r-----
08.06.2011 - 16:05:31,73
akzeptierte DBEs:
0 1 2 3 4 5 6

CH3NO DBE: 1
C2H7N DBE: 0
H3N3 DBE: 1

3 von 16 Summenformeln

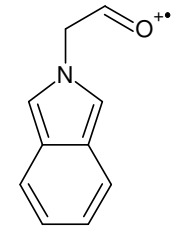

Monoisotopic Mass = 159.067865 Da

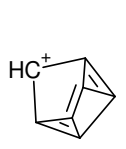

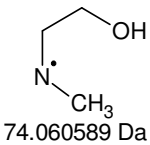

74.060589 Da

Monoisotopic Mass = 85.007276 Da

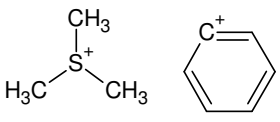

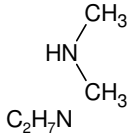

C_2H_7N
45.057849 Da

+MSn [F3]: 85,2 Th as well as 130 -> (85) und 159 -> 85

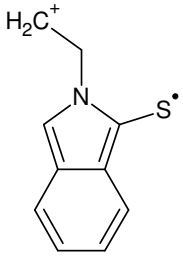

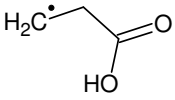

73.028954 Da

Monoisotopic Mass = 175.045021 Da

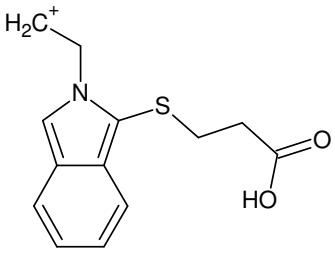

Monoisotopic Mass = 248.073975 Da

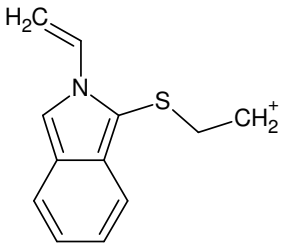

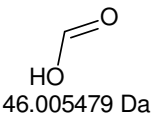

46.005479 Da

Monoisotopic Mass = 202.068496 Da

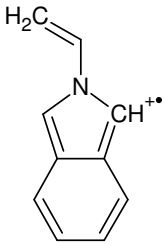

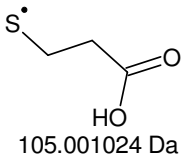

105.001024 Da

Monoisotopic Mass = 143.072951 Da

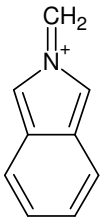

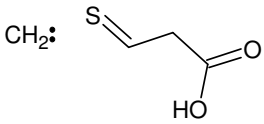

118.008849 Da

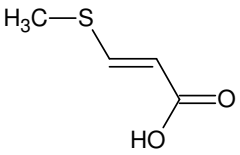

Monoisotopic Mass = 130.065126 Da

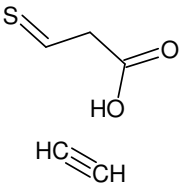

130.008849 Da

Monoisotopic Mass = 118.065126 Da

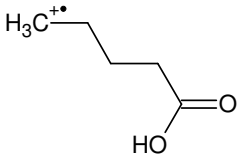

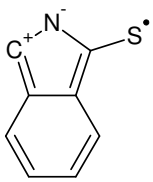

146.006444 Da

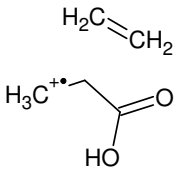

Monoisotopic Mass = 102.067531 Da

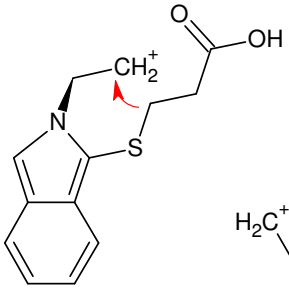

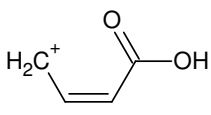

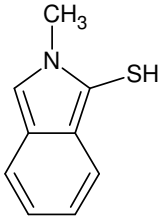

163.045569 Da

Monoisotopic Mass = 85.028406 Da

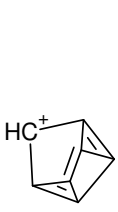

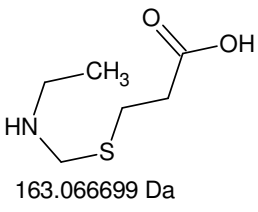

163.066699 Da

Monoisotopic Mass = 85.007276 Da

+MSn [F3] : 175 <-248 -> 202, 143, 130, 118, 102, 85

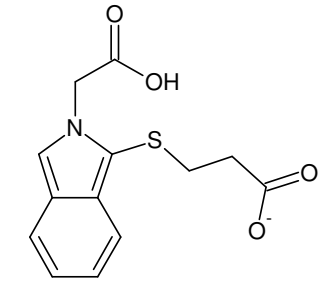

Monoisotopic Mass = 278.049251 Da

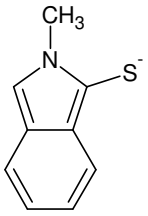

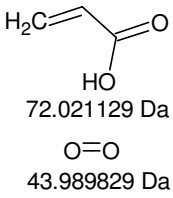

72.021129 Da

O=O

43.989829 Da

Monoisotopic Mass = 162.038293 Da

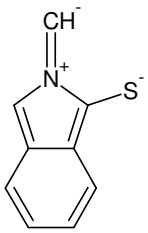

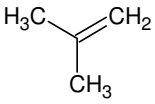

56.0626 Da

Monoisotopic Mass = 160.022643 Da

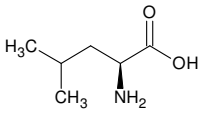

L-Leucin

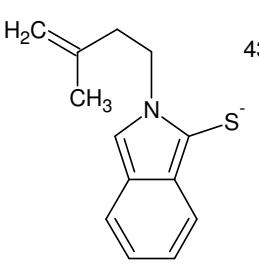

O=O

43.989829 Da

Monoisotopic Mass = 216.085243 Da

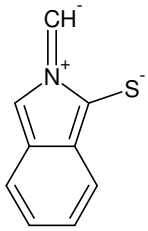

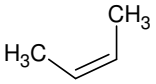

56.0626 Da

Monoisotopic Mass = 160.022643 Da

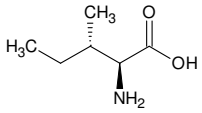

L-Isoleucine

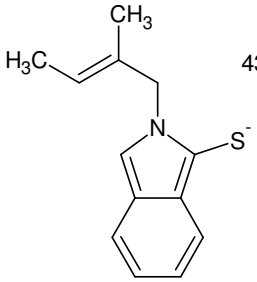

O=O

43.989829 Da

Monoisotopic Mass = 216.085243 Da

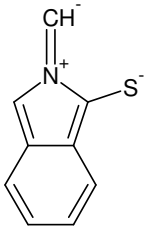

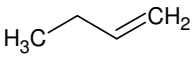

56.0626 Da

Monoisotopic Mass = 160.022643 Da

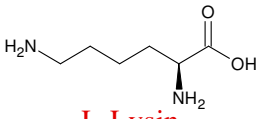

L-Lysin

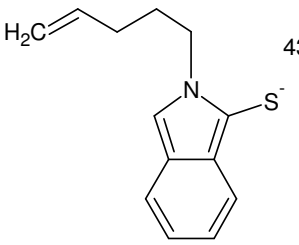

O=O

43.989829 Da

Monoisotopic Mass = 216.085243 Da

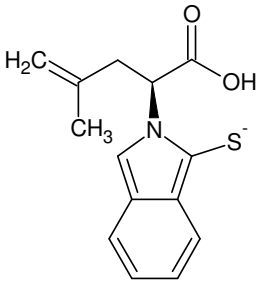

Monoisotopic Mass = 260.075072 Da

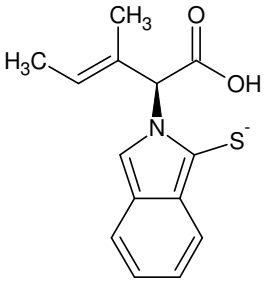

Monoisotopic Mass = 260.075072 Da

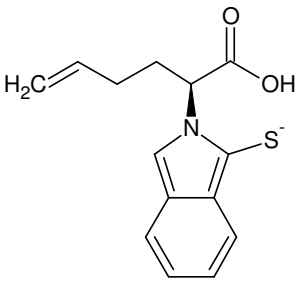

Monoisotopic Mass = 260.075072 Da

-MSn [F3]: 160 <- 216 <- 260 {I/II}

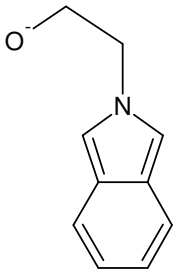

56 Da mit S:
Gefundene Verbindungen: 5
$CH_{12}S$ MG=56,0659672
C_2S MG=55,972072
H_8OS MG=56,0295838
$H_{10}NS$ MG=56,053392
$H_{24}S$ MG=56,1598624

Monoisotopic Mass = 160.076788 Da
kein Fragment mit 56 Da und S konstruierbar;
-216 Th spaltet aber 34 Da (H_2S) ab.

Gefundene Verbindungen: 8
CH_6O MG=34,0418626
CH_8N MG=34,0656708
C_2H_{10} MG=34,078246
H_2O_2 MG=34,0054792
H_2S MG=33,9877212
H_4NO MG=34,0292874
H_6N_2 MG=34,0530956
$H_{18}O$ MG=34,1357578

Ion -215,7 Th
Gefundene Verbindungen: 95
CH11O10S MG=215,0072926
CH11O12 MG=215,0250506
...
H11N2O9S MG=215,0185256
H11N2O11 MG=215,0362836

-----D--B--E--f-i-l-t-e-r-----
02.05.2011 - 15:22:17,75
akzeptierte DBEs:
0 1 2 3 4 5 6

C2HNO9S	DBE: 3	MG=214,9372056
C2HNO11	DBE: 3	MG=214,9549636
C3H5NO8S	DBE: 2	MG=214,973589
C3H5NO10	DBE: 2	MG=214,991347
C4H9NO7S	DBE: 1	MG=215,0099724
C4H9NO9	DBE: 1	MG=215,0277304
C5H13NO6S	DBE: 0	MG=215,0463558
C5H13NO8	DBE: 0	MG=215,0641138
C7H5NO5S	DBE: 6	MG=214,988844
C7H5NO7	DBE: 6	MG=215,006602
C8H9NO4S	DBE: 5	MG=215,0252274
C8H9NO6	DBE: 5	MG=215,0429854
C9H13NO3S	DBE: 4	MG=215,0616108
C9H13NO5	DBE: 4	MG=215,0793688

Spannweite: 0,142163 Da
=> Messung: 215,7 == 216

14 von 95 Summenformeln

-MSn [F3]: 160 <- 216 <- 260 {II/II}

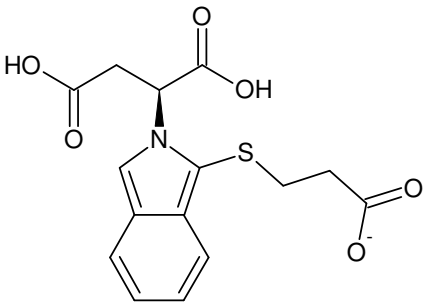

OPA-Asp
Monoisotopic Mass = 336.054731 Da
=> kein Fragment mit 92 Da möglich
(2-Propensäure - 72 Da - wird bereits früher abgespalten.)

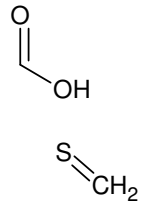

91.993199 Da

351,8 - 259,7 = 92,1
423,9 - 331,8 = 92,1
Gefundene Verbindungen: 113
CH2NO2S MG=91,9806252
CH2NO4 MG=91,9983832
(...)
N2O4 MG=91,985808
N2S2 MG=91,950292

-----D--B--E--f-i-l-t-e-r-----
08.06.2011 - 13:42:01,53
akzeptierte DBEs:
0 1 2 3 4 5 6

CH4N2OS DBE: 1
CH4N2O3 DBE: 1
CH8N4O DBE: 0
COS2 DBE: 2
CO3S DBE: 2
CO5 DBE: 2
C2H4O2S DBE: 1
C2H4O4 DBE: 1
C2H4S2 DBE: 1
C2H8N2O2 DBE: 0
C2H8N2S DBE: 0
C3H8OS DBE: 0
C3H8O3 DBE: 0
C3N4 DBE: 6
C4N2O DBE: 6
C5H4N2 DBE: 5
C5O2 DBE: 6
C5S DBE: 6
C6H4O DBE: 5
C7H8 DBE: 4
H4N4O2 DBE: 1
H4N4S DBE: 1
H8N6 DBE: 0
N2O2S DBE: 2
N2O4 DBE: 2
N2S2 DBE: 2

26 von 113 Summenformeln

92,1 Da; Δ 0,5 Da
ohne S:
Gefundene Verbindungen: 73
CH2NO4 MG=91,9983832
CH4N2O3 MG=92,0221914
(...)
H46NO2 MG=92,3528356
N2O4 MG=91,985808

-----D--B--E--f-i-l-t-e-r-----
08.06.2011 - 13:48:12,75
akzeptierte DBEs:
-2 -1 0 1 2 3 4 5 6

CH4N2O3 DBE: 1
CH8N4O DBE: 0
CO5 DBE: 2
C2H4O4 DBE: 1
C2H8N2O2 DBE: 0
C2H12N4 DBE: -1
C3H8O3 DBE: 0
C3H12N2O DBE: -1
C3N4 DBE: 6
C4N2O DBE: 6
C4H12O2 DBE: -1
C4H16N2 DBE: -2
C5H4N2 DBE: 5
C5O2 DBE: 6
C5H16O DBE: -2
C6H4O DBE: 5
C7H8 DBE: 4
H4N4O2 DBE: 1
H8N6 DBE: 0
N2O4 DBE: 2

20 von 73 Summenformeln

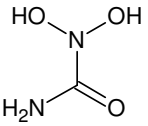
$CH_4N_2O_3$
92.022192 Da

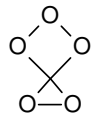
CO_5
91.974573 Da

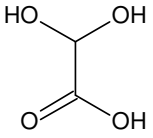
$C_2H_4O_4$
92.010959 Da

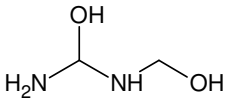
$C_2H_8N_2O_2$
92.058578 Da

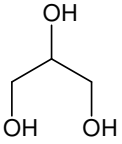
$C_3H_8O_3$
92.047344 Da

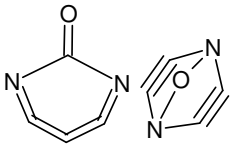
C_4N_2O
92.001063 Da

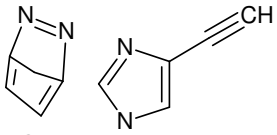
$C_5H_4N_2$
92.037448 Da

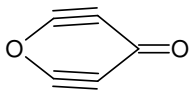
C_5O_2
91.989829 Da

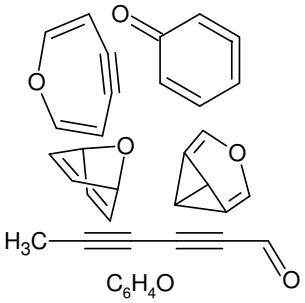
C_6H_4O
92.026215 Da

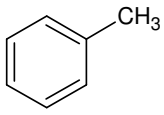
C_7H_8
92.0626 Da

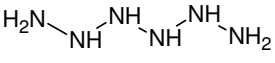
H_8N_6
92.081044 Da

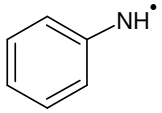
C_6H_6N
92.050024 Da

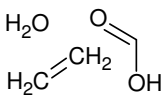
$C_3H_8O_3$
92.047344 Da

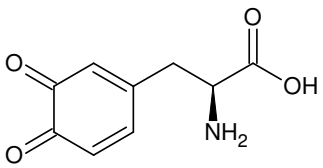
o-Dopachinon
Monoisotopic Mass = 195.053158 Da

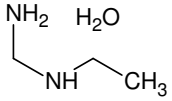
$C_3H_{12}N_2O$
92.094963 Da

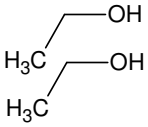
$C_4H_{12}O_2$
92.08373 Da

-MSn [F3]: 92 Da

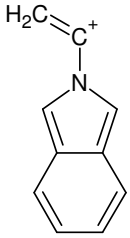

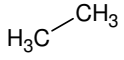

30.04695 Da

Monoisotopic Mass = 142.065126 Da

172,1 - 142,1 = **30,0**

Gefundene Verbindungen: 7

CH_2O MG=30,0105642
CH_4N MG=30,0343724
C_2H_6 MG=30,0469476
H_2N_2 MG=30,0217972
$H_{14}O$ MG=30,1044594
$H_{16}N$ MG=30,1282676
NO MG=29,997989

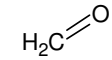

CH_2O
30.010565 Da

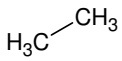

C_2H_6
30.04695 Da

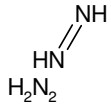

H_2N_2
30.021798 Da

Gefundene Verbindungen: 8

CH5O MG=33,034038
CH7N MG=33,0578462
C2H9 MG=33,0704214
HO2 MG=32,9976546
HS MG=32,9798966
H3NO MG=33,0214628
H5N2 MG=33,045271
H17O MG=33,1279332

-----D--B--E--f-i-l-t-e-r-----
08.06.2011 - 17:53:31,23
akzeptierte DBEs:
-1 0 1 2 3 4 5 6 7 8

CH7N DBE: -1
H3NO DBE: 0

2 von 8 Summenformeln

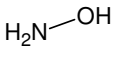

H_3NO
33.021464 Da

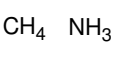

CH_7N
33.057849 Da

HS
32.979895 Da

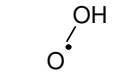

HO_2
32.997654 Da

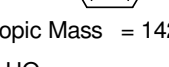

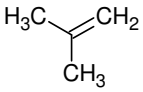

56.0626 Da

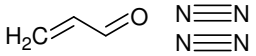

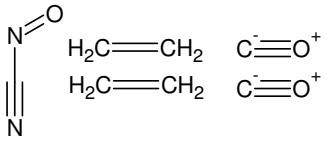

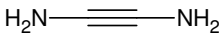

H_2O
18.010565 Da

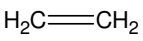

28.0313 Da

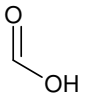

46.005479 Da

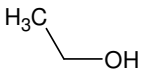

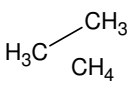

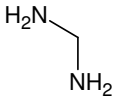

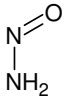

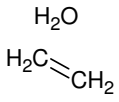

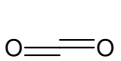

43.989829 Da

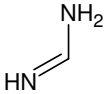

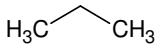

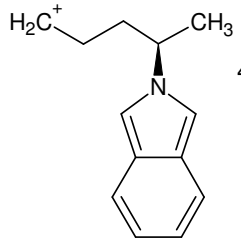

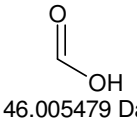

46.005479 Da

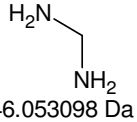

46.053098 Da

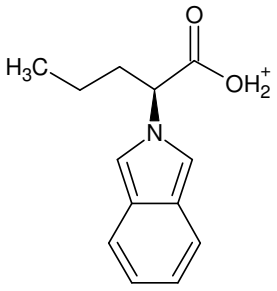

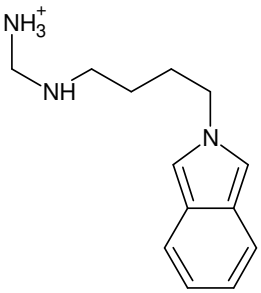

Monoisotopic Mass = 172.112076 Da Monoisotopic Mass = 218.117555 Da Monoisotopic Mass = 218.165174 Da

18 Da (H_2O) sind aus dieser Struktur nicht abspaltbar.

+MSn [F3]: 218,1 Th

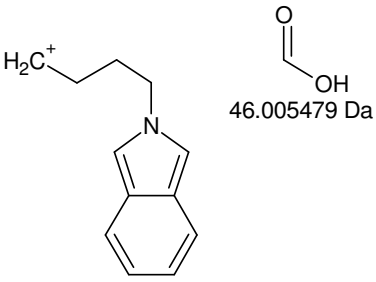

Monoisotopic Mass = 172.112076 Da

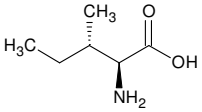

L-Isoleucin

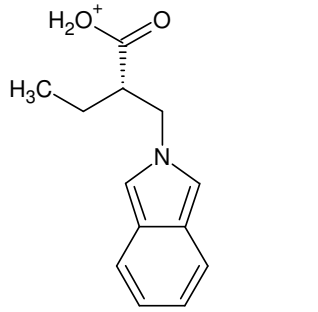

Monoisotopic Mass = 218.117555 Da

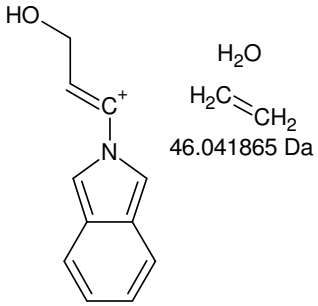

Monoisotopic Mass = 172.07569 Da

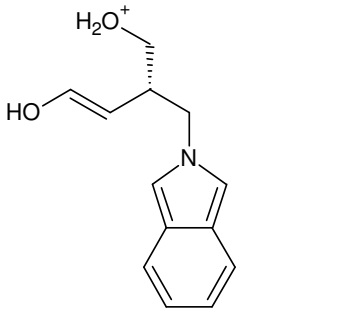

Monoisotopic Mass = 218.117555 Da

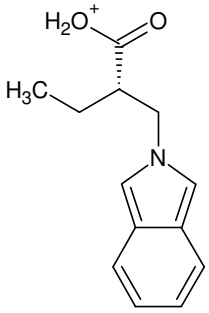

+ 56 Da; Aus dem Ergebnis müssen 33 Da abspaltbar sein (H_2NOH, HS). =>
1 mögliche Summenformel für 56 Da

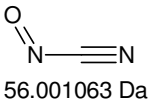

Monoisotopic Mass = 218.117555 Da

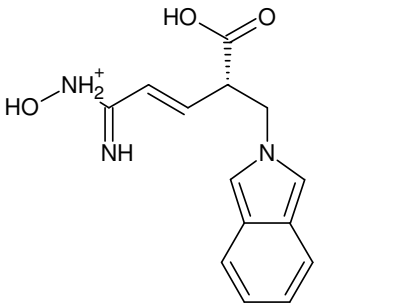

Monoisotopic Mass = 274.118618 Da

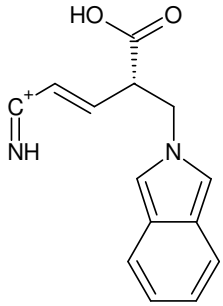

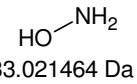

Monoisotopic Mass = 241.097154 Da

+MSn [F3]: 218,1 Th : Ile

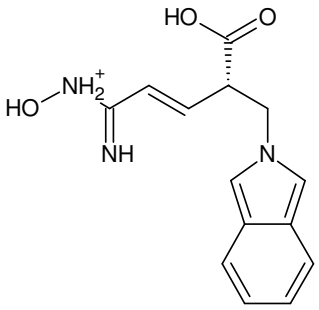

Monoisotopic Mass = 274.118618 Da

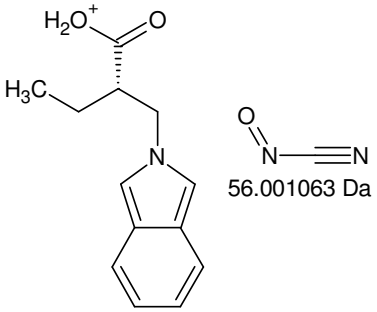

Monoisotopic Mass = 218.117555 Da

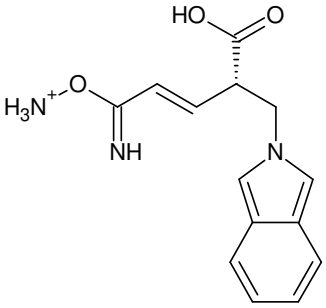

Monoisotopic Mass = 274.118618 Da

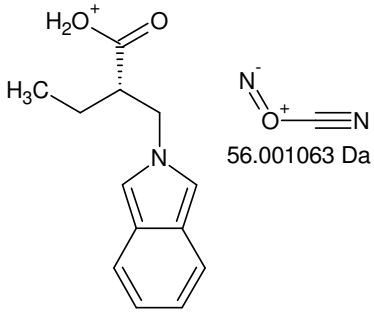

Monoisotopic Mass = 218.117555 Da

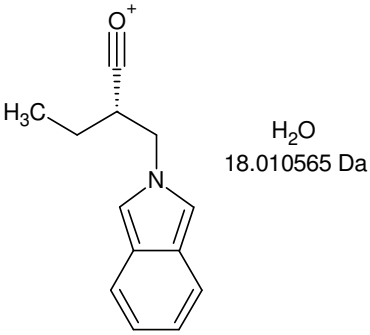

Monoisotopic Mass = 200.10699 Da

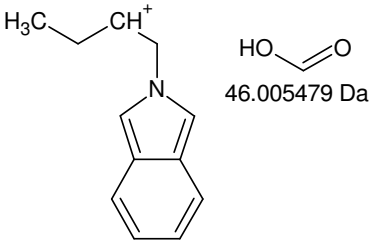

Monoisotopic Mass = 172.112076 Da

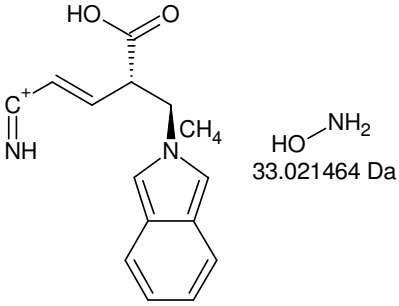

Monoisotopic Mass = 241.097154 Da

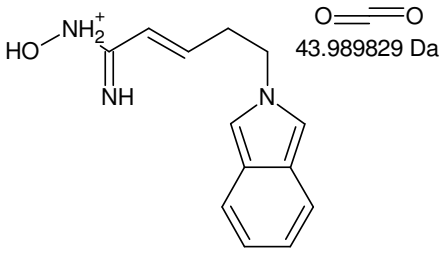

Monoisotopic Mass = 230.128789 Da

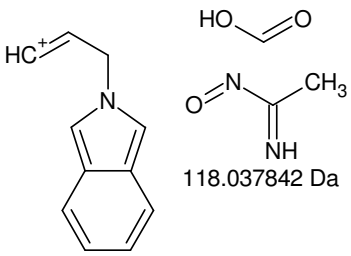

Monoisotopic Mass = 156.080776 Da

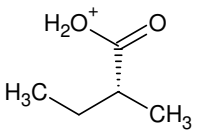

Monoisotopic Mass = 103.075356 Da

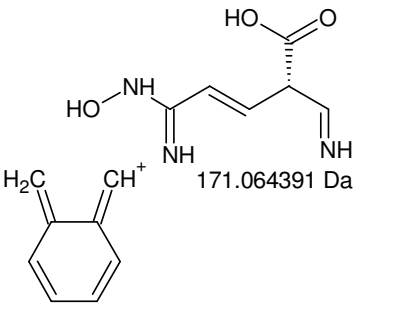

Monoisotopic Mass = 103.054227 Da

+MSn [F3]: 274 -> 218 -> 200, 172 and 274 -> 241, 230, 156, 103

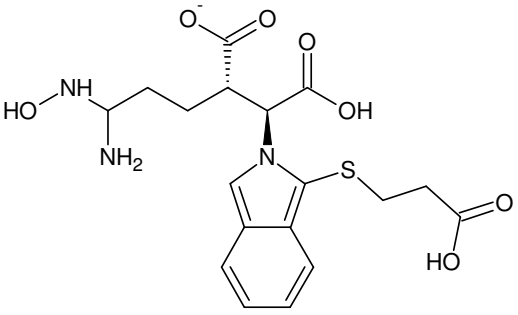

Monoisotopic Mass = 424.118394 Da

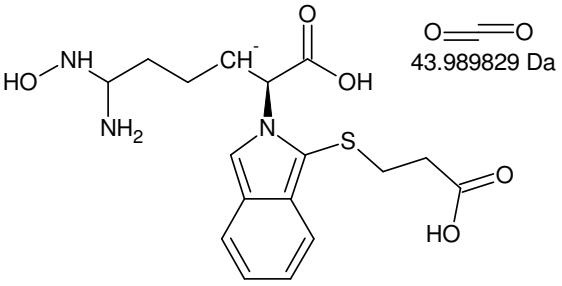

Monoisotopic Mass = 380.128564 Da

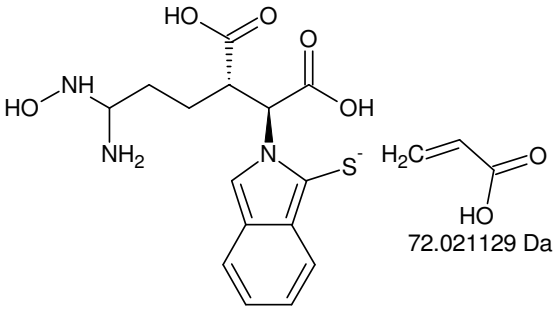

Monoisotopic Mass = 352.097264 Da

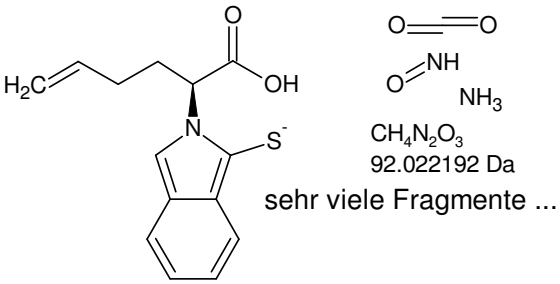

Monoisotopic Mass = 260.075072 Da

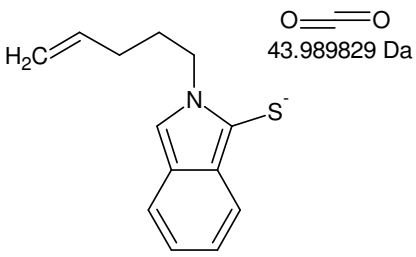

Monoisotopic Mass = 216.085243 Da

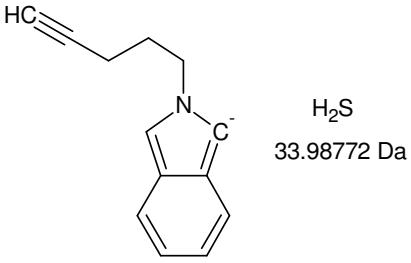

Monoisotopic Mass = 182.097523 Da

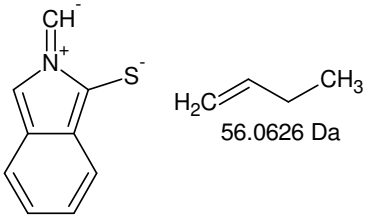

Monoisotopic Mass = 160.022643 Da

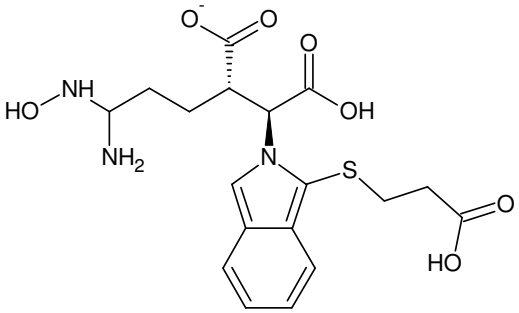

Monoisotopic Mass = 424.118394 Da

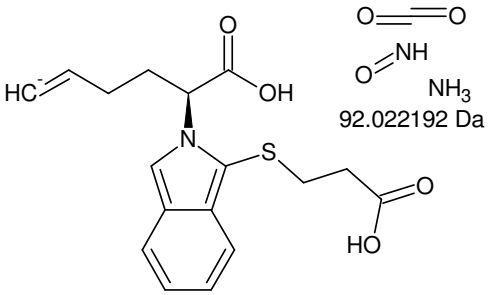

Monoisotopic Mass = 332.096202 Da

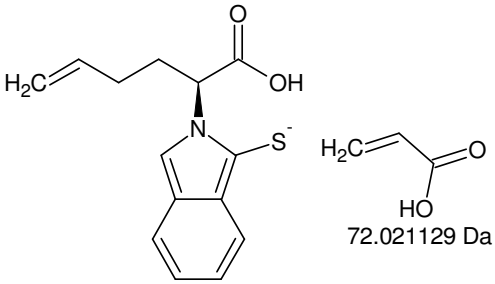

Monoisotopic Mass = 260.075072 Da

-MSn [F3]: 424 -> 380 and 424 -> 352 -> 260 -> 216 -> 182, 160 as well as 424 -> 332 -> 260

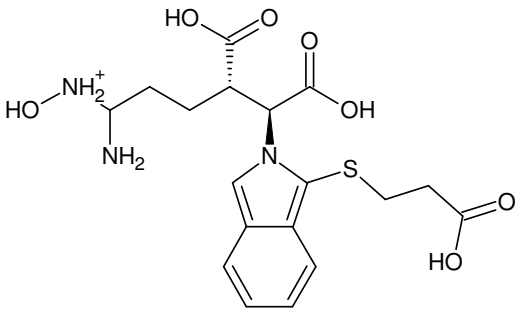

Monoisotopic Mass = 426.132947 Da

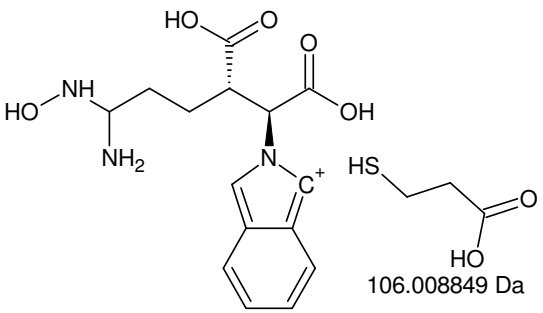

Monoisotopic Mass = 320.124097 Da

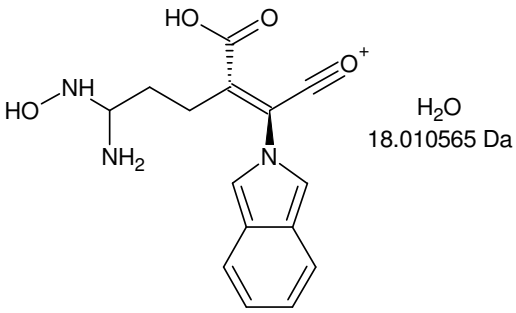

Monoisotopic Mass = 302.113532 Da

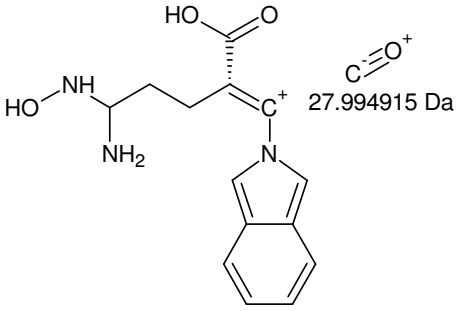

Monoisotopic Mass = 274.118618 Da

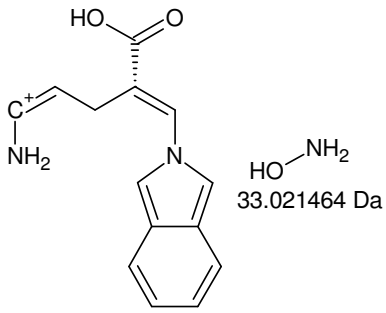

Monoisotopic Mass = 241.097154 Da

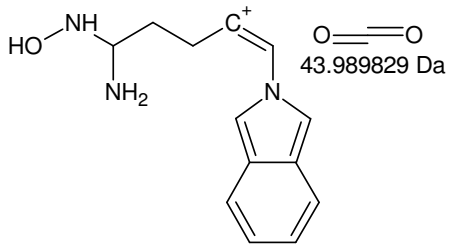

Monoisotopic Mass = 230.128789 Da

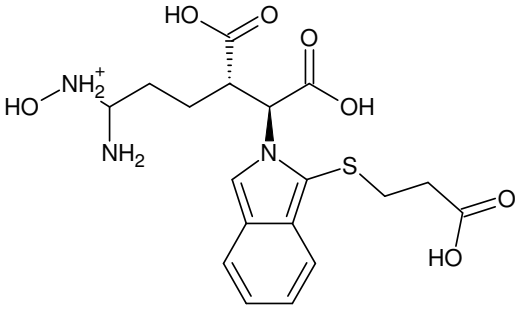

Monoisotopic Mass = 426.132947 Da

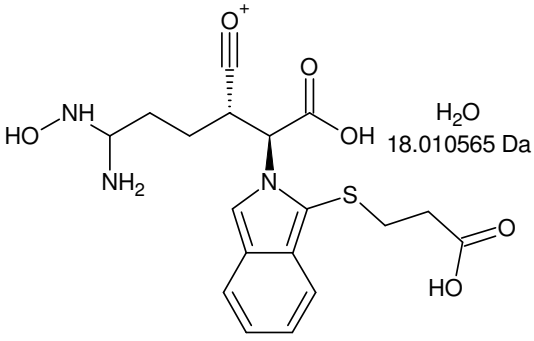

Monoisotopic Mass = 408.122382 Da

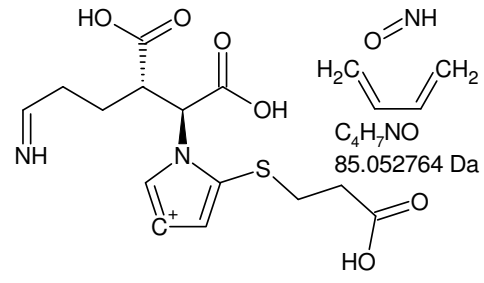

Monoisotopic Mass = 341.080183 Da

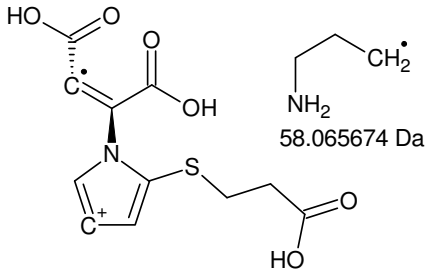

Monoisotopic Mass = 283.014508 Da

+MSn [F3]: 426 -> 320 -> 302 -> 274 -> 241, 230 and 426 -> 408, 341 -> 283

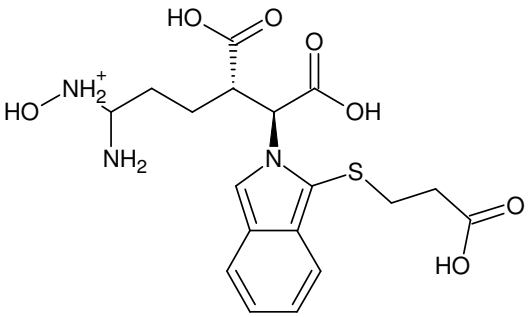

Monoisotopic Mass = 426.132947 Da

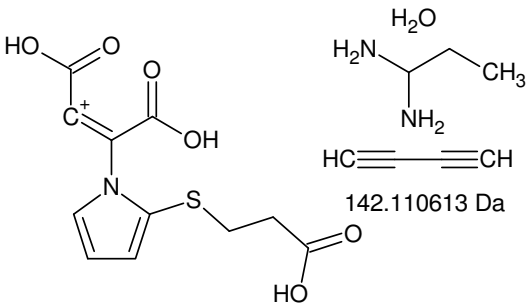

142.110613 Da

Monoisotopic Mass = 284.022333 Da

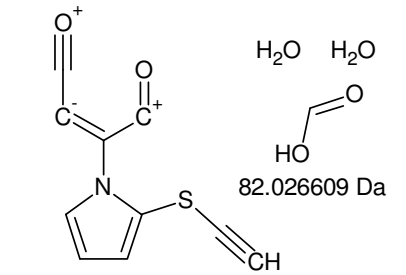

82.026609 Da

Monoisotopic Mass = 201.995725 Da

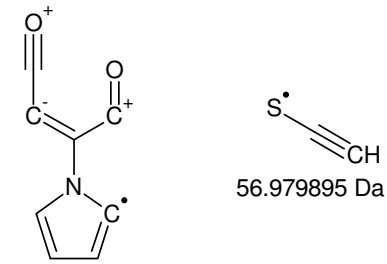

56.979895 Da

Monoisotopic Mass = 145.01583 Da

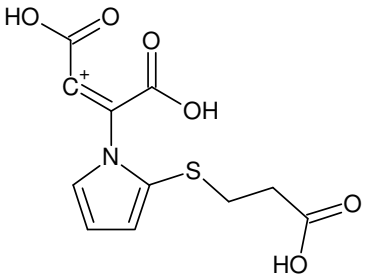

Monoisotopic Mass = 284.022333 Da

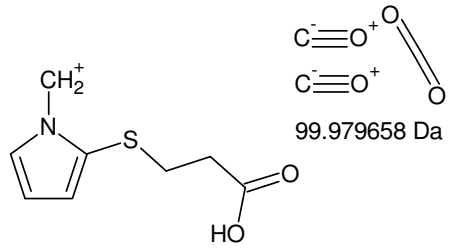

99.979658 Da

Monoisotopic Mass = 184.042675 Da

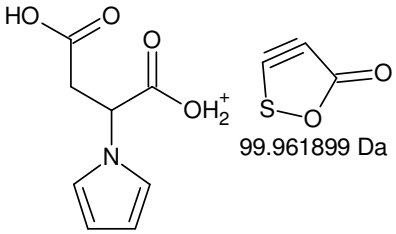

99.961899 Da

Monoisotopic Mass = 184.060434 Da

+MSn [F3]: 426 -> 284 -> 202 -> 145 and [426 -> 284] -> 184

F4

The signal of interest had the form of a shoulder on the rising edge of a bigger peak.

+MS^n

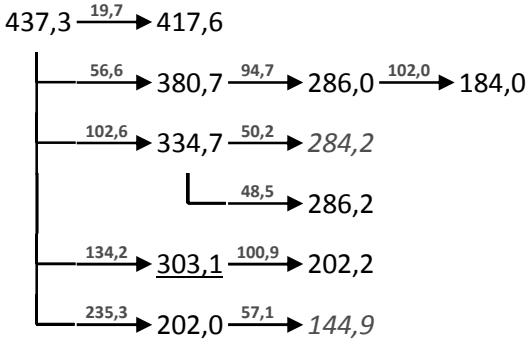

-MS^n

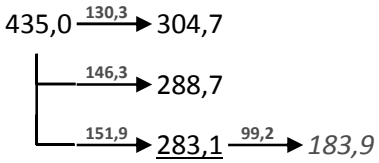

isotopic fingerprint (MS^2, 8 Th isolation width):

peak area / % of monoisotopic	**+1**	**+2**	**+3**
measured (437,3 Th):	45,7	26,0	-
measured (-434,8 Th):	45,5	-	-

Figure XIII-XXX MS^n analysis of F4

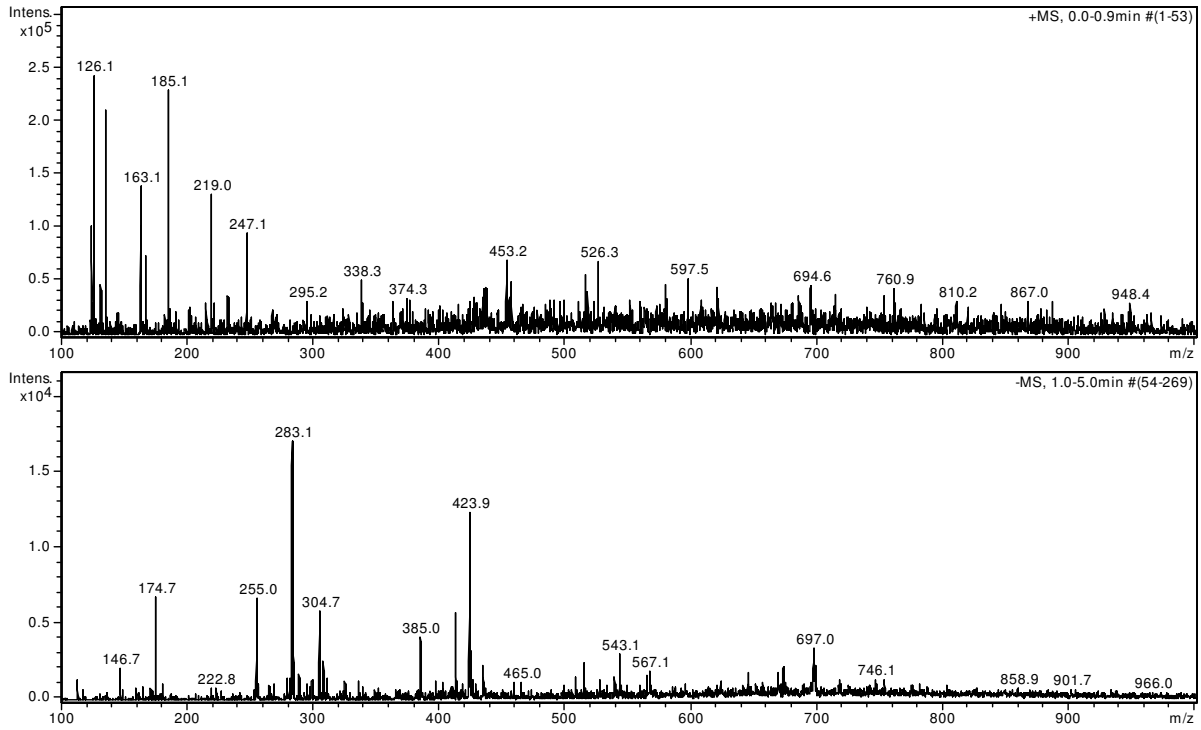

Figure XIII-XXXI F4: 12,5 – 12,9 min, 0,5 ‰ FA, 66 % ACN in ddH_2O (diluted 1:2 with ACN); full scan MS^1

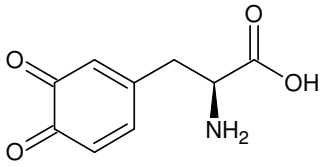

o-Dopachinon
Monoisotopic Mass = 195.053158 Da

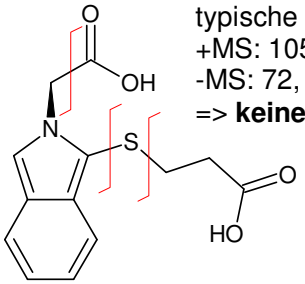

Monoisotopic Mass = 279.056528 Da

typische Fragmente fehlen:
+MS: 105, 106, 46 Da
-MS: 72, 44 Da
=> **keine** 3-Mercaptopropionsäureseitenkette

414,3 - 297,1 = **117,2**
Gefundene Verbindungen: 229
CHN4OS MG=116,9871076
CHN4O3 MG=117,0048656
(..)
H57N2S MG=117,4242222
H59N3O MG=117,4657884

-----D--B--E--f-i-l-t-e-r-----
14.06.2011 - 10:56:52,32
akzeptierte DBEs:
0 1 2 3 4 5 6 7 8

CH3N5O2	DBE: 3
CH3N5S	DBE: 3
CH7N7	DBE: 2
C2H3N3OS	DBE: 3
C2H3N3O3	DBE: 3
C2H7N5O	DBE: 2
C3H3NO2S	DBE: 3
C3H3NO4	DBE: 3
C3H3NS2	DBE: 3
C3H7N3O2	DBE: 2
C3H7N3S	DBE: 2
C3H11N5	DBE: 1
C4H7NOS	DBE: 2
C4H7NO3	DBE: 2
C4H11N3O	DBE: 1
C5H11NO2	DBE: 1
C5H11NS	DBE: 1
C5H15N3	DBE: 0
C6H3N3	DBE: 7
C6H15NO	DBE: 0
C7H3NO	DBE: 7
C8H7N	DBE: 6
H3N7O	DBE: 3

23 von 229 Summenformeln

min. C1O2:

CH3N5O2	DBE: 3
C2H3N3O3	DBE: 3
C3H3NO2S	DBE: 3
C3H3NO4	DBE: 3
C3H7N3O2	DBE: 2
C4H7NO3	DBE: 2
C5H11NO2	DBE: 1

7 von 59 Summenformeln

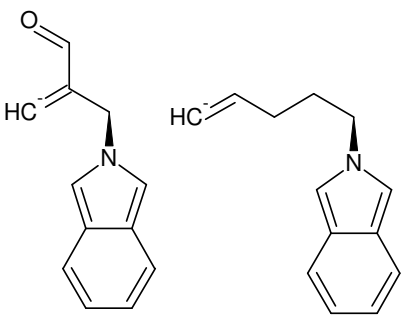

184.076788 Da 184.113173 Da

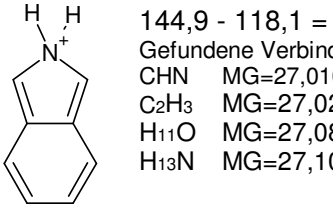

Monoisotopic Mass = 412.142307 Da

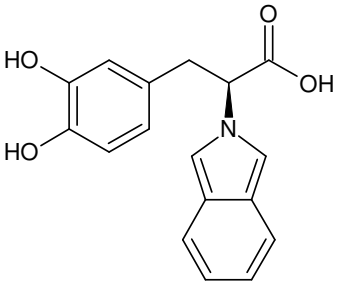

Monoisotopic Mass = 297.100108 Da

144,9 - 118,1 = **26,8**
Gefundene Verbindungen: 4
CHN MG=27,0108986
C_2H_3 MG=27,0234738
$H_{11}O$ MG=27,0809856
$H_{13}N$ MG=27,1047938

Monoisotopic Mass = 118.065126 Da

144,9 - 115,0 = **29,9**
Gefundene Verbindungen: 7
CH_2O MG=30,0105642
CH_4N MG=30,0343724
C_2H_6 MG=30,0469476
H_2N_2 MG=30,0217972
$H_{14}O$ MG=30,1044594
$H_{16}N$ MG=30,1282676
NO MG=29,997989

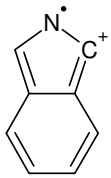

Monoisotopic Mass = 115.041651 Da

183,9 - 116,1 = **67,8**
Gefundene Verbindungen: 45
CH8OS MG=68,0295838
CH8O3 MG=68,0473418
(...)
H24N2O MG=68,1888534
H26N3 MG=68,2126616

-----D--B--E--f-i-l-t-e-r-----
14.06.2011 - 10:09:52,82
akzeptierte DBEs:
0 1 2 3 4 5 6 7 8

CN4	DBE: 4
C2N2O	DBE: 4
C3H4N2	DBE: 3
C3O2	DBE: 4
C3S	DBE: 4
C4H4O	DBE: 3
C5H8	DBE: 2

7 von 45 Summenformeln

304,7 - 283,1 = 21,6

Gefundene Verbindungen: 3
H_6O MG=22,0418626
CH_{10} MG=22,078246
H_8N MG=22,0656708

=> - Na^+, $+H^+$?

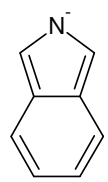

Monoisotopic Mass = 116.050573 Da

Insulin B enthält kein Methionin.

MS^n [F4]: 414 Da {I/II}

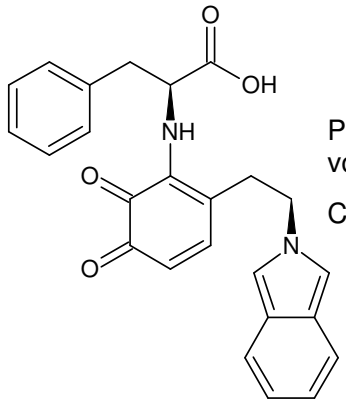

Phe ist der N-Terminus von Insulin B.

Chinon reoxidiert

Monoisotopic Mass = 414.157957 Da

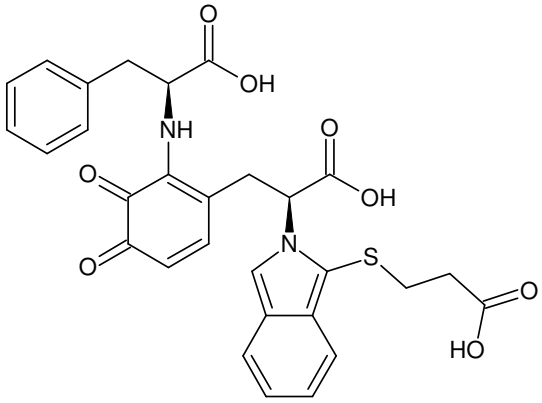

Monoisotopic Mass = 562.140986 Da

Molekülpeaks und Fragmente stimmen mit **keinem** der Signale der Probe K BoT1 r 18h (Kollagen mit BoT1) überein.

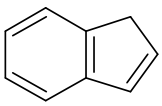

1*H*-Inden

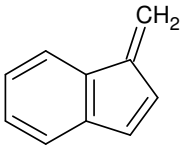

Benzofulven
1-Methyliden-1*H*-inden
(intensiv gefärbt - allerdings auch bei 280nm; Dort wurde aber kein Signal gefunden.)

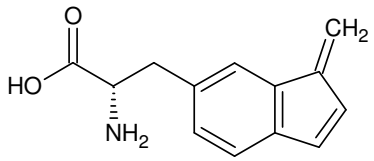

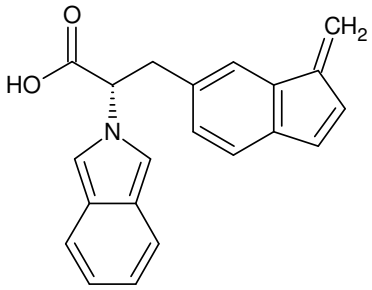

MS^n [F4]: 414 Da {II/II}

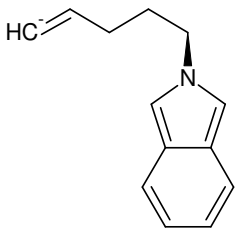

Monoisotopic Mass = 184.113173 Da

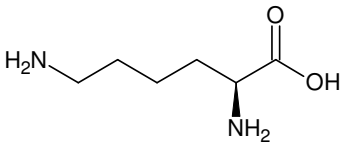

L-Lysin

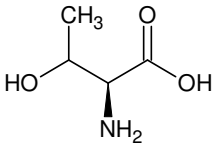

L-Threonin

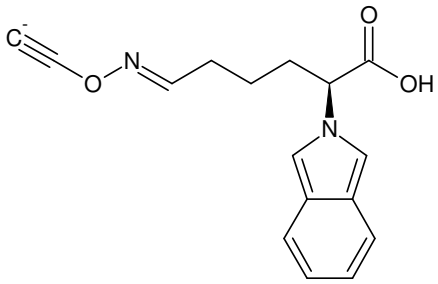

Monoisotopic Mass = 283.108816 Da

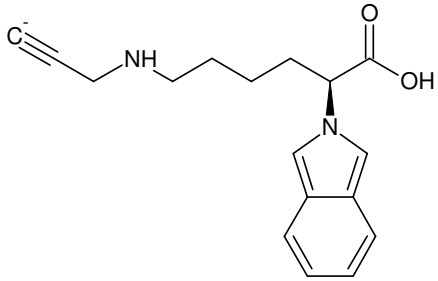

Monoisotopic Mass = 283.145201 Da

99,2 - 44,0 = **55,2**
Gefundene Verbindungen: 24
CHN3 MG=55,0170466
CH11O2 MG=55,0759006
(...)
H25NO MG=55,193604
H27N2 MG=55,2174122

-----D--B--E--f-i-l-t-e-r-----
14.06.2011 - 10:36:46,59
akzeptierte DBEs:
0 1 2 3 4 5 6 7 8

CHN3 DBE: 3
C2HNO DBE: 3
C3H5N DBE: 2

3 von 24 Summenformeln

283,1 - 183,9 = **99,2**
Gefundene Verbindungen: 133
CHN5O MG=99,0181096
CH3N6 MG=99,0419178
(...)
H41N3O MG=99,3249456
H43N4 MG=99,3487538

-----D--B--E--f-i-l-t-e-r-----
14.06.2011 - 10:46:02,00
akzeptierte DBEs:
0 1 2 3 4 5 6 7 8

CHN5O DBE: 4
C2HN3O2 DBE: 4
C2HN3S DBE: 4
C2H5N5 DBE: 3
C3HNOS DBE: 4
C3HNO3 DBE: 4
C3H5N3O DBE: 3
C4H5NO2 DBE: 3
C4H5NS DBE: 3
C4H9N3 DBE: 2
C5H9NO DBE: 2
C6H13N DBE: 1
C7HN DBE: 8
HN7 DBE: 4

14 von 133 Summenformeln

130,3 - 44,0 = **86,3**
Gefundene Verbindungen: 92
CH2N4O MG=86,0228602
CH4N5 MG=86,0466684
(...)
H44N3 MG=86,3535044
N5O MG=86,010285

-----D--B--E--f-i-l-t-e-r-----
14.06.2011 - 10:34:56,71
akzeptierte DBEs:
0 1 2 3 4 5 6 7 8

CH2N4O DBE: 3
C2H2N2O2 DBE: 3
C2H2N2S DBE: 3
C2H6N4 DBE: 2
C3H2OS DBE: 3
C3H2O3 DBE: 3
C3H6N2O DBE: 2
C4H6O2 DBE: 2
C4H6S DBE: 2
C4H10N2 DBE: 1
C5H10O DBE: 1
C6H14 DBE: 0
C7H2 DBE: 7
H2N6 DBE: 3

14 von 92 Summenformeln

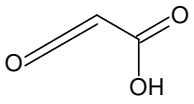

$C_3H_2O_3$
86.000394 Da

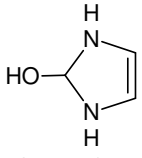

$C_3H_6N_2O$
86.048013 Da

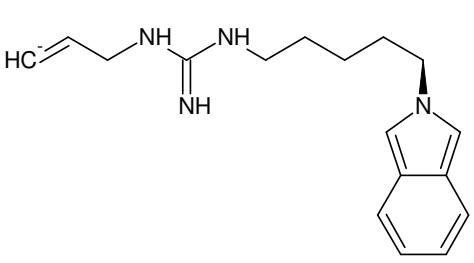

Monoisotopic Mass = 283.19282 Da

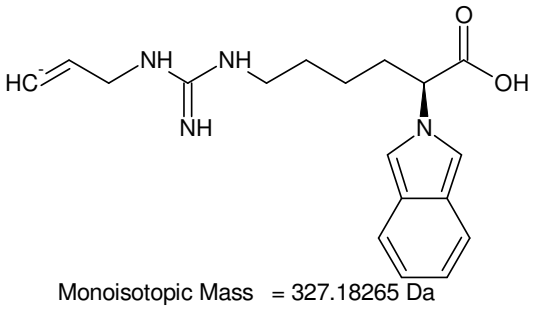

Monoisotopic Mass = 327.18265 Da

-MSn [F4]: 184 <- 283 <? 435 {I/II}

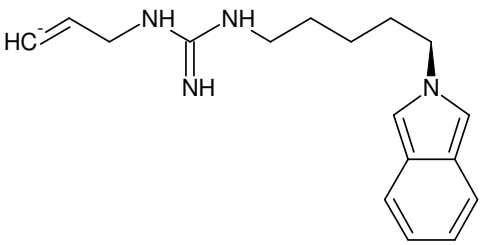

Monoisotopic Mass = 283.19282 Da

mit CO_2:

Gefundene Verbindungen: 73
CH2N6O2 MG=130,0239232
CH6O7 MG=130,0113526
(...)
C7NO2 MG=129,992904
C8H2O2 MG=130,0054792

-----D--B--E--f-i-l-t-e-r-----
14.06.2011 - 14:57:55,67
akzeptierte DBEs:
0 1 2 3 4 5 6 7 8

CH2N6O2	DBE: 4
C2H2N4O3	DBE: 4
C3H2N2O4	DBE: 4
C3H6N4O2	DBE: 3
C4H2O5	DBE: 4
C4H6N2O3	DBE: 3
C5H6O4	DBE: 3
C5H10N2O2	DBE: 2
C6H10O3	DBE: 2
C7H14O2	DBE: 1
C8H2O2	DBE: 8

11 von 73 Summenformeln

435,0 - 304,7 = **130,3**

Gefundene Verbindungen: 324
CH2N6O2 MG=130,0239232
CH2N6S MG=130,0061652
(...)
N7O2 MG=130,011348
N7S MG=129,99359

-----D--B--E--f-i-l-t-e-r-----
14.06.2011 - 14:46:10,01
akzeptierte DBEs:
0 1 2 3 4 5 6 7 8

CH2N6O2	DBE: 4
CH2N6S	DBE: 4
CH6N8	DBE: 3
C2H2N4OS	DBE: 4
C2H2N4O3	DBE: 4
C2H6N6O	DBE: 3
C3H2N2O2S	DBE: 4
C3H2N2O4	DBE: 4
C3H2N2S2	DBE: 4
C3H6N4O2	DBE: 3
C3H6N4S	DBE: 3
C3H10N6	DBE: 2
C4H2OS2	DBE: 4
C4H2O3S	DBE: 4
C4H2O5	DBE: 4
C4H6N2OS	DBE: 3
C4H6N2O3	DBE: 3
C4H10N4O	DBE: 2
C5H6O2S	DBE: 3
C5H6O4	DBE: 3
C5H6S2	DBE: 3
C5H10N2O2	DBE: 2
C5H10N2S	DBE: 2
C5H14N4	DBE: 1
C6H2N4	DBE: 8
C6H10OS	DBE: 2
C6H10O3	DBE: 2
C6H14N2O	DBE: 1
C7H2N2O	DBE: 8
C7H14O2	DBE: 1
C7H14S	DBE: 1
C7H18N2	DBE: 0
C8H2O2	DBE: 8
C8H2S	DBE: 8
C8H6N2	DBE: 7
C8H18O	DBE: 0
C9H6O	DBE: 7
C10H10	DBE: 6
H2N8O	DBE: 4
H2O2S3	DBE: 0
H2O4S2	DBE: 0
H2O6S	DBE: 0
H2O8	DBE: 0
H2S4	DBE: 0

44 von 324 Summenformeln

-MSn [F4]: [184 <- 283] <? 435 {II/II}

F5

+MS^n

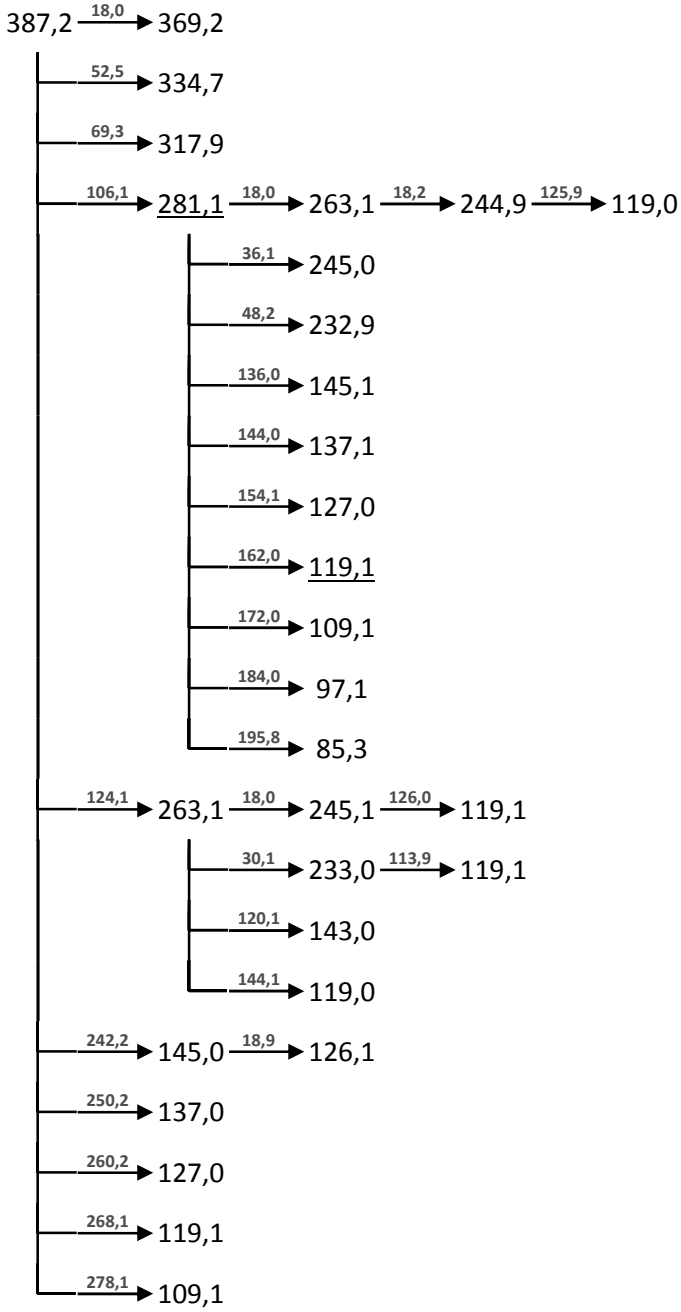
387,2
18,0
369,2
52,5
334,7
69,3
317,9
106,1
281,1
18,0
263,1
18,2
244,9
125,9
119,0
36,1
245,0
48,2
232,9
136,0
145,1
144,0
137,1
154,1
127,0
162,0
119,1
172,0
109,1
184,0
97,1
195,8
85,3
124,1
263,1
18,0
245,1
126,0
119,1
30,1
233,0
113,9
119,1
120,1
143,0
144,1
119,0
242,2
145,0
18,9
126,1
250,2
137,0
260,2
127,0
268,1
119,1
278,1
109,1

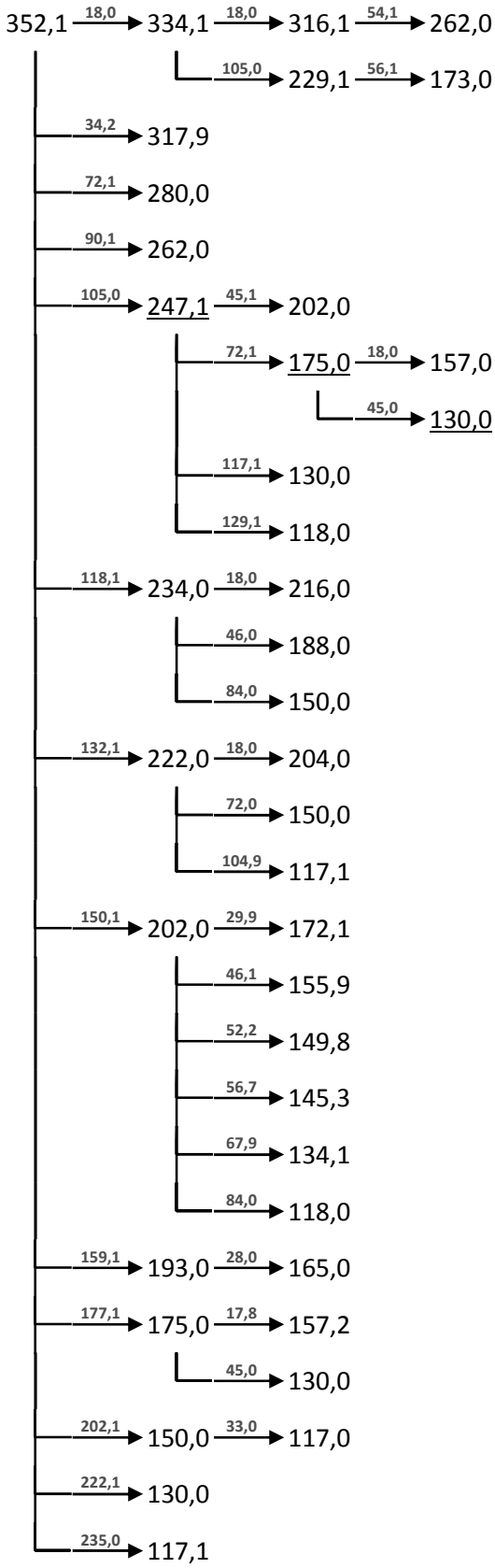
352,1
18,0
334,1
18,0
316,1
54,1
262,0
105,0
229,1
56,1
173,0
34,2
317,9
72,1
280,0
90,1
262,0
105,0
247,1
45,1
202,0
72,1
175,0
18,0
157,0
45,0
130,0
117,1
130,0
129,1
118,0
118,1
234,0
18,0
216,0
46,0
188,0
84,0
150,0
132,1
222,0
18,0
204,0
72,0
150,0
104,9
117,1
150,1
202,0
29,9
172,1
46,1
155,9
52,2
149,8
56,7
145,3
67,9
134,1
84,0
118,0
159,1
193,0
28,0
165,0
177,1
175,0
17,8
157,2
45,0
130,0
202,1
150,0
33,0
117,0
222,1
130,0
235,0
117,1

-MS^n

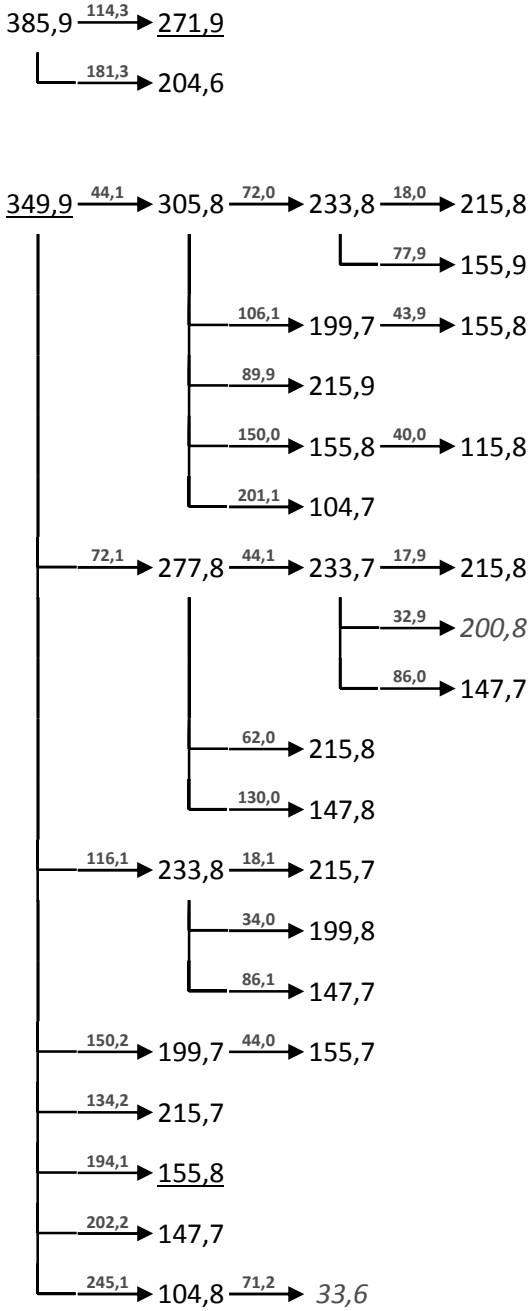

isotopic fingerprint:

peak area / % of monoisotopic	**+1**	**+2**	**+3**
measured (387,2 Th):	29,3	27,2	11,2
measured (-385,2 Th):	23,2	26,8	-
theoretical ($C_{17}H_{22}NO_5S^+$):	20,1	7,5	1,2
measured (-349,9 Th):	18,6	23,3	5,7
measured (352,1 Th):	22,9	(36,6)	8,3

Figure XIII-XXXII MS^n analysis of F5

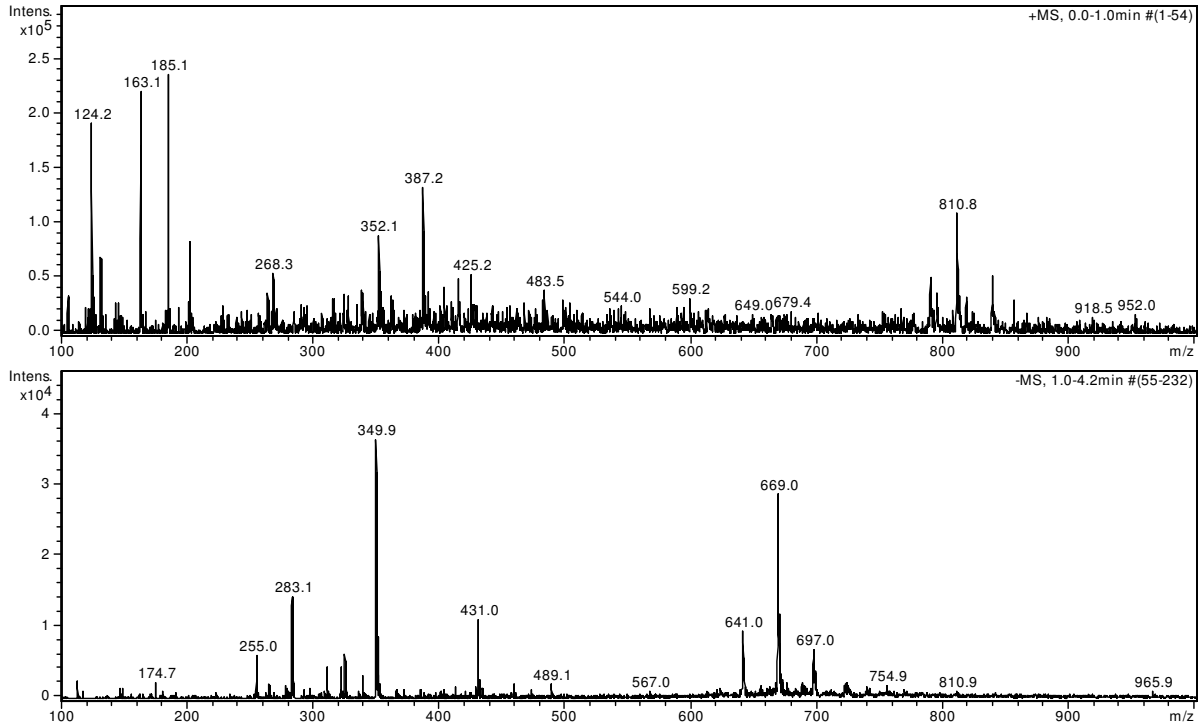

Figure XIII-XXXIII F5: 16,1 – 16,6 min, 0,5 ‰ FA, 67 % ACN in ddH_2O (diluted 1:2 with ACN); full scan MS^1

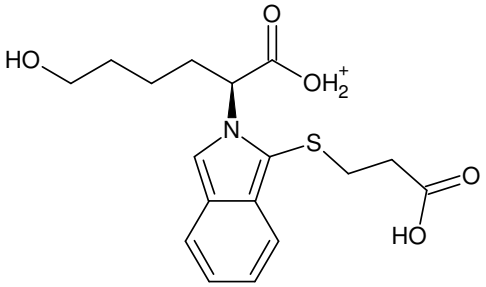

Monoisotopic Mass = 352.121319 Da

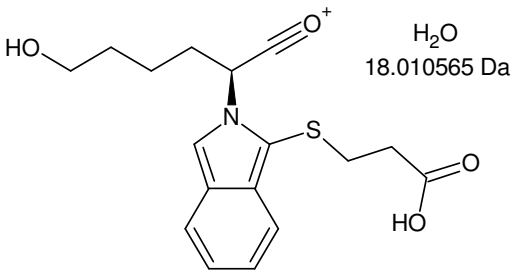

Monoisotopic Mass = 334.110755 Da

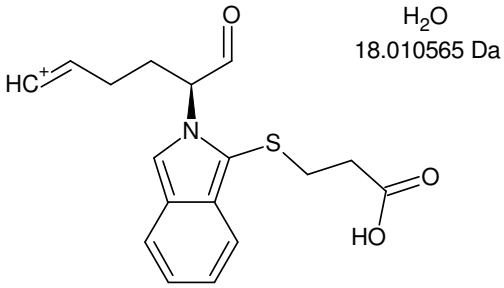

Monoisotopic Mass = 316.10019 Da

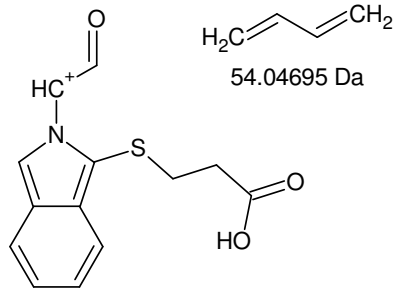

Monoisotopic Mass = 262.05324 Da

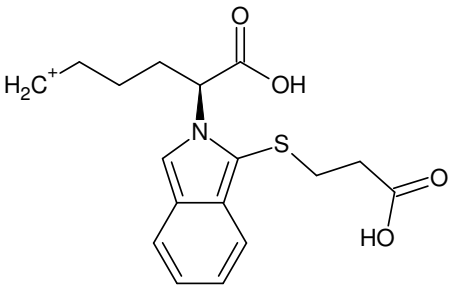

Monoisotopic Mass = 334.110755 Da

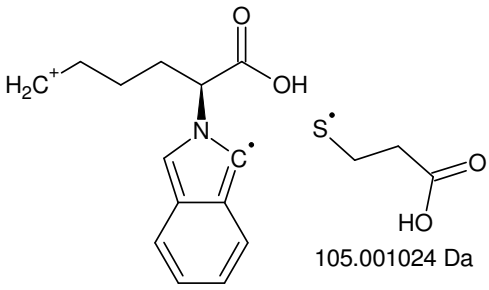

Monoisotopic Mass = 229.10973 Da

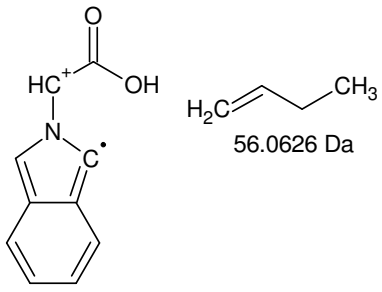

Monoisotopic Mass = 173.04713 Da

+MSn [F5]: 352 ->334 -> 316 -> 262 and [352 -> 334] -> 229 -> 173

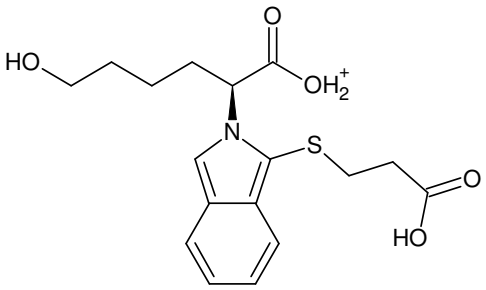

Monoisotopic Mass = 352.121319 Da

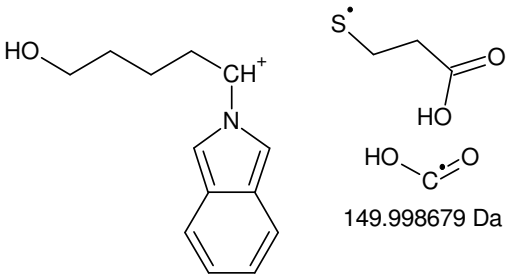

Monoisotopic Mass = 202.122641 Da

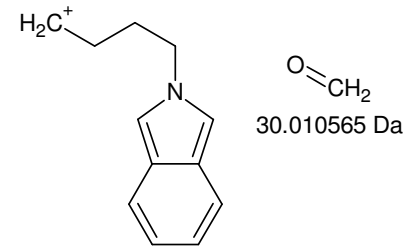

Monoisotopic Mass = 172.112076 Da

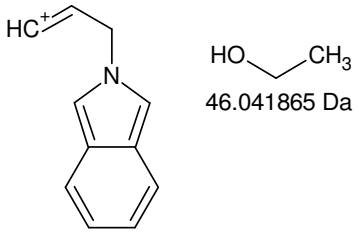

Monoisotopic Mass = 156.080776 Da

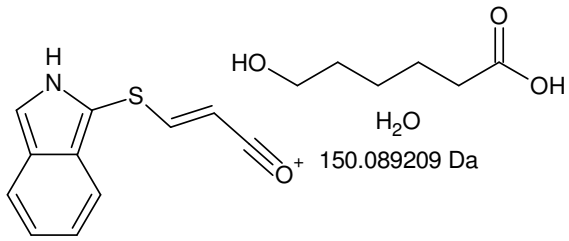

Monoisotopic Mass = 202.03211 Da

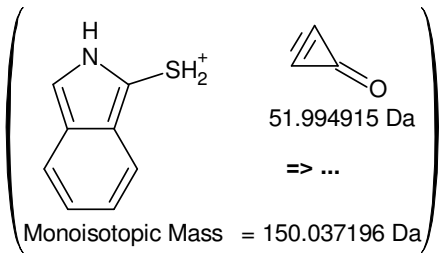

Monoisotopic Mass = 150.037196 Da

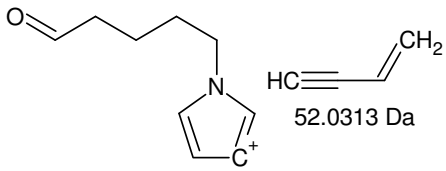

Monoisotopic Mass = 150.09134 Da

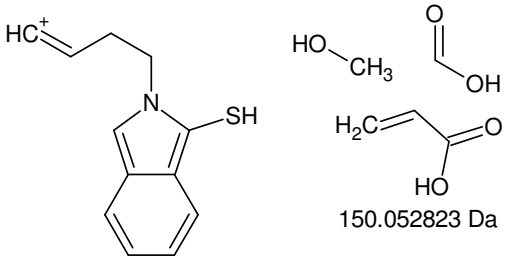

Monoisotopic Mass = 202.068496 Da

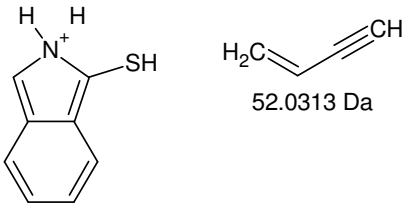

Monoisotopic Mass = 150.037196 Da

+MSn [F5]: 352 ->202 -> 172, 156, 150

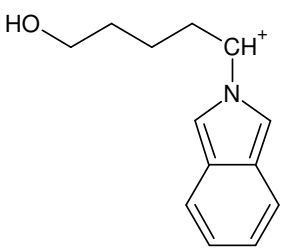

Monoisotopic Mass = 202.122641 Da

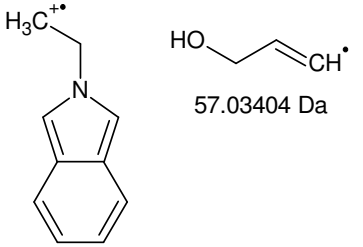

Monoisotopic Mass = 145.088601 Da

202 - 134 = **68**
Gefundene Verbindungen: 45
CH8OS MG=68,0295838
CH8O3 MG=68,0473418
(...)
H24N2O MG=68,1888534
H26N3 MG=68,2126616

-----D--B--E--f-i-l-t-e-r-----
17.05.2011 - 17:12:18,75
akzeptierte DBEs:
0
1
2
3
4
5
6

CN4 DBE: 4
C2N2O DBE: 4
C3H4N2 DBE: 3
C3O2 DBE: 4
C3S DBE: 4
C4H4O DBE: 3
C5H8 DBE: 2

7 von 45 Summenformeln

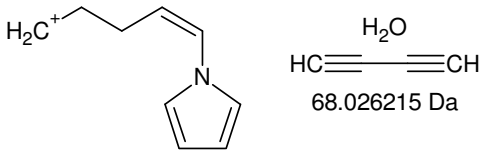

Monoisotopic Mass = 134.096426 Da

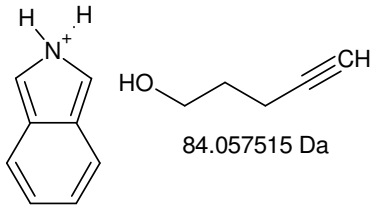

Monoisotopic Mass = 118.065126 Da

+MSn [F5]: 352 ->202 -> 145, 134, 118

F6

+MS^n

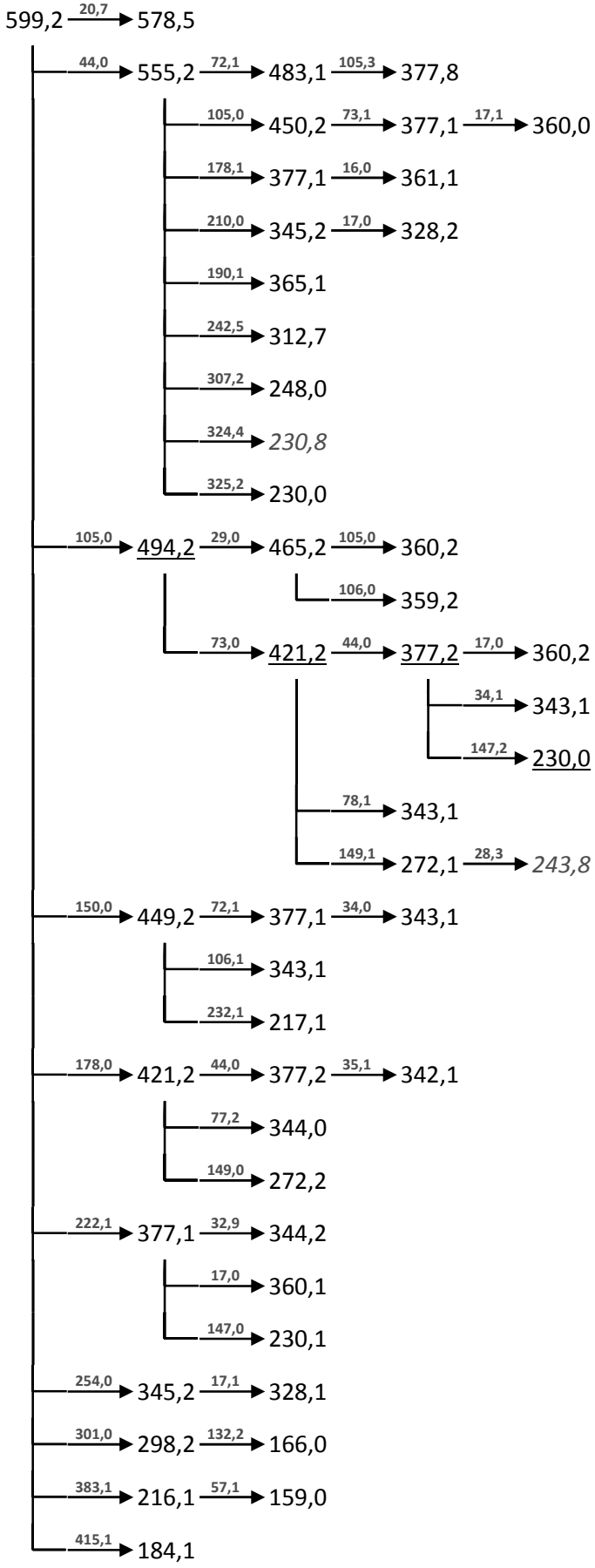
599,2 20,7 578,5
44,0 555,2 72,1 483,1 105,3 377,8
105,0 450,2 73,1 377,1 17,1 360,0
178,1 377,1 16,0 361,1
210,0 345,2 17,0 328,2
190,1 365,1
242,5 312,7
307,2 248,0
324,4 230,8
325,2 230,0
105,0 494,2 29,0 465,2 105,0 360,2
106,0 359,2
73,0 421,2 44,0 377,2 17,0 360,2
34,1 343,1
147,2 230,0
78,1 343,1
149,1 272,1 28,3 243,8
150,0 449,2 72,1 377,1 34,0 343,1
106,1 343,1
232,1 217,1
178,0 421,2 44,0 377,2 35,1 342,1
77,2 344,0
149,0 272,2
222,1 377,1 32,9 344,2
17,0 360,1
147,0 230,1
254,0 345,2 17,1 328,1
301,0 298,2 132,2 166,0
383,1 216,1 57,1 159,0
415,1 184,1

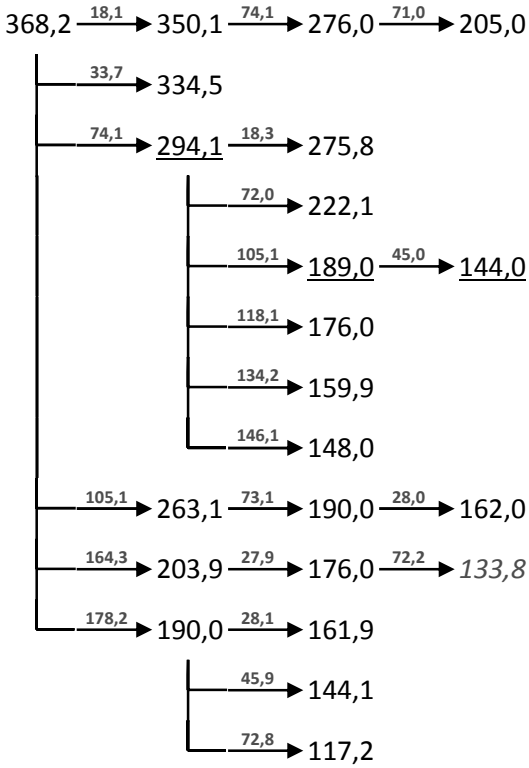
368,2
18,1
350,1
74,1
276,0
71,0
205,0
33,7
334,5
74,1
294,1
18,3
275,8
72,0
222,1
105,1
189,0
45,0
144,0
118,1
176,0
134,2
159,9
146,1
148,0
105,1
263,1
73,1
190,0
28,0
162,0
164,3
203,9
27,9
176,0
72,2
133,8
178,2
190,0
28,1
161,9
45,9
144,1
72,8
117,2

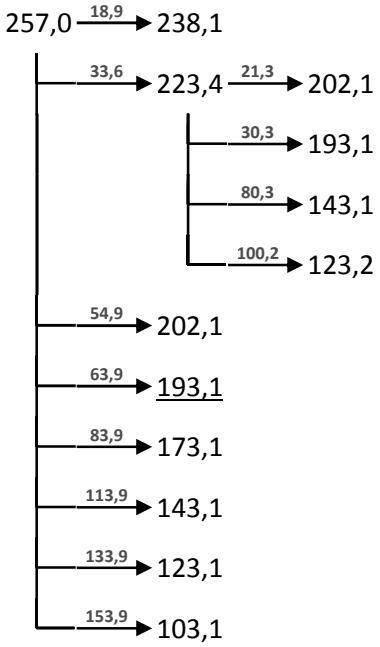
257,0
18,9
238,1
33,6
223,4
21,3
202,1
30,3
193,1
80,3
143,1
100,2
123,2
54,9
202,1
63,9
193,1
83,9
173,1
113,9
143,1
133,9
123,1
153,9
103,1

-MS^n

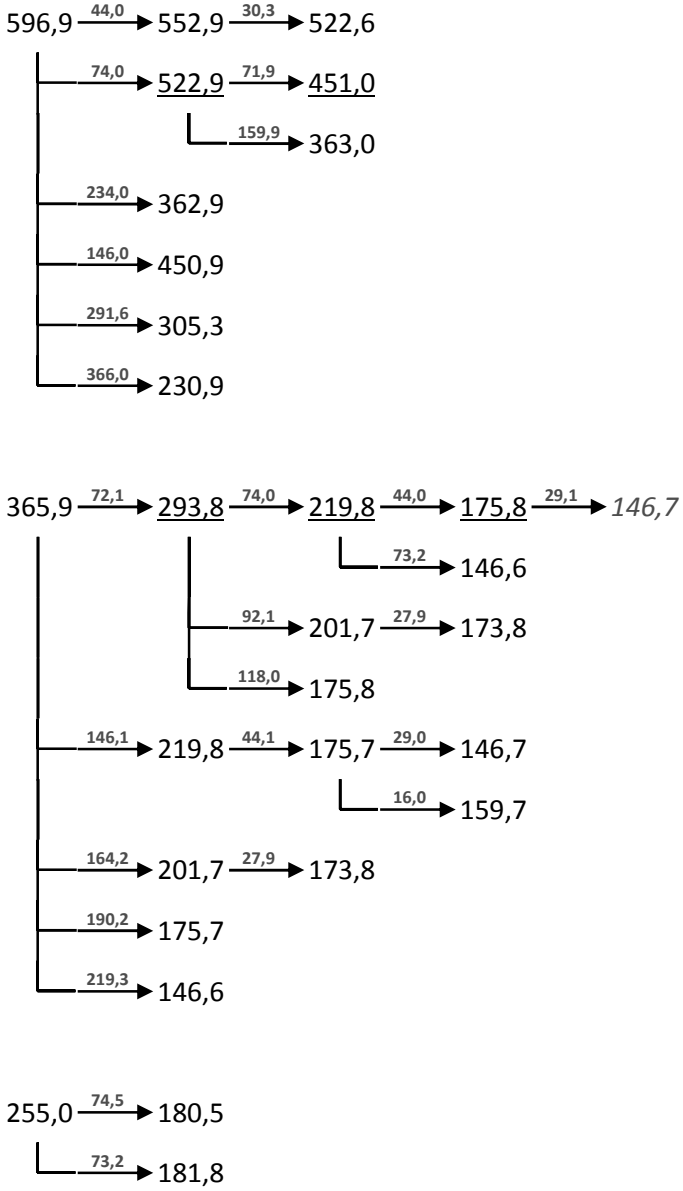

isotopic fingerprint:

peak area / % of monoisotopic	**+1**	**+2**	**+3**
theoretical ($C_{27}H_{27}N_4O_8S_2^+$):	33,0	16,0	4,0
measured (599,3 Th):	37,4	17,0	6,7
measured (-596,9 Th):	52,3	21,0	-
theoretical ($C_{17}H_{22}NO_6S^+$):	20,1	7,7	1,2
measured (368,1 Th):	21,0	-	-
measured (-365,9 Th):	19,8	8,7	2,2
measured (256,9 Th):	27,1	-	-
measured (-255,0 Th):	16,0	5,0	4,2

Figure XIII-XXXIV MS^n analysis of F6

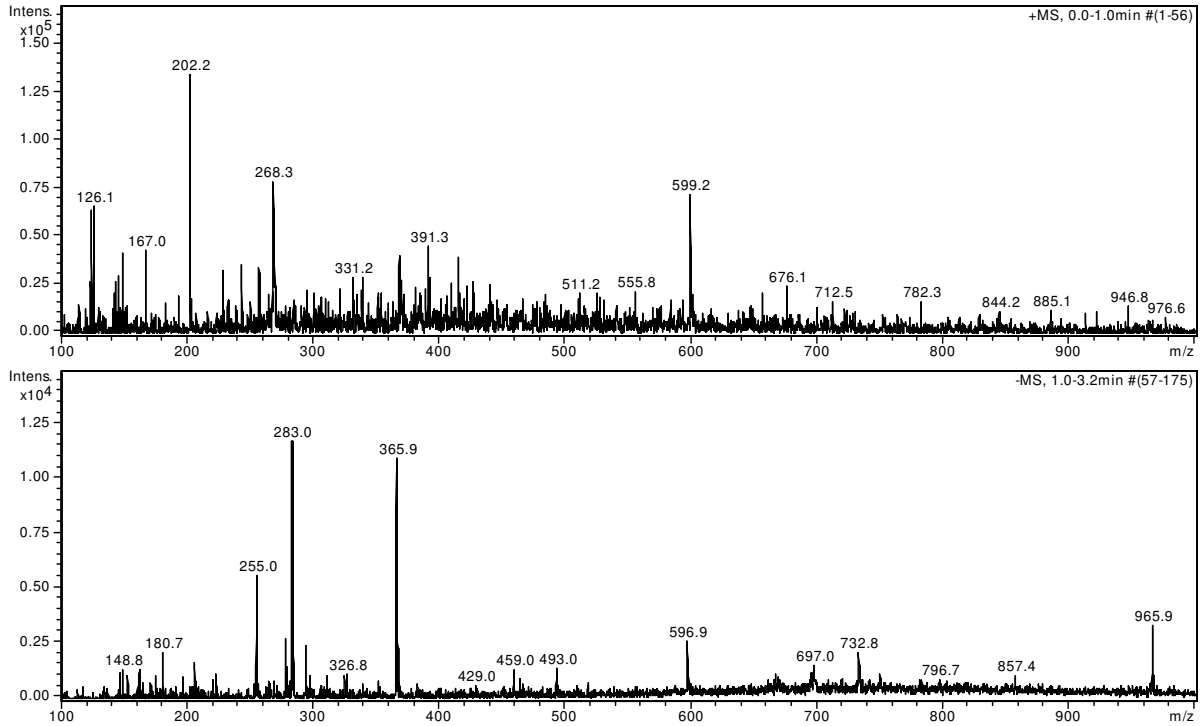

Figure XIII-XXXV F6: 20,1 – 20,4 min, 1 ‰ FA, 36 % ACN in ddH_2O; full scan MS^1

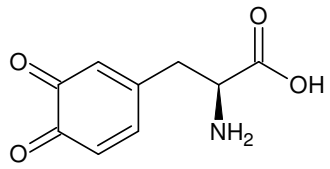

o-Dopachinon
Monoisotopic Mass = 195.053158 Da

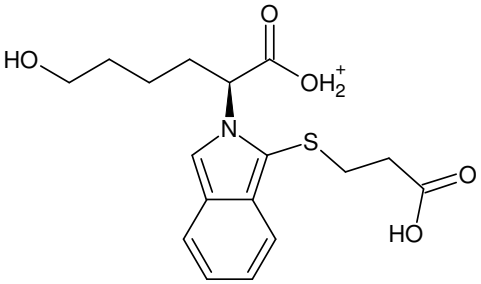

Monoisotopic Mass = 352.121319 Da

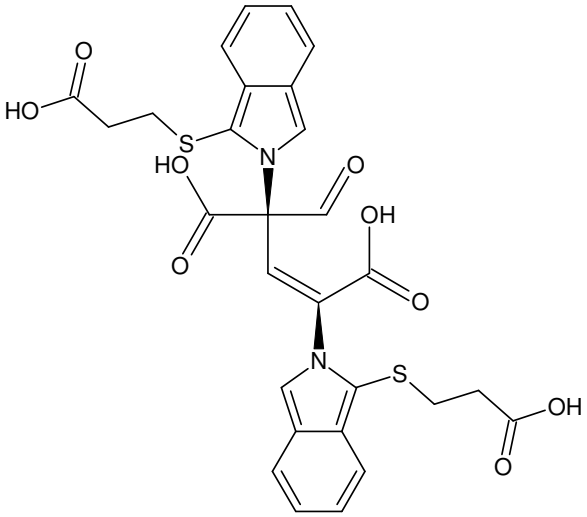

Monoisotopic Mass = 596.09232 Da
AKP Ser-Ser ist um 2 Da zu leicht.

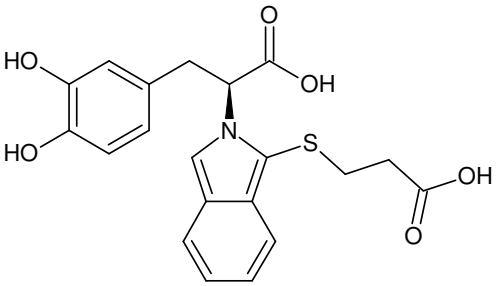

Monoisotopic Mass = 401.093307 Da

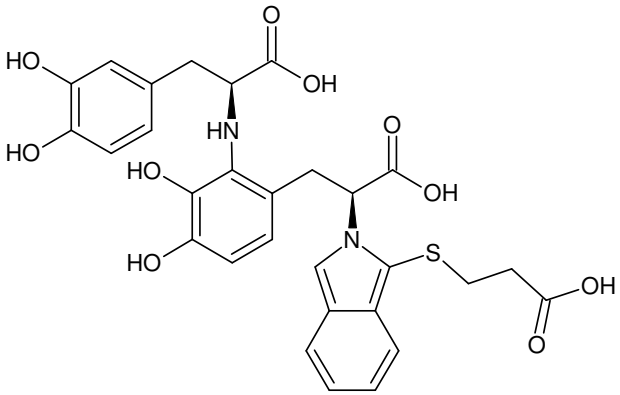

Monoisotopic Mass = 596.146465 Da

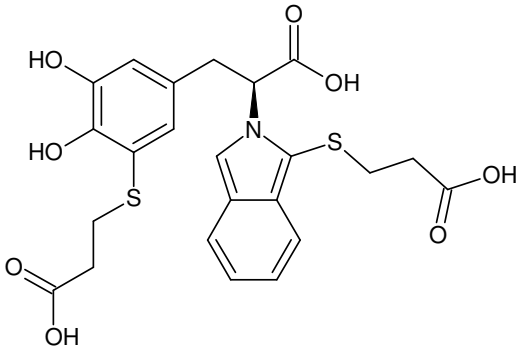

Monoisotopic Mass = 505.086507 Da

MS^n [F6]: 598 Da

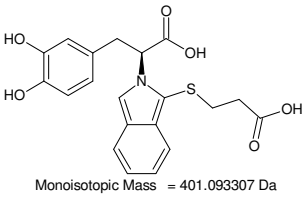

Monoisotopic Mass = 401.093307 Da

ohne S, genau ein N:
Gefundene Verbindungen: 76
CH11NO10 MG=197,0382946
CH27NO9 MG=197,1685732
(...)
H71NO7 MG=197,5230256
H86NO6 MG=196,6454796

-----D--B--E--f-i-l-t-e-r-----
14.06.2011 - 16:02:08,76
akzeptierte DBEs:
1 2 3 4 5 6 7 8

C3H3NO9	DBE: 3
C4H7NO8	DBE: 2
C5H11NO7	DBE: 1
C7H3NO6	DBE: 7
C8H7NO5	DBE: 6
C9H11NO4	DBE: 5
C10H15NO3	DBE: 4
C11H19NO2	DBE: 3
C12H23NO	DBE: 2
C13H27N	DBE: 1
C14H15N	DBE: 8

11 von 76 Summenformeln

mit $C_3H_5O_2S$:
Gefundene Verbindungen: 133
C3H5N2O2S3 MG=196,951317
C3H5N2O4S2 MG=196,969075
(...)
C9H25O2S MG=197,157517
C10H13O2S MG=197,0636218

-----D--B--E--f-i-l-t-e-r-----
14.06.2011 - 16:05:50,79
akzeptierte DBEs:
1 2 3 4 5 6 7 8

C3H7N3O3S2	DBE: 2
C3H7N3O5S	DBE: 2
C3H11N5O3S	DBE: 1
C4H7NO2S3	DBE: 2
C4H7NO4S2	DBE: 2
C4H7NO6S	DBE: 2
C4H11N3O2S2	DBE: 1
C4H11N3O4S	DBE: 1
C5H11NO3S2	DBE: 1
C5H11NO5S	DBE: 1
C7H7N3O2S	DBE: 6
C8H7NO3S	DBE: 6
C9H11NO2S	DBE: 5

13 von 133 Summenformeln

598,2 - 401,1 = **197,1**
Gefundene Verbindungen: 1274
CHN4O2S3 MG=196,9261666
CHN4O4S2 MG=196,9439246
(...)
H96N6O MG=196,7645206
H98N7 MG=196,7883288

-----D--B--E--f-i-l-t-e-r-----
14.06.2011 - 15:45:03,59
akzeptierte DBEs:
1 2 3 4 5 6 7 8

CH3N5OS3	DBE: 3	C5H7N7O2	DBE: 6
CH3N5O3S2	DBE: 3	C5H7N7S	DBE: 6
CH3N5O5S	DBE: 3	C5H11NOS3	DBE: 1
CH3N5O7	DBE: 3	C5H11NO3S2	DBE: 1
CH3N13	DBE: 7	C5H11NO5S	DBE: 1
CH7N7OS2	DBE: 2	C5H11NO7	DBE: 1
CH7N7O3S	DBE: 2	C5H11N9	DBE: 5
CH7N7O5	DBE: 2	C6H3N3OS2	DBE: 7
CH11N9OS	DBE: 1	C6H3N3O3S	DBE: 7
CH11N9O3	DBE: 1	C6H3N3O5	DBE: 7
C2H3N3O2S3	DBE: 3	C6H7N5OS	DBE: 6
C2H3N3O4S2	DBE: 3	C6H7N5O3	DBE: 6
C2H3N3O6S	DBE: 3	C6H11N7O	DBE: 5
C2H3N3O8	DBE: 3	C7H3NO2S2	DBE: 7
C2H3N3S4	DBE: 3	C7H3NO4S	DBE: 7
C2H3N11O	DBE: 7	C7H3NO6	DBE: 7
C2H7N5O2S2	DBE: 2	C7H3NS3	DBE: 7
C2H7N5O4S	DBE: 2	C7H7N3O2S	DBE: 6
C2H7N5O6	DBE: 2	C7H7N3O4	DBE: 6
C2H7N5S3	DBE: 2	C7H7N3S2	DBE: 6
C2H11N7O2S	DBE: 1	C7H11N5O2	DBE: 5
C2H11N7O4	DBE: 1	C7H11N5S	DBE: 5
C2H11N7S2	DBE: 1	C7H15N7	DBE: 4
C3H3NOS4	DBE: 3	C8H7NOS2	DBE: 6
C3H3NO3S3	DBE: 3	C8H7NO3S	DBE: 6
C3H3NO5S2	DBE: 3	C8H7NO5	DBE: 6
C3H3NO7S	DBE: 3	C8H11N3OS	DBE: 5
C3H3NO9	DBE: 3	C8H11N3O3	DBE: 5
C3H3N9O2	DBE: 7	C8H15N5O	DBE: 4
C3H3N9S	DBE: 7	C9H11NO2S	DBE: 5
C3H7N3OS3	DBE: 2	C9H11NO4	DBE: 5
C3H7N3O3S2	DBE: 2	C9H11NS2	DBE: 5
C3H7N3O5S	DBE: 2	C9H15N3O2	DBE: 4
C3H7N3O7	DBE: 2	C9H15N3S	DBE: 4
C3H7N11	DBE: 6	C9H19N5	DBE: 3
C3H11N5OS2	DBE: 1	C10H15NOS	DBE: 4
C3H11N5O3S	DBE: 1	C10H15NO3	DBE: 4
C3H11N5O5	DBE: 1	C10H19N3O	DBE: 3
C4H3N7OS	DBE: 7	C11H19NO2	DBE: 3
C4H3N7O3	DBE: 7	C11H19NS	DBE: 3
C4H7NO2S3	DBE: 2	C11H23N3	DBE: 2
C4H7NO4S2	DBE: 2	C12H23NO	DBE: 2
C4H7NO6S	DBE: 2	C13H27N	DBE: 1
C4H7NO8	DBE: 2	C14H15N	DBE: 8
C4H7NS4	DBE: 2	H3N7O2S2	DBE: 3
C4H7N9O	DBE: 6	H3N7O4S	DBE: 3
C4H11N3O2S2	DBE: 1	H3N7O6	DBE: 3
C4H11N3O4S	DBE: 1	H3N7S3	DBE: 3
C4H11N3O6	DBE: 1	H7N9O2S	DBE: 2
C4H11N3S3	DBE: 1	H7N9O4	DBE: 2
C5H3N5O2S	DBE: 7	H7N9S2	DBE: 2
C5H3N5O4	DBE: 7	H11N11O2	DBE: 1
C5H3N5S2	DBE: 7	H11N11S	DBE: 1

106 von 1274 Summenformeln

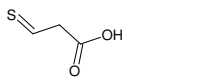

Molecular Formula = $C_3H_4O_2S$
Monoisotopic Mass = 103.993199 Da

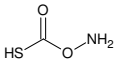

92.988448 Da

CH_3NO_2S
92.988448 Da

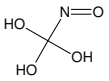

CH_3NO_4
93.006208 Da

CH_3NS_2
92.970689 Da

$C_4H_3N_3$
93.032697 Da

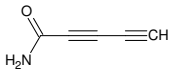

C_5H_3NO
93.021464 Da

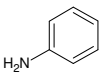

C_6H_7N
93.057849 Da

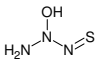

H_3N_3OS
92.999682 Da

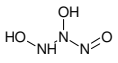

$H_3N_3O_3$
93.017441 Da

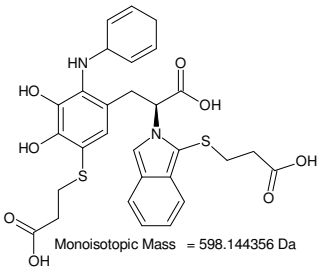

Monoisotopic Mass = 598.144356 Da

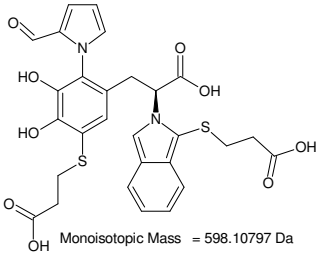

Monoisotopic Mass = 598.10797 Da

197,1 - 104,0 = **93,1**
Gefundene Verbindungen: 113
CHOS2 MG=92,9468836
CHO3S MG=92,9646416
(...)
H47NO2 MG=93,3606602
H47NS MG=93,3429022

-----D--B--E--f-i-l-t-e-r-----
14.06.2011 - 16:17:13,32
akzeptierte DBEs:
1 2 3 4 5 6 7 8

CH3NO2S	DBE: 1
CH3NO4	DBE: 1
CH3NS2	DBE: 1
C4H3N3	DBE: 5
C5H3NO	DBE: 5
C6H7N	DBE: 4
H3N3OS	DBE: 1
H3N3O3	DBE: 1

8 von 113 Summenformeln

MS^n [F6]: 598 Da – o-Dopachinon

Arg - Gly: Argininanteil leicht reduziert (nicht sign.), Glycinanteil bei Behandlung mit BoT2 sign. angestiegen

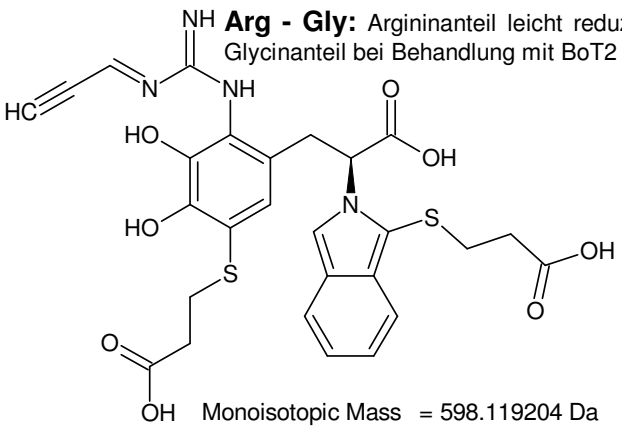

Monoisotopic Mass = 598.119204 Da

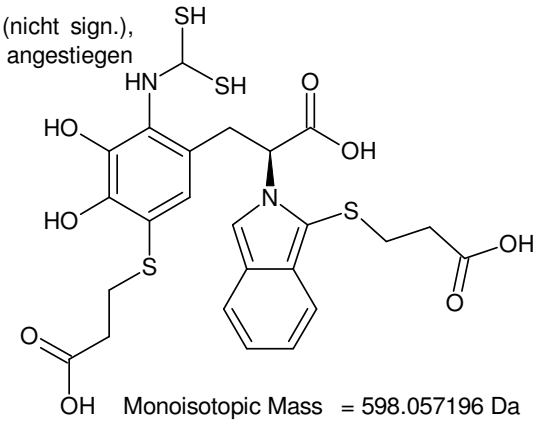

Monoisotopic Mass = 598.057196 Da

599,2 - 578,5 = **20,7**
Gefundene Verbindungen: 3
H_5O MG=21,034038
CH_9 MG=21,0704214
H_7N MG=21,0578462

ungewöhnlichstes Fragment => größtes Diskriminierungs-potential

H_2 H_2O $H^{\bullet}$
H_5O
21.03404 Da

$CH_3^{\bullet}$ H_2 H_2 H_2
CH_9
21.070425 Da

NH_3 H_2 H_2
H_7N
21.057849 Da

20,0 Da
Gefundene Verbindungen: 3
H_4O MG=20,0262134
CH_8 MG=20,0625968
H_6N MG=20,0500216

H_2O H_2
H_4O
20.026215 Da

CH_4 H_2 H_2
CH_8
20.0626 Da

$NH_2^{\bullet}$ H_2 H_2
H_6N
20.050024 Da

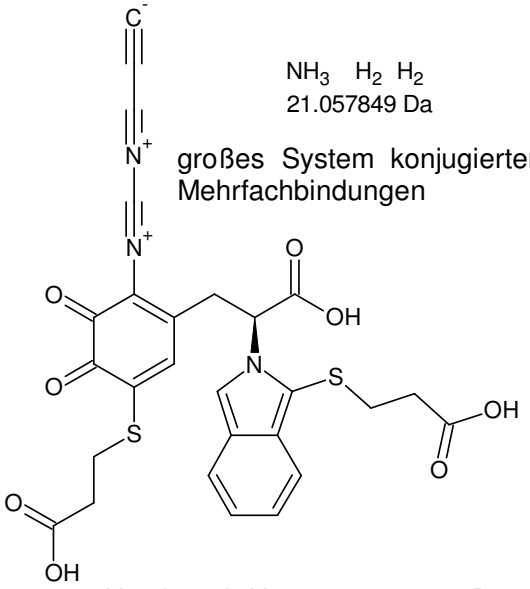

NH_3 H_2 H_2
21.057849 Da

großes System konjugierter Mehrfachbindungen

Monoisotopic Mass = 578.068631 Da

+MSn [F6]: 598 Da and 599 -> 578

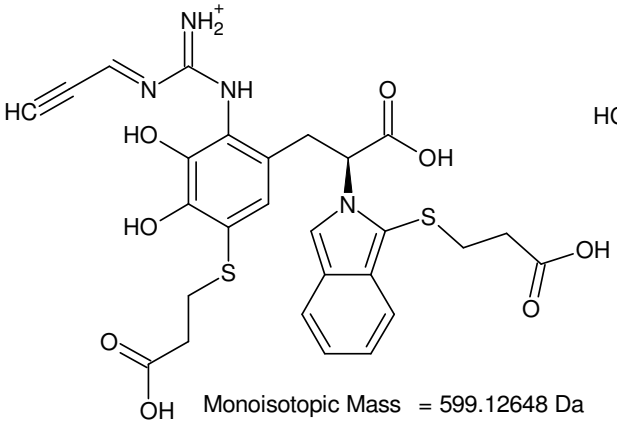

Monoisotopic Mass = 599.12648 Da

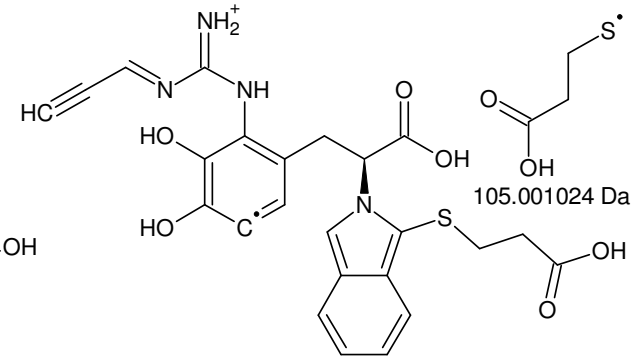

105.001024 Da

Monoisotopic Mass = 494.125456 Da

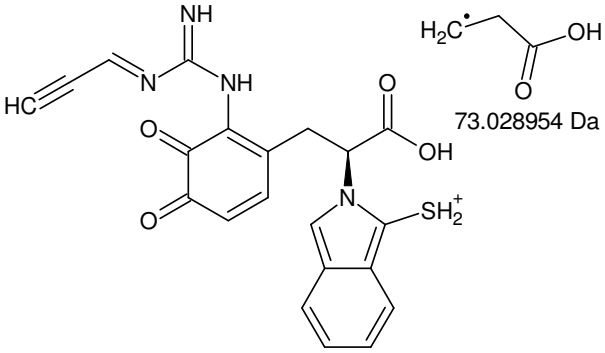

73.028954 Da

Monoisotopic Mass = 421.096501 Da

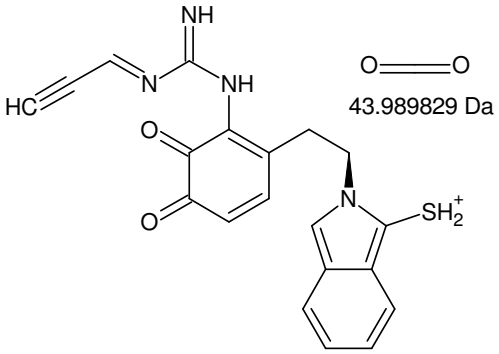

43.989829 Da

Monoisotopic Mass = 377.106672 Da

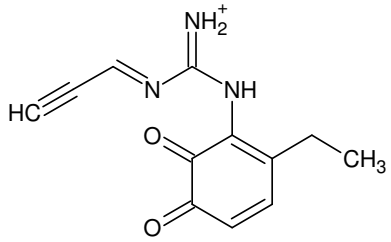

Monoisotopic Mass = 230.092403 Da

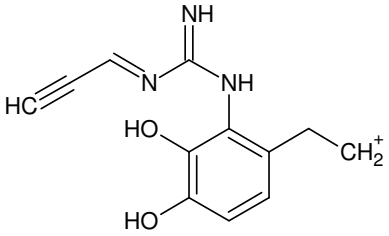

Monoisotopic Mass = 230.092403 Da

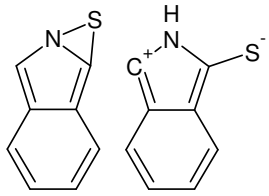

147.01427 Da

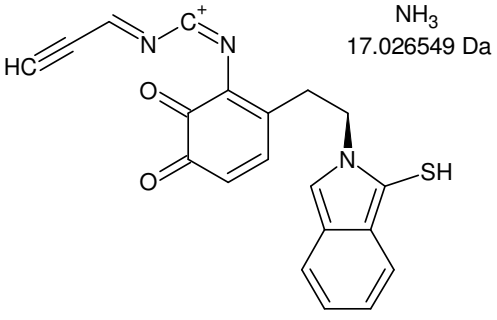

17.026549 Da

Monoisotopic Mass = 360.080123 Da

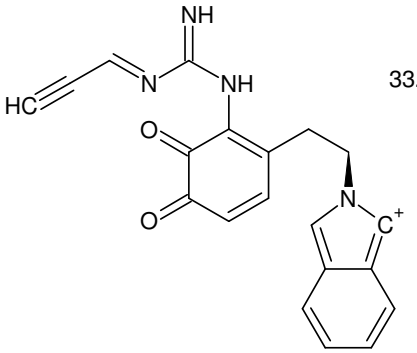

33.98772 Da

Monoisotopic Mass = 343.118952 Da

+MSn [F6]: 599 -> 494 -> 421 -> 377 -> 230, 360, 343

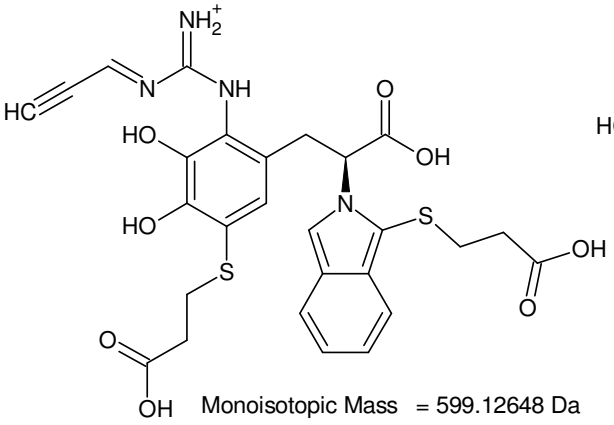

Monoisotopic Mass = 599.12648 Da

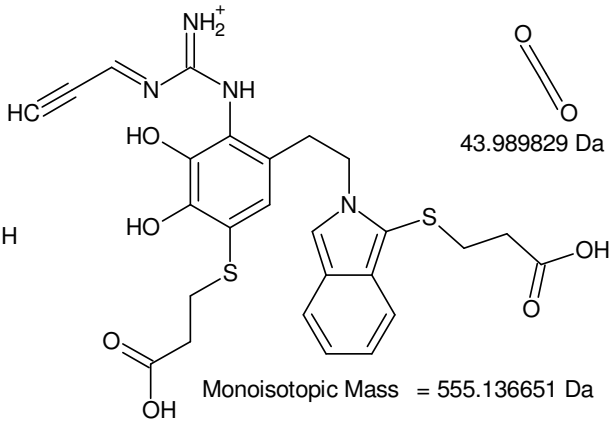

43.989829 Da

Monoisotopic Mass = 555.136651 Da

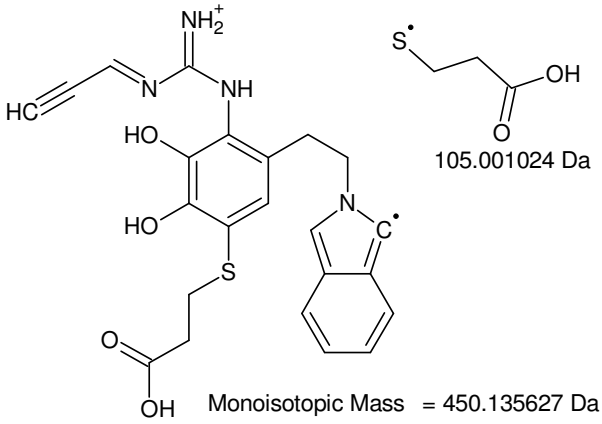

105.001024 Da

Monoisotopic Mass = 450.135627 Da

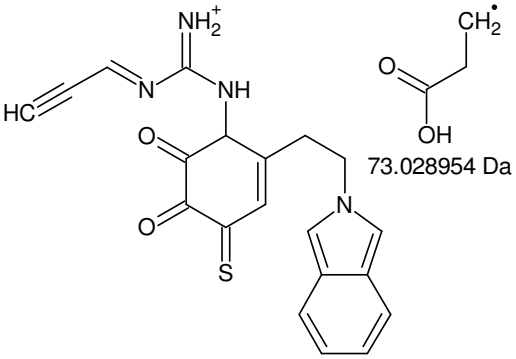

73.028954 Da

Monoisotopic Mass = 377.106672 Da

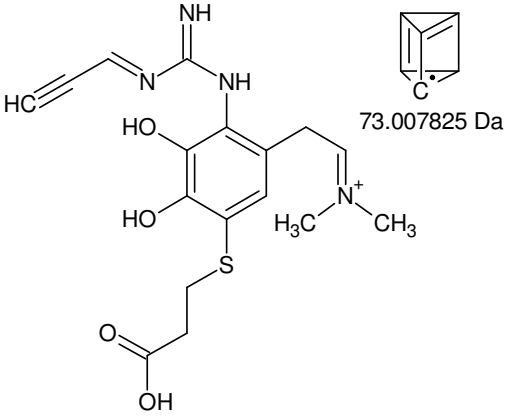

73.007825 Da

Monoisotopic Mass = 377.127802 Da

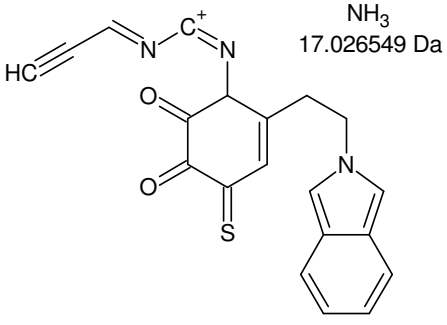

NH_3
17.026549 Da

Monoisotopic Mass = 360.080123 Da

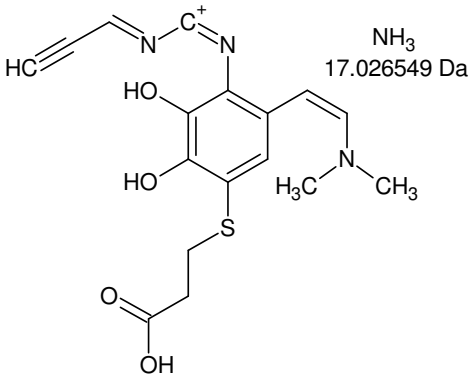

NH_3
17.026549 Da

Monoisotopic Mass = 360.101252 Da

+MSn [F6]: 599 -> 555 -> 450 -> 377 -> 360

597 - 522 = **75**

Gefundene Verbindungen: 59

CHNOS	MG=74,9778856
CHNO3	MG=74,9956436
(...)	
H29NS	MG=75,2020594
H33N3	MG=75,2674338

-----D--B--E--f-i-l-t-e-r-----
16.06.2011 - 15:32:00,69
akzeptierte DBEs:
0 1 2 3 4 5 6 7 8

CHNOS	DBE: 2
CHNO3	DBE: 2
CH5N3O	DBE: 1
C2H5NO2	DBE: 1
C2H5NS	DBE: 1
C2H9N3	DBE: 0
C3H9NO	DBE: 0
C5HN	DBE: 6
HN3O2	DBE: 2
HN3S	DBE: 2
H5N5	DBE: 1

11 von 59 Summenformeln

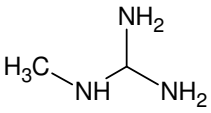

$C_2H_9N_3$
75.079647 Da

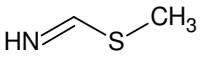

C_2H_5NS
75.014269 Da

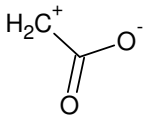

NH_3

$C_2H_5NO_2$
75.032028 Da

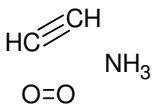

NH_3
O=O

$C_2H_5NO_2$
75.032028 Da

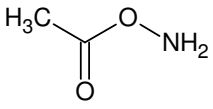

75.032028 Da

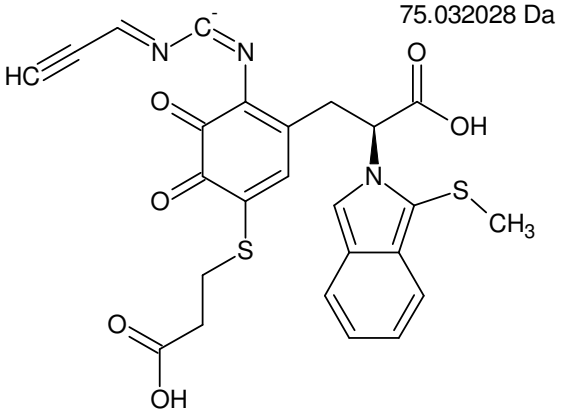

Monoisotopic Mass = 522.079899 Da

-MSn [F6]: 597 -> 522

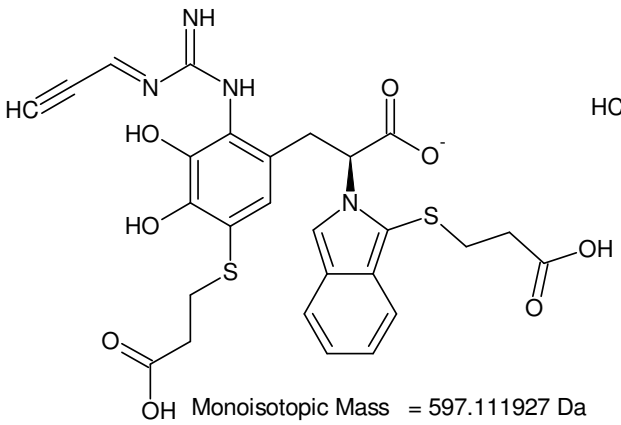

Monoisotopic Mass = 597.111927 Da

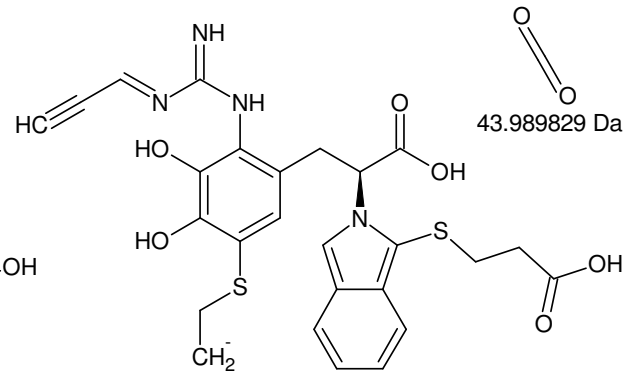

43.989829 Da

Monoisotopic Mass = 553.122098 Da

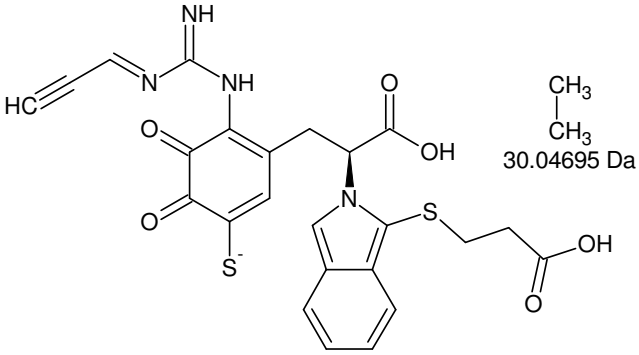

30.04695 Da

Monoisotopic Mass = 523.075148 Da

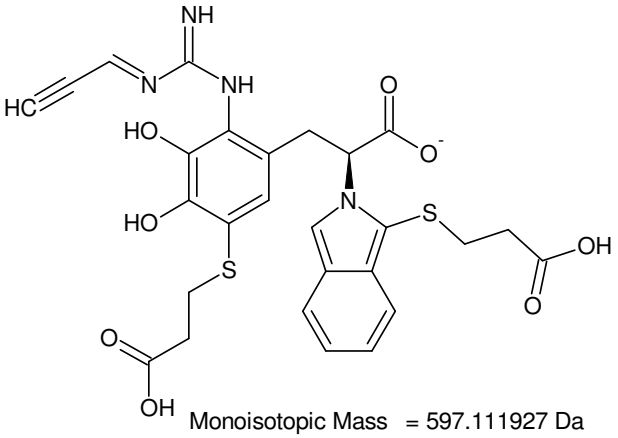

Monoisotopic Mass = 597.111927 Da

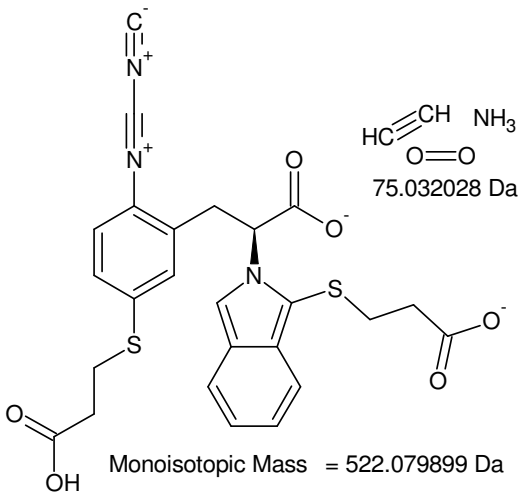

75.032028 Da

Monoisotopic Mass = 522.079899 Da

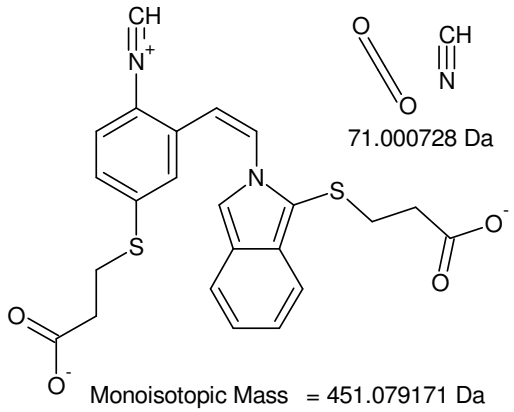

71.000728 Da

Monoisotopic Mass = 451.079171 Da

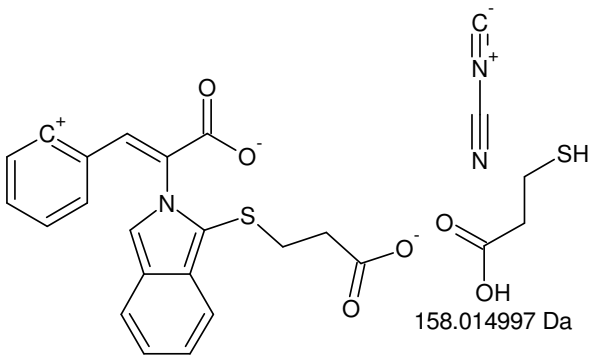

158.014997 Da

Monoisotopic Mass = 364.064902 Da

-MSn [F6]: 597 -> 553 -> 523 und 597 -> 522 -> 451, 364

Molekülpeaks und Fragmente stimmen mit BoT#8 (Probe V) überein.

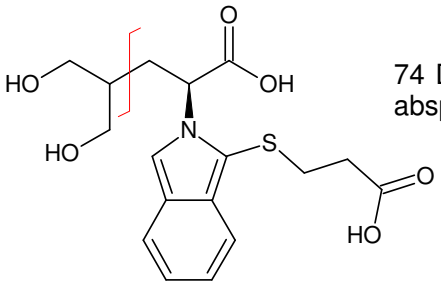

74 Da nach 72 Da abspaltbar.

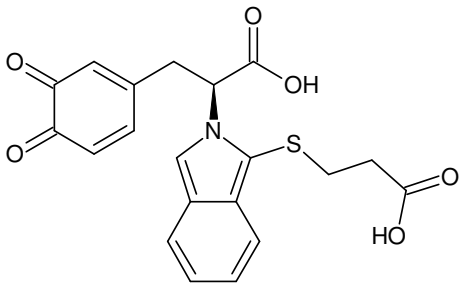

Monoisotopic Mass = 399.077657 Da

BoT#8

Monoisotopic Mass = 367.108957 Da

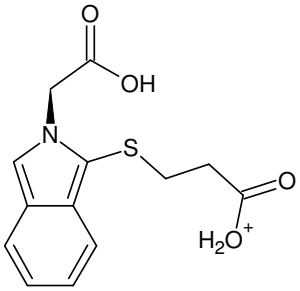

Monoisotopic Mass = 280.063804 Da

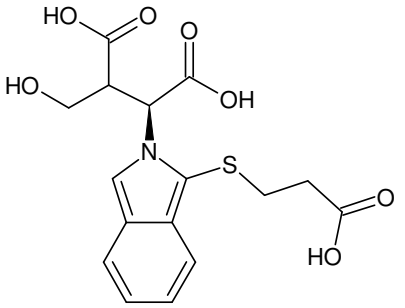

Monoisotopic Mass = 367.072572 Da

74 Da nach 72 Da nicht mehr abspaltbar.

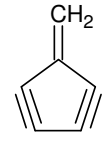

74.01565 Da

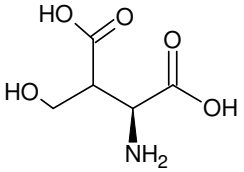

Monoisotopic Mass = 163.048072 Da

MS^n [F6]: 367 Da

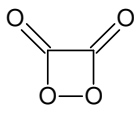

C_2O_4
87.979658 Da

368,2 - 280,1 = **88,1**
Gefundene Verbindungen: 99
CH2N3O2 MG=88,0147012
CH2N3S MG=87,9969432
(...)
N4O2 MG=88,002126
N4S MG=87,984368

Valin, dihydroxiliert und oxidiert

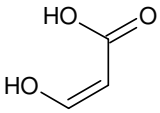

$C_3H_4O_3$
88.016044 Da

dihydroxyliertes **Leucin**

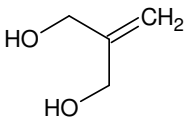

$C_4H_8O_2$
88.052429 Da

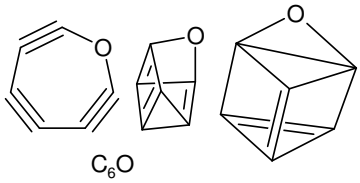

C_6O
87.994915 Da

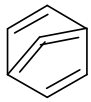

C_7H_4
88.0313 Da

-----D--B--E--f-i-l-t-e-r-----
17.06.2011 - 15:21:33,29
akzeptierte DBEs:
1 2 3 4 5 6 7 8

CH4N4O DBE: 2
CN2OS DBE: 3
CN2O3 DBE: 3
C2H4N2O2 DBE: 2
C2H4N2S DBE: 2
C2H8N4 DBE: 1
C2O2S DBE: 3
C2O4 DBE: 3
C2S2 DBE: 3
C3H4OS DBE: 2
C3H4O3 DBE: 2
C3H8N2O DBE: 1
C4H8O2 DBE: 1
C4H8S DBE: 1
C5N2 DBE: 7
C6O DBE: 7
C7H4 DBE: 6
H4N6 DBE: 2
N4O2 DBE: 3
N4S DBE: 3

20 von 99 Summenformeln

bisher (Probe V und BoT#8, siehe V) nicht erfasste Fragmente:

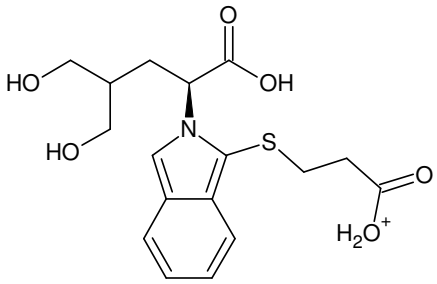

Monoisotopic Mass = 368.116234 Da

368,2 - 334,5 = **33,7**
Gefundene Verbindungen: 8
CH_6O MG=34,0418626
CH_8N MG=34,0656708
C_2H_{10} MG=34,078246
H_2O_2 MG=34,0054792
H_2S MG=33,9877212
H_4NO MG=34,0292874
H_6N_2 MG=34,0530956
$H_{18}O$ MG=34,1357578
=> 33,7 === 34,0(1)

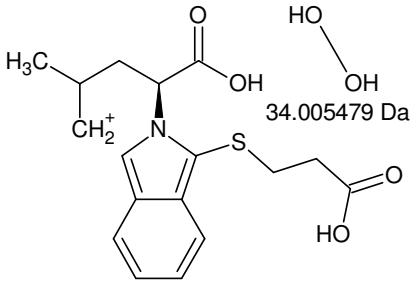

34.005479 Da

Monoisotopic Mass = 334.110755 Da

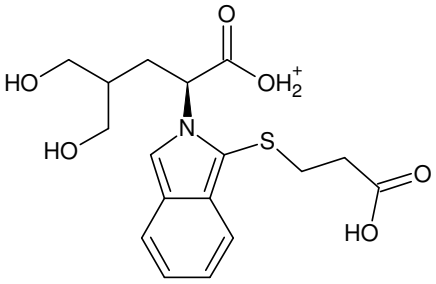

Monoisotopic Mass = 368.116234 Da

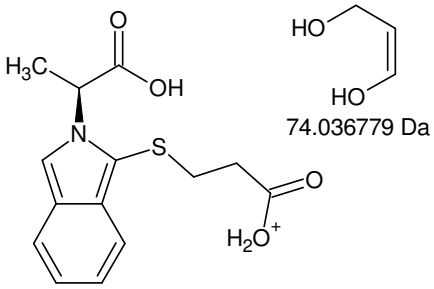

74.036779 Da

Monoisotopic Mass = 294.079454 Da

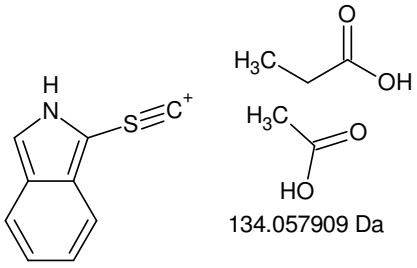

134.057909 Da

Monoisotopic Mass = 160.021546 Da

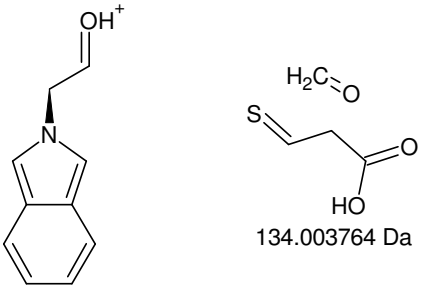

134.003764 Da

Monoisotopic Mass = 160.07569 Da

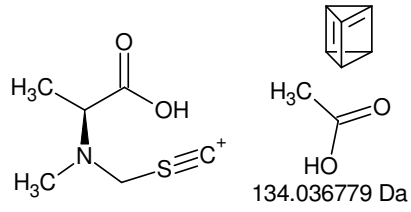

134.036779 Da

Monoisotopic Mass = 160.042675 Da

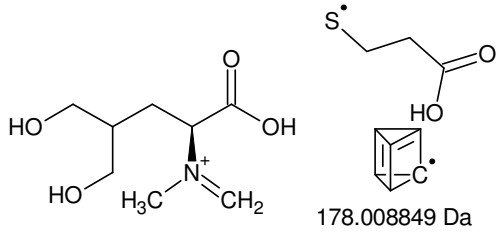

178.008849 Da

Monoisotopic Mass = 190.107384 Da

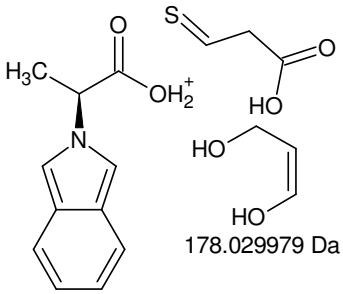

178.029979 Da

Monoisotopic Mass = 190.086255 Da

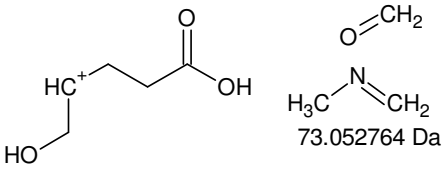

73.052764 Da

Monoisotopic Mass = 117.054621 Da

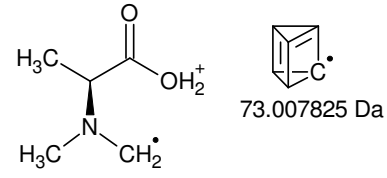

73.007825 Da

Monoisotopic Mass = 117.07843 Da

+MSn [F6]: 368 -> 334 as well as 368 -> 294 -> 160 and [368 -> 190] -> 117

F7

+MS^n

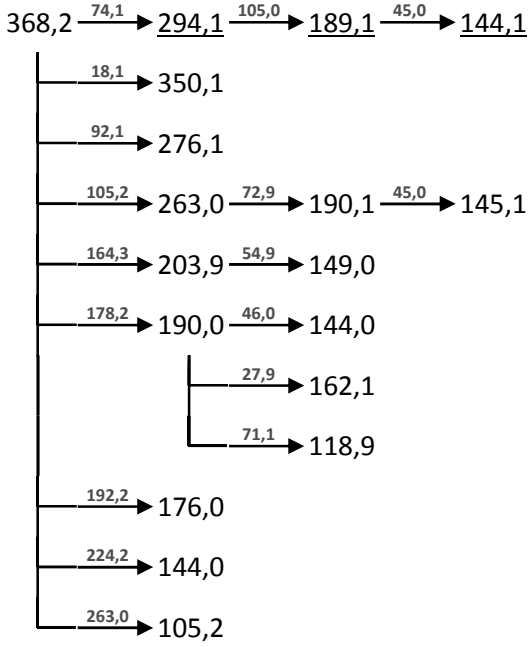

-MS^n: No fragmentation information could be retrieved as the sample was depleted right after the isolation step for -365,9 Th.

isotopic fingerprint:

peak area / % of monoisotopic	**+1**	**+2**	**+3**
theoretical ($C_{17}H_{22}NO_6S^+$):	20,1	7,7	1,2
measured (368,1 Th):	36,2	11,7	-
measured (-365,9 Th):	20,0	3,4	-

Figure XIII-XXXVI MS^n analysis of F7

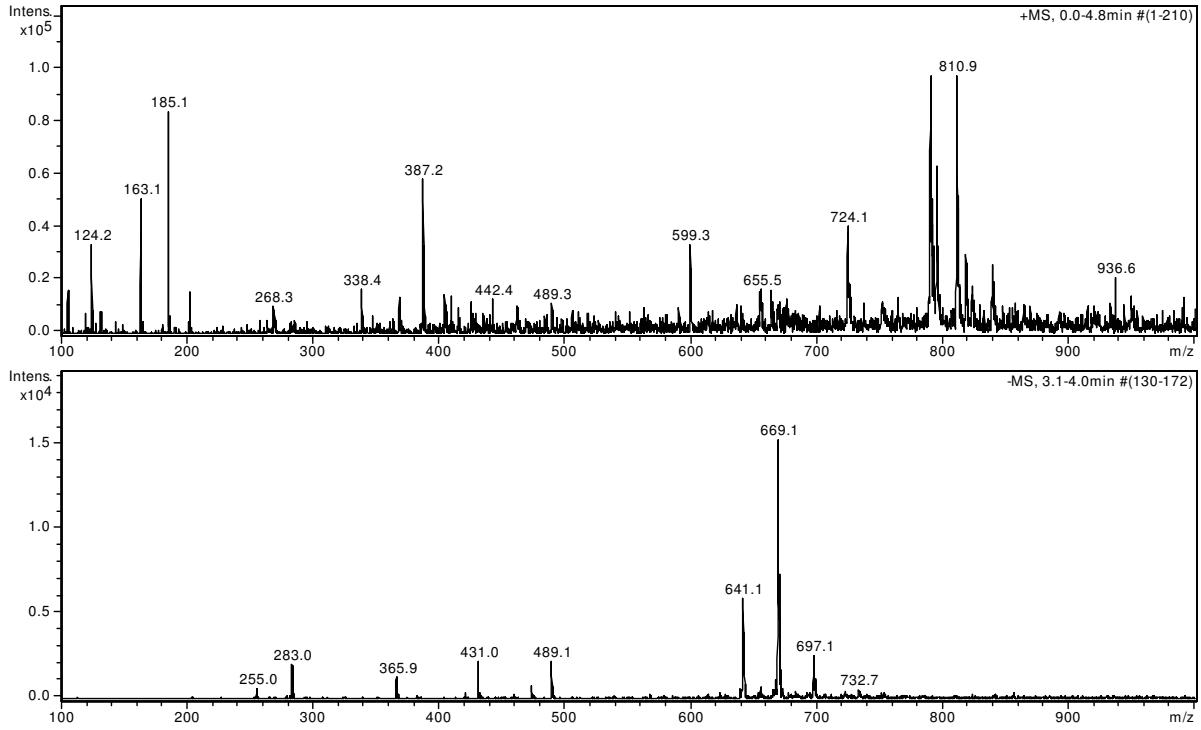

Figure XIII-XXXVII F7: 20,6 – 20,9 min, 0,5 ‰ FA, 68 % ACN in ddH_2O (diluted 1:2 with ACN); full scan MS^1

367 Da (F7) == 367 Da (F6)

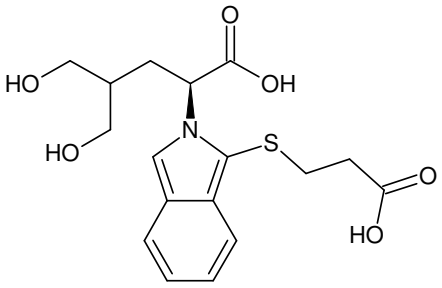

BoT#8
Monoisotopic Mass = 367.108957 Da

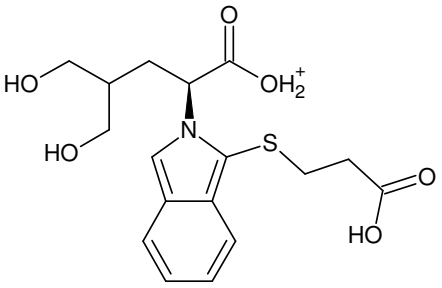

Monoisotopic Mass = 368.116234 Da

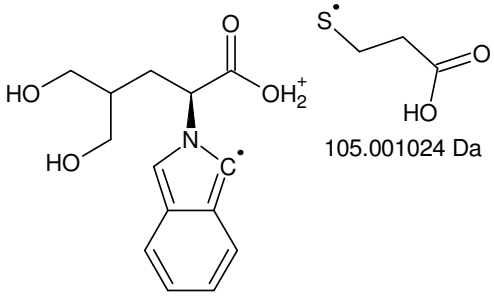

105.001024 Da

Monoisotopic Mass = 263.115209 Da

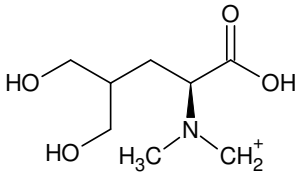

73.007825 Da

Monoisotopic Mass = 190.107384 Da

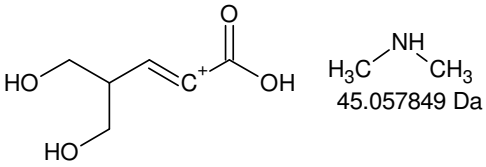

45.057849 Da

Monoisotopic Mass = 145.049535 Da

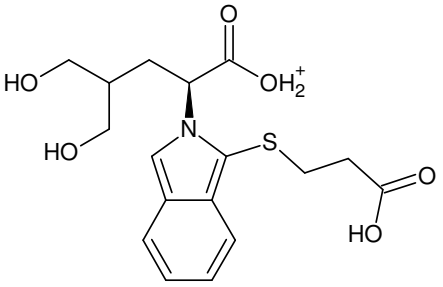

Monoisotopic Mass = 368.116234 Da

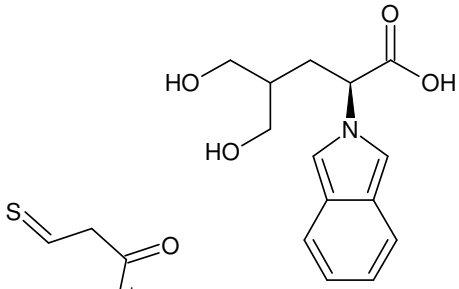

263.115758 Da

Monoisotopic Mass = 105.000476 Da

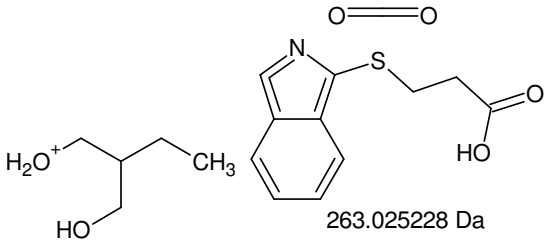

263.025228 Da

Monoisotopic Mass = 105.091006 Da

+MSn [F7]: 367 Da; 368 -> 263 -> 190 -> 145 and 368 -> 105

60 Da

Gefundene Verbindungen: 34
CH2NO2 MG=60,0085532
CH2NS MG=59,9907952
(...)
N2O2 MG=59,995978
N2S MG=59,97822

-----D--B--E--f-i-l-t-e-r-----
20.06.2011 - 12:45:42,52
akzeptierte DBEs:
-1 0 1 2 3 4 5 6 7 8

CH4N2O	DBE: 1
COS	DBE: 2
CO3	DBE: 2
C2H4O2	DBE: 1
C2H4S	DBE: 1
C2H8N2	DBE: 0
C3H8O	DBE: 0
C4H12	DBE: -1
C5	DBE: 6
H4N4	DBE: 1
N2O2	DBE: 2
N2S	DBE: 2

12 von 34 Summenformeln

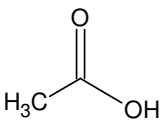

$C_2H_4O_2$
60.021129 Da

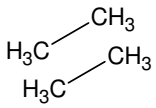

C_4H_{12}
60.0939 Da

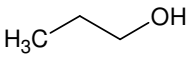

C_3H_8O
60.057515 Da

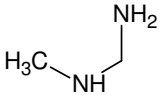

$C_2H_8N_2$
60.068748 Da

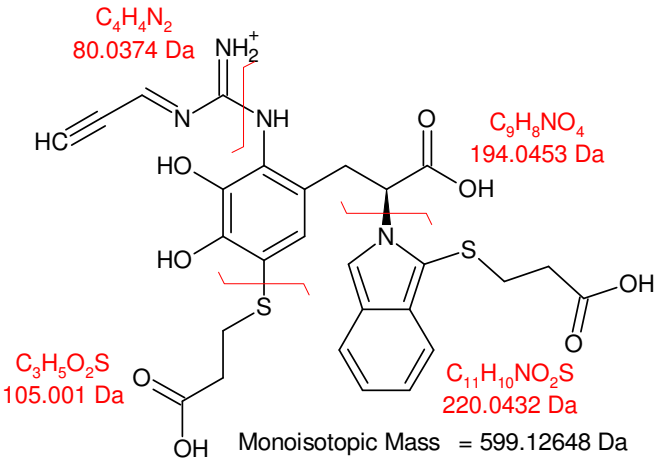

Monoisotopic Mass = 599.12648 Da

nach Zerfall der Verbindung:
4 x 60 Da

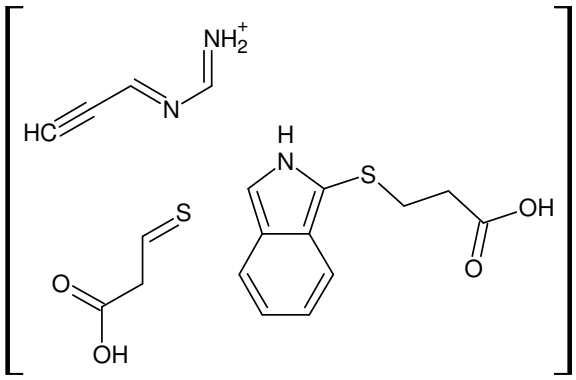

Monoisotopic Mass = 406.088973 Da

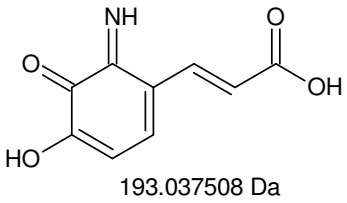

193.037508 Da

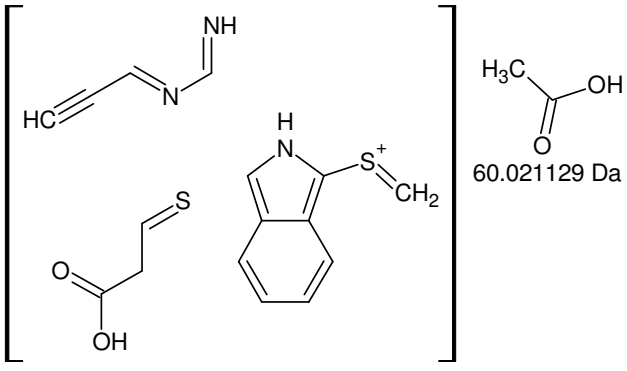

60.021129 Da

Monoisotopic Mass = 346.067843 Da

+MSn [F7]: 599 -> 406 -> 346

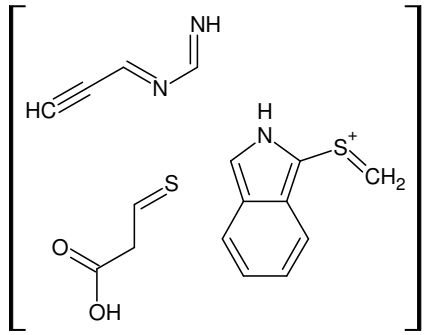

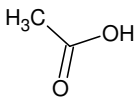

60.021129 Da

Monoisotopic Mass = 346.067843 Da

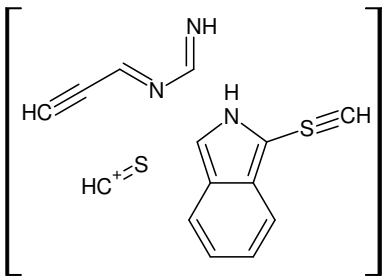

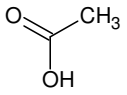

60.021129 Da

Monoisotopic Mass = 286.046714 Da

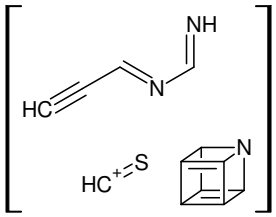

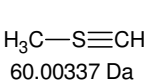

60.00337 Da

Monoisotopic Mass = 226.043344 Da

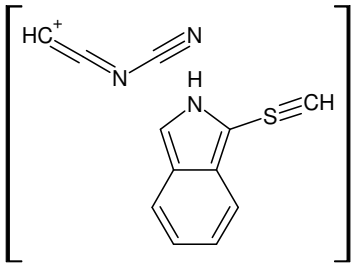

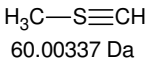

60.00337 Da

Monoisotopic Mass = 226.043344 Da

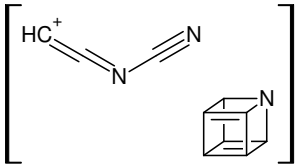

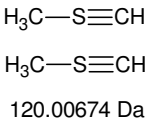

120.00674 Da

Monoisotopic Mass = 166.039974 Da

+MSn [F7]: [599 -> 406 -> 346] -> 286 -> 226, 166

F8

No signals in compliance with the predefined selection rules ($[M\pm p]^{\pm}$) could be found in the full scan mass spectra of fraction 8.

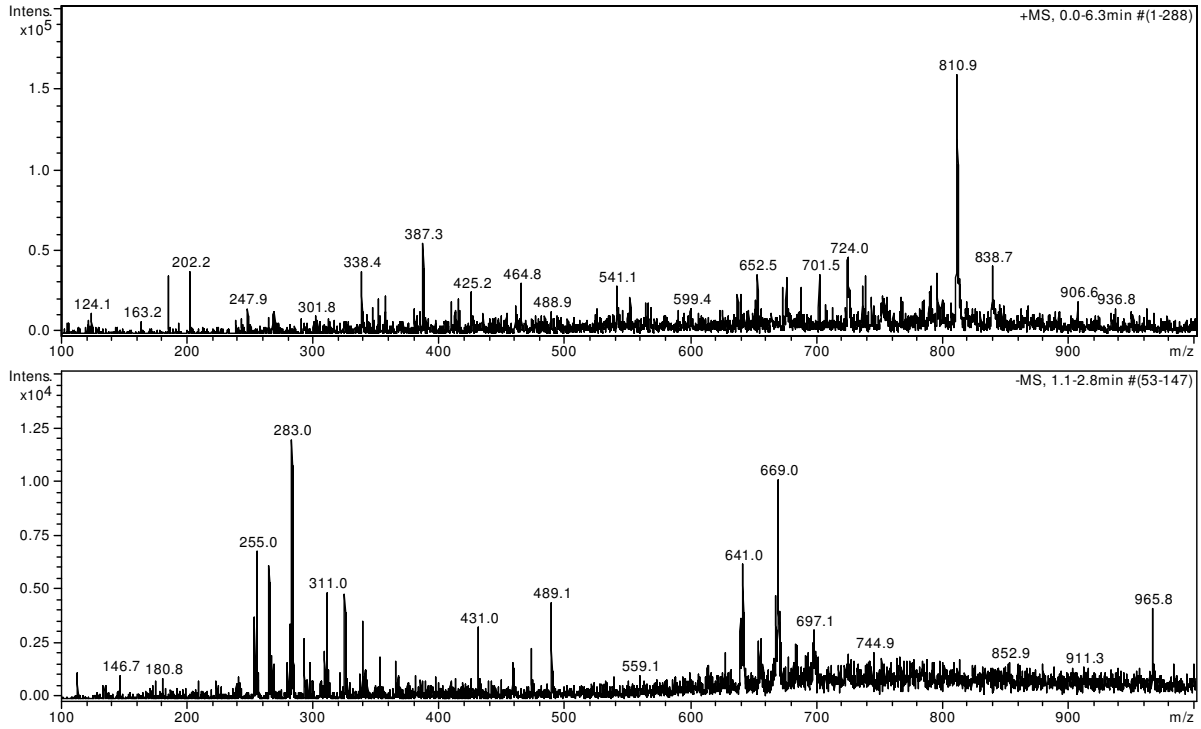

Figure XIII-XXXVIII F8: 21,7 – 22,2 min, 1 ‰ FA, 37 % ACN in ddH_2O; full scan MS^1

F9

+MS^n

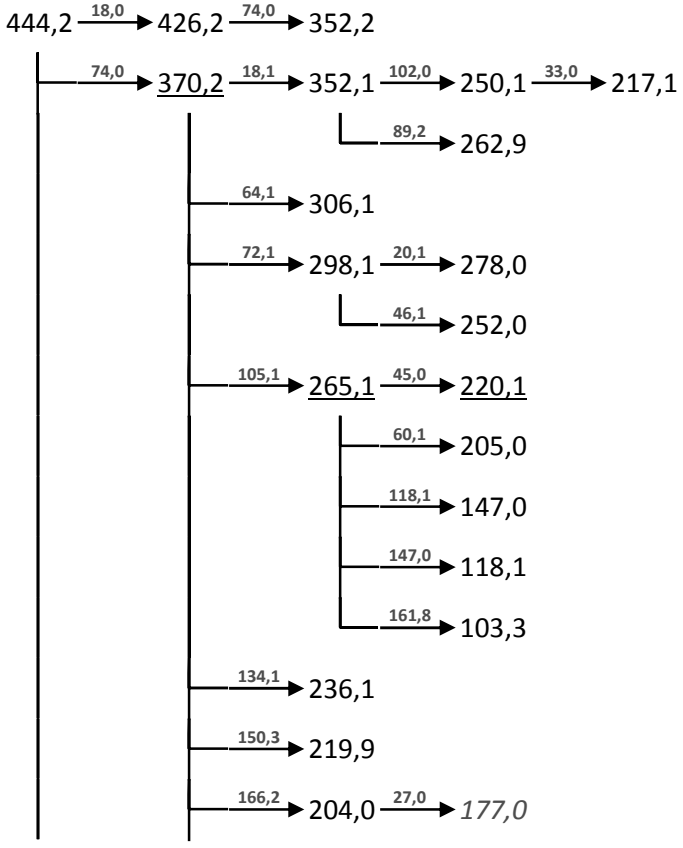

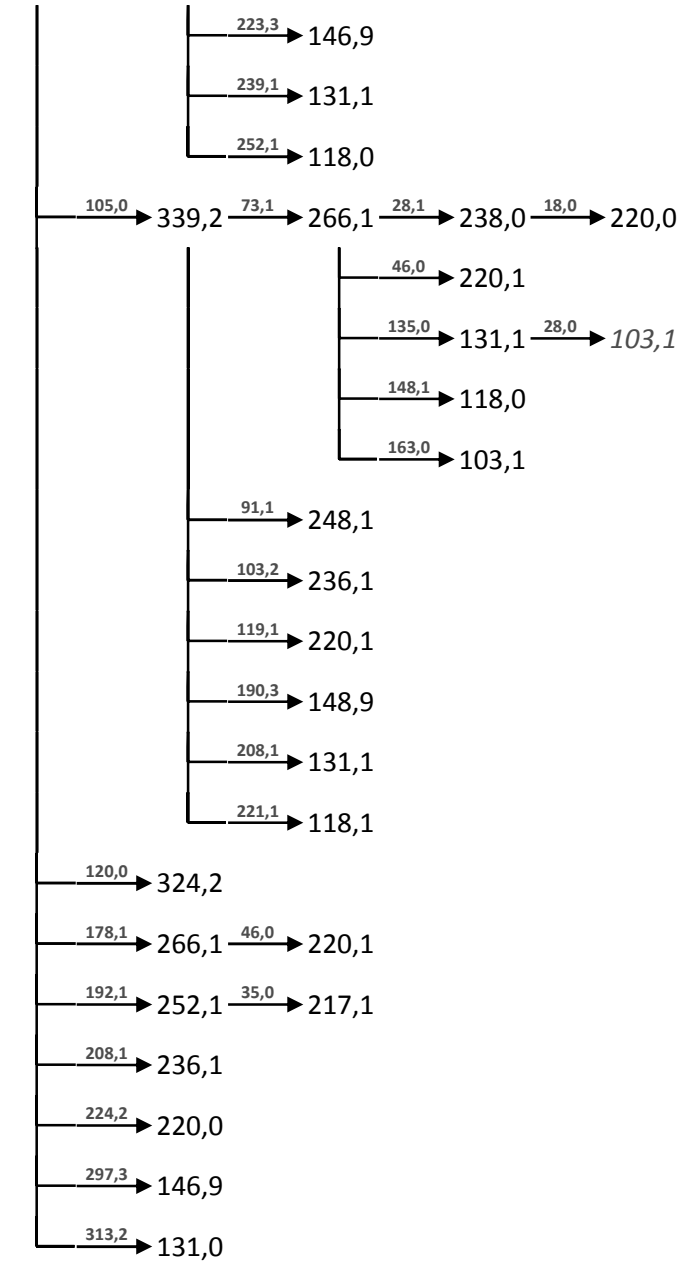
223,3
146,9
239,1
131,1
252,1
118,0
105,0
339,2
73,1
266,1
28,1
238,0
18,0
220,0
46,0
220,1
135,0
131,1
28,0
103,1
148,1
118,0
163,0
103,1
91,1
248,1
103,2
236,1
119,1
220,1
190,3
148,9
208,1
131,1
221,1
118,1
120,0
324,2
178,1
266,1
46,0
220,1
192,1
252,1
35,0
217,1
208,1
236,1
224,2
220,0
297,3
146,9
313,2
131,0

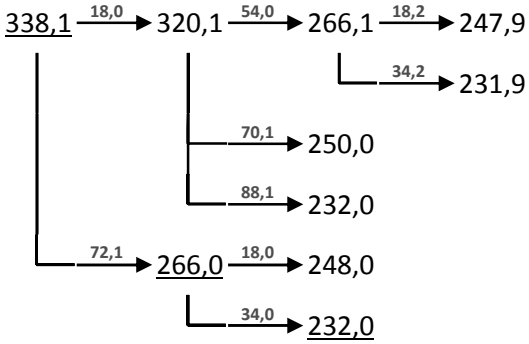
338,1
18,0
320,1
54,0
266,1
18,2
247,9
34,2
231,9
70,1
250,0
88,1
232,0
72,1
266,0
18,0
248,0
34,0
232,0

-MS^n

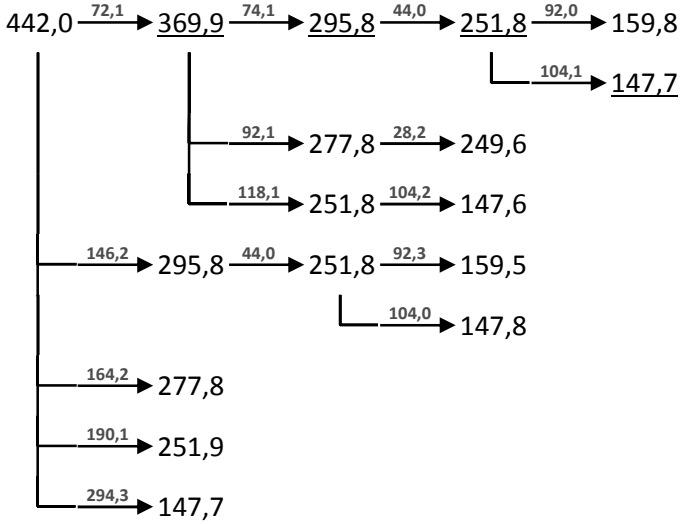

isotopic fingerprint:

peak area / % of monoisotopic	**+1**	**+2**	**+3**
theoretical ($C_{22}H_{22}NO_7S^+$):	25,6	9,1	1,7
measured (444,3 Th):	37,7	26,7	14,9
measured (-442,0 Th):	31,7	10,3	5,1
theoretical ($C_{15}H_{16}NO_6S^+$):	17,8	7,3	1,1
measured (338,2 Th):	23,5	10,3	4,4
measured (-335,9 Th):	61,4	17,8	-

Figure XIII-XXXIX MS^n analysis of F9

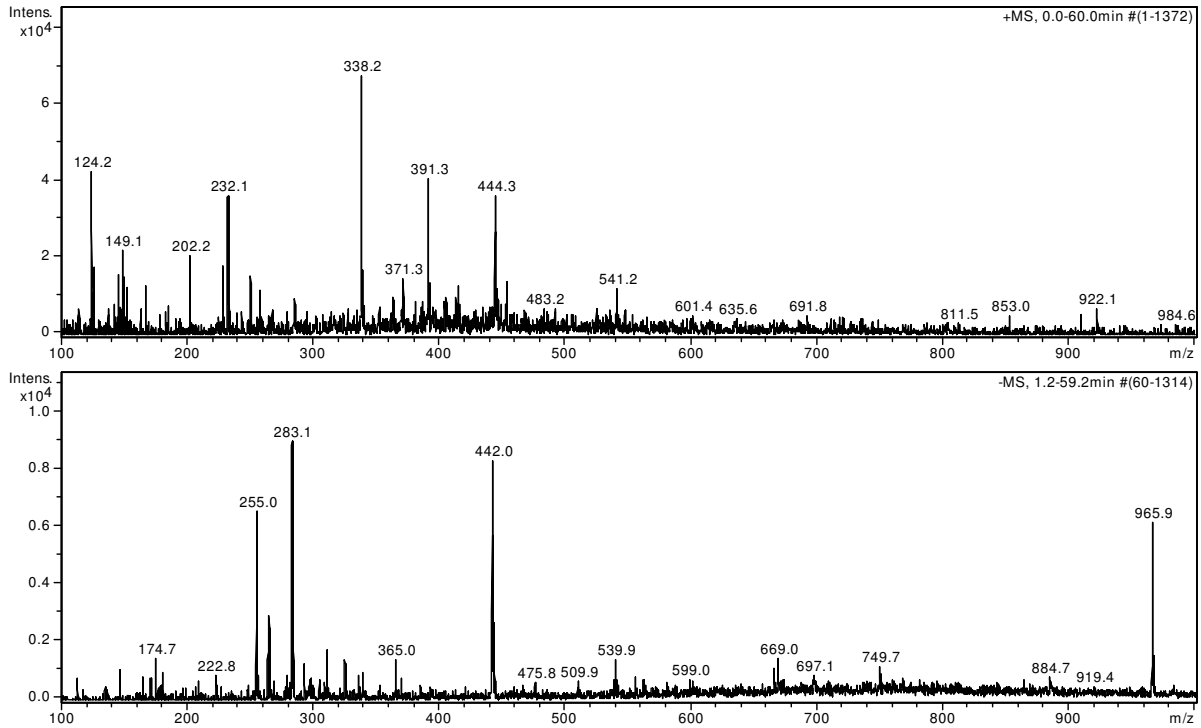

Figure XIII-XL F9: 33,15 – 33,85 min, 1 ‰ FA, 43 % ACN in ddH_2O; full scan MS^1

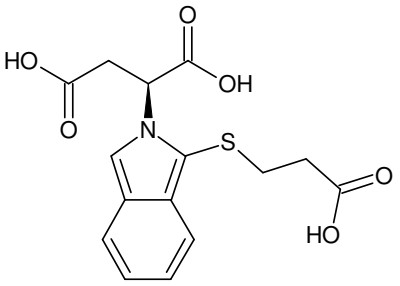

OPA-Asp
Monoisotopic Mass = 337.062007 Da

320,1 - 266,1 = **54,0**
Gefundene Verbindungen: 25
CH10O2 MG=54,068076
CH10S MG=54,050318
CH12NO MG=54,0918842
CH14N2 MG=54,1156924
CH26O MG=54,1983546
CH28N MG=54,2221628
CN3 MG=54,009222
C2H2N2 MG=54,0217972
C2H14O MG=54,1044594
C2H16N MG=54,1282676
C2NO MG=53,997989
C3H2O MG=54,0105642
C3H4N MG=54,0343724
C3H18 MG=54,1408428
C4H6 MG=54,0469476
H6OS MG=54,0139346
H6O3 MG=54,0316926
H8NO2 MG=54,0555008
H8NS MG=54,0377428
H10N2O MG=54,079309
H12N3 MG=54,1031172
H22O2 MG=54,1619712
H22S MG=54,1442132
H24NO MG=54,1857794
H26N2 MG=54,2095876

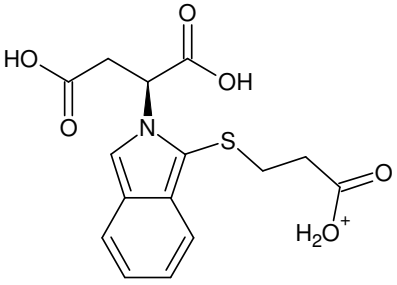

Monoisotopic Mass = 338.069284 Da

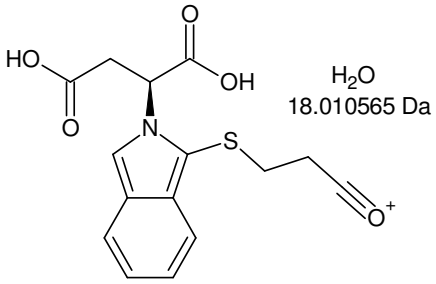

Monoisotopic Mass = 320.058719 Da

-----D--B--E--f-i-l-t-e-r-----
20.06.2011 - 17:06:02,13
akzeptierte DBEs:
-1 0 1 2 3 4 5 6 7 8

C2H2N2 DBE: 3
C3H2O DBE: 3
C4H6 DBE: 2

3 von 25 Summenformeln

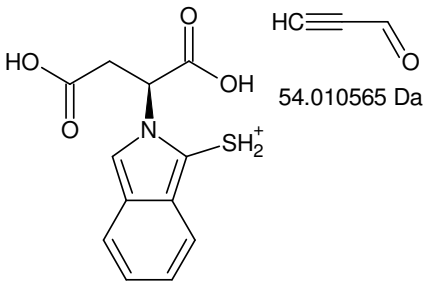

Monoisotopic Mass = 266.048154 Da

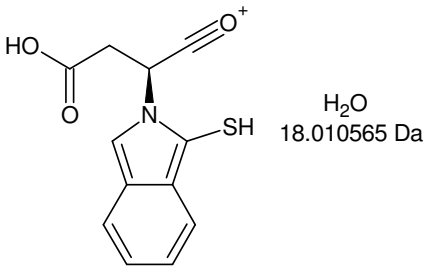

Monoisotopic Mass = 248.03759 Da

18,0 Da
Gefundene Verbindungen: 3
H2O MG=18,0105642
CH6 MG=18,0469476
H4N MG=18,0343724

266,1 - 231,9 = **34,2**
Gefundene Verbindungen: 8
CH6O MG=34,0418626
CH8N MG=34,0656708
C2H10 MG=34,078246
H2O2 MG=34,0054792
H2S MG=33,9877212
H4NO MG=34,0292874
H6N2 MG=34,0530956
H18O MG=34,1357578

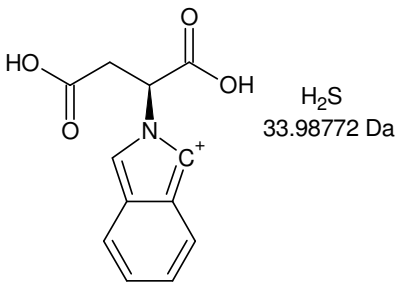

Monoisotopic Mass = 232.060434 Da

kein Einfluss der Seitenkette

-----D--B--E--f-i-l-t-e-r-----
20.06.2011 - 17:08:45,64
akzeptierte DBEs:
-1 0 1 2 3 4 5 6 7 8

CH6O DBE: -1
H2O2 DBE: 0
H2S DBE: 0
H6N2 DBE: -1

4 von 8 Summenformeln

+MSn [F9]: 337 Da: OPA-Asp; 338 -> 320 -> 266 -> 248, 232

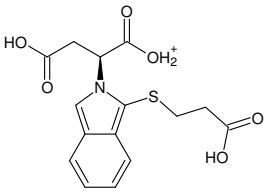

Monoisotopic Mass = 338.069284 Da

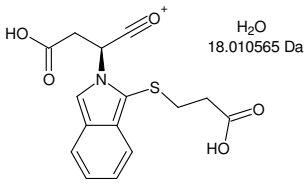

Monoisotopic Mass = 320.058719 Da

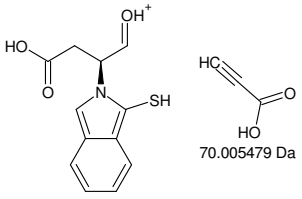

Monoisotopic Mass = 250.05324 Da

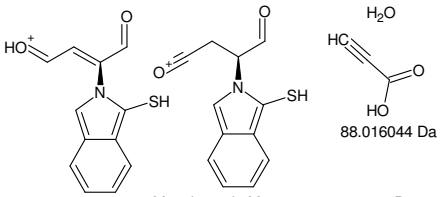

Monoisotopic Mass = 232.042675 Da

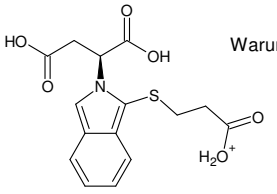

Monoisotopic Mass = 338.069284 Da

Warum nicht -105 Da?

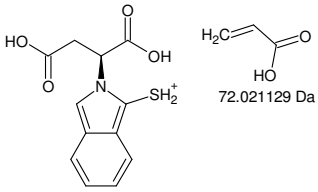

Monoisotopic Mass = 266.048154 Da

Aus diesen Fragmenten lässt sich keine (direkte) Diskriminierungskapazität bezüglich der Seitenkette ableiten.

- keine Funktionalitäten außer Carboxy

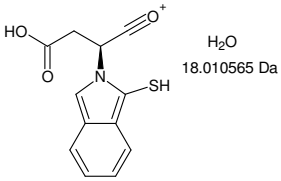

Monoisotopic Mass = 248.03759 Da

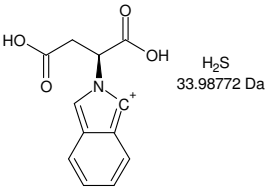

Monoisotopic Mass = 232.060434 Da

320,1 - 250,0 = **70,1**

Gefundene Verbindungen: 49

CH2N4	MG=70,0279452
CH10OS	MG=70,045233
(...)	
H28N3	MG=70,2283108
N5	MG=70,01537

-----D--B--E--f-i-l-t-e-r-----
20.06.2011 - 17:35:50,30
akzeptierte DBEs:
-1 0 1 2 3 4 5 6 7 8

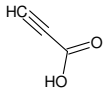

CH2N4	DBE: 3
C2H2N2O	DBE: 3
C3H2O2	DBE: 3
C3H2S	DBE: 3
C3H6N2	DBE: 2
C4H6O	DBE: 2
C5H10	DBE: 1

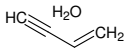

7 von 49 Summenformeln

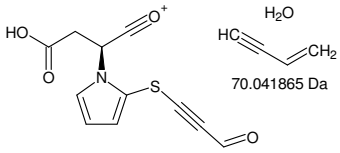

Monoisotopic Mass = 250.016854 Da

+MSn [F9]: 338 -> 320 -> 250, 232 and 338 -> 266 -> 248, 232

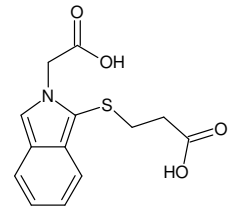

Monoisotopic Mass = 279.056528 Da

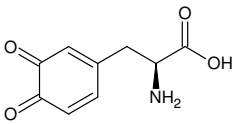

o-Dopachinon
Monoisotopic Mass = 195.053158 Da

443,2 - 279,1 = **164,1**
Gefundene Verbindungen: 698
CH2N5OS2 MG=163,9700782
CH2N5O3S MG=163,9878362
(...)
N6O3S MG=163,975261
N6O5 MG=163,993019

-----D--B--E--f-i-l-t-e-r-----
21.06.2011 - 10:42:06,07
akzeptierte DBEs:
1 2 3 4 5 6 7 8

CH4N6O2S	DBE: 3		
CH4N6O4	DBE: 3	C4N6S	DBE: 8
CH4N6S2	DBE: 3	C5H4N6O	DBE: 7
CH8N8O2	DBE: 2	C5H8O2S2	DBE: 2
CH8N8S	DBE: 2	C5H8O4S	DBE: 2
CH12N10	DBE: 1	C5H8O6	DBE: 2
CN4O2S2	DBE: 4	C5H8S3	DBE: 2
CN4O4S	DBE: 4	C5H12N2O2S	DBE: 1
CN4O6	DBE: 4	C5H12N2O4	DBE: 1
CN4S3	DBE: 4	C5H12N2S2	DBE: 1
C2H4N4OS2	DBE: 3	C5N4OS	DBE: 8
C2H4N4O3S	DBE: 3	C5N4O3	DBE: 8
C2H4N4O5	DBE: 3	C6H4N4O2	DBE: 7
C2H8N6OS	DBE: 2	C6H4N4S	DBE: 7
C2H8N6O3	DBE: 2	C6H8N6	DBE: 6
C2H12N8O	DBE: 1	C6H12OS2	DBE: 1
C2N2OS3	DBE: 4	C6H12O3S	DBE: 1
C2N2O3S2	DBE: 4	C6H12O5	DBE: 1
C2N2O5S	DBE: 4	C6N2O2S	DBE: 8
C2N2O7	DBE: 4	C6N2O4	DBE: 8
C2N10	DBE: 8	C6N2S2	DBE: 8
C3H4N2O2S2	DBE: 3	C7H4N2OS	DBE: 7
C3H4N2O4S	DBE: 3	C7H4N2O3	DBE: 7
C3H4N2O6	DBE: 3	C7H8N4O	DBE: 6
C3H4N2S3	DBE: 3	C7OS2	DBE: 8
C3H8N4O2S	DBE: 2	C7O3S	DBE: 8
C3H8N4O4	DBE: 2	C7O5	DBE: 8
C3H8N4S2	DBE: 2	C8H4O2S	DBE: 7
C3H12N6O2	DBE: 1	C8H4O4	DBE: 7
C3H12N6S	DBE: 1	C8H4S2	DBE: 7
C3N8O	DBE: 8	C8H8N2O2	DBE: 6
C3O2S3	DBE: 4	C8H8N2S	DBE: 6
C3O4S2	DBE: 4	C8H12N4	DBE: 5
C3O6S	DBE: 4	C9H8OS	DBE: 6
C3O8	DBE: 4	C9H8O3	DBE: 6
C3S4	DBE: 4	C9H12N2O	DBE: 5
C4H4N8	DBE: 7	C10H12O2	DBE: 5
C4H4OS3	DBE: 3	C10H12S	DBE: 5
C4H4O3S2	DBE: 3	C10H16N2	DBE: 4
C4H4O5S	DBE: 3	C11H16O	DBE: 4
C4H4O7	DBE: 3	C12H20	DBE: 3
C4H8N2OS2	DBE: 2	H4N8OS	DBE: 3
C4H8N2O3S	DBE: 2	H4N8O3	DBE: 3
C4H8N2O5	DBE: 2	H8N10O	DBE: 2
C4H12N4OS	DBE: 1	N6OS2	DBE: 4
C4H12N4O3	DBE: 1	N6O3S	DBE: 4
C4N6O2	DBE: 8	N6O5	DBE: 4

93 von 698 Summenformeln

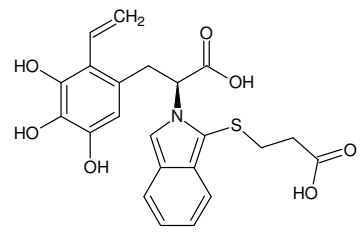

Monoisotopic Mass = 401.093307 Da

443,2 - 401,1 = **42,2**
Gefundene Verbindungen: 13

CH2N2	MG=42,0217972
CH14O	MG=42,1044594
CH16N	MG=42,1282676
CNO	MG=41,997989
C2H2O	MG=42,0105642
C2H4N	MG=42,0343724
C2H18	MG=42,1408428
C3H6	MG=42,0469476
H10S	MG=42,050318
H12NO	MG=42,0918842
H10O2	MG=42,068076
H14N2	MG=42,1156924
N3	MG=42,009222

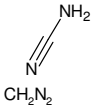

CH_2N_2
42.021798 Da

-----D--B--E--f-i-l-t-e-r-----
21.06.2011 - 10:20:02,74
akzeptierte DBEs:
1 2 3 4 5 6 7 8

CH2N2	DBE: 2
C2H2O	DBE: 2
C3H6	DBE: 1

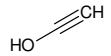

C_2H_2O
42.010565 Da

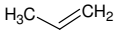

C_3H_6
42.04695 Da

3 von 13 Summenformeln

Monoisotopic Mass = 443.103872 Da

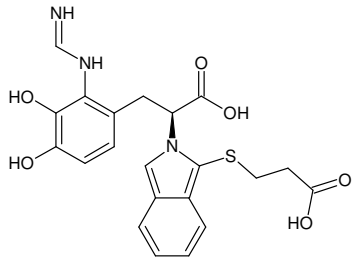

Monoisotopic Mass = 443.115105 Da

MS^n [F9]: 443 Da

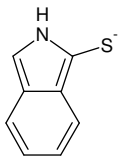

Monoisotopic Mass = 148.022643 Da

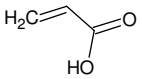

72.021129 Da

43.989829 Da

251,8 - 147,7 = 104,1

Gefundene Verbindungen: 163
CH2N3OS MG=103,9918582
CH2N3O3 MG=104,0096162
(...)
N4OS MG=103,979283
N4O3 MG=103,997041

-----D--B--E--f-i-l-t-e-r-----
21.06.2011 - 12:17:59,60
akzeptierte DBEs:
-1 0 1 2 3 4 5 6 7 8

CH4N4O2	DBE: 2
CH4N4S	DBE: 2
CH8N6	DBE: 1
CN2O2S	DBE: 3
CN2O4	DBE: 3
CN2S2	DBE: 3
C2H4N2OS	DBE: 2
C2H4N2O3	DBE: 2
C2H8N4O	DBE: 1
C2OS2	DBE: 3
C2O3S	DBE: 3
C2O5	DBE: 3
C3H4O2S	DBE: 2
C3H4O4	DBE: 2
C3H4S2	DBE: 2
C3H8N2O2	DBE: 1
C3H8N2S	DBE: 1
C3H12N4	DBE: 0
C4H8OS	DBE: 1
C4H8O3	DBE: 1
C4H12N2O	DBE: 0
C4N4	DBE: 7
C5H12O2	DBE: 0
C5H12S	DBE: 0
C5H16N2	DBE: -1
C5N2O	DBE: 7
C6H4N2	DBE: 6
C6H16O	DBE: -1
C6O2	DBE: 7
C6S	DBE: 7
C7H4O	DBE: 6
C8H8	DBE: 5
H4N6O	DBE: 2
N4OS	DBE: 3
N4O3	DBE: 3

35 von 163 Summenformeln

369,9 - 295,8 = 74,1

Gefundene Verbindungen: 60
CH2N2O2 MG=74,0116272
CH2N2S MG=73,9938692
(...)
N3O2 MG=73,999052
N3S MG=73,981294

-----D--B--E--f-i-l-t-e-r-----
21.06.2011 - 10:53:59,49
akzeptierte DBEs:
-1 0 1 2 3 4 5 6 7 8

CH2N2O2	DBE: 2
CH2N2S	DBE: 2
CH6N4	DBE: 1
C2H2OS	DBE: 2
C2H2O3	DBE: 2
C2H6N2O	DBE: 1
C3H6O2	DBE: 1
C3H6S	DBE: 1
C3H10N2	DBE: 0
C4H10O	DBE: 0
C5H14	DBE: -1
C6H2	DBE: 6
H2N4O	DBE: 2

13 von 60 Summenformeln

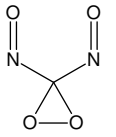

CN_2O_4
103.985806 Da

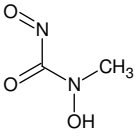

$C_2H_4N_2O_3$
104.022192 Da

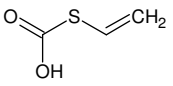

$C_3H_4O_2S$
103.993199 Da

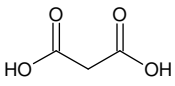

$C_3H_4O_4$
104.010959 Da

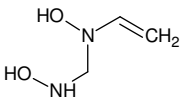

$C_3H_8N_2O_2$
104.058578 Da

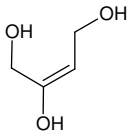

$C_4H_8O_3$ - Glu, Val
104.047344 Da

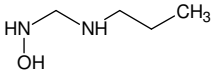

$C_4H_{12}N_2O$
104.094963 Da

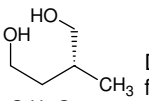

$C_5H_{12}O_2$
104.08373 Da

DBE fehlt

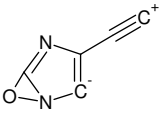

C_5N_2O - His
104.001063 Da

$CH_2N_2O_2$
74.011627 Da

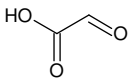

$C_2H_2O_3$
74.000394 Da

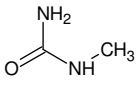

$C_2H_6N_2O$
74.048013 Da

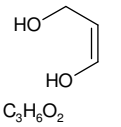

$C_3H_6O_2$
74.036779 Da

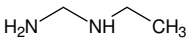

$C_3H_{10}N_2$
74.084398 Da

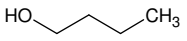

$C_4H_{10}O$
74.073165 Da

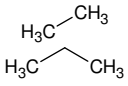

C_5H_{14}
74.10955 Da

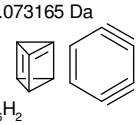

C_6H_2
74.01565 Da

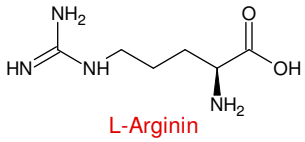

L-Arginin

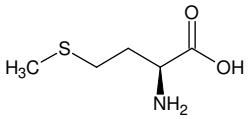

L-Methionin

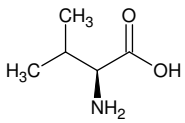

L-Valin

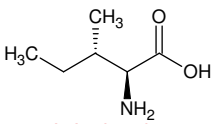

L-Isoleucin

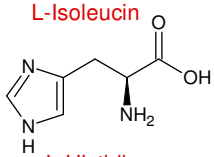

L-Histidin

1 DBE wird zur "Montage" benötigt.

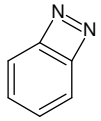

$C_6H_4N_2$
104.037448 Da

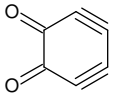

C_6O_2
103.989829 Da

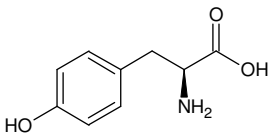

L-Tyrosin

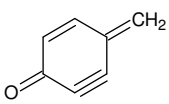

C_7H_4O
104.026215 Da

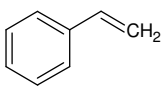

C_8H_8 - Phe
104.0626 Da

-MSn [F9]: 148 <- 252 <- 296 <- 370 <- 442: fragments (268 <- 370 cp. F3: 92Da)

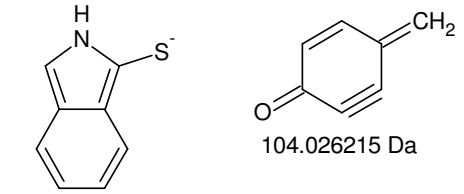

Monoisotopic Mass = 148.022643 Da

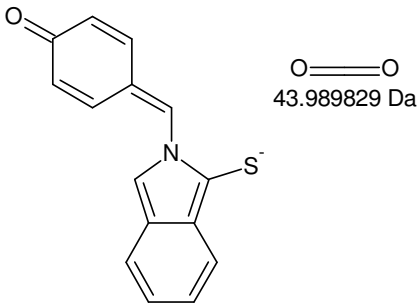

Monoisotopic Mass = 252.048858 Da

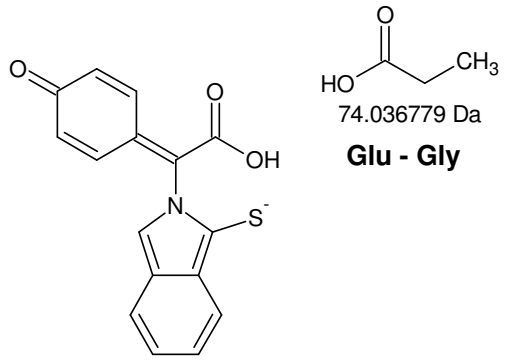

Glu - Gly

Monoisotopic Mass = 296.038687 Da

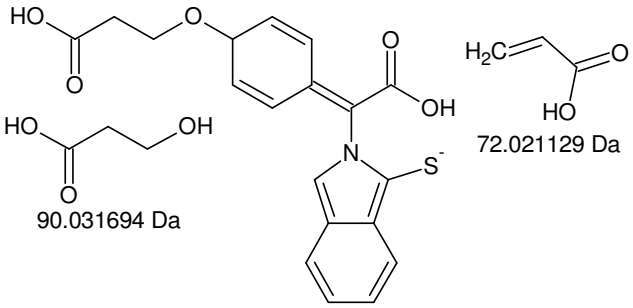

Monoisotopic Mass = 370.075466 Da

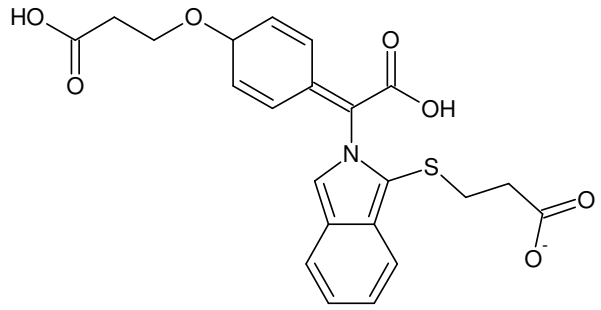

Monoisotopic Mass = 442.096596 Da

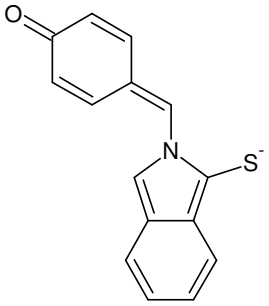

Monoisotopic Mass = 252.048858 Da

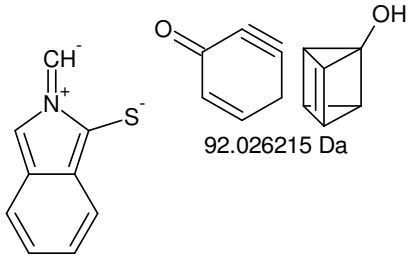

Monoisotopic Mass = 160.022643 Da

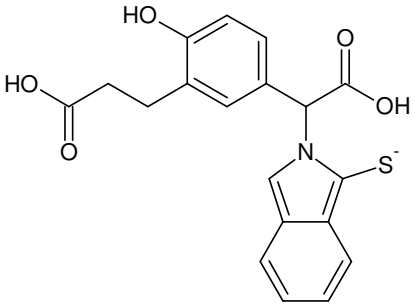

Monoisotopic Mass = 370.075466 Da

-92 Da, -28 Da nicht realisierbar

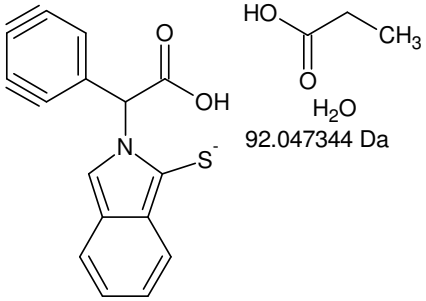

Monoisotopic Mass = 278.028122 Da

Aus dieser Struktur können 28 Da nicht abgespalten werden.

X –MSn [F9]: 148 <- 252 <- 296 <- 370 <- 442

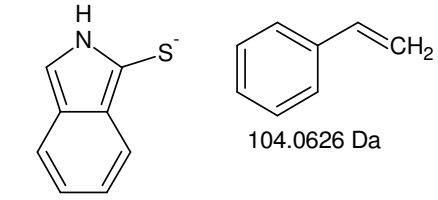

Monoisotopic Mass = 148.022643 Da

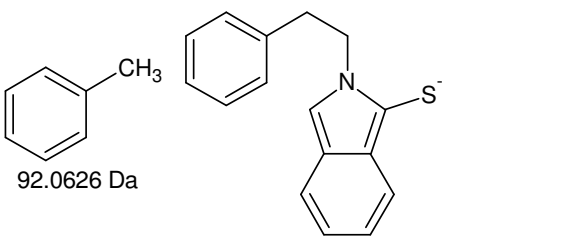

Monoisotopic Mass = 252.085243 Da

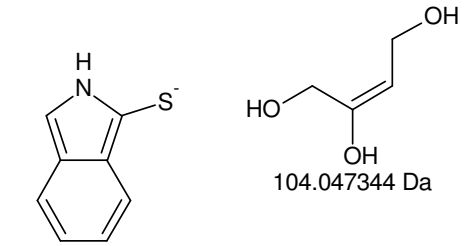

Monoisotopic Mass = 148.022643 Da

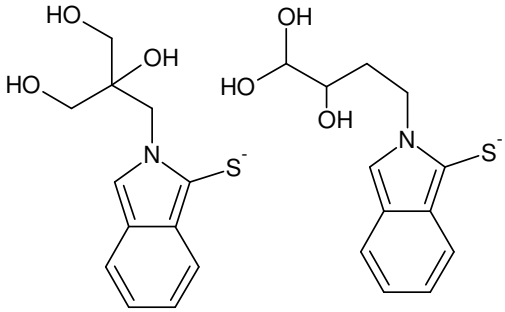

Monoisotopic Mass = 252.069987 Da

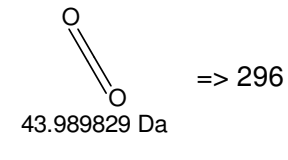

=> 296

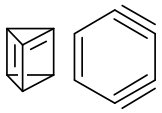

=> 370

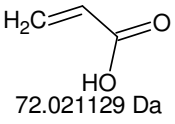

=> 442

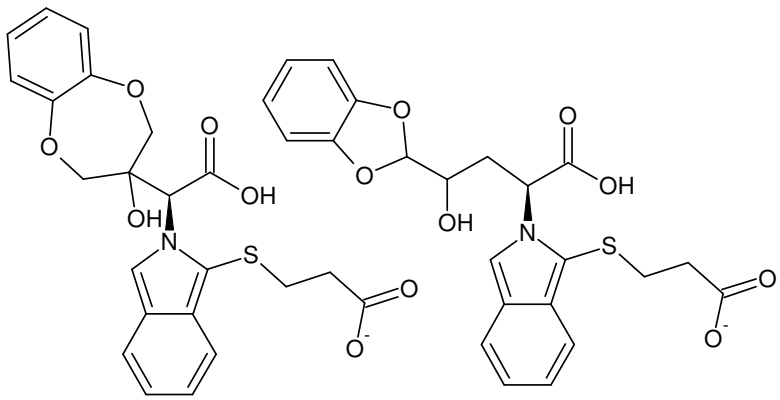

Monoisotopic Mass = 442.096596 Da

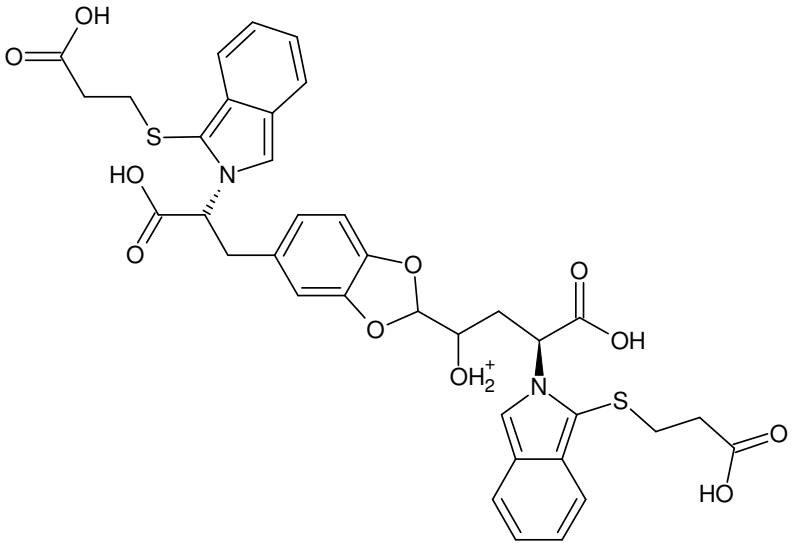

Monoisotopic Mass = 735.167676 Da

-MSn [F9]: 148 <- 252 <- 296 <- 370 <- 442: Glu-Tyr {I/II}

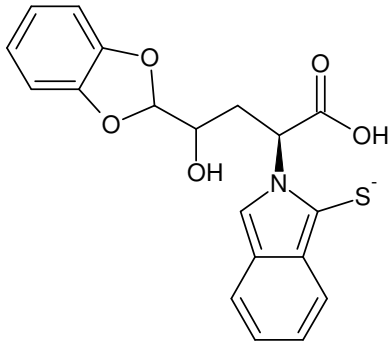

92.026215 Da

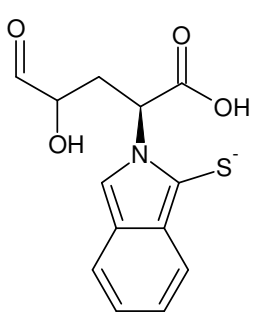

27.994915 Da

Monoisotopic Mass = 370.075466 Da

Monoisotopic Mass = 278.049251 Da

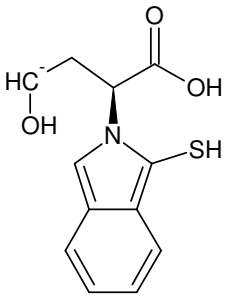

Monoisotopic Mass = 250.054337 Da

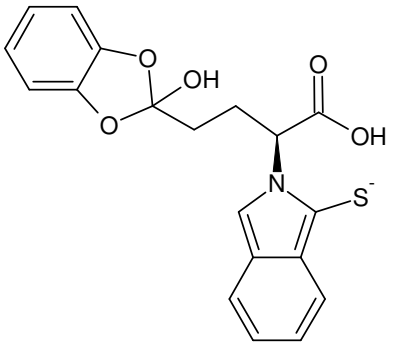

92.026215 Da

Monoisotopic Mass = 370.075466 Da

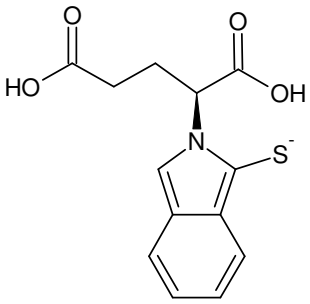

Monoisotopic Mass = 278.049251 Da

Aus dieser Struktur ist eine Abspaltung von 28 Da nicht zu erwarten.

-MSn [F9]: 148 <- 252 <- 296 <- 370 <- 442: Glu-Tyr {II/II}

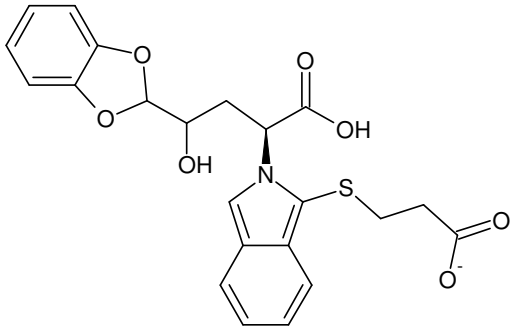

Monoisotopic Mass = 442.096596 Da

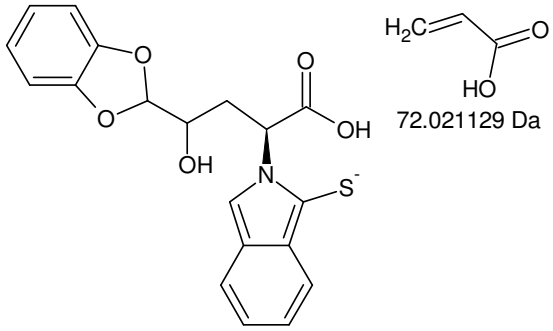

72.021129 Da

Monoisotopic Mass = 370.075466 Da

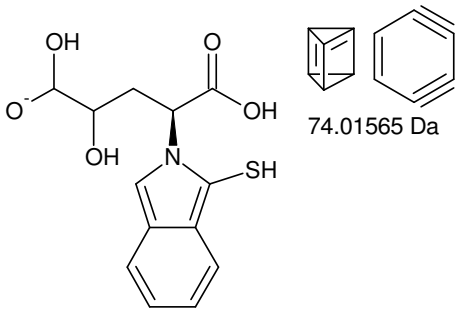

74.01565 Da

Monoisotopic Mass = 296.059816 Da

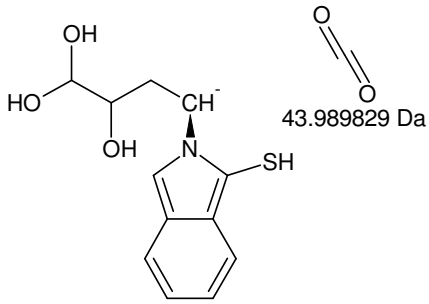

43.989829 Da

Monoisotopic Mass = 252.069987 Da

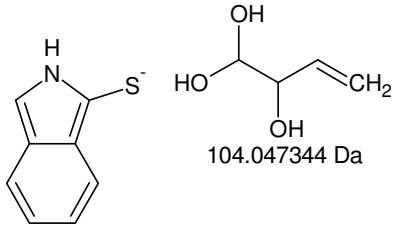

104.047344 Da

Monoisotopic Mass = 148.022643 Da

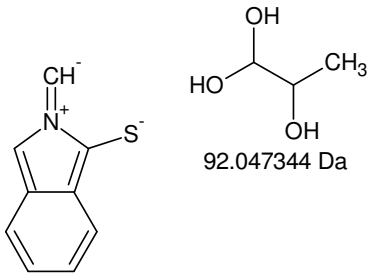

92.047344 Da

Monoisotopic Mass = 160.022643 Da

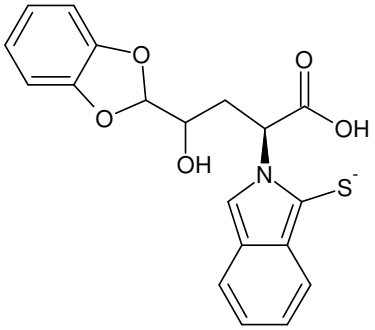

Monoisotopic Mass = 370.075466 Da

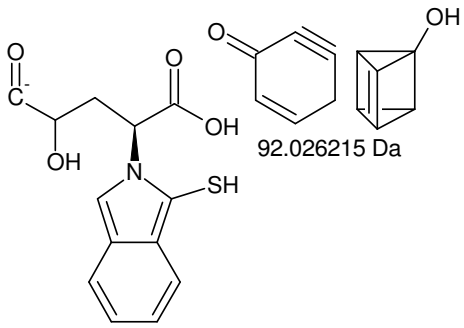

92.026215 Da

Monoisotopic Mass = 278.049251 Da

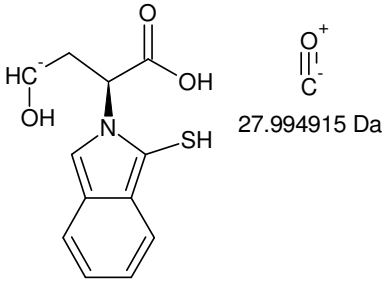

27.994915 Da

Monoisotopic Mass = 250.054337 Da

-MSn [F9]: 442 -> 370 -> 296 -> 252 -> 148, 160 and 370 -> 278 -> 250

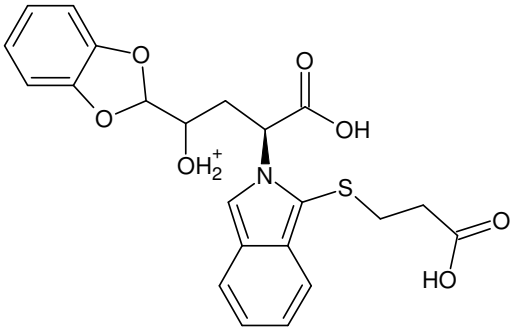

Monoisotopic Mass = 444.111148 Da

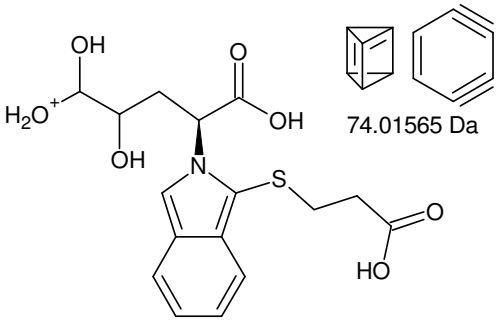

74.01565 Da

Monoisotopic Mass = 370.095498 Da

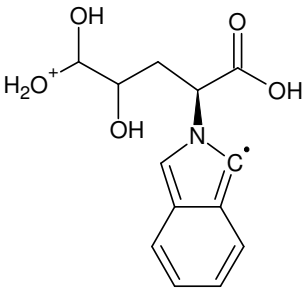

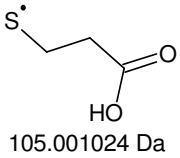

105.001024 Da

Monoisotopic Mass = 265.094474 Da

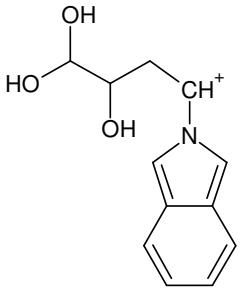

44.997654 Da

Monoisotopic Mass = 220.09682 Da

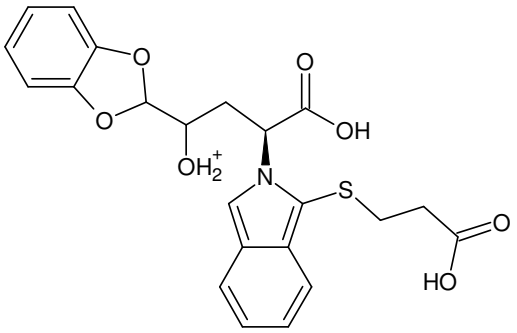

Monoisotopic Mass = 444.111148 Da

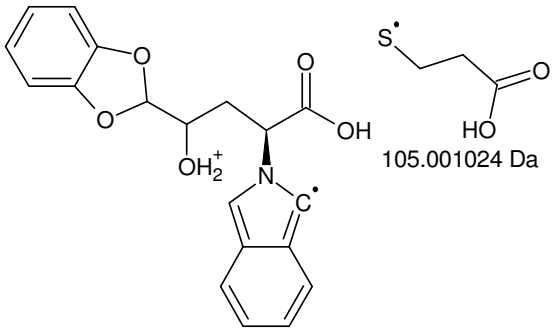

105.001024 Da

Monoisotopic Mass = 339.110124 Da

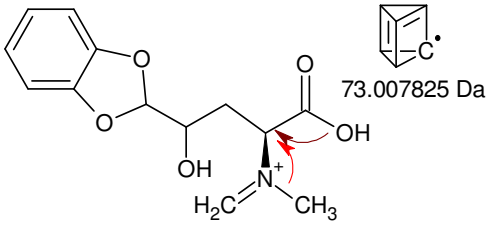

73.007825 Da

Monoisotopic Mass = 266.102299 Da

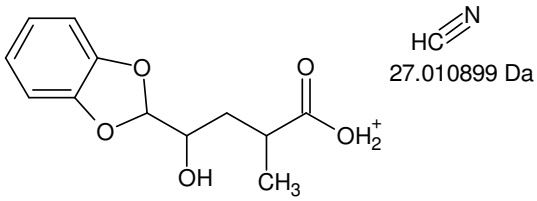

27.010899 Da

Monoisotopic Mass = 239.0914 Da

266,1 - 238,9 = **27,2**
Gefundene Verbindungen: 4
CHN MG=27,0108986
C_2H_3 MG=27,0234738
$H_{11}O$ MG=27,0809856
$H_{13}N$ MG=27,1047938

27.010899 Da

238,9 - 220,0 = **18,9**
Gefundene Verbindungen: 3
H_3O MG=19,0183888
CH_7 MG=19,0547722
H_5N MG=19,042197

$H^{\bullet}$ H_2O
19.01839 Da

NH_3 H_2
19.042199 Da

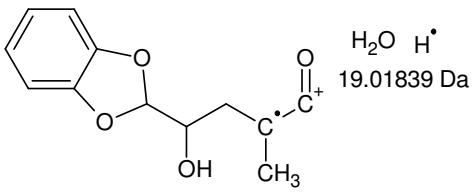

H_2O $H^{\bullet}$
19.01839 Da

Monoisotopic Mass = 220.07301 Da

+MSn [F9]: 444 -> 370 -> 265 -> 220 as well as 444 -> 339 -> 266 -> 239 -> 220

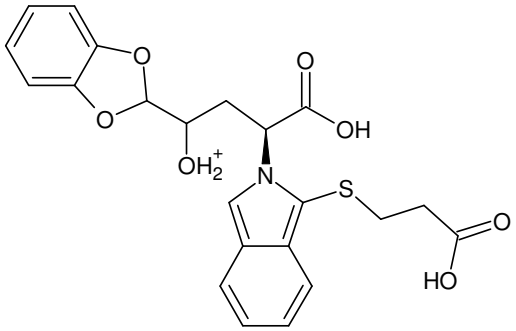

Monoisotopic Mass = 444.111148 Da

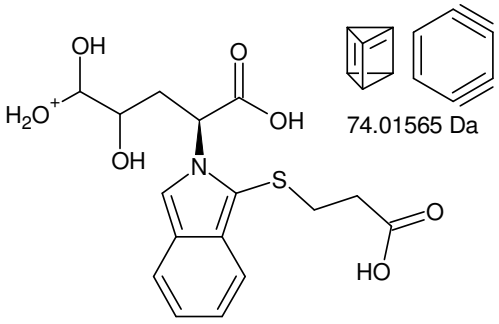

74.01565 Da

Monoisotopic Mass = 370.095498 Da

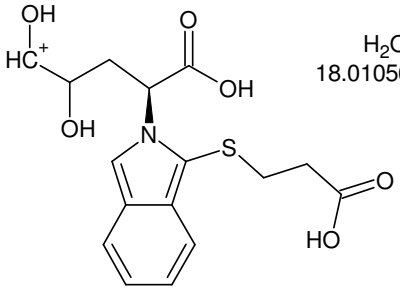

H_2O
18.010565 Da

Monoisotopic Mass = 352.084934 Da

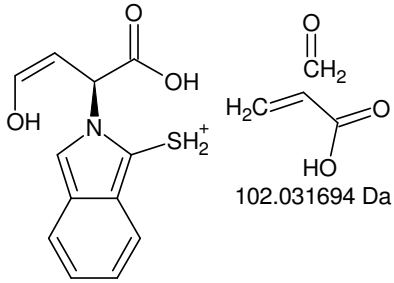

102.031694 Da

Monoisotopic Mass = 250.05324 Da

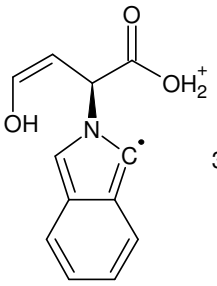

$HS^{\bullet}$
32.979895 Da

Monoisotopic Mass = 217.073345 Da

250,1 - 217,1 = **33,0**

Gefundene Verbindungen: 8

CH5O	MG=33,034038
CH7N	MG=33,0578462
C2H9	MG=33,0704214
HO2	MG=32,9976546
HS	MG=32,9798966
H3NO	MG=33,0214628
H5N2	MG=33,045271
H17O	MG=33,1279332

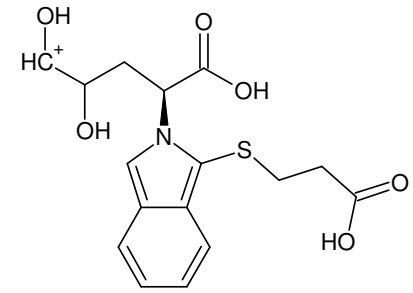

Monoisotopic Mass = 352.084934 Da

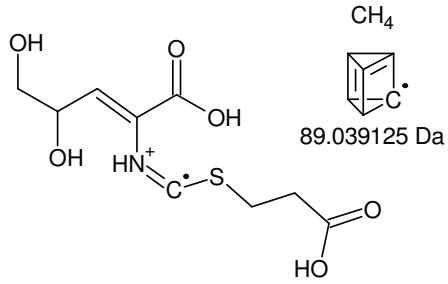

CH_4
89.039125 Da

Monoisotopic Mass = 263.045809 Da

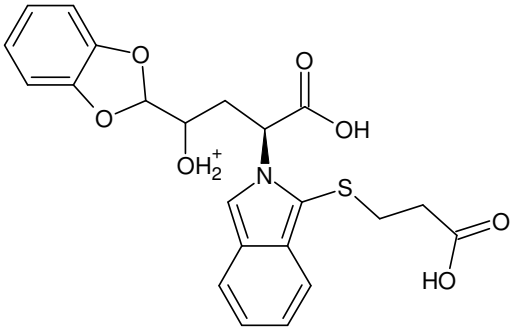

Monoisotopic Mass = 444.111148 Da

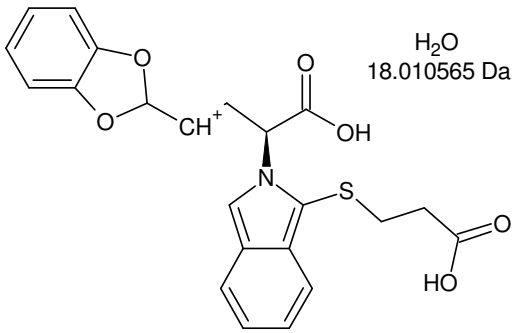

H_2O
18.010565 Da

Monoisotopic Mass = 426.100584 Da

+MSn [F9]: 444 -> 370 -> 352 -> 250 -> 217 as well as 352 -> 263 und 444 -> 426

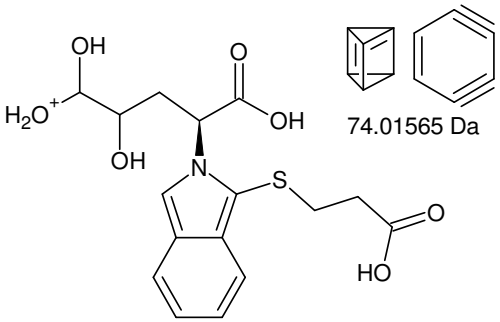

Monoisotopic Mass = 370.095498 Da

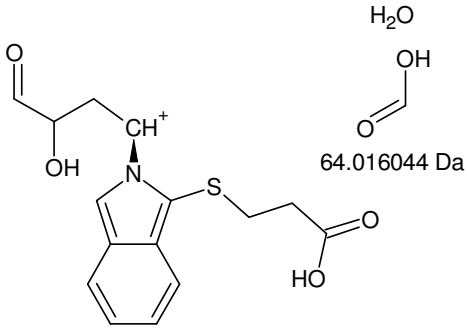

Monoisotopic Mass = 306.079454 Da

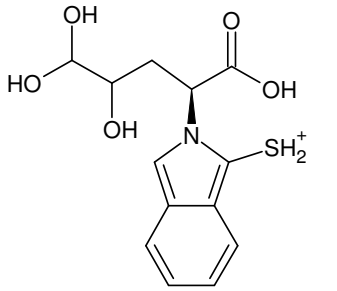

Gefundene Verbindungen: 3
H_4O MG=20,0262134
CH_8 MG=20,0625968
H_6N MG=20,0500216

Monoisotopic Mass = 298.074369 Da

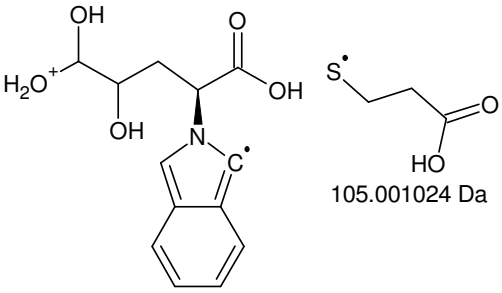

Monoisotopic Mass = 265.094474 Da

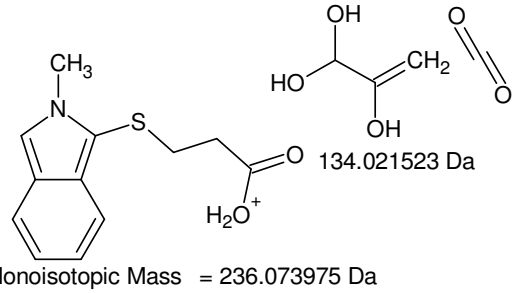

Monoisotopic Mass = 236.073975 Da

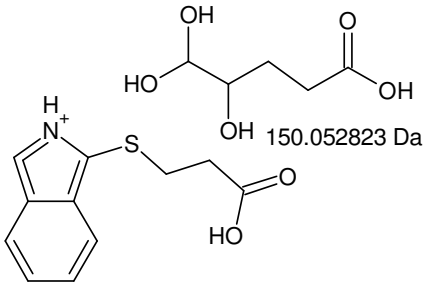

Monoisotopic Mass = 220.042675 Da

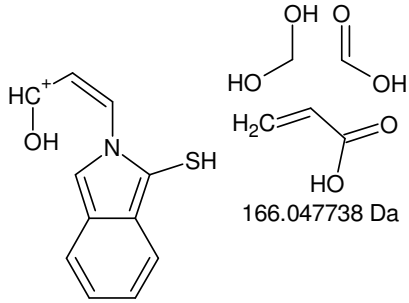

Monoisotopic Mass = 204.04776 Da

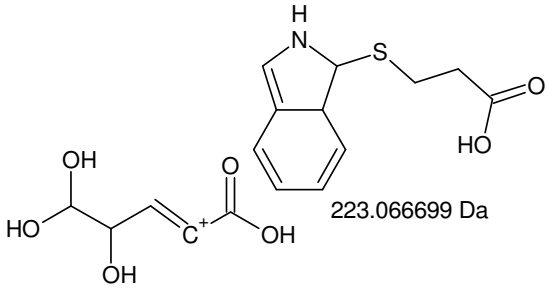

Monoisotopic Mass = 147.0288 Da

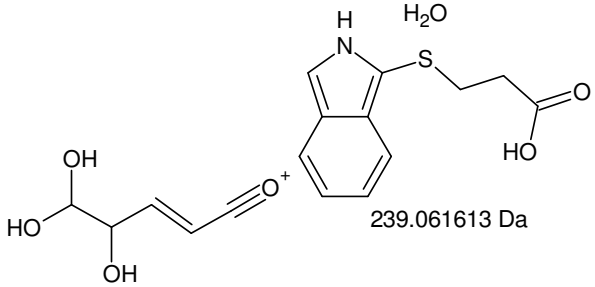

Monoisotopic Mass = 131.033885 Da

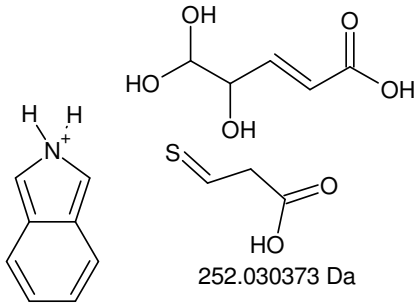

Monoisotopic Mass = 118.065126 Da

+MSn [F9]: [444 -> 370] -> 306, 298, 265, 236, 220, 204, 147, 131, 118

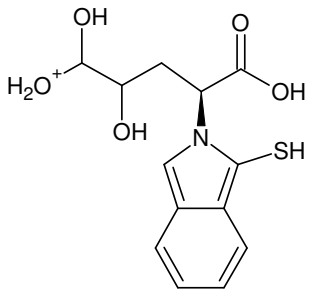

Monoisotopic Mass = 298.074369 Da

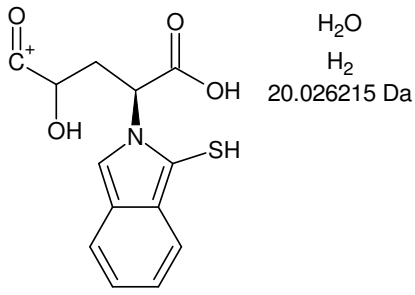

Monoisotopic Mass = 278.048154 Da

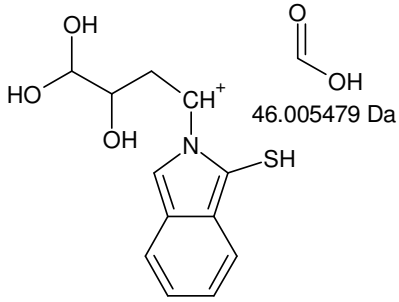

Monoisotopic Mass = 252.06889 Da

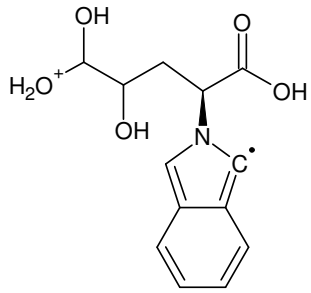

Monoisotopic Mass = 265.094474 Da

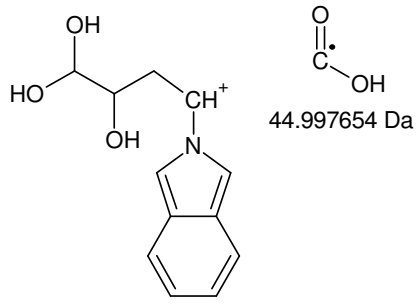

Monoisotopic Mass = 220.09682 Da

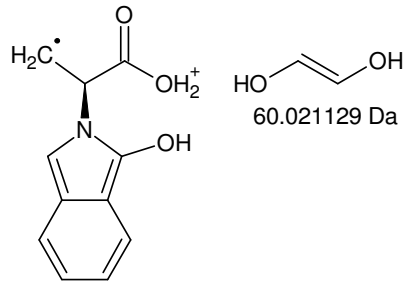

Monoisotopic Mass = 205.073345 Da

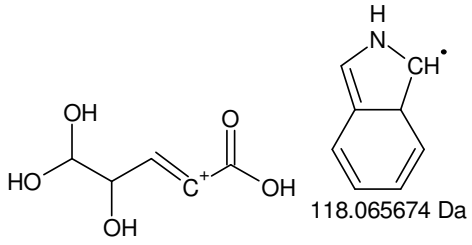

Monoisotopic Mass = 147.0288 Da

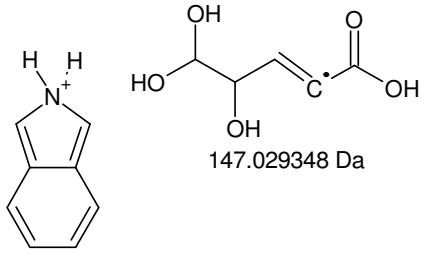

Monoisotopic Mass = 118.065126 Da

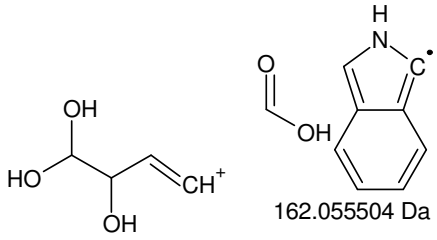

Monoisotopic Mass = 103.03897 Da

+MSn [F9]: [444 -> 370 -> 298] -> 278, 252 and [444 -> 370 -> 265] -> 220, 205, 147, 118, 103

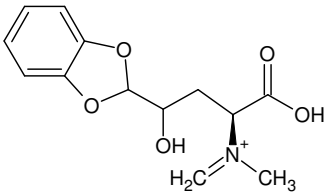

Monoisotopic Mass = 266.102299 Da

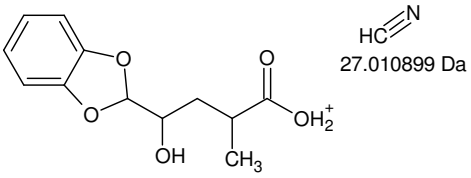

Monoisotopic Mass = 239.0914 Da

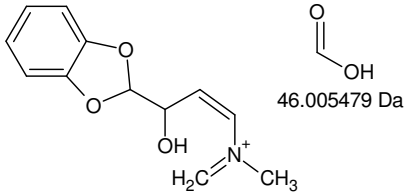

Monoisotopic Mass = 220.09682 Da

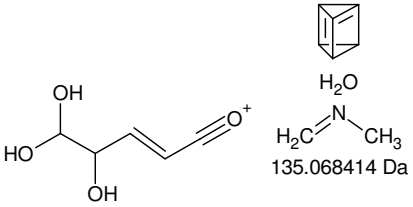

Monoisotopic Mass = 131.033885 Da

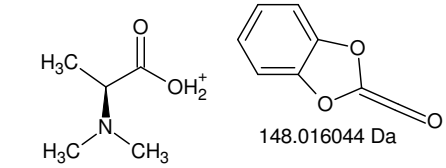

Monoisotopic Mass = 118.086255 Da

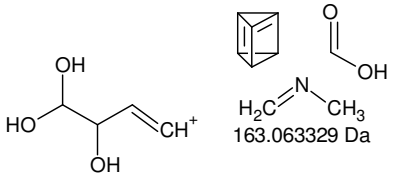

Monoisotopic Mass = 103.03897 Da

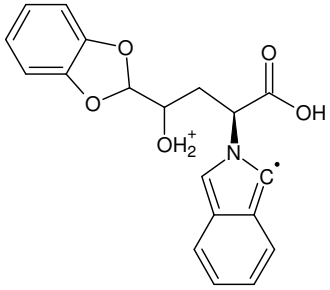

Monoisotopic Mass = 339.110124 Da

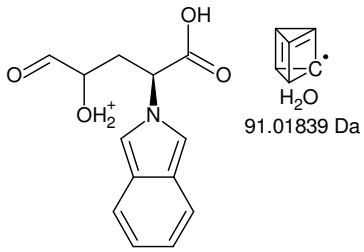

Monoisotopic Mass = 248.091734 Da

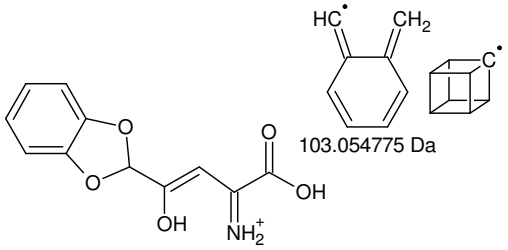

Monoisotopic Mass = 236.055349 Da

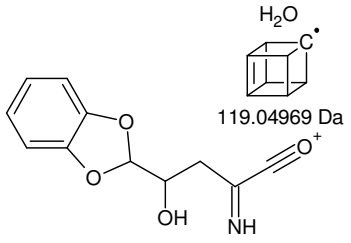

Monoisotopic Mass = 220.060434 Da

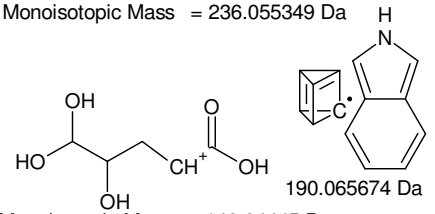

Monoisotopic Mass = 149.04445 Da

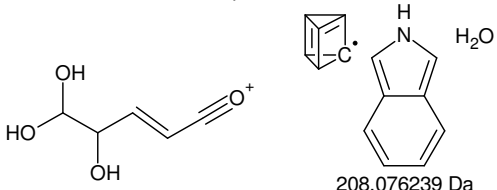

Monoisotopic Mass = 131.033885 Da

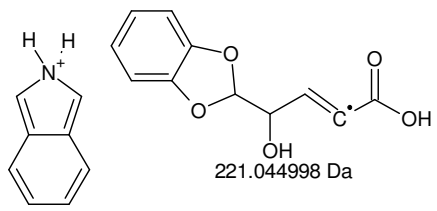

Monoisotopic Mass = 118.065126 Da

+MSn [F9]: [444 -> 339 -> 266] -> 239, 220, 131, 118, 103 and [444 -> 339] -> 248, 236, 220, 149, 131, 118

F10

In the fragmentation tree of 415 Th none of the typical fragments for 3-mercaptopropionic acid (+MS^n: 105, 106, 46 Da; -MS^n: 72, 44 Da) were found. The respective compound is therefore most likely not an OPA-derivative but has a different structure which renders any attempts at deducing a structure for it not exactly impossible but highly speculative in nature.

+MS^n

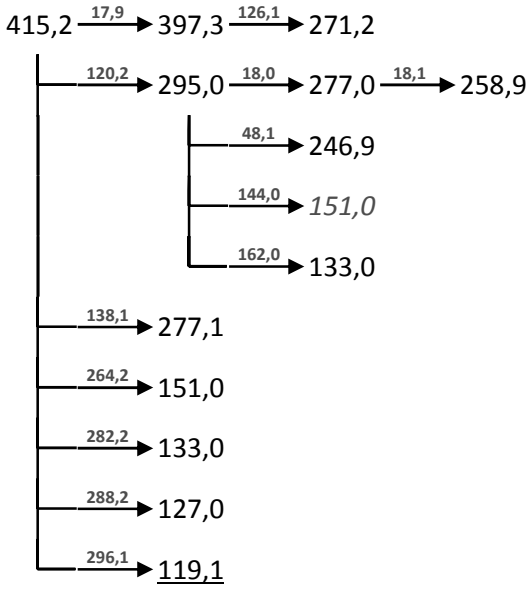

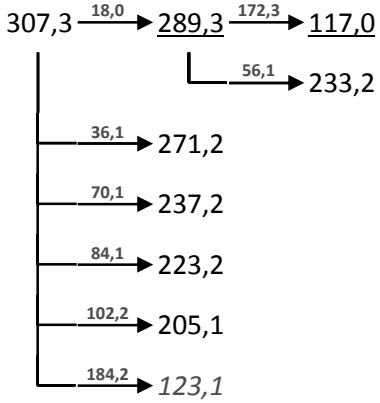

-MS^n

The abundance of the signals in question didn't suffice for a successful cycle of isolation and subsequent fragmentation.

isotopic fingerprint:

peak area / % of monoisotopic	**+1**	**+2**	**+3**
measured (415,4 Th):	29,2	10,1	5,9
measured (-413,1 Th):	17,3	-	-
measured (307,3 Th):	(75,5)	(9,4)	(25,8)
measured (-304,7 Th):	5,6	(25,8)	(4,1)

Figure XIII-XLI MS^n analysis of F10

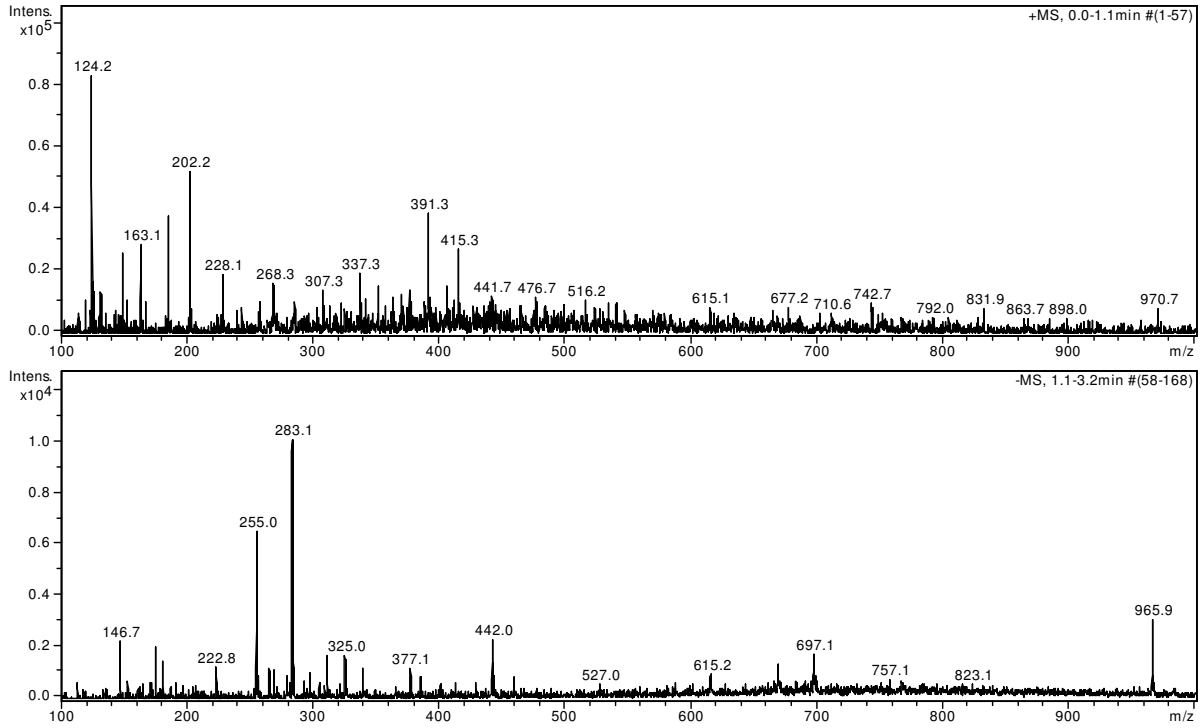

Figure XIII-XLII F10: 56,75 – 57,45 min, 1 ‰ FA, 56 % ACN in ddH_2O; full scan MS^1

XIII.III. 7 AS with N-Boc-L-Tyr and AbT in sodium phosphate buffer

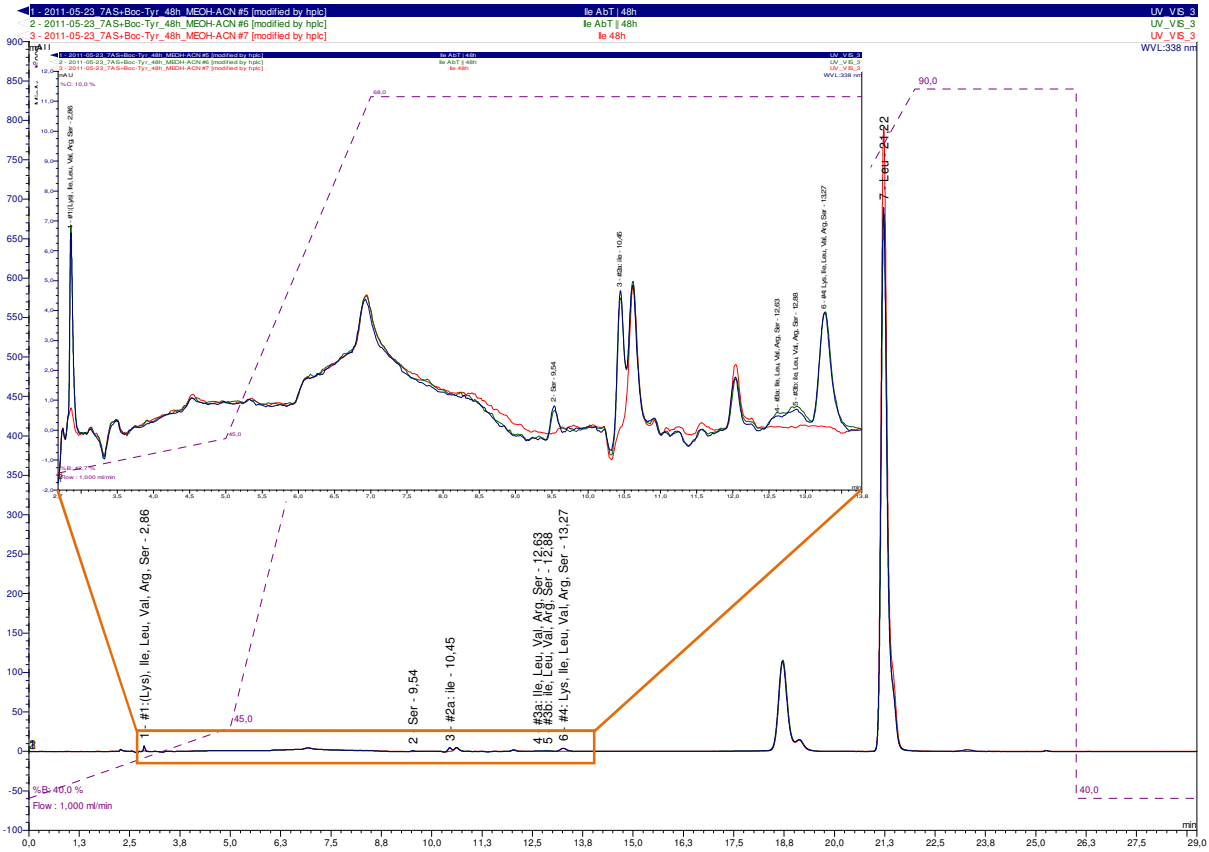

Figure XIII-XLIII Ile + Boc-Tyr with 2 U l^{-1} AbT, 24h; RP-HPLC-UVD after OPA-derivatisation

A == ddH_2O, B == ACN:MeOH:ddH_2O 45:45:10 (v+v+v),C == FA, 1% in ddH_2O (265 mM)

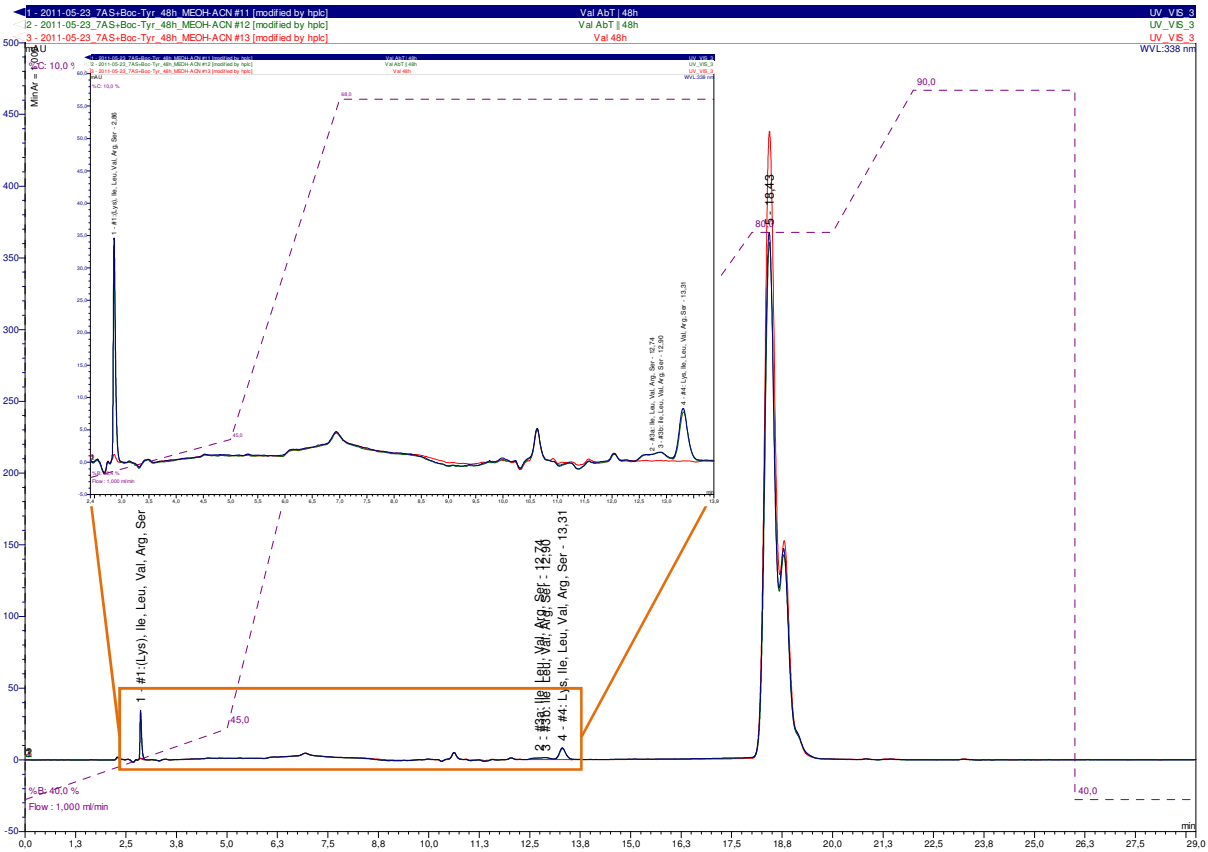

Figure XIII-XLIV Val + Boc-Tyr with 2 U l^{-1} AbT, 24h; RP-HPLC-UVD after OPA-derivatisation

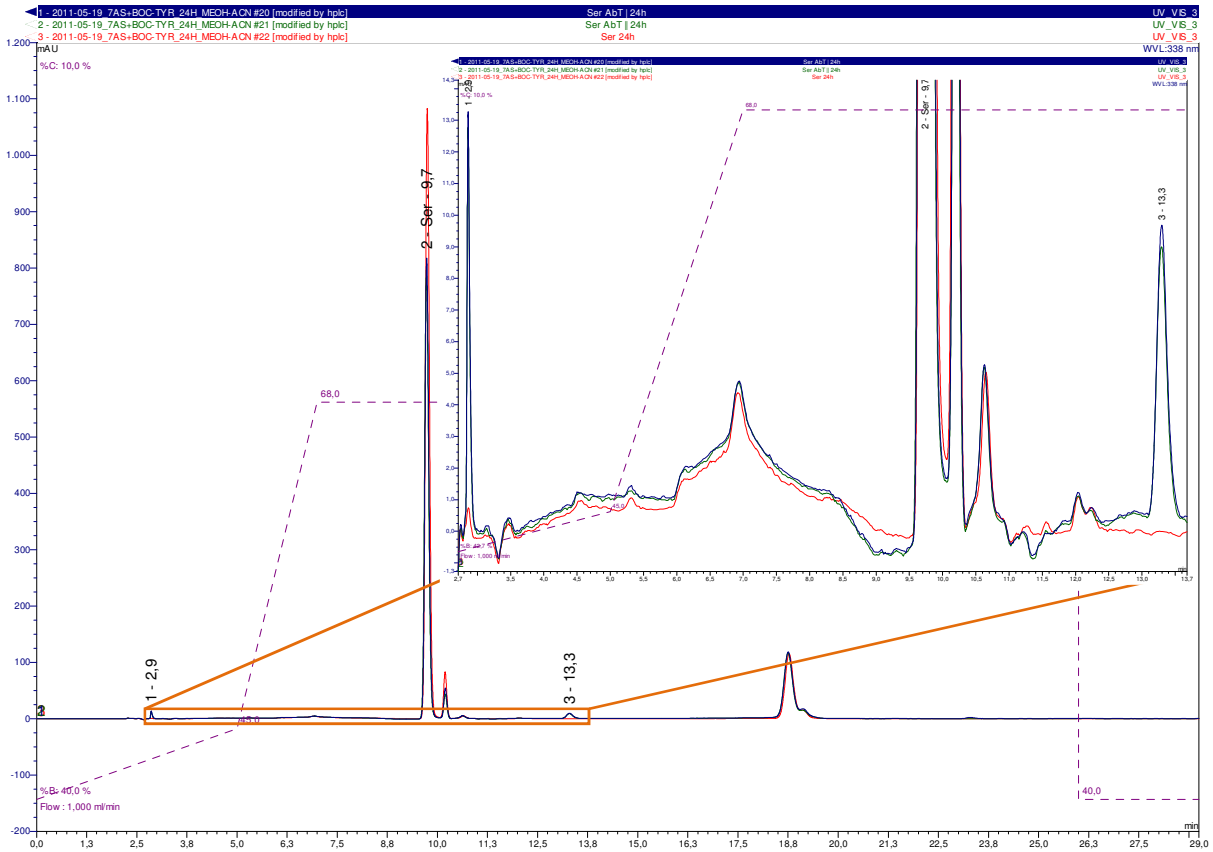

Figure XIII-XLV Ser + Boc-Tyr with 2 U l^{-1} AbT, 24h; RP-HPLC-UVD after OPA-derivatisation

XIII.III.I. Arg 274 nm 8 min

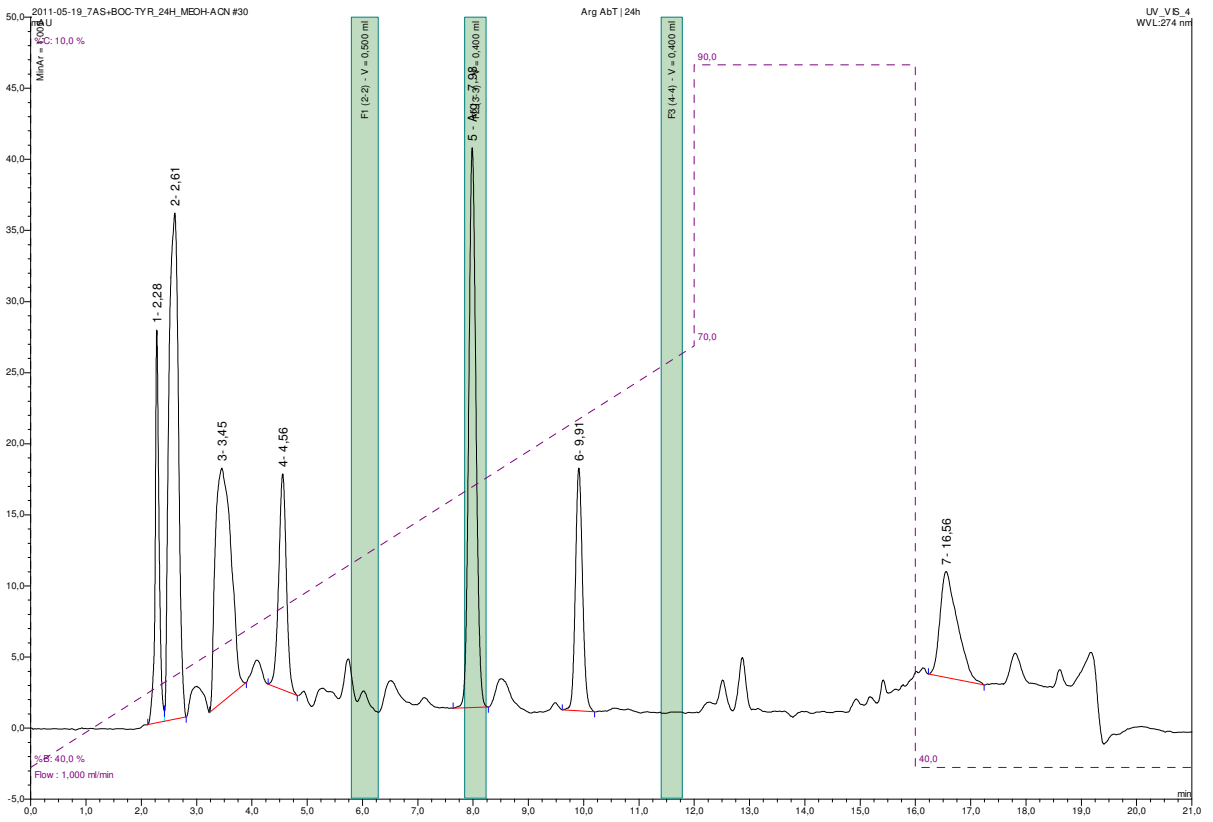

Figure XIII-XLVI Arg AbT | 24h; not derivatised: Fraction 2 was subjected to MS^n analysis.

+MS^n

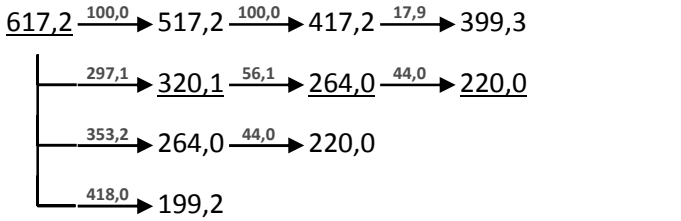
617,2
100,0
517,2
100,0
417,2
17,9
399,3
297,1
320,1
56,1
264,0
44,0
220,0
353,2
264,0
44,0
220,0
418,0
199,2

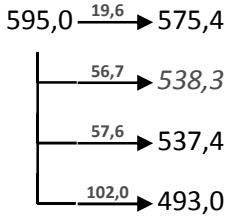
595,0
19,6
575,4
56,7
538,3
57,6
537,4
102,0
493,0

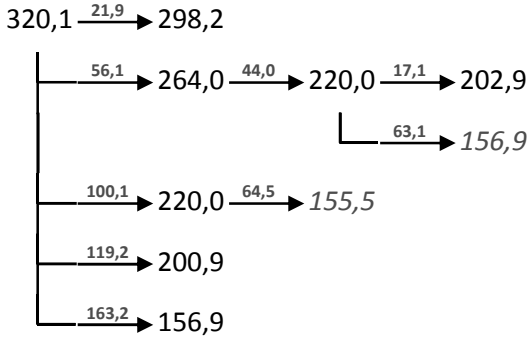
320,1
21,9
298,2
56,1
264,0
44,0
220,0
17,1
202,9
63,1
156,9
100,1
220,0
64,5
155,5
119,2
200,9
163,2
156,9

-MS^n

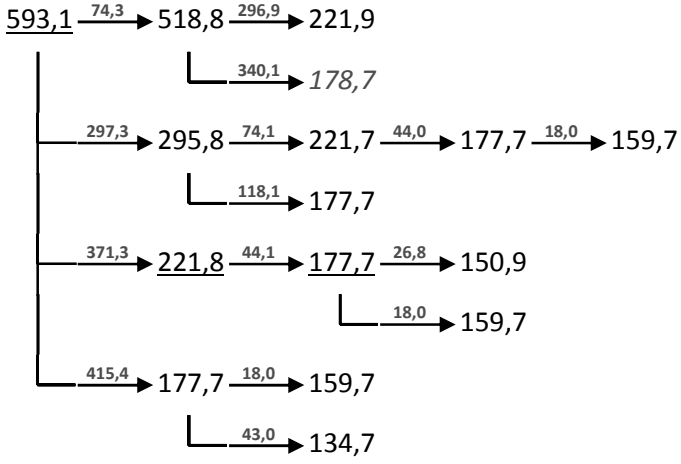
593,1
74,3
518,8
296,9
221,9
340,1
178,7
297,3
295,8
74,1
221,7
44,0
177,7
18,0
159,7
118,1
177,7
371,3
221,8
44,1
177,7
26,8
150,9
18,0
159,7
415,4
177,7
18,0
159,7
43,0
134,7

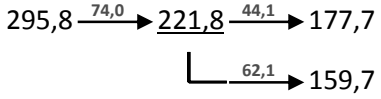
295,8
74,0
221,8
44,1
177,7
62,1
159,7

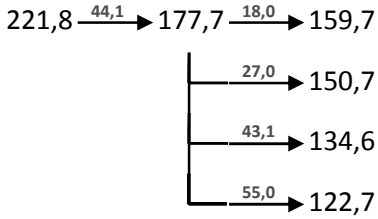

isotopic fingerprint:

peak area / % of monoisotopic	**+1**	**+2**	**+3**
theoretical ($C_{28}H_{37}N_2O_{12}^-$):	32,0	7,4	1,3
measured (-593,1 Th):	26,0	6,5	1,1
measured (595,0 Th):	26,6	4,5	1,7
theoretical ($C_{14}H_{18}NO_6^-$):	16,1	2,4	0,3
measured (-295,9 Th):	17,4	2,7	0,3
measured (298,1 Th):	(42,4)	(29,7)	(16,4)

Figure XIII-XLVII MS^n analysis of Arg 274 nm 8 min

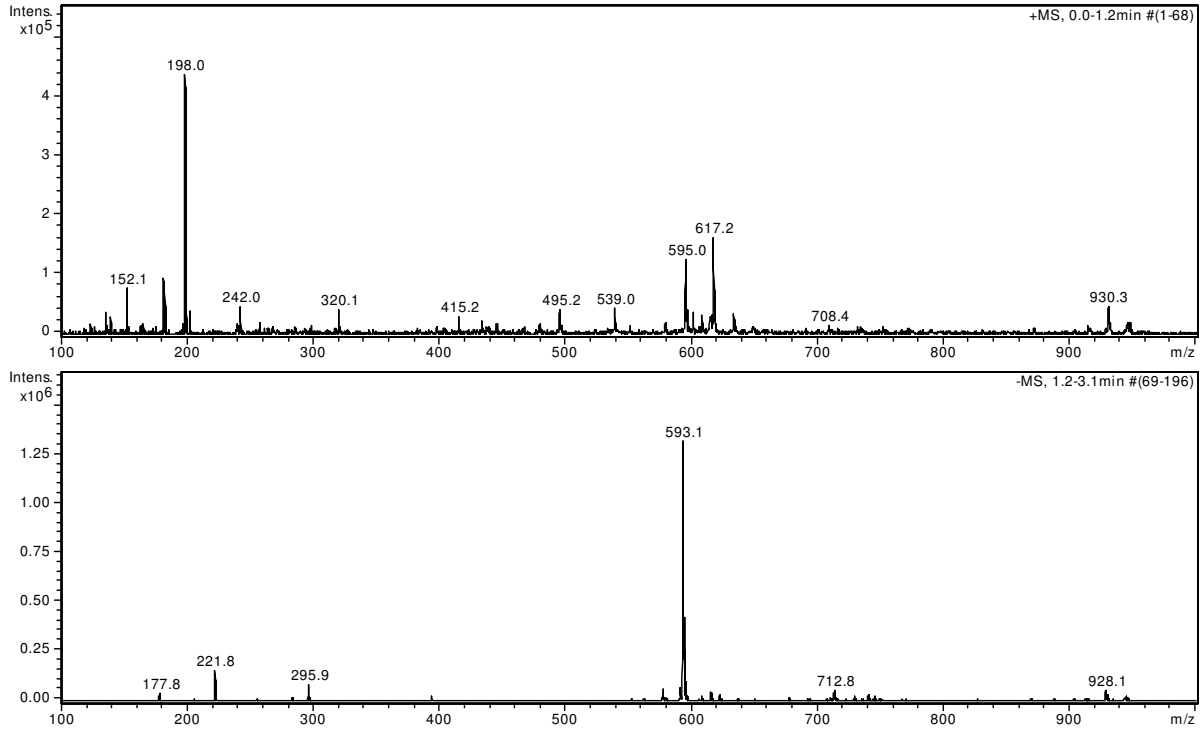

Figure XIII-XLVIII Arg 274 nm 8 min: 27 % MeOH, 27 % ACN, 1 ‰ FA in ddH_2O; full scan MS^1

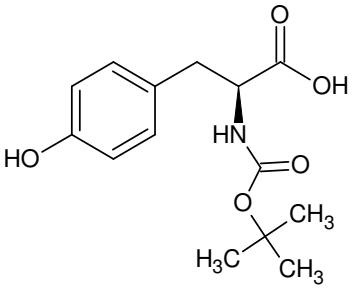

L-Boc-Tyr-OH

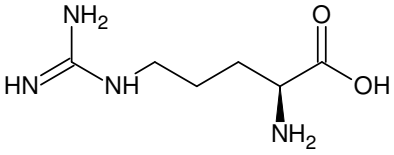

L-Arg

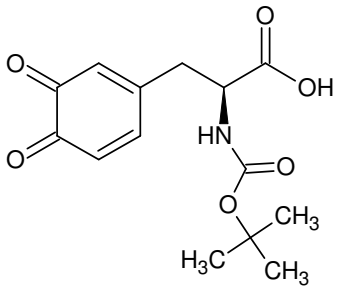

Monoisotopic Mass = 295.105587 Da

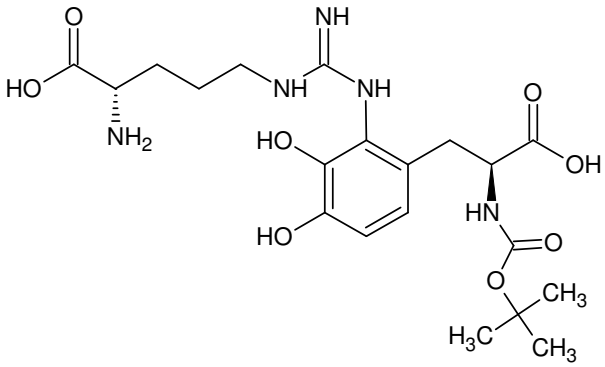

Monoisotopic Mass = 469.217263 Da

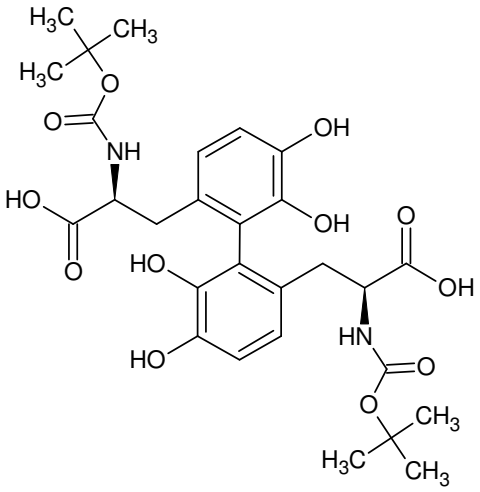

Monoisotopic Mass = 592.226825 Da

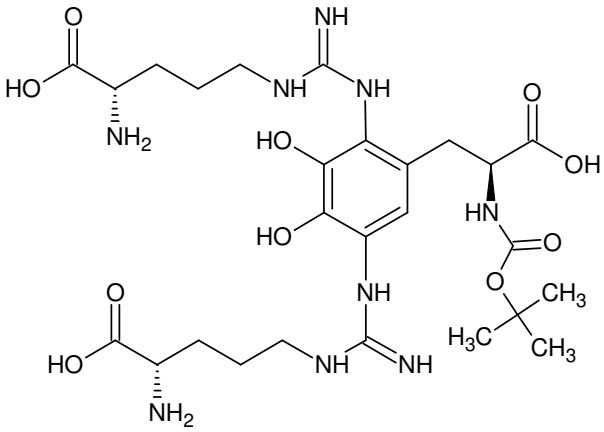

Monoisotopic Mass = 641.313289 Da

MS^n [Arg 274 nm 8 min]: quinone reactions

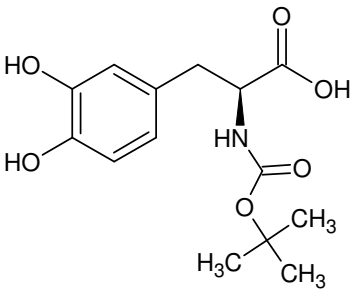

Monoisotopic Mass = 297.121237 Da

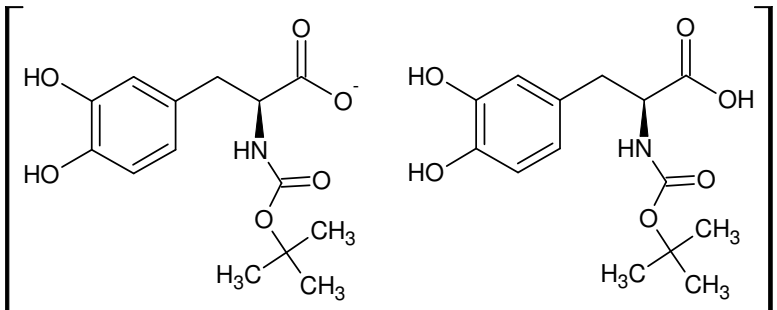

Monoisotopic Mass = 593.235198 Da

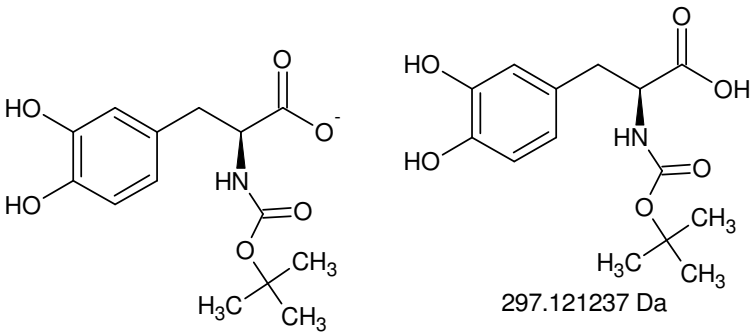

297.121237 Da

Monoisotopic Mass = 296.113961 Da

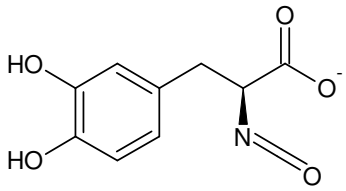

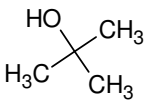

74.073165 Da

Monoisotopic Mass = 222.040796 Da

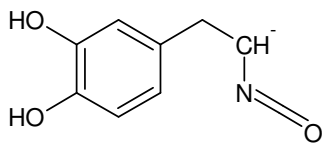

43.989829 Da

Monoisotopic Mass = 178.050967 Da

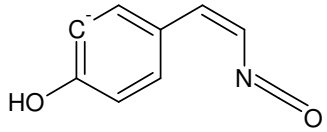

H_2O
18.010565 Da

Monoisotopic Mass = 160.040402 Da

-MSn [Arg 274 nm 8 min]:297 Da as well as 593 -> 296 -> 222 -> 178 -> 160

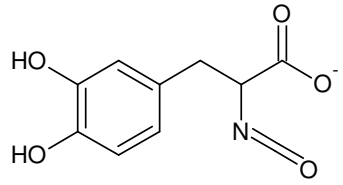

Monoisotopic Mass = 222.040796 Da

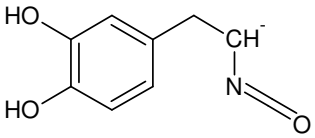

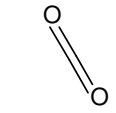

43.989829 Da

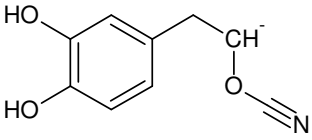

Gefundene Verbindungen: 4
CHN MG=27,0108986
C_2H_3 MG=27,0234738
$H_{11}O$ MG=27,0809856
$H_{13}N$ MG=27,1047938

Monoisotopic Mass = 178.050967 Da

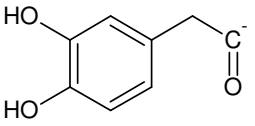

27.010899 Da

Monoisotopic Mass = 151.040068 Da

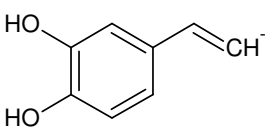

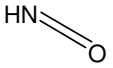

43.005814 Da

Monoisotopic Mass = 135.045153 Da

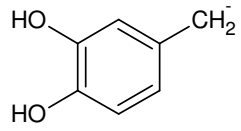

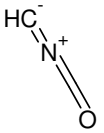

55.005814 Da

Monoisotopic Mass = 123.045153 Da

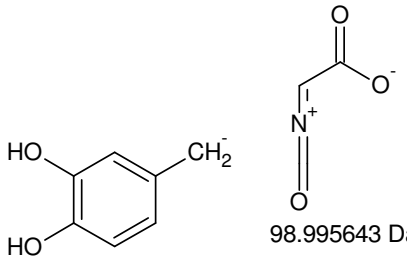

98.995643 Da

Monoisotopic Mass = 123.045153 Da

-MSn [Arg 274 nm 8 min]: [593 -> 296 -> 222] -> 178 -> 151, 135, 123

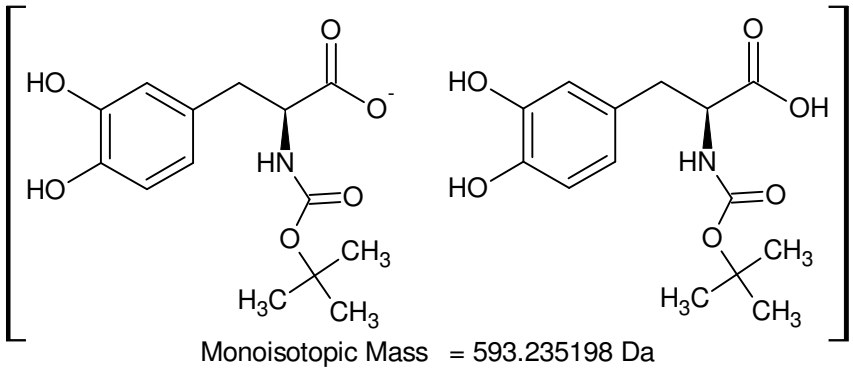

Monoisotopic Mass = 593.235198 Da

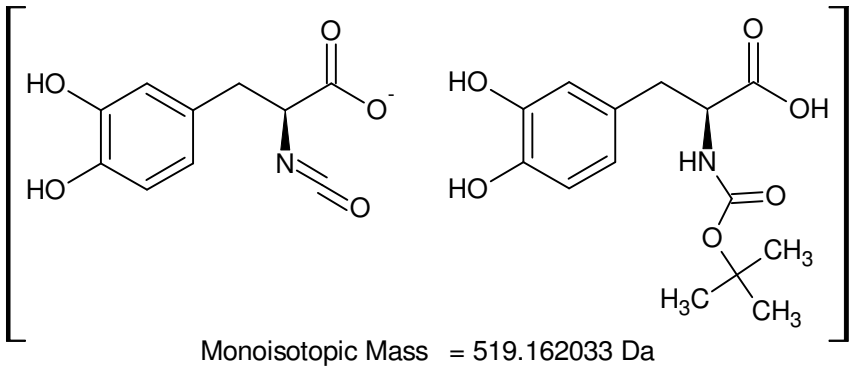

Monoisotopic Mass = 519.162033 Da

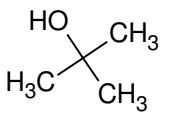

74.073165 Da

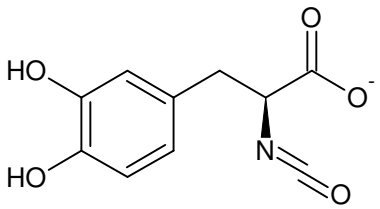

Monoisotopic Mass = 222.040796 Da

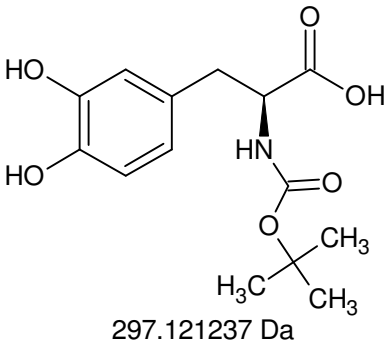

297.121237 Da

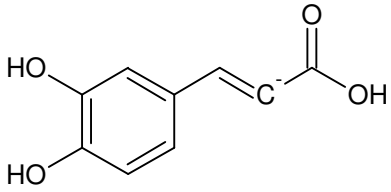

Monoisotopic Mass = 179.034982 Da

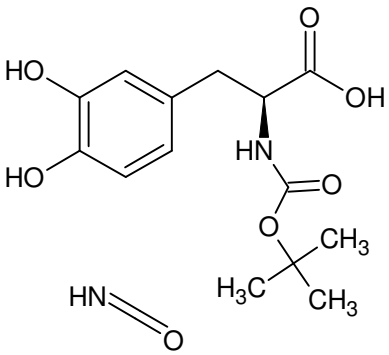

340.127051 Da

-MSn [Arg 274 nm 8 min]: 593 -> 519 -> 222, 179

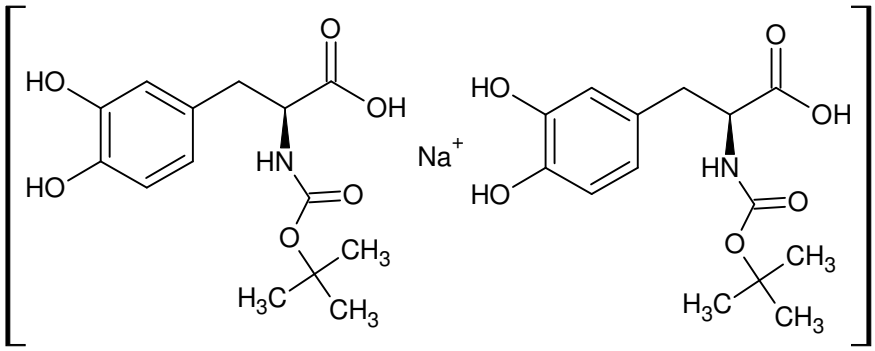

Monoisotopic Mass = 617.231696 Da

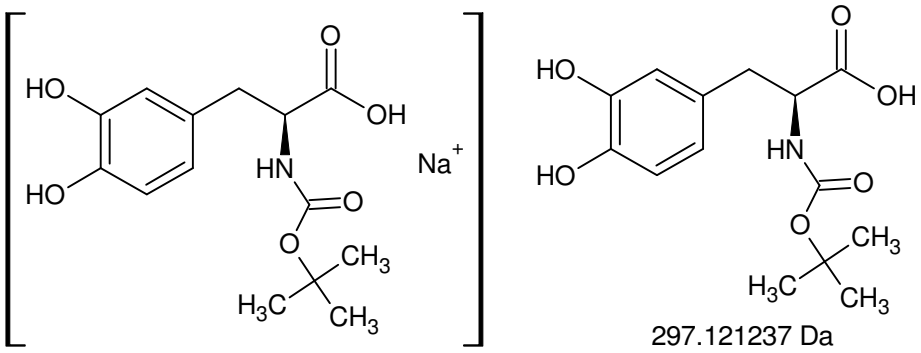

297.121237 Da

Monoisotopic Mass = 320.110459 Da

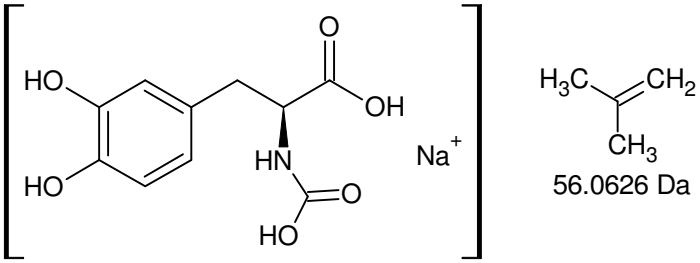

56.0626 Da

Monoisotopic Mass = 264.047858 Da

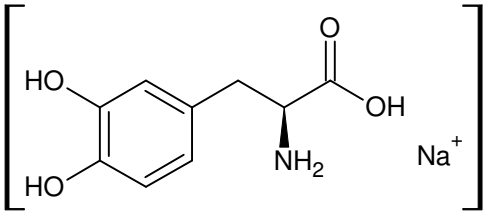

43.989829 Da

Monoisotopic Mass = 220.058029 Da

+MSn [Arg 274 nm 8 min]: 617 -> 320 -> 264 -> 220

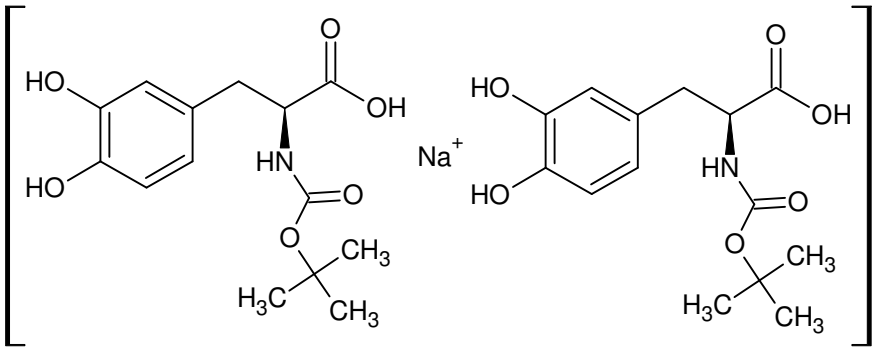

Monoisotopic Mass = 617.231696 Da

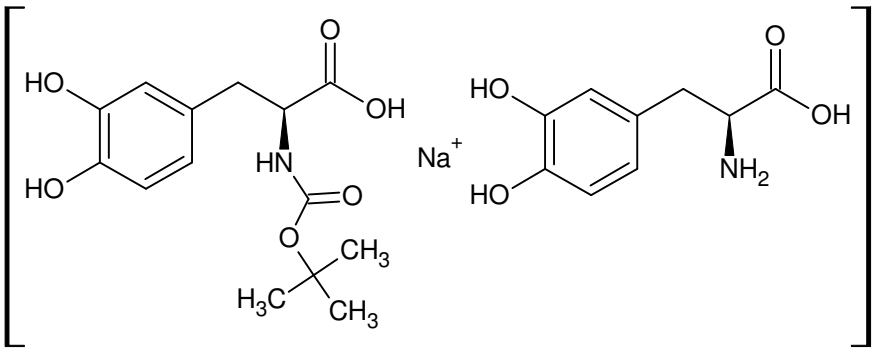

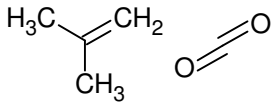

100.052429 Da

Monoisotopic Mass = 517.179267 Da

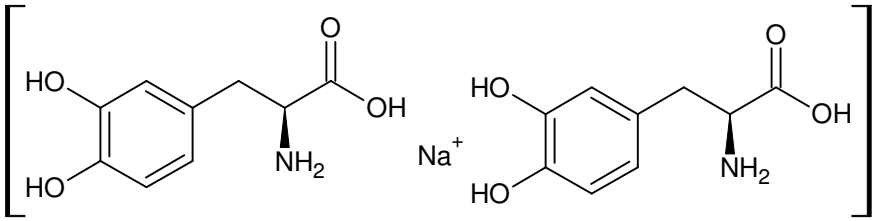

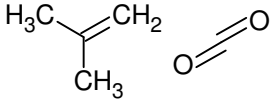

100.052429 Da

Monoisotopic Mass = 417.126837 Da

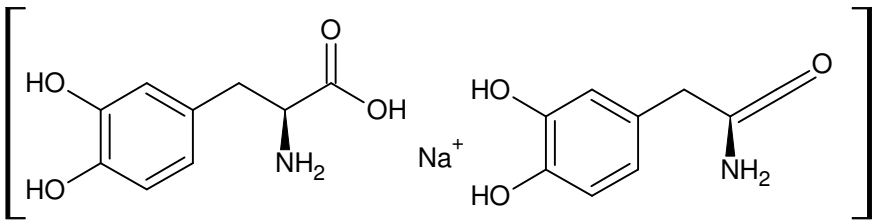

H_2O
18.010565 Da

Monoisotopic Mass = 399.116272 Da

+MSn [Arg 274 nm 8 min]: 617 -> 517 -> 417 -> 399

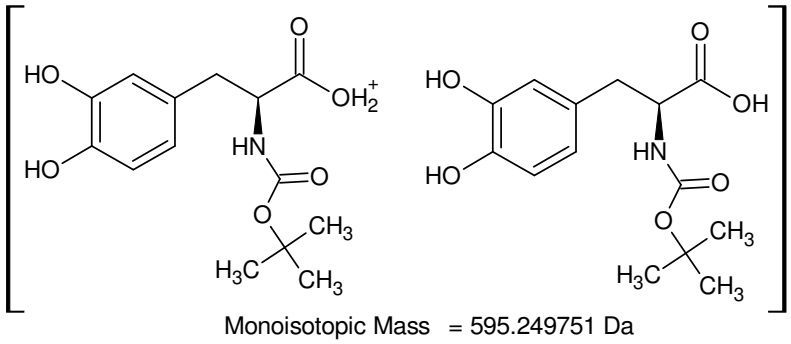

Gefundene Verbindungen: 3
H_4O MG=20,0262134
CH_8 MG=20,0625968
H_6N MG=20,0500216

Monoisotopic Mass = 595.249751 Da

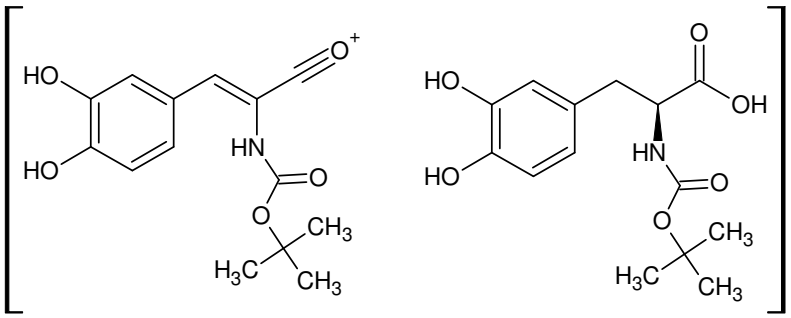

H_2O H_2
20.026215 Da

Monoisotopic Mass = 575.223536 Da

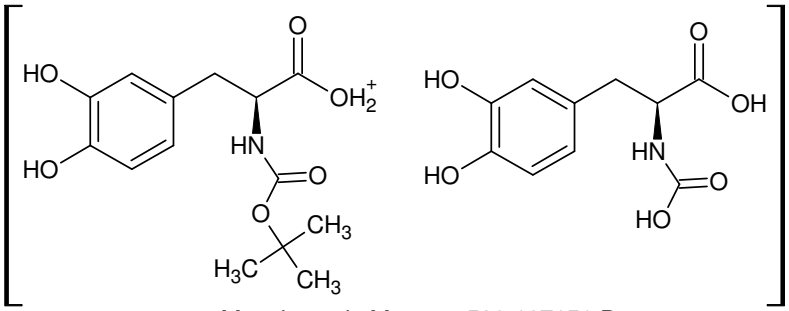

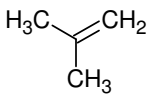

56.0626 Da

Monoisotopic Mass = 539.187151 Da

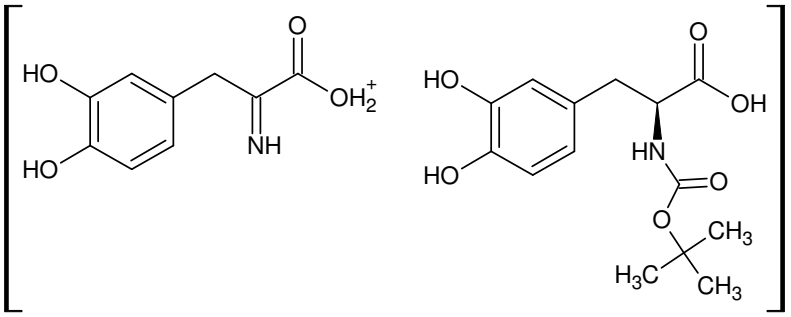

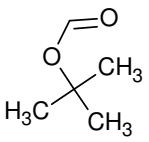

102.06808 Da

Monoisotopic Mass = 493.181672 Da

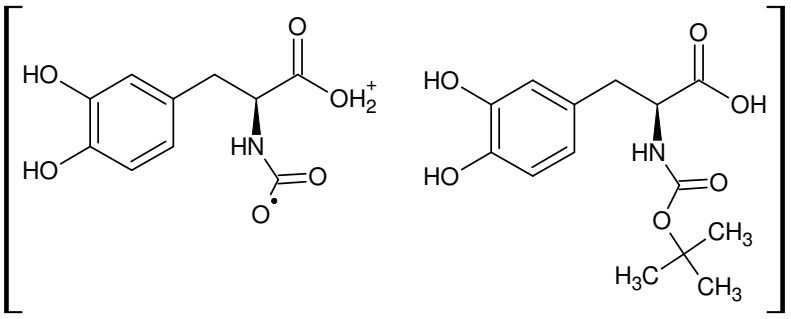

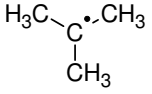

57.070425 Da

Monoisotopic Mass = 538.179326 Da

+MSn [Arg 274 nm 8 min]: 595 -> 575, 539, 493, (538)

XIII.III.II. **Arg 595 nm 6,8 min**

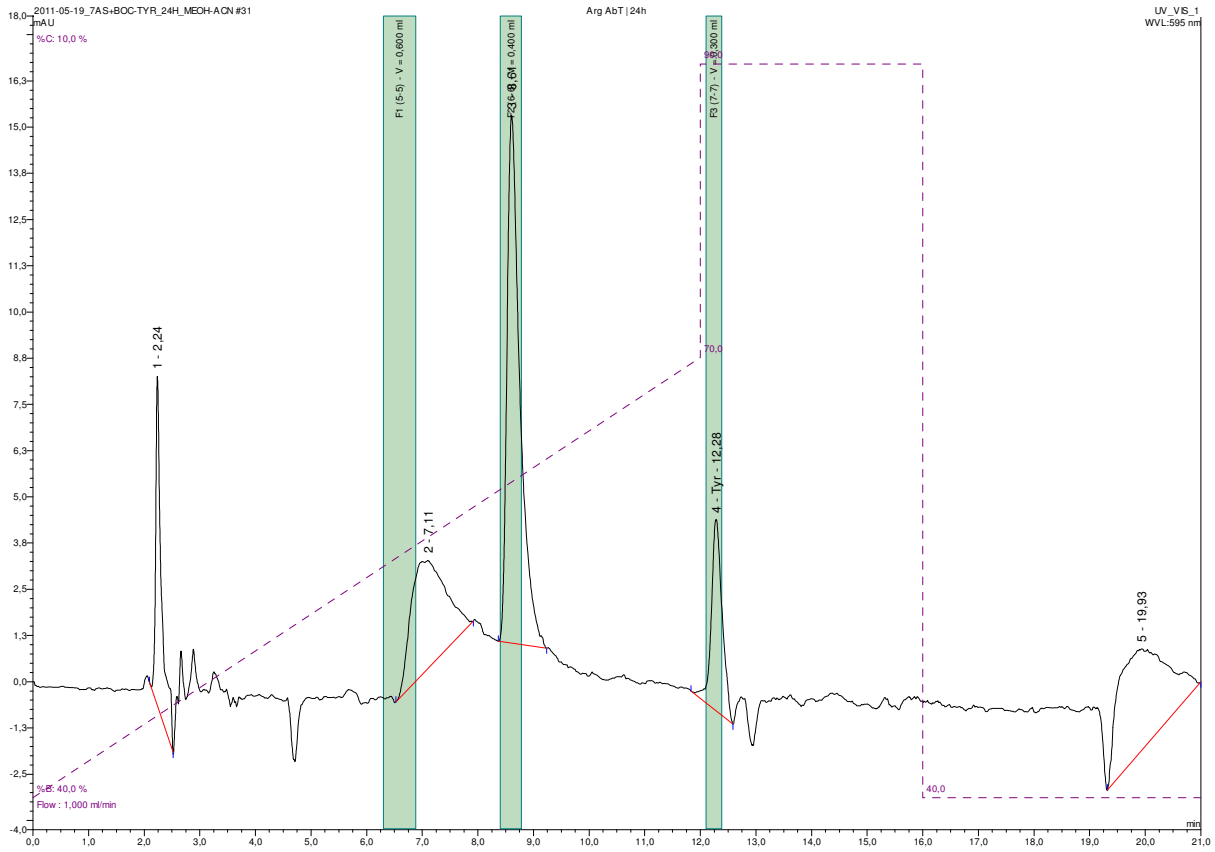

Figure XIII-XLIX Arg AbT | 24h; not derivatised: All three fractions were analysed using IT-MS^n.

+MS^n

403,2 —17,0→ 386,2 —56,0→ 330,2

403,2 —56,0→ **347,2** —17,1→ 330,1 —44,0→ 286,1 —17,0→ 269,1

347,2 —42,1→ 244,0

403,2 —44,1→ **303,1** —17,0→ **286,1** —17,0→ 269,1

303,1 —42,0→ **244,1** —17,0→ 227,1

303,1 —42,0→ 261,1 —17,0→ 244,1

303,1 —59,0→ 244,1 —17,1→ 227,0

303,1 —44,2→ 199,9

403,2 —61,1→ 286,1 —17,0→ 269,1 —17,1→ *252,0*

286,1 —42,1→ 244,0 —17,0→ 227,0

286,1 —28,8→ *215,2*

-MS^n

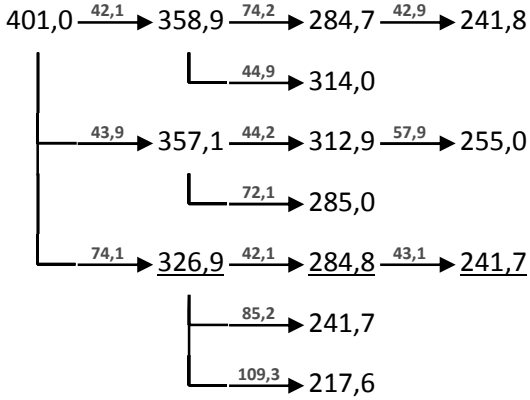

isotopic fingerprint:

peak area / % of monoisotopic	**+1**	**+2**	**+3**
theoretical ($C_{19}H_{23}N_4O_6^+$):	22,6	3,7	0,5
measured (403,2 Th):	34,4	14,4	11,7
measured (-401,0 Th):	25,1	14,9	5,6

Figure XIII-L MS^n analysis of Arg 595 nm 6,8 min

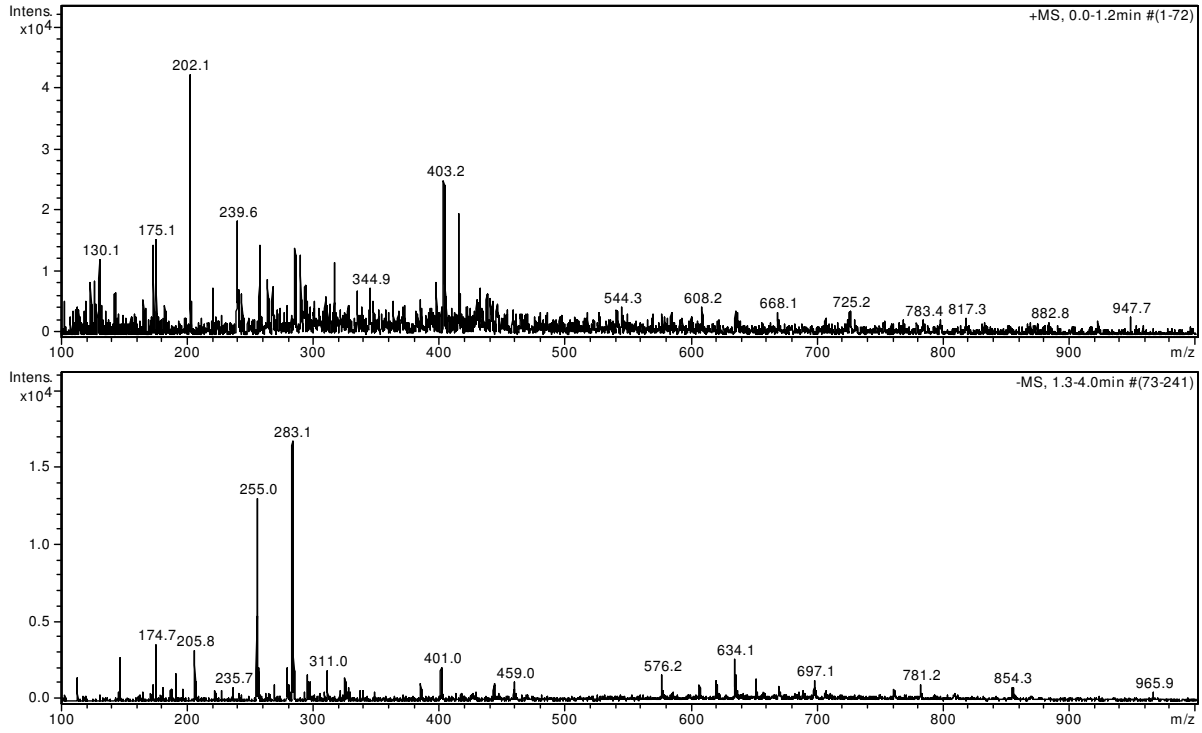

Figure XIII-LI Arg 595 nm 6,8 min: fraction 1; 25 % MeOH, 25 % ACN, 1 ‰ FA in ddH_2O; full scan MS^1

gerade nominelle Masse => gerade Anzahl an N-Atomen

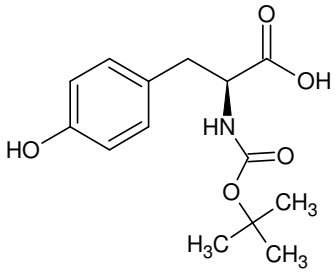

L-Boc-Tyr-OH

Monoisotopic Mass = 281.126323 Da

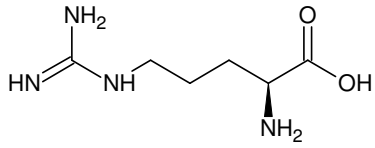

L-Arginin

Monoisotopic Mass = 174.111676 Da

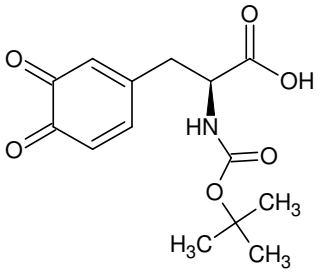

Monoisotopic Mass = 295.105587 Da

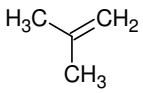

56.0626 Da

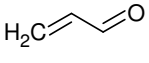

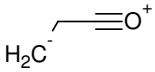

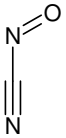

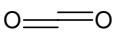

43.989829 Da

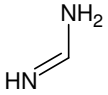

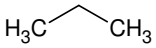

NH_3

17.026549 Da

$HO^{\bullet}$

$CH_3^{\bullet}$ H_2

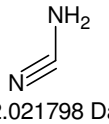

42.021798 Da

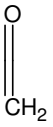

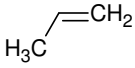

NH_3

17.026549 Da

$HO^{\bullet}$

=> freie Aminogruppe (Guanidino?) & Boc

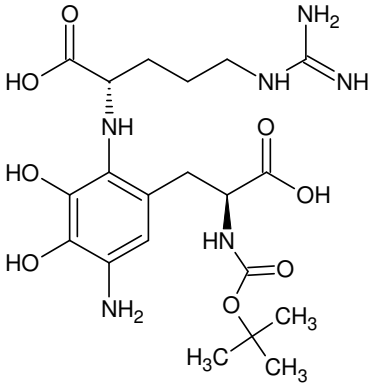

Monoisotopic Mass = 484.228162 Da

Gefundene Verbindungen: 13

CH2N2	MG=42,0217972
CH14O	MG=42,1044594
CH16N	MG=42,1282676
CNO	MG=41,997989
C2H2O	MG=42,0105642
C2H4N	MG=42,0343724
C2H18	MG=42,1408428
C3H6	MG=42,0469476
H10S	MG=42,050318
H12NO	MG=42,0918842
H10O2	MG=42,068076
H14N2	MG=42,1156924
N3	MG=42,009222

-----D--B--E--f-i-l-t-e-r-----

13.07.2011 - 11:47:13,71

akzeptierte DBEs:

-1 0 1 2 3 4 5 6 7 8

CH_2N_2	DBE: 2
C_2H_2O	DBE: 2
C_3H_6	DBE: 1

3 von 13 Summenformeln

Gefundene Verbindungen: 23

CH_2N_3	MG=56,0248712
$CH_{12}O_2$	MG=56,0837252
$CH_{14}NO$	MG=56,1075334
$CH_{16}N_2$	MG=56,1313416
$CH_{28}O$	MG=56,2140038
CN_2O	MG=56,001063
C_2H_2NO	MG=56,0136382
$C_2H_4N_2$	MG=56,0374464
$C_2H_{16}O$	MG=56,1201086
$C_2H_{18}N$	MG=56,1439168
C_2O_2	MG=55,98983
C_3H_4O	MG=56,0262134
C_3H_6N	MG=56,0500216
C_3H_{20}	MG=56,156492
C_4H_8	MG=56,0625968
H_8O_3	MG=56,0473418
$H_{10}NO_2$	MG=56,07115
$H_{12}N_2O$	MG=56,0949582
$H_{14}N_3$	MG=56,1187664
$H_{24}O_2$	MG=56,1776204
$H_{26}NO$	MG=56,2014286
$H_{28}N_2$	MG=56,2252368
N_4	MG=56,012296

-----D--B--E--f-i-l-t-e-r-----

06.06.2011 - 9:30:28,35

akzeptierte DBEs:

0 1 2 3 4 5 6

CN_2O	DBE: 3
$C_2H_4N_2$	DBE: 2
C_2O_2	DBE: 3
C_3H_4O	DBE: 2
C_4H_8	DBE: 1
N_4	DBE: 3

6 von 23 Summenformeln

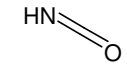

43.005814 Da

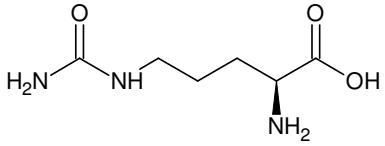

L-Citrullin

Monoisotopic Mass = 175.095691 Da

+MSn [Arg 595 nm 6,8 min]: main fragmentation route 403 Th

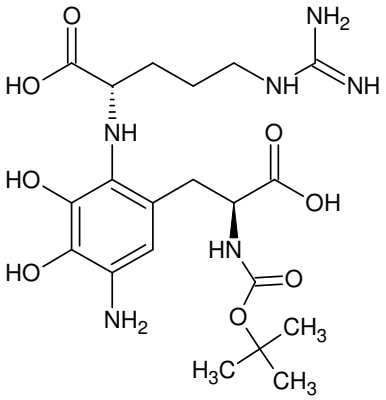

Molecular Formula = $C_{20}H_{32}N_6O_8$
Monoisotopic Mass = 484.228162 Da

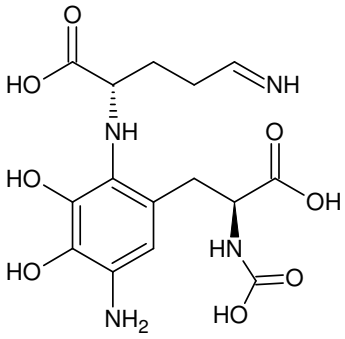

Molecular Formula = $C_{15}H_{20}N_4O_8$
Monoisotopic Mass = 384.128114 Da

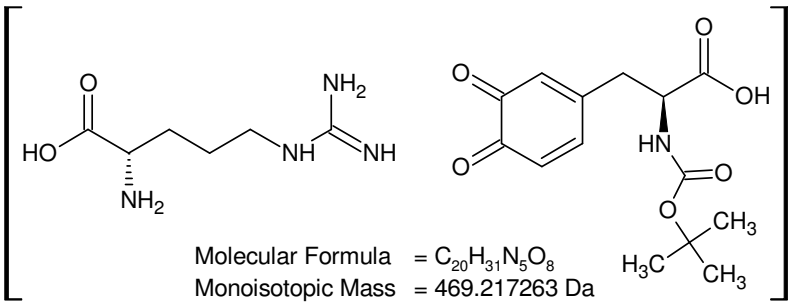

Molecular Formula = $C_{20}H_{31}N_5O_8$
Monoisotopic Mass = 469.217263 Da

469 + 1 - 403 = 67
Gefundene Verbindungen: 31
CH7O3 MG=67,0395172
CH9NO2 MG=67,0633254
(...)
H23N2O MG=67,1810288
H25N3 MG=67,204837

-----D--B--E--f-i-l-t-e-r-----
13.07.2011 - 15:25:40,48
akzeptierte DBEs:
-2 -1 0 1 2 3 4 5 6 7 8

C_2HN_3 DBE: 4
C_3HNO DBE: 4
C_4H_5N DBE: 3
H_5NO_3 DBE: -1
CH_9NO_2 DBE: -2
H_9N_3O DBE: -2

6 von 31 Summenformeln

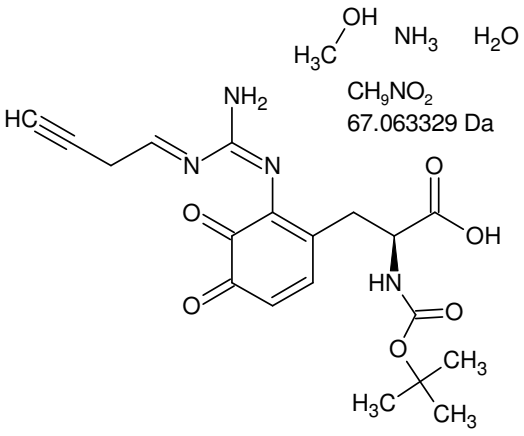

CH_9NO_2
67.063329 Da

Molecular Formula = $C_{19}H_{22}N_4O_6$
Monoisotopic Mass = 402.153934 Da

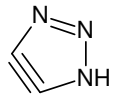

C_2HN_3
67.017047 Da

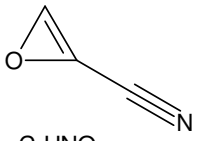

C_3HNO
67.005814 Da

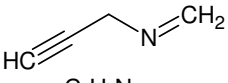

C_4H_5N
67.042199 Da

NH_3 H_2O $O{=}O$
H_5NO_3
67.026943 Da

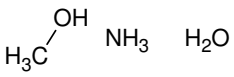

CH_9NO_2
67.063329 Da

NH_3 NH_3 NH_3 **O:**
H_9N_3O
67.074562 Da

402 Da [Arg 595 nm 6,8 min]: Arg & o-Dopachinone

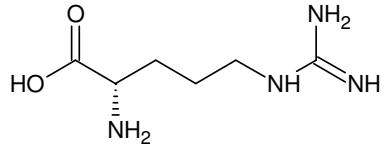

Molecular Formula = $C_6H_{14}N_4O_2$
Monoisotopic Mass = 174.111676 Da

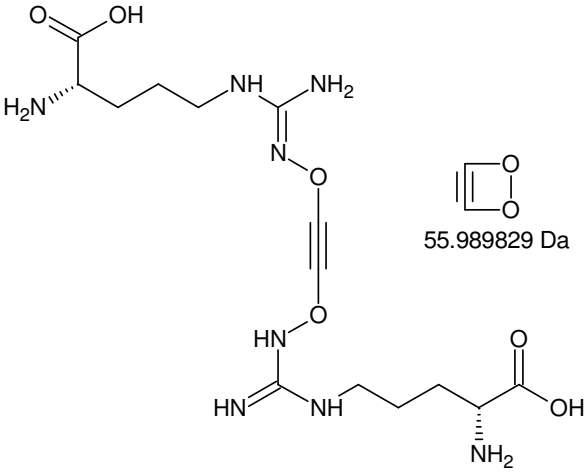

Monoisotopic Mass = 402.197531 Da

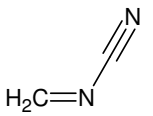

$C_2H_2N_2$
54.021798 Da

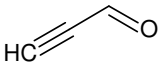

C_3H_2O
54.010565 Da

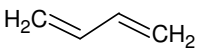

C_4H_6
54.04695 Da

$H_2O\ H_2O\ H_2O$

H_6O_3
54.031694 Da

55.989829 Da

2*174 - 402 = **-54**
Gefundene Verbindungen: 25

CH10O2	MG=54,068076
CH10S	MG=54,050318
(...)	
H24NO	MG=54,1857794
H26N2	MG=54,2095876

-----D--B--E--f-i-l-t-e-r-----
26.07.2011 - 11:10:35,52
akzeptierte DBEs:
-2 -1 0 1 2 3 4 5 6 7 8

$C_2H_2N_2$	DBE: 3
C_3H_2O	DBE: 3
C_4H_6	DBE: 2
H_6OS	DBE: -2
H_6O_3	DBE: -2

5 von 25 Summenformeln

Die beobachteten Fragmente 56 Da, 44 Da (+MSn) sowie 74 Da und 43 Da (-MSn) sind mit diesem Strukturtyp nur schwer zu erklären (kein Boc).

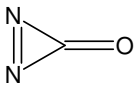

CN_2O
56.001063 Da

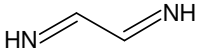

$C_2H_4N_2$
56.037448 Da

C_2O_2
55.989829 Da

C_2S
55.97207 Da

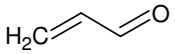

C_3H_4O
56.026215 Da

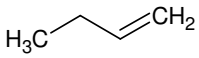

C_4H_8
56.0626 Da

N_4
56.012296 Da

2*174 - 402 - 2 = **-56**
Gefundene Verbindungen: 28

CH2N3	MG=56,0248712
CH12O2	MG=56,0837252
(...)	
H28N2	MG=56,2252368
N4	MG=56,012296

-----D--B--E--f-i-l-t-e-r-----
18.08.2011 - 15:25:53,28
akzeptierte DBEs:
-2 -1 0 1 2 3 4 5 6 7 8

CN_2O	DBE: 3
$C_2H_4N_2$	DBE: 2
C_2O_2	DBE: 3
C_2S	DBE: 3
C_3H_4O	DBE: 2
C_4H_8	DBE: 1
N_4	DBE: 3

7 von 28 Summenformeln

402 Da [Arg 595 nm 6,8 min]: 2x Arg

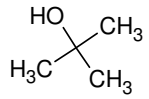

74.073165 Da

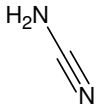

42.021798 Da

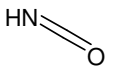

43.005814 Da

42 Da +/- 0,5 Da
Gefundene Verbindungen: 13

CH2N2	MG=42,0217972
CH14O	MG=42,1044594
CH16N	MG=42,1282676
CNO	MG=41,997989
C2H2O	MG=42,0105642
C2H4N	MG=42,0343724
C2H18	MG=42,1408428
C3H6	MG=42,0469476
H10S	MG=42,050318
H12NO	MG=42,0918842
H10O2	MG=42,068076
H14N2	MG=42,1156924
N3	MG=42,009222

-----D--B--E--f-i-l-t-e-r-----
18.08.2011 - 15:43:32,97
akzeptierte DBEs:
-2 -1 0 1 2 3 4 5 6 7 8

CH_2N_2	DBE: 2
C_2H_2O	DBE: 2
C_3H_6	DBE: 1

3 von 13 Summenformeln

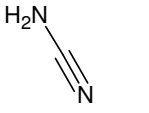

CH_2N_2
42.021798 Da

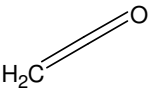

C_2H_2O
42.010565 Da

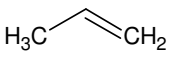

C_3H_6
42.04695 Da

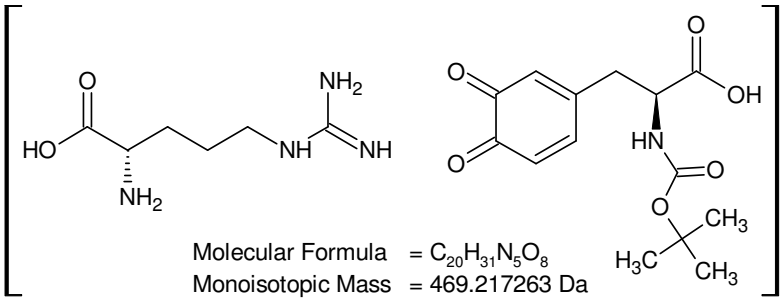

Molecular Formula = $C_{20}H_{31}N_5O_8$
Monoisotopic Mass = 469.217263 Da

CH_9NO_2
67.063329 Da

NH_3 NH_3 NH_3 O:
H_9N_3O
67.074562 Da

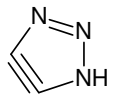

C_2HN_3
67.017047 Da

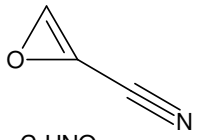

C_3HNO
67.005814 Da

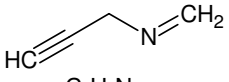

C_4H_5N
67.042199 Da

NH_3 H_2O O=O
H_5NO_3
67.026943 Da

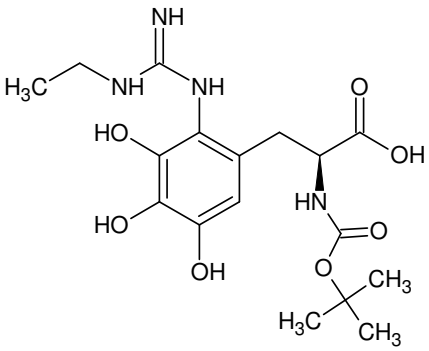

Monoisotopic Mass = 398.180149 Da

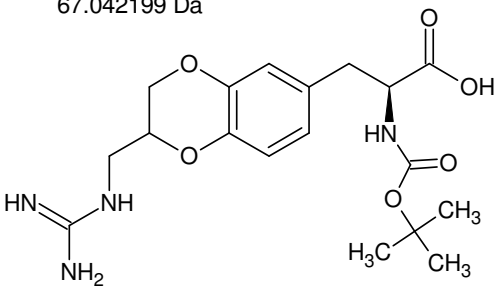

Monoisotopic Mass = 394.185235 Da

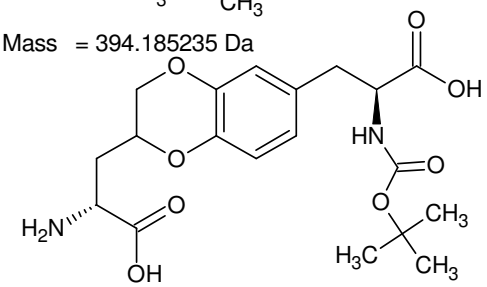

Monoisotopic Mass = 410.168916 Da

402 Da [Arg 595 nm 6,8 min]: fragment 42 Da, main fragmentation route -MSn

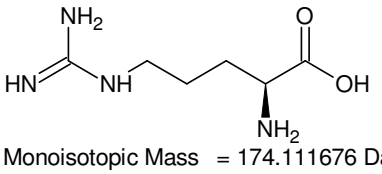

Monoisotopic Mass = 174.111676 Da

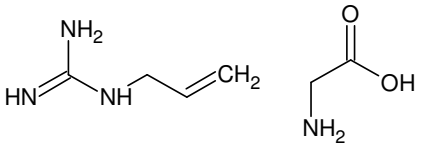

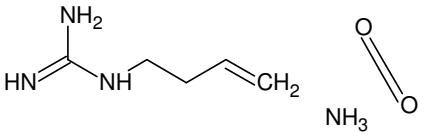

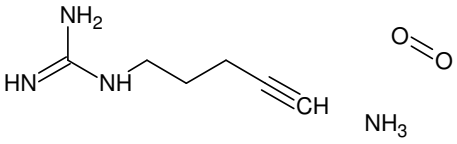

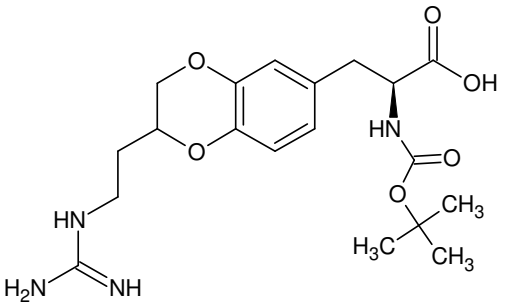

Monoisotopic Mass = 408.200885 Da

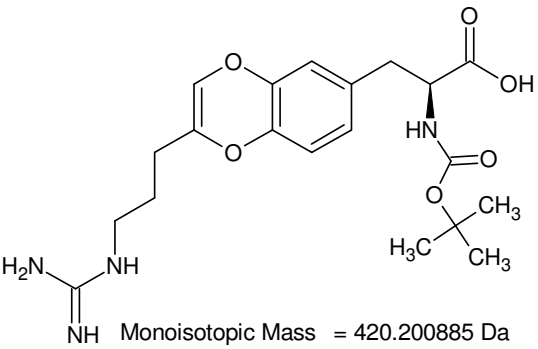

Monoisotopic Mass = 420.200885 Da

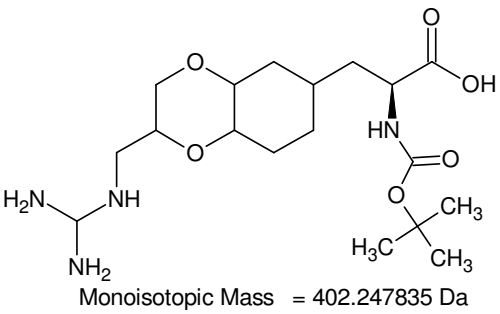

Monoisotopic Mass = 402.247835 Da

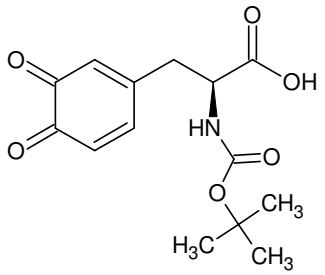

Monoisotopic Mass = 295.105587 Da

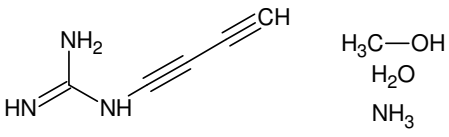

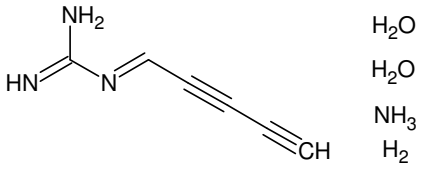

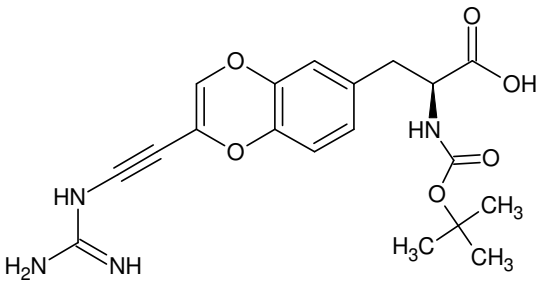

Monoisotopic Mass = 402.153934 Da

Unsättigung woher - durch Chinon?

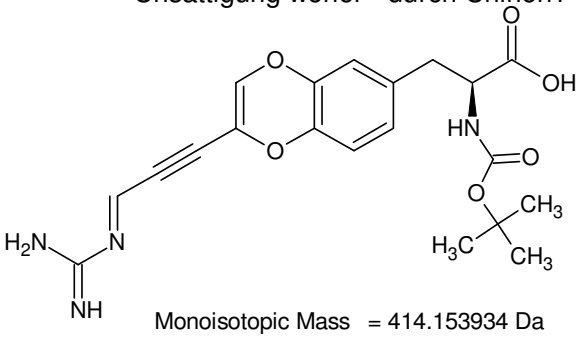

Monoisotopic Mass = 414.153934 Da

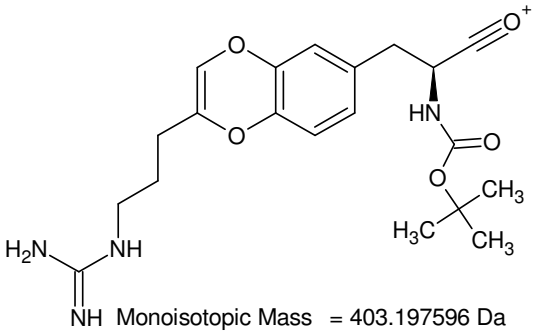

Monoisotopic Mass = 403.197596 Da

aber: -MS^n auf M-2 => $[M-H]^-$; konsekutiver Verlust von 2 x 44 Da im negativen Modus

MS^n [Arg 595 nm 6,8 min]: 402 Da {I/II}

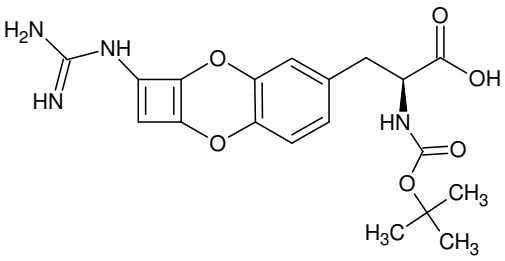

Monoisotopic Mass = 402.153934 Da

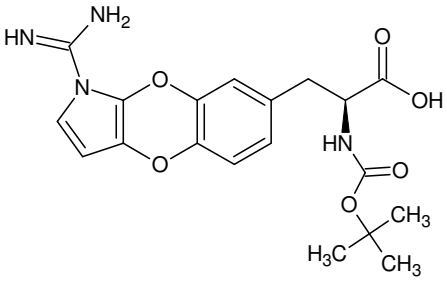

Monoisotopic Mass = 402.153934 Da

kein Fragment mit 26 oder 28 Da beobachtet

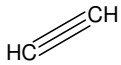

26.01565 Da

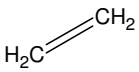

28.0313 Da

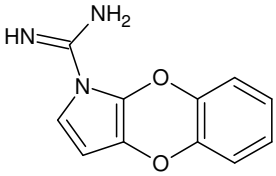

1*H*-[1,4]benzodioxino[2,3-*b*]pyrrol-1-carboximidamid
Absorptionsbande bei 625 nm? - fulvenartige Grenzstruktur (geladen) möglich
Unsättigung im Zuge der Aromatisierung?

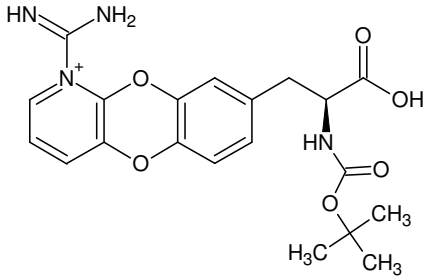

Monoisotopic Mass = 415.161211 Da

MS^n [Arg 595 nm 6,8 min]: 402 Da {II/II}

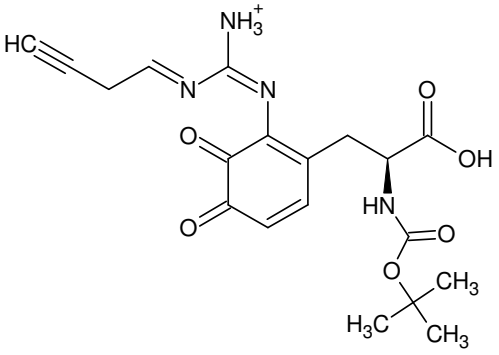

Monoisotopic Mass = 403.161211 Da

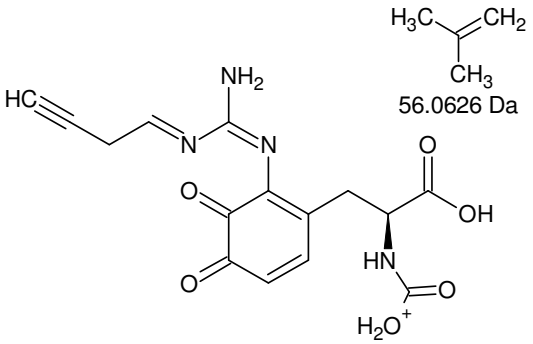

Monoisotopic Mass = 347.098611 Da

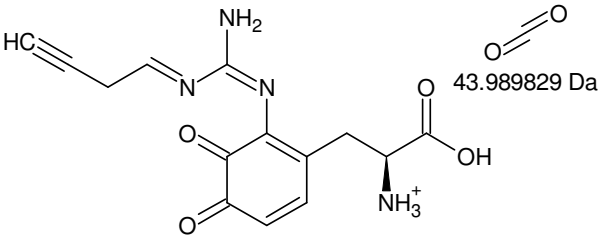

Monoisotopic Mass = 303.108781 Da

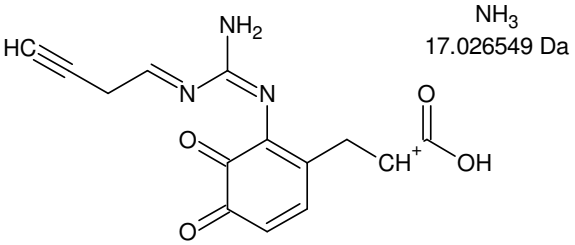

Monoisotopic Mass = 286.082232 Da

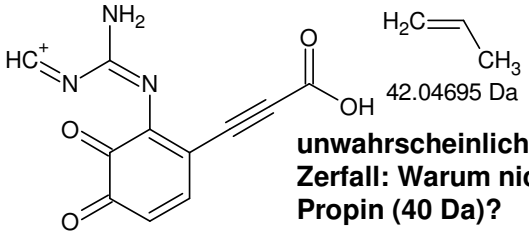

unwahrscheinlicher Zerfall: Warum nicht Propin (40 Da)?

Monoisotopic Mass = 244.035282 Da

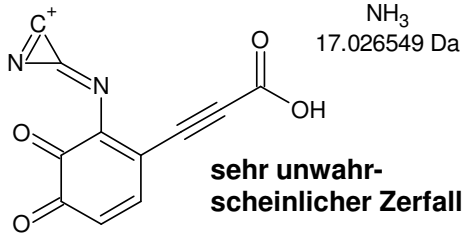

sehr unwahr-scheinlicher Zerfall

Monoisotopic Mass = 227.008733 Da

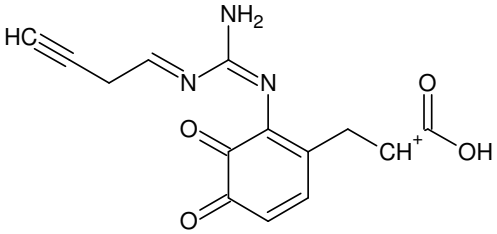

Monoisotopic Mass = 286.082232 Da

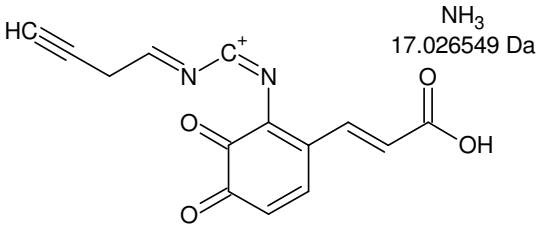

Monoisotopic Mass = 269.055683 Da

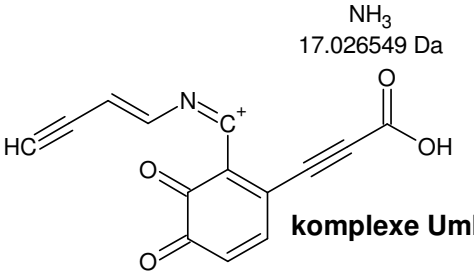

komplexe Umlagerung

Monoisotopic Mass = 252.029134 Da

X +MSn [Arg 595 nm 6,8 min]: 403 -> 347 -> 303 -> 286 ?> 244 -> 227 as well as 286 -> 269 X> (252) and 244 -> (215), 200 and also 403 -> 386 -> 330 {I/II}

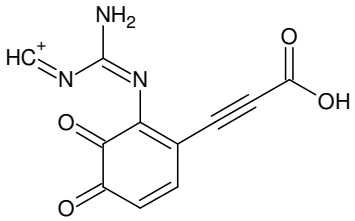

Monoisotopic Mass = 244.035282 Da

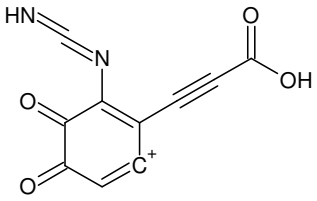

29.026549 Da

Monoisotopic Mass = 215.008733 Da

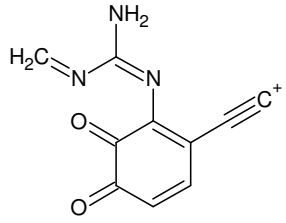

43.989829 Da

Monoisotopic Mass = 200.045453 Da

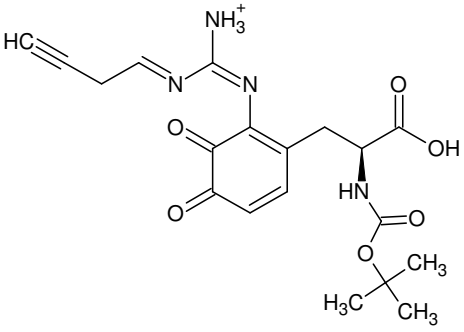

Monoisotopic Mass = 403.161211 Da

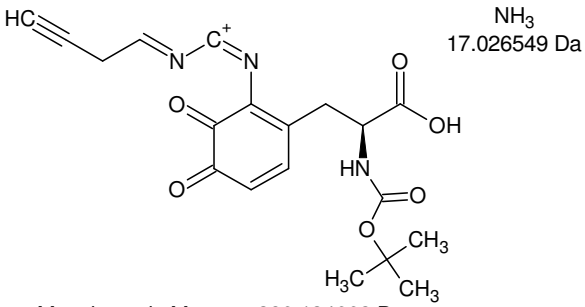

17.026549 Da

Monoisotopic Mass = 386.134662 Da

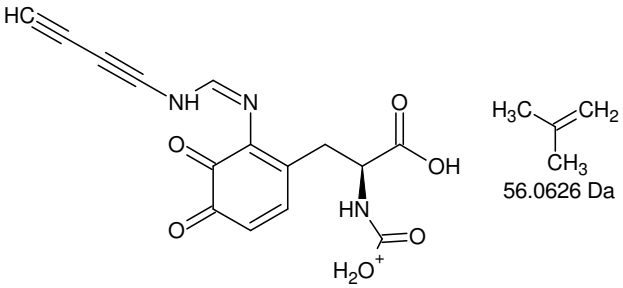

56.0626 Da

Monoisotopic Mass = 330.072062 Da

X +MSn [Arg 595 nm 6,8 min]: 403 -> 347 -> 303 -> 286 ?> 244 -> 227 as well as 286 -> 269 X> (252) and 244 -> (215), 200 and also 403 -> 386 -> 330 {II/II}

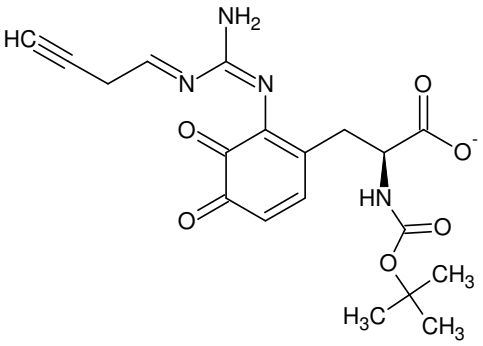

Monoisotopic Mass = 401.146658 Da

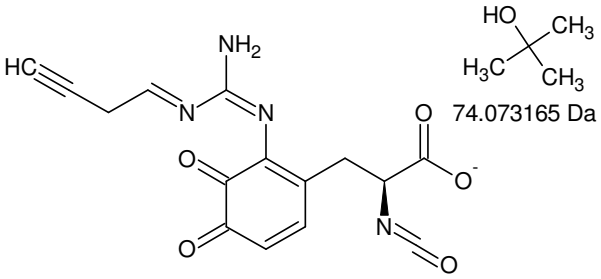

Monoisotopic Mass = 327.073493 Da

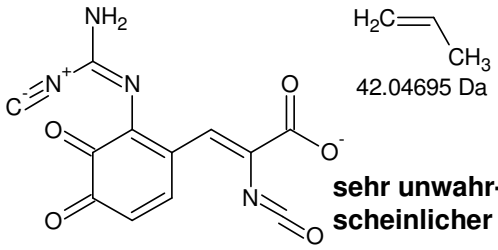

sehr unwahr-scheinlicher Zerfall

Monoisotopic Mass = 285.026543 Da

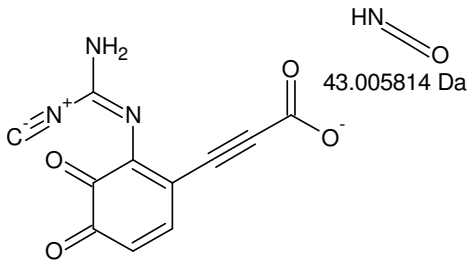

Monoisotopic Mass = 242.020729 Da

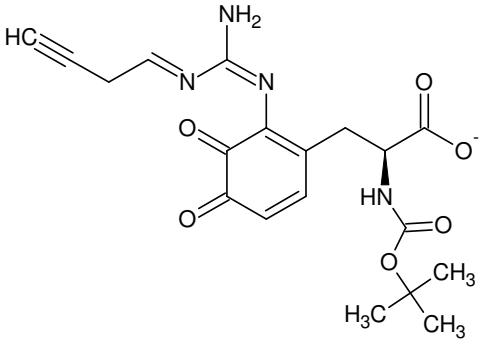

Monoisotopic Mass = 401.146658 Da

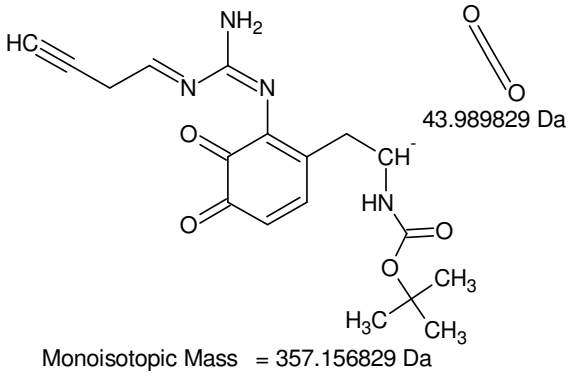

Monoisotopic Mass = 357.156829 Da

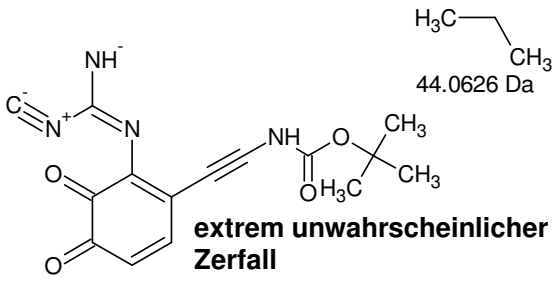

extrem unwahrscheinlicher Zerfall

Monoisotopic Mass = 313.094229 Da

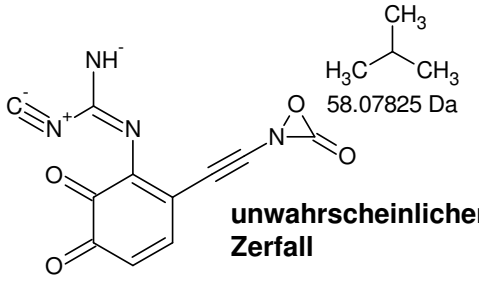

unwahrscheinlicher Zerfall

Monoisotopic Mass = 255.015978 Da

X -MSn [Arg 595 nm 6,8 min]: 401 -> 327 ?> 285 -> 242 and 401 -> 357 X> 313 -> 255 as well as 401 -> 359 ?> 314 {I/II}

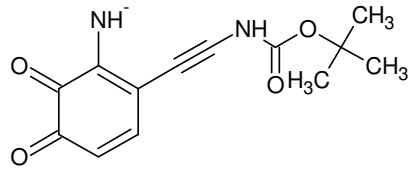

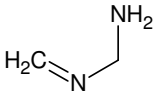

58.053098 Da

Monoisotopic Mass = 261.088081 Da

3 DBE zu wenig

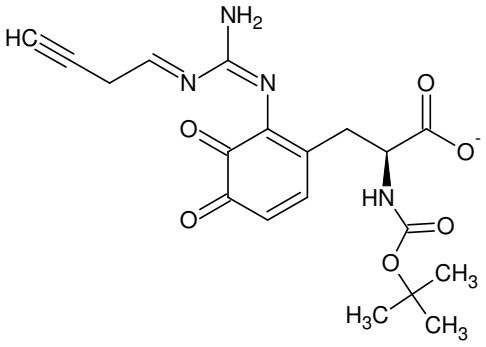

Monoisotopic Mass = 401.146658 Da

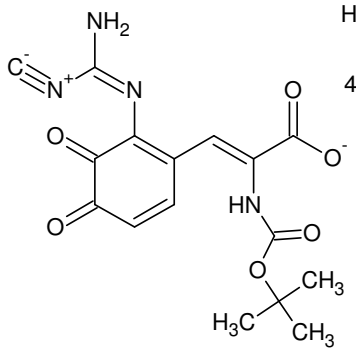

42.04695 Da

sehr unwahr-scheinlicher Zerfall

Monoisotopic Mass = 359.099708 Da

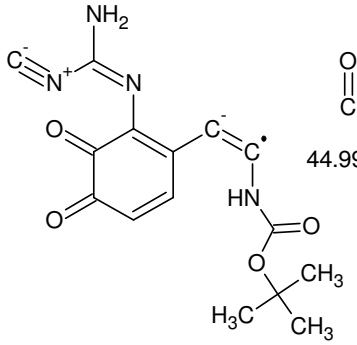

44.997654 Da

unwahrscheinlicher Zerfall: warum nicht -44 Da (CO_2)

Monoisotopic Mass = 314.102054 Da

X -MSn [Arg 595 nm 6,8 min]: 401 -> 327 ?> 285 -> 242 and 401 -> 357 X> 313 -> 255 as well as 401 -> 359 ?> 314 {I/II}

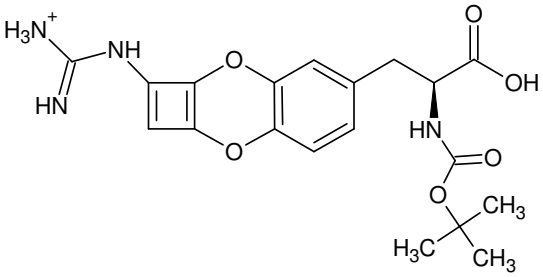

Monoisotopic Mass = 403.161211 Da

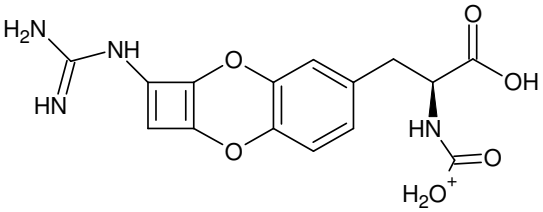

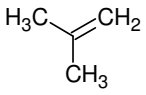

56.0626 Da

Monoisotopic Mass = 347.098611 Da

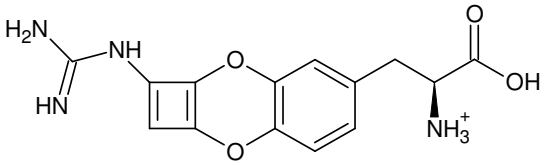

43.989829 Da

Monoisotopic Mass = 303.108781 Da

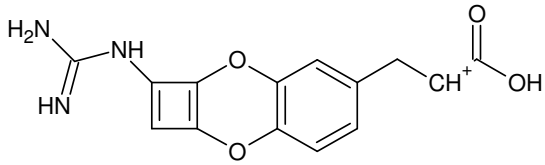

NH_3
17.026549 Da

Monoisotopic Mass = 286.082232 Da

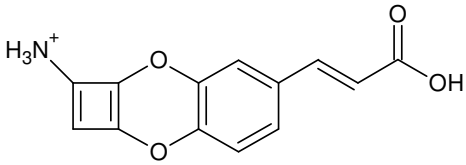

42.021798 Da

Monoisotopic Mass = 244.060434 Da

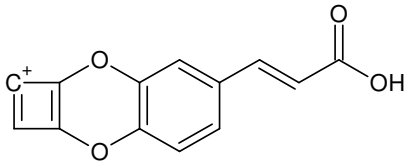

Monoisotopic Mass = 227.033885 Da

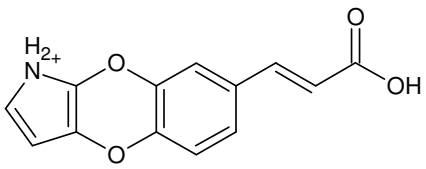

Monoisotopic Mass = 244.060434 Da

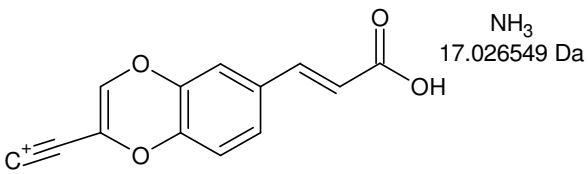

NH_3
17.026549 Da

Monoisotopic Mass = 227.033885 Da

Ladungslokalisation am N vorherrschend

+MSn [Arg 595 nm 6,8 min]: 403 -> 347 -> 303 -> 286 -> 244 -> 227 and 286 -> 269 -> (252) as well as 244 -> (215), 200 and also 403 -> 386 -> 330 {I/II}

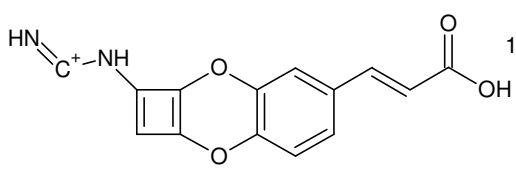

Monoisotopic Mass = 269.055683 Da

NH_3
17.026549 Da

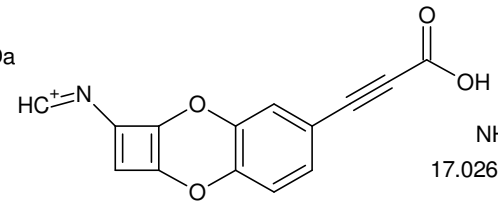

NH_3
17.026549 Da

Monoisotopic Mass = 252.029134 Da

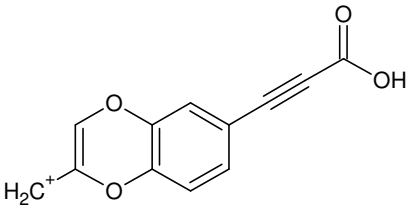

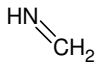

29.026549 Da

Monoisotopic Mass = 215.033885 Da

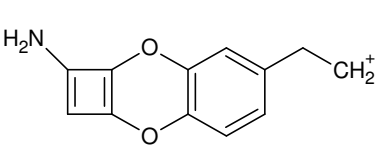

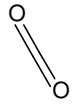

43.989829 Da

Monoisotopic Mass = 200.070605 Da

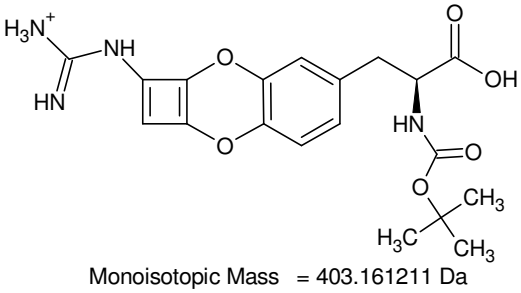

Monoisotopic Mass = 403.161211 Da

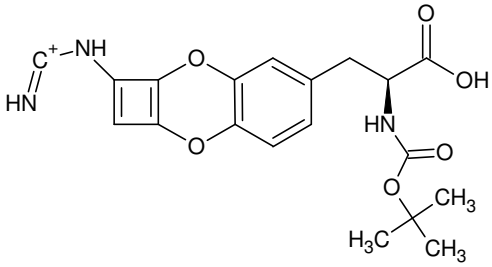

NH_3
17.026549 Da

Monoisotopic Mass = 386.134662 Da

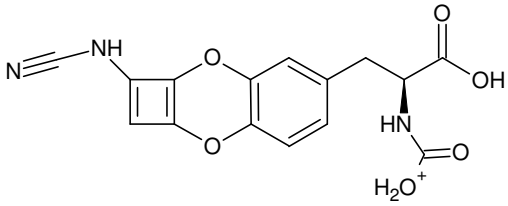

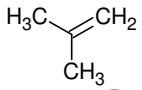

56.0626 Da

Monoisotopic Mass = 330.072062 Da

+MSn [Arg 595 nm 6,8 min]: 403 -> 347 -> 303 -> 286 -> 244 -> 227 and 286 -> 269 -> (252) as well as 244 -> (215), 200 and also 403 -> 386 -> 330 {II/II}

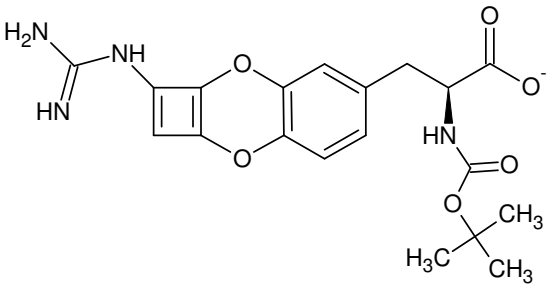

Monoisotopic Mass = 401.146658 Da

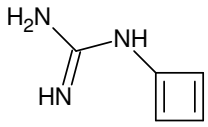

109.063997 Da

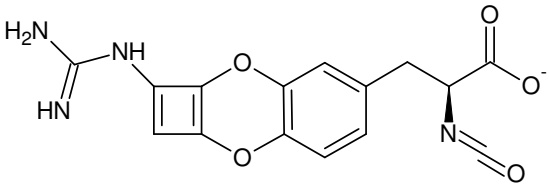

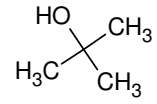

74.073165 Da

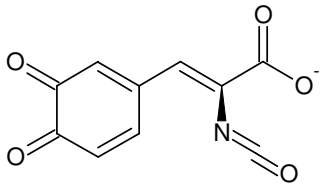

Monoisotopic Mass = 327.073493 Da

Monoisotopic Mass = 218.009496 Da

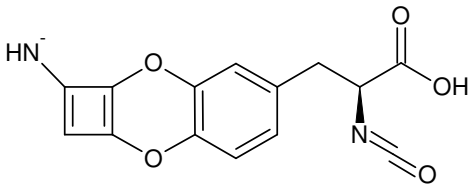

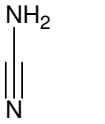

42.021798 Da

Monoisotopic Mass = 285.051695 Da

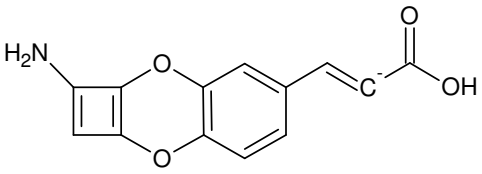

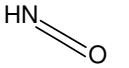

43.005814 Da

Warum bleibt der Stickstoff am 4-Ring im System?

=> 5-Ring?

Monoisotopic Mass = 242.045881 Da

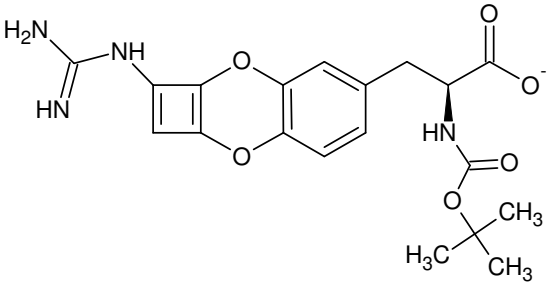

Monoisotopic Mass = 401.146658 Da

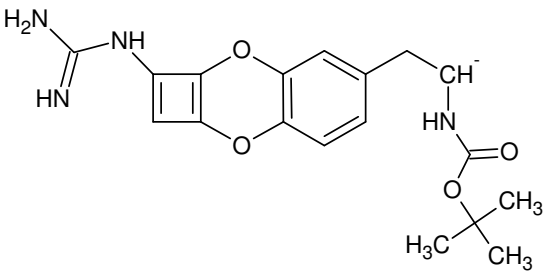

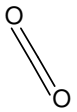

43.989829 Da

Monoisotopic Mass = 357.156829 Da

-MSn [Arg 595 nm 6,8 min]: 401 -> 327 -> 285 -> 242 and 401 -> 357 -> 313 -> 255 as well as 401 -> 359 ?> 314 {I/II}

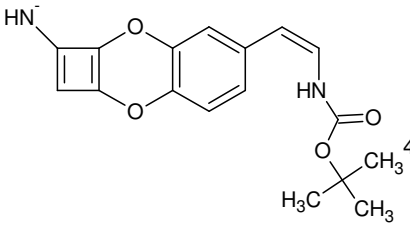

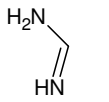

44.037448 Da

Monoisotopic Mass = 313.119381 Da

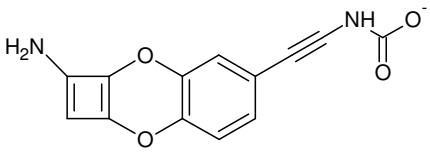

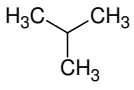

58.07825 Da

Monoisotopic Mass = 255.04113 Da

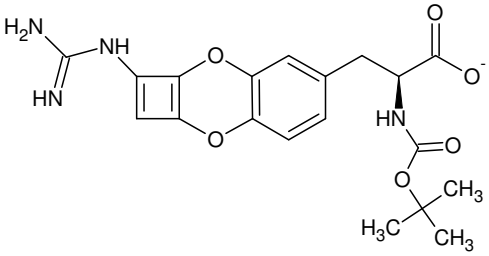

Monoisotopic Mass = 401.146658 Da

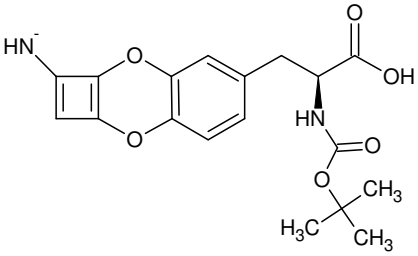

42.021798 Da

Monoisotopic Mass = 359.12486 Da

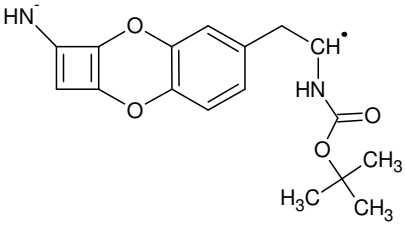

44.997654 Da

Monoisotopic Mass = 314.127206 Da

unwahrscheinlicher Zerfall: warum nicht -44 Da (CO_2)?

Ladung auf der anderen Seite des Moleküls lokalisiert?

Messfehler?
Spektrum von -MS4(-359 Th):

m/z	I (cnts)
312.9	10
314.0	62
358.0	12

=> **Δ = 44 Da**

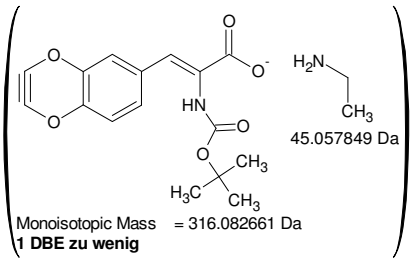

45.057849 Da

Monoisotopic Mass = 316.082661 Da
1 DBE zu wenig

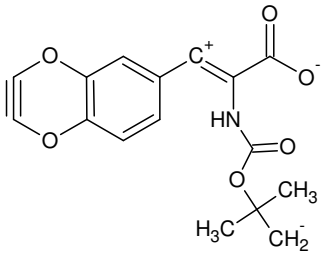

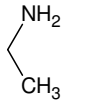

45.057849 Da

Monoisotopic Mass = 314.067011 Da

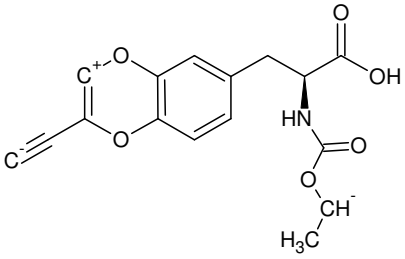

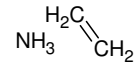

45.057849 Da

Monoisotopic Mass = 314.067011 Da

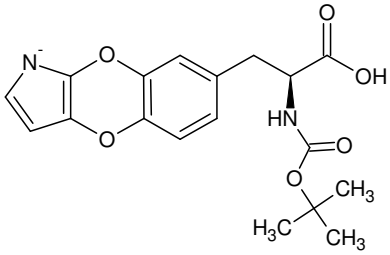

Monoisotopic Mass = 359.12486 Da

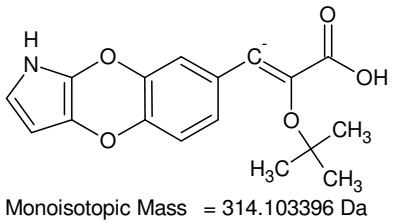

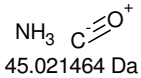

45.021464 Da

Monoisotopic Mass = 314.103396 Da

-MSn [Arg 595 nm 6,8 min]: 401 -> 327 -> 285 -> 242 and 401 -> 357 -> 313 -> 255 as well as 401 -> 359 ?> 314 {II/II}

XIII.III.III. Arg 595 nm 8,6 min

+MS^n

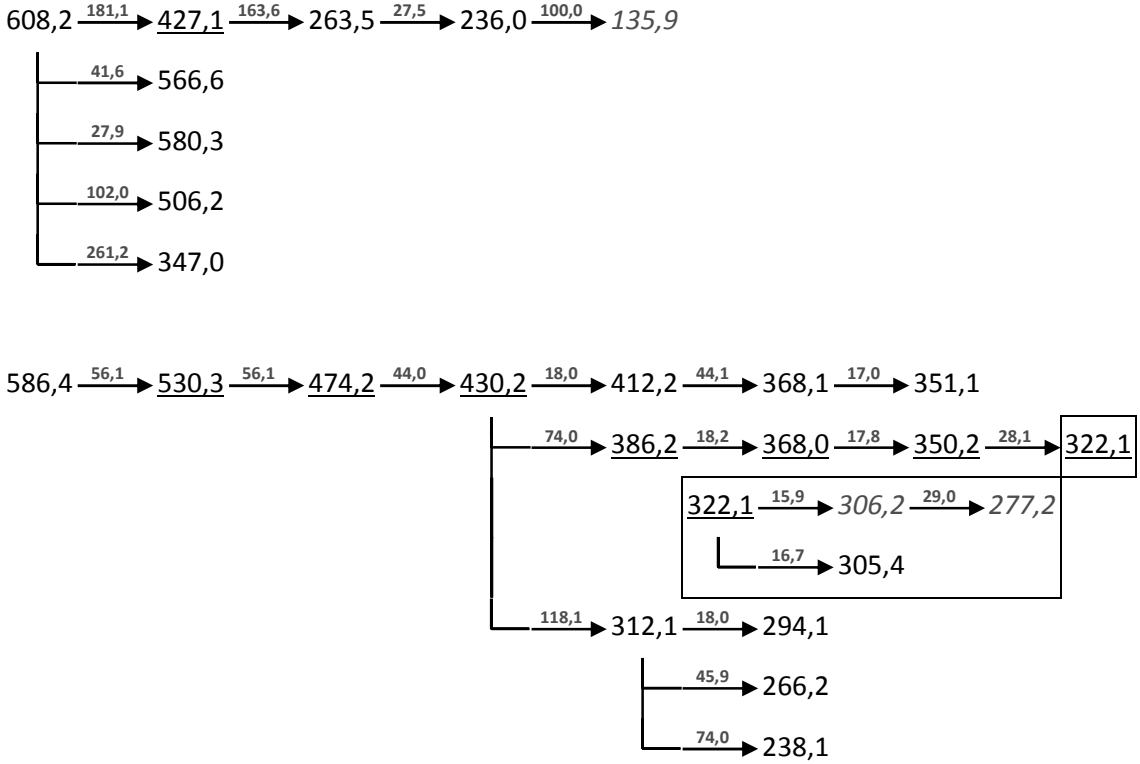

-MS^n

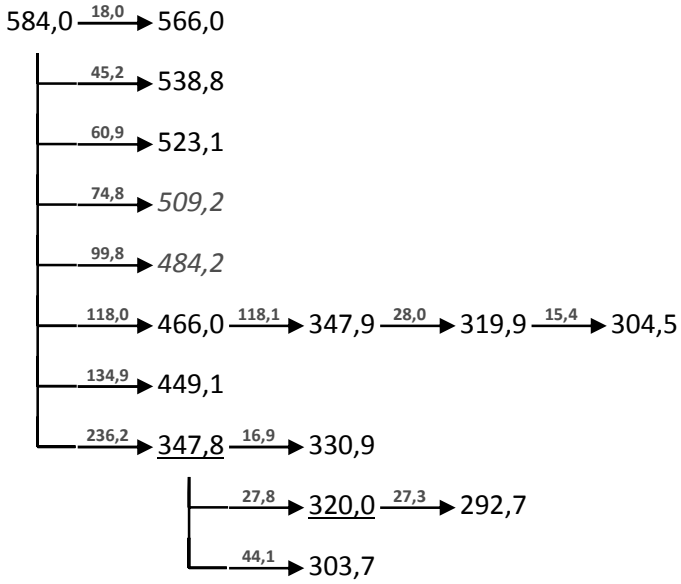

isotopic fingerprint:

peak area / % of monoisotopic	**+1**	**+2**	**+3**
theoretical ($C_{29}H_36N_3O_{10}^+$):	33,4	7,5	1,3
measured (586,4 Th):	32,1	10,2	3,6
measured (-584,0 Th):	20,1	7,3	0,5

Figure XIII-LII MS^n analysis of Arg 595 nm 8,6 min

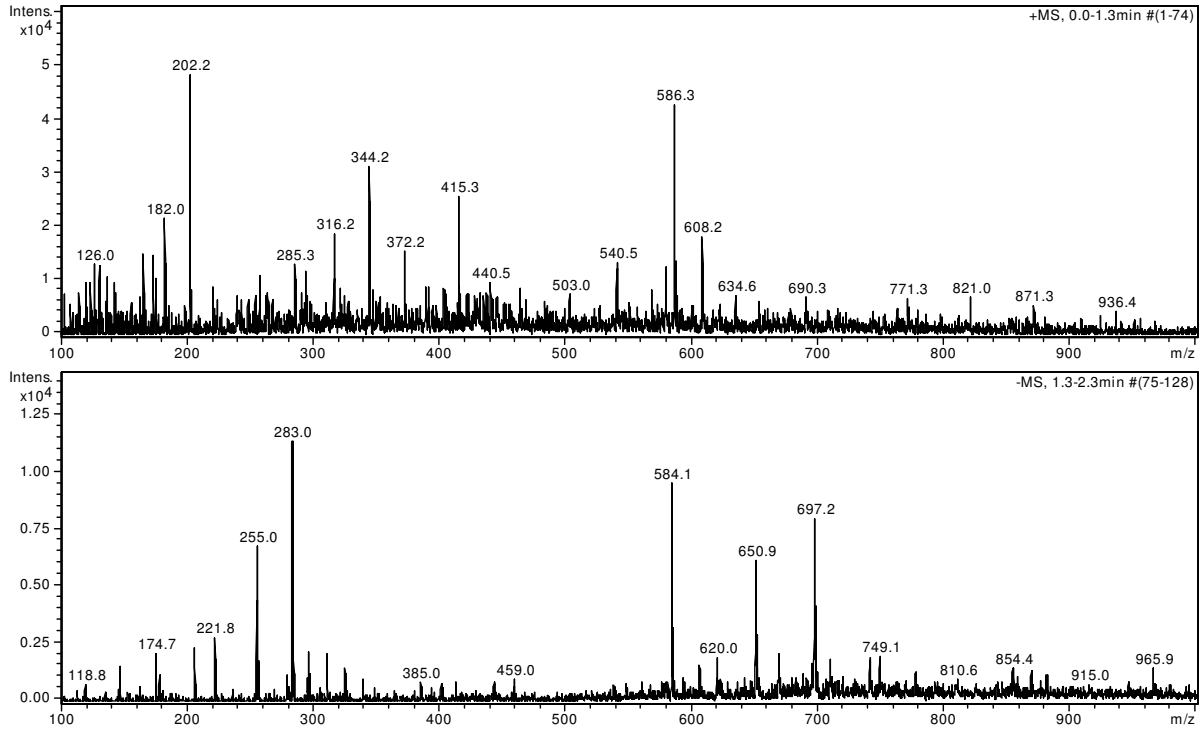

Figure XIII-LIII Arg 595 nm 8,6 min: fraction 2; 27 % MeOH, 27 % ACN, 1 ‰ FA in ddH_2O; full scan MS^1

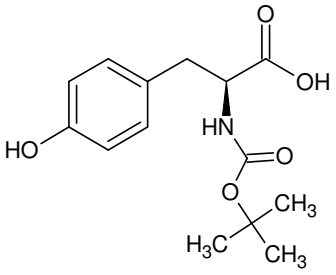

L-Boc-Tyr-OH
Monoisotopic Mass = 281.126323 Da

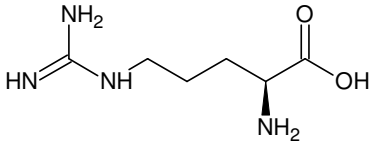

L-Arginin
Monoisotopic Mass = 174.111676 Da

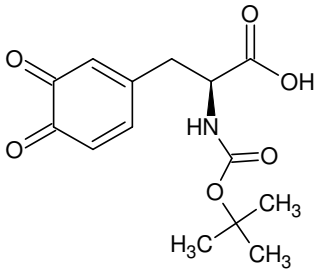

Monoisotopic Mass = 295.105587 Da

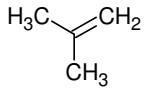

56.0626 Da

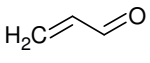

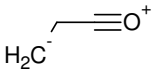

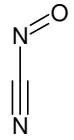

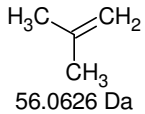

56.0626 Da

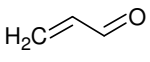

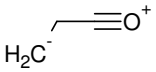

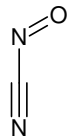

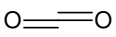

43.989829 Da

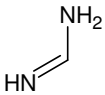

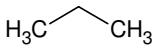

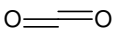

43.989829 Da

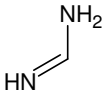

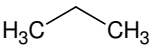

H_2O
18.010565 Da

H_2O
18.010565 Da

praktische keine strukturelle Information => keine funktionellen Gruppen an aliphatischen Seitenketten

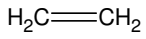

28.0313 Da

NH_3
17.026549 Da

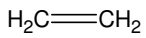

28.0313 Da

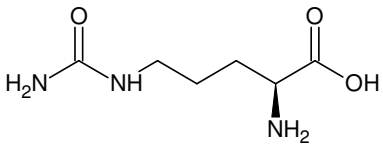

L-Citrullin
Monoisotopic Mass = 175.095691 Da

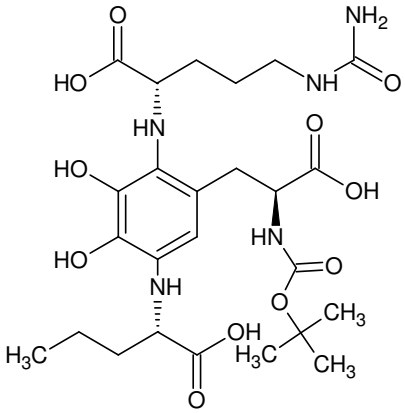

Monoisotopic Mass = 585.264607 Da

Gefundene Verbindungen: 23

CH_2N_3	MG=56,0248712
$CH_{12}O_2$	MG=56,0837252
$CH_{14}NO$	MG=56,1075334
$CH_{16}N_2$	MG=56,1313416
$CH_{28}O$	MG=56,2140038
CN_2O	MG=56,001063
C_2H_2NO	MG=56,0136382
$C_2H_4N_2$	MG=56,0374464
$C_2H_{16}O$	MG=56,1201086
$C_2H_{18}N$	MG=56,1439168
C_2O_2	MG=55,98983
C_3H_4O	MG=56,0262134
C_3H_6N	MG=56,0500216
C_3H_{20}	MG=56,156492
C_4H_8	MG=56,0625968
H_8O_3	MG=56,0473418
$H_{10}NO_2$	MG=56,07115
$H_{12}N_2O$	MG=56,0949582
$H_{14}N_3$	MG=56,1187664
$H_{24}O_2$	MG=56,1776204
$H_{26}NO$	MG=56,2014286
$H_{28}N_2$	MG=56,2252368
N_4	MG=56,012296

-----D--B--E--f-i-l-t-e-r-----
06.06.2011 - 9:30:28,35
akzeptierte DBEs:
0 1 2 3 4 5 6

CN_2O	DBE: 3
$C_2H_4N_2$	DBE: 2
C_2O_2	DBE: 3
C_3H_4O	DBE: 2
C_4H_8	DBE: 1
N_4	DBE: 3

6 von 23 Summenformeln

Gefundene Verbindungen: 6

CH_2N	MG=28,0187232
CO	MG=27,994915
C_2H_4	MG=28,0312984
$H_{12}O$	MG=28,0888102
$H_{14}N$	MG=28,1126184
N_2	MG=28,006148

585 Da [Arg 595 nm 8,6 min]: main fragmentation route +MSn

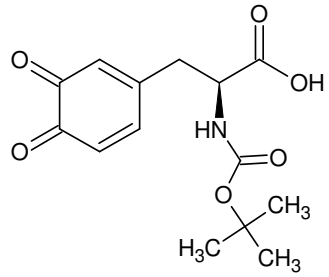

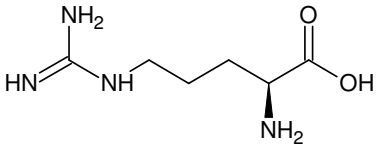

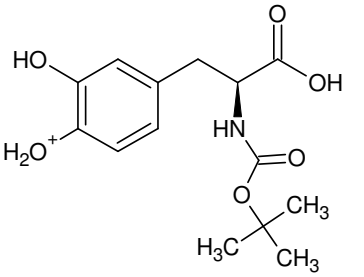

Monoisotopic Mass = 298.128514 Da

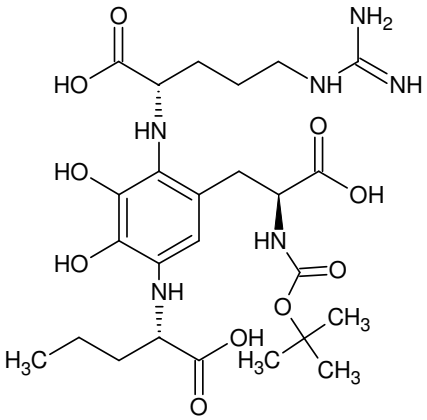

Monoisotopic Mass = 584.280592 Da

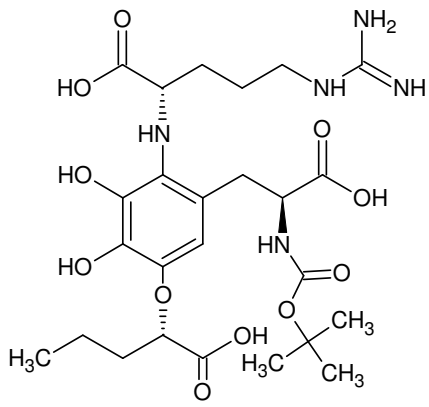

Monoisotopic Mass = 585.264607 Da

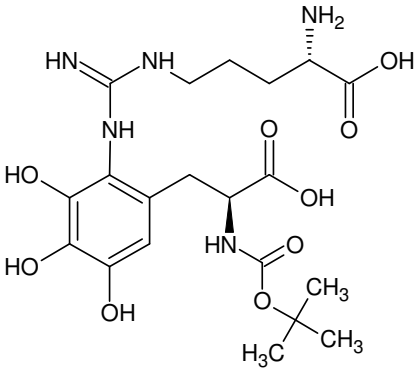

Monoisotopic Mass = 485.212178 Da

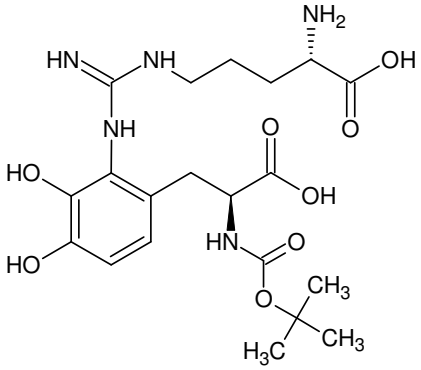

Monoisotopic Mass = 469.217263 Da

Gefundene Verbindungen: 91

CH2N5O	MG=100,0259342
CH4N6	MG=100,0497424
(...)	
H44N4	MG=100,3565784
N6O	MG=100,013359

-----D--B--E--f-i-l-t-e-r-----
06.06.2011 - 11:23:33,54
akzeptierte DBEs:
0 1 2 3 4 5 6

CH4N6	DBE: 3
CN4O2	DBE: 4
C2H4N4O	DBE: 3
C2N2O3	DBE: 4
C3H4N2O2	DBE: 3
C3H8N4	DBE: 2
C3O4	DBE: 4
C4H4O3	DBE: 3
C4H8N2O	DBE: 2
C5H8O2	DBE: 2
C5H12N2	DBE: 1
C6H12O	DBE: 1
C7H16	DBE: 0
N6O	DBE: 4

14 von 91 Summenformeln

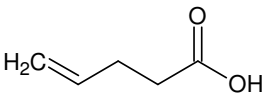

100.052429 Da

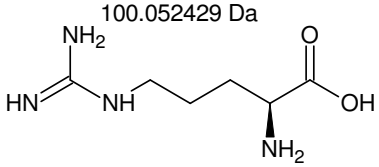

Gefundene Verbindungen: 133

CH2N5O2	MG=116,0208492
CH4N6O	MG=116,0446574
(...)	
H58N3O	MG=116,4579638
N6O2	MG=116,008274

-----D--B--E--f-i-l-t-e-r-----
06.06.2011 - 11:41:45,03
akzeptierte DBEs:
0 1 2 3 4 5 6

CH4N6O	DBE: 3
CN4O3	DBE: 4
C2H4N4O2	DBE: 3
C2H8N6	DBE: 2
C2N2O4	DBE: 4
C3H4N2O3	DBE: 3
C3H8N4O	DBE: 2
C3O5	DBE: 4
C4H4O4	DBE: 3
C4H8N2O2	DBE: 2
C4H12N4	DBE: 1
C5H8O3	DBE: 2
C5H12N2O	DBE: 1
C6H12O2	DBE: 1
C6H16N2	DBE: 0
C7H16O	DBE: 0
C9H8	DBE: 6
H4N8	DBE: 3
N6O2	DBE: 4

19 von 133 Summenformeln

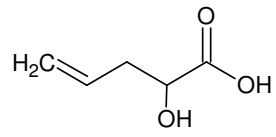

116.047344 Da

585 Da [Arg 595 nm 8,6 min]: 586 Th

CD

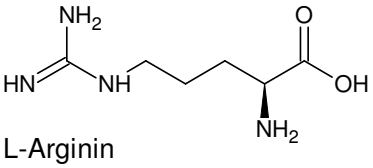

L-Arginin
Monoisotopic Mass = 174.111676 Da

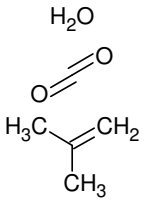

$C_5H_{10}O_3$
18.062994 Da

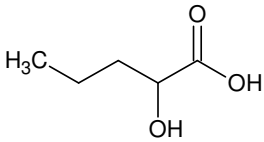

$C_5H_{10}O_3$
118.062994 Da

585 - 295 - 174 + 2 = **118**
Gefundene Verbindungen: 241
CH2N4OS MG=117,9949322
CH2N4O3 MG=118,0126902
(...)
N5OS MG=117,982357
N5O3 MG=118,000115

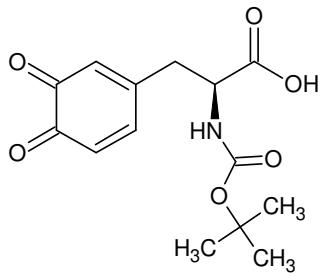

Monoisotopic Mass = 295.105587 Da

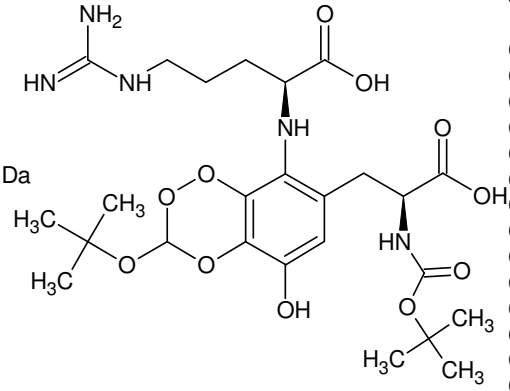

Monoisotopic Mass = 585.264607 Da

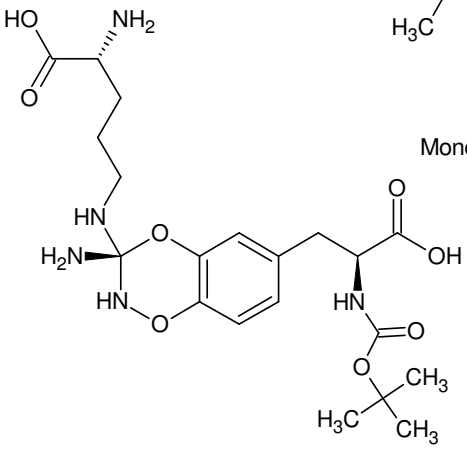

Monoisotopic Mass = 469.217263 Da

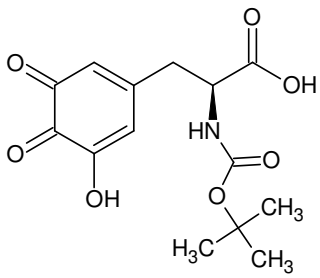

Monoisotopic Mass = 311.100502 Da

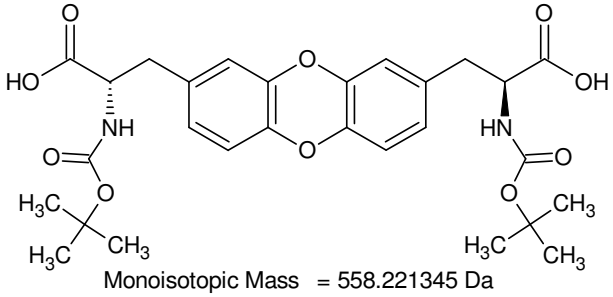

Monoisotopic Mass = 558.221345 Da

-----D--B--E--f-i-l-t-e-r-----
19.08.2011 - 11:30:14,76
akzeptierte DBEs:
-2 -1 0 1 2 3 4 5 6 7 8

CH2N4OS	DBE: 3
CH2N4O3	DBE: 3
CH6N6O	DBE: 2
C2H2N2O2S	DBE: 3
C2H2N2O4	DBE: 3
C2H2N2S2	DBE: 3
C2H6N4O2	DBE: 2
C2H6N4S	DBE: 2
C2H10N6	DBE: 1
C3H2OS2	DBE: 3
C3H2O3S	DBE: 3
C3H2O5	DBE: 3
C3H6N2OS	DBE: 2
C3H6N2O3	DBE: 2
C3H10N4O	DBE: 1
C4H6O2S	DBE: 2
C4H6O4	DBE: 2
C4H6S2	DBE: 2
C4H10N2O2	DBE: 1
C4H10N2S	DBE: 1
C4H14N4	DBE: 0
C5H2N4	DBE: 7
C5H10OS	DBE: 1
C5H10O3	DBE: 1
C5H14N2O	DBE: 0
C6H2N2O	DBE: 7
C6H14O2	DBE: 0
C6H14S	DBE: 0
C6H18N2	DBE: -1
C7H2O2	DBE: 7
C7H2S	DBE: 7
C7H6N2	DBE: 6
C7H18O	DBE: -1
C8H6O	DBE: 6
C8H22	DBE: -2
C9H10	DBE: 5
H2N6O2	DBE: 3
H2N6S	DBE: 3
H6N8	DBE: 2
H6OS3	DBE: -2
H6O3S2	DBE: -2
H6O5S	DBE: -2
H6O7	DBE: -2

43 von 241 Summenformeln

585 - 558 = **27**
Gefundene Verbindungen: 4
CHN MG=27,0108986
C_2H_3 MG=27,0234738
$H_{11}O$ MG=27,0809856
$H_{13}N$ MG=27,1047938

585 Da [Arg 595 nm 8,6 min]

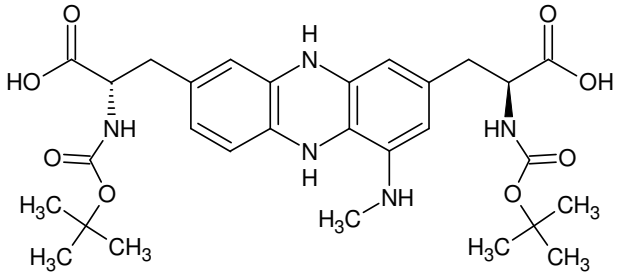

Monoisotopic Mass = 585.279863 Da

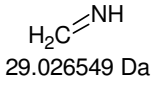

29.026549 Da

Gefundene Verbindungen: 6

CHO	MG=29,0027396
CH_3N	MG=29,0265478
C_2H_5	MG=29,039123
HN_2	MG=29,0139726
$H_{13}O$	MG=29,0966348
$H_{15}N$	MG=29,120443

Fragment 29 Da beobachtet

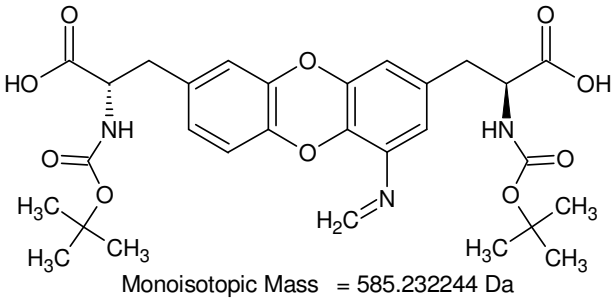

Monoisotopic Mass = 585.232244 Da

Chromophor zu klein

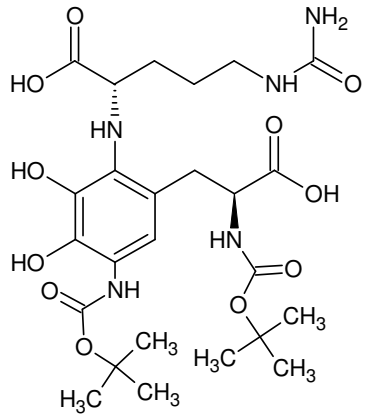

Monoisotopic Mass = 585.264607 Da

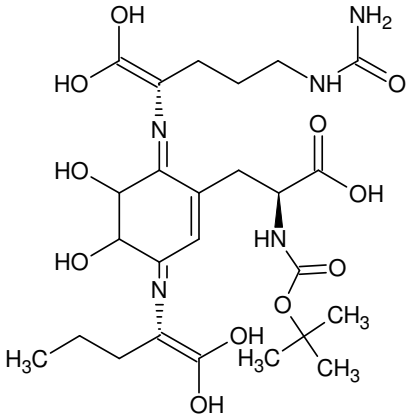

Monoisotopic Mass = 585.264607 Da

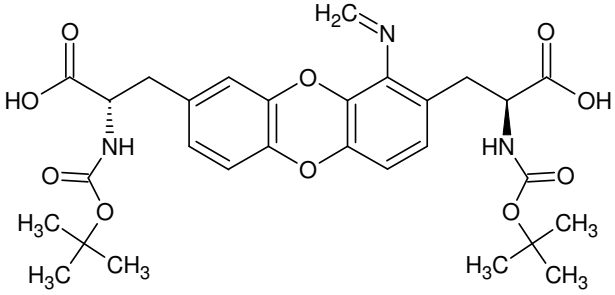

Monoisotopic Mass = 585.232244 Da

585Da [Arg 595 nm 8,6 min]

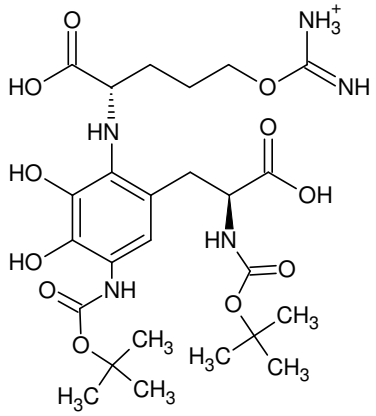

Monoisotopic Mass = 586.271884 Da

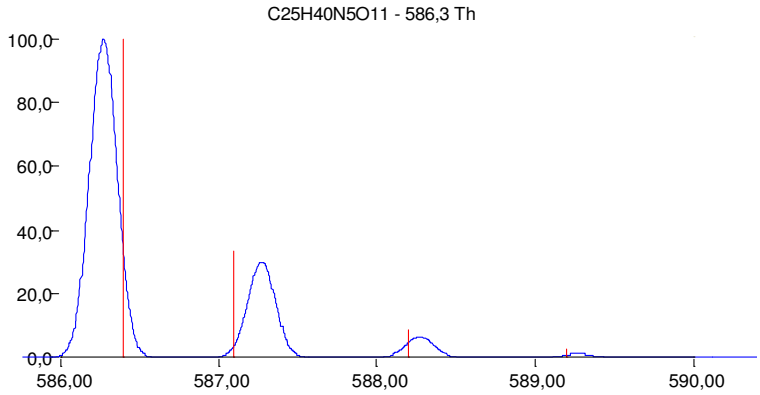

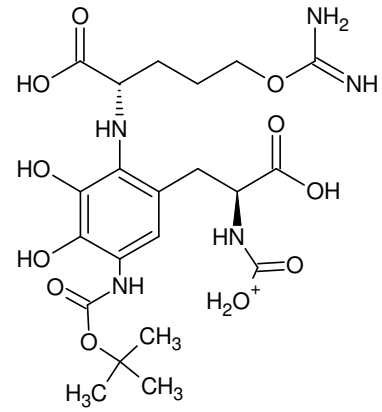

Monoisotopic Mass = 530.209283 Da

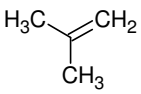

56.0626 Da

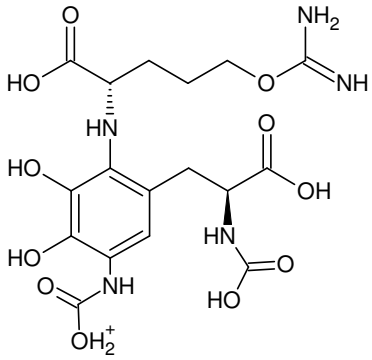

Monoisotopic Mass = 474.146683 Da

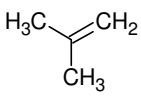

56.0626 Da

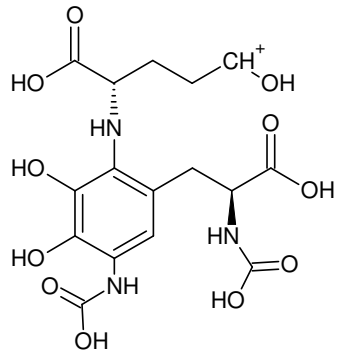

Monoisotopic Mass = 430.109235 Da

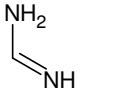

44.037448 Da

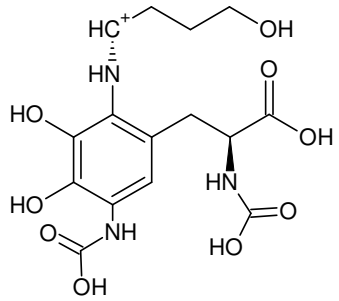

Monoisotopic Mass = 386.119406 Da

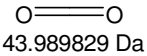

43.989829 Da

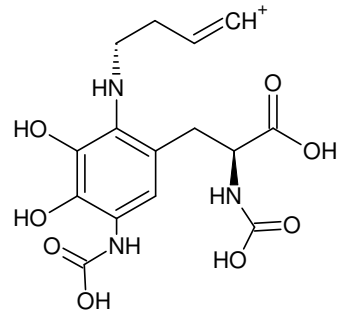

Monoisotopic Mass = 368.108841 Da

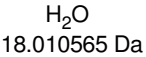

18.010565 Da

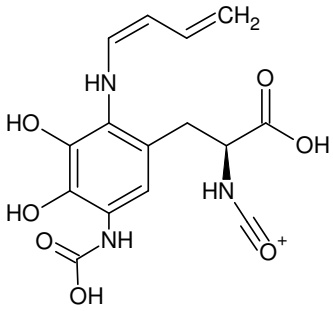

Monoisotopic Mass = 350.098276 Da

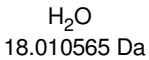

18.010565 Da

+MSn [Arg 595 nm 8,6 min]: 586 -> 530 -> 474 -> 430 -> 386 -> 368 -> 350

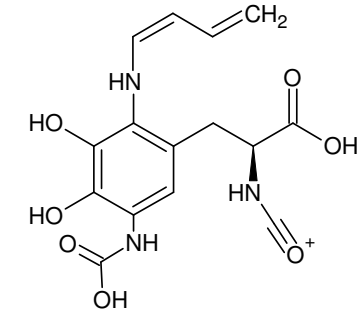

Monoisotopic Mass = 350.098276 Da

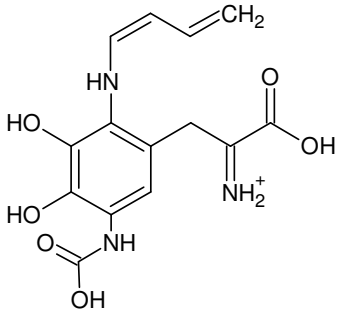

27.994915 Da

Monoisotopic Mass = 322.103362 Da

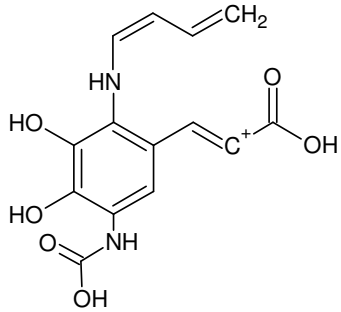

NH_3
17.026549 Da

Monoisotopic Mass = 305.076813 Da

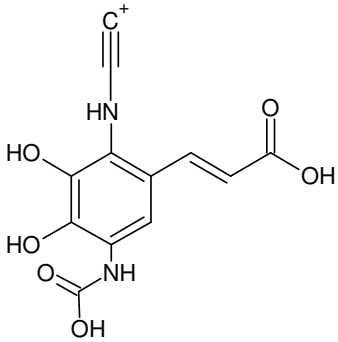

28.0313 Da

Monoisotopic Mass = 277.045512 Da

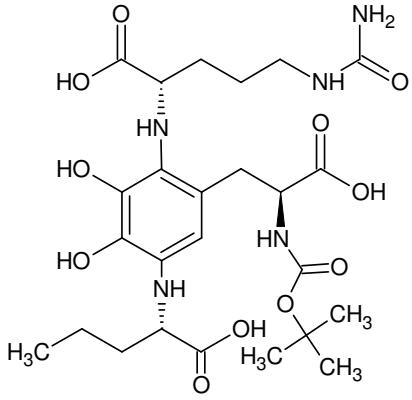

Monoisotopic Mass = 585.264607 Da

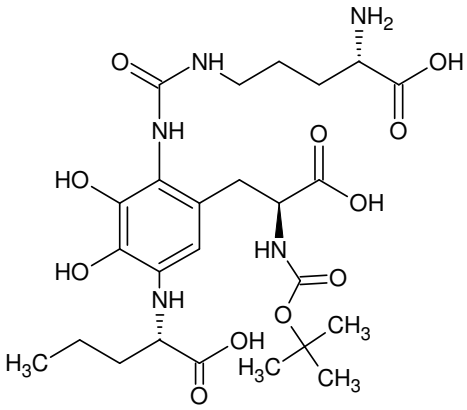

Monoisotopic Mass = 585.264607 Da

+MSn [Arg 595 nm 8,6 min]: [586 -> 530 -> 474 -> 430 -> 386 -> 368 ->] 350 -> 322 -> 305 (-> 277) and 585 Da

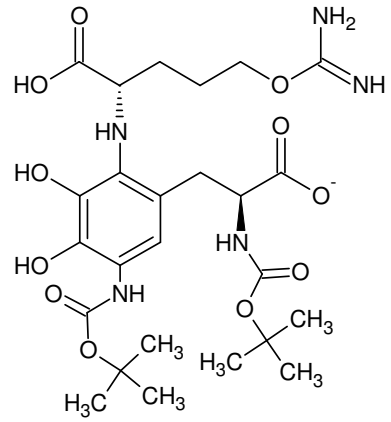

Monoisotopic Mass = 584.257331 Da

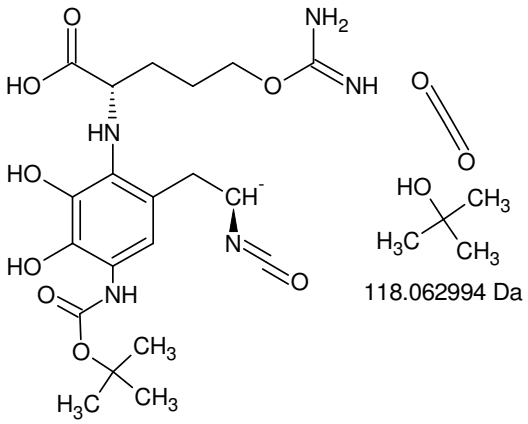

118.062994 Da

Monoisotopic Mass = 466.194336 Da

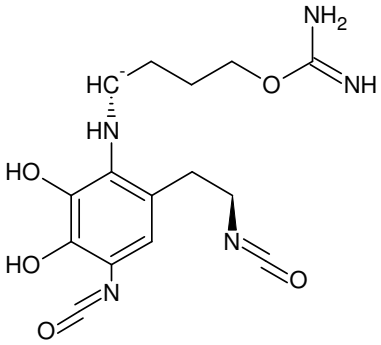

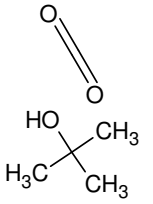

118.062994 Da

Monoisotopic Mass = 348.131342 Da

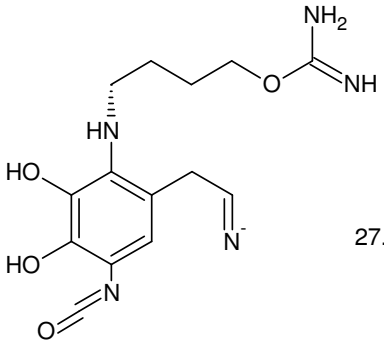

27.994915 Da

Monoisotopic Mass = 320.136428 Da

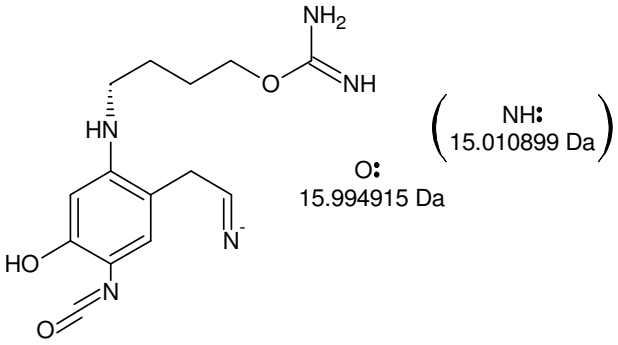

NH: 15.010899 Da

O: 15.994915 Da

Monoisotopic Mass = 304.141513 Da

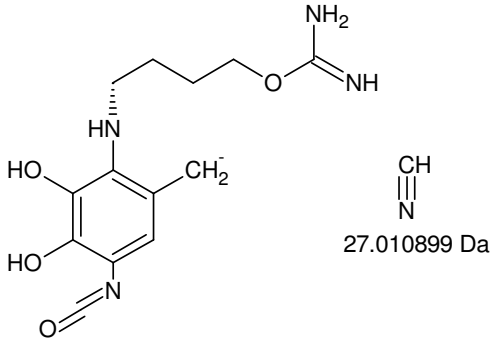

27.010899 Da

Monoisotopic Mass = 293.125529 Da

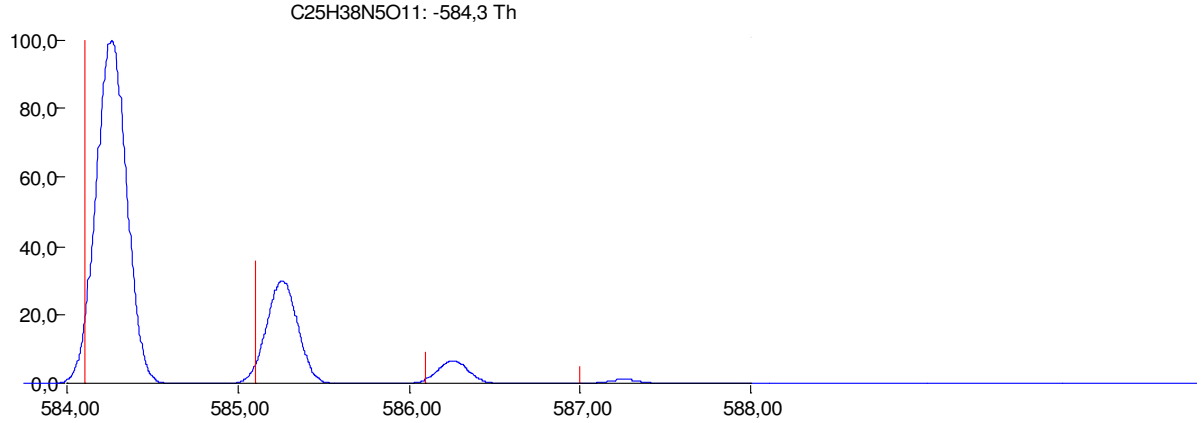

-MSn [Arg 595 nm 8,6 min]: 584 -> 466 -> 348 -> 320 -> 304, 293

Unterschied der Proben Arg 595nm 8,6min & Arg 595nm 12,3min: [586 -> 530 -> 474 -> 430 ->] 386 -> 368 -> **350** (412 -> 368-> 351) bei 8,6min und 386 -> 368 -> **351** (412-> 368 -> 350) bei 12,3min => **Isomere?**

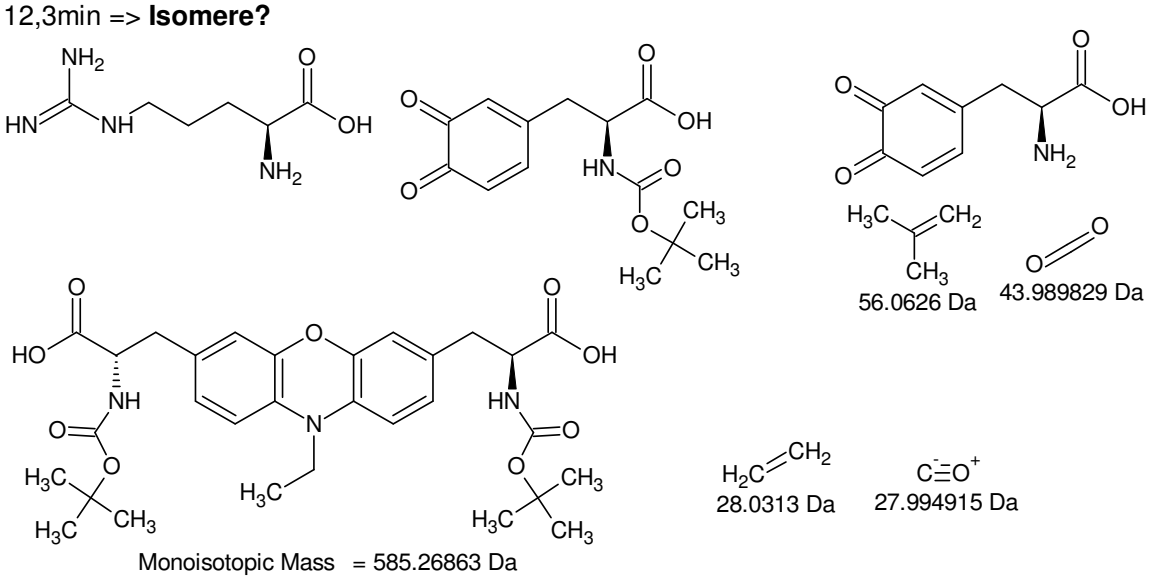

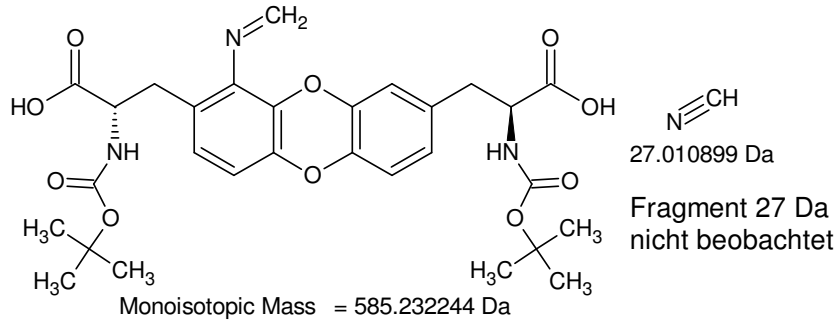

Arginin: pK_s(Guanidino-NH_2) = 13,2, pI = 11,76

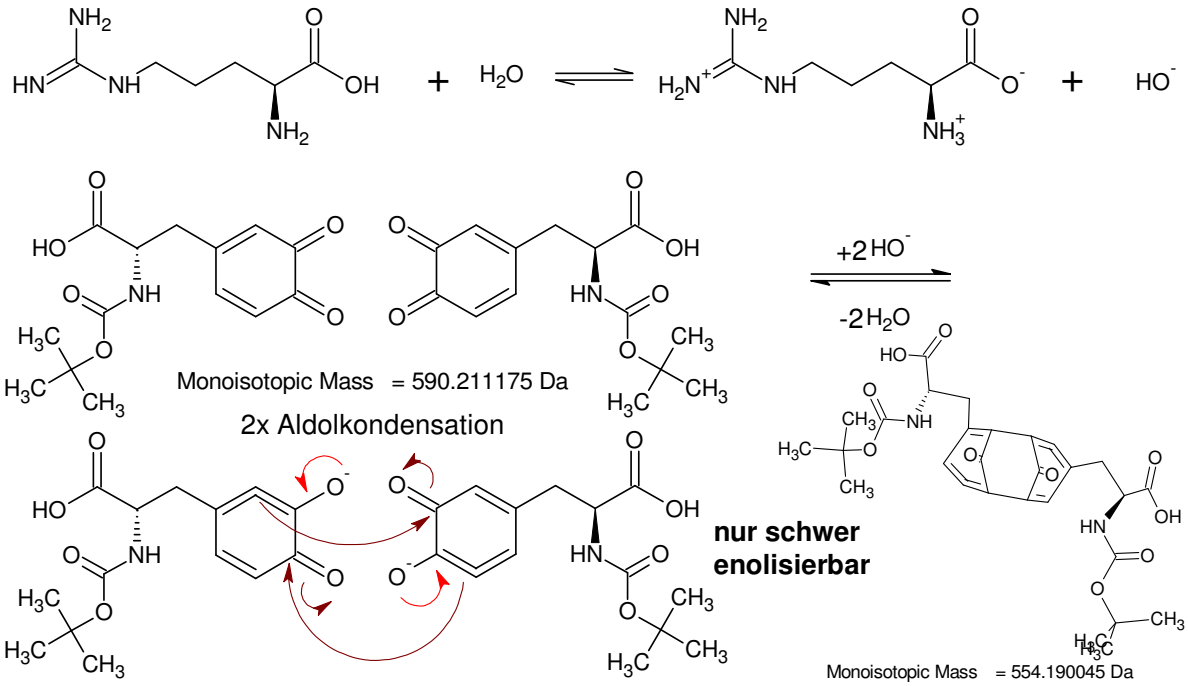

585 Da [Arg 595 nm 8,6 min]

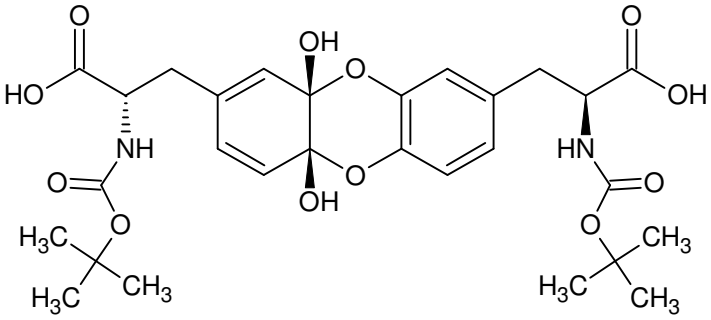

Monoisotopic Mass = 592.226825 Da

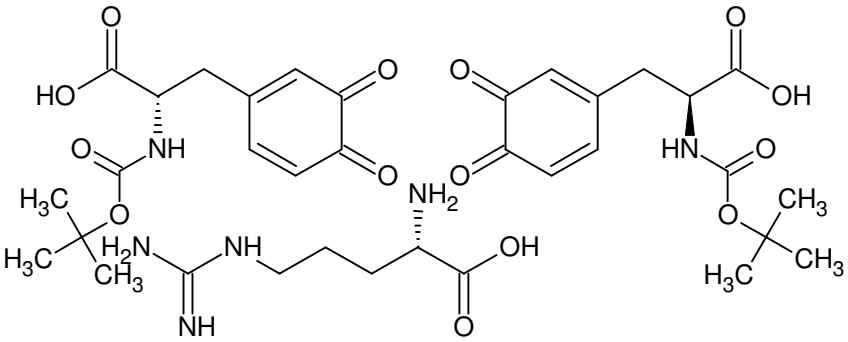

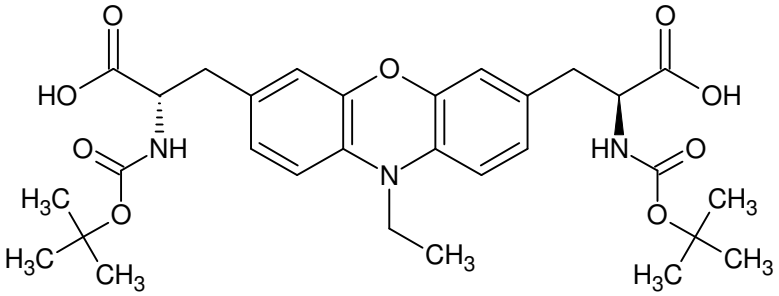

Monoisotopic Mass = 585.26863 Da

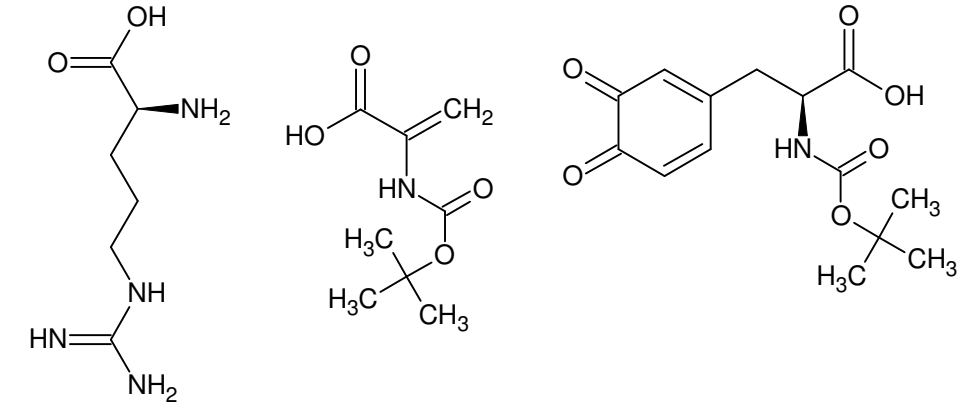

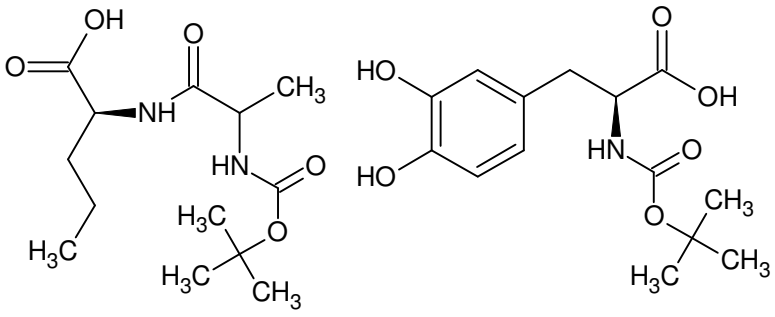

Monoisotopic Mass = 585.289759 Da

585 Da [Arg 595 nm 8,6 min]

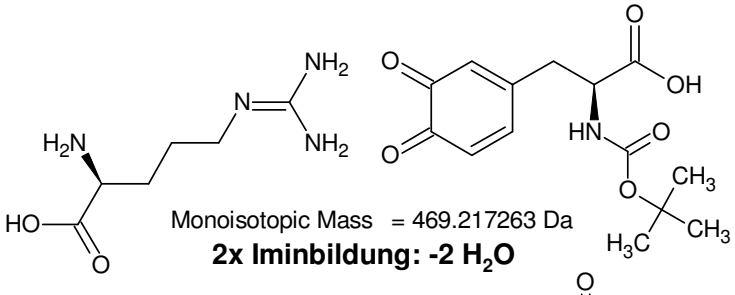

Monoisotopic Mass = 469.217263 Da

2x Iminbildung: -2 H_2O

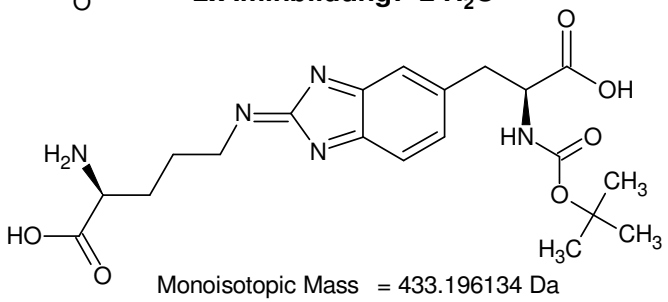

Monoisotopic Mass = 433.196134 Da

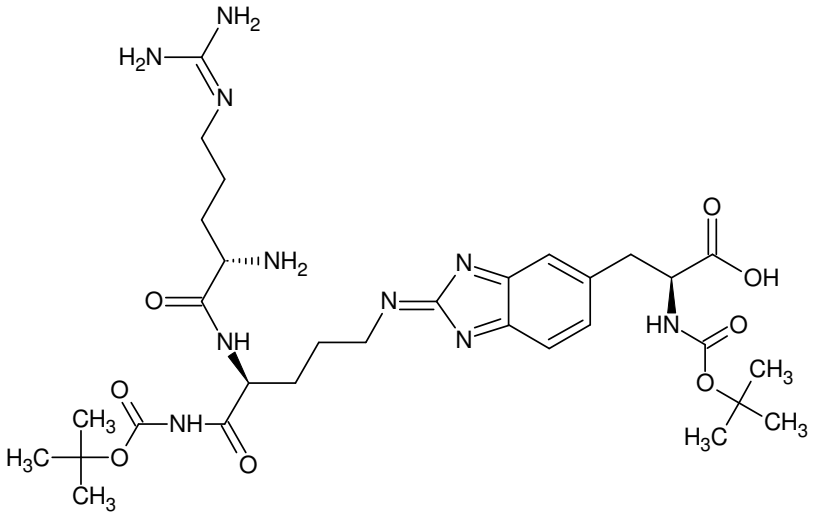

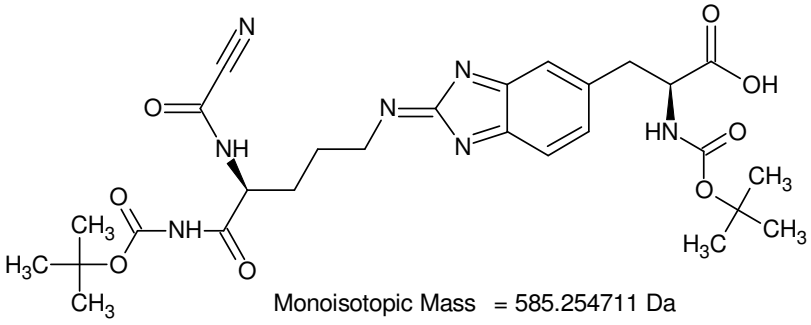

Monoisotopic Mass = 585.254711 Da

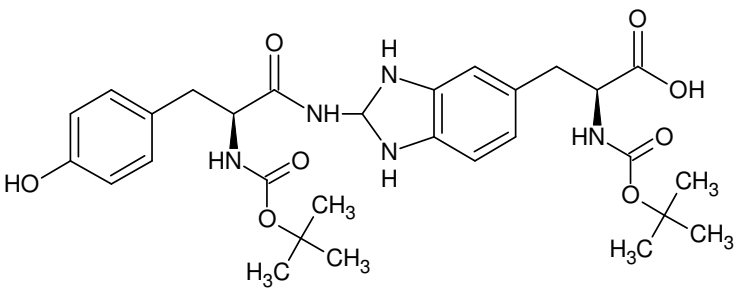

Monoisotopic Mass = 585.279863 Da

585 Da [Arg 595 nm 8,6 min]

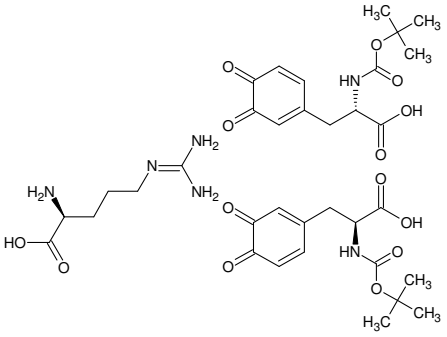

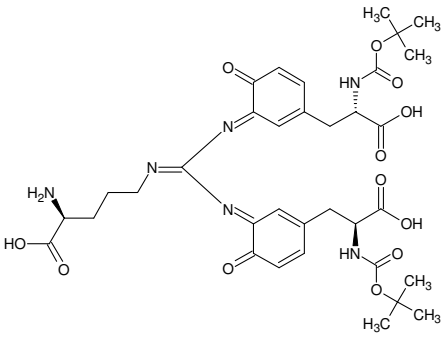

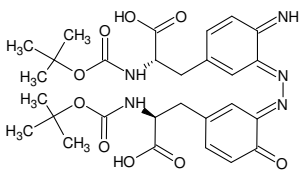

Monoisotopic Mass = 585.243478 Da

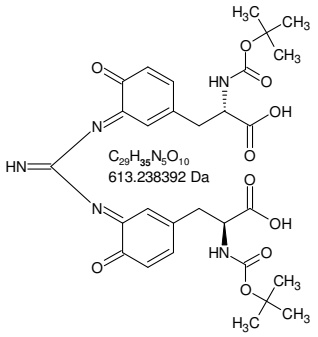

$C_{29}H_{35}N_5O_{10}$
613.238392 Da

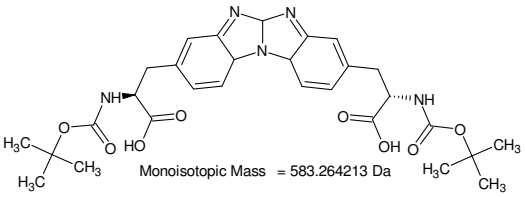

Monoisotopic Mass = 583.264213 Da

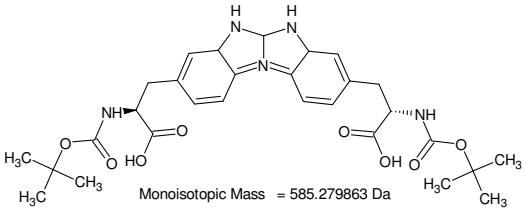

Monoisotopic Mass = 585.279863 Da

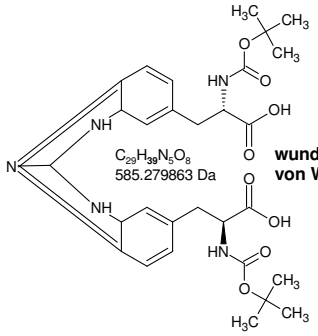

$C_{29}H_{39}N_5O_8$
585.279863 Da

wunderbare Vermehrung von Wasserstoffatomen

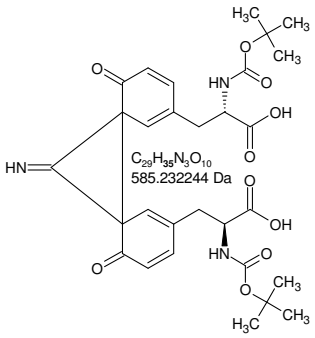

$C_{29}H_{35}N_3O_{10}$
585.232244 Da

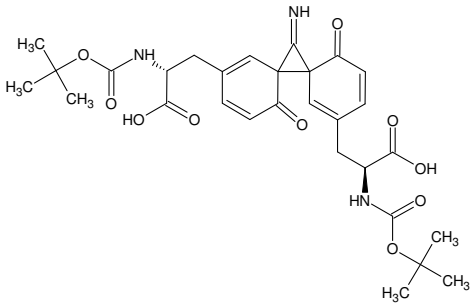

585 Da [Arg 595 nm 8,6 min]

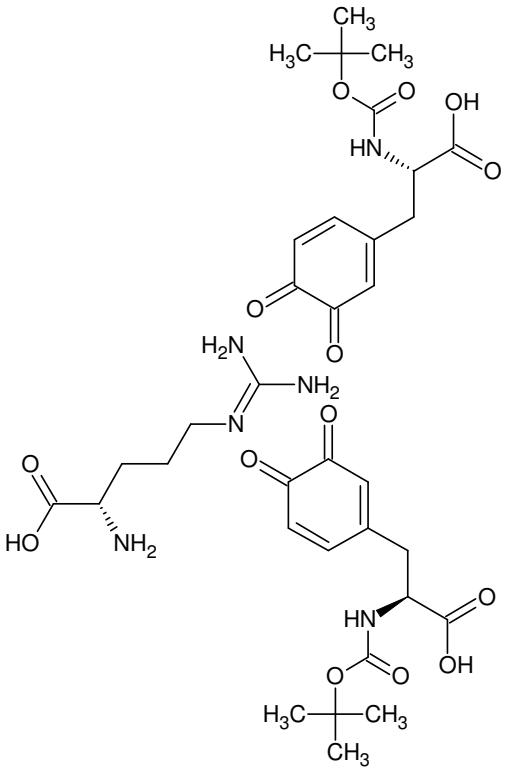

Monoisotopic Mass = 764.32285 Da

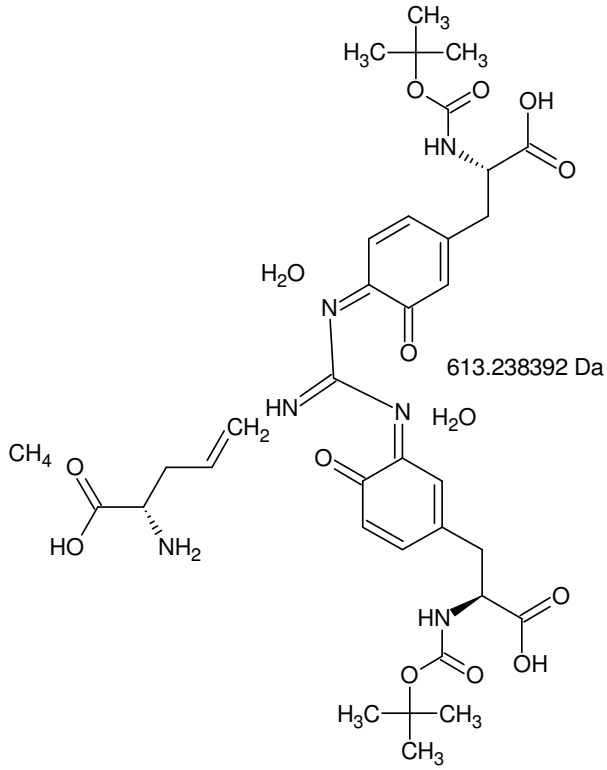

613.238392 Da

Monoisotopic Mass = 764.32285 Da

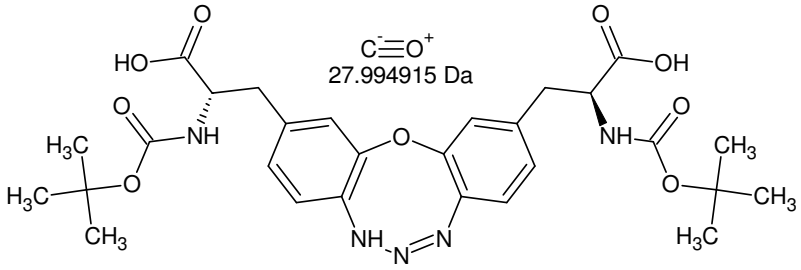

27.994915 Da

Monoisotopic Mass = 585.243478 Da

kondensierte Systeme: keine Isomere möglich wenn S_0 im Molekül

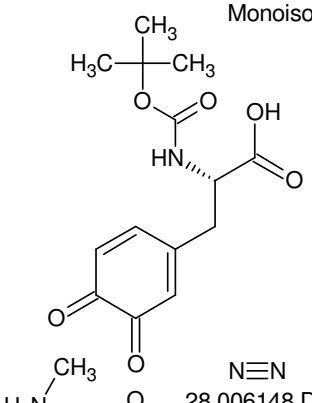

28.006148 Da

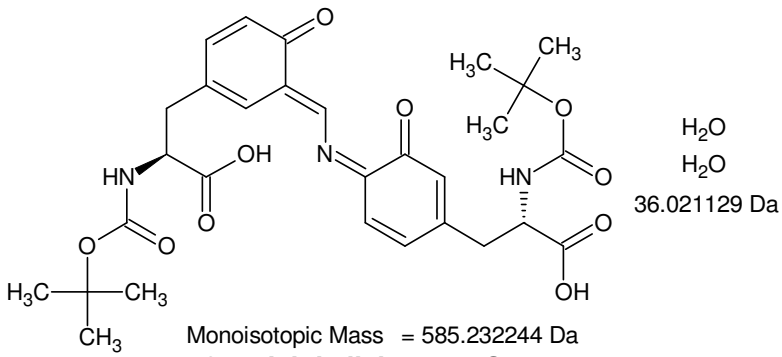

36.021129 Da

Monoisotopic Mass = 585.232244 Da

großes delokalisiertes π-System

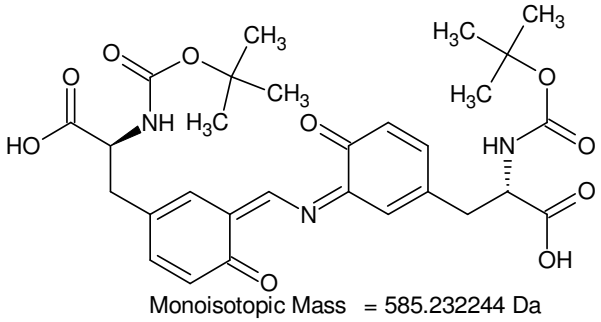

Monoisotopic Mass = 585.232244 Da

Isomer

585 Da [**Arg 595 nm 8,6 min**]

CDX

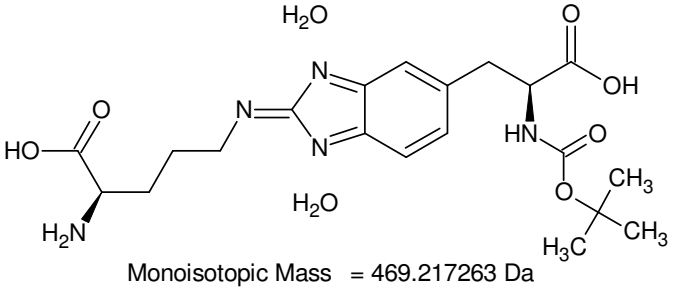

Monoisotopic Mass = 469.217263 Da

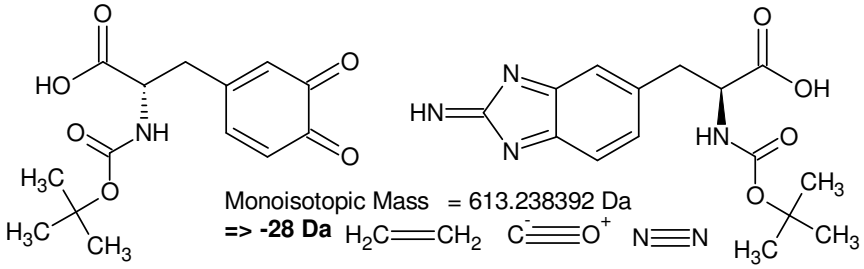

Monoisotopic Mass = 613.238392 Da

=> -28 Da $H_2C{=}CH_2$ $C{\equiv}O^+$ $N{\equiv}N$

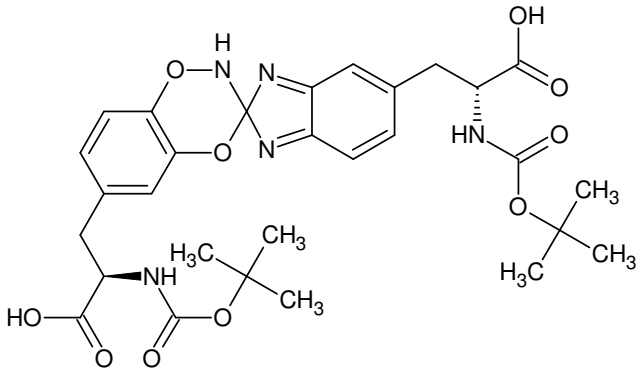

Diels-Alder

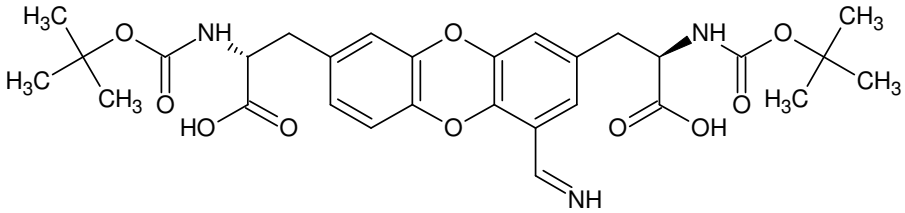

$N{\equiv}N$
28.006148 Da

Monoisotopic Mass = 585.232244 Da

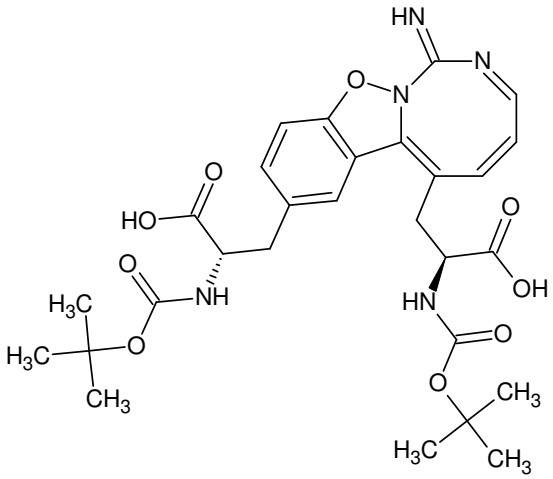

$C{\equiv}O^+$
27.994915 Da

Monoisotopic Mass = 585.243478 Da

585 Da [**Arg 595 nm 8,6 min**]

653,2 - 586,3 = **66,9**
650,9 - 584,1 = **66,8**
(akzeptierte Fragmentmassen jeweils Suchmasse +/- 0,5 Da; gefundene Formeln identisch mit Summenformeln für 67 Da)
Gefundene Verbindungen: 41
CH7OS MG=67,0217592
CH7O3 MG=67,0395172
(...)
H23N2O MG=67,1810288
H25N3 MG=67,204837

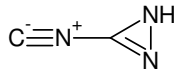

C_2HN_3
67.017047 Da

O=O NH_3 H_2O
H_5NO_3
67.026943 Da

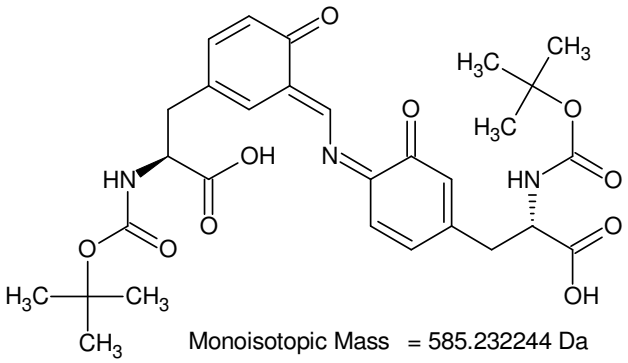

Monoisotopic Mass = 585.232244 Da

-----D--B--E--f-i-l-t-e-r-----
25.08.2011 - 13:58:20,87
akzeptierte DBEs:
-2 -1 0 1 2 3 4 5 6 7 8

CH_9NO_2 DBE: -2
CH_9NS DBE: -2
C_2HN_3 DBE: 4
C_3HNO DBE: 4
C_4H_5N DBE: 3
H_5NOS DBE: -1
H_5NO_3 DBE: -1
H_9N_3O DBE: -2

8 von 41 Summenformeln

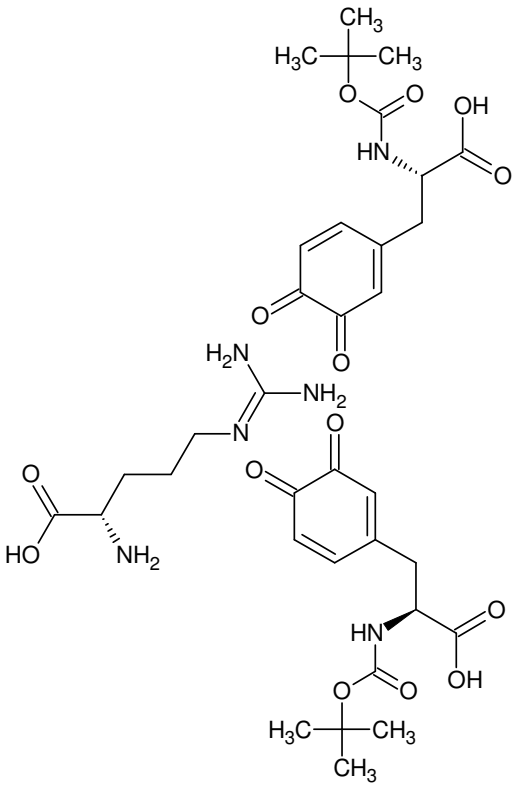

Monoisotopic Mass = 764.32285 Da

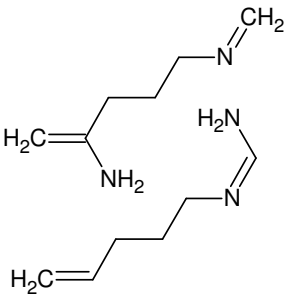

112.100048 Da

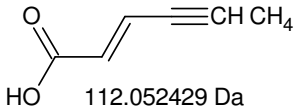

112.052429 Da

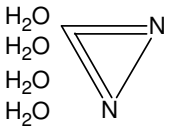

112.048407 Da

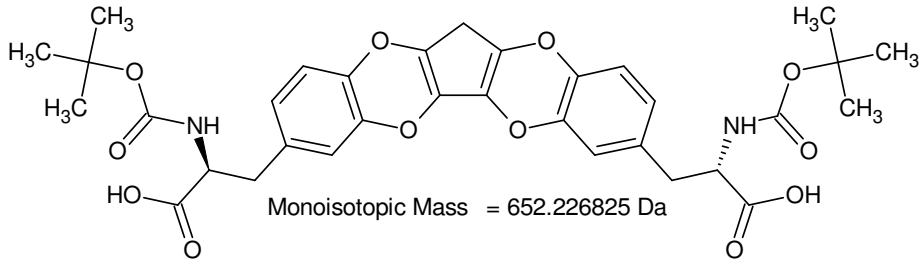

Monoisotopic Mass = 652.226825 Da

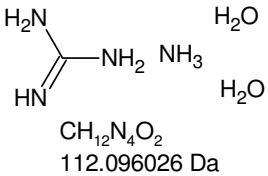

$CH_{12}N_4O_2$
112.096026 Da

652 Da [**Arg 595 nm 8,6 min**] **{I/III}**

764 - 652 = **112**
Gefundene Verbindungen: 209
CH2N7 MG=112,0371672
CH4O2S2 MG=111,9652724
(..)
O3S2 MG=111,928889
O7 MG=111,964405

-----D--B--E--f-i-l-t-e-r-----
25.08.2011 - 15:26:02,61
akzeptierte DBEs:
-2 -1 0 1 2 3 4 5 6 7 8

CH4O2S2 DBE: 0
CH4O4S DBE: 0
CH4O6 DBE: 0
CH4S3 DBE: 0
CH8N2O2S DBE: -1
CH8N2O4 DBE: -1
CH8N2S2 DBE: -1
CH12N4O2 DBE: -2
CH12N4S DBE: -2
CN6O DBE: 5
C2H4N6 DBE: 4
C2H8OS2 DBE: -1
C2H8O3S DBE: -1
C2H8O5 DBE: -1
$C_2H_{12}N_2OS$ DBE: -2
$C_2H_{12}N_2O_3$ DBE: -2
C2N4O2 DBE: 5
C2N4S DBE: 5
C3H4N4O DBE: 4
C3H12O2S DBE: -2
C3H12O4 DBE: -2
C3H12S2 DBE: -2
C3N2OS DBE: 5
C3N2O3 DBE: 5
C4H4N2O2 DBE: 4
C4H4N2S DBE: 4
C4H8N4 DBE: 3
C4O2S DBE: 5
C4O4 DBE: 5
C4S2 DBE: 5
C5H4OS DBE: 4
C5H4O3 DBE: 4
C5H8N2O DBE: 3
C6H8O2 DBE: 3
C6H8S DBE: 3
C6H12N2 DBE: 2
C7H12O DBE: 2
C8H16 DBE: 1
C9H4 DBE: 8
H4N2OS2 DBE: 0
H4N2O3S DBE: 0
H4N2O5 DBE: 0
H8N4OS DBE: -1
H8N4O3 DBE: -1
H12N6O DBE: -2
N8 DBE: 5
OS3 DBE: 1
O5S DBE: 1
O3S2 DBE: 1
O7 DBE: 1

50 von 209 Summenformeln

genau **2x O**:
Gefundene Verbindungen: 37
CH4O2S2 MG=111,9652724
CH8N2O2S MG=112,0306468
(...)
H48O2S MG=112,3374828
H52N2O2 MG=112,4028572

-----D--B--E--f-i-l-t-e-r-----
25.08.2011 - 15:46:27,67
akzeptierte DBEs:
-2 -1 0 1 2 3 4 5 6 7 8

$CH_4O_2S_2$ DBE: 0
$CH_8N_2O_2S$ DBE: -1
$CH_{12}N_4O_2$ DBE: -2
$C_2N_4O_2$ DBE: 5
$C_3H_{12}O_2S$ DBE: -2
$C_4H_4N_2O_2$ DBE: 4
C_4O_2S DBE: 5
$C_6H_8O_2$ DBE: 3

8 von 37 Summenformeln

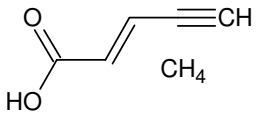

$C_6H_8O_2$
112.052429 Da

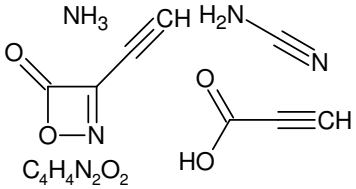

$C_4H_4N_2O_2$
112.027277 Da

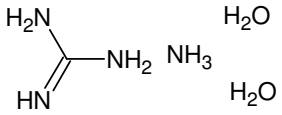

$CH_{12}N_4O_2$
112.096026 Da

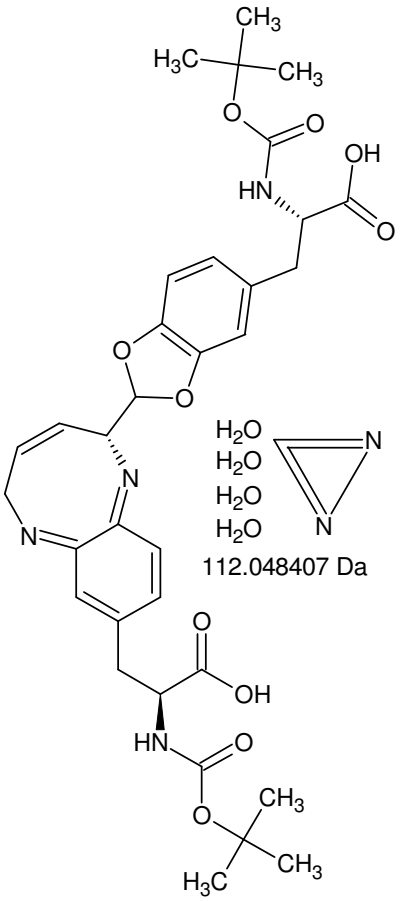

112.048407 Da

Monoisotopic Mass = 652.274444 Da

652 Da [**Arg 595 nm 8,6 min**] **{II/III}**

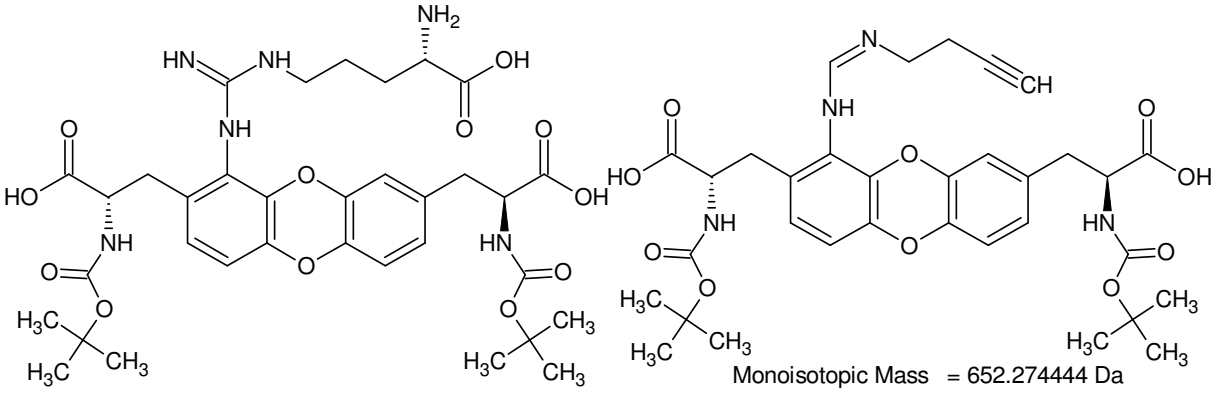

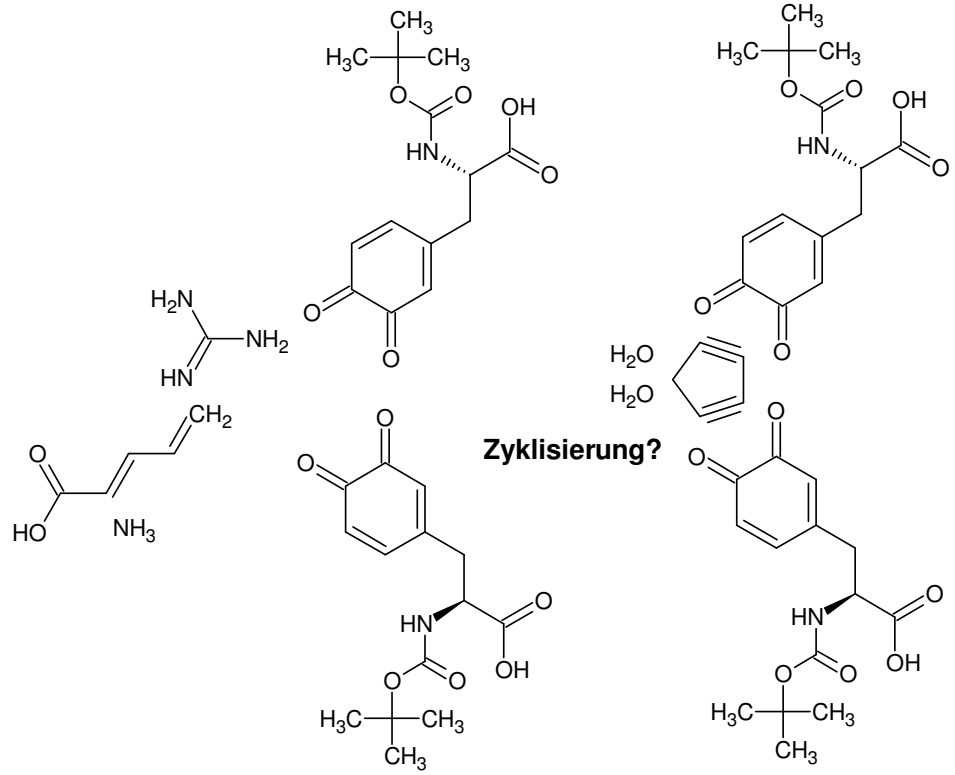

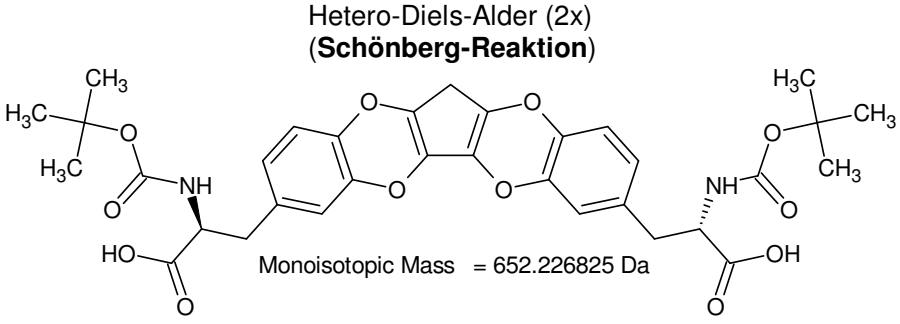

652 Da [**Arg 595 nm 8,6 min**] **{III/III}**

312,1 - 238,1 = **74,0**
368,1 - 294,1 = **74,0**
Gefundene Verbindungen: 60
CH2N2O2 MG=74,0116272
CH2N2S MG=73,9938692
(...)
N3O2 MG=73,999052
N3S MG=73,981294

-----D--B--E--f-i-l-t-e-r-----
25.08.2011 - 16:27:10,19
akzeptierte DBEs:
-2 -1 0 1 2 3 4 5 6 7 8

$CH_2N_2O_2$	DBE: 2
CH_2N_2S	DBE: 2
CH_6N_4	DBE: 1
C_2H_2OS	DBE: 2
$C_2H_2O_3$	DBE: 2
$C_2H_6N_2O$	DBE: 1
$C_3H_6O_2$	DBE: 1
C_3H_6S	DBE: 1
$C_3H_{10}N_2$	DBE: 0
$C_4H_{10}O$	DBE: 0
C_5H_{14}	DBE: -1
C_6H_2	DBE: 6
H_2N_4O	DBE: 2

13 von 60 Summenformeln

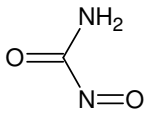
$CH_2N_2O_2$
74.011627 Da

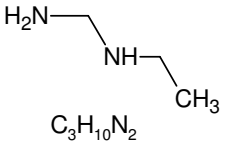
$C_3H_{10}N_2$
74.084398 Da

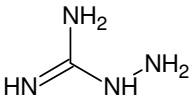
CH_6N_4
74.059246 Da

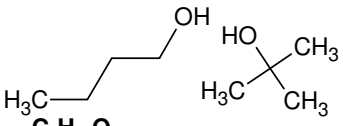
$C_4H_{10}O$
74.073165 Da

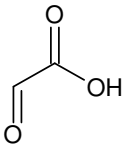
$C_2H_2O_3$
74.000394 Da

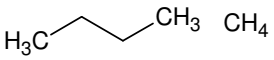
C_5H_{14}
74.10955 Da

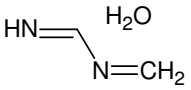
$C_2H_6N_2O$
74.048013 Da

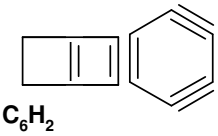
C_6H_2
74.01565 Da

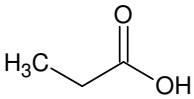
$C_3H_6O_2$
74.036779 Da

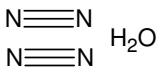
H_2N_4O
74.022861 Da

46 + 28 = 74

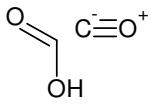
$C_2H_2O_3$
74.000394 Da

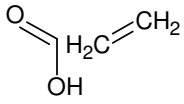
$C_3H_6O_2$
74.036779 Da

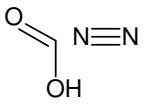
$CH_2N_2O_2$
74.011627 Da

18 + 28 = 46

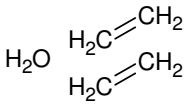
$C_4H_{10}O$
74.073165 Da

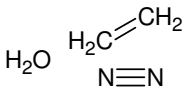
$C_2H_6N_2O$
74.048013 Da

118 - 74 = **44**
Gefundene Verbindungen: 16
CH2NO MG=44,0136382
CH4N2 MG=44,0374464
(...)
H16N2 MG=44,1313416
N2O MG=44,001063

-----D--B--E--f-i-l-t-e-r-----
30.08.2011 - 13:06:39,33
akzeptierte DBEs:
-2 -1 0 1 2 3 4 5 6 7 8

CH_4N_2	DBE: 1
CO_2	DBE: 2
CS	DBE: 2
C_2H_4O	DBE: 1
C_3H_8	DBE: 0
N_2O	DBE: 2

6 von 16 Summenformeln

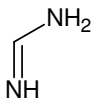
CH_4N_2
44.037448 Da

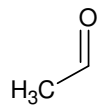
C_2H_4O
44.026215 Da

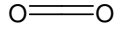
CO_2
43.989829 Da

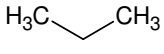
C_3H_8
44.0626 Da


CS
43.97207 Da

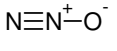
N_2O
44.001063 Da

MS^n [Arg 595 nm 8,6 min]: fragment 74 Da

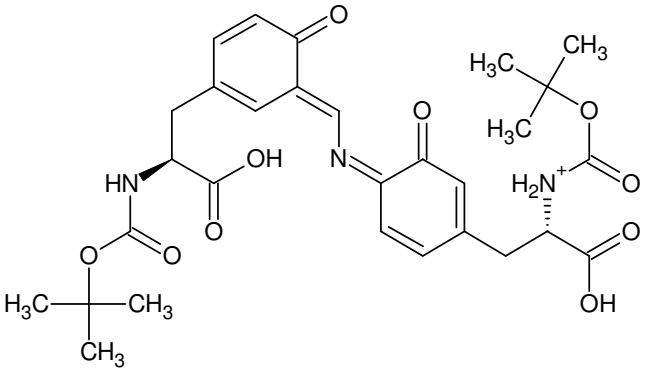

Monoisotopic Mass = 586.239521 Da

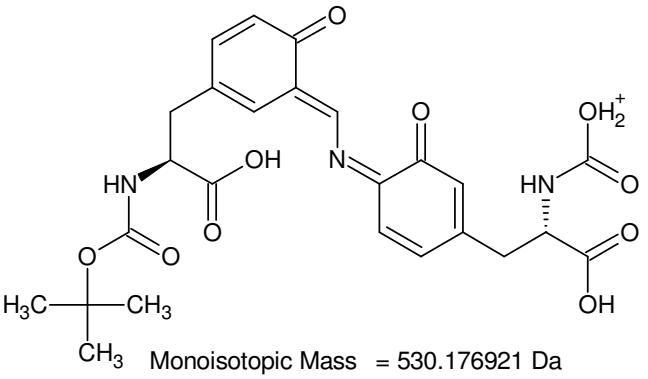

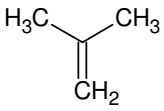

56.0626 Da

Monoisotopic Mass = 530.176921 Da

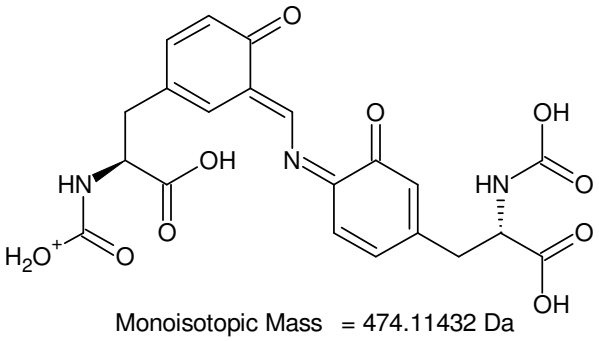

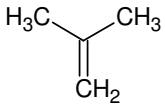

56.0626 Da

Monoisotopic Mass = 474.11432 Da

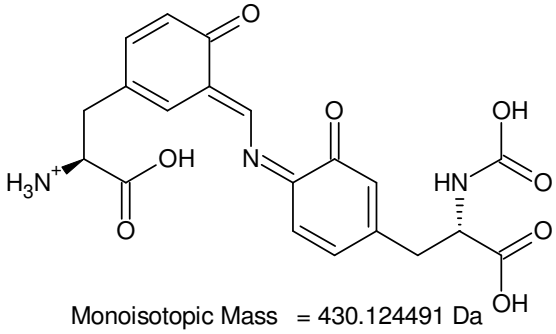

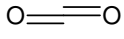

43.989829 Da

Monoisotopic Mass = 430.124491 Da

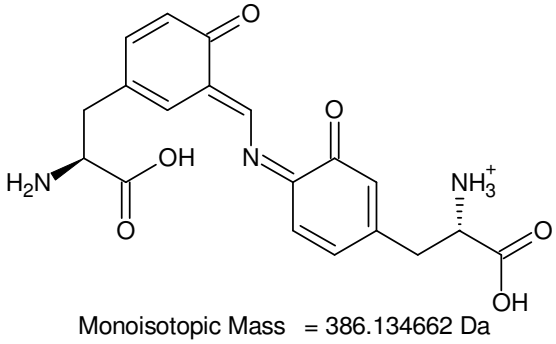

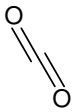

43.989829 Da

Monoisotopic Mass = 386.134662 Da

+MSn [Arg 595 nm 8,6 min]: 586 -> 530 -> 474 -> 430 -> 386 -> 368

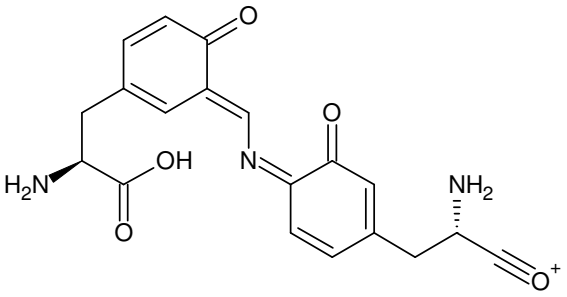

Monoisotopic Mass = 368.124097 Da

H_2O
18.010565 Da

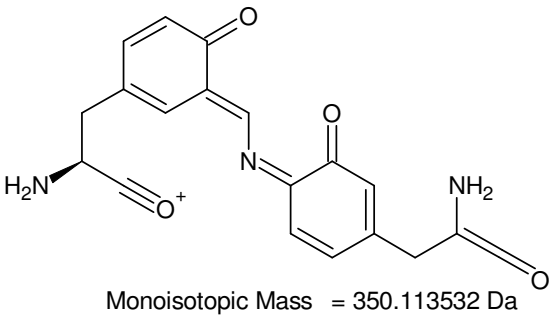

Monoisotopic Mass = 350.113532 Da

H_2O
18.010565 Da

noch einmal Wasser aus einer Carboxygruppe? - bereits ungesättigt!

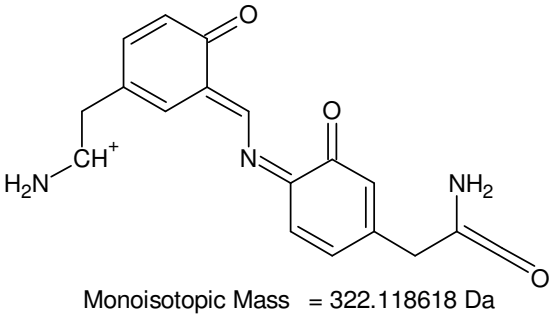

Monoisotopic Mass = 322.118618 Da

$C\equiv O^+$
27.994915 Da

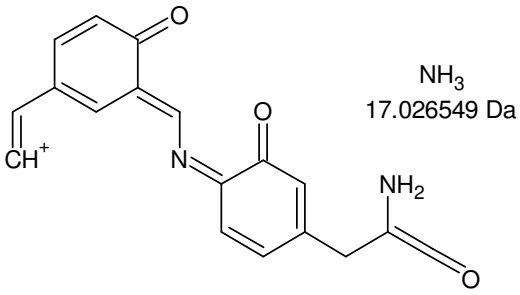

Monoisotopic Mass = 305.092069 Da

NH_3
17.026549 Da

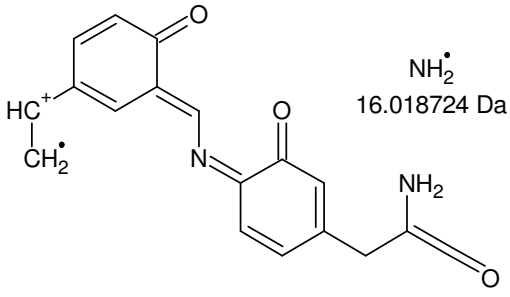

Monoisotopic Mass = 306.099894 Da

$NH_2^{\bullet}$
16.018724 Da

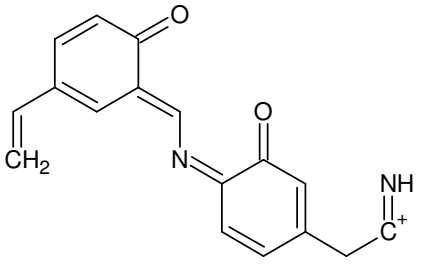

Monoisotopic Mass = 277.097154 Da

$HC^{\bullet}=O$
29.00274 Da

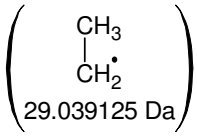

29.039125 Da

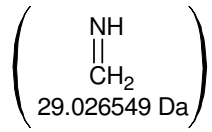

29.026549 Da

+MSn [Arg 595 nm 8,6 min]: [586 -> 530 -> 474 -> 430 -> 386 -> 368] ?> 350 -> 322 ->305, (306 -> 277)

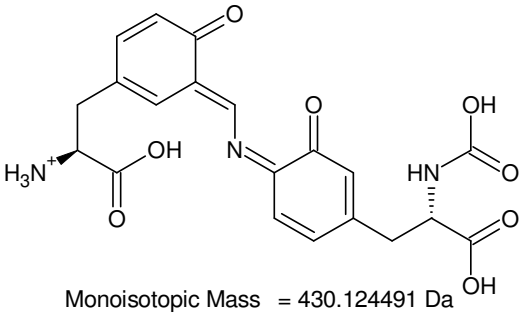

Monoisotopic Mass = 430.124491 Da

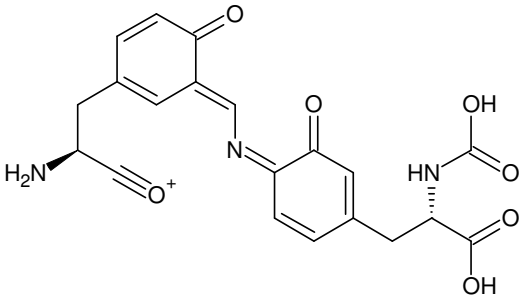

H_2O
18.010565 Da

Monoisotopic Mass = 412.113926 Da

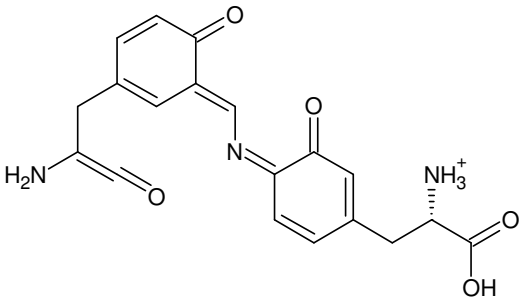

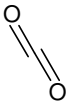

43.989829 Da

Monoisotopic Mass = 368.124097 Da

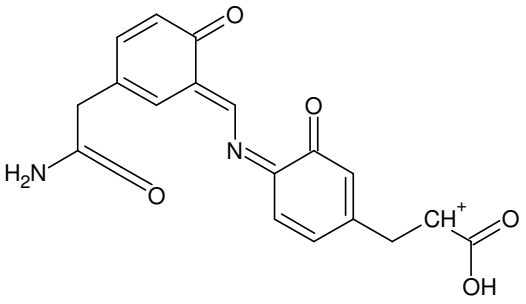

NH_3
17.026549 Da

Monoisotopic Mass = 351.097548 Da

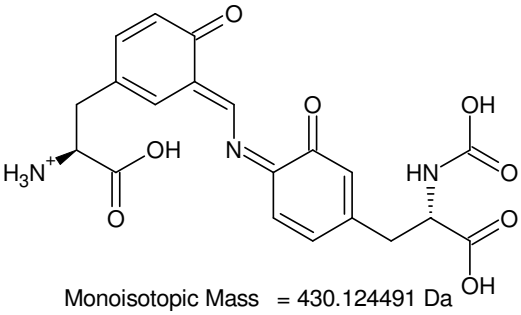

Monoisotopic Mass = 430.124491 Da

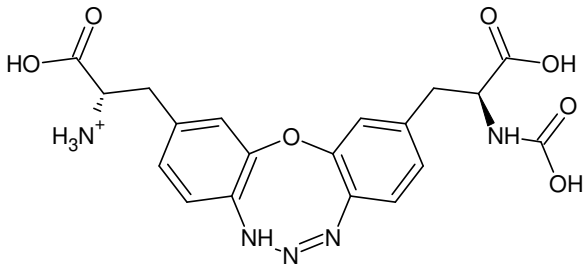

Monoisotopic Mass = 430.135724 Da

Die Seitengruppen sind identisch.

=> keine diskriminative Information
über die Koppelregion verfügbar

+MSn [Arg 595 nm 8,6 min]: 430 -> 412 -> 368 -> 351

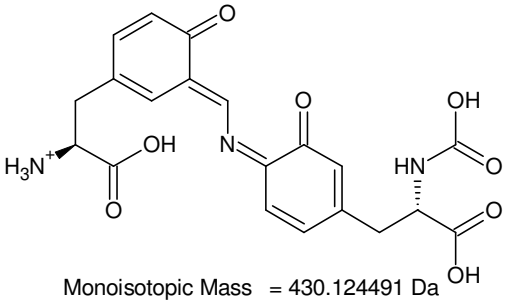

Monoisotopic Mass = 430.124491 Da

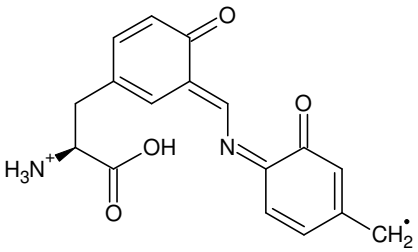

Monoisotopic Mass = 312.110458 Da

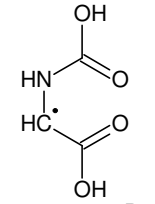

118.014033 Da

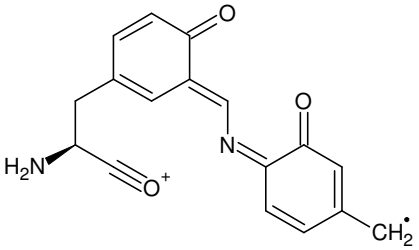

Monoisotopic Mass = 294.099894 Da

H_2O
18.010565 Da

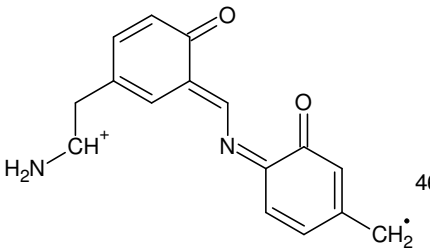

Monoisotopic Mass = 266.104979 Da

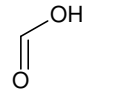

46.005479 Da

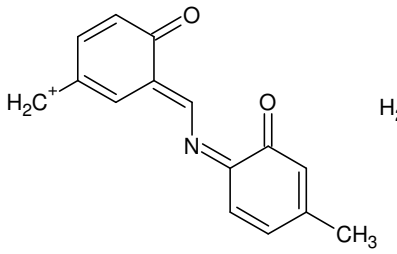

Monoisotopic Mass = 238.086255 Da

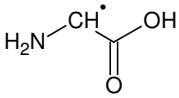

74.024203 Da

+MSn [Arg 595 nm 8,6 min]: 430 ?> 312 -> 294, 266, 238

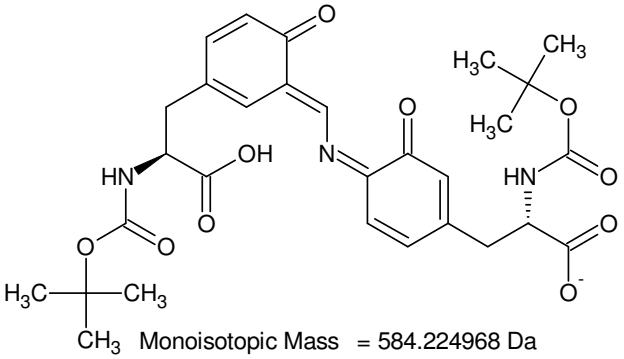

Monoisotopic Mass = 584.224968 Da

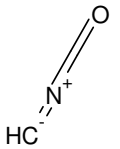

55.005814 Da

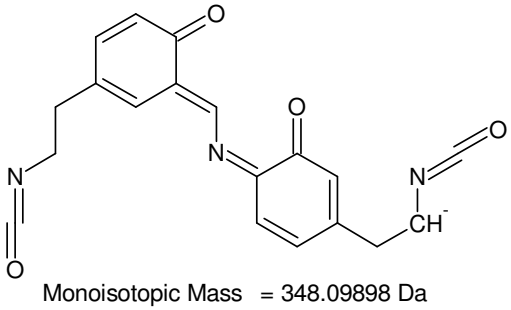

Monoisotopic Mass = 348.09898 Da

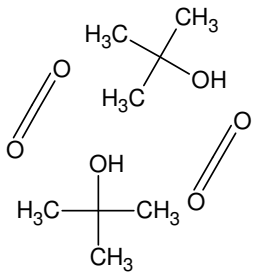

236.125988 Da

118 * 2 = 236

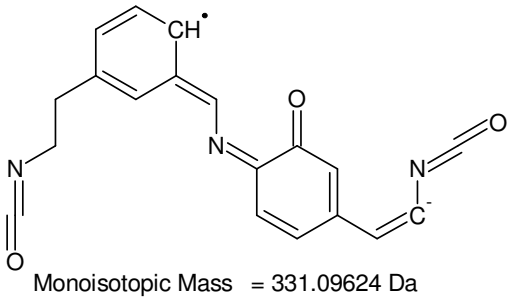

Monoisotopic Mass = 331.09624 Da

HO•
17.00274 Da

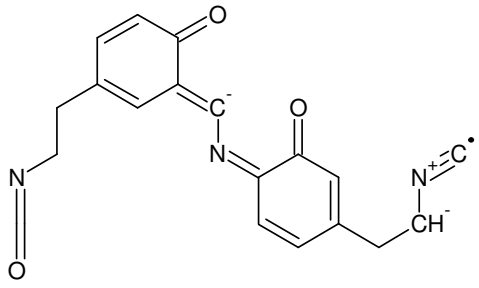

Monoisotopic Mass = 331.09624 Da

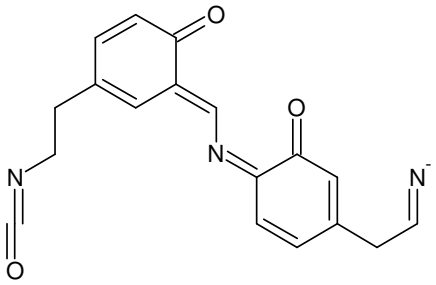

Monoisotopic Mass = 320.104065 Da

27.994915 Da

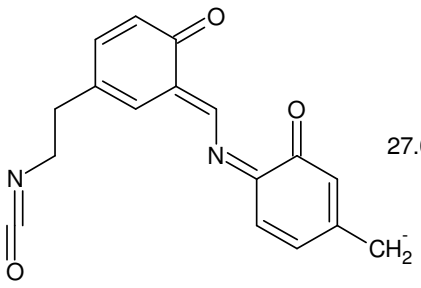

Monoisotopic Mass = 293.093166 Da

27.010899 Da

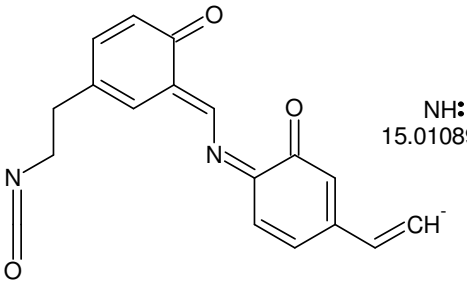

Monoisotopic Mass = 305.093166 Da

NH:
15.010899 Da

-MSn [Arg 595 nm 8,6 min]: 584 -> 348 ?> 331, X304, 320 -> (293), 305

74 + 44 = 118

430,2 - 312,1 = **118,1**
584,0 - 466,0 = **118,0**
386,2 - 268,0 = **118,2**
584,0 - 465,9 = **118,1**
Gefundene Verbindungen: 139
CH2N4O3 MG=118,0126902
CH4N5O2 MG=118,0364984
(...)
H60N3O MG=118,473613
N5O3 MG=118,000115

-----D--B--E--f-i-l-t-e-r-----
25.08.2011 - 18:43:05,89
akzeptierte DBE:
-2 -1 0 1 2 3 4 5 6 7 8

$CH_2N_4O_3$ DBE: 3
CH_6N_6O DBE: 2
$C_2H_2N_2O_4$ DBE: 3
$C_2H_6N_4O_2$ DBE: 2
$C_2H_{10}N_6$ DBE: 1
$C_3H_2O_5$ DBE: 3
$C_3H_6N_2O_3$ DBE: 2
$C_3H_{10}N_4O$ DBE: 1
$C_4H_6O_4$ DBE: 2
$C_4H_{10}N_2O_2$ DBE: 1
$C_4H_{14}N_4$ DBE: 0
$C_5H_2N_4$ DBE: 7
$C_5H_{10}O_3$ DBE: 1
$C_5H_{14}N_2O$ DBE: 0
$C_6H_2N_2O$ DBE: 7
$C_6H_{14}O_2$ DBE: 0
$C_6H_{18}N_2$ DBE: -1
$C_7H_2O_2$ DBE: 7
$C_7H_6N_2$ DBE: 6
$C_7H_{18}O$ DBE: -1
C_8H_6O DBE: 6
C_8H_{22} DBE: -2
C_9H_{10} DBE: 5
$H_2N_6O_2$ DBE: 3
H_6N_8 DBE: 2
H_6O_7 DBE: -2

26 von 139 Summenformeln

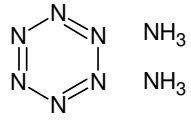

H_6N_8
118.071542 Da

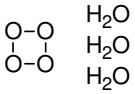

H_6O_7
118.011353 Da

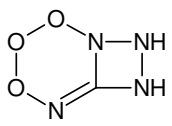
$CH_2N_4O_3$
118.01269 Da

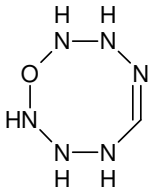
CH_6N_6O
118.060309 Da

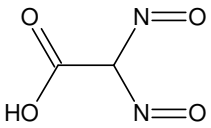
$C_2H_2N_2O_4$
118.001457 Da

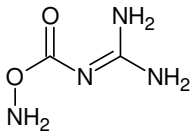
$C_2H_6N_4O_2$
118.049075 Da

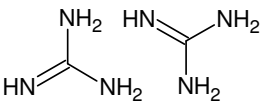
$C_2H_{10}N_6$
118.096694 Da

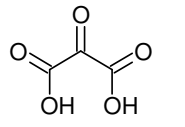
$C_3H_2O_5$
117.990223 Da

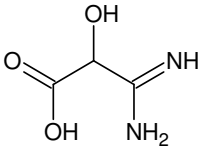
$C_3H_6N_2O_3$
118.037842 Da

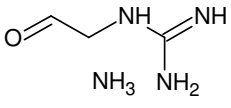
$C_3H_{10}N_4O$
118.085461 Da

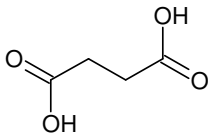
$C_4H_6O_4$
118.026609 Da

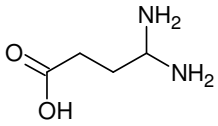
$C_4H_{10}N_2O_2$
118.074228 Da

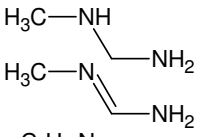
$C_4H_{14}N_4$
118.121846 Da

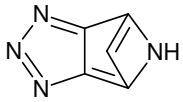
$C_5H_2N_4$
118.027946 Da

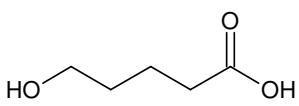
$C_5H_{10}O_3$
118.062994 Da

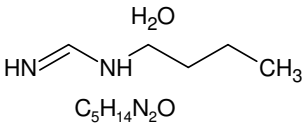

$C_5H_{14}N_2O$
118.110613 Da

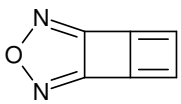
$C_6H_2N_2O$
118.016713 Da

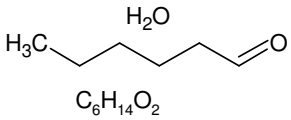

$C_6H_{14}O_2$
118.09938 Da

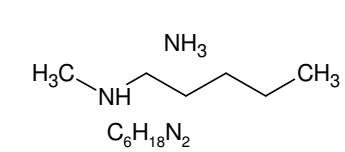

$C_6H_{18}N_2$
118.146999 Da

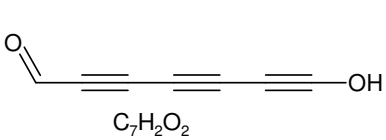
$C_7H_2O_2$
118.005479 Da

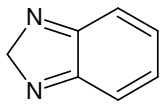
$C_7H_6N_2$
118.053098 Da

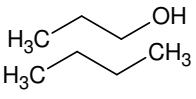
$C_7H_{18}O$
118.135765 Da

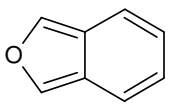
C_8H_6O
118.041865 Da

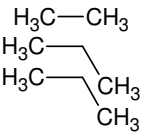
C_8H_{22}
118.172151 Da

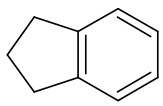
C_9H_{10}
118.07825 Da

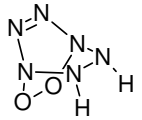
$H_2N_6O_2$
118.023923 Da

MS^n [Arg 595 nm 8,6 min]: fragment 118 Da

584 $-^{118}>$ 466 $-^{118}>$ 348 $-^{28}>$ 320 $-^{27}>$ 293

$-^{15}>$ 305

$-^{43}>$ 305

$-^{44}>$ 304

$-^{17}>$ 331

15 Da +/- 0,5 Da
Gefundene Verbindungen: 2
CH_3 MG=15,0234738
HN MG=15,0108986

17 Da +/- 0,5 Da
Gefundene Verbindungen: 3
HO MG=17,0027396
CH_5 MG=17,039123
H_3N MG=17,0265478

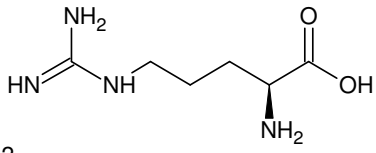

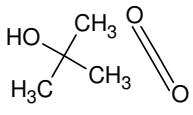

118.062994 Da

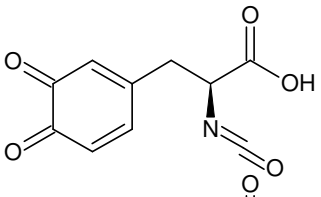

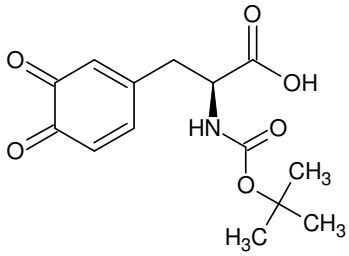

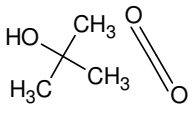

118.062994 Da

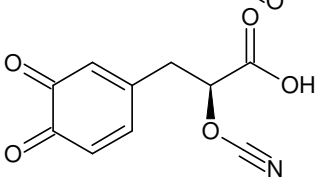

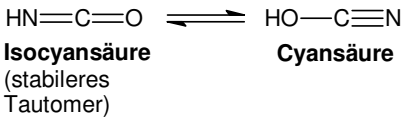

Isocyansäure (stabileres Tautomer)

Cyansäure

27.994915 Da

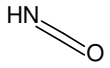

43.005814 Da

43.989829 Da

17.00274 Da

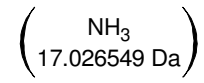

17.026549 Da

NH**:**
15.010899 Da

27.010899 Da

Diese Zerfallsroute ist zur Gänze mit der Boc-Gruppe erklärbar. => keine strukturelle Information über die Kopplungsregion. (Höchstens ein Hinweis auf eine freie Aminogruppe, welche dann allerdings auch bereits schon weiter unten im Zerfallsbaum gut sichtbar sein sollte.)

-MS^2(584.0)

m/z	I
347.9	3322
348.8	167
466.0	2330
466.9	173
584.0	449
.....	.....
565.0	9
565.2	7
567.0	**10**
569.2	9

-MS^3(584 -> **466**): 449 **nicht im Spektrum**

-MS^3(584 -> **348**): 330.6 (10), **331.6 (12)** und 332.1 (19)

zweite Spektrenserie: **kein Signal** von 325 - 345

=> **Eine freie Aminogruppe hätte deutlich intensivere Signale bewirkt.**

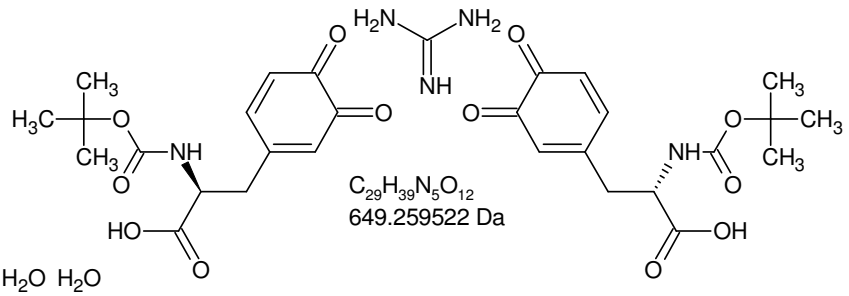

$C_{29}H_{39}N_5O_{12}$
649.259522 Da

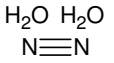

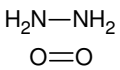

Chromophore isoliert

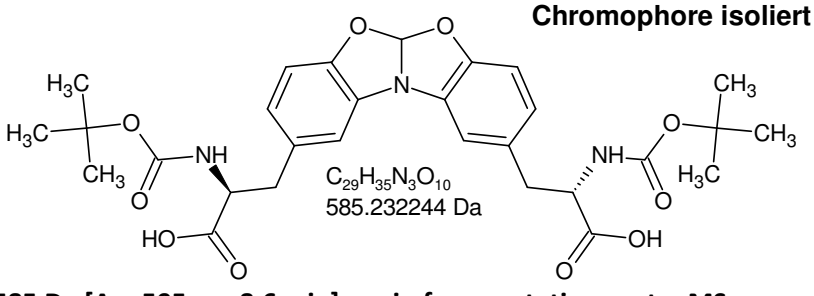

$C_{29}H_{35}N_3O_{10}$
585.232244 Da

585 Da [Arg 595 nm 8,6 min]: main fragmentation route -MSn

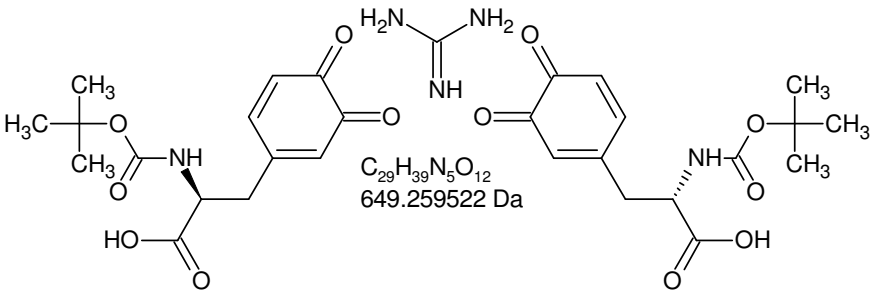

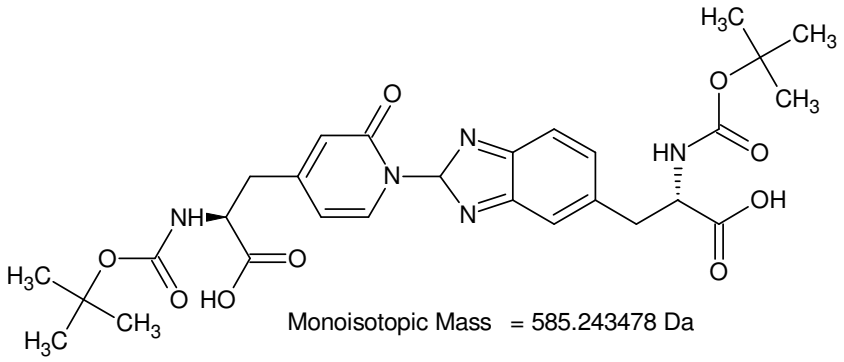

H_2O H_2O
36.021129 Da

$C\equiv O^+$
27.994915 Da

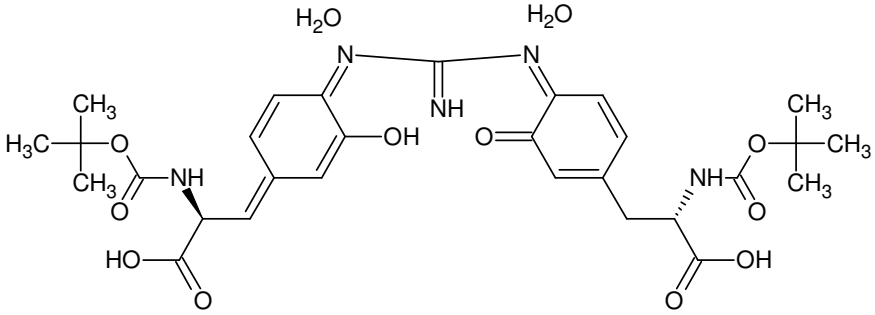

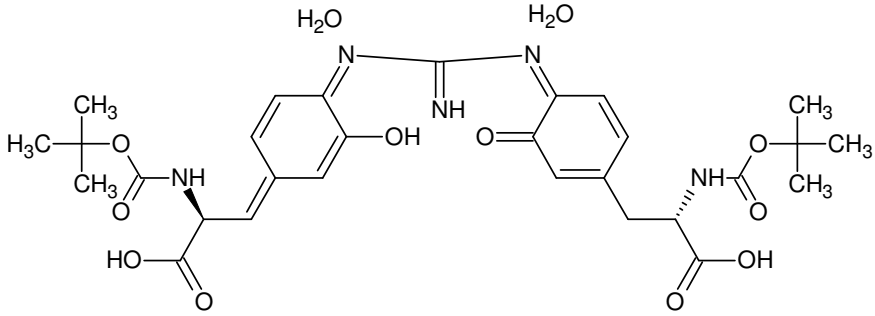

Aldolkondensation

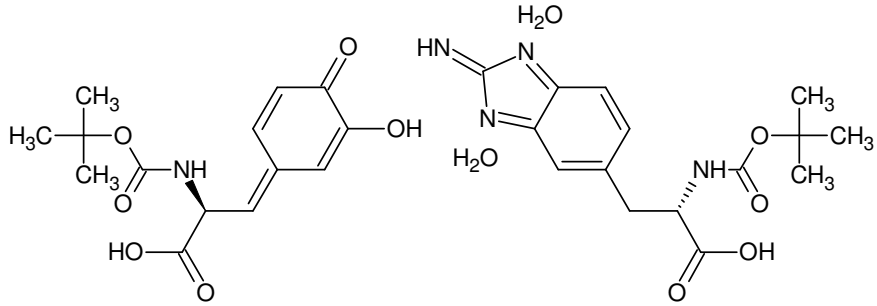

Aldolkondensation

Die 2. Oxogruppe ist nicht enolisierbar.

585 Da [Arg 595 nm 8,6 min]

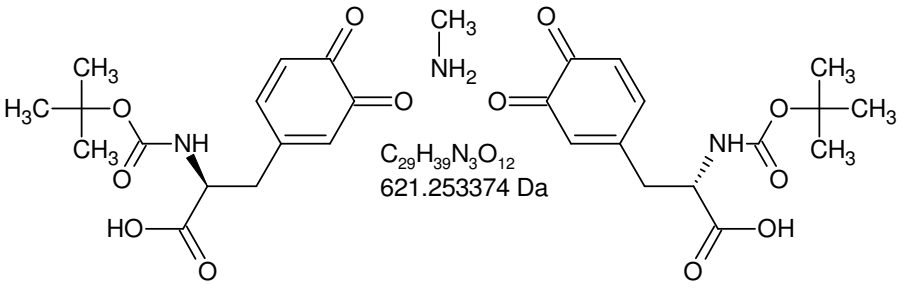

CH_3-NH_2:
Decarboxylationsprodukt von Glycin oder jeder anderen Aminosäure nach Seitenkettenverlust

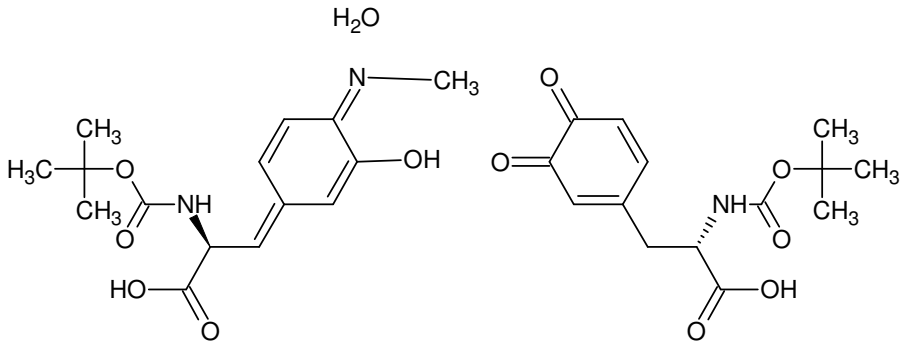

Iminbildung: -H_2O;
Produkt säurelabil ("Schiff'sche Base")

Enolisierung

Reihenfolge umgekehrt? - Nur eine der beiden Oxogruppen ist enolisierbar während beide Imine bilden können.

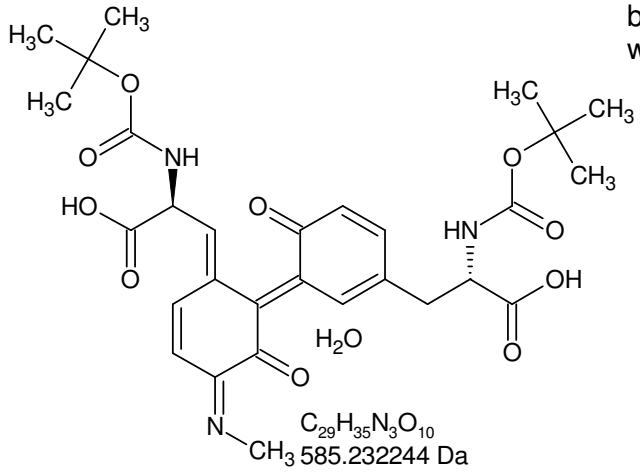

Aldolkondensation: -H_2O;

zwei Möglichkeiten für die Oxokomponente -> Isomere; basenkatalysiert?

=> erweiterte chinoide Struktur, Alkyl-N zeitigt (als auxochrome Gruppe) einen starken bathochromen Effekt.

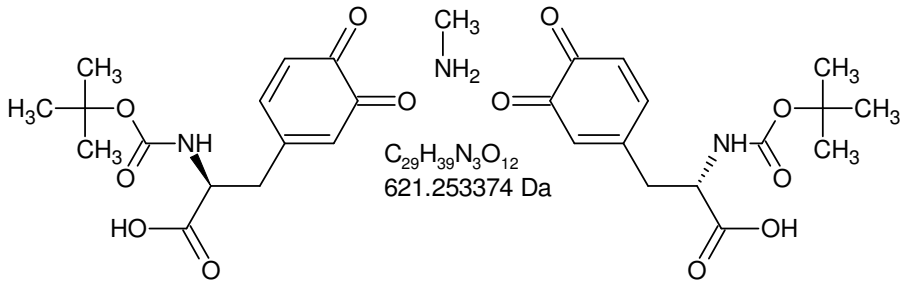

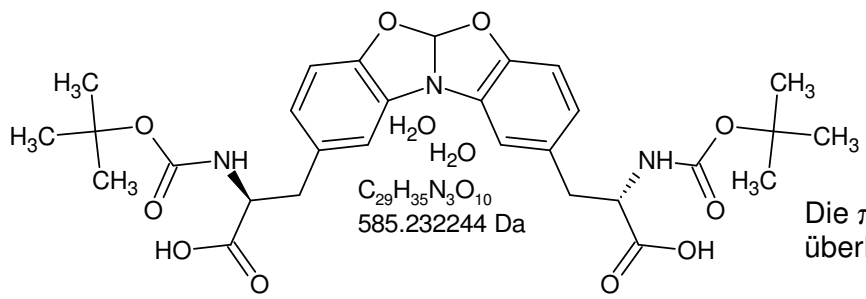

Die π-Systeme der Chromophore überlappen sich nicht.

585 Da [Arg 595 nm 8,6 min]

621 - 585 = **36**
Gefundene Verbindungen: 8
CH8O MG=36,0575118
CH10N MG=36,08132
C2H12 MG=36,0938952
C3 MG=36
H4O2 MG=36,0211284
H4S MG=36,0033704
H6NO MG=36,0449366
H8N2 MG=36,0687448

-----D--B--E--f-i-l-t-e-r-----
31.08.2011 - 11:57:23,98
akzeptierte DBE:
-2 -1 0 1 2 3 4 5 6 7 8

CH_8O DBE: -2
C_3 DBE: 4
H_4O_2 DBE: -1
H_4S DBE: -1
H_8N_2 DBE: -2

5 von 8 Summenformeln

CH_4 H_2 H_2O
CH_8O
36.057515 Da

C_3
36 Da

H_2O H_2O
H_4O_2
36.021129 Da

H_2S H_2
H_4S
36.00337 Da

NH_3 NH_3 H_2
H_8N_2
36.068748 Da

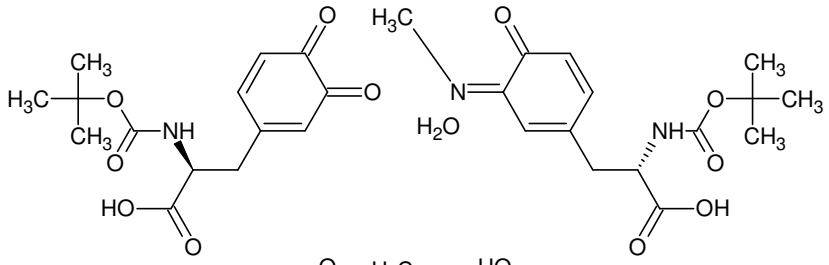

Iminbildung

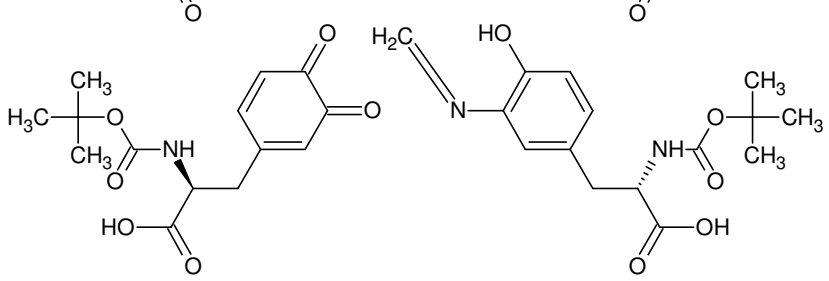

Rearomatisierung

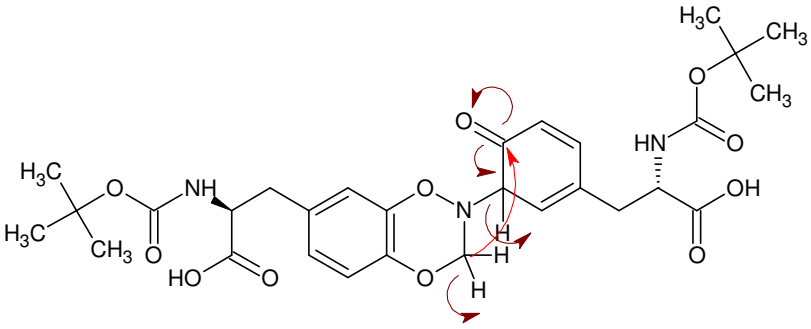

Hetero-Diels-Alder-Reaktion

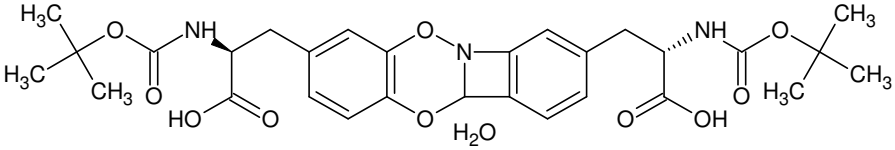

$C_{29}H_{35}N_3O_{10}$
585.232244 Da

Wasserelimination unter Bildung eines 4-Ringes?
Die Chromophore sind voneinander elektronisch isoliert.

585 Da [Arg 595 nm 8,6 min]

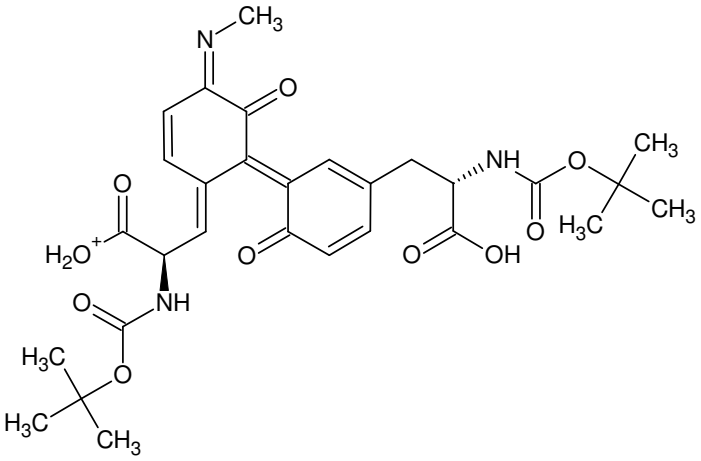

Monoisotopic Mass = 586.239521 Da

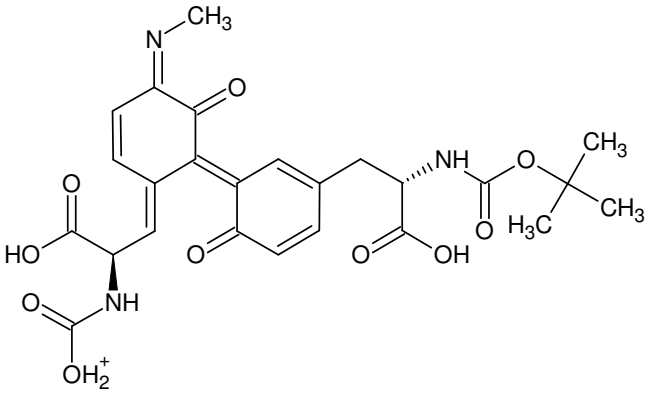

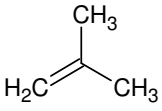

56.0626 Da

Monoisotopic Mass = 530.176921 Da

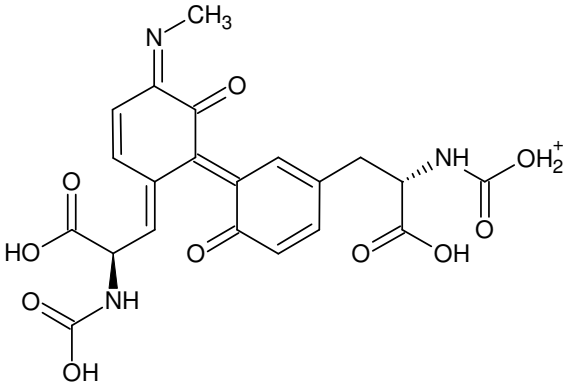

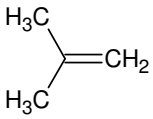

56.0626 Da

Monoisotopic Mass = 474.11432 Da

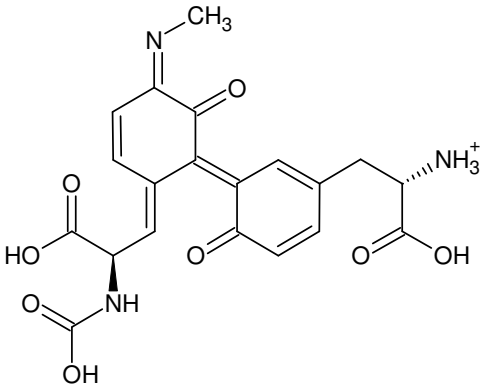

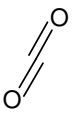

43.989829 Da

Monoisotopic Mass = 430.124491 Da

+MSn [Arg 595 nm 8,6 min]: 586 -> 530 -> 474 -> 430

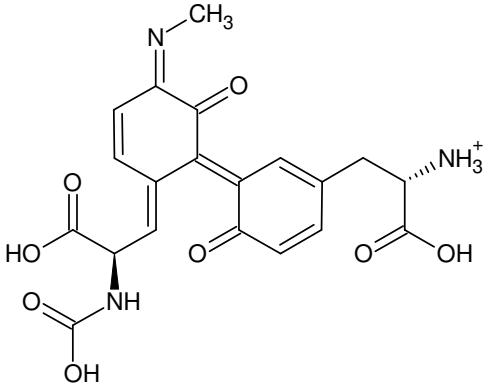

Monoisotopic Mass = 430.124491 Da

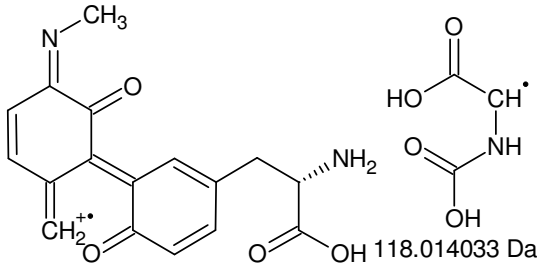

118.014033 Da

Monoisotopic Mass = 312.110458 Da

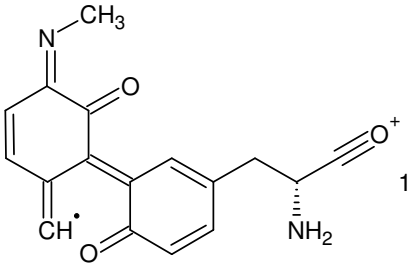

H_2O
18.010565 Da

Monoisotopic Mass = 294.099894 Da

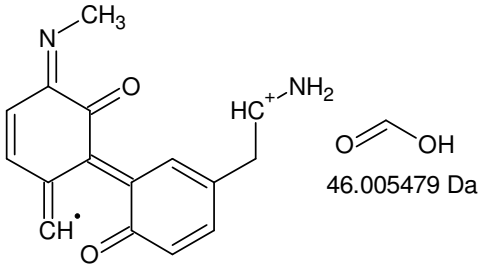

46.005479 Da

Monoisotopic Mass = 266.104979 Da

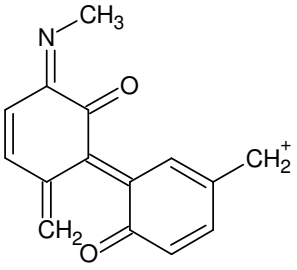

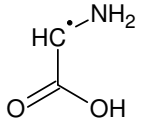

74.024203 Da

intensivstes Signal ausgehend von 312 Th

Monoisotopic Mass = 238.086255 Da

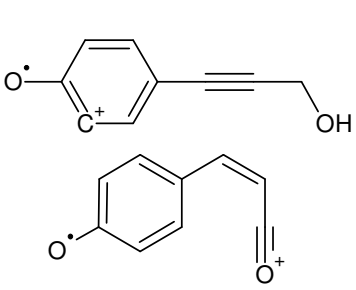

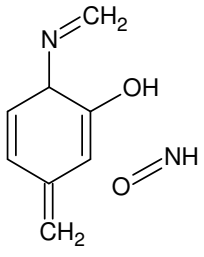

166.074228 Da

Monoisotopic Mass = 146.036231 Da

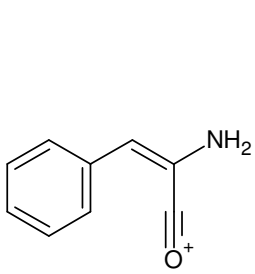

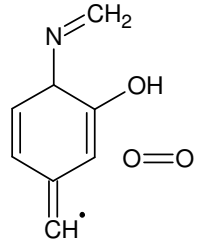

166.050418 Da

Monoisotopic Mass = 146.06004 Da

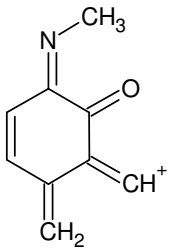

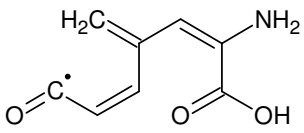

166.050418 Da

Monoisotopic Mass = 146.06004 Da

+MSn [Arg 595 nm 8,6 min]: [586 -> 530 -> 474 -> 430] -> 312 -> 294, 266, 238, (146)

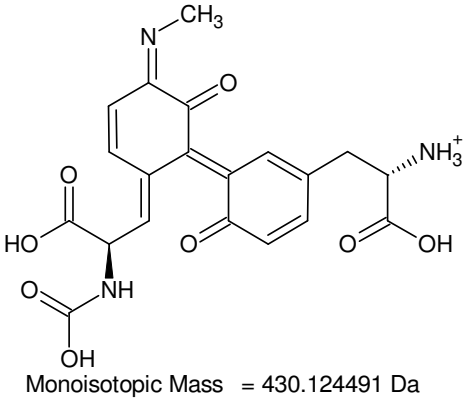

Monoisotopic Mass = 430.124491 Da

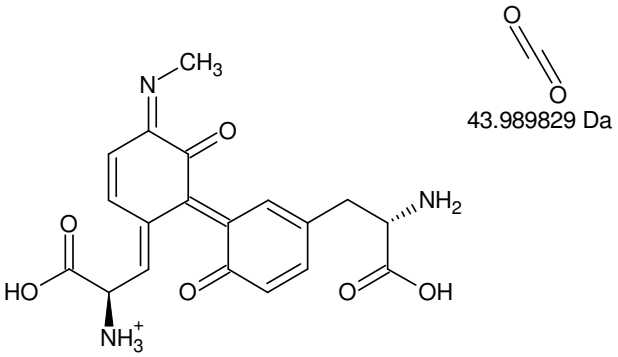

Monoisotopic Mass = 386.134662 Da

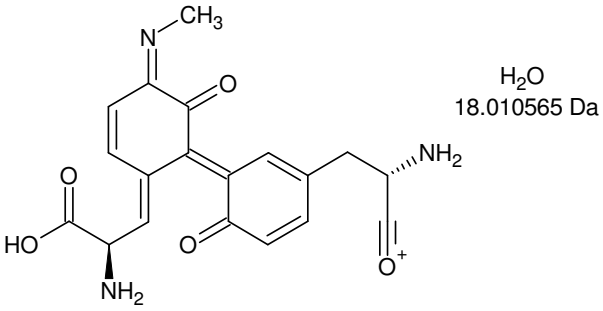

Monoisotopic Mass = 368.124097 Da

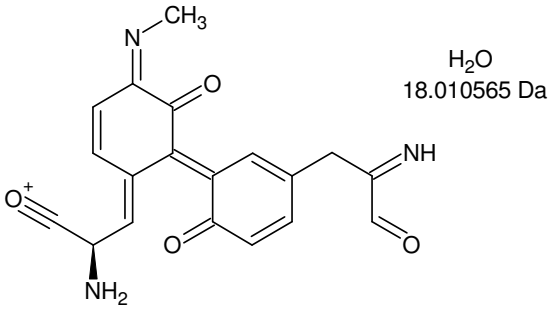

Monoisotopic Mass = 350.113532 Da

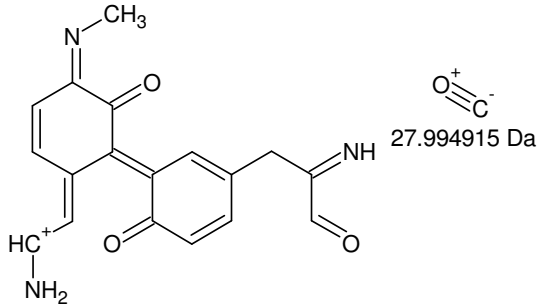

Monoisotopic Mass = 322.118618 Da

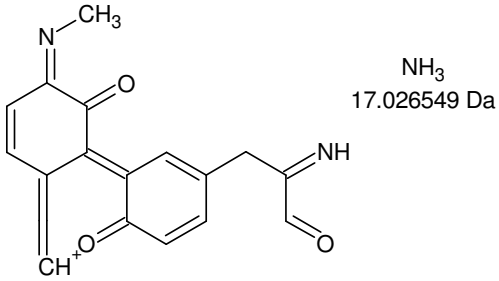

Monoisotopic Mass = 305.092069 Da

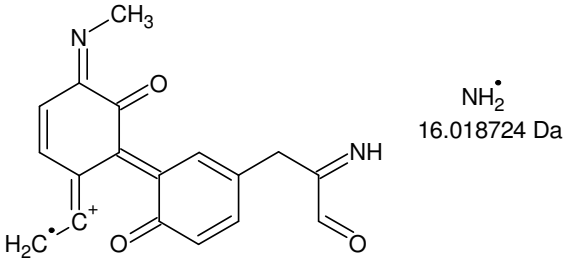

Monoisotopic Mass = 306.099894 Da

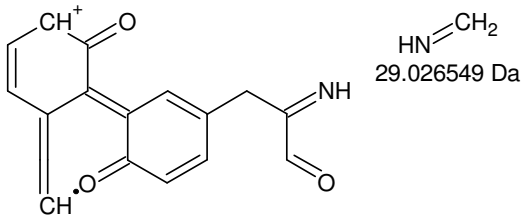

Monoisotopic Mass = 277.073345 Da

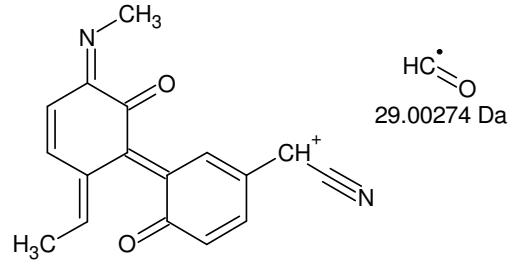

Monoisotopic Mass = 277.097154 Da

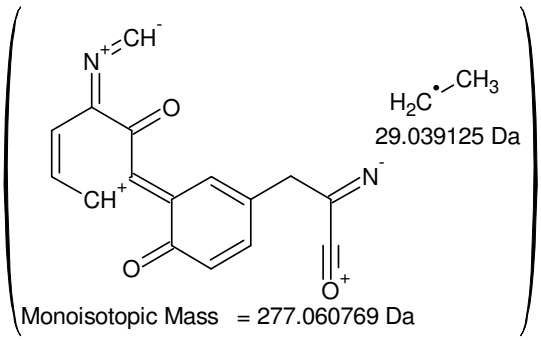

Monoisotopic Mass = 277.060769 Da

+MSn [Arg 595 nm 8,6 min]: [586 -> 530 -> 474 -> 430] -> 386 -> 368 ?> 350 -> 322 -> 305, (306 -> 277)

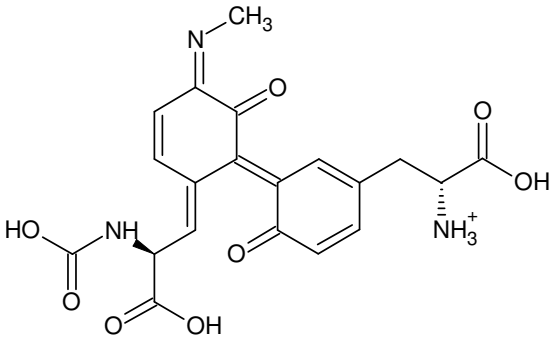

Monoisotopic Mass = 430.124491 Da

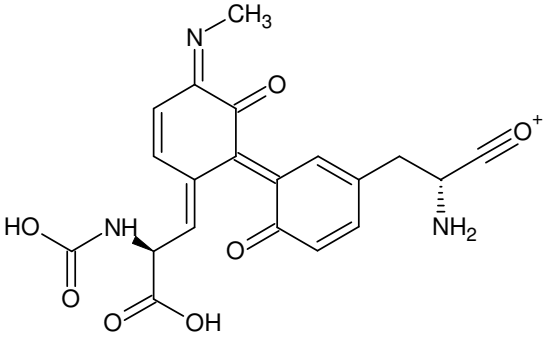

H_2O
18.010565 Da

Monoisotopic Mass = 412.113926 Da

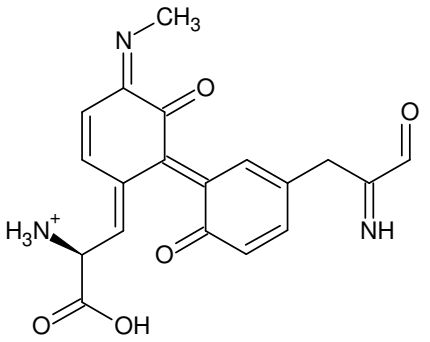

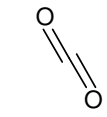

43.989829 Da

Monoisotopic Mass = 368.124097 Da

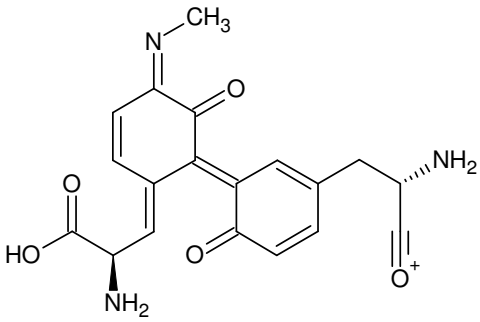

Monoisotopic Mass = 368.124097 Da

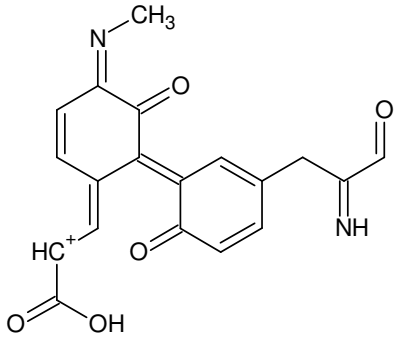

NH_3
17.026549 Da

Monoisotopic Mass = 351.097548 Da

+MSn [Arg 595 nm 8,6 min]: [586 -> 530 -> 474 -> 430] -> 412 -> 368 -> 351

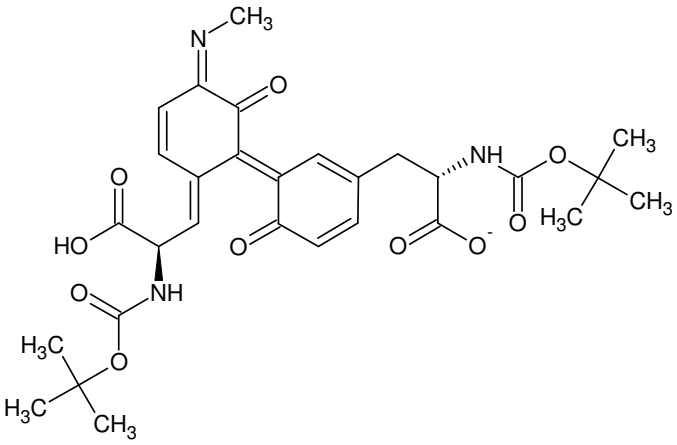

Monoisotopic Mass = 584.224968 Da

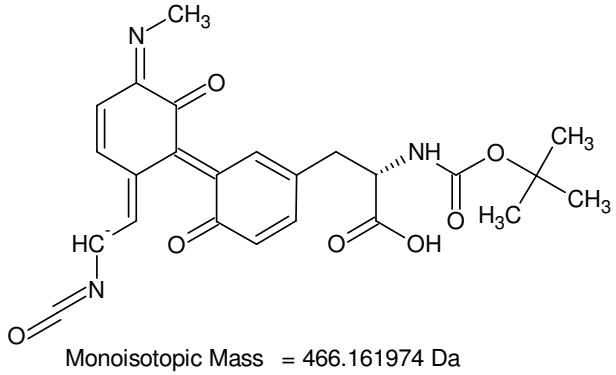

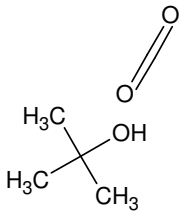

118.062994 Da

Monoisotopic Mass = 466.161974 Da

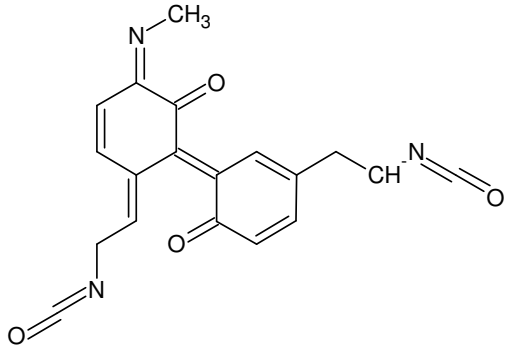

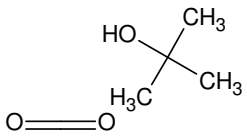

118.062994 Da

Monoisotopic Mass = 348.09898 Da

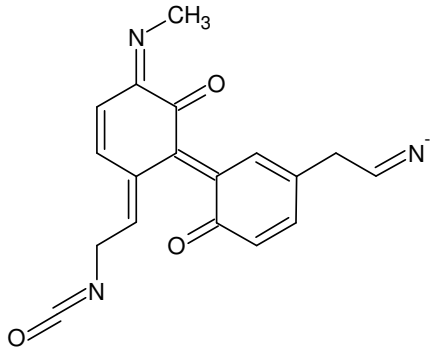

27.994915 Da

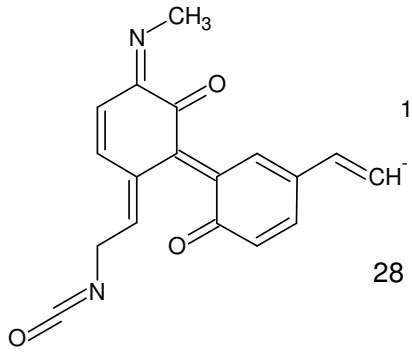

NH: 15.010899 Da

28 + 15 = 43

Monoisotopic Mass = 320.104065 Da

Monoisotopic Mass = 305.093166 Da

-MSn [Arg 595 nm 8,6 min]: 584 -> 466 -> 348 -> 320 -> 305

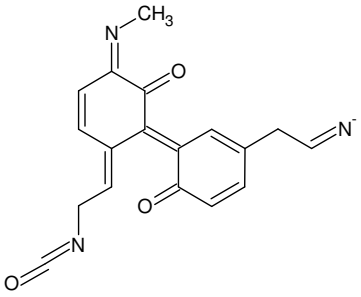

Monoisotopic Mass = 320.104065 Da

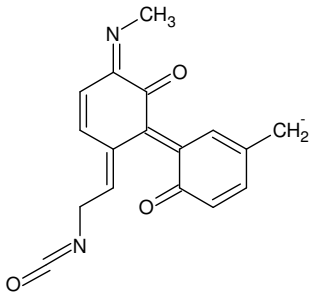

Monoisotopic Mass = 293.093166 Da

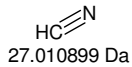

27.010899 Da

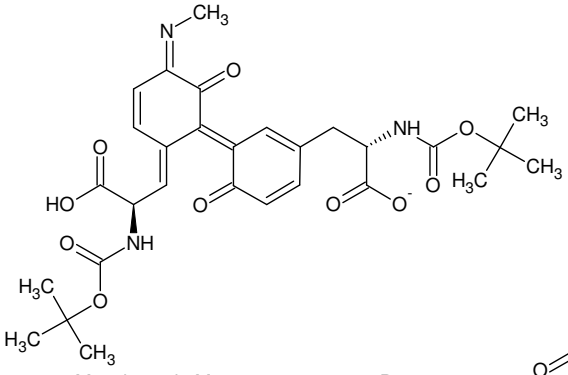

Monoisotopic Mass = 584.224968 Da

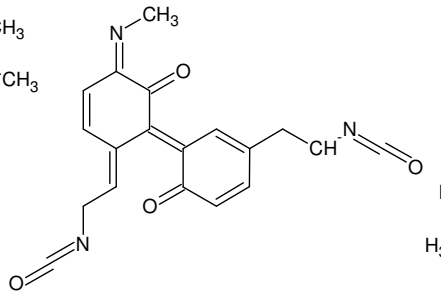

Monoisotopic Mass = 348.09898 Da

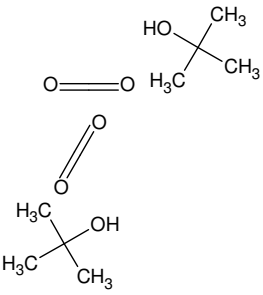

236.125988 Da

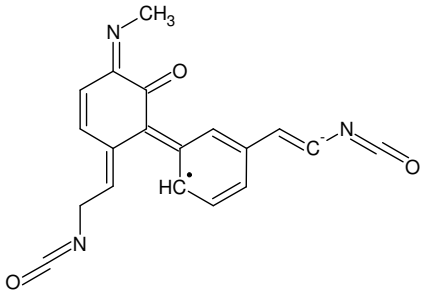

Monoisotopic Mass = 331.09624 Da

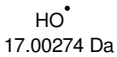

17.00274 Da

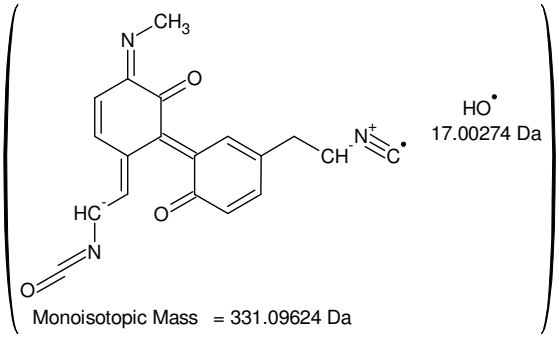

Monoisotopic Mass = 331.09624 Da

17.00274 Da

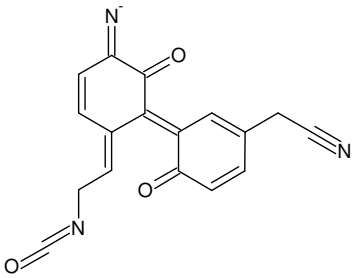

Monoisotopic Mass = 304.072765 Da

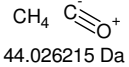

44.026215 Da

-MSn [Arg 595 nm 8,6 min]: [584 -> 466 -> 348 -> 320] -> 293 and 584 -> 348 ?> 331, 304

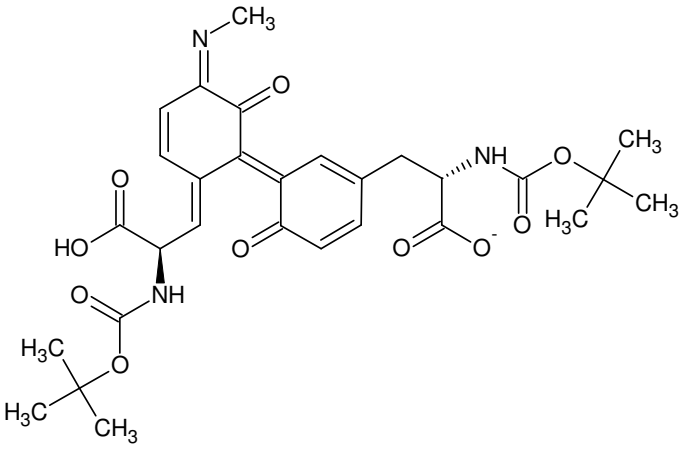

Monoisotopic Mass = 584.224968 Da

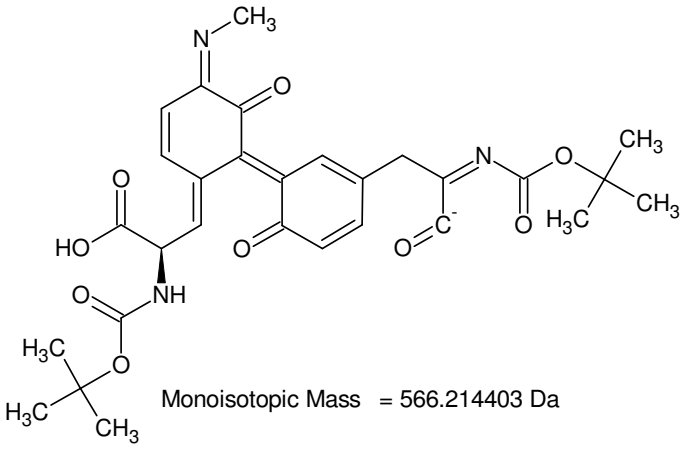

H_2O
18.010565 Da

Monoisotopic Mass = 566.214403 Da

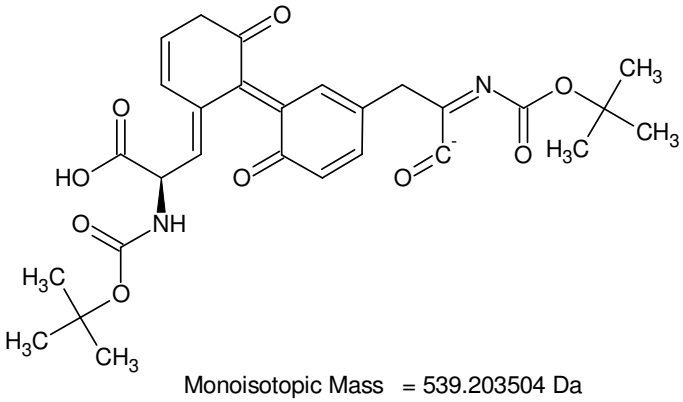

$N{\equiv}CH$ H_2O
45.021464 Da

Monoisotopic Mass = 539.203504 Da

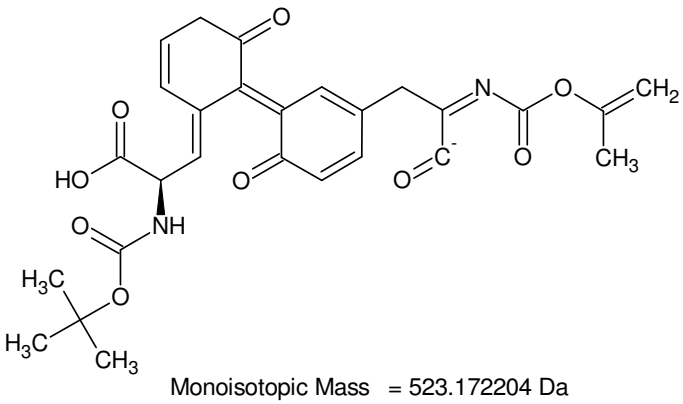

$N{\equiv}CH$ H_2O CH_4
61.052764 Da

$O{=}NH_3{=}O$
61.016378 Da

Monoisotopic Mass = 523.172204 Da

-MSn [Arg 595 nm 8,6 min]: 584 -> 566, 539, 523, 510, (484), 449

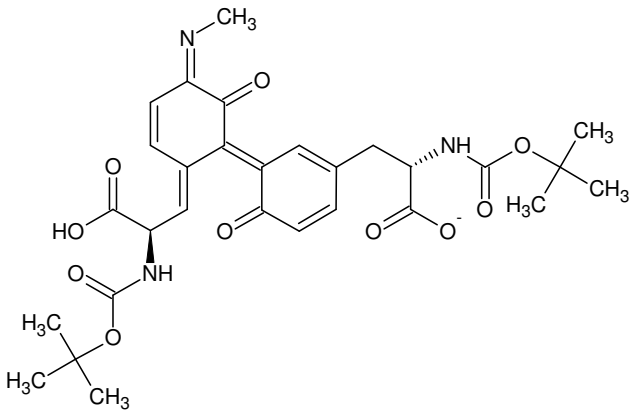

Monoisotopic Mass = 584.224968 Da

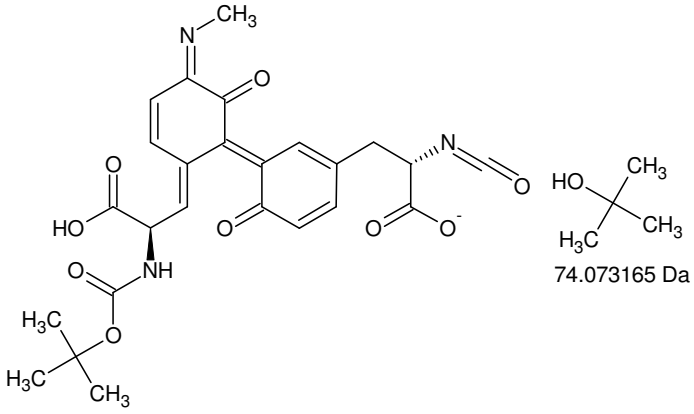

74.073165 Da

Monoisotopic Mass = 510.151803 Da

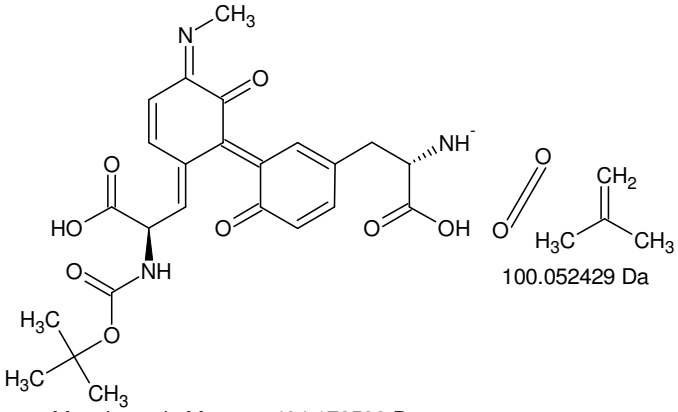

100.052429 Da

Monoisotopic Mass = 484.172538 Da

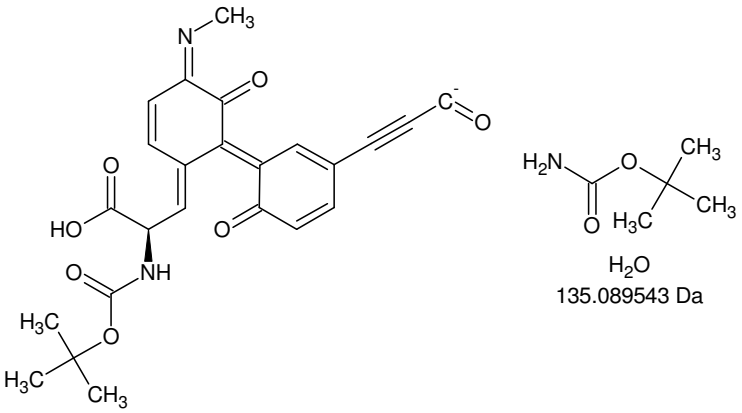

135.089543 Da

Monoisotopic Mass = 449.135425 Da

-MSn [Arg 595 nm 8,6 min]: 584 -> 510, (484), 449

XIII.III.IV. Arg 595 nm 12,3 min

+MS^n

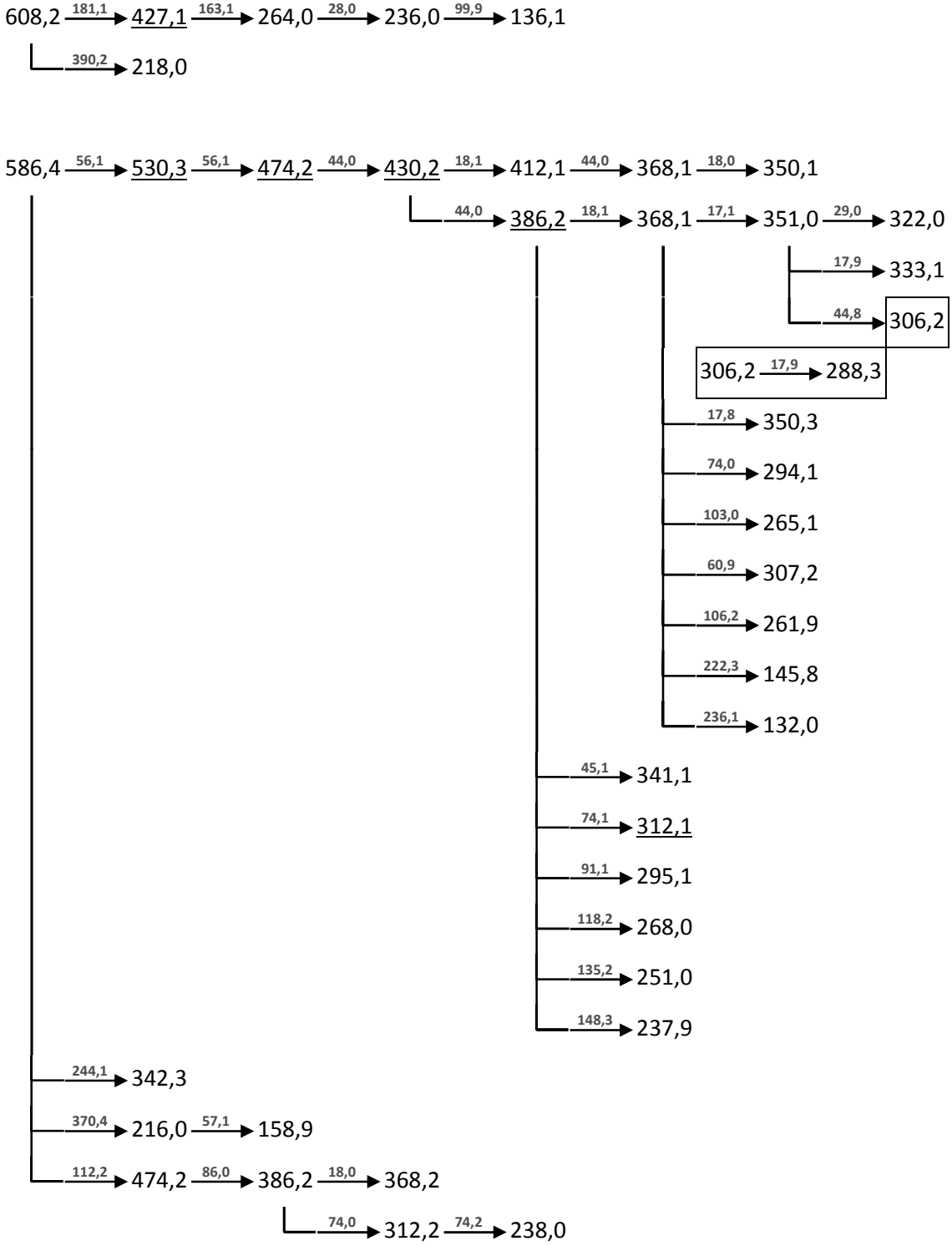

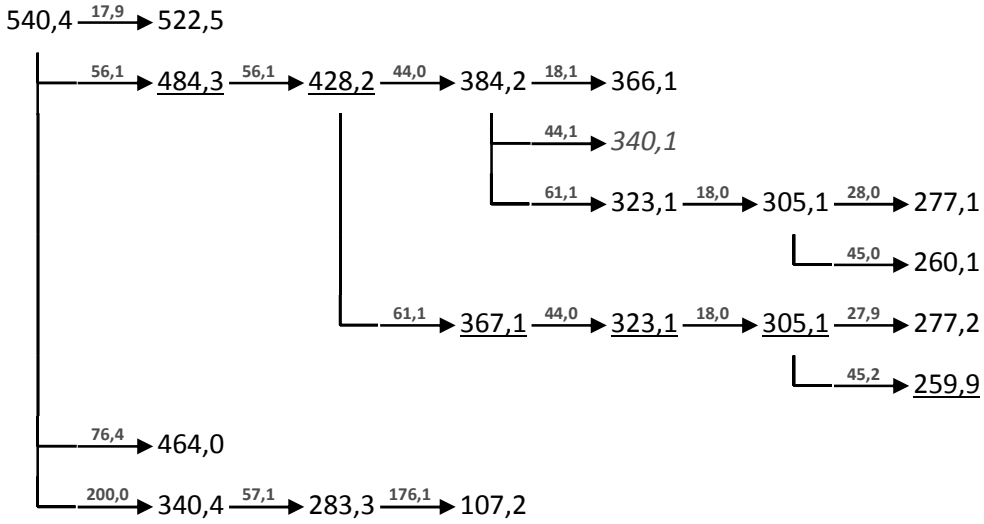

-MS^n

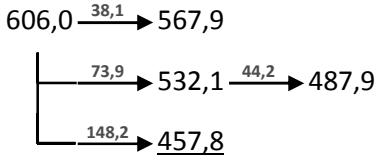

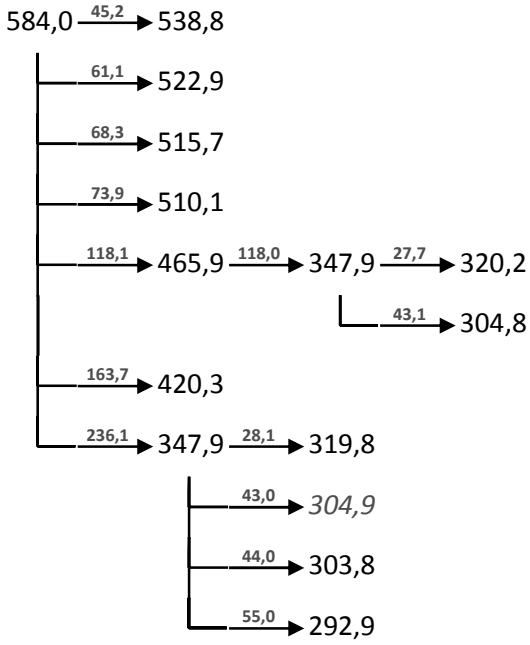

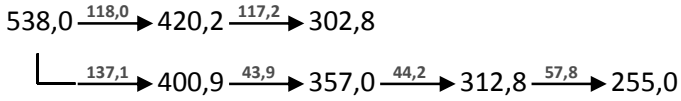

isotopic fingerprint:

peak area / % of monoisotopic	**+1**	**+2**	**+3**
theoretical ($C_{29}H_{36}N_3O_{10}^+$):	33,4	7,5	1,3
measured (586,3 Th):	34,6	4,1	1,1
measured (-584,0 Th):	44,9	13,9	8,0

measured (540,4 Th):	50,1	24,2	6,0
measured (-538,0 Th):	38,6	16,7	-

Figure XIII-LIV MS^n analysis of Arg 595 nm 12,3 min

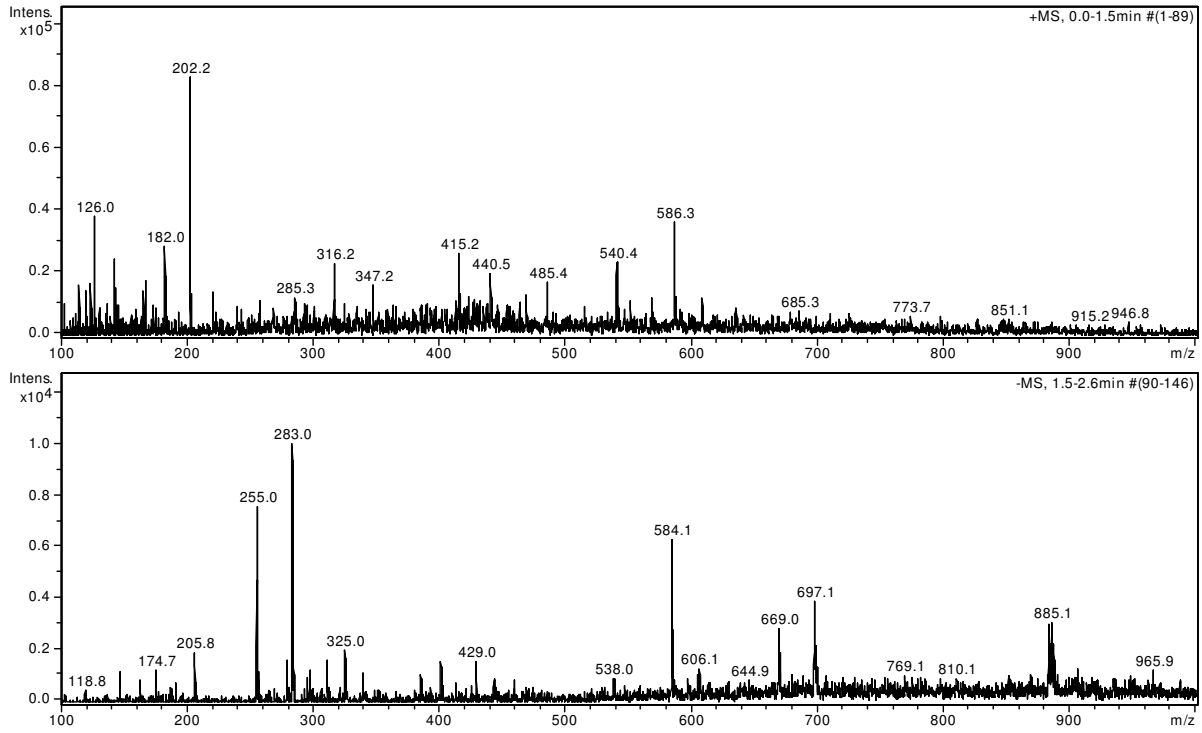

Figure XIII-LV Arg 595 nm 12,3 min: fraction 3; 31 % MeOH, 31 % ACN, 1 ‰ FA in ddH_2O; full scan MS^1

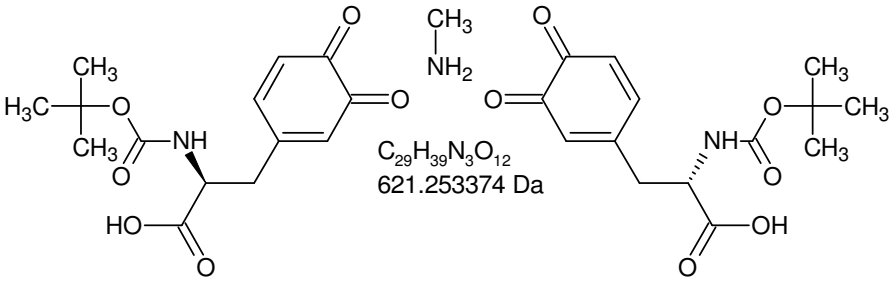

$C_{29}H_{39}N_3O_{12}$
621.253374 Da

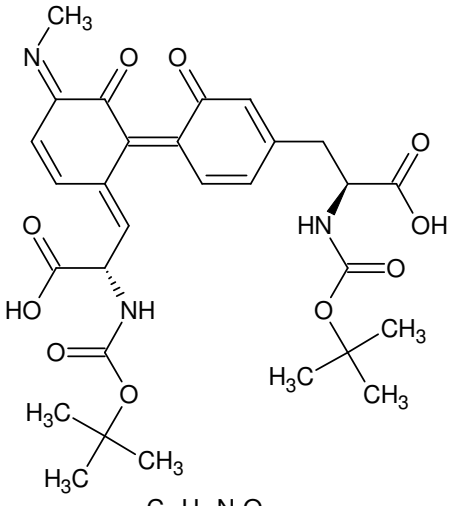

$C_{29}H_{35}N_3O_{10}$
585.232244 Da

H_2O
H_2O
36.021129 Da

anderes Isomer
(Aldolkondensationsprodukt) der Struktur aus Arg_595nm_8,6min

585 Da [Arg 595 nm 12,3 min]

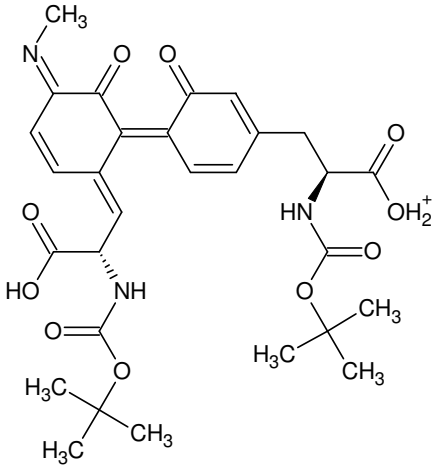

Monoisotopic Mass = 586.239521 Da

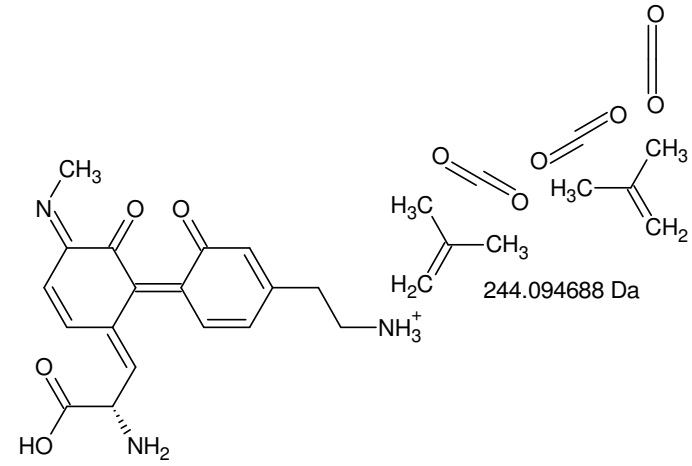

Monoisotopic Mass = 342.144833 Da

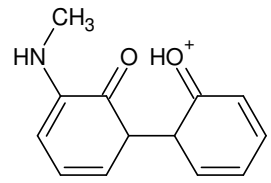

Monoisotopic Mass = 216.101905 Da

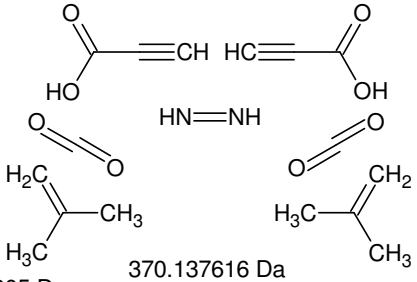

370.137616 Da

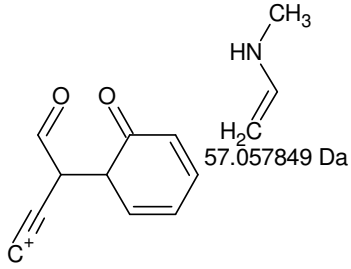

Monoisotopic Mass = 159.044056 Da

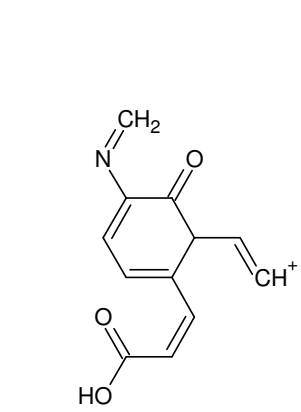

Monoisotopic Mass = 216.06552 Da

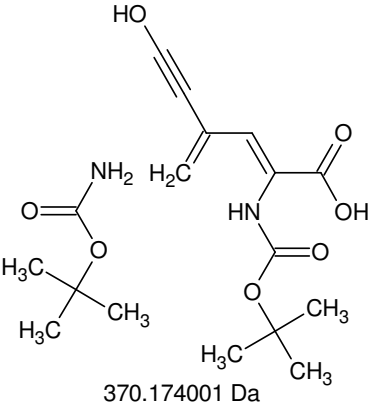

370.174001 Da

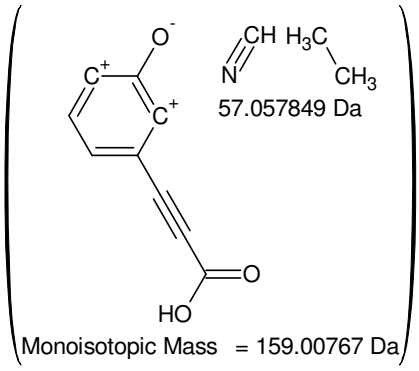

Monoisotopic Mass = 159.00767 Da

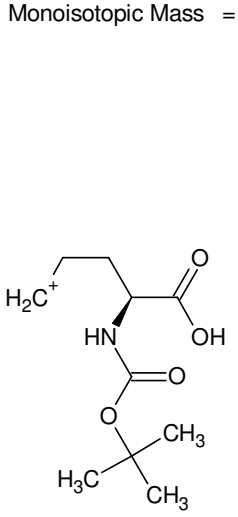

Monoisotopic Mass = 216.123034 Da

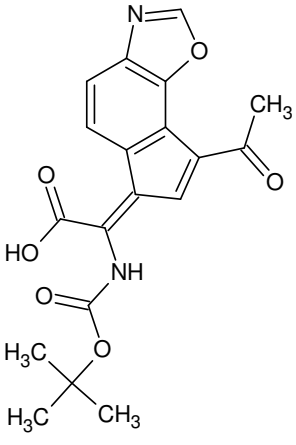

370.116486 Da

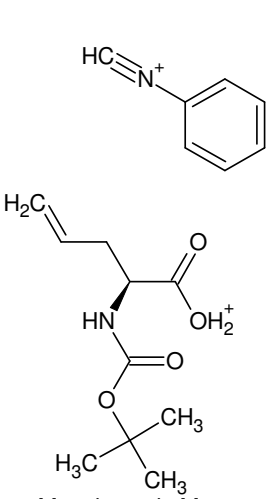

Monoisotopic Mass = 216.123034 Da

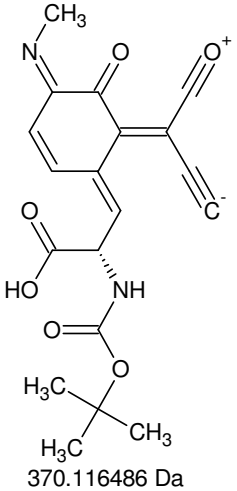

370.116486 Da

+MSn [Arg 595 nm 12,3 min]: 586 -> (342), 216 -> 159, (102) {I/II}

216,0 - 158,9 = **57,1**
Gefundene Verbindungen: 28
CHN2O MG=57,0088876
CH3N3 MG=57,0326958
(...)
H27NO MG=57,2092532
H29N2 MG=57,2330614

-----D--B--E--f-i-l-t-e-r-----
31.08.2011 - 17:37:23,53
akzeptierte DBE:
-2 -1 0 1 2 3 4 5 6 7 8

CH_3N_3 DBE: 2
C_2H_3NO DBE: 2
C_3H_7N DBE: 1

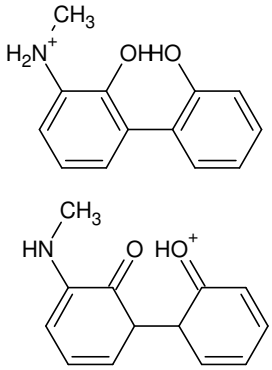

Monoisotopic Mass = 216.101905 Da

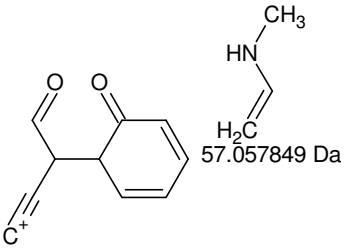

57.057849 Da

Monoisotopic Mass = 159.044056 Da

3 von 28 Summenformeln

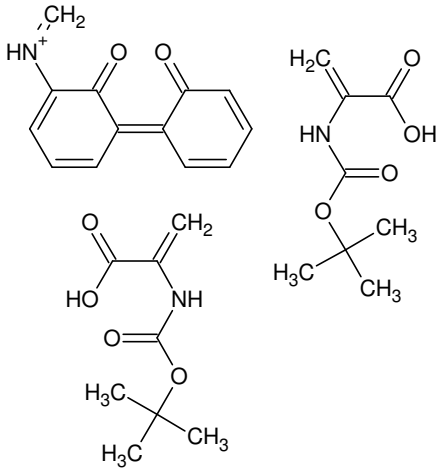

Monoisotopic Mass = 586.239521 Da

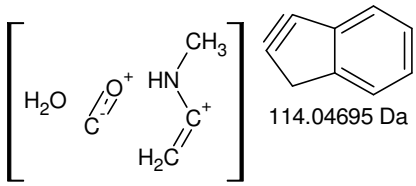

114.04695 Da

Monoisotopic Mass = 102.054955 Da

+MSn [Arg 595 nm 12,3 min]: 586 -> (342), 216 -> 159, (102) {II/II}

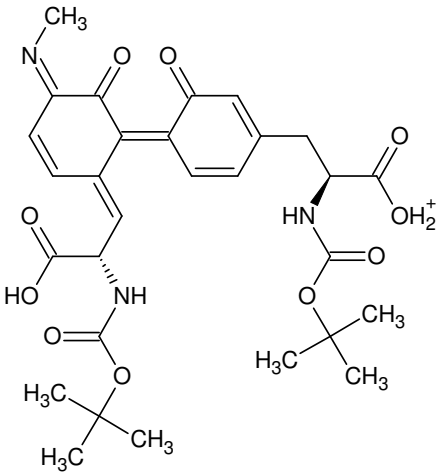

Monoisotopic Mass = 586.239521 Da

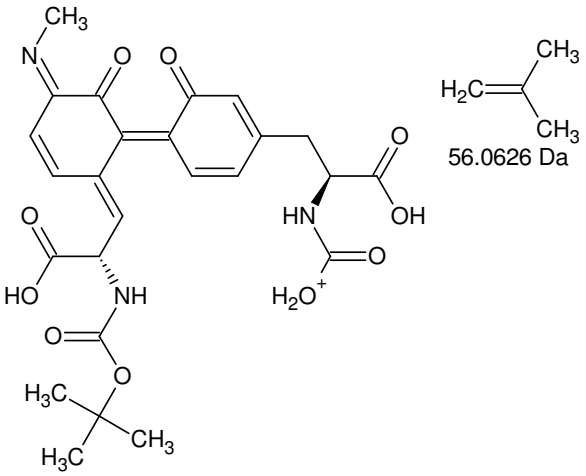

Monoisotopic Mass = 530.176921 Da

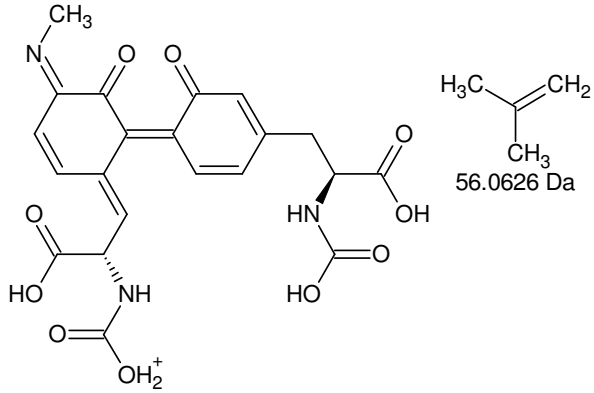

Monoisotopic Mass = 474.11432 Da

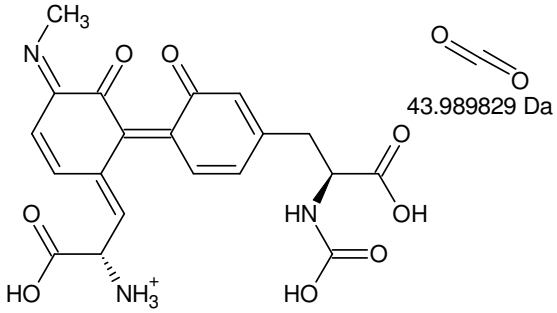

Monoisotopic Mass = 430.124491 Da

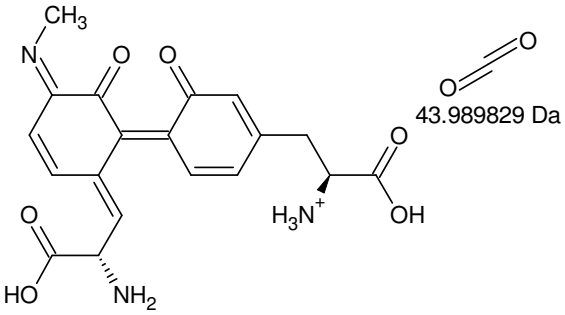

Monoisotopic Mass = 386.134662 Da

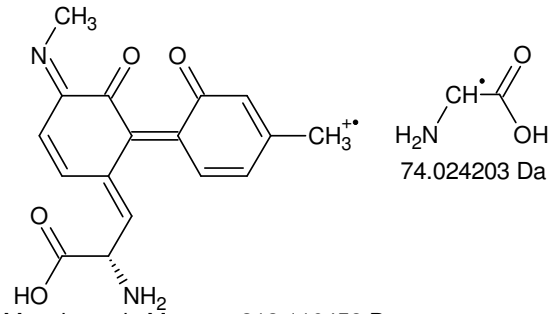

Monoisotopic Mass = 312.110458 Da

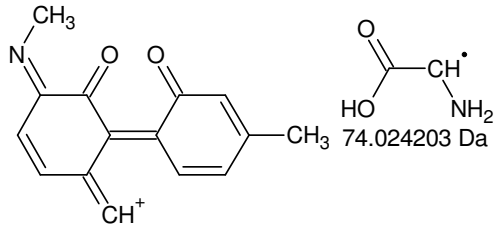

Monoisotopic Mass = 238.086255 Da

+MSn [Arg 595 nm 12,3 min]: 586 -> 530 -> 474 -> 430 -> 386 -> 312 -> 238

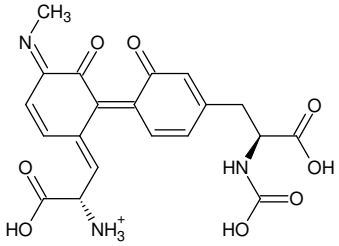

Monoisotopic Mass = 430.124491 Da

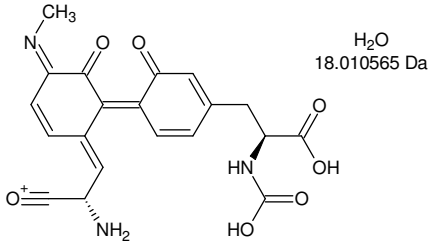

Monoisotopic Mass = 412.113926 Da

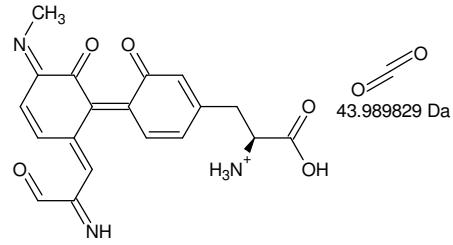

Monoisotopic Mass = 368.124097 Da

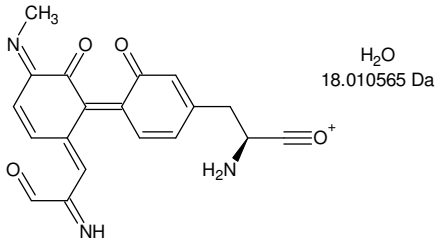

Monoisotopic Mass = 350.113532 Da

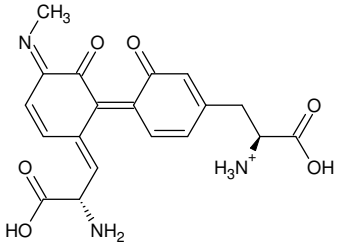

Monoisotopic Mass = 386.134662 Da

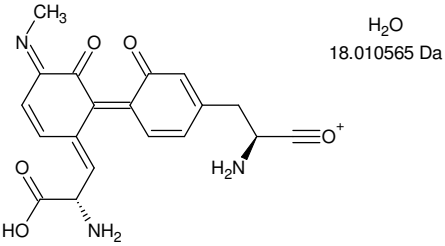

Monoisotopic Mass = 368.124097 Da

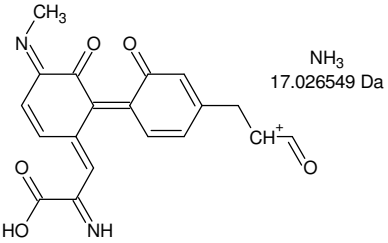

Monoisotopic Mass = 351.097548 Da

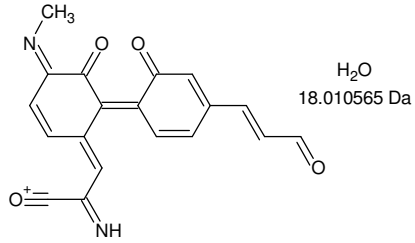

Monoisotopic Mass = 333.086983 Da

351,0 - 306,2 = **44,8**
Gefundene Verbindungen: 16
CHO2 MG=44,9976546
CHS MG=44,9798966
(...)
H15NO MG=45,115358
H17N2 MG=45,1391662

-----D--B--E--f-i-l-t-e-r-----
31.08.2011 - 18:47:13,68
akzeptierte DBE:
-2 -1 0 1 2 3 4 5 6 7 8

CH_3NO DBE: 1
C_2H_7N DBE: 0
H_3N_3 DBE: 1

3 von 16 Summenformeln

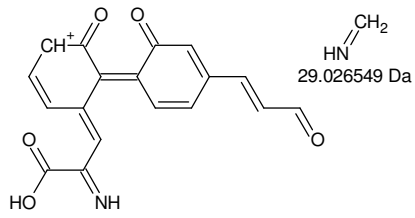

Monoisotopic Mass = 322.070999 Da

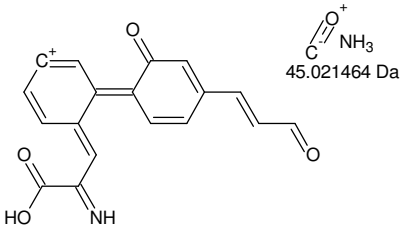

Monoisotopic Mass = 306.076084 Da

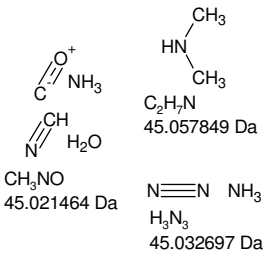

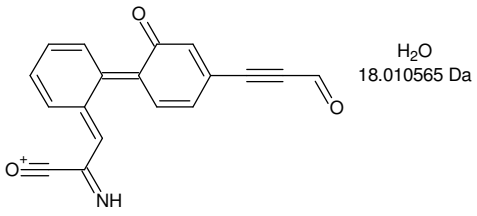

Monoisotopic Mass = 288.06552 Da

+MSn [Arg 595 nm 12,3 min]: [586 -> 530 -> 474 -> 430] -> 412 -> 368 -> 350 and [586 -> 530 -> 474 -> 430 -> 386] -> 368 -> 351 -> 333, 322, 306 -> 288

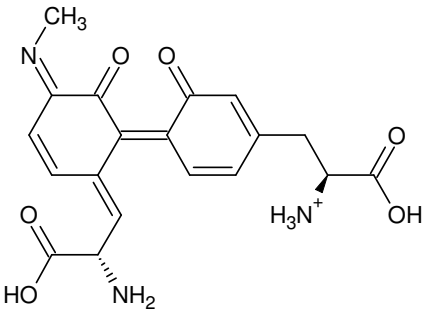

Monoisotopic Mass = 386.134662 Da

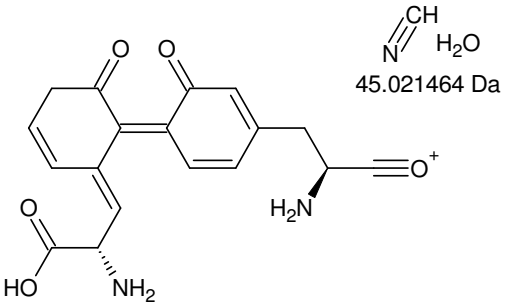

Monoisotopic Mass = 341.113198 Da

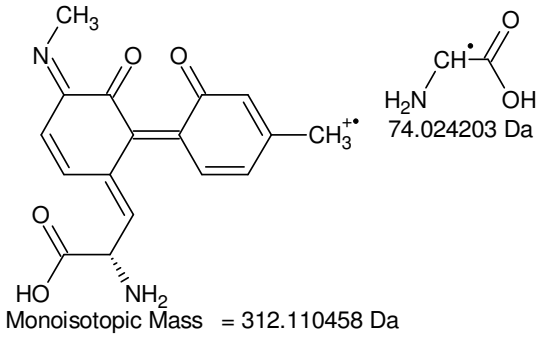

Monoisotopic Mass = 312.110458 Da

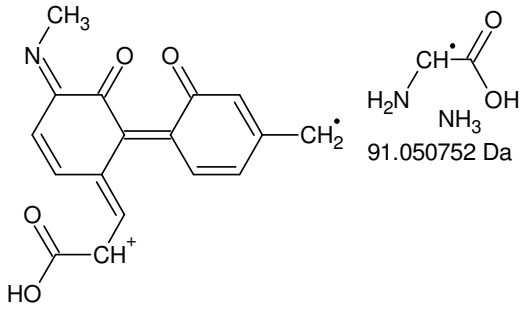

Monoisotopic Mass = 295.083909 Da

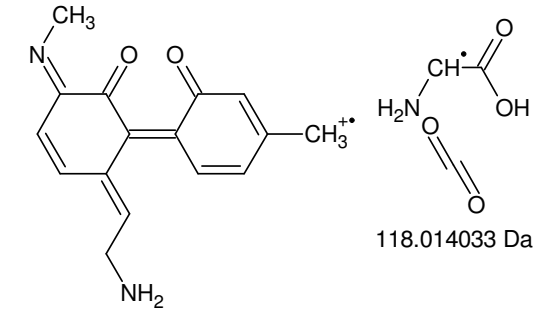

Monoisotopic Mass = 268.120629 Da

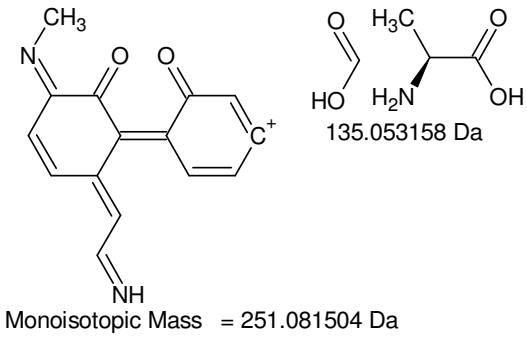

Monoisotopic Mass = 251.081504 Da

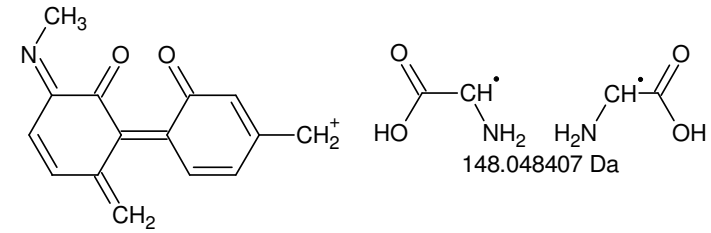

Monoisotopic Mass = 238.086255 Da

+MSn [Arg 595 nm 12,3 min]: [586 -> 530 -> 474 -> 430 -> 386] -> 341, 312, 295, 268, 251, 238

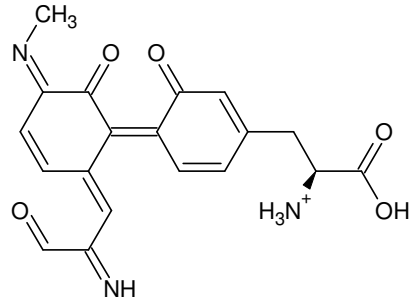

Monoisotopic Mass = 368.124097 Da

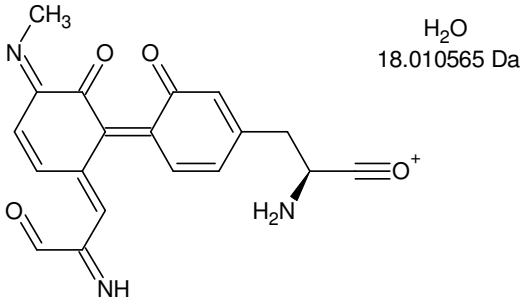

Monoisotopic Mass = 350.113532 Da

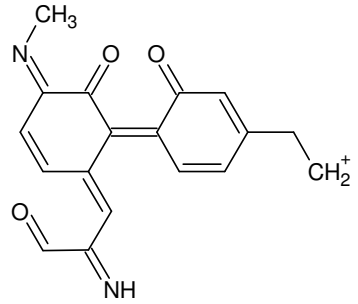

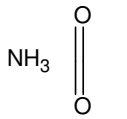

Monoisotopic Mass = 307.107719 Da

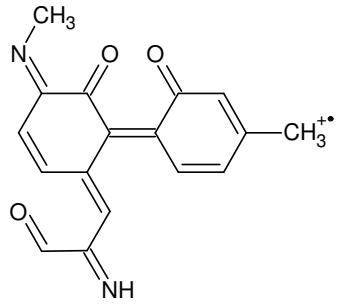

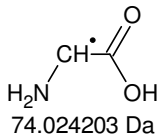

Monoisotopic Mass = 294.099894 Da

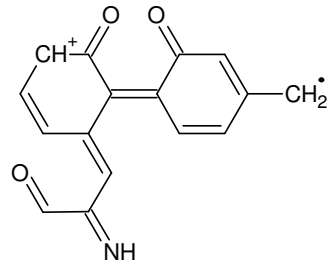

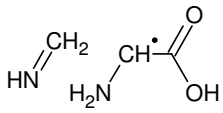

Monoisotopic Mass = 265.073345 Da

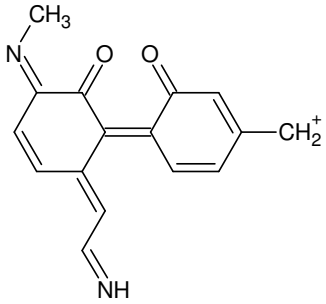

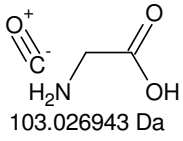

Monoisotopic Mass = 265.097154 Da

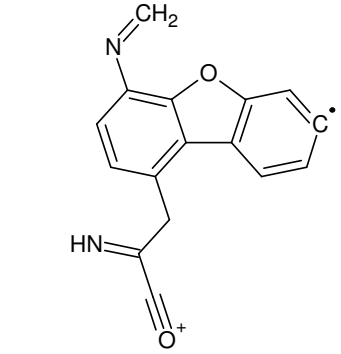

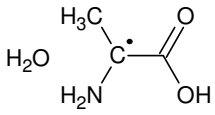

Monoisotopic Mass = 262.073679 Da

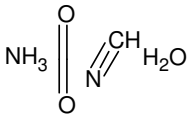

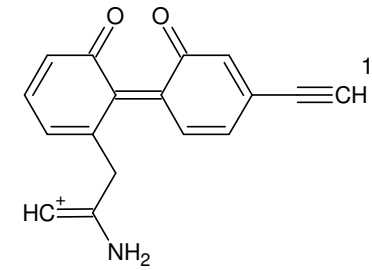

Monoisotopic Mass = 262.086255 Da

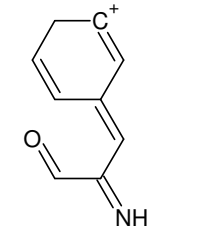

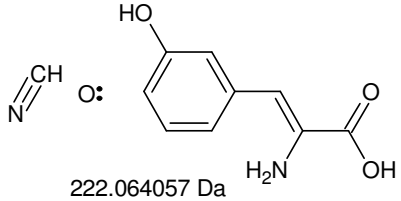

Monoisotopic Mass = 146.06004 Da

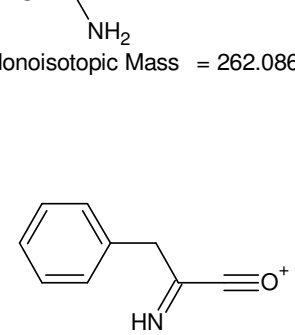

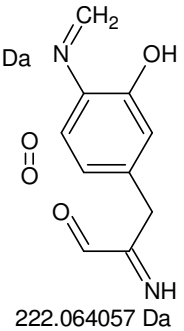

Monoisotopic Mass = 146.06004 Da

+MSn [Arg 595 nm 12,3 min]: [586 -> 530 -> 474 -> 430 -> 386 -> 368] -> 350, 307, 294, 265, 262, 146

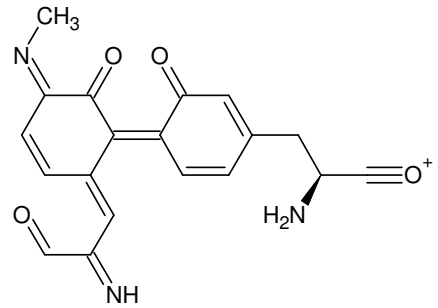

Monoisotopic Mass = 350.113532 Da

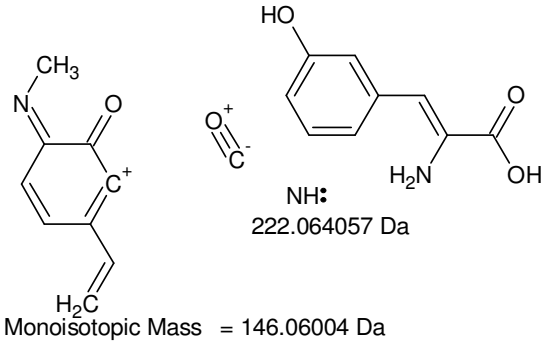

222.064057 Da

Monoisotopic Mass = 146.06004 Da

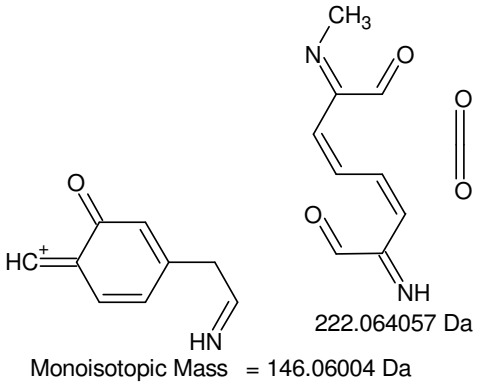

222.064057 Da

Monoisotopic Mass = 146.06004 Da

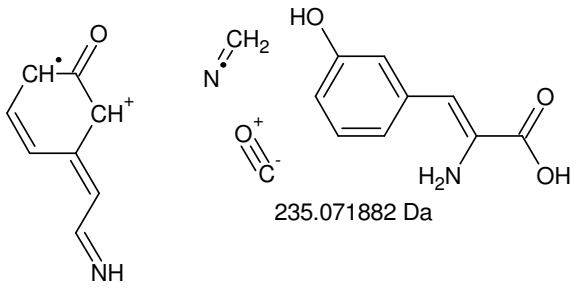

235.071882 Da

Monoisotopic Mass = 133.052215 Da

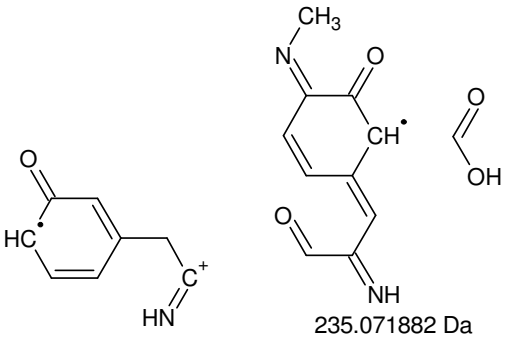

235.071882 Da

Monoisotopic Mass = 133.052215 Da

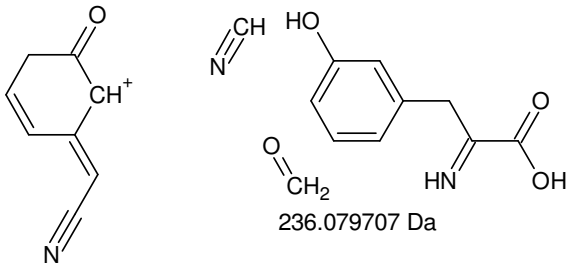

236.079707 Da

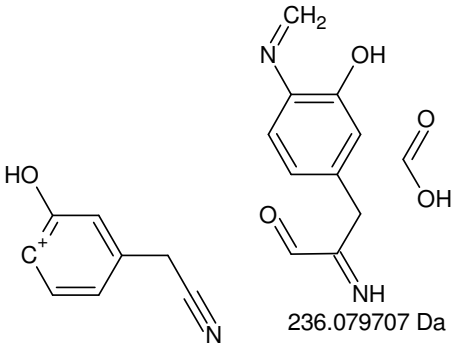

236.079707 Da

Monoisotopic Mass = 132.04439 Da

+MSn [Arg 595 nm 12,3 min]: [586 -> 530 -> 474 -> 430 -> 386 -> 368] -> 146, (133), 132

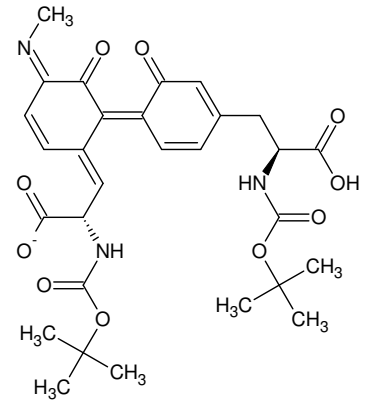

Monoisotopic Mass = 584.224968 Da

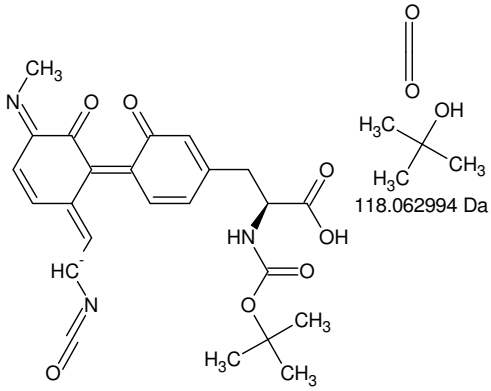

118.062994 Da

Monoisotopic Mass = 466.161974 Da

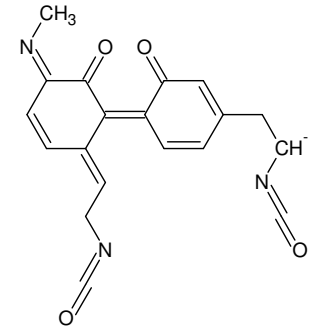

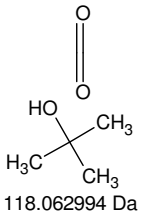

118.062994 Da

Monoisotopic Mass = 348.09898 Da

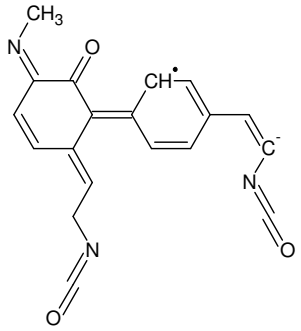

17.00274 Da

Monoisotopic Mass = 331.09624 Da

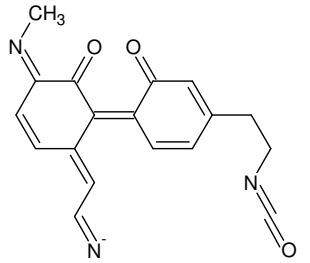

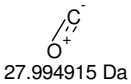

27.994915 Da

Monoisotopic Mass = 320.104065 Da

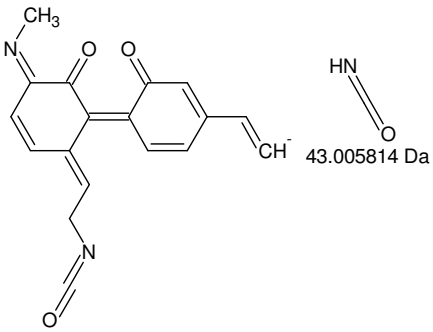

43.005814 Da

Monoisotopic Mass = 305.093166 Da

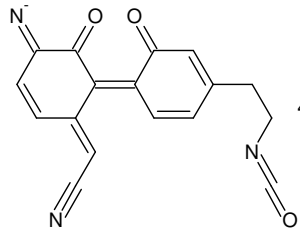

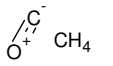

44.026215 Da

Monoisotopic Mass = 304.072765 Da

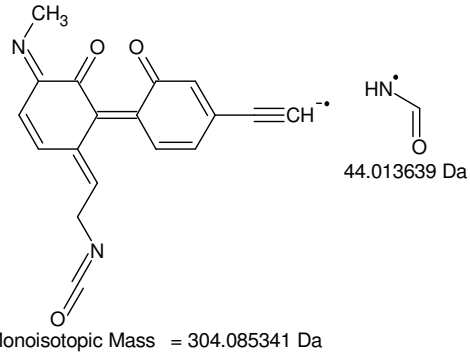

44.013639 Da

Monoisotopic Mass = 304.085341 Da

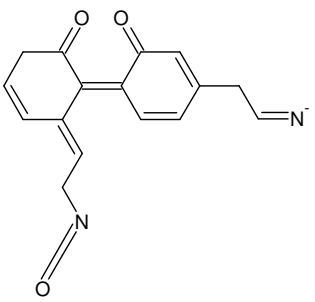

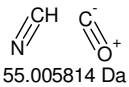

55.005814 Da

Monoisotopic Mass = 293.093166 Da

-MSn [Arg 595 nm 12,3 min]: 584 -> 466 -> 348 -> (331), 320, 305, 304, 293

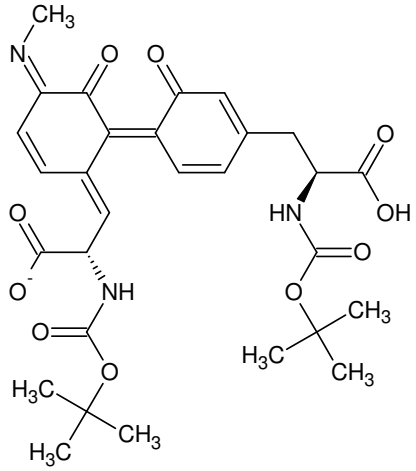

Monoisotopic Mass = 584.224968 Da

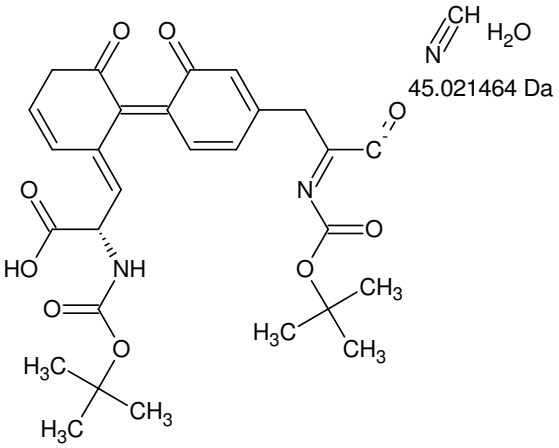

45.021464 Da

Monoisotopic Mass = 539.203504 Da

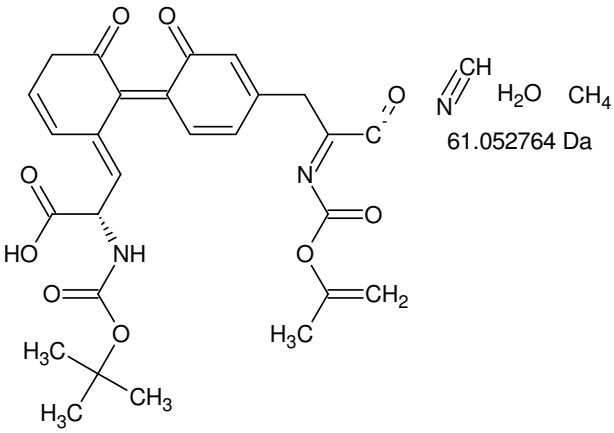

61.052764 Da

Monoisotopic Mass = 523.172204 Da

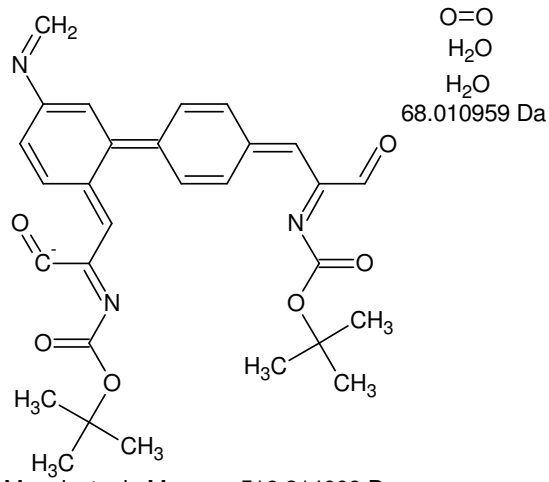

68.010959 Da

Monoisotopic Mass = 516.214009 Da

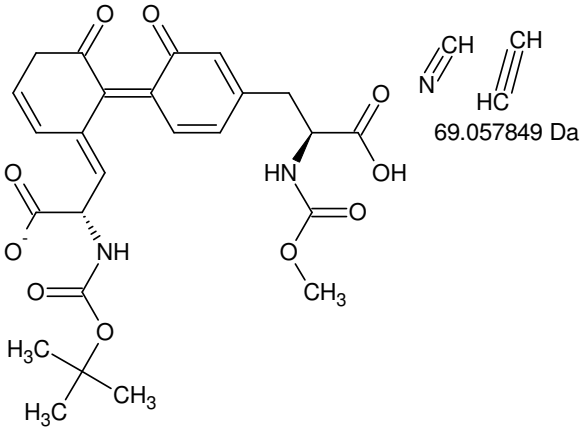

69.057849 Da

Monoisotopic Mass = 515.167119 Da

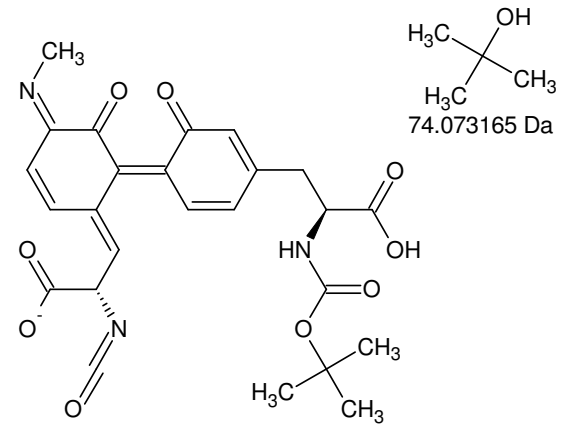

74.073165 Da

Monoisotopic Mass = 510.151803 Da

-MSn [Arg 595 nm 12,3 min]: 584 -> 539, 523, (516), (515), 510, (422), (420)

584,0 - 515,7 = **68,3**
Gefundene Verbindungen: 34
CH8O3 MG=68,0473418
CH10NO2 MG=68,07115
(...)
H24N2O MG=68,1888534
H26N3 MG=68,2126616

-----D--B--E--f-i-l-t-e-r-----
01.09.2011 - 14:55:03,93
akzeptierte DBE:
-2 -1 0 1 2 3 4 5 6 7 8

CH_8O_3 DBE: -2
CN_4 DBE: 4
C_2N_2O DBE: 4
$C_3H_4N_2$ DBE: 3
C_3O_2 DBE: 4
C_4H_4O DBE: 3
C_5H_8 DBE: 2
H_4O_4 DBE: -1
$H_8N_2O_2$ DBE: -2

9 von 34 Summenformeln

H_2O H_2O H_3C-OH CH_8O_3 68.047344 Da

H_2O H_2O $O=O$ H_4O_4 68.010959 Da

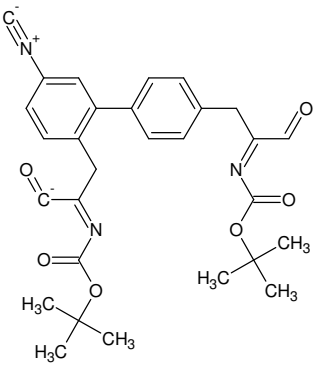

Monoisotopic Mass = 516.214009 Da

69 - 27 = **42**
-----D--B--E--f-i-l-t-e-r-----
01.09.2011 - 15:06:19,71
akzeptierte DBE:
-2 -1 0 1 2 3 4 5 6 7 8

CH_2N_2 DBE: 2
C_2H_2O DBE: 2
C_3H_6 DBE: 1

3 von 12 Summenformeln

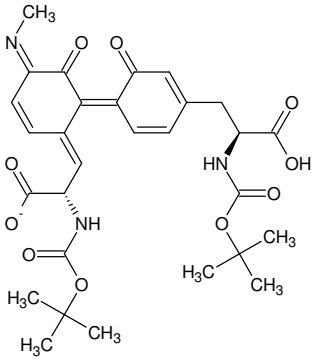

Monoisotopic Mass = 584.224968 Da

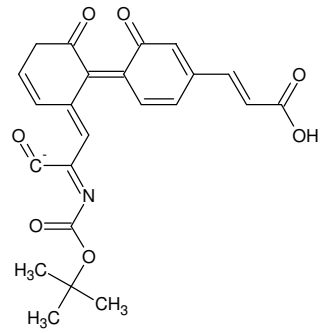

Monoisotopic Mass = 422.124526 Da

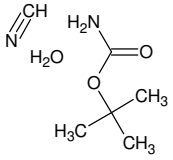

162.100442 Da

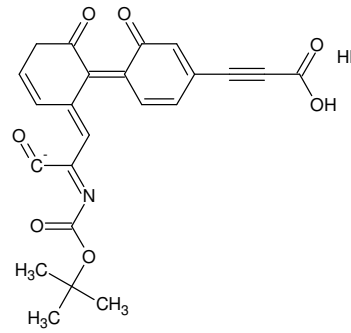

Monoisotopic Mass = 420.108876 Da

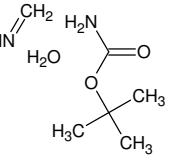

164.116092 Da

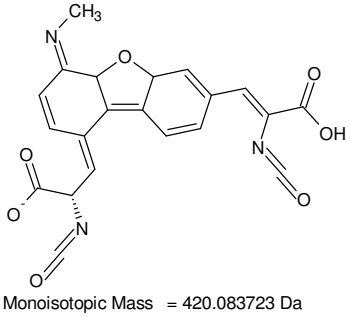

Monoisotopic Mass = 420.083723 Da

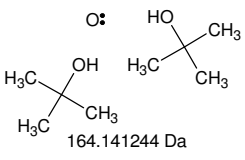

164.141244 Da

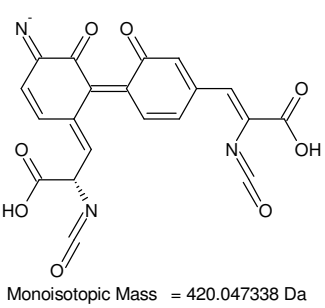

Monoisotopic Mass = 420.047338 Da

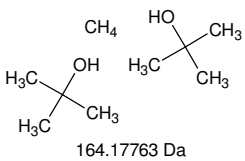

164.17763 Da

-MSn [Arg 595 nm 12,3 min]: 584 -> {516}, (422), (420)

XIII.III.V. **OPA-Ser 13,3 min**

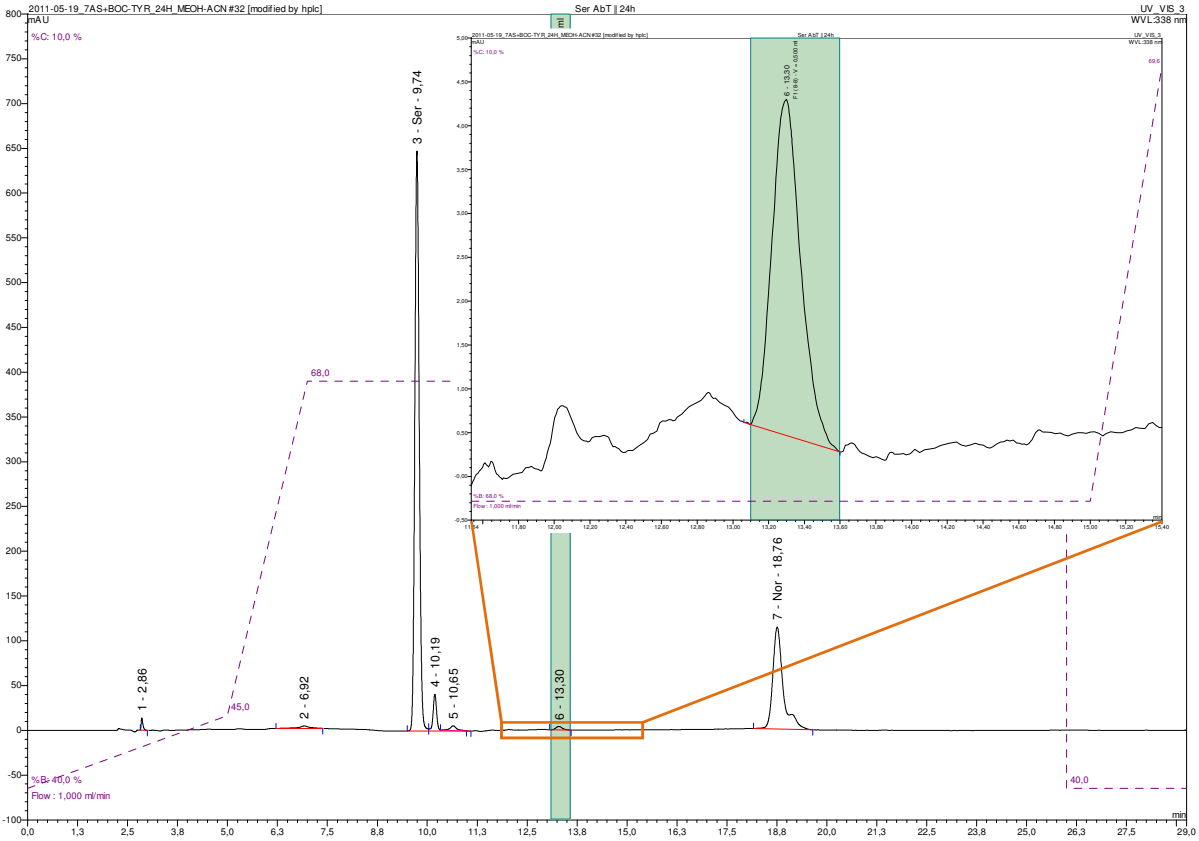

Figure XIII-LVI Ser AbT || 24h; OPA-derivatised

+MS^n

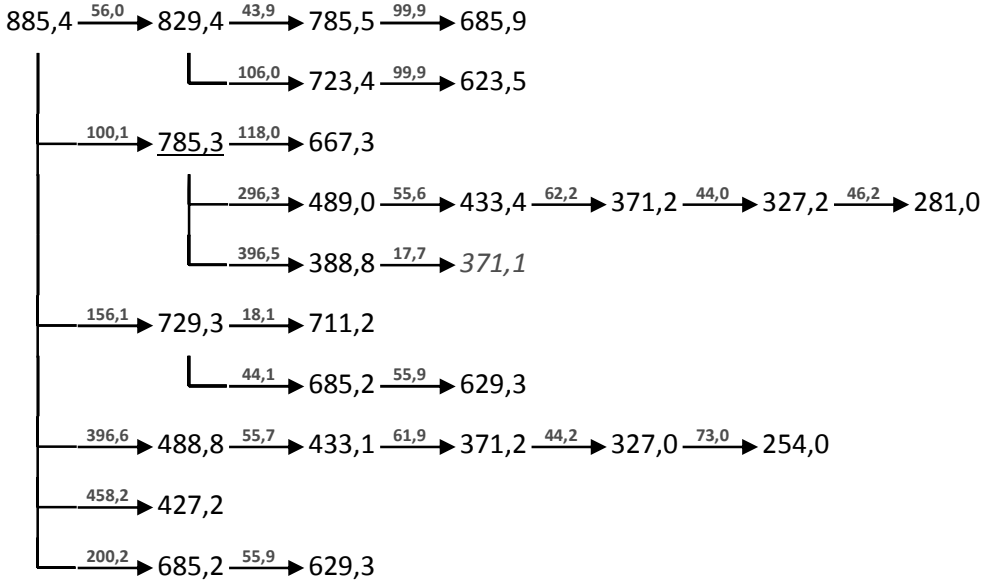

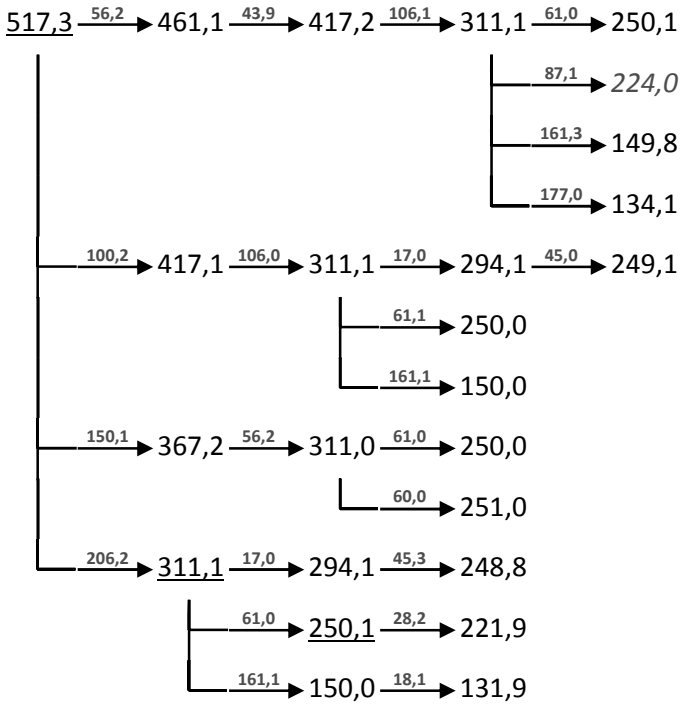
517,3
56,2
461,1
43,9
417,2
106,1
311,1
61,0
250,1
87,1
224,0
161,3
149,8
177,0
134,1
100,2
417,1
106,0
311,1
17,0
294,1
45,0
249,1
61,1
250,0
161,1
150,0
150,1
367,2
56,2
311,0
61,0
250,0
60,0
251,0
206,2
311,1
17,0
294,1
45,3
248,8
61,0
250,1
28,2
221,9
161,1
150,0
18,1
131,9

-MS^n

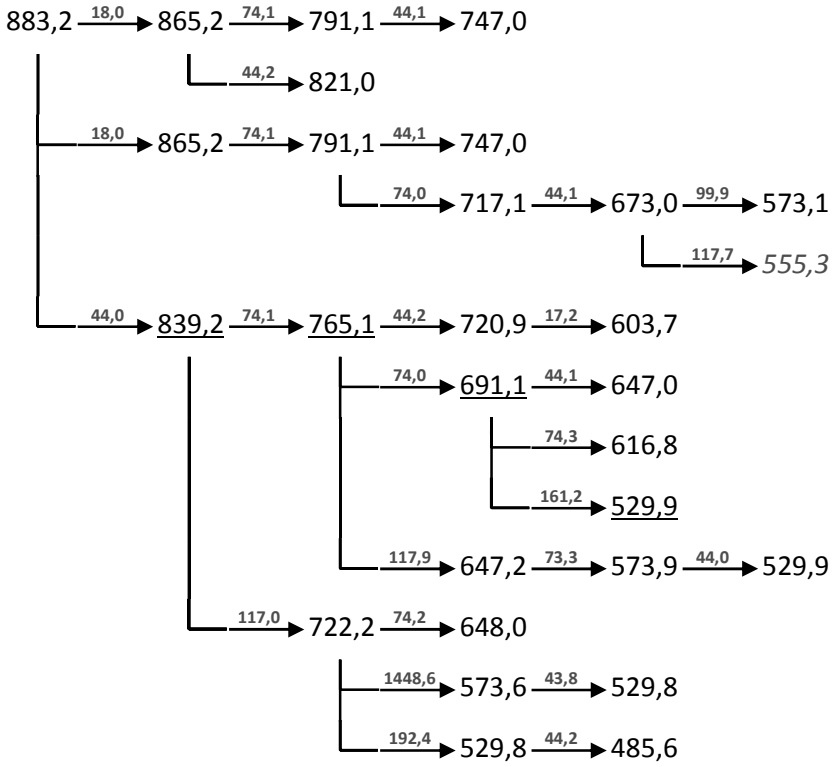
883,2
18,0
865,2
74,1
791,1
44,1
747,0
44,2
821,0
18,0
865,2
74,1
791,1
44,1
747,0
74,0
717,1
44,1
673,0
99,9
573,1
117,7
555,3
44,0
839,2
74,1
765,1
44,2
720,9
17,2
603,7
74,0
691,1
44,1
647,0
74,3
616,8
161,2
529,9
117,9
647,2
73,3
573,9
44,0
529,9
117,0
722,2
74,2
648,0
1448,6
573,6
43,8
529,8
192,4
529,8
44,2
485,6

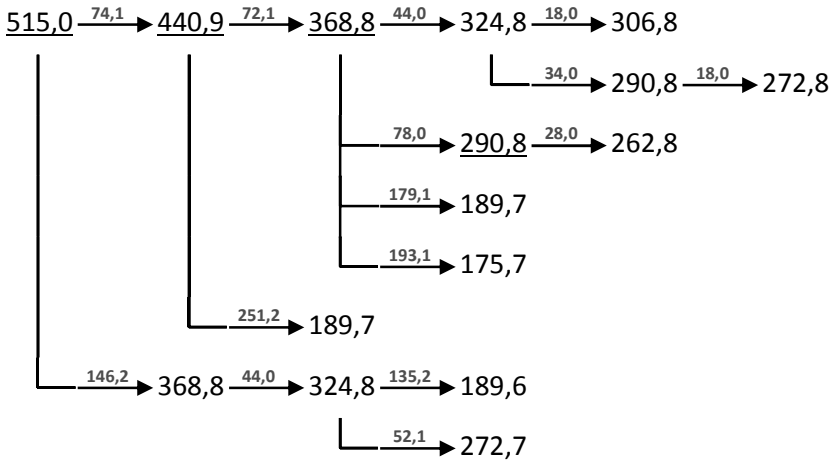

isotopic fingerprint:

peak area / % of monoisotopic	**+1**	**+2**	**+3**
theoretical ($C_{41}H_{47}N_4O_{16}S^-$):	47,9	19,1	5,4
measured (-883,2 Th):	44,0	26,0	9,7
measured (885,4 Th):	36,5	21,8	7,2
theoretical ($C_{25}H_{27}N_2O_8S^-$):	29,3	10,3	2,1
measured (-515,0 Th):	27,4	9,4	2,9
measured (517,3 Th):	27,0	16,1	4,1

Figure XIII-LVII MS^n analysis of OPA-Ser 13,3 min

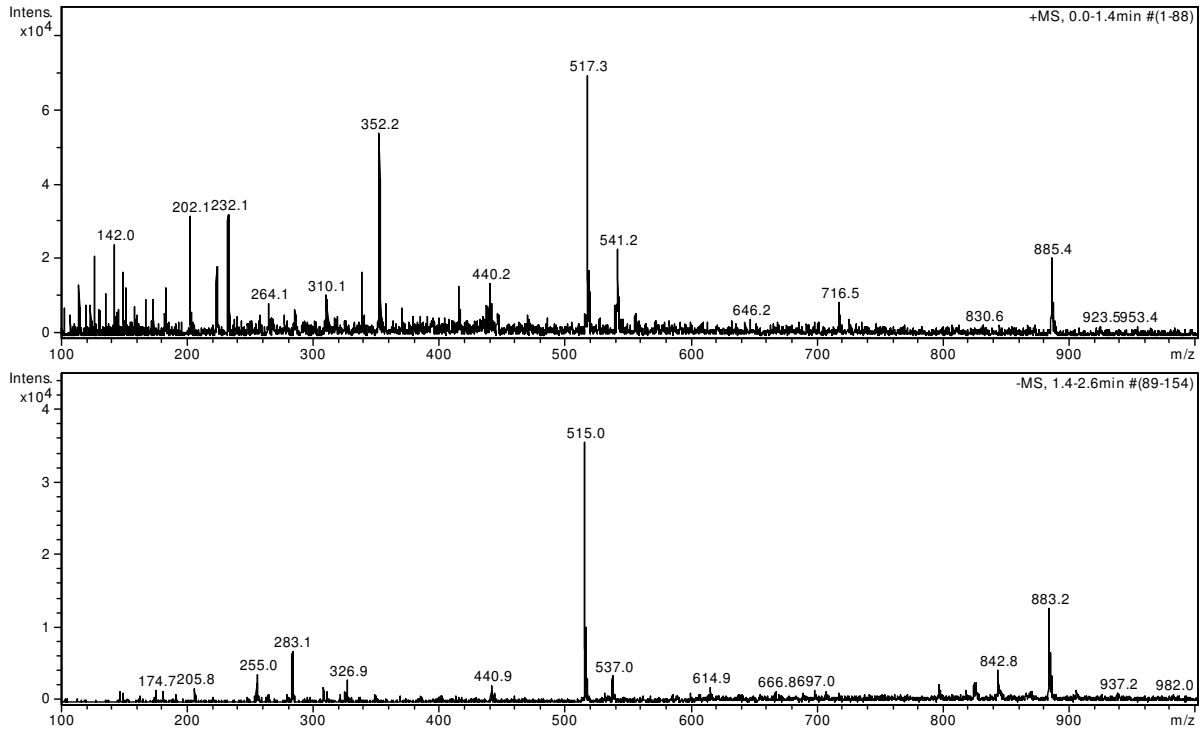

Figure XIII-LVIII OPA-Ser 13,3 min: 31 % MeOH, 31 % ACN, 1 ‰ FA in ddH_2O; full scan MS^1

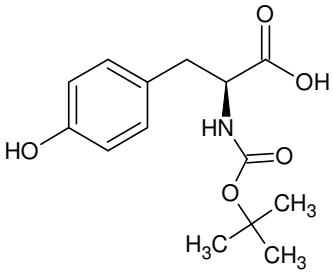

L-Boc-Tyr-OH

Monoisotopic Mass = 281.126323 Da

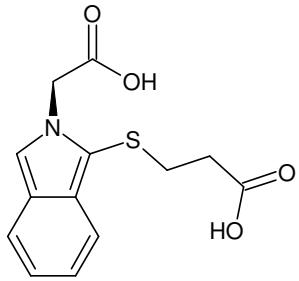

OPA-Gly

Monoisotopic Mass = 279.056528 Da

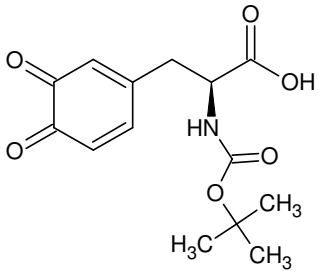

Monoisotopic Mass = 295.105587 Da

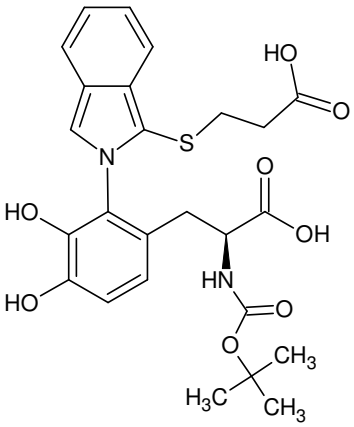

Monoisotopic Mass = 516.156636 Da

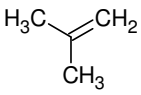

56.0626 Da

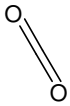

43.989829 Da

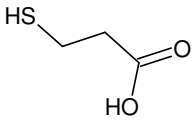

106.008849 Da

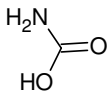

61.016378 Da

Gefundene Verbindungen: 16

CH_2NO	MG=44,0136382
CH_4N_2	MG=44,0374464
$CH_{16}O$	MG=44,1201086
$CH_{18}N$	MG=44,1439168
CO_2	MG=43,98983
CS	MG=43,972072
C_2H_4O	MG=44,0262134
C_2H_6N	MG=44,0500216
C_2H_{20}	MG=44,156492
C_3H_8	MG=44,0625968
H_2N_3	MG=44,0248712
$H_{12}O_2$	MG=44,0837252
$H_{12}S$	MG=44,0659672
$H_{14}NO$	MG=44,1075334
$H_{16}N_2$	MG=44,1313416
N_2O	MG=44,001063

Das zugehörige Signal (RP-HPLC, 13,3 min @ 338 nm) findet sich in allen vermessenen Proben (6 AS: Lys, Ile, Leu, Val, Arg, Ser).

=> keine Aminosäureseitenketten in der Bildung der Verbindung involviert

größtes gemeinsames Fragment:

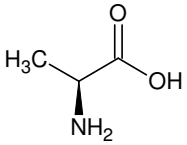

L-Alanine **(Ala)**

516 Da [OPA-Ser 13,3 min]

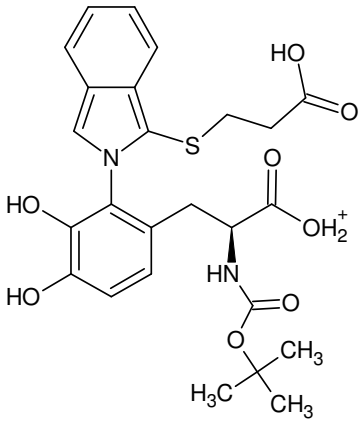

Monoisotopic Mass = 517.163912 Da

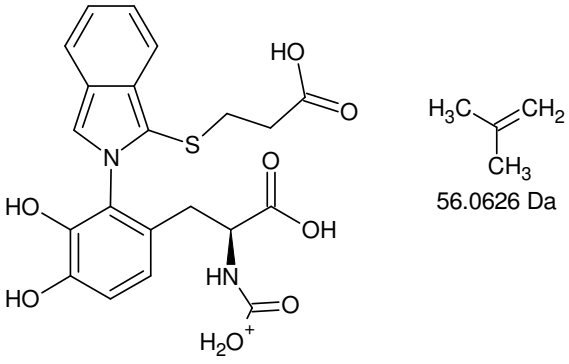

Monoisotopic Mass = 461.101312 Da

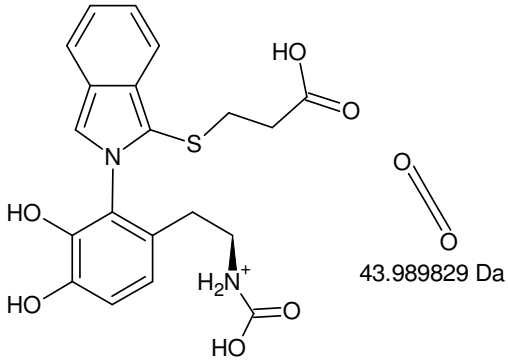

Monoisotopic Mass = 417.111483 Da

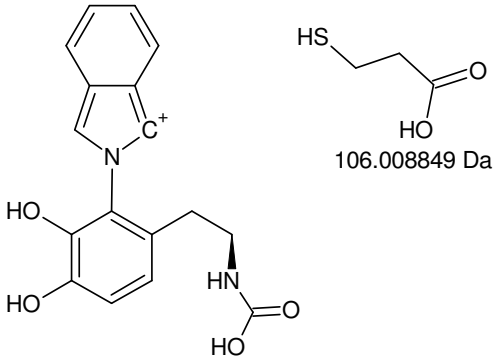

Monoisotopic Mass = 311.102633 Da

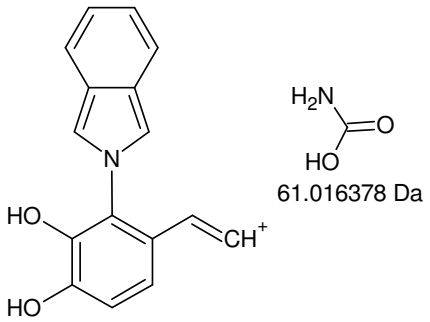

Monoisotopic Mass = 250.086255 Da

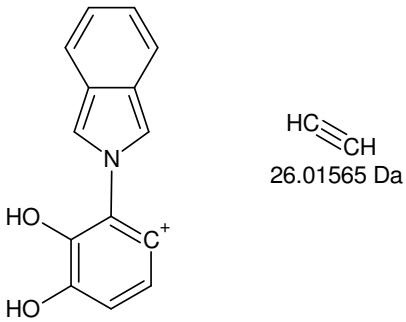

Monoisotopic Mass = 224.070605 Da

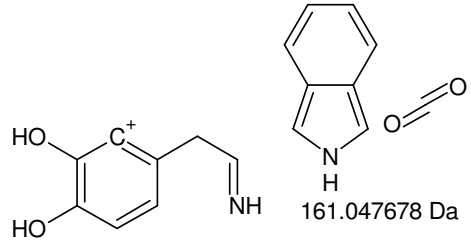

Monoisotopic Mass = 150.054955 Da

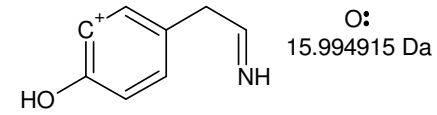

Monoisotopic Mass = 134.06004 Da

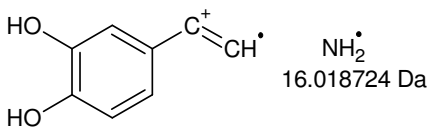

Monoisotopic Mass = 134.036231 Da

+MSn [OPA-Ser 13,3 min]: 517 -> 461 -> 417 -> 311 -> 250, 224, 150, 134

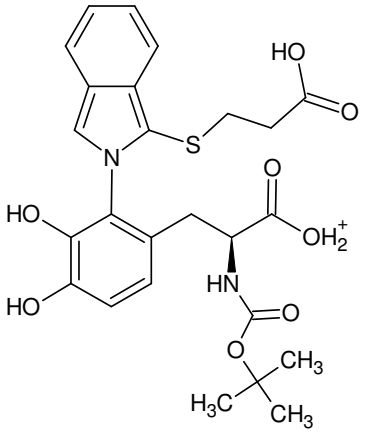

Monoisotopic Mass = 517.163912 Da

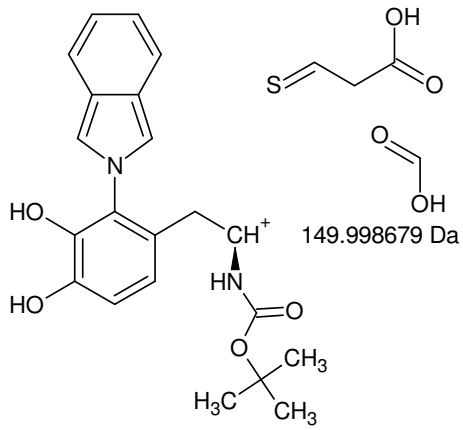

149.998679 Da

Monoisotopic Mass = 367.165234 Da

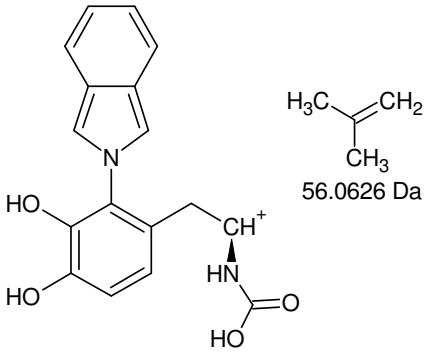

56.0626 Da

Monoisotopic Mass = 311.102633 Da

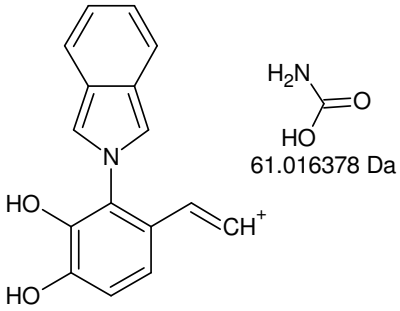

61.016378 Da

Monoisotopic Mass = 250.086255 Da

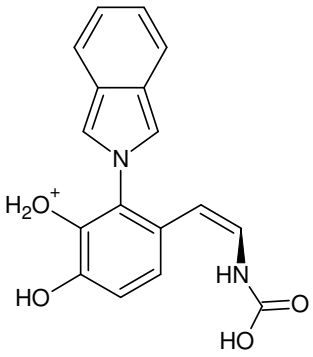

Monoisotopic Mass = 311.102633 Da

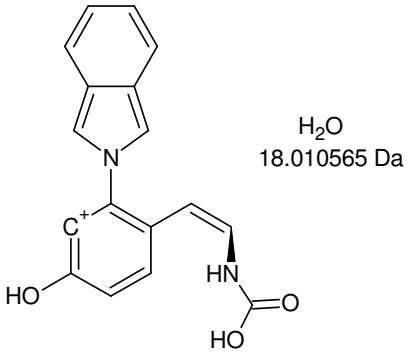

18.010565 Da

Monoisotopic Mass = 293.092069 Da

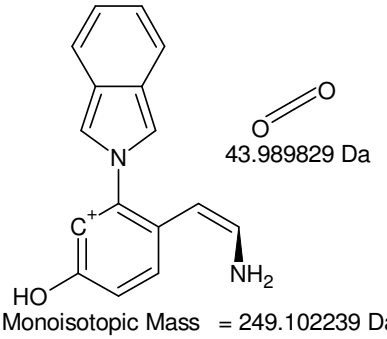

43.989829 Da

Monoisotopic Mass = 249.102239 Da

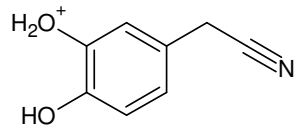

Monoisotopic Mass = 150.054955 Da

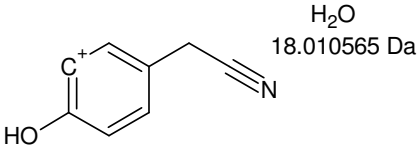

18.010565 Da

Monoisotopic Mass = 132.04439 Da

+MSn [OPA-Ser 13,3 min]: 517 -> 367 -> 311 -> 250 and 311 -> 293 -> 249 and (311 -> 150) -> 132

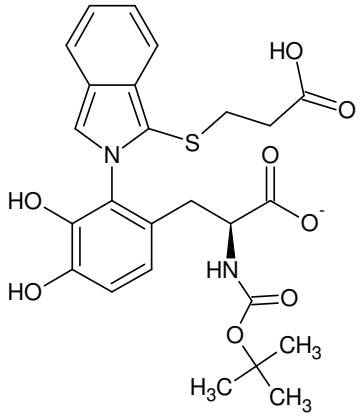

Monoisotopic Mass = 515.149359 Da

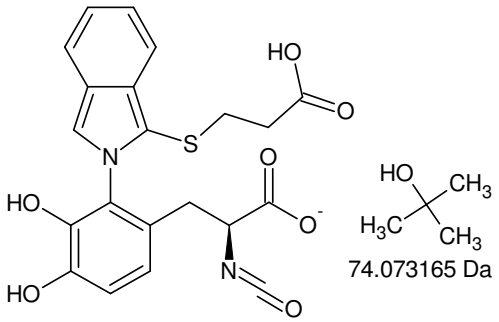

74.073165 Da

Monoisotopic Mass = 441.076194 Da

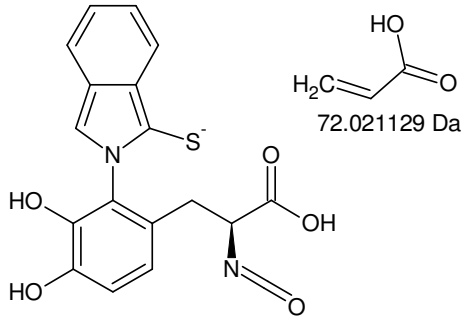

72.021129 Da

Monoisotopic Mass = 369.055065 Da

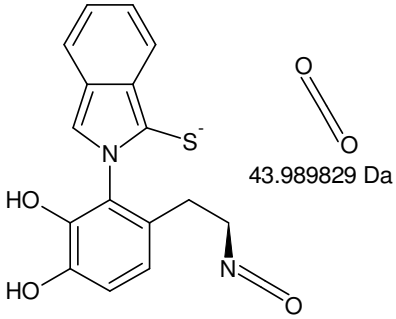

43.989829 Da

Monoisotopic Mass = 325.065236 Da

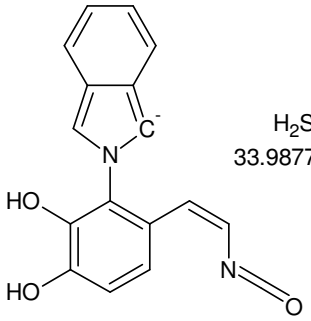

33.98772 Da

Monoisotopic Mass = 291.077516 Da

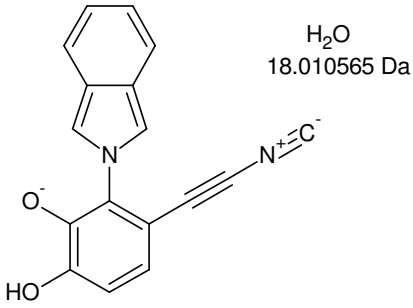

18.010565 Da

Monoisotopic Mass = 273.066951 Da

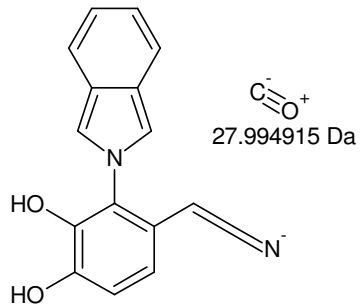

27.994915 Da

Monoisotopic Mass = 263.082601 Da

-MSn [OPA-Ser 13,3 min]: 515 -> 441 -> 369 -> 325 -> 291 -> 273, 263

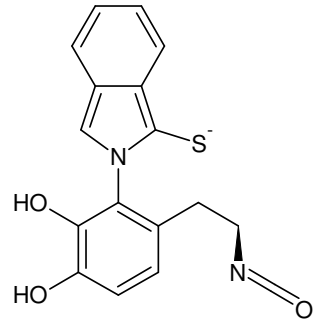

Monoisotopic Mass = 325.065236 Da

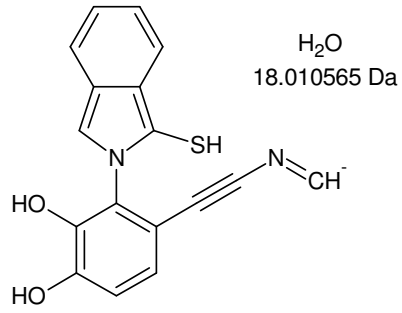

Monoisotopic Mass = 307.054671 Da

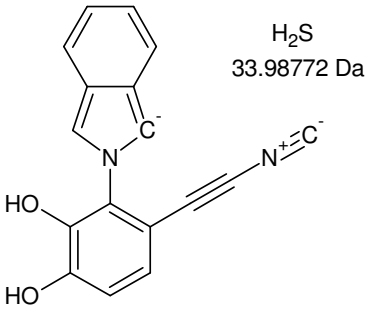

Monoisotopic Mass = 273.066951 Da

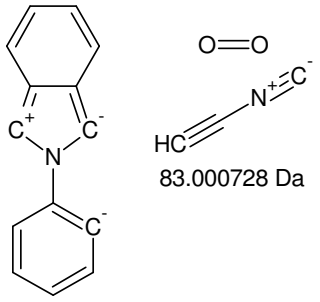

Monoisotopic Mass = 190.066223 Da

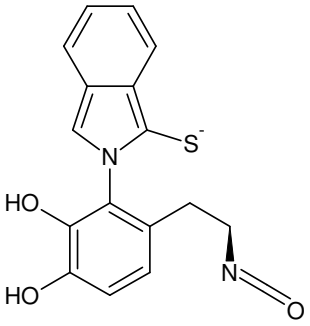

Monoisotopic Mass = 325.065236 Da

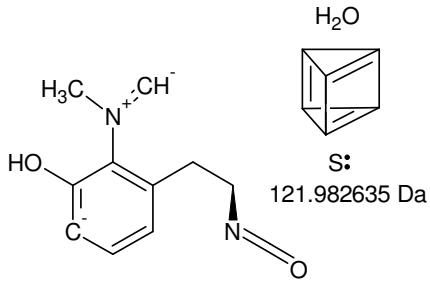

Monoisotopic Mass = 203.082601 Da

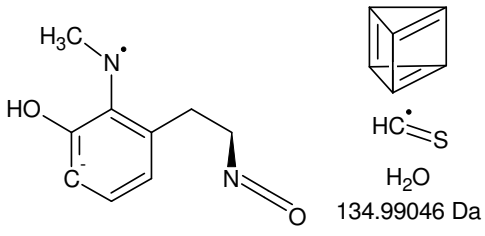

Monoisotopic Mass = 190.074776 Da

-MSn [OPA-Ser 13,3 min]: (515 -> 441 -> 369 -> 325) -> 307, (203,) 273, 190

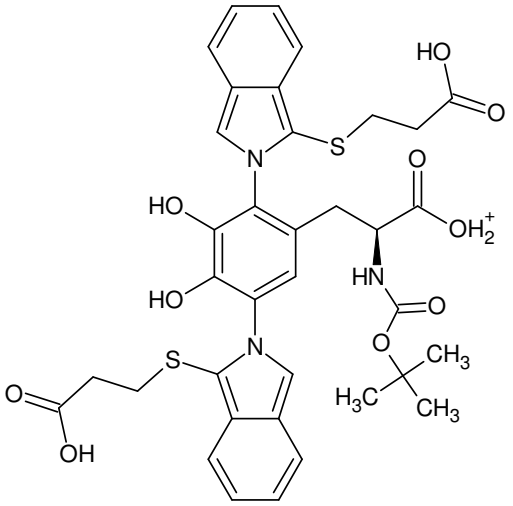

Monoisotopic Mass = 736.199311 Da

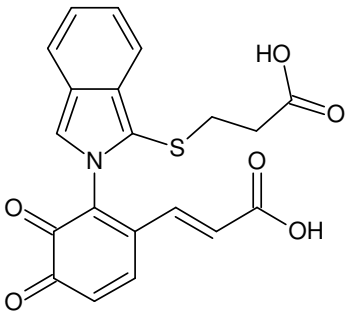

397.062007 Da

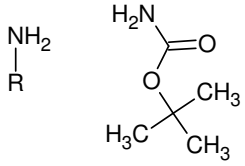

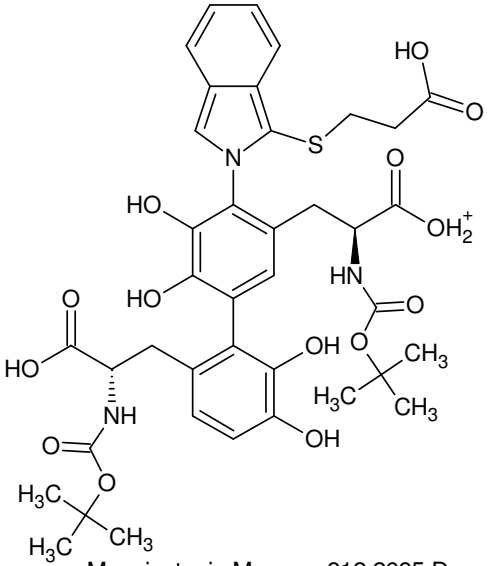

Monoisotopic Mass = 812.2695 Da

keine Fluoreszenz von Dityrosin ($\lambda_{em,max}$ = 404 nm, $\lambda_{ex,max}$ = 326 nm) beobachtet

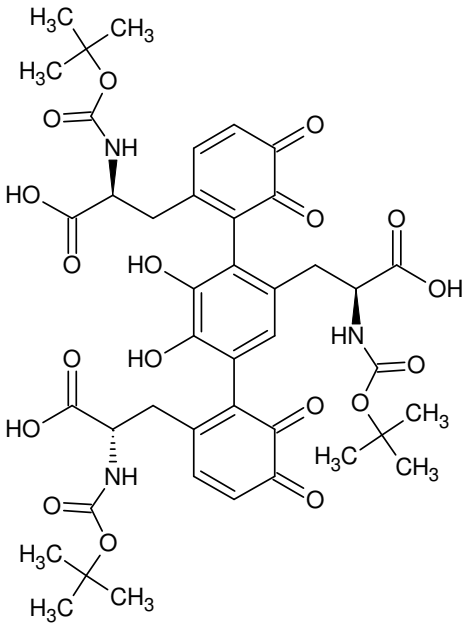

Monoisotopic Mass = 883.301112 Da

gerade nominelle Masse => gerade Anzahl an N-Atomen;

Absorptionsbande bei 338nm beobachtet

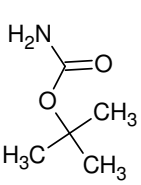

117.078979 Da

117.057849 Da

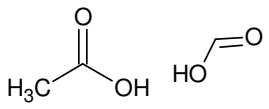

106.026609 Da

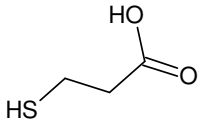

106.008849 Da

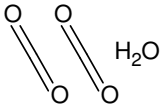

105.990223 Da

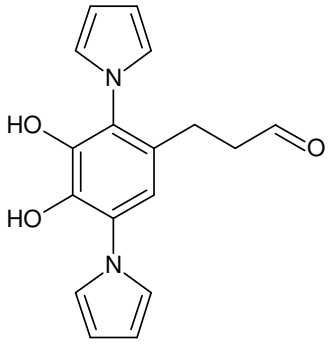

296.116092 Da

884 Da [OPA-Ser 13,3 min]

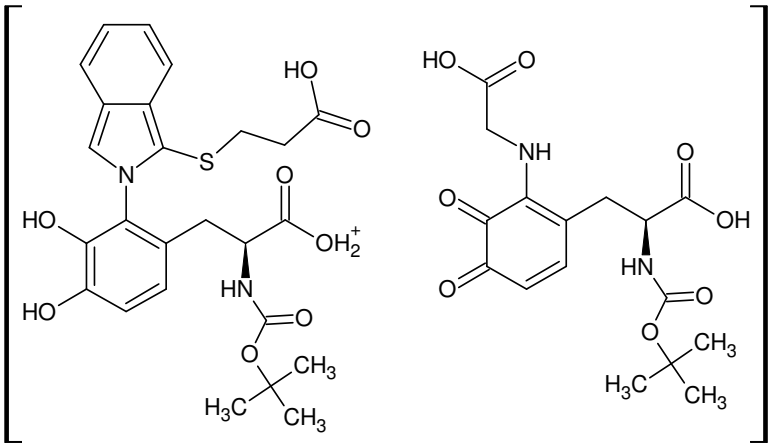

Monoisotopic Mass = 885.285878 Da

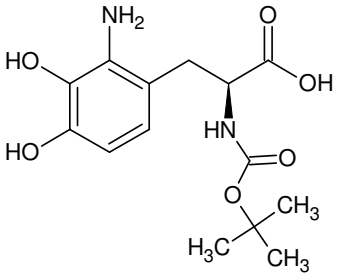

Monoisotopic Mass = 312.132136 Da

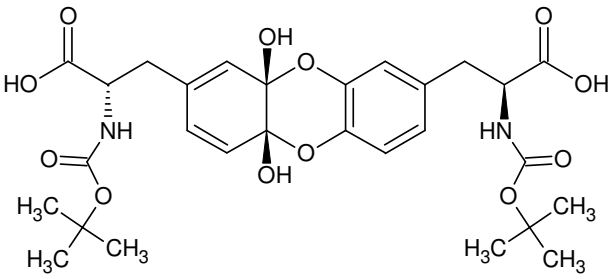

Monoisotopic Mass = 592.226825 Da

Hetero-Diels-Alder-Reaktion von Boc-Dopachinon mit Boc-Tyr-$(OH)_2$

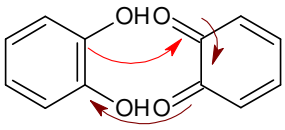

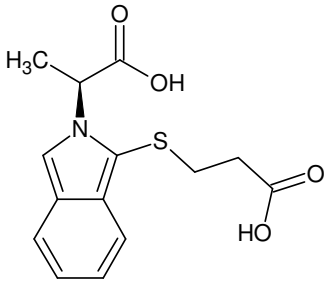

Monoisotopic Mass = 293.072178 Da

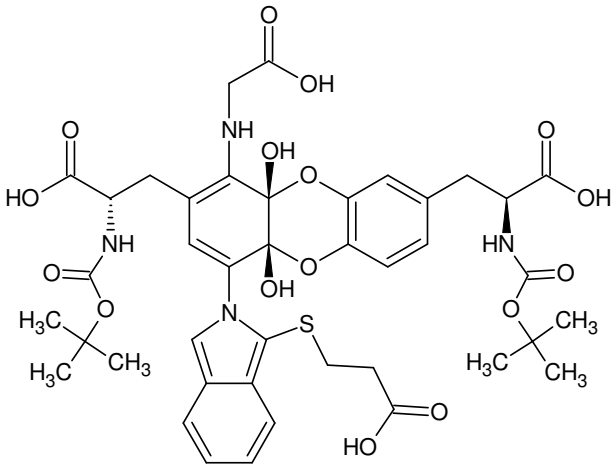

Monoisotopic Mass = 884.278601 Da

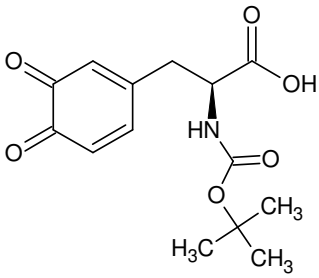

Monoisotopic Mass = 295.105587 Da

aber: **Fragment 72 Da bei -MS^n nicht beobachtet** => sterische Hinderung?

884 Da [OPA-Ser 13,3 min]

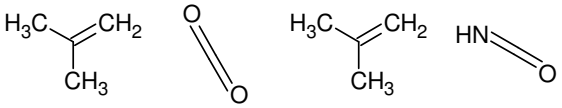

56.0626 Da 43.989829 Da 56.0626 Da 43.005814 Da

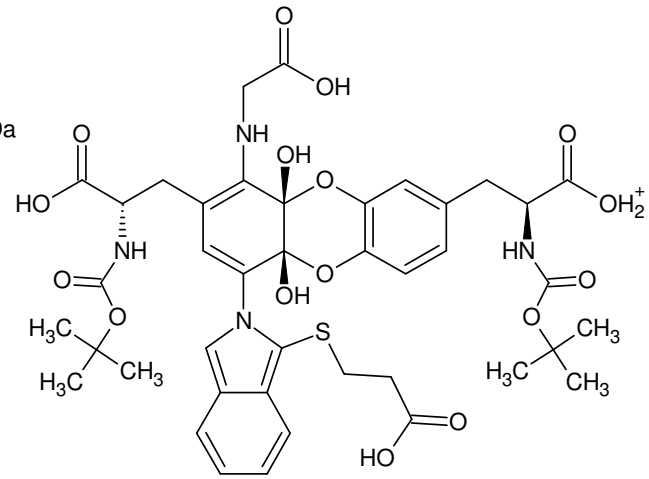

Monoisotopic Mass = 885.285878 Da

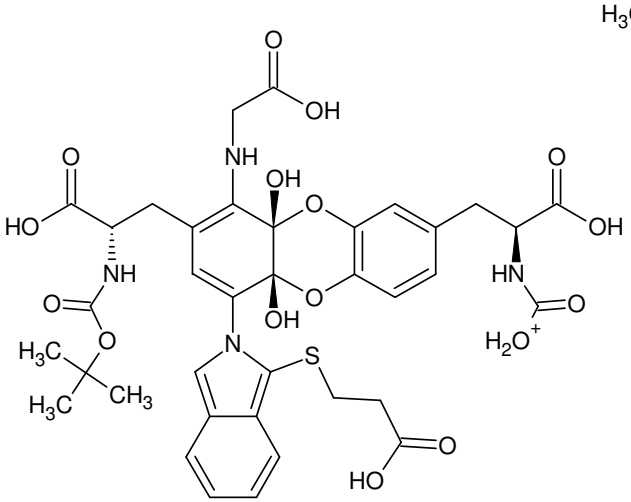

Monoisotopic Mass = 829.223278 Da

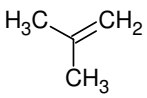

56.0626 Da

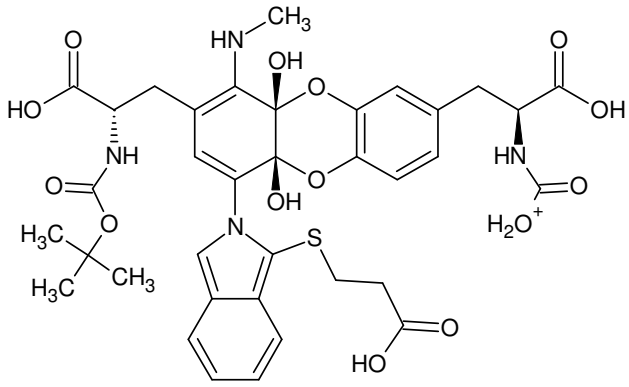

Monoisotopic Mass = 785.233448 Da

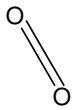

43.989829 Da

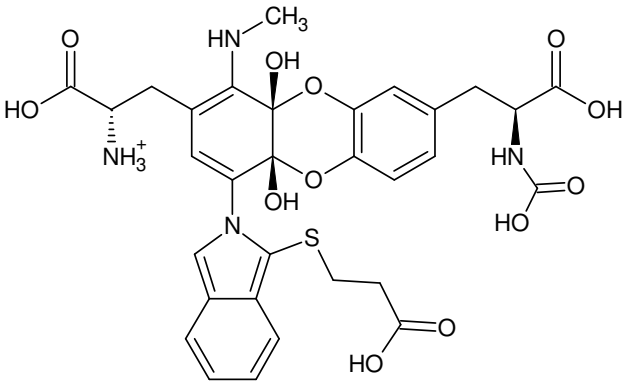

Monoisotopic Mass = 685.181019 Da

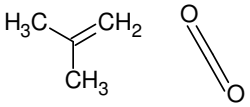

100.052429 Da

+MSn [OPA-Ser 13,3 min]: 885 -> 829 -> 785 -> 685

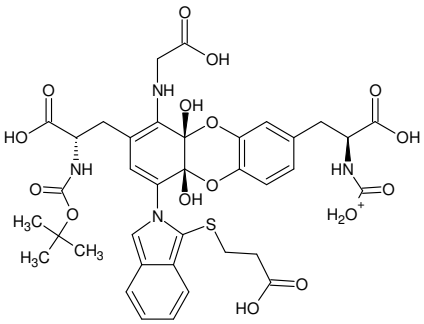

Monoisotopic Mass = 829.223278 Da

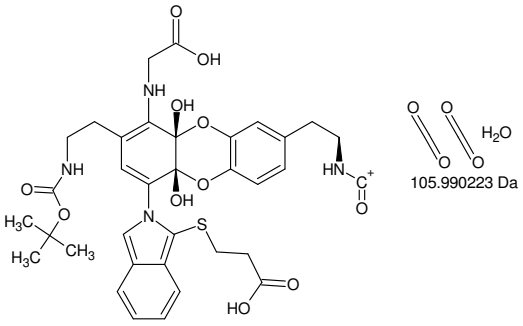

Monoisotopic Mass = 723.233054 Da

105.990223 Da

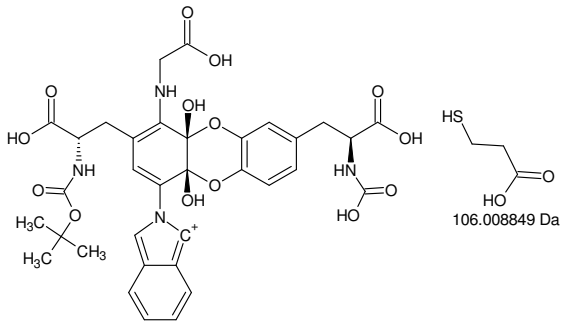

Monoisotopic Mass = 723.214428 Da

106.008849 Da

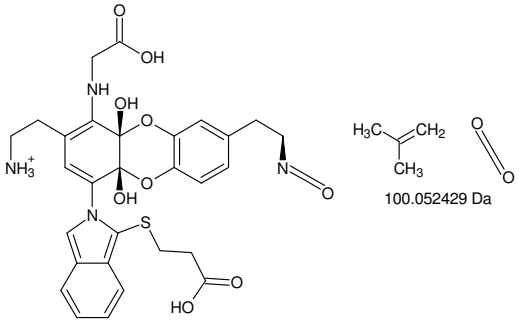

Monoisotopic Mass = 623.180625 Da

100.052429 Da

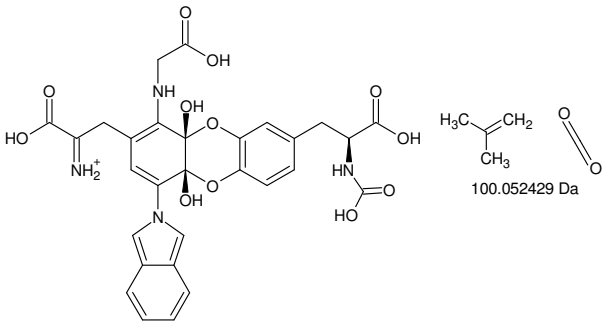

Monoisotopic Mass = 623.161999 Da

100.052429 Da

+MSn [OPA-Ser 13,3 min]: [885 -> 829] -> 723 -> 623

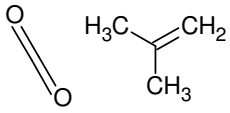

100.052429 Da

Gefundene Verbindungen: 37
CH2OS MG=61,9826362
CH2O3 MG=62,0003942
(...)
NOS MG=61,970061
NO3 MG=61,987819

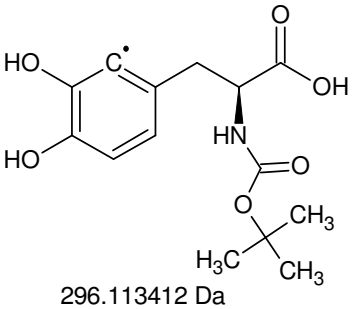

296.113412 Da

-----D--B--E--f-i-l-t-e-r-----
26.05.2011 - 13:15:32,90
akzeptierte DBEs:
0 1 2 3 4 5 6

CH_2OS	DBE: 1
CH_2O_3	DBE: 1
CH_6N_2O	DBE: 0
$C_2H_6O_2$	DBE: 0
C_2H_6S	DBE: 0
C_5H_2	DBE: 5
$H_2N_2O_2$	DBE: 1
H_2N_2S	DBE: 1
H_6N_4	DBE: 0

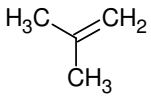

56.0626 Da

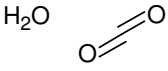

62.000394 Da

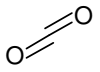

43.989829 Da

9 von 37 Summenformeln

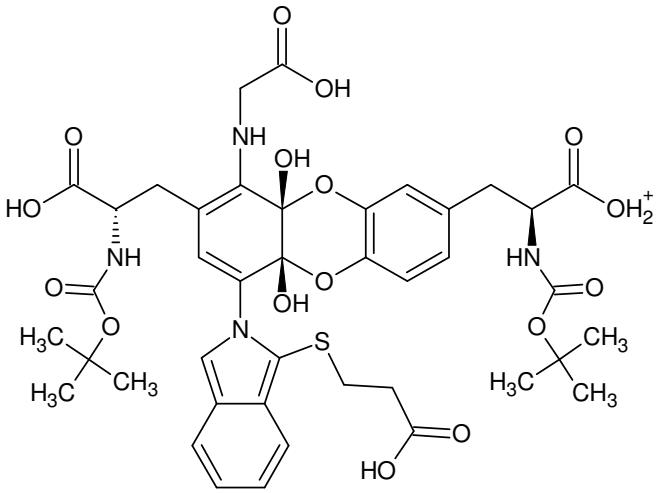

Monoisotopic Mass = 885.285878 Da

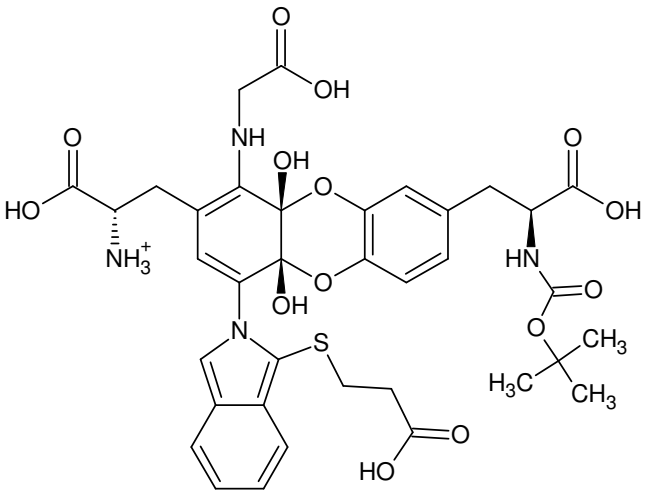

Monoisotopic Mass = 785.233448 Da

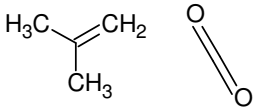

100.052429 Da

+MSn [OPA-Ser 13,3 min]: 885 -> 785

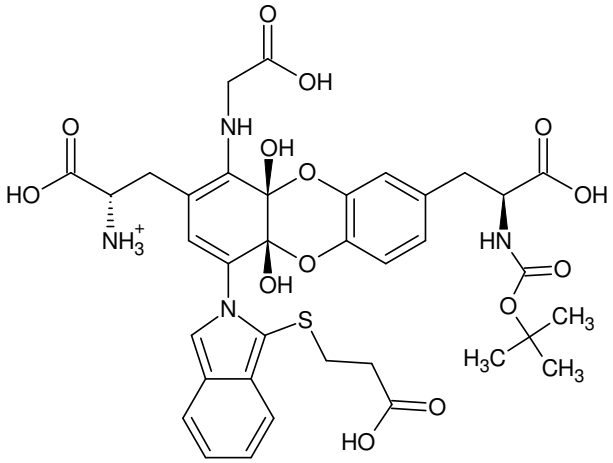

Monoisotopic Mass = 785.233448 Da

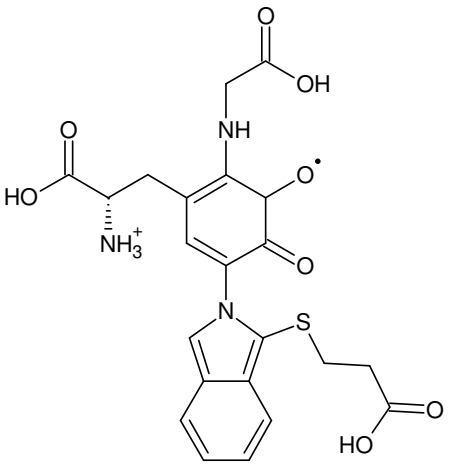

Monoisotopic Mass = 489.120036 Da

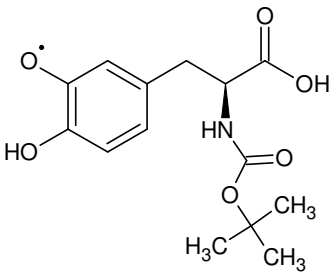

296.113412 Da

retro Diels-Alder

56 Da nicht mehr abspaltbar

- 100 Da zusätzlich nicht mehr möglich

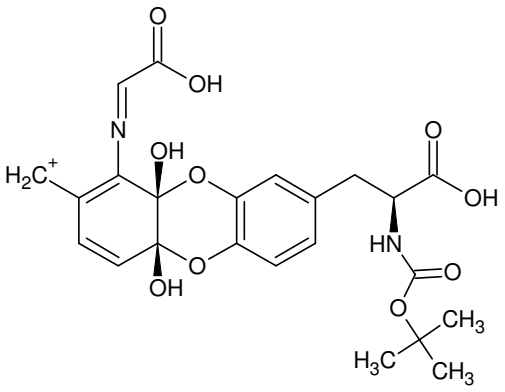

Monoisotopic Mass = 489.150371 Da

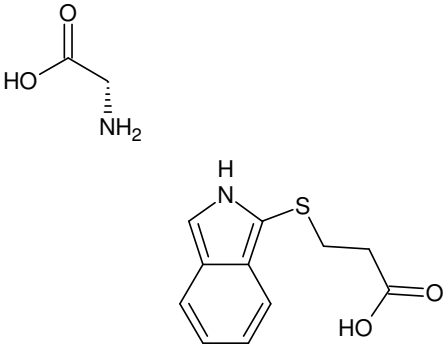

Monoisotopic Mass = 296.083077 Da

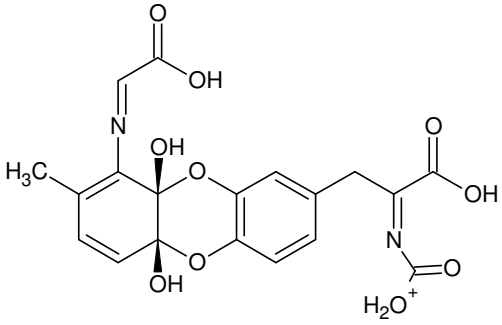

Monoisotopic Mass = 433.087771 Da

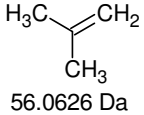

56.0626 Da

+MSn [OPA-Ser 13,3 min]: [885 -> 785] -> 489 -> 433

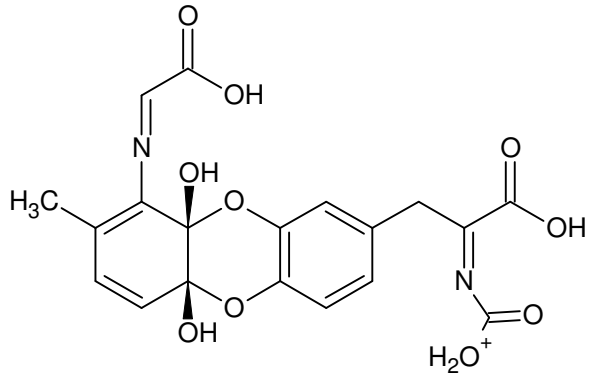

Monoisotopic Mass = 433.087771 Da

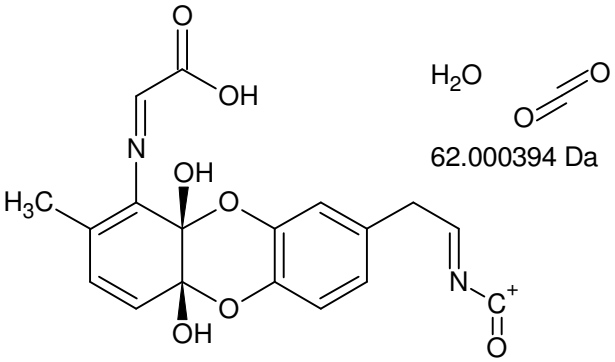

H_2O

62.000394 Da

Monoisotopic Mass = 371.087377 Da

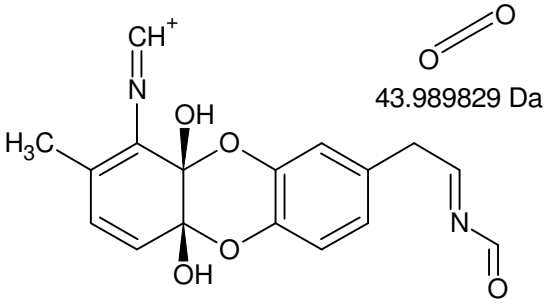

43.989829 Da

Monoisotopic Mass = 327.097548 Da

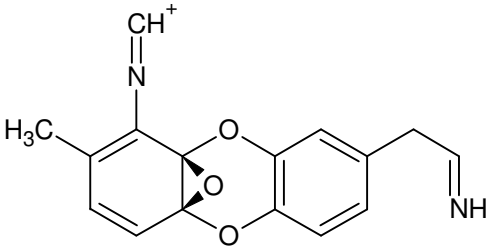

Monoisotopic Mass = 281.092069 Da

46.005479 Da

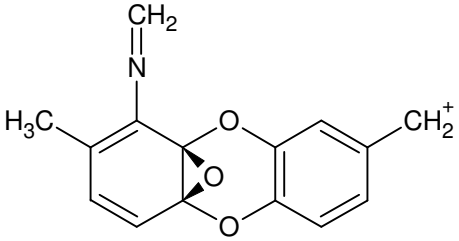

Monoisotopic Mass = 254.08117 Da

27.010899 Da

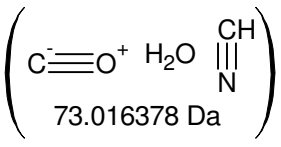

73.016378 Da

+MSn [OPA-Ser 13,3 min]: [885 -> 785 -> 489 -> 433] -> 371 -> 327 -> 281, 254

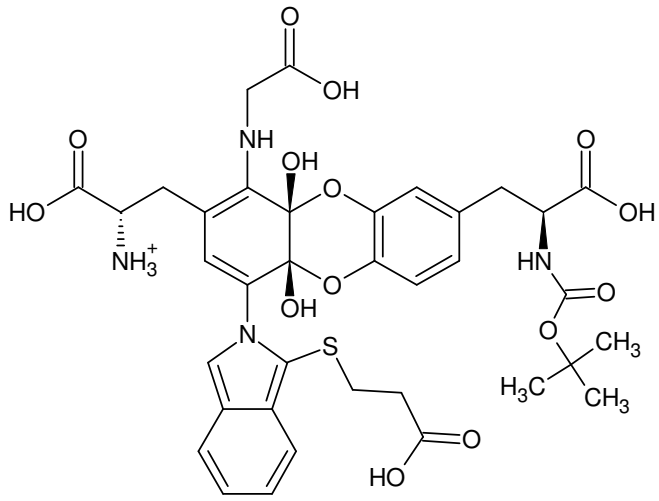

Monoisotopic Mass = 785.233448 Da

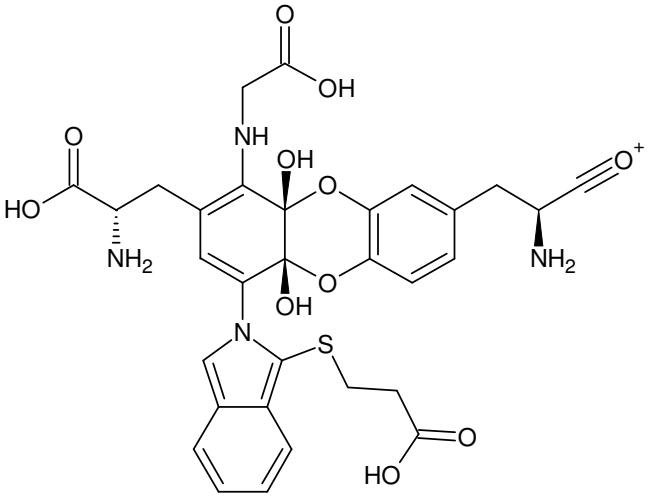

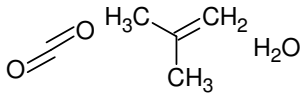

118.062994 Da

Monoisotopic Mass = 667.170454 Da

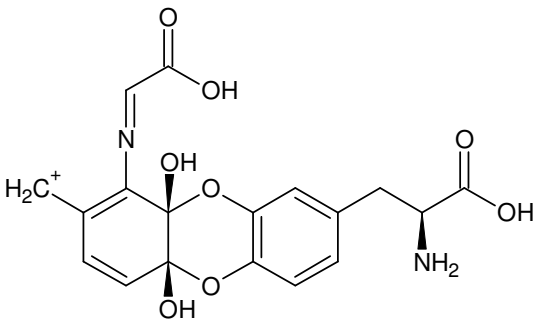

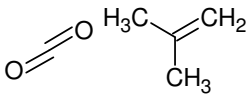

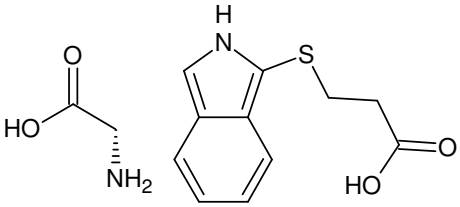

396.135506 Da

Monoisotopic Mass = 389.097942 Da

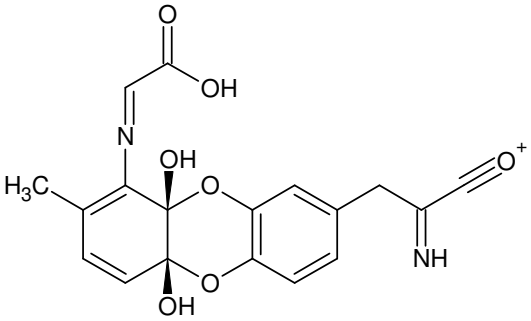

H_2O

18.010565 Da

Monoisotopic Mass = 371.087377 Da

-MSn [OPA-Ser 13,3 min]: [885 -> 785] -> 667, 389 -> 371

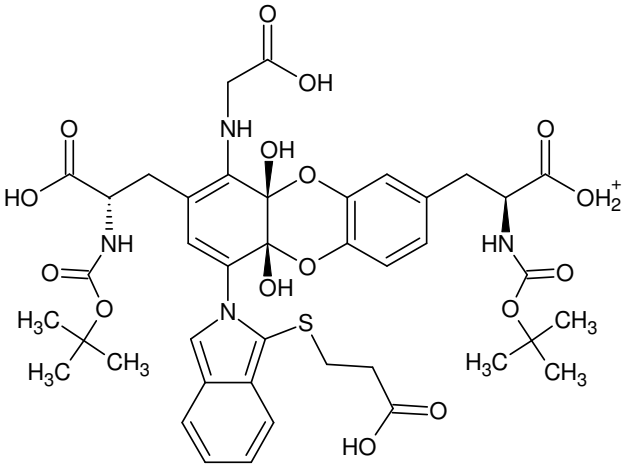

Monoisotopic Mass = 885.285878 Da

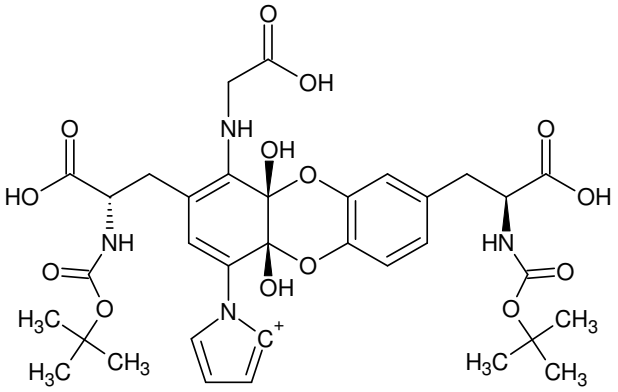

Monoisotopic Mass = 729.261378 Da

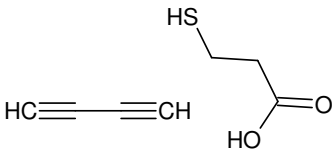

156.024499 Da

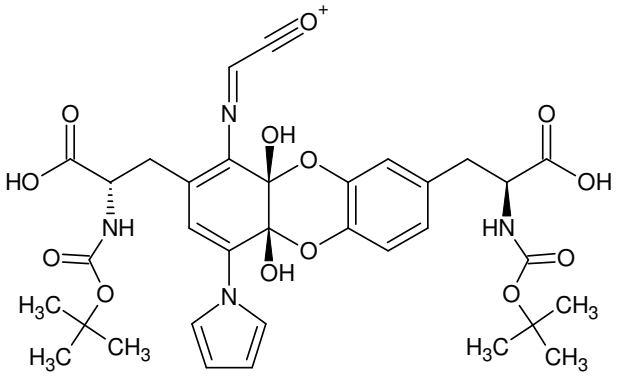

Monoisotopic Mass = 711.250814 Da

H_2O
18.010565 Da

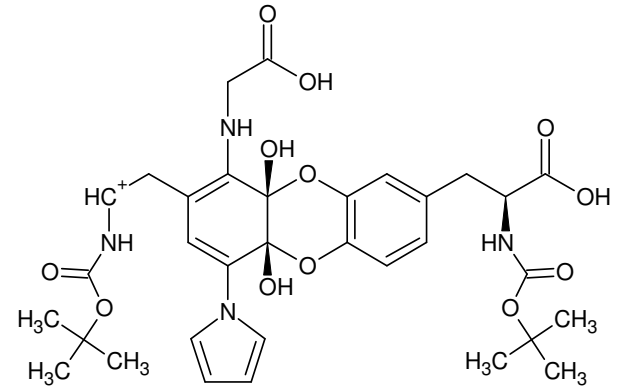

Monoisotopic Mass = 685.271549 Da

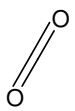

43.989829 Da

+MSn [OPA-Ser 13,3 min]: 885 -> 729 -> 711, 685

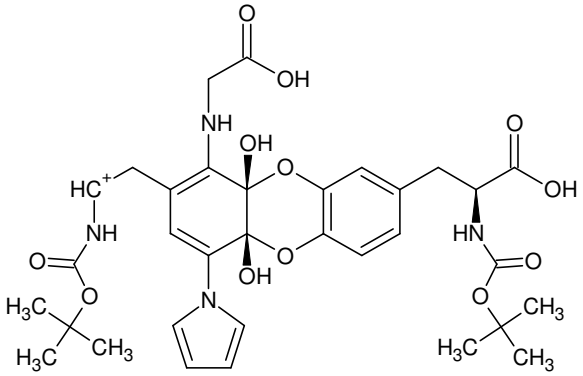

43.989829 Da

Monoisotopic Mass = 685.271549 Da

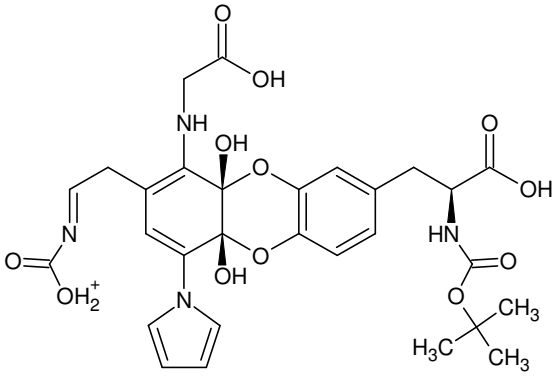

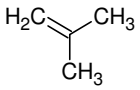

56.0626 Da

Monoisotopic Mass = 629.208949 Da

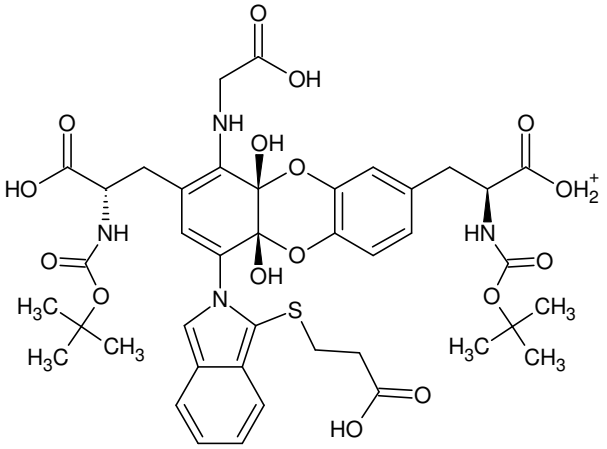

Monoisotopic Mass = 885.285878 Da

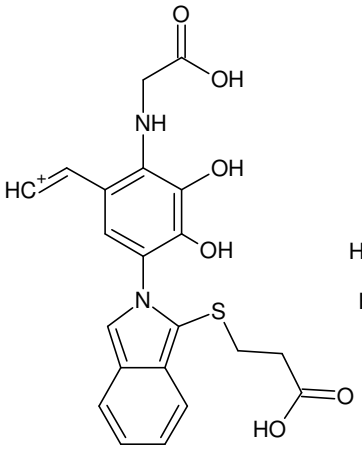

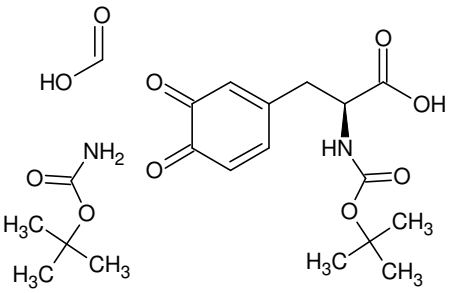

458.190045 Da

Monoisotopic Mass = 427.095833 Da

+MSn [OPA-Ser 13,3 min]: [885 -> 729 -> 685] -> 629 and 885 -> 427

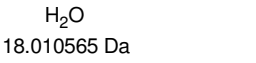

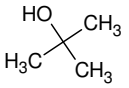

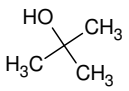

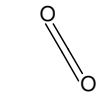

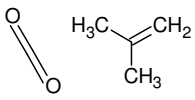

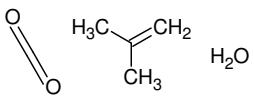

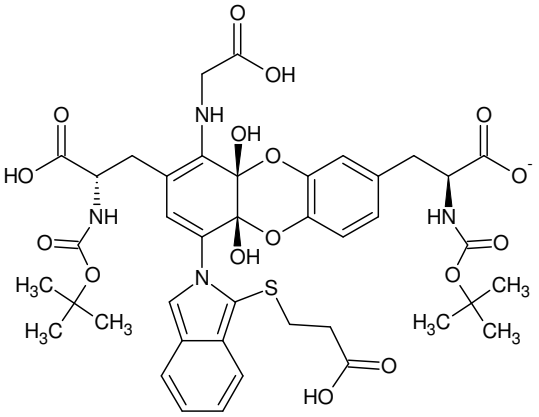

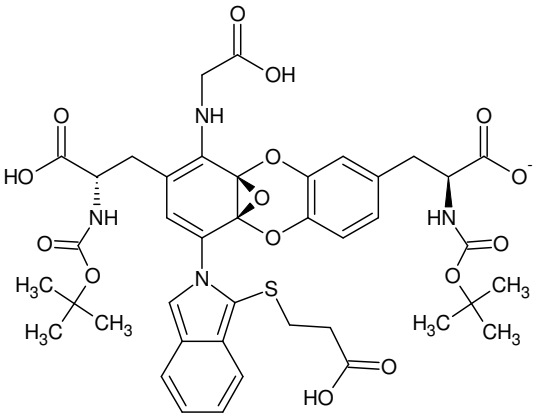

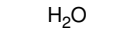

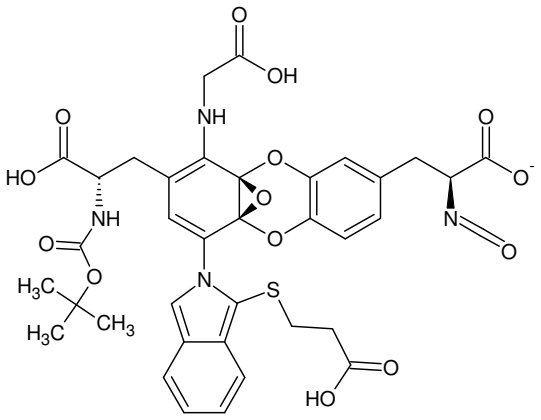

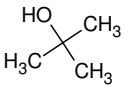

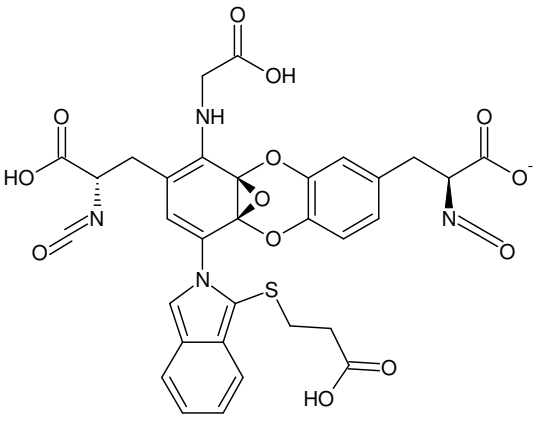

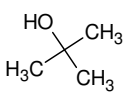

-MSn [OPA-Ser 13,3 min]: 883 -> 865 -> 791 -> 717

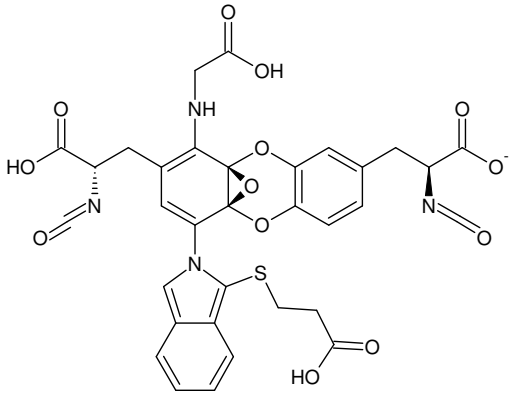

Monoisotopic Mass = 717.11443 Da

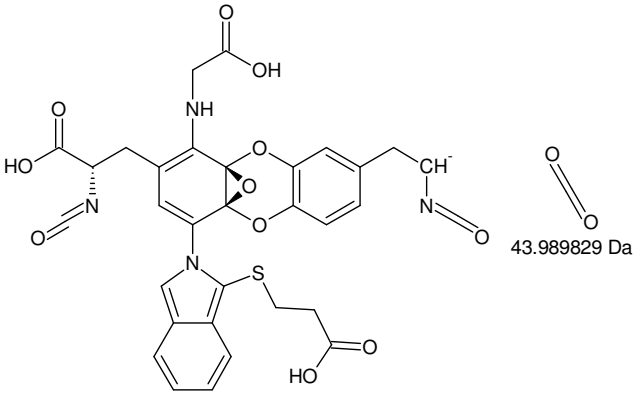

Monoisotopic Mass = 673.124601 Da

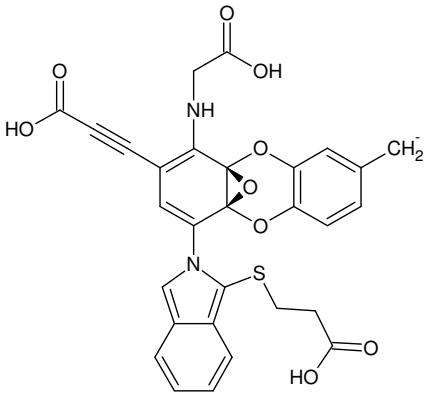

Monoisotopic Mass = 573.097324 Da

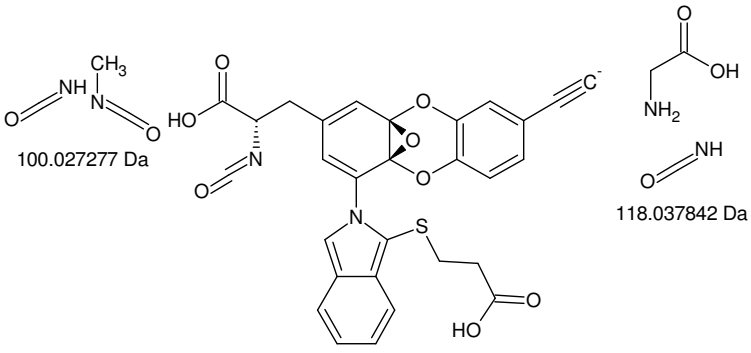

Monoisotopic Mass = 555.086759 Da

-MSn [OPA-Ser 13,3 min]: [883 -> 865 -> 791 -> 717] -> 673 -> 573, 555

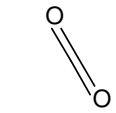

43.989829 Da

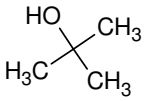

74.073165 Da

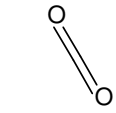

43.989829 Da

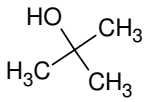

74.073165 Da

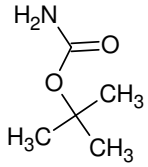

117.078979 Da

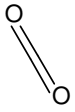

43.989829 Da

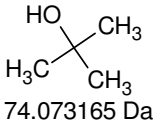

74.073165 Da

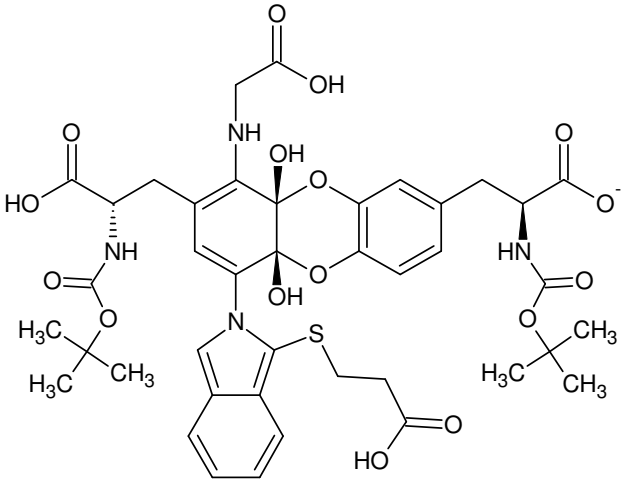

Monoisotopic Mass = 883.271325 Da

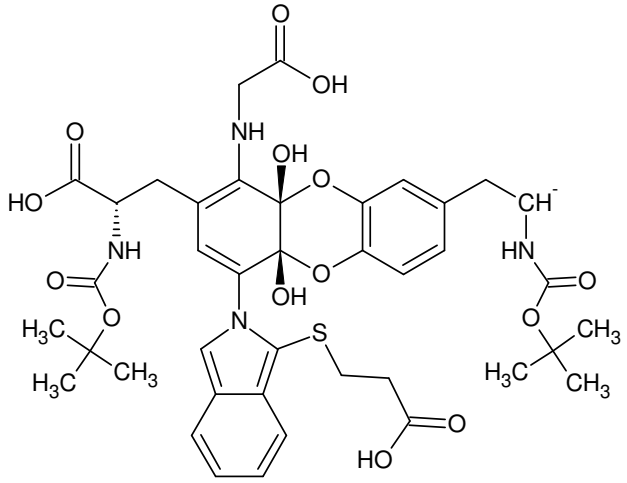

Monoisotopic Mass = 839.281496 Da

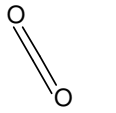

43.989829 Da

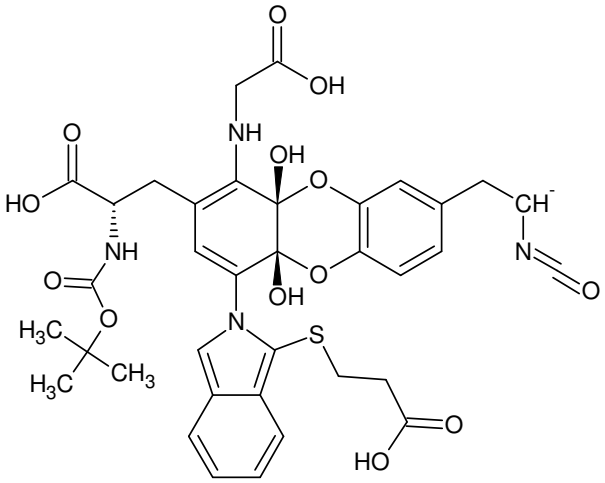

Monoisotopic Mass = 765.208331 Da

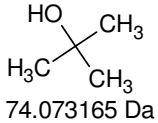

74.073165 Da

-MSn [OPA-Ser 13,3 min]: 883 -> 839 -> 765

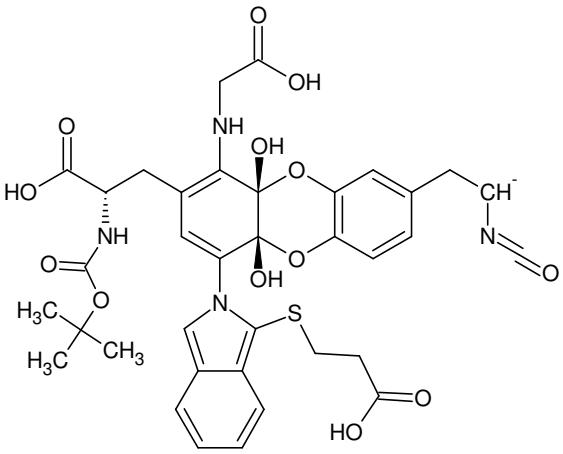

Monoisotopic Mass = 765.208331 Da

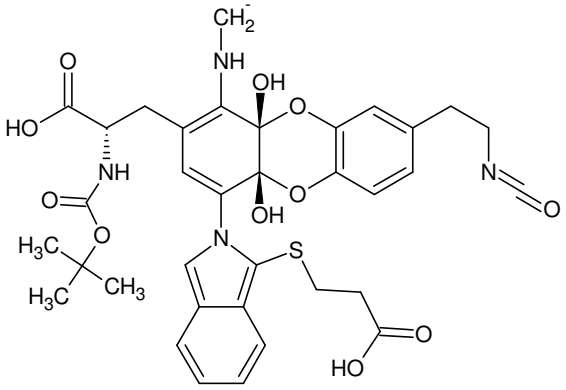

Monoisotopic Mass = 721.218502 Da

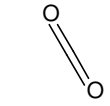

43.989829 Da

Das Fragment 17 Da taucht in den +MS^n-Messungen nicht auf.

=> keine freie Aminogruppe

In den -MSn-Messungen gibt es auch kein Fragment mit 17 Da.:
-720,9 Th - -603,7 Th = -**117,2 Da**

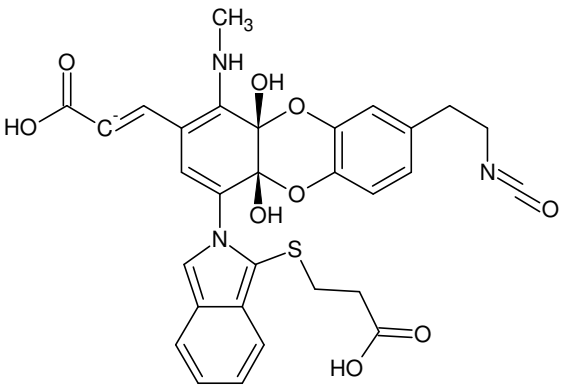

Monoisotopic Mass = 604.139523 Da

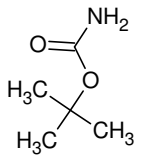

117.078979 Da

-MSn [OPA-Ser 13,3 min]: [883 -> 839 -> 765] -> 721 -> 604

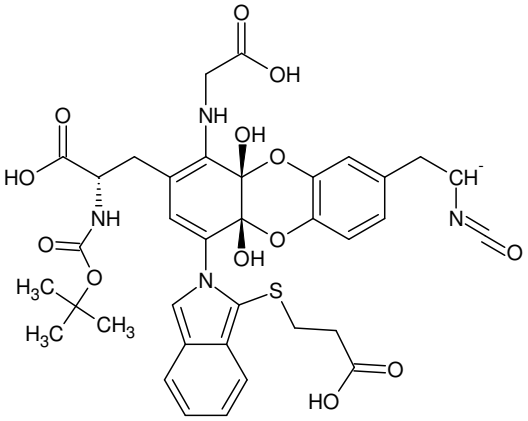

Monoisotopic Mass = 765.208331 Da

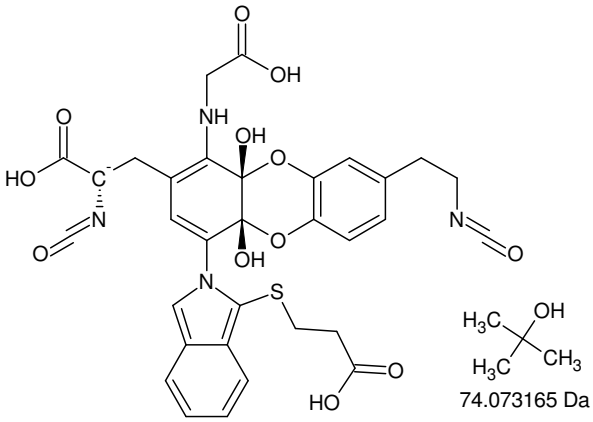

Monoisotopic Mass = 691.135166 Da

74.073165 Da

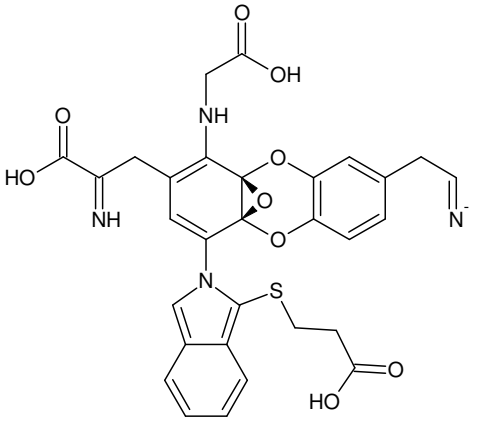

Monoisotopic Mass = 617.134772 Da

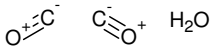

74.000394 Da

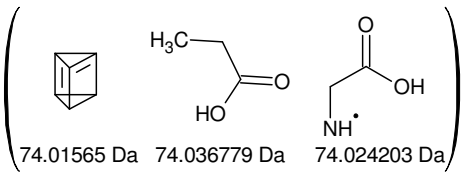

74.01565 Da 74.036779 Da 74.024203 Da

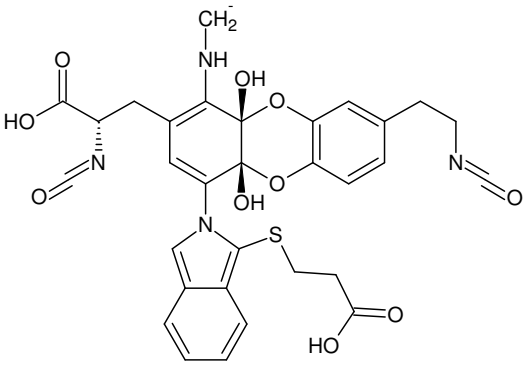

Monoisotopic Mass = 647.145337 Da

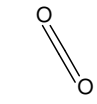

43.989829 Da

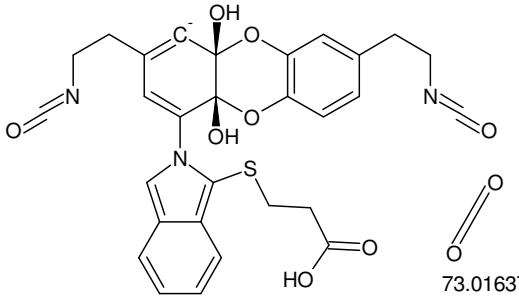

Monoisotopic Mass = 574.128958 Da

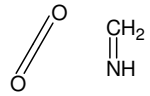

73.016378 Da

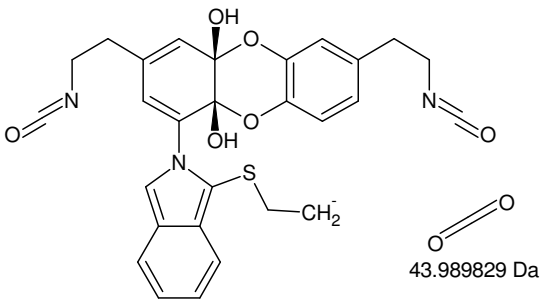

Monoisotopic Mass = 530.139129 Da

43.989829 Da

-MSn [OPA-Ser 13,3 min]: [883 -> 765] -> 691 -> 617, 647 -> 574 -> 530

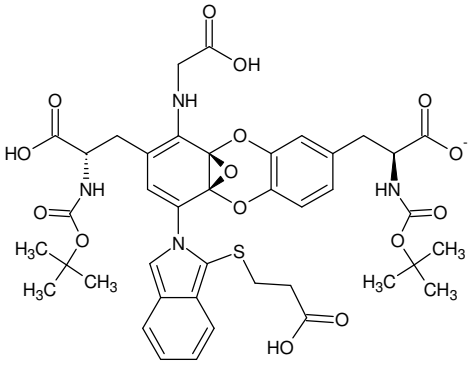

Monoisotopic Mass = 865.26076 Da

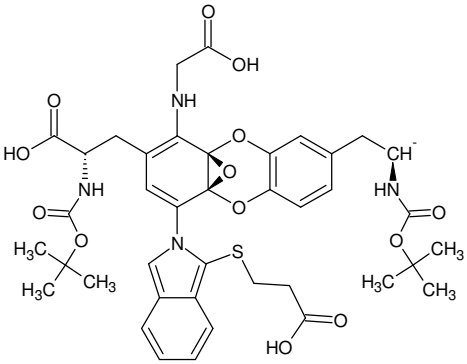

43.989829 Da

Monoisotopic Mass = 821.270931 Da

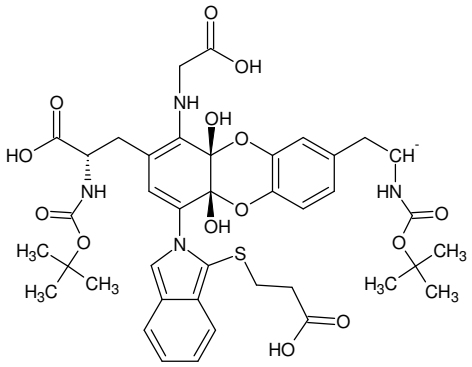

Monoisotopic Mass = 839.281496 Da

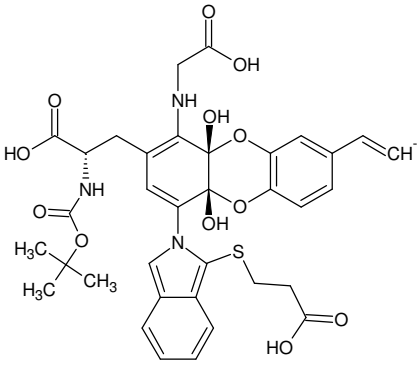

117.078979 Da

Monoisotopic Mass = 722.202517 Da

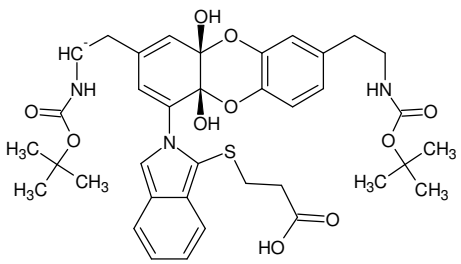

117.006208 Da

Monoisotopic Mass = 722.275288 Da

-MSn [OPA-Ser 13,3 min]: [883 -> 865] -> 821 and [883 -> 839] -> 722 -> 648, 574 -> 530 -> 486

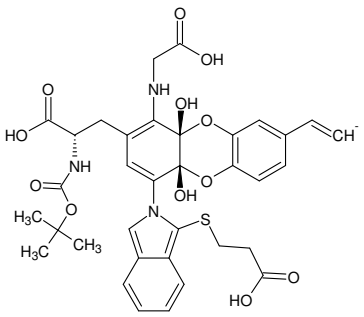

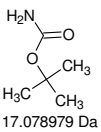

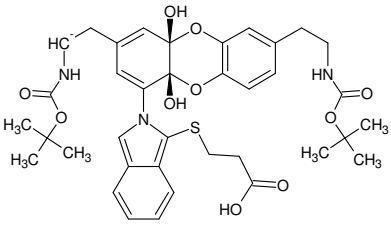

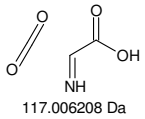

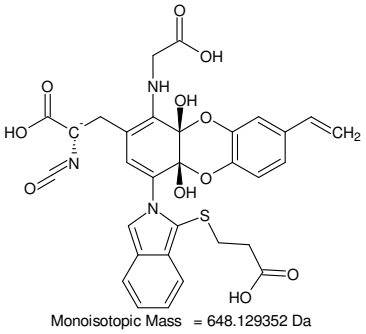

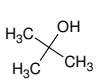

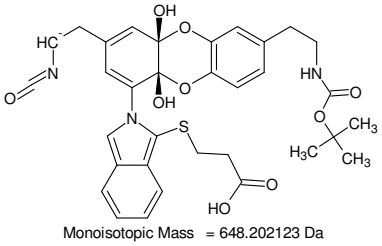

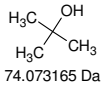

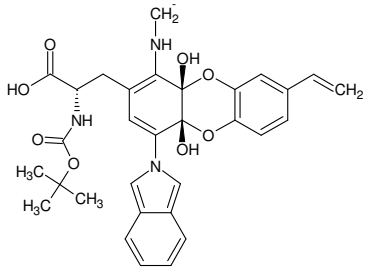

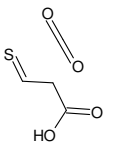

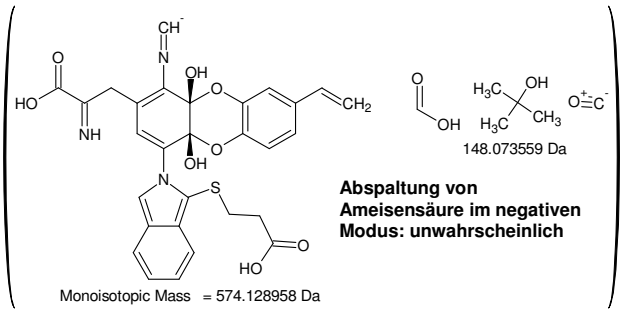

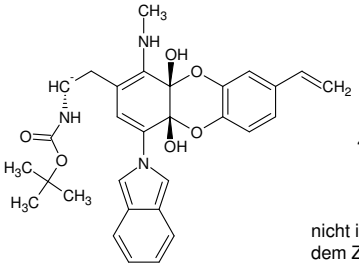

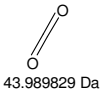

nicht identisch mit -530 Th aus dem Zerfallspfad über -765 Th

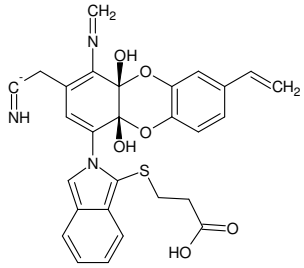

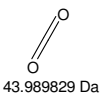

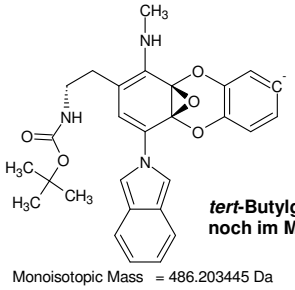

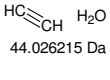

***tert*-Butylgruppe immer noch im Molekül?**

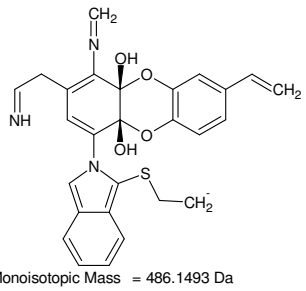

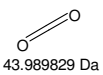

-MSn [OPA-Ser 13,3 min]: [883 -> 839 -> 722] -> 648, 574 -> 530 -> 486

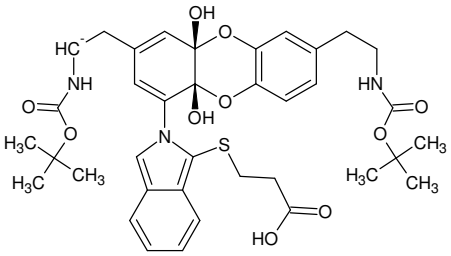

Monoisotopic Mass = 722.275288 Da

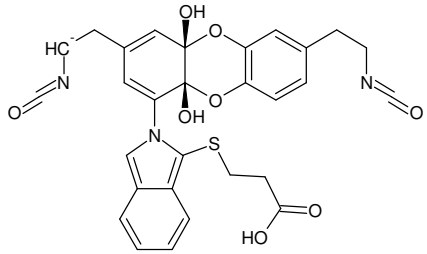

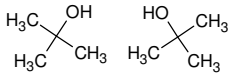

148.14633 Da

Monoisotopic Mass = 574.128958 Da

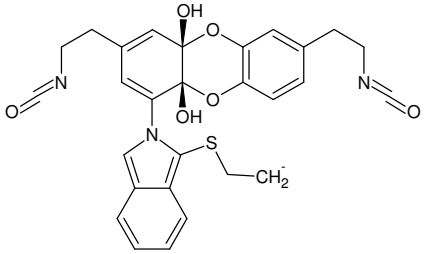

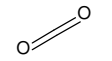

43.989829 Da

Monoisotopic Mass = 530.139129 Da

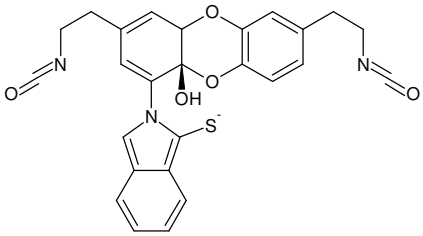

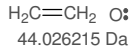

44.026215 Da

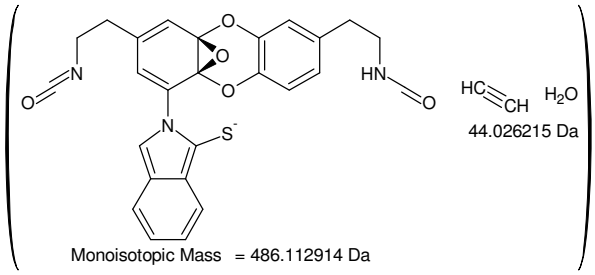

44.026215 Da

Monoisotopic Mass = 486.112914 Da

Monoisotopic Mass = 486.112914 Da

-MSn [OPA-Ser 13,3 min]: [883 -> 839 -> 722] -> 574 -> 530 -> 486

XIII.III.VI. **OPA-Val 2,9 min**

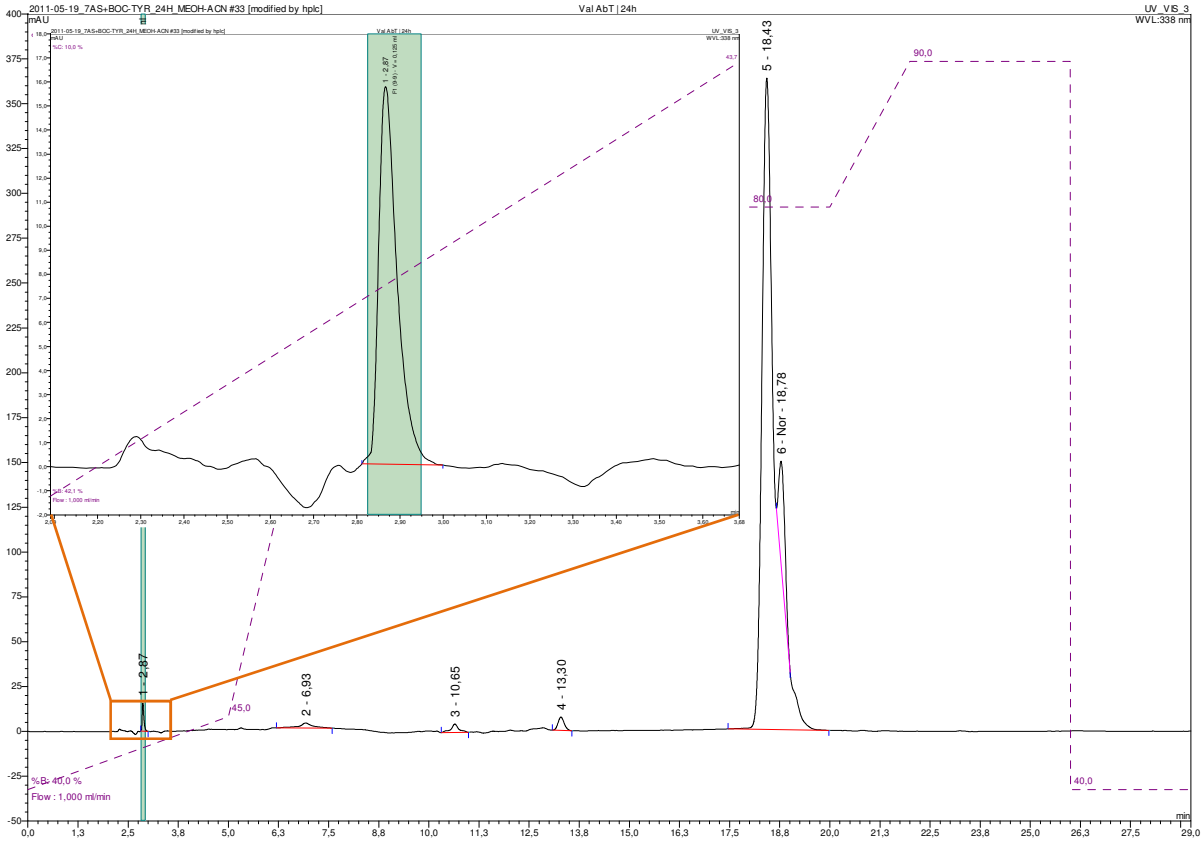

Figure XIII-LIX Val AbT | 24h;OPA-derivatised

+MS^n

973,0 —31,2→ 941,8
- —100,1→ 872,9
- —129,1→ 843,9
- —210,0→ 763,0 —232,1→ 530,6

741,0 —48,0→ 693,0 —46,1→ 646,9 —69,1→ 577,8 —148,9→ 428,9
- 646,9 —105,6→ 541,3
- —110,0→ 631,0
- —157,6→ 583,4
- —173,0→ 568,0
- —210,0→ 531,0 —254,1→ 276,9 —72,1→ 204,8

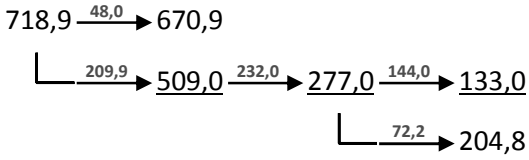
718,9
48,0
670,9
209,9
509,0
232,0
277,0
144,0
133,0
72,2
204,8

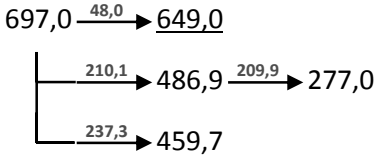
697,0
48,0
649,0
210,1
486,9
209,9
277,0
237,3
459,7

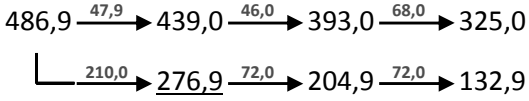
486,9
47,9
439,0
46,0
393,0
68,0
325,0
210,0
276,9
72,0
204,9
72,0
132,9

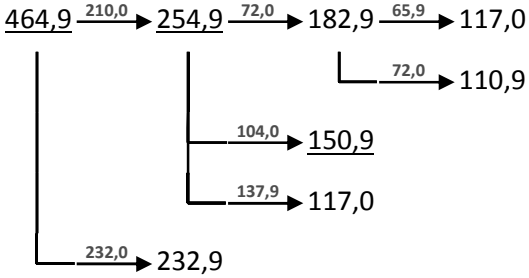
464,9
210,0
254,9
72,0
182,9
65,9
117,0
72,0
110,9
104,0
150,9
137,9
117,0
232,0
232,9

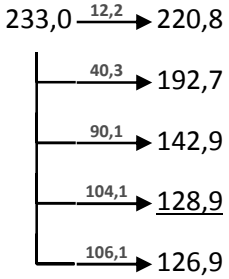
233,0
12,2
220,8
40,3
192,7
90,1
142,9
104,1
128,9
106,1
126,9

-MS^n

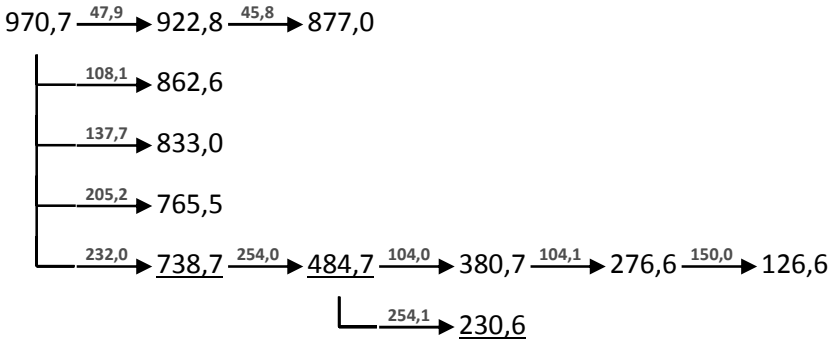
970,7
47,9
922,8
45,8
877,0
108,1
862,6
137,7
833,0
205,2
765,5
232,0
738,7
254,0
484,7
104,0
380,7
104,1
276,6
150,0
126,6
254,1
230,6

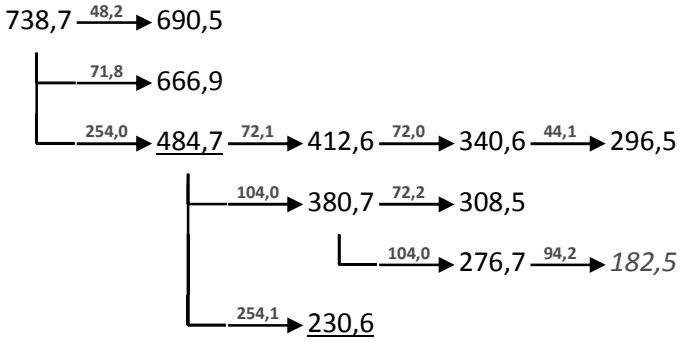
738,7
48,2
690,5
71,8
666,9
254,0
484,7
72,1
412,6
72,0
340,6
44,1
296,5
104,0
380,7
72,2
308,5
104,0
276,7
94,2
182,5
254,1
230,6

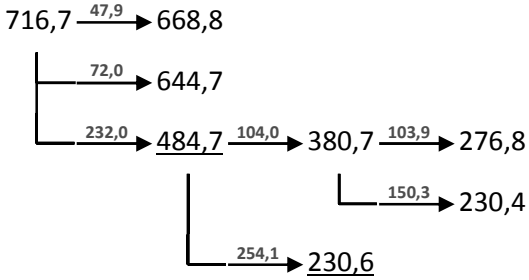
716,7
47,9
668,8
72,0
644,7
232,0
484,7
104,0
380,7
103,9
276,8
150,3
230,4
254,1
230,6

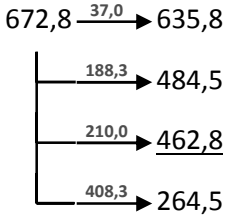
672,8
37,0
635,8
188,3
484,5
210,0
462,8
408,3
264,5

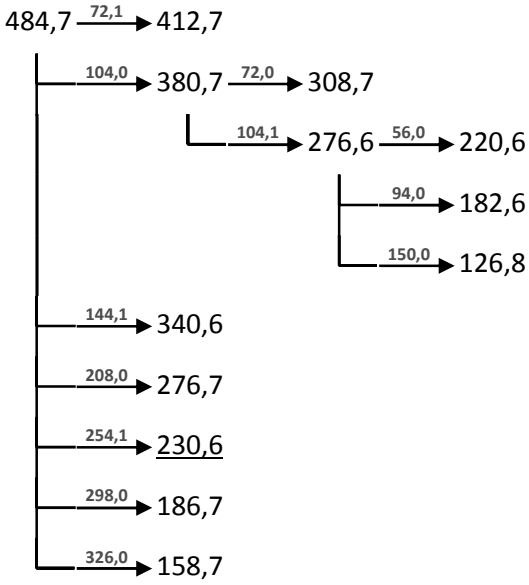
484,7
72,1
412,7
104,0
380,7
72,0
308,7
104,1
276,6
56,0
220,6
94,0
182,6
150,0
126,8
144,1
340,6
208,0
276,7
254,1
230,6
298,0
186,7
326,0
158,7

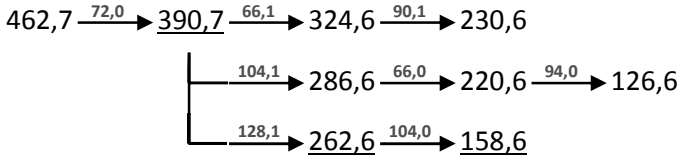

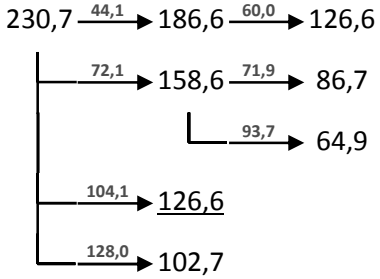

isotopic fingerprint:

peak area / % of monoisotopic	**+1**	**+2**	**+3**
theoretical ($C_{36}H_{35}N_8Na_6O_{16}^+$):	42,0	12,3	2,7
measured (972,8 Th):	52,1	-	-
measured (-970,8 Th):	24,4	-	-
theoretical ($C_{27}H_{26}N_6Na_5O_{12}^+$):	32,3	7,5	1,3
measured (740,9 Th):	40,2	-	-
measured (-738,8 Th):	25,6	-	-
theoretical ($C_{27}H_{27}N_6Na_4O_{12}^+$):	32,3	7,5	1,3
measured (718,9 Th):	15,9	-	-
measured (-716,7 Th):	26,1	-	-
theoretical ($C_{18}H_{18}N_4Na_3O_8^+$):	21,5	3,9	0,5
measured (486,9 Th):	20,3	-	-
measured (-484,8 Th):	19,6	-	-
theoretical ($C_{18}H_{19}N_4Na_2O_8^+$):	21,5	3,9	0,5
measured (465,0 Th):	18,3	-	-
measured (-462,8 Th):	11,5	-	-
theoretical ($C_9H_{10}N_2NaO_4^+$):	10,8	1,4	0,1
measured (233,0 Th):	8,5	-	-
measured (-230,7 Th):	5,1	-	-

Figure XIII-LX MS^n analysis of OPA-Val 2,9 min

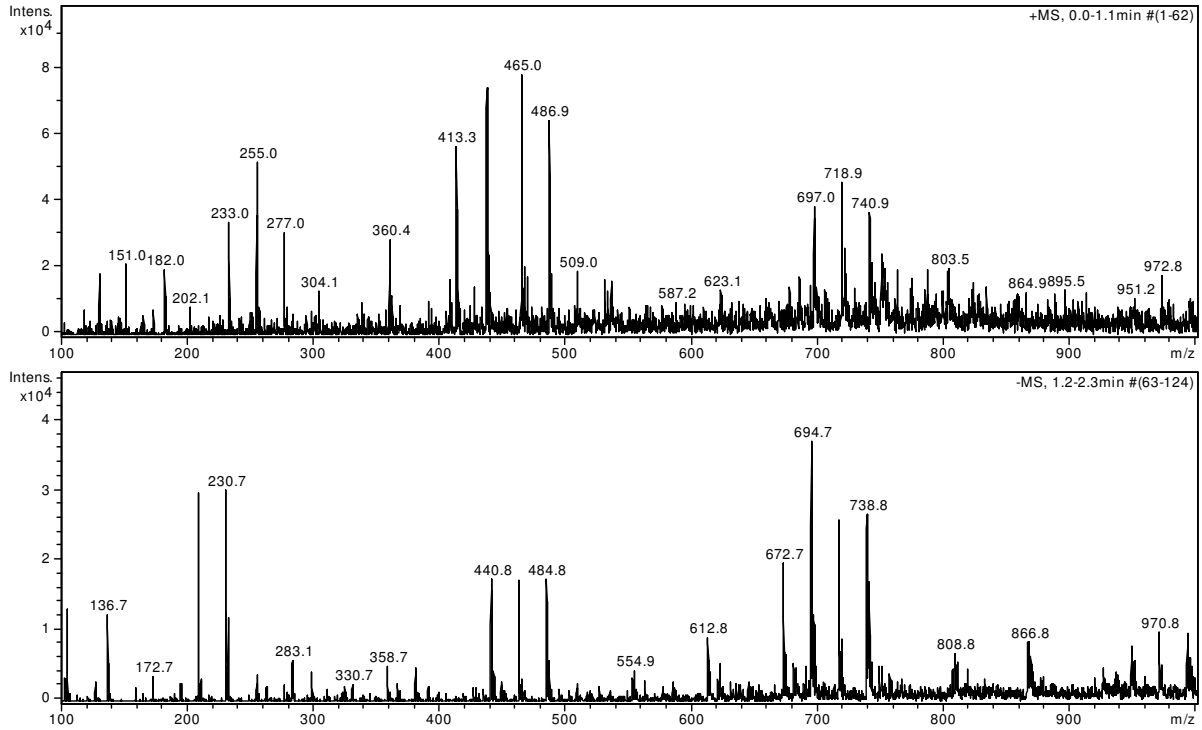

Figure XIII-LXI OPA-Val 2,9 min: 3 % MeOH, 87 % ACN, 0,1ȯ ‰ FA in ddH_2O (diluted 1:6 with ACN); full scan MS^1

Cluster mit Natrium
Gefundene Verbindungen: 3
H_6O MG=22,0418626
CH_{10} MG=22,078246
H_8N MG=22,0656708

Differenz der stärksten Signale (719 Th, 465 Th; -695 Th, -441 Th) = **254 Th**

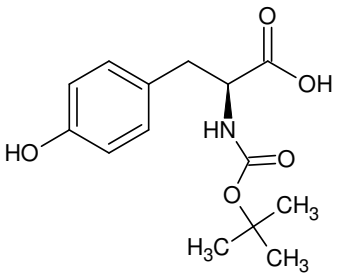

L-Boc-Tyr-OH

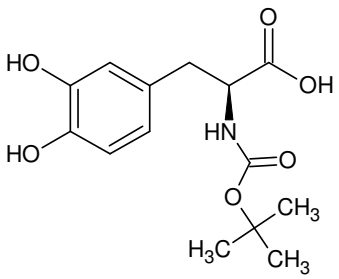

Monoisotopic Mass = 297.121237 Da

211 Th, -187 Th

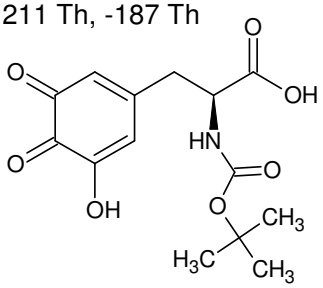

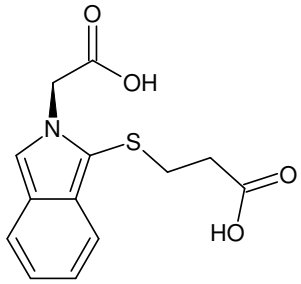

OPA-Gly
Monoisotopic Mass = 279.056528 Da

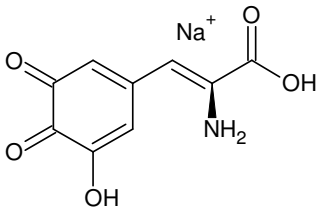

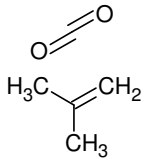

100.052429 Da

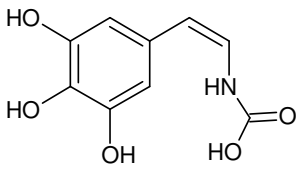

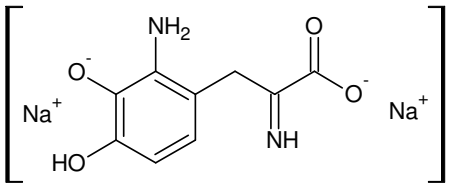

Monoisotopic Mass = 254.027947 Da

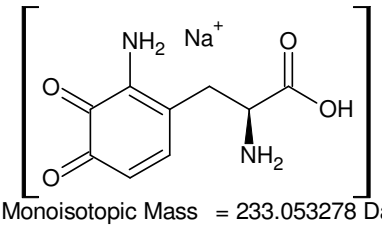

Monoisotopic Mass = 233.053278 Da

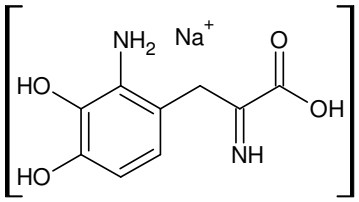

Monoisotopic Mass = 233.053278 Da

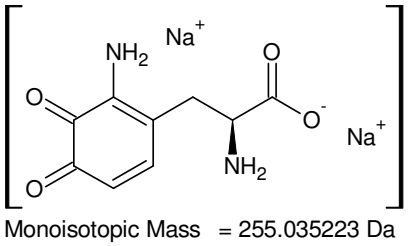

Monoisotopic Mass = 255.035223 Da

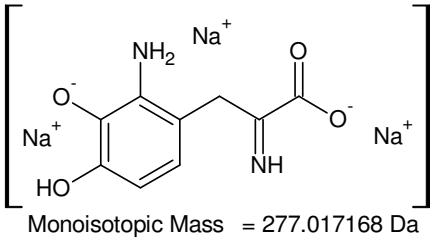

Monoisotopic Mass = 277.017168 Da

[OPA-Val 2,9 min]: Cluster with 3x Na

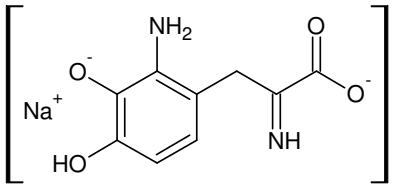

Monoisotopic Mass = 231.038725 Da

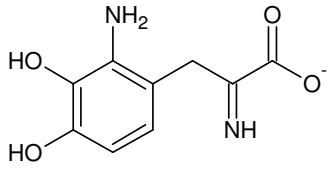

Monoisotopic Mass = 209.05678 Da

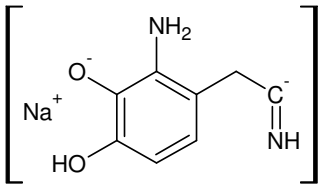

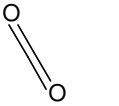

43.989829 Da

Monoisotopic Mass = 187.048896 Da

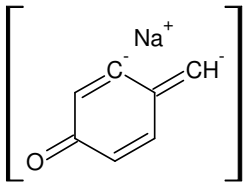

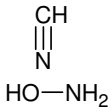

60.032363 Da

Monoisotopic Mass = 127.016533 Da

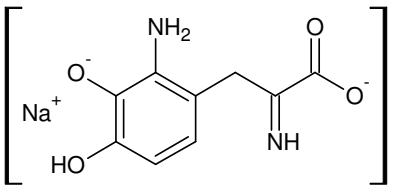

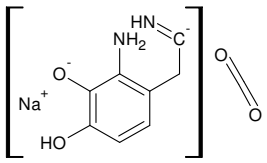

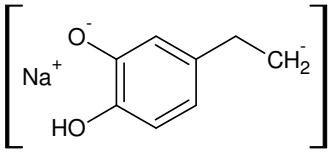

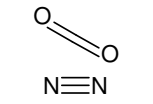

71.995977 Da

Monoisotopic Mass = 231.038725 Da

Monoisotopic Mass = 159.042748 Da

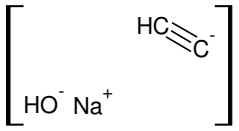

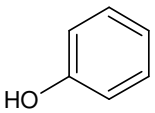

94.041865 Da

Monoisotopic Mass = 65.024693 Da

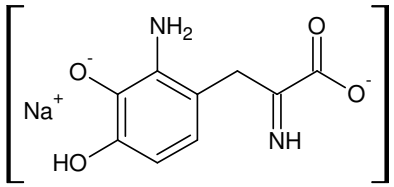

Monoisotopic Mass = 231.038725 Da

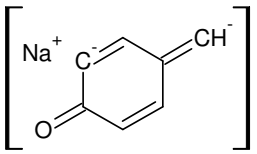

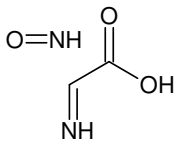

104.022192 Da

Monoisotopic Mass = 127.016533 Da

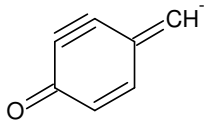

Na-H

23.997595 Da

Monoisotopic Mass = 103.018938 Da

-MSn [OPA-Val 2,9 min]: 231 -> 187 -> 127 as well as 231 -> 159 -> (65) and 231 -> 127, 103

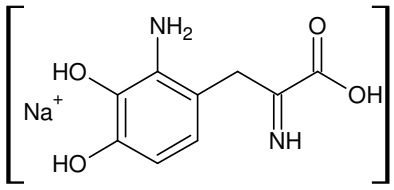

Monoisotopic Mass = 233.053278 Da

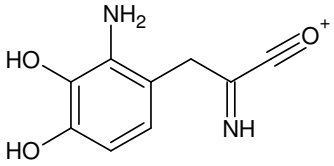

Na^+HO^-
39.99251 Da

Monoisotopic Mass = 193.060769 Da

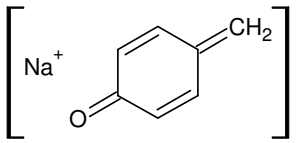

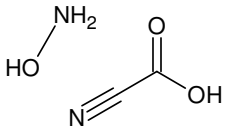

104.022192 Da

Monoisotopic Mass = 129.031086 Da

+MSn [OPA-Val 2,9 min]: 233 -> 193, 129

Gefundene Verbindungen: 15
CH_5Na MG=40,028893
$CH_{12}O$ MG=40,0888102
$CH_{14}N$ MG=40,1126184
CN_2 MG=40,006148
C_2H_2N MG=40,0187232
C_2H_{16} MG=40,1251936
C_2O MG=39,994915
C_3H_4 MG=40,0312984
H_3NNa MG=40,0163178
HNaO MG=39,9925096
H_8O_2 MG=40,0524268
H_8S MG=40,0346688
$H_{12}N_2$ MG=40,1000432
$H_{10}NO$ MG=40,076235
$H_{17}Na$ MG=40,1227882

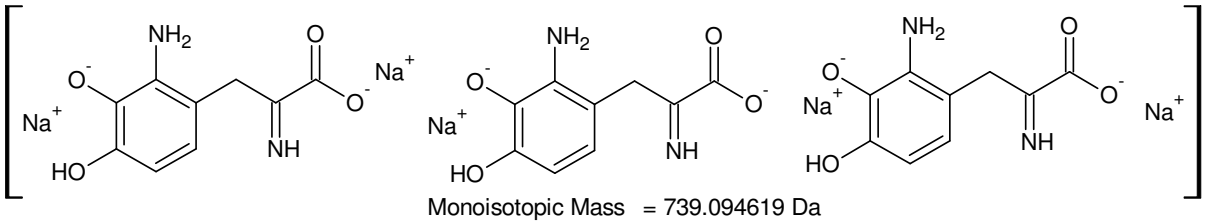

Monoisotopic Mass = 739.094619 Da

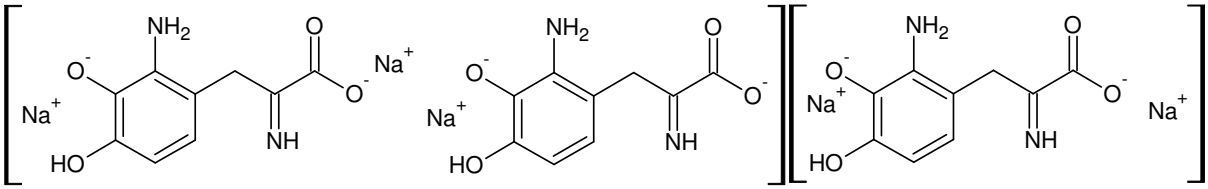

Monoisotopic Mass = 485.066672 Da

254.027947 Da

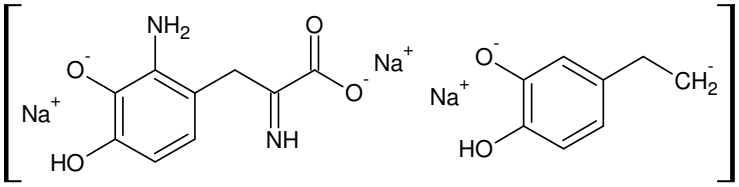

Monoisotopic Mass = 413.070695 Da

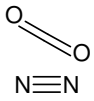

71.995977 Da

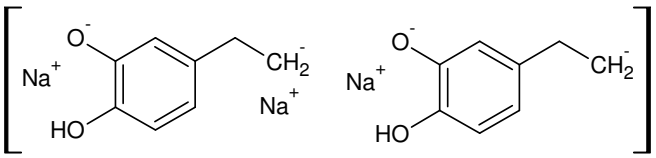

Monoisotopic Mass = 341.074718 Da

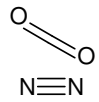

71.995977 Da

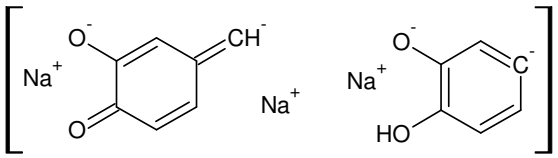

Monoisotopic Mass = 297.012117 Da

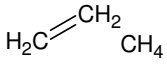

44.0626 Da

Gefundene Verbindungen: 20
CH_2NO MG=44,0136382
CH_4N_2 MG=44,0374464
CH_9Na MG=44,0601914
$CH_{16}O$ MG=44,1201086
$CH_{18}N$ MG=44,1439168
CO_2 MG=43,98983
CS MG=43,972072
C_2H_4O MG=44,0262134
C_2H_6N MG=44,0500216
C_2H_{20} MG=44,156492
C_3H_8 MG=44,0625968
H_2N_3 MG=44,0248712
H_5NaO MG=44,023808
H_7NNa MG=44,0476162
$H_{12}O_2$ MG=44,0837252
$H_{14}NO$ MG=44,1075334
$H_{12}S$ MG=44,0659672
$H_{16}N_2$ MG=44,1313416
$H_{21}Na$ MG=44,1540866
N_2O MG=44,001063

-MSn [OPA-Val 2,9 min]: 739 -> 485 -> 413 -> 341 -> 297

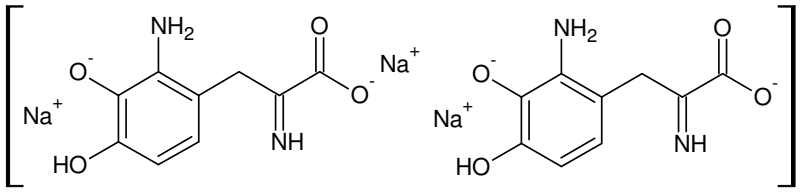

Monoisotopic Mass = 485.066672 Da

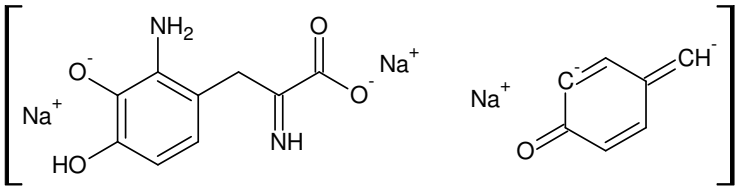

Monoisotopic Mass = 381.04448 Da

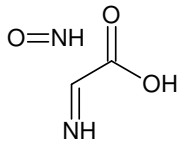

104.022192 Da

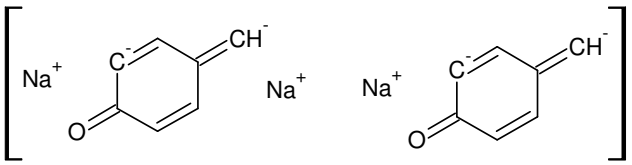

Monoisotopic Mass = 277.022288 Da

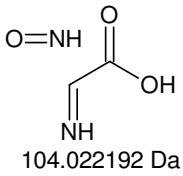

104.022192 Da

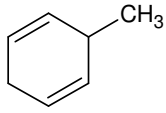

94.07825 Da

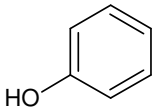

94.041865 Da

zu viele H

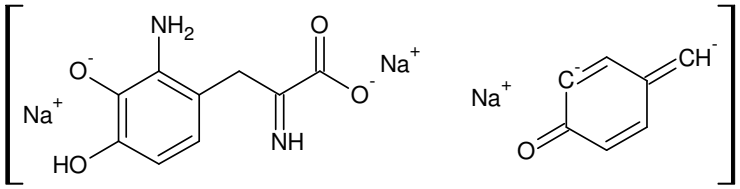

Monoisotopic Mass = 381.04448 Da

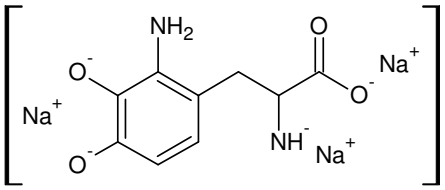

Monoisotopic Mass = 277.018265 Da

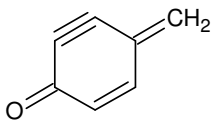

104.026215 Da

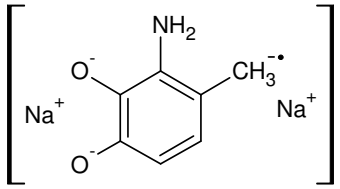

Monoisotopic Mass = 183.027767 Da

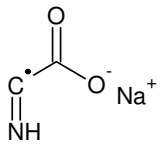

93.990498 Da

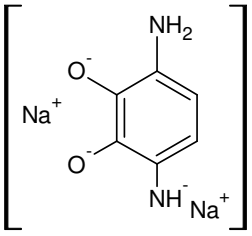

Monoisotopic Mass = 183.015191 Da

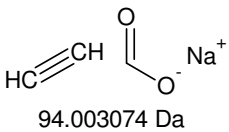

94.003074 Da

-MSn [OPA-Val 2,9 min]: [739 -> 485] -> 381 -> 277 -> 183

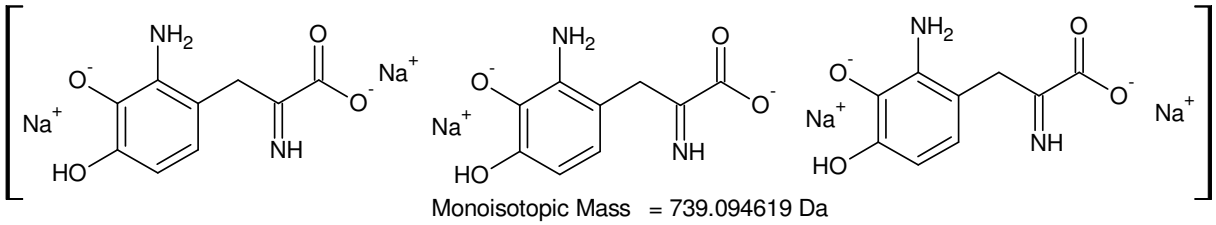

Monoisotopic Mass = 739.094619 Da

Gefundene Verbindungen: 27

CH_4O_2	MG=48,0211284	
CH_4S	MG=48,0033704	
CH_6NO	MG=48,0449366	
CH_8N_2	MG=48,0687448	
$CH_{13}Na$	MG=48,0914898	
$CH_{20}O$	MG=48,151407	
$CH_{22}N$	MG=48,1752152	Na—H
C_2HNa	MG=47,9975946	Na—H
C_2H_8O	MG=48,0575118	47.99519 Da
$C_2H_{10}N$	MG=48,08132	
C_2H_{24}	MG=48,1877904	
C_3H_{12}	MG=48,0938952	
C_4	MG=48	
H_2Na_2	MG=47,9951892	
H_2NO_2	MG=48,0085532	
H_2NS	MG=47,9907952	
H_4N_2O	MG=48,0323614	
H_6N_3	MG=48,0561696	
H_9NaO	MG=48,0551064	
$H_{11}NNa$	MG=48,0789146	
$H_{16}O_2$	MG=48,1150236	
$H_{16}S$	MG=48,0972656	
$H_{18}NO$	MG=48,1388318	
$H_{25}Na$	MG=48,185385	
$H_{20}N_2$	MG=48,16264	
OS	MG=47,966987	
O_3	MG=47,984745	

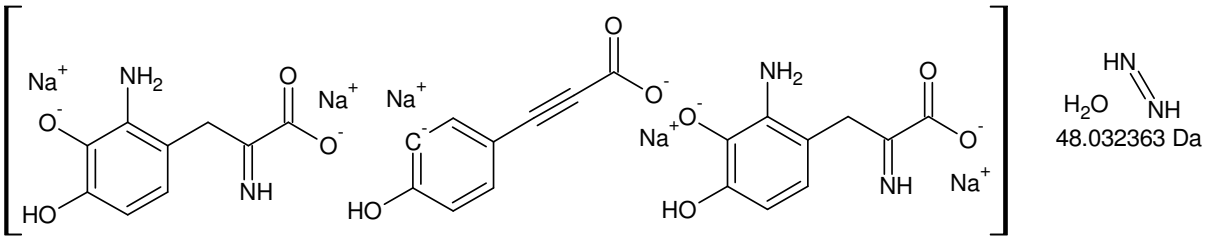

48.032363 Da

Monoisotopic Mass = 691.062256 Da

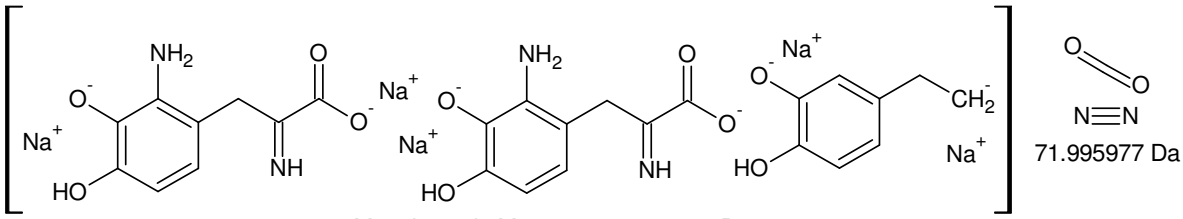

71.995977 Da

Monoisotopic Mass = 667.098642 Da

-MSn [OPA-Val 2,9 min]: 739 -> 691, 667

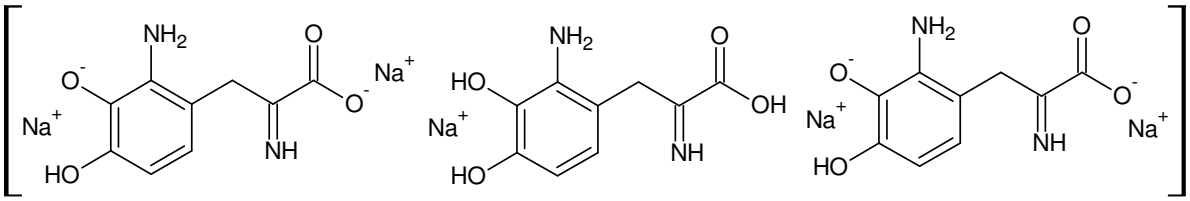

Monoisotopic Mass = 741.109172 Da

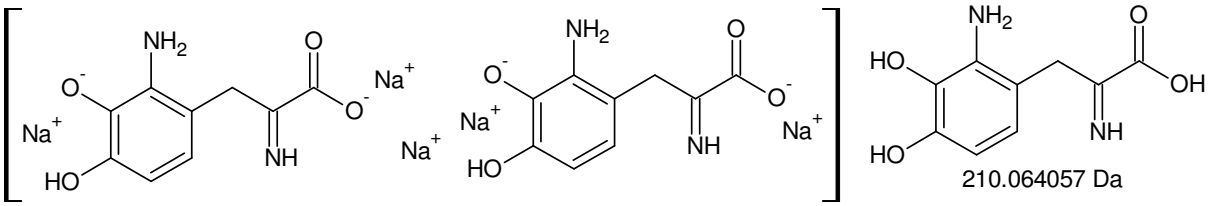

Monoisotopic Mass = 531.045115 Da

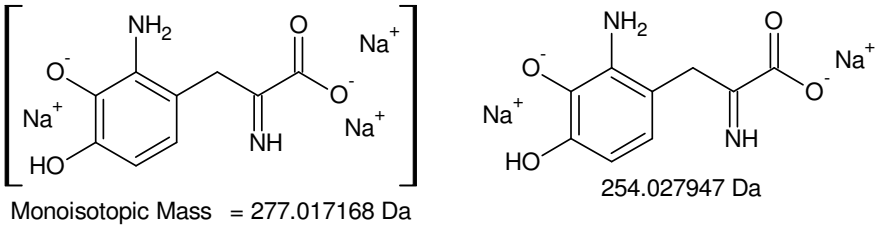

Monoisotopic Mass = 277.017168 Da

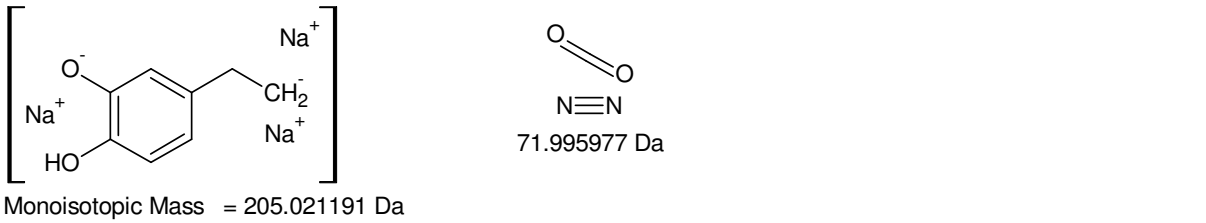

+MSn [OPA-Val 2,9 min]: 741 -> 531 -> 277 -> 205

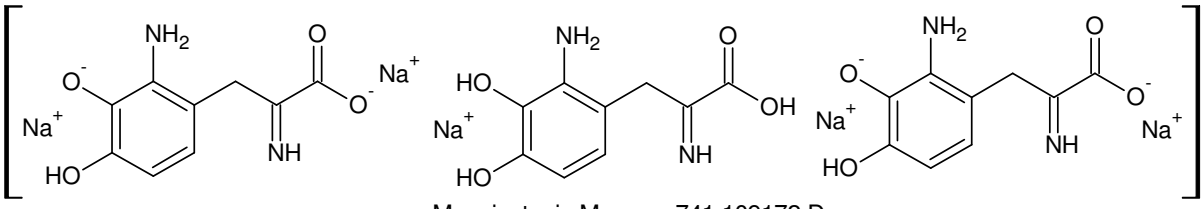

Monoisotopic Mass = 741.109172 Da

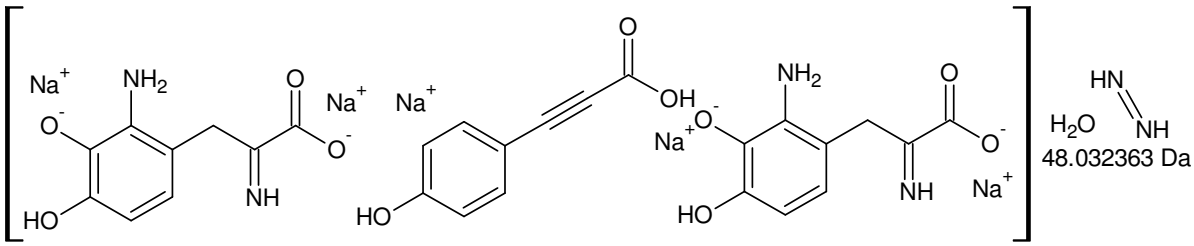

Monoisotopic Mass = 693.076809 Da

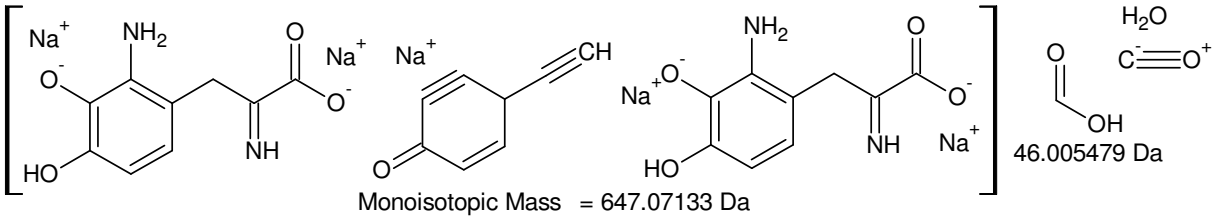

Monoisotopic Mass = 647.07133 Da

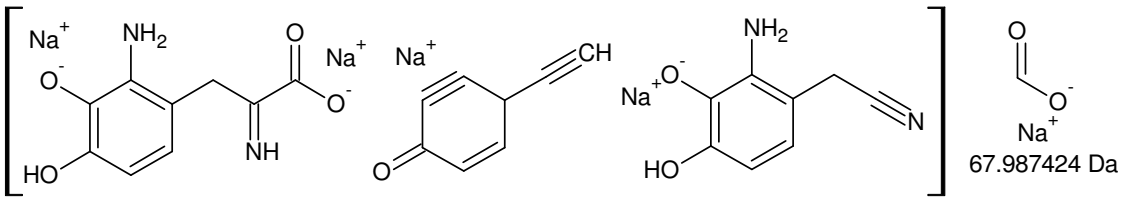

Monoisotopic Mass = 579.083905 Da

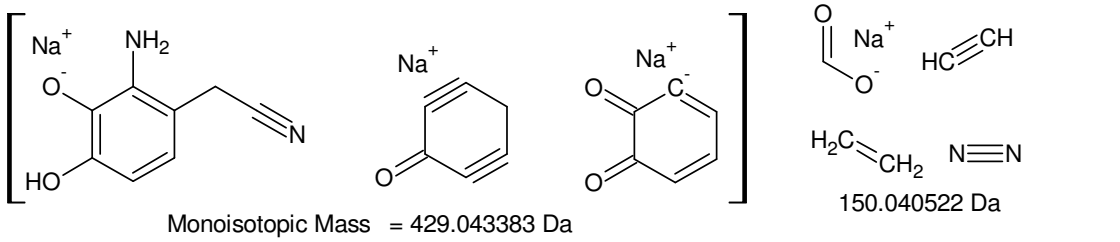

Monoisotopic Mass = 429.043383 Da

+MSn [OPA-Val 2,9 min]: 741 -> 693 -> 647 -> 579 -> 429

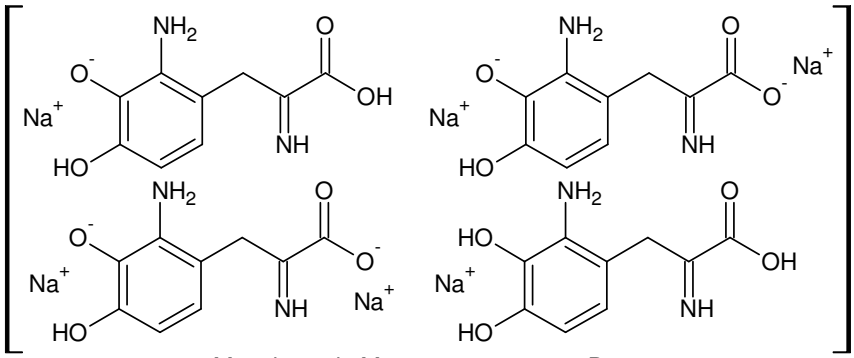

Monoisotopic Mass = 973.155173 Da

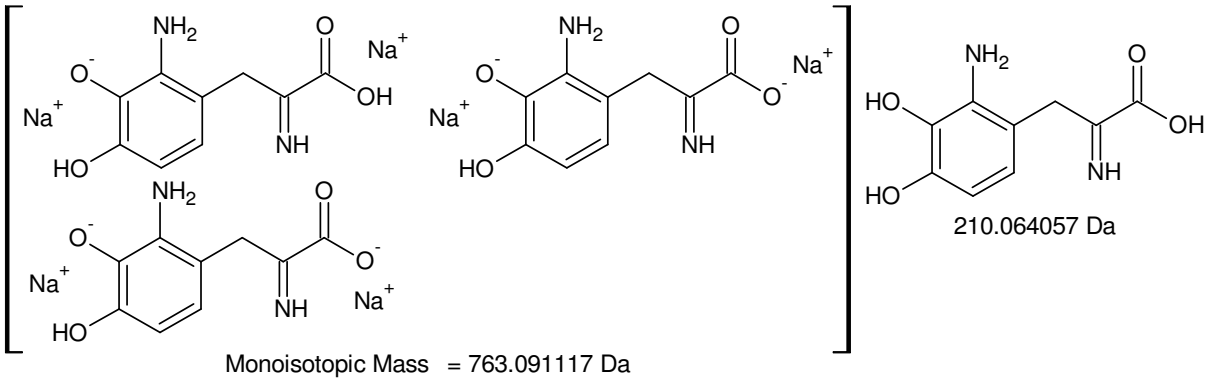

Monoisotopic Mass = 763.091117 Da

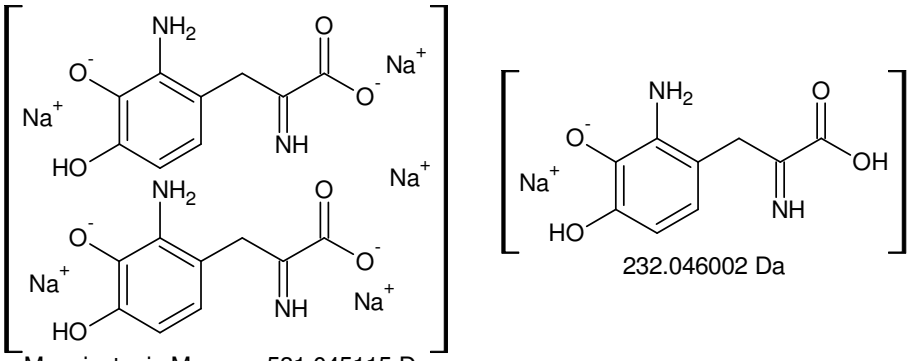

Monoisotopic Mass = 531.045115 Da

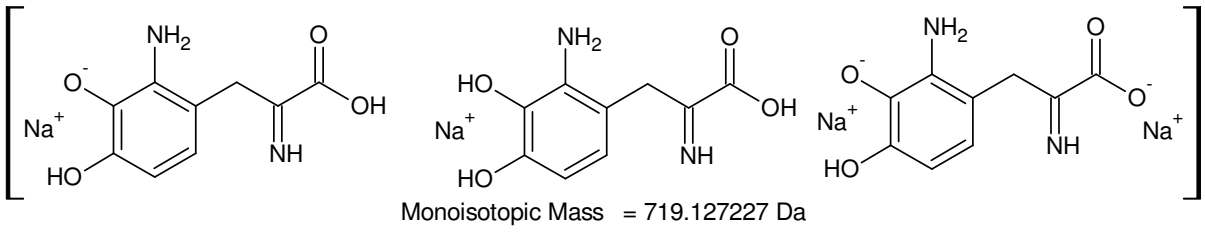

Monoisotopic Mass = 719.127227 Da

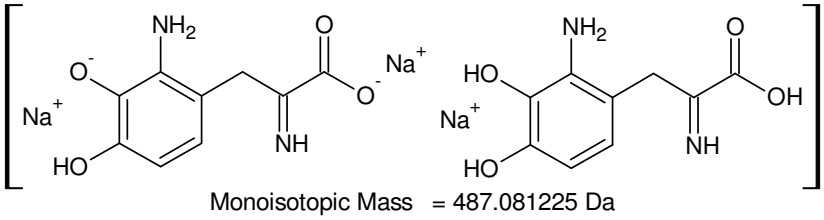

Monoisotopic Mass = 487.081225 Da

+MSn [OPA-Val 2,9 min]: 973 -> 763 -> 531 and 719 Th, 487 Th

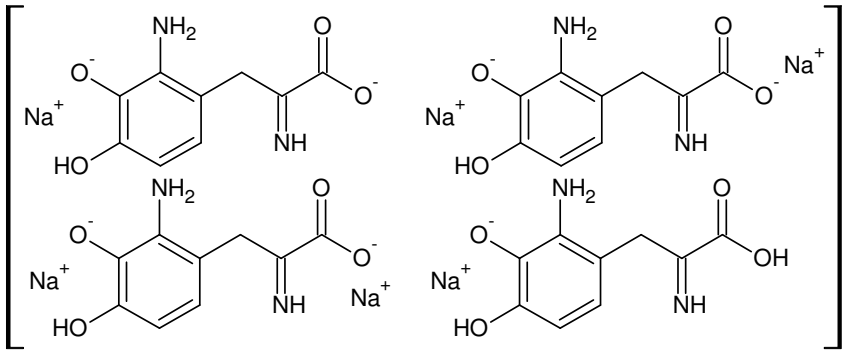

Monoisotopic Mass = 971.140621 Da

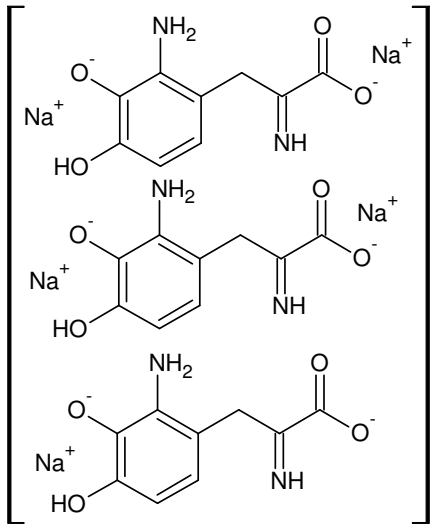

Monoisotopic Mass = 739.094619 Da

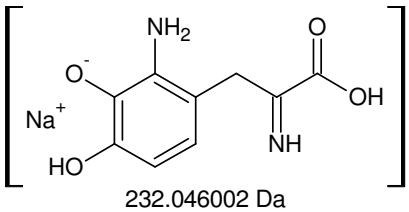

232.046002 Da

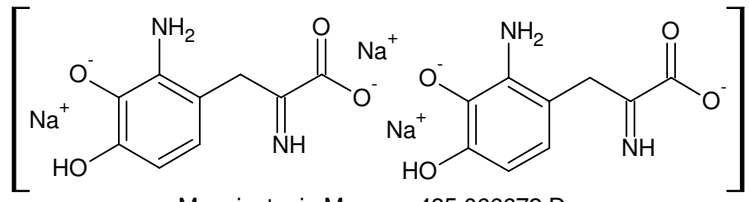

Monoisotopic Mass = 485.066672 Da

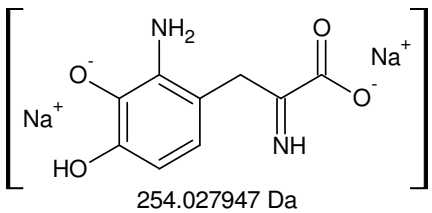

254.027947 Da

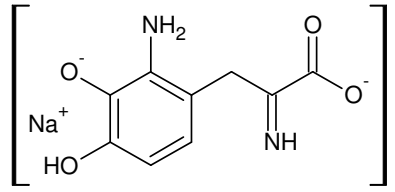

Monoisotopic Mass = 231.038725 Da

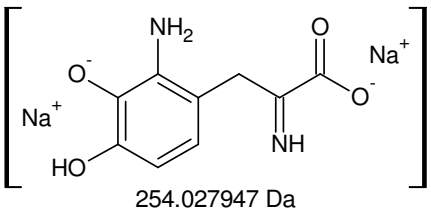

254.027947 Da

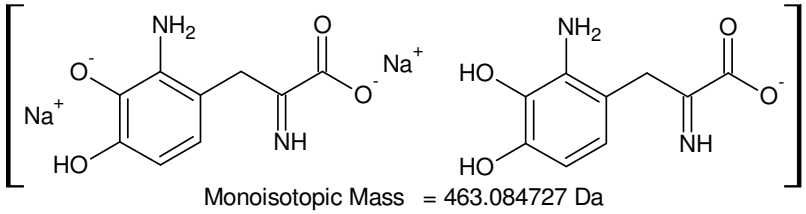

Monoisotopic Mass = 463.084727 Da

-MSn [OPA-Val 2,9 min]: 971 -> 739 -> 485 -> 231 and -463 Th

XIII.III.VII. OPA-Ile 10,4 min decomposed

The signal was not stable in the presence of methanol.

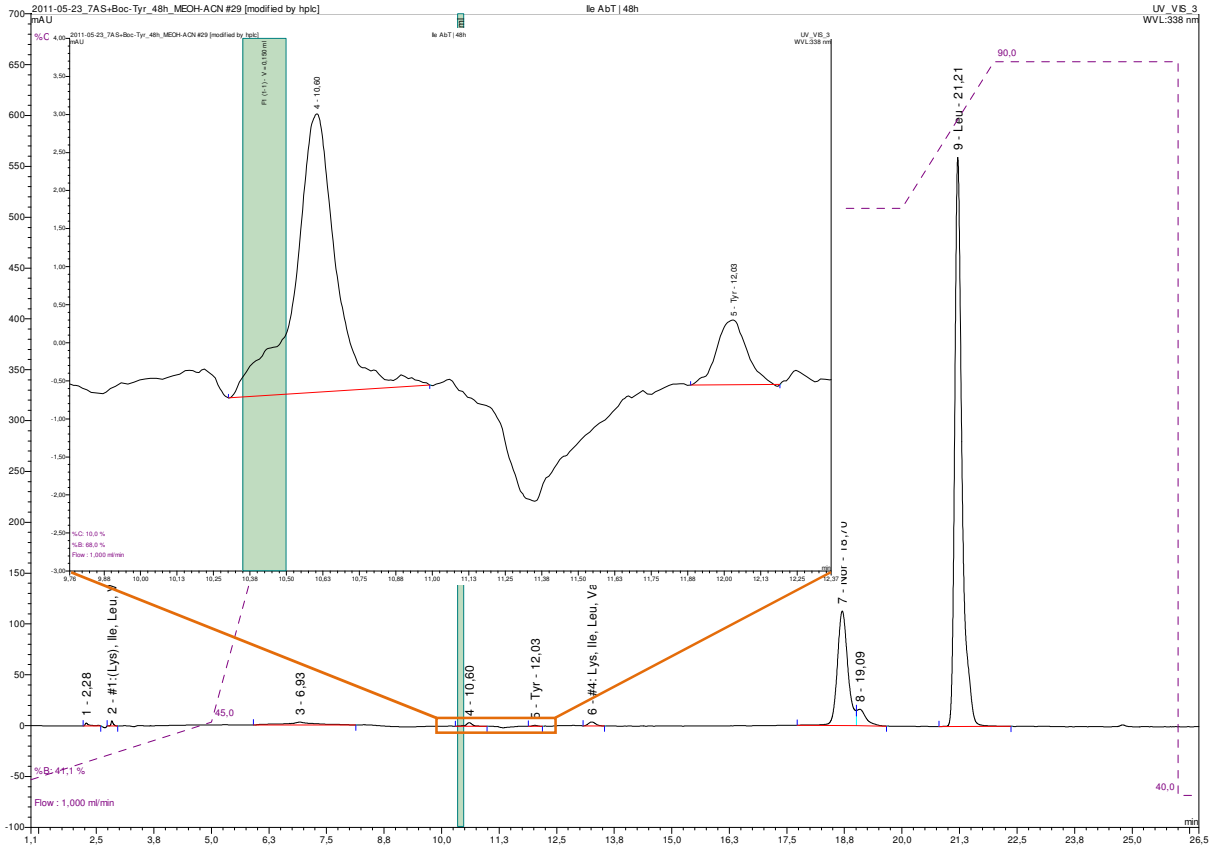

Figure XIII-LXII Ile AbT | 48h; derivatised with OPA (amino acid solution 30 h with 50 % (v+v) methanol @ 25°C)

+MS^n

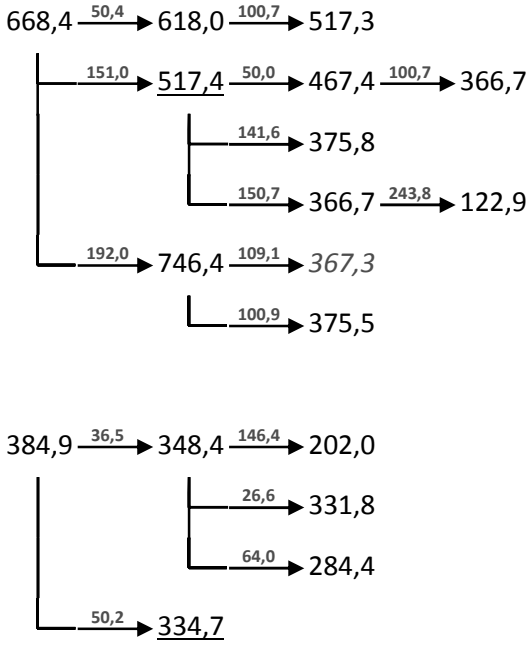

-MS^n

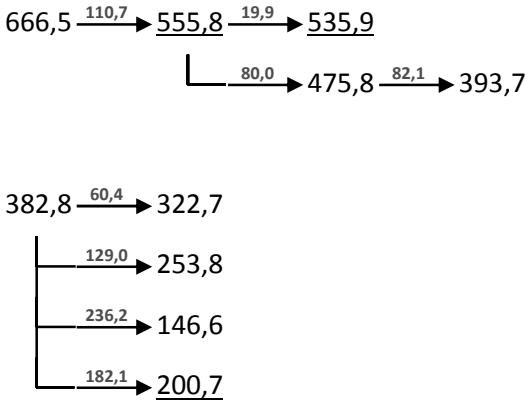

isotopic fingerprint:

peak area / % of monoisotopic	**+1**	**+2**	**+3**
measured (668,5 Th):	18,5	13,3	12,8
measured (-666,7 Th):	30,3	26,9	10,9
measured (384,8 Th):	44,6	13,9	6,9
measured (-382,8 Th):	19,5	-	-

Figure XIII-LXIII MS^n analysis of OPA-Ile 10,4 min decomposed

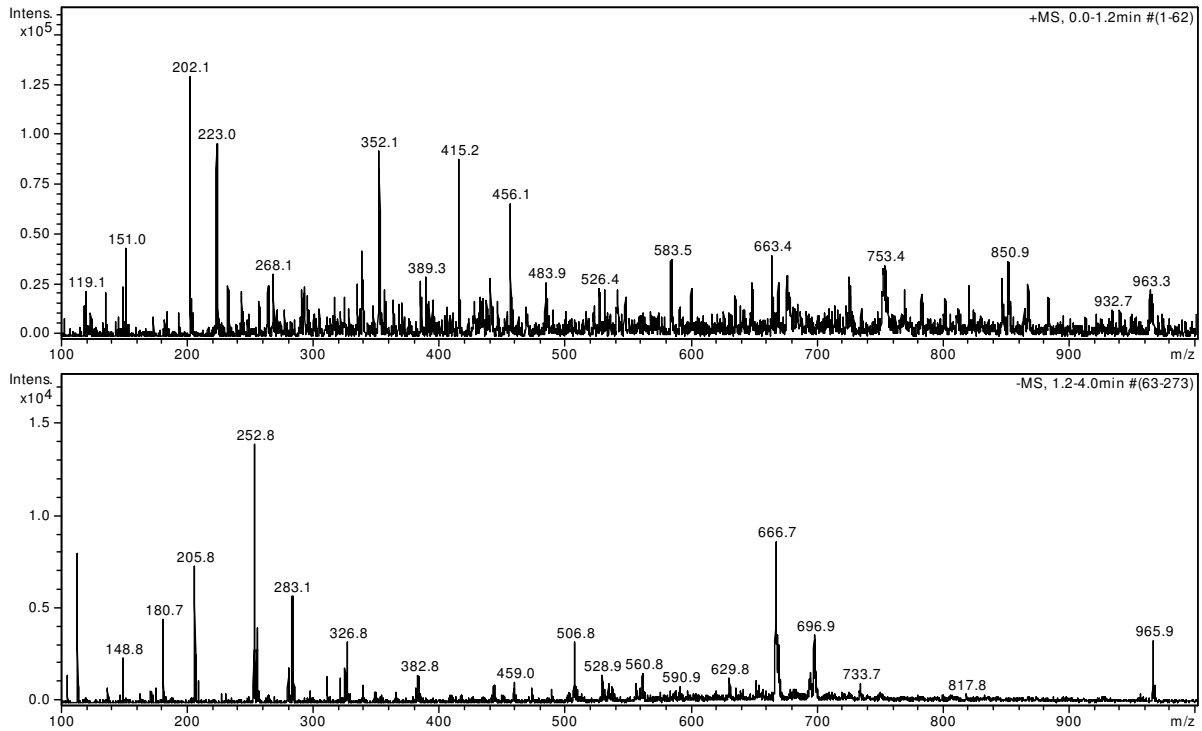

Figure XIII-LXIV OPA-Ile 10,4 min decomposed: 31 % MeOH, 31 % ACN, 1 ‰ FA in ddH_2O; full scan MS^1

XIII.III.VIII. OPA-Ile 10,4 min

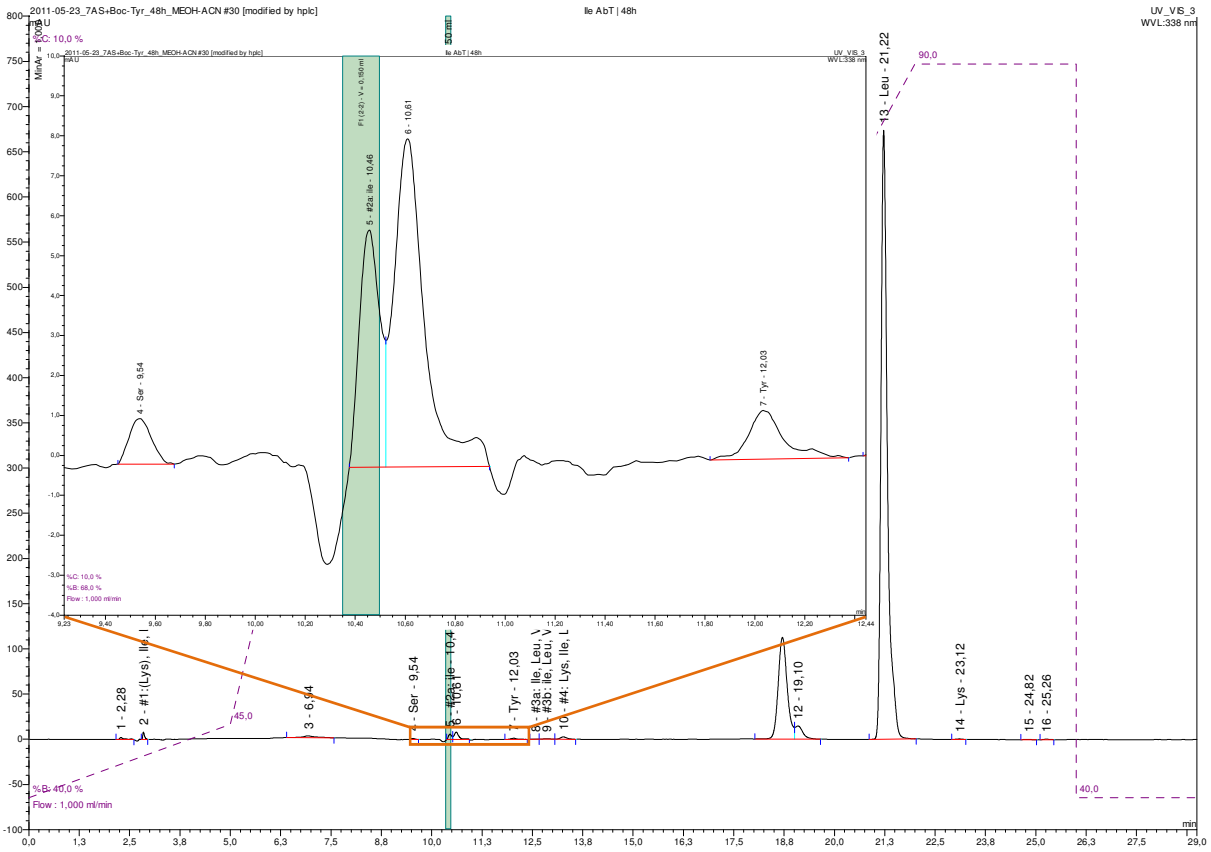

Figure XIII-LXV Ile AbT | 48h; derivatised with OPA (50 % (v+v) methanol added 15 min before the measurement)

+MS^n

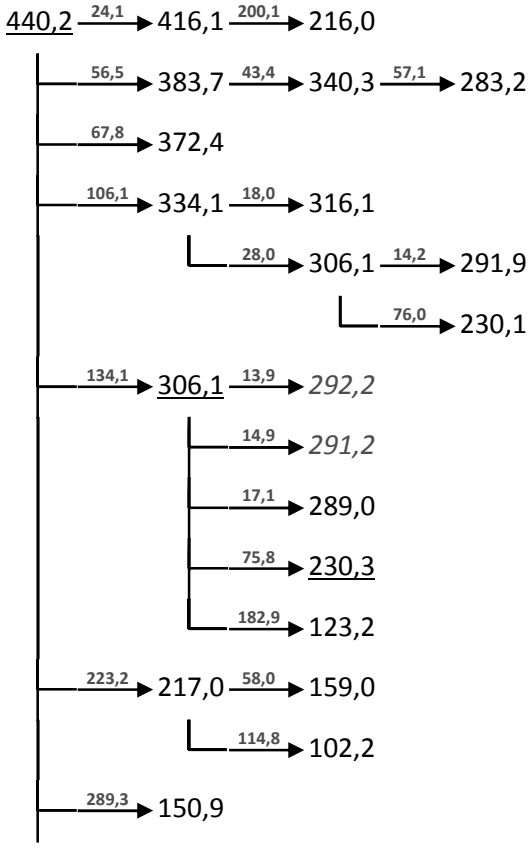

CDXC

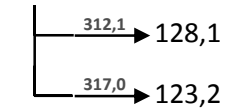

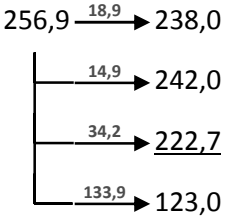

-MS^n

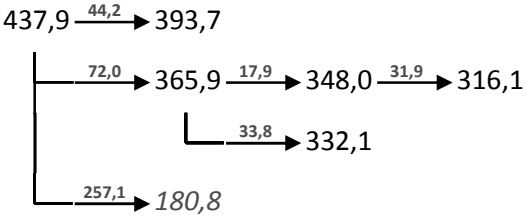

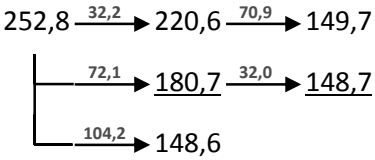

isotopic fingerprint:

peak area / % of monoisotopic	**+1**	**+2**	**+3**
theoretical ($C_{23}H_{22}NO_6S^+$):	26,6	9,2	1,8
measured (440,2 Th):	36,8	23,4	7,2
measured (-437,9 Th):	56,5	29,4	-
measured (256,8 Th):	14,9	13,4	2,2
measured (-255,0 Th):	18,0	0,7	-

Figure XIII-LXVI MS^n analysis of OPA-Ile 10,4 min

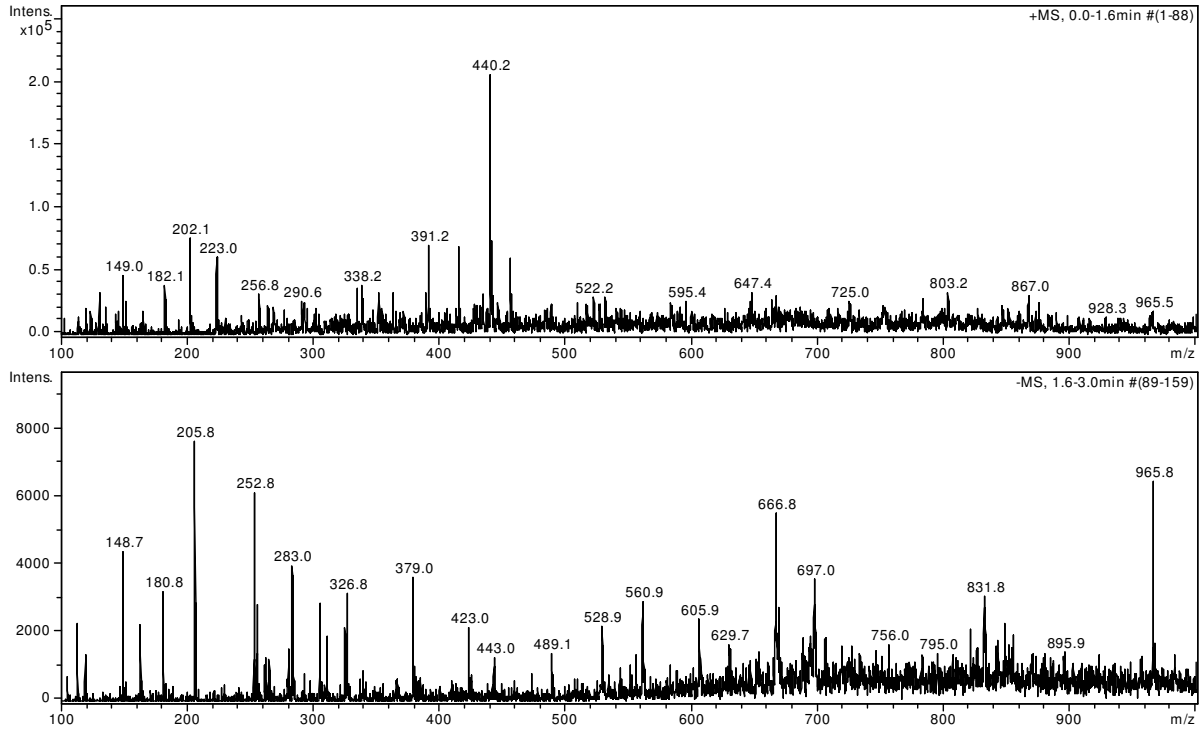

Figure XIII-LXVII OPA-Ile 10,4 min: 10 % MeOH, 89 % ACN, 0,3̇ ‰ FA in ddH_2O (diluted 1:3 with ACN); full scan MS^1

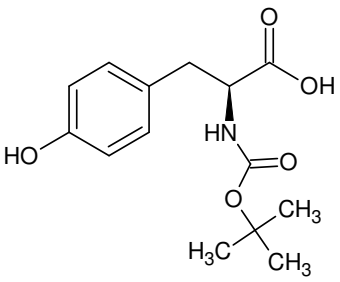

L-Boc-Tyr-OH
Monoisotopic Mass = 281.13 Da

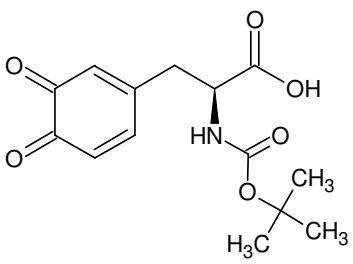

L-Boc-Dopachinon
Monoisotopic Mass = 295.11 Da

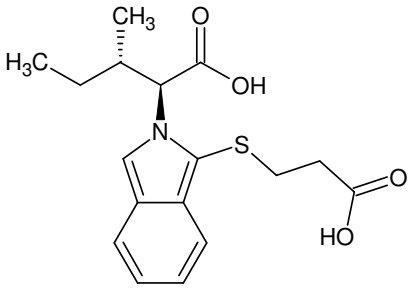

OPA-Ile
Monoisotopic Mass = 335.12 Da

Das Signal (RP-HPLC, 10,4 min @ 338 nm) tritt **nur bei mit AbT behandeltem (Iso)leucin** auf.

Das Produkt ist in Anwesenheit von MeOH nicht stabil.

{kein Signal @ 228 nm (sehr gering) => eher kein Isoindol
Signal @ 338 nm vorhanden => **Chinon?**}

Aber: Neutralverluste 106 Da (+MS) bzw. 72 Da (-MS) => **3-Mercaptopropionsäure**
keine Markerfragmente von Boc (56 Da und 100 Da in +MS, 74 Da in -MS)

Die Ionisierung im positiven Modus liefert ein brauchbares Signal, im negativen Modus zeigt sich nur Rauschen.

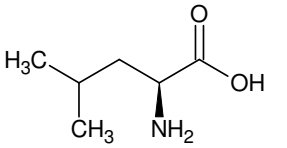

Leu

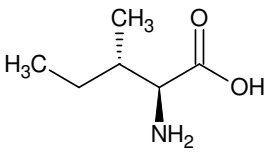

Ile

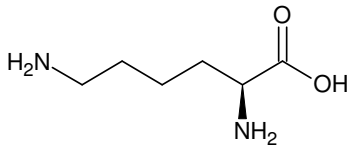

Lys

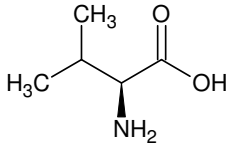

Val

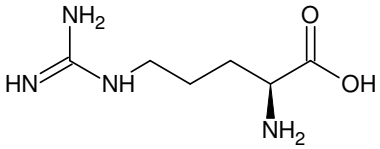

Arg

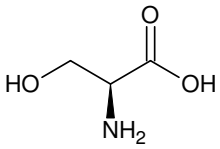

Ser

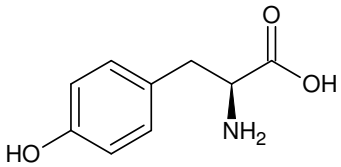

Tyr

439 Da [OPA-Ile 10,4 min] {I/III}

439 - 335 = **104**
Gefundene Verbindungen: 163
CH2N3OS MG=103,9918582
CH2N3O3 MG=104,0096162
(...)
N4OS MG=103,979283
N4O3 MG=103,997041

-----D--B--E--f-i-l-t-e-r-----
31.05.2011 - 17:07:10,42
akzeptierte DBEs:
1 2 3 4 5 6

CH4N4O2	DBE: 2
CH4N4S	DBE: 2
CH8N6	DBE: 1
CN2O2S	DBE: 3
CN2O4	DBE: 3
CN2S2	DBE: 3
C2H4N2OS	DBE: 2
C2H4N2O3	DBE: 2
C2H8N4O	DBE: 1
C2OS2	DBE: 3
C2O3S	DBE: 3
C2O5	DBE: 3
C3H4O2S	DBE: 2
C3H4O4	DBE: 2
C3H4S2	DBE: 2
C3H8N2O2	DBE: 1
C3H8N2S	DBE: 1
C4H8OS	DBE: 1
C4H8O3	DBE: 1
C6H4N2	DBE: 6
C7H4O	DBE: 6
C8H8	DBE: 5
H4N6O	DBE: 2
N4OS	DBE: 3
N4O3	DBE: 3

25 von 163 Summenformeln

439-295 = **144**
Gefundene Verbindungen: 459
CH2N7O2 MG=144,0269972
CH2N7S MG=144,0092392
(...)
O7S MG=143,936477
O9 MG=143,954235

-----D--B--E--f-i-l-t-e-r-----
01.06.2011 - 15:55:17,01
akzeptierte DBEs:
1 2 3 4 5 6

CH4N8O	DBE: 4
CN6OS	DBE: 5
CN6O3	DBE: 5
C2H4N6O2	DBE: 4
C2H4N6S	DBE: 4
C2H8N8	DBE: 3
C2N4O2S	DBE: 5
C2N4O4	DBE: 5
C2N4S2	DBE: 5
C3H4N4OS	DBE: 4
C3H4N4O3	DBE: 4
C3H8N6O	DBE: 3
C3N2OS2	DBE: 5
C3N2O3S	DBE: 5
C3N2O5	DBE: 5
C4H4N2O2S	DBE: 4
C4H4N2O4	DBE: 4
C4H4N2S2	DBE: 4
C4H8N4O2	DBE: 3
C4H8N4S	DBE: 3
C4H12N6	DBE: 2
C4O2S2	DBE: 5
C4O4S	DBE: 5
C4O6	DBE: 5
C4S3	DBE: 5
C5H4OS2	DBE: 4
C5H4O3S	DBE: 4
C5H4O5	DBE: 4
C5H8N2OS	DBE: 3
C5H8N2O3	DBE: 3
C5H12N4O	DBE: 2
C6H8O2S	DBE: 3
C6H8O4	DBE: 3
C6H8S2	DBE: 3
C6H12N2O2	DBE: 2
C6H12N2S	DBE: 2
C6H16N4	DBE: 1
C7H12OS	DBE: 2
C7H12O3	DBE: 2
C7H16N2O	DBE: 1
C8H16O2	DBE: 1
C8H16S	DBE: 1
C11H12	DBE: 6
H4N10	DBE: 4
N8O2	DBE: 5
N8S	DBE: 5
OS4	DBE: 1
O3S3	DBE: 1
O5S2	DBE: 1
O7S	DBE: 1
O9	DBE: 1

51 von 459 Summenformeln

439 - 295 = **144** (ohneS)
Gefundene Verbindungen: 234
CH2N7O2 MG=144,0269972
CH4N8O MG=144,0508054
(...)
N8O2 MG=144,014422
O9 MG=143,954235

-----D--B--E--f-i-l-t-e-r-----
01.06.2011 - 16:09:14,26
akzeptierte DBEs:
1
2
3
4
5
6

CH4N8O	DBE: 4
CN6O3	DBE: 5
C2H4N6O2	DBE: 4
C2H8N8	DBE: 3
C2N4O4	DBE: 5
C3H4N4O3	DBE: 4
C3H8N6O	DBE: 3
C3N2O5	DBE: 5
C4H4N2O4	DBE: 4
C4H8N4O2	DBE: 3
C4H12N6	DBE: 2
C4O6	DBE: 5
C5H4O5	DBE: 4
C5H8N2O3	DBE: 3
C5H12N4O	DBE: 2
C6H8O4	DBE: 3
C6H12N2O2	DBE: 2
C6H16N4	DBE: 1
C7H12O3	DBE: 2
C7H16N2O	DBE: 1
C8H16O2	DBE: 1
C11H12	DBE: 6
H4N10	DBE: 4
N8O2	DBE: 5
O9	DBE: 1

25 von 234 Summenformeln

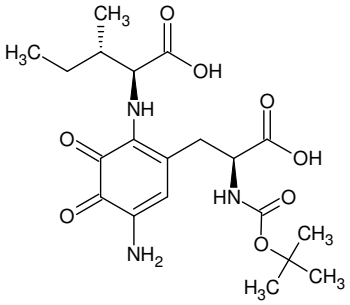

Monoisotopic Mass = 439.195465 Da

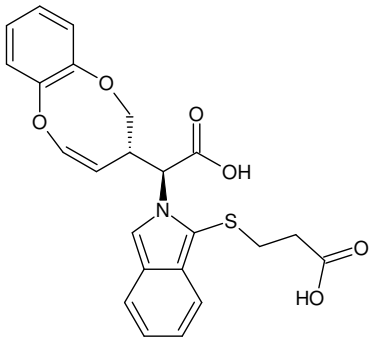

Monoisotopic Mass = 439.108957 Da

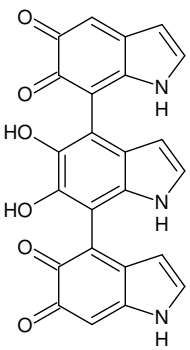

Monoisotopic Mass = 439.080435 Da

439 Da [OPA-Ile 10,4 min] {II/III}

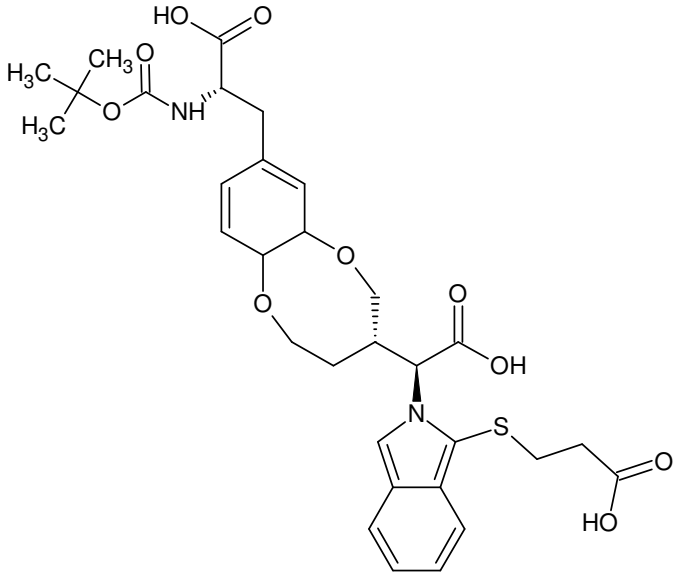

Monoisotopic Mass = 630.224715 Da

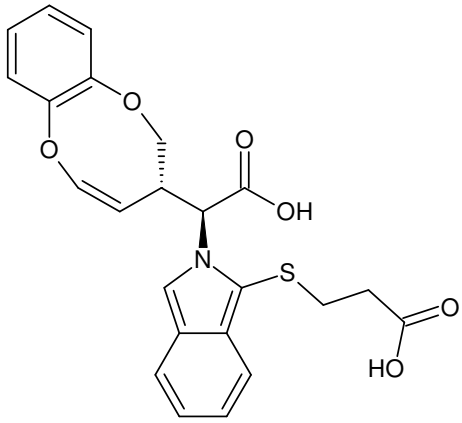

Monoisotopic Mass = 439.108957 Da

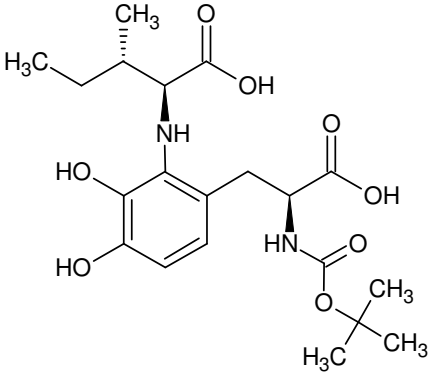

Monoisotopic Mass = 426.200216 Da

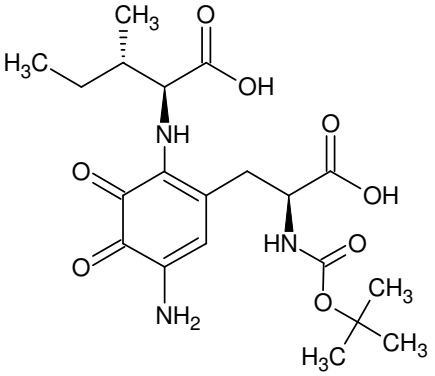

Monoisotopic Mass = 439.195465 Da

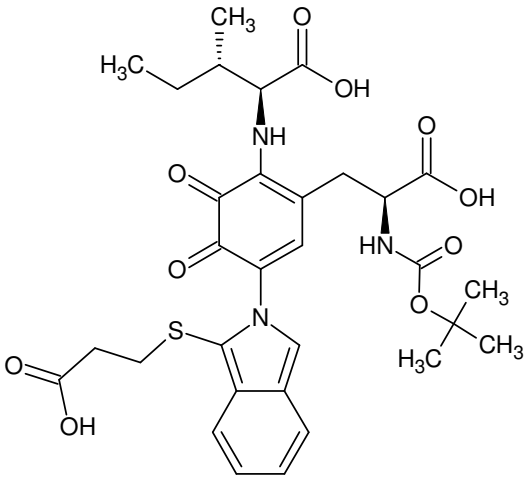

Monoisotopic Mass = 643.219964 Da

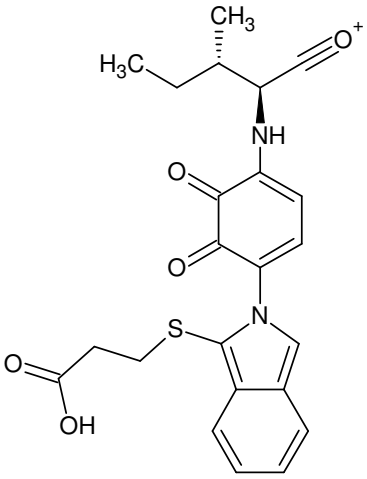

Monoisotopic Mass = 439.132218 Da

439 Da [OPA-Ile 10,4 min] {III/III}

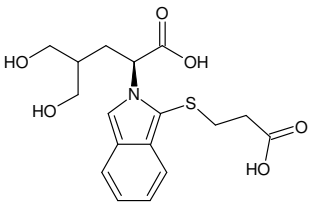

BoT#8
Monoisotopic Mass = 367.108957 Da

439 - 367 = **72**
Gefundene Verbindungen: 55
CH2N3O MG=72,0197862
CH4N4 MG=72,0435944
(...)
H30N3 MG=72,24396
N4O MG=72,007211

-----D--B--E--f-i-l-t-e-r-----
10.08.2011 - 14:04:54,13
akzeptierte DBEs:
0 1 2 3 4 5 6 7 8

CH_4N_4	DBE: 2
CN_2O_2	DBE: 3
CN_2S	DBE: 3
$C_2H_4N_2O$	DBE: 2
C_2OS	DBE: 3
C_2O_3	DBE: 3
$C_3H_4O_2$	DBE: 2
C_3H_4S	DBE: 2
$C_3H_8N_2$	DBE: 1
C_4H_8O	DBE: 1
C_5H_{12}	DBE: 0
C_6	DBE: 7
N_4O	DBE: 3

13 von 55 Summenformeln

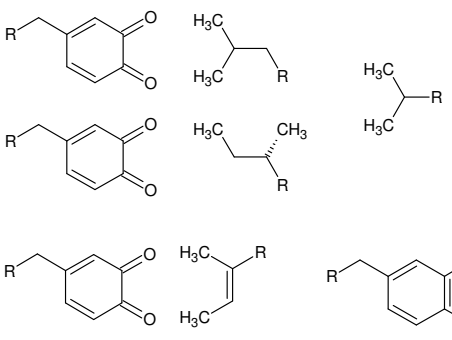

Unterschied Ile, Leu - Val:
zusätzliche Methylengruppe
=> DB?
Laut SEQC (Mopac2009, PM6)
kann das Chinon den
verzweigten Aliphaten reduzieren
(unter Bildung eines Diradikals).

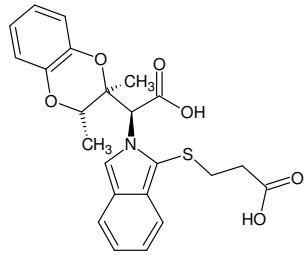

Monoisotopic Mass = 441.124607 Da

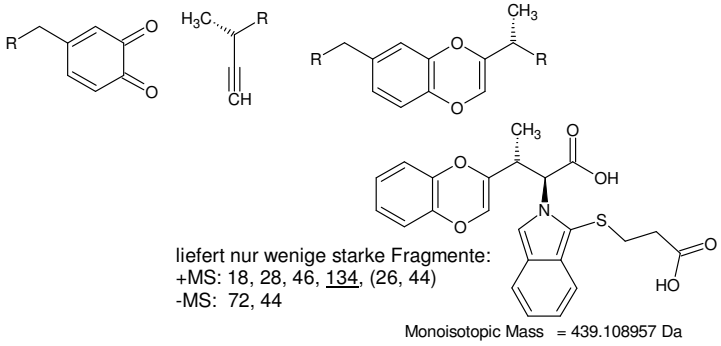

liefert nur wenige starke Fragmente:
+MS: 18, 28, 46, 134, (26, 44)
-MS: 72, 44

Monoisotopic Mass = 439.108957 Da

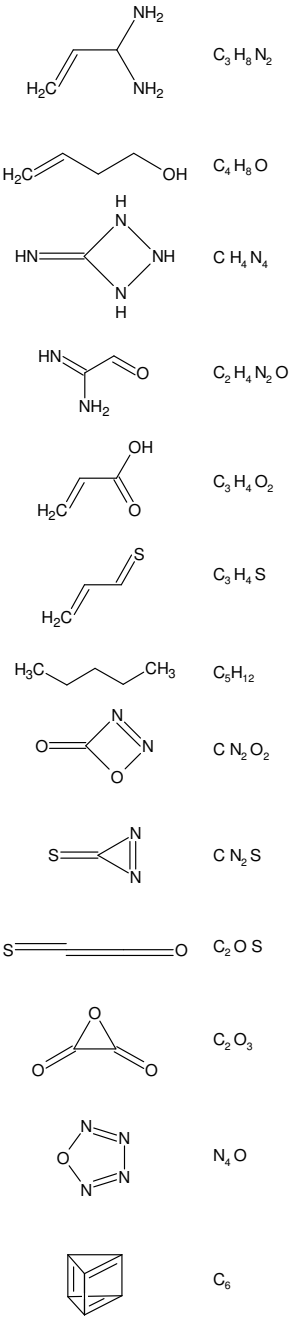

439 Da [OPA-Ile 10,4 min]: Fragment 72 Da

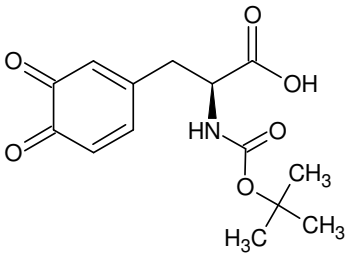

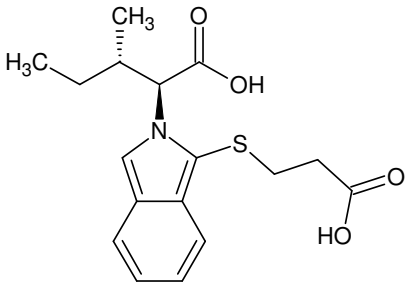

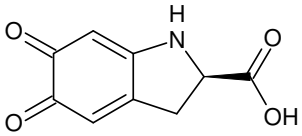

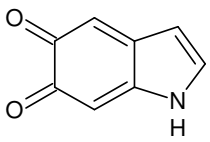

Indol-5,6-chinon

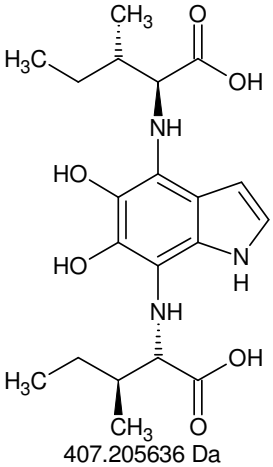

407.205636 Da

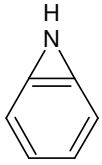

91.042199 Da

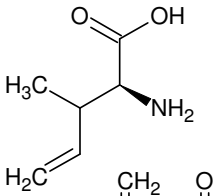

NH_3 H_2 H_2

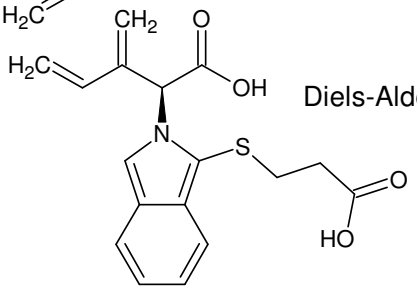

Diels-Alder

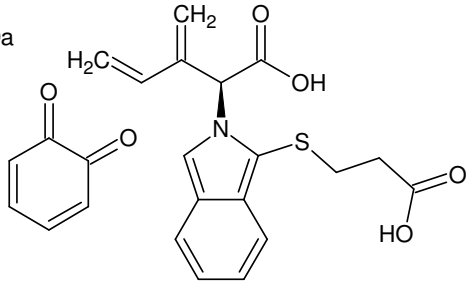

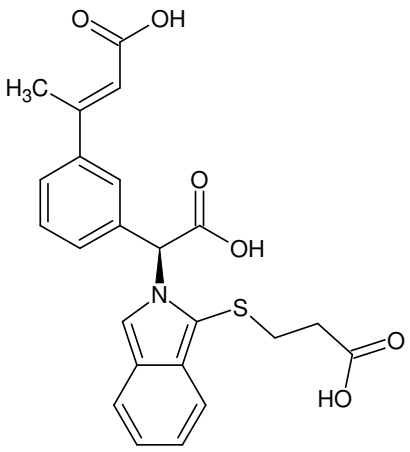

Monoisotopic Mass = 439.108957 Da

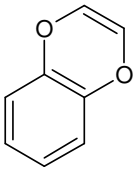

134.036779 Da

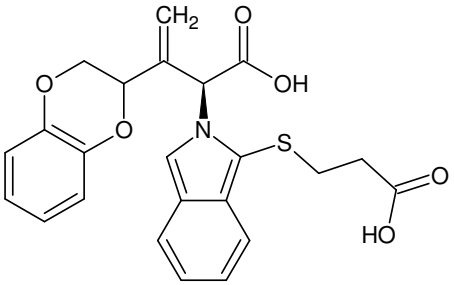

Monoisotopic Mass = 439.108957 Da

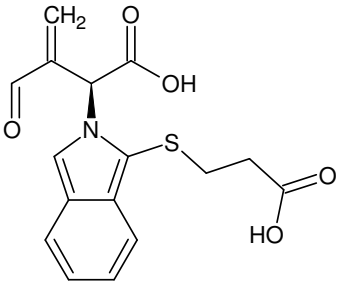

Monoisotopic Mass = 333.067093 Da

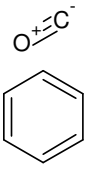

106.041865 Da

CH_2:
14.01565 Da

439 Da [OPA-Ile 10,4 min]

230 Th finden sich (nur) im Fragmentationsbaum von **OPA-Arg** und von 599 Th in Probe **F6**.

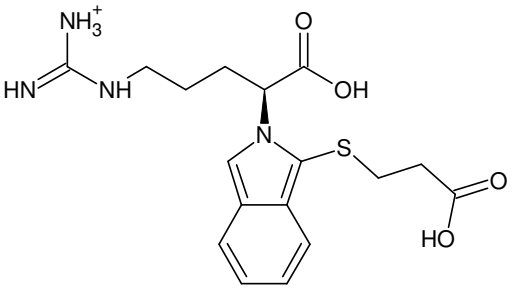

OPA-Arg: $[M+H]^+$

Monoisotopic Mass = 379.143452 Da

OPA-Arg

+MS^n:

379,1 -> <u>335,1</u> -> 282,1 -> (245,6)
-> 230,1 -> 114,1
-> 263,1
-> 247,1
-> <u>231,1</u>
-> 229,1
-> 187,0
-> 112,1
-> 273,1
-> 231,1
-> 229,1

-MS^n:

376,9 -> 332,8
-> 304,8 -> 260,7 -> 243,7 -> 201,6
-> 147,6
-> 218,7 -> 147,6
-> 147,6
-> <u>260,8</u>
-> 218,7
-> 147,7

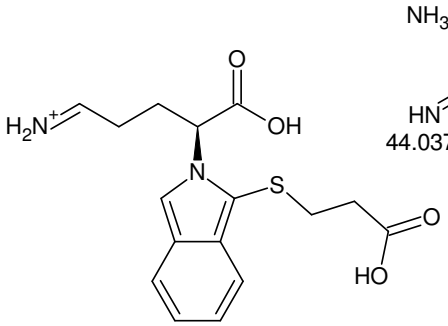

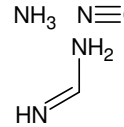

44.037448 Da

Monoisotopic Mass = 335.106003 Da

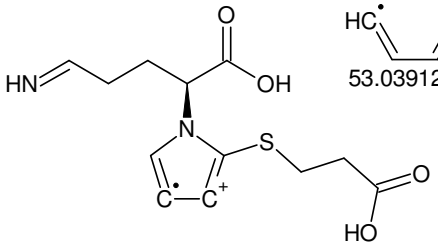

53.039125 Da

Monoisotopic Mass = 282.066878 Da

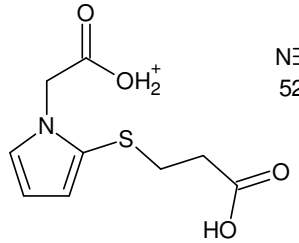

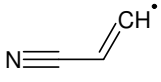

52.018724 Da

Monoisotopic Mass = 230.048154 Da

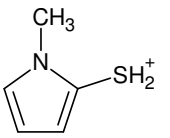

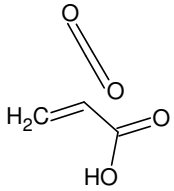

116.010959 Da

Monoisotopic Mass = 114.037196 Da

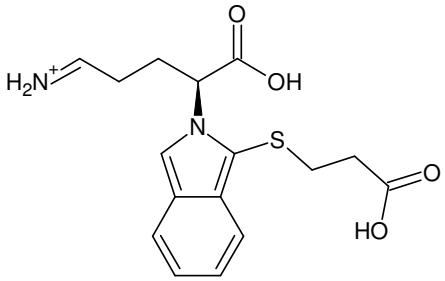

Monoisotopic Mass = 335.106003 Da

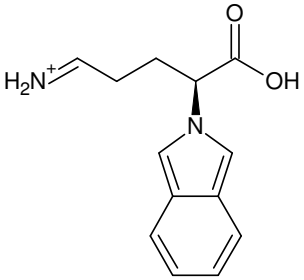

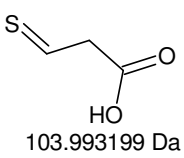

103.993199 Da

Monoisotopic Mass = 231.112804 Da

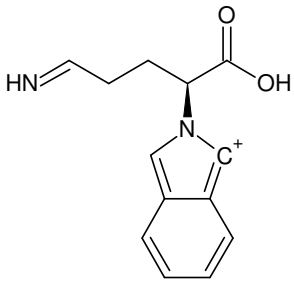

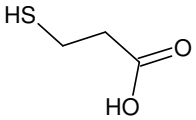

106.008849 Da

Monoisotopic Mass = 229.097154 Da

230 Th [OPA-Ile 10,4 min]: OPA-Arg 379 -> 335 -> 282 -> 231 -> 114 and 335 -> 231, 229

-MS^n

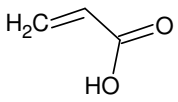

72.021129 Da

+MS^n

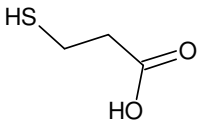

106.008849 Da

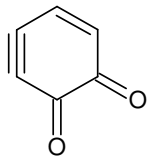

H_2O

18.010565 Da

=> aliphatische Hydroxygruppe?

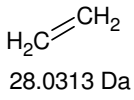

28.0313 Da

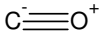

H_2O

18.010565 Da

S:

31.97207 Da

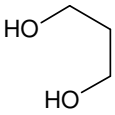

76.052429 Da

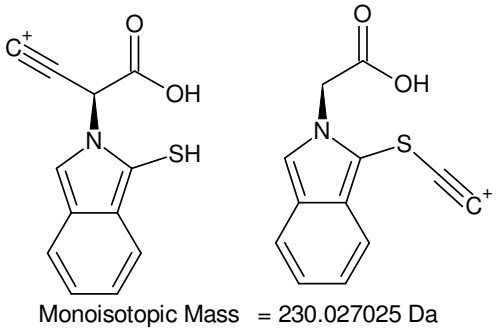

Monoisotopic Mass = 230.027025 Da

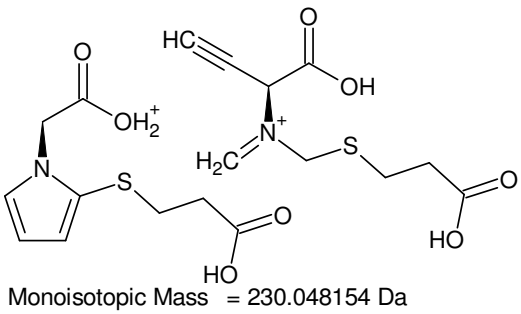

Monoisotopic Mass = 230.048154 Da

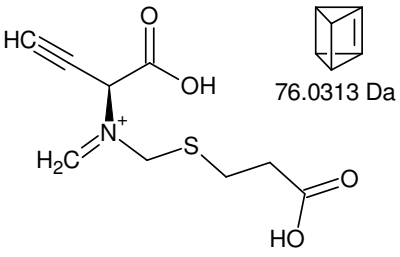

76.0313 Da

Monoisotopic Mass = 230.048154 Da

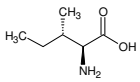

28.0313 Da

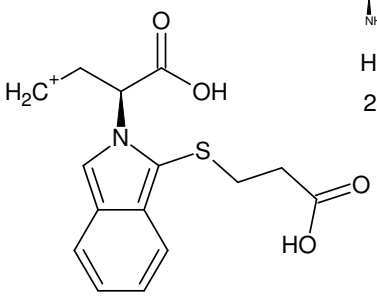

Monoisotopic Mass = 306.079454 Da

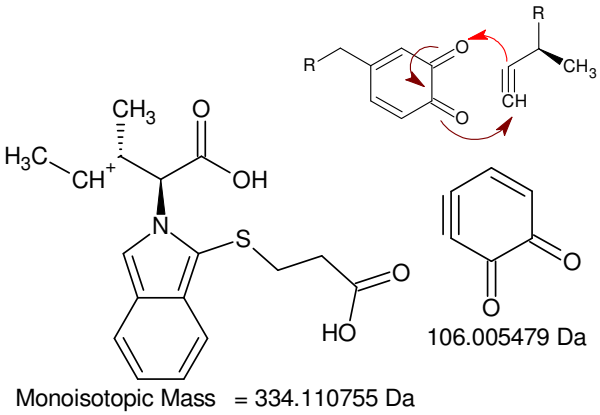

106.005479 Da

Monoisotopic Mass = 334.110755 Da

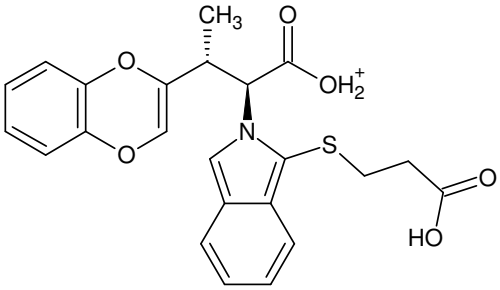

Monoisotopic Mass = 440.116234 Da

+MSn [OPA-Ile 10,4 min]: 230 <- 306 <- 334 <- 440 {I/II}

76 Da +/- 0,5 Da:
Gefundene Verbindungen: 47
CH2NO3 MG=76,0034682
CH4N2O2 MG=76,0272764
(...)
H34N3 MG=76,2752584
N2O3 MG=75,990893

-----D--B--E--f-i-l-t-e-r-----
10.08.2011 - 17:29:01,89
akzeptierte DBEs:
-1 0 1 2 3 4 5 6 7 8

$CH_4N_2O_2$ DBE: 1
CH_8N_4 DBE: 0
CO_4 DBE: 2
$C_2H_4O_3$ DBE: 1
$C_2H_8N_2O$ DBE: 0
$C_3H_8O_2$ DBE: 0
$C_3H_{12}N_2$ DBE: -1
$C_4H_{12}O$ DBE: -1
C_4N_2 DBE: 6
C_5O DBE: 6
C_6H_4 DBE: 5
H_4N_4O DBE: 1
N_2O_3 DBE: 2

13 von 47 Summenformeln

440,2 - 334,1 = **106,1**
Gefundene Verbindungen: 106
CH2N2O4 MG=106,0014572
CH4N3O3 MG=106,0252654
(...)
H50N4 MG=106,403526
N3O4 MG=105,988882

-----D--B--E--f-i-l-t-e-r-----
11.08.2011 - 12:03:06,01
akzeptierte DBEs:
-2 -1 0 1 2 3 4 5 6 7 8

$CH_2N_2O_4$ DBE: 2
$CH_6N_4O_2$ DBE: 1
$CH_{10}N_6$ DBE: 0
$C_2H_2O_5$ DBE: 2
$C_2H_6N_2O_3$ DBE: 1
$C_2H_{10}N_4O$ DBE: 0
$C_3H_6O_4$ DBE: 1
$C_3H_{10}N_2O_2$ DBE: 0
$C_3H_{14}N_4$ DBE: -1
$C_4H_2N_4$ DBE: 6
$C_4H_{10}O_3$ DBE: 0
$C_4H_{14}N_2O$ DBE: -1
$C_5H_2N_2O$ DBE: 6
$C_5H_{14}O_2$ DBE: -1
$C_5H_{18}N_2$ DBE: -2
$C_6H_2O_2$ DBE: 6
$C_6H_6N_2$ DBE: 5
$C_6H_{18}O$ DBE: -2
C_7H_6O DBE: 5
C_8H_{10} DBE: 4
$H_2N_4O_3$ DBE: 2
H_6N_6O DBE: 1

22 von 106 Summenformeln

ohne N:
-----D--B--E--f-i-l-t-e-r-----
11.08.2011 - 12:26:52,46
akzeptierte DBEs:
-2 -1 0 1 2 3 4 5 6 7 8

$C_2H_2O_5$ DBE: 2
$C_3H_6O_4$ DBE: 1
$C_4H_{10}O_3$ DBE: 0
$C_5H_{14}O_2$ DBE: -1
$C_6H_2O_2$ DBE: 6
$C_6H_{18}O$ DBE: -2
C_7H_6O DBE: 5
C_8H_{10} DBE: 4

8 von 26 Summenformeln

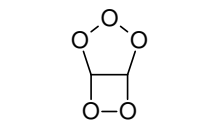

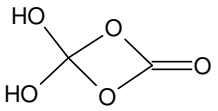

$C_2H_2O_5$
105.990223 Da

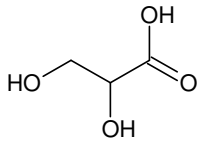

$C_3H_6O_4$
106.026609 Da

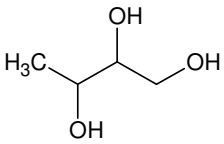

$C_4H_{10}O_3$
106.062994 Da

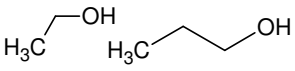

$C_5H_{14}O_2$
106.09938 Da

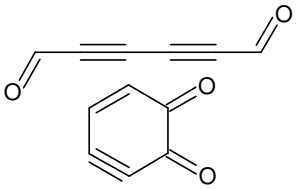

$C_6H_2O_2$
106.005479 Da

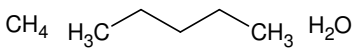

$C_6H_{18}O$
106.135765 Da

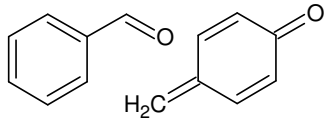

C_7H_6O
106.041865 Da

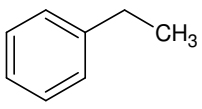

C_8H_{10}
106.07825 Da

+MSn [OPA-Ile 10,4 min]: 230 <- 306 <- 334 <- 440 {II/II}

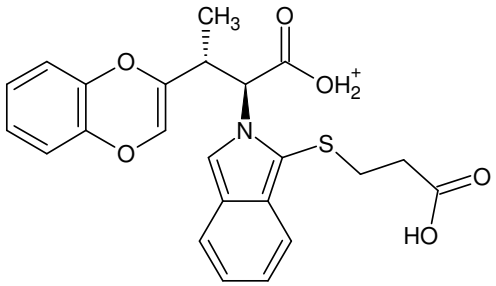

Monoisotopic Mass = 440.116234 Da

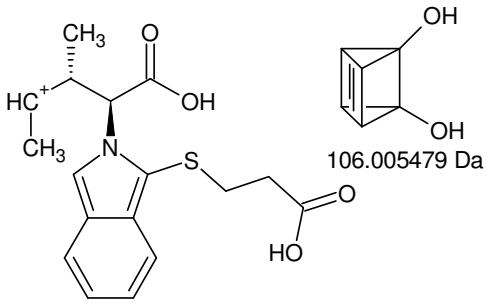

106.005479 Da

Monoisotopic Mass = 334.110755 Da

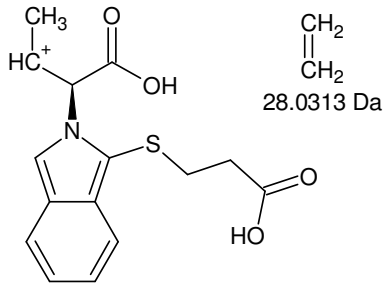

28.0313 Da

Monoisotopic Mass = 306.079454 Da

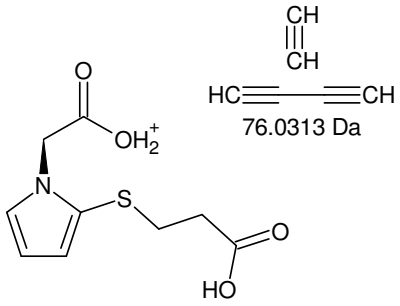

76.0313 Da

Monoisotopic Mass = 230.048154 Da

Die diesem Ast des Zerfallsbaumes zugeordnete Wahrscheinlichkeit ist bescheiden.:
306,2 Th: **81764** cnts; 384,0 Th: **222** cnts; {385,1 Th: 880 cnts}

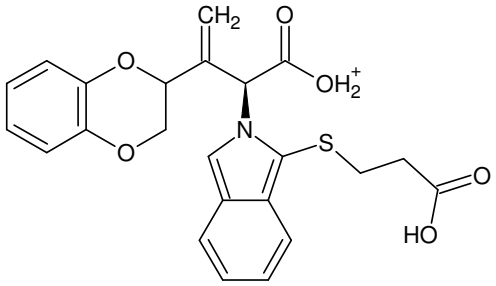

Monoisotopic Mass = 440.116234 Da

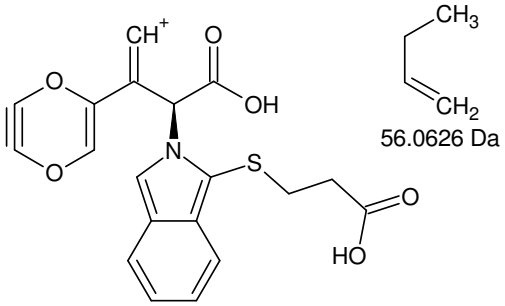

56.0626 Da

Monoisotopic Mass = 384.053634 Da

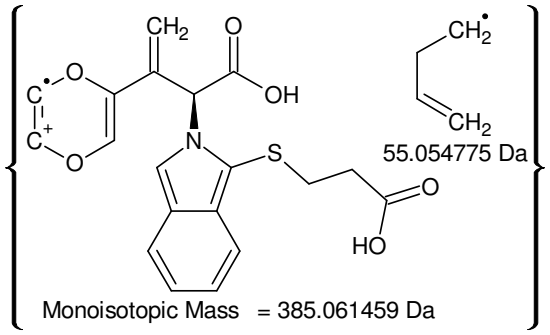

55.054775 Da

Monoisotopic Mass = 385.061459 Da

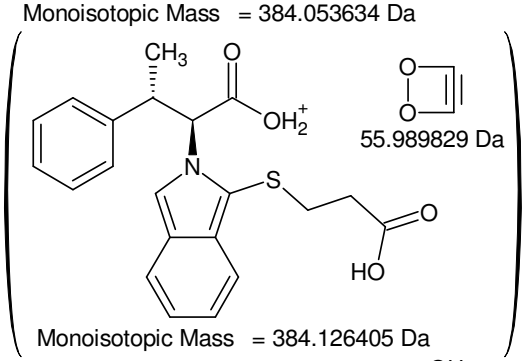

55.989829 Da

Monoisotopic Mass = 384.126405 Da

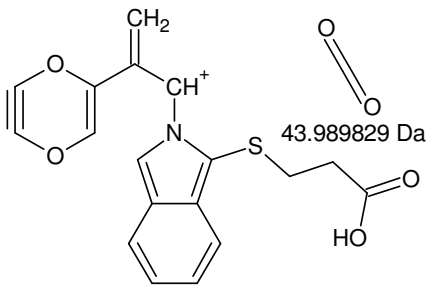

43.989829 Da

Monoisotopic Mass = 340.063804 Da

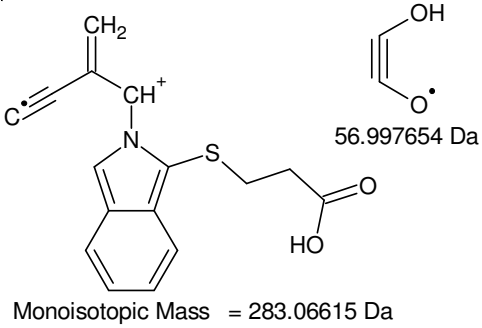

56.997654 Da

Monoisotopic Mass = 283.06615 Da

+MSn [OPA-Ile 10,4 min]: 440 -> 334 -> 306 -> 230 and 440 -> 384 -> 340 -> 283

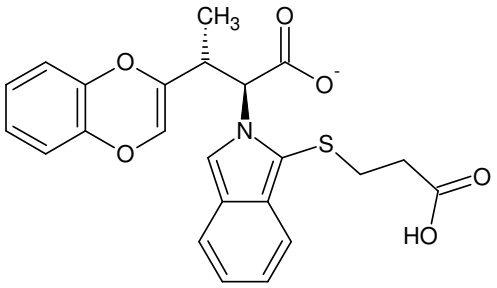

Monoisotopic Mass = 438.101681 Da

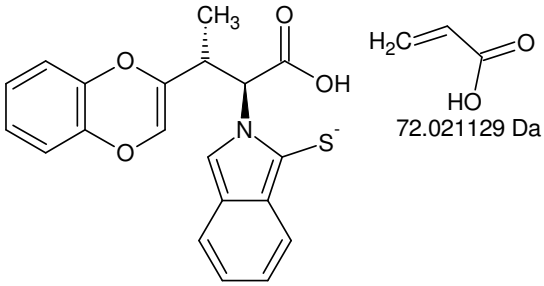

Monoisotopic Mass = 366.080552 Da

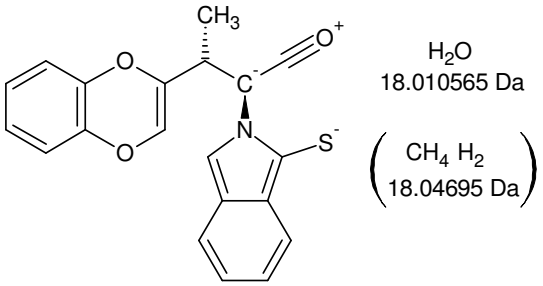

Monoisotopic Mass = 348.069987 Da

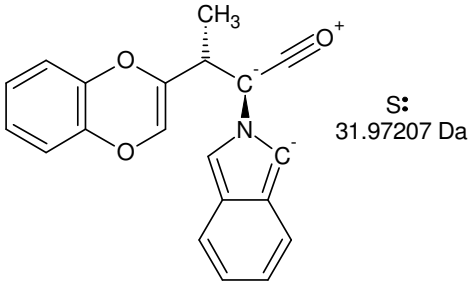

Monoisotopic Mass = 316.097917 Da

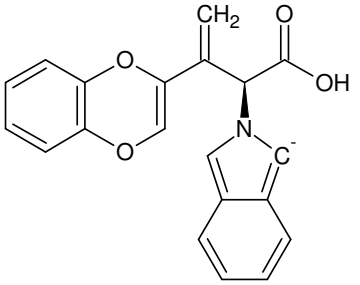

Monoisotopic Mass = 332.092832 Da

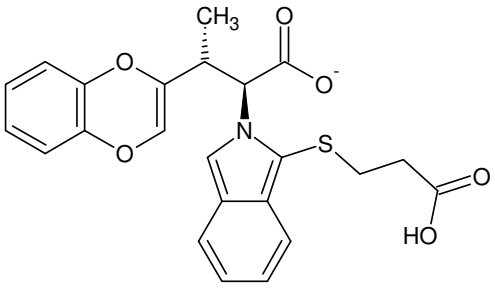

Monoisotopic Mass = 438.101681 Da

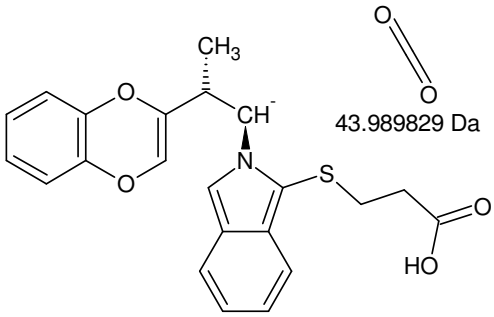

Monoisotopic Mass = 394.111852 Da

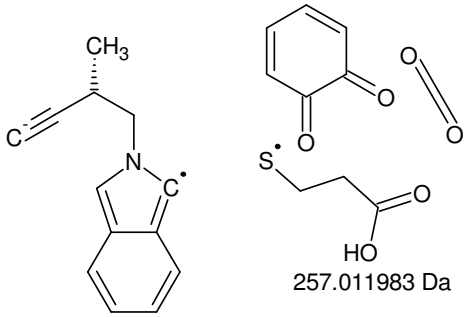

Monoisotopic Mass = 181.089698 Da

retro-Diels-Alder

-MSn [OPA-Ile 10,4 min]: 438 -> 366 -> 348 -> 316 and 438 -> 394, (181)

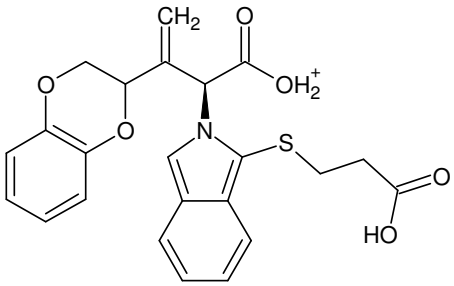

Monoisotopic Mass = 440.116234 Da

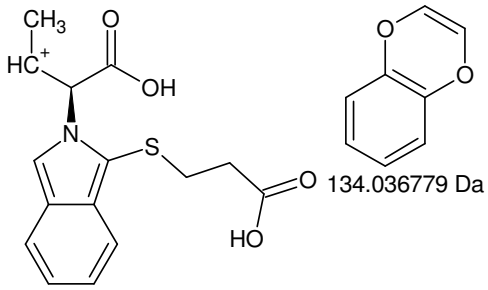

134.036779 Da

Monoisotopic Mass = 306.079454 Da

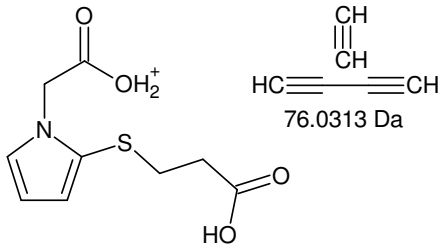

76.0313 Da

Monoisotopic Mass = 230.048154 Da

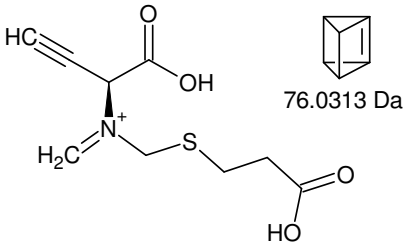

76.0313 Da

Monoisotopic Mass = 230.048154 Da

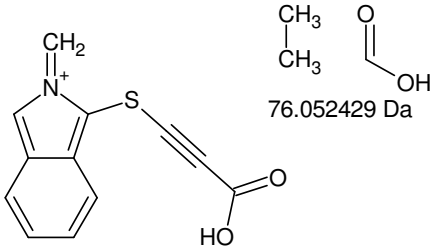

76.052429 Da

Monoisotopic Mass = 230.027025 Da

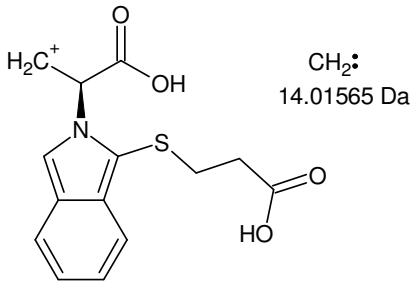

14.01565 Da

Monoisotopic Mass = 292.063804 Da

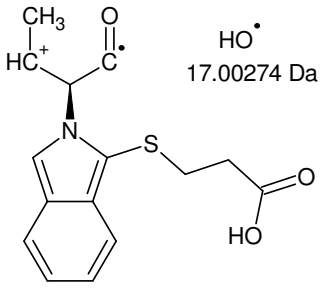

17.00274 Da

Monoisotopic Mass = 289.076715 Da

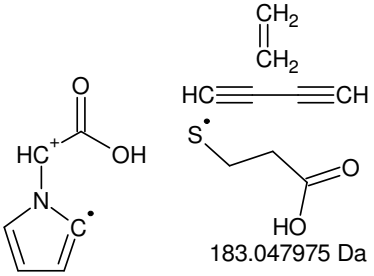

183.047975 Da

Monoisotopic Mass = 123.03148 Da

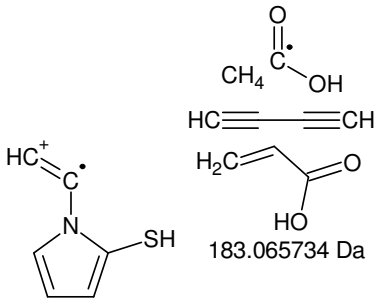

183.065734 Da

Monoisotopic Mass = 123.013721 Da

+MSn [OPA-Ile 10,4 min]: 440 -> 306 -> 230, 292, (289), 123

XIII.III.IX. **OPA-Ile 12,9 min**

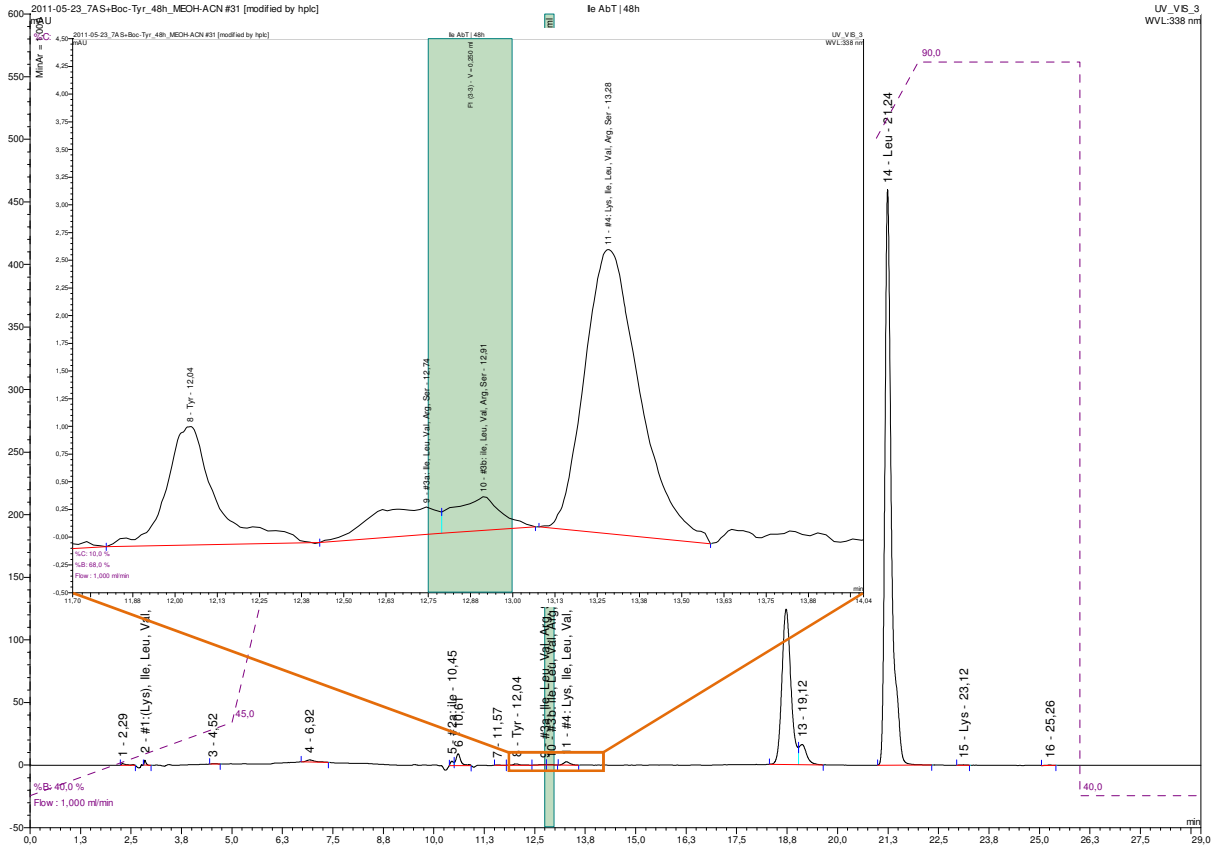

Figure XIII-LXVIII Ile AbT | 48h; derivatised with OPA (50 % (v+v) methanol added 75 min before the measurement)

+MS^n

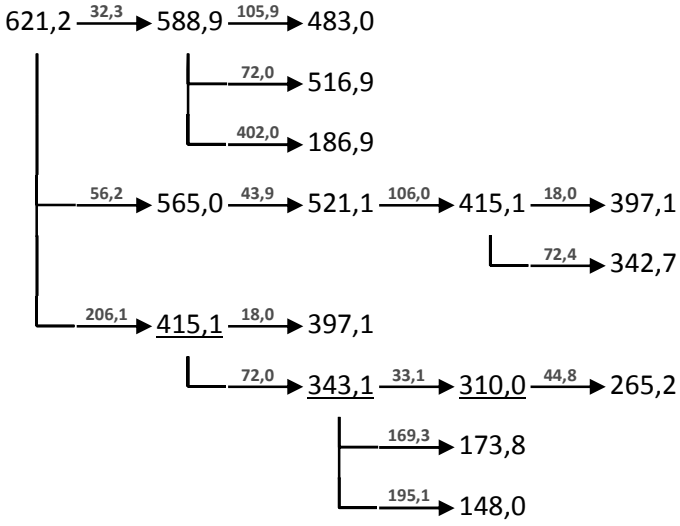

-MS^n

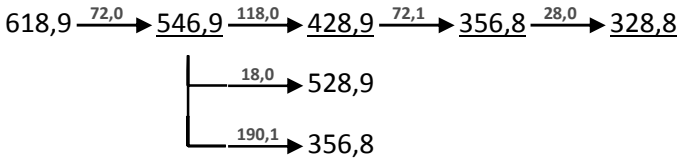

isotopic fingerprint:

peak area / % of monoisotopic	**+1**	**+2**	**+3**
theoretical ($C_{28}H_{33}N_2O_{10}S_2^+$):	33,5	16,5	4,2
measured (620,5 Th):	44,6	-	-
measured (-619,0 Th):	51,9	43,0	19,1

Figure XIII-LXIX MS^n analysis of OPA-Ile 12,9 min

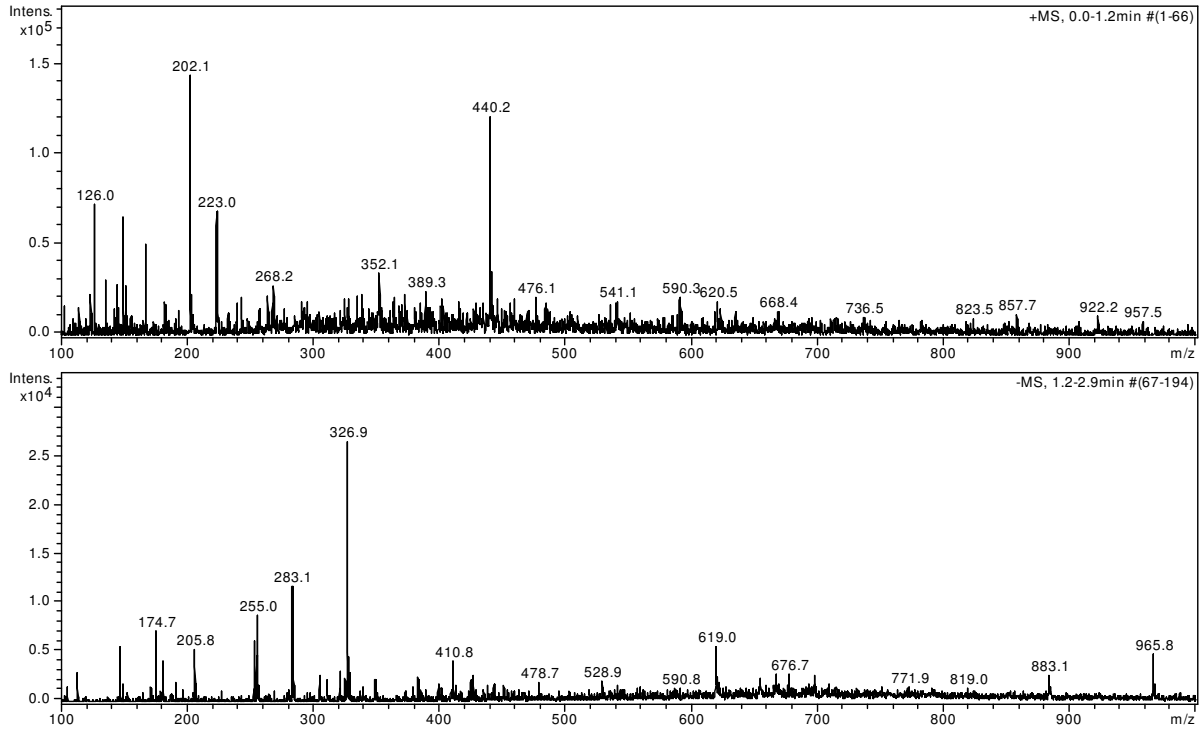

Figure XIII-LXX OPA-Ile 12,9 min: 31 % MeOH, 31 % ACN, 1 ‰ FA in ddH_2O; full scan MS^1

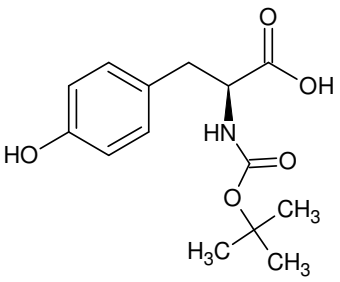

L-Boc-Tyr-OH
Monoisotopic Mass = 281.13 Da

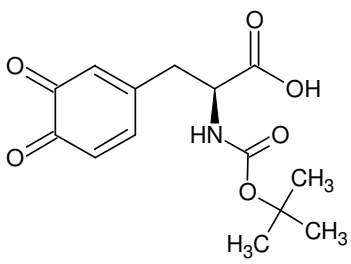

L-Boc-Dopachinon
Monoisotopic Mass = 295.11 Da

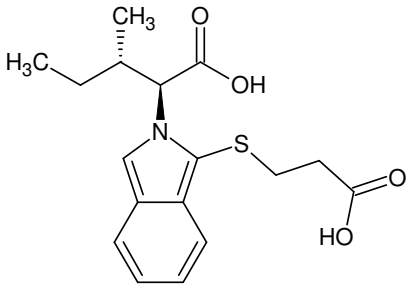

OPA-Ile
Monoisotopic Mass = 335.12 Da

Das zugehörige Signal (RP-HPLC, 12,9 min @ 338nm) tritt bei **Ile, Leu, Val, Arg und Ser** auf und ist im UVD eher bescheiden (0,35 mAU Signalhöhe; unmodifiziertes Ile: 460 mAU).

Die Ionisierung ist sowohl im positiven als auch im negativen Modus mäßig effizient, die Zielsignale (621 Th & - 619 Th) zählen zu den kleineren Signalen im Spektrum.

Aus der geraden nominellen Masse folgt eine **gerade Anzahl an N-Atomen**, was einen symmetrischen Aufbau des Moleküls zulässt.

In den Fragmentierungsbäumen finden sich sowohl die Markerfragmente für 3-Mercaptopropionsäure am Isoindolgerüst (+MS: 106 Da, -MS: 72 Da) als auch für Boc (+MS: 56 Da, -MS: (118: 74+44); 74 Da und 43 Da nicht beobachtet).

größtes gemeinsames Fragment (Ile, Leu, Val, Arg, Ser):

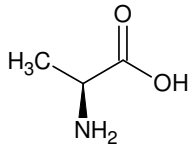

L-Alanine **(Ala)**

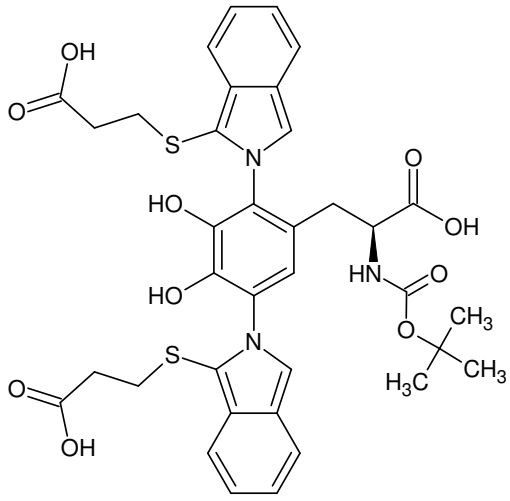

Monoisotopic Mass = 735.192034 Da

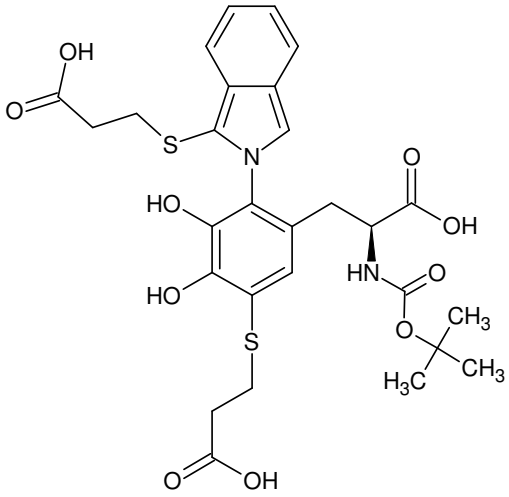

Monoisotopic Mass = 620.149835 Da

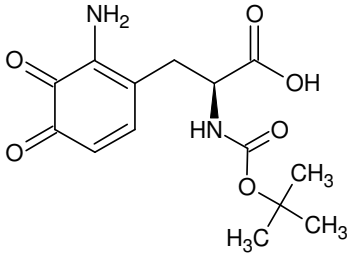

Monoisotopic Mass = 310.116486 Da

Ausgangsverbindung vor der OPA-Derivatisierung

620 Da [OPA-Ile 12,9 min]

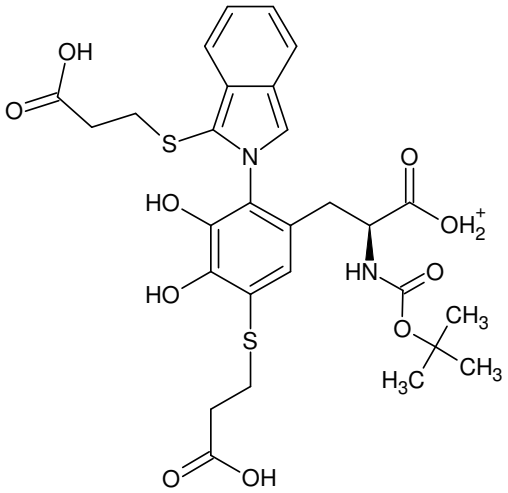

Monoisotopic Mass = 621.157112 Da

621,2 - 588,9 = **32,3**
Gefundene Verbindungen: 8
CH4O MG=32,0262134
CH6N MG=32,0500216
C2H8 MG=32,0625968
H2NO MG=32,0136382
H4N2 MG=32,0374464
H16O MG=32,1201086
O2 MG=31,98983
S MG=31,972072

-----D--B--E--f-i-l-t-e-r-----
11.08.2011 - 14:14:07,76
akzeptierte DBEs:
-2 -1 0 1 2 3 4 5 6 7 8

CH_4O DBE: 0
C_2H_8 DBE: -1
H_4N_2 DBE: 0
O_2 DBE: 1
S DBE: 1

5 von 8 Summenformeln

$H_3C—OH$
methanol

CH_4 CH_4
methane

$H_2N—NH_2$
hydrazine

O═O
dioxygen

S:
sulfanylidene

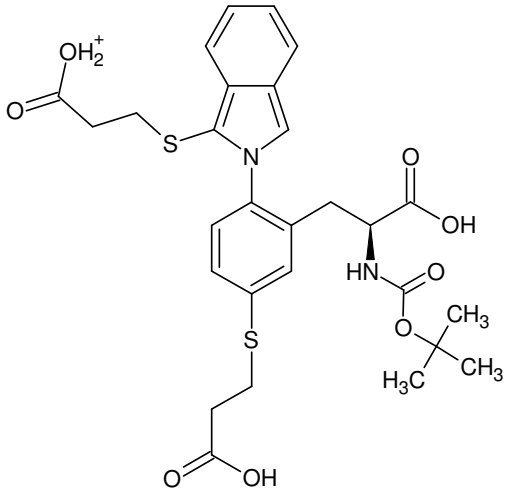

O═O
31.989829 Da

Monoisotopic Mass = 589.167282 Da

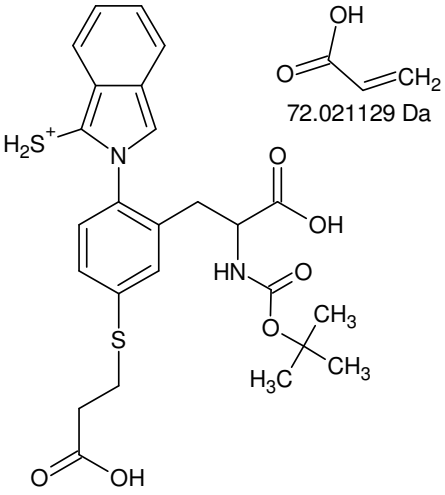

72.021129 Da

Monoisotopic Mass = 517.146153 Da

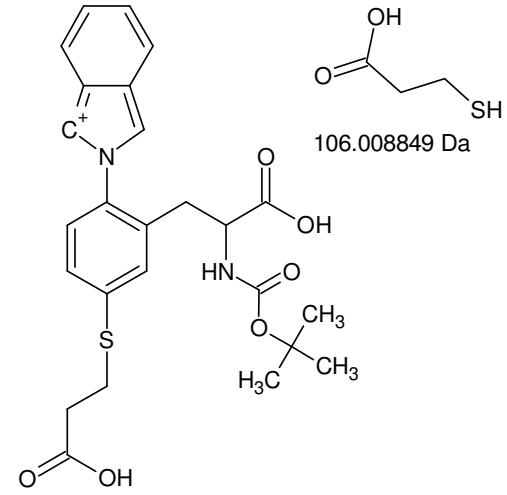

106.008849 Da

Monoisotopic Mass = 483.158433 Da

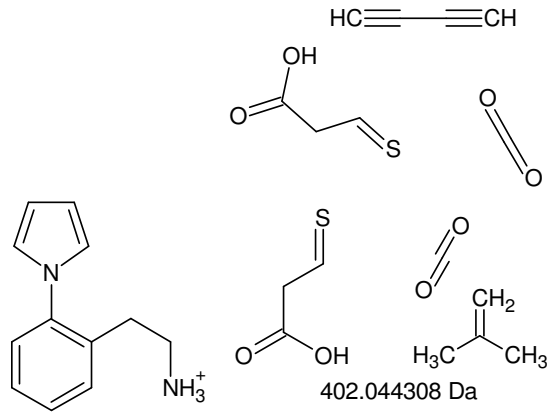

402.044308 Da

Monoisotopic Mass = 187.122975 Da

+MSn [OPA-Ile 12,9 min]: 621 -> 589 -> 517, 483, 187

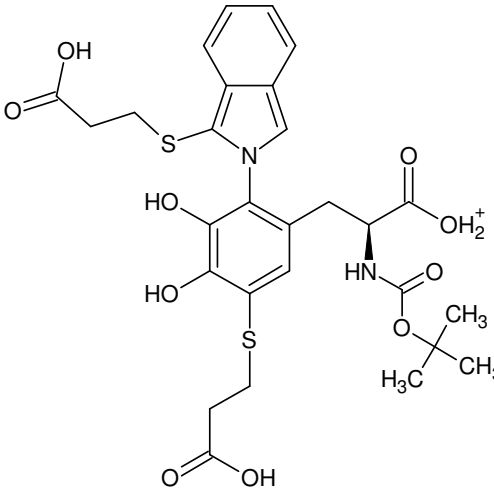

Monoisotopic Mass = 621.157112 Da

Gefundene Verbindungen: 28
CH2N3 MG=56,0248712
CH12O2 MG=56,0837252
(...)
H28N2 MG=56,2252368
N4 MG=56,012296

-----D--B--E--f-i-l-t-e-r-----
11.08.2011 - 16:32:31,17
akzeptierte DBEs:
-2 -1 0 1 2 3 4 5 6 7 8

CN_2O	DBE: 3
$C_2H_4N_2$	DBE: 2
C_2O_2	DBE: 3
C_2S	DBE: 3
C_3H_4O	DBE: 2
C_4H_8	DBE: 1
N_4	DBE: 3

7 von 28 Summenformeln

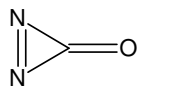

CN_2O
56.001063 Da

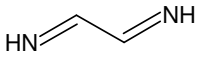

$C_2H_4N_2$
56.037448 Da

C_2O_2
55.989829 Da

C_2S
55.97207 Da

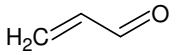

C_3H_4O
56.026215 Da

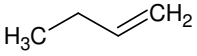

C_4H_8
56.0626 Da

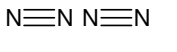

N_4
56.012296 Da

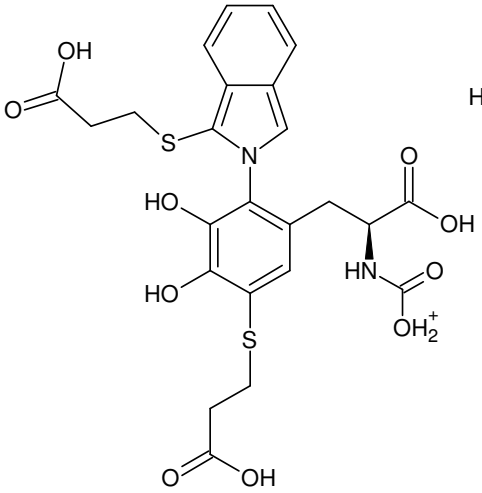

Monoisotopic Mass = 565.094511 Da

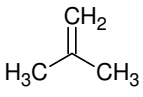

56.0626 Da

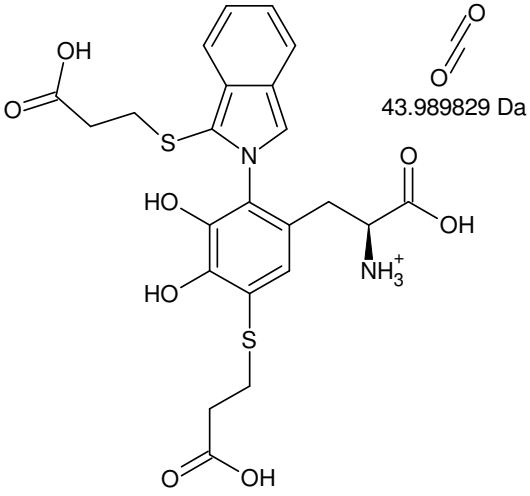

Monoisotopic Mass = 521.104682 Da

43.989829 Da

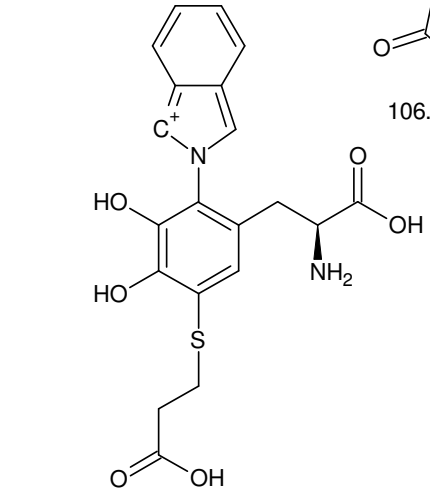

Monoisotopic Mass = 415.095833 Da

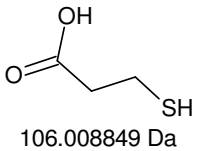

106.008849 Da

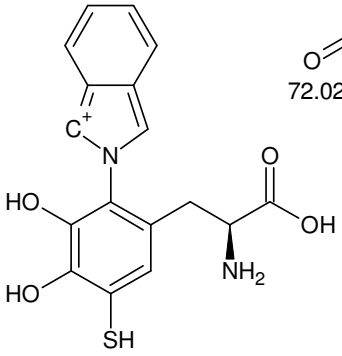

Monoisotopic Mass = 343.074703 Da

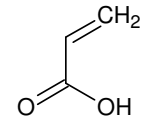

72.021129 Da

+MSn [OPA-Ile 12,9 min]: 621 -> 565 -> 521 -> 415 -> 343

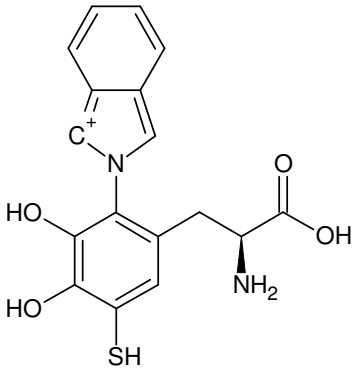

Monoisotopic Mass = 343.074703 Da

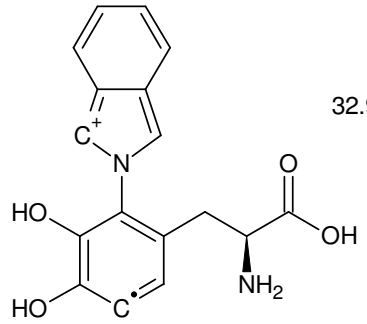

HS•
32.979895 Da

Monoisotopic Mass = 310.094808 Da

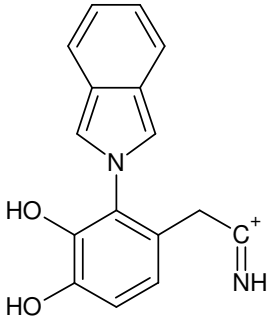

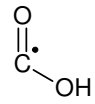

44.997654 Da

Monoisotopic Mass = 265.097154 Da

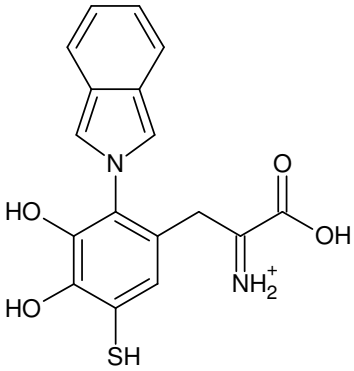

Monoisotopic Mass = 343.074703 Da

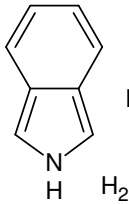

H_2O

H_2S

169.056134 Da

Anellierung analog der Bildung von Leucodopachrom

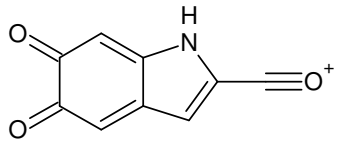

Monoisotopic Mass = 174.018569 Da

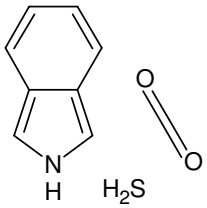

H_2S

195.035399 Da

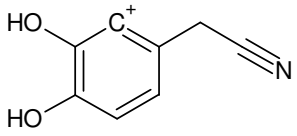

Monoisotopic Mass = 148.039305 Da

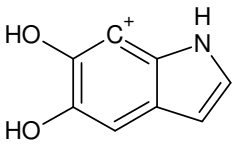

Monoisotopic Mass = 148.039305 Da

+MSn [OPA-Ile 12,9 min]: [621 -> 565 -> 521 -> 415 -> 343] -> 310 -> 265 und 343 -> 174, 148

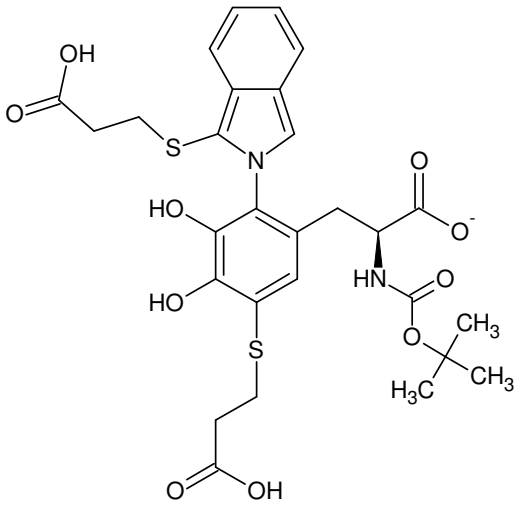

Monoisotopic Mass = 619.142559 Da

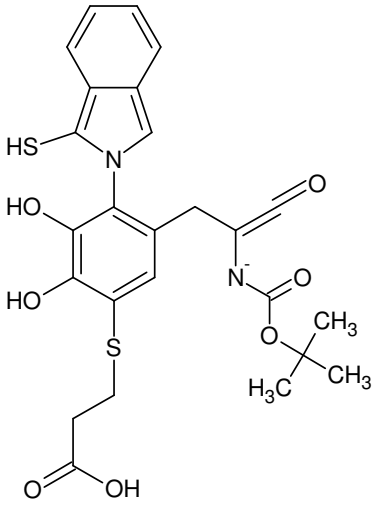

H_2O
18.010565 Da

Monoisotopic Mass = 529.110865 Da

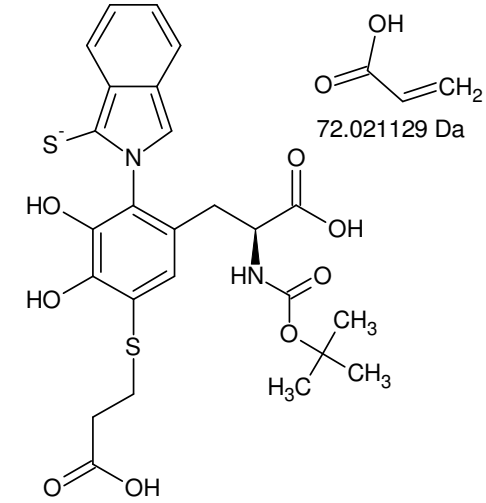

72.021129 Da

Monoisotopic Mass = 547.121429 Da

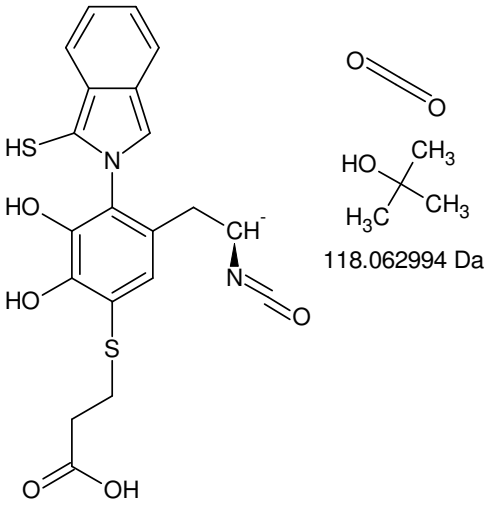

118.062994 Da

Monoisotopic Mass = 429.058435 Da

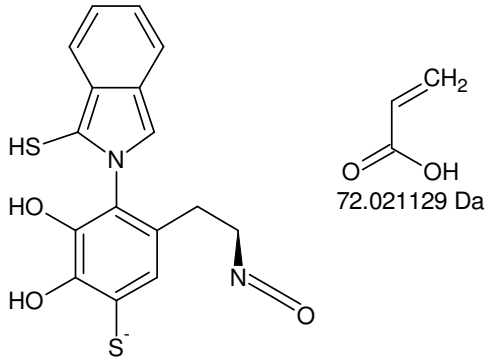

72.021129 Da

Monoisotopic Mass = 357.037306 Da

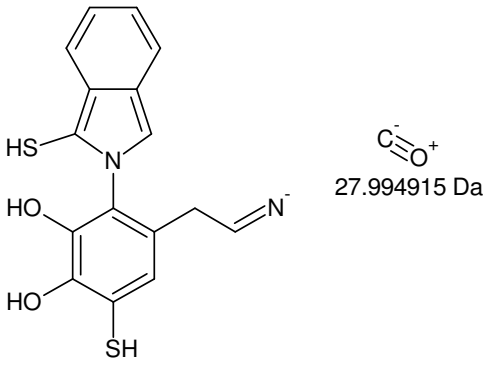

27.994915 Da

Monoisotopic Mass = 329.042391 Da

-MSn [OPA-Ile 12,9 min]: 619 -> 529, 547 -> 429 -> 357 -> 329

14. References

[1] Renate Czaker. Extracellular matrix (ECM) components in a very primitive multicellular animal, the dicyemid mesozoan Kantharella antarctica. *The Anatomical Record*, 259 (1): 52 – 59, 2000. ISSN 1097-0185. doi: 10.1002/(SICI)1097-0185(20000501)259:1<52::AID-AR6>3.0.CO;2-J. <url>.

[2] B. Runnegar. Collagen gene construction and evolution. *Journal of Molecular Evolution*, 22: 141 – 149, 1985. ISSN 0022-2844. doi: 10.1007/BF02101692. <url>.

[3] Bernd Schierwater, Michael Eitel, Wolfgang Jakob, Hans-Jürgen Osigus, Heike Hadrys, Stephen L Dellaporta, Sergios-Orestis Kolokotronis, and Rob DeSalle. Concatenated Analysis Sheds Light on Early Metazoan Evolution and Fuels a Modern "Urmetazoon" Hypothesis. *PLoS Biol*, 7 (1): e1000020, 01 2009. doi: 10.1371/journal.pbio.1000020. <url>. PMCID: PMC 2631068.

[4] Adolf Seilacher, Pradip K. Bose, and Friedrich Pflüger. Triploblastic Animals More Than 1 Billion Years Ago: Trace Fossil Evidence from India. *Science*, 282 (5386): 80 – 83, 1998. doi: 10.1126/science.282.5386.80. <url>.

[5] Kai-Michael Wess. *Charakterisierung des Kollagens im Ligamentum deltoideum beim kongenitalen Klumpfuß und beim gesunden Fuß*. PhD thesis, Medizinische Fakultät der Heinrich Heine Universität Düsseldorf, 2009. <url>. urn:nbn:de:hbz:061-20091019-111335-8.

[6] Johanna Myllyharju and Kari I. Kivirikko. Collagens, modifying enzymes and their mutations in humans, flies and worms. *Trends in Genetics*, 20 (1): 33 – 43, 2004. ISSN 0168-9525. doi: 10.1016/j.tig.2003.11.004. <url>.

[7] Darwin J. Prockop, Kari I. Kivirikko, Leena Tuderman, and Norberto A. Guzman. The Biosynthesis of Collagen and Its Disorders. *New England Journal of Medicine*, 301 (1): 13 – 23, 1979. doi: 10.1056/NEJM197907053010104. <url>.

[8] J Bella, M Eaton, B Brodsky, and HM Berman. Crystal and molecular structure of a collagen-like peptide at 1.9 A resolution. *Science*, 266 (5182): 75 – 81, 1994. doi: 10.1126/science.7695699. <url>. PMID: 7695699.

[9] Mirja-Liisa Sassi. *Carboxyterminal degradation products of type I collagen*. PhD thesis, Faculty of Medicine, Department of Clinical Chemistry, University of Oulu, 2001. <url>. ISBN Print: 951-42-6490-8 ISBN 951-42-6491-6 (PDF).

[10] Nicole Pischon. *Bedeutung der extrazellulären Kollagenmodifikationen für die Osteoblastendifferenzierung und Entstehung von Knochengewebe*. PhD thesis, Medizinische Fakultät Charité - Universitätsmedizin Berlin, 2009. <url>.

[11] R. Puxkandl, I. Zizak, O. Paris, J. Keckes, W. Tesch, S. Bernstorff, P. Purslow, and P. Fratzl. Viscoelastic properties of collagen: synchrotron radiation investigations and structural model. *Philosophical Transactions of the Royal Society of London. Series B: Biological Sciences*, 357 (1418): 191 – 197, 2002. doi: 10.1098/rstb.2001.1033. <url>.

[12] Karl A. Piez, Elizabeth A. Eigner, and Marc S. Lewis. The Chromatographic Separation and Amino Acid Composition of the Subunits of Several Collagens. *Biochemistry*, 2 (1): 58–66, 1963. doi: 10.1021/bi00901a012. <url>.

[13] K. Gelse, E. Pöschl, and T. Aigner. Collagens—structure, function, and biosynthesis. *Advanced Drug Delivery Reviews*, 55 (12): 1531 – 1546, 2003. ISSN 0169-409X. doi: 10.1016/j.addr.2003.08.002. <url>. <ce:title>Collagen in drug delivery and tissue engineering</ce:title>.

[14] Kari I. Kivirikko and Raili Myllylä. [10] Posttranslational enzymes in the biosynthesis of collagen: Intracellular enzymes. In Dixie W. Frederiksen Leon W. Cunningham, editor, *Structural and Contractile Proteins Part A: Extracellular Matrix*, volume 82 of *Methods in Enzymology*, pages 245 – 304. Academic Press, 1982. doi: 10.1016/0076-6879(82)82067-3. <url>.

[15] Michael Tronnier Yahya Açil Peter P Fietzek Wilfried Schmeller Peter K Müller Jürgen Brinckmann, Holger Notbohm and Boris Bätge. Overhydroxylation of Lysyl Residues is the Initial Step for Altered Collagen Cross-Links and Fibril Architecture in Fibrotic Skin. *Journal of Investigative Dermatology*, 113: 617 – 621, 1999. doi: 10.1046/j.1523-1747.1999.00735.x. <url>.

[16] Sabine Frank, Richard A Kammerer, Diane Mechling, Therese Schulthess, Ruth Landwehr, James Bann, Yuan Guo, Ariel Lustig, Hans Peter Bächinger, and Jürgen Engel. Stabilization of short

collagen-like triple helices by protein engineering. *Journal of Molecular Biology*, 308 (5): 1081 – 1089, 2001. ISSN 0022-2836. doi: 10.1006/jmbi.2001.4644. <url>.

[17] Christopher A Miles, Lynda Knott, Ian G Sumner, and Allen J Bailey. Differences between the thermal stabilities of the three triple-helical domains of type IX collagen. *Journal of Molecular Biology*, 277 (1): 135 – 144, 1998. ISSN 0022-2836. doi: 10.1006/jmbi.1997.1603. <url>.

[18] Shumpei Sakakibara, Katsuhiko Inouye, Keiko Shudo, Yasuo Kishida, Yuji Kobayashi, and Darwin J. Prockop. Synthesis of (Pro-Hyp-Gly)n of defined molecular weights Evidence for the stabilization of collagen triple helix by hydroxypyroline. *Biochimica et Biophysica Acta (BBA) - Protein Structure*, 303 (1): 198 – 202, 1973. ISSN 0005-2795. doi: 10.1016/0005-2795(73)90164-5. <url>.

[19] Peter M. Royce and Michael J. Barnes. Comparative studies on collagen glycosylation in chick skin and bone. *Biochimica et Biophysica Acta (BBA) - General Subjects*, 498 (1): 132 – 142, 1977. ISSN 0304-4165. doi: 10.1016/0304-4165(77)90094-0. <url>.

[20] Naoko Nagai, Masanori Hosokawa, Shigeyoshi Itohara, Eijiro Adachi, Takatoshi Matsushita, Nobuko Hosokawa, and Kazuhiro Nagata. Embryonic Lethality of Molecular Chaperone Hsp47 Knockout Mice Is Associated with Defects in Collagen Biosynthesis. *The Journal of Cell Biology*, 150 (6): 1499 – 1506, 2000. doi: 10.1083/jcb.150.6.1499. <url>.

[21] Mehmet Ilhan Uzel, Ian C. Scott, Hermik Babakhanlou-Chase, Amitha H. Palamakumbura, William N. Pappano, Hsiang-Hsi Hong, Daniel S. Greenspan, and Philip C. Trackman. Multiple Bone Morphogenetic Protein 1-related Mammalian Metalloproteinases Process Pro-lysyl Oxidase at the Correct Physiological Site and Control Lysyl Oxidase Activation in Mouse Embryo Fibroblast Cultures. *Journal of Biological Chemistry*, 276 (25): 22537 – 22543, 2001. doi: 10.1074/jbc.M102352200. <url>.

[22] J. D. Prockop. Collagens: Molecular Biology, Diseases, and Potentials for Therapy. *Annual Review of Biochemistry*, 64 (1): 403 – 434, 1995. doi: 10.1146/annurev.bi.64.070195.002155. <url>.

[23] Joseph P. R. O. Orgel, Thomas C. Irving, Andrew Miller, and Tim J. Wess. Microfibrillar structure of type I collagen in situ. *Proceedings of the National Academy of Sciences*, 103 (24): 9001 – 9005, 2006. doi: 10.1073/pnas.0502718103. <url>.

[24] John A. Trotter Karl E. Kadler, David F. Holmes and John A. Chapman. Collagen fibril formation. *Biochemical Journal*, 316: 1 – 11, 1996. <url>. PMCID: PMC1217307.

[25] Fritz Verzár. Das Altern des Kollagens. *Helvetica physiologica et pharmacologica acta*, 14: 207 – 227, 1956. PMID: 13345221.

[26] F. Verzár. Aging of the collagen fiber. *International Review of Connective Tissue Research*, 2: 243 – 300, 1964. PMID: 5334763.

[27] A. J. Bailey and D. Lister. Thermally Labile Cross-links in Native Collagen. *Nature*, 220: 280 – 281, 1968. doi: 10.1038/220280a0. <url>.

[28] Simon P. Robins and Allen J. Bailey. The chemistry of the collagen cross-links. The mechanism of stabilization of the reducible intermediate cross-links. *Biochemical Journal*, 149: 381 – 385, 1975. <url>. PMCID: PMC1165631.

[29] Massami Shimokomaki Simon P. Robins and Allen J. Bailey. The chemistry of the collagen cross-links. Age-related changes in the reducible components of intact bovine collagen fibres. *Biochemical Journal*, 131: 771 – 780, 1973. <url>. PMCID: PMC1177537.

[30] T. Housley, M.L. Tanzer, E. Henson, and P.M. Gallop. Collagen crosslinking: Isolation of hydroxyaldol-histidine, a naturally-occurring crosslink. *Biochemical and Biophysical Research Communications*, 67 (2): 824 – 830, 1975. ISSN 0006-291X. doi: 10.1016/0006-291X(75)90887-6. <url>.

[31] Herbert M. Kagan and Wande Li. Lysyl oxidase: Properties, specificity, and biological roles inside and outside of the cell. *Journal of Cellular Biochemistry*, 88 (4): 660 – 672, 2003. ISSN 1097-4644. doi: 10.1002/jcb.10413. <url>.

[32] Robert C. Siegel. Collagen cross-linking. Synthesis of collagen cross-links in vitro with highly purified lysyl oxidase. *Journal of Biological Chemistry*, 251 (18): 5786 – 5792, 1976. <url>.

[33] Robert C. Siegel and Josef C. Fu. Collagen cross-linking. Purification and substrate specificity of lysyl oxidase. *Journal of Biological Chemistry*, 251 (18): 5779 – 5785, 1976. <url>.

[34] Sheldon R. Pinnell and George R. Martin. The cross-linking of collagen and elastin: enzymatic conversion of lysine in peptide linkage to alpha-aminoadipic-delta-semialdehyde (allysine) by an

extract from bone. *Proceedings of the National Academy of Sciences of the United States of America (PNAS)*, 61: 708 – 716, 1968. <url>. PMCID: PMC225217.

[35] Daisaburo Fujimoto, Kin ya Akiba, and Nobuo Nakamura. Isolation and characterization of a fluorescent material in bovine achilles tendon collagen. *Biochemical and Biophysical Research Communications*, 76 (4): 1124 – 1129, 1977. ISSN 0006-291X. doi: 10.1016/0006-291X(77)90972-X. <url>.

[36] Daisaburo Fujimoto, Takahiko Moriguchi, Torao Ishida, and Hiroshi Hayashi. The structure of pyridinoline, a collagen crosslink. *Biochemical and Biophysical Research Communications*, 84 (1): 52 – 57, 1978. ISSN 0006-291X. doi: 10.1016/0006-291X(78)90261-9. <url>.

[37] Werner Henkel John E. Scott, Rui-ging Qian and Robert W. Glanville. An Ehrlich chromogen in collagen cross-links. *Biochemical Journal*, 209: 263 – 264, 1983. <url>. PMCID: PMC1154082.

[38] J. E. Scott, E. W. Hughes, and A. Shuttleworth. A collagen-associated Ehrlich chromogen: a pyrrolic cross-link? *Bioscience Reports*, 1: 611 – 618, 1981. ISSN 0144-8463. doi: 10.1007/BF01116276. <url>.

[39] Ian K. Hornstra, Shonyale Birge, Barry Starcher, Allen J. Bailey, Robert P. Mecham, and Steven D. Shapiro. Lysyl Oxidase Is Required for Vascular and Diaphragmatic Development in Mice. *Journal of Biological Chemistry*, 278 (16): 14387 – 14393, 2003. doi: 10.1074/jbc.M210144200. <url>.

[40] Andrew H. Kang, Barbara Faris, and Carl Franzblau. The in vitro formation of intermolecular cross-links in chick skin collagen. *Biochemical and Biophysical Research Communications*, 39 (1): 175 – 182, 1970. ISSN 0006-291X. doi: 10.1016/0006-291X(70)90774-6. <url>.

[41] John F. Tarlton Lynda Knott and Allen J. Bailey. Chemistry of collagen cross-linking: biochemical changes in collagen during the partial mineralization of turkey leg tendon. *Biochemical Journal*, 322: 535 – 542, 1997. <url>. PMCID: PMC1218223.

[42] Marvin L. Tanzer, Timothy Housley, Linda Berube, Robert Fairweather, Carl Franzblau, and Paul M. Gallop. Structure of Two Histidine-containing Cross-Links from Collagen. *Journal of Biological Chemistry*, 248 (2): 393 – 402, 1973. <url>.

[43] Mitsuo Yamauchi, David T. Woodley, and Gerald L. Mechanic. Aging and cross-linking of skin collagen. *Biochemical and Biophysical Research Communications*, 152 (2): 898 – 903, 1988. ISSN 0006-291X. doi: 10.1016/S0006-291X(88)80124-4. <url>.

[44] Gerald L. Mechanic, Elton P. Katz, Masayuki Henmi, Claudia Noyes, and Mitsuo Yamauchi. Locus of a histidine-based, stable trifunctional, helix to helix collagen cross-link: stereospecific collagen structure of type I skin fibrils. *Biochemistry*, 26 (12): 3500 – 3509, 1987. doi: 10.1021/bi00386a038. <url>.

[45] Mitsuo Yamauchi, Philip Prisayanh, Zia Haque, and David T Woodley. Collagen Cross-Linking in Sun-Exposed and Unexposed Sites of Aged Human Skin. *Journal of Investigative Dermatology*, 97: 937 – 941, 1991. doi: 10.1111/1523-1747.ep12491727. <url>.

[46] David R. Eyre, Mercedes A. Paz, and Paul M. Gallop. Cross-Linking in Collagen and Elastin. *Annual Review of Biochemistry*, 53 (1): 717 – 748, 1984. doi: 10.1146/annurev.bi.53.070184.003441. <url>.

[47] Michael Tronnier Holger Notbohm Boris Bätge Wilfried Schmeller Michel H. J. Koch-Peter K. Müller Jürgen Brinckmann, Yahya Açil and Helmut H. Wolff. Altered X-Ray Diffraction Pattern Is Accompanied by a Change in the Mode of Cross-Link Formation in Lipodermatosclerosis. *Journal of Investigative Dermatology*, 107: 589 – 592, 1996. doi: 10.1111/1523-1747.ep12582991. <url>.

[48] Jerold A. Last, Lucas G. Armstrong, and Karen M. Reiser. Biosynthesis of collagen crosslinks. *International Journal of Biochemistry*, 22 (6): 559 – 564, 1990. ISSN 0020-711X. doi: 10.1016/0020-711X(90)90031-W. <url>.

[49] Ian R. Dickson David R. Eyre and Kirk Van Ness. Collagen cross-linking in human bone and articular cartilage Age-related changes in the content of mature hydroxypyridinium residues. *Biochemical Journal*, 252: 495 – 500, 1988. <url>. PMCID: PMC1149171.

[50] Allen J Bailey, Robert Gordon Paul, and Lynda Knott. Mechanisms of maturation and ageing of collagen. *Mechanisms of Ageing and Development*, 106 (1-2): 1 – 56, 1998. ISSN 0047-6374. doi: 10.1016/S0047-6374(98)00119-5. <url>.

[51] D R Sell and V M Monnier. Structure elucidation of a senescence cross-link from human extracellular matrix. Implication of pentoses in the aging process. *Journal of Biological Chemistry*, 264 (36): 21597 – 21602, 1989. <url>.

[52] Ulrich Valcourt, Blandine Merle, Evelyne Gineyts, Stéphanie Viguet-Carrin, Pierre D. Delmas, and Patrick Garnero. Non-enzymatic Glycation of Bone Collagen Modifies Osteoclastic Activity and Differentiation. *Journal of Biological Chemistry*, 282 (8): 5691 – 5703, 2007. doi: 10.1074/jbc.M610536200. <url>.

[53] Wolfgang Friess. Collagen – biomaterial for drug delivery. *European Journal of Pharmaceutics and Biopharmaceutics*, 45 (2): 113 – 136, 1998. ISSN 0939-6411. doi: 10.1016/S0939-6411(98)00017-4. <url>.

[54] M. Geiger, R.H. Li, and W. Friess. Collagen sponges for bone regeneration with rhBMP-2. *Advanced Drug Delivery Reviews*, 55 (12): 1613 – 1629, 2003. ISSN 0169-409X. doi: 10.1016/j.addr.2003.08.010. <url>.

[55] Chi H. Lee, Anuj Singla, and Yugyung Lee. Biomedical applications of collagen. *International Journal of Pharmaceutics*, 221 (1-2): 1 – 22, 2001. ISSN 0378-5173. doi: 10.1016/S0378-5173(01)00691-3. <url>.

[56] Zbigniew Ruszczak and Wolfgang Friess. Collagen as a carrier for on-site delivery of antibacterial drugs. *Advanced Drug Delivery Reviews*, 55 (12): 1679 – 1698, 2003. ISSN 0169-409X. doi: 10.1016/j.addr.2003.08.007. <url>.

[57] Eugene Khor. Methods for the treatment of collagenous tissues for bioprostheses. *Biomaterials*, 18 (2): 95 – 105, 1997. ISSN 0142-9612. doi: 10.1016/S0142-9612(96)00106-8. <url>.

[58] Miho Maeda, Shunsuke Tani, Akihiko Sano, and Keiji Fujioka. Microstructure and release characteristics of the minipellet, a collagen-based drug delivery system for controlled release of protein drugs. *Journal of Controlled Release*, 62 (3): 313 – 324, 1999. ISSN 0168-3659. doi: 10.1016/S0168-3659(99)00156-X. <url>.

[59] MI) Varani James (Ann Arbor MI) Helmreich David L. (Ann Arbor-MI) Hillegas, William J. (Ann Arbor. Collagen-coated polystyrene microcarrier beads, February 1991. <url>. US Patent 4994388.

[60] Yoshihiro Ito, Ji Zheng, and Yukio Imanishi. Serum-free cell culture on insulin-immobilized porous collagen beads. *Biotechnology and Bioengineering*, 45 (2): 144 – 148, 1995. ISSN 1097-0290. doi: 10.1002/bit.260450208. <url>.

[61] M. Yamaguchi, Y. Shirai, Y. Inouye, M. Shoji, M. Kamei, S. Hashizume, and S. Shirahata. Changes in monoclonal antibody productivity of recombinant BHK cells immobilized in collagen gel particles. *Cytotechnology*, 23: 5–12, 1997. ISSN 0920 - 9069. doi: 10.1023/A:1007959400666. <url>.

[62] H. Petite, I. Rault, A. Huc, Ph. Menasche, and D. Herbage. Use of the acyl azide method for cross-linking collagen-rich tissues such as pericardium. *Journal of Biomedical Materials Research*, 24 (2): 179 – 187, 1990. ISSN 1097-4636. doi: 10.1002/jbm.820240205. <url>.

[63] L.H.H. Olde Damink, P.J. Dijkstra, M.J.A. van Luyn, P.B. van Wachem, P. Nieuwenhuis, and J. Feijen. Cross-linking of dermal sheep collagen using a water-soluble carbodiimide. *Biomaterials*, 17 (8): 765 – 773, 1996. ISSN 0142-9612. doi: 10.1016/0142-9612(96)81413-X. <url>.

[64] Marcel Nimni, Sol Bernick, David Cheung, Delia Ertl, Satoru Nishimoto, Wendelin Paule, Carl Salka, and Basil Strates. Biochemical differences between dystrophic calcification of cross-linked collagen implants and mineralization during bone induction. *Calcified Tissue International*, 42: 313 – 320, 1988. ISSN 0171-967X. doi: 10.1007/BF02556366. <url>.

[65] W. G. Bradley and G. L. Wilkes. Some Mechanical Property Considerations of Reconstituted Collagen for Drug Release Supports. *Artificial Cells, Blood Substitutes and Biotechnology*, 5 (2): 159 – 175, 1977. doi: 10.3109/10731197709118671. <url>.

[66] Robert J. Ruderman, Clarence W. R. Wade, William D. Shepard, and Fred Leonard. Prolonged resorption of collagen sponges: Vapor-phase treatment with formaldehyde. *Journal of Biomedical Materials Research*, 7 (2): 263 – 265, 1973. ISSN 1097-4636. doi: 10.1002/jbm.820070213. <url>.

[67] L. H. H. Olde Damink, P. J. Dijkstra, M. J. A. Luyn, P. B. Wachem, P. Nieuwenhuis, and J. Feijen. Glutaraldehyde as a crosslinking agent for collagen-based biomaterials. *Journal of Materials Science: Materials in Medicine*, 6: 460 – 472, 1995. ISSN 0957-4530. doi: 10.1007/BF00123371. <url>.

[68] Milos Chvapil, Donald P. Speer, Hana Holubec, Thomas A. Chvapil, and David H. King. Collagen fibers as a temporary scaffold for replacement of ACL in goats. *Journal of Biomedical Materials Research*, 27 (3): 313 – 325, 1993. ISSN 1097-4636. doi: 10.1002/jbm.820270305. <url>.
[69] R. Tu, C.-L. Lu, K. Thyagarajan, E. Wang, H. Nguyen, S. Shen, C. Hata, and R. C. Quijano. Kinetic study of collagen fixation with polyepoxy fixatives. *Journal of Biomedical Materials Research*, 27 (1): 3 – 9, 1993. ISSN 1097-4636. doi: 10.1002/jbm.820270103. <url>. PMID: 8420998.
[70] J N Rodríguez-López, J Tudela, R Varón, F García-Carmona, and F García-Cánovas. Analysis of a kinetic model for melanin biosynthesis pathway. *Journal of Biological Chemistry*, 267 (6): 3801 – 3810, 1992. <url>.
[71] Howard S. Mason and Charles I. Wright. The chemistry of melanin v. oxidation of dihydroxyphenylalanine by tyrosinase. *Journal of Biological Chemistry*, 180 (1): 235–247, 1949. <url>.
[72] John M. Pawelek. After Dopachrome? *Pigment Cell Research*, 4 (2): 53 – 62, 1991. ISSN 1600-0749. doi: 10.1111/j.1600-0749.1991.tb00315.x. <url>.
[73] Itzhack Polacheck and Kyung Joo Kwon-Chung. Melanogenesis in Cryptococcus neoformans. *Journal of General Microbiology*, 134 (4): 1037 – 1041, 1988. doi: 10.1099/00221287-134-4-1037. <url>.
[74] George Zonios, Aikaterini Dimou, Ioannis Bassukas, Dimitrios Galaris, Argyrios Tsolakidis, and Efthimios Kaxiras. Melanin absorption spectroscopy: new method for noninvasive skin investigation and melanoma detection. *Journal of Biomedical Optics*, 13 (1): 014017–1 – 014017–8, 2008. ISSN 10833668. doi: 10.1117/1.2844710. <url>.
[75] Luis A. Burzio and J. Herbert Waite. Reactivity of peptidyl-tyrosine to hydroxylation and cross-linking. *Protein Science*, 10 (4): 735 – 740, 2001. ISSN 1469-896X. doi: 10.1110/ps.44201. <url>. PMCID: PMC2373961.
[76] R. Lantto, E. Puolanne, K. Kruus, J. Buchert, and K. Autio. Tyrosinase-Aided Protein Cross-Linking: Effects on Gel Formation of Chicken Breast Myofibrils and Texture and Water-Holding of Chicken Breast Meat Homogenate Gels. *Journal of Agricultural and Food Chemistry*, 55 (4): 1248 – 1255, 2007. doi: 10.1021/jf0623485. <url>. PMID: 17243701.
[77] Kan Shinpo Shosuke Ito, Toshiaki Kato and Keisuke Fujita. Oxidation of tyrosine residues in proteins by tyrosinase. Formation of protein-bonded 3,4-dihydroxyphenylalanine and 5-S-cysteinyl-3,4-dihydroxyphenylalanine. *Biochemical Journal*, 222: 407 – 411, 1984. <url>. PMCID: PMC1144193.
[78] Luis A. Burzio and J. Herbert Waite. Cross-Linking in Adhesive Quinoproteins: Studies with Model Decapeptides. *Biochemistry*, 39 (36): 11147 – 11153, 2000. doi: 10.1021/bi0002434. <url>.
[79] Lynda M. McDowell, Luis A. Burzio, J. Herbert Waite, and Jacob Schaefer. Rotational Echo Double Resonance Detection of Cross-links Formed in Mussel Byssus under High-Flow Stress. *Journal of Biological Chemistry*, 274 (29): 20293 – 20295, 1999. doi: 10.1074/jbc.274.29.20293. <url>.
[80] Lorena G Fenoll, José Neptuno Rodríguez-López, Francisco García-Molina, Francisco García-Cánovas, and José Tudela. Michaelis constants of mushroom tyrosinase with respect to oxygen in the presence of monophenols and diphenols. *The International Journal of Biochemistry & Cell Biology*, 34 (4): 332 – 336, 2002. ISSN 1357-2725. doi: 10.1016/S1357-2725(01)00133-9. <url>.
[81] Karen Gronskov, Jakob Ek, and Karen Brondum-Nielsen. Oculocutaneous albinism. *Orphanet Journal of Rare Diseases*, 2 (1): 43, 2007. ISSN 1750-1172. doi: 10.1186/1750-1172-2-43. <url>. PMID: 17980020.
[82] Yuji Yamaguchi and Vincent J. Hearing. Physiological factors that regulate skin pigmentation. *BioFactors*, 35 (2): 193 – 199, 2009. ISSN 1872-8081. doi: 10.1002/biof.29. <url>. PMCID: PMC2793097.
[83] Juan C. Espín, Ramón Varón, Lorena G. Fenoll, M. Angeles Gilabert, Pedro A. García-Ruíz, José Tudela, and Francisco García-Cánovas. Kinetic characterization of the substrate specificity and mechanism of mushroom tyrosinase. *European Journal of Biochemistry*, 267 (5): 1270 – 1279, 2000. ISSN 1432-1033. doi: 10.1046/j.1432-1327.2000.01013.x. <url>.
[84] G.W. Felton, K.K. Donato, R.M. Broadway, and S.S. Duffey. Impact of oxidized plant phenolics on the nutritional quality of dietar protein to a noctuid herbivore, Spodoptera exigua. *Journal of Insect Physiology*, 38 (4): 277 – 285, 1992. ISSN 0022-1910. doi: 10.1016/0022-1910(92)90128-Z. <url>.

[85] G. W. Felton, K. Donato, R. J. Del Vecchio, and S. S. Duffey. Activation of plant foliar oxidases by insect feeding reduces nutritive quality of foliage for noctuid herbivores. *Journal of Chemical Ecology*, 15: 2667 – 2694, 1989. ISSN 0098-0331. <url>. 10.1007/BF01014725.

[86] Roohi Aslam Bilal Mustafa Maleeha Maria, Nazish Bostan and Waseem Safdar. Type III Multicopper Proteins: A Critical Review. *International Journal of Biotechnology,*, 4: 575 – 581, 2011. <url>.

[87] James C. Sacchettini Thomas Klabunde, Christoph Eicken and Bernt Krebs. Crystal structure of a plant catechol oxidase containing a dicopper center. *Nature Structural Biology*, 5: 1084 – 1090, 1998. doi: 10.1038/4193. <url>. PMID: 9846879.

[88] Wangsa T. Ismaya, Henriëtte J. Rozeboom, Amrah Weijn, Jurriaan J. Mes, Fabrizia Fusetti, Harry J. Wichers, and Bauke W. Dijkstra. Crystal Structure of Agaricus bisporus Mushroom Tyrosinase: Identity of the Tetramer Subunits and Interaction with Tropolone. *Biochemistry*, 50 (24): 5477 – 5486, 2011. doi: 10.1021/bi200395t. <url>.

[89] Mor Sendovski, Margarita Kanteev, Vered Shuster Ben-Yosef, Noam Adir, and Ayelet Fishman. First Structures of an Active Bacterial Tyrosinase Reveal Copper Plasticity. *Journal of Molecular Biology*, 405 (1): 227 – 237, 2011. ISSN 0022-2836. doi: 10.1016/j.jmb.2010.10.048. <url>.

[90] Shinobu Itoh and Shunichi Fukuzumi. Monooxygenase Activity of Type 3 Copper Proteins. *Accounts of Chemical Research*, 40 (7): 592 – 600, 2007. doi: 10.1021/ar6000395. <url>.

[91] Malte Rolff, Julia Schottenheim, Heinz Decker, and Felix Tuczek. Copper-O2 reactivity of tyrosinase models towards external monophenolic substrates: molecular mechanism and comparison with the enzyme. *Chem. Soc. Rev.*, 40: 4077 – 4098, 2011. doi: 10.1039/C0CS00202J. <url>.

[92] Chiyuki Morioka, Yoshimitsu Tachi, Shinnichiro Suzuki, and Shinobu Itoh. Significant Enhancement of Monooxygenase Activity of Oxygen Carrier Protein Hemocyanin by Urea. *Journal of the American Chemical Society*, 128 (21): 6788 – 6789, 2006. doi: 10.1021/ja061631h. <url>. PMID: 16719449.

[93] Heinz Decker and Thomas Rimke. Tarantula Hemocyanin Shows Phenoloxidase Activity. *Journal of Biological Chemistry*, 273 (40): 25889 – 25892, 1998. doi: 10.1074/jbc.273.40.25889. <url>.

[94] Erol Akyilmaz, Emine Yorganci, and Engin Asav. Do copper ions activate tyrosinase enzyme? A biosensor model for the solution. *Bioelectrochemistry*, 78 (2): 155 – 160, 2010. ISSN 1567-5394. doi: 10.1016/j.bioelechem.2009.09.007. <url>.

[95] Christopher J. Cooksey, Peter J. Garratt, Edward J. Land, Stan Pavel, Christopher A. Ramsden, Patrick A. Riley, and Nico P. M. Smit. Evidence of the Indirect Formation of the Catecholic Intermediate Substrate Responsible for the Autoactivation Kinetics of Tyrosinase. *Journal of Biological Chemistry*, 272 (42): 26226 – 26235, 1997. doi: 10.1074/jbc.272.42.26226. <url>.

[96] Harry W. Duckworth and Joseph E. Coleman. Physicochemical and Kinetic Properties of Mushroom Tyrosinase. *Journal of Biological Chemistry*, 245 (7): 1613 – 1625, 1970. <url>.

[97] Juan Carlos Espín, Jeroen van Leeuwen, and Harry J. Wichers. Kinetic Study of the Activation Process of a Latent Mushroom (Agaricus bisporus) Tyrosinase by Serine Proteases. *Journal of Agricultural and Food Chemistry*, 47 (9): 3509 – 3517, 1999. doi: 10.1021/jf9813539. <url>.

[98] Víctor Falguera, Jordi Pagán, and Albert Ibarz. A kinetic model describing melanin formation by means of mushroom tyrosinase. *Food Research International*, 43 (1): 66 – 69, 2010. ISSN 0963-9969. doi: 10.1016/j.foodres.2009.08.013. <url>.

[99] L.G. Fenoll, M.J. Peñalver, J.N. Rodríguez-López, R. Varón, F. García-Cánovas, and J. Tudela. Tyrosinase kinetics: discrimination between two models to explain the oxidation mechanism of monophenol and diphenol substrates. *The International Journal of Biochemistry & Cell Biology*, 36 (2): 235 – 246, 2004. ISSN 1357-2725. doi: 10.1016/S1357-2725(03)00234-6. <url>.

[100] Lorena G. Fenoll, José Neptuno Rodríguez-López, Francisco García-Sevilla, Pedro Antonio García-Ruiz, Ramón Varón, Francisco García-Cánovas, and José Tudela. Analysis and interpretation of the action mechanism of mushroom tyrosinase on monophenols and diphenols generating highly unstable o-quinones. *Biochimica et Biophysica Acta (BBA) - Protein Structure and Molecular Enzymology*, 1548 (1): 1 – 22, 2001. ISSN 0167-4838. doi: 10.1016/S0167-4838(01)00207-2. <url>.

[101] Francisco Garcia-Carmona, Edelmira Valero, and Juana Cabanes. Effect of l-proline on mushroom tyrosinase. *Phytochemistry*, 27 (7): 1961 – 1964, 1988. ISSN 0031-9422. doi: 10.1016/0031-9422(88)80077-3. <url>.
[102] Ramón Varon Jose Tudela Francisco Garcia-Cánovas Jose Luis Muñoz-Muñoz, Francisco Garcia-Molina and Jose N. Rodríguez-López. Kinetic cooperativity of tyrosinase. A general mechanism. *Acta Biochimica Polonica*, 58: 303 – 311, 2011. <url>.
[103] José N. Rodríguez-López P. A. García-Ruiz Francisco García-Cánovas Lorena G. Fenoll, María José Peñalver and José Tudela. Deuterium isotope effect on the oxidation of monophenols and o-disphenols by tyrosinase. *Biochemical Journal*, 380 (3): 643–650, 2004. doi: 10.1042/BJ20040136. <url>. cited By (since 1996) 12.
[104] Jose Muñoz-Muñoz, Francisco Garcia-Molina, Ramón Varon, Jose Tudela, Francisco Garcia-Cánovas, and Jose Rodríguez-López. New features of the steady-state rate related with the initial concentration of substrate in the diphenolase and monophenolase activities of tyrosinase. *Journal of Mathematical Chemistry*, 48: 347 – 362, 2010. ISSN 0259-9791. doi: 10.1007/s10910-010-9675-5. <url>.
[105] Russell L. Jolley, Leonard H. Evans, Nobuo Makino, and Howard S. Mason. Oxytyrosinase. *Journal of Biological Chemistry*, 249 (2): 335 – 345, 1974. <url>.
[106] Nobuo Makino, Paul McMahill, Howard S. Mason, and Thomas H. Moss. The Oxidation State of Copper in Resting Tyrosinase. *Journal of Biological Chemistry*, 249 (19): 6062 – 6066, 1974. <url>.
[107] Shigenobu Kasai Mika Tada, Masahiro Kohno and Yoshimi Niwano. Generation Mechanism of Radical Species by Tyrosine-Tyrosinase Reaction. *Journal of Clinical Biochemistry and Nutrition*, 47: 162 – 166, 2010. doi: 10.3164/jcbn.10-48. <url>. PMCID: PMC2935156.
[108] Minao Furumura Richard A. Spritz, Lingling Ho and Vincent J. Hearing Jr. Mutational Analysis of Copper Binding by Human Tyrosinase. *Journal of Investigative Dermatology*, 109: 207 – 212, 1997. doi: 10.1111/1523-1747.ep12319351. <url>.
[109] Luis A. Burzio and J.Herbert Waite. The Other Topa: Formation of 3,4,5-Trihydroxyphenylalanine in Peptides. *Analytical Biochemistry*, 306 (1): 108 – 114, 2002. ISSN 0003-2697. doi: 10.1006/abio.2002.5690. <url>.
[110] Te-Sheng Chang. An Updated Review of Tyrosinase Inhibitors. *International Journal of Molecular Sciences*, 10 (6): 2440 – 2475, 2009. ISSN 1422-0067. doi: 10.3390/ijms10062440. <url>.
[111] Francisco García-Molina, Jose Luis Muñoz-Muñoz, Francisco Martínez-Ortiz, Pedro Antonio García-Ruíz, Jose Tudela, Francisco García-Cánovas, and Jose Neptuno Rodríguez-López. Tetrahydrofolic Acid Is a Potent Suicide Substrate of Mushroom Tyrosinase. *Journal of Agricultural and Food Chemistry*, 59 (4): 1383 – 1391, 2011. doi: 10.1021/jf1035433. <url>.
[112] Young Mi Ha, Yun Jung Park, Ji Yeon Lee, Daeui Park, Yeon Ja Choi, Eun Kyeong Lee, Ji Min Kim, Jin-Ah Kim, Ji Young Park, Hye Jin Lee, Hyung Ryong Moon, and Hae Young Chung. Design, synthesis and biological evaluation of 2-(substituted phenyl)thiazolidine-4-carboxylic acid derivatives as novel tyrosinase inhibitors. *Biochimie*, 94 (2): 533 – 540, 2012. ISSN 0300-9084. doi: 10.1016/j.biochi.2011.09.002. <url>.
[113] Mercedes Jiménez and Francisco García-Carmona. Hydrogen peroxide-dependent 4-t-butylphenol hydroxylation by tyrosinase — a new catalytic activity. *Biochimica et Biophysica Acta (BBA) - Protein Structure and Molecular Enzymology*, 1297 (1): 33 – 39, 1996. ISSN 0167-4838. doi: 10.1016/0167-4838(96)00094-5. <url>.
[114] Mercedes Jiménez and Francisco García-Carmona. Hydroxylating Activity of Tyrosinase and Its Dependence on Hydrogen Peroxide. *Archives of Biochemistry and Biophysics*, 373 (1): 255 – 260, 2000. ISSN 0003-9861. doi: 10.1006/abbi.1999.1519. <url>.
[115] Francisco Martinez-Ortiz José Tudela Manuel Acosta Ramón Varón-Francisco García-Cánovas José Neptuno Rodríguez-López, Marino Bañón-Arnao. Catalytic oxidation of 2,4,5-trihydroxyphenylalanine by tyrosinase: identification and evolution of intermediates. *Biochimica et Biophysica Acta (BBA) - Protein Structure and Molecular Enzymology*, 1160 (2): 221 – 228, 1992. ISSN 0167-4838. doi: 10.1016/0167-4838(92)90011-2. <url>.
[116] Jose L. Muñoz-Muñoz, Francisco García-Molina, Pedro A. García-Ruiz, Milagros Molina-Alarcón, Jose Tudela, Francisco García-Cánovas, and Jose N. Rodríguez-López. Phenolic substrates

and suicide inactivation of tyrosinase: kinetics and mechanism. *Biochem J*, 416 (3): 431 – 440, 2008. doi: 10.1042/BJ20080892. <url>.

[117] Jose Luis Muñoz-Muñoz, Francisco Garcia-Molina, Pedro Antonio Garcia-Ruiz, Ramon Varon, Jose Tudela, Jose N. Rodriguez-Lopez, and Francisco Garcia-Canovas. Catalytic oxidation of o-aminophenols and aromatic amines by mushroom tyrosinase. *Biochimica et Biophysica Acta (BBA) - Proteins & Proteomics*, 1814 (12): 1974 – 1983, 2011. ISSN 1570-9639. doi: 10.1016/j.bbapap.2011.07.015. <url>.

[118] Jose Luis Muñoz-Muñoz, Jose Berna, Francisco Garcia-Molina, Pedro Antonio Garcia-Ruiz, Jose Tudela, Jose N. Rodriguez-Lopez, and Francisco Garcia-Canovas. Unravelling the suicide inactivation of tyrosinase: A discrimination between mechanisms. *Journal of Molecular Catalysis B: Enzymatic*, 75 (0): 11 – 19, 2012. ISSN 1381-1177. doi: 10.1016/j.molcatb.2011.11.001. <url>.

[119] Francisco Martínez Ortiz, JoséTudela Serrano, JoséNeptuno Rodríguez López, Ramón Varón Castellanos, JoséAntonio Lozano Teruel, and Francisco García-Cánovas. Oxidation of 3,4-dihydroxymandelic acid catalyzed by tyrosinase. *Biochimica et Biophysica Acta (BBA) - Protein Structure and Molecular Enzymology*, 957 (1): 158 – 163, 1988. ISSN 0167-4838. doi: 10.1016/0167-4838(88)90169-0. <url>.

[120] Antonio Rescigno, Frédéric Bruyneel, Alessandra Padiglia, Francesca Sollai, Andrea Salis, Jaqueline Marchand-Brynaert, and Enrico Sanjust. Structure–activity relationships of various amino-hydroxy-benzenesulfonic acids and sulfonamides as tyrosinase substrates. *Biochimica et Biophysica Acta (BBA) - General Subjects*, 1810 (8): 799 – 807, 2011. ISSN 0304-4165. doi: 10.1016/j.bbagen.2011.05.002. <url>.

[121] José Neptuno Rodríguez-López, Lorena G. Fenoll, María J. Peñalver, Pedro Antonio García-Ruiz, Ramón Varón, Francisco Martínez-Ortíz, Francisco García-Cánovas, and José Tudela. Tyrosinase action on monophenols: evidence for direct enzymatic release of o-diphenol. *Biochimica et Biophysica Acta (BBA) - Protein Structure and Molecular Enzymology*, 1548 (2): 238 – 256, 2001. ISSN 0167-4838. doi: 10.1016/S0167-4838(01)00237-0. <url>.

[122] Pillaiyar Thanigaimalai, Ki-Cheul Lee, Vinay K. Sharma, Cheonik Joo, Won-Jea Cho, Eunmiri Roh, Youngsoo Kim, and Sang-Hun Jung. Structural requirement of phenylthiourea analogs for their inhibitory activity of melanogenesis and tyrosinase. *Bioorganic & Medicinal Chemistry Letters*, 21 (22): 6824 – 6828, 2011. ISSN 0960-894X. doi: 10.1016/j.bmcl.2011.09.024. <url>.

[123] Nobuo Makino and Howard S. Mason. Reactivity of Oxytyrosinase toward Substrates. *Journal of Biological Chemistry*, 248 (16): 5731 – 5735, 1973. <url>.

[124] Álvaro Sánchez-Ferrer, José Neptuno Rodríguez-López, Francisco García-Cánovas, and Francisco García-Carmona. Tyrosinase: a comprehensive review of its mechanism. *Biochimica et Biophysica Acta (BBA) - Protein Structure and Molecular Enzymology*, 1247 (1): 1 – 11, 1995. ISSN 0167-4838. doi: 10.1016/0167-4838(94)00204-T. <url>.

[125] Louis P. Hammett. The Effect of Structure upon the Reactions of Organic Compounds. Benzene Derivatives. *Journal of the American Chemical Society*, 59 (1): 96 – 103, 1937. doi: 10.1021/ja01280a022. <url>.

[126] Shin-ichi Yamazaki and Shinobu Itoh. Kinetic Evaluation of Phenolase Activity of Tyrosinase Using Simplified Catalytic Reaction System. *Journal of the American Chemical Society*, 125 (43): 13034 – 13035, 2003. doi: 10.1021/ja036425d. <url>.

[127] Liviu M. Mirica, Michael Vance, Deanne Jackson Rudd, Britt Hedman, Keith O. Hodgson, Edward I. Solomon, and T. Daniel P. Stack. Tyrosinase Reactivity in a Model Complex: An Alternative Hydroxylation Mechanism. *Science*, 308 (5730): 1890 – 1892, 2005. doi: 10.1126/science.1112081. <url>.

[128] Michael Fountoulakis and Hans-Werner Lahm. Hydrolysis and amino acid composition analysis of proteins. *Journal of Chromatography A*, 826 (2): 109 – 134, 1998. ISSN 0021-9673. doi: 10.1016/S0021-9673(98)00721-3. <url>.

[129] Tim Rogalinski, Kaiyue Liu, Tobias Albrecht, and Gerd Brunner. Hydrolysis kinetics of biopolymers in subcritical water. *The Journal of Supercritical Fluids*, 46 (3): 335 – 341, 2008. ISSN 0896-8446. doi: 10.1016/j.supflu.2007.09.037. <url>.

[130] Kang S. Lee and Dennis G. Drescher. Fluorometric amino-acid analysis with o-phthaldialdehyde (OPA). *International Journal of Biochemistry*, 9 (7): 457 – 467, 1978. ISSN 0020-711X. doi: 10.1016/0020-711X(78)90075-7. <url>.
[131] John W. Henderson Jr. and Anne Brooks. Improved Amino Acid Methods using Agilent ZORBAX Eclipse Plus C18 Columns for a Variety of Agilent LC Instrumentation and Separation Goals. Technical report, Agilent Technologies, Inc., 2010. <url>. Agilent Application Note 5990-4547EN.
[132] Clare L. Hawkins, Philip E. Morgan, and Michael J. Davies. Quantification of protein modification by oxidants. *Free Radical Biology and Medicine*, 46 (8): 965 – 988, 2009. ISSN 0891-5849. doi: 10.1016/j.freeradbiomed.2009.01.007. <url>.
[133] H. H. Richmond, G. S. Myers, and George F Wright. The Reaction between Formaldehyde and Ammonia. *Journal of the American Chemical Society*, 70 (11): 3659 – 3664, 1948. doi: 10.1021/ja01191a034. <url>.
[134] U. K. Laemmli. Cleavage of Structural Proteins during the Assembly of the Head of Bacteriophage T4. *Nature*, 227 (5259): 680 – 685, 1970. doi: 10.1038/227680a0. <url>.
[135] Dmitry S. Kryndushkin, Ilya M. Alexandrov, Michael D. Ter-Avanesyan, and Vitaly V. Kushnirov. Yeast [PSI+] Prion Aggregates Are Formed by Small Sup35 Polymers Fragmented by Hsp104. *Journal of Biological Chemistry*, 278 (49): 49636 – 49643, 2003. doi: 10.1074/jbc.M307996200. <url>.
[136] Z. Hodny, R. Struzinsky, and Z. Deyl. Silver staining of collagen type I after sodium dodecylsulphate polyacrylamide gel electrophoresis: effect of Maillard reaction. *Journal of Chromatography B: Biomedical Sciences and Applications*, 578 (1): 53 – 62, 1992. ISSN 0378-4347. doi: 10.1016/0378-4347(92)80224-E. <url>.
[137] Timothy V. Updyke and Sheldon C. Engelhorn. System for pH-neutral stable electrophoresis gel, 2000. <url>. US Patent 6162338.
[138] Myungkoo Suh Donghoon Kang, Yong Song Gho and Chulhun Kang. Highly Sensitive and Fast Protein Detection with Coomassie Brilliant Blue in Sodium Dodecyl Sulfate-Polyacrylamide Gel Electrophoresis. *Bulletin of the Korean Chemical Society (BKCS)*, 23: 1511 – 1512, 2002. doi: 10.5012/bkcs.2002.23.11.1511. <url>.
[139] Ernest W. Willoughby and Andrea Lambert. A sensitive silver stain for proteins in agarose gels. *Analytical Biochemistry*, 130 (2): 353 – 358, 1983. ISSN 0003-2697. doi: 10.1016/0003-2697(83)90599-7. <url>.
[140] K. J. R. Rosman and P. D. P. Taylor. Isotopic Compositions of the Elements 1997. *Journal of Physical and Chemical Reference Data*, 27: 1275, 1998. doi: 10.1063/1.556031. <url>.
[141] Michal Holčapek, Robert Jirásko, and Miroslav Lísa. Basic rules for the interpretation of atmospheric pressure ionization mass spectra of small molecules. *Journal of Chromatography A*, 1217 (25): 3908 – 3921, 2010. ISSN 0021-9673. doi: 10.1016/j.chroma.2010.02.049. <url>.
[142] Tobias Kind and Oliver Fiehn. Advances in structure elucidation of small molecules using mass spectrometry. *Bioanalytical Reviews*, 2: 23 – 60, 2010. ISSN 1867-2086. doi: 10.1007/s12566-010-0015-9. <url>. PMCID: PMC3015162.
[143] Karsten Levsen, Hans-Martin Schiebel, Johan K. Terlouw, Karl J. Jobst, Manfred Elend, Alfred Preiß, Herbert Thiele, and Arnd Ingendoh. Even-electron ions: a systematic study of the neutral species lost in the dissociation of quasi-molecular ions. *Journal of Mass Spectrometry*, 42 (8): 1024 – 1044, 2007. ISSN 1096-9888. doi: 10.1002/jms.1234. <url>.
[144] Avi Weissberg and Shai Dagan. Interpretation of ESI(+)-MS-MS spectra—Towards the identification of “unknowns”. *International Journal of Mass Spectrometry*, 299 (2-3): 158 – 168, 2011. ISSN 1387-3806. doi: 10.1016/j.ijms.2010.10.024. <url>.
[145] M. Klessinger and W. Lüttke. Theoretische und spektroskopische Untersuchungen an Indigo-Farbstoffen — II: Das chromophore System der Indigo-Farbstoffe. *Tetrahedron*, 19, Supplement 2 (0): 315 – 335, 1963. ISSN 0040-4020. doi: 10.1016/S0040-4020(63)80023-X. <url>.
[146] Mark A. Thompson and Michael C. Zerner. A theoretical examination of the electronic structure and spectroscopy of the photosynthetic reaction center from Rhodopseudomonas viridis. *Journal of the American Chemical Society*, 113 (22): 8210 – 8215, 1991. doi: 10.1021/ja00022a003. <url>.

[147] Mohd.Shahid Khan and Zahid H Khan. Electronic absorption spectra of amino substituted anthraquinones and their interpretation using the ZINDO/S and AM1 methods. *Spectrochimica Acta Part A: Molecular and Biomolecular Spectroscopy*, 59 (7): 1409 – 1426, 2003. ISSN 1386-1425. doi: 10.1016/S1386-1425(02)00360-8. <url>.

[148] Shenfeng Yuan and Zhirong Chen. Study on the prediction of electronic absorption spectrum for cyanine compounds. *Journal of Molecular Structure: THEOCHEM*, 717 (1-3): 81 – 84, 2005. ISSN 0166-1280. doi: 10.1016/j.theochem.2004.12.018. <url>.

[149] Muhannad Altarsha, Gérald Monard, and Bertrand Castro. Quantum computations of the UV–visible spectra of uric acid and its anions. *Journal of Molecular Structure: THEOCHEM*, 761 (1-3): 203 – 207, 2006. ISSN 0166-1280. doi: 10.1016/j.theochem.2006.01.008. <url>.

[150] Denis Jacquemin, Cyril Peltier, and Ilaria Ciofini. Visible spectrum of naphthazarin investigated through Time-Dependent Density Functional Theory. *Chemical Physics Letters*, 493 (1-3): 67 – 71, 2010. ISSN 0009-2614. doi: 10.1016/j.cplett.2010.04.071. <url>.

[151] Claude Millot, Rachel Schurhammer, Etienne Engler, and Georges Wipff. Simulation and UV–visible spectra of organic dyes in subcritical and supercritical carbon dioxide. *Journal of Molecular Liquids*, 153 (1): 37 – 45, 2010. ISSN 0167-7322. doi: 10.1016/j.molliq.2009.11.008. <url>.

[152] Luis Serrano-Andrés and Björn O. Roos. A Theoretical Study of the Indigoid Dyes and Their Chromophore. *Chemistry – A European Journal*, 3 (5): 717 – 725, 1997. ISSN 1521-3765. doi: 10.1002/chem.19970030511. <url>.

[153] Yunsheng Xue, Yi Liu, Lin An, Ling Zhang, Yimin Yuan, Jie Mou, Ling Liu, and Youguang Zheng. Electronic structures and spectra of quinoline chalcones: DFT and TDDFT-PCM investigation. *Computational and Theoretical Chemistry*, 965 (1): 146 – 153, 2011. ISSN 2210-271X. doi: 10.1016/j.comptc.2011.01.042. <url>.

[154] R. Graham Cooks and Alan L. Rockwood. The 'Thomson'. A suggested unit for mass spectroscopists. *Rapid Communications in Mass Spectrometry*, 5: 93, 1991. doi: 10.1002/rcm.1290050210. <url>.

[155] Florian Rasche, Aleš Svatoš, Ravi Kumar Maddula, Christoph Böttcher, and Sebastian Böcker. Computing Fragmentation Trees from Tandem Mass Spectrometry Data. *Analytical Chemistry*, 83 (4): 1243 – 1251, 2011. doi: 10.1021/ac101825k. <url>.

[156] R.E. Childs and W.G. Bardsley. The steady-state kinetics of peroxidase with 2,2'-azino-di-(3-ethyl-benzthiazoline-6-sulphonic acid) as chromogen. *Biochemical Journal*, 145: 93 – 103, 1975. <url>. PMCID: PMC1165190.

[157] Christian Johannes and Andrzej Majcherczyk. Laccase activity tests and laccase inhibitors. *Journal of Biotechnology*, 78 (2): 193 – 199, 2000. ISSN 0168-1656. doi: 10.1016/S0168-1656(00)00208-X. <url>.

[158] Riitta Partanen, Mika Torkkeli, Maarit Hellman, Perttu Permi, Ritva Serimaa, Johanna Buchert, and Maija-Liisa Mattinen. Loosening of globular structure under alkaline pH affects accessibility of β-lactoglobulin to tyrosinase-induced oxidation and subsequent cross-linking. *Enzyme and Microbial Technology*, 49 (2): 131 – 138, 2011. ISSN 0141-0229. doi: 10.1016/j.enzmictec.2011.04.010. <url>.

[159] Emilia Selinheimo, Deirdre NiEidhin, Charlotte Steffensen, Jacob Nielsen, Anne Lomascolo, Sonia Halaouli, Eric Record, David O'Beirne, Johanna Buchert, and Kristiina Kruus. Comparison of the characteristics of fungal and plant tyrosinases. *Journal of Biotechnology*, 130 (4): 471 – 480, 2007. ISSN 0168-1656. doi: 10.1016/j.jbiotec.2007.05.018. <url>.

[160] Svend Olav Andersen. The cross-links in resilin identified as dityrosine and trityrosine. *Biochimica et Biophysica Acta (BBA) - General Subjects*, 93 (1): 213 – 215, 1964. ISSN 0304-4165. doi: 10.1016/0304-4165(64)90289-2. <url>.

[161] Martin Paul Bucknall. *Dityrosine as a biomarker of free radical induced oxidative damage in diseases of ageing*. PhD thesis, School of Medical Sciences, University of New South Wales, Sydney 2052, 2006. <url>.

[162] Holger Eickhoff, Günther Jung, and Anton Rieker. Oxidative phenol coupling—tyrosine dimers and libraries containing tyrosyl peptide dimers. *Tetrahedron*, 57 (2): 353 – 364, 2001. ISSN 0040-4020. doi: 10.1016/S0040-4020(00)00942-X. <url>.

[163] C. Giulivi, N. J. Traaseth, and K. J. A. Davies. Tyrosine oxidation products: analysis and biological relevance. *Amino Acids*, 25: 227 – 232, 2003. ISSN 0939-4451. doi: 10.1007/s00726-003-0013-0. <url>.
[164] Edward P.L. Hunter, Marc F. Desrosiers, and Michael G. Simic. The effect of oxygen, antioxidants, and superoxide radical on tyrosine phenoxyl radical dimerization. *Free Radical Biology and Medicine*, 6 (6): 581 – 585, 1989. ISSN 0891-5849. doi: 10.1016/0891-5849(89)90064-6. <url>.
[165] Benny Sabroe Welinder, Peter Roepstorff, and Svend Olav Andersen. The crustacean cuticle—IV. Isolation and identification of cross-links from Cancer pagurus cuticle. *Comparative Biochemistry and Physiology Part B: Comparative Biochemistry*, 53 (4): 529 – 533, 1976. ISSN 0305-0491. doi: 10.1016/0305-0491(76)90212-1. <url>.
[166] Dean A. Malencik, James F. Sprouse, Chris A. Swanson, and Sonia R. Anderson. Dityrosine: Preparation, Isolation, and Analysis. *Analytical Biochemistry*, 242 (2): 202 – 213, 1996. ISSN 0003-2697. doi: 10.1006/abio.1996.0454. <url>.
[167] Dong-Ik Lee, Sangpill Hwang, Jee Yun Choi, Ik-Sung Ahn, and Chang-Ha Lee. A convenient preparation of dityrosine via Mn(III)-mediated oxidation of tyrosine. *Process Biochemistry*, 43 (9): 999 – 1003, 2008. ISSN 1359-5113. doi: 10.1016/j.procbio.2008.04.020. <url>.
[168] Thomas M. Annesley. Ion Suppression in Mass Spectrometry. *Clinical Chemistry*, 49 (7): 1041 – 1044, 2003. doi: 10.1373/49.7.1041. <url>.
[169] Vincent Stroobant Edmond de Hoffmann. *Mass Spectrometry: Principles and Applications, 3rd Edition*. Wiley-Interscience, 2007. doi: ISBN: 978-0-470-03310-4. <url>.
[170] Moddie D. Taylor and Malcolm B. Templeman. The Vapor Phase Dissociation of Some Carboxylic Acids. III.1 Trifluoroacetic Acid and Trifluoroacetic Acid-d2,3. *Journal of the American Chemical Society*, 78 (13): 2950 – 2953, 1956. doi: 10.1021/ja01594a008. <url>.
[171] Bernd O. Keller, Jie Sui, Alex B. Young, and Randy M. Whittal. Interferences and contaminants encountered in modern mass spectrometry. *Analytica Chimica Acta*, 627 (1): 71 – 81, 2008. ISSN 0003-2670. doi: 10.1016/j.aca.2008.04.043. <url>.
[172] Svend Olav Andersen. Characterization of a new type of cross-linkage in resilin, a rubber-like protein. *Biochimica et Biophysica Acta*, 69 (0): 249 – 262, 1963. ISSN 0006-3002. doi: 10.1016/0006-3002(63)91258-7. <url>.
[173] Theresa DiMarco and Cecilia Giulivi. Current analytical methods for the detection of dityrosine, a biomarker of oxidative stress, in biological samples. *Mass Spectrometry Reviews*, 26 (1): 108 – 120, 2007. ISSN 1098-2787. doi: 10.1002/mas.20109. <url>.
[174] A. J. Lea. A Neutral Solvent for Melanin. *Nature*, 156: 478, 1945. doi: 10.1038/156478a0. <url>.
[175] Irwin W. Sizer. The action of tyrosinase on proteins. *Journal of Biological Chemistry*, 163 (1): 145 – 157, 1946. <url>.
[176] Michael E. Jung and Tsvetelina I. Lazarova. Efficient Synthesis of Selectively Protected l-Dopa Derivatives from l-Tyrosine via Reimer−Tiemann and Dakin Reactions. *The Journal of Organic Chemistry*, 62 (5): 1553 – 1555, 1997. doi: 10.1021/jo962099r. <url>.
[177] Howard B. Bensusan. Investigation of crosslinks in collagen following an enzymic hydrolysis. *Biochimica et Biophysica Acta (BBA) - Protein Structure*, 285 (2): 447 – 452, 1972. ISSN 0005-2795. doi: 10.1016/0005-2795(72)90331-5. <url>.
[178] Timothy J. Housley, Marvin L. Tanzer, and Howard B. Bensusan. Release of reducible crosslinks of collagen by total enzymic hydrolysis. *Biochimica et Biophysica Acta (BBA) - Protein Structure*, 365 (2): 405 – 413, 1974. ISSN 0005-2795. doi: 10.1016/0005-2795(74)90013-0. <url>.
[179] Andrew H. Kang and Jerome Gross. Relationship between the Intra and Intermolecular Cross-links of Collagen. *Proceedings of the National Academy of Sciences of the United States of America*, 67: 1307 – 1314, 1970. <url>.
[180] David A. Slatter, R. Gordon Paul, Martin Murray, and Allen J. Bailey. Reactions of Lipid-derived Malondialdehyde with Collagen. *Journal of Biological Chemistry*, 274 (28): 19661 – 19669, 1999. doi: 10.1074/jbc.274.28.19661. <url>.

[181] Marvin L. Tanzer and Gerald Mechanic. Collagen reduction by sodium borohydride: Effects of reconstitution, maturation and lathyrism. *Biochemical and Biophysical Research Communications*, 32 (5): 885 – 892, 1968. ISSN 0006-291X. doi: 10.1016/0006-291X(68)90324-0. <url>.
[182] D. P. Reinhard J. Brinckmann Y. Gaber, K. Tiedemann. Veränderungen der Quervernetzungen im kollagenen Bindegewebe bei Dermatoliposklerose. *Phlebologie*, 33: 8 – 11, 2004. <url>.
[183] Paul M. Gallop, Olga O. Blumenfeld, Edward. Henson, and Arthur L. Schneider. Isolation and identification of α-amino aldehydes in collagen. *Biochemistry*, 7 (6): 2409 – 2430, 1968. doi: 10.1021/bi00846a051. <url>.
[184] M.M. Kreevoy and R.W. Jacobson. The rate of decomposition of sodium borohydride in basic aqueous solutions. *Ventronn Alembic*, 15: 2 – 3, 1979.
[185] Gordon W. Gribble. Sodium borohydride in carboxylic acid media: a phenomenal reduction system. *Chemical Society Reviews*, 27: 395 – 404, 1998. doi: 10.1039/A827395Z. <url>.
[186] Edward L. Howes Robert H. DeBellis Arthur Sohler Ines Mandl, John D. MacLennan. Isolation and characterization of proteinase and collagenase from Cl. histolyticum. *The Journal of Clinical Investigation*, 32: 1323 – 1329, 1953. <url>. PMCID: PMC438478.
[187] Louis Pillemer and M. C. Hutchinson. The determination of the albumin and globulin contents of human serum by methanol precipitation. *Journal of Biological Chemistry*, 158 (1): 299 – 301, 1945. <url>.
[188] D. Wessel and U.I. Flügge. A method for the quantitative recovery of protein in dilute solution in the presence of detergents and lipids. *Analytical Biochemistry*, 138 (1): 141 – 143, 1984. ISSN 0003-2697. doi: 10.1016/0003-2697(84)90782-6. <url>.
[189] S. Jus, I. Stachel, W. Schloegl, M. Pretzler, W. Friess, M. Meyer, R. Birner-Gruenberger, and G.M. Gübitz. Cross-linking of collagen with laccases and tyrosinases. *Materials Science and Engineering: C*, 31 (5): 1068 – 1077, 2011. ISSN 0928-4931. doi: 10.1016/j.msec.2011.03.007. <url>.
[190] B. Madhan, V. Subramanian, J. Raghava Rao, Balachandran Unni Nair, and T. Ramasami. Stabilization of collagen using plant polyphenol: Role of catechin. *International Journal of Biological Macromolecules*, 37 (1-2): 47 – 53, 2005. ISSN 0141-8130. doi: 10.1016/j.ijbiomac.2005.08.005. <url>.
[191] P. L. Gordon, C. Huang, R. C. Lord, and I. V. Yannas. The Far-Infrared Spectrum of Collagen. *Macromolecules*, 7 (6): 954 – 956, 1974. doi: 10.1021/ma60042a052. <url>.
[192] S.D Figueiró, Júlio C Góes, R.A Moreira, and A.S.B Sombra. On the physico-chemical and dielectric properties of glutaraldehyde crosslinked galactomannan–collagen films. *Carbohydrate Polymers*, 56 (3): 313 – 320, 2004. ISSN 0144-8617. doi: 10.1016/j.carbpol.2004.01.011. <url>.
[193] Malte Rolff and Felix Tuczek. How Do Copper Enzymes Hydroxylate Aliphatic Substrates? Recent Insights from the Chemistry of Model Systems. *Angewandte Chemie International Edition*, 47 (13): 2344 – 2347, 2008. ISSN 1521-3773. doi: 10.1002/anie.200705533. <url>.
[194] Heather R. Lucas, Lei Li, Amy A. Narducci Sarjeant, Michael A. Vance, Edward I. Solomon, and Kenneth D. Karlin. Toluene and Ethylbenzene Aliphatic C−H Bond Oxidations Initiated by a Dicopper(II)-μ-1,2-Peroxo Complex. *Journal of the American Chemical Society*, 131 (9): 3230 – 3245, 2009. doi: 10.1021/ja807081d. <url>. PMID: 19216527.
[195] Christian Würtele, Ole Sander, Volker Lutz, Thomas Waitz, Felix Tuczek, and Siegfried Schindler. Aliphatic C−H Bond Oxidation of Toluene Using Copper Peroxo Complexes That Are Stable at Room Temperature. *Journal of the American Chemical Society*, 131 (22): 7544 – 7545, 2009. doi: 10.1021/ja902327s. <url>. PMID: 19441813.
[196] C. Nick Pace, Felix Vajdos, Lanette Fee, Gerald Grimsley, and Theronica Gray. How to measure and predict the molar absorption coefficient of a protein. *Protein Science*, 4 (11): 2411 – 2423, 1995. ISSN 1469-896X. doi: 10.1002/pro.5560041120. <url>.
[197] Rhoda Elison Hirsch and Ronald L. Nagel. Conformational studies of hemoglobins using intrinsic fluorescence measurements. *Journal of Biological Chemistry*, 256 (3): 1080 – 1083, 1981. <url>.
[198] William Ramsay Taylor. The classification of amino acid conservation. *Journal of Theoretical Biology*, 119 (2): 205 – 218, 1986. ISSN 0022-5193. doi: 10.1016/S0022-5193(86)80075-3. <url>. PMID: 3461222.

[199] Yoshiko Kuboe, Hitomi Tonegawa, Kousaku Ohkawa, and Hiroyuki Yamamoto. Quinone Cross-Linked Polysaccharide Hybrid Fiber. *Biomacromolecules*, 5 (2): 348 – 357, 2004. doi: 10.1021/bm034363d. <url>. PMID: 15002994.

[200] G Kumar, J.F Bristow, P.J Smith, and G.F Payne. Enzymatic gelation of the natural polymer chitosan. *Polymer*, 41 (6): 2157 – 2168, 2000. ISSN 0032-3861. doi: 10.1016/S0032-3861(99)00360-2. <url>.

[201] Claudia Thalmann and Thomas Lötzbeyer. Enzymatic cross-linking of proteins with tyrosinase. *European Food Research and Technology*, 214: 276 – 281, 2002. ISSN 1438-2377. doi: 10.1007/s00217-001-0455-0. <url>.

[202] Tefsit Bekele, Meha H. Shah, Jamison Wolfer, Ciby J. Abraham, Anthony Weatherwax, and Thomas Lectka. Catalytic, Enantioselective [4 + 2]-Cycloadditions of Ketene Enolates and o-Quinones: Efficient Entry to Chiral, α-Oxygenated Carboxylic Acid Derivatives. *Journal of the American Chemical Society*, 128 (6): 1810 – 1811, 2006. doi: 10.1021/ja058077g. <url>. PMID: 16464078.

[203] Daniel H. Paull, Jamison Wolfer, James W. Grebinski, Anthony Weatherwax, and Thomas Lectka. Catalytic, Asymmetric Inverse Electron Demand Hetero Diels-Alder Reactions of o-Benzoquinone Derivatives and Ketene Enolates. *CHIMIA International Journal for Chemistry*, 61 (5): 240 – 246, May 2007. doi: 10.2533/chimia.2007.240. <url>.

[204] Jose Luis Muñoz-Muñoz, Francisco Garcia-Molina, Ramon Varon, Pedro A. Garcia-Ruíz, Jose Tudela, Francisco Garcia-Cánovas, and Jose Neptuno Rodríguez-López. Suicide inactivation of the diphenolase and monophenolase activities of tyrosinase. *IUBMB Life*, 62 (7): 539 – 547, 2010. ISSN 1521-6551. doi: 10.1002/iub.348. <url>.

[205] Luciana Pereira Artur Cavaco-Paulo Eva Almansa, Andreas Kandelbauer and Georg M. Gübitz. Influence of Structure on Dye Degradation with Laccase Mediator Systems. *Biocatalysis and Biotransformation*, 22: 315 – 324, 2004. doi: 10.1080/10242420400024508. <url>.

[206] Zhiwei Huang, Harvey Lui, X. K. Chen, Abdulmajeed Alajlan, David I. McLean, and Haishan Zeng. Raman spectroscopy of in vivo cutaneous melanin. *Journal of Biomedical Optics*, 9 (6): 1198 – 1205, 2004. doi: 10.1117/1.1805553. <url>.

[207] J.E. Purcell, J.H. Kelley, E. Kwan, C.G. Sheu, and H.R. Weller. Energy levels of light nuclei. *Nuclear Physics A*, 848 (1-2): 1 – 74, 2010. ISSN 0375-9474. doi: 10.1016/j.nuclphysa.2010.08.012. <url>.

[208] The Advisory Group on Ionising Radiation (AGIR) on behalf of the Health Protection Agency. *Review of Risks from Tritium. Report of the independent Advisory Group on Ionising Radiation (RCE-4)*. Health Protection Agency (UK), 2007. ISBN 978-0-85951-610-5. <url>.